

**Horst E. Friedrich  
Barry L. Mordike  
(Eds.)**

# Magnesium Technology

**Metallurgy, Design Data,  
Applications**

Friedrich · Mordike  
Magnesium Technology



Horst E. Friedrich · Barry L. Mordike

# Magnesium Technology

Metallurgy, Design Data, Applications

With 590 Figures



Springer

Professor  
Dr.-Ing. Horst E. Friedrich  
Institut für Fahrzeugkonzepte (FK)  
Deutsches Zentrum für Luft- und Raumfahrt (DLR) e.V.  
in der Helmholtz-Gemeinschaft  
Pfaffenwaldring 38–40  
70569 Stuttgart  
Germany  
*e-mail: Horst.Friedrich@dlr.de*

Professor  
Dr. Barry L. Mordike  
Institut für Werkstoffkunde und Werkstofftechnik  
TU Clausthal  
Agricolastrasse 6  
38678 Clausthal-Zellerfeld  
Germany  
*e-mail: barrymordike@hotmail.com*

Library of Congress Control Number 2005931991

ISBN-10 3-540-20599-3 Springer Berlin Heidelberg New York  
ISBN-13 978-3-540-20599-9 Springer Berlin Heidelberg New York

This work is subject to copyright. All rights are reserved, whether the whole or part of the material is concerned, specifically the rights of translation, reprinting, reuse of illustrations, recitation, broadcasting, reproduction on microfilms or in any other ways, and storage in data banks. Duplication of this publication or parts thereof is only permitted under the provisions of the German Copyright Law of September 9, 1965, in its current version, and permission for use must always be obtained from Springer-Verlag. Violations are liable to prosecution under the German Copyright Law.

**Springer is a part of Springer Science+Business Media**  
springeronline.com

© Springer-Verlag Berlin Heidelberg 2006  
Printed in Germany

The use of general descriptive names, registered names, trademarks, etc. in this publication does not imply, even in the absence of a specific statement, that such names are exempt from the relevant protection laws and regulations and therefore free for general use.

Cover design: deblik Berlin  
Typesetting: Fotosatz-Service Köhler GmbH, Würzburg

Printed on acid-free paper 02/3141 xv – 5 4 3 2 1 0

---

## Preface/Foreword

Magnesium was discovered and isolated as a chemical element in 1808 by Sir Humphrey Davy. The problem with its isolation was associated with its reactivity, which has haunted all those interested in using magnesium as components. The applications today must also consider the problems of corrosion. If we consider other properties e.g. elastic rigidity we find that the elastic constants are significantly lower than those of other metals. The yield strength or ultimate tensile strength is also poorer than most constructional metals.

The significant event at the beginning of the twentieth century was aviation and this changed the rules – it was the specific yield strength which was important and indeed much work was undertaken in the two wars to develop magnesium alloys for aviation. Magnesium had come of age and was used extensively in military aircraft during the Second World War. Thereafter, there was a slump in its use and apart from isolated applications was unable to compete with other metals, both from an economic and also technological standpoint.

In the nineteen-nineties a concentrated effort was made to solve many of the problems, which limited the widespread application of magnesium alloys. This effort was essentially global with producers and car manufacturers uniting so that magnesium becomes recognised as a structural material. One group was USA and Canada, another was Australia with CAST, Israel, Norsk Hydro, MEL and Germany. In this book we have authors covering all aspects of magnesium technology. For the first time in 50 years we are able to show which advances in component development have been made possible since the tome by Emley of MEL. The authors come from Germany, USA, Norway, Canada, Israel, Switzerland and the UK and have covered the following topics on a chapter or sub-chapter basis.

There have not been many books on magnesium. The first was Beck's "Magnesium und seine Legierungen", published in the 1930's, which was hurriedly translated into English. This was followed 25 years later by Emley's book, Principles of "Magnesium Technology". This was a comprehensive revue of the state of the art. Since that time there has been the ASM Handbook which provided a useful collation of the properties of magnesium alloys but did not attempt to update Emley.

There are nine chapters in this book. The first chapter covers the history until 1945 and also from 1945 to about 1990. The second chapter covers an extensive survey of 30 pages of various production technologies of magnesium. This is followed by a detailed presentation of the physical metallurgy, physical and mechanical constants, deformation behaviour, strengthening mechanisms, classifi-

cation of alloys, binary and higher phase diagrams, various MEL alloys and highly creep resistant alloys. Chapter 4 is devoted to melting, alloying and refining. Chapter 5 is a contribution by several authors of 70 pages to a detailed description of present day magnesium casting alloys. Chapter 6 covers the technology of magnesium and its alloys. This chapter of 200 pages discusses many aspects e.g. sand casting, casting defects, inspection, identification and elimination of defects. This is followed by a discussion of die casting, also squeeze casting and semi-solid casting with their associated properties. Rolling of magnesium and sheet metal forming is a recent important extension to magnesium technology. Extrusion is also discussed with alloy developments and novel extrusion methods. An important topic in this chapter is magnesium matrix composites. Joining and welding processes are also covered in this chapter. Alternative processes to welding, such as adhesive bonding technology, clinching, riveting, direct screwing, folding, hybrid joining are relatively new methods of joining magnesium. Machining of reinforced and un-reinforced magnesium alloys concludes this chapter.

Chapter 7 is dedicated to corrosion and surface protection and represents a chapter in which significant advances have been made and where some problems have been eliminated. Chapter 8 shows examples of automobile applications in Europe and North America together with concepts of life cycle inventory of vehicles, other applications such as hand tools, sports equipment, electronic equipment and aerospace. Barriers to magnesium are also discussed. In chapter 9 the problem of setting up a secondary recycling strategy for magnesium is discussed.

This book for the first time shows a wide spectrum of applications. Obviously, the automobile applications are particularly important as they could guarantee that a sufficient volume of magnesium is produced; ensuring that unit prices are low. The price competition is keen and there is still much to be achieved with wrought products, in particular.

Significant advances have been made in corrosion protection, joining technologies and recycling.

Horst E. Friedrich

Barry L. Mordike

---

## **Dr. Horst E. Friedrich**

Prof. Dr. H. E. Friedrich studied engineering at the Technical University of Munich. After working in the engineering and consultancy sectors, he took up a senior management position in the aeronautical industry in 1986. He was responsible for new methods of construction and new materials, aircraft engines and optimising product development times. In 1996, Prof. Friedrich joined Volkswagen AG in Wolfsburg as head of vehicle research, where at last he was head of Group research for materials technology and vehicle concepts. He specialised in innovative materials and construction methods, and concept vehicles for future vehicle specifications.

Since March 2004 he is director of the Institute of Vehicle Concepts at the German Aerospace Center in Stuttgart and professor at the University of Stuttgart. The research fields are Alternative Power Trains and Energy Conversion as well as Light Weight Design and Hybrid Construction methods.

Prof. Dr. Friedrich worked as Director of the Board of the International Magnesium Association (IMA) and has a lectureship at the Technical University of Berlin for materials and design in the transportation industry.

## **Prof. Dr Barry L. Mordike**

Barry Mordike studied Physical Metallurgy at Birmingham University and completed his studies with BSc(Hons) Class1 in 1956. He then undertook research for his PhD in the Cavendish Laboratory, Department of Physics, University of Cambridge, completing his PhD in Summer 1959. He then continued research in the Institut für Metallphysik, Universität Göttingen as 'Wissenschaftlicher Assistent' to Prof. Peter Haasen. In September 1966 he took up a post as Senior Lecturer (C4 Professur) in the Department of Metallurgy, University of Liverpool, where he stayed until the end of 1976. In Dec 1976 he was appointed to the newly created Chair of Materials Engineering and Technology at the Technical University of Clausthal. He remained at Clausthal until he became Emeritus Professor in October 1999.

Apart from his academic pursuits he created in 1989 a technology transfer company, Zentrum für Funktionswerkstoffe g.G.m.b.H( Clausthal) with the aid of Government funding. This enabled projects to be completed where industrial competence and confidentiality were necessary. In 2002 Prof. V. Neubert took over from him as General Manager.

Initially, his research interests concentrated on fundamental problems such as deformation processes, initiation of fatigue, crystal growth, strengthening mechanisms in metals. He changed his emphasis and developed interests in more applied research. Prior to going to Clausthal he started to work on magnesium alloys (1972), some aspects being supported by MEL (Elektron), Powder Metal-



lurgy (1973) and Laser Technology (1976). At Clausthal, he rapidly built up a considerable research potential and covered a wide range of subjects.

The period 1976 to 1999 will be remembered for its contribution to developing Laser Treatment of Materials, Magnesium 1972 – present day, Powder Metallurgy and Composite Materials, Surface Engineering, in particular, Plasma Immersion Technology.

---

## List of Contributors

*Eli Aghion*

Department of Materials Engineering, Ben Gurion University of the Negev,  
P.O.B. 653, Beer Sheva 84105, Israel  
e-mail: egyon@bgu.ac.il

*Terje Kr. Aune*

Advanced Magnesium Technologies Ltd, Level 9, 303 Coronation Drive, Milton,  
Queensland 4064, Australia

*Robert E. Brown*

226 Deer Trace, Prattville, Alabama 36067, USA  
e-mail: magman6@aol.com

*Dieter Brungs*

Eversberg, Ober den Eschen 9, 59872 Meschede, Germany

*Bernard Closset*

Modal Technologies Inc., 8 Chemin de l'Ancien-Tir, 1252 Meinier, Switzerland  
e-Mail: closset@deckpoint.ch

*Gerald Cole*

25800 Romany Way, Franklin, MI 48025-1197, USA  
e-mail: geraldcole@peoplepc.com

*Günter H. Deinzer*

Entwicklung/Werkstoffe AUDI Ingolstadt, Germany  
e-mail: guenter.deinzer@audi.de

*Berend Denkena*

Institut für Fertigungstechnik und Werkzeugmaschinen,  
Produktionstechnisches Zentrum, Universität Hannover, Schönebecker Allee 2,  
30823 Garbsen, Germany  
e-mail: denkena@ifw.uni-hannover.de

*Hajo Dieringa*

GKSS-Forschungszentrum Geesthacht GmbH, Institut für Werkstoffforschung,  
Max-Planck-Straße 1, 21502 Geesthacht, Germany  
e-mail: hajo.dieringa@gkss.de

*Dan Eliezer*

Department of Materials Engineering, Ben Gurion University of the Negev,  
P.O.B. 653, Beer Sheva 84105, Israel  
e-mail: deliezer@bgumail.bgu.ac.il

*Steve Erickson*

e-mail: serickson@iglide.net

*Horst E. Friedrich*

Institut für Fahrzeugkonzepte (FK), Deutsches Zentrum für Luft- und  
Raumfahrt (DLR) e.V. in der Helmholtz-Gemeinschaft, Pfaffenwaldring 38-40,  
70569 Stuttgart, Germany  
e-mail: horst.friedrich@dlr.de

*Francis H. Froes*

University of Idaho, Institute for Materials and Advanced Processes,  
College of Engineering, McClure Building, Room 437, Moscow,  
Idaho 83844-3026, USA  
e-mail: imap@uidaho.edu

*Gilad Golub*

Environmental Services Co. Ltd, Ramat Hovav, P.O. Box 5743, Beer Sheva 84156,  
Israel

*Kurt Harbodt*

Reiherstraße 44, 50997 Köln, Germany  
e-mail: kharbodt@t-online.de

*Otto-Diedrich Hennemann*

Fraunhofer Institut, Fertigungstechnik und angewandte Materialforschung,  
Wiener Straße 12, 28359 Bremen, Germany  
e-mail: hen@ifam.fhg.de

*Jim Hillis*

1027 Riverview Ranch Dr., Brazoria, TX 77422, USA  
e-Mail: jehillis@direcway.com

*Norbert Hort*

GKSS-Forschungszentrum Geesthacht GmbH, Institut für Werkstoffforschung,  
Max-Planck-Straße 1, 21502 Geesthacht, Germany  
e-mail: norbert.hort@gkss.de

*Peter Juchmann*

Salzgitter Magnesium-Technologie AG, Eisenhüttenstr. 99, 38239 Salzgitter,  
Germany

e-mail: juchmann.p@salzgitter-ag.de

*Karl Ulrich Kainer*

GKSS-Forschungszentrum Geesthacht GmbH, Institut für Werkstoffforschung,  
Max-Planck-Straße 1, 21502 Geesthacht, Germany

e-mail: karl.kainer@gkss.de

*Catrin Kammer*

METALL-Fachzeitschrift für Metallurgie, Kielsche Str. 43B, 38642 Goslar,  
Germany

e-mail: kammer@t-online.de

*Helmut Kaufmann*

ARC, Leichtmetallkompetenzzentrum Ranshofen GmbH, Postfach 26,  
5282 Ranshofen, Austria

e-mail: helmut.kaufmann@arcs.ac.at

*John F. King*

19, Brookside Crescent, Greenmount, Bury, BL8 4BG, United Kingdom

e-mail: jking.mel@btopenworld.com

*Simon Kleiner*

EMPA, Feuerwerkerstr. 39, 3602 Thun, Switzerland

e-mail: simon.kleiner@empa.ch

*Sanday Thakar Kumar*

Singapore Institute of Manufacturing Technology, Forming Technology Group,  
71, Nanyang Drive, Singapore 638075

e-mail: thankur@SIM Tech.a-star.edu.sg

*Peter Kurze*

AHC-Oberflächentechnik GmbH & Co. KG OGH, Postfach 00 21 49,  
50151 Kerpen, Germany

e-mail: info@ahc-surface.com

*Pavel Lukáč*

Department of Metalphysics, Faculty of Mathematics and Physics,  
Charles University, Ke Karlovu 5, 12116 Praha 2, Czechia

e-mail: lukac@met.mff.cuni.cz

*Andreas Mertz*

Am Stockfeld 24, 66539 Neunkirchen, Germany

e-mail: amertz@gmx.net

*Gerson Meschut*

Wilhelm Böllhof GmbH & Co. KG, Archimedesstraße, 33649 Bielefeld,  
Germany  
e-mail: gmeschut@boellhof.com

*Barry L. Mordike*

Institut für Werkstoffkunde und Werkstofftechnik, TU Clausthal,  
Agricolastraße 6, 38678 Clausthal-Zellerfeld, Germany  
e-mail: barrymordike@hotmail.com

*Mihriban Pekguleryuz*

McGill University, Department of Mining and Metallurgical Engineering,  
3610 University Street, Monreal, QC H3A 2B2, Canada  
e-mail: mihriban.pekguleryuz@mcgill.ca

*Christian Podolsky*

Pfalzstr.10, 30173 Hannover, Germany

*Michael Rethmeier*

Volkswagen AG, Wolfsburg, Germany  
e-mail: michael.rethmeier@volkswagen.de

*Soenke Schumann*

Volkswagen AG, Konzernforschung, Werkstofftechnik/Metalle, Brieffach 1511,  
38436 Wolfsburg, Germany  
e-mail: soenke.schumann@volkswagen.de

*Hans Kurt Tönshoff*

Universität Hannover Institute of Production Engineering  
and Machine Tools (IFW), Schlosswender Straße 5, 30159 Hannover, Germany  
e-mail: toenshoff@ ifw.uni-hannover.de

*Håkon Westengen*

Norsk Hydro ASA, Research Centre Porsgrunn, Forskingsparken Heroya,  
3907 Porsgrunn, Norway  
e-mail: hakon.westengen@hydro.com

*Jens Winkler*

Continental AG, Jädekamp 30, 30419 Hannover, Germany  
e-mail: jens.winkler@conti.de



---

# Contents

<b>1</b>	<b>History . . . . .</b>	<b>1</b>
1.1	History until 1945	
	<i>Kurt Harbott</i> . . . . .	1
1.1.1	Asia . . . . .	1
1.1.2	Australia . . . . .	2
1.1.3	Europe . . . . .	2
1.1.4	North America . . . . .	8
1.2	History Since 1945	
	<i>Robert E. Brown</i> . . . . .	12
1.2.1	Production . . . . .	12
1.2.2	Applications . . . . .	20
	References . . . . .	28
<b>2</b>	<b>Production Technologies of Magnesium</b>	
	<i>Gilad Golub, Eli Aghion</i> . . . . .	29
2.1	Introduction . . . . .	29
2.2	Raw Materials for Magnesium Production . . . . .	30
2.2.1	Magnesite . . . . .	31
2.2.2	Dolomite . . . . .	31
2.2.3	Bischofite . . . . .	31
2.2.4	Carnallite . . . . .	31
2.2.5	Serpentine . . . . .	32
2.2.6	Sea Water . . . . .	32
2.3	Electrochemical Methods . . . . .	33
2.3.1	Preparation of Magnesium Chloride Salts from Natural Raw Materials . . . . .	33
2.3.2	Drying Magnesium Chloride Salts . . . . .	35
2.3.3	Electrolysis of Magnesium Salts . . . . .	36
2.3.3.1	Type of Electrolytes for Electrolysis . . . . .	36
2.3.3.2	Thermal Balance of the Electrolysis Cell . . . . .	37
2.3.3.3	Increasing the Magnesium Output by Means of Artificial Cooling . . . . .	39

2.3.4	Types of Electrodes in the Electrolysis Cells . . . . .	39
2.3.5	Structure of the Electrolysis Cells . . . . .	41
2.3.6	Operation of Electrolysis Cell . . . . .	42
2.3.7	Refining Raw Magnesium Produced by Electrochemical Methods	43
2.3.8	Industrial Methods for Electrochemical Production . . . . .	44
2.3.8.1	DSM and Russian Process . . . . .	44
2.3.8.2	The Dow Process . . . . .	46
2.3.8.3	The MagCorp (now US Mag) Process . . . . .	47
2.3.8.4	The Hydro Magnesium Process . . . . .	47
2.3.8.5	The Magnola Process . . . . .	49
2.3.8.6	The AMC Process . . . . .	50
2.4	Thermal Reduction Methods . . . . .	52
2.4.1	Preparation of Raw Material and Thermal Reduction Method . .	52
2.4.2	Industrial Methods with Thermal Reduction . . . . .	52
2.4.2.1	Silicothermic Processes . . . . .	52
2.4.2.2	Aluminothermic Processes . . . . .	56
2.4.2.3	Carbothermic Process . . . . .	57
2.4.3	Collection and Refining the Raw Magnesium Produced by Thermal Reduction . . . . .	58
2.5	Advantages and Disadvantages of Electrolytic Production Versus Thermal Reduction Methods . . . . .	59
	References . . . . .	60
<b>3</b>	<b>Physical Metallurgy</b>	
	<i>Barry L. Mordike, Pavel Lukač</i> . . . . .	63
3.1	Introduction . . . . .	63
3.2	Properties of Pure Magnesium . . . . .	63
3.2.1	Atomic Properties . . . . .	63
3.2.2	Electron States . . . . .	64
3.2.3	Lattice Parameters . . . . .	64
3.2.4	Thermal Expansion . . . . .	65
3.2.5	Density . . . . .	65
3.2.6	Thermodynamic Properties . . . . .	65
3.2.7	Diffusion . . . . .	65
3.2.8	Thermal Conduction . . . . .	66
3.2.9	Elastic Moduli . . . . .	68
3.2.10	Damping Capacity . . . . .	68
3.2.11	Deformation Behavior . . . . .	74
3.2.12	Strengthening Mechanisms . . . . .	75
3.2.12.1	Dislocation Strengthening . . . . .	76
3.2.12.2	Solid Solution Hardening . . . . .	76
3.2.12.3	Precipitation Strengthening . . . . .	77

3.2.12.4	Dispersion Strengthening . . . . .	78
3.2.12.5	Strengthening by Grain Size Refinement . . . . .	78
3.3	Magnesium Alloys . . . . .	79
3.3.1	Common Alloying Elements . . . . .	80
3.3.1.1	Aluminum . . . . .	80
3.3.1.2	Calcium . . . . .	80
3.3.1.3	Lithium . . . . .	80
3.3.1.4	Manganese . . . . .	81
3.3.1.5	Rare Earths . . . . .	81
3.3.1.6	Silicon . . . . .	81
3.3.1.7	Silver . . . . .	81
3.3.1.8	Thorium . . . . .	81
3.3.1.9	Yttrium . . . . .	81
3.3.1.10	Zinc . . . . .	81
3.3.1.11	Zirconium . . . . .	81
3.3.2	Elements Used for Manufacturing Purposes or Impurities . . . .	82
3.3.2.1	Beryllium . . . . .	82
3.3.2.2	Copper . . . . .	82
3.3.2.3	Iron . . . . .	82
3.3.2.4	Nickel . . . . .	82
3.3.2.5	Tin . . . . .	82
3.3.3	Classification of Alloys . . . . .	82
3.4	Phase Diagrams . . . . .	84
3.4.1	Conventional Alloys . . . . .	84
3.4.1.1	Magnesium-Aluminum . . . . .	84
3.4.1.2	Magnesium-Zinc . . . . .	84
3.4.1.3	Magnesium-Manganese . . . . .	85
3.4.1.4	Super Light Weight Alloys . . . . .	86
3.4.1.5	High Performance Alloys . . . . .	87
3.4.1.6	Magnesium-Scandium . . . . .	88
3.4.1.7	Magnesium-Zirconium . . . . .	89
3.4.2	Higher Systems . . . . .	90
3.5	Commercial Alloy Systems . . . . .	92
3.5.1	Magnesium Die Casting Alloys (Zirconium Free) . . . . .	93
3.5.2	Permanent Mould, Sand and Investment Casting Alloys . . . .	94
3.5.2.1	Magnesium-Zinc-Zirconium . . . . .	94
3.5.2.2	Magnesium-Rare Earth-Zinc-Zirconium (ZK61 and ZK62) . . .	94
3.5.2.3	Magnesium-Silver . . . . .	96
3.5.2.4	Magnesium-Yttrium Alloys . . . . .	96
3.5.3	Further Development . . . . .	96
3.5.4	Highly Creep Resistant Alloys . . . . .	97
	References . . . . .	102
	Appendix . . . . .	105

<b>4</b>	<b>Melting, Alloying and Refining</b>	<b>109</b>
4.1	Zirconium-Free Alloys <i>Mihriban Pekguleryuz</i>	109
4.1.1	Mg-Al, Mg-Al-Zn, and Mg-Al-Si Alloys	109
4.1.1.1	Flux Melting and Refining	109
4.1.1.2	Fluxless Melting, and Alloying (the use of Cover gases)	113
4.1.1.3	Alloying of Mg with Al, Zn, Si	115
4.1.1.4	Manganese	116
4.1.1.5	Beryllium	119
4.1.1.6	Silicon	121
4.1.2	Mg-Al-(Rare-Earth) Alloys	121
4.1.3	Mg-Al-(Alkaline Earth) Alloys	122
4.1.3.1	Calcium	123
4.1.3.2	Strontium	123
4.1.4	Mg-Li Alloys	124
4.2	Alloys Containing Zirconium <i>John F. King</i>	128
4.2.1	Introduction	128
4.2.2	Mechanism of Grain Refinement by Zirconium	128
4.2.3	Effect of Other Alloying Elements	131
4.2.3.1	Incompatible Elements	131
4.2.3.2	Compatible Alloy Systems	132
4.2.4	Methods of Introducing Zirconium	133
4.2.4.1	Products Available	133
4.2.4.2	Basic Principles of Zr Grain Refinement	133
4.2.4.3	Zirconium Grain Refining in Fluxed Melts	135
4.2.4.4	Zirconium Grain Refining in Flux-Free Melts	137
4.2.4.5	Methods of Assessing Grain Refinement	138
4.2.5	Melting, Alloying Procedures for Other Elements	139
	References	141
<b>5</b>	<b>Magnesium Casting Alloys</b>	<b>145</b>
5.1	Casting Alloys <i>Håkon Westengen, Terje Kr. Aune</i>	145
5.1.1	Introduction	145
5.1.2	Alloying Principles	146
5.1.2.1	Properties of Pure Magnesium	146
5.1.2.2	Alloy Preparation	146
5.1.2.3	Alloying Elements and Their Influence	149
5.1.3	Casting Methods	162
5.1.4	Alloys for Diecasting	166
5.1.4.1	Compositions	166
5.1.4.2	Microstructures (Hydro Magnesium)	167

5.1.4.3	Properties . . . . .	171
5.1.5	Alloys for Sand Casting . . . . .	198
5.1.5.1	Compositions . . . . .	198
5.1.5.2	Properties . . . . .	199
5.2	Wrought Alloys	
	<i>Catrin Kammer</i> . . . . .	204
5.2.1	Magnesium – Aluminum . . . . .	208
5.2.2	Magnesium – Manganese (M-alloys) . . . . .	210
5.2.3	Magnesium – Aluminum – Zinc (AZ-alloys) . . . . .	210
5.2.4	Magnesium – Zinc – Zirconium (ZK-Alloys) . . . . .	212
5.2.5	Magnesium – Zinc – Rare Earth (ZE-Alloys) . . . . .	212
5.2.6	Magnesium – Yttrium – Rare Earth (WE-Alloys) . . . . .	212
5.2.7	Magnesium – Thorium, Zirconium or Manganese (HK- and HM-Alloys) . . . . .	213
5.2.8	Magnesium – Lithium – Alloys (LA-Alloys) . . . . .	213
5.2.9	Other Wrought Alloys . . . . .	214
	References . . . . .	214
<b>6</b>	<b>Technology of Magnesium and Magnesium Alloys . . . . .</b>	<b>219</b>
6.1	Casting . . . . .	219
6.1.1	Sand Casting	
	<i>John F. King</i> . . . . .	219
6.1.1.1	Introduction . . . . .	219
6.1.1.2	Sand Systems . . . . .	220
6.1.1.3	Design of Running Systems . . . . .	223
6.1.1.4	Mould Preparation and Assembly . . . . .	226
6.1.1.5	Identification and Elimination of Defects . . . . .	228
6.1.1.6	Sand Casting Techniques . . . . .	229
6.1.1.7	Heat Treatment . . . . .	231
6.1.1.8	Inspection of Castings . . . . .	232
6.1.2	Die Casting	
	<i>Dieter Brungs, Andreas Mertz</i> . . . . .	234
6.1.2.1	Die Casting Process for Magnesium . . . . .	234
6.1.2.2	Design Guidelines for Magnesium Die Castings . . . . .	247
6.1.2.3	Properties of Magnesium Die Castings . . . . .	252
6.1.2.4	Environmental Impact . . . . .	257
6.1.3	Squeeze Casting, Thixocasting and Rheocasting	
	<i>Helmut Kaufmann, Simon Kleiner</i> . . . . .	258
6.1.3.1	Introduction . . . . .	258
6.1.3.2	Squeeze Casting . . . . .	259
6.1.3.3	Semi-Solid Casting . . . . .	261
6.2	Forming . . . . .	269



6.2.1	Rolling and Shut Forming <i>Peter Juchmann</i> . . . . .	269
6.2.1.1	Situation and Potential of Magnesium Sheet . . . . .	269
6.2.1.2	Forming of Magnesium and Magnesium Alloys . . . . .	272
6.2.1.3	Magnesium Rolling . . . . .	274
6.2.1.4	Magnesium Sheet . . . . .	276
6.2.1.5	Sheet Metal Forming . . . . .	278
6.2.1.6	Prototyping and Application Perspectives . . . . .	284
6.2.1.7	Concluding Remarks and Outlook . . . . .	287
6.2.2	Extrusion, Forging <i>Bernard Closset</i> . . . . .	289
6.2.2.1	Production of Cast Stock . . . . .	289
6.2.2.2	Extrusion . . . . .	294
6.2.2.3	Magnesium Extrusion Fundamentals . . . . .	299
6.2.2.4	Alloy Developments . . . . .	310
6.2.2.5	Novel Extrusion Methods . . . . .	312
6.2.2.6	Bending of Magnesium Extrusions . . . . .	314
6.3	Magnesium Matrix Composites <i>Norbert Hort, Hajo Dieringa, Sanday T. Kumar, Karl Ulrich Kainer</i> . . . . .	315
6.3.1	Introduction . . . . .	315
6.3.2	Reinforcements . . . . .	319
6.3.2.1	Particle-Reinforcement . . . . .	320
6.3.2.2	Fibre-Reinforcement . . . . .	321
6.3.2.3	Whisker . . . . .	322
6.3.2.4	Hybrids . . . . .	322
6.3.3	Manufacturing . . . . .	323
6.3.3.1	Ingot Metallurgy . . . . .	323
6.3.3.2	Powder Metallurgy . . . . .	326
6.3.4	Interfaces . . . . .	329
6.3.5	Alloys and Composites . . . . .	331
6.3.6	Machining and Recycling . . . . .	333
6.3.7	Corrosion . . . . .	334
6.4	Joining . . . . .	335
6.4.1	Motivation and Requirements <i>Gerson Meschut</i> . . . . .	335
6.4.2	Joining Magnesium <i>Günter H. Deinzer</i> . . . . .	336
6.4.3	Welding and Other Thermal Processes <i>Günter H. Deinzer, Michael Rethmeier</i> . . . . .	349
6.4.3.1	Weldability of Magnesium Alloys . . . . .	349
6.4.3.2	TIG Welding . . . . .	349
6.4.3.3	MIG Welding . . . . .	349
6.4.3.4	Laser-Beam Welding . . . . .	356

6.4.3.5	Electron-Beam Welding . . . . .	359
6.4.3.6	Friction Welding . . . . .	359
6.4.3.7	Brazing and Soldering . . . . .	364
6.4.4	Adhesive Bonding <i>Otto-Diedrich Hennemann</i> . . . . .	365
6.4.4.1	Introduction . . . . .	365
6.4.4.2	Adhesives . . . . .	367
6.4.4.3	Pre-treatment . . . . .	369
6.4.4.4	Adhesive Bonding Technology . . . . .	371
6.4.4.5	Strength and Testing . . . . .	372
6.4.4.6	Development Tendencies . . . . .	373
6.4.5	Mechanical and Hybrid Joining <i>Gerson Meschut</i> . . . . .	374
6.4.5.1	Clinching . . . . .	374
6.4.5.2	Riveting . . . . .	377
6.4.5.3	Direct Screwing (Self-piercing/-Tapping) . . . . .	385
6.4.5.4	Folding . . . . .	392
6.4.5.5	Hybrid Joining . . . . .	394
6.4.5.6	Conclusion and OutView . . . . .	396
6.5	Machining <i>Hans Kurt Tönshoff, Berend Denkena, Jens Winkler, Christian Podolsky</i> . . . . .	398
6.5.1	Machining . . . . .	398
6.5.1.1	Machining of not Reinforced Magnesium Alloys . . . . .	399
6.5.1.2	Machining of Reinforced Mg Alloys . . . . .	406
6.5.1.3	Cooling Lubricants . . . . .	409
6.5.2	Burnishing . . . . .	411
	References . . . . .	418
7	<b>Corrosion and Surface Protections</b> . . . . .	431
7.1	Surface Treatments and Protection <i>Peter Kurze</i> . . . . .	431
7.1.1	Introduction . . . . .	431
7.1.2	Passivation Properties of Magnesium-Based Materials in Air . . . . .	432
7.1.2.1	Resistance of the Passivated Layer to Chemicals . . . . .	433
7.1.3	Surface Treatment of Magnesium-Based Materials . . . . .	433
7.1.3.1	Principles and Prerequisites for Optimum Surface Protection . . . . .	433
7.1.3.2	Preliminary Treatment . . . . .	437
7.1.3.3	Conversion Coatings Provided by Electroless Electrochemical Surface Treatment . . . . .	439
7.1.3.4	Conversion Coatings Provided by Anodic Oxidation . . . . .	450
7.1.3.5	Conversion Coatings Provided by Anodic Plasma-Chemical Reaction in the Electrolyte . . . . .	455

7.1.3.6	Galvanic-deposit coatings . . . . .	466
7.1.3.7	Application of Coatings Using Physical Methods . . . . .	467
7.1.3.8	Organic Coating Systems . . . . .	467
7.2	Corrosion	
	<i>Jim Hillis</i> . . . . .	469
7.2.1	Introduction . . . . .	469
7.2.2	Magnesium Protective Films . . . . .	469
7.2.3	Metallurgical Factors in the Corrosion of Alloys . . . . .	470
7.2.4	Stress Corrosion . . . . .	481
7.2.5	Corrosion Fatigue . . . . .	482
7.2.6	Common Causes of Corrosion Failure . . . . .	484
7.2.7	Environmental Factors . . . . .	488
7.2.7.1	Acidity/Alkalinity . . . . .	488
7.2.7.2	Specific Ions/Salts . . . . .	488
7.2.7.3	Elevated Temperature . . . . .	489
7.2.7.4	Organic Compounds . . . . .	489
7.2.8	Galvanic Corrosion/Selection of Fasteners . . . . .	490
	References . . . . .	494
<b>8</b>	<b>Engineering Requirements, Strategies and Examples . . . . .</b>	<b>499</b>
8.1	Automotive Applications in Europe	
	<i>Soenke Schumann, Horst E. Friedrich</i> . . . . .	499
8.1.1	Introduction . . . . .	499
8.1.2	Potential Use of Magnesium in Vehicles . . . . .	503
8.1.3	Automotive Applications – Examples . . . . .	506
8.1.3.1	Drive train Train Applications . . . . .	506
8.1.3.2	Interior Applications . . . . .	519
8.1.3.3	Body . . . . .	527
8.1.3.4	Chassis . . . . .	554
8.1.4	Life Cycle Assessment . . . . .	559
8.1.4.1	Life Cycle Inventory of Vehicles . . . . .	560
8.1.4.2	Life Cycle Inventory of Magnesium . . . . .	563
8.1.5	Strategy and Outlook . . . . .	565
8.2	Automotive Applications in North America	
	<i>Gerald Cole</i> . . . . .	569
8.2.1	Transportation Industry . . . . .	569
8.2.1.1	Introduction and Background . . . . .	569
8.2.1.2	Magnesium in the 1970s . . . . .	570
8.2.1.3	Magnesium in the 1980s . . . . .	570
8.2.1.4	Magnesium in the 1990s . . . . .	571
8.2.1.5	Magnesium in NA vs Europe . . . . .	573
8.2.1.6	Engineering Magnesium Applications . . . . .	589
8.2.2	Non-Automotive Uses for Magnesium . . . . .	593

8.2.2.1	Electronics/Communication . . . . .	593
8.2.2.2	Hand Tools . . . . .	593
8.2.2.3	Sports Equipment . . . . .	594
8.2.2.4	Aerospace . . . . .	594
8.2.3	Magnesium Manufacturing in North America . . . . .	594
8.2.3.1	Semi-Solid Metal Casting (SSM) . . . . .	595
8.2.3.2	Thixomolding (TXM) . . . . .	595
8.2.3.3	Magnesium Can Replace Polymers . . . . .	597
8.2.3.4	Magnesium Can be Fabricated into Macro-composites of Plastics and Metals . . . . .	597
8.2.3.5	Alloys Designed Especially for SSM and TXM . . . . .	597
8.2.3.6	Redesigning Parts and Assemblies . . . . .	598
8.2.3.7	Thermal Management and Improvement of TXM . . . . .	598
8.2.3.8	Summary . . . . .	599
8.2.4	Magnesium R&D in North America . . . . .	600
8.2.4.1	USCAR Programs . . . . .	600
8.3	Magnesium Aerospace <i>Francis H. Froes, Dan Eliezer, Eli Aghion</i> . . . . .	603
8.3.1	Background . . . . .	603
8.3.2	Past Aerospace Use . . . . .	607
8.3.3	Barriers to Magnesium Use in Aerospace . . . . .	617
8.4	Consumer Applications of Magnesium <i>Steve Erickson</i> . . . . .	620
8.4.1	Logistics . . . . .	621
8.4.2	Power Hand Tools . . . . .	621
8.4.3	Lawn and Garden Equipment . . . . .	623
8.4.4	Concrete Handling Tools and Equipment . . . . .	623
8.4.5	Computers and Computer Hardware . . . . .	624
8.4.6	Electronic Equipment . . . . .	625
8.4.7	Optical Equipment . . . . .	625
8.4.8	Sports Equipment . . . . .	626
8.4.9	Galvanic Applications . . . . .	627
8.4.10	Miscellaneous Consumer Applications . . . . .	628
	References . . . . .	629
9	<b>Recycling</b> <i>Håkon Westengen</i> . . . . .	633
9.1	Introduction . . . . .	633
9.2	Classification System . . . . .	634
9.2.1	Process Overview . . . . .	635
9.2.2	Class 1 . . . . .	636
9.2.2.1	Flux-based Systems . . . . .	637
9.2.2.2	In-house Recycling . . . . .	638

9.2.2.3	In-cell Recycling . . . . .	639
9.2.3	Class 2 . . . . .	640
9.2.4	Class 3 . . . . .	640
9.2.5	Class 4 . . . . .	641
9.2.6	Class 5 . . . . .	641
9.2.7	Class 6 . . . . .	642
9.2.8	Class 7 . . . . .	643
9.2.9	Class 8 . . . . .	645
9.3	Recycling Using Flux . . . . .	645
9.3.1	Principles . . . . .	645
9.3.1.1	Thermodynamic Restrictions . . . . .	647
9.4	Fluxless Refining . . . . .	647
9.4.1	Principles . . . . .	648
9.4.2	Systems Involving Filters . . . . .	649
9.5	Contamination Control . . . . .	650
9.5.1	Additional Sources of Trace Elements and Inclusions During Recycling . . . . .	651
9.5.2	Effects and Removal of Some Trace Elements . . . . .	652
9.5.2.1	Nickel . . . . .	652
9.5.2.2	Iron . . . . .	653
9.5.2.3	Copper . . . . .	653
9.5.2.4	Cobalt . . . . .	653
9.5.2.5	Hydrogen . . . . .	655
9.5.2.6	Other Elements . . . . .	655
9.5.3	Effects of Inclusions . . . . .	656
9.5.4	Measurements of Inclusions . . . . .	656
9.6	Concluding Remarks . . . . .	659
	References . . . . .	660
	<b>Subject Index . . . . .</b>	<b>665</b>

---

# 1 History

## 1.1 History until 1945

*Kurt Harbodt*

The history of elementary magnesium started in 1755, when Joseph Black, a Scottish chemist, discovered that magnesia contained a new element, magnesium. Black was unable to isolate this element.

Magnesia had previously been known as “white stone” or “white earth” (magnesia lithos or magnesia carnea). It is generally accepted that the name originates from an area in Thessaly, Northern Greece, where in ancient times the material had been excavated and exported to countries around the Mediterranean.

Actually, the British chemist and scientist Sir Humphrey Davy is honored as the discoverer, because it was he who isolated the metal in 1808, when he decomposed wet magnesium sulphate by electrolysis using a voltaic cell and a mercury cathode.

Exactly 20 years later the Frenchman Antoine Alexandre Brutun Bussy isolated the metal by fusing dehydrated magnesium chloride with potassium at elevated temperatures.

Then Michael Faraday, the famous British scientist and a former assistant to Sir Humphrey, reduced dehydrated magnesium chloride by electrolysis and obtained pure metallic magnesium in 1833.

A German, Robert-Wilhelm Bunsen, after having developed the carbon-zinc electric cell in 1841, produced metallic magnesium in 1852, also starting from fused and dehydrated magnesium chloride.

Besides smaller attempts in some European countries (see below), magnesium found steady interest only in Germany, which, in 1868, was the only producer in the world, using the metal mostly as powder or ribbon for flashlights and other pyrotechnical purposes, and as a reducing agent in the production of aluminum.

As future developments and activities varied considerably in different parts of the world, we will now present the history according to country and continent.

### 1.1.1 Asia

In Japan Riken Metal Manufacturing Co started magnesium production in 1931. Negotiations between IG Farben, UBE Industries, Mitsubishi Shoji Kaisha and

Sumitomo Copper and Steel Rolling Works in Osaka did not result in a licensing agreement.

In 1938 a licensing agreement between IG Farben and the Japanese companies Mitsui Bussan Kaisha and Denki Kagaku Kogyo KK was negotiated to produce magnesium through thermic reduction based on [1] in the territories of Japan, Korea, Mandschukuo and Formosa. As a copy of the final contract couldn't be found the result is unknown, but during World War II six producers are reported in Japan, one in Formosa (Taiwan) and one in Korea, three using magnesite from Korea and Mandschukuo the others sea water as raw materials. The total yearly production was estimated at approximately 3,000 tons per year.

In 1952 a Japanese delegation again approached Bayer Leverkusen, one of the successors of IG-Farben, and showed interest in the silicothermic process. It is known that between 1978 and 1993 producers like Furukawa, UBE and Japan Chem and Met used silicothermic processes (Pidgeon and Magnetherm) for the production of metallic magnesium.

### 1.1.2 Australia

The US Bureau of Mines circular 8201 reports a magnesium production of averaging 255 t for the years 1940–1944 and 855 t (average) for the time 1945–1949. Broken Hill Proprietary Company (BHP) used the process of Murex Limited of Rainham in Essex, England. This process used calcium carbide to reduce calcined magnesite. It was a 1,000 ton plant, but never reached full capacity.

### 1.1.3 Europe

In Austria F.J. Hansgirg developed the carbothermic process, a direct reduction of MgO by coal. The patent [2] was granted to Österreichisch-Amerikanische Magnesit AG, an affiliate of American Metals Corporation (ALCOA group).

The pilot plant at Radenthein never became efficient because of the great amount of subsidiary equipment necessary and the dangerous handling of the pyrophoric Mg powder.

In 1938 IG Farben planned, together with the Austrian Donau-Chemie Vienna, the building of a 20,000 tons per year magnesium plant at Mossbierbaum. Before completion the plant was destroyed by bombing.

An agreement between IG Farben and Österreichische Magnesit AG, now located in Munich, was reached in 1940 concerning the further development of the carbothermic process.

In France a small production was started in 1857 by Deville and Caron. They replaced potassium by metallic sodium and added calciumfluoride.

In 1915, during World War I, the Société d'Electro-Chimie et des Aciéries Electrique began producing magnesium at Clavaux, Isère, and in 1922 Alais, Froges et Camerque (later Pechiney) built a plant at Epierre, Savoie. The latter company together with Ugine, founded, in cooperation with IG Farben, the Société Général du Magnesium in 1931, which set up plants in St. Auban and Jarrie. The production of these plants during World War II averaged 3,000 tons per year. After the

war the Auban plant was closed but Jarrie remained in operation until 1963 with a yearly output of about 1,500 t.

A unit for reduction of magnesia with calcium carbide by the Murex process was also exploited in 1942–44 at the plant of Societe des Produits Azotes at Lanermezan (Hautes-Pyrenees).

Germany, without doubt, was the country where the development of magnesium found the greatest interest and support.

On 9 April 1885 Aluminium und Magnesiumfabrik Hemelingen, near Bremen, was founded and started production of magnesium in 1886, applying the Graetzel cell [3] to produce aluminum and magnesium in an electrolytic process. Carnallite ( $\text{MgCl}_2$ , KCl) was used as raw material and  $\text{MgCl}_2$ , NaCl and KCl served as electrolyte (42%  $\text{MgCl}_2$ ; 32% KCl; 26% NaCl). Direct production of aluminum could not be achieved by this process but the magnesium was used partly to reduce cryolite ( $\text{Na}_3\text{AlF}_6$ ) from Greenland. The total magnesium production between 1886 and 1890 was 60 t while only 39 t of aluminum were produced.

In 1873 the German government in Berlin issued a first regulation, called “Regulation for the Protection against Fires involving powders of Magnesium, Aluminium and their alloys in Foundries, Warehouses and other works”.

Another electrolysis unit was built at Bitterfeld in 1896 by Chemische Fabrik Griesheim Elektron, which acquired the Graetzel process. The production ran until 1928, when the IG Farben or Oxychloride process was invented.

It was Griesheim that created the brand name Elektron on the occasion of the Air Fair at Frankfurt in 1909, a name later used extensively by IG Farben throughout the world.

In the same year G. Pistor and P. Rakowics of Chemische Fabrik Griesheim received a patent for an Al and Zn bearing alloy for structural applications (AZ). The US [4] was granted 26 July 1910.

On occasion of the International Air Transport Fair (ILA) at Frankfurt in 1909 (Fig. 1.1) this alloy was presented, accompanied by a 75HP Adler airship motor with a magnesium crankcase. The part had been cast by Elektron Co. GmbH at Spandau (Berlin).

Until 1915 Germany remained the sole producer of magnesium, mainly for military and pyrotechnical purposes. This fact was the reason why magnesium was called “the German metal”. In 1900 the production amounted to 10 t.

In spite of the high energy input of 35–40 KWh/kg the consumption boomed during World War I because of the high need in military ordinance such as flares, tracer bullets and aircraft parts. World production rose from 320 t in 1915 to 1,200 t in 1918; with Germany increasing output from 80 to 500 t.

The establishment of a new company in 1925 named IG Farben also included Messrs. Griesheim Elektron and the new group took over the magnesium production at Bitterfeld in 1927.

1928 the new IG Farben- or Oxychloride process decreased the consumption of electricity per kg of Mg considerably and led to a surplus of very pure chlorine that could be used in IG’s chemical business. Large-scale production started in 1931 in Bitterfeld, using brown coal as the energy resource and the brines from the nearby potash mine at Staßfurt as raw material. Production there rose from 1,270 t in 1933 to 4,000 t in 1940.





**Fig. 1.1.** Magnesium pavilion of the “Chemische Fabrik Griesheim-Elektron (CFGE)” at the International Air Transport Fair (ILA) in Frankfurt, Germany (1909)

In 1924 magnesium alloys (AZ; 2,5–3,0% Al; 3,0–4,0% Zn) were used for the first time as pistons in automobiles, the pistons being die cast by Elektron Metall Bad Cannstatt (the company in Berlin had been acquired by the Mahle group). Henry Ford, while vacationing in Baden-Baden, visited these die casting facilities in 1930 and arranged further discussions with Ford’s executive vice president, Mr. Wibel.

A number of magnesium parts were used in airships, such as:

- Bow point, holding the mooring on the ship’s side, connecting all girdles
- Piece on the cabin of command, holding the anchor cable sheaves of pulleys
- Fittings of the steering gear and fuel distribution
- Cabin tables, easy chairs, plain chairs, doors, ladders, etc.

Magnesium castings were introduced into cars on a larger scale by Professor Porsche. One of the first applications was in the 8-cylinder, air-cooled Tatra motor, produced in Nesselsdorf, Czechia. Later, Porsche worked for Austro-Daimler

in Vienna and then founded his own engineering office in Stuttgart on Kronenstraße (Institut für Maschinenelemente), where he was asked to design the famous Volkswagen beetle, which contained at least 20 kg of magnesium. For the production of this car, a new city was founded in 1938: "City of the KdF-car near Fallersleben". The name was changed to Wolfsburg in 1945.

On 3 June 1933 a German Patent [1] for the continuous production of metallic magnesium through thermic reduction was granted to IG Farben which applied, in 1935 and 1936, for some amendments, including the reduction with silicon, which led to the patents 689122, 689712, 670714 and others.

The German government, heavily arming its forces and trying to depend on national resources, encouraged and financially supported the increase in the production of magnesium. Many cast parts were used in military vehicles and airplanes, but the metal also found uses in flares and incendiary bombs.

In 1934 the German Ministry for Air Transport financed a new IG Farben production facility at Aken near Dessau. The loan had to be paid back by 0.10 RM/kg magnesium delivered. This biggest plant had a capacity of 7,400 t in 1935 and ended with a capacity of 9,800 t in 1940.

In 1935 the German company Wintershall, after 6 years of research, started production at Großheringen, using fused carnallite ( $\text{KCl}$ ;  $\text{MgCl}_2 \cdot 6 \text{H}_2\text{O}$ ). The name of the process was MAGNEWIN. Production: 2,000 tons per year. As Wintershall had problems achieving the by-product chlorine in an appropriate purity and concentration a licensing agreement with IG Farben was drafted in 1944. In this agreement Wintershall was limited to a maximum production of 7,500 tons per year.

In 1939 the Staßfurth plant of IG Farben started production with an initial quantity of 3,580 t metal produced. In this year the German production was approximately 18,000 mt with a total world production of 30,000 t. (England 5,000 t; France 2,000 t; Italy 500 t; Japan 1,500 t; USA 2,500 t; USSR not available).

In Great Britain magnesium was first produced in 1864 by John Mathey of Penticroft with his Magnesium Metal Co. Ltd. in the town of Salford near Manchester. The small scale production ceased in 1908.

Major C.J.P. Ball, later founder of MEL, first became acquainted with magnesium for structural applications during his service as an officer in the army of occupation in Germany after World War I.

He, with his company F.A. Hughes & Co. Ltd., began, by an agreement with IG Farben, to explore the British market in 1920. In 1922 he convinced Sterling Metals Ltd of Coventry to start experimental work for sand castings with Elektron Metal.

After corrosion resistance and other properties had been improved considerably in 1926 by adding Manganese to alloys the Air Ministry granted the first DTD specification no. 59.

A regulation set in operation in 1928, licensing commercial vehicles by weight, led to an increasing demand of magnesium parts like crankcases, gearboxes and axle casings.

Two other companies, Birmingham Aluminium Casting Co. Ltd. and J. Stone & Co. Ltd. of Deptford joined Sterling Metals in 1929 and 1934, respectively.

An agreement between IG Farben and Hughes & Co. London/James Booth & Co. Birmingham was finalized, concerning “wrought products” including pressings and forgings.

In 1927 IG Farben was approached by the British government, which expressed its interest in building a magnesium production plant in the UK. So in 1933 IG Farben transferred the patent rights for the production and the fabrication processes to Hughes & Co. Ltd.

Founded in 1934, Magnesium Elektron (MEL) built and operated a magnesium production plant from 1936 in Clifton Junction under license from IG Farben with an initial capacity of 1,500 t.

The British government, in 1936, acknowledged the importance of magnesium for airplanes and other military applications and asked MEL to increase capacity. New negotiations with IG Farben began before the startup of Clifton Junction to increase the capacity by 2,500 t – Clifton Junction II – this new capacity coming on stream in 1938. Later, another production site was added at Lowerhouse near Burley (Basic Magnesium, Inc.).

At the beginning MEL used Greek magnesite as raw material but in 1939, when war became imminent, magnesia was extracted from sea water (British Periclas Ltd., Hattlepool) and dolomite substituted for the magnesite. That is why MEL claims to be the first company in the world using sea water as a source for raw material.

In 1936 Murex set up a 1,000 t production at Rainham based on the carbothermic process, but by coal replaced by calcium carbide as the reducing agent. Later, after being instructed by the government, it built an additional plant at Moss End, Larnak, with a capacity of 5,000 t which came on stream in 1942.

The carbothermic Radenthein process also was applied by Magnesium Metal Co. in their plant at Swansea but never reached planned capacity.

Technical difficulties also prevented production at capacity (5,000 t) in the plant erected by International Alloy Ltd. at Cardiff between 1940 and 1943. Here, aluminum and ferrosilicon was used as the reducing agent.

All plants in Germany were closed after the war with the exception of Magnesium Elektron. This company produced about 80% of the British magnesium during the war and still is an important producer, particularly active in special alloys.

In Italy 1935 SAMIS (S.A. Magnesio Italiana Sulcis) built a plant in San Giovanni Suergin/Sardinia, using the electrolytic Blumenfeld process. The first owner was G. Caproni, an industrialist in the aircraft industry. The company was later taken over by S.A. Nazionale Cogne, a state owned company. Production: 500 tons per year.

According to an agreement between IG Farben (via ELSA) and Cogne in January 1939 the production in Sardinia was closed down and a new production established in Aosta.

IG received 47% of SAMIS, its affiliate ELSA another 4%. Planned was a silicothermic process with rotary furnaces. In 1942 the company was asked by the government to increase production to 600 tons per year.

In 1939 Società Magnesio e Leghe di Magnesio started production in Bolzano, applying a silicothermic process developed by Amati and later simplified by

Ravelli. The raw material was dolomite. Production during the war approached 2,000 tons per year.

In 1942 IG Farben, Cogne and SAVA founded Compagnia Industriale del Magnesio Anonima (CIMA) for an electrolytic production in Chioggia. The project never was realized.

In 1935 a delegation from Norsk Hydro visited the German Ministry of Economy in Berlin and asked for a licence to produce magnesium, using the excess electric power available. The proposal was rejected because IG Farben did not want to have a competitor producing the metal mainly for export.

In May 1937, Norsk Hydro while visiting the Marine Chemicals Company San Francisco showed interest in the DOW process.

In 1941, after the occupation of Norway by the Nazis, the “Reich” confiscated the Norwegian aluminium industry, most of the companies being affiliates of foreign owners.

Mr. Koppenberg from Junkers was established as “trustee”.

In January 1941 talks started between the Norwegian attorney Bjarne Eriksen (representing Norsk Hydro-Elektrisk Kvaelfstofaktieselskab Oslo, A/S Rjukanfos and A/S Svaelffos) and Mr. Haefliger of IG Farben to found Nordisk Magnesium Elektron Aksjelskap, with an estimated investment of Nkr 30 million.

The German Ministry of Air Transport (Air Force), wanting to hold control on such a company, turned down the project and instead, via the Bank der Deutschen Luftfahrt, founded Nordag in Oslo which, together with IG Farben and Norsk Hydro, founded Nordisk Lettmetall in Herøyen. Alumina, Aluminium, Cryolite, Chlorine and Magnesium were produced by this company. The power had to be delivered by Norsk Hydro, which had a majority of Norwegian, British and French shareholders.

In a very controversial discussion between the German Ministry of Air Transport and the German “trustee” in Berlin on 30 April 1941 IG Farben succeeded that the foundation of Nordisk Lettmetall was realised in accordance with Norwegian law and that the Norwegian partners were not forced but could participate only voluntarily. IG also reached an agreement that the French shareholders were not excluded from the necessary capital increase by a German governmental act (refusal of a currency transfer permit) but, in an arrangement with the French Banque de Paris et Pays Bas could sell their options to IG Farben at a fair price.

Nordisk Lettmetall was founded in Oslo on 2 May 1941 with a capital of Nkr 45 million. The chairman of the supervisory board was Dr. Axel Aubert, president of Norsk Hydro. The executive board consisted of Dr. Moschel from IG Farben as president, Bjarna Eriksen, vice president legal and Dr. Alf Bryn, vice president administration.

A 10,000 tons per year electrolytic magnesium plant and a 12,000 tons per year aluminium plant were later planned. The raw material for magnesium would be magnesium carbonate extracted from sea water through precipitation with lime. Before magnesium could be produced the allies destroyed the work under construction in 1944 by bombing.

Russia in 1930 acquired a licence for the production of aluminium from Pechiney. In this agreement the French committed themselves to transferring the

knowledge of producing magnesium. This transfer should have been completed in 1932. The first magnesium production started in 1936 at Solikamsk in the Perm Region of Russia and production reached during World War II, 5,000 t, produced in three plants: Solikamsk, Avisma and Zaparoshe in the Ukraine.

Talks between the Russian embassy in Berlin and IG Farben/Ministry of Economy in 1941 to license the magnesium processes (electrolytic and electrothermic) under a “works support agreement” had been discussed on the occasion of a lunch on 19 May 1941 with the result that “at present the parties are not in the position to sign a licensing or works support agreement”.

Switzerland saw the start of magnesium production in 1926 at Société pour la Fabrication du Magnesium at Martigny-Bourge. This was a 250-ton-per-year plant when built and it was expanded to an output of 700 tons per year in 1944 and shut down in 1947. Production was restarted in 1953 and it produced about 300 tons per year until 1959 when it was closed.

#### 1.1.4 North America

During World War I eight companies in North America were producing magnesium; after the war the number dropped to two, both in the US: Dow Chemical using the Dow electrolytic process and American Magnesium Corporation (Alcoa) using the fluoride process.

In Canada Shawinigan Electro Metals Co. in Shawinigan, Québec, ran a production from 1915 to 1919, using magnesite from Kilmar, Québec. Energy consumption of this process was a staggering 50 KWh/kg. An ingenious Norwegian, Christian Backer, was general manager. He later founded the Norwegian company De Norske Saltverker AS to produce magnesium and extract salts from seawater in a village outside Bergen/Norway.

One of the most significant achievements in the production of magnesium was the development of the Pidgeon process by the Canadian scientist Lloyd M. Pidgeon in 1939, who based his work on former IG Farben patents. This silicothermic process generated a particularly pure magnesium metal from dolomite.

In 1941 the Canadian government funded a 5,000 tons per year plant at Haley, Ontario, piloted and brought to full production by Lloyd Pidgeon. After the war, Dominion Magnesium Co. Ltd. bought this plant. Later the operation became part of the Timminco group.

In the United States General Electric had a magnesium plant at Schenectady, NY since 1914.

The Dow Chemical Co. had put effort into magnesium since 1915. Herbert H. Dow developed an electrolytic cell, called “the bathtub.” The company built its first plant in 1916 at Midland, Michigan. As raw material they used the by-product magnesium chloride from deep-well brines at Midland.

Another amongst the eight companies producing magnesium during World War I was Aviation Material Corporation at Niagara Falls, NY, later known as American Magnesium Corporation (AMC).

Those two companies, Dow and AMC, remained the only producers after the war, with Dow having a more efficient and cheaper production process.

As in the 1920s the US magnesium industry was protected by the prohibitive import duties of the Fordney-Mc-Cumber tariff and, with Dow owning all process rights, IG Farben looked for its own production in the US. They joined forces with AMC (ALCOA group) and founded the Magnesium Development Company (MDC) on 23 October 1931, with IG Farben being a 50% shareholder. But ALCOA used this agreement only strategically to reach an understanding with Dow.

Through the indirect connection with IG Farben via MDC it came to an understanding which was formalized through a cross licensing agreement between Dow, ALCO and MDC on 1 February 1934.

In this contract Dow agreed not to export to Europe before 1938 with the exception of one client, the Murex group in England. IG Farben bought magnesium from Dow (5 September 1934). Part of the agreement was also that in case of a joint production a maximum quantity of 4,000 t was allowed; a higher quantity needed the approval of IG Farben.

On 24 June 1934 a contract was signed between Dow and AMC, in which Dow committed itself to deliver magnesium to AMC at prices lower than AMC's production costs.

The cross-licensing agreement was cancelled by a US court in 1941, in a suit against those companies, being charged with "alleged conspiracy to monopolize and restrain competition in the production, use and sale of magnesium, thus violating section 1 and 2 of the Act of 2 July 1890, known as the Sherman Antitrust Law."

In the National Defense program of 1939, the US government acknowledged the great importance of magnesium alloys for aircraft and other military purposes. So it not only encouraged the industry to build new magnesium plants but also partly financed these new facilities.

Dow doubled the production in Midland in 1940 and constructed a new production plant in Freeport, Texas, partly financially supported by the British government. The 18,000 tons per year plant used sea water as the source of magnesium.

In an unbelievably short period, new capacities came on stream. Between 1940 and 1942, 15 new plants were built in the US, most of them government owned, such as those in Velasco, Texas; Austin, Texas; Lake Charles, Louisiana; Marysville, Michigan, 50% of Freeport. One of them, the 50,000 tons per year Basic Magnesium Inc at Henderson near Las Vegas, Nevada was built in less than one year as a venture between Basic Refractories of Cleveland and MEL, applying the MEL/IG Farben technology.

Other plants using the silicothermic process were in Spokane, Washington; Wingdale, NY; Dearborn, Michigan; Luckey, Ohio; Manteca, California and Canaan, Connecticut.

The Permanente Metals Co, Permanente, California (Kaiser), a partly government funded operation used the carbothermic Radenthein process, never reached the planned capacity of 24,000 t and, after having produced 11,500 short tons of ingot, ceased production. It was never reopened and was dismantled after the war, like most of the other plants.

The production in the US rose from approximately 2,500 short tons in 1939 to more than 184,000 tons in 1943, being reduced to 157,000 t in 1944 and to





**Fig. 1.2.** First airplane nearly completely designed with magnesium-Northrop XP-56

33,000 t in 1945. But, due to technical problems, the production/capacity ratio was fairly poor with an average of just below 65%.

It might be of interest, that in 1940 the first airplane, almost completely designed for magnesium, had been constructed, the Northrop XP-56 (Fig. 1.2). Others, such as the B36 Bomber (Fig. 1.3) contained many magnesium parts.

In 1944 world capacity was estimated 432,000 t from 41 plants in 13 countries with 16 plants in the US, amounting to approximately 280,000 t capacity. Production in 1944 is reported with 210,000 t.

## Additional references

- |                    |   |
|--------------------|---|
| Catrin Kammer:     | Magnesium Taschenbuch,<br>Aluminium Verlag, Düsseldorf 2000                         |
| Gottfried Plumpe:  | Die IG Farben Industrie AG<br>Duncker u. Humboldt, Berlin 1990                      |
| Peter Hayes:       | Industry and ideology. IG Farben in the Nazi era<br>Cambridge University Press 1987 |
| US Bureau of Mines | Information Circular 8201; 1963   |
| Wolfgang Büchen    | Die Deutsche Magnesiumgewinnung von 1886–1945<br>Erzmetall 48/1995                  |

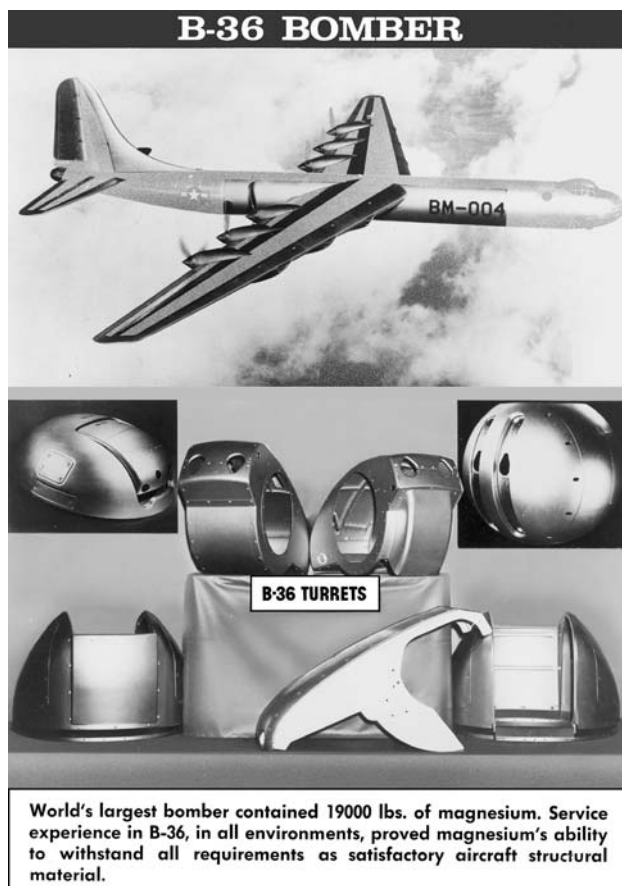


Fig. 1.3. B-36 Bomber

Stan B. Hirst

Early History of Magnesium in the United Kingdom

01.02.2001-04-24

Encyclopaedia Britannica

*Archives:*

Zentralarchiv Bayer AG, Leverkusen

Unternehmensarchiv BASF AG, Ludwigshafen

Protocols and documents of the IG Farben process

Frankfurt 1947/48.



## 1.2 History Since 1945

*Robert E. Brown*

### 1.2.1 Production

After World War II, production of magnesium decreased drastically. Germany was prohibited from producing magnesium. Most of the German magnesium production plants happened to be in what was defined as the Soviet Occupation zone of Germany and Austria. The magnesium plants at Aken, Germany and Moosbieniaum, Austria were dismantled and taken to the USSR. Similarly, all production of magnesium ceased in Japan by 1946 due, in part, to material shortages.

As the war ended, Dow closed its original 18,000 tons per year plant in Midland, Michigan because of the improved economics of the Freeport, Texas plant. The Midland plant had used salt brines from deep wells for its source of magnesium chloride. The Freeport (and Velasco) plants used sea water. Due to curtailment of magnesium production near the end of the war, five of the government-owned plants were shut down by mid-1944 and all government plants were shut down by November 1945. Kaiser closed its carbothermic plant at Permanente in 1945. Dow's Freeport plant remained the only plant in the US producing magnesium in 1946.

**United Kingdom.** There was a large surplus of magnesium in inventory in the United Kingdom. British operators started to close their plants and by 1947 there was no magnesium production in the United Kingdom. Except for a brief government-subsidized Magnesium Elektron restart during the Korean situation and a small amount of production for a short period, no further electrolytic magnesium was produced in Britain. The electric power price was five times the 1938 figure, so, in 1963, MEL built a 5,000 tons per year Pidgeon process plant to produce magnesium from dolomite at Hopton Junction. This plant was not successful due to impurities in the ore. MEL has continued to be a leading developer of magnesium alloys. In recent years, they have built a recycling operation in England that has now reached 10,000 tons per year and are just starting up a second recycling plant in the Czech Republic which could also reach 10,000 tons per year.

**France.** After the war, the plant at Saint-Auban, France was shut down leaving only the 1,500 tons per year Jarrie plant operating. In 1959, a single furnace pilot plant was built at Beaudean to test the magnetherm process, which was developed in a long research program started before World War II. In 1964, Pechiney completed construction of a 3,500 tons per year magnetherm process plant that replaced the Jarrie I.G. process plant, which was shut down. The new plant at Marignac started production in 1964. In 1970, it had four 2,200 kW furnaces, with each furnace producing 3.5 tons of metal per day. A fifth and sixth furnace of 4,500 kW were added in 1970 and 1971 respectively. The larger furnaces produced 6.5 tons of metal per day. The four smaller furnaces were expanded and the plant capacity was raised to first 14,000 tons per year in 1981 and then through process

improvements to 20,000 tons in 1990. The magnesium production furnaces at Marignac were shut down in 2002, but the melting and casting facility continues to operate doing recycling and converting magnesium bought on the open market.

**Canada.** In 1945, the Aluminum Company of Canada (Alcan) built a 1,000 tons per year electrolytic plant at Arvida, Quebec to produce magnesium from magnesium chloride produced from brucite. In 1951, the plant capacity was increased to 4,000 tons per year.

The original Alcan magnesium plant used an I.G. Farben cell. Brucite was changed to magnesium chloride using a shaft kiln with carbon and chlorine. Chlorine was obtained from the Alcan caustic chlorine plant. In 1959, in a complex deal, Alcan agreed to swap aluminum with Dow Chemical in exchange for magnesium and caustic and therefore the magnesium production operation was shut down.

Alcan had been experimenting with a modified I.G. cell with no diaphragm. The cells were running at 28,000 amps in 1959 when the plant was closed and sold to Osaka Titanium. A joint research and development pact was formed with Osaka leading to the further development of the Alcan Cell by Dr. Olivio Sivilotti.

The cell went from a 28,000 to a 40,000 amp tapered anode cell, which was used by Oremet and Timet and ultimately went to 80,000 amps. At one stage, Osaka started to change the 80,000 amp cell for a 100,000 amp cell. However, new multipolar cells came out at this time and Osaka constructed a building for 24 of the multipolar cells. These were  $3 \times 140$  kA cells for one setting. Today, Alcan and Sumitomo Sittix (formerly Osaka Titanium) are licensing the technology for primary magnesium production. Noranda's new production plant in Danville, which was opened in 2001, was the first commercial application of the multi-polar technology in primary magnesium production. The Australian Magnesium Corporation's project, which is currently in the basic engineering phase, will be the second application of the technology.

Dominion Magnesium purchased the original Pidgeon process plant from the government of Canada in 1945. A magnesium sand casting facility called Haley Industries was built next to the magnesium metal production plant. An extrusion press was installed at Dominion Magnesium in 1948. The 5,000 tons per year Pidgeon process silicothermic plant, which is at present owned by Timminco, has been modernized and expanded to 10,000 tons per year and continues to produce primarily magnesium along with calcium, strontium and barium. Dr. Lloyd Pidgeon of the National Research Council of Canada developed the silicothermic process as mentioned by IG Farben in some of their 1930s magnesium work. The ability of Dr. Pidgeon and a small group of researchers to transfer the pilot results to a full commercial plant within 18 months was a great accomplishment resulting in the process being named the Pidgeon process. The process uses a briquetted charge of calcined dolomite and ferrosilicon that is placed in a 10-foot long horizontal retort. The retort is externally heated to 2,200°F in a furnace and a vacuum pulled in the retort. The silicon of the FeSi reduces the MgO in the charge and the resulting magnesium vapors flow to a condenser in the portion that extends from the furnace. This is a cyclic process with the retorts being

charged and discharged several times per day. The Chinese were introduced to the Pidgeon process by lectures and seminars. Since then, they have built hundreds of silicothermic plants based on the Pidgeon process and are now the world's largest magnesium producing country.

In 1986, Alcoa (51%) and MPLC(49%) announced a new 50,000 tons per year magnesium plant to be built in Alberta, Canada. The plant was going to be developed in three phases, the first being 12,500 t. A special process to produce anhydrous magnesium chloride was used. The heart of the feed preparation process was a single reactor that converted raw magnesite directly into anhydrous magnesium chloride. Common magnesite was used as a raw material with no beneficiation. The rough crushed rock was poured into a single stage vertical reactor where it descended by gravity into increasing temperatures in a process similar to a blast furnace. The magnesite was then mixed with a stream of chlorine and carbon monoxide gases yielding molten anhydrous magnesium chloride at the base of the reactor. This molten material was fed directly into a modified Russian-type electrolytic cell. The process was said to be very simple, economical and efficient. Materials Processing Licensing Corporation developed the feed process. The magnesium technology was later consolidated in a company called Magnesium International Corporation. Alcoa backed out of the venture and Alberta Natural Gas took their place. The province of Alberta gave the project a loan guarantee up to US\$ 180 million. The 12,500 tons per year plant was started up in early 1990 and closed in April 1991. It was eventually sold off and demolished.

Norsk Hydro had been making many advances in the science and technology of magnesium production. Electrolytic cells had been upgraded to a high level of productivity with a high regard for the environment. The company had been looking around the world for many years at potential magnesium projects. In 1985, Norsk Hydro did a feasibility study for a new magnesium plant to be located in Quebec. The Canadian governments contributed C\$ 500,000 toward the study which was completed in June 1986. A very favorable power contract was negotiated with Hydro-Quebec. The plant was to be located in the Becancour Industrial park on the St. Lawrence River and would be a 50,000 tons per year plant with a capital cost of US\$ 285 million. The feed for the plant was to be produced from magnesite. After several years of testing, design and construction, the plant started with a design of 45,000 tons per year. Its cost exceeded the estimates by a large amount. The plant was immediately the subject of anti-dumping actions in the USA sponsored by MagCorp which said the plant was being subsidized by its power contract and by the Canadian government, both national and provincial. In the immediate years after the start up, the Becancour plant suffered many problems both operational and commercial. It added 10,000 tons per year of recycling capacity in 1995. The plant now operates in the 40,000 tons per year range plus 5,000–7,000 t of recycled metal.

Noranda had been involved in a number of studies and reviews of possible magnesium production in Quebec. In 1988, Noranda and Lavalin Industries established a 50/50 joint venture to evaluate the possible production of magnesium from asbestos waste tailings. The study, funded by the Quebec and Canadian governments, included a pilot plant for producing anhydrous magnesium chloride and was completed in 1990. Noranda eventually became the major partner of a

proposed 50,000 tons per year smelter to be located in the Thetford Mines area of Quebec. In 1995, Noranda announced a commitment to build a magnesium demonstration plant and announced joint venture partners as Aisin Seiki Corp, Ltd. (Toyota) (16%), SNC Lavalin (16%), Société Générale de Financement du Quebec (SGF) (16%) and Noranda Metallurgy, Inc. (52%). The pilot plant started in late 1996. Eventually both SNC Lavalin and Aisin Seiki dropped out of the venture leaving Noranda (80%) and SGF (20%). In late 1997, Noranda announced that they would build a 58,000 tons per year plant at Danville, Quebec. Noranda licensed the electrolytic technology from Alcan and installed the latest cells available. The plant capacity at 60% alloy and 40% pure magnesium was announced to be 63,000 tons. Electrolytic production was started in 2000. The plant has experienced many problems and was closed in 2003 and put into a standing status.

**United States.** In 1951, the Korean War created a need for the United States to revive magnesium production. Titanium Metals Corporation of America leased part of the Basic Magnesium plant in Henderson, Nevada in 1950 to produce titanium. Part of the electrolytic plant was reactivated to produce magnesium for titanium reduction by recycling the byproduct of the reduction of titanium tetrachloride with magnesium. This by-product was anhydrous magnesium chloride. Dow Chemical increased the output of its Freeport plant to 24,000 tons per year. Seven government-owned magnesium plants were reactivated and by the end of 1951 were producing at 70% of rated capacity. These plants were either shut down or sold by 1957. Dow bought the Velasco electrolytic magnesium production facilities which consisted of two 18,000 tons per year electrolytic magnesium plants with Dow 22 electrode E-cells. Dow continued to operate the plants intermittently for a number of years. New England Lime Company (Nelco) purchased the silicothermic process plant at Canaan, Connecticut and produced magnesium for the US Atomic Energy Commission and also produced calcium.

After the Korean War and its related defense activities, production continued for a brief period to build a strategic stockpile. After the stockpile objective of 195,000 short tons was reduced to 165,000 short tons, production dropped each year until the 1960s. The US Government felt that there was a sufficient domestic supply of magnesium as new producers started into production, so the stockpiled magnesium metal was sold by auction starting in 1962 and continuing until 1978, when all of the stockpile had been sold.

In 1972, Dow built a new 25,000 tons per year magnesium production plant based on a modified Dow cell technology. The plant was never a success and was closed within two years. Dow shut down their entire magnesium operations in 1999 after trying, unsuccessfully, for several years to find a buyer for the 60,000 tons per year Freeport, Texas plant.

In 1956, Brooks and Perkins, a large magnesium fabricator, decided they wanted to have an independent supply of magnesium. In a joint (50–50) venture with Dominion Magnesium (now Timminco) design and engineering was started on a 7,500 tons per year Pidgeon process plant to be built in Selma, Alabama. Dominion Magnesium dropped out of the project citing the lack of money. The project stalled for about two years, until Calumet and Hecla, an old line copper company agreed to join the venture, but on a 70% majority basis. Alabama

Metallurgical Corp started magnesium production in October 1959. The plant was expanded to 10,000 tons per year and produced metal until December 1969, when it was permanently closed.

Standard Magnesium Corporation was a company built in Tulsa, Oklahoma in the late 1950s. Founded by Roger Wheeler, they refined scrap magnesium, sludges and drosses. The company produced anodes for cathodic protection and later added an extrusion press for making water heater anodes and extruded shapes for bakery racks and other commercial parts. The plant was sold to Kaiser Aluminum, who had plans to build a primary magnesium plant on the Pacific Coast in the state of Washington or Oregon. This plan was essentially stopped by Dow Chemical, who announced in 1965 that they would lower the price of magnesium for aluminum alloying to 30 cents per pound from 36 cents per pound over a five-year period.

Wheeler left Kaiser and returned to Tulsa and started his own magnesium operation called American Magnesium. It was to be a 25,000 short tons per year primary production plant in Snyder, Texas and would use brines from an underground lake for the magnesium credits. The plant was built and started in 1969 using a spray drier for producing cell feed which then went to a chlorinator to complete the drying of the material and removal of oxide. The electrolytic cell was a modified IG cell based on the MEL Basic Magnesium plant in Henderson, Nevada. There were many problems with the cell and Wheeler purchased Russian cell technology for the plant and had Russian technicians come to Texas to install and start up the cells. The plant continued to struggle with environmental problems. Although the plant was located in a very rural area of Texas, the plant emissions were blamed for much of the severely rusted barbed wire on the cattle farms. This created many complaints and finally heavy rain flooded the evaporation ponds and severely diluted most of the feed that was being prepared. On 27 May 1981, during a shut down period, Wheeler was assassinated and the plant was never restarted.

Alcoa became very concerned when the price of magnesium started to increase in 1971. By 1974, with the price going to 90 cents per pound, the company obtained a license from Pechiney for the Magnetherm process and started engineering and construction of a Magnetherm plant near a dolomite deposit that was used for the WWII silicothermic plant at Spokane, Washington (Bagley process). The original plant was to have nine furnaces that had a charge of calcined dolomite, alumina, and ferrosilicon and aluminum scrap. The original capacity was to be 30,000 short tons per year, but this was increased by process improvements over the years to 45,000 tons per year. The plant became uneconomical as the selling price of magnesium dropped and the plant was closed in October 2001.

In 1961, the general manager the Chevrolet Division of General Motors (GM), contacted the New York office of Norsk Hydro that was managed by Sven Fougner. GM wished to find a secure supply of magnesium from a source other than Dow. Fougner had also been contacted by technical people from the Great Salt Lake about the potential for a magnesium plant using brine from the lake for feed for a magnesium and chlorine plant. Norsk Hydro joined in a feasibility study and also made a list of companies for partners that would be acceptable to

GM. National Lead was one of the major companies and became part of the venture. In 1963, Norsk withdrew from the project and National Lead (NL Industries) took over the project. Pilot plant tests were run on magnesium chloride prepared from brine from the Great Salt Lake. The electrolytic tests were run in an MEL type IG Farben cell at the Titanium Metals Corporation plant. Engineering and design and construction were by Ralph M. Parsons and a 45,000 tons per year plant was built, starting up in 1969. After many process problems, Norsk Hydro was retained to modify the plant and upgrade the electrolytic cells. NL Industries was in the process of rationalization and sold the magnesium plant to Amax in 1980. The plant continued to experience both operational difficulties and many other problems. In 1989, the plant was sold to the Renco Group and renamed Magnesium Corporation of America. As the world price of magnesium was increasing quite rapidly, the plant became profitable in the early 1990s, but had many environmental problems. The 40,000 tons per year plant was refinanced by Renco Metals in 1996 and 30 new, upgraded cells of their own design were used to upgrade one cell building starting in the year 2000. These cells are said to be much more environmentally friendly and more efficient. Renco Metals asked for Chapter 11 bankruptcy protection in August 2001. In June 2002, US Magnesium LLC purchased the assets of MagCorp in a sale by the bankruptcy court of the Southern District of New York. The plant has continued in operation throughout this period.

**Japan.** In 1954, Furakawa Magnesium Company built a Pidgeon Process pilot plant at Oyama, Japan. A 2,000 tons per year production plant was built in 1956. They expanded the plant to 3,000 tons per year in 1959 and further expanded that to 5,000 tons per year. This plant was closed in 1989.

Ube Industries built a 5,000 tons per year silicothermic plant in Yamaguchi Prefecture in 1964, which later expanded to 8,000 tons per year. This plant used a synthetic dolomite made from sea water magnesia and calcined limestone. Ube closed the plant in Sept 1994. Ube formed a joint venture with two Japanese trading companies, Mitsui and Kanematsu, and with Chinese interests. The joint venture company was called Nanjing Ube Magnesium Company. Part of the Ube magnesium production equipment was moved to the Chinese mainland. The new plant started production in 1995 at an annual rate of 4,000 tons per year. An existing 700 tons per year Pidgeon process plant operated by the Chinese partner, Nanjing Hwahong, was also transferred to the new joint venture.

In 1988, Japan Metals and Chemicals built a 3,000 tons per year magnesium production plant at Takaoka in Western Honshu. JMC had licensed Pechiney magnetherm technology, with dolomite for the operation to be imported from South Korea. The plant had a very short life and was closed in 1992.

**Norway.** In 1950, Norsk Hydro began reconstruction of the German-built IG process plant at Heroya, Norway, with 12,000 tons per year capacity. In 1960, the plant capacity was expanded to 14,000 tons per year. Further expansion to 18,000 tons per year took place in 1963–65. A new 24,000 tons per year plant was brought on stream in 1962 making the total production capacity 42,000 tons per year. Each of the two Norsk Hydro primary magnesium plants (Norway and Be-



cancour) added large recycling facilities, which operate in conjunction with the primary operations. The primary magnesium production in Norway was closed in 2002, but recycling and some melting and casting continues at the Norwegian plant.

**Italy.** In Italy, there was a magnesium production plant in Bolzano that used ferrosilicon to reduce calcined dolomite in a special Amati process furnace as modified by Edward Ravelli. The plant produced magnesium during WWII and was closed for several years. It started production again in 1950. Operations were expanded and improved, reaching a record output of 10,700 metric tons in the year 1981. The plant continued at high levels of production for several years, but production was slowly reduced until the plant was closed in 1992 due to high costs of production.

**Brazil.** Brasmag has built a magnesium production plant using a Ravelli furnace in Minas Gerais, Brazil. It started production in 1982 with two furnaces, then added two more furnaces reaching 2,000 tons per year. More improved furnaces were added to raise the plant capacity to 6,000 tons per year in 1985. Further improvements were made and the production increased. The highest production reached was 9,700 t in 1995. The plant is still in operation in 2004.

**Israel.** Dead Sea Magnesium Ltd. was established as a partnership of Dead Sea Works Ltd. (DSW) of Israel (65%) and Volkswagen AG of Germany (35%). DSW was a member of Israel Chemicals Ltd. (ICL) group. In late 1999, ICL bought all of the DSW shares. Construction of a 25,000 tons per year magnesium production plant was started in 1994 at Sodom and Production begun in 1996. The plant was designed by a consortium of the Aluminum Magnesium Institute of Russia (VAMI) and the Ukrainian Titanium Institute (UTI). The plant uses carnallite harvested from the Dead Sea as the basis for the cell feed. The plant uses the flowline technology system. Additional funds were invested by the partners to debottleneck the original plant and the capacity has been raised to 34,000 tons per year. One of the significant facts about DSM, is that it was established as an R&D oriented company. Its Magnesium Research Institute (MRI) leads technological developments in magnesium extraction processes and magnesium applications, including development of new Mg alloys, which is carried out cooperatively with VW.

**Yugoslavia.** Magnohrom built a 5,000 tons per year magnesium production plant using the Magnetherm process in the Kosovo region of Serbia in 1979. Production at the Bela Sterna plant was 5,000 tons per year in 1985. The plant was expanded and reached a peak production in 1992 of 8,000 tons per year. The plant suffered from sanctions imposed in 1992 against Serbia and Montenegro. Production declined and the plant closed in 1999 due to disruption of oil supply by NATO activities. The plant, now listed as being located in Serbia, has resumed low-level production.

**Russia** is the largest magnesium producer in the CIS. Magnesium and magnesium alloy is produced at JSC Avisma and Solikamsk. Avisma (formerly Berezniki

Titanium and Magnesium) has been in operation since 1943 and is the largest Russian producer of magnesium (approximately 36,000 tons per year), but much of the metal produced here is used in titanium production with about 17,000 tons per year to be sold as magnesium. Solikamsk is the world's oldest continuously operating magnesium production plant. It was started in 1934 and continues today. It produces about 20,000 tons per year. All of which is sold into the market either as pure magnesium or as alloy.

**Kazakhstan** has the JSC UKTMK magnesium production plant (formerly Ust.Kamenogorsk titanium and magnesium combine). The plant was commissioned in 1965 and has an annual capacity of 40,000 tons per year. However, there have been shortages in raw materials and the production has been considerably reduced. Most of the magnesium produced is used to produce titanium.

**Ukraine** has two magnesium plants. The Zaporozhyre Titanium and Magnesium Works has been in operation since 1935. It has a capacity of 45,000 tons per year. There is a lack of raw materials so the actual production was much less. Production has been closed for several years. The Kulush magnesium plant has a capacity of 24,000 tons per year. It has been privatized as part of the Oriana chemical complex and is now known as JSC Oriana. Production in recent years has been very small.

**India.** There were two silicothermic Pidgeon process plants in India. Tamil Nadu Magnesium is a 600 tons per year Pidgeon plant built in the 1970s and was closed in recent years. The Southern Magnesium and Chemicals built a 1,000 tons per year Pidgeon process plant at Bangalore. It was closed in 2003.

**China.** Fushan Aluminum was the first light metal smelter in China. Construction started in 1936 and production of aluminum started in 1938. Between 1951 and 1954, Soviet technicians helped to construct the newer aluminum pot lines and during this time introduced magnesium technology to Fushan. Fushan was set up similar to the Soviet non-ferrous plants in that it was ultimately producing aluminum, magnesium and titanium at its plant site.

The Minhe Magnesium plant in Qinghai Province was built in 1970. It was originally designed to produce ferrosilicon. In 1984, the government agency, CNNC, approved a magnesium plant for Minhe Xian. The magnesium plant started operations in 1987. Magnesium metal was produced by the electrolysis of anhydrous magnesium chloride. The magnesium chloride was produced by chlorination of magnesium carbonate. The raw material came from Haicheng, Liaoning Province. The plant was designed for an annual output of 4,000 tons of magnesium metal.

The first metal produced by the Pidgeon process was made in Nanjing in 1978, but the costs of production were much higher than the costs of the electrolytic magnesium. In 1988, Shenyang Al and Mg Engineering and Research Institute completed the design and installation of the first magnesium plant using the Pidgeon process. It was located in Tongshan, Hubei Province with a design capacity of 500 tons.



After this plant was started, two more Pidgeon plants were built in Ningxia with a total capacity of 2,000 tons per year. Additional Pidgeon plants were built in Shanxi and Henan provinces. By 1997, the number of magnesium production plants using the Pidgeon process was over 200. Plant sizes varied from 100 to 3,000 tons per year.

In 1995, Ube Industries announced that they would join two Japanese trading companies to form a joint venture for magnesium metal production in China. The joint venture was called Nanjing Hwahong Magnesium Industry Corporation and built a plant in Nanjing called Nanjing-Ube Magnesium Company. The venture took over the management of the existing Nanjing Hwahong magnesium plants, one rated at 500 tons per year; another rated at 700 tons per year. The new plant that was built using some of the equipment from the shuttered Ube Magnesium plant in Japan and new equipment was rated at 3,300 tons per year. Ube Industries supplied the technology. Ube had operated a Pidgeon process plant in Japan for many years and the facility had a rated capacity of 9,000 tons per year when it was closed in September 1994.

At this time, it was estimated in the West (2), that there were 30 magnesium producing plant, in China and that the total capacity was 30,000 tons. Later review of published numbers by semi-official Chinese groups indicate that this was just about correct. The greatest area of inaccuracy was the understanding of what was happening and how quickly it could happen.

As the industry grew, the magnesium plants grew in areas with good dolomite and available fuel for firing the retort furnaces. The plants in Ningxia use pulverized coal and some gas. Electricity is required for ferrosilicon production. There is hydro power on the Yellow River and coal fired power stations also.

China had record numbers of plants being built and during the peak of small plants in operation there were nearly 300 separate operating magnesium plants. Many of these were high cost plants and closed as the selling price of magnesium dropped and caused many of the small plants to lose money. Many of the older smaller plants had operating costs at about US\$ 1,950 per ton. As the selling price went below that level many plants closed. Also there were some forced consolidations and some improved design and operating practices.

Nearly all of the magnesium produced in China today uses the Pidgeon process. The most modern plants cost under US\$ 500 per installed ton and cash costs to operate run under US\$ 2000 per metric ton.

### 1.2.2 Applications

After World War II the magnesium industry attempted to develop magnesium for a number of applications, but failed in the most part. The most successful peacetime application for magnesium was in the original German Volkswagen car that was designed by Ferdinand Porsche. The VW Beetle used large magnesium alloy die castings for the crankcase and the transmission housing (both cast in halves) plus a number of smaller castings. Each Beetle contained more than 20 kg of magnesium alloy. Only a few new projects were discussed world wide in the post-war period. Germany was forbidden to make or use magnesium under the "Use-Verbot" put into the document of surrender. This lasted for several years until



Fig. 1.4. Hand grinding of castings in the 1940s

Volkswagen received permission to start using magnesium again in 1949 up to 1951. It obtained the magnesium alloy from Norsk Hydro in Norway and from Dow in Texas, and several other sources, including Russia. By 1974, Volkswagen was casting nearly 50,000 tons of magnesium each year.

Many of the other applications developed during the war could not be quickly converted to civilian uses. Some of the uses such as aircraft wheels and aircraft engine castings and troop carrying buses were modified and then used for the basis of civilian industries. However, the majority lost out and the wartime fabrication plants closed. Magnesium associations were set up to help the magnesium industry find peacetime uses. The Magnesium Industry Council in the UK and The Magnesium Association in North America attempted to help develop new uses. However there was too little demand for magnesium and too much production and foundry capacity, so most of the producers and fabricators, which were established for wartime business eventually closed. One of the businesses that was successful was the use of extruded magnesium for corrosion protection in hot water heaters. Magnesium dockboards, hand trucks, chain saws and bakery racks also became profitable businesses (Figs. 1.5–1.7 illustrate some other applications).

Dow eventually purchased a plant site at Madison, Illinois to house a new wrought products production facility. The world's largest extrusion press



**Fig. 1.5.** Magnesium lawn-mower housing (1965)



**Fig. 1.6.** Fire chief meeting 1948 – cooking steaks on a magnesium griddle supported on magnesium ingot pieces



Fig. 1.7. Magnesium products in the sixties

(14,000 tons) was leased (and later purchased) from the government. It was a press that was built for the German magnesium industry, but was not completed before the war's end. Extrusion and rolling mill equipment was moved from Midland, Michigan. During the 1950s, Dow produced a large amount of sheet that was used in aircraft and rocket construction.

A very large user of magnesium sheet and extrusions was Samsonite luggage made by Shwayder Brothers. The original Samsonite hard luggage had a deep drawn magnesium sheet for both sides and the frames were extruded magnesium. A special pebbled coating of plastic was used to protect the magnesium sides. As the quality of plastic improved and price of magnesium went up, Shwayder replaced the magnesium sheet with plastic, but magnesium extrusions are still used for the frames.

Dow helped develop products for the magnesium sheet that it rolled. The Met Lab also helped design alloy compositions to create the right properties for some very technical uses of magnesium. Magnesium sheet was used on many rockets, including the Vanguard, Jupiter, Titan 1, Polaris, Thor-able Star and the Atlas Agena (Fig. 1.8). Dow worked with the Metropolitan Body Company in 1955. This group built Metro-Lite delivery bodies on an International truck chassis. Floor and roof rails were 0.156 in-thick magnesium. The dent resistance of magnesium was very good. Pound for pound, magnesium resists denting better than other metals used in construction. Magnesium sheet for lithographic printing has been a mainstay of the magnesium sheet business. It is more easily handled and etched when compared to aluminum.

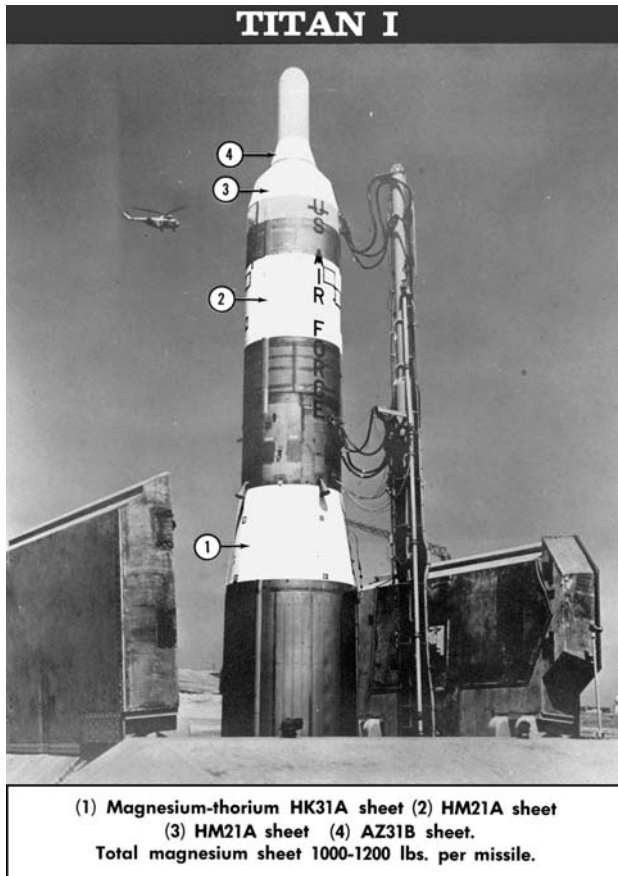


Fig. 1.8. Titan I rocket

Despite all of the work Dow did on magnesium, the Madison plant never achieved magnesium product production that was anywhere near the rated capacity. Spectrulite Consortium Inc. (SCI) now owns the plant. SCI continues as the only major magnesium rolling operation in the world. SCI was purchased by magnesium Electron in 2003.

There was a great amount of sheet being used and a company that got its start in the wartime production of magnesium fabricated parts, Brooks and Perkins (B&P), built a magnesium rolling mill in 1952 in the Detroit area. They had purchased a three-stand rolling mill from Alcoa. It was installed in Livonia and originally used to make sheet and fabrications for the Korean War effort. The company decided to expand the rolling mill and build a magnesium casting plant to produce the slabs, etc. for the rolling and extrusion operations. Brooks and Perkins went on to become one of the largest and most innovative groups to produce magnesium fabrications and aerial delivery systems. Brooks and Perkins was the originator of the construction of the 7,000 tons

per year Pidgeon process plant in Alabama in 1959 and owned 30% for a number of years.

Much of the work that B & P did was novel and supported by government contracts. As the price of magnesium increased, B & P was forced to convert more and more of their products into aluminum. The demand for cargo container systems for the large jet passenger planes increased dramatically. The price of magnesium made its use prohibitive and most of the systems were developed from aluminum extrusions and sheet.

Brooks and Perkins also perfected the art of metal spinning for magnesium. Using magnesium sheet, the company made structural shapes, including many aircraft parts, by spinning.

In the post war period, until today, the major new applications in magnesium did not come from work by the magnesium community. Many of the new applications were given to the industry.

The use of magnesium as an alloying agent to strengthen aluminum received a big boost as the aluminum beverage can business expanded rapidly. The 3004 body stock alloy contains about 1.2% magnesium and the 5182 lid stock alloy contains 4% magnesium. Aluminum auto body sheet also contains over 1% magnesium. This use was solely the development of the aluminum industry and magnesium went along for the ride.

Desulfurization of steel has also helped the industry, although most of the powders or granules now used in desulfurization mixes, come from China. The steel industry researchers themselves mainly developed this procedure.

Die casting of magnesium is the fastest growing segment of the magnesium industry and is growing globally. Much of this use has been the result of a demand for environmentally friendly cars. The world's die casters have responded to the demands and new designs of the auto industry. The builders of die casting machinery have also contributed to magnesium's growth by creating bigger and more complex parts. With hot chamber die casting, machine builders created a new and faster process for the production of magnesium alloy castings.

For a number of years, Dow Chemical offered die casting alloy at a price that was five cents below the price of pure magnesium. This practice originally started when pure magnesium sold for 36 cents per pound. It was the industry contribution to encourage the development of die casting. The same pricing relationship applied for many years, die cast alloy selling for less than pure magnesium. However, that difference is no longer evident and magnesium die casting alloy usually sells for a higher price than pure magnesium.

In recent years, the entire process of building cars has changed. The automobile manufacturers do less actual part design and procurement of metal or castings. They tend to buy components. This is now putting much of the burden of part development on the Tier One suppliers. And, in cases where the Tier One does not have a casting facility, it passes the burden of design and development on to the die casters.



**Table 1.1.** Major magnesium projects since 1950

	Company	Location	Mg Source	Process	Type	Initial Capacit	Comment
1951	Norsk Hydro	Porsgrunn	Sea Water	Electrolytic	I.G. Farben	18,000	1, 17
1959	Alabama Metallurgical	Selma, Al	Dolomite	Thermal	Pidgeon	7,500	2, 17
1960	Furakawa	Japan	Dolomite	Thermal	Pidgeon	5,000	3, 17
1964	Pechiney	France	Dolomite	Thermal	Magnetherm	9,000	4, 17
1964	Ube Kosan	Japan	Dolomite	Thermal	Pidgeon	5,000	5, 17
1965	Ust Kamenogorst	Kazakstan	Purchased MgCl <sub>2</sub>	Electrolytic	VAMI	40,000	
1965	MEL	U. K.	Dolomite	Thermal	Pidgeon	10,000	6, 17
1969	Nat. Lead	Utah	Brine	Electrolytic	Modif IG	40,000	7, 17
1970	Am Magnes	Texas	Brine	Electrolytic	Modif IG	25,000	8, 17
1972	Dow Chem	Texas	Sea H <sub>2</sub> O	Electrolytic	Dow Cell	25,000	9, 17
1975	NoWst Alloy	Addy WA	Dolomite	Thermal	Magnetherm	30,000	10, 17
1989	MagCan	Canada	Magnesite	Electrolytic	MPLC	12,500	11, 17
1989	Norsk Hydro	Canada	Magnesite	Electrolytic	Norsk Hyd	45,000	12
2001	Noranda	Canada	Serpentine Tailings	Electrolytic	Alcan multi-polar	63,000	13, 17
1996	Dead Sea Mg	Israel	Carnallite Brine	Electrolytic	VAMI/UTI	30,000	14
1997	AusMagCorp	Quenslnd	Magnesite	Electrolytic	Alcan multi-polar	1,500	15, 17
2001	AusMagCorp	Quenslnd	Magnesite	Electrolytic	Alcan multi-polar	97,000	15
1987	Minhe	China	Carnallite	Electrolytic	VAMI	4,000	
1990	Various	China	Dolomite	Thermal	Pidgeon	500 to 20,000	16

*Comments*

1. Primary production closed 2002. Output in 2000 at 43,000 tons per year + 10,000 tpy recycling.
2. Pidgeon process plant was put out of business in 1969 by Dow lowering price from 36 to 30 cents.
3. Plant became uneconomic, labor, electricity and process costs became too high.
4. Plant at Marginac has been expanded to 17,000 tons per year capacity but electrical costs were high. Pechiney has ceased magnesium production at the plant in 2002.
5. Made dolomite from seawater magnesia and limestone. Process became too costly. Moved plant to China in a joint venture deal.
6. MEL built Pidgeon Process plant and it was not successful due to impurities in their dolomite deposit.
7. National Lead sold to Amax who sold to Renco. Plant was modified in 2001 by changing out NH type of cells in one building and installing a Mag-Corp developed cell, which seems to be doing very well.

8. Magnesium electrolytic cells were not efficient, bought Russian cell technology, had environmental problems, fixed much of that, then evaporation ponds flooded, owner assassinated, sold out to MPLC.
9. Dow built a Mag-Chlor plant to produce magnesium and strong chlorine; it did not run well and was closed and demolished after about one year of operation.
10. Alcoa established a magnesium production plant using Pechiney Magnetherm technology. The plant is located just north of the old Spokane World War II magnesium plant that used the same dolomite deposit. Plant efficiency and capacity had been expanded to 45,000 tons per year by Alcoa applied research. Used magnesite to "sweeten" the charge. Plant was shutdown in late 2001.
11. MagCan was designed and built to process magnesite using a carbo-chlorination process developed by MPLC and piloted in England. The plant used the modified Russian electrolytic cells developed by American Mag. Failed within one year due to combination of technical and partner reasons.
12. Norsk Hydro built a new plant in Canada to use magnesite. Process was developed in Norway. The plant was late and over budget and the operations took a long time to get running well. The plant was built in North America to access the auto industry and aluminum alloying. Anti dumping charges virtually barred the shipment of magnesium from this plant to the US, causing the plant to run at half capacity for several years and lose money. Plans to expand are on hold.
13. Noranda has a new plant based on a process using serpentine tailings for feed material. The process was piloted and now the 63,000 commercial plant has started. Work on the process development took about ten years before the pilot plant operation. Full scale commercial plant experienced start up difficulties normally expected with electrolytic plants using new dehydration technology. The main problem of getting high quality  $\text{MgCl}_2$  to feed the electrolytic cells was a long and costly problem. Plant was temporarily closed in April 2003.
14. Dead Sea Magnesium uses technology supplied by the Russian VAMI and the Ukrainian Titanium Institute. It has continuous flow line concepts and is presently struggling with high energy costs.
15. Australian Magnesium (Queensland Metals) has been working on the magnesium process for producing magnesium from magnesite for over 10 years. A 1,500 tons per year demonstration plant was started in 1998 and has produced several tons of magnesium per day to prove the process and provide data for the feasibility study. The financing for a 97,000 tons per year smelter is being completed. Detailed engineering and site preparation is starting on the commercial plant. It is scheduled to start producing metal in 2005. Ford Motor has signed an off-take agreement for half of the production for 10 years. Base price is said to be US\$ 1.30. Ford also put A\$ 40 million into the project to help build the demonstration plant. Project had a huge projected cost over run and was stopped in 2003. Ford withdrew their support.
16. Chinese companies in several provinces built Pidgeon process magnesium plants, most had small capacities. There were an estimated 300 of these plants at the peak of building in 1995. The decreasing magnesium sales price has forced consolidation and rationalization of many of the separate plants.
17. Plant that was built, operated and closed.



## References

1. IG Farben German Pat. 122163 (1932, 1933)
2. Österreichisch-Amerikanische Magnesit AG, Pat. DRP 661010 (1938)
3. Aluminium und Magnesium Fabrik Hemelingen German Pat. 26962 (1885)
4. G. Pistor; P. Rakowicz U.S. Pat. 965.485 (1910)

---

## 2 Production Technologies of Magnesium

*Eli Aghion, Gilad Golub*

### 2.1 Introduction

One of the features of the magnesium industry is the wide variety of production processes. Relative to an industry, which has been manufacturing a product commercially for close to one hundred years, it is somewhat strange that there are over 10 different processes for producing magnesium. Unlike many other industries, there is no one particular dominant technology used for most of the world's production.

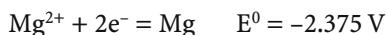
The large number of production technologies stems from the differences in basic parameters of the production processes. Below are the basic parameters, which differentiate the various production methods.

#### (A) Raw materials

There are six sources of raw materials for the production of magnesium: magnesite, dolomite, bischofite, carnallite, serpentine and sea water. These sources differ in the magnesium content, in production methods, and in their origin. Some are mined from mines, some in open mining, others originate in various processes carried out on sea water and salt lakes, and another material originates from the waste of the asbestos production process.

#### (B) Materials and method of reduction

Magnesium always appears in nature in ionic form with the following electron arrangement:  $1S^22S^22P^63S^2$ . This arrangement is characterized by the low ionization energies relative to the two most external electrons, which are at the 3S level. This is the reason why univalent or trivalent magnesium is not found in nature, only bivalent. The low standard reduction potential of magnesium is the reason why no metallic magnesium is found in nature [1]:



All production technologies, therefore, require a reduction agent which can transfer two electrons to the magnesium. The reduction agents are: electric current operated at the appropriate potential, coal in various forms, silicone-based materials (FeSi),  $\text{CaC}_2$ , and aluminum. The accepted division in literature, for thermal and electrochemical technologies stems in fact from this central feature. All the electrochemical technologies use direct current electricity form, which passes through the electrolysis cells and discharges chlorine and magnesium ions into

gaseous chlorine and metallic magnesium. The thermal methods are based on heating of magnesia in the presence of various reduction materials, to a variety of temperatures. At a particular temperature the reduction reaction takes place and the magnesium becomes metal, usually in its gaseous form.

### (C) Production temperatures

Maximum temperatures in the various production processes are in the range of 655–1,900°C, which is a very large temperature range for a production process of one particular material. In general, electrochemical production processes take place within the lower production temperature range, usually between 655–720°C, while the thermal reduction production processes take place within the higher temperature ranges, usually between 900–1900°C.

### (D) By-products

The by-products from the various methods are, in fact dependant on the composition of the raw materials. If the basic raw material is bischofite or carnallite, we shall obtain, in addition to magnesium, chlorine and by-products related to the components of the original material. In the case of Carnallite, in addition to chlorine there will be KCl-rich salt (70%), which serves in the production of fertilizers.

With processes in which the basic raw material does not contain chlorine, no surplus chlorine will be produced, since the chlorine produced will be recycled into the production process. Most processes will actually require the addition of chlorine from external sources such as magnesium chloride or HCl.

This chapter details extensively the basic parameters used in the various production methods. The chapter will also provide examples of commercial production technologies in existence around the world, while tracking the relative advantages and disadvantages that characterize these technologies.

## 2.2 Raw Materials for Magnesium Production

The raw materials for the production of magnesium come from different magnesium sources. Since these materials begin as natural raw materials, they will never appear in their pure form. In all cases they will be accompanied by additional materials, depending on their source. Table 2.1 details the chemical formulas of the raw materials on their pure form.

**Table 2.1.** Raw materials and their molecular formula

Material	Chemical formula
Magnesite	$\text{MgCO}_3$
Dolomite	$\text{MgCO}_3 \cdot \text{CaCO}_3$
Bischofite	$\text{MgCl}_2 \cdot 6\text{H}_2\text{O}$
Carnallite	$\text{MgCl}_2 \cdot \text{KCl} \cdot 6\text{H}_2\text{O}$
Serpentine	$3\text{MgO} \cdot 2\text{SiO}_2 \cdot 2\text{H}_2\text{O}$
Sea water	$\text{Mg}_{(\text{aq})}^{2+}$

### 2.2.1 Magnesite

In nature, this material is composed mainly from carbonated magnesium and contains low concentrations of calcium, iron and manganese as impurities. Magnesite belongs to the calcite group, which is a group of carbonates that are similar in their physical characteristics. Magnesite is usually produced when rocks rich in magnesium come into contact with carbonate-rich solutions thereby producing a first degree metamorphosis. The Magnesite does not normally produce crystals with a defined form. It has a crystalline structure similar to calcite and it is white.

Magnesite is common in Brazil, Austria, Korea, China and the West Coast of the United States of America, and it is extracted by mining. The magnesium concentration by weight is 28.8%.

### 2.2.2 Dolomite

This is composed mainly of the double salts of magnesium and calcium carbonate, and contains low concentrations of iron and manganese as impurities. Dolomite is usually colorless and looks like small diamond-shaped crystals. Dolomite is formed as a result of calcite transformations in the presence of magnesium ions.

Dolomite rock is useful in the chemical industry for the preparation of magnesium and serves as construction and decoration stone. Common deposits can be found in England, Germany, Brazil, Norway and Mexico.

The magnesium concentration in dolomite by weight is 28.8%.

### 2.2.3 Bischofite

A colorless mineral in the shape of chips or crystals. Bischofite is obtained as a by-product of the potash production process, which is produced both through mining and from the sea. It is extracted from solutions of salt water, for example, seawater and water from the Great Salt Lake. In order to extract bischofite the water is partly removed from the solution by solar evaporation and then the other salts are crystallized.

The magnesium weight percentage in bischofite is 11.96%.

### 2.2.4 Carnallite

Carnallite serves mainly as raw material for the production of potash and as ore for magnesium. It is produced in the sediment of evaporation ponds, where seawater has been concentrated and exposed to continued evaporation. The process of carnallite formation requires special climatic conditions, which will enable continued and intensive natural evaporation. In addition, the formation basin must have a special form. Typical conditions of this kind are found in the Dead Sea, where carnallite appears as large masses and is not crystal-shaped. Carnallite is especially light, with a specific weight of only 1.6 g/cm<sup>3</sup>.

Industrial actions connected with the manufacture of carnallite are environmentally friendly. Carnallite manufacture at the Dead Sea uses mainly solar

energy to cause precipitation. The salination in ponds saves about 10 million tons of fuel a year.

Carnallite as a raw mineral is common in the following regions: Mexico, USA, Germany, Russia, China, Iran and Israel.

The magnesium weight percentage in carnallite is 8.75%.

### 2.2.5 Serpentine

A group of silicate minerals with similar chemical characteristics but a different structure. This group is produced from magnesium-rich minerals and is composed mainly of greenish magnesium hydroxide silicates. The best-known minerals in the serpentine group are called chrysotil and they contain the following main formula:  $\text{Mg}_3[\text{Si}_2\text{O}_5](\text{OH})_4$ . Most of the minerals in the serpentine group are composed of asbestos fibers and, therefore, form the main source of commercial asbestos, used for the insulation of houses and buildings. The serpentine structure includes layers of tetrahedral silicates with layers of  $\text{Mg}(\text{OH})_2$  between the layers. Serpentine is a component of metamorphous rocks. The raw material for serpentine is mined and is common to the following regions: Italy, Russia, Canada. Serpentine is obtained as a main by-product in asbestos production processes.

The magnesium weight percentage in serpentine is 26.33%.

### 2.2.6 Sea Water

The magnesium ion is the third most common component in sea water. Its concentration varies between different seas (see Table 2.2). Magnesium ions are the product of erosion. The magnesium hydroxides and carbonates that form have low solubility in seawater and therefore as a result of their settling to the bottom they become the building blocks for coral reefs. In addition, they have an important ecological function in that they accumulate high concentrations of  $\text{CO}_2$ , keeping this gas out of the atmosphere. The low solubility of these salts is used to produce magnesium from seawater, and is achieved by adding a precipitation agent, such as  $\text{Ca}(\text{OH})_2$ . The relative ion concentrations appear in Table 2.2.

**Table 2.2.** Composition of general sea water and Dead Sea water

Material	Sea water composition [%]	Dead Sea water composition [%]
Magnesium	0.129	4.2
Chlorine	1.95	20.8
Potash	0.038	0.75
Bromine	0.067	0.6
Sodium	1.077	3.5
Calcium	0.0412	1.6

## 2.3 Electrochemical Methods

It is possible to divide the magnesium production technologies into two main types: electrochemical methods and thermal reduction methods. The difference between these methods stems from the reduction process of the magnesium ion to metallic magnesium. For the electrochemical methods the reduction is carried out with electric current fed into the electrolyte cells. In the case of thermal methods, the reduction is carried out by means of various reducing materials at high temperatures [2–4].

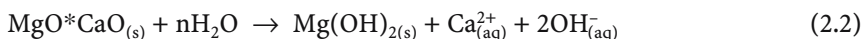
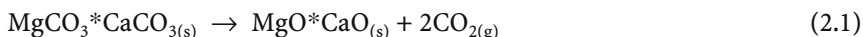
In the chapters dealing with the magnesium production processes we shall examine most of the methods that exist in the world for the commercial production of magnesium. In addition, we will present production processes that are currently not used, such as the carbothermic and Dow processes, as well as innovative processes, such as the Magnola process, the Heggie process and the AMC process.

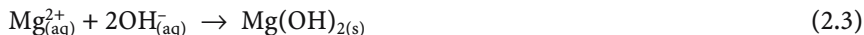
### 2.3.1 Preparation of Magnesium Chloride Salts from Natural Raw Materials

The basic raw materials for the production of magnesium with the electrochemical process are generally divided into two: salts containing chloride and raw materials that must be transformed into salts containing chloride. Eventually, all the materials will become either bischofite or carnallite prior to drying and feeding into the electrolysis cells.

The production process employed by Dead Sea Magnesium (DSM) is based on raw material obtained directly from the Dead Sea through processes of dehydration and crystallization. This process is thought to be the most efficient and economic of all the production processes for raw materials, since it is based on evaporation with the help of solar energy on open ponds [5]. Magcorp uses a similar method with the waters of the Great Salt Lake, from which it produces magnesium chloride-rich solutions. Various manufacturers from the former Soviet Union produce artificial carnallite from bischofite or magnesium sulfate. The artificial carnallite is produced through the addition of spent electrolyte from the electrolysis process, which contains about 70% KCl to magnesium chloride-rich solutions [6]. With this process, the carnallite settles, and is separated, by means of crystallizers, back to the production process. The production of magnesium directly from raw materials containing chloride is advantageous, since for each ton of magnesium, 2.5 t of chlorine, which are produced during the electrolysis process can be sold. With all other production processes, it is necessary to manufacture HCl with an intermediate process in order to complete the process of preparation of the raw materials for the electrolysis [2–4].

The Dow process of production of magnesium chloride was originally based on the roasting of dolomite in kilns and its addition to seawater containing magnesium ions (this fundamental process is still used today at a hydro magnesium plant in Norway). The process is carried out according to Eqs. (2.1–2.3).





Later, NaOH solutions began to be used with the Dow process. The source of these is in chlorine production processes from NaCl electrolysis; hydroxide ions from the base react in a similar manner to Eq. (2.3). In the second stage the reaction is caused between  $\text{Mg}(\text{OH})_{2(\text{s})}$  and HCl (see Eq. (2.4)) [7].



The HCl source in the Dow process is in the by-product of the production processes of PVC and other chloro-organic materials. Another possibility is the production of HCl by burning of chlorine from the electrolysis process with hydrogen or methane. The practical significance is that all the chlorine manufactured in the electrolysis cells is recycled into the magnesium production process. The solution created during this stage contains silica and other solids in addition to the sulfates. In order to sink the sulfates as gypsum, calcium ions are then added to this solution, the solids are filtered from the solution and the clean solution is sent to the next stage.

In the hydro magnesium process used in Canada the raw material for the process is magnesite, which is mined in mines (mainly in China). The magnesite is dissolved in a hot HCl solution, thus arriving at a magnesium chloride-rich solution:



The acid solution must be hot for an efficient melting process. The basic ore of the magnesite is rich in various metallic impurities, sulfates and boron, which can be a problem at the electrolysis stage. Therefore, already at this stage a number of processes are carried out, whose purpose is to separate the impurities from the magnesium chloride [2, 4].

In the AMC process, the preliminary stage is fundamentally similar to the hydro magnesium Canadian process.

The source of the acid in both cases is a reaction of all the chlorine created during the electrolysis process with hydrogen or methane.

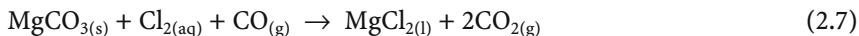
In the Magnola process the original raw material is serpentine. This material, as in the hydro magnesium and AMC processes, reacts with HCl whose source is in chlorine from the electrolysis cells [10–13], according to the following reaction, where the silica and other insoluble materials are separated from the solution:



Since the serpentine contains large quantities of iron, manganese, etc., additional settling and cleaning processes are carried out, with the final goal being to obtain a clean solution of magnesium chloride.

The commercial electrolytic processes produce by this stage a total of two materials: carnallite and a magnesium chloride-rich solution.

During the history of magnesium production there were a number of additional processes with which attempts were made to produce directly anhydrous magnesium chloride, attempting to bypass the drying stage. None of these processes survived commercially; the most famous of them is the process described by Eq. (2.7), which was at one time carried out at Magcan Canada [23].



The process was carried out at temperatures of 800°C, and the melted magnesium chloride flowed from the bottom of the reaction reactor.

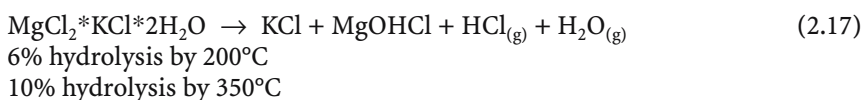
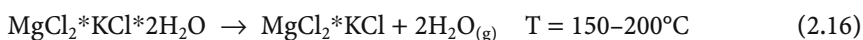
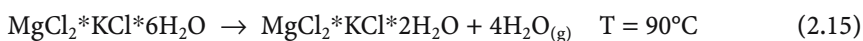
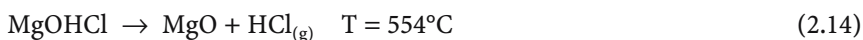
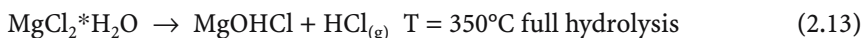
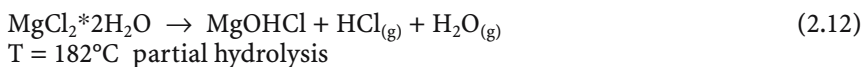
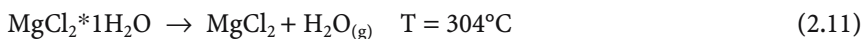
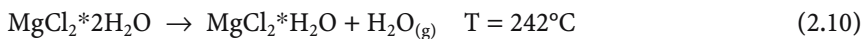
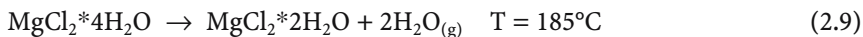
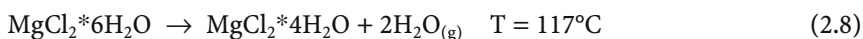
### 2.3.2 Drying Magnesium Chloride Salts

Carnallite, bischofite and their solutions contain large quantities of water. Carnallite and bischofite are hydrate salts containing six molecules of water per crystal and at times even additional water in attached form. The use of these materials in the electrolysis process requires the removal of all the water prior to the electrolysis. Carnallite and bischofite tend to decompose in the hydrolysis reaction to magnesium oxide and HCl, at relatively low temperatures, and, therefore, the drying process is actually the most complicated and hardest stage in the electrolysis methods for the production of magnesium. In this matter it should be stated that most magnesium production R&D in the last decades has focused on the drying process for extraction of anhydrous magnesium chloride with low content of magnesium oxide.

The three negative characteristics of a hydrolysis reaction are:

1. The creation of magnesium oxide, which will later be concentrated as sludge in the electrolysis cells, will react with the graphite anodes and will harm the energy efficiency of the process.
2. Losses of magnesium chloride during the process.
3. The requirement to handle the acid gases produced during the reaction.

The advantage in using carnallite is the fact that the hydrolysis of this material is significantly lower than the hydrolysis of bischofite, and even the decomposition temperatures of its various hydrates are lower. The following are the decomposition and hydrolysis temperatures of carnallite and bischofite [2]:





The products of the drying stage can appear in two forms. One form is that of a solid material, the other is molten salts. In addition to this difference there are “sensitive” electrolysis cells, which require material with a particularly low concentration of magnesium oxide (0.05–0.1%) and more “resistant” electrolysis cells that can also work with raw materials containing 0.6% magnesium oxide. These differences, of course, influence the character of the required drying process.

### 2.3.3 Electrolysis of Magnesium Salts

The electrolysis stage is performed in the electrolysis cells. At this stage there are a number of main points that characterize the process. In this chapter we shall focus on these points while reviewing the various electrolysis cells and their features. We shall concentrate on the following points: the composition of the electrolyte, the thermal balance of the cell, the type of electrodes, the structure of the cell, a comparison table that includes the main production parameters, and the cell operation.

#### 2.3.3.1 Type of Electrolytes for Electrolysis

The optimal electrolyte for the production of magnesium must have low resistance, high density, and a low price. Magnesium chloride does not have high conductivity and, therefore, the accepted values for its use are relatively low (8–25%), this despite the fact that it is in fact the material undergoing electrolysis. The other materials are determined according to other technological constraints [6].

In general, there are two types of electrolytes: a substitute electrolyte and a constant electrolyte.

**Substitute electrolyte.** This kind of electrolyte is used in the DSM process today and in the former Soviet Union. In this case, the electrolyte composition is determined mostly by the raw material carnallite. The substitute electrolyte is constantly extracted from the cells and it is, therefore, impossible to use high cost materials or such that require special treatment prior to introduction into the cells. The electrolyte in this case is of a low density and high resistance relative to a constant electrolyte. The only material which is added in large quantities is sodium chloride for purpose of improving the electric conductivity of the electrolyte. It must be remembered that any addition requires heating and melting, which are wasted when the addition is extracted from the electrolysis cells. With this technology, for each ton of magnesium produced, some 5 t of spent electrolyte are extracted from the cell [5, 6].

**Constant electrolyte.** This electrolyte exists in all the processes in which magnesium chloride is the material added to the cell. In this case the products are magnesium and chlorine only and there is no spent electrolyte extracted from the cell. The only electrolyte that exits the cell is the electrolyte attached to the metallic magnesium and, therefore, the loss of electrolyte is at a level of 1–2% only. Thus, the composition of the electrolyte is, in fact, an optimization of three

**Table 2.3.** Data on various electrolytes [6, 14]

Electrolyte type/ Parameter	Substitute electrolyte	Constant electrolyte	Li base electrolyte
Compositions [%]	MgCl <sub>2</sub> 8–18 KCl 64–70 NaCl 19–23 CaF <sub>2</sub> 0.3–0.5	MgCl <sub>2</sub> 15–25 CaCl <sub>2</sub> 20–25 NaCl 55–60 CaF <sub>2</sub> 1	MgCl <sub>2</sub> 15–25 CaCl <sub>2</sub> 20–25 NaCl 35–40 LiCl 18–20 CaF <sub>2</sub> 1
Density [g/ml]	1.60–1.61	1.75–1.76	1.68–1.69
Conductivity [ $\Omega \cdot \text{cm}^{-1}$ ]	1.87	2.46	3.65

main parameters: density, electric conductivity and price. Since these parameters are similar the world over, one can say that the electrolyte composition in the AMC process, NH process (Canada), MagCorp process and NH process (Norway) is very similar. In the electrolyte composition (see Table 2.3) there is no KCl, unlike the composition of the first type of electrolyte. This is not surprising since it is known that KCl does not contribute to the increase in density and it has a higher resistance than NaCl. The function of the calcium chloride is weighting since it, too, is of a high resistance. This type of electrolyte is heavier and magnesium of a lower density will separate more easily from the electrolyte in the electrolysis cells.

In the past, in order to reduce the electrical resistance of the electrolyte, lithium chloride was added to the electrolyte. It was, indeed found that this material significantly decreased the resistance of the electrolyte, but its high price negated the possibility of using it on a regular basis in commercial processes [6, 15].

A small quantity of CaF<sub>2</sub> is added to all the electrolytes used in the electrolysis cells. This material is added to the electrolyte in order to assist in the growth of the metallic magnesium drops and the wetting of the cathode surface. In the absence of CaF<sub>2</sub>, or another source of fluoride ions, there is a drop in the efficiency of the process [6].

### 2.3.3.2 Thermal Balance of the Electrolysis Cell

The electrolysis cells, as can be seen in Table 2.4, work in a limited temperature range close to 700°C. In order to maintain this temperature, it is necessary to constantly balance the amount of heat generated in the cell with the amount of heat cleared from the cell. The amount of heat generated in the cell is, in fact, all the electric energy introduced into the cell minus the energy required for the decomposition of the magnesium chloride into magnesium and chlorine. The theoretical energy value for the above decomposition is about 7 kWh/kg of magnesium [10]. From Table 2.4, it is possible to see that most of the processes require almost twice the energy for production. This difference in energy constitutes the heat generated in the cell [2–4, 6].

**Table 2.4.** General comparison of electrolysis technologies [2–4, 6, 7, 10–12, 17–24]

Parameter/ Company	DSM	Dow	Magcorp	Hydro magnesium	Magnola	AMC
Cell technology	Russian (VAMI) diaphragmless	Dow cell	Alcan diaphragmless	Hydro diaphragmless cell	Alcan MPC-EX	Alcan MPC-MKIII
Production TPY	600–650	600–700	550–600	1400–1500	2200–2300	1350–1450
Current/Voltage [kA/V]	200/4.8	200/7.0	180/4.5	400/5.3	160/17	150–170/12
Mg [kWh/kg]	13–14	18–19	13–15	12–13	10.5–11.5	11–12
Electrode technology	Mono-polar	Mono-polar	Mono-Polar	Mono-polar	Multi-polar	Multi-polar
Life span (years)	3–6	2	4–5	6	2	2–3
Cell temperature [°C]	680–700	710–720	680–700	700–720	655–665	655–665
Feeding	Molten carnallite	Solid MgCl <sub>2</sub> *2H <sub>2</sub> O 27% H <sub>2</sub> O	Molten MgCl <sub>2</sub>	Solid MgCl <sub>2</sub>	Molten MgCl <sub>2</sub> electrolyte	Solid MgCl <sub>2</sub>
MgO in feeding [%]	0.2–0.6		0.1–0.3	< 0.1	0.03–0.1	0.1

The causes for the loss of energy can be found in the technology. The main cause is the electrical resistance of the cell. The resistance of the cell is the sum of the resistances of the cathode, the anode, and mainly of the electrolyte (between the cathode and the anode). The resistance of the electrolyte depends on the distance between the cathode and the anode, and the electrolyte properties (as they appear in Table 2.3), on the conditions of the surface of the anode and cathode, and on the temperatures. A further important cause, which leads to a loss of energy is the current efficiency. The main factor, which influences the efficiency of the current, is the exothermal back reaction between the gaseous chlorine and magnesium.

### **2.3.3.3 Increasing the Magnesium Output by Means of Artificial Cooling**

The manner of heat removal from the cell changes according to the type of cell. In general more magnesium can be produced from any given electrolytic cell by simultaneously increasing the current and removing more heat. Below are the various means that remove or use heat in a cell [3, 4, 6]:

- Melting solid feed material. Some of the electrolysis cells are fed by solid magnesium chloride, and the melting of this material requires a great deal of energy, thus cooling the cell [16].
- Heat losses by surface cooling. There are cells in which the heat is removed by natural convection only and there are cells in which forced air is used in order to increase the heat removal.
- Anode cooling. In most electrolysis cells where anodes are introduced from the cell roof, cooling of the upper part of anode is carried out by water. The anodes, which are made of graphite are excellent conductors of heat and thus they enable the removal of a large amount of heat from the cell, precisely in the spot where heat is created (between the anode and cathode).
- A dedicated installation for the cooling of the electrolyte. The Alcan cells contain a large heat exchanger, which is capable of removing over 1 MWh heat out of the cell. This heat exchanger (Fig. 2.1) removes the heat with the assistance of forced air. The heat exchanger is also used for financial reasons. For example, when the price of electricity is low (night price), more magnesium can be produced from the cells by putting the heat exchanger into operation [17, 24].

The Alcan cells work in a narrow range of temperatures (see Table 2.4). This range is also obtained by using heating electrodes. There is a link between the efficiency of the current and the temperature; in principle, the lower the temperature the higher the current efficiency. The limit is the temperature at which magnesium solidifies, which is 650°C. Except for the alcan multipolar cells there are usually no heating installations for electrolysis cells and, therefore, in order to avoid the solidification of the cell, most of the cells work at a large temperature gap of 50°C from the magnesium solidification temperature.

### **2.3.4 Types of Electrodes in the Electrolysis Cells**

Two types of electrodes exist in the electrolysis cells, mono-polar and multi-polar (see Table 2.4). The differences between them stem from the way in which

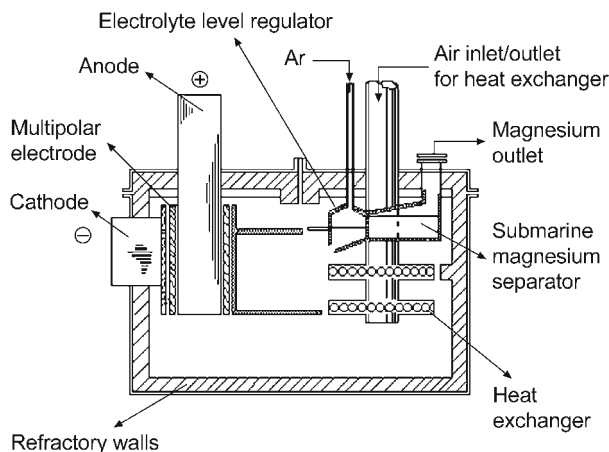


Fig. 2.1. Alcan cell, schematic vertical cross section [23, 24]

the electricity flows through them and in their electric connections [7, 25] (see Fig. 2.2). In mono-polar electrodes the electrons flow from the anode (made of graphite) to the cathode which is made of metal. In multi-polar electrodes there are about 3–5 bipoles (usually made of graphite [17–24]. The current, which passes through, polarizes them, thus enabling the performance of electrolysis over their integral surface. The significance is that with multi-polar electrodes, each electron is used a number of times and therefore the voltage in multi-polar electrodes is higher.

The main advantages of multi-polar electrodes lies in the saving of expensive electric connectors and a greater production per area unit. The main disadvantage lies usually in a low current efficiency due to leakage, which is caused by the ends and work at higher voltages. Alcan cells contain a number of important modifications, the most important of which enables a 5–15 mm distance between bipoles as against a distance of 7–12 cm between an anode and a cathode in mono-polar electrodes. The large difference in distance has a vast influence over

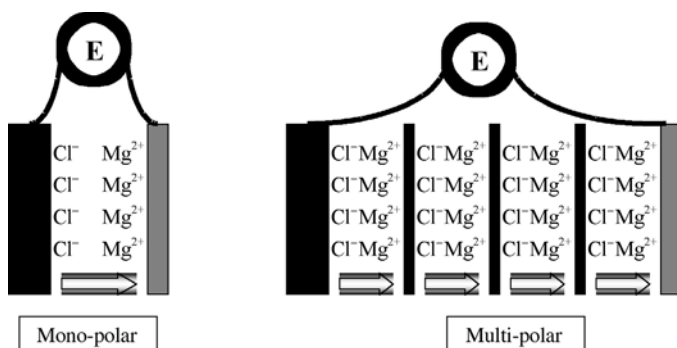


Fig. 2.2. Electrode technology

the resistance, voltage and required consumption of electricity for magnesium production (see also Table 2.4) [2–4, 6, 17–24].

### 2.3.5 Structure of the Electrolysis Cells

All the electrolysis cells are divided into the electrochemical area containing anodes and cathodes, and the service area where the raw material feed takes place and the magnesium is gathered.

This can be seen in Figs. 2.1 and 2.3. Except for the Dow cell, which is made of steel and its shell is directly connected to the cathodes, all the other electrolysis cells are made mainly from ceramic refractory materials. The reason for this is the harsh corrosive conditions, which exist in the electrolysis cells. These conditions prevent the possibility of using unprotected metal in the electrolysis cell.

In all the cells (except for the Dow cells) the cathode entry is on the sides of the cell body, and the anode entry in most cells is from above. The advantage in an upper entry of the anode is the possibility of changing them when they wear out. An added advantage is the ability to cool them with the aid of water easily and without disturbing the flow routine in the cell. The main disadvantage in anodes with an upper entry is the increased wearing out caused to the part of the anode above the melt. Due to the high price of graphite anodes this disadvantage is fundamental. In DSM's electrolysis cells, the anodes entry is at the bottom of the cell and their life span is the same as the cell's life span; when they wear out the cell usually should be disassembled and rebuilt.

In Alcan electrolysis cells [17–24] and hydro magnesium cells [16], there is only one electrode area and next to it a service area (see Fig. 2.1). In the electrolysis cells of DSM, Russian manufacturers and MagCorp, there are rows of electrodes with the service area in between them (see Fig. 2.3) [6, 30].

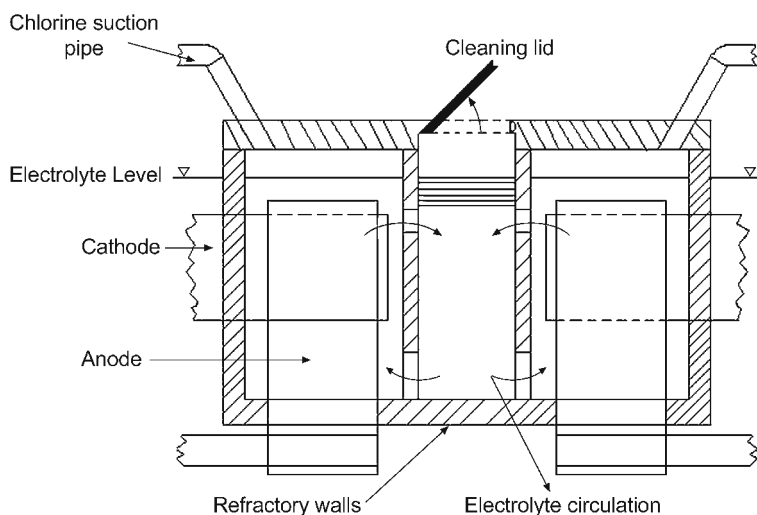


Fig. 2.3. Bottom anodes entry cell, schematic vertical cross section [2–6, 8]

In all the cells between the service area and the electrode area there is an inner wall. This wall contains openings in both its lower and its upper parts, enabling the flow of electrolyte.

In the electrolysis cells of DSM, Dow, Russian manufacturers and MagCorp there is a service opening, which allows the cleaning of sludge (mainly magnesium oxide) when required which sometimes accumulates at the bottom of the cells [6, 30].

Since the raw materials, fed into the Dow cells contains large quantities of water, the graphite anodes suffer particularly fast erosion. These anodes, that have a circular cross section, differ from the rectangular anodes in other electrolysis cells and, therefore, can be adapted (they can be lowered following erosion), which takes place at short intervals. Raw materials, which contain a large amount of water cause erosion of the anodes and are also responsible for the relatively low energy efficiency in the production of Dow cells (see Table 2.4) [8, 31, 32].

Alcan cells are considered to be the most sophisticated of the existing cells, but their main disadvantage is their great sensitivity to the production process. Alcan cells must be fed with raw materials with very low levels of impurities and with an extremely low level of magnesium oxide (see Table 2.4) [2, 4]. Despite that, their customary life span is the shortest. The compensation for the cost involved in rebuilding lies in the high output of alcan cells to cell cube volume, and in the low energy consumption in the production of magnesium (see Table 2.4). In the alcan cell service area there is a device whose function is to safeguard a constant level of the electrolyte and also a submersible device to which the metallic magnesium adheres in the cell and from which it is pumped out [23]. An alcan cell also has the means for heating and cooling as previously mentioned, which enable the regulating of the temperature more precisely [23].

### 2.3.6 Operation of Electrolysis Cell

The main factor that significantly eases the gathering of magnesium is the relatively high density of the electrolyte from which the magnesium, whose density is lower, is gathered. This makes separation from the electrolyte easier, which takes place in all electrolysis cells by suction with a vacuum ladle a number of times each day. The suction of the magnesium, introduction of raw material, and, if required, the suction of the spent electrolyte is performed entirely within the service area in the electrolysis cells. Inside the electrolysis cell there is constant movement of material, caused by the upward movement of chlorine bubbles following their formation. This movement causes the metallic magnesium, which is formed in the electrode region to flow through small openings in the upper part of the partition separating the different parts in the cell to the service area in which the magnesium is gathered, as can be seen in Fig. 2.3.

The electrolysis cells must be fed with raw material at all times. Therefore metallic magnesium and the chlorine produced within it, and at times the spent electrolyte, must be removed frequently. Despite these basic facts, there are differences in the operation of the cells between the various methods. What is common to all the processes is the constant chlorine suction from the electrolysis cells. The materials feed differs from plant to plant. At hydro magnesium

(Canada) the material is fed as a solid all the time, with the aid of a constant feed system, which includes a silo and pneumatic launch. With the magnola process, the magnesium chloride-rich electrolyte goes through the overflow from the chlorinator on a constant basis. At Magcorp the molten magnesium chloride is fed in ladles to each electrolysis cell a number of times per day.

In magnesium production plants in Russia, where the raw material is carnallite, in addition to maintaining the carnallite feed to each cell, it is also necessary to extract the spent electrolyte at the completion of the process a number of times per day [6].

DSM has the most efficient operating method: instead of performing a molten carnallite feed into each magnesium cell several times a day, DSM works with a method called flow line [33, 34]. This method is based on the connection of dozens of electrolysis cells into one line, with channels. At the beginning of the electrolysis cells, the molten carnallite is fed into the head cell in which an electrochemical refining of the impure electrolyte also takes place. At the end of the electrolysis cells there is a separation cell. This cell assists in the gathering and separation of the metallic magnesium from the electrolyte. Some of the spent electrolyte is transferred to a granulator where it becomes solid and is sold for fertilizer production, while the other part of the electrolyte is pumped back into the head cell and is mixed with primary raw material – molten carnallite. The magnesium, too, is constantly pumped from the separation cell with the aid of vacuum ladles. Thus, instead of performing the operations in each cell separately, they are performed only in the first and last cells. The channels connecting the electrolysis cells have an additional function, they assist in the cooling of the electrolyte thus increasing the output of the cell. Between the first cell of the flowline and the last cell there is a slight difference in height, which enables the gravitational flow from cell to cell.

### 2.3.7 Refining Raw Magnesium Produced by Electrochemical Methods

Most of the magnesium plants using electrochemical technology, contain dedicated facilities for the constant refining and the casting of the metallic magnesium. These installations usually have a capacity of 15–30 t. Molten raw magnesium arriving from the electrolysis area is fed into these refining facilities at a temperature of about 700°C.

These facilities are called Continuous Refining Furnace (CRF). Their main function is to clean the magnesium from the impurities it contains. A secondary function is to enable constant casting on the ingots casting conveyors. The CRF refines the magnesium with the aid of additional weighted salts, which are added to it. Examples of round and rectangular shaped CRFs can be seen in Figs. 2.4 and 2.5.

The raw magnesium, which arrives from the electrolysis cells, contains up to 2% electrolyte, magnesium oxide, and nitrides. This material is fed into the CRF in ladles with a few tons capacity. In the CRF the magnesium is refined of impurities by a settling process with the aid of higher density salts [37], and a cell structure which causes the magnesium to move slowly according to the FIFO principle. The chloride and magnesium oxide contents after cleaning are significantly lower.



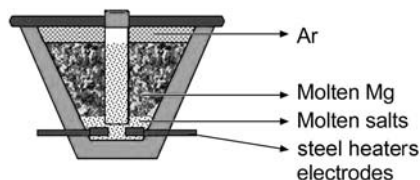


Fig. 2.4. Continuous refining furnace – circular shape [35, 36]

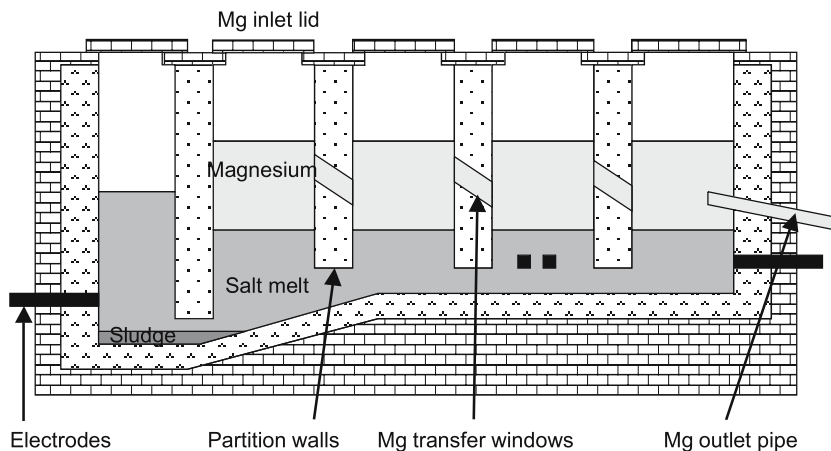


Fig. 2.5. Continuous refining furnace – rectangular shape [35]

The weighted salts enable heating with electrodes that are introduced from the bottom of the installation. The protective gas in the upper part of the CRF serves to protect the magnesium from reacting with oxygen.

The round CRF must be cleaned from the central shaft, every few days. This cleaning includes removal of the surplus electrolytes and magnesium oxide-rich sludge that accumulates inside, and also a replenishing of the weighted salts mix.

### 2.3.8 Industrial Methods for Electrochemical Production

For a more thorough familiarization of the commercial processes used in the production of magnesium worldwide, we shall define below the various processes, according to the main production methods used.

#### 2.3.8.1 DSM and Russian Process

According to the DSM process [5, 6, 26–30] (see Fig. 2.6) the dehydration process is divided into two parts: first we introduce the carnallite, which contains six molecules of water per crystal, and water is absorbed into the fluidized bed dryers.

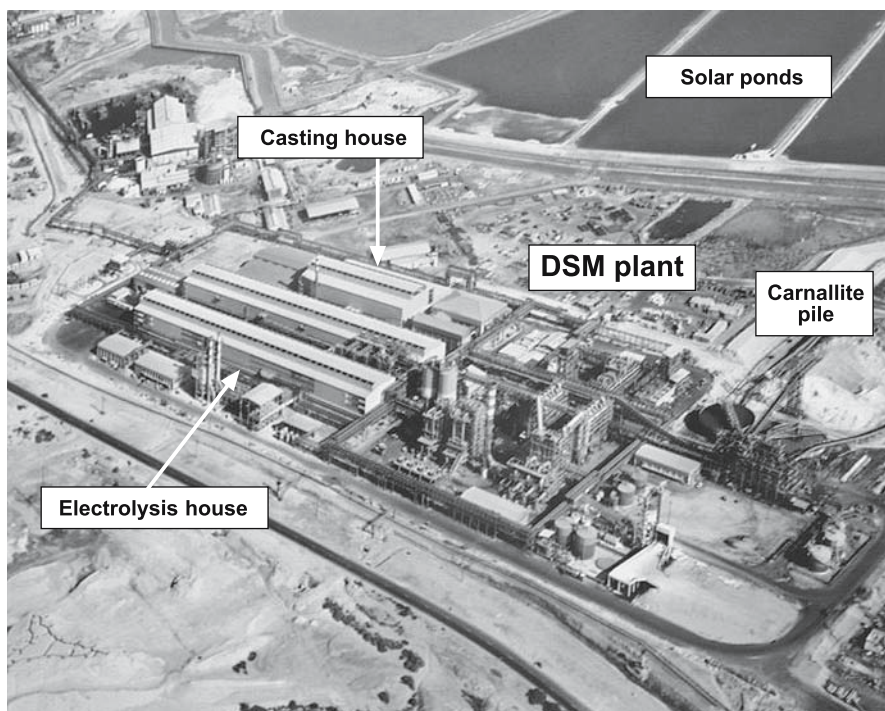
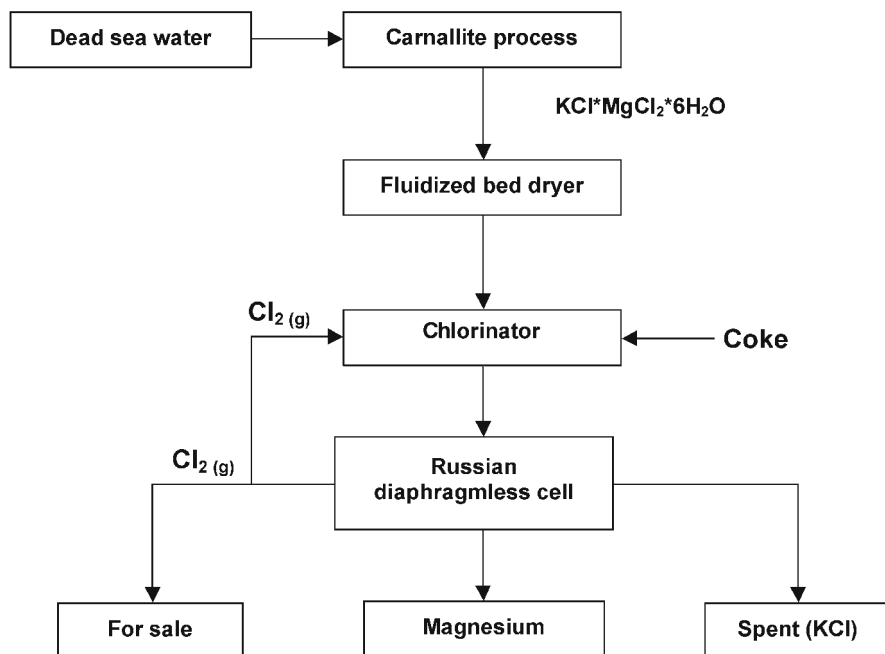


Fig. 2.6. DSM/russian flow processes

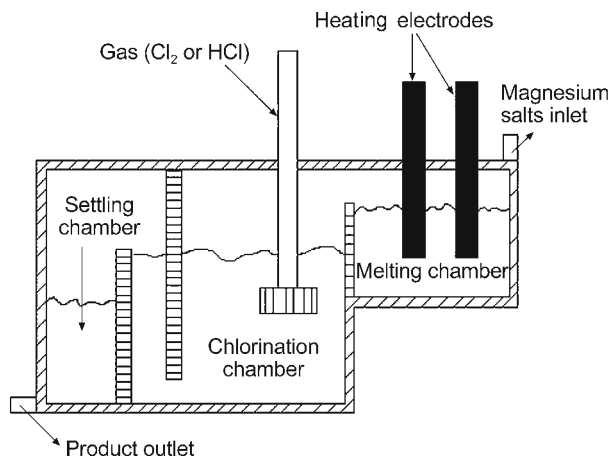


Fig. 2.7. (General) schematic description of a three-part chlorinator

The material in the fluidized bed dryers undergoes a number of heating stages in which the temperature rises from 130 to 200°C. During the process some 95% of the water is extracted from the carnallite, concurrently with the hydrolysis and the emission of a small amount of acid. The product of this stage is dry carnallite, which contains 3–6% water and 1–2% magnesium oxide.

Then the dry carnallite with a number of additives is transferred to the chlorinator. The chlorinator is an installation whose function is to melt down the carnallite, to remove from it all the water and to significantly reduce the quantity of magnesium oxide it contains. The chlorinator is made up of three chambers, as can be seen in Fig. 2.7. The melting of the carnallite takes place in the first chamber; in the second chamber chlorine is introduced for a reaction, and the following reaction occurs:



At this stage only one third of the chlorine produced in the electrolysis cells is used, while the remaining two thirds are made liquid and sold to chlorine consumers.

The material remains for some time in the third chamber, which is also known as the settling chamber. In this chamber, the remains of magnesium oxide and other insoluble materials sink to the bottom as sludge, while the molten and clean carnallite is transferred to the electrolysis stage. At this point the magnesium oxide concentration is reduced to 0.2–0.6%. The working temperature in the chlorinator is about 700–750°C.

### 2.3.8.2 The Dow Process

The process developed at Dow [2–4, 7, 8, 31, 32] (see Fig. 2.8) is unique, due to the fact that the material fed into the electrolysis cells still contains a significant amount of water – about 27%. A solution of magnesium chloride is introduced

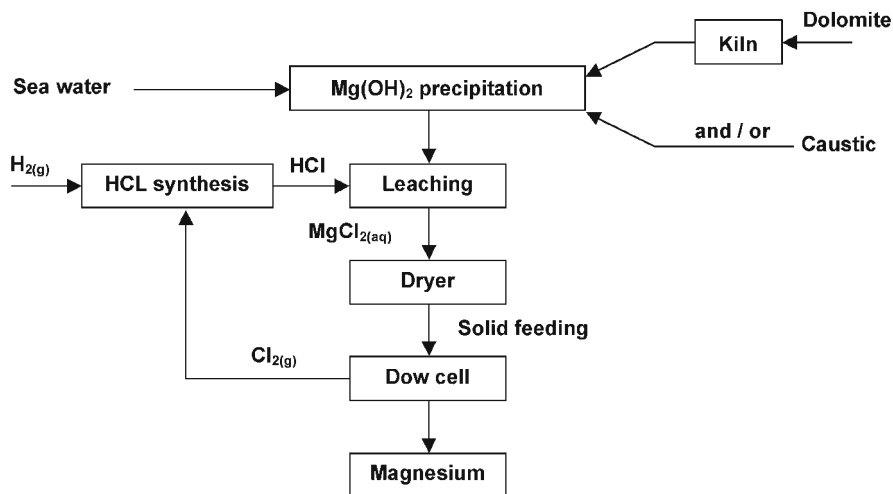


Fig. 2.8. Dow processes

directly into the spray dryer and comes into direct contact with burning gases, predominantly natural gas. During this process only reactions (2.8) and (2.9) take place. The products of this stage are granules of  $\text{MgCl}_2 \cdot 2\text{H}_2\text{O}$ . The additional dehydration is, in fact, carried out in the electrolysis cell, by the chlorine, which is created in the cell and the graphite anodes, which are used up at a fast rate.

### 2.3.8.3 The MagCorp (now US Mag) Process

During the preliminary drying process (see Fig. 2.9) the magnesium chloride solution is sent to the spray dryers, which are operated through burning gasses from the gas turbine electricity production. The magnesium chloride is dried to a fine powder, which contains, at the end of the drying process, 4% magnesium oxide and 4% water. This material is then sent to the chlorinator, as in the process carried out at DSM. The MagCorp chlorinator uses two thirds of the amount of chlorine manufactured in the cells and coke according to reaction (2.18). The reason for the larger amount of chlorine required in the MagCorp chlorination process (twice as much) compared with DSM, lies in the differences in the hydrolysis reaction between bischofite and carnallite. The working temperature is about  $815^\circ\text{C}$ , and it, too, is a result of the differences between the melting temperature of carnallite and magnesium chloride. The concentration of magnesium oxide in the product is 0.1–0.3% [2, 4, 6].

### 2.3.8.4 The Hydro Magnesium Process

In the hydro Magnesium process (see Fig. 2.10), during the preliminary drying process, the magnesium chloride solution is heated in the evaporator by the residual heat from the process until almost pure bischofite with a water content

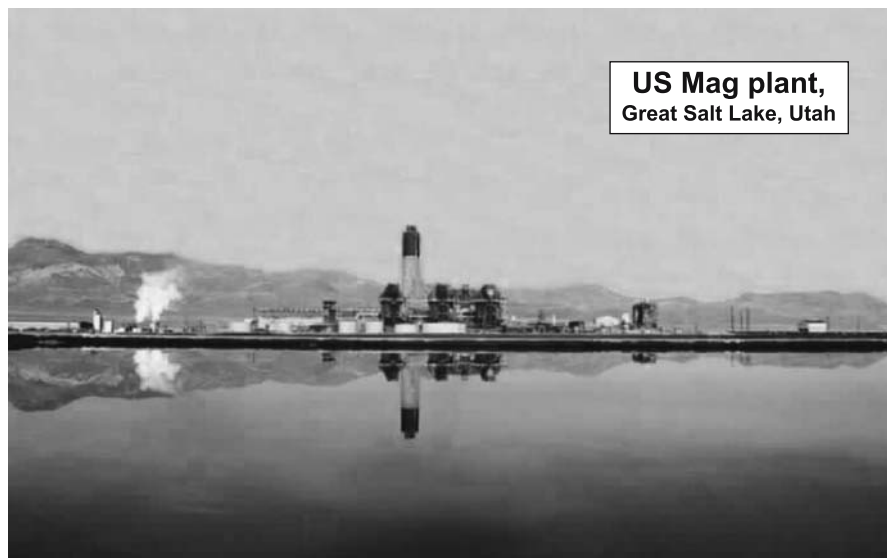
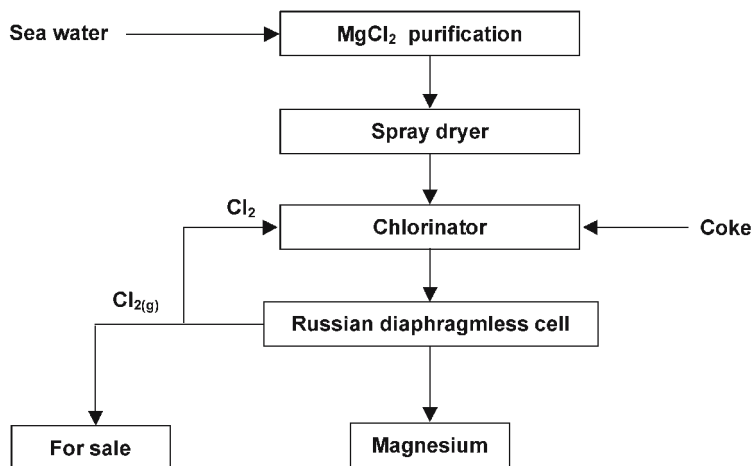


Fig. 2.9. MagCorp processes

of 45–50% is obtained ( $\text{MgCl}_2 \cdot 6\text{H}_2\text{O}$ ) [2, 4, 38–44]. The bischofite, which is melted during this process is turned into prills in the prilling tower. One of the main reasons for the transfer to prills is the wish to reduce the quantities of dust during the next drying stages.

The next drying stage is performed in a fluidized bed dryer. At this stage, the bischofite with six molecules of water is dried by hot air to  $\text{MgCl}_2 \cdot 2\text{H}_2\text{O}$ , as described in Eqs. (2.8) and (2.9). The last stage of drying, to extract anhydrous magnesium chloride is carried out by gaseous HCl drying at temperatures of about 330°C. The reason for performing this stage with heated gaseous HCl is the diffi-

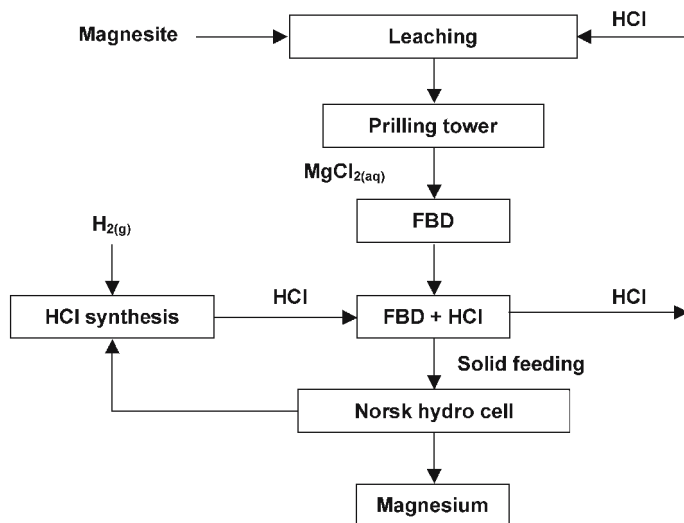
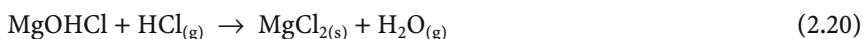


Fig. 2.10. Hydro magnesium processes (Canada)

culty in preventing hydrolysis, and the wish to obtain solid and dry magnesium chloride with magnesium oxide qualities of about 0.1%. From Eqs. (2.19) and (2.20) it appears that the use of gaseous HCl will fundamentally reduce the hydrolysis reactions, thus reducing the concentration of magnesium oxide in the product. A further point is that opposite reactions to hydrolysis take place with HCl (Eq. (2.19) and (2.20)), which also reduce the concentration of magnesium oxide.



The HCl from the drying process is transferred to the raw materials extraction and preparation process, according to Fig. 2.10.

### 2.3.8.5 The Magnola Process

A magnesium chloride-rich solution (27%) is poured into the spray dryer. In this installation, with the aid of hot gases, by burning of natural gas, the magnesium chloride is dried to  $\text{MgCl}_2 \cdot 2\text{H}_2\text{O}$ , Eqs. (2.8) and (2.9), as in the hydro magnesium drying process [10–12, 45–47]. The main difference lies in the fact that in the magnola process drying is carried out in one stage (see Fig. 2.11). The “price” is the relatively high percentage of hydrolysis, which causes a concentration of magnesium oxide of up to about 2%. During the second stage the material is transferred to a unique chlorinator called “super chlorinator”. The melting process is carried out as follows: an electrolyte low in magnesium chloride is pumped from the electrolysis cell to the chlorinator where it assists in the melting of magnesium chloride hydrate; this electrolyte returns to the electrolysis cell richer in

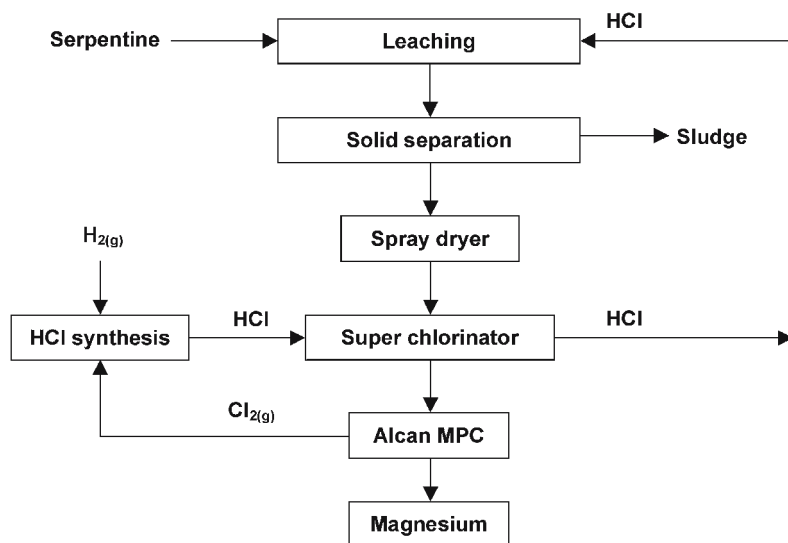


Fig. 2.11. Magnola processes

magnesium chloride in the overflow. The reason for the melting in the electrolyte is the relatively high melting temperature of pure magnesium chloride; melting in the electrolyte enables the melting temperature to be decreased 200–300°C. The electrolyte temperature is about 650°C, and this is also the temperature at which the material is returned to the electrolysis cell, with the assistance of heating by the graphite electrodes.

The chlorinator is fed with dry, gaseous HCl, which is produced from all the chlorine manufactured in the electrolysis cells. Feeding is carried out with the assistance of a number of graphite mixers, which are introduced from the chlorinator ceiling. These mixers assist in dispersing the HCl and improve the efficiency of the following reaction:



The high concentration of HCl in the melt and above the melt prevents the back hydrolysis reaction between the water vapors to the magnesium chloride. The concentration of magnesium oxide in the electrolyte returning to the electrolysis cell is about 0.05%.

The HCl discharged from the two drying stages is received in watery solutions and transferred back to the extraction process, according to Fig. 2.11, thus closing the process circle for the production of magnesium from raw material that does not contain chlorine.

### 2.3.8.6 The AMC Process

This company developed an innovative unique process, which apparently bypasses the problem of the hydrolysis reaction. At the completion of the drying

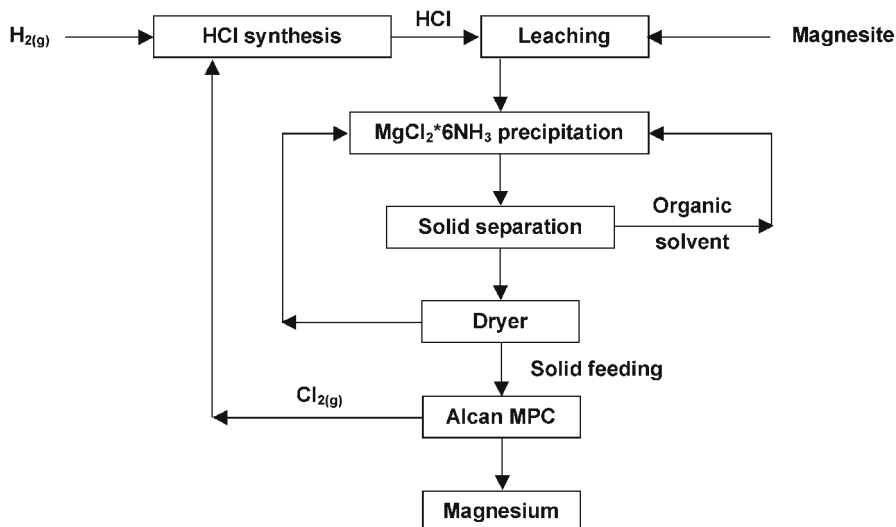
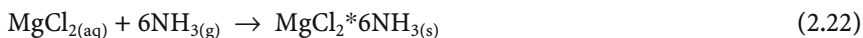


Fig. 2.12. AMC processes

process, a powdery anhydrous magnesium chloride is obtained, with a concentration of magnesium oxide lower than 0.1% [9, 48–50].

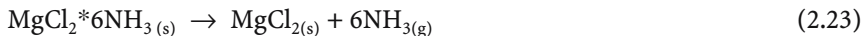
It is possible to track the drying process in Fig. 2.12.

In the preliminary stage, an organic solvent ethylene glycol and/or methanol are added to the concentrated magnesium chloride solution. Gaseous ammonia is then bubbled into the solution and the settling reaction (2.22) takes place:



This reaction creates  $\text{MgCl}_2 \cdot 6\text{NH}_{3(\text{s})}$ , which is the ammonia based analog of bischofite, with water exchanged for ammonia molecules. The settling process will only take place in a solution that contains a major organic component. The  $\text{MgCl}_2 \cdot 6\text{NH}_{3(\text{s})}$  that settles is separated and filtered from the solution. The remaining solution undergoes refining in which the organic solvent is separated and sent for reuse in the process.

The  $\text{MgCl}_2 \cdot 6\text{NH}_{3(\text{s})}$  is transferred to a drying furnace, in which it is heated to a temperature of about 550°C. The reason for this high temperature is that the ammonia molecules are linked tighter to the magnesium chloride than water molecules. During the heating process the material decomposes to ammonia and magnesium chloride (see Eq. (2.23)). In this case, unlike the bischofite drying process, there is no hydrolysis problem at all since there are no water molecules.



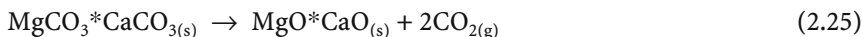
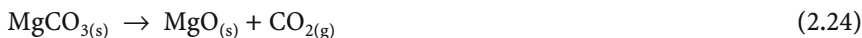
The ammonia is cooled, cleaned and returned the process. The anhydrous solid magnesium chloride is sent to the electrolysis cells.



## 2.4 Thermal Reduction Methods

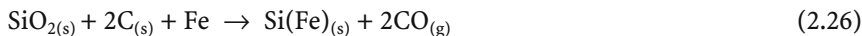
### 2.4.1 Preparation of Raw Material and Thermal Reduction Method

The only ores used in the production of magnesium with thermal reduction technology are dolomite and magnesite. These ores are extracted through customary mining methods, mainly through open mining. The ore extracted from the mine undergoes calcination at temperatures of 700–1,000°C. At this temperature the material releases CO<sub>2</sub> gas, according to Eqs. (2.24) and (2.25), for magnesite and dolomite, respectively [3]:



Following calcination the material is ground into a fine powder.

Another main raw material that is used in thermal reduction is an alloy of silicon and iron called Ferrosilicon. The silicon content in this alloy is 65–85%, and at times the mix also contains small quantities of aluminum. The preparation of the ferrosilicon is carried out by reducing silica with coal, containing iron (scrap iron), at high temperatures [3]:



An additional material, which was used in the past as a thermal reduction agent, is Calcium carbide. The process of preparation of this material is relatively simple, but it requires high temperatures of about 1,800–2,000°C. Below is the reaction used in the production of this material:



Another raw material used in the magnetherm process is bauxite. This material undergoes calcination at temperatures of about 1,200°C before it is introduced into reaction, according to Eq. (2.28) [4]:



Additional raw materials used as additives or reduction agents, such as aluminum, alumina and coal usually undergo grinding or chipping only.

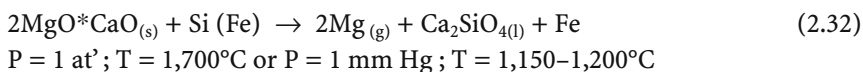
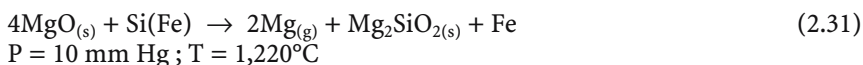
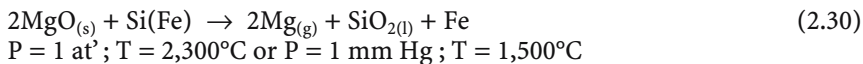
The heating and reduction processes differ between thermal technologies, with thermodynamics eventually determining the reaction temperature. The thermodynamics of the reduction reaction depends on reactants, products and reaction conditions, such as pressure, temperature and the presence of other additives. The reactions described below are organized according to the reducing material used.

### 2.4.2 Industrial Methods with Thermal Reduction

#### 2.4.2.1 Silicothermic Processes

These processes are the main and almost the only thermal processes by which magnesium is produced commercially [2–4]. In general, this category contains

three main processes, which differ mainly in the manner of heating. Following are the main reactions of these processes at different temperatures and pressures:



### ***The Pidgeon Process***

This process [51–61] was developed in the 1940s in Ontario Canada, by Prof. Pidgeon and the Timminco company. Lately, this process has received new attention and constitutes a central process in the magnesium production at a large number of Chinese manufacturers (see Figs. 2.13 and 2.14).

The reaction that takes place is reaction (2.32). A schematic illustration of the retort used in this process is shown in Fig. 2.14. The dimensions of the retort are 2.7–3.3 m with a diameter of 28–35 cm. The capacity of the retort is about 120 kg.

The source of energy in the process carried out in China is normally coal, while the calcination process and the heating furnaces require 14–20 t of coal for the production of one ton of magnesium.

On completion of the process a magnesium crown is obtained, weighing 12–20 kg, which is then extracted from the upper part of the retort. Due to the usually high temperature, the magnesium in this case will contain high concentrations of aluminum, manganese, iron and other impurities. The above process can also be carried out with magnesite as an alternative to dolomite; the working conditions are almost identical and the reaction in this case is Eq. (2.31).

Another version of the above process is carried out at a higher temperature, according to the reaction appearing in Eq. (2.30). The advantage of this reaction is the higher output from each retort (up to about 80%), while the disadvantages in this case are many. The main one being the higher temperature required for the process, 1,500°C, about 300°C more than with the regular process. Work at a higher temperature usually causes the evaporation of impurities and a lower quality of material. In addition, there is accelerated amortization of tools, and this in addition to the higher cost of energy and the need for accessibility to magnesite.

### ***The Magnetherm Process***

This technology was developed in the 1950s and 1960s by the large aluminum production company Pechiney [2, 4, 62–68]. Later, it was also used by Northwest Alloys in the United States (see Fig. 2.15). The main characteristic of this technology is the heating and production furnace in which the heating takes place with electrodes using alternating current. Such heating requires liquid slag, which will conduct electricity, and therefore, in addition to Dolomite, which

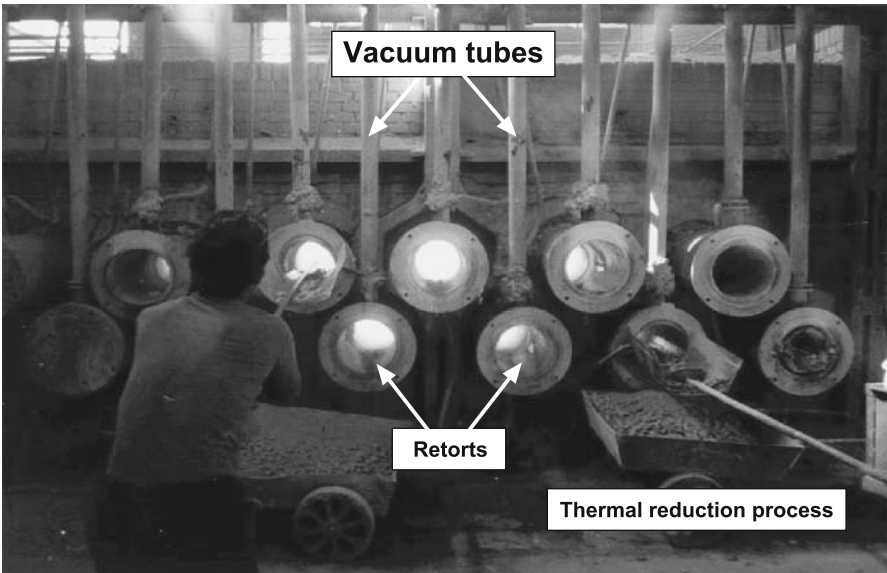
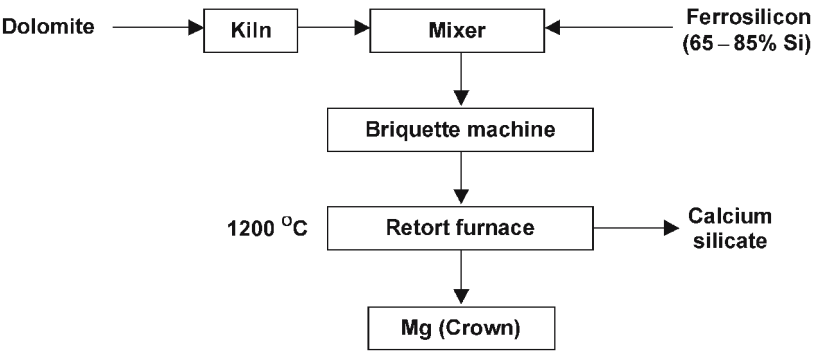


Fig. 2.13. Pidgeon processes

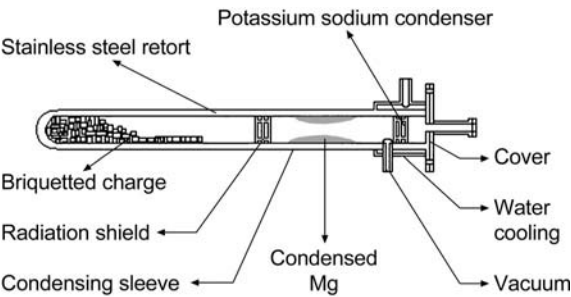


Fig. 2.14. A retort used in the pidgeon process



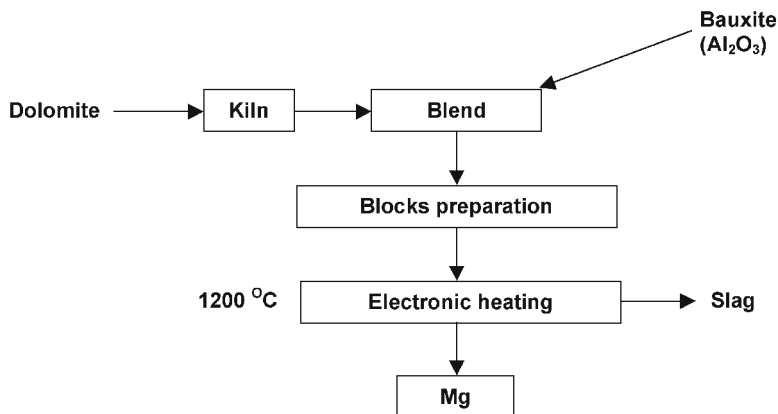


Fig. 2.17. Bolzano processes

the temperature is the addition of metallic aluminum as an alternative to silicon. The use of aluminum in these processes will be detailed in the aluminothermic processes.

Production in a furnace with the Magnetherm process is in batch form and a complete cycle lasts normally 16–24 h. The magnesium fumes rise and accumulate in the cooled condenser in the liquid or solid state. The furnace usually produces between 3 and 8 t of magnesium a day, according to its size. As a rule, 7 t of raw material are required in order to produce 1 t of magnesium.

### **The Bolzano Process**

This production process [4, 69–71] was developed at a magnesium plant near the town of Bolzano, Italy, and today it is also used by the Brasmag company in Brazil (see Fig. 2.17). The heating process in a Bolzano furnace is also different from other silicothermic processes. In this process, dolomite powder that has undergone calcination is compressed with the ferrosilicon reduction agent into large blocks, which are connected to electric heating conductors. The heat in this case passes directly only to the blocks and not to the entire furnace. The process works with a relatively low temperature of  $1,200^\circ\text{C}$  and a pressure of 3 mm Hg. The energy consumption of the heating process is considered to be low compared with the other thermal process used to produce magnesium today. The energy consumption in the furnace is only 7–7.3 kWh/kg of magnesium. The other production parameters are very similar to the Magnetherm process.

#### **2.4.2.2 Aluminothermic Processes**

In this process, aluminum serves as the reduction material for the production of magnesium. In the main reaction, the reduction of dolomite is carried out with

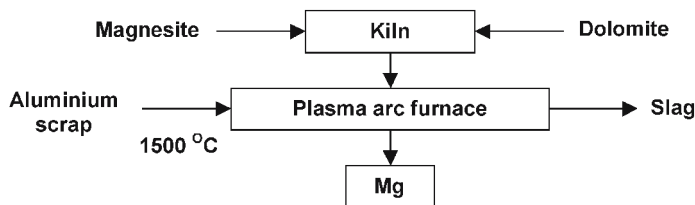
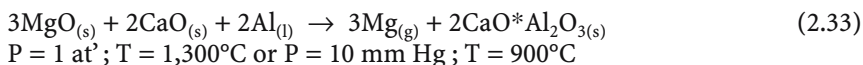


Fig. 2.18. Heggie processes

aluminum (with the addition of some magnesite) that has undergone calcination as shown in Eq. (2.33):



The advantages of this process are many, and they stem mainly from the fact that the reaction is carried out at a relatively low temperature, which is, in fact, the lowest of all the thermal processes. The main disadvantage of the process is in the high cost of aluminum, and therefore, the only process in which aluminum serves as a partial reduction agent is the magnetherm process [2, 4, 62–68]. Hence it is usually operated by companies that also own very large aluminum plants. These companies generally also manufacture (as a by-product) large quantities of aluminum scrap and aluminum rich waste which can be used for this process.

An innovative process which is based on this reaction, is the Heggie [9, 72], which is described in Fig. 2.18. The process is based on the use of Dolomite and magnesite that have undergone calcination, and aluminum scrap as reduction material. The furnace used is the Heggie process and works according to the working principles of the DC transferred arc plasma furnace. This process is supposed to work at atmospheric pressure and under argon atmosphere at temperatures of about  $1,500^{\circ}\text{C}$ . The way the Heggie furnace works enables the relatively high work temperature to exist only in a restricted area of the electric arc. The developers of the process claim that the Heggie furnace consumes only 6 kWh in order to manufacture 1 kg of magnesium.

### 2.4.2.3 Carbothermic Process

The principle behind the carbothermic process [2–4, 73–77] from a thermodynamic point of view is that it is better to react the magnesium oxide directly with coke, rather than reacting the coke with silica and produce silicon, and react the silicon with magnesium oxide in order to produce magnesium (as is carried out in all silicothermic methods). However, it appears that in practice the reactions with coal are not an economical method of producing magnesium. The problem lies mainly in the high activation energy required for the reaction (Eq. 2.34).



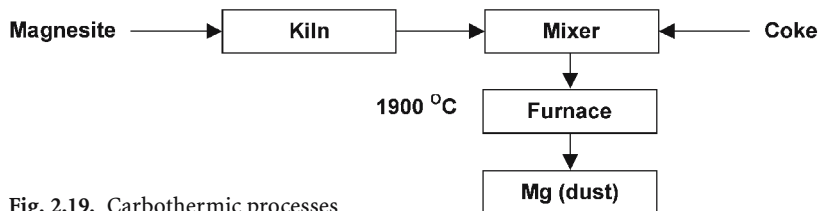


Fig. 2.19. Carbothermic processes

Due to this high activation energy the equilibrium reaction takes place only at a temperature of 1,854°C. In addition to the high activation energy, when magnesium is being produced and slow cooling is attempted, a reverse reaction of the products takes place, and therefore, it is necessary to carry out a very fast cooling of the gases. Such cooling creates very fine magnesium powder, which makes the continuation of the production process much harder. Despite these production difficulties, magnesium was produced commercially during the World War II in California, USA. The flow chart of the process is shown in Fig. 2.19.

Another possibility is reduction with  $\text{CaC}_2$  [3, 76, 77].

The production process with this reduction agent is relatively simple and can be carried out at temperatures of 1,120–1,140°C in a retort similar to the Pidgeon process, under a low vacuum. Two plants in England, which successfully produced magnesium worked with this process during World War II. The main problem with this process is its high cost, which stems mainly from the high cost of calcium carbide. The production ratio is three tons of calcium carbide for one ton of magnesium.

#### 2.4.3 Collection and Refining the Raw Magnesium Produced by Thermal Reduction

The solid raw magnesium, which is obtained using the thermal reduction processes, usually contains impurities. The main impurities include, among others, magnesium oxide and magnesium nitride. In addition to these impurities, the magnesium also contains metallic impurities that are generally not obtained with the electrochemical methods, such as sodium and a small amount of potassium [2–4].

The crude magnesium, which is obtained as a solid in thermal reduction processes, is melted in large furnaces made of steel and heated externally. At times these furnaces are built of refractory materials and are gas or fuel heated. On melting fluxes containing a large amount of magnesium chloride are added to the furnace, and then the following reactions, which refine the magnesium from the metallic impurities such as alkali metals, take place as follows:



The magnesium oxides and nitrides settle to the bottom due to their relatively high specific gravity [3].

2.5 Advantages and Disadvantages of Electrolytic Production Versus Thermal Reduction Methods

Assuming that energy costs, personnel, sources of financing and environmental ordinances around the world were identical, it would be reasonable that most of the magnesium plants would be established according to the availability of raw materials and energy, as well as according to accessibility and customary production technologies. However, it is in fact possible to see that magnesium production plants are established or closed according to differences in the above parameters or in connection with the utilization of cheap resources in developing countries.

A glance at the magnesium market in the last decade points to the fact that the main revolution in the field of magnesium production has occurred in China. This revolution is based on production with Pidgeon technology, which is considered to be the most basic technology for commercial production of magnesium. This method, developed in the 1930s and 1940s, and which had almost completely disappeared, has begun to flourish again over the last decade, despite the existence of other, more advanced thermal methods, which were developed in the 1950s and 1960s as a preferred alternative to Pidgeon technology. The use of Pidgeon technology in China involves the burning of coal as the source of energy for the process. The amount of coal required to produce 1 t of magnesium is 20–25 t for the preparation of FeSi, calcination of dolomite, heating the retorts, and re-melting and casting the magnesium ingots [78].

This energy consumption in China for the production of magnesium is almost double that required for the electrochemical processes common to the developed countries. The burning of such large quantities of coal is not compatible with environmental concerns, since it is accompanied by the discharge of very large quantities of SO<sub>x</sub> into the atmosphere.

Table 2.5. Comparison between electrolytic and thermal reduction processes

Comparative parameter	Electrolytic technology	Thermal reduction technology
Raw material	Magnesite Dolomite Bischofite Carnallite Serpentine Sea water	Dolomite
Energy sources	Hydro power, gas, Fuel	Coal, gas
Energy consumption per ton of Mg [MWh]	18–28	45–80
Operational conditions	Continuous process	Batch process
Capital investment per ton Mg [US\$]	10,000–18,000	Up to 2000
Operational man power	X	Up to 5X



The personnel required for production with the Pidgeon technology stands at a ratio of 4–5 times that required for production in the electrochemical plants common to the West. The advantage of this technology is the cheap investment required for the production of magnesium, which is about one tenth of the investment required for the production of magnesium in the new electrochemical plants. In addition, there is also a financial advantage in that it is possible to build plants with small outputs: 500–3,000 TPY, which can justify the basic investment in infrastructures.

A summary of the comparison between electrolytic and thermal reduction processes for magnesium production is shown in Table 2.5. This clearly indicates that although the capital investment for electrolytic production is higher compared to thermal reduction process, the operating costs for magnesium production by thermal reduction are significantly higher and certainly not justified if compared by the same economic criteria.

## References

1. CRC handbook of Chemistry and Physics, 61 ed., 1980–81, CRC Press Inc., pp. D-156
2. Kipouros GJ and Sadoway DR (1987) in Mamantov, Mamantov, Braunstein (Eds.), *Advances in Molten Salt Chemistry*, V. 6, Elsevier, Amsterdam, pp. 127–209
3. Emley EF (1966) *Principles of Magnesium Technology*, Pergamon, London
4. Kirk-Othmer (1992) *Encyclopedia of Chemical Technology*, V. 15, John Wiley & Sons, New York
5. Olami R (1994) IMA-51 Proceedings, p. 59
6. Strelets KhL (1997) *Electrolytic Production of Magnesium* translated by J. Schmorak, Keter, Jerusalem, also available as TT 76-50003, U.S. Dept. Commerce, NTIS, Springfield VA
7. Wilson CB (1966) IMA-53 Proceedings, p. 52
8. Krenzke FJ (1972) in Hampel CA (Ed.), *'The Encyclopedia of Electrochemistry'*, Krieger, Huntington NY, pp. 783–787
9. Salomon & Smith & Barney Report, October 1999
10. Stanley RW, Berube M, Celik C, Oosako Peacy YJ, Avedesian M (1996) IMA-53 Proceedings, p. 58
11. The Magnola process, [www.noranda.com](http://www.noranda.com)
12. Magnola and Magnesium, [www.mining-journal.com/mininginfo/projects/magnola.htm](http://www.mining-journal.com/mininginfo/projects/magnola.htm)
13. Harris GB and Peacey JG (1992), U.S. Pat. 5091161
14. Janz GG. Thermodynamic and Transport Properties for Molten Salts: Correlation Equations for Critically Evaluated Density, Surface Tension, Electrical Conductance, and Viscosity Data, *J. of Physical and Chemical Reference Data*, V. 17, Suppl. 2
15. Williams EJ, Dean LG and McCutchen CW (1960) Brit. Pat. 849969
16. Andreassen KA, Boyum Q, Johnsen HK, Ognedal LB, Solheim PR (1981) U.S. Pat. 4308116
17. Sivilotti OG (1985) U.S. Pat. 4518475
18. Sivilotti OG (1985) U.S. Pat. 4560449
19. Sivilotti OG (1983) U.S. Pat. 4420381
20. Sivilotti OG (1986) U.S. Pat. 4604177
21. Sivilotti OG (1990) U.S. Pat. 4960501
22. Sivilotti OG (1985) U.S. Pat. 4514269
23. Sivilotti OG (1997) U.S. Pat. 5660710
24. Christensen J, Creber D, Holywell G, Moriya A and Yamaguchi M (1997) in Aghion E and Eliezer D (Eds.) *Proceedings on the First Israeli International Conference on Magnesium Science & Technology*, Dead Sea, Israel, pp. 9–14
25. Blue RD, Hunter RM and Neipert MP (1949) U.S. Pat. 2468022
26. Petrunko AN and Lobanov VS (1977) *Light Metal Age*, 35, 16, 18, 20, 21

27. Donskikh PA, Korotkov YA and E.F. Michailov EF (1985) *Tsvetnye Metally* (Engl. trans.), 26(6), 68–70
28. Saburov LN, Teterin VV, Mikhailov EF and Penskii V (1985) *Tsvetnye Metally* (Engl. trans.), 26(8), 83–84
29. Reznikov IL, Sandler GY, Svidlo VP and Krayukhin AB (1985) *Tsvetnye Metally* (Engl. trans.) 26(9), 51–53
30. Muzhzhavlev KD et al. (1977) U.S. Pat. 4,058,448
31. Gilroy D (1971) in Kuhn AT (Ed.) *Industrial Electrochemical Processes*, Elsevier, Amsterdam, pp. 175–217
32. Beck TR and Ruggeri RT (1981) in Gerischer H and Tobias CW (Eds.) *Advances in Electrochemistry and Electrochemical Engineering*, Vol. 12, Wiley, New York, pp. 263–354
33. Zabelin IV et al. (1984) U.S. Pat. 4,483,753
34. Shekhotsov G, Shchegolev V, Devyatkin V, Tatakin A and Zabelin I (2000), in Aghion E and Eliezer D (Eds.) ‘Proceedings on the Second Israeli International Conference on Magnesium Science & Technology’, Dead Sea, Israel, pp. 57–61
35. Barannik and I. Sikorskaya I (1997), in Aghion E and Eliezer D (Eds.) ‘Proceedings on the First Israeli International Conference on Magnesium Science & Technology’, Dead Sea, Israel, pp. 15–20
36. Kosarev SP, Didrikh NV, Yasev VD, Raskatov VG, Romanenko ON, Trukhin AF (1978) Can. Pat. 1022978
37. Golub G, Katsnelson G, Zinn M, Aghion E (2000) U.S. Pat. 6,132,490
38. Boyum O, Eriksen KE, Solberg P, Tveten KW (1973) U.S. Pat. 3742100
39. Blaker I, Boyum O, Anton K, Skipperud R, Tveten KW (1973) U.S. 3760050
40. Wallevik O, Ronhaug JB (1983) U.S. Pat. 4385931
41. Mejdell GT, Baumann HM, Tveten KW (1992) U.S. Pat. 5112584
42. Tveten KW, Mejdell GT, Marcussen JB (1992) U.S. Pat. 5120514
43. Mezzeta G (1991) *Light Metal Age*, 49, 12
44. Andreassen KA and Stiansen KB (1975) U.S. Pat. 3,907,651
45. Peacey JG, Kennedy MW, Walker TP (1996) U.S. Pat. 5565080
46. White C, Berube M (1999) U.S. Pat. 5980854
47. Peacey JG, Kennedy MW, Walker TP (1995) WO Pat. 95/31401
48. Sivillotti OG (1995) U.S. Pat. 5439563
49. Sivillotti OG, Sang JV, Lemay RJR (1996) U.S. Pat. 5514359
50. Amundsen K, Eklund HR, Schmidt R (2000) U.S. Pat. 6042794
51. Pidgeon LM (1944) *Trans. Can. Inst. Min. Met.*, 47, 17
52. Pidgeon LM and Alexander WA (1944) *Trans. AIME*, 159, 315
53. Pidgeon LM (1946) *Trans. Can. Inst. Min. Met.*, 49, 621
54. Humes WB (1944) *Trans. AIME*, 159, 353
55. Mayer A (1944) *Trans. AIME*, 159, 363
56. Pierce WM, Waring RK, Fetterolf LD and Mahler G (1944) *Trans. AIME*, 159, 377
57. Schrier E (1952) *Chem. Eng.*, 59 (4), 148
58. Froats A (1979) in McMinn CJ (Ed.), ‘*Light Metals 1980*’, TMS/AIME, Warrendale PA, pp. 969–979
59. Brit. Pat. 606644, 606637
60. Toguri JM and Pidgeon LM (1962) *Canadian J. Chem.*, 40, 1769
61. Toguri JM and Pidgeon LM (1961) *Canadian J. Chem.*, 39, 540
62. Faure C and Marchal J (1964) *J. Metals*, 16, 721
63. Trocme F (1971) in Edgeworth TG (Ed.), ‘*Light Metals 1971*’, TMS/AIME, Warrendale PA, pp. 669–677
64. Logerot JM and Mena AM (1980) *Extractive Metallurgy: Latest Developments of the Magnetherm Process*, TMS Paper Selection, CM-80-74, TMS/AIME, Warrendale PA, pp. 29
65. Christini RA, Roiles R, Bowman KA and Ballain MD (1984) U.S. Pat. 4,478,637
66. Bowman KA, Christini RA and Ballain MD (1985) U.S. Pat. 4,498,927
67. Brit. Pat. 908531

68. Christini RA (1979) in McMinn CJ (ed.), "Light Metals 1980", AIME, Warrendale PA, pp. 981–995
69. Bettanini C, Zanier S and Enrici M (1980) U.S. Pat. 4,238,223
70. Ravelli S et al. (1981) U.S. Pat. 4,264,778
71. S. Afr. Pat. 8704237, (1987)
72. Exploration & Project development Summary, [www.mtgrace.com/exploration.html](http://www.mtgrace.com/exploration.html)
73. Dungan TA (1944) Trans. AIME, 159, 308
74. Hansgirg FJ (1943) Iron Age, 152 (21), 56; 152 (22), 52
75. Hansrig FJ (1948) U.S. Pat. 2,437,815
76. Miller GL (1952) Vacuum, 2, 19
77. Production of magnesium and magnesia, 2nd. Nat. Expend. Rep. HMSO, pp. 1934–44
78. Komesaroff M (2000) Metal Bulletin Monthly, p. 58

---

## 3 Physical Metallurgy

*Barry L. Mordike, Pavel Lukáč*

### 3.1 Introduction

Magnesium was discovered and isolated by Sir Humphrey in 1808, but it took about 100 years before a real demand for magnesium developed. The uses of magnesium as a structural material were, however, very few. The bulk was used as an alloying element in aluminium alloys. Other uses, such as deoxidation of steel, chemical and pyrotechnics, outweighed structural uses.

Since the 1939–45 war, when there had been a surge in the use of magnesium in structural uses (228,000 tonnes per year in 1944) [1], mainly for aircraft, it took another 40 years to reach the same level in 1992. There had been attempts to use magnesium but these were relatively few, e.g., the legendary VW Beetle. A magnesium alloy was used as canning material in the Calder Hall nuclear power station (1953) where extreme creep resistance and low neutron cross section were required.

Since 1993/5 there has been renewed interest in using magnesium based alloys in automobile and other household and sport applications. The driving force is the weight savings. Magnesium is substantially less dense than aluminium. It is also relatively expensive to produce, not as easily worked as aluminium, relatively few developed alloys exist, no secondary recycling procedure has been developed and there are questions as to corrosion resistance and safety; all factors which prevent its wide acceptance. Unless the automobile industry embraces its use, magnesium will not become economically viable in other fields.

### 3.2 Properties of Pure Magnesium

Magnesium is classified as an alkaline earth metal. It is found in Group 3 of the periodic table. It thus has a similar electronic structure to Be, Ca, Sr, Ba and Rd.

#### 3.2.1 Atomic Properties

Element Symbol	Mg
Atomic Number	12
Atomic Weight	24.3050
Atomic Diameter	0.320 nm
Atomic Volume	14.0 cm <sup>3</sup> /mol

Atomic Isotopes	78.99% $^{24}\text{Mg}$
10.0%	$^{25}\text{Mg}$
11.01%	$^{26}\text{Mg}$ [2]

### 3.2.2 Electron States

In free atoms  $1s^2, 2s^2, 2p^6, 3s^2$   
Valency 2

The crystal structure is hexagonal close packed. Figure 3.1 shows the magnesium unit cell, illustrating the basal plane and planes of the  $\{11\bar{2}2\}$  and  $\{\bar{1}100\}$  zones.

### 3.2.3 Lattice Parameters

The lattice parameters of pure magnesium estimated at room temperature are:  $a = 0.32092$  nm and  $c = 0.52105$  nm [3]. The  $c/a$  ratio is 1.6236 which is close to the ideal value of 1.633. Therefore, magnesium may be considered as perfectly closed packed. The lattice parameters of pure magnesium increase with increasing temperature as given in Table 3.1 [4, 5].

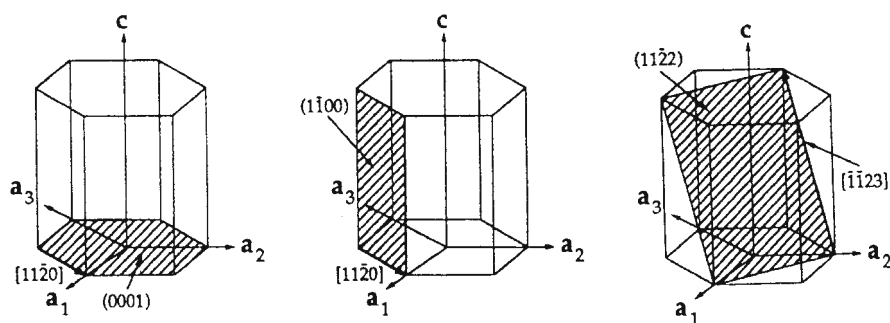


Fig. 3.1. Unit cell and major planes and directions

Table 3.1. Effect of temperature on the lattice parameters of pure magnesium

Temperature [°C]	a [nm]	c [nm]
10	0.32081	0.52091
25	0.32088	0.52099
30	0.32100	0.52120
46	0.32106	0.52128
98	0.32152	0.52191
160	0.32211	0.52308
180	0.32214	0.52310
200	0.32217	0.52327
310.5	0.32313	0.52529
455	0.32485	0.52769
506.8	0.32551	0.52879
597	0.32665	0.53067

The temperature dependence of the lattice parameters can be expressed as

$$a = 0.32075 + (7.045 \Delta T + 0.0047 \Delta T^2) \times 10^{-6} \text{ nm}$$

and

$$c = 0.52076 + (11.758 \Delta T + 0.0080 \Delta T^2) \times 10^{-6} \text{ nm}$$

where  $\Delta T$  is the temperature in  $^{\circ}\text{C}$ .

3.2.4 Thermal Expansion

The coefficient of linear thermal expansion  $\alpha_T$  of polycrystalline magnesium depends on the temperature range. According to Baker [6] (see also [7]) the coefficient of linear thermal expansion can be expressed as a function of temperature in the following form:

$$\alpha_T = (25.0 + 0.0188 \Delta T) \times 10^{-6} \text{ }^{\circ}\text{C}^{-1}.$$

This relation is valid at temperatures between 0 and  $550^{\circ}\text{C}$  and  $\Delta T$  is in  $^{\circ}\text{C}$ .

The mean values of the coefficients of linear thermal expansion for various temperature ranges are given in Table 3.2.

3.2.5 Density

The density of magnesium at  $20^{\circ}\text{C}$  is  $1.738 \text{ g/cm}^3$ . At the melting point of  $650^{\circ}\text{C}$  this is reduced to  $1.65 \text{ g/cm}^3$ . On melting there is an expansion in volume of 4.2%.

3.2.6 Thermodynamic Properties

The specific heat capacity  $C_p$  at constant pressure at  $20^{\circ}\text{C}$  is  $1.025 \text{ kJ/kgK}$  [8]. It increases with increasing temperature. The temperature dependence of  $C_p$  in units of  $\text{J/molK}$  can be expressed in the temperature range from 298 to  $923 \text{ K}$  as  $C_p = 26.19 - 1.01 \times 10^{-3} T - 1.60 \times 10^5/T + 8.41 \times 10^{-6} T^2$  [7].

3.2.7 Diffusion

Volume diffusion is very important at higher temperatures, especially at  $T > 0.6 T_m$ , where  $T_m$  is the absolute melting point. At lower temperatures pipe diffusion, i.e., diffusion along dislocation cores, may become more significant. Grain boundary diffusion plays a role in polycrystals because the grain boundary acts as a low energy channel for the movement of atoms. A similar situation exists in composites at the interfaces between the matrix and the reinforcement.

In an isotropic solid as is the case for cubic symmetry, the diffusion coefficient  $D$  has the same value in all directions. In uniaxial single crystals, of close packed

Table 3.2. Mean coefficients of linear thermal expansion of polycrystalline magnesium

T [ $^{\circ}\text{C}$ ]	20–100	20–200	20–300	20–400	20–500
$\alpha_T$ [ $^{\circ}\text{C}^{-1}$ ]	$26.1 \times 10^{-6}$	$27.1 \times 10^{-6}$	$28.0 \times 10^{-6}$	$29.0 \times 10^{-6}$	$29.9 \times 10^{-6}$

hexagonal magnesium,  $D$  is the same for all directions perpendicular to the  $c$  axis and is often denoted by  $D_{\perp}$ .  $D$  in the direction of the  $c$  axis is denoted by  $D_{\parallel}$ . If the concentration gradient lies at an angle  $\theta$  to the  $c$  axis, then the diffusion coefficient in this direction can be expressed as

$$D(\theta) = D_{\perp} \sin^2 \theta + D_{\parallel} \cos^2 \theta. \quad (3.1)$$

Thus the values of  $D_{\parallel}$  and  $D_{\perp}$  can be determined by measuring  $D(\theta)$  for different values of  $\theta$ . The temperature dependence of the diffusion coefficient is given by

$$D = D_0 \exp(-Q/RT) \quad (3.2)$$

where  $D_0$  is the frequency factor,  $Q$  is the activation energy,  $R$  is the gas constant and  $T$  is the absolute temperature.  $D_0$  and  $Q$  depend on the diffusion process and alloy composition but are independent of temperature.

The values of  $D_0$  and  $Q$  for Mg single crystals are given in Table 3.3.

### 3.2.8 Thermal Conduction

In many applications of materials at elevated temperatures, the thermal expansion and rate of heat transfer are very important. Operating temperatures, resistance to the thermal stresses and other limitations on the materials are directly related to the heat transfer and heat conduction.

The thermal conductivity in an isotropic solid is defined as

$$\mathbf{q} = -K \text{ grad } T \quad (3.3)$$

where  $\mathbf{q}$  is a vector of the heat flow rate across the unit cross section perpendicular to  $\mathbf{q}$  (i.e., the energy transported per unit time through unit area),  $T$  is the absolute temperature,  $K$  is the thermal conductivity, and the negative sign indicates that heat flows down a temperature gradient, i.e., from hotter to colder regions. In metallic materials heat is transferred by coupling between lattice vibrations and/or movement of electrons and collisions with atoms and lattice defects. The thermal conductivity can be considered to be the sum of two components: the phonon thermal conductivity depending on the phonon mean free path and the electronic thermal conductivity depending on the electron mean free path. The electron scattering and therefore the electron free path and the electronic thermal conductivity are significantly influenced by crystal defects such as impurities (foreign atoms), dislocations, grain boundaries. The main variables that should effect the thermal conductivity are the temperature level, the chemical composition and the volume fraction and the arrangement of the various phases present in the material.

**Table 3.3.** Self-diffusion data for Mg single crystals

Purity; Ref.	$D_{0\parallel}$ [ $\text{cm}^2/\text{s}$ ]	$D_{0\perp}$ [ $\text{cm}^2/\text{s}$ ]	$Q_{\parallel}$ [kJ/mol]	$Q_{\perp}$ [kJ/mol]
99.9% [9, 10]	1.5	1.0	136.1	134.8
99.99% [11]	1.78	1.75	139.0	138.2

In pure metals, the lattice (phonon) component of the thermal conductivity is small and the electronic contribution is dominant. According to the Wiedemann-Franz law the electronic component of the thermal conductivity  $K_e$  is related to the electrical conductivity  $\sigma_e$  at a temperature  $T$  by the expression

$$K_e = \sigma_e L_e T \tag{3.4}$$

where  $L_e = 2.45 \times 10^{-8} \text{ W}\Omega\text{K}^{-2}$  is the Lorenz number. This relation may be used for alloys only as a first approximation. In some cases the electrical conductivity which can be measured more easily is used for the calculation of the total thermal conductivity in dilute alloys. Thus, using the relation (3.4), Aune and Westengen [12, 13] have calculated the thermal conductivity of AZ91, AM20, AM50, AS21 and AE42 alloys.

The thermal conductivity of pure magnesium measured at elevated temperatures decreases with increasing temperature. At very low temperatures the thermal conductivity exhibits high values. The values of the thermal conductivity listed in [14, 15] are given in Table 3.4.

Table 3.5 [7] presents the values of the thermal conductivity calculated from the electrical resistivity of magnesium [6].

The values of the thermal conductivity listed in Table 3.5 were calculated using the following equation [16]

$$K = 22.6 T/\varrho_e + 0.0167 T \tag{3.5}$$

where  $\varrho_e$  is the electrical resistivity in units of  $\text{n}\Omega\text{m}$  and  $T$  is the absolute temperature. The measured values of the thermal conductivity of magnesium are close to the calculated ones.

**Table 3.4.** Temperature variation of the thermal conductivity of magnesium [14, 15]

T [K]	1	2	3	4	5	6	7
K [W/mK]	986	1960	2900	3760	4500	5080	5470
T [K]	8	9	10	15	20	30	40
K [W/mK]	5670	5700	5580	4110	2720	1290	719
T [K]	50	60	70	80	90	100	150
K [W/mK]	465	327	249	202	178	169	161
T [K]	200	250	300	350	400	500	600
K [W/mK]	169	157	156	155	153	151	149

**Table 3.5.** Calculated thermal conductivity values of magnesium [7]

T [K]	273	293	311	366	422	477
K [W/mK]	155.3	154.5	154.1	153.7	153.2	152.8
T [K]	533	589	644	700		
K [W/mK]	152.8	153.2	153.7	154.1		



### 3.2.9 Elastic Moduli

The deformation behavior of a metal depends on the applied stress. If the applied stress is low, then the metal behaves elastically, i.e., there is a linear relation between the stress and the strain. In this case the metal changes its dimensions in response to the applied force (stress) but there are no residual dimensional changes by removing the stress. In one dimension the applied uniaxial stress  $\sigma$  is linearly related to the longitudinal strain  $\varepsilon$ . This relation is known as Hooke's law.

In one dimension, Hooke's law can be written either as

$$\sigma = C\varepsilon \quad (3.6)$$

or as

$$\varepsilon = S\sigma \quad (3.7)$$

where  $C$  is known as the stiffness and  $S$  is called the compliance. The stiffness (in one dimension) is known as Young's modulus and usually written as  $E$ .

The elastic properties of an isotropic material are characterised by Young's modulus  $E$ , shear modulus  $G$ , bulk modulus  $K$  and Poisson's ratio  $\nu$ .

Some relations can be useful when only two elastic constants are known. They are

$$E = 2G(1 + \nu) = 3K(1 - 2\nu) = 9GK/(3K + G) \quad (3.8)$$

or it is easy to remember

$$3/E = 1/G + 1/3K \quad (3.8a)$$

$$G = E/2(1 + \nu) = 3K(1 - 2\nu)/2(1 + \nu) = 3KE/(9K - E) \quad (3.9)$$

$$K = E/3(1 - 2\nu) = 2G(1 + \nu)/3(1 - 2\nu) = GE/3(3G - E) \quad (3.10)$$

$$\nu = (E - 2G)/2G = (3K - 2G)/2(3K + G) = 1/2 - E/6K \quad (3.11)$$

The shear modulus and Poisson's ratio may be estimated from the velocity of ultrasonic waves propagating through samples. The following relations are used to calculate the elastic characteristics assuming that the sample is isotropic and homogeneous

$$G = \rho_s v_s^2 \quad (3.12)$$

$$\nu = [2 - (v_l/v_s)^2]/2[1 - (v_l/v_s)^2] \quad (3.13)$$

and

$$E = 2G(1 + \nu) \quad (3.14)$$

where  $\rho_s$  is the specimen density and  $v_l$  and  $v_s$  are the longitudinal wave velocity and the shear wave velocity, respectively. Poisson's ratio is 0.35. The elastic constant  $E$  at 20°C is 44 GPa.

### 3.2.10 Damping Capacity

It is often stated in the literature that magnesium has good damping properties. This can be true, but damping depends on many factors, e.g., purity, grain size, alloy composition, amplitude, temperature and frequency. Therefore, a universal statement that magnesium based materials have good damping properties is not

true. Experiments are necessary to establish to what extent damping occurs for each particular case.

In a perfectly elastic solid, stress and strain are related by Hooke's law. In a real (polycrystalline) material, Hooke's law is not obeyed, not even at stresses below the conventional elastic limit. When vibrations are induced in the material elastic strain energy is dissipated. Elastic waves, i.e., the periodically changing local strain, are attenuated with the resultant generation of heat. The rate of attenuation can be of practical importance, for example, because it can lead to reduced noise and vibrations in a material. The damping capacity of a metal thus characterises the ability to dissipate elastic energy. The damping capacity characterises a time-dependent response to an applied load. There are usually two main types of damping: anelastic and hysteretic. If there is a lag between the application of stress and the attainment of the resultant equilibrium strain, then the metal exhibits "anelastic" behavior. Processes responsible for this behavior give rise to an energy loss. Under vibration the energy loss reaches a maximum (peak) at a certain (critical) frequency of vibration.

During deformation of a hysteretic solid the stress-strain curve on loading is not coincident with that of unloading as would occur with reversible dislocation movement. The energy loss is proportional to the area between the loading and unloading curves. In this case the energy loss is independent of the load cycle frequency. Damping of this kind could be of particular interest to engineers. In the case of metals there is a limit to the energy which can be sensibly dissipated as the dislocation movement becomes irreversible at higher stresses (strains) and can act as a source of fatigue failure.

The specific damping capacity is defined as the ratio of vibrational strain energy dissipated during one cycle of vibration to that of the previous cycle. It is usually measured on a cylindrical specimen in torsion and is given in per cent. The specific damping capacity of commercial magnesium alloys was estimated to be between 0.4% for QE22 to 7.4% for a Mg-Zn-Th-Zr alloy; it is higher than that of commercial aluminium alloys.

There are various mechanisms by which the energy can be absorbed within a stressed material. These mechanisms all contribute to the internal friction in the material.

Anelastic damping as a function of temperature and/or frequency has been used to identify several atomic processes. Measurements of the damping peaks have been used to provide information on precipitation and ordering phenomena and on properties of point defects, dislocations and grain boundaries. Some diffusion data can also be obtained. Thus anelastic damping is of interest to physical metallurgists [17, 18]. The following characteristics have been used in the measurements of damping (internal friction):

The logarithmic decrement  $\delta$  which expresses the reduction in amplitude of vibration of a freely decaying system during one cycle is defined as

$$\delta = \ln(A_n/A_{n+1}) \quad (3.15)$$

where  $A_n$  and  $A_{n+1}$  are the values of the freely decaying amplitude. Measurement of the logarithmic decrement at small strains (stresses) is a sensitive method of determining the microstructure of the material.

The logarithmic decrement  $\delta$  of free decay of a vibrating specimen may be expressed as

$$\delta = \pi (\Delta E/E) [\omega \tau / (1 + \omega^2 \tau^2)] \quad (3.16)$$

where  $\omega$  is the angular frequency,  $\Delta E/E$  is the modulus defect and  $\tau$  is the relaxation time. The equation is valid for a relaxation process that is governed by a single relaxation time. The relaxation time depends on the temperature according to an Arrhenius equation of the form

$$\tau = \tau_0 \exp (Q_r/RT) \quad (3.17)$$

where  $\tau_0$  is a constant,  $Q_r$  is the activation energy controlling the relaxation process,  $R$  is the gas constant and  $T$  is the absolute temperature. The maximum value of damping – damping peak  $\delta_p$  – is reached if  $\omega \tau = 1$ . The modulus defect is a measure of the strength of the relaxation and it can be orientation dependent, especially in hexagonal metals.

Several damping peaks were observed. Their position in the temperature scale depends on the activation energy. In metals and alloys the following main types were observed:

The Zener-type peak (ZP) is observed in substitution solid solutions due to the stress-induced redistribution of solute atoms.

The Snoeck-type peak (SP) is a result of the stress-induced redistribution of solute atoms in interstitial solid solution. The interaction of interstitial solute atoms with substitutional solute atoms results in a modified Snoeck-type peaks in ternary alloys.

Bordoni peaks (BP) – a large number of BPs are observed at low temperatures in cold worked pure metals due to the movement of dislocations.

Hasiguti peaks (HP) are formed at higher temperatures because of the interaction of dislocations with point defects.

The K stler-type peaks (KP) are observed in cold worked alloys as a result of the interaction of dislocations with interstitial solute atoms.

It should be noted that the stress-induced migration of grain boundaries and/or sub-grain boundaries (polygonisation) gives rise to high temperature damping peaks.

The modulus defect is very often calculated using the equation

$$\Delta E/E = 2\delta_p/\pi = 2(Q^{-1})_{\max} \quad (3.18)$$

where  $(Q^{-1})_{\max}$  is the peak value of  $Q^{-1}$ . The temperature positions of the damping peaks are listed in Table 3.6. The mechanism which is considered to cause the peak is also given.

The damping behavior of a material is often characterised by other terms such as the loss factor  $\eta$  and the quality factor  $Q^{-1}$ . The numerical relationship between the logarithmic decrement and these other factors is  $\eta = Q^{-1} = \delta/\pi$ .

The dependence of the logarithmic decrement on the strain (stress) amplitude of vibration can help to identify changes in the microstructure in both magnesium alloys and in magnesium metal matrix composites due to thermal or mechanical loading.

**Table 3.6.** Damping peaks in magnesium alloys

Composition	Peak temp. [K]	Freq. [Hz]	Activation energy [kJ/mol]	Modulus defect	Mechanisms	Ref.
99.97%	493	0.46	–	$8 \times 10^{-2}$	GB	19
99.992%, CW	20	$4 \times 10^4$	–	$3 \times 10^{-3}$	BP(?)	20
99.992%, CW	100	$4 \times 10^4$	–	–	BP	21
99.99%, CW	180	$10^3$	28.9	–	PD-D	22
	225		42.3	–	PD-D	
Not given	37	$1.5 \times 10^7$	0.9	–	DM-BS	23
	106.5		8.7	–	DM-NBS	
	155.5		40.5	–	–	
Mg-1.88Li	51	$1.5 \times 10^7$	1.74	–	DM-BS	23
	99.5		9.60	–	DM-NBS	
	154.5		126	–	–	
Mg-0.0048N	46	$1.5 \times 10^7$	1.0	–	DM-BS	24
	116		22	–	DM-NBS	
	154.5		35	–	–	
99.996%	20	$10^4$	–	$4 \times 10^{-4}$	GB(?)	24
	40–240	$10^4$	–	$10^{-3}$	DM-BS	
Mg-Al, Zn, Cd, Tl, In	0–300	$1.5 \times 10^{-2}$	–	Complex	D-D	25
		0.75	–			
99.9999%	40	1–2	–	$3 \times 10^{-3}$	BP1	26
99.9999%,*	80	1–2	–	$1 \times 10^{-2}$	BP2	26
High purity	15	1	–	–	P1 sub1	27
	40		–	–	BP1	
	80	1	–	–	BP2	
High purity	105	1	–	–	HP1	27
	220		–	–	HP2	
	420	1	–	–	P sub 2	

\* Cold work at 10 K; CW- cold work at room temperature; GB, mechanism associated with grain boundaries; BP1 and BP2, Bordoni peak 1 and 2; HP1 and HP2, Hashiguti peak 1 and 2; P1 sub1 and P sub 2, P peaks; DM-BS, dislocation motion in basal slip system; DM-NBS, dislocation motion in non-basal system; PD-D, point defects-dislocations interaction; D-D, dislocation-dislocation interaction.

When an MMC is subjected to temperature changes thermal stresses arise at the interfaces between the matrix and the reinforcement as a result of the considerable mismatch between the thermal expansion coefficients of the matrix and the reinforcement. Even moderate temperature changes can produce thermal stresses that exceed the matrix yield stress. Consequently, new dislocations are generated at the interfaces causing thermal fatigue, microstructural changes, matrix plastic deformation and irreversible shape changes. Damping and/or stress relaxation measurements can detect these microstructural changes in the matrix. The dislocation density at the interface was found to be significantly higher than elsewhere in the matrix. A higher dislocation density in the composite material

produces a higher level of the internal stress. An increase in the dislocation density near reinforcement fibres has been calculated as [28]:

$$\varphi = \frac{Bf\Delta\alpha\Delta T}{b(1-f)d} \quad (3.19)$$

where  $f$  is the volume fraction of the reinforcement,  $d$  is its minimum size,  $b$  is the magnitude of the Burgers vector of dislocations and  $B$  is a geometrical constant. When the thermal stresses reach the yield stress, plastic zones form in the matrix close to the interfaces.

Damping measurements can be used as a non-destructive method of investigation.

Figure 3.2 shows the plots of the logarithmic decrement versus the strain amplitude on a logarithmic scale for ZC63 alloy reinforced with 24.9 vol.%  $\delta$ - $\text{Al}_2\text{O}_3$  short fibres (Saffil) with a mean diameter of 3  $\mu\text{m}$  and a mean length about of 87  $\mu\text{m}$ . The logarithmic decrement of the composite was measured before (depicted as received) and after one thermal cycle between room temperature and various increasing upper temperatures.

It can be seen from Fig. 3.2 that the strain amplitude dependence of the logarithmic decrement exhibits two regions. The logarithmic decrement  $\delta$  can be expressed as

$$\delta = \delta_0 + \delta_H(\epsilon) \quad (3.20)$$

where  $\delta_0$  is the amplitude independent component, found at low amplitudes. The component  $\delta_H$  depends on the strain amplitude  $\epsilon$  and is determined usually by dislocation vibrations. The value of the amplitude dependent logarithmic decrement before thermal cycling is much lower than that after thermal cycling, and  $\delta$  in the strain amplitude dependent region increases very strongly with increasing upper temperature of the cycle. The value of the critical strain  $\epsilon_{cr}$  at which the logarithmic decrement begins to increase with strain amplitude after thermal cycling is much lower than that before thermal cycling. Recovery of the cycled composite occurs very slowly. After several days the measured logarithmic decrement is still very high [29]. Thermal cycling leads to irreversible structural changes.

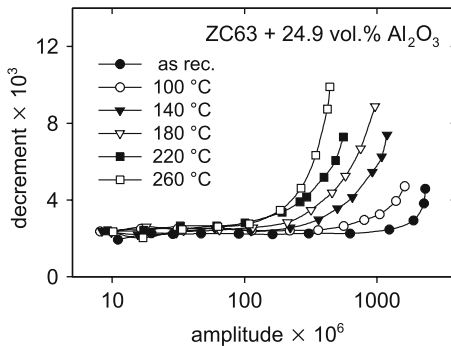


Fig. 3.2. Strain amplitude dependence of the logarithmic decrement

According to the Granato-Lücke theory [30] the dislocation structure is assumed to consist of segments of length  $L_N$  along which weak pinning points are distributed randomly. The mean distance between two weak pinning points is  $\ell$  with  $\ell \ll L_N$ . The mean total density of dislocations is  $\rho$ . The periodic stress  $\sigma = \sigma_0 \sin \omega t$  is applied. At  $T = 0$  and at a sufficiently high stress the dislocation is able to breakaway from the weak pinning points. Only the ends of the longer segments  $L_N$  are assumed to be unbreakable pinning points. The stress required for the breakaway of dislocations is determined by the largest double loop in a segment and depends strongly on the statistical distribution of the pinning points. With increasing temperature, the stress for breakaway is decreased because the process is thermally activated [31]. At higher temperatures the breakaway can occur at lower stress than is possible for the double loop, but higher activation energies are required because the break away occurs simultaneously from several neighbouring pinning points. The stress dependence of  $\delta_H$  can be approximated

$$\delta_H = \frac{\rho L_N}{6} \frac{\nu}{\omega} \left( \frac{3\pi kT}{2U_0} \right)^{1/2} \left( \frac{\ell^3 \sigma_0^2}{U_0 G} \right)^{1/2} \exp \left[ -\frac{4}{3} \frac{U_0}{kT} \left( \frac{U_0 G}{\ell^3} \right)^{1/2} \frac{1}{\sigma_0} \right] \quad (3.21)$$

where  $G$  the shear modulus,  $\sigma_0$  the amplitude of the applied stress and  $\omega$  its angular frequency,  $\nu$  the attempt frequency,  $U_0$  the activation energy,  $k$  the Boltzmann constant and  $T$  the absolute temperature. It can be seen that this relationship has a similar form to the original equation given by Granato and Lücke [30].

Quantitative estimates using simplifying assumptions lead to the expression for the strain amplitude dependence of the logarithmic decrement

$$\delta_H = (C_1/\epsilon) \exp(-C_2/\epsilon) \quad (3.22)$$

where

$$C_1 = \rho F_B L_N^3 / 6bE\ell^2 \quad \text{and} \quad C_2 = F_B / bE\ell \quad (3.23)$$

Here  $F_B$  is the binding force between a dislocation and a solute atom (weak pinning point),  $E$  is the unrelaxed modulus,  $\epsilon$  is the strain amplitude and  $\ell$  is the mean distance between weak pinning points.

The  $\delta_H$  component depends exponentially on the stress amplitude. With increasing upper temperature of the thermal cycles the decrement component  $\delta_H$  increases too. This can be due to an increase in dislocation density (see Eq. (3.19)), while the number of solute atoms remains constant and hence the effective distance between two weak pinning points is higher. The increase in both microphysical parameters, i.e., dislocation density  $\rho$  as well as the dislocation segments  $\ell$ , leads to the observed increase in the decrement component  $\delta_H$ . It is very probable that a stress-assisted thermally activated redistribution of the weak pinning points may occur during thermal cycling.

Dislocations created owing to the difference of the thermal expansion coefficients of the matrix and the reinforcing fibres are the main reason for the increasing value of the decrement with increasing temperature of thermal treatment. Dislocation unpinning and repinning processes seem to be thermally activated.

It is obvious from these comments that such measurements can be used to study microstructural changes in magnesium alloys and composites. It also becomes evident that only pure magnesium can be classed as a high damping material. The alloys show a wide range of damping capacity.

### 3.2.11 Deformation Behavior

In order to prepare materials with the required mechanical properties it is very important to understand the mechanisms determining both yielding and work (strain) hardening of polycrystals. According to von Mises [32] more than 5 independent slip systems must operate for polycrystals to deform uniformly and without failure at the grain boundaries. Magnesium is close packed hexagonal and there are not five independent slip systems available. The number of the independent basal slip systems is thus less than that required. It is necessary that other, non-basal slip systems are activated or that deformation occurs by twinning. The low temperature brittleness of magnesium may be a result of the restricted number of independent and easily operated slip systems.

Therefore, the deformation behavior of polycrystalline magnesium and its alloys is determined by the activity of non-basal slip systems. Apart from basal slip, first order prismatic slip systems and second order pyramidal slip systems play a significant role in the deformation behavior of Mg and its alloys. To improve plasticity of magnesium, it is necessary to increase the activity of non-basal slip systems. It is clear that the activity of a non-basal slip system, i.e., the critical resolved shear stress (CRSS) for non-basal slip, depends on solute atoms, precipitates as well as on temperature. However, the investigation of the CRSS for both prismatic and pyramidal slip systems has not attracted as much attention as it deserves. The activity of non-basal slip systems is a complex function of the test temperature and the concentration of solute atoms. In contrast to basal slip, the CRSS for glide in the second order pyramidal system exhibits an anomalous or positive temperature dependence [33–35]. The CRSS for (first order) prismatic slip system decreases very strongly with increasing temperature [36, 37]. The CRSS for prismatic slip at room temperature is about 100 times higher than that of basal slip, whereas at 300°C it is only four times higher. The concentration dependence of the CRSS for prismatic slip for Mg-Zn is more complex and it is different at various temperatures [37]. The results for Mg-Al single crystals give the same trends in the temperature and concentration dependence of the CRSS for prismatic slip. A decrease in the CRSS for prismatic slip with increasing concentration indicates solution softening.

A non-monotonic temperature dependence of the CRSS has been reported for the prismatic slip system in Mg-In and Mg-Li alloys [38, 39]. At room temperature the CRSS for prismatic slip in a Mg-In alloy increases practically linearly with the addition of In, whereas it is independent of the In concentration below room temperature [40].

The CRSS for second-order pyramidal slip system in Mg-Li alloys increases with increasing temperature in the range from 77–293 K. The CRSS for pyramidal slip in Mg-Li alloys is lower than that in pure Mg. It decreases with the addition of lithium in a non-monotonic manner [41, 42]. The CRSS of Mg-

7.5 at. % Li measured at room temperature is about a half of that of pure magnesium.

An analysis of the stress dependence of the work hardening rate could help in understanding the deformation behavior of polycrystalline magnesium alloys. This analysis of the hardening behavior as a function of temperature has yet to be made.

Electron microscopy investigations showed that the presence of edge basal dislocations is characteristic of non-deformed Mg single crystals [43]. At the beginning of deformation, isolated basal dislocations with edge orientation were observed. With increasing strain screw dislocations may cross slip. Double cross slip of screw dislocations from the basal plane through the prismatic planes to the basal plane is typical of Mg single crystals deformed at room temperature. During deformation the motion of dislocations in the non-basal (pyramidal) slip systems have been assumed and observed [44, 45]. Different dislocation reactions can take place. Some dislocation reactions may produce obstacles as with the generation of long-range stress fields; other dislocation reactions may result in softening.

The macroscopic work hardening behavior is the result of the sum of two microscopic effects: storage and annihilation of dislocations. We may consider the processes of storage of dislocations as both dislocation forest and impenetrable (non-dislocation) obstacles (such as small particles, precipitates, grain boundaries). According to TEM observations, it can be considered that the dominant recovery process is cross slip of screw dislocation segments. The activity of cross slip increases with increasing temperature. At higher temperatures the strong decrease in the strain hardening rate may be caused by the operation of further recovery processes in addition to cross slip, very likely dislocation climb aided by diffusion.

Twinning should be also considered as a deformation mechanism, even if it is intense at low temperatures and at low strains. Twinning in the initial stage of plastic deformation may reorient the basal planes which become more favourable for slip. Both twinning and the presence of  $c+a$  dislocations (i.e., dislocations in the pyramidal slip system) is in agreement with observations [45].

### 3.2.12 Strengthening Mechanisms

Plastic deformation of magnesium polycrystals occurs, under most conditions, by glide of dislocations. Under special conditions, mechanical twinning occurs. The onset of plastic deformation occurs when the resolved shear stress (the stress acting on the slip plane in the slip direction) reaches a critical value. This is at a certain value of the applied stress – the yield stress,  $\sigma_y$ . Polycrystals contain crystal defects such as vacancies, foreign atoms, dislocations in various slip systems, precipitates, dispersoids, etc. The crystal defects restrict the dislocation movement or in other words, the crystal defects are obstacles hindering mobile dislocations. Therefore, the deformation behavior of polycrystals is influenced by the presence of crystal defects. Strength of a material is a result of strengthening mechanisms due to defects in the material.



### 3.2.12.1 Dislocation Strengthening

Plastic deformation is the result of the movement and multiplication of dislocations. The yield stress of Mg polycrystals depends on all dislocations in the polycrystal as described by the following relationship:

$$\sigma_{yD} = M\alpha Gb\varrho^{1/2} \quad (3.24)$$

Here  $G$  is the shear modulus,  $b$  is the magnitude of the Burgers vector,  $\varrho$  is the dislocation density,  $M$  is the Taylor factor and  $\alpha$  is a constant in the range 0.1 to 0.5. The constant  $\alpha = 0.2$  has been estimated for the interaction between the dislocation forest and basal dislocations in magnesium single crystals at 300 K [46].

### 3.2.12.2 Solid Solution Hardening

Solute atoms are also responsible for the strengthening of materials. Solute atoms in Mg or in Mg alloys change the lattice constants (both the  $a$  and  $c$  parameter) and modify the binding forces. In a very dilute solid solution the moving dislocation interacts with a solute atom. The interaction intensity can be described by the relative change in the lattice parameter (the size misfit parameter)  $\delta = (da/dc)/a$  and the relative change in the modulus (modulus misfit parameter)  $\eta = (dG/dc)/G$ . In both expressions  $c$  is the atomic solute concentration. The mobile dislocations interact with many solute atoms. The interaction force between a dislocation and a solute atoms depends on the distance between the dislocation and the atom. The minimum force is given by a statistical sum of the interactions of many solute atoms. The yield stress of dilute Mg based alloys can be expressed as described by Fleischer [47]

$$\sigma_{yS} = \sigma_{y0} + Z_F G(|\delta| + \beta|\eta|)^{3/2} c^{1/2} \quad (3.25)$$

or according to Labusch [48]

$$\sigma_{yS} = \sigma_{y0} + Z_L G(\delta^2 + \beta^2 \eta^2)^{2/3} c^{2/3} \quad (3.26)$$

In both equations  $\sigma_{y0}$  is the yield stress of pure magnesium,  $Z_L$  and  $Z_F$  are constants and  $\beta$  is between 1/20 and 1/16. It can be concluded from the published experimental results [49] that the value of the solution hardening rate increases from that for Mg-Li through Mg-Al to that for Mg-Zn. The strengthening effect of the various solutes arises from the concentration dependence of both lattice parameter and elastic constants. The concentration dependence of the lattice parameter for some Mg base alloys has been determined [50] or the size factor may be estimated as computed by King [51]. On the other hand, the concentration dependence of elastic constants has been measured only for a few Mg alloy systems. In the case where the concentration dependence of the shear modulus  $G$  is not known, an approximate value of  $\eta$  can be calculated using the equation [47, 52]

$$\eta = 2(G_1 - G)/(G_1 + G) \quad (3.27)$$

where  $G_1$  is the shear modulus of the alloying metal.

In commercial alloys many different solute atoms are present, e.g., in ternary or quaternary alloys. The solute atoms then cause different interactions because the strength of the solute atoms as obstacles is not the same. Various relationships for the superposition of two kinds of obstacles have been discussed [53].

### 3.2.12.3 Precipitation Strengthening

The strength of precipitate strengthened polycrystalline magnesium alloys depends on the size, distribution and volume fraction of the precipitates and on the nature of the interface between the precipitates and the matrix (coherent or incoherent). Dislocations may be able to cut fine precipitates but cannot shear through larger incoherent precipitates. The dislocations then bow out between precipitates. The stress at which the precipitate particles are overcome can be expressed by a more general formula

$$\sigma_{yp} = MF/bL \quad (3.28)$$

where  $L$  is the average particle spacing along the dislocation line and  $F$  is the mean obstacle strength [54, 55].

In the case of particle shearing, the obstacle strength depends on the main interaction mechanism between shearable precipitates and the mobile dislocations (for instance the creation of new interfaces or a difference in the stacking fault energy between the precipitates and the matrix) and it can be written in the following form

$$F_0 = K_p G b R \quad (3.29)$$

where  $K_p$  is the parameter depending on the mechanism considered and  $R$  is the average radius of precipitates. However, the mean obstacle strength  $F$  depends on the precipitate size distribution. The average particle spacing depends on the particle volume fraction  $f$  and on  $R$ . The yield stress for the case that all precipitates are sheared is given by

$$\sigma_{yp} = Z_p M G K_p^{3/2} (fR/b)^{1/2} \quad (3.30)$$

where  $Z_p$  is a constant.

In the case of bowing dislocations between precipitate particles (incoherent precipitates), the obstacle strength is constant

$$F_0 = G b^2. \quad (3.31)$$

The yield stress for the case that all precipitates are by-passed is given as

$$\sigma_{y0} = 2 M G b / L_p \quad (3.32)$$

where  $L_p$  is the average interparticle spacing in the glide plane. This stress is called the Orowan stress. The average particle spacing along the dislocation line is larger than the average interparticle spacing in the glide plane and then the yield stress is expressed as

$$\sigma_{y0} = Z_0 M G b f^{1/2} / R \quad (3.33)$$

where  $Z_0$  is a constant about 0.6.

The critical radius of precipitates for the transition between the shearing and by-pass modes is the radius at which the obstacles strengths are identical for both mechanism, i.e.,

$$R_c = \frac{b}{K_p} \cdot \left( \frac{Z_o}{Z_p} \right)^{2/3} \text{ where } \frac{Z_o}{Z_p} \text{ is almost one.} \quad (3.34)$$

This radius controls the peak strength of the material.

Usually in practice, the strength of an alloy is given by the contribution of dislocation hardening, solute hardening and precipitation hardening. Then the yield stress of the alloys can be calculated as

$$\sigma_{ya} = \sigma_{ys} + [(\sigma_{yD})^2 + (\sigma_{yP})^2]^{1/2}. \quad (3.35)$$

#### 3.2.12.4 Dispersion Strengthening

The strength of dispersion strengthened materials depends on the size, distribution and volume fraction of dispersoids. Mobile dislocations cannot cut the incoherent dispersoids and the yield stress of the material is very close to the Orowan stress given by the relation (3.32) or (3.33).

#### 3.2.12.5 Strengthening by Grain Size Refinement

A finer grain size may contribute significantly to the strength. The yield stress increases with decreasing grain size. The grain size dependence of the yield stress (and tensile strength) can be expressed through the Hall-Petch relationship [56–58]

$$\sigma_{yd} = \sigma_0 + K_y d^{-1/2} \quad (3.36)$$

where  $d$  is the average grain diameter,  $\sigma_0$  is a constant and  $K_y$  is the stress intensity factor for plastic yielding. The value of  $K_y$  depends on temperature, texture, composition and preparation [59–64]. Considering the results published on the grain size dependence of the yield stress of Mg and Mg alloys one obtains a  $K_y$  value of about 210 MPa  $\mu\text{m}^{1/2}$ .

It is important to note that, in the case of Mg and Mg alloys,  $\sigma_0$  is related to the critical resolved shear stress (CRSS) for the easiest (basal) slip system operating within the grain volume, whereas  $K_y$  is associated with the CRSS for the non-basal (more difficult) slip systems required to operate near the grain boundaries in order to maintain the continuity of deformation [65]. Then

$$\sigma_0 = M \tau_0 \quad (3.37)$$

where  $M$  is the Taylor orientation factor and it is very difficult to calculate its value for hexagonal metals; very often  $M = 4$  to 6.5 is used for magnesium and its alloys. The yield stress is a sum of the individual strengthening mechanisms.

The stress intensity factor  $K_y$  as a function of the CRSS for non-basal slip,  $\tau_{NB}$ , is given by [65]

$$K_y = CM [M^* G b / (1 - \nu)]^{1/2} \tau_{NB}^{1/2} \quad (3.38)$$

**Table 3.7.** Mechanical properties of cp-Mg in N/mm<sup>2</sup>

	Yield stress (tensile)	Yield stress (compression)	Ultimate tensile stress	Hardness HB
Sand cast cp Mg	21	21	90	30
Extruded cp Mg	69–105	34–55	165–205	35
Rolled sheet	115–140	105–115	180–220	45–47
Annealed sheet	90–105	69–83	160–195	40–41

where C is a numerical constant,  $M^*$  is the Sachs orientation factor for the accommodating system,  $\nu$  is Poisson’s constant and G and b have their usual meaning.

The values of both  $\sigma_0$  and  $K_y$  decrease with increasing temperature. The temperature dependence of  $\sigma_0$  for Mg polycrystals is parallel to the temperature dependence of the CRSS for basal glide of Mg single crystal. The temperature dependence of  $K_y^2$  is parallel to the CRSS for prismatic slip in Mg [66]. This supports the view that, for Mg and Mg alloys,  $\sigma_0$  for polycrystals is related to the CRSS for basal glide and is affected by all obstacles to dislocation motion and  $K_y$  is related to the CRSS for non-basal slip. In other words, the temperature dependence and the value of the yield stress of Mg polycrystals are influenced by the temperature and concentration dependences of CRSS for both basal slip and non-basal slip. The temperature dependence of the yield stress of a Mg alloy should be more complex than that of the CRSS for basal slip of a single crystal. This is due to a non-monotonic dependence of the CRSS for non-basal slip (in some solid solutions) on the test temperature.

The mechanical properties thus depend in general on the state of the material, how it was produced and to what thermo-mechanical treatments it was subjected [7]. Some typical values are given in the Table 3.7.

The mechanical properties of pure magnesium are not sufficient for normal technical applications. In addition, the crystal structure limits as we saw above the deformability. The possible slip planes are shown in Fig. 3.1. At room temperature slip takes place on the basal plane (0001) and in the  $\langle 11\bar{2}0 \rangle$  direction. Secondary slip occurs in the  $\langle 11\bar{2}0 \rangle$  direction on the  $\{10\bar{1}0\}$  vertical faces. At elevated temperatures slip occurs in the  $\langle 11\bar{2}0 \rangle$  direction on the  $\{10\bar{1}1\}$  pyramidal planes, and on the  $\{11\bar{2}2\}$  planes and  $\langle \bar{1}\bar{1}23 \rangle$  direction thus enabling technical processes such as hot rolling and extrusion.

The outlining principles for development of commercial alloys have been presented above in so far as mechanical properties are concerned. Despite the advantages of magnesium the difficulties and limitations of such a development are immediately apparent.

**3.3 Magnesium Alloys**

Magnesium must be alloyed with other metals if it is to be employed for engineering applications. The classification of alloys employed has traditionally been

made primarily according to mode of manufacture with subdivisions indicating composition and application. Consequently the first classification is, for example, sand casting, permanent mold, die casting, forging, extrusion, rolling (sheet and plate). Thereafter subdivisions according to composition are made.

The development of alloys for specific applications, e.g., creep resistance follows analogous considerations to those adopted for fcc and bcc metals. Magnesium is hcp, which must be borne in mind in relation to ductility. Although there are about 25 metals with an appropriate atomic size to form alloys there is in reality few appropriate alloying elements. The solubility is often restricted by the relative – valency effect and because of the chemical affinity for elements such as silicon and tin, which leads to the formation of stable compounds. Alloying behaviour is discussed in detail in references [67–69].

Consequently there are only about ten elements which can be considered as alloying elements. Those elements which dissolve may be expected to modify the ductility, the elastic properties and harden by solid solution hardening. Only dissolved additions can modify the elastic constants unless composites are considered.

When intermetallics are formed they restrict the ductility and often such alloys can only be used as casting alloys. The formation of intermetallics can be exploited to improve the creep resistance providing the precipitates can form with the right size and distribution. The precipitation sequence and precipitation process are critical in determining the suitability of an alloy for applications in which creep resistance is necessary.

### **3.3.1 Common Alloying Elements**

#### **3.3.1.1 Aluminum**

Aluminum is the most commonly used alloying element and forms the basis of the die casting alloys. The maximum solubility is 11.5 at % (12.7 mass %) and alloys in excess of 6 mass % can be heat treated. Aluminum improves strength, the optimum combination of strength and ductility being observed at about 6%. Alloys are readily castable. The creep resistance is limited due to the poor thermal stability of the  $\text{Mg}_{17}\text{Al}_{12}$  phase.

#### **3.3.1.2 Calcium**

Alloying with calcium is becoming more common in the development of cheap creep resistant alloys – essentially replacing  $\text{Mg}_{17}\text{Al}_{12}$  with  $\text{Al}_{12}\text{Ca}$ . Otherwise Ca can act as a deoxidant in the melt or in subsequent heat treatment. It improves the roll ability of sheet but >0.3 mass % can reduce the weld ability.

#### **3.3.1.3 Lithium**

The only alloying element to reduce the density of alloys below that of magnesium. Furthermore it is soluble up to 17.0 at % (5.5 mass %), a value retained largely at room temperature. The second phase is body centred cubic (11 mass %), which enables the production of wrought products, either  $\alpha + \beta$  or

$\beta$  phase. Addition of Li decreases the strength but increases the ductility. The elastic constants are also improved somewhat.

#### **3.3.1.4 Manganese**

Manganese is usually not employed alone but with other elements, e.g., Al. In this case compounds  $MnAl$ ,  $MnAl_6$  or  $MnAl_4$  are formed. It reduces the solubility of iron and produces relatively innocuous compounds. It increases the yield strength and improves salt water corrosion resistance of  $MgAl$  and  $MgAlZn$  alloys. Binary alloys (M1A) are used in forgings or extruded bars. The maximum amount of manganese is 1.5–2 mass %.

#### **3.3.1.5 Rare Earths**

Rare Earths are added to magnesium alloys to improve the high temperature strength and creep resistance. They are usually added as Mischmetal (so have a mass % of cerium and other rare earths (mainly lanthanum and neodymium)) or didymium (85% neodymium and 15% praseodymium).

#### **3.3.1.6 Silicon**

Silicon increases the fluidity of molten alloys. In the presence of iron it will reduce the corrosion resistance. It is employed in very few alloys (AS21 and AS41).

#### **3.3.1.7 Silver**

Silver increases the age hardening response and high temperature properties of thorium or rare earth containing alloys e.g. QE22 and QH21.

#### **3.3.1.8 Thorium**

The addition of thorium confers creep resistance – up to 350°C. It improves cast ability. Alloys are weldable. It's use is being phased out due to thorium being radioactive.

#### **3.3.1.9 Yttrium**

Yttrium is used in conjunction with rare earths to improve high temperature strength and creep resistance up to 300°C.

#### **3.3.1.10 Zinc**

Zinc is one of the commonest alloying additions. It is used in conjunction with Al (e.g., AZ91 or with zirconium, thorium or rare earths).

#### **3.3.1.11 Zirconium**

Grain refining agent. Can be used with alloys containing zinc, rare earths, thorium, yttrium or a combination thereof but not in alloys containing aluminum

or manganese as these form stable compounds with zirconium. It also forms stable compounds with iron, silicon, carbon, nitrogen, oxygen and hydrogen in the melt. Only dissolved zirconium is effective as grain refiner.

### **3.3.2 Elements Used for Manufacturing Purposes or Impurities**

#### **3.3.2.1 Beryllium**

Beryllium is only slightly soluble. It is used to decrease oxidation of the melt. It can cause grain coarsening.

#### **3.3.2.2 Copper**

Copper adversely affects corrosion properties if present in an amount greater than 0.05 mass %. It will improve high temperature strength.

#### **3.3.2.3 Iron**

A very harmful impurity as it reduces corrosion resistance. For good corrosion resistance, upper limit of 0.005 mass % is specified.

#### **3.3.2.4 Nickel**

Also a harmful impurity. Reduces greatly corrosion resistance even at small amounts. As with iron an upper limit of 0.005 mass % is specified for good resistance.

#### **3.3.2.5 Tin**

Small amounts of tin, in conjunction with small amounts of aluminum, serve to improve ductility and reduces the tendency to cracking during forging.

It thus becomes apparent how few elements are available for producing the desired properties. As the search for new and better alloys continues, other, mostly unusual, alloying elements are being investigated for example scandium, strontium, terbium, gadolinium.

### **3.3.3 Classification of Alloys**

The traditional classification according to the production method is still used as stated above. The first subdivision is then according to the composition. The limited number of alloying elements has resulted in the majority of alloys being based on the alloying elements aluminum, manganese, rare earths (or similar), zinc and for Al, Mn free alloys, zirconium.

The convention to depict the main elements in an alloy is given in Table 3.8. Thus AZ91 signifies 9% Al and 1% Zn. Older publications may contain other letters, e.g., MEL use of T for Thorium e.g. ZTI.

**Table 3.8.** Convention for alloy elements designation

Letter	Alloying elements
A	Aluminum
C	Copper
E	Rare earth metals
H	Thorium
K	Zirconium
L	Lithium
M	Manganese
Q	Silver
S	Silicon
Y	Yttrium
Z	Zinc

The global composition (rounded figures) may be expanded to provide additional information or variants by adding a letter after the last composition number, A etc., e.g., AZ 91A, B, ... E. X describes an experimental alloy.

Further information can be provided as shown in Table 3.9; fabrication details, e.g., as fabricated, annealed, aged. To differentiate from the other information a hyphen is inserted. Examples are ZK 61A – T5, AM 100 A – T61.

**Table 3.9.** Temper designations for magnesium alloys

General divisions	
F	As fabricated
O	Annealed recrystallised (wrought products only)
H	Strain hardened
T	Thermally treated to produce stable tempers. Other than F, O or H
W	Solution heat treated (unstable temper)
Subdivisions of H	
H1, plus one or more digits	Strain hardened only
H2, plus one or more digits	Strain hardened and then partially annealed
H3 , plus one or more digits	Strain hardened and then stabilised
Subdivisions of T	
T1	Cooled and naturally aged
T2	Annealed (cast products only
T3	Solution heat treated and then cold worked
T4	Solution heat treated
T5	Cooled and artificially aged
T6	Solution heat treated and artificially aged
T7	Solution heated and stabilised
T8	Solution heat treated, cold worked, and artificially aged
T9	Solution heat treated , artificially aged and cold worked
T10	Cooled, artificially aged, and cold worked



## 3.4 Phase Diagrams

### 3.4.1 Conventional Alloys

Properties of materials can be classified as structure insensitive or structure sensitive. Structure insensitive properties are those which are largely uninfluenced by the microstructure, e.g., density, electrical properties, thermal conductivity, specific heat. Such properties are determined by the chemical composition and atomic properties. The structure sensitive properties, on the other hand, are all mechanical properties.

The metallurgist describes a material not only by the chemical composition but also by the phases present. This can be done for binary and ternary systems relatively simply in the form of phase diagrams. The phase diagram represents the equilibrium state but is not capable of providing information regarding the physical shape or dispersion of the phases or phases which might appear in non equilibrium processing.

They are particularly useful tools in interpreting microstructures, planning heat treatment such as age hardening or thermo mechanical treatments.

In the following pages, the most important phase diagrams for magnesium binary alloy systems will be presented and discussed. In commercial alloys additional alloying elements are added for a variety of reasons, e.g., modifying the Mg solid solubility of the primary alloying element, modifying the precipitation mode of phases, or creating different intermetallic phases. The complex systems have been rarely investigated fully. To facilitate understanding and fill in gaps in our knowledge attempts are being made to calculate phase diagrams or obtain information relevant to alloy development. These will be discussed below.

#### 3.4.1.1 Magnesium-Aluminum

Aluminum is one of the most important alloying elements in magnesium. Several systems contain Al up to 10 mass %, e.g., AZ, AE, AM and AS. Figure 3.3 shows the Mg-Al system. Al is one of the few metals that dissolve easily in magnesium. Above the solubility limit  $\text{Mg}_{17}\text{Al}_{12}$ , a brittle intermetallic, precipitates out. The solubility limit of aluminum at the eutectic temperature is 11.5 at.% (12 mass %) and falls to about 1% at room temperature. Consequently, the  $\text{Mg}_{17}\text{Al}_{12}$  plays a dominant role in determining the properties (Fig. 3.4). The commercial alloys based on Mg-Al involve further alloying additions of zinc, e.g., AZ91, AZ81 and AZ63.

#### 3.4.1.2 Magnesium-Zinc

Zinc is an important alloying element but rarely serves as the major alloying element (ZK, ZH, ZM, ZC and ZE series of alloys). The binary phase diagram (Fig. 3.5) shows a eutectic at 51.3 mass %. There is 6.2 mass % solubility at the eutectic temperature.

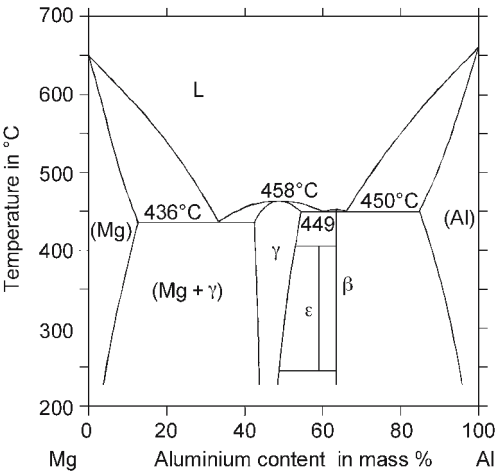


Fig. 3.3. Phase diagram of Mg-Al binary alloy

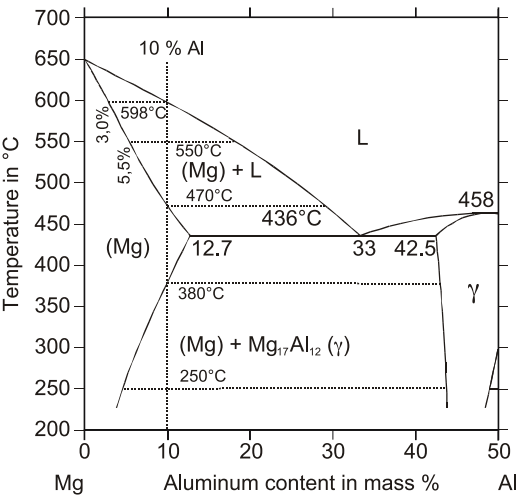


Fig. 3.4. Magnesium-rich section of Mg-Al system

3.4.1.3 Magnesium-Manganese

Manganese is an important major addition for many magnesium alloys. More recently it has become important in the development of high performance creep alloys. The Mg-Mn phase diagram is unusual in several aspects, e.g., in that there is a peritectic reaction in which magnesium (Fig. 3.6) precipitates out at 653°C from  $L + \alpha \text{ Mn}$ . The solubility of Mn in solid magnesium is more than in the liquid (2.2 mass % c.f. 2.0 mass %). With decreasing temperature the solubility decreases causing more precipitation of manganese.

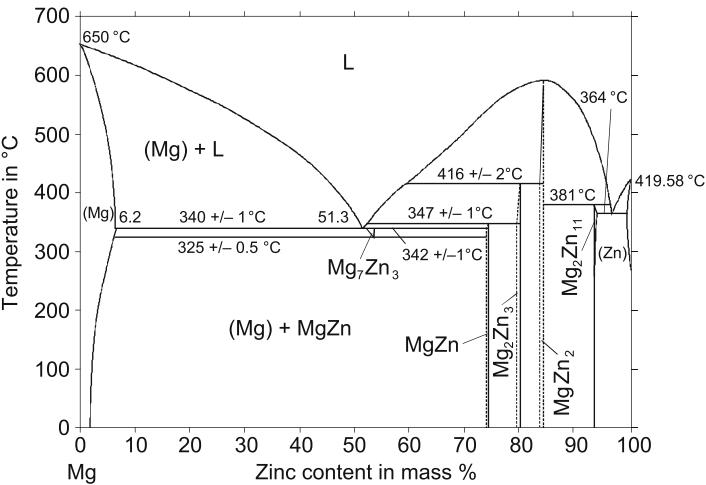


Fig. 3.5. Phase diagram of Mg-Zn system

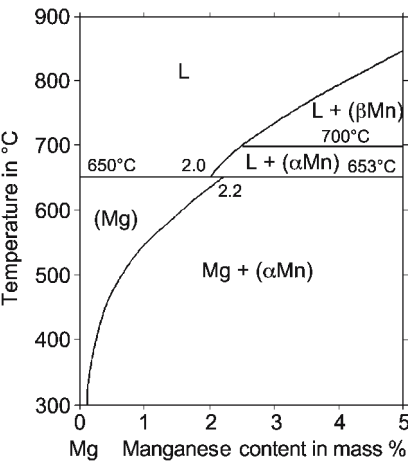


Fig. 3.6. Magnesium-manganese phase diagram up to 5 mass % Mn

3.4.1.4 Super Light Weight Alloys

Lithium is the only alloying element which decreases the density of magnesium. The phase diagram (Fig. 3.7) shows a eutectic at 588°C with a solubility limit of lithium in magnesium of 5.5 mass %, which is largely retained at lower temperatures. The second phase  $\beta$ , bcc, is also stable down to room temperature opening the possibility of producing  $\alpha + \beta$  and  $\beta$  workable alloys. This was investigated by the USAF in 1958 [70].

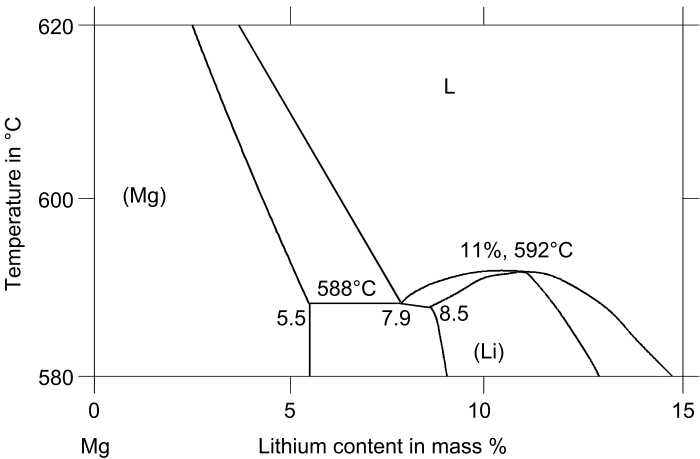


Fig. 3.7. Mg-Li phase diagram up to 15 mass % Li

3.4.1.5 High Performance Alloys

The attainment of superior properties requires completely different alloying additions. Rare Earths and similar alloying elements were employed for alloys designated QE, WE, HK and experimental alloys with scandium. Figure 3.8 shows the Mg-Nd phase diagram. The Nd is usually in the form of a Mischmetal-neodymium-praseodymium.

The purpose of the Nd is to form stable precipitates. The rare earth is used with silver in the QE series, producing alloys with a good creep resistance up to 200°C (Fig. 3.9).

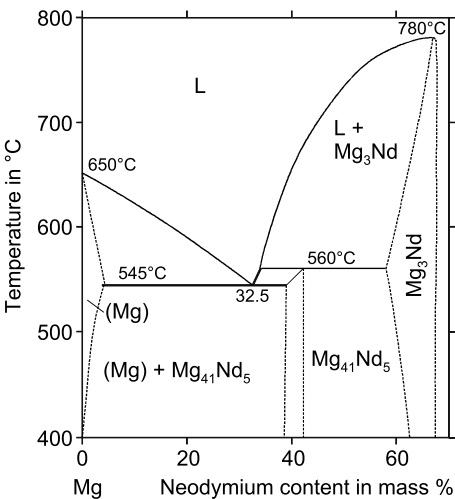


Fig. 3.8. Magnesium neodymium phase diagram up to 70 mass % Nd [71]

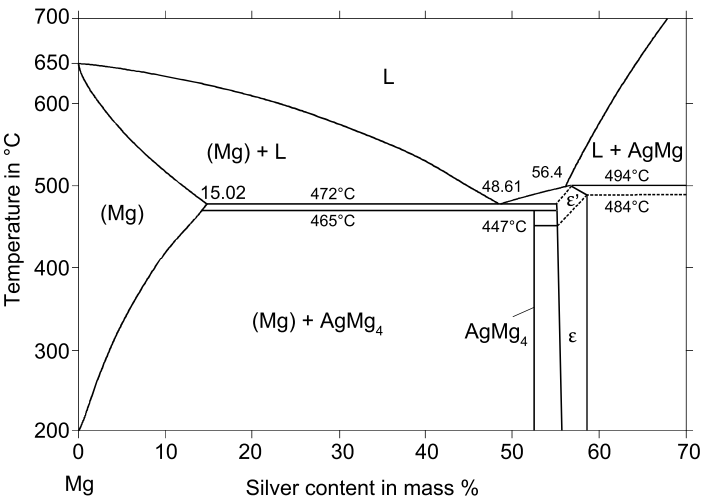


Fig. 3.9. Magnesium-Silver phase diagram up to 70 mass % Ag [72]

Alternatively magnesium is alloyed with yttrium and rare earth elements. This results in the WE series. Figure 3.10 shows the magnesium-yttrium phase diagram. There is a relatively high solubility of yttrium in magnesium (12.47 mass %).

3.4.1.6 Magnesium-Scandium

Scandium has been considered lately as an alloying addition which could be used to obtain better creep properties. The Mg-Sc system (Fig. 3.11) shows a peritectic and a strong increase in melting point. The diagram shown was determined by a combination of experimental and thermodynamic analysis [74].The previ-

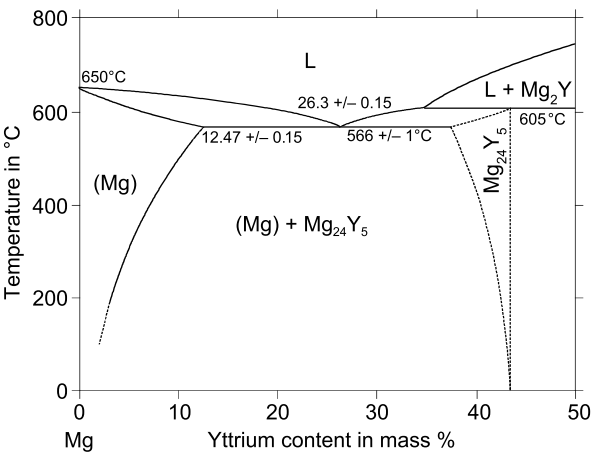


Fig. 3.10. Magnesium-Yttrium phase diagram up to 50 mass % Y [73]

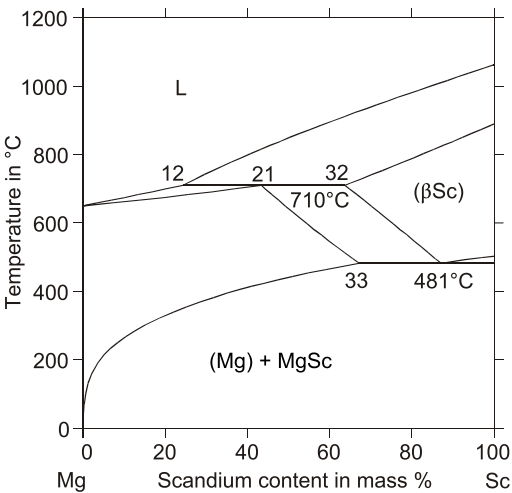


Fig. 3.11. Mg-Sc phase diagram up to 50 mass % Sc [74]

ously accepted diagram was shown to be erroneous. Although the falling solubility suggests the possibility of age hardening the MgSc forms very slowly and is incoherent. A strong effect is observed only after the addition of Mn.

3.4.1.7 Magnesium-Zirconium

Zirconium is a very effective grain refiner for magnesium and can be used with all alloys except those containing aluminum or manganese. The phase diagram is shown in Fig. 3.12. The solubility of zirconium in magnesium is 3.8 mass % at the melting temperature and decreases to 0.2 mass % at room temperature.

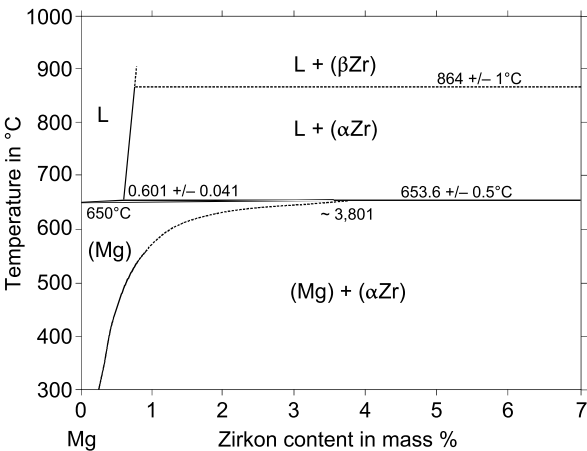


Fig. 3.12. Mg-Zr phase diagram up to 7 mass % Zr [75]

It is considered that zirconium is a good refiner because it has the same crystal structure and the lattice parameters are virtually identical.

### 3.4.2 Higher Systems

Tertiary equilibrium diagrams have been determined for many systems. MgAlZn, MgLiAl, MgScMn, MgAlSc have been discussed in the Magnesium Pocket Book [76]. It is more probable that ternary and higher phase diagrams contain errors. It is expensive and time consuming to repeat the experimental work. Schmid-Fetzer and his group at the TU Clausthal in Germany have developed thermodynamic modeling which enables existing data to be assessed and if necessary corrected. Likewise the relevant information for new systems can be calculated [77].

The Calphad method, which is employed here, involves modeling all relevant experimental data of a system such as phase equilibria and thermodynamic data, enthalpies and chemical activities. Then it is possible to determine the phase equilibria for any given state (temperature, concentration and pressure) in the system.

The technique will be demonstrated with Mg-Sc-Mn and Mg-Sc-Mn-Gd. An isothermal section was calculated for the Mg-Sc-Mn system (Figs. 3.13 and 3.14) [77].

It can be seen that the magnesium solid solution, over a wide range of composition for small manganese contents, is in equilibrium with the  $\text{Mn}_2\text{Sc}$  phase. The other two MnSc intermetallics are of no significance. This was confirmed in practice. The  $\text{Mn}_2\text{Sc}$  phase precipitates as a fine dispersion and is coherent and leads to marked strengthening.

The Calphad method can also be applied to quaternary systems. Phase diagrams can be generated which can be read easily. Figure 3.15 shows a vertical section from the Mg-Mn-Gd-Sc system for constant Mn and Gd with variable Sc

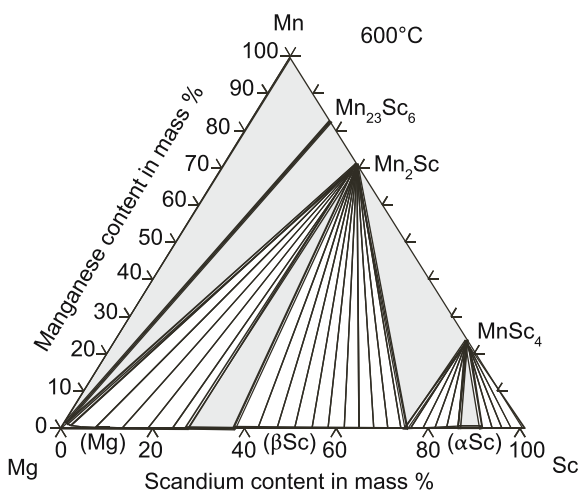


Fig. 3.13. Mg-Sc-Mn system – Isothermal section at 600°C

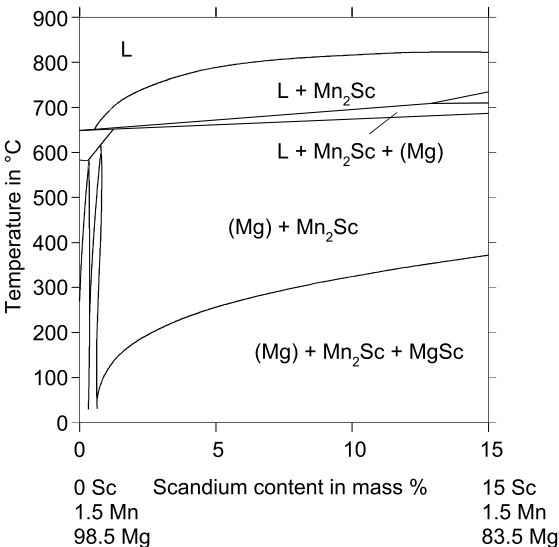


Fig. 3.14. Mg-Sc-Mn systems. Vertical section for Mn 1.5 mass %, variable Sc

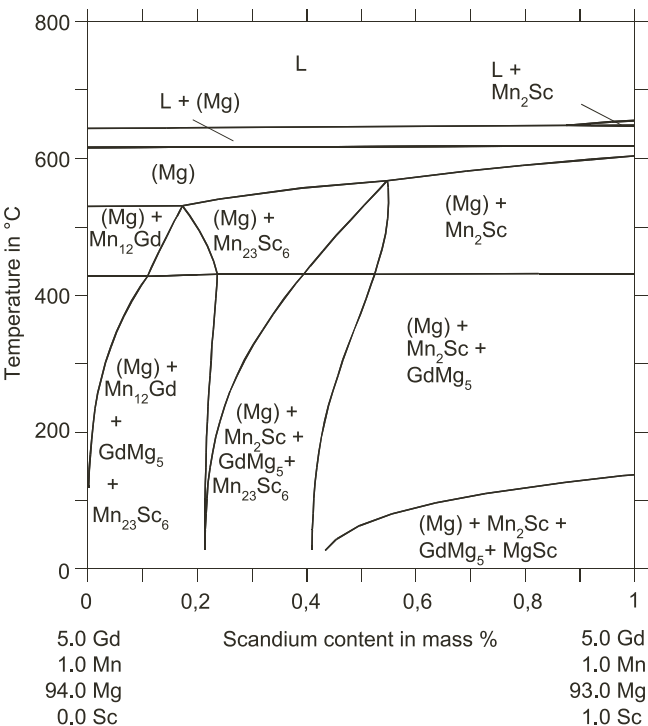


Fig. 3.15. Mg-Mn-Gd-Sc system T-x vertical section constant Mn 1 mass %, Gd 5 mass %



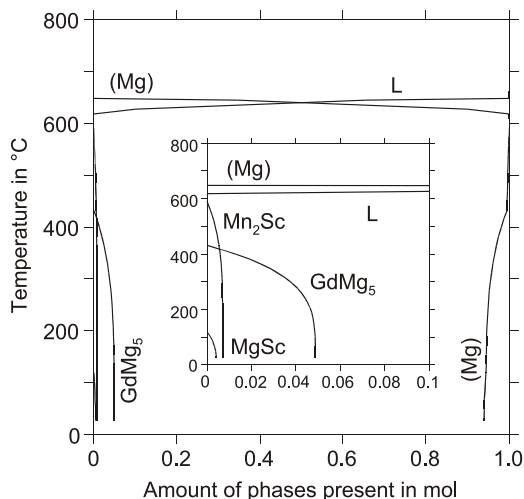


Fig. 3.16. Mg-Mn-Gd-Sc system

from 0 to 1 mass %. This system was studied as a further development of the MgScMn system where one of the aims was to reduce the amount of scandium.

The following information can be read from the diagram:

- 1) The liquidus temperature is below 700°C, which enables simpler and more economical melting technology.
- 2) At concentrations below 0.9 mass % Sc the phase which first precipitates is the magnesium solid solution.
- 3) A homogeneous magnesium solution enables solutionising and ageing treatments.
- 4) A series of multi phase fields lie below the Mg field, which offer many possible heat treatments to achieve optimum results.

It is also possible to calculate the amount present of the various phases. Figure 3.16 shows the amount of the phases present in an alloy MgMn1Gd5Sc0,8 as a function of temperature.

Thermodynamic modelling has thus changed radically the approach to alloy development replacing many hours of tedious experimental work by theoretical prediction.

### 3.5 Commercial Alloy Systems

There are five basic groups of alloy system commercially available. These use the alloying elements, manganese, aluminum, zinc, zirconium and rare earths. Rare earths are used where better high temperature properties are required. A classification can be made according to composition but it is still instructive to use the method of production.

3.5.1 Magnesium Die Casting Alloys (Zirconium Free)

Die casting is by far the most common production method accounting for ~ 70% of the magnesium used. The process is well understood with a high rate of production. It is suitable for intricately shaped components. The rapid quench ensures a fine grain structure but can cause entrapment of gas (porosity) which renders the components unsuitable for heat treatment and also unweldable. Die casting is ideally suited for thin walled components, which necessitates the use of low viscosity alloys. Typical die casting alloys are listed in Table 3.10 together with some typical properties.

The most common alloys are based on the magnesium- aluminum system. All alloys listed in Table 3.10 as die casting alloys have aluminum as the major element.

The strength at low aluminum contents is produced by solid solution hardening. At higher concentrations the strength is derived from the formation of  $Mg_{17}Al_{12}$ . Increasing the  $Mg_{17}Al_{12}$  content reduces the ductility. In a straight Mg-Al system the best mechanical properties are observed for 6 mass % Al and if porosity can be avoided. They can be solutionised and aged. There must always be a compromise in die casting alloys: reducing the aluminum content reduces the castability and only relatively simple dies can be filled. Increasing the aluminum content improves the castability and strength at the expense of ductility. The  $Mg_{17}Al_{12}$  intermetallic forms discontinuously at the grain boundaries. It melts at about 460°C and softens at temperatures of 110–120°C sufficiently to permit grain boundary sliding when additional slip systems are also active.

It can also be seen in Table 3.10 that all alloys contain Mn. Mn improves the corrosion resistance and also provides greater ductility and fracture toughness. There exists a series AM20, AM50 and AM60 to cover the range of properties required. The improvement in the properties arises from a better distribution of the  $Mg_{17}Al_{12}$ , i.e., reduction in the amount on the boundary.

The AS alloys AS21 and AS41 are alloys which rely on the formation of  $Mg_2Si$  in a fine form on the grain boundaries to reduce the creep rate. It also has the effect of reducing the amount of  $Mg_{17}Al_{12}$ .  $Mg_2Si$  is also used to harden some aluminum alloys. As the equilibrium diagram shows, it is relatively stable. In order to obtain  $Mg_2Si$  it is necessary to cool quickly; a limitation on the size of the sections.

Table 3.10. Room temperature mechanical properties of die casting alloys

	Al	Mn	Zn	Other	Yield strength [N/mm <sup>2</sup> ]	Tensile strength [N/mm <sup>2</sup> ]	Elongation [%]	Hardness HB
AE42	4.0	0.1		2.5 RE	145	230	11	60
AM20	2.1	0.1			90	210	20	45
AM50	4.9	0.26			125	230	15	60
AM60	6.0	0.13			130	240	13	65
AS21	2.2	0.1		1.0 Si	120	220	13	55
AS41	4.2	0.2		1.0 Si	140	240	15	60
AZ91	9.0	0.13	0.7		160	250	7	70

AS21 has the better creep resistance compared to AS41 but is less fluid and more difficult to cast.

AZ91 contains in addition to aluminum, zinc, which improves the strength. Zinc increases the tendency to microporosity. The corrosion resistance is satisfactory.

Other attempts to improve the creep resistance of MgAl have included calcium additions but the improvement is accompanied by a tendency to hot cracking.

More recent attempts have been made to improve the properties by adding rare earths, e.g., AE42. The alloys are only suitable for die casting otherwise on slow cooling coarse  $Al_2RE$  compounds form. The RE is added in one of the forms of mischmetal. The magnesium forms a compound with one or more of the rare earths in the mischmetal.

There are no die casting alloys containing zirconium as it forms compounds with aluminum and manganese.

### **3.5.2 Permanent Mould, Sand and Investment Casting Alloys**

Table 3.11 shows the alloys for general casting purposes. They can be divided into two groups: zirconium-free and zirconium-containing alloys. Zirconium is added for grain refining purposes.

The first group, zirconium free, can be considered to be extensions of the Mg-Al group or Mg-Al-Zn with small additions of Mn. Zirconium cannot be used with the MgAl or Mg-Al-Zn alloys as it forms compounds with Al and Mn. Other methods must be used therefore to refine the structure, e.g., superheating, nucleation by carbon and using strontium.

The requirements of pressure die casting alloys and the nature of the process exclude the use of heat treatable alloys. Development of alloys for other casting processes concentrate on overcoming the limitations of the Mg-Al and Mg-Al-Zn with respect to strength, particularly creep resistance. Nearly all AM, AZ alloys in Table 3.11 are heat treated. Nevertheless  $Mg_{17}Al_{12}$ , which stabilizes the grain boundaries, softens at  $\sim 460^\circ C$  enabling grain boundary sliding.

The second group of alloys includes the very important group of high performance alloys with rare earth as the significant alloying element.

#### **3.5.2.1 Magnesium-Zinc-Zirconium**

There are two alloys in commercial use ZK51 and ZK61. The former is used in the T5 temper and the stronger alloy in T5 or T6. Their widespread application is limited by microporosity.

#### **3.5.2.2 Magnesium-Rare Earth-Zinc-Zirconium (ZK61 and ZK62)**

These alloys contain either the neodymium mischmetal or the cheaper cerium based mischmetal. Castability does not present any problems. Ageing is used to improve the mechanical properties particularly the creep properties.

**Table 3.11.** Nominal composition of sand, investment and permanent mould casting alloys

	Al	Zn	Mn	RE	Y	Zr	Other	Yield [N/mm <sup>2</sup> ]	UTS [N/mm <sup>2</sup> ]	Elongation [%]	Hardness HB
AM100A-T6	10.0		0.1 min					150	275	1	69
AZ63A-T6	6.0	3.0	0.15					130	275	5	73
AZ81A-T4	8.0	0.7	0.13					83	275	15	55
AZ91C	8.0	0.7	0.13					145	275	6	66
AZ91E-T6	9.0	2.0	0.1					145	275	6	66
AZ92A	9.0	2.0	0.1					150	275	3	84
EQ21A-T6				2.0		0.6	1.5 Ag 0.1 Cu	195	235	2	65–85
EZ33A-T6		2.7		3.3		0.6		110	160	2	50
QE22A-T6				2.0		0.6	2.5 Ag	195	260	3	80
WE43A-T6				3.4	4.0	0.7		165	250	2	75–95
WE54A-T6				3.5	5.0	0.5		172	250	2	75–95
ZE41A-T5		4.2		1.2				140	205		62
ZE63A-T6		5.7		2.5		0.7		190	300	10 3–5	60 85
ZK51A-T5		4.6				0.7		165	205		65
ZK61A-T5		6.0				0.7		185	310		68
ZK61A-T6		6.0				0.7		180	310	10	70

### 3.5.2.3 Magnesium-Silver

After the development of Mg-RE-Zr alloys ways were sought to improve the strength of these aged hardened alloys. Nd containing rare earth was preferred and silver was added. Substitution of the silver by another group I metal, e.g., copper did not produce the same effect. The properties produced exceeded those of available contemporary alloys at temperatures up to 250°C. The composition most frequently used is QE22 which is used in the fully solutionised and age hardened state. Silver, in sufficient quantity, modifies the precipitation process possibly by increasing the volume fraction of precipitate. The precise sequence of precipitates is not known, but leads to an equilibrium phase with a composition discerned to be  $\text{Mg}_{12}\text{Nd}_2\text{Ag}$  [78]. This alloy is used in the aerospace industry, particularly for applications at elevated temperatures.

### 3.5.2.4 Magnesium-Yttrium Alloys

Yttrium is an element with a high solid solubility in magnesium and has the potential for age hardening. Initially work was carried out on MgYZnRE alloys [79]. The zinc was added to reduce the solubility of the expensive yttrium. The mechanical properties were, however, not as good as the Mg-Y-Nd-Zr alloys. These alloys have better high temperature strength than QE alloys and furthermore better corrosion properties. It is possible, in order to reduce the costs, to use an yttrium-containing mischmetal with 75% Y and heavy earths, e.g., gadolinium and erbium. The alloys, WE54 and WE43, are capable of resisting creep at operating temperatures up to 300°C and at the same time exhibiting good room temperature properties. The precipitation process is again complex [80]. Two alloys are commercially available WE54 (Mg-5.25 Y-3.5 RE (1.5-2 Nd)-0.45 Zr) and WE43 (Mg4Y-2.25 Nd RE  $\geq$  0.14 Zr). WE43 is more stable during prolonged use at elevated temperatures. Table 3.11 gives the mechanical properties. The WE alloys are steadily replacing the QE22 due to high strengths at elevated temperatures and higher corrosion resistance.

### 3.5.3 Further Development

Figure 3.17 shows schematically the developments necessary in alloy development to meet the increasing demands on magnesium alloys. There are obvious limitations in high performance alloys as many of the desired property profiles are more easily attained in aluminum alloys and the only benefit that magnesium can bring is the weight saving. At the other end of the scale the super light alloys are being challenged by polymeric materials, particularly fibre reinforced polymers. Nevertheless, apart from possible future developments in high temperature creep resistance, the results of this research may lead to new developments in alloys for temperatures up to 200°C. In the case of magnesium-lithium alloys they need to be strengthened without losing the weight benefit and this work is on going [81].

The field in Fig. 3.17 where the most potential for improvement lies, is in production techniques, not solely for improvement in ductility as shown but in pro-

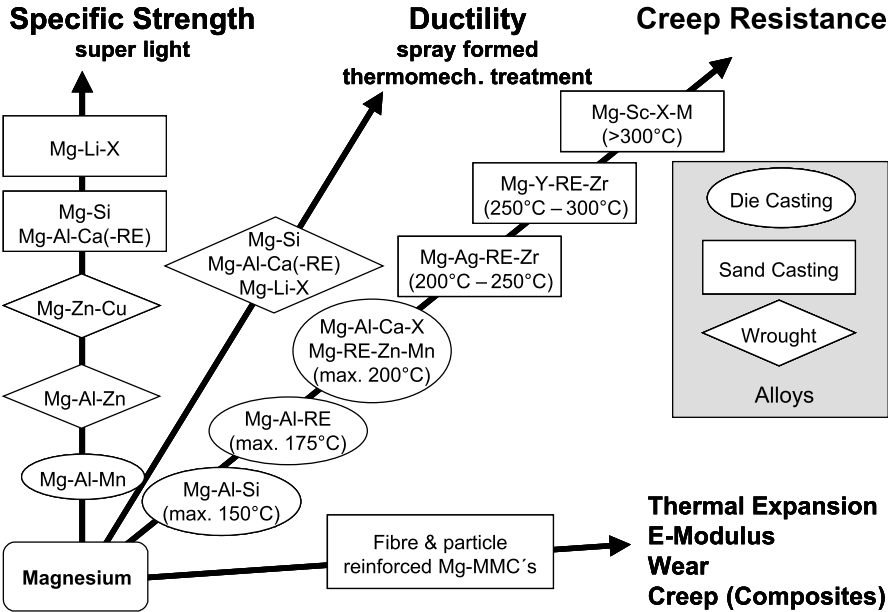


Fig. 3.17. Necessary development in alloys

ducing components with a better microstructure and hence generally better properties. Such techniques would be thixocasting [82] spray forming [83], squeeze casting [84] and thermo mechanical treatments. Independently of this, joining is an important aspect.

3.5.4 Highly Creep Resistant Alloys

In order to replace the WE series work commenced on scandium containing alloys. The earliest such work to be reported was in the USSR. More recently this has been investigated in Germany. The problems caused by insufficient thermodynamic data has been discussed above. Table 3.12 shows the range of alloys studied to date.

Scandium was chosen because it increases the melting point of magnesium alloys (peritectic reaction), forms stable intermetallic compounds and diffuses slowly in magnesium. The results on Mg-Sc binary alloys have been published elsewhere [85–87]. Since the results of the binary alloys were promising, ternary and quaternary alloys were studied whereby the alloys chosen had compositions amenable to age hardening. The alloys were produced by squeeze casting. The microstructures are shown in Fig. 3.18 and 3.19. They exhibit the typical features of cast structures but compared to sand or ingot casting the microstructure is much finer. Mn<sub>2</sub>Sn precipitates were detected in the grain boundaries and within the grains both in the as cast and T5 treated conditions. The addition of Ce led to the formation of additional precipitates, mainly in the grain boundaries (Figs. 3.19).

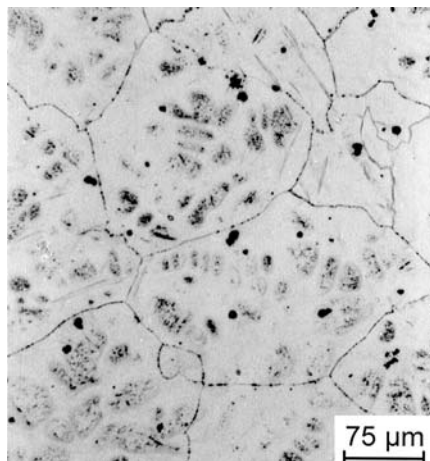
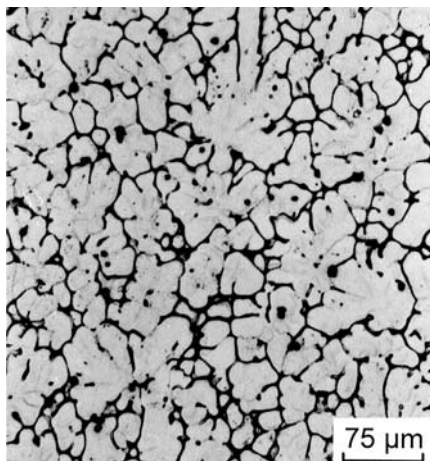
**Table 3.12.** Composition of cast alloys in mass %

Binary	Ternary
Mg-3.2Sc	Mg-15.2Sc-1.4Mn
Mg-7.4Sc	Mg-5.9Sc-1.6Mn
Mg-10.1Sc	Quaternary
Mg-11.1Sc	Mg-9Sc-3.2 Ce-1.5Mn
Mg-14.5Sc*	Mg-6.3Sc-4.2 Ce-1.5Mn
Mg-19.1Sc*	Mg-5.1Gd-0.3 Sc-1.5Mn
Mg-4.5Gd	Mg-9.6Gd-0.9 Sc-1.3Mn
Mg-9.3Gd	Mg-2.8Ce-0.9 Sc-1.1Mn
Mg-14.6Gd	Mg-3.9Y-0.7 Sc-1.1Mn

All alloys except \* prepared by squeeze casting at IWW TU Clausthal, otherwise melted by MEL, Manchester, UK.

Calculations had predicted that neither a T4 nor a T6 treatment would be possible in both the ternary and quaternary alloys chosen. The optimum was a T5 treatment between 250 and 350°C. The ageing response is strong due to the formation of  $\text{Mn}_2\text{Sc}$  and  $\text{Mg}_{12}\text{Ce}$  precipitates. The mechanical properties, yield strength and secondary creep rate are shown in Figs. 3.20, 3.21 and 3.22.

The yield stress is thus significantly higher than QE22 T6 (80 N/mm<sup>2</sup>) but of the same order as WE43 T6 (160 N/mm<sup>2</sup>). The creep rate in the cast state for the new alloys was comparable to those of WE43. The addition of Ce reduced the creep rate significantly in the T5 state due to  $\text{Mg}_{12}\text{Ce}$  precipitates. These new alloys showed secondary creep rates of  $1\text{--}2 \times 10^{-8} \text{ s}^{-1}$  at 350°C compared to  $1 \times 10^{-6} \text{ s}^{-1}$  for WE43 T6 and at 400°C  $\text{MgSc15Mn1}$  in the T5 condition a rate of  $1.7 \times 10^{-6} \text{ s}^{-1}$  compared to  $1 \times 10^{-4} \text{ s}^{-1}$  for WE43 T6. Since the Sc content did not influence markedly the

**Fig. 3.18.** MgSc6Mn1 cast state**Fig. 3.19.** MgSc6Ce4Mn1 cast state

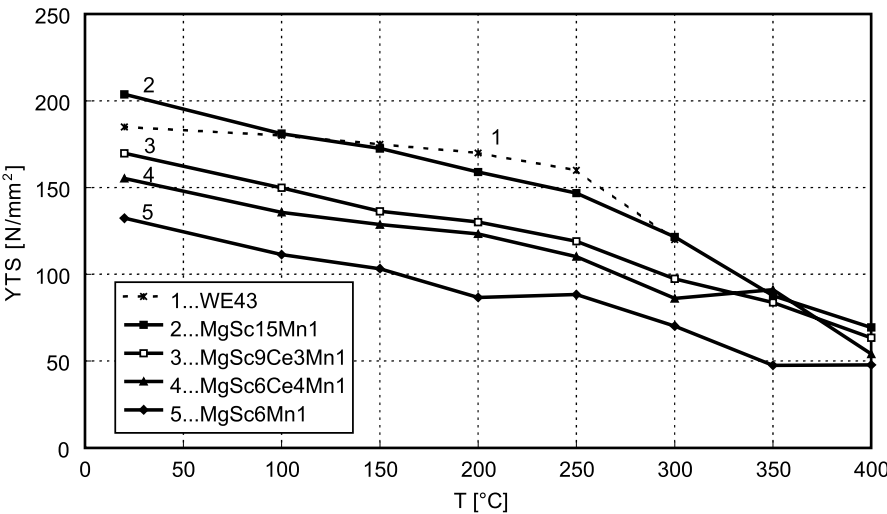


Fig. 3.20. Yield strength of Mg-Sc based alloys

secondary creep rate other alloys were produced: binary Mg-Gd alloys, quaternary MgGdScMn and a Mg-Y-Sc-Mn as given in Table 3.13.

The choice of gadolinium was new. Figure 3.23 shows a comparison of secondary creep rates of binary Mg-Gd alloys in the as cast and T6 states together with WE43 and QE22 at 200°C 60 N/mm<sup>2</sup>.

The creep rates for the quaternary alloys in the as-cast state are compared to WE43 T6 at 350°C and 30 N/mm<sup>2</sup> in Fig. 3.24.

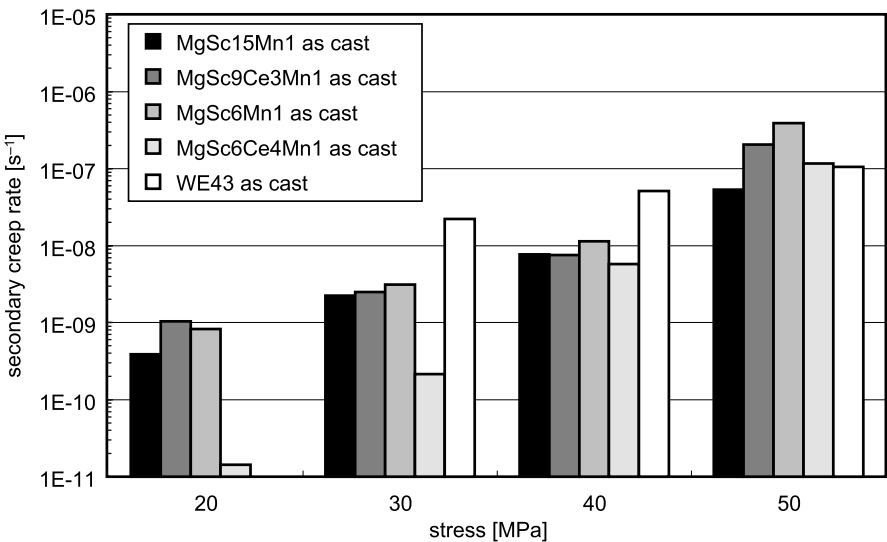


Fig. 3.21. Secondary creep rate of Mg-Sc-(Ce)-Mn alloys (as cast, 300°C)



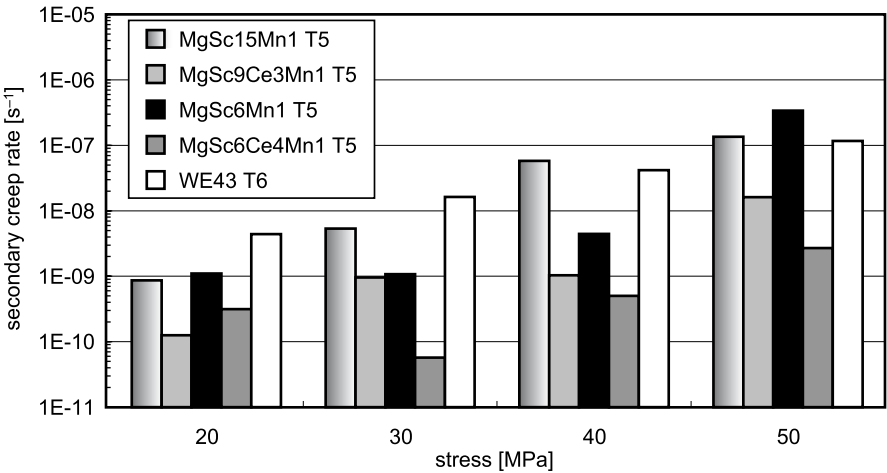


Fig. 3.22. Secondary creep rate of Mg-Sc-(Ce)-Mn alloys (T5, 300°C)

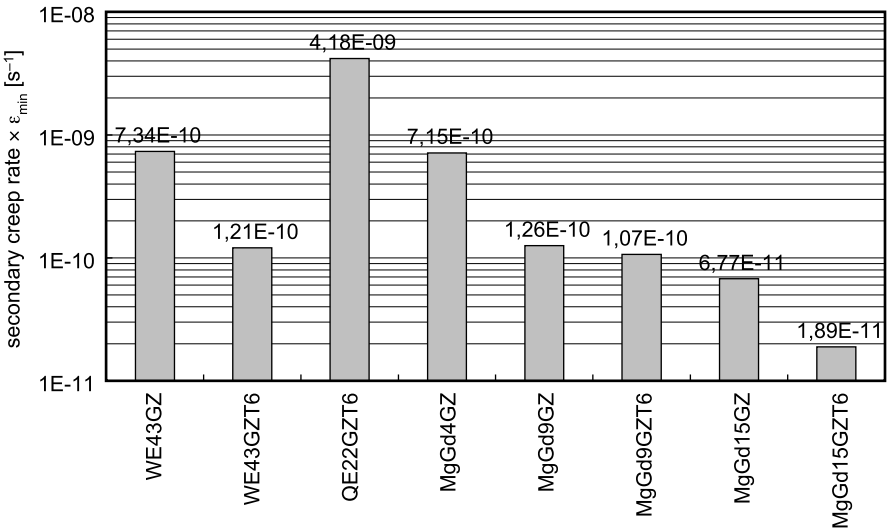


Fig. 3.23. Comparison of secondary creep rate of Mg-Gd with WE43 and QE22 at 200°C. GZ is cast condition

Table 3.13. Secondary creep rate of Mg-Gd-Sc-Mn, Mg-Y-Sc-Mn, Mg-Ce-Sc-Mn alloys

Alloy	$\epsilon$ [s <sup>-1</sup> ]
MgGd10Sc0,8Mn1	$2.67 \times 10^{-8}$
MgGd5Sc0,3Mn1	$2.49 \times 10^{-8}$
MgY4Sc1Mn1	$6.62 \times 10^{-8}$
MgCe3Sc1Mn1	$1.54 \times 10^{-8}$
WE43 T6	$1.10 \times 10^{-6}$

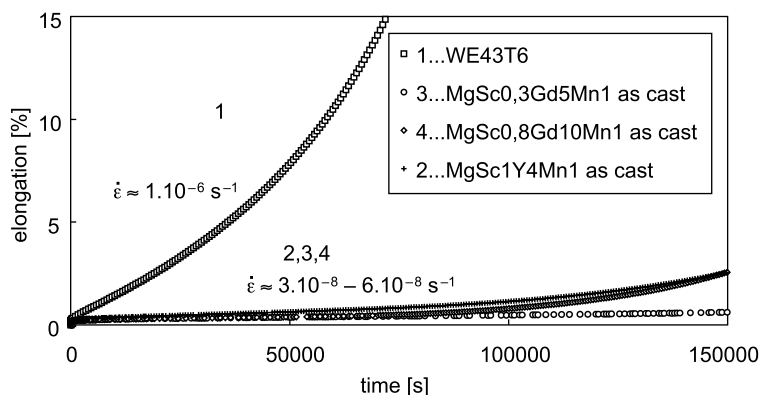


Fig. 3.24. Comparison of creep rate of quaternary alloys with WE43 at 350°C

The creep rates are listed in Table 3.13. The creep rates are almost two orders of magnitude lower than that of WE43 T6.

The thermal stability of the mechanical properties and hence of the microstructure is essential for alloys to be employed at temperatures above 250°C. An arrangement of interlocking plate-shaped precipitates on all three prismatic planes is thought to account for the outstanding high temperature properties of Mg-Th-based alloys. This triangular configuration can be very resistant to coarsening and ensures the highest strengthening. A similar precipitate morphology is found in Mg-RE alloys with cbco metastable plates and Mg<sub>5</sub>Gd type stable plates. Table 3.14 shows the increase in hardness and yield stress produced by age hardening in some of the alloys listed and compared to the stress increase calculated  $\Delta\tau$  using equations taking into account the shape, volume fraction and size of particles as determined by electron microscopy. Such values have only an indicative value. It is clear that the triangular configuration produces the highest hardening in Mg-Gd and Mg-Y-Nd alloys. The same volume fraction and size of basal plates would increase the stress by only half as much if they were present as prismatic cbco plates as in MgGd15 [88].

The low Sc contents show however that a basal dispersion of plates can be effective obstacles to cross slip of basal dislocations at elevated temperatures. Similarly they can be equally effective obstacles in the non-basal prismatic slip system as the prismatic plates are common to the basal slip system.

Combination of alloying rare earths with elements decreasing the solubility of rare earths in Mg and simultaneously forming thermally stable plate shaped particles on the basal planes is clearly a promising method of developing creep resistant magnesium alloys.

**Table 3.14.** Increase in hardness and yield stress of quaternary alloys

Alloy	Treated	Phase	Vol. fract.	Size $\varnothing$	[nm] thickness t	$\Delta HV$	$\Delta R_{p0.2}$ [MPa]	$\Delta \tau$ [MPa]
MgGd15	T4 iso- chr. 280°C	cbco, prism. plates	0.0118	20	5	35	–	55
	T6	cbco, prism. plates	0.0180	15	5	46	65	78
	T4 iso- chr. 240°C	cbco spheres	0.0033	~ 4		35	–	47
	T6 crept 350°C/ 60 MPa	Mg <sub>5</sub> Gd plates	0.1	1300	90	–	15	20
WE63	T4+ 300°C	fcc plates	0.16	830	110	16	27	34
MgSc15Mn1	T5	Mn <sub>2</sub> Sc spheres	0.0010	~ 4.5		23	36	23
MgSc6Ce4Mn1	T5	Mn <sub>2</sub> Sc bas. plates	0.0031	25	5	13	24	11
MgGd5Sc0.3 Mn1	T5	Mn <sub>2</sub> Sc bas. plates	0.0019	12	3	18	8	15
		Mn,Gd bas. plates	0.0027	65	1,5			5
MgGd10Sc0.8 Mn1	T5	cbco prism. plates	0.01	23	4	35	–	52

$\varnothing$  is a diameter of plates, t is thickness of plate. One size only given implies sphere.

## Acknowledgements

The authors would like to thank Dr. Alexandra Rudajevova, Prof. Bohoš Smola, Prof. Ivana Stulikova and Prof. Zuzanka Trojanova for discussions, provision of results and diagrams. We are glad to acknowledge Aluminium-Verlag, Düsseldorf, for permission to reproduce phase diagrams.

## References

1. Magnesium and Magnesium Alloys. ASM Specialty Handbook. (Eds. Avedesian MM, Baker H), ASM International, Materials Park, OH, 1999, pp. 3–6
2. Magnesium and Magnesium Alloys. ASM Specialty Handbook. (Eds. Avedesian MM, Baker H), ASM International, Materials Park, OH, 1999, pp. 7–11

3. Phase Diagrams of Binary Magnesium Alloys. (Eds. Nayeb-Hashemi AA, Clark JB), ASM International, Materials Park, OH, 1988, p.1
4. Raynor GV, Hume-Rothery W (1939), J. Inst. Met. 65, 379
5. Busk RS (1952) Trans. AIME 194, 207
6. Baker H (1967) Physical Properties of Magnesium and Magnesium Alloys. The Dow Chemical Company, Midland, MI
7. Magnesium and Magnesium Alloys. ASM Specialty Handbook. (Eds. Avedesian MM, Baker H), ASM International, Materials Park, OH, 1999
8. McDonald RA, Stull DR (1955) Am. Chem. Soc. 77, 5293
9. Shewmon P (1989), Diffusion in Solids. 2nd ed., TMS, Warrendale, PA
10. Peterson NL (1979) J. Nucl. Mater. 69/70, 3
11. Combronde J, Brebec G (1971) Acta Metall. 19, 1393
12. Aune TK, Westengen H (1995) SAE Technical Paper 950424, Detroit
13. Aune TK, Westengen H (1996) Giesserei – Praxis, Nr. 19/20, 398
14. CRC Handbook of Chemistry and Physics. (Ed. Lide DR Jr.), 78th ed., CRC Press, Boca Raton, FL, 1997, pp. 12-193 – 12-194
15. Collins JG, White GK (1964) Progress in Low Temperature Physics, Vol. 4, North Holland, Amsterdam, pp. 450
16. Bungardt W, Kallenbach R (1950) Metall. 4, 317 and 365
17. Zener C (1948) Elasticity and Anelasticity of Metals. Chicago University Press, Chicago,
18. Nowick AS, Berry BS (1972) Anelastic Relaxation in Crystalline Solids. Academic Press, New York
19. Ke TS (1947) Phys. Rev. 72, 41
20. Caswell HL (1958) J. Appl. Phys. 29, 1210
21. Sack HS (1962) Acta Met. 10, 455
22. Hashiguti RR, Igata N, Kamoshita G (1962) Acta Met. 10, 442
23. Koda S, Kamigaki K, Kayano H (1963) J. Phys. Soc. Japan 18, (Suppl. 1), 195
24. Tsui RTC, Sack HS (1967) Acta Met 15, 1715
25. Roberts JM (1968) Trans. JIM 9, (Suppl.), 69
26. Seyed Reihani SM, Fantozzi G, Esnouf C, Revel G (1979) Scripta Met. 13, 1011
27. Fantozzi G, Esnouf C, Seyed Reihani SM, Revel G (1984) Acta Metall. 32, 2175
28. Arsenaault RJ, Shi N (1986) Mater. Sci. Eng. A81, 175
29. Trojanová Z, Lukáč P, Riehemann W, Mordike BL (2002) Mater. Sci. Eng. 324A, 122
30. Granato AV, Lücke K (1956) J. Appl. Phys. 27, 583 and 789
31. Granato AV, Lücke K (1981) J. Appl. Phys. 52, 7136
32. von Mises R (1928) Z. Angew. Math. Mech. 8, 161
33. Stohr JF, Poirier J (1972) Phil. Mag. 25, 1313
34. Obara T, Yoshinaga H, Morozumi S (1973) Acta Metall. 21, 845
35. Ando S, Nakamura K, Takashima K, Tonda H (1962) J. Japan Institute Light Metals 42, 765
36. Flynn PW, Mote J, Dorn JE (1961) Trans. AIME 221, 1148
37. Akhtar A, Teghtsoonian E (1969) Acta Metall. 17, 1351
38. Escaravage C, Bach P, Champier G (1979) in: Proc. 2nd International Conference on the Strength of Metals and Alloys. ASM, Pacific Grove, p. 299
39. Urakami A, Meshii A, Fine MF (1970) in: Proc. 2nd International Conference on the Strength of Metals and Alloys. ASM, Pacific Grove, p. 272
40. Ahmadiéh A, Mitchell J, Dorn JE (1965) Trans. AIME 233, 1130
41. Ando S, Tonda H (2000) Mater. Sci. Forum 350–351, 43
42. Ando S, Tonda H (2000) Mater. Trans. JIM 41, 1188
43. Lavrentev FF, Salita OP, Lukáč P (1982) Acta Universitatis Carolinae, Mathematica et Physica 23, 33
44. Lukáč P (1985) Czech. J. Phys. B35, 275
45. Zhang P, Watzinger B, Kong QP, Blum W (2000) Key Eng. Mater. 171–174, 609
46. Lavrentev FF (1980) Mater. Sci. Eng. 46, 191
47. Fleischer RL (1964) in: Strengthening of Metals. (Ed. Peckner D), Reinhold, New York, p. 29

48. Labusch R (1970) *Phys. Stat. Sol.* 41, 659
49. Lukáč P (1992) *Phys. Stat. Sol. (a)* 131, 377
50. Pearson WB (1958) *Handbook of Lattice Spacing and Structure of Metals and Alloys*. Pergamon Press, London
51. King HV (1966) *J. Mater. Sci.* 1, 79
52. Hashin Z (1962) *J. Appl. Mech.* 29, 143
53. Brown LM, Ham RK (1971) in: *Strengthening Methods in Crystals*. (Eds. Kelly A, Nicholson RB), Applied Science, London, p. 9
54. Gerold V (1979) in: *Dislocations in Solids*. Vol. 4. (Ed. Nabarro FRN), North-Holland, Amsterdam, p. 219
55. Reppich B (1993) in: *Materials Science and Technology*. Vol. 6. (Eds. Cahn R, Haasen P, Kramer EJ), VCH, Weinheim, p. 311
56. Hall EO (1951) *Proc Phys. Soc. (London)* 64B, 747
57. Petch NJ (1953) *J. Iron Steel Inst.* 174, 25
58. Armstrong RW, Codd I, Douthwaite RM, Petch NJ (1962) *Phil. Mag.* 7, 45
59. Hauser FE, Landon PR, Dorn JE (1956) *Trans. AIME* 206, 589
60. Wilson DV (1970) *J. Inst. Metals* 98, 133
61. Sambasiva Rao G, Prasad YVRK (1982) *Metall. Trans.* 13A, 2219
62. Sambasiva Rao G, Prasad YVRK (1983) *J. Mater. Sci.* 18, 2385
63. Nussbaum G, Sainfort P, Regazzoni G, Gjestland H (1989) *Scripta Metall.* 23, 1079
64. Jones H (1994) *Key Eng. Mater.* 97–98, 1
65. Armstrong RW (1968) *Acta Metall.* 16, 347
66. Flynn PW, Mote J, Dorn JE (1961) *Trans. AIME* 221, 1148
67. Hume-Rothery W, Raynor GE (1956) *Structure of Metals and Alloys*, Institute of Metals, London
68. Raynor GW (1959) *Physical Metallurgy of Magnesium and its Alloys*. Pergamon Press, New York, p. 103
69. Roberts CS (1969) *Magnesium and its Alloys*, J. Wiley and Sons, New York, p. 17
70. Jackson PJ, Frost PO (1967) NASA Report SP-5068
71. Delfino S, Saccorè A, Ferro R (1990), *Metall. Trans.* 21A, 2109–2114
72. *Binary Alloy Phase Diagrams*, 2nd Edition. (Ed. Massalski TB), ASM International, Materials Park, OH, 1996, p. 41
73. *Binary Alloy Phase Diagrams*, 2nd Edition. (Ed. Massalski TB), ASM International, Materials Park, OH, 1996, p. 1559
74. Pisch A, Schmid-Fetzel R, Cacciamani G, Riani P, Saccone A, Ferro R (1998) *Z. Metallkunde* 89, 474–477
75. *Binary Alloy Phase Diagrams*, 2nd Edition (Ed. Massalski TB), ASM International, Materials Park, OH, 1996, p. 1566
76. *Magnesium Taschenbuch*, Aluminium Verlag Düsseldorf, (Ed. C Kammer), 2000, p. 125
77. von Buch F, Lietzau J, Mordike BL, Pisch A, Schmid-Fetzer R (1999) *Mater. Sci. Eng.* A263, 1–7
78. Polmear IL (1992) in: *Magnesium Alloys and their Applications*. (Eds. Mordike BL, Hehmann F), DGM Informationsgesellschaft, Oberursel, pp. 201–212
79. Mordike BL, Henning W (1987) in: *Proc. of London Conference on Magnesium Technology*, (Ed. Baker H), Institute of Metals, London, 1987, p. 54
80. Lorimer GW (1987) in: *Proc. of London Conference on Magnesium Technology*, (Ed. Baker H), Institute of Metals, London, p. 47–53
81. Juchmann P (1998) *Beitrag zur Eigenschaftsentwicklung von Mg-Werkstoffen durch Lithium*. PhD Thesis, Hannover, VDI Fortschritt Berichte Reihe 5, Nr. 554
82. Hartmann (2000) in: *Kammer C, Magnesium Taschenbuch*, Aluminium Verlag, Düsseldorf, pp. 519–524
83. Ebert T, Mordike BL (2001), *Materialwissenschaft und Werkstofftechnik* 32, 36
84. Hartmann D (2000) in: *C. Kammer, Magnesium Taschenbuch*, Aluminium Verlag, Düsseldorf, pp. 516

85. von Buch F, Mordike BL (1998) in: Magnesium 97. (EDS. Aghion E, Eliezer D) Magnesium Research Institute, Beer Sheva, pp. 163
86. Mordike BL (2002) Mater. Sci. Eng. A324, 1033
87. Mordike BL (2001) J. Mater. Processing, Technology 117, 391
88. Smola B, Stulikova I, Fon Buch F, Mordike BL (2002) Mater. Sci. Eng. A324, 113
89. Magnesium and Magnesium Alloys. ASM Specialty Handbook. (Eds. Avedesian MM, Baker H), ASM international, Materials Park, OH, 1999
90. Aune TK, Westengen H (1996) Giesserei – Praxis, Nr. 19/20, 398
91. Rudajevová A, Kiehn J, Kainer KU, BMordike BL, Lukáč P (1999) Scripta mater. 40, 57
92. Rudajevová A, Lukáč P (1999) Phys. Stat. Sol. (a) 175, 547
93. Rudajevová A, von Buch F, Mordike BL (1999) J. Alloys Comp, vol. 292, p. 27
94. Hasselman DPH, Johnson LF (1987) J. Comp. Mater. 21, 508

## Appendix

Table 3.15 presents the values of the thermal conductivity for some commercially produced magnesium alloys based on aluminum as the major alloying element. The values were estimated at room temperature.

The temperature dependence of the thermal conductivity of cp-Mg, AZ91 is given in Table 3.16 [91] and QE22, the most widely used Mg-Ag casting alloy, is given in Table 3.17 [92]. The values of the thermal conductivity were estimated by using flash method.

Addition of an alloying element to magnesium causes a decrease in the thermal conductivity of the alloy with increasing alloying element content. Rudajevová et al. [93] measured the temperature dependence of the thermal conductivity of some Mg-Sc alloys using flash method. The values of the thermal conductivity of the alloys at room temperature, their chemical composition and preparation are given in Table 3.18.

**Table 3.15.** Thermal conductivity for various cast magnesium alloys [89, 90]

Alloy	AZ91	AM20	AM50	AM60	AS21	AS41	AE42
K [W/mK]	51	94	65	61	84	68	84

**Table 3.16.** Temperature influence on the thermal conductivity of AZ91 alloy

T [°C]	20	50	100	150	200	250
K [W/mK]	51.2	54.7	59.9	65.4	70.8	77.1

**Table 3.17.** The values of the thermal conductivity in W/mK of cp-Mg and QE22 alloy

T [°C]	20	50	100	150	200	250	300
cp-Mg	135.1	137.5	142.1	141.8	140.2	140.1	140.6
QE22	116.4	118.8	122.3	123.6	124.8	126.2	125.8

**Table 3.18.** Composition of Mg-Sc alloys and their thermal conductivity at RT

Alloy designation	Sc content [mass %]	K [W/mK] at RT	Casting route
MgS4	3.23	55.7	squeeze casting
MgSc8	7.42	30.9	squeeze casting
MgSc12	10.14	27.7	squeeze casting
MgSc16	11.11	24.7	squeeze casting
MgSc12 MEL	14.54	20	sand casting
MgSc16 MEL	19.09	17	ingot casting

**Table 3.19.** Thermal conductivity of Mg-Sc alloys at selected temperatures

T [°C]	20	50	100	150	200	250	300
Mg4Sc	55.7	58.5	62.6	68.9	72.0	75.2	78.7
Mg8Sc	30.9	32.6	36.4	39.8	42.7	46.5	49.4
Mg12Sc	27.7	29.2	32.3	36.1	39.2	42.1	45.2
Mg16Sc	24.7	26.3	29.2	32.7	25.6	38.4	41.4

**Table 3.20.** Thermal conductivity of AZ91 alloy and AZ91 composite (MMC)

K [W/mK]	50°C	100°C	150°C	200°C	250°C	300°C
AZ91	55.6	60.5	64.7	68.0	71.4	72.8
AZ91MMC	35.5	38.7	40.7	43.9	43.2	46.4

**Table 3.21.** Thermal conductivity of SiCp/QE22 composites

T [°C]	20	50	100	150	200	250	300
10SiC/QE22	110.7	112.8	116.0	119.2	119.9	120.4	121.1
15SiC/QE22	109.2	110.1	113.2	113.8	113.9	113.8	114.4
25SiC/QE22	106.1	106.6	107.8	107.8	106.6	105.5	104.5

The values of the thermal conductivity of some Mg-Sc alloys at selected temperatures are listed in Table 3.19 [93].

The temperature variation of the thermal conductivity of specimens of AZ91 alloy reinforced with 22.6 vol.% short Saffil fibres is listed in Table 3.20 [91]. Table 3.20 presents also the thermal conductivity of unreinforced AZ91 alloy; the specimens were prepared by squeeze casting.

The temperature dependences of the thermal conductivity of QE22 alloy and QE22 alloys reinforced by 10, 15 and 25 vol.% SiC particles are given in Table 3.21 [92].

The thermal conductivity of a composite is a complex function of the thermal conductivity of the matrix, thermal conductivity of particles (fibres) and their radius, and also the thermal conductance of the interface.

The ratio of the thermal conductivity of a composite  $K_c$  to the thermal conductivity of the matrix  $K_m$  i.e.  $K_c/K_m$  can be calculated from the thermal conductivity of both components of the composite and the volume fraction of particles knowing the thermal conductance of the interface,  $h$ , (thermal conductance is the inverse of the thermal boundary resistance) from the relation (A) deduced by Hasselman and Johnson [94] for composites with spherical particles

$$\frac{K_c}{K_m} = \frac{\left[ 2f \left( \frac{K_p}{K_m} - \frac{K_p}{r.h} - 1 \right) + \frac{K_p}{K_m} + 2 \frac{K_p}{r.h} + 2 \right]}{\left[ f \left( 1 - \frac{K_p}{K_m} + \frac{K_p}{r.h} \right) + \frac{K_p}{K_m} + \frac{K_p}{r.h} + 2 \right]} \quad (3.39)$$

where  $K_p$  is the thermal conductivity of particles and  $r$  is their radius. A similar relation has been also derived for the fibre composite when the heat flow is perpendicular to fibres [95]:

$$\frac{K_c}{K_m} = \frac{\left[ f \left( \frac{K_f}{K_m} - \frac{K_f}{r.h} - 1 \right) + \frac{K_f}{K_m} + \frac{K_f}{r.h} + 1 \right]}{\left[ f \left( 1 - \frac{K_f}{K_m} + \frac{K_f}{r.h} \right) + \frac{K_f}{K_m} + \frac{K_f}{r.h} + 1 \right]} \quad (3.40)$$

where  $K_f$  is the thermal conductivity of fibres and  $r$  is their radius.



---

## 4 Melting, Alloying and Refining

### 4.1 Zirconium-Free Alloys

*Mihriban Pekgülyüz*

With the automotive, electronic and consumer goods industries embracing magnesium in their applications, magnesium alloys that do not contain zirconium have gained a higher market share than alloys which do. The zirconium-free alloys include important alloy classes such as Mg-Al, Mg-Al-Zn, Mg-Al-Si, Mg-Al-(Rare-Earths), Mg-Al-(Alkaline Earths), Mg-Li and alloys that contain a number of rare alloying elements such as combinations of rare earths, alkaline earths and lanthanides. While Mg-Al, Mg-Al-Zn and Mg-Al-Si are commercial, the other alloy systems are either semi-commercial or being developed.

#### 4.1.1 Mg-Al, Mg-Al-Zn, and Mg-Al-Si Alloys

The main alloying elements in these alloys are two or more of the elements from the following list: Al, Zn, Mn, Be, Si. Addition of Al, Zn, and Si are straightforward [1] while Mn and Be require more control. Magnesium can be melted and alloyed to produce Mg-Al based alloys using electric resistance, gas-fired and induction furnaces with mild steel crucibles.

As in all magnesium alloys, Mg-Al based alloy melts must be protected against oxidation and burning during melting, alloying and casting. The Mg-Al alloy-melt forms a porous  $\text{MgO-Al}_2\text{O}_3$  surface layer, which does not offer resistance to oxidation and burning. Fluxes (employing molten salt mixtures) or fluxless-melting techniques (using protective gas mixtures, such as  $\text{SO}_2$ , or  $\text{SF}_6$  mixed with  $\text{CO}_2$ , dry air or  $\text{N}_2$ ) can be used depending on alloy compositions and processing conditions.

##### 4.1.1.1 Flux Melting and Refining

Flux melting, alloying and refining of Mg-Al based alloys has had a long historical development. This can be found in detail in Emley's classic book on magnesium technology [1, pp. 72–73]. Early fluxes consisted of  $\text{MgCl}_2$ , which would solidify above the melting point of Mg. This led to chloride inclusions in the melt (Fig. 4.1).

In order to solve these problems a number of methods were developed. Flux compositions were usually adjusted to melt below the melting point of the alloys

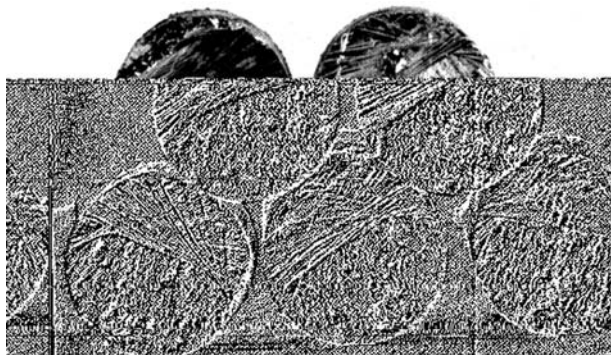


Fig. 4.1. Flux inclusion in cast magnesium alloy: a severe problem in early days of magnesium melting, alloying and casting [1, p. 72]

so that they spread-out and protect the solid metal from oxidation prior to melting. Alkaline earth metal chlorides such as  $\text{BaCl}_2$  were added to adjust the melting point. Another early method involved the addition of porous substances such as  $\text{MgO}$  to absorb the chlorides. These techniques did not provide the optimum solution but added to the overall knowledge base on flux melting of  $\text{Mg}$ .

$\text{BaCl}_2$  was also commonly part of the composition of early fluxes due to its high density, which would encourage the flux and the flux-oxide particulates to settle to the bottom. The elimination of  $\text{BaCl}_2$  due to environmental regulations prompted wider use of inspissated (thick) flux to promote separation by agglomeration due to the surface tension or tacky character of the salt phase. Between 1922 and 1938, the development of thickened (inspissated fluxes) consisting of  $\text{MgCl}_2$  and thickening agents such as  $\text{MgO}$  and  $\text{MgF}_2$  were developed. The flux could provide a thin viscous protective layer on the melt surface and avoided the risk of chloride inclusions arising from the use of excess flux. Dow Chemical contributed to the development of the flux melting process of magnesium from the early days. Dow used molten fluxes an amount of 20–50% of the charge weight. Initially,  $\text{MgCl}_2$ - $\text{NaCl}$  eutectic compositions were used but later adjusted to form a flux layer that floated on top of the melt. This still led to trace levels of flux inclusions in the cast metal.

The modern flux technique developed by Dow gave rise to a number of commercially available fluxes for magnesium. The composition could be varied – high potassium flux (M134) has lower density, which made a better cover flux than high  $\text{MgCl}_2$  (M-130). At Dow, only M130 was typically used in the open pots and the protection of melts was achieved by adding the flux after significant oxidation had occurred. In essence this created an inspissated flux in-place on the melt surface, which would provide protection for hours if it was not alloyed to dry-out. Magnesium Elektron also developed an alternate technique of using a two-flux process, which uses a fluid protective flux for melting and an inspissated thick flux applied to the melt surface when the melting is complete.

The mechanism of the chloride flux in preventing oxidation and burning of magnesium melts is relatively well understood [1, p. 100]. This involves the wet-

ting of the underlying metal surface with very thin chloride films, thereby preventing the adsorption of oxygen molecules and consequent scale formation. This usually means that even if you have a non-continuous layer of powdered flux sprinkled on liquid magnesium, the vapours arising from the melting of magnesium chloride or calcium chloride of the flux is sufficient for the formation of a protective thin chloride film on the melt surface, which is not directly covered. Fluid fluxes also have a high affinity for the oxide phase – so they wet both the oxide on the solid metal prior to melting as well as the oxide on the melt surface.

The protective function of the fluxes can also be explained by the Pilling and Bedworth factor [2]

$$F = W_o d_m / W_m d_o \quad (4.1)$$

where  $W_o$  = molecular weight of the surface oxide

$W_m$  = atomic weight of the metal

$d_o$  = density of the oxide

$d_m$  = density of the metal.

According to this, a surface oxide is protective if its factor is above 1.0. This theory has an additional complication when applied to liquid metals, because of the compression of the surface film due to surface tension. Delauvaut [3] has shown that the factor changes if various elements are incorporated into the surface film (see Table 4.1).

The function of flux is not only for protecting against oxidation and burning but also for refining (i.e., removing oxides and non-metallic inclusions) from the melt. This is achieved by appropriate use of fluid and inspissated fluxes. The presence of oxides in cast magnesium can be traced back to, among other factors, insufficient skimming of the melt surface before pouring, pump removal of metal where the inlet is too close to the bottom of the crucible thus picking up settled oxides, insufficient settling time after application of inspissated fluxes, and turbulence during pouring (Fig. 4.2). Nitride inclusions may also be found if the alloy has nitride forming elements such as sodium and barium. These oxide and nitride inclusions tend to settle to the bottom in fluxed melts (Fig. 4.3).

Flux inclusions occur if unabsorbed protective flux remains on the metal surface, the flux is too fluid, there is brittle or powdery flux due to long handling, pouring is too fast or if there is incomplete removal of the flux adhering to the lip of the pot before pouring. Here stirring of the metal is needed to help the re-

**Table 4.1.** Protection coefficient of surface films on magnesium melts

Surface film formed	Protection Coefficient
$Mg + O = MgO$	0.71
$Mg + H_2O = MgO + H_2$	0.71
$3Mg + N_2 = Mg_3N_2$	0.79
$Mg + S = MgS$	1.26
$3Mg + 2BF_3 = 3MgF_2 + 2B$	1.32
$Mg + 2HF = MgF_2 + H_2$	1.32
$3MgO + 2BF_3 = B_2O_3 + 3MgF_2$	3.1

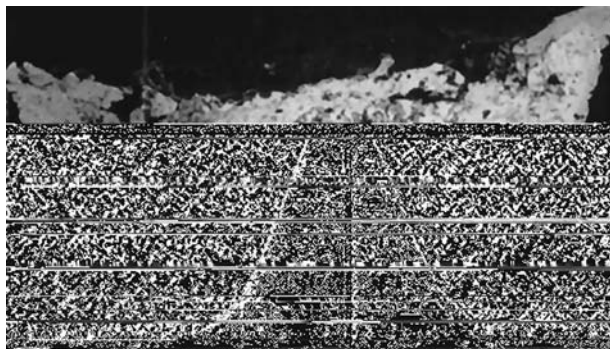


Fig. 4.2. Polished section of an ingot (Mg-8% Al), showing the oxide inclusions in the absence of a refining flux [1]

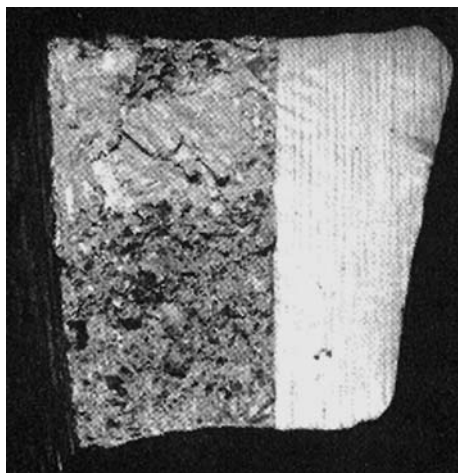


Fig. 4.3. Fracture surface of an ingot cast at 750°C showing the settling of the oxides [1]

fining process. As the metal is stirred, the agitation of the metal brings the excess fluid flux, oxides, and inspissated flux together into a single thickened phase, which coalesces and settles to the bottom. When the balance of fluid flux, oxides and inspissated flux is correct, the melt will be left free of both oxide and flux and the settled phase will be pasty or custard-like. If too little flux is present the settled phase will be crumbly and dry in appearance. If the flux content is too high the settled phase will remain fluid and free flowing. In both of the latter two cases, the melt will likely remain contaminated by suspended flux-oxide inclusions.

Hence, to perform both its functions, the inspissated flux has to have the following properties [1]:

- (a) The flux must have a consistency that allows it to be drawn back before pouring without leaving a film or particles on the exposed metal surface.

- (b) The flux must be homogeneous and not separate into a dry surface level and a more fluid layer below.
- (c) It should be able to absorb excessive amount of oxides without becoming too dry.
- (d) It should be able to absorb a fluid protective flux.
- (e) The flux should not be too sensitive to temperatures up to 950°C changing consistency or becoming brittle and powdery upon prolonged holding in the furnace.
- (f) The flux should have good wetting and spreading characteristics and not lose wetability with time at temperature.
- (g) It should have a low hygroscopicity.
- (h) An inspissated flux that is used both for protection and refining should be capable of being partly stirred through the metal and should not adhere readily to the sides or the bottom of the crucible.
- (i) Density can be important for both fluid and inspissated fluxes. In fluid fluxes, lower densities are necessary to keep the flux on the surface of the melt. Higher density may aid in the separation of the flux and flux-oxides from the metal. In years past the addition of  $\text{BaCl}_2$ , a heavy salt, was used for this purpose but today environmental controls on barium salts have eliminated this option in most regions of the world.

The compositions that give rise to various flux attributes are discussed by Emley [1, pp. 117–124] in detail. Some compositions are given in Table 4.2. The general design rules that emerge are that some fluoride is normally desirable for homogeneity; a stoichiometric excess of  $\text{MgCl}_2$  over the fluorides (other than  $\text{MgF}_2$ ) is required to avoid temperature sensitivity and loss of wetability and protective bases free from  $\text{MgCl}_2$  should be inspissated with  $\text{MgF}_2$ .

#### **4.1.1.2 Fluxless Melting, and Alloying (the use of Cover gases)**

The fluxless-method of melt-protection during melting and alloying of Mg-Al based alloys have been developed since the 1970s. Mixtures of  $\text{CO}_2$ ,  $\text{CO}_2$ -air, or air alone combined with 0.3 to 0.5%  $\text{SF}_6$  have been successfully used for melt protection in casting operations thus essentially eliminating the problems due to flux inclusions. Due to the global warming potential of  $\text{SF}_6$ , which is 24,000 times that of  $\text{CO}_2$ , alternative protective gases are currently under development. One alternative is the use of 1–2%  $\text{SO}_2$  in either nitrogen or in air. The toxicity and the corrosiveness of the  $\text{SO}_2$  gas necessitates adherence to good engineering practices and designs to properly manage the industrial hygiene and safety issues of this gas mixture. All aspects of the design require review from bulk storage of the  $\text{SO}_2$  to the final mixing and use. Good ventilation systems are normally required.

When melting in the absence of fluxes, the oxides formed tend to float at or near the surface due to their porous character and their association with the gases liberated during the melting operation. In most processes it is desirable to refine the melt by removing these oxides. Removal of the oxides is critical in the recycling of scrap metal. Presently there are only a handful of foundries that practice fluxless recycling of magnesium scrap. Fluxless refining can be effectively

**Table 4.2.** Chemical composition of various refining fluxes

Protective base, wt %				Inspissating agents, wt %							General type	Comments
MgCl <sub>2</sub>	CaCl <sub>2</sub>	NaCl	KCl	BaCl <sub>2</sub>	BaF <sub>2</sub>	MgF <sub>2</sub>	CaF <sub>2</sub>	MgO	SiO <sub>2</sub>	C		
–	41	26	9	–	–	24	–	–	–	–	MgCl <sub>2</sub> free	CaCl <sub>2</sub> rich
–	19	11	7.5	37.5	–	25	–	–	–	–	Oxide free	BaCl <sub>2</sub> rich
–	–	17	26	40	–	17	–	–	–	–		CaCl <sub>2</sub> free
65	–	–	–	–	–	35	–	–	–	–	No alkali metal chlorides, oxide free	
38	–	–	31	–	–	31	–	–	–	–	Oxide free	KCl rich
29	20	12	6	–	–	–	33	–	–	–	Oxide free	Ba free
29	–	–	8	39	24	–	–	–	–	–	Oxide free	Ba rich
31	7	6	25	–	–	–	21	5	–	–	Standard inspissated	Elrasal D
34	15	10	7	–	–	–	21	13	–	–		Melrasal E
50	–	–	20	–	–	–	15	15	–	–		Dow 310

achieved with standard Mg-Al alloys by flushing argon gas throughout the melt. This will accelerate the floatation of the oxides to the melt surface where they can then be removed. Work has also been done using baffled furnace designs with high residence times, which allows the oxides to float to the melt surface naturally as a result of the hydrogen content in the melt. Hydrogen results from the thermal decomposition of the hydrous oxide skins and also the decomposition of residual hydrocarbon lubricants on the scrap surfaces [4–6].

The mechanism of melt protection with these gases is not completely understood. It is postulated that fluorine offers the best protection by being incorporated into the surface film and changing its Pilling and Bedworth factor to above 1.0, which means the surface film is continuous and protective (Table 4.3). Sulphur or sulphur dioxide also provides protection but the role of sulphur gases is also poorly understood in relationship to providing a barrier to oxygen in the environment.  $\text{SF}_6$ , being a source of both sulphur and fluorine, provides a very effective barrier. Other gases such as carbon dioxide or argon are less effective (although heavier than air at ambient temperatures) at the temperatures used in processing magnesium melts. They can not form an effective gaseous barrier to the diffusion of air to the melt surface and they do not form protective films on the metal surface. Carbon dioxide has been used in a limited fashion in foundries, but it requires a continuous flow of fresh  $\text{CO}_2$  onto the melt surface and strict temperature control. At elevated melt temperatures the carbon dioxide will react rapidly, forming carbon monoxide and magnesium oxide. New gas protection systems are under development to address the environmental effects associated with the exceptionally high global warming potential (GWP) of  $\text{SF}_6$ . To date, the best candidates appear to be a few select fluorocarbons, which are of low toxicity, low GWP, and are of limited environmental impact [7].

#### 4.1.1.3 Alloying of Mg with Al, Zn, Si

Aluminum, zinc and silicon are added directly to liquid magnesium at temperatures around 680–750°C [1, 8]. All three elements are normally added in elemental form. Recoveries range between 70–90%. If large melts are involved, the additions are usually placed in a perforated metal basket, and the melt stirred for homogeneity. Care must be exercised when adding aluminum to be positive that the ingot does not maintain direct contact with the steel crucible. Because of its limited solubility and high melting-temperature elemental silicon is the most dif-

**Table 4.3.** Protection coefficient of surface films on magnesium melts [3]

Surface film formed	Protection coefficient
$\text{Mg} + \text{S} = \text{MgS}$	1.26
$3\text{Mg} + 2\text{BF}_3 = 3\text{MgF}_2 + 2\text{B}$	1.32
$\text{Mg} + 2\text{HF} = \text{MgF}_2 + \text{H}_2$	1.32
$3\text{Mg} + \text{N}_2 = \text{Mg}_3\text{N}_2$	0.79
$\text{Mg} + \text{CO}_2 = 2\text{MgO} + \text{C}$	0.9
$2\text{Mg} + \text{CO} = \text{MgO} + \text{C}$	1.08



difficult to alloy and typically requires more time and agitation to complete the desired addition. Both fluxes and protective gas mixtures can be successfully used in making these alloy additions. For the alloys to meet today's high purity standards, the alloy ingredients must be carefully selected for purity.

#### 4.1.1.4 Manganese

Manganese is added to the alloys mainly for corrosion resistance. In Mg-Al alloys, manganese combines with the detrimental impurity iron and precipitates it to the bottom of the melt as a Fe-Mn-Al intermetallic. The precipitated intermetallic has been identified as  $\text{Al}_5(\text{Mn,Fe})_2$ . In addition to reducing the soluble iron content in the alloy melt, the manganese addition also passivates the residual iron that remains in solution provided the content is less than a critical limit for the alloy, referred to as the critical Fe/Mn ratio. This is discussed in additional detail in the chapter titled Corrosion [9]. Manganese additions can be problematic since the melting point of manganese is high and the solubility of manganese is reduced with aluminum in the melt. Various manganese additives and addition techniques can be used. Mn can be added as anhydrous  $\text{MnCl}_2$  flake, or as electrolytic manganese in the form of flake or briquettes.

For  $\text{MnCl}_2$  additions, anhydrous flake should be employed at high melt temperature (700–730°C). The melt surface is skimmed and the  $\text{MnCl}_2$  flake is stirred into the melt. Use of  $\text{MnCl}_2$  powder is discouraged because of very low alloy efficiency and high HCL emissions. Mn enters the alloy through the reaction ( $\text{MnCl}_2 + \text{Mg} = \text{MgCl}_2 + \text{Mn}$ ) with a wide range of recoveries from 35–90%. Recovery is heavily dependent on the quality of the reagent and on whether the melt protection is flux or mixed gases. The use of  $\text{MnCl}_2$  flake is common due to the ease in making the alloy addition but has drawbacks of HCL emissions during the reagent addition due to reaction of the chlorides with moisture in the air and frequent removal of sludge accumulation due to low alloying efficiencies. Also, because  $\text{MgCl}_2$  is generated in the reaction of the  $\text{MnCl}_2$  with the melt, this is not the reagent of choice where a flux-free product is critical. Figure 4.4 shows the rapidly quenched surface layer of the melt obtained during  $\text{MnCl}_2$  addition under flux protection [1]. It can be seen that Mn is found in the form of massive particles while some of the Mn is embedded in the flux phase. Manganese then dissolves into the magnesium melt from these intermetallic particles lowering the Fe content of the alloy to acceptable levels. Figure 4.5 shows a graph of Mn recovery from these Mn massive reaction products at melt temperatures of 750–800°C. The lower alloying efficiency may be due to the entrapment of the Mn particles in the flux phase and can be minimised through stirring of the surface layer. Mn can also be added in the form of electrolytic pure manganese (99.7–99.8% purity) as shown in Table 4.4. This may come in the form of powdered or flaked manganese packed in super sacs, drums or bags. For fluxed melts the melt temperature is kept at 750–800°C and the metal is stirred vigorously for some time. For best results the flake size needs to be controlled which means that finer flakes need to be removed or compacted. The solubility of Mn is generally high in pure Mg (about 2% at the melting point) but is greatly influenced by aluminum [2, 3]. The solubility of Mn in a Mg-Al alloys is shown in Fig. 4.6.



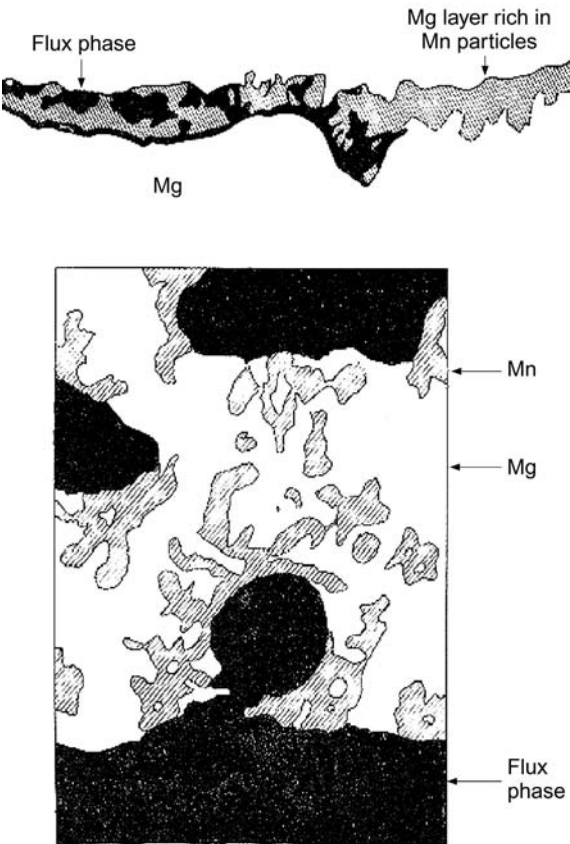


Fig. 4.4. Sections through layer formed when MnCl<sub>2</sub> is sprinkled on molten magnesium [1, p. 163]

Table 4.4. Typical chemical compositions of Mn additives

Additive	% Element									Others
	Mn	Al	Si	Fe	Ni	Cu	S	P	Se	
Pure Mn powder	99.8	–	0.0046	0.02	–	–	0.02	0.0035	0.07	Mn powder size –40 to –320 mesh
75/25 Mn/Al	75.0	24.4	0.016	0.086	0.002	0.003	–	–		Briquette

A final method that can be discussed is adding a liquid Al-Mn alloy into magnesium melts to get alloying efficiencies greater than 90%. This requires the preparation of the Mn-Al liquid alloy in a separate crucible, which is then transferred to the Mg melt. Since aluminium reduces the solubility of Mn in Mg [10], the addition of Mn prior to the addition of Al can be an option. However, this is

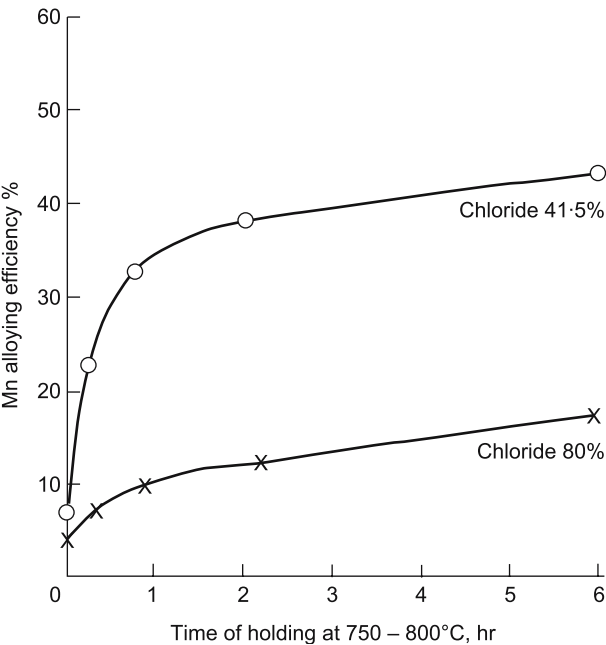


Fig. 4.5. Manganese pick-up from chloride coated particles [1, p. 164]

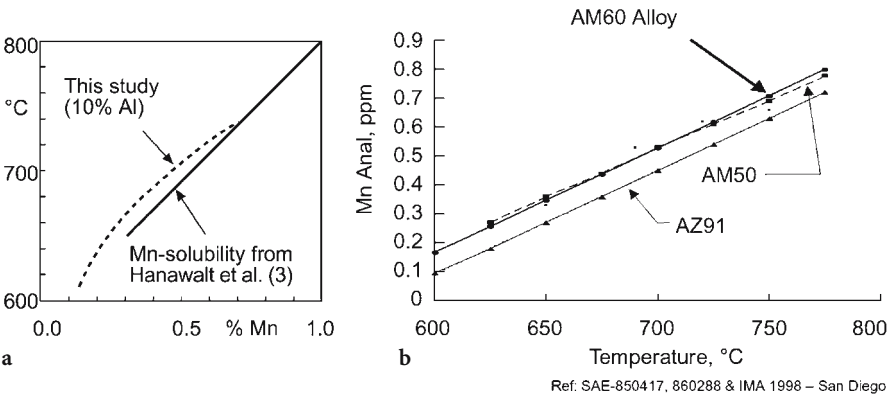


Fig. 4.6a, b. a Mn solubility in Mn-10% Al alloy [10]; b Mn solubility in AZ91, AM50 and AM60 alloys [9]

not always possible and Mn usually needs to be added towards the end, or at the end, in order to precipitate out Fe introduced by other alloying elements.

In Mg-Al based alloys, Mn precipitates out Fe in the form of Mn-Al-Fe intermetallic compounds, which settle to the bottom of the melt and are incorporated into the sludge phase (Fig. 4.7). Slight variations are observed in the Mn-Fe ratios of the intermetallics from various locations in the sludge phase.

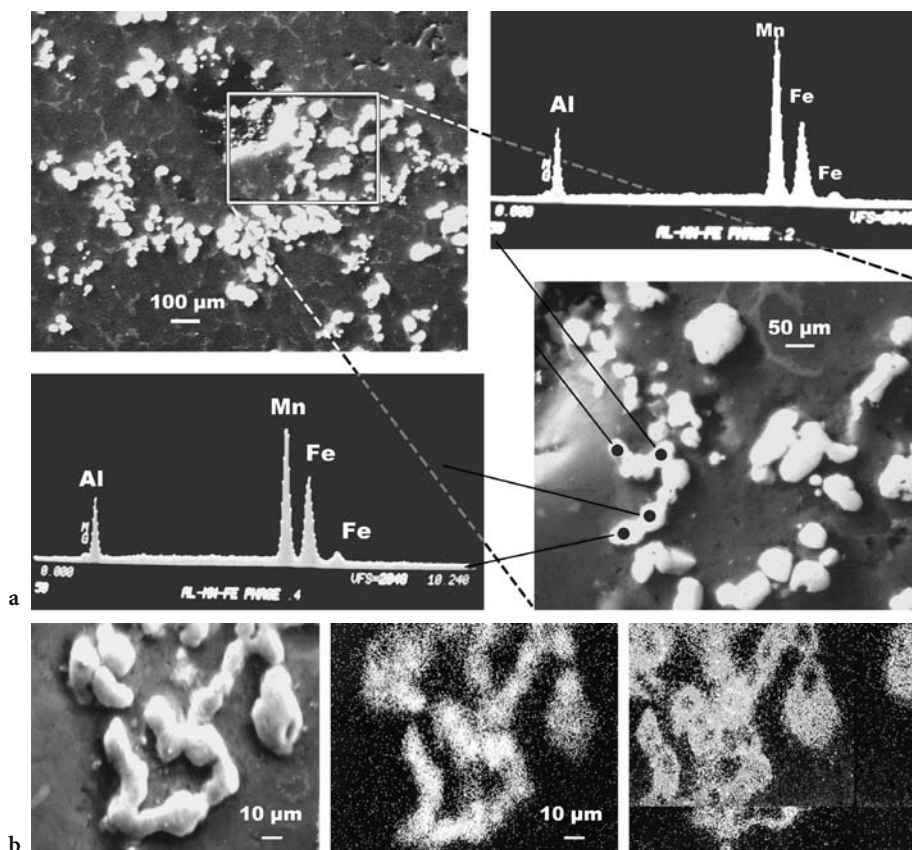


Fig. 4.7a, b. a Scanning electron micrographs and EDX analysis of the sludge phase containing Mn-Al-Fe intermetallics; b SEM image of the Mn-Al-Fe particle and the corresponding Fe and Mn elemental maps

#### 4.1.1.5 Beryllium

Beryllium is added to magnesium die cast alloys at trace levels of 5–30 ppm for improved oxidation resistance of the molten metal [11]. Laboratory experiments show that the degree of oxidation after five hours of melt holding at 700°C for AZ91 with no Be is three times that for AZ91 containing 9 ppm Be. The exact role of Be in reducing the melt oxidation rate is not well understood. Various theories exist on the effect of Be in changing the stability of the surface oxide layer [12]. Its incorporation into the melt surface oxide is through the formation of a mixed BeO-MgO layer [12]. Its surface protective role has been attributed to the densification of the oxide film. This film is flexible and resists the vapour pressure of magnesium. Spielberg et al. [12] further explain the behaviour of Be during alloying. The density of Be being much higher than Mg, Be in excess of solid solubility first settles to the bottom of the melt and then forms  $\text{MgBe}_{13}$  intermetallics

which move upwards with melt convection. Be dissolves from these intermetallics continuously repairing the mixed surface oxide layer providing continued protection. Beryllium also lowers the surface tension of magnesium providing additional protection.

The most convenient way of adding Be which will be discussed here is through an Al-5% Be master alloy. Recoveries of Be depend on the Al and Mn content of the melt, the iron pick-up and the settling conditions.

The solubility of Be in molten Mg is limited (0.005%) and increases with Al content, but decreases with the Mn content. Be precipitates iron from Mg melts. If high melt temperatures are used, excessive Fe pick-up from the crucibles would result in excessive Be removal to the sludge and hence in low recoveries in the melt processing. One method to increase Be recovery is to first reduce the Fe levels in the melt with Mn and then make the Be addition. The combination of higher melt temperature and low iron will give the best alloy efficiency.

Microstructural investigation of cast Mg-Al based alloys via secondary ion mass spectroscopy (SIMS) shows that Be is associated with Mn as well as Al and sometimes with Si in the bulk of the metal (Fig. 4.8).

Because of the toxicity of beryllium, the use is strictly controlled according to health and safety regulations [13–15]. While the levels found in commercial mag-

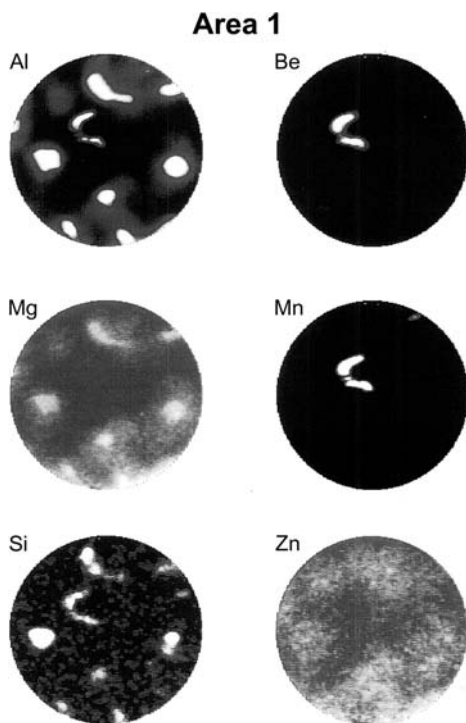


Fig. 4.8. SIMS analysis of AZ91D alloy ingot showing the presence of Be associated with Al, Mn and Si in the alloy [16]

nesium alloys are low, alloying operations that involve additives containing substantial amounts of Be during alloy production should follow very strict rules. It is known that, though it is rare, some individuals exposed to Be dust may form a sensitivity to it which upon further exposure may develop into Be-induced diseases. It is, fortunately, easy to identify individuals who are at risk by a simple blood test. Guidelines for handling Be should be followed when Be additives are handled. Any activity that could create dusts that contain Be should be monitored for proper industrial hygiene controls. Activities that should be considered for review include things such as alloy additions, handling of sludges, cleaning or repair of melt tools and equipment. There are also efforts to find replacements for Be for the oxidation-reduction of magnesium melts.

#### 4.1.1.6 Silicon

Silicon can be introduced into molten magnesium as elemental metallic silicon. This may be in the form of briquettes packed in plastic bags or as loose crystalline elemental material, both of which come in various grades (Table 4.5). For magnesium alloys the key issue is the control of the Fe content, therefore the silicon addition should be made prior to the Mn in order to control the iron content of the final product.

Due to the high melting point of Si, high melt temperatures (850–800°C for fluxed melts or 700–750 for flux free melts) and stirring need to be employed. An alternative route may be the addition of silicon via an Al-Si master alloy for easy melting and high recovery. Al-Si eutectic or hypereutectic may be selected depending on the Al and Si contents of the magnesium alloy.

#### 4.1.2 Mg-Al-(Rare-Earth) Alloys

Rare-earth elements, which include elements, such as Ce, Nd, Pr, are added to Al containing alloys of magnesium for improved creep resistance [17, 18]. The most economical route is to use mischmetal, which has a naturally occurring combination of rare earth elements and is available in the form of lumps of various sizes. The additive can oxidize readily in moist atmosphere and reacts violently with water. It should always be stored under a coating of a non-corrosive wax or oil. Mischmetal usually contains 85–90% total rare earth content. Typical compositions of mischmetal are shown in Table 4.6.

**Table 4.5.** Typical chemical compositions of silicon metal

Chemical composition	Min. % Si	Maximum %				
		Fe	Ca	Al	Ti	P
Standard	98.5	0.4	0.3	0.7	0.04	0.003
High purity	99.0	0.35	0.01	0.3	0.04	0.003
High purity, low iron	99.0	0.27	0.03	0.3	0.04	0.003
High purity, low iron	99.0	0.2	0.02	0.2	–	0.004
Very high purity, low iron	99.2	0.15	0.01	0.1	–	0.0025

**Table 4.6.** Typical compositions of mischmetal

Total rare earth metal		Iron	Calcium, Sodium, Barium, Phosphorous, Magnesium, Sulfur, Silicon, Chloride and others		
85 to 90%		6 to 10%	1 to 3%		
Individual elements in total rare earth metal					
Cerium	Lanthanum	Neodymium	Praseodymium	Samarium	Other heavies
40 to 45%	20 to 25%	15 to 20%	4 to 6%	1 to 4%	1 to 2%

The melting point of the additive varies between 600 and 900°C according to the percentage of iron. Care should be taken to make the addition under good melt protection. Cerium or lanthanum are also commercially available at higher cost if the addition of only one rare earth element is preferred.

Standard magnesium foundry fluxes react with rare earths resulting in poor melt recovery. The use of protective gas atmospheres that do not react with rare earth elements may improve recovery values. If fluxes are used 70% recoveries can be obtained if the rare earth addition is made just prior to ingot or part casting. Upon remelting under flux, an additional 10% loss is encountered. Rare earth may lead to excessive oxidation of the melt and care should be exercised to protect the alloy well to avoid oxide inclusions especially for applications where fatigue resistance is critical.

**4.1.3 Mg-Al(Alkaline Earth) Alloys**

Many Mg-Al based alloys containing alkaline earth elements Ca and/or Sr have emerged in the 1990s and 2000 [19–31]. Ca and Sr are added for improved creep resistance [27]. Some of these alloys also contain rare earth elements [25]. The alloys may also contain Zn [24], Si, Mn, and the addition techniques are the same as in the previous sections. It is preferable to add the other alloying elements first and then to introduce the alkaline earth elements though it is also possible to add these elements simultaneously with the others. The addition of calcium and strontium can be carried out in the form of master alloys as well as pure metal. Master alloy additives are usually easier to handle and store.

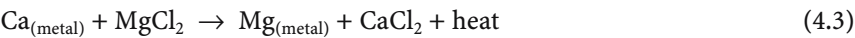
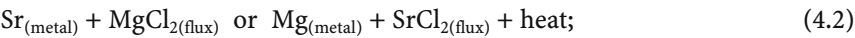
It should be noted that standard magnesium foundry fluxes containing  $MgCl_2$  are not compatible with these alloys. This includes the addition of manganese as  $MnCl_2$  since the reaction products include  $MgCl_2$ . Due to the higher chemical activity of Ca and Sr, they react with the  $MgCl_2$  salt and are lost as salts to the bottom of the crucible. This reaction is shown below and progresses rapidly.

If fluxes or  $MnCl_2$  is used in the melt then the Ca and Sr additions should be made at the very end after skimming the metal surface. Excess amounts are needed to reach target values and the melt should not be held for long periods. Care should be taken not to disturb the sludge while pouring the metal into ingots or injecting into dies. Periodic analytical sampling is required to monitor the

**Table 4.7.** Typical chemical composition of 30/70 Ca/Mg master alloy

% Element					
Ca	Al	Fe	Zn	Mn	Balance
30.2	0.23	0.0977	0.029	0.003	Mg

alkaline earth composition in the presence of chlorides, possibly including an end of cast sample. If processed flux free, the Sr and Ca is stable in the melt similar to other alloy ingredients.



**4.1.3.1 Calcium**

Calcium is added for creep resistance [23, 24, 26, 30] and the levels may range from 0.01 to 3%. Calcium can be introduced as a Mg-Ca master alloy. Fifteen, 20 and 30% Ca master alloys are commercially available. Table 4.7 shows a composition of a typical Ca master alloy. Recommended addition temperatures for these master alloys depend on the Ca content. And range from 680–720°C. Dissolution or mixing time of 15–30 minutes after the addition is recommended. Recoveries are quite high around 80–90% under fluxless alloying conditions.

As mentioned above, standard magnesium fluxes react with calcium so flux free melt protection is the preferred method for Ca additions. Specially formulated fluxes may be available in the future to alleviate the reactivity problem and allow the calcium addition to be fully equilibrated with the other alloy elements so that a good quality low iron alloy can be produced and/or recycled under flux based operating conditions.

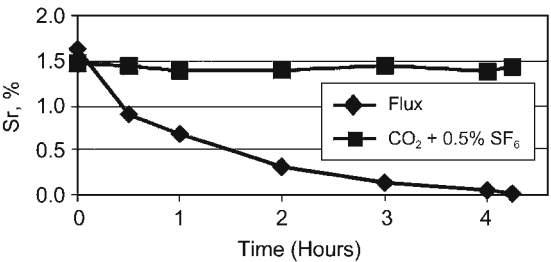
**4.1.3.2 Strontium**

Strontium is added for creep resistance in diecasting [28, 29, 31] and gravity casting alloys or to reduce micro- shrinkage porosity in gravity cast alloys [32]. The Sr level in the alloy may range from 0.02% to 3%. Sr can be introduced as Sr-Al master alloys or pure Sr metal. The master alloys are either low Sr (10%) or high Sr (90%). The most efficient way of adding strontium is a 90%Sr-10%Al master alloy (Table 4.8). This master alloy comes in the form of waffles or packed in aluminum tubes to avoid excessive oxidation (brittle dark grey) of the additive. The preferred alloying temperature is around 675–700°C and results in 85–95% recovery. The low Sr master alloys (e.g., 10–90 Sr/Al and 15–85 Sr/Al) can be used if the alloy has substantial aluminum and low Sr levels. High melt temperature of 725–775°C is required for high alloying efficiency. Mg-Sr master alloys can also be developed for commercial production.

**Table 4.8.** Chemical compositions of typical strontium additives

Additive	Element %										Others
	Sr	Al	Ca	Fe	Cu	Ni	Mn	Si	Ba	Zn	
90Mg-10Sr	balance	8–12	0.1 max	<<0.2	0.0035	0.0033	0.0052	0.02 max	0.5 max	0.004	Mg: 0.2 max
Pure Sr	balance	<0.01	0.01	0.01	<0.01	–	–	<0.001	0.1	–	Mg: 0.01
10Sr-90Al	9–11	balance	0.03	0.3	–	–		0.2	0.1	–	0.05 max*
15Sr-85Al	14–16	balance	0.05	0.3	–	–		0.2	0.1	–	0.05 max*

\* Total 0.15%.



**Fig. 4.9.** Strontium loss from a Mg-5Al-2Sr alloy melt held under flux (M130 Flux). Note that the same alloy melt shows very good stability when held under CO<sub>2</sub> + 0.5% SF<sub>6</sub> cover-gas

Standard foundry fluxes react with Sr, as noted above, lowering the alloying efficiency drastically (see Fig. 4.9). Flux-free melt protection is recommended for alloy preparation. If fluxes are used, strontium should be added at the very end and the alloying process should be optimized with respect to time and temperature to avoid excessive holding under flux. Specially formulated fluxes may be available in the future to minimize this problem, as with the Ca alloys. Production of high purity alloy, free of oxide and chloride contaminants, will require significant agitation and equilibration periods in order to assure effective alloying and iron reduction following the Sr addition.

Pure Sr can also be used as an additive, however the tenacious white oxide that forms on the metal can reduce recovery. To minimize the oxidation, pure Sr needs to be stored under argon and dipped in oil during manipulation before addition. The recovery rates depend on the temperature of the melt as shown in Fig. 4.10.

**4.1.4 Mg-Li Alloys**

Lithium is extremely difficult to add because of its high reactivity. The techniques for preparing and handling Mg-Li alloys have been developed over the years [33–



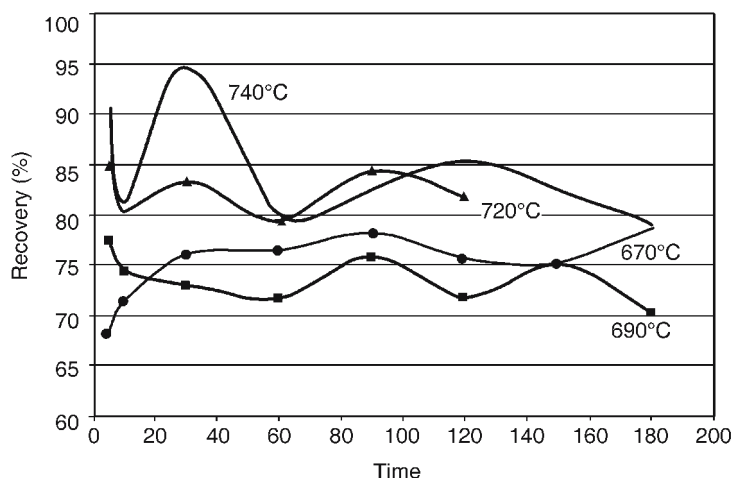


Fig. 4.10. Pure strontium recovery in Mg-5% Al melt

37]. The first melting practice used in North America was developed at Battelle Labs [33, 34] and consisted of melting Mg-Li under a LiCl-LiF flux in the proportion of 75/25 or 82/18 depending on the alloy composition. If the alloy contains Cd a change to the 82/18 ratio is recommended to avoid excess flux viscosity.

A crucible with a diameter about one-third of its height is used to prepare the melts. The flux is melted first to remove all traces of water from the hygroscopic flux ingredients. The magnesium and other alloying elements excluding lithium are then added and allowed to dissolve. The molten flux is lighter than the liquid metal and floats on the top providing surface protection. Lithium is added by means of an inverted cup plunged into the melt. After the lithium has melted, the cup is removed and the melt is thoroughly stirred. After the Li addition the density of the alloy phase becomes less than that of the molten flux, but a small amount of flux still remains on the metal surface providing protection (Fig. 4.11).

A complication of the use of fluxes seems to be sodium contamination of the melt [35], which decreases the ductility of the alloy. To avoid this problem the quantity of flux used needs to be 35% of the weight charge except when very large quantities of a charge are prepared. Bubbling nitrogen can also help remove sodium.

Dow Magnesium used variations of the flux-melting process. It was felt that the optimum melting and casting process needed to make use of flux to clean the metal and allow for scrap recycling. However, protection of a large surface area may be difficult by flux alone [36]. An inert gas atmosphere or vacuum should also be utilized to avoid excessive oxidation of the melt.

Battelle Labs also developed the technique for melting Mg-Li under argon or in a partial vacuum [34], which was widely used [36]. This method uses a capped mild steel crucible, which is purged with argon when cold, after which

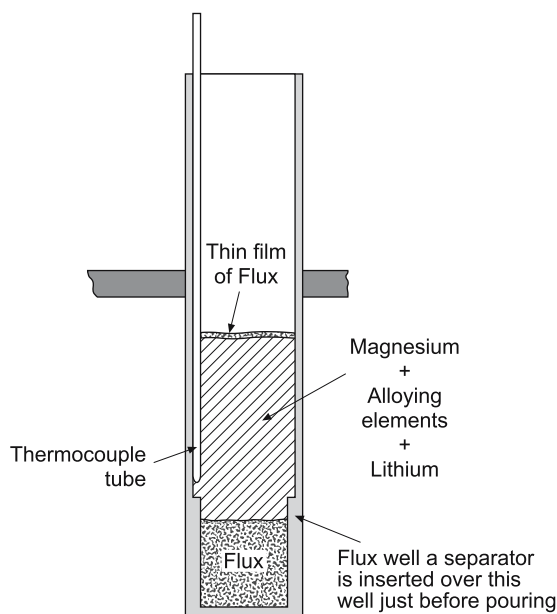


Fig. 4.11. Melting crucible showing the relative positions of flux and metal after lithium addition [33]

the charge is loaded and melted. Magnesium is melted and all the other ingredients, which have similar melting points (Al, Zn, Cd, Ag, Si), are added around 700–750°C allowing dissolution time after each addition. Manganese, if introduced as a master alloy, can also be included in this group. Lithium is added last and at the lowest temperature possible (680–700°C). The use of agitation is recommended.

Pure lithium metal is supplied in rod form by various metal suppliers (Table 4.9). The purity of the lithium used especially with respect to sodium is critical for alloy properties.

Casting and pouring of the Mg-Li base alloy also requires special equipment. Completely closed melting and pouring systems have been developed that incorporate features such as charging port, stirring rod, pouring tube, inert gas pressure regulator (Fig. 4.12). A variation of this has also been produced to develop a counter-gravity mold pouring technique with a two-part mold fitted above the furnace (Fig. 4.13).

Alternative methods for making Mg-Li base alloys are also occasionally used [40]. These involve separate melting of magnesium and lithium. A mild steel crucible is used for melting magnesium under flux, aluminum additions are made and then the melt is degassed and grain refined at 725–750°C. Lithium is melted in low carbon stainless steel or tantalum crucibles and kept at a 200°C under a 75%LiCl–25%LiF flux cover. The molten magnesium is then added to molten lithium through a funnel piercing the flux cover.

Table 4.9. Typical chemical composition of pure lithium

Li	Ne	Ce	Fe	Si	Cl	N	K
99.8%	100 ppm	190 ppm	100 ppm	100 ppm	60 ppm	300 ppm	300 ppm

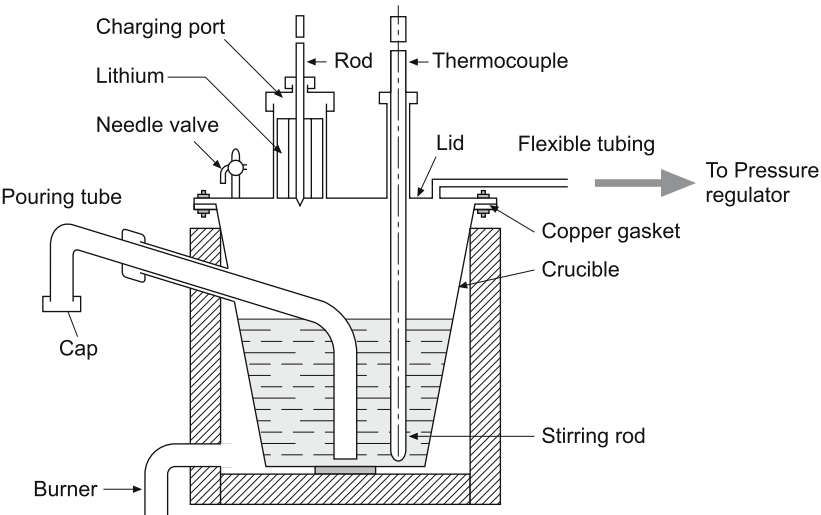


Fig. 4.12. Schematic drawing showing the melting furnace set-up for Mg-Li base alloys [38]

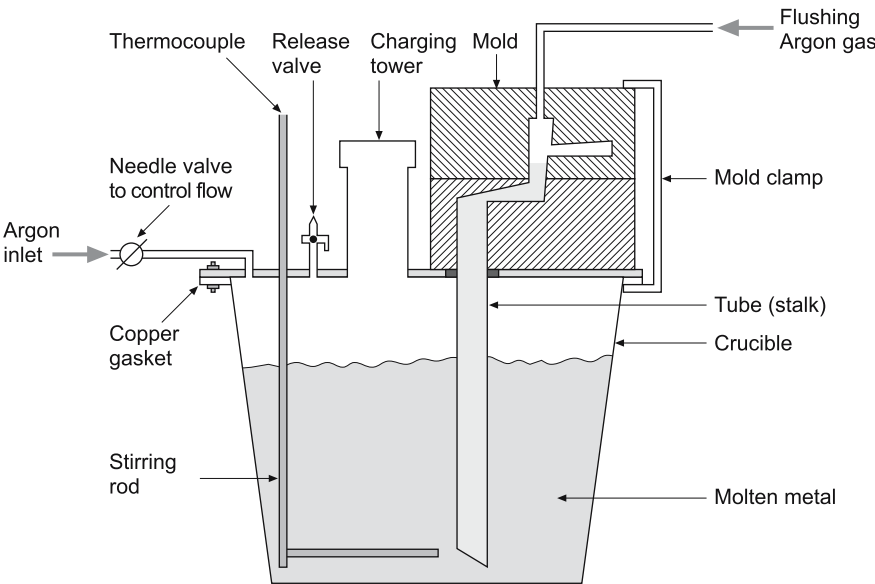


Fig. 4.13. Schematic of Mg-Li base alloy melting and casting set-up [39]

4.2 Alloys Containing Zirconium

John F. King

4.2.1 Introduction

The grain refining effect of zirconium was discovered in Germany in the late 1940s [41–43]. This introduced the possibility of significantly improving mechanical and casting properties of magnesium alloys by grain refinement.

The subsequent development, by Magnesium Elektron in the UK, of effective and practical means of introducing zirconium into magnesium eventually led to the development of new families of alloys based on combinations of elements not previously possible.

This development, driven by the needs of jet aircraft engines, resulted in a continuous improvement in strength and particularly elevated temperature resistance, culminating in current alloys such as WE43 (Mg-4%Y-3%RE (Rare Earth)–0.5%Zr) which have high strength and long term temperature stability at temperatures as high as 250°C.

The history of the development of techniques for introducing zirconium into magnesium up to the 1960s has been eloquently described by Emley [44]. While most of the basic techniques had been established at that time, further development and refinement have taken place. This chapter aims to summarise the current state of the art for melting alloying and refining of zirconium-containing magnesium alloys.

4.2.2 Mechanism of Grain Refinement by Zirconium

Melting and alloying of Mg-Zr alloys to produce alloys with satisfactory properties depends on an understanding of the mechanism of the grain refining effect of zirconium.

Although the precise mechanism is still the subject of investigation [45–47], there are a number of key factors which contribute to the grain refinement process.

- The similarity of lattice parameters between magnesium and zirconium (see Table 4.10.)
- The presence of a peritectic reaction between Zr and Mg close to the freezing point (see Fig. 4.14.)
- The need for the liquid magnesium to be saturated by zirconium at or just above the freezing point.

Table 4.10. Lattice parameters of Mg and Zr

Element	a [nm]	c [nm]	c/a	Structure
Mg	0.320	0.514	1.606	HCP
Zr	0.323	0.520	1.610	HCP

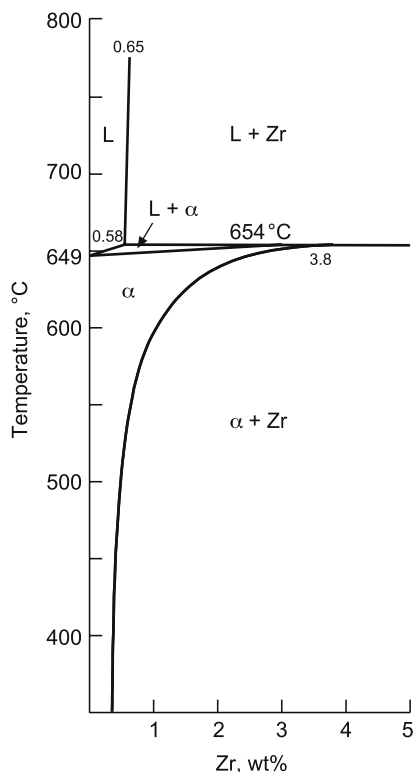


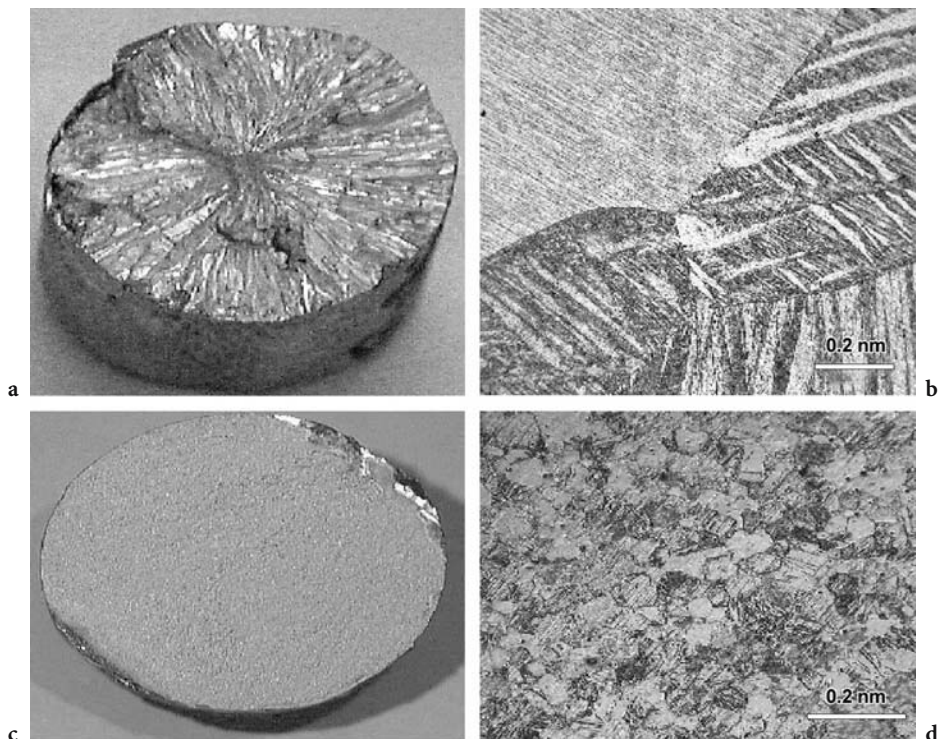
Fig. 4.14. Equilibrium phase diagram for Mg-Zr system

The overall process leading to the fine-grained structure in Mg-Zr alloys may be described with reference to the equilibrium diagram (Fig. 4.14).

For alloys, which are saturated with Zr in the liquid phase, cooling will allow some precipitation of  $\alpha$ -Zr particles as the freezing temperature is approached. At the peritectic temperature (approx. 654°C), suspended Zr particles can form nuclei for the peritectic reaction between Zr particles and Zr-saturated Mg liquid to produce solid  $\alpha$ -Mg with high Zr content.

The close similarity between lattice parameters of Mg and Zr should allow this reaction to occur readily on suitable Zr particles between the peritectic temperature and the equilibrium freezing point of Mg (650°C). Initial solid crystals of  $\alpha$ -Mg will grow by surrounding the Zr nucleating particle and absorbing Zr from the particle or the surrounding liquid until Zr depletion in the surrounding liquid inhibits further growth. This then allows further nucleation and growth to occur from additional precipitated particles within the liquid until further growth is inhibited by growth of neighbouring crystals. The result on final solidification is a relatively homogeneous distribution of fine hexagonal grains, reflecting the hexagonal crystal structure and consequent growth mode of the two components (see Fig. 4.15).

The basic process summarised above has been verified by several researchers [47–49]. Particularly, the presence of the characteristic Zr-rich coring, and a cen-



**Fig. 4.15a – d.** Effect of Zr addition on grain size and structure of pure magnesium. **a** Pure magnesium (fracture); **b** Pure magnesium (microstructure); **c** Pure magnesium with a 0.7% zirconium addition (fracture); **d** Pure magnesium with a zirconium addition (microstructure)

tral Zr particle have been illustrated and related to the metallographic grain structure (see Fig. 4.16). Practically, it is well known that Zr addition to pure magnesium or appropriate alloys reduces the grain size by an order of magnitude or more compared to non-Zr containing alloys, with consequent beneficial effects on mechanical properties and casting characteristics.

A fuller explanation of the mechanism needs to take account of other factors observed in the processing of Mg-Zr alloys such as the effect of other alloying elements and trace impurities and the indication that only Zr soluble in the liquid Mg alloy appear to take part in the grain refinement process. For example, in Fig. 4.17, typical Zr rich coring in a Mg-RE-Zn-Zr alloy was shown to be rod-like precipitate with the approximate composition  $Zr_2Zn$  [50].

Further work in this area is still required.

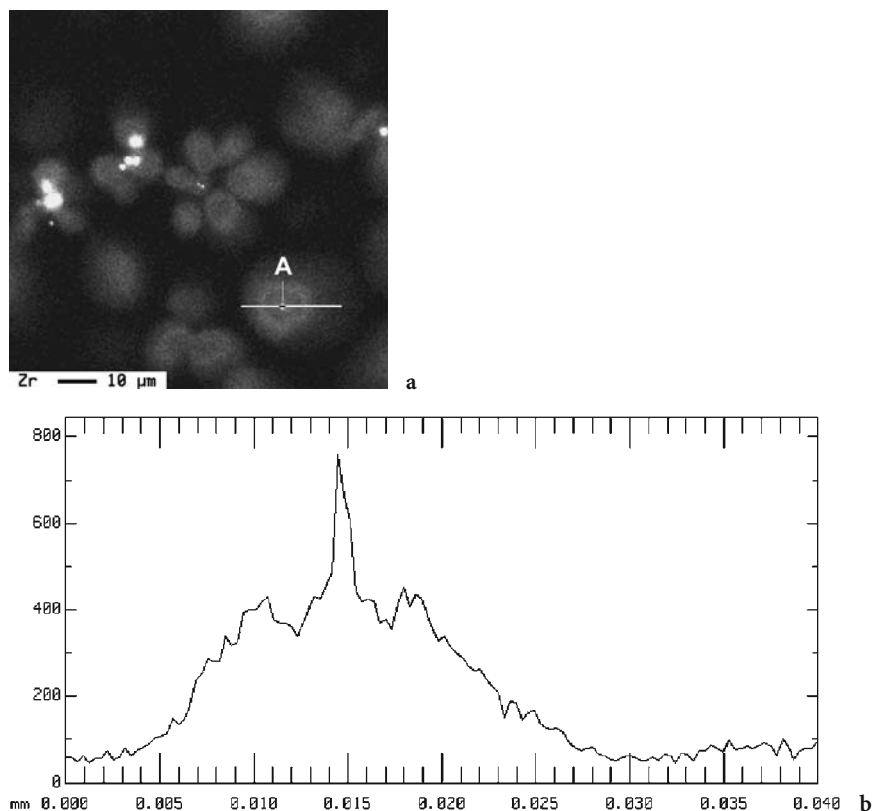


Fig. 4.16a, b. a X-ray map showing distribution of Zr in grain refined pure Mg, b line scan across particle A showing Zr distribution

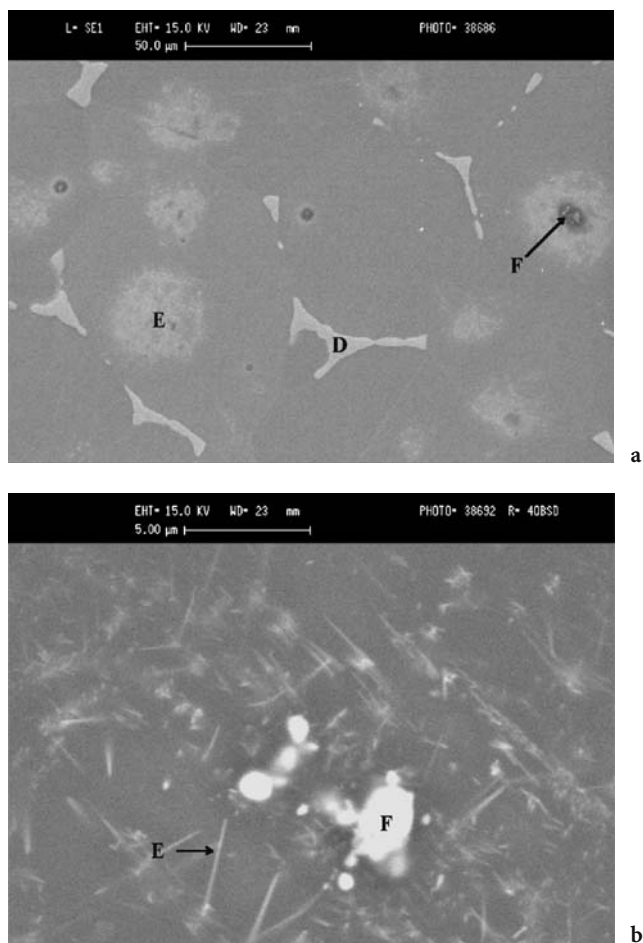
### 4.2.3 Effect of Other Alloying Elements

#### 4.2.3.1 Incompatible Elements

Because maximum solubility of Zr is necessary to ensure effective grain refinement, certain metallic elements, which form stable high melting point compounds with Zr, cannot be present in Mg-Zr alloys. These include Al, Si, Fe, Ni, Mn, Sn, Co and Sb.

Elements such as Al, Si and Mn are major alloying additions for commercial non-zirconium magnesium alloys, but cannot be used with Zr. In fact, contamination with these readily available elements, as might arise from inadvertent mixing of scrap, must be scrupulously avoided in the foundry.

Another important inhibiting element for Zr refined alloys is hydrogen. Zirconium forms stable hydrides with hydrogen, which can be absorbed from furnace gases or generated by breakdown of moisture during melting of oxidised scrap or use of damp fluxes. Once formed, zirconium hydride cannot be decom-



**Fig. 4.17a, b.** Structure of as-cast Mg-RE-Zn-Zr alloy. **a** Secondary electron SEM image showing intergranular phase D, Zr-rich clusters E, and globular precipitates F, **b** back scattered SEM image at a higher magnification showing the rod like precipitates E ( $Zr_2Zn$ ) within a Zr-rich cluster containing a globular precipitate F

posed within the temperature envelope of normal melting procedures and essentially removes effective zirconium from the system.

#### 4.2.3.2 Compatible Alloy Systems

Although alloying of magnesium with aluminium provides the majority of the current commercial alloys because of its relatively high solubility, solid solution hardening effect, and flexibility of properties by heat treatment, its use is precluded with Zr-containing alloys. Fortunately, however, there are a number of other elements, which also demonstrate significant solubility in magnesium, and



can provide an even wider range of properties. Significant among these are Zn, Ag, Th, and a wide range of rare-earth elements (RE).

This has led to the development of new families of alloys distinct from the non-Zr alloys such as Mg-Zn-Zr, Mg-Zn-RE-Zr, Mg-Ag-RE-Zr, Mg-Y-RE-Zr.

Mg-Th-Zr and Mg-Zn-Th-Zr alloys were also once widely used for high temperature aerospace applications, although are now obsolete due to radioactivity issues.

Properties of the current alloys are described in detail elsewhere in this publication.

Specific issues of alloying and metal handling are described in this chapter.

#### **4.2.4 Methods of Introducing Zirconium**

##### **4.3.4.1 Products Available**

The high melting temperature of metallic zirconium, coupled with the presence of a highly stable oxide barrier film, make it almost impossible to alloy directly with magnesium. Early practical techniques relied on direct reduction of Zr-containing salt mixtures in molten magnesium to form active Zr, which then readily alloyed in situ with the melt. Typical salts were chloride- or fluoride-based, resulting in formation of  $\text{MgCl}_2$  or  $\text{MgF}_2$ , which were difficult to remove from the melt.

Subsequently, metallic hardeners were developed, again manufactured by direct reduction of Zr halides in molten magnesium followed by suitable treatment to remove excessive salts. The history of these methods was reviewed in detail by Emley [44].

Since the 1960s only metallic hardeners have seen significant use for processing of Mg-Zr alloys. A variety of hardeners with Zr content varying between 15 and 65% are available. Quality and efficiency vary widely. The key to an effective hardener is to ensure that the contained Zr is in an “active” form that is readily soluble when added to molten magnesium or alloy, and contains the fewest contaminants, usually residual halides from the production process.

The most widely used hardener worldwide is the proprietary product Zirmax manufactured by Magnesium Elektron in the UK. This product contains nominally 33 wt% Zr in a relatively homogeneous distribution of fine particles mostly 5  $\mu\text{m}$  or less in dimensions in a matrix of magnesium (Fig. 4.18). Because the Zr particles were formed in situ within the magnesium matrix during the processing of the hardener their surfaces are not passivated by oxide films or other external contaminants and are almost totally “active” so that when diluted or alloyed into a magnesium alloy melt they can dissolve rapidly with minimum losses.

##### **4.2.4.2 Basic Principles of Zr Grain Refinement**

Several key factors must be considered to achieve optimum grain refinement.

1. Optimum grain refinement requires that the magnesium alloy melt must be saturated with Zr at the temperature at which the melt will be cast. Most Mg-

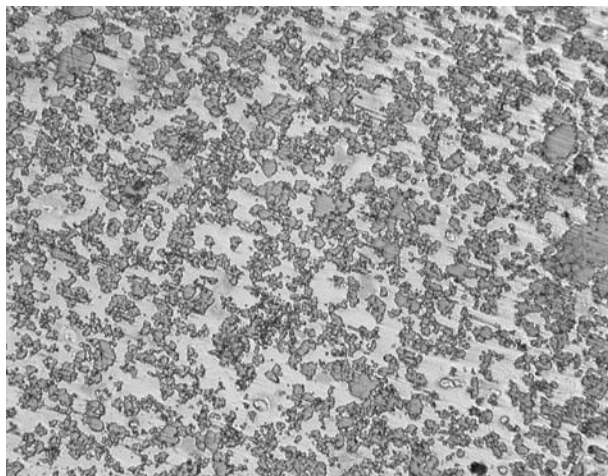


Fig. 4.18. Structure of Zirmax Mg-33% Zr Hardener (original magnification  $\times 400$ )

Zr alloys are sand or gravity cast. Casting temperatures are typically in the range 760–800°C. Zr alloying temperatures in the range 780–800°C are therefore preferred.

2. Even with efficient hardeners such as Zirmax, dissolution rate of Zr into the Mg alloy tends to be slower than the actual melting rate of the hardener. This results in initial suspension then settling of active Zr particles into a Zr rich layer at the bottom of the crucible. Re-stirring or “puddling” of this layer back into intimate contact with the melt is an essential part of the alloying process. This may be achieved manually or mechanically by suitably designed stirrers.
3. Once saturation with Zr has been achieved, Zr will be continually lost from solution by reaction with iron from the crucible, hydrogen pick-up, reaction with other contaminants or precipitation due to temperature cycling. It is therefore essential to ensure that an excess of active Zr is available in the melt to compensate for ongoing losses. This is normally achieved by adding excess hardener which will form a Zr-rich layer at the bottom of the crucible acting as a reservoir for Zr. To avoid losses, the melt should normally be poured from the crucible with the Zr residue or heel in place. This currently dictates that melting of Mg-Zr alloys is carried out as a batch process and that a significant heel of metal is retained in the crucible after casting.
4. Only Zr in solution in the molten Mg alloy is effective in the grain refining process. Since some degree of precipitation and reaction of Zr with contaminants is inevitable, Zr may be present in the melt in both soluble and “insoluble” forms. Estimation of Zr content for grain size control therefore requires a technique which differentiates between the two types. Direct estimation of grain size in test samples before casting is recommended (see later). Spectrographic analysis of samples is not appropriate for this purpose.

### 4.2.4.3 Zirconium Grain Refining in Fluxed Melts

Melt processing temperatures and the degree of metal disturbance or agitation are usually higher for Mg-Zr alloys than the non-Zr alloys. Flux-free melting is therefore more difficult, and a significant proportion of melts are still processed with fluxes. The general principles of flux melting, as described for non-Zr alloys in Sect. 4.1 also apply to Mg-Zr alloys. There are however a number of issues that are specific to the use of flux in Mg-Zr alloys.

The need for puddling or stirring of the melt to ensure all available Zr is suspended at some stage also results in suspension of all Zr-rich insoluble particles and other contaminants such as oxides. Some of these may be of similar density to the liquid melt and slow to settle. The purpose of flux refining is to ensure that suspended particles in the melt are wetted by the flux and settled. This process appears more difficult in Mg-Zr alloys using normal fluxes recommended for Mg-Al type alloys, and chloride contamination in the form of fine suspended partially fluxed Zr rich particles may persist in the melt and be transferred into the cast product. The traditional solution to this problem has been to use higher density fluxes containing high levels  $\text{BaCl}_2$  specially formulated for Mg-Zr alloys. The typical composition of two such fluxes, manufactured by Magnesium Elektron, is shown in Table 4.11.

Flux 1 (HE) is inspissated with  $\text{CaF}_2$  and formulated to minimize the activity of free  $\text{MgCl}_2$  while providing a suitable balance of wettability and viscosity. This flux can be used for all Mg-Zr alloys with the exception of Y-RE-Zr alloys, which require special flux free melting techniques.

Flux 2 (TE) is inspissated with  $\text{MgF}_2$ , which permits a higher free  $\text{MgCl}_2$  content. This flux was formerly used for Th containing alloys, in which presence of RE was undesirable; any trace RE in the melt is removed by reaction with  $\text{MgCl}_2$ . It is still often preferred for melting and alloying of silver containing alloys such as QE22 (MSR).

Use and disposal of  $\text{BaCl}_2$  containing fluxes is now subject to environmental legislation in many countries. Where such regulations apply, appropriate authorisations are necessary. If  $\text{BaCl}_2$  containing fluxes cannot be used,  $\text{BaCl}_2$  free alternatives such as Flux 3 (UE) may be necessary, but greater care is required to ensure flux refining is carefully carried out, and adequate time allowed for settling.

Melting, alloying and grain refining using fluxes is essentially a single batch process. Excess Zr, settled inclusions and some alloy, are all entrained in the fluxy heel in the bottom of the crucible, which cannot be efficiently re-used in the next melt.

**Table 4.11.** Melting and Refining Fluxes for Mg-Zr alloys

Designation	$\text{MgCl}_2$ (%)	KCl (%)	NaCl (%)	$\text{BaCl}_2$ (%)	$\text{CaF}_2$ (%)	$\text{MgF}_2$ (%)	$\text{CaCl}_2$ (%)
1. HE	35	8	–	44	13	–	–
2. TE	32	8	–	40	–	20	–
3. UE	34	3	27	–	15	–	21

After casting, residue metal is normally cast into ingots for separate recycling, while the fluxy residue is scraped out for disposal.

A typical melting procedure in a foundry making sand or gravity castings in Mg-Zr alloy ZE41 (RZ5) may be summarized as follows:

1. Example charge:

ZE41 ingot + clean casting recycle scrap	100 kg
Zirmax (nominal 33 wt% Zr)	5 kg
Ce-rich Mischmetal	0.2 kg
Pure Zn (adjustment as required)	

Note: Zr addition equivalent to approx 1.6 wt% to compensate for losses during melting, contamination, precipitation, etc. Excess normally high to ensure adequate initial level without further reprocessing.

Additions can be reduced based on experience.

RE can be added as mischmetal or Mg-RE hardener.

2. Clean, red-hot mild steel crucible coated with flux on bottom and sides by dusting. Ingot and scrap charged and melted. When fully molten, surface protected with thin layer of flux.
3. Preheated Zr hardener and RE addition added at 720–740°C, melt heated to around 780°C and held at this temperature.
4. Surface flux layer cleaned off with any accumulated oxide film and replaced with fresh flux cover. Melt stirred or “puddled” at 780°C with a suitable tool to lift metal from the viscous Zr-rich layer at the bottom into contact with the melt for sufficient time to ensure full alloying (e.g., several minutes). Surface protected by sprinkling fresh flux during stirring.
5. Melt held at 780°C, sample taken by preheated ladle from the melt and poured into cast iron chill bar mould for estimation of grain size (see below).  
Note: If examination of test bar fracture indicates inadequate grain refinement, the puddling operation is repeated and grain size rechecked.  
If still not satisfactory, melt contamination is indicated and remedial measures are necessary (ie; further Zr addition or cast off for offline rectification).
6. If grain size is judged satisfactory, a sample for analytical control is cast by ladle then any loose flux around the top of the crucible is cleaned off and melt surface flux layer replaced in preparation for pouring. Melt temperature continues to be held at 780°C or is allowed to slowly adjust to casting temperature if different. Large temperature fluctuations likely to cause convection currents in the settled melt should be avoided.
7. The melt is held for a minimum of 15 min after cleaning to allow any dislodged flux agglomerations to settle and for the surface flux layer to harden.  
Note: If the melt is held for longer than 40 min, rechecking of grain size is recommended before proceeding.
8. Crucible is transferred to the pouring station if not poured in situ. Flux cover around the pouring lip of the crucible is cut away and removed using a suitable mild steel tool. At this point, liquid metal surface at the pouring point is protected by powdered sulphur or SO<sub>2</sub> (if permissible) Alternatively CO<sub>2</sub>/SF<sub>6</sub> protective gas mixture is applied to the area through an appropriate distributor.

9. Metal is poured from the crucible, maintaining a constant pouring stream, and protecting the melt surface, pouring stream and casting cavity with the appropriate protective gas. A metal heel of at least 10% of the initial melt volume is retained in the crucible to avoid pour-over of flux or settled particles from the bottom of the crucible.
10. Residual metal is cast into ingots for later recycling and the fluxy residue is scraped into a suitable container for disposal. With correct melt treatment, the fluxy residue should be a viscous mass easily scraped from the crucible. A fiery powdery residue indicates inadequate flux usage and poor flux refining. A very fluid residue suggests excessive flux usage. With good practice, flux usage equivalent to 5–8% of the total metal charge is usual.

#### 4.2.4.4 Zirconium Grain Refining in Flux-Free Melts

Since the development of melt protection by  $\text{SF}_6$  containing gases, techniques have been adapted for use with Mg-Zr alloys. The higher processing temperatures, batch processing and metal stirring requirements make these alloys more difficult to protect than commercial Mg-Al based alloys. Conventional steel crucibles are used with loose fitting lids with suitable entry ports for charging or metal processing.  $\text{CO}_2$  is used as the carrier gas with relatively high concentrations of  $\text{SF}_6$  (e.g., 0.5–2.0 vol%). Flow rates are adjusted depending on the melt processing (e.g., low flow for melt down and holding, high flow for alloying, puddling and pouring. Typical flow rates for various crucible sizes in a practical industrial system are indicated in Table 4.12.

In practice, precise flow rates will depend on the specific configuration of melting equipment, effectiveness of sealing and distribution of gas. Gas flow and usage will be minimised on the basis of experience.

While  $\text{CO}_2/\text{SF}_6$  is currently the preferred gas mixture, environmental concerns dictate that use of  $\text{SF}_6$  will be phased out in future. Suitable alternatives for crucible melting of Mg-Zr alloys are still to be defined.

Melting, alloying and grain refining operations in flux free melts are similar to those in fluxed melts. However, certain changes are necessary.

1. Since no flux refining process is carried out, particulates suspended in the melt (Zr rich and oxides) settle more slowly by gravity. Longer times must be allowed for this settling to occur. This could vary between 15 min for small melts and 40 min for larger melts. Even then, settling (particularly of oxides) may be

**Table 4.12.** Typical gas mixture and flow rates for foundry melting of Mg-Zr alloys

Crucible dia [mm]	Low flow [l/min]	High flow [l/min]
300	3.5	10
500	3.5	30
750	5.0	50

Constant gas mixture:  $\text{CO}_2 + 1.75 \text{ vol\% SF}_6$ .

incomplete in the lower part of the melt. To compensate for this, a larger heel should be retained in the crucible after pouring. Where high quality castings or billets are being poured, a simple filtering system is also normally incorporated in the casting running system or billet casting launder.

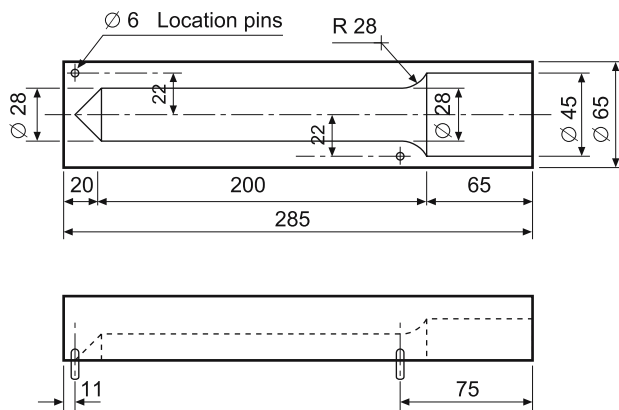
2. With good flux free melting practice, higher metal yields can be achieved. Alloying losses due to reaction with fluxes (e.g., RE elements) and entrainment of metal in the flux heel are eliminated. Apart from the heel of retained metal, only a small heel of settled oxide and excess Zr particulate remain. It is therefore possible to utilize the retained metal and any retained active Zr by recharging metal for the next melt directly into the remaining heel. This permits Zirconium hardener additions to be progressively reduced in sequential melts.

For example, in a foundry melting ZE41 (RZ5) charges of ingot and recycle scrap for sand or gravity casting where a minimum final Zr content of 0.7 wt% is required, recommended additions of Zirmax for a 3 or 4 melt cycle may be: melt 1: 5 wt%, melt 2: 4 wt%, melt 3,4: 3 wt%. For experienced and competent foundries, Zirmax additions can be reduced even further, although some additional hardener is always required for each melt.

#### 4.2.4.5 Methods of Assessing Grain Refinement

As previously indicated, only Zr in solution in magnesium contributes to grain refinement. While chemical or spectrographic analysis are necessary for overall control of composition, spectrographic analysis particularly is not able to differentiate between “soluble” and “insoluble” Zr. Since grain refinement is the key purpose of Zr addition, a direct assessment of grain refinement is regarded as the preferred method of judging correct Zr levels.

For this, the method almost universally used is that developed by Magnesium Elektron. A simple 28 mm diameter bar is chill cast into a cast-iron two piece die (see Fig. 4.19) by hand ladling from the melt after treatment. After cooling, a small

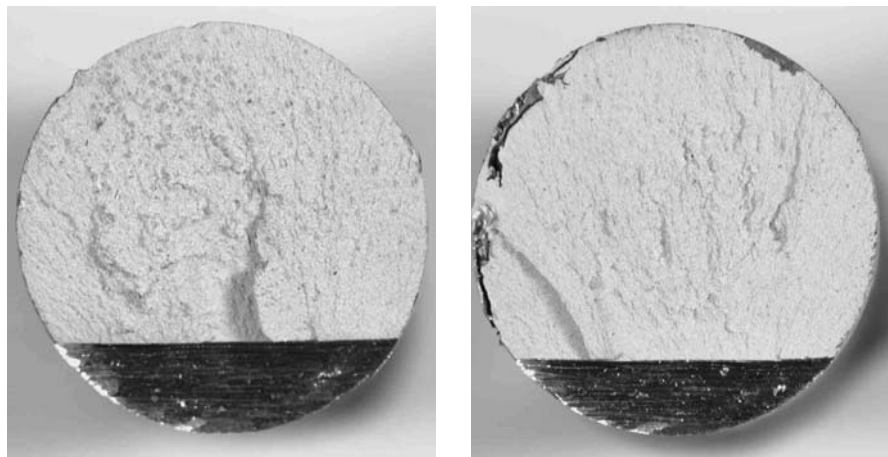


Dimensions in mm, Material: Cast iron



Fig. 4.19. Chill mould for grain size estimation sample





**Fig. 4.20.** Comparison of acceptable (*right*) and unacceptable (*left*) grain sizes in ZE41 (RZ5) alloy fracture test bars

notch is cut into the bar 25–40 mm from the bottom and the bar is fractured at the notch. The fracture surface has a characteristic appearance depending on the actual grain size and, to a lesser extent, the alloy composition. (This is illustrated in Figs. 4.15 and 4.20). With relatively little experience it is easy to judge whether grain refinement is satisfactory by visual examination (see Fig. 4.20). Fractures may be compared against prepared standards showing a range of grain sizes as correlated with metallographic measurement. This simple assessment is rapid and can be carried out inline in the foundry. More sophisticated foundries with metallographic polishing and microscope facilities may also measure grain size directly as a quality control tool.

For this type of test bar, an average grain size of 30  $\mu\text{m}$  or less would be indicative of satisfactory grain refinement.

#### 4.2.5 Melting, Alloying Procedures for Other Elements

Major alloying elements commonly used in Zr-refined magnesium alloys are Zn, Ag, Y, and a range of RE elements. With the exception of Y-containing alloys, fluxed or flux free melting procedures previously described can be applied with few problems. Alloys can be produced directly from virgin materials but many users prefer to use pre-alloyed ingot as a starting material, as control of composition is simpler, particularly where relatively small volume melts are made on a batch basis in a number of alloys, as is often the case in sand foundries making aerospace castings. However, even with use of alloyed ingot, compositional adjustments may still be required using elemental additions.

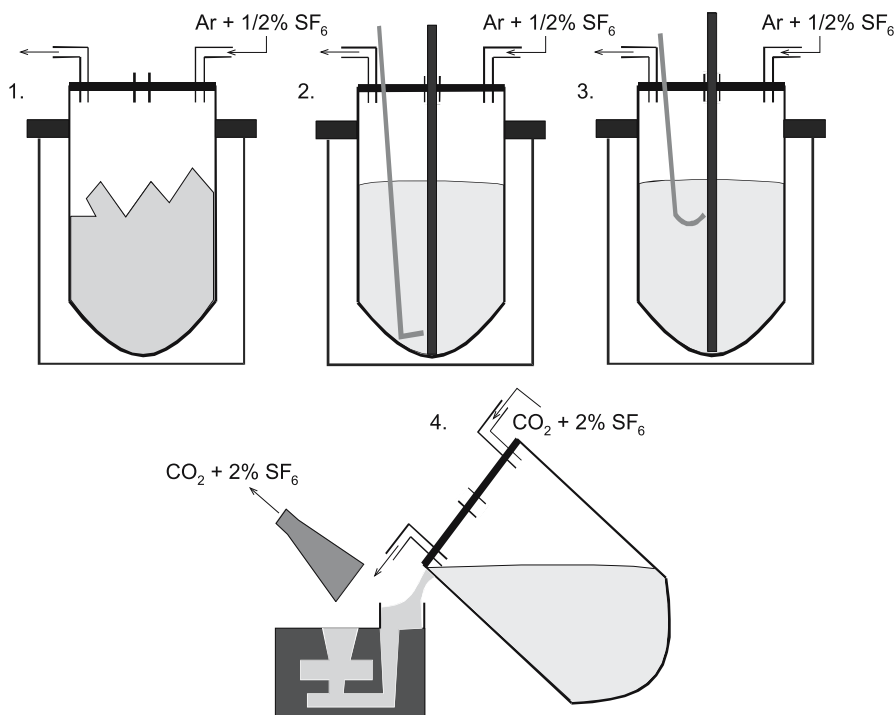
Metallic zinc and silver alloy easily with magnesium with almost 100% efficiency and are usually added in this form. High purity metal is used (e.g., 99.95% Zn, 99.9% Ag). Impurities which may react with Zr should be avoided. Additions are usually made in a steel alloying basket that is immersed below the surface of

the melt and gently agitated until the contents have fully dissolved. The melt is then stirred mechanically to ensure the alloying is complete.

A range of RE elements are used in magnesium alloys. Current commercially used Mg-Zn-RE-Zr alloys contain a RE blend derived from Ce-rich Mischmetal. The typical composition recommended is: total RE 97.5% min, Ce approx. 50%, La 20–30%, with the remainder being substantially Nd and Pr. Impurities such as Fe, Si and Al should be minimized.

Mg-Ag-RE-Zr alloys require a Nd rich RE fraction. Historically Nd rich mischmetals were available containing around 70% Nd, with the remainder substantially Pr, with minor amounts of Ce and La. More recently, RE alloys are extensively fractionated to produce pure RE elements for a wide variety of applications. Pr has specific applications and Nd additions used in Mg-Ag-RE-Zr alloys are now often almost pure Nd (e.g., 95–99% Nd). This variation does not appear to be critical to alloy properties.

Both RE types alloy fairly easily with Mg, and would again be allowed to dissolve in the melt in an alloying basket with the melt in the temperature range 720–780°C. In fluxed melts, RE elements will react with  $\text{MgCl}_2$  in the flux to form the relevant chloride. With good melting practice the losses experienced should not exceed 10%. It is normal practice to take losses at this level into account when cal-



**Fig. 4.21.** Basis metal handling of Mg-Y alloys. (1) Charge and melt-down, (2) Grain-refine, (3) Analysis, grain-size check, (4) Pour



culating the initial alloying addition. In flux free melting, only small oxidation losses around 2–5% are observed.

Mg-Y-RE-Zr alloys contain yttrium, a Nd-rich RE fraction and a heavy RE fraction (i.e., Gd, Dy, Er, Tb, etc.). The HRE fraction is derived from the use of a relatively low cost Y/HRE concentrate in the manufacturing of the alloy. The Y to (Y + HRE) ratio in commercially available alloys is 75–80%. The alloying behaviour of Y and HRE are virtually identical. Neither can be melted and alloyed using conventional flux or flux-free techniques without heavy losses. A practical inert gas melting system has been developed for melting and alloying and casting, as illustrated in Fig. 4.21. A sealed crucible is used with an inert gas mixture of Ar + 0.5 vol% SF<sub>6</sub>. While sealed during melting and holding, simple entry lids are provided for alloying and mechanical melt processing. During these operations, gas flow rate is increased to minimize oxidation. Presence of SF<sub>6</sub> in the event of air leakage promotes rapid formation of a protective oxide film on the metal surface.

Using this technique, Y and HRE losses are restricted to around 5–8%. Argon based inert gases are not protective for open casting, so a conventional CO<sub>2</sub>/SF<sub>6</sub> gas is substituted at this stage, oxidation losses being minimal for the short duration of this operation.

Losses of the Nd-rich fraction during melting are negligible.

Yttrium and HRE are preferably added in the form of a Mg-Y/RE hardener, containing typically 20–25% Y, when melting these alloys in foundry operations. The high melting points of the pure elements result in very slow dissolution in molten Mg even at 800°C. This incurs high losses, making compositional control of the alloy difficult.

## References to Chapter 4.1

1. Emley EF (1966) *Principle of Magnesium Technology*, Pergammon Press, pp. 92–167
2. Pilling NB and Bedworth JD (1923) *Journal of Institute of Metals*, Vol. 29, pp. 529–534
3. Devault R “Etudes des phenomenes superficiels dans l’oxydation de quelques metaux fondus”, PhD Thesis, Centre de documentation universitaire, Tournier et Constans, Paris, France
4. Housh SE and V. Petrovich V (1990) *Magnesium Refining: A Fluxless Alternative*, SAE Technical Paper 920071, Detroit
5. Leyendecker T and Schroder D (1998) *Economical Process for In-House Remelting in Magnesium Diecasting Shops*, Proceedings of the 55th Annual IMA Conference, International Magnesium Association, McLean, VA, May, pp. 16–18
6. Hillis JE and Mercer II EW (2000) *Separation of Non-Metallic Contaminants in Fluxless Melting and Refining of Magnesium Alloys*, Technical Paper #2000-01-1125, Society of Automotive Engineers, Detroit, MI
7. Tranelli G, Pettersen G, Aarstad K, Thorvald AE, Solheim I, Syvertsen M, Oye B (2001) *A Systematic Approach for Identifying Replacements to SF<sub>6</sub>/SO<sub>2</sub> in the Magnesium industry-An IMA/SINTEF-NTNU Cooperative Project Proc. IMA 2001 Magnesium Conference*, May, Brussels, pp. 69–73
8. *Alloy Phase Diagrams* (1992) Baker H, Ed., ASM Handbook, Vol. 3
9. Hillis JE, Mercer WE and Murray RW (1998) *Compositional Requirements for Quality Performance with High Purity Magnesium Alloys*, Proceedings of the IMA, The International Magnesium Association, McLean, VA, pp. 74–98

10. Thorvaldsen A and Aliravci CA (1994) Solubility of Manganese in Liquid Mg-Al Alloys, Light Metals Processing and Applications, CIM, Aug
11. Standard Specification for Magnesium Alloys in Ingot Form for Sand Castings, Permanent Mold Castings, and Die Castings, B 93/B 93M-98, Annual Book of ASTM Standards, Vol. 2.02, Aluminum and Magnesium Alloys, ASTM International, West Conshohocken, PA, pp. 46-49
12. Spielberg W, Wellmann B (1992) The Effects of Beryllium Additions on Magnesium and Magnesium Containing Alloys, Magnesium Alloys and Their Applications, B. L. Mordike and F. Hehmann, Eds. DGM, Garmische-Partenkirchen, pp. 259-267.
13. American National Standards Institute (1970) Acceptable concentrations of beryllium and beryllium compounds. New York: ANSI; ANSI Z37.29
14. Vainio H, Rice JM (1997) Editorial: Beryllium Revisited. J. Occup. Env. Med. 39(3): 203
15. Eisenbud M (1990) Health Problems in the Beryllium Industry. In: An Environmental Odyssey: People, Pollution, Politics in the Life of a Practical Scientist. Seattle, WA: University of Washington Press; 48-54
16. Davis B (2001) Research Report 00701MG.DAV, submitted to Noranda Inc.
17. Waltrip JS (1990) Fresh Look at Some Old Magnesium Diecasting Alloys For elevated Temperature Applications, Proc. 47th Ann. World Magnesium Conf., IMA, Cannes, May, pp. 124-129
18. Mercer WE (1990) Magnesium Die cast Alloys for Elevated Temperature Applications, SAE 900788
19. Pekgülyüz MO, Avedesian MM (1992) Magnesium Alloying – Some Potentials for Alloy Development, Jour. Japan Inst. Light Metals, Vol. 42, No. 11, pp. 679-686
20. Pekgülyüz MO, Avedesian MM (1992) Magnesium Alloying – Some Metallurgical Aspects, Proc. Intl. Conf. Magnesium Alloys and Their Applications, Mordike BL and Hehman F, Eds. Deutsche Gesellschaft für Materialkunde, Garmisch, Germany, April, pp. 213-220
21. Pekgülyüz MO, Luo A, Vermette P and Avedesian MM (1993) Magnesium Alloy Development, Proc. 50th Ann. World Magnesium Conf., IMA, Washington, D.C., May, pp. 20-27
22. Luo AA, Pekgülyüz MO (1994) Cast Magnesium Alloys for Elevated Temperature Applications – A Review, Jour. Materials Science, Vol. 29, pp. 313-319
23. Pekgülyüz MO and Luo A (1996) Creep Resistant Magnesium Alloys for Diecasting, ITM Inc., International Patent Application WO 96/25529
24. Luo A, Shinoda T (1998) A New Magnesium Alloy for Automotive Powetrain Applications, SAE 980086
25. Pekgülyüz MO (1999) Development of Creep Resistant Magnesium Diecasting Alloys – An Overview, Proc. Aalen Conf. Magnesium Technology, Aalen, Germany, Sep.
26. Pekgülyüz MO and Renaud J (2000) Creep Resistance in Mg-Al-Ca Alloys, 2000 Magnesium Technology, H. Kaplan, J. Hryn and B. Clow, Eds. TMS, pp. 279-284
27. Koike S, Washizu K, Tanaka S, Baba T, Kikawa K (2000) Development of Lightweight Oil Pans Made of a Heat-Resistant Magnesium Alloy for Hybrid Engines SAE 2000-01-1117
28. Pekgülyüz MO (2000) Development of Creep Resistant Magnesium Diecasting Alloys, Magnesium Alloys 2000, Materials Science Forum, Y. Kojima, T. Aizawa, S. Kamado, Eds. Trans. Tech. Publication, Switzerland, pp. 131-130
29. Pekgülyüz MO, Baril E (2001) Development of Creep Resistant Magnesium-Aluminum-Strontium Alloys, 2001 Magnesium Technology, J. Hryn, Ed., TMS, New Orleans, March, pp. 119-136
30. Luo AA and B. Powell B (2001) Tensile and Compressive Creep of Magnesium-Aluminum-Calcium Based Alloys, 2001 Magnesium Technology, J. Hryn, Ed., TMS, New Orleans, March, pp. 137-144
31. Labelle P, Pekgülyüz M, Don Argo, Dierks M, Sparks T, Waltematte T (2001) Heat Resistant Magnesium Alloys for Power-Train Applications, Society of Automotive Engineers SAE Paper 2001-01-0424
32. Gruzleski JE and Abdulcelil Aliravci (1992) Low Porosity, Fine-Grain Sized Strontium-Treated Magnesium Alloy Castings, US Patent 5,143,564, Sep. 1

33. Jackson JH, Frost PD, Loonam AC, Eastwood LW and Lorig CH (1949) Magnesium-Lithium Base Alloys – Preparation, Fabrication, and General Characteristics, Metallurgical Transactions, Vol. 182, pp. 149–168
34. Frost PD (1965) Technical and Economic Status of Magnesium Lithium Alloys, Technology Utilization Report to Industrial and Defense Management, National Aeronautics and Space Administration, Washington, DC, August, p. 38
35. Frost PD, Jackson JH, Loonam AC and Lorig CH (1959) The Effect of Sodium Contamination on Magnesium-Lithium Base Alloys, Journal of Metals, Trans AIME, Vol. 188, pp. 1171–1172
36. Vyatkin IP, Mushkov V, Kechin VA and Elkin FM (1972) Technological Features Related to the Preparation of Magnesium-Lithium Alloys, Sov. Journal of Non-Ferrous Metals, June Vol. 13, No. 6, pp. 48–49
37. Saia A and Edelman RE (1962) Silicon Effect on Magnesium Lithium Based Alloys, AFS Transactions, pp. 909–914
38. Saia A and Edelman RE (1962) Producing Magnesium-Lithium Alloy Castings, Foundry, Vol. 90 Aug. pp. 38–41
39. Saia A and Edelman RE and Gilmore HL (1967) The gating and Riser of Counter-Gravity Poured Magnesium-Lithium Castings, Modern Casting, Vol. 52, No. 1, July, pp. 105–114
40. Singh RK, Sudhakar B and Chakravorty CR (1989) Producing Magnesium-Lithium Alloys Castings, Indian Foundry Journal, Vol. 35, No. 5, pp. 21–24

## References to Chapter 4.2

41. Sauerwald F (1947) Z. Anorg. Chem. 255, 212
42. Sauerwald F (1949) Z. Anorg. Chem. 258, 296
43. Sauerwald F (1949) Z. Metallkunde. 40, 41
44. Emley EF (1966) Principles of Magnesium Technology Pergamon Press Ltd. pp. 126–156
45. Tamura Y, Kon N, Motegi T, Sato E (1998) J. Jpn. Inst. Light Metals. 48, pp. 185–189
46. Qian M, Zheng L, Graham D, Frost M, StJohn DH (2001) J. Light Metals, Vol. 1, pp. 157–165
47. Davis B (2001) Study of Zr Grain refinement in Magnesium and Alloys by Sedimentation Techniques. Univ. Oxford. 2001. Magnesium Elektron Sponsored Post-Doc Project Report (Unpublished)
48. Emley EF (1966) “Principles of Magnesium Technology” Pergamon Press Ltd., pp. 254–261
49. StJohn DH, Dahle AK, Abbot T, Nave MD, Qian M (2003) “Solidification of cast Magnesium Alloys” Magnesium Technology 2003, Ed. Kaplan HI, TMS, pp. 95–100
50. Forward CT, Bettles C (2000) CAST, Australia (private communication, Jan 2000)

# 5 Magnesium Casting Alloys

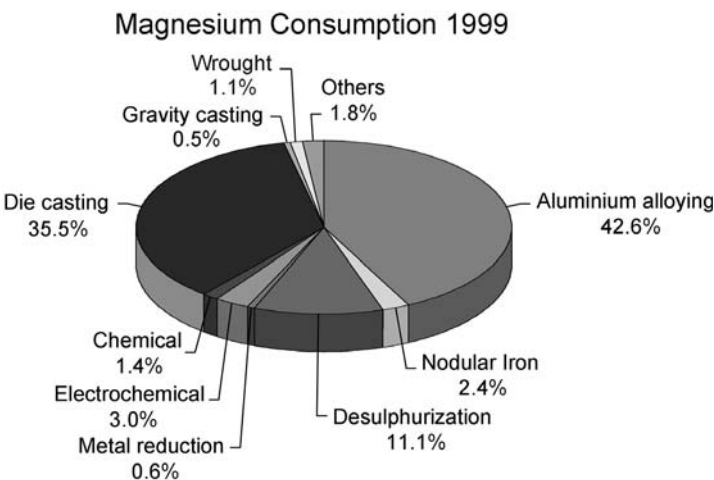
## 5.1 Casting Alloys

*Håkon Westengen, T. K. Aune*

### 5.1.1 Introduction

The global annual magnesium production in 1999 was around 375,000 metric tons according to statistics from the International Magnesium Association [1]. The consumption of the various market segments is illustrated in Fig. 5.1. The die casting segment is growing in excess of 15% per year and is now challenging the aluminium alloying segment as the largest single market segment. Gravity casting includes sand and permanent mould casting and amounts to approximately 2,000 tons per year, with a limited annual growth.

The magnesium die casting market is driven mainly by automotive applications [2]. There is also certain growth in applications for the “3C” market (Communications, Computers and Cameras) and for handheld tools [3]. Traditionally the workhorse alloy has been AZ91. This alloy shows superior castability and good mechanical properties, combined with good corrosion resistance for the high



**Fig. 5.1.** Market segments for magnesium 1999 [1]

purity versions of the alloy. Typical applications include transmission casings, valve covers, intake manifolds, brackets, pumps, etc. Most of the 3C applications and handheld tool parts are also made from AZ91.

Introduction of the high-ductility, energy absorbing alloys in the AM-series is a major driving force behind the expansion of the automotive use of magnesium diecastings [4–8]. These alloys are used for components that are subjected to deformation during a crash. Examples of applications include steering wheel cores, instrument panel substrates, seats, doors, body parts, etc.

Engine parts exposed to temperatures exceeding 120°C represent a potentially large market for magnesium die castings. Major efforts are undertaken to improve the creep resistance of magnesium die casting alloys to allow for operating temperatures exceeding 150°C [9]. It is a paradox that while a series of magnesium sand casting alloys with superior creep properties are available for applications with working temperatures reaching 250°C or even more [10], there is still a lack of good die casting alloys with adequate creep properties in the temperature range of 150–200°C for automotive engine applications.

The sand and permanent mould casting alloys are used for rather specialised applications. Racing wheels, engine blocks and certain parts for helicopters and aircraft constitute the majority of applications. In addition to AZ91, a series of special alloys containing Zr as grain refining additive, are available. Examples are provided by ZE41, EZ33, QE21 and WE 43 [10, 11].

## 5.1.2 Alloying Principles

### 5.1.2.1 Properties of Pure Magnesium

Table 5.1 lists some important physical properties of pure magnesium. Pure magnesium is mainly used as an alloying element in aluminium, for steel desulphurization, production of nodular cast iron, as a reducing agent in titanium and zirconium production and as a chemical in various processes. It follows from Table 5.2 that pure magnesium is soft and mechanically weak.

### 5.1.2.2 Alloy Preparation

Pure magnesium has a hexagonal crystal structure with lattice parameters  $a = 0.32092$  nm and  $c = 0.52105$  nm [13, 14]. The ideal  $c:a$  ratio for close packed spheres is 1.633. For magnesium at room temperature the value is 1.6236. This shows that magnesium has a nearly perfectly close packed hexagonal structure with an atomic diameter of 0.32 nm.

If nonconventional methods are applied to produce the materials, alloys with an extremely wide range of compositions and microstructures can be made [15, 16]. Such techniques may involve mechanical alloying, cospraying, sintering, fibre- or particulate composites, etc. However, in the vast majority of applications, conventional molten metal processing is used. In such cases extensive liquid solubility of the alloying elements is a prerequisite.

The liquid solubility of elements in magnesium thus plays a decisive role in determining their usefulness as alloying elements. Interactions between the

**Table 5.1.** Physical properties of pure magnesium (99.9 wt%) [12]

Property	Value
Melting point	650°C ± 2
Boiling point	1107°C ± 10
Latent heat of fusion	0.37 MJ/kg
Latent heat of evaporation	5.25 MJ/kg
Heat of combustion	25.1 MJ/kg
Specific heat	
at 20°C	1030 J/(kg K)
at 600°C	1178 J/(kg K)
Electrical resistivity at 20°C	4.45 μΩ cm
Thermal conductivity at 25°C	155 W/(kg K)
Linear coefficient of thermal expansion at 20°C	25.2 × 10 <sup>-6</sup> K <sup>-1</sup>
Density	
at 20°C	1.738 g/cm <sup>3</sup>
at 600°C	1.622 g/cm <sup>3</sup>
at 650°C (solid)	1.65 g/cm <sup>3</sup>
at 650°C (liquid)	1.58 g/cm <sup>3</sup>
Volume change during solidification	4.2%
Volume change during cooling 650–20°C	5%

**Table 5.2.** Mechanical properties of pure magnesium (99.9 wt%) [12]

	Tensile strength MPa	Tensile yield strength MPa	Compressive yield stress MPa	Elongation % 50 mm	Brinell hardness 500 kp/10 mm
Sand cast, thickness 13 mm	90	21	21	2–6	30
Extrusion, thickness 13 mm	165–205	69–105	34–55	5–8	35
Hard rolled sheet	180–220	115–140	105–115	2–10	45–47
Annealed sheet	160–195	90–105	69–83	3–15	40–41

different elements in the liquid determine the level of liquid solubility. Large differences in electronegativity will promote formation of stable compounds that tend to reduce the liquid solubility [14]. This is reflected in the phase diagrams. Some elements such as silicon, manganese and zirconium have the solubility, however, the temperatures necessary to dissolve substantial amounts are high, limiting the practical amounts. Figure 5.2 indicates the level of liquid solubility of alloying elements in binary magnesium alloys [17, 18].

When several alloying elements are added, the situation becomes extremely complex, and it is often observed that the liquid solubility of an element is sup-

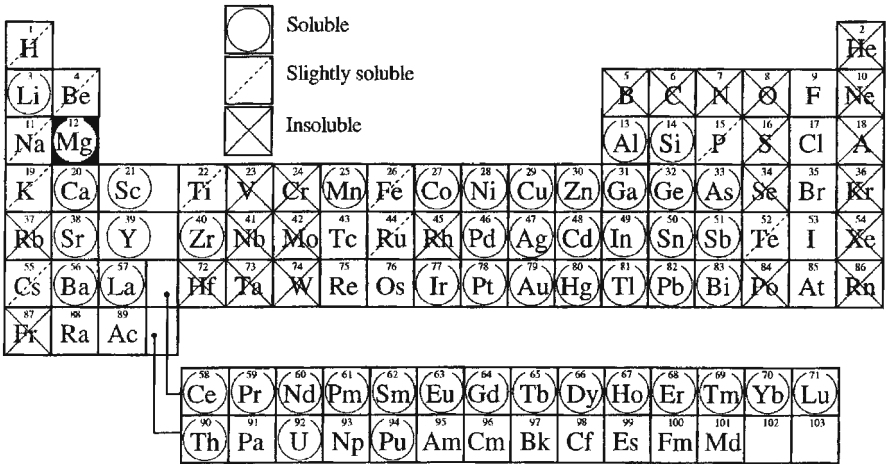


Fig. 5.2. Liquid solubility of elements in binary magnesium alloys [17, 18]

pressed by third or more element additions. Thermodynamically stable intermetallic particles suppress the liquid solubility. Even if elements in group 2a, 3a, 3b and 4a of the periodic table generally show a high liquid solubility in magnesium, combinations of alloying elements may reduce the liquid solubility dramatically. An example is provided by a recently developed alloy, containing 2 wt% Al, 1 wt% Si and additions of rare earth (RE) elements as well as manganese [19]. In this alloy the liquid solubility of both manganese and RE-elements are in the range 0.1 wt%. In binary alloys these elements have extensive liquid solubility. Another, very useful example of suppression of the liquid solubility is the reduction in Fe-solubility with Mn-additions to Mg-Al alloys. This is exploited to produce high purity alloys [20, 21].

A further important aspect of alloy design is the solid solubility of the alloying elements [14]. A prerequisite for extensive solid solubility is that the atomic size of the alloying elements does not deviate more than approximately 15% from that of magnesium, Fig. 5.3. With a few exceptions this general rule apply.

As for the liquid solubility, the stability of the intermetallic constituents plays a decisive role in determining the solid solubility. Most of the intermetallics are extremely stable, a fact that reduces the solid solubility to low levels for most of the binary systems. Figure 5.4 summarises the solid and liquid solubility of alloying elements in binary magnesium alloys.

Also the solid solubility will usually be reduced by addition of more alloying elements. A typical example is provided by the Mg-Zn-RE system. A commercial alloy ZE63 was developed for special high temperature applications. This alloy could not be solution treated due to the low solid solubility of Zn in the presence of RE-elements. To remedy this situation, a special heat treatment schedule, involving treatment in hydrogen atmosphere at elevated temperature was developed. Hydrogen diffuses rapidly in magnesium, and forms extremely stable compounds with RE, thus releasing Zn bound in intermetallic particles. The Zn in solid solution could then be utilised fully in subsequent age hardening heat treatment.

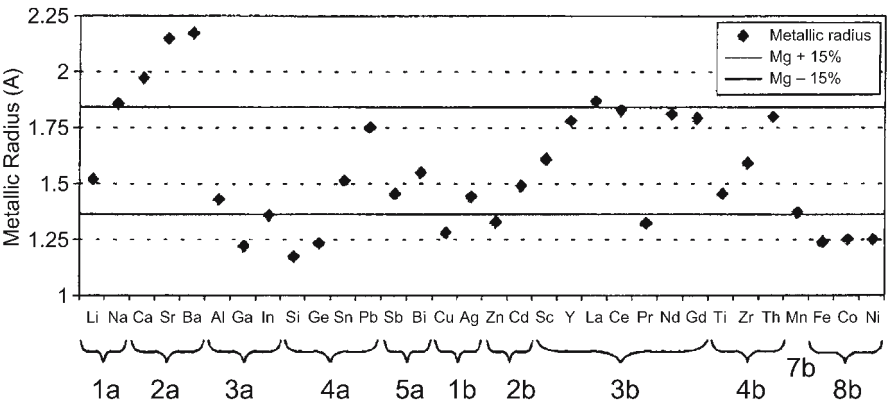


Fig. 5.3. Atomic sizes of the elements [14]

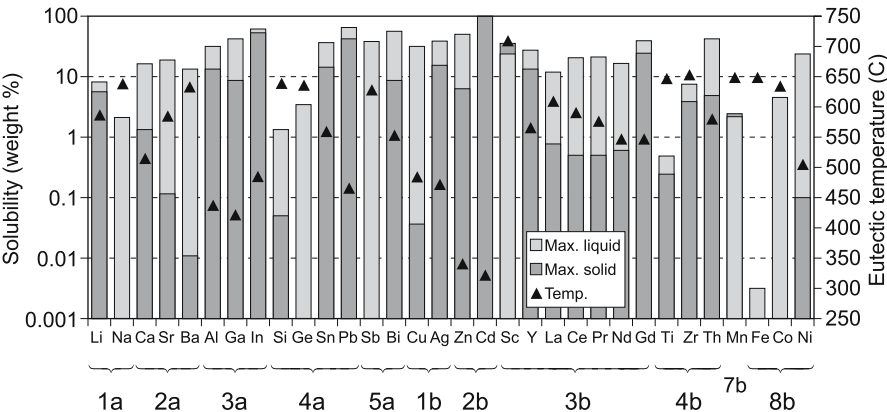


Fig. 5.4. Solid and liquid solubility of alloying elements in binary magnesium alloys. Note that the left axis is exponential. Max. liquid solubility is identical with the concentration at the eutectic or peritectic point. The eutectic temperatures are indicated on the right axis [17–19]

### 5.1.2.3 Alloying Elements and Their Influence

#### General

Pure magnesium is hardly used as a construction material. Alloying elements are used to influence a wide variety of properties, both to increase the manufacturability and the product properties. From a practical point of view, casting alloys are tailored both to the applied casting method and to the product requirements. Product requirements will also to a large extent depend on actual design of the part. Ideally a casting alloy should fulfil the whole range of properties, however, in practice there will always be some compromising.

Factors to be considered: Molten metal reactivity, castability, grain structure control, mechanical properties, corrosion properties, physical properties, machinability, formability, weldability etc.



In the following we will discuss how some of these properties of magnesium alloys are influenced by alloying elements, and practical approaches to optimise performance.

### ***Molten metal reactivity***

Magnesium alloys have a high affinity for oxygen and nitrogen in the atmosphere [22]. The vapour pressure of molten metal is high, and the oxide layer formed on the molten metal surface is porous and non-protective. The reactivity of the metal is reduced by certain alloying elements, in particular beryllium, which is active at levels down to 5 ppm [22]. This is due to enrichment of beryllium in the surface layer. Beryllium has a very low solubility, which decreases with falling temperatures. Beryllium therefore tends to precipitate out of the liquid at temperatures approaching the liquidus temperature. Also, due to the high tendency to segregate to the surface, the beryllium content decreases with time as it is incorporated into the surface oxide. Beryllium is commonly added in concentrations 5–15 ppm in die casting alloys. In sand casting alloys, beryllium must be limited due to its negative effect on grain size. Beryllium is classified as a carcinogenic substance, and care must be taken during handling of the material. It is usually added as aluminium-1 wt% beryllium hardener, and working gloves should always be used to avoid direct contact with the skin.

Other alloying elements, such as aluminium, also reduce the oxidation rate of molten alloy. Similarly calcium is reported to depress the reactivity. In practice alloying additions are not sufficient to protect against excessive oxidation. Salt fluxes or protective gases are used as additional remedies.

### ***Purity control***

A prerequisite to obtain the excellent corrosion properties of current magnesium alloys is careful control of the impurity levels. Elements such as Fe, Ni, and Cu are highly detrimental to corrosion properties, see Fig. 5.5 [20], and strict specification limits apply for these elements (ASTM Standard, EU Standard).

Fe is removed by a process utilising the fact that the solubility of Fe in molten magnesium is suppressed by Mn-additions [20, 21]. As an example, the standard alloy AZ91D is produced according to the following principles: the basic material is pure magnesium with minimum purity of 99.90%. Mn is added at an elevated temperature to a level exceeding the final specification. Following an addition of Mn, aluminium and Zn is added, and the temperature of the molten alloy is then lowered to the casting temperature. Be is added and before casting the alloy is equilibrated at the casting temperature. During the alloying and equilibrating process, Mn, Al, and Fe are precipitated as intermetallic compounds that settle to the sludge in the bottom of the furnace. The process allows full control of the Fe-content to levels well below the specification limits for high purity alloys. In the same process, some Ni is removed, however, Ni-removal by Mn-additions is not fully efficient to purify contaminated metal to levels below high purity specifications. At present there are no established methods to control Ni and Cu other than controlling the purity of basic alloy constituents [23].

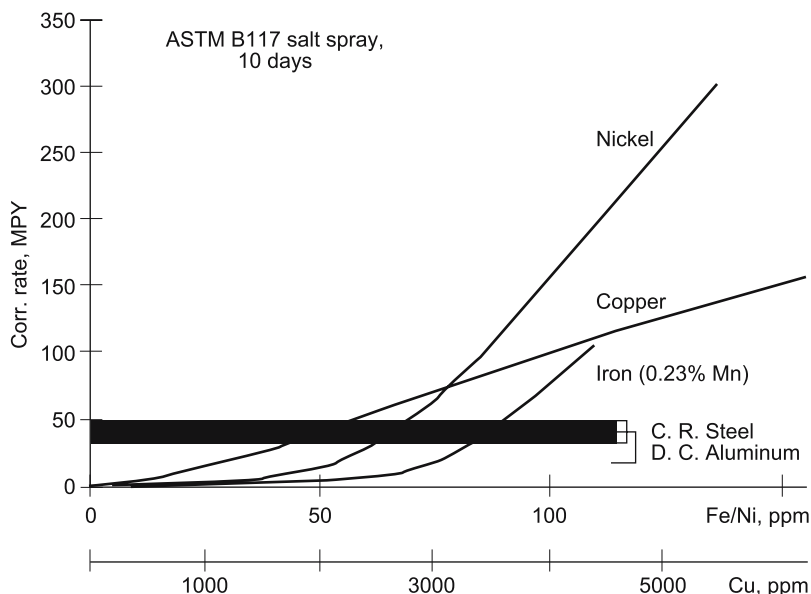


Fig. 5.5. Influence of impurities on corrosion rate. Performance vs. impurity content. Cold rolled steel and die cast aluminium as reference [20]

Molten metal purification by reducing the solubility of the impurities is also an additional effect of the grain refining additive Zr. Fe is precipitated in Zr-containing intermetallics to levels that improve the corrosion rate of the alloys. Other elements that interact with Fe are rare earth elements, especially when present in Al-containing alloys. The corrosion rate is determined by several factors including size, distribution, type and composition of the intermetallic particles precipitated during cooling from the casting temperature. By controlling such factors, alloys can be composed that show superior corrosion properties.

### Grain refining

Magnesium alloys, except for some special Li-containing alloys, all exhibit a hexagonal crystal structure. This means that at ambient temperatures, the number of operating slip systems limits the formability of the metal. This is due to localised slip and build-up of stresses at the grain boundaries in locations where the localised deformation occurs. The larger the grain size, the larger the build-up of stresses [22]. The result is that coarse-grained alloys show only limited formability at ambient temperatures. Also the yield strength is low due to the extremely high stress concentration factors resulting from localisation of slip. A further effect of grain refinement, is the improvement in flowability, and hence mould filling characteristics, see next paragraph.

Grain refining can be achieved by different methods, superheating, trace element additions, peritectic additions, constitutional grain refining or rapid

solidification. In wrought alloys grain refining can be achieved by thermo-mechanical treatment.

Superheating was traditionally used for sand and permanent mould casting of Mg-Al alloys [22]. The molten metal was heated to temperatures in the range 850°C before it was cooled to the casting temperature and poured. The mechanism of the grain refining process has never been fully explained, however, it has been argued that pickup of carbon from the steel crucibles and subsequent formation of carbon-containing nuclei during cooling is the probable mechanism. This is supported by the fact that addition of carbon-containing substances like wax-fluorspar, hexachloroethane or simply finely dispersed carbon black promote grain refining. Carbon is only present as a trace element, but apparently, a sufficiently high number of nuclei, probably  $\text{AlC}_4$ , is formed to promote grain refining. The grain size accomplished by these methods is in the range 100–200  $\mu\text{m}$ . This is sufficient to obtain better mould filling characteristics, reduced porosity level and reduction of hot cracking as well as somewhat improved mechanical properties.

Grain refining by addition of Zr is extremely efficient [24], in fact it is the most efficient grain refining additive ever reported for metallic alloys. The grain structure observed in sand or permanent mould castings consists of spherical grains, with a size characteristic for the cooling rate. It is typically possible to achieve grain sizes in the range 10–100  $\mu\text{m}$ , depending upon the cooling conditions. Figure 5.6 shows the effect of Zr-refining of pure magnesium. It follows that both strength and ductility increase dramatically with increasing Zr-content up to about 0.6 wt%. The spherical grain structure promotes extremely good flow

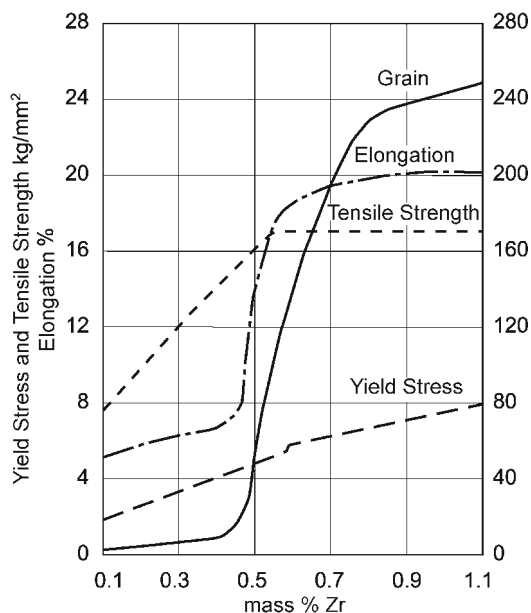
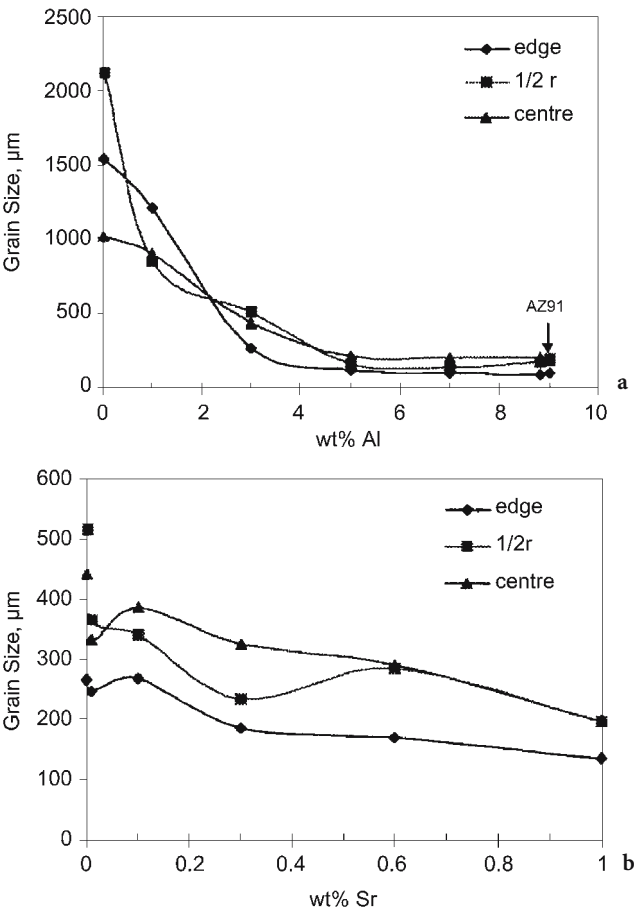


Fig. 5.6. Effect of Zr-additions to sand cast binary Mg-Zr alloys, on mechanical properties and grain size [24]

characteristics, and a series of alloys have been developed in which all depends on the grain refining action of Zr. The probable mechanism is that primary particles containing Zr are formed in the molten alloy. These intermetallic particles have a crystal structure that acts as a potent substrate for growth of the  $\alpha$ -Mg by the peritectic reaction  $\text{Liq} + \text{MgZr} \rightarrow \alpha\text{-Mg}$ . Zr is compatible with a number of alloying elements such as Zn, Ag, Nd, Ce, Y, Th, etc. However, it is not compatible with the most common alloying element Al. This is due to the formation of the highly stable  $\text{Al}_3\text{Zr}$  intermetallic, which reduces the liquid solubility of Zr to negligible levels.

It is well known that a certain grain refining effect is obtained by adding alloying elements, especially if the partition coefficient is less than one, as is common for eutectic systems. This kind of grain refining is due to a slow-down of the growth rate because of solute build-up. Even if the nucleation rate is not influ-



**Fig. 5.7.** **a** Effect of aluminium content on grain size [25]. **b** Effect of strontium content on grain size. Mg-3 wt% Al alloy [25]

enced, this will lead to the formation of a finer grain structure. In the binary Mg-Al-system it has been shown that the effect is considerable, Fig. 5.7 [25]. It has also been reported that additions of Sr to Mg-Al alloys, causes a significant grain refining effect.

### ***Mould filling characteristics***

The ability to fill casting moulds or dies is a complex phenomenon, involving a variety of alloy specific factors, including melting point, solidification interval, amount of eutectic constituents, grain refining, surface energy etc. When the alloy properties are combined with the casting process in use, the castability may be defined as a qualitative factor describing the ability to form quality parts with a high reproducibility. There are obvious problems to define a standardised 'castability' test. At best a test setup, like a spiral mould filling test, is capable of ranking different alloys in a relative way.

There are, however, some criteria that a good casting alloy should fulfil:

- The composition of the molten metal should be stable at the casting temperature.
- The amount of eutectic constituents should be large enough to allow feeding until the end of solidification.
- The eutectic should preferably consist of a ductile continuous phase with an isolated second phase in the form of particles, rods or plates.
- The solidification interval should not be excessively large.
- The grain structure should be refined either chemically or by rapid cooling.
- The surface energy should be low enough to fill details of the mould.
- The alloy should not react with the die/mould material to cause sticking or other damage.
- The alloying elements should provide the necessary mechanical, physical and corrosion properties.

Magnesium alloys are fulfilling these requirements to a variable degree.

Some alloying elements are unstable in the liquid state. This is especially so for Be, which tends to diffuse to the surface and react with oxygen together with magnesium and aluminium. If the temperature of the molten metal is decreased, Be also tends to precipitate due to the low solubility.

The aluminium content in molten alloys is slowly reduced due to the formation of Al-rich oxides on the metal surface. Other elements that are unstable or sensitive to variations in the temperature of the melt are Zr and Mn. Mn is stable as long as the temperature is kept constant. However, the grain refining effect of Zr is only lasting for a short time after addition. Zr-grain refined alloys are always used in batch production.

The amount of eutectic constituents is usually low in Mg-alloys, compared to typical Al-based casting alloys. In general this implies that the castability as experienced in common casting processes such as sand and permanent mould casting is somewhat limited. However, the Zr- containing alloys containing elements such as Zn, Rare Earth, Ag and Y secure a fairly good castability because of the extremely efficient grain refining effect of Zr combined with relatively high vol-

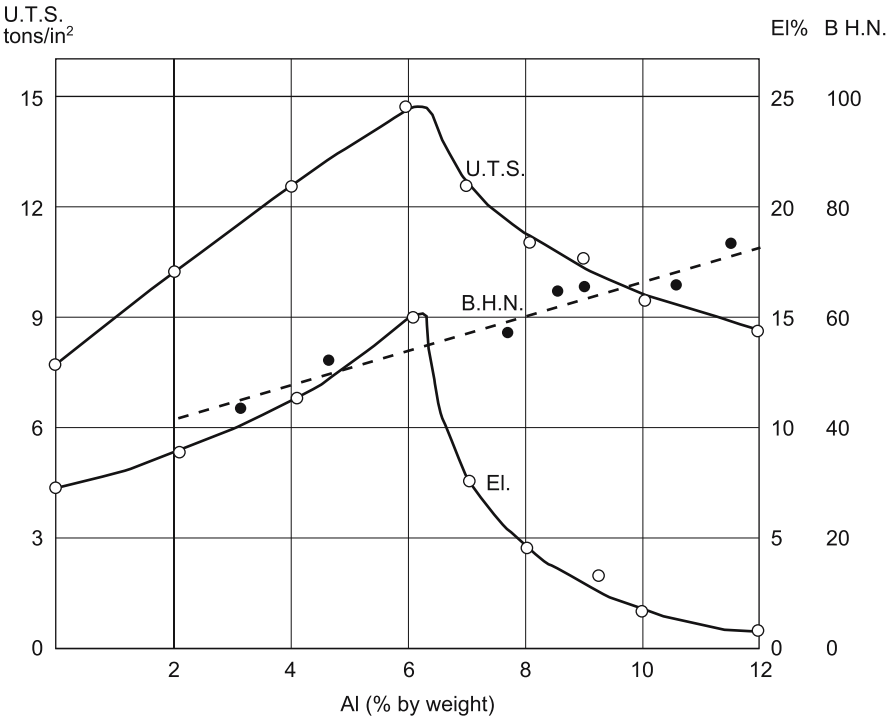


Fig. 5.8. Effect of aluminium content on ductility. Sand cast samples, as cast condition [26]

ume fractions of eutectic phase. The Mg-Al alloys derive their castability through non-equilibrium solidification as discussed in the next paragraph. Non-equilibrium solidification increases the amount of eutectic constituents considerably, compared to the situation at equilibrium solidification.

In Mg-Al alloys the eutectic consists of  $\alpha$ -Mg and  $\beta$ -Mg<sub>17</sub>Al<sub>12</sub>. The continuous phase is  $\beta$ -Mg<sub>17</sub>Al<sub>12</sub> which is brittle. This means that alloys with high amounts of aluminium tends to become brittle, and the maximum Al-content in commercial alloys is limited to about 10 wt%. From a castability point of view an alloy with up to 30 wt% aluminium would have been preferred. Such an alloy would, however, be as brittle as glass. The embrittling effect of the eutectic is illustrated in Fig. 5.8.

**Solidification**

Solidification in commercial casting processes occurs under non-equilibrium conditions. For most cases the Scheil equation gives a good description of the process [27]. This relation is based on the assumption that no diffusion occurs in the solidified material, and full mixing takes place in the molten metal. The Scheil equation can be modified to take into account some diffusion in the solid state during solidification.

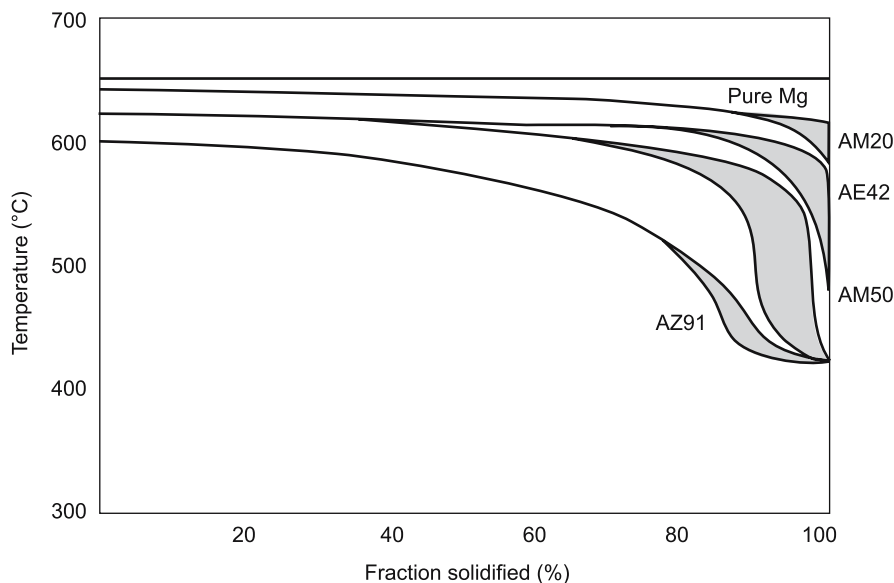


Fig. 5.9. Fraction solidified as a function of temperature, Mg-Al alloys [28]

For the Mg-Al alloys, it is common to observe eutectic constituents even when the Al-content is as low as 2 wt%. This supports the view that solidification is well expressed by the Scheil equation. Figure 5.9 shows a typical fraction solidified as a function of the temperature for Mg-Al alloys with different Al-contents.

When the Scheil equation is obeyed, there will always be a certain amount of eutectic constituents. This also means that the solidification interval of the Mg-Al alloys is very wide, Fig. 5.10. Of the commercial Mg-Al alloys, AZ91 has the highest eutectic fraction, around 10% resulting in good castability.

In some cases the solidification interval can be changed by alloying additions. Examples are provided by additions of rare earth elements or Cu to Mg-Zn alloys. This is due to a change in the solidification paths, and formation of ternary eutectics.

Based on thermodynamic data, the solidification pattern and phases formed may be calculated. Examples are provided in [29].

The scale of the microstructure is directly influenced by the cooling rate. As for most metallic alloys there is a direct relation between the local cooling rate and the secondary dendrite arm spacing. For AZ91 the following relation has been reported [30]:

$$\text{DAS } (\mu\text{m}) = 35.5 R^{-0.31} \quad (5.1)$$

where DAS is secondary dendrite arm spacing, and R is cooling rate in deg/sec through the solidification range.

There is also a correlation between the average grain size and the cooling rate, although less pronounced. In general, the grain size decreases with increasing cooling rate. As discussed earlier, the grain size may be further influenced by de-

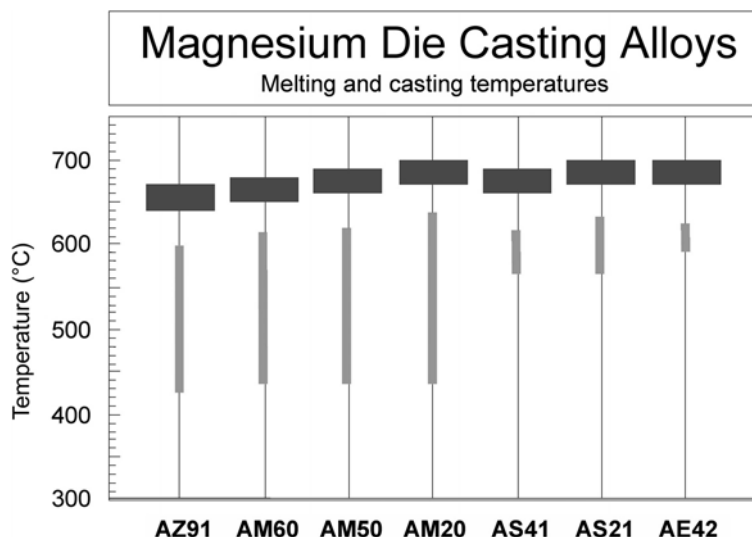


Figure 5.10. Solidification interval Mg-Al type alloys [28]

liberate grain refining additives. In a die cast part, it is generally observed that the strength and ductility decrease with increasing section thickness, Fig. 5.11 [31]. This can be attributed to the accompanying coarsening of the grain and dendrite structure. It has been claimed that this effect is amplified by the fact that solidification starts already during die filling, and a certain volume fraction of floating crystals are formed during feeding, ending up in the central parts of the cross section. A bimodal grain size distribution results [32].

### **Physical properties**

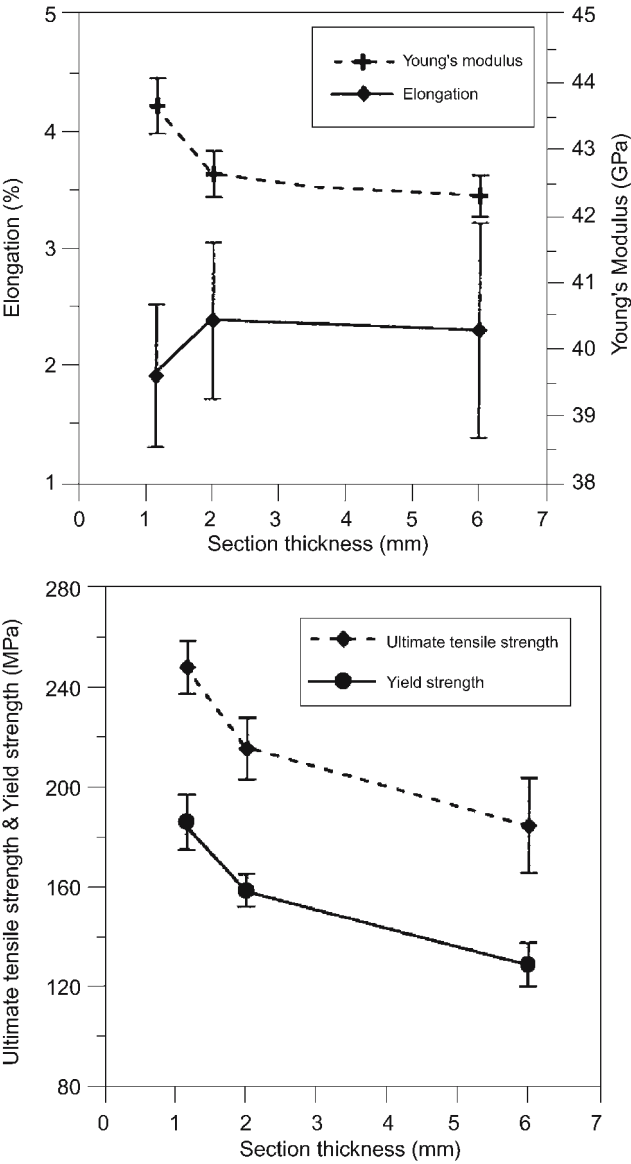
Alloying elements have a strong influence on physical properties. Some examples are provided here:

**Density.** Figure 5.12 shows the influence of alloying elements on the density of magnesium with additions of binary elements [26]. The common alloying elements increase the density of the alloys, however lithium additions dramatically reduce the density. Alloys with density  $< 1 \text{ g/cm}^3$  can be manufactured.

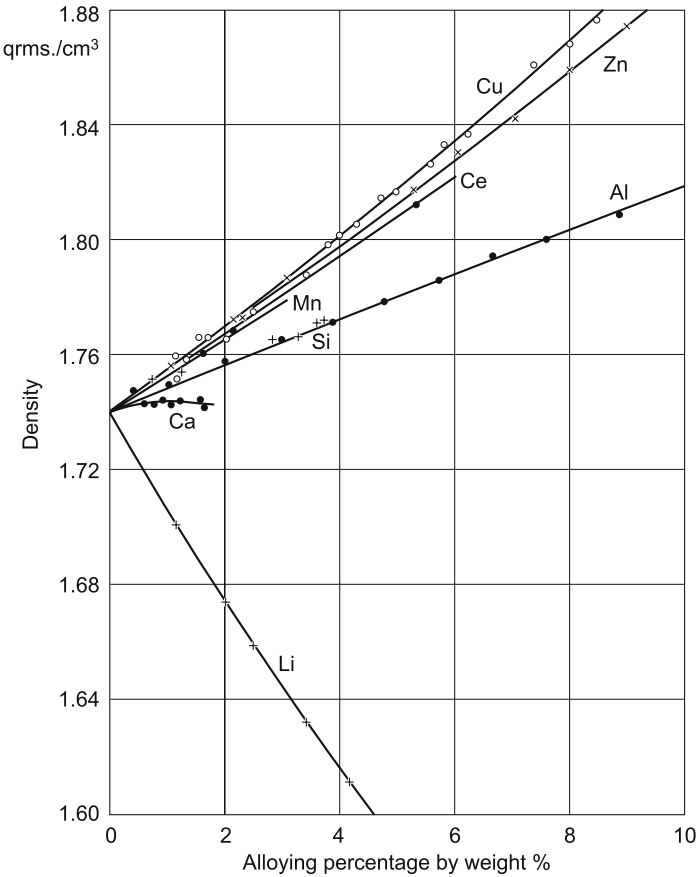
**Electrical resistivity.** Figure 5.13 shows the influence of alloying on the electrical resistivity [26]. The electrical resistivity is quite sensitive to alloying elements. Electrons are scattered at solute elements, second phase particles and other lattice defects occurring as a result of the alloying.

**Thermal conductivity.** The thermal conductivity and the electrical conductivity are strongly interrelated. According to the Wiedemann-Franz law the ratio of the thermal conductivity to the electrical conductivity is only temperature depen-





**Fig. 5.11.** Variation of mechanical properties with section thickness. Die cast AZ91D samples [31]



**Figure 5.12.** Influence of alloying elements on the density of magnesium at room temperature [26]

dent. This means that as the electrical resistivity increases due to alloying additions a corresponding decrease in the thermal conductivity will be expected. This is illustrated in Fig. 5.14 [26].

**Damping capacity.** The damping capacity of a metal reflects the ability to dissipate vibration energy. A simple way of characterising the damping capacity is to measure the decay of mechanical vibrations. The average logarithmic decrement  $\delta$  is defined as

$$\delta = N^{-1} \ln (A_1/A_{N+1}) \tag{5.2}$$

where  $N$  is an arbitrary number of oscillations and  $A_1$  and  $A_{N+1}$  are the oscillation amplitudes at start and after  $N$  oscillations. Figure 5.15 shows the average logarithmic decrement and hardness of some cast magnesium alloys [33]. The measurements are made in torsion on solid circular samples with diameter 6 mm,

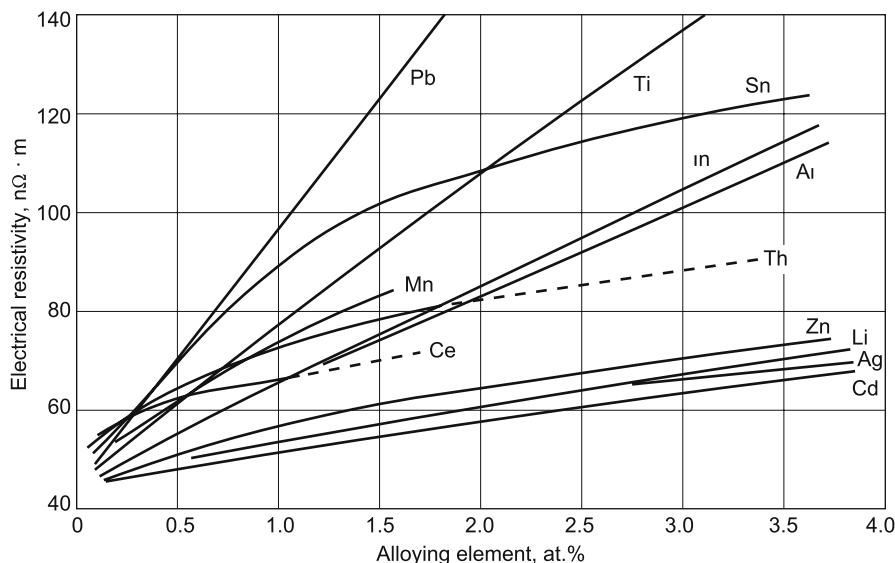


Fig. 5.13. Electrical resistivity for binary magnesium alloys as a function of alloying additives [26]

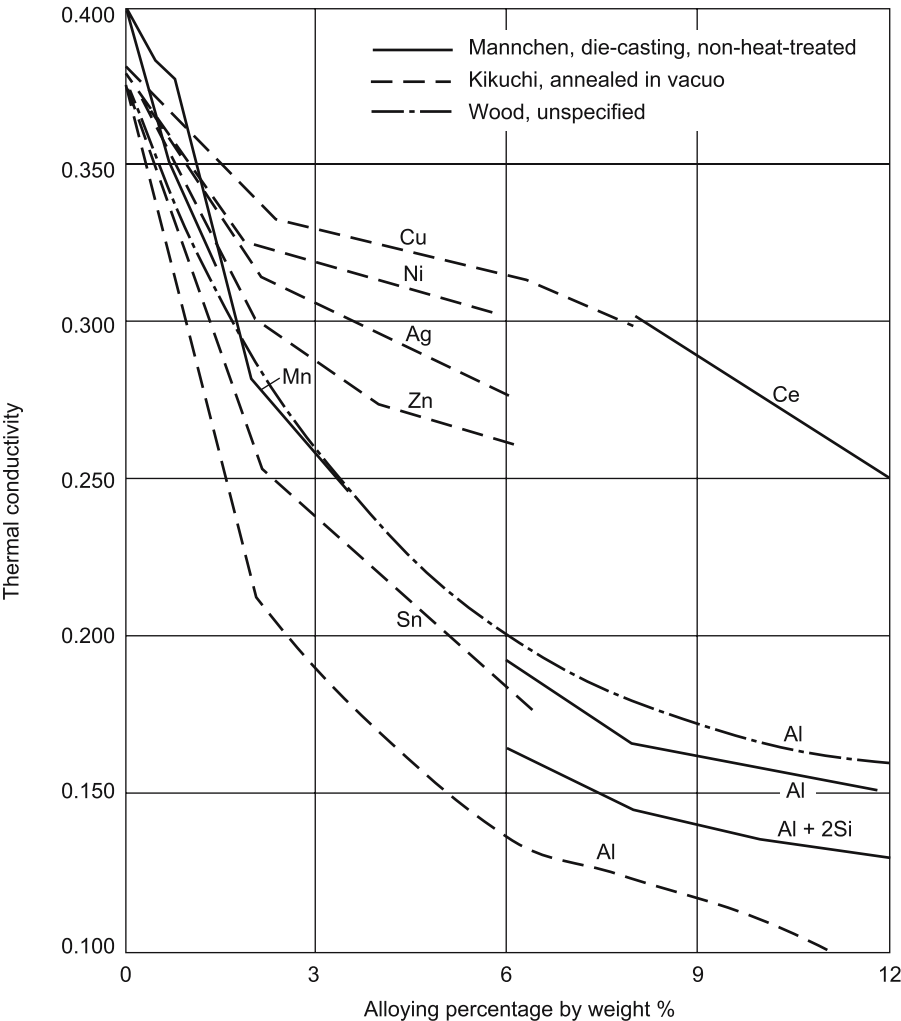
length 50 mm. It follows that the damping capacity decreases rapidly with additions of alloying elements which increase the hardness of the material. This includes aluminium and manganese. Zirconium in small amounts does not significantly influence the damping capacity. Binary magnesium zirconium alloys have found some limited use as high damping material.

### Mechanical properties

The mechanical properties of magnesium can be widely influenced by alloying. The strength of cast magnesium alloys is obtained by one or more of the well known hardening mechanisms: solid solution hardening, grain size or Hall Petch hardening, age hardening and dispersion hardening.

The influence of alloying elements on hardness is shown in Fig. 5.16 [26]. These diagrams illustrate that the hardening effect is far from linear. This is to be expected since the elements have a wide variation in solid solubility. Hence the alloying elements are partly present in solid solution, partly as intermetallic constituents. It is, however, interesting to see that there is a fairly good correlation between strength and total wt% of added elements, Fig. 5.17. The data in Fig. 5.17 are from die casting trials with a multitude of different alloys [19].

The most common hardening elements are aluminium, zinc, silicon, rare earth elements, silver and yttrium. Aluminium, zinc, silver and yttrium exhibit a high solid solubility, and the solid solubility decreases with falling temperature. This is a prerequisite for age hardening, and alloys containing these elements can be heat treated to the T4, T5 or T6 condition.



**Fig. 5.14.** Thermal conductivity of binary magnesium alloys as a function of alloying additives [26]

Some of the alloying elements form high density, stable dispersions of precipitates, capable of stabilising the structure under load at elevated temperature. Such elements include Ce, Nd, Pr, Y, Ca, Sr, Si and heavy rare earth elements such as Gd and Tb. While some of these elements have a low liquid solubility, forming precipitates during solidification, elements like Y, Gd and Tb have extensive liquid solubility and also a considerable solid solubility. The solid solubility is reduced on decreasing the temperature.

This allows for a controlled heat treatment, including solution treatment and ageing, to optimise the dispersion  $f/r$ , where  $f$  is volume fraction of particles and  $r$  the mean radius of the particles. Alloys with 3–4 wt% Y show extremely good

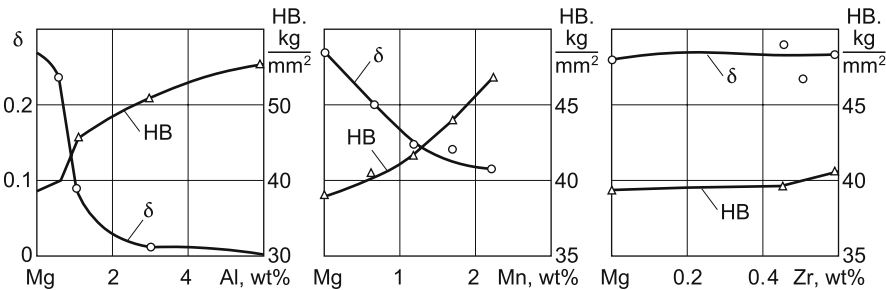


Fig. 5.15. Effect of alloying with aluminium, manganese and zirconium on damping capacity and hardness [33]

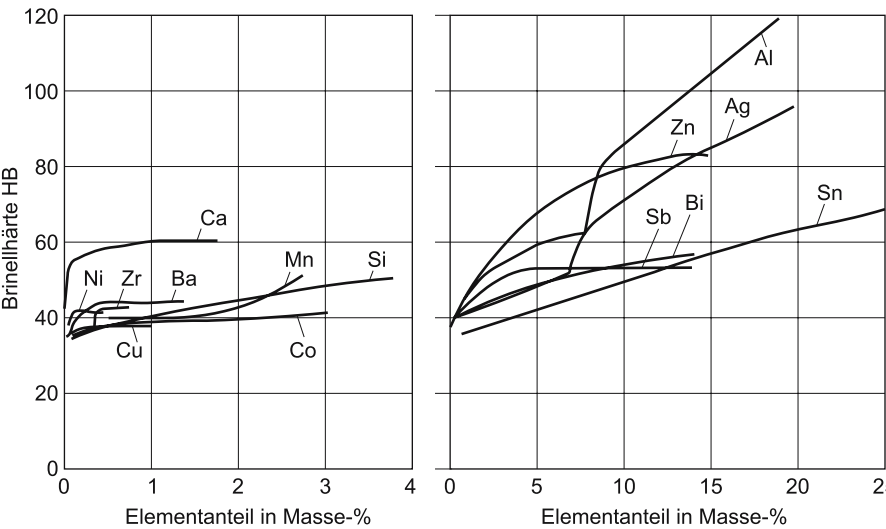


Fig. 5.16. Influence of alloying elements on hardness [26]

creep properties, and parts with working temperatures reaching 250–300°C can be produced in alloys such as WE43 [10].

### 5.1.3 Casting Methods

As discussed in Chap. 6.1, a multitude of shape casting methods are available for casting magnesium. These include sand casting, plaster mould casting, permanent mould casting, high pressure die casting, squeeze casting and various semi-solid casting methods. Each of these casting methods exhibits certain characteristic features which combined with the alloy used and part geometry determine the properties of the cast product.

For aluminium, it has been a common understanding that porosity free permanent mould castings provide the ultimate properties. Such parts can be heat treated to the fully aged condition. Squeeze casting and thixotropic casting

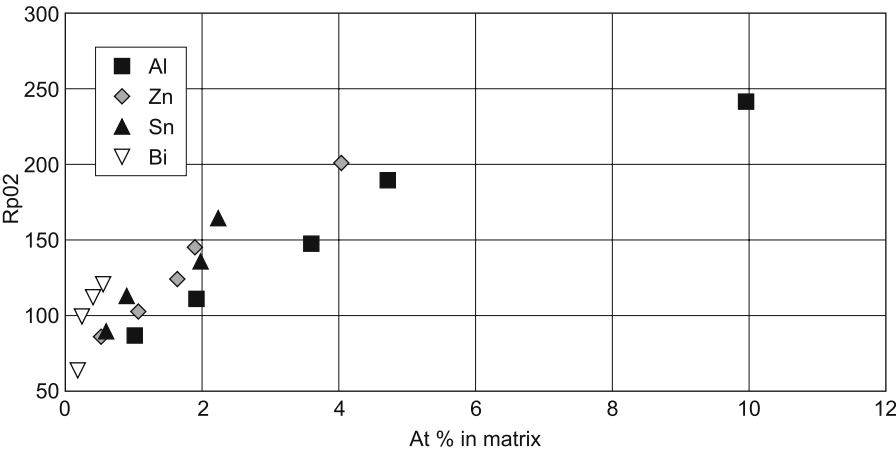


Fig. 5.17. Flow stress as a function of at % added alloying elements. Die cast samples [19]

are special versions of permanent mould castings, where the content of porosity is minimised by use of controlled mould filling and application of high pressures during solidification. High pressure die casting has until recently been considered as an inferior casting method from a quality point of view. The merits of the process were mainly attributed to its low cost and high volume production of near net shape parts. The wide specification limits of the common aluminium die casting alloy, A380 is another positive element to reduce cost.

Development of improved die casting processes and tailoring of alloys, has opened up multitude of new applications [34]. This is exemplified by the extensive use of die cast parts in the body of the Audi A2 and A8. Contrary to the traditional die cast parts, which are commonly used in cars, the body parts of Audi A2 and A8 constitute structural members which must fulfil strict requirements towards energy absorption during crash conditions. Figure 5.18 is a schematical classification of die cast light metal parts. For aluminium, most of the traditional die cast parts falls into category 1 and 2. The space frame parts are examples of large thin-walled multifunction parts with strict property requirements, category 3. The successful development of applications in category 3 has definitely changed the conception of high pressure die cast parts as inferior to other types of castings. It has also changed the attitude towards development of die casting alloys. The property requirements can only be met by advanced alloys, tailored to the specific characteristics of the process [35].

Magnesium die cast applications have generally been more advanced than aluminium, and most of the current applications are in category 3 and 4 in Fig. 5.18. These are the categories where the material price has the lowest impact on competitiveness. The added value during die casting is much higher for these product categories than for category 1 and 2. However, the recent material price ratio between aluminium and magnesium die casting alloys is now favouring many magnesium applications also in category 1 and 2.

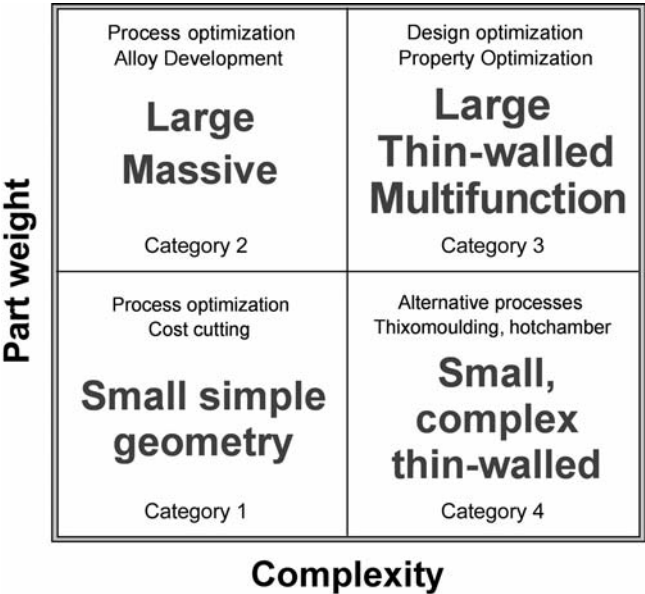


Fig. 5.18. Schematical classification of diecast parts

The renaissance of the magnesium die cast market during the last two decades can largely be attributed to two factors:

- I: The conscious reinvention and standardisation of high purity alloys
- II: Exploitation of the high ductility offered by the AM series of alloys with reduced aluminium content.

As discussed earlier, refinement of the grain and dendrite structure caused by rapid cooling is extremely beneficial for the mechanical properties. This is fully exploited in thin walled die cast parts, where cooling rates are typically in the range 100–1000°C/s. Figure 5.19 shows schematically the influence of cooling rate on the tensile properties of defect free samples. Since the various casting methods exhibit typical cooling rates, this is tentatively indicated in the diagram. In real castings, various defects caused by improper feeding or impurities will occur, reducing the ductility of the material. With reference to Fig. 5.19, it can be noted that even if a thin walled die cast part may contain more casting defects than an optimally cast permanent mould casting, the die cast part will show superior properties due to the finer grain size. As the wall thickness increases, the advantage of die casting diminishes, and for heavy wall thickness, permanent mould castings may compare favourably.

The effect of cooling rate on the grain size is also the main reason why thixotropic casting and squeeze casting do not outperform high pressure die casting for most applications. Thixomolding is a special process, where granules are fed into a heated screw, in a way similar to plastic injection moulding [36]. Semisolid slurry is injected into a die at high speeds. Figure 5.20 [37] shows that the mechanical properties improve as the amount of solid is decreases. When the

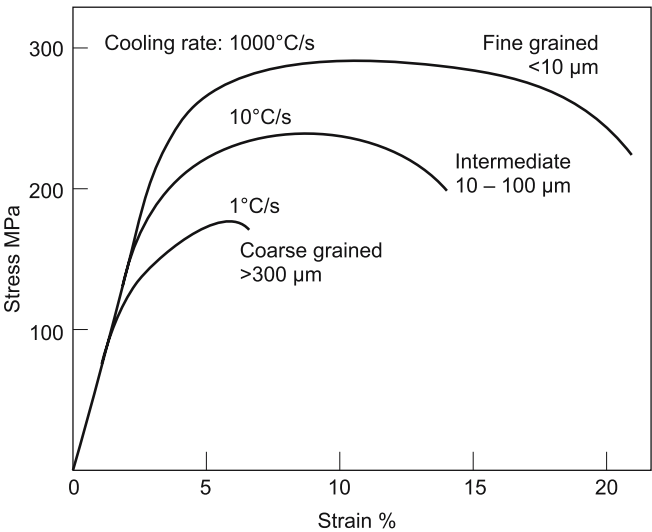


Fig. 5.19. Effect of cooling rate on tensile stress-strain curves, schematic

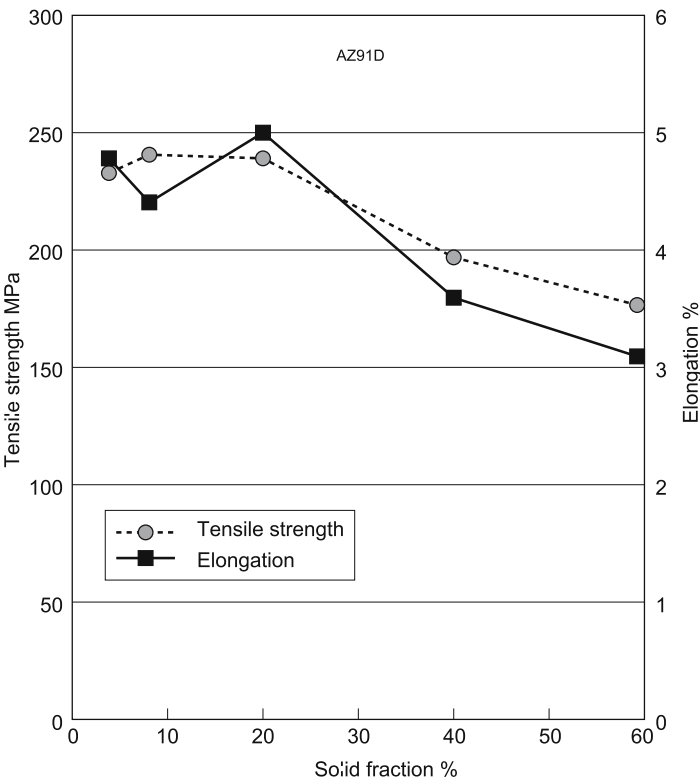


Fig. 5.20. Tensile strength and elongation to fracture of thixomoulded AZ91D vs. volume fraction solid [37]



amount of solid is reduced below 20%, the properties obtained are similar to those obtained by ordinary hot chamber die castings of good quality.

It should be noted that special alloys containing Zr as a grain refiner, are less sensitive to cooling rate during solidification. For these alloys, Zr-additions have the same effect on the structure as high cooling rates.

5.1.4 Alloys for Diecasting

5.1.4.1 Compositions

Magnesium alloys combine low component weight with cost competitive manufacturing. Thin walls, net shapes, high casting rates and long die life are typical advantages to be gained from using magnesium diecastings. Other advantages include excellent machinability, good damping capacity and electromagnetic interference (EMI) and radio frequency interference (RFI) shielding properties. High purity alloys and modern design techniques to avoid galvanic corrosion qualify magnesium for corrosive environments.

AZ91 is the most commonly used magnesium based alloy for pressure die casting, with excellent castability and good strength. Typically used for automobile and computer parts, mobile telephones, sporting goods, housings and covers, brackets, chain saw parts, handheld tools, household equipment, etc.

AM60 and AM50 are alloys with outstanding ductility and energy absorbing properties combined with good strength and castability. Typical uses are automotive seat frames, steering wheels, instrument panels, brackets, fans, etc.

AM20 is an alloy recognised for its ductility and impact strength. Typical uses are automotive safety parts where the highest possible ductility is required.

AS41, AS21 and AE42 are alloys with good creep properties up to about 150°C. Decreased aluminium content in AS21 compared to AS41 results in increased creep resistance and ductility, and in some decrease in tensile strength and castability. All three alloys offer good mechanical properties at room temperature.

Typical compositions of magnesium die casting alloys are listed in Table 5.3. All values are given in weight percent. Complete information is given in the relevant international (ISO) [38], European (EN) [39] and US (ASTM) [35, 40, 41] standards.

Table 5.3. Typical composition of magnesium diecasting alloys [%]

Alloy	Al	Zn	Mn	Si	RE <sup>a</sup>
AZ91, MgAl9Zn1	9	0.7	0.3		
AM60, MgAl6Mn	6		0.4		
AM50, MgAl5Mn	5		0.4		
AM20, MgAl2Mn	2		0.4		
AS41, MgAl4Si	4		0.4	1	
AS21, MgAl2Si	2		0.4	1	
AE42, MgAl4RE2	4				2.5

<sup>a</sup> Rare earths.

### 5.1.4.2 Microstructures (Hydro Magnesium)

#### Aluminum

Magnesium and aluminum are fully soluble in the liquid state, and the eutectic reaction takes place at 437°C, forming a mixture of  $\alpha$  (Mg) and  $\beta$  ( $\text{Mg}_{17}\text{Al}_{12}$ ), see Figs. 5.21 and 5.22. The binary phase  $\text{Mg}_{17}\text{Al}_{12}$  is brittle, and alloys with a large volume fraction of eutectic have reduced practical interest due to their brittleness. The form of this  $\beta$ -phase depends on whether the alloy contains zinc or not. If zinc is not present, a massive compound with islands of magnesium solid solution is formed. In alloys with zinc a completely divorced compound is formed. The precipitation of  $\beta$  from solid solution can be continuous or discontinuous. During cooling of alloys with more than about 8% Al (depending on cooling rate), such precipitation starts at grain boundaries and has a lamellar form (Fig. 5.21).

#### Zinc

If aluminum is present, zinc is dissolved mainly in the  $\beta$ -phase. If the ratio of zinc to aluminum exceeds 1 to 3, the  $\text{Mg}_{17}\text{Al}_{12}$  phase is transformed to  $\text{Mg}_{32}(\text{AlZn})_{49}$ .

#### Manganese

If no aluminum is present, manganese appears as primary elemental particles. With the presence of aluminum, a Mn-Al compound is formed. If sufficient iron

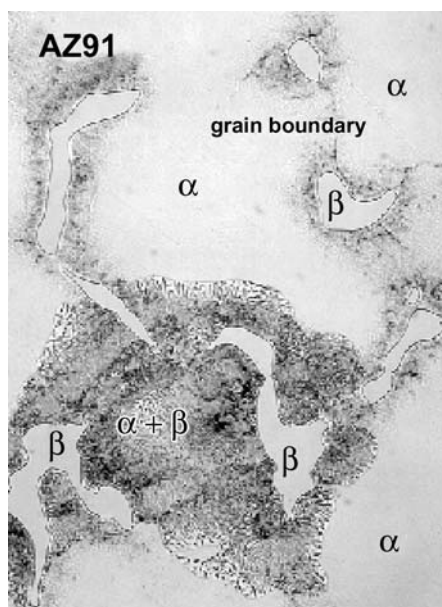


Fig. 5.21.  $\alpha$  (Mg) and  $\beta$  ( $\text{Mg}_{17}\text{Al}_{12}$ ) in AZ91

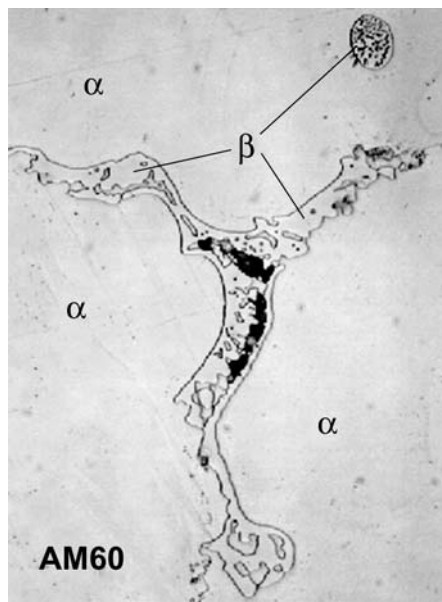


Fig. 5.22.  $\alpha$  (Mg) and  $\beta$  ( $\text{Mg}_{17}\text{Al}_{12}$ ) in AM60

is present, a Mn-Al-Fe compound is formed. The manganese-rich phases appear in a variety of shapes, from irregular to needles (Fig. 5.23).

### **Silicon**

Addition of Si causes the formation of finely dispersed  $\text{Mg}_2\text{Si}$  particles. This phase is shaped either as a polygon or Chinese characters at higher concentrations of Si (Fig. 5.24).

### **Rare earth elements**

In AE42 a dispersion of  $\text{Al}_4\text{RE}$  and  $\text{AlMnRE}$  intermetallics are formed (Fig. 5.25).

### **Oxides**

Oxides are formed as films or clusters (Figs. 5.26 and 5.27).

### **Examples of microstructures**

The microstructure of an alloy depends on the alloy composition, solidification and cooling rates and patterns, as well as heat treatment. The structure of a die casting alloy with a high solidification rate is much more finely distributed than that of a gravity cast alloy. The pictures (Figs. 5.28–5.31) show examples of optical micrographs of die cast alloys.

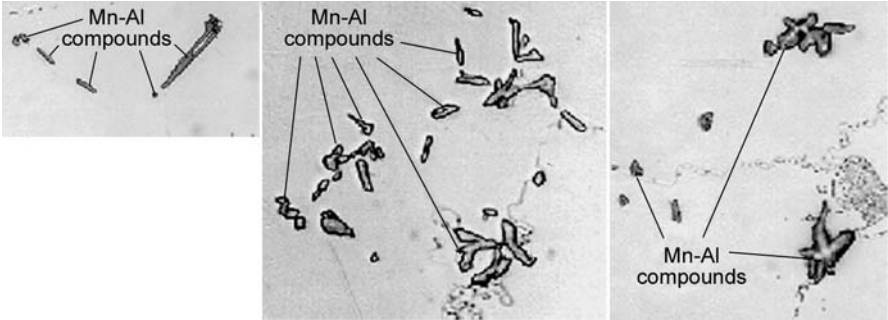


Fig. 5.23. Mn-Al compounds of different shapes

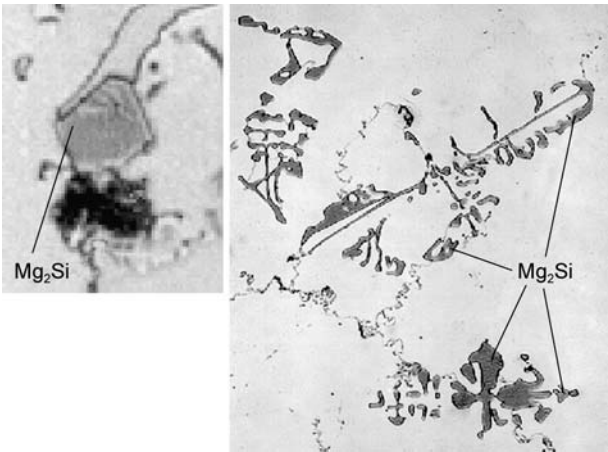


Fig. 5.24. Mg<sub>2</sub>Si particles

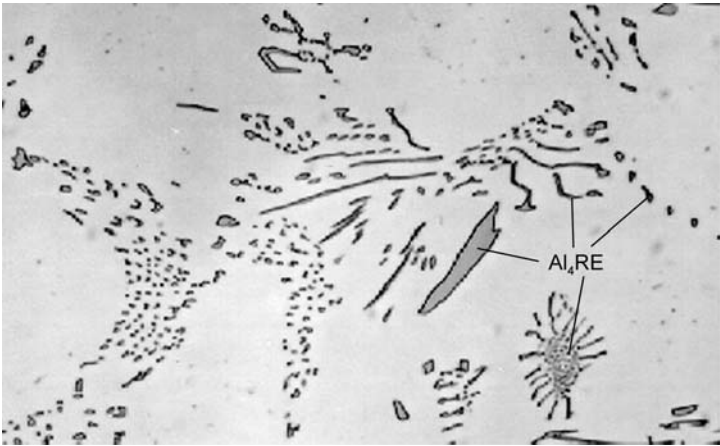


Fig. 5.25. Al<sub>4</sub>RE intermetallics

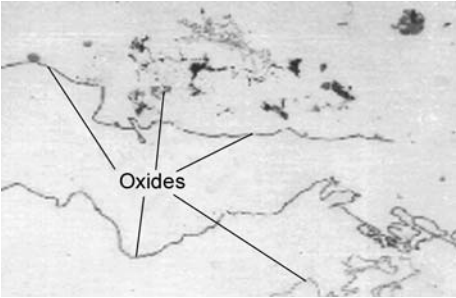


Fig. 5.26. Oxide films

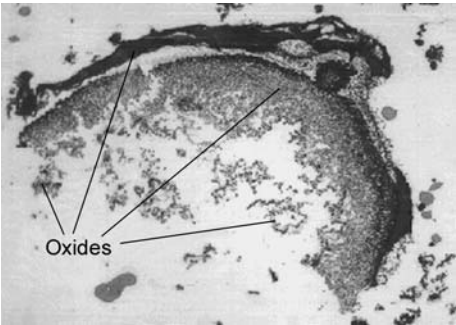


Fig. 5.27. Oxide clusters

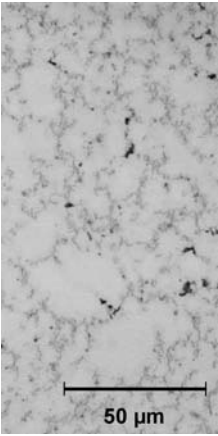


Fig. 5.28. Alloy AZ91

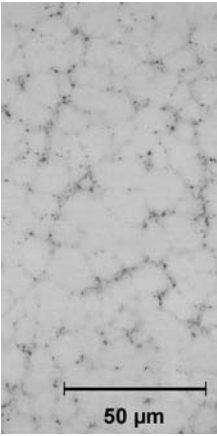


Fig. 5.29. Alloy AM50

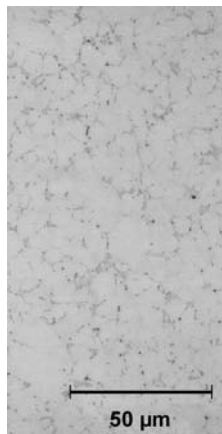


Fig. 5.30. Alloy AS21

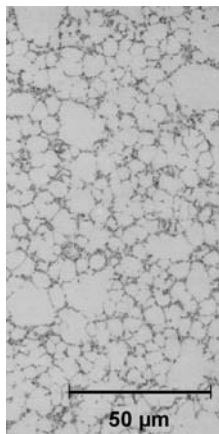


Fig. 5.31. Alloy AE42

### 5.1.4.3 Properties

#### *Introduction*

The mechanical properties of high pressure die cast components are less predictable than those of components made from wrought materials. This is caused by the rather inhomogeneous material structure due to changing solidification conditions. The properties depend strongly on the manufacturing route and the variables involved. Almost all mechanical property data that are available today are based on the testing of separately die cast test bars. A geometrically complex casting, however, exhibits a range of property values. The influence of process conditions on the microstructure and mechanical properties of magnesium die castings is described by Sannes and Westengen [42].

Tabulated mechanical properties are usually based upon the testing of separately die cast specimens. Even such specimens show variations in properties depending upon the actual casting conditions. These values must be understood as examples of what might be expected when casting parts with cross-sections, structure and quality comparable to those of the test bars. Castability is reduced with reduced aluminium content in the alloy, which might entail reduced property values compared to what might be expected.

The designer's dilemma is to describe mechanical properties to a complex shape casting. This is usually done by introducing design safety factors. Material property research programs should emphasise the relation between manufacturing characteristics, material structure and quality, and component properties. Superior product performance can only be obtained by fully exploiting the synergy of optimum design, processing route and material selection.

Information about property data for magnesium and magnesium based alloys are also provided by Busk [43], Kainer [44], Avedesian et al. [45] and Kammer [46]. Table 5.4 shows typical mechanical property values at room temperature for a range of die cast magnesium based alloys [47].

**Table 5.4.** Typical mechanical properties at room temperature [47]

Property	Unit	AZ91	AM60	AM50	AM20	AS41	AS21	AE42
Ultimate Tensile Strength, $R_m$	MPa	250	240	230	210	240	220	230
Tensile Yield Strength, $R_{p0.2}$ (0.2% offset)	MPa	160	130	125	90	140	120	145
Compressive Yield Strength	MPa	148	nm	113	74	nm	106	103
Fracture Elongation ( $L_0 = 50$ mm)	%	7	13	15	20	15	13	11
Elastic Modulus, tension	GPa	45	45	45	45	45	45	45
Elastic Modulus, shear	GPa	17	nm	nm	nm	nm	nm	nm
Brinell hardness	HBS 1/5	70	65	60	45	60	55	60
Impact strength (Charpy un-notched test bars)	J	9	18	18	18	16	12	12

Mean values obtained from separately cast test bars produced on a 400 t cold chamber machine, using a six-cavity die. 6 mm round tensile test bars and  $10 \times 10 \times 55$  impact test bars.  
nm: not measured.

### ***Tensile properties***

Since magnesium alloys do not exhibit a definite elastic region, there is no real yield point on the stress – strain curve; the 0.2% offset tensile yield strength value is only a selected point on the curve, and is not connected to a distinct change in the course of the curve.

An illustrative way to demonstrate ductility is to perform a “pig tail test” at room temperature. A test bar is bent to fracture, and the shape of the twisted bar gives a picture of the ductility of the alloy (Fig. 5.32) [47–49].

Typical stress – strain curves for die cast magnesium based alloys at room temperature are shown in Fig. 5.33 [47–49]. At lower aluminium contents the alloys show a tendency to form of a yield point and the work hardening rate is decreased. Due to the embrittling effect of the  $\beta$ -Mg<sub>17</sub>Al<sub>12</sub> phase, ductility is reduced when the aluminium content increases. The effect of temperature on tensile properties is shown in Figs. 5.34–5.36 [47–49]. Stress – strain curves at various temperatures are shown in Figs. 5.37–5.42. All these data are based on separately die cast 6 mm round tensile test bars with  $L_0 = 50$  mm.

The strain rate sensitivity at low and intermediate test speeds is shown in Figs. 5.43 and 5.44 [49]. The influence of test speed was measured by changing the crosshead speed for AZ91 and AM50 in steps from 0.5–200 mm/min at room temperature. Alloy AZ91 showed no effect of test speed on ultimate tensile strength and fracture elongation values, while the tensile yield strength values (0.2% off-



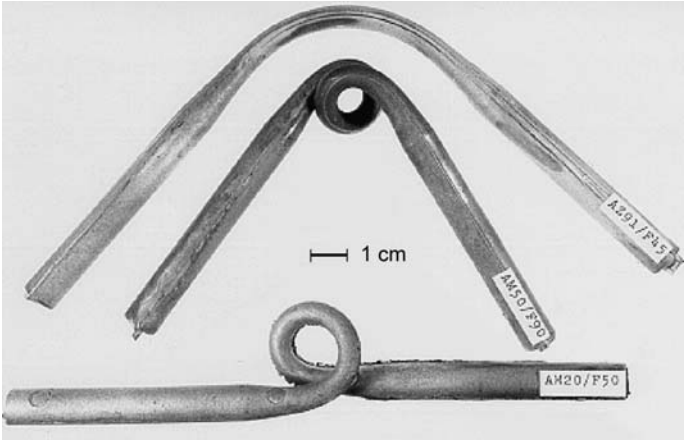


Fig. 5.32. “Pig tail test” of 6 mm round tensile test bars at room temperature. Alloys from top: AZ91, AM50 (vacuum assisted die cast), and AM20

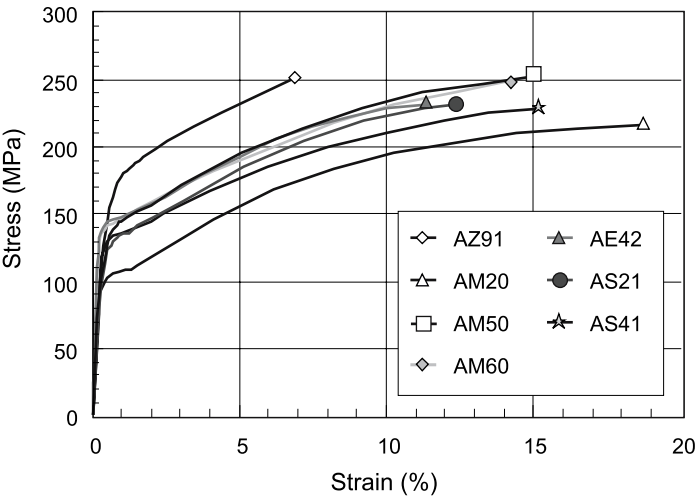


Fig. 5.33. Stress – Strain curves at room temperature

set) increased with increasing speed. For alloy AM60 the results did not prove any effect of speed on the ultimate tensile strength value. The tensile yield strength increased with increasing speed and the elongation values decreased with increasing speed, especially >10 mm/min.

The strain rate sensitivity at high strain rates is shown in Figs. 5.45 and 5.46 [5–7, 49]. In this investigation the strain rate was varied from 15–130 s<sup>-1</sup>, a range typical of deformation at crash. All tests were undertaken at room temperature. The test results show no significant differences between the fracture elongation values at different strain rates ranging from 15–130 s<sup>-1</sup> for the magnesium alloys



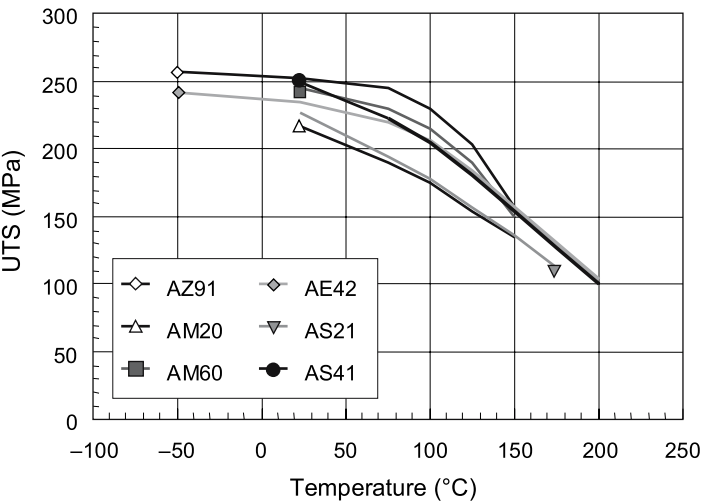


Fig. 5.34. Ultimate tensile strength ( $R_m$ ) values as a function of temperature

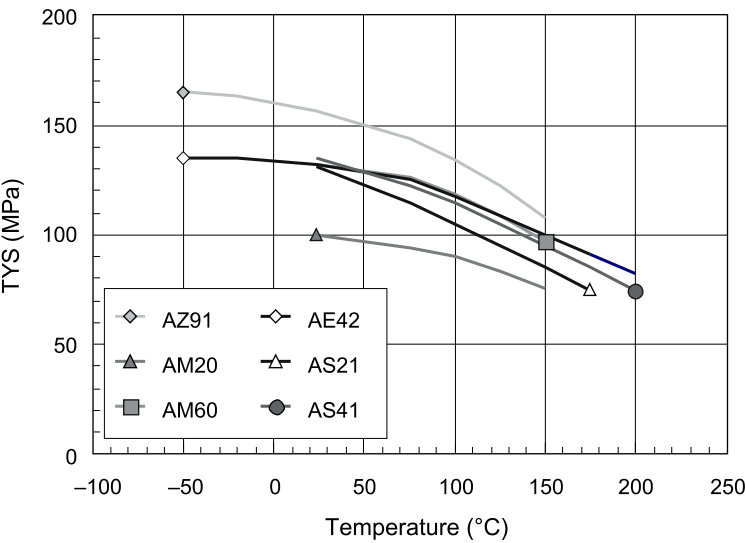


Fig. 5.35. Tensile yield strength ( $R_{p0.2}$ ) values as a function of temperature

AZ91D, AM60B and AM50A. All three alloys showed significantly higher ultimate tensile strength values at  $130\text{ s}^{-1}$  compared to the  $15\text{ s}^{-1}$  strain rate. The increase in the mean value was of the order of 17%.

The effect of the aluminium content on the tensile properties of AM type alloys at room temperature is shown in Figs. 5.47 and 5.48 and in Table 5.5 [8]. These results show that there are relatively small changes in tensile properties by

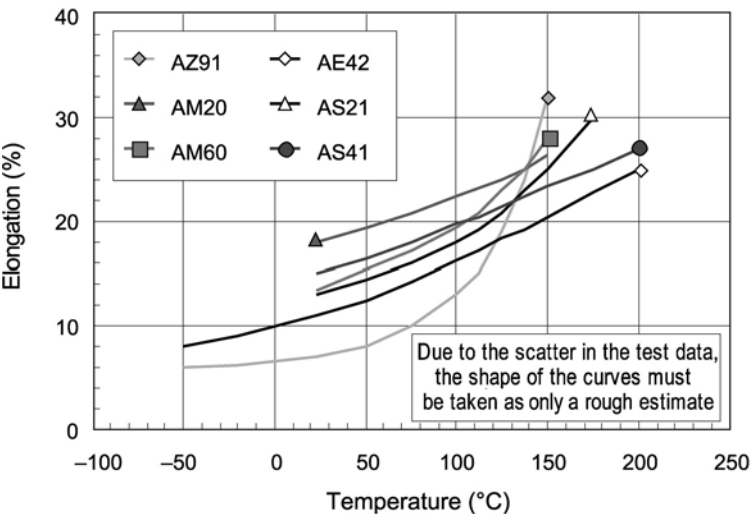


Fig. 5.36. Fracture elongation values as a function of temperature

Table 5.5. Tensile properties as a function of the aluminium content in AM type alloys

% Al	UTS [MPa]	TYS [MPa]	Elong. [%]
2	217 (3)	99 (7)	18.8 (2.0)
4.8	229 (12)	116 (3)	15.2 (1.7)
5.3	249 (6)	123 (3)	16.0 (1.3)
5.8	253 (8)	125 (5)	16.1 (1.4)
6.4	250 (12)	131 (6)	14.3 (2.9)
6.9	248 (14)	132 (5)	12.8 (2.5)
7.5	258 (10)	151 (9)	8.7 (1.8)
8	245 (7)	159 (18)	5.4 (1.6)

Room temperature values. Standard deviation values in parentheses.

reducing the aluminium content below 6%. The ultimate tensile strength, tensile yield strength and fracture elongation values do not change more than 10–20% when going from 6% Al down to 2% Al. Increasing the aluminium content from 6–8% increases the ultimate tensile strength and tensile yield strength values by about 3% and 21% respectively, along with decreasing the fracture elongation value by almost 70%.

The effect of wall thickness on tensile properties at room temperature is shown in Fig. 5.49 [50]. Wall thicknesses from 2.5–10 mm were included in this investigation. The tensile properties decrease significantly with increasing wall thickness, for all alloys included. This is due to a coarser microstructure and higher porosity.

Pressure die castings are usually not subjected to heat treatment due to porosity and risk of blistering and surface damage. However, in order to demonstrate

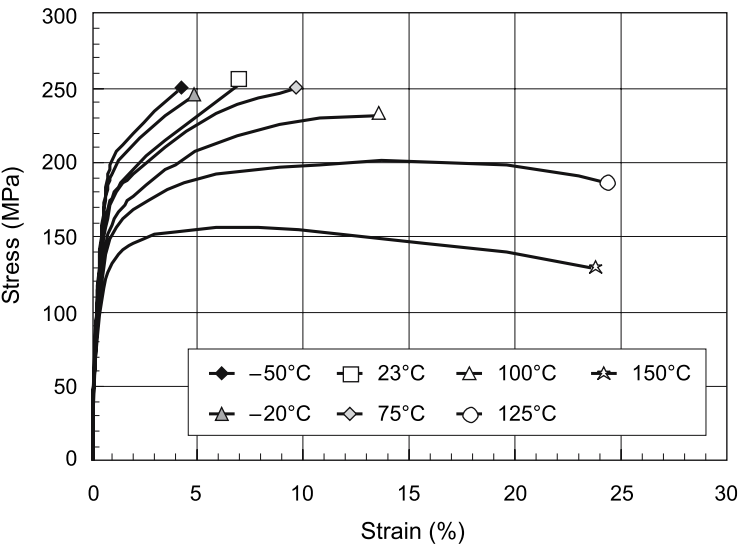


Fig. 5.37. Temperature stress – strain curves for alloy AZ91

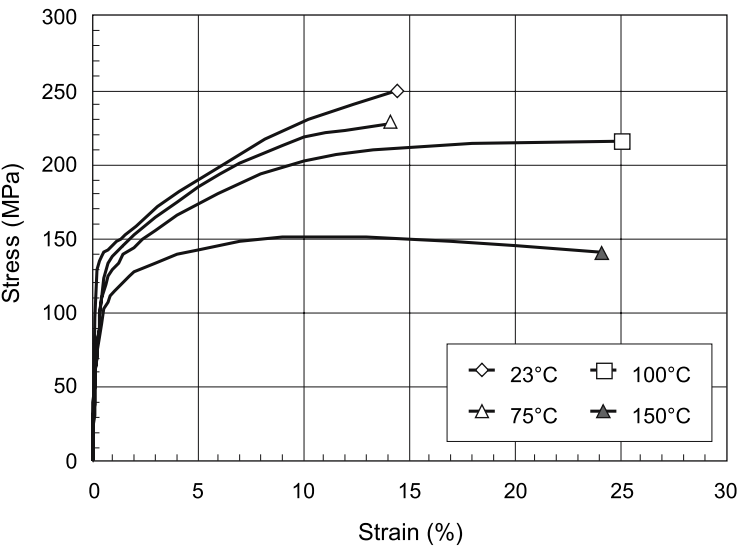


Fig. 5.38. Temperature stress – strain curves for alloy AM60

the effect of heat treatment on tensile properties, the result of a trial with alloy AZ91 is shown in Fig. 5.50 [49]. The graph shows stress – strain curves representing as cast, solution heat treated (T4: 415°C for 24 hours), and artificially aged (T6: T4 + 205°C for 15 hours) test bars. By using a T4 type heat treatment it is possible to increase the ductility with almost 100%, but at the expense of a lower tensile yield strength value.

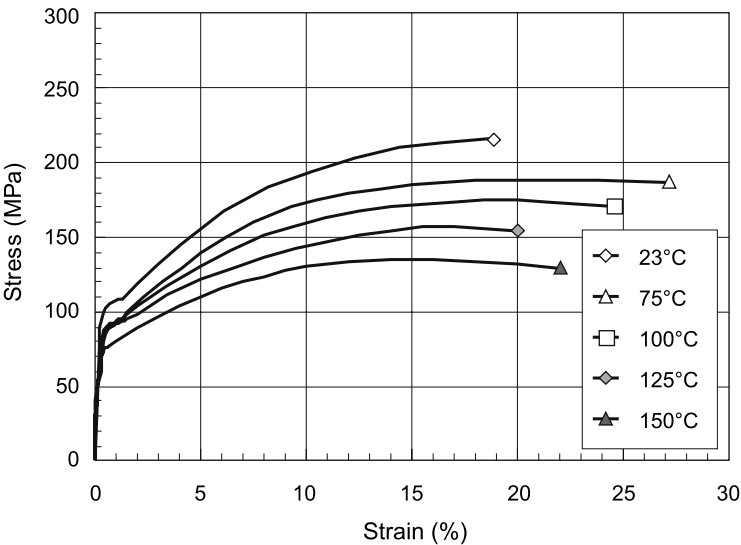


Fig. 5.39. Temperature stress – strain curves for alloy AM20

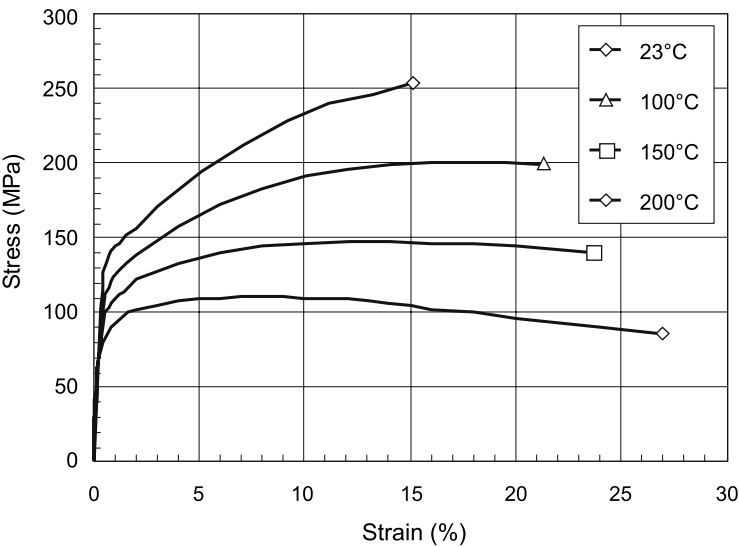


Fig. 5.40. Temperature stress – strain curves for alloy AS41

The elastic modulus for alloy AZ91 vs. temperature is shown in Fig. 5.51 [48, 49]. The line and the filled circles represent the elastic modulus values obtained from tensile tests. The open circles are based on Piezo-electric measurements on gravity cast AZ91 samples. It is difficult to obtain good elastic data from ordinary tensile tests due to the shape of the stress – strain curve, but the tensile test data correspond well with the Piezo-electric data up to about 90°C. These elastic data

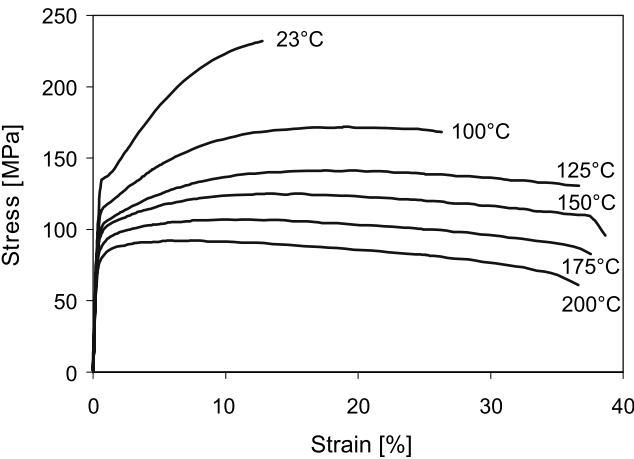


Fig. 5.41. Temperature stress – strain curves for AS21X

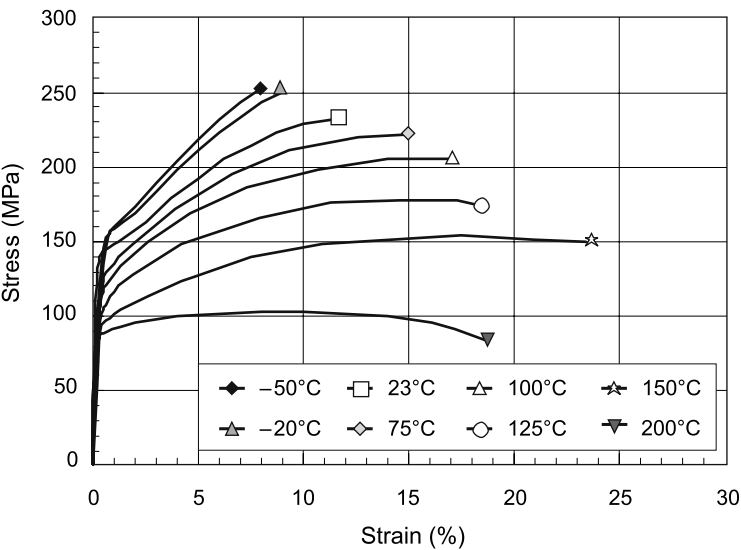


Fig. 5.42. Temperature stress – strain curves, alloy AE42

for AZ91 compares well with those presented by Sakkinen [58], showing 39 GPa at 150°C. Schindelbacher and Rösch [50] investigated the Young’s modulus in the temperature range from RT up to 150°C for the alloys AZ91, AM60, AM20, AE42 and AS41. The results are shown in Fig. 5.52.

During the lifetime of a vehicle it will typically be subject to a number of sunny days which can raise the cabin temperature significantly, with material aging as a possible effect. The effect of aging on alloy properties is affected by alloy com-

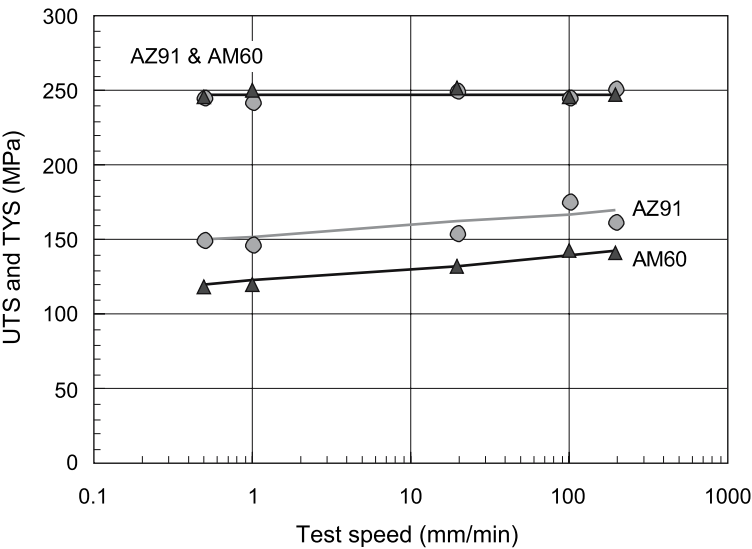


Fig. 5.43. Ultimate and tensile yield strength

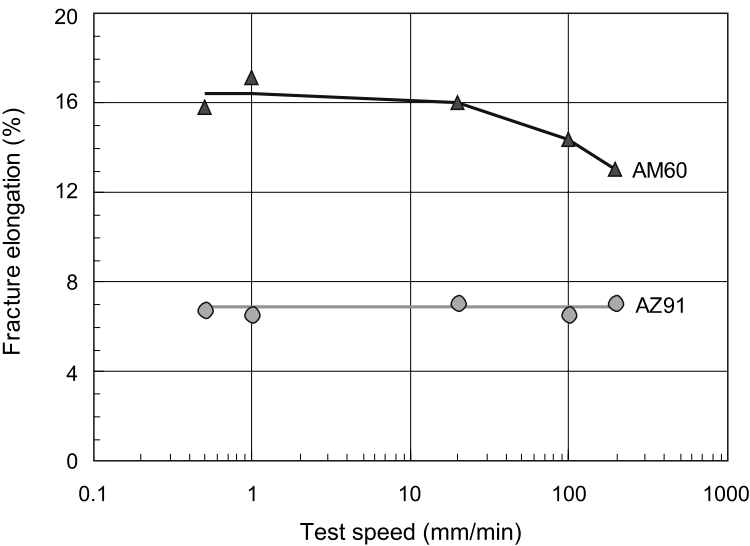


Fig. 5.44. Total fracture elongation ( $L_o = 50$  mm)

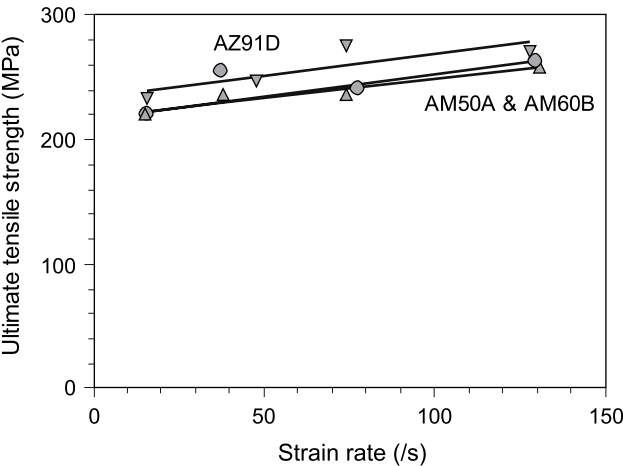


Fig. 5.45. High strain rate ultimate tensile data

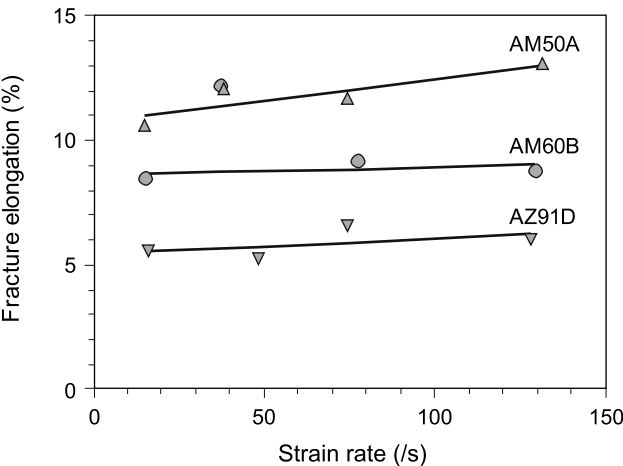


Fig. 5.46. High strain rate fracture elongation data

position, cooling rate and structure as a result of casting parameters, and stress relief due to the elevated temperature.

For AM-type alloys aluminium is the element that has the largest effect on aging properties. The amount of Al determines the formation of the binary  $\beta$ -phase  $Mg_{17}Al_{12}$ . Increased Al content and thereby an increased amount of  $\beta$ -phase, increases the strength of the alloy, but reduces the ductility. A matrix supersaturated in aluminium at the aging temperature is necessary to obtain an aging effect. The ability of an alloy to show precipitation in the solid state is determined by inhomogeneities and non-equilibrium conditions in the alloy structure. The level of stress in a cast sample is determined by the processing parameters. Stress

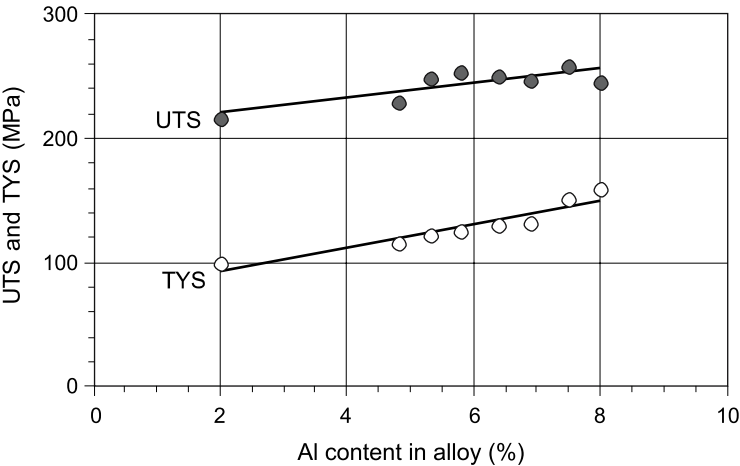


Fig. 5.47. Ultimate tensile strength and tensile yield strength (0.2% offset)

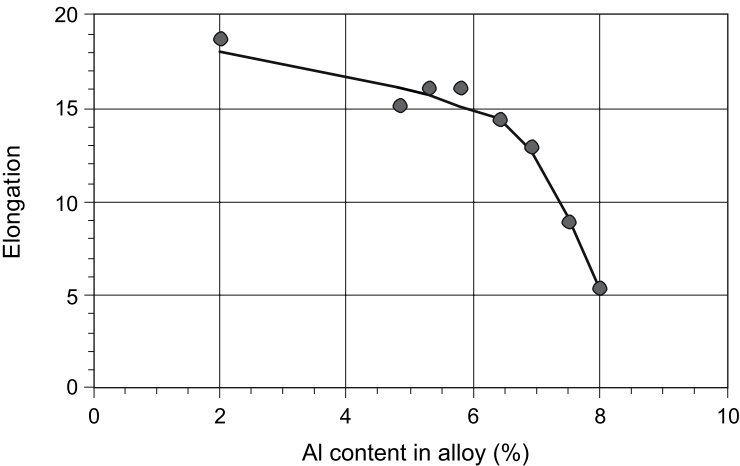


Fig. 5.48. Effect of aluminium content on fracture elongation

relief will contribute to increased ductility. Due to the complexity of the die casting process it is difficult to maintain complete control of the resultant alloy structure. This may give a marked contribution to the data scatter and complicate the adaptation of aging property models.

The effect of aging has been reported by a number of authors [16, 51–54]. They report up to 30% reduction in fracture elongation values after 2,000 hours at about 110°C. The results from a recent investigation are summarised in Table 5.6 [47].



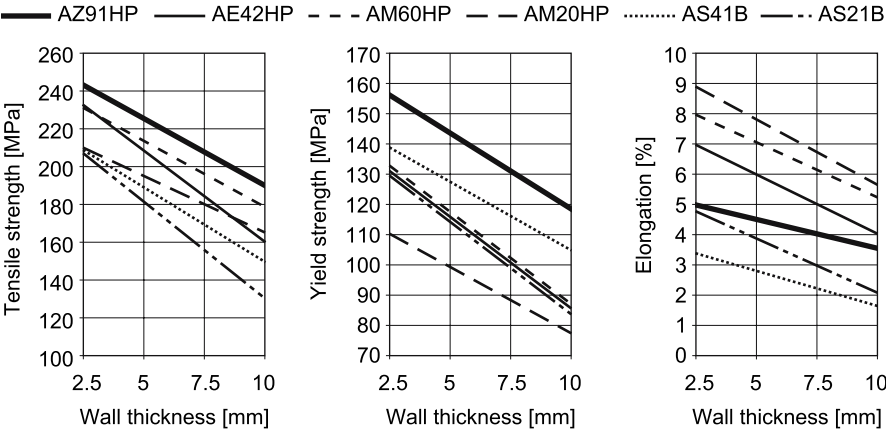


Fig. 5.49. Effect of wall thickness at room temperature

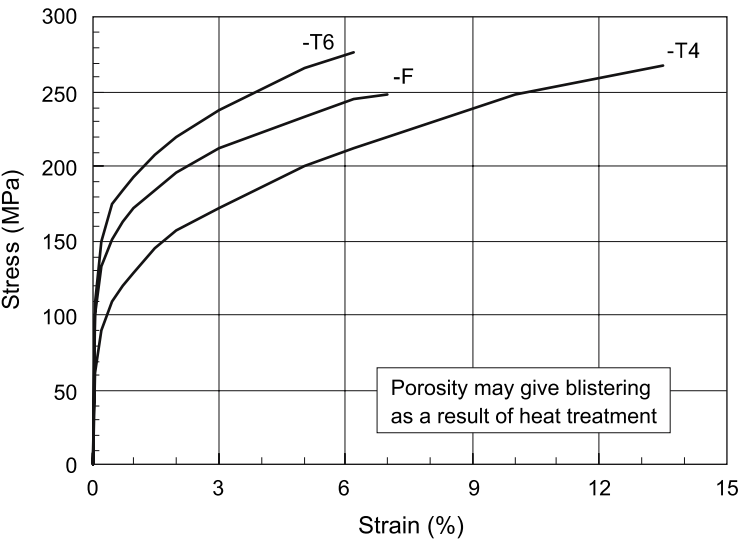


Fig. 5.50. Effect of heat treatment on the tensile properties of high pressure die cast AZ91 6 mm round test bars

**Compression properties**

A material's compressive strength describes its resistance to external compressive forces. Figure 5.53 shows the compression curves for AZ91D and AM50A at room temperature for compression values up to 1%. Figure 5.54 shows the effect of temperature on the compression yield strength (0.2% offset). For the alloy AZ91D the room temperature CYS value is similar to the TYS value, for alloy AM50A the room temperature CYS value is lower than the corresponding TYS value. The compression test strain rate used was  $0.00005\text{ s}^{-1}$  [5, 7, 47].

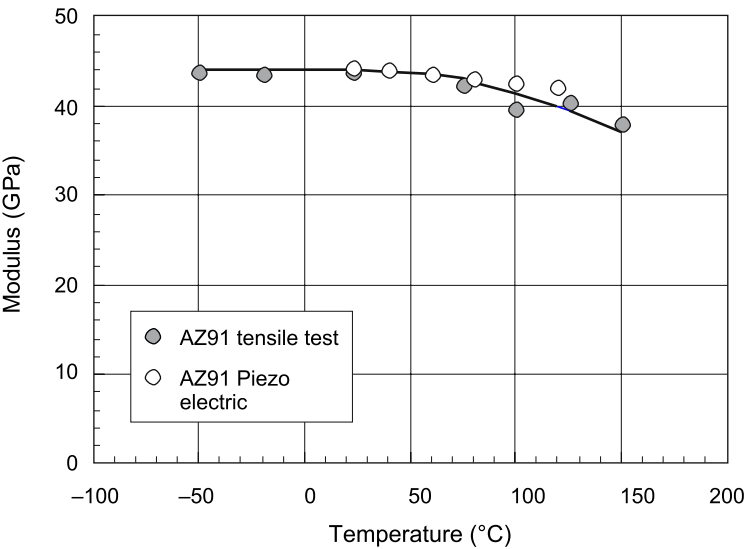


Fig. 5.51. The elastic modulus (tension) for AZ91

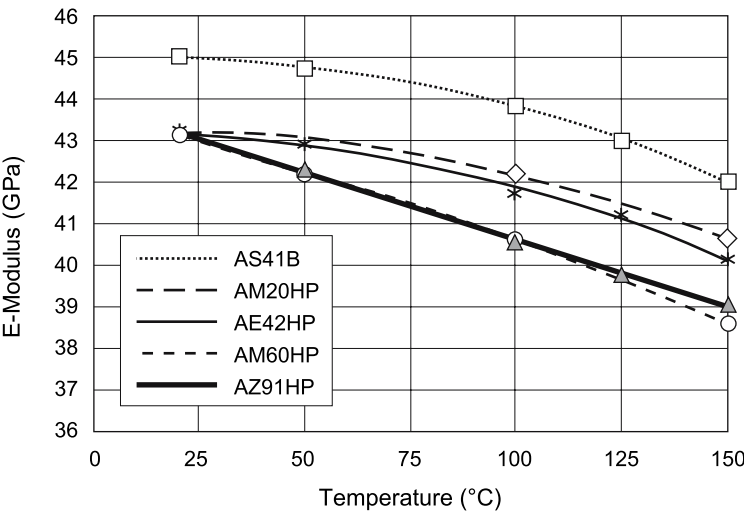
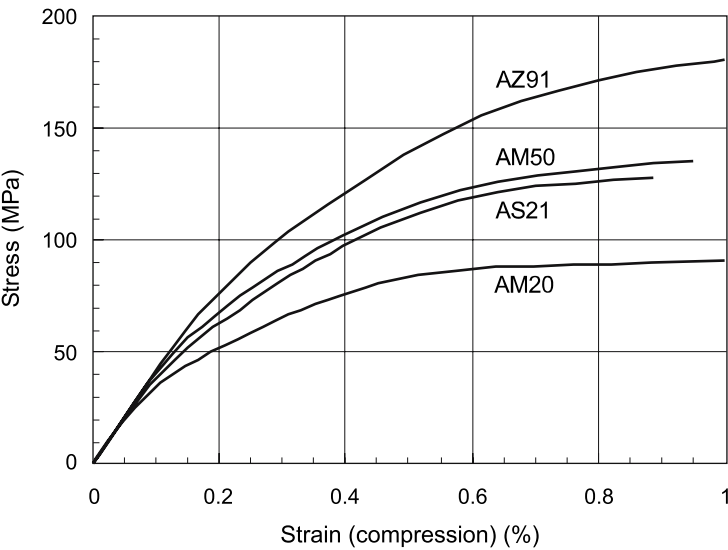


Fig. 5.52. The elastic modulus (tension) for a range of alloys

**Table 5.6.** Aging of AM50 and AM60 alloys

Aging temperature [°C]	Summary
75	No effect on tensile properties for none of the alloy compositions
100	Up to 6% and 17% increase in ultimate and tensile yield strength, respectively. Up to 40% reduction in fracture elongation value
125	Up to 11% and 20% increase in ultimate and tensile yield strength, respectively. Up to 40% reduction in fracture elongation value

Alloys with from 4.5% Al to 6.5% Al. Aging time up to 2,000 hours.



**Fig. 5.53.** Compression curves at room temperature

***Fatigue properties***

Designing for fatigue performance requires extensive knowledge of the material properties, component geometry and dynamic loading conditions. Constant amplitude SN curves for AZ91, AM60 and AM50 at room temperature are shown in Fig. 5.55. The effect of the mean stress parameter R is shown for alloy AM60 in Fig. 5.56 [5, 7]. Both the inclination and the SN-level are similar for the AM60 and AM50 alloys. It is proven that these two curves are similar by statistic comparison of the two data sets. Alloy AZ91 falls slightly below the curves for the two other alloys.

The fatigue life is described by the equation

$$N = C \cdot \Delta\sigma^{-b} \tag{5.3}$$

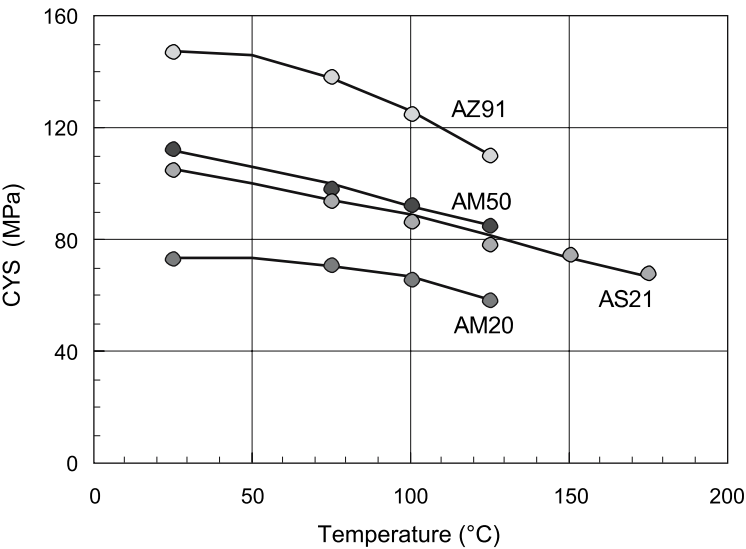


Fig. 5.54. Compression yield strength vs. temperature

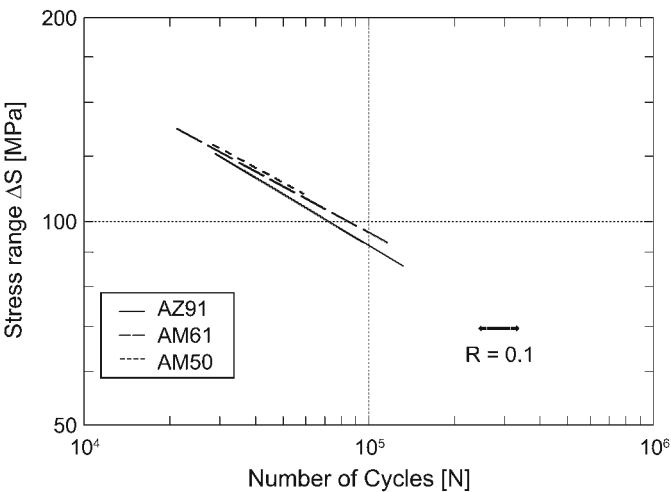


Fig. 5.55. Mean SN lines for AZ91, AM60 and AM50. R = 0.1

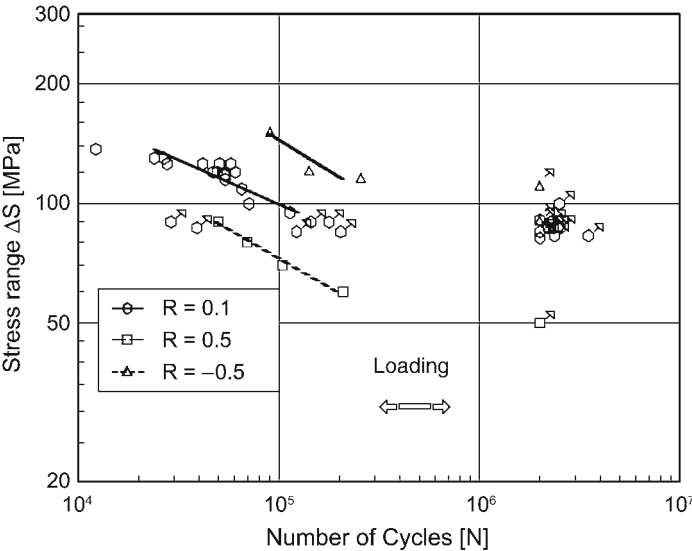


Fig. 5.56. Effect of mean stress parameter R, alloy AM60

Table 5.7. Mean and design fatigue properties at constant amplitude

Alloy	Mean values		Design values			
	b	C	$\Delta\sigma_E$	b	C	$\Delta\sigma_E$
AM50	4.38	$5.28 \cdot 10^{13}$	90	4.38	$2.96 \cdot 10^{13}$	74
AM60	4.40	$5.28 \cdot 10^{13}$	91	4.40	$2.39 \cdot 10^{13}$	72
AZ91	4.00	$0.71 \cdot 10^{13}$	86	4.00	$0.51 \cdot 10^{13}$	70

and the calculated values (b and C) corresponding to the SN-curves in Fig. 5.56 are listed in Table 5.7 together with the endurance limit values ( $\Delta\sigma_E$ ). Design values based on a 97.5% survival level are included in the Table 5.7.

**Impact properties**

Impact testing provides information about material performance in rapid strain situations. The impact value is greatly affected by the metal flow and the solidification conditions. For example, increasing the volume of the overflows for a Charpy test bar in an otherwise unchanged die geometry resulted in increased absorbed energy from 10 J to 23 J (alloy AM60 [4, 7]).

The temperature dependency of impact strength for Charpy-type test bars with a cast-in notch is shown in Fig. 5.57 [48]. The temperature effect is minor for all alloys except AM20 for temperatures up to 150°C. For Alloy AM20 the impact strength increases with increasing temperature above room temperature. The in-

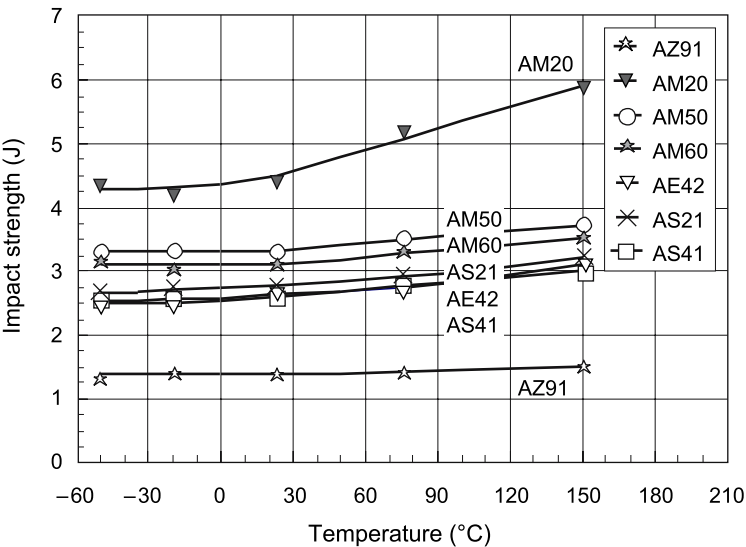


Fig. 5.57. Effect of temperature. 10×10×55 mm impact test bars with 2 mm cast-in notch (Charpy-type)

crease in impact strength with temperature is due to increased test bar deflection before fracture.

Figure 5.58 shows the impact strength of Charpy type impact test bars (10×10×55 mm) as a function of the aluminium content in the alloy [8]. The difference in impact toughness between test bars, with machined and cast notch geometry, reflects the difference in overall test bar quality and porosity. Samples with a machined-in notch will generally exhibit lower impact strength than those

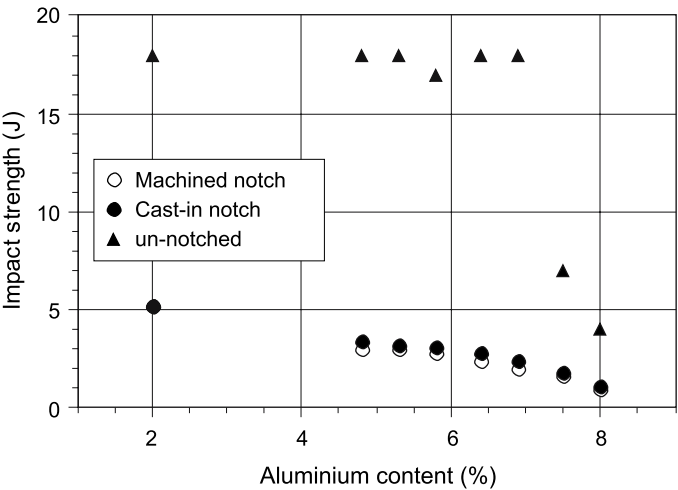


Fig. 5.58. Impact strength as a function of the aluminium content in AM type alloys

with a cast-in notch. This is due to the physical removal of the dense surface layer, or skin, in the notch area of the machined test bar. The almost identical curves for machined and cast-in notches in Fig. 5.58 confirm the low porosity in these samples. The un-notched bar impact strength is almost unchanged when increasing the aluminium content from 2% to about 7%, while the notched bars show decreased impact strength with increased aluminium content over the entire range investigated. The un-notched bar impact values show a behaviour much like the fracture elongation values. The difference in impact value between an un-notched sample and a sample with machined-in notch reflects the amount of energy needed to initiate a crack in an un-notched sample. The energy is almost constant for aluminium content between 2% and 7%. At higher aluminium concentrations the required crack initiation energy is considerably reduced. This shift in energy requirement is explained by changes in alloy brittleness and surface condition. The un-notched test bar has a 25% larger fracture cross-section to overcome than the notched bars. The un-notched test bar data values shown in Fig. 5.61 are corrected for this difference in cross section.

The graphs in Figs. 5.59 and 5.60 illustrate the effect of a machined notch on the energy absorption at room temperature. The results are based on separately die cast 10×10×55 mm Charpy type test bars, and include un-notched bars as well as bars with machined-in notch (the pendulum speed was 3.9 m/s, [4, 7]).

**Hardness properties**

The Brinell hardness value of a material is a measure of its resistance to permanent deformation by indentation. The hardness values presented in Fig. 5.61 [48] are based on measurements of flat 3-mm-thick die cast plates, with the surface

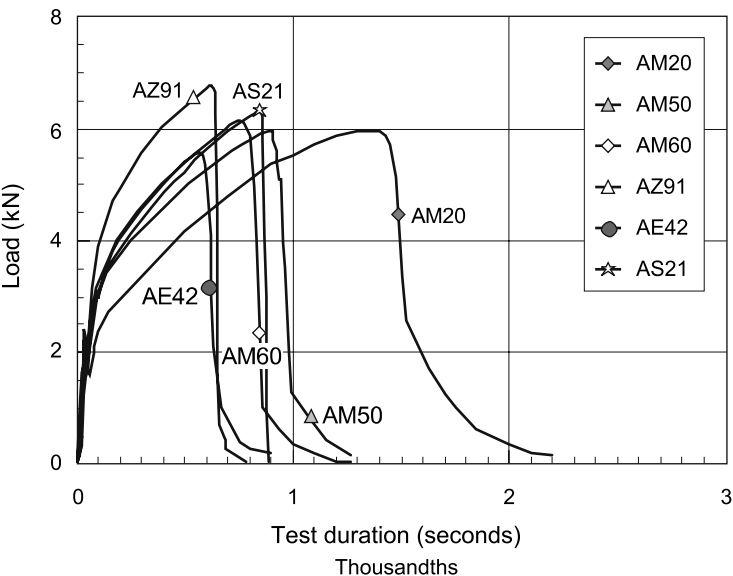


Fig. 5.59. Impact curves. Un-notched test bars, room temperature

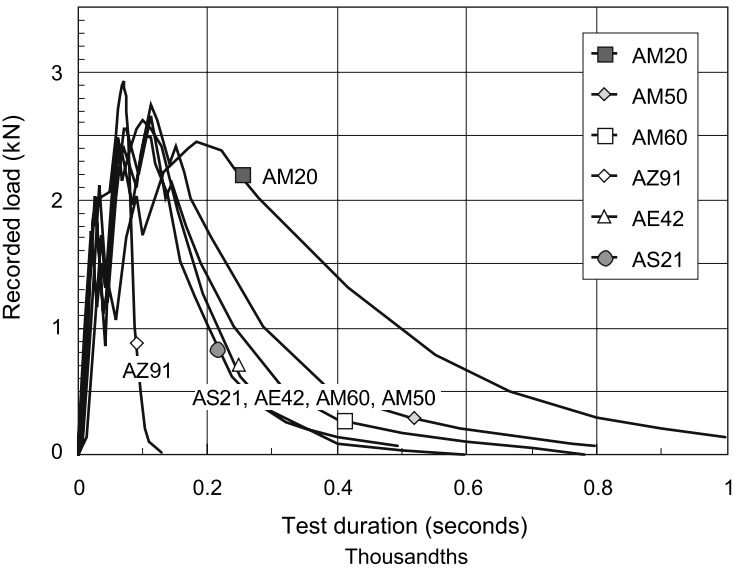


Fig. 5.60. Impact curves. 2 mm machined notch, room temperature

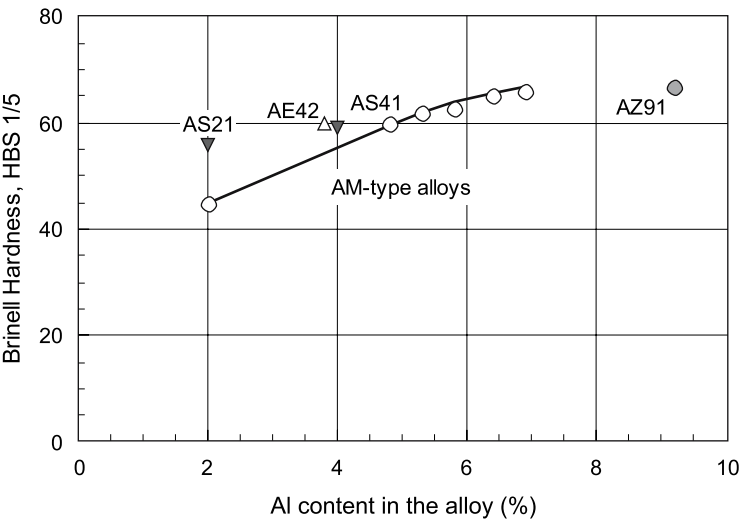


Fig. 5.61. Brinell Hardness of die cast alloys



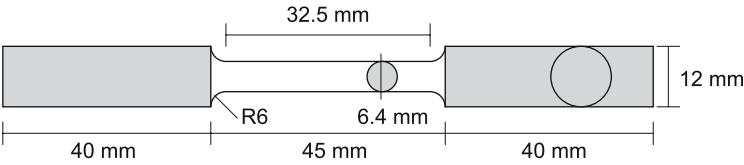


Fig. 5.62. Torsion test bar configuration

slightly ground to obtain a more accurate measurement of the indentation. The open circles and the line in the graph show the hardness of AM-type alloys as a function of the aluminium content in the alloy.

**Torsion properties**

A torsion (shear) test gives information about the shear stress that a material is capable of sustaining. The test bar used for the torsion test is shown in Fig. 5.62. Torque – torsion graphs for the alloys AZ91, AM60 and AM50 at room temperature are shown in Figs. 5.63–5.65. The results include torsion speeds from 0.5–25 rev/s. All curves have a “knee” whose location and sharpness depend upon alloy composition and revolution speed. The location is shifted towards both higher torque and higher torsion values with increasing speed of revolution. Torque – torsion curves for the more ductile AM60B and AM50A alloys generally exhibit a knee at a lower torque, but withstand appreciable more torsion (degree of twist) prior to failure, compared to AZ91 [4, 7, 47].

**Creep properties**

Creep is defined as the time dependent part of the strain that results from exposure to a constant load and temperature. Creep deformation is divided in three

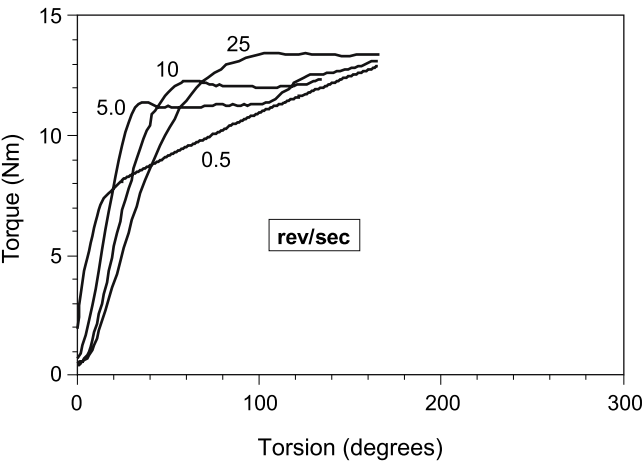


Fig. 5.63. Torque – torsion curves for AZ91

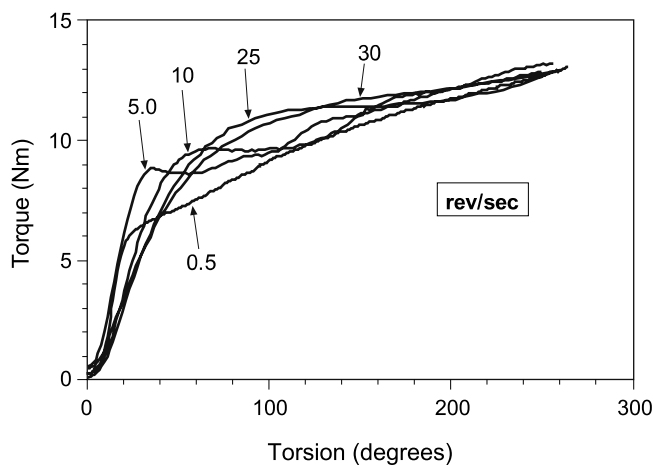


Fig. 5.64. Torque – torsion curves for AM60

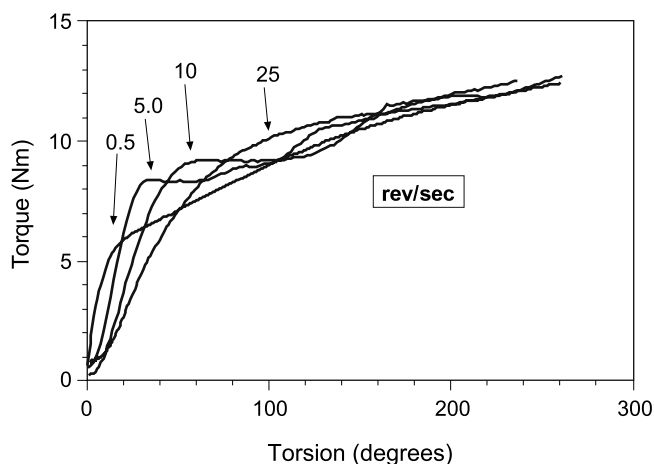


Fig. 5.65. Torque – torsion curves for AM50

stages. The primary creep stage is characterised by a creep rate decreasing with time. The secondary creep stage represents a steady-state creep region characterised by a constant creep rate. In the tertiary creep stage the deformation accelerates rapidly and failure occurs. Creep tests for 1,000 hours are often used, but a fairly good screening is obtained after 100 hours.

The dominant creep deformation mechanisms vary with stress and temperature [55]. For Mg die casting alloys under practical application conditions, creep deformation is relevant in the temperature range 100–200°C, and with mechanical stresses in the range up to yield strength of the alloys. However, also creep deformation at ambient temperature has been reported [56, 57]. Adapting creep

data for Mg die cast alloys to power law creep calculations,

$$\dot{\epsilon}_s = A\sigma^n e^{-\frac{Q_c}{RT}} \quad (5.4)$$

reveals  $n > 1$  for the test conditions where creep deformation is significant [56, 58–62]. This indicates that dislocation movement is the dominating deformation process [63].

There is a significant compression-tension asymmetry in the creep response of Mg die cast alloys, with higher deformation rates in tension than in compression [58, 59, 62]. This is explained in two ways. First, the precipitation reaction of supersaturated  $\alpha$  Mg(Al) to  $\alpha + \beta$  results in a lattice dilation and will be enhanced under tension and suppressed under compression. Second, the strain induced by the precipitation reaction will increase the creep strain measured in tension and decrease it in compression. In addition there may be cavity growth in tension, which will be suppressed in compression. The majority of the creep data reported in the literature is from tensile creep tests.

The microstructure of die cast Mg alloys consists of a grain interior of  $\alpha$ -Mg(Al) solid solution, and a grain boundary zone (grain “mantle”), which is eutectic Mg-Al (Al-enriched  $\alpha$  Mg + pockets of  $\beta$  –  $\text{Mg}_{17}\text{Al}_{12}$ ) and with AlMn particles. The creep resistant alloys within the Mg-Al base system obtain their creep resistance by a relatively low content of Al, and addition of elements, which form stable intermetallic phases within the grain mantle. AS41 and AS21 contains around 1% Si, which forms  $\text{Mg}_2\text{Si}$  particles. AE42 contains 2–3% Cerium-rich Mischmetal (RE), which forms  $\text{Al}_{11}\text{RE}_3$ . In both cases the intermetallic phases are distributed in the grain boundary zone, and their effect on creep is primarily to inhibit grain boundary sliding. In the case of Mg-Al-RE, the formation of  $\text{Al}_{11}\text{RE}_3$  also reduces the effective amount of Al, which otherwise would lead to Al-enrichment in the grain boundary zone. The grain interior is not significantly influenced by the addition of either Si or RE.

Typical creep properties of die cast magnesium alloys, obtained from separately die cast test bars are shown in Figs. 5.66–5.71 [47].

### **Physical properties**

Solidification simulation tools makes it possible to increase the quality and efficiency of the mould design phase and thereby contribute to reduced production costs. The availability of relevant and reliable input physical data determines the quality of the simulation results. Examples of physical properties are listed in Table 5.8 [47].

Alloy density values as a function of temperature, and linear thermal expansion relative to room temperature values are found in Figs. 5.72 and 5.73 [47]. Specific heat and thermal conductivity values as a function of temperature are shown in Figs. 5.74 and 5.75 [64, 65].

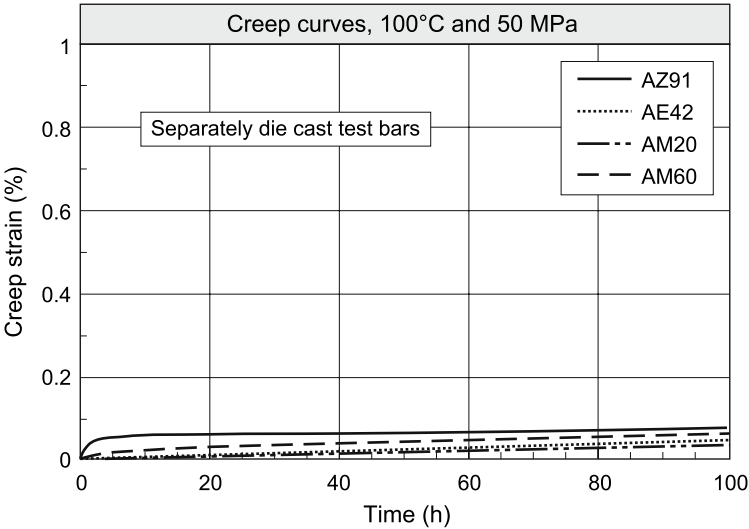


Fig. 5.66. 100°C and 50 MPa

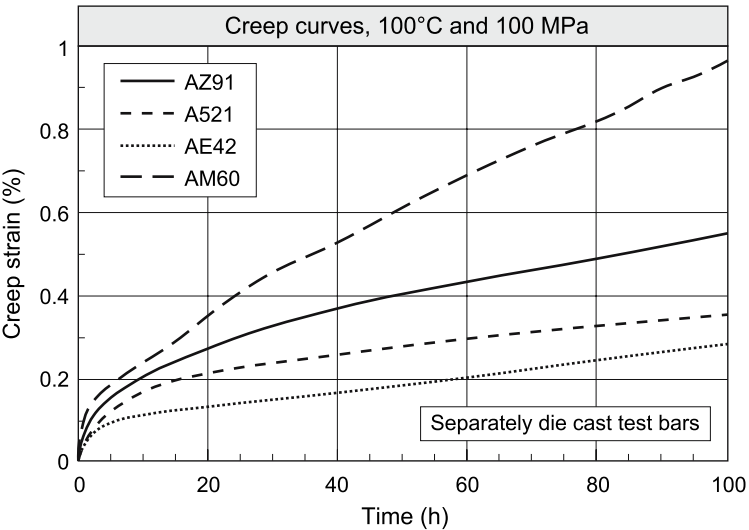


Fig. 5.67. 100°C and 100 MPa

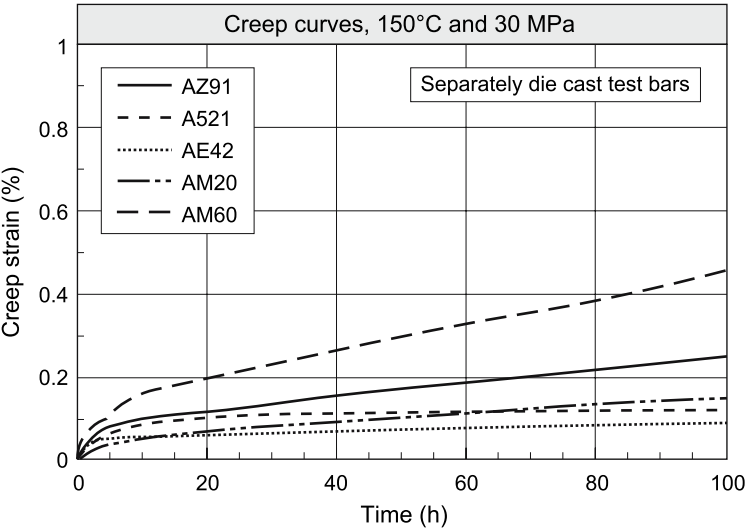


Fig. 5.68. 150°C and 30 MPa

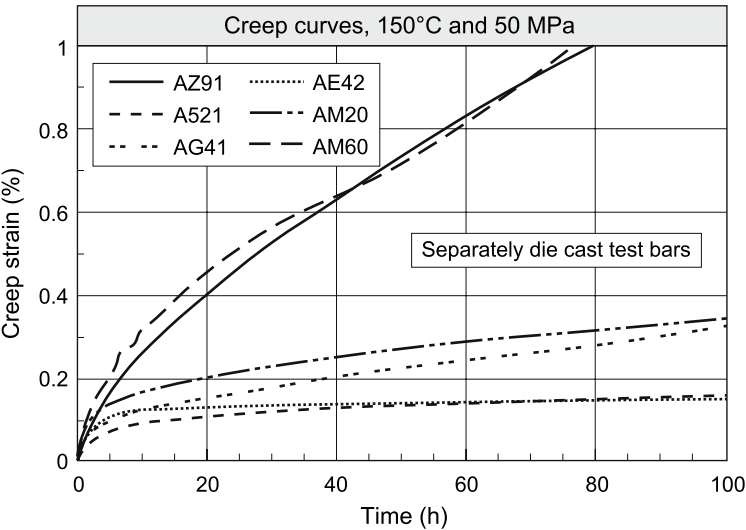


Fig. 5.69. 150°C and 50 MPa

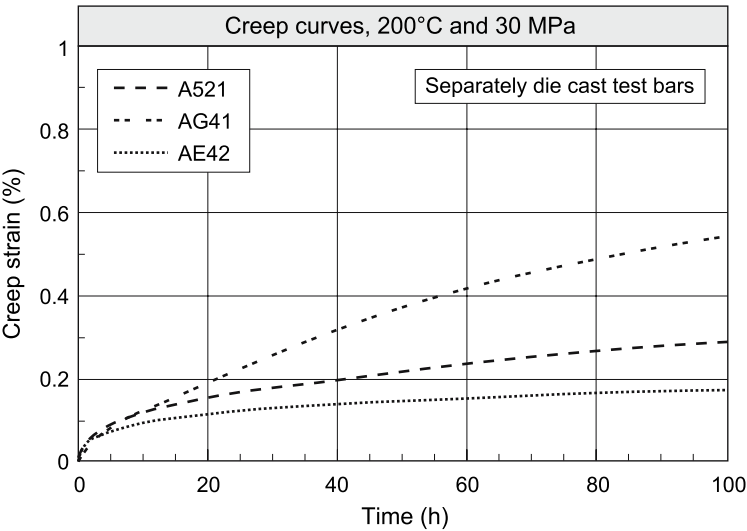


Fig. 5.70. 200°C and 30 MPa

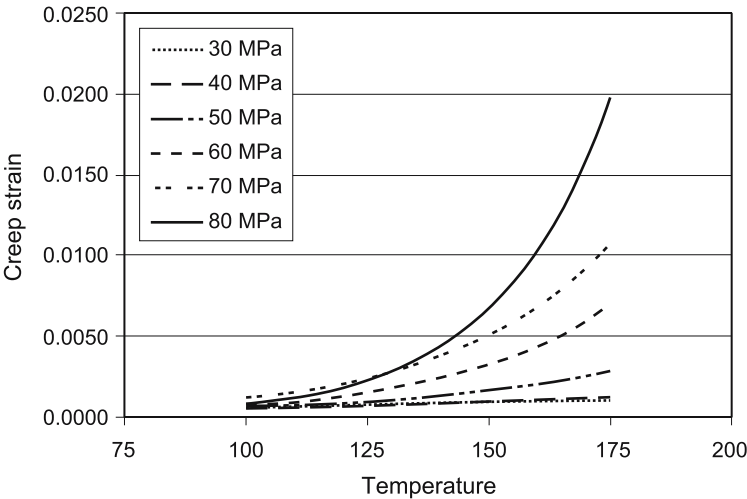


Fig. 5.71. Creep strain after 100 hours for AS21

Table 5.8. Typical physical properties [47]

Property	Unit	AZ91	AM60	AM50	AM20	AS41	AS21	AE42
Density at 20°C	g/cm <sup>3</sup>	1.81	1.80	1.77	1.75	1.77	1.76	1.79
Liquidus temperature	°C	598	615	620	638	617	632	625
Incipient melting temp.	°C	420–435	420–435	420–435	420–435	(420–435)	(420–435)	(590)
Linear thermal exp. coeff. 20–100°C	µm/m·K	26.0	26.0	26.0	26.0	26.1	26.1	26.1
Specific heat of fusion	kJ/kg	370	370	370	370	370	370	370
Specific heat at 20°C	kJ/kg·K	1.02	1.02	1.02	1.02	1.02	1.02	1.02
Thermal conductivity at 20°C	W/K·m	51	61	65	94	68	84	84
Electrical conductivity at 20°C	MS/m	6.6	nm	9.1	13.1	nm	10.8	11.7

nm: not measured.  
Values in brackets are estimated.

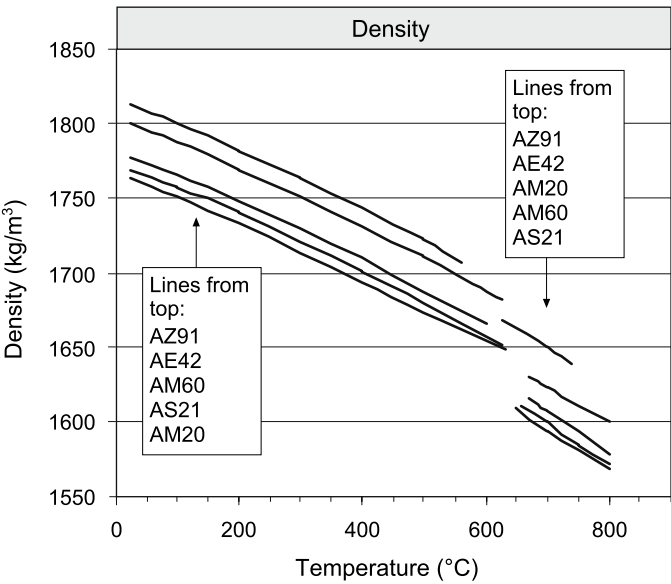


Fig. 5.72. Alloy density

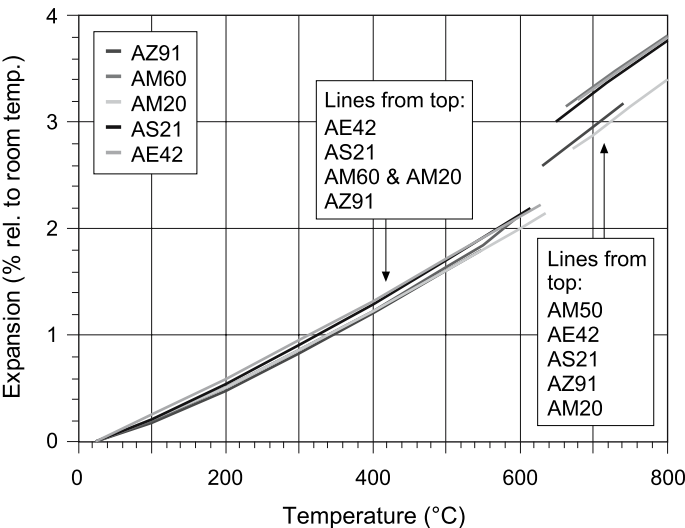


Fig. 5.73. Linear thermal expansion relative to room temperature

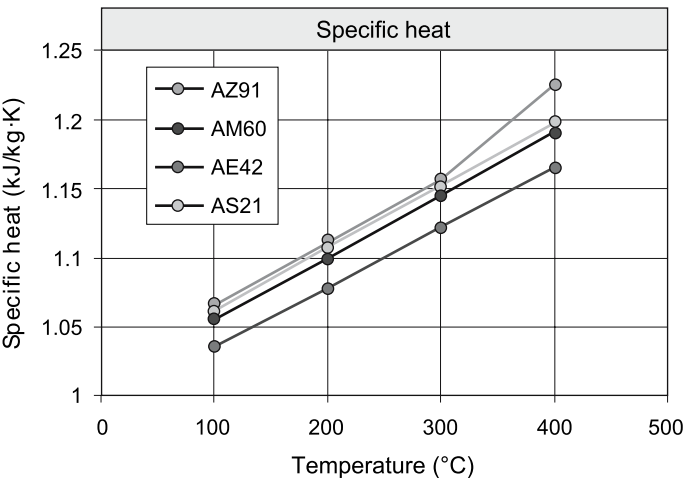


Fig. 5.74. Specific heat



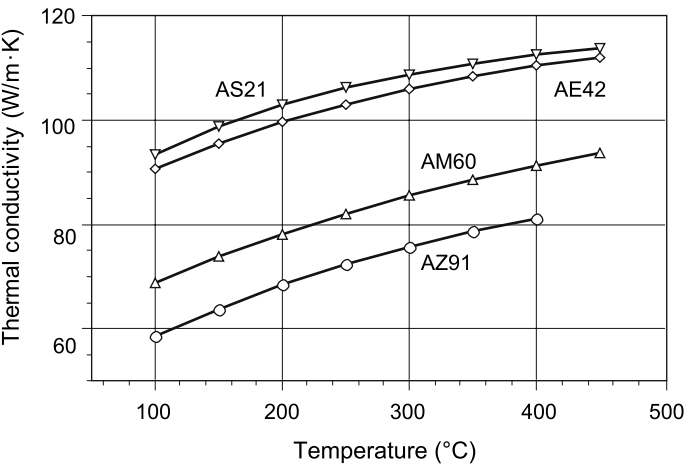


Fig. 5.75. Thermal conductivity

5.1.5 Alloys for Sand Casting

5.1.5.1 Compositions

The typical compositions of magnesium sand casting alloys are listed in Table 5.9. All values are given in weight percent. Complete information is given in the relevant international (ISO), European (EN) and US (ASTM) standards.

Alloy AZ91 is a general purpose alloy with good founding properties. Used in as cast, solution heat treated and solution and precipitation heat treated conditions.

Alloy AZ81 is a general purpose alloy. Good founding properties. Good ductility, strength and impact resistance. Mainly used in as cast and solution heat treated conditions.

ZC63 is a high strength, pressure tight commercial alloy. Mainly used in solution and precipitation heat treated condition.

Table 5.9. Typical composition of magnesium sand casting alloys

Alloy	% Al	% Zn	% Mn	% RE	% Zr	% Ag	% Y	% Cu
AZ81, A8, MgAl8Zn1	8.0	0.7	0.3					
AZ91, MgAl9Zn1	9.0	0.7	0.3					
ZC63, MgZn6Cu3Mn	6.0		0.5					2.5
RZ5, ZE41, MgZn4RE1Zr		4.2		1.3	0.7			
ZRE1, EZ33, MgRE3Zn2Zr		2.5		3.0	0.6			
MSR-B, MgAg2RE2Zr				2.5	0.6	2.5		
EQ21, MgRE2Ag1Zr				2.0	0.6	1.5		0.07
WE54, MgY5RE4Zr				3.5	0.5		5.25	
WE43, MgY4RE3Zr				3.0	0.5		4.0	

Alloy RZ5 is easily cast, weldable, pressure tight, with useful strength at elevated temperatures. Mainly used in precipitation heat treated condition.

Alloy ZRE1 is creep-resistant up to 250°C. Excellent castability. Pressure tight and weldable. Mainly used in precipitation heat treated conditions.

MSR-B and EQ21 are heat treatable alloys with high yield strength up to 200°C. Pressure tight and weldable. Mainly used in solution and precipitation heat treated conditions.

Alloy WE54 shows high strength at elevated temperatures. Mainly used in solution and precipitation heat treated conditions.

Alloy WE43 shows excellent retention of strength after long exposures at 250°C. Good castability, weldable. Mainly used in solution and precipitation heat treated conditions.

5.1.5.2 Properties

Minimum mechanical property values for sand cast alloys are listed in Table 5.10 [66]. The tensile properties quoted are the specification minima for that alloy and condition, bracketed values are for information only. The values are valid for separately cast test bars and may not be realised in certain portions of castings. Elongation values are based on a gauge length of  $5.65 \cdot \sqrt{A}$ , except in the case of thin material. Endurance values for  $50 \cdot 10^6$  reversals in rotating-bending-type tests (semicircular notch, radius 1.2 mm).

Fatigue (rotating bending) and creep properties of alloy RZ5 at elevated temperatures are shown in Figs. 5.76 and 5.77 [66]. The creep graph shows the stress/time relationship for specified creep strains at 150°C.

Fatigue (rotating bending) and creep properties of alloy ZRE1 at elevated temperatures are shown in Figs. 5.78 and 5.79 [66]. The creep graph shows the stress/time relationship for specified creep strains at 250°C.

Fatigue (rotating bending) and creep properties of alloy WE54 at elevated temperatures are shown in Figs. 5.80 and 5.81 [66]. The creep graph shows the stress/time relationship for 0.2% creep strain at 200 and 250°C. Table 5.11 shows typical tensile properties at various temperatures.

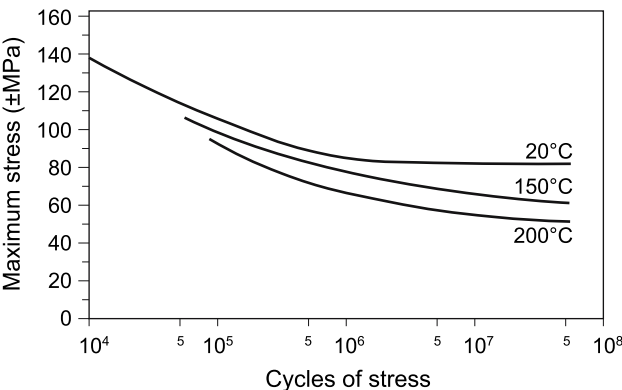


Fig. 5.76. Fatigue of RZ5 (–75)

**Table 5.10.** Mechanical properties of sand cast magnesium alloys at room temperature

Alloy	Cond.	Tensile properties			Compression prop.		Fatigue properties	
		R <sub>p0.2</sub> MPa	R <sub>m</sub> MPa	A %	R <sub>p0.2</sub> MPa	R <sub>m</sub> MPa	Unnotched MPa	Notched MPa
AZ81	-F	(85)	140	2	75–90	280–340	75–85	58–65
	-T4	80	200	7	75–90	325–415	75–90	60–70
AZ91	-F	(95)	125	–	85–110	280–340	77–85	58–65
	-T4	80	200	4	75–110	185–432	77–92	65–77
	-T6	120	215	–	110–140	385–465	70–77	58–62
ZC63	-T6	125	210	2	104	206	90	–
RZ5	-T5	135	200	3	130–150	330–365	90–105	75–90
ZRE1	-T5	95	140	3	85–120	275–340	66–75	50–55
MSR-B	-T6	185	240	2	165–200	310–385	100–110	60–70
EQ21	-T6	175	240	2	165–200	310–385	100–110	60–70
WE54	-T6	185	255	2	167–175	410	95–100	–
WE43	-T6	172	220	2	187	323	85	–

Cond. = temper conditions; R<sub>p0.2</sub> = 0.2% proof stress; R<sub>m</sub> = ultimate tensile/compression strength; A = fracture elongation; -F = as cast condition; -T4 = solution heat treated; -T5 = precipitation treated; -T6 = solution and precipitation heat treated.

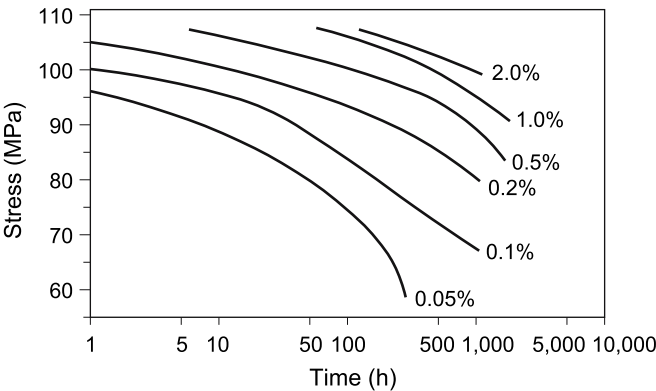


Fig. 5.77. Creep of RZ5 at 150°C (-T5)

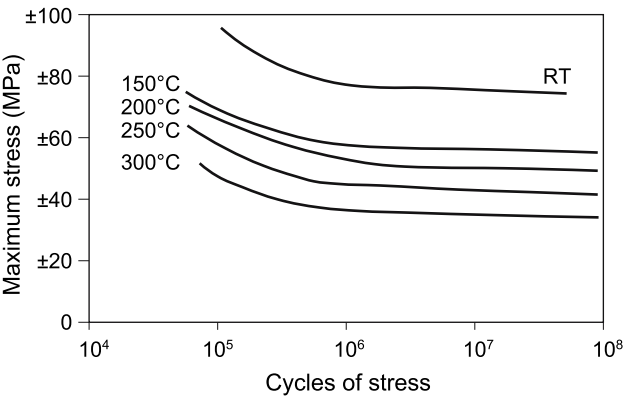


Fig. 5.78. Fatigue of ZRE1 (-T5)

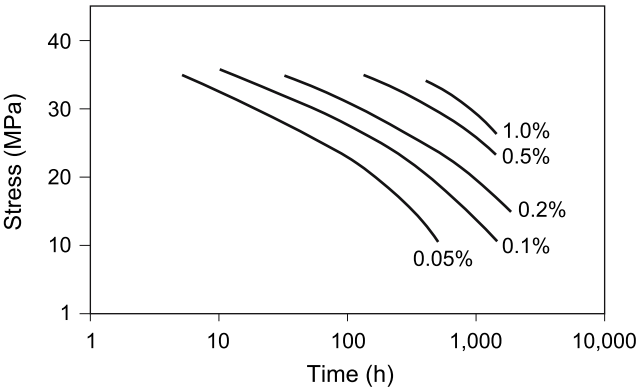


Fig. 5.79. Creep of ZRE1 at 250°C (-T5)

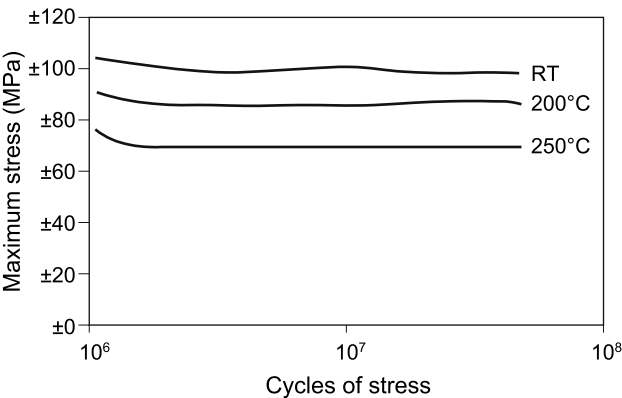


Fig. 5.80. Fatigue of WE54 (-T6)

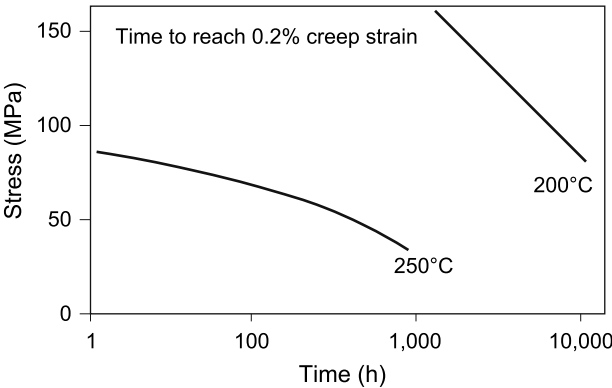


Fig. 5.81. Creep of WE54 (-T6)

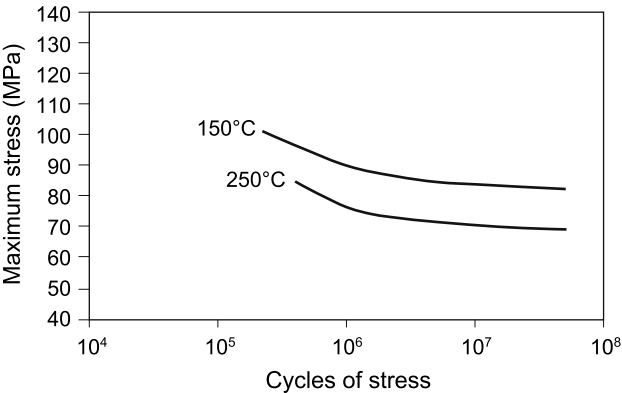


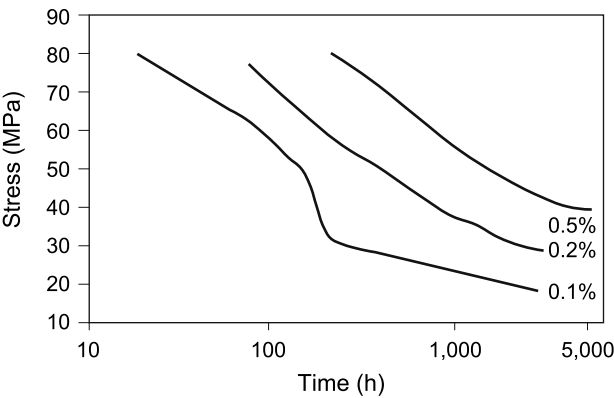
Fig. 5.82. Fatigue of WE43 (-T6)

**Table 5.11.** Typical tensile properties of alloy WE54 (-T6 condition)

Temperature [°C]	0.2% Proof stress [Mpa]	Tensile strength [Mpa]	Elongation [%]
20	205	280	4.0
100	197	260	4.5
150	195	255	5.0
200	183	241	6.5
250	175	230	9.0

Fatigue (rotating bending) and creep properties of alloy WE43 at elevated temperatures are shown in Figs. 5.82 and 5.83 [49]. The creep graph shows the stress/time relationship for specified creep strains at 250°C. Table 5.12 shows the tensile properties of samples taken from actual WE43 castings.

Examples of physical properties of sand cast alloys are listed in Table 5.13 [66]. More information is found in Sect. 5.1.4.



**Fig. 5.83.** Creep of WE43 (-T6)

**Table 5.12.** Tensile properties of alloy WE43 (-T6 condition)

Temperature [°C]	Number of tests	0.2% Proof stress [Mpa]	Tensile strength [Mpa]	Elongation [%]
20	215	Minimum 149	200	2
		Average 178	250	7
		Maximum 215	293	17
250	56	Minimum 134	187	2
		Average 155	211	18
		Maximum 193	235	36

**Table 5.13.** Physical properties of magnesium sand cast alloys

Alloy	Specific gravity [20°C]	Coeff. of thermal exp. [20–200°C] $10^{-6} \text{ K}^{-1}$	Thermal conductivity [20°C] $\text{W} \cdot \text{m}^{-1} \cdot \text{K}^{-1}$	Electrical resistivity [20°C] $\text{n}\Omega \cdot \text{m}$	Specific heat [20–100°C] $\text{J} \cdot \text{kg}^{-1} \cdot \text{K}^{-1}$
AZ81	1.81	27.2	84	134	1000
AZ91	1.83	27.0	84	141	1000
ZC63	1.87	27.0	123	54	960
RZ5	1.84	27.1	109	68	960
ZRE1	1.80	26.8	100	73	1050
MSR-B	1.82	26.7	113	68	1000
EQ21	1.81	26.7	113	68	1000
WE54	1.85	24.6	52	173	960
WE43	1.84	26.7	51	148	966

## 5.2 Wrought Alloys

*Catrin Kammer*

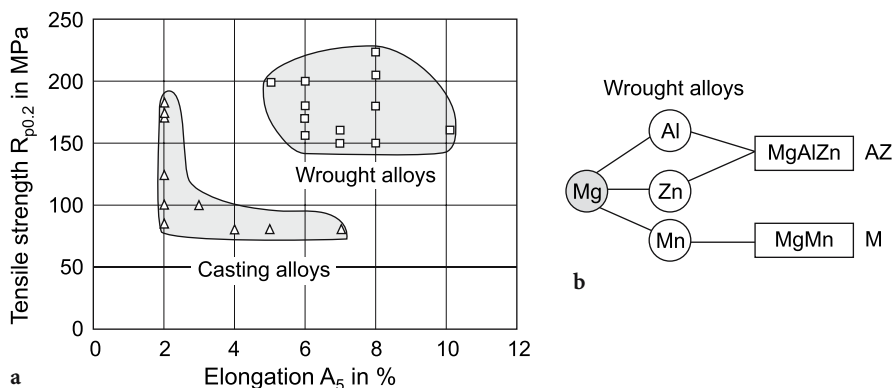
The development of magnesium alloys started shortly after the first industrial production of this light metal. In the 1930's a first peak in research and applications was reached. Magnesium wrought alloys were used during the Second World War against the background of military applications. Thereafter, the research and development for wrought alloys was slow, in particular due to the fact that magnesium alloys were considered unsuitable for aircraft applications or were even forbidden. In specific niches, magnesium wrought alloys were present, for example, in transportation and in sports equipment. Research was limited until the 1990's when it saw a new boom.

However, there was no steady development as there was in the case of aluminum wrought alloys. This is the reason for the small number of magnesium alloys compared to the huge number of aluminum alloys. Thus, aluminum has a competitive edge in research and development [67, 68].

As in the case of aluminum alloys, one differentiates between magnesium alloys as cast or wrought alloys. Workability, i.e., the capability for plastic deformation, is of paramount importance with wrought alloys, whereas casting alloys should be readily pourable and exhibit good mould-filling characteristics. Magnesium has excellent casting properties, but deformation is more difficult, especially at room temperature. Therefore more casting alloys are available than wrought alloys.

On the other hand, wrought magnesium alloys have specific advantages, for example they are leak proof because they are not porous. Excellent mechanical properties can be achieved by special thermomechanical treatment (see Fig. 5.84a).

This leads to some differences in alloy content, but not as significant as in the case of aluminum alloys. It is not possible to say that the alloying content in casting alloys is always higher than in wrought alloys.



**Fig. 5.84.** Overview of magnesium wrought alloys [68]. **a** Ratio strength to elongation for magnesium wrought and cast alloys. **b** Main alloying elements of magnesium wrought alloys

- **Casting alloys** contain up to 10% aluminum, up to 6.5% zinc, up to 0.5% manganese, up to 1.5% silicon and traces of copper, nickel and iron. Special alloys have additions of rare earth elements up to 4%. Also possible are additions of silver (up to 3%) and zirconium (up to 1%). Newly developed alloys can have contents of rare earth elements up to 10% and high levels of lithium.
- **Wrought alloys** have up to 10% aluminum, up to 2% manganese, up to 1.5% zinc (and seldomly up to 6% zinc), less silicon (in the order of 0.1%) and traces of copper, nickel and iron.

Main alloying elements of magnesium alloys are aluminum, zinc and manganese (see Fig. 5.84b). They mainly improve the strength at room temperature and at higher temperatures. As in the case of aluminum alloys, the different alloying elements can bring a significant change in the mechanical properties caused by solid solution strengthening, precipitation hardening or a combination of both processes. Beside this, they can improve the corrosion resistance.

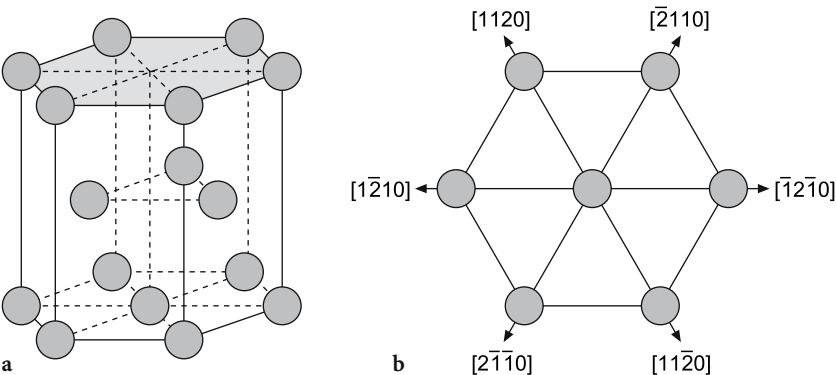
Other important advantages of all types of magnesium alloys are two well known properties: the low density and the good damping behavior.

Section 5.2.1–5.2.9 will show the composition, classification and properties of the most important magnesium wrought alloys.

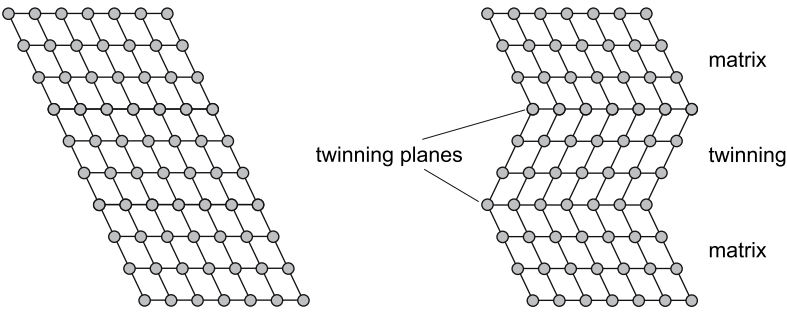
As already said, wrought alloys are only a small group within the magnesium alloys of technical use. The reason for this is seen in the low deformability room temperature, due to the hexagonal crystal lattice (Fig. 5.85). In spite of this, magnesium can be deformed by the classic deformation processes, for example, extruding, rolling and forging, at temperatures above about 200 to 225°C depending on the alloy composition [69]. Up to this temperature (225°C for pure magnesium) there is only gliding in the basic plane (0001) of the hexagonal lattice. The slip plane is defined by the direction of the closed-packed atomic direction (see Fig. 5.85) [70–72].

In addition to gliding in the basis plane, twinning is a second mechanism of deformation at room temperature (see Fig. 5.86).





**Fig. 5.85.** Slip planes and slip directions in the hexagonal closed packing. **a** Basic plane (0001), **b** directions in the basis plane



**Fig. 5.86.** Twinning

At a temperature above 225°C further *pyramidal* slip planes are activated (Fig. 5.87). This is caused by the higher mobility of the atoms at this temperature. These additional gliding planes bring a clear improvement to the formability [73, 74].

Among the magnesium wrought alloys used today, several groups can be identified, not all of which are included in DIN 1729 (see Table 5.14). In many cases ASTM conform alloys are used (Table 5.15 and 5.16).

**Table 5.14.** Composition of magnesium wrought alloys [75]

Alloy Chem.	Num.	Composition in mass-%							Other (total)
		Si	Cu	Al	Zn	Fe	Ni	Mn	
MgAl <sub>7</sub> Zn	3.5312	0.1	0.1	2.5–3.5	0.5–1.5	0.03	0.005	0.05–0.4	0.1
MgAl <sub>7</sub> Zn	3.5612	0.1	0.1	5.5–7.0	0.5–1.5	0.03	0.005	0.15–0.4	0.1
MgAl <sub>8</sub> Zn	3.5812	0.1	0.05	7.8–9.2	0.2–0.8	0.005	–	0.12–0.3	0.3
MgMn <sub>2</sub>	3.5200	0.10	0.05	0.05	0.03	0.005	0.001	1.2–2.0	0.10

**Table 5.15.** Composition of magnesium wrought alloys for plate and sheet [76]

Alloy											
ASTM	UNS	Al	Mn	Zn	Th	Si	Cu	Ni	Fe	Special	Other (total)
AZ31B	M11311	2.5–3.5	0.20–1.0	0.6–1.4	–	0.10	0.05	0.005	0.005	0.04 Ca	0.30
AZ31C	M11312	2.4–3.6	0.15–1.0	0.50–1.5	–	0.10	0.10	0.03	–	–	0.30
HK31A	M13310	–	–	0.30	2.5–4.0	–	0.10	0.01	–	0.40–1.0 Zr-	0.30
HM21A	M13210	–	0.45–1.1	–	1.5–2.5	–	–	–	–	–	0.30
ZE10A	M16100	–	–	1.0–1.5	–	–	–	–	–	0.12–0.22-RE	0.30
LA141A	M14141	1.0–1.5	0.15	–	–	0.004	0.005	0.005	0.005	0.005 Na 13.0–15.0 Li	0.30

**Table 5.16.** Composition of magnesium wrought alloys for forgings and extrusions according to [77]

ASTM	UNS	Al	Mn	Zn	Si	Cu	Ni	Fe	Special	Other, total
Forgings B91/B92										
AZ31B	M11311	2.5–3.5	0.20–1.0	0.6–1.4	0.10	0.05	0.005	0.005	0.04 Ca	0.30
AZ61A	M11610	5.8–7.2	0.15–0.5	0.40–1.5	0.10	0.05	0.005	0.005	–	0.30
AZ80A	M11800	7.8–9.2	0.12–0.5	0.20–0.8	0.10	0.05	0.005	0.005	–	0.30
HM21A	M13210	–	0.45–1.1	–	–	–	–	–	1.5–2.5 Th	0.30
ZK60A	M16600	–	–	4.8–6.2	–	–	–	–	0.45 Zr min.	0.30
Extrusions B107/B 107M-94										
AZ31B	M11311	2.5–3.5	0.20–1.0	0.6–1.4	0.10	0.05	0.005	0.005	0.04 Ca	0.30
AZ31C	M11312	2.3–3.6	0.15–1.0	0.05–1.5	0.10	0.10	0.03	–	–	0.30
AZ61A	M11610	5.8–7.2	0.15–0.5	0.40–1.5	0.10	0.05	0.005	0.005	–	0.30
AZ80A	M11800	7.8–9.2	0.12–0.5	0.20–0.8	0.10	0.05	0.005	0.005	–	0.30
M1A	M15100	–	1.2–2.0	–	0.10	0.05	0.01	–	0.30	0.30
ZK40A	M16400	–	–	3.5–4.5	–	–	–	–	0.45 Zr min.	0.30
ZK60A	M16600	–	–	4.8–6.2	–	–	–	–	0.45 Zr min.	0.30

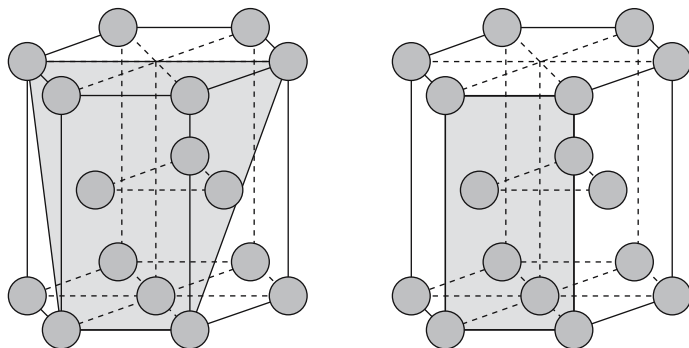


Fig. 5.87. Pyramidal and prismatic gliding

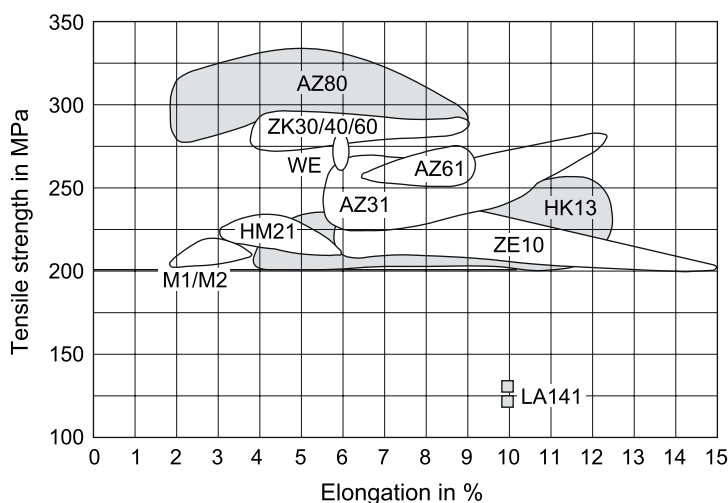


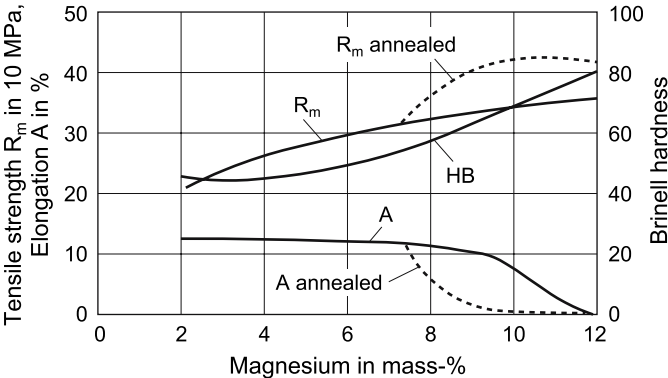
Fig. 5.88. Combination of properties available with magnesium wrought alloys (compilation according to ASTM and DIN, see also Tables 5.14 to 5.16) [75, 76]

With thermal treatments, the properties can be varied over a large area (see Fig. 5.88). That is why the few magnesium wrought alloys must cover a large spectrum of properties.

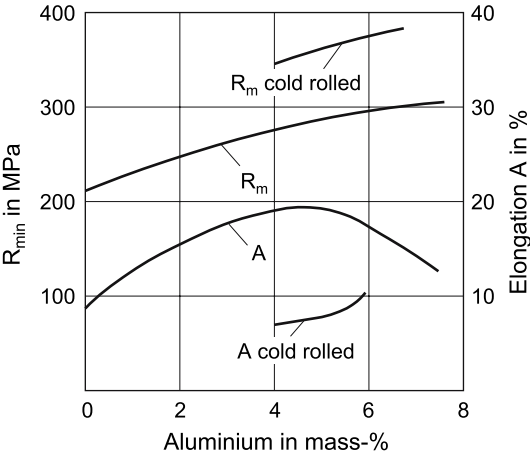
In the following sections the mechanical properties will be the main topic of discussion.

### 5.2.1 Magnesium – Aluminum

For magnesium, aluminum is an ideal alloying element. The best mechanical properties in the case of wrought alloys are achieved in the range of 9 to 10% aluminum. The reason for this is the (at least partial) homogenization of the material caused by the elevated temperature before and/or after the deformation.



**Fig. 5.89.** Influence of aluminum on the mechanical properties of magnesium [78]; F – extruded; T6 – Solution heat treatment 420°C/2 h/Water cooling, ageing 200°C/12 h



**Fig. 5.90.** Influence of aluminum on the strength of magnesium (rolled) [67]

Magnesium alloys with an aluminum content up to 7% can be hot rolled. If the alloy content is lower, cold rolling after hot rolling is possible – without a significant decrease in ductility. An increase in the aluminum content causes difficulties in processing.

On annealing homogenized alloys just under the solubility line, further improvement of the tensile strength can be obtained, but simultaneously the elongation will decrease (see Figs. 5.89 and 5.90).

For extrusions and forgings, alloys are used containing approximately 10% aluminum. They have a high tensile strength and proof stress [78].

### 5.2.2 Magnesium – Manganese (M-alloys)

Pure magnesium-manganese alloys such as MgMn1,5 and MgMn2 are counted as alloys for general use with medium strength values [78]. The alloying content is limited to a maximum of 2.5% manganese.

The influence of the manganese content on the mechanical properties is rather low (see Fig. 5.91). In rolled condition alloys with more than approximately 1.5% manganese a higher strength is observed.

The alloy MgMn2 (M2) with two % manganese is standardized in DIN 1729 [75] (see Table 5.14). This alloy is of good formability. Examples of mechanical properties are given in Table 5.17, properties for extrusions in Table 5.18. Table 5.18 shows the properties of alloys after thermomechanical treatments, tested transverse or lengthwise. The differences in the results depend on the testing direction (L- and T-values) and can be explained by the deformation mechanisms in the hexagonal lattice (number of available slip planes).

The alloy is suited for extrusion and can be welded. The corrosion resistance is good. This alloy is used for cladding and for anodes. Besides this, in North America an alloy M1 (with 1% Mn) is used for the production of extrusions. This alloy can be rolled, too.

### 5.2.3 Magnesium – Aluminum – Zinc (AZ-alloys)

Zinc results in an improvement in strength, especially if the content is higher than 3%. The effect of additions of zinc in rolled samples is shown in Fig 5.92. Examples of the mechanical properties are given in Table 5.17, properties for extrusions in Table 5.18.

Due to the fact that aluminum can result in high strengths of the alloys, the group AZ can produce high to very high strengths (see Fig. 5.88).

The most important alloys can be characterized as follows:

- AZ31 (MgAl3Zn) shows a medium strength. The alloy is formable and weldable [75]. The material is suited for parts with a moderate mechanical stress

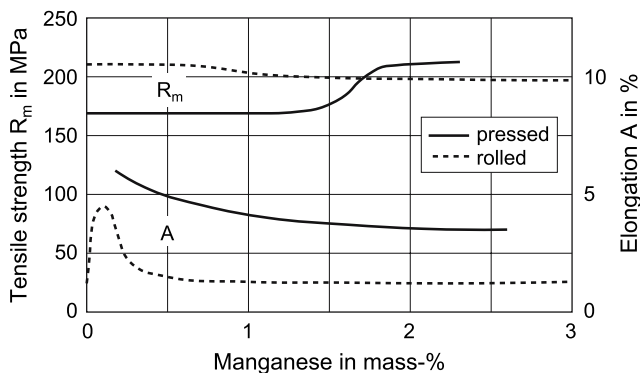
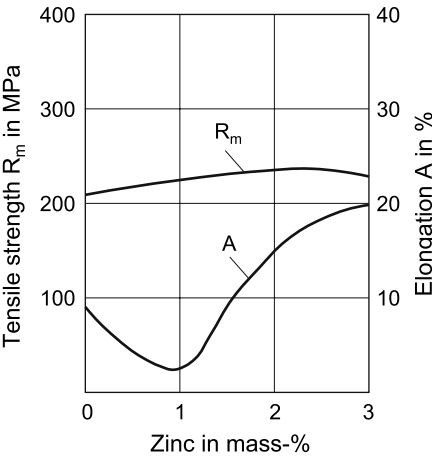


Fig. 5.91. Influence of additions of manganese on the mechanical properties of magnesium (Aitchison, Haughton und Prytherch) [67]

**Table 5.17.** Magnesium wrought alloy – extrusions and forgings, examples for mechanical properties

	Alloy	Composition	Mech. properties			Use
			$R_{p0,2}$ [MPa]	$R_m$ [MPa]	$A_5$ [%]	
M	M2	Mg-2Mn	160	215	4	alloy for extrusion at high press output, middle strength values, weldable, corrosion resistant
AZ	AZ31	Mg-3Al-1Zn	160	240	10	alloy for extrusion and forging middle to high strength values, corrosion resistant in HP condition
	AZ61	Mg-6Al-1Zn	190	270	9	
	AZ80	Mg-8Al-0.5Zn	215	300	8	
ZK	ZK30	Mg-3Zn-0.6Zr	215	300	9	alloy for extrusion and forging middle to high strength values, good deformability
	ZK60	Mg-6Zn-0.6Zr	235	315	8	
WE	WE43	Mg-4Y-3SE-0.5Zr	160	260	6	alloy for extrusion and forging, good strength at elevated temperatures
	WE54	Mg-5,25Y-3,5SE-0,5Zr	180	280	6	



**Fig. 5.92.** Influence of additions of zinc on the mechanical properties of magnesium (rolled) [68]

while the corrosion resistance must be good. According to the ASTM standard, the alloy is suited for forging. In the case of extrusion the material AZ31B can be processed at velocities up to 20 m/min [79].

- AZ61 (MgAl6Zn) has higher strength values. The material is conditionally weldable. As a HP-alloy (high purity alloy) the material has a high corrosion resistance [75]. Applications are parts with moderate to stress level. According to ASTM forging is possible.

- AZ80 (MgAl8Zn) is the alloy with the highest strength. It is used for parts with the highest mechanical stress [75]. In the high purity condition, the corrosion resistance is very good. In the ASTM-standard, the alloy is recommended for the production of forgings.

Important: In the case of extrusion processes, the press speed of these high alloying contents containing alloys (AZ61A and AZ80) is limited to maximum values of 5–3 m/min, otherwise hot cracks can occur. In general, the higher the alloying content, the lower the extrusion speed must be [79].

### 5.2.4 Magnesium – Zinc – Zirconium (ZK-Alloys)

Magnesium – Zinc – Zirconium alloys are ZK30, ZK40 and ZK60 and are contained in the ASTM-standards, but not in the DIN. The alloys have medium to high strength. They are used for extrusions and for forging. The formability of zirconium containing alloys is good (see Fig. 5.88) [68]. Examples of mechanical properties are given in Table 5.17 and properties for extrusions in Table 5.18.

### 5.2.5 Magnesium – Zinc – Rare Earth (ZE-Alloys)

The alloy ZE10 (ASTM = B90) is suited for the production of plate and sheet. It has a medium strength, but high elongation (ductility, see Fig. 5.88). The additions of zirconium cause a clear improvement in the mechanical properties (high tensile strength without significant decrease in ductility) due to a grain refinement. Mg-Zn-Zr-alloys for extrusion have no additions of rare earth elements [68].

### 5.2.6 Magnesium – Yttrium – Rare Earth (WE-Alloys)

The Alloys WE43 (Mg-4Y-3SE-0.5Zr) and WE54 (Mg-5.25Y-3.5SE-0.5Zr) are not standardized in the DIN and ASTM. Both are suited for extrusion and forging.

**Table 5.18.** Mechanical properties of extrusions, in different thermal treatments, testing lengthwise (L) or transverse (T) [68]

Alloy	Condition	Tensile (L)			Tensile (T)		
		R <sub>p0.2</sub> [MPa]	R <sub>m</sub> [MPa]	A <sub>5</sub> [%]	R <sub>p0.2</sub> [MPa]	R <sub>m</sub> [MPa]	A <sub>5</sub> [%]
M2	F	180	250	4	–	–	–
AZ31	F	180	250	14	110	225	13
AZ61	F	220	300	12	137	294	12
AZ80	F	240	340	10	170	323	11
ZK30	T6	240	290	14	220	280	16
ZK60	T6	280	320	12	250	310	14
WE43	T6	170	260	12	165	250	14
WE54	T6	190	280	10	185	275	13

The strength at elevated temperatures is good. This alloys are used for forging and extrusion with good strength values at elevated temperatures. Examples for mechanical properties are given in Table 5.17, properties for extrusions in Table 5.18.

### 5.2.7 Magnesium – Thorium, Zirconium or Manganese (HK- and HM-Alloys)

Usually additions of thorium lead to a solid solution strengthening. That is why these alloys cover a wide area of properties, as shown in Fig. 5.88. According to the ASTM the alloys are suited for the production of plate and sheet and for the production of forgings.

### 5.2.8 Magnesium – Lithium – Alloys (LA-Alloys)

This group of alloys is relatively new. Lithium, with its excellent low density ( $0.534 \text{ g/cm}^3$ ), reduces the density of magnesium alloys in a significant way. Besides this, the formability of magnesium is improved. Dependent on the alloying content there are two main reasons for the activation additional slip planes [79]:

- In the case of homogeneous alloys (up to approximately 7% Li) lithium, with its similar atomic radius ( $\text{Li: } 2.05 \cdot 10^{-10} \text{ m; Mg: } 1.72 \cdot 10^{-10} \text{ m}$ ), is built into the hexagonal crystal lattice of magnesium. In this hexagonal solid solution the  $c/a$  proportion will be lower. This leads to the activation of additional slip planes [80].
- Another point is the good solubility of magnesium in lithium. That explains why magnesium-based alloys with the krz-structure of lithium are possible. In this case more slip planes are activated [80].

These two mechanisms are the reason for the improvement of ductility and formability of magnesium by additions of lithium. Sometimes a very good formability is achieved – anomalous for magnesium. Therefore, these alloys are

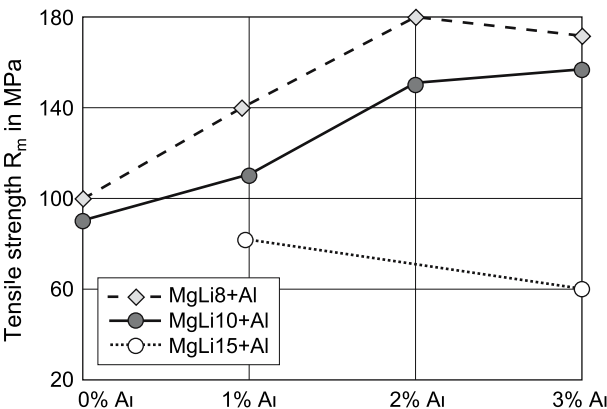


Fig. 5.93. Tensile strength of three different Mg-Li-alloys with different aluminum contents [80]



predestined for use as wrought alloys. However, the strength of pure Mg-Li-alloys is relatively low, especially in the case of higher lithium contents. This is caused by dynamic recovery (cross slip of dislocations, creep processes).

A counter measure is possible by additions of aluminum. This causes the appearance of the granular AlLi-precipitation (AlLi, Li<sub>2</sub>MgAl) and to solid solution strengthening. This can also be seen in Fig. 5.93. Here an alloy with 8% lithium and 3% aluminum show the highest strengths. A further improvement of the content brings no additional effect. Above 8% even a decrease in strength was registered. Optimal are contents between 1 and 3%. One alloy of this type is included in the ASTM standards. The alloy LA141 (with 14% lithium and 1% aluminum) at 10% elongation (T7, Sheet, plate, ASTM B90), but the strength is relatively low ( $R_m \sim 130$  MPa;  $R_{p0.2} \sim 100$  MPa).

### 5.2.9 Other Wrought Alloys

A new development is a Mg-Zn-Cu-Mn-alloy. After extrusion it reaches tensile strengths up to 350 MPa (T6 condition) [79]. In the 1930s the American Magnesium Corp. (AMC) developed tin containing magnesium wrought alloys.

## References to Chapter 5.1

1. International Magnesium Association Statistics 1999, IMA, 1303 Vincent Place, McLean, Virginia 221001, USA
2. Schumann S, Friedrich F (1998) The use of magnesium in cars – Today and in Future. In Mordike BL, Kainer KU (Eds) Werkstoff Informationsgesellschaft, Frankfurt, Germany, pp. 3–13
3. Ohshima E (1996) Application of Die Cast Magnesium to AVCC. In Proc. Conf. International Magnesium Association, Ube City, Japan. IMA, 1303 Vincent Place, McLean, Virginia 221001 USA, pp. 1–16
4. Aune TK, Albright DL, Westengen H (1990) Properties of Die Cast Magnesium Alloys of Varying Aluminium Content, SAE paper 900792, Warrendale PA, USA
5. Aune TK, Albright D, Ørjasæter O, Nerdahl OK (2000) Elements of the Fatigue Process in Magnesium Die Casting Alloys. In Kaplan HI, Hryn JN, Clow B (eds) Magnesium Technology 2000. TMS-AIME, Warrendale, PA, USA, pp. 319–323
6. Aune TK, Westengen H (2000) High performance die castings – Utilizing Magnesium's properties. In Kainer KU (Ed) Magnesium Alloys and their applications. Wiley-VCH Weinheim, Germany, pp. 540–547
7. Aune TK, Westengen H, Albright D (2000) High Performance Die Castings – Utilising Magnesium's Properties. In Kainer KU (ed) Magnesium Alloys and their Applications. Wiley VCH Verlag GmbH, Weinheim, Germany, pp. 540–547
8. Aune TK, Westengen H, Ruden T (1993) Mechanical Properties of Energy Absorbing Magnesium Alloys, SAE paper 930418, Warrendale PA, USA
9. King JF (1998) Development of Magnesium Diecasting Alloys. In Mordike BL, Kainer KU (Eds) Werkstoff Informationsgesellschaft, Frankfurt, Germany, pp. 37–47
10. King JF (2000) Development of practical high temperature magnesium Casting alloys. In Kainer KU (ed) Magnesium Alloys and their applications. Wiley-VCH Weinheim, Germany, pp. 14–22
11. Unsworth W (1989) The role of rare earth elements in the development of magnesium base alloys. Int. J. of materials and Product Technology, Vol. 4, no. 4, pp. 359–378
12. Metals Handbook, 10th edn., Vol. 2 (1990) Properties and selection: nonferrous alloys and special-purpose materials. ASM International, Materials Park, OH, USA

13. Polmear IJ (1995) *Light Alloys. Metallurgy of the light metals*, 3<sup>rd</sup> Edition, Arnold, London, England
14. Roberts CSR (1958) *Magnesium and Its Alloys*. Wiley, New York, USA
15. Westengen H (1991) Current trends in magnesium alloy development. In Hirano K, Oikawa H, Ikeda K (eds) *Science and Engineering of Light Metals*. Japan Institute of Light Metals, Tokyo, Japan, pp. 77–84
16. Westengen H, Wei L-Y, Aune T, Albright D (1998) Effect of Intermediate Temperature Aging on Mechanical Properties and Microstructure of Die cast AM-Alloys. In Mordike BL, Kainer KU (eds) *Magnesium Alloys and their Applications*, Werkstoff-Informationsgesellschaft mbH, Frankfurt, Germany, pp. 209–214
17. Binary Alloy Phase Diagrams 2<sup>nd</sup> Ed. (1996) ASM International, Materials Park, OH, USA
18. Nayeb-Hashemi AA, Clark JB (1988) *Phase Diagrams of Binary Magnesium Alloys*. ASM International, Materials Park, OH, USA
19. Pettersen K, Bakke P (2001) Norsk Hydro, Internal report. To be published
20. Hillis MM (1998) Compositional requirements for quality performance with high purity. In Proc. Conf. International Magnesium Association, Coronado Calif. USA, IMA, 1303 Vincent Place, McLean, Virginia 221001 USA, pp. 74–81
21. Holta O, Westengen H, Røen J (1997) High purity magnesium die casting alloys: Impact of metallurgical principles on industrial practice. In Lorimer GW (ed) *Proc. 3rd Int. Magnesium Conf.* Institute of Materials, London, UK, pp. 75–88
22. Emley EF (1966) *Principles of Magnesium Technology*. Pergamon, Oxford, UK
23. Bakke P, Sannes S, Albright, DL (1999) Effects of Ni, Cu, Si and Co on the corrosion properties of permanent mould cast medaillons and die cast plates of magnesium alloy AZ91. SAE Technical Paper 1999-01-0926. SAE International, Warrendale PA, USA
24. Schickl G (1954) *Magnesium Taschenbuch*. VEB Verlag Technik, Berlin, Germany
25. Lee YC, Dahle AK, StJohn DH (2000) Grain refinement of magnesium. In Kaplan HJ, Hryn JN, and Clow BB (eds) *Magnesium Technology 2000*, TMS, Warrendale, Pennsylvania, USA, pp. 211–218
26. Beck A (1940) *The Technology of Magnesium and its Alloys* (Translated from German). FA Hughes & Co. Ltd, London, UK
27. *Metals Handbook* (1988) 9th edn., Vol. 15, Casting. ASM International, Materials Park, OH, USA
28. *Hydro Magnesium* (1996) Die cast magnesium alloys. Data Sheet
29. Han Q, Kenik EA, Agnew SR, Viswanathan S (2001) Solidification behaviour of commercial magnesium alloys. In Hryn J (ed) *Magnesium Technology 2001*, TMS, Warrendale, Pennsylvania, USA, pp. 81–86
30. Dube D, Couture A, Carbonneau, Y, Fiset M, Angers R, Tremblay R (1998) Secondary dendrite arm spacings in magnesium alloy AZ91D. From plaster moulding to laser remelting. *Int. J. Cast Metals Res.*, 11, pp. 139–144
31. Sequeira WP, Dunlop GL, Murray MT (1997) Effect of section thickness and microstructure on the mechanical properties of high pressure die cast magnesium alloy AZ91D. In Lorimer GW (ed) *Proc. Third Int. Magnesium Conference*, Institute of Metals, 1 Carlton House Terrace, London, UK, pp. 63–73
32. Bowles AL, Griffiths JR, Davidson CJ (2001) Ductility and the skin effect in high pressure die cast Mg-Al alloys. In Hryn J (ed) *2001 Magnesium Technology 2001*, TMS, Warrendale, Pennsylvania, USA, pp. 161–168
33. Drits ME, Rokhlin LL, Sherwedine VV, Shulga YN (1972) Influence of certain factors on energy Dissipation during elastic vibrations in magnesium alloys. *Problillemys Procnosit.*, Vol. 3, no. 10
34. Koch H, Klos R, Hielscher U (2000) *Eisenarme Aluminium-Druckgusslegierungen als Substitutionswerkstoff für Stahlblechkonstruktionen im Automobilbau*. Giesserei-Praxis No. 4
35. ASTM B 94: Standard Specification for Magnesium-Alloy Die Castings. American Society for Testing and Materials, West Conshohocken, PA 19428-2959, USA

36. Decker R, Carnahan R, Vining R, Walukas D, LeBeau S, Prewitt N (1998) Thixomolding® Mg Based Alloys. In Mordike BL, Kainer KU (Eds) Werkstoff Informationsgesellschaft, Frankfurt, Germany, pp. 545–553
37. Czerwinski F, Pinet PJ, Overbeeke J (2001) The influence of primary solid content on the tensile properties of a thixomolded AZ91D magnesium alloy. In Hryn J (ed) 2001 Magnesium Technology 2001, TMS, Warrendale, Pennsylvania, USA, pp. 99–102
38. ISO 16220: Magnesium and magnesium alloys – Magnesium alloy ingots and castings. International Organization for Standardization, Case postale 56, CH-1211 Geneva 20, Switzerland
39. EN 1753: Magnesium and magnesium alloys – Magnesium alloy ingots and castings. European Committee for Standardization, Rue de Stassart 36, B-1050 Brussels, Belgium
40. ASTM B 80: Standard Specification for Magnesium-Alloy Sand Castings. American Society for Testing and Materials, West Conshohocken, PA 19428-2959, USA
41. ASTM B 93: Standard Specification for Magnesium Alloys in Ingot Form for Sand Castings, Permanent Mold Castings, and Die Castings. American Society for Testing and Materials, West Conshohocken, PA 19428-2959, USA
42. Sannes S, Westengen H (1998) The Influence of Process Conditions on the Microstructure and Mechanical Properties of Magnesium Die Castings. In Mordike BL, Kainer KU (eds) Magnesium Alloys and their Applications, Werkstoff-Informationsgesellschaft mbH, Frankfurt, Germany, pp. 223–228
43. Busk RS (1987) Magnesium Products Design. Marcel Dekker, New York
44. Kainer KU (2000) Magnesium – Eigenschaften, Anwendungen, Potentiale, Wiley-VCH
45. Avedesian MM, Baker H (eds) (1999) ASM Speciality Handbook Magnesium and Magnesium Alloys. ASM International
46. Kammer C (ed) (2000) Magnesium Taschenbuch. Aluminium-Verlag, Düsseldorf
47. Hydro Magnesium technical brochures and internal reports. Hydro Magnesium, Avenue Marcel Thiry 83, B-1200 Brussels, Belgium
48. Aune TKr (1995) Magnesium Die Casting – Alloys and Properties. IMA Automotive Seminar, Frankfurt, October 1995
49. Aune TKr, Westengen H (1995) Property Update on Magnesium Die Casting Alloys. SAE Technical Paper 950424. SAE International, Warrendale, PA, USA
50. Schindelbacher G, Rösch R (1998) Mechanical properties of magnesium die casting alloys at elevated temperatures and microstructure in dependence of wall thickness. In Mordike BL, Kainer KU (eds) Magnesium Alloys and their Applications, Werkstoff-Informationsgesellschaft mbH, Frankfurt, Germany, pp. 247–252
51. Basner TG, Evans M, Sakkinen DJ (1993) The Effect of Extended Time Aging on the Mechanical Properties of Vertical Vacuum Cast Aluminium-Manganese and Aluminium-Rare Earth Magnesium Alloys. SAE Technical Paper 930419. SAE International, Warrendale, PA, USA
52. Finkel A, Regev M, Aghion E, Bamberger M, Rosen A (1997) Aging Study of AZ91D Casts. In Aghion E, Eliezer D (eds) Magnesium 1997. Proceedings of the Dead Sea Magnesium Conference, pp. 121–126
53. Sakkinen DJ, Evans M (1993) The Effect of Aging on Magnesium Die Casting Alloys. NADCA document T93-112. Cleveland, October 1993, pp. 305–313
54. Suman C (1990) The Effects on Direct Aging on Mechanical Properties and Corrosion Resistance of Diecast Magnesium Alloys AZ91D and AM60B. SAE Technical Paper 900794. SAE Technical Paper 940779. SAE International, Warrendale, PA, USA
55. Ashby MF (1972) A first report on deformation-mechanism maps. Acta Met, Vol 20, July 1972, pp. 887–897
56. Miller WK (1988) Creep of die cast AZ91 Magnesium at room temperature and low stress. GM research publication GMR-6219. General Motors, Warren, Michigan 48090, USA
57. Suman C (1991) Creep of Diecast Magnesium Alloys AZ91D and AM60B. SAE Technical Paper 910416. SAE International, Warrendale, PA, USA
58. Agnew SR, Liu KC, Kenik EA, Viswanathan S (2000) Tensile and Compressive Creep Behavior of Die Cast Magnesium Alloy AM60B. In Kaplan HI, Hryn JN, Clow B (eds) Magnesium Technology 2000. TMS-AIME, Warrendale, PA, USA, pp. 285–290

59. Agnew SR, Viswanathan S, Payzant, Han Q, Liu KC, Kenik EA (2000) Tensile and Compressive Creep Behavior of Magnesium Die Casting Alloys Containing Aluminium. In Kainer KU (ed) *Magnesium Alloys and their Applications*. Wiley VCH Verlag GmbH, Weinheim, Germany, pp. 687–692
60. Chen FC, Jones JW, McGinn TA, Kearns JE, Nielsen AJ, Allison JE (1997) Bolt-Load Retention and Creep of Die-Cast Magnesium Alloys. SAE Technical Paper 970325. SAE International, Warrendale, PA, USA
61. Dargusch MS, Pettersen K, Dunlop GL (1997) The Microstructure and Creep Behaviour of Die Cast Magnesium AZ91 and AS21 Alloys. Proceedings of the 19th. International Die Casting Congress, Minneapolis, USA. Nov, 1997, pp. 131–137
62. Sohn KY, Wayne Jones J, Allison JE (2000) The effect of Calcium on Creep and Bolt load retention Behavior of Die-cast AM50 Alloy. In Kaplan HI, Hryn JN, Clow B (eds) *Magnesium Technology 2000*. TMS-AIME, Warrendale, PA, USA, pp. 271–278
63. Evans RW, Wilshire B (1993) *Introduction to Creep*. The Institute of Materials, 1 Carlton House Terrace, London SW1Y 5DB, England
64. Kaschnitz E, Funk W (1997) Thermophysikalische Eigenschaften von Magnesiumlegierungen – Teil 1: Wärmeleitfähigkeit. *Giesserei-Praxis* Nr. 7/8, pp. 179–181
65. Kaschnitz E, Funk W (1997) Thermophysikalische Eigenschaften von Magnesiumlegierungen – Teil 3: Spezifische Wärmekapazität. *Giesserei-Praxis* Nr. 11/12, pp. 260–261
66. *Magnesium Elektron technical brochures and internal reports*. Magnesium Elektron, Swinton, Manchester M27 8DD, England

## References to Chapter 5.2

67. Beck A (1939) *Magnesium und seine Legierungen*. Springer, Berlin Heidelberg New York
68. Kammer C (2000) *Magnesium-Taschenbuch*. Aluminium-Verlag, Düsseldorf
69. Wilkinson RG, Winter DB (1941) Deep Drawing and Pressing of Magnesium Alloy Sheet. *Sheet Metal Industries*. 15, 8, p. 1039/1042
70. Roberts CS (1960) *Magnesium and its Alloys*. Wiley, New York
71. Raynor GV (1959) *The Physical Metallurgy of Magnesium and Its Alloys*. Pergamon, London
72. Chapman A (1963) Ph.D. Thesis. University of Birmingham
73. Reed-Hill RE, Robertson WD (1957) Deformation of Magnesium Single Crystals by Non-basal Slip. *J Metal*, 9, 4, p. 496/502
74. Reed-Hill RE, Robertson WD (1958) Pyramidal Slip in Magnesium. *Society of AIME-Trans.*, V. 212, p. 256
75. [DIN 1729-1]
76. [ASTM B90/B90M-93]
77. ASTM B107/B 107M-94
78. Schumann H (1991) *Metallographie*. Deutscher Verlag für Grundstoffindustrie Leipzig. 13. Edition
79. Habashi F (1998) *Alloys*. Wiley, Weinheim
80. Schemme K (1991) Magnesiumwerkstoffe für die 90er Jahre. *Aluminium* 67, 2, p. 167/178

## Additional Readings

- ASM Specialty Handbook (1999) *Magnesium and Magnesium Alloys*. ASM International, Materials Park, OH, USA
- Busk RS (1987) *Magnesium Products Design*. Marcel Dekker, New York, USA
- Kainer KU (2000) *Magnesium Eigenschaften, Anwendungen Potenziale*, Wiley-VCH, Weinheim, Germany
- Kammer C (2000) *Magnesium Taschenbuch*, Aluminium-Verlag, Düsseldorf, Germany
- Magnesium Technology* (1987) Proc. Conf. Baker C, Lorimer GW, Unsworth WE (eds), Institute of Metals, London, UK

- Magnesium alloys and their applications (2000) Proc. Conf. Kainer KU(Ed) Wiley-VCH Weinheim, Germany
- Magnesium alloys and their applications (1998) Proc. Conf. Mordike BL, Kainer KU (eds), Werkstoff Informationsgesellschaft, Frankfurt, Germany
- Magnesium Alloys and their Applications (1992) Proc. Conf Mordike BL, Hehmann F (eds), DGM Informationsgesellschaft, Oberursel, Germany

# 6 Technology of Magnesium and Magnesium Alloys

## 6.1 Casting

### 6.1.1 Sand Casting

*John F. King*

#### 6.1.1.1 Introduction

Sand casting is one of the oldest fabrication techniques for metallic components. The process is highly developed and used for many commercial metals and alloys for applications ranging from highly automated and high volume processes for Al and cast iron alloys, to highly complex low volume components in a wide range of alloys, including magnesium.

Sand casting has been used for magnesium alloy components since the earliest isolation and industrial uses of the metal. The basic principles of sand casting for magnesium alloys do not differ greatly from those of other commercial materials. However, to produce castings of satisfactory quality, it is necessary to take into account some of the significant differences in physical properties between magnesium and other common metals, such as are listed in Table 6.1 [1].

- a) Molten magnesium reacts readily with many basic moulding materials including silica sand and moisture. Moisture must be minimised and suitable inhibitors used to prevent adverse reaction between the metal and the moulds.

**Table 6.1.** Comparative physical properties of magnesium and other metals

	Mg	Al	Cu	Zn	Ni	Fe
Melting Point (°C)	650	660	1083	420	1453	1537
Boiling Point (°C)	1103	2480	2590	907	3000	3070
Density (kg · m <sup>-3</sup> )	1740	2700	8960	7140	8900	7870
Coeff of Linear Expansion (×10 <sup>6</sup> /°K)	26.0	23.5	17.0	31	13.3	12.1
Thermal Conductivity (Wm <sup>-1</sup> K <sup>-1</sup> )	156	238	393	113	88	71
Specific Heat (J · Kg <sup>-1</sup> K <sup>-1</sup> )	1025	900	377	377	460	460
Volume Heat Capacity (J · m <sup>-3</sup> × 10 <sup>-3</sup> )	1783	2430	3378	2692	4094	3620
Latent Heat of Fusion per unit Vol. (J · m <sup>-3</sup> × 10 <sup>-6</sup> )	624	1039	1829	790	2702	2078

- b) Molten magnesium oxidises readily forming voluminous oxides, which may be entrained in the metal. Moulds must be designed for smooth metal flow without turbulence.
- c) Density of magnesium is lower than other conventional casting metals. In simple gravity casting, there is therefore relatively little metallostatic pressure to fill the mould. Moulds must be highly permeable and/or well vented to encourage metal flow in thinner sections and to avoid the risk of mis-runs or “blowing” of gas from the mould into the metal.
- d) To compensate for low volume heat capacity, risers need to be relatively large to provide adequate feeding.

### 6.1.1.2 Sand Systems

Sand systems normally consist of a suitable sand, a binder and an appropriate magnesium reaction inhibitor. Historically, “green” sand mixes were used, with water based natural binders. However, these have now been mainly replaced by chemically bonded systems.

The binder for green sand mixes is normally bentonite, which is a natural clay. This is mixed with water to provide an acceptable degree of workability. Because of the high water content, a highly effective inhibitor is required in green sand mixes. A mix of powdered sulphur and boric acid ( $\text{HBO}_3$ ) has traditionally been used.

A typical facing mix for parts of the mould in direct contact with magnesium would be:

Bentonite	4%
Sulphur	5%
Boric Acid	1%
Water	4%
Sand	Remainder

On filling the mould, sulphur reacts rapidly to produce  $\text{SO}_2$ , which provides the inhibiting effect. Sulphur content can be reduced in parts of the mould not in direct magnesium contact and such mixes can be used for facing, or complete mould manufacture by hand or machine. However, significant quantities of  $\text{SO}_2$  are released and all sulphur containing mixes are now considered undesirable for large-scale use for environmental reasons.

Sulphur content can be minimised but not entirely eliminated by addition of other inhibitors such as potassium fluoroborate ( $\text{KBF}_4$ ).

More recently, with the potential use of magnesium alloy sand castings for high volume automotive production, use of green sand systems has been further considered, since such mixes are easy to use, inexpensive and present relatively minor long term recycling or disposal problems. Satisfactory mixes with very low moisture content have been achieved by use of further additives such as urea [2].

There is a wide range of chemically bonded systems available for sand casting, as shown in Table 6.2.

As a general rule, self-setting processes are used for mould making, while heated or gas-hardening processes are used for core making.

**Table 6.2.** Foundry sand binder processes

Process	Type	Examples
Heated	Oil Sand Croning Shell Hot Box Warm Box	
Self setting	Ester Hardened Silicates Phenolic Urethane Phenolic-acid hardened Phenolic-alkali hardened Urea-furan Phenolic-furan Phenolic/urea-furan	"Pepset", "Novathane"  "Alphaset"
Gas hardened	CO <sub>2</sub> /Silicate Process Amine/Phenolic Urethane SO <sub>2</sub> Process Phenolic-gas hardened	 "Isocure" "Isoaset" "Betaset", "Novaset"

A wide range of binders have been used for magnesium casting. Since water is often a reaction product of the chemical hardening process, those with minimum water content are preferred.

Binder content is typically around 1% of the total mix. This can be varied depending on the strength or collapsibility required in the mould or core. Specific parameters will normally be determined by the foundry, in conjunction with the specific material supplier, based on experience.

Washed, dried and graded silica sands are predominantly used for magnesium sand casting moulds. Sieve gradings between 50 AFS and 100 AFS can be used. For general use, 60 AFS grade sand gives a satisfactory level of permeability. For finer surface detail, 80–90 AFS sands can be used, but permeability is reduced.

Zircon and chromite sands can also be used satisfactorily with chemical binder systems. For magnesium alloys, these are used primarily as facing sand on thicker sections of castings if additional chilling is required. Olivine sands can also be used.

Molten magnesium will react readily with moisture and at higher temperatures also with the silica sand itself.



These reactions are effectively inhibited by sulphur/SO<sub>2</sub>, or by compounds which can break down to release fluoride ions to form non-reactive MgF<sub>2</sub>. In the latter case, breakdown at a relatively low temperature is necessary for effective inhibition. Typical breakdown temperatures are listed in Table 6.3.

For sand casting applications, inhibitor combinations commonly used are listed in Table 6.4.



**Table 6.3.** Breakdown Temperatures for Fluorine Containing Compounds

Compound	Approx. Breakdown Temp. [°C]
Fluoroboric acid $\text{HBF}_4$	70
Fluorosilicic acid $\text{H}_2\text{SiF}_6$	70
Magnesium fluorosilicate $\text{MgSiF}_6$	120
Zinc fluorosilicate $\text{ZnSiF}_6$	160
Ammonium bifluoride $\text{NH}_4\text{HF}_2$	175 <sup>a</sup>
Sodium bifluoride $\text{NaHF}_2$	180 <sup>a</sup>
Ammonium fluoroborate $\text{NH}_4\text{BF}_4$	350
Sodium fluoroborate $\text{NaBF}_4$	385
Potassium fluorosilicate $\text{K}_2\text{SiF}_6$	430
Potassium fluoroborate $\text{KBF}_4$	530
Sodium fluoride $\text{NaF}$	585
Potassium fluorozirconate $\text{K}_2\text{ZrF}_6$	590
Potassium fluorotitanate $\text{K}_2\text{TiF}_6$	780
Potassium aluminium fluoride $\text{KAlF}_4$	1025
Magnesium fluoride $\text{MgF}_2$	1260
Calcium fluoride $\text{CaF}_2$	1300

<sup>a</sup> Release  $\text{HF}$ .

Remainder release other F' containing compounds above stated temperature.

**Table 6.4.** Inhibitor additions for sand casting

Inhibitor	Addition [%]	Comment
Sulphur	1–2	Very effective, but introduces $\text{SO}_2$ into foundry atmosphere
$\text{KBF}_4$	1–2	Effective, but can produce fluorine or $\text{HF}$ fume
50% $\text{KBF}_4$ / 50% $\text{HBO}_3$	2	Reduced fluoride v $\text{KBF}_4$ alone
$\text{K}_2\text{SiF}_6$	1–2	Less effective than $\text{KBF}_4$
75% $\text{K}_2\text{SiF}_6$ / 25% S	1–2	More effective than $\text{K}_2\text{SiF}_6$ alone where $\text{SO}_2$ is permissible
$\text{Na}_2\text{SiF}_6$	1–2	Similar to $\text{K}_2\text{SiF}_6$ . Does not affect Al alloys cast in same sand

Use of decomposable or soluble 'F' containing compounds is now problematic from the point of view of recycling and ultimate disposal. In thermal recycling, fluorine compounds tend to "frit" with the sand and binders at the recycling temperature, preventing attrition for re-use and there are environmental restrictions on disposal of sands containing F' compounds.

For this reason, some castings are now made in moulds without inhibitors, but which are coated with an inhibited mould coat. This can be achieved in relatively thin walled castings, but caution is required for larger casting sections where cooling rates are slower, increasing the risk of "burn out" of the inhibitor coating.

Reaction of magnesium with silica sand is then exothermic with the potential for violent reaction.

### 6.1.1.3 Design of Running Systems

First essentials in making good quality magnesium casting are to ensure the casting is filled with the minimum of turbulence and that the filling or gating system is designed to avoid or trap any entrained oxide or inclusions that may occur during pouring.

All aspects of the mould design should be considered. As illustrated in Fig. 6.1, effective measures are:

- 1) Pouring streams should be as short as possible and well protected to avoid development of thick oxide skins
- 2) Pouring bushes should always be used, rather than pouring metal directly into the downsprue. Bushes should be designed so that partial filling can be established before metal flows into the downsprue. This avoids turbulent flow (Fig. 6.2)
- 3) Downsprues should be tapered with cross-sectional area at the bottom being less than the top. This ensures the sprue remains full throughout filling and avoids aspirating air. Rectangular sprues are preferable to round ones as they prevent vortex formation
- 4) A well should be provided beneath the sprue to trap any drossy oxide from the start of pouring. These often contain a vertical perforated steel screen and wire wool (Fig. 6.3)
- 5) Filters can be incorporated in the running system. Most effective are 5–10 ply knitted mild steel mesh pads or ceramic foam filters. Ceramic filters should be high  $\text{Al}_2\text{O}_3$  or  $\text{ZrO}_2$  and fully sintered to avoid reaction. In both cases, filters should be fitted in an enlarged section of the runner to avoid any choking effect. Filters are not always necessary. Metal poured from melts correctly prepared with fluxes can normally be poured clean (i.e., free of oxides or inclusions), pro-

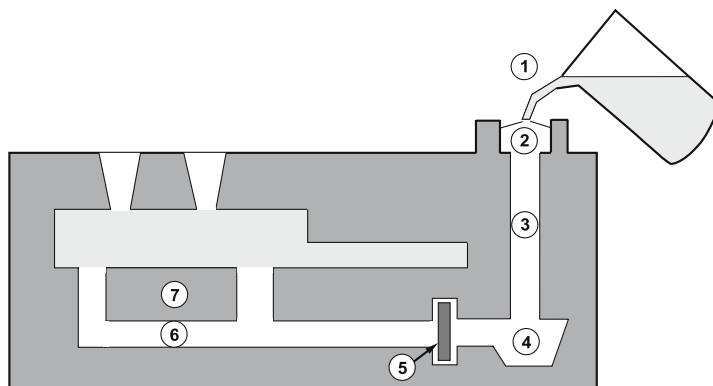
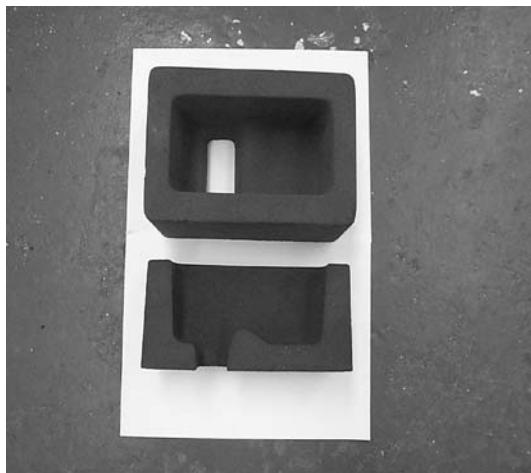
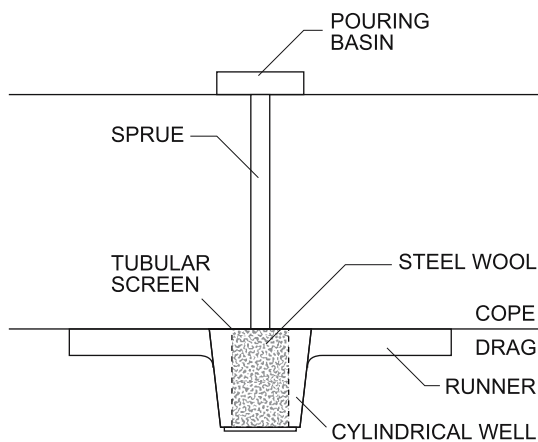


Fig. 6.1. Key factors for mould design



**Fig. 6.2.** Effective pouring bush with weir



**Fig. 6.3.** Typical sprue well (schematic)

- vided the running system is well designed. However, fluxless melts may contain some unsettled oxides and should always be poured with filters in the system
- 6) Metal should be fed into the lowest section of the casting and allowed to rise up through the casting. Cascading flow should be avoided
  - 7) Casting filling should be unpressurised, i.e., total cross sectional areas within the running system should decrease progressively from the casting entry to the downsprue. An ideal ratio is 1-2-3 for downsprue-runners-gates. All runners and gates should be smooth and generously radiused where possible

Having devised a running system to deliver clean metal to the casting, the next requirement is to design the gating, chilling and risering of the mould cavity itself to prevent misruns, promote optimum directional solidification and adequate feeding to minimise micro-shrinkage.

Casting characteristics of magnesium alloys can vary widely and there are a number of important distinctions to make. As indicated elsewhere, there are two major families of casting alloys.

- 1) **Mg-Al Alloys.** Alloys such as AZ91 are widely used commercially for all casting processes including sand casting. These alloys have a wide freezing range (e.g., 110–160°C). Solidification occurs by formation of branched dendrites, which ultimately results in trapping and shrinkage of residual eutectic phase within the dendrite arms causing microporosity. Although the fluidity of these alloys is excellent, as judged by casting distance in simple spiral test castings (Table 6.5), soundness depends critically on grain refinement and extensive use of chills is necessary to promote fine grain and minimise porosity. Porosity-free structures are difficult to achieve and porosity tends to be interconnected and outcropping.
- 2) **Mg-Zr Alloys.** Zr refined alloys in general freeze at higher temperatures than Mg-Al alloys and have a narrower freezing range (e.g., 75–100°C). However, solidification occurs by formation of spheroidal cells, which is more influenced by the Zr refining mechanism than by chill rate. During solidification, bulk feeding by the solidifying “slurry” can occur. Provided directional solidification and feeding are maintained, microporosity is not a major feature and tends to be fine and isolated.

Magnesium has the lowest density and volume heat capacity of any commercial casting alloys (Table 6.1). This has a significant effect on feeding distances in a solidifying casting. This feeding distance depends on:

- Alloy
- Temperature gradient
- Section thickness

In Table 6.5, spiral test fluidity and feeding distances in horizontally cast chilled and unchilled 25 mm thick plates are compared for a number of alloys.

**Table 6.5.** Casting characteristics of magnesium alloys

Alloy	Composition	Fluidity factor <sup>a</sup>	Feeding distance <sup>b</sup>	
			unchilled [mm]	chilled [mm]
AZ91	Mg-9% Al-1% Zn-Mn	1.0	60	150
EZ33 (ZRE1)	Mg-3% RE-2.6% Zn-Zr	NA	150	200
ZE41 (RZ5)	Mg-4.2% Zn-1.3% RE-Zr	0.8	100	150
QE22 (MSR)	Mg-2.5% Ag-2.0% RE-Zr	0.7	75	125
WE43	Mg-4% Y-3% RE-Zr	1.0	100	150

<sup>a</sup> Average cast length of twin spiral castings of trapezoidal section poured under standard conditions (values normalised to AZ91 as unity).

<sup>b</sup> Length of porosity free volume from end of 200 mm × 200 mm × 25 mm thick plate with full width riser at opposite end (25 mm square section chill on end of chilled plate).

The practical implication of the above is that casting system design may vary significantly depending on the alloy. Where chills are used, they are normally aluminium or cast iron, depending on the degree of chill required (cast iron most effective). Chills are normally scored to avoid gas entrapment and cleaned, coated and thoroughly preheated to minimise risk of gas blows from any residual moisture on the surface. Chills are normally at least twice the thickness of the section to be chilled.

Riser design is important for magnesium castings. The purpose of the riser is to supply liquid metal to feed the casting. They must therefore be the last portion of the casting to solidify. Previous considerations indicate that tall risers may be ineffective, but volume must be sufficient to ensure an adequate reservoir of liquid metal.

Ideally, the hottest metal should be supplied to the risers. However, this is not always possible in bottom-filled castings. A number of possible solutions are illustrated diagrammatically in Fig. 6.4.

Risers are best extended to atmosphere at the top of the mould to maximise metallostatic head. However, this can require significant metal volume and create hot spots within the casting due to excessive flow of hot metal. To counteract this, smaller diameter risers can be created by incorporating insulating ceramic fibre sleeves in the mould. Sleeves must contain inhibitors as for mould materials, to avoid reaction. Such sleeves are available commercially.

#### **6.1.1.4 Mould Preparation and Assembly**

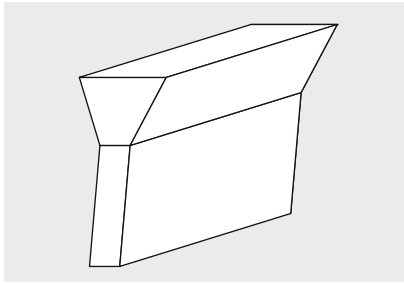
Simplest sand moulds consist of an upper section (cope) and a lower section (drag), which form the upper and lower sections of the casting cavity. Separate sand sections or cores may be incorporated within the mould to form more complex internal features within the casting, including channels and internal pipelines.

Using green sand, the mould is usually formed within a rigid lightweight moulding box against a permanent pattern. Premixed sand is poured into the box and rammed or squeezed manually or by machines to the necessary degree of compaction to ensure integrity and dimensional stability. Extent of squeezing or ramming determines the permeability of the mould, which is necessary to allow gas to escape rapidly as the metal fills the mould.

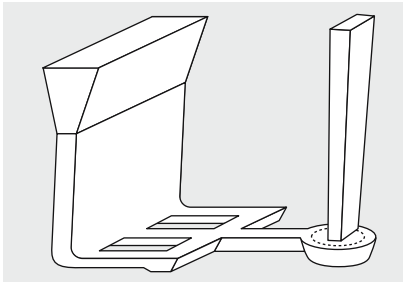
Chemically bonded sands are easier to handle and less dependent on moulding skills to achieve the required consistency. As with green sand, moulds are made by filling and compacting the premixed sand composition against a pattern in a suitable box. However, once hardened, the moulds can be removed from the box for final assembly.

For more complex casting, moulds may consist of multiple components with intermediate sections and many internal cores. In fact, some moulds are now made by complete assembly of a series of pre-formed cores made and assembled with a high degree of accuracy (core box assembly technique).

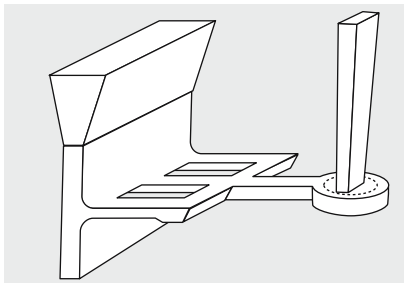
In general, mould manufacturing and assembly techniques are similar to those used for other cast metals, particularly aluminium-based alloys. However, for magnesium alloys, particular attention must be given to ensuring mould cavities



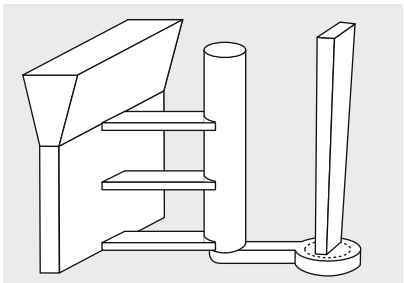
Top Pouring (inclusions will result)



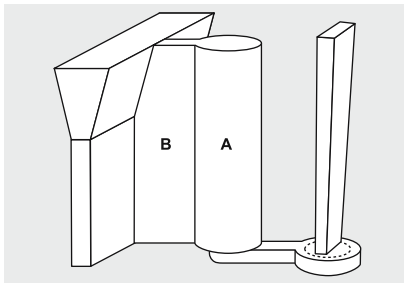
Gating System (results in cold feed metal)



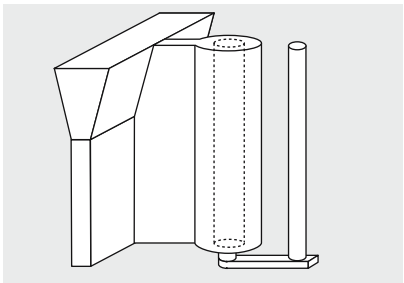
Gating subjected to Metal Tumbling



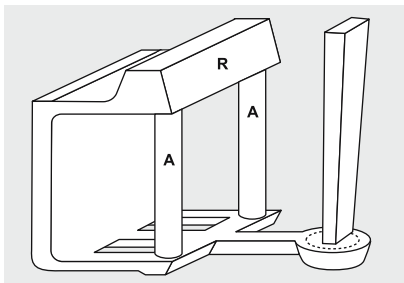
Step Gating can be effective providing flow pattern in upper gates is not established prematurely



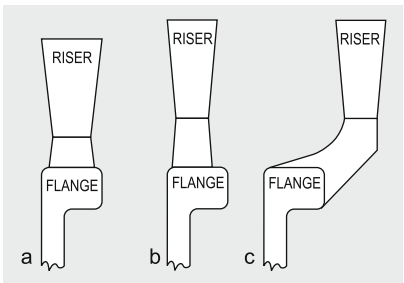
Slit Gate takes Hot Metal into Riser



Tubular Screen guarantees Horizontal Flow through Slit Gate



Side Risers A, with Bottom Gating transfers Hot Metal to Feeder R



Porosity Results with a & b, but not c

Fig. 6.4. Riser options

are free of moisture before casting. Moisture within the mould can cause reactions with the molten metal during filling, resulting in oxide defects or even gas porosity. Preheating of the assembled moulds to around 100°C is recommended to avoid this (and also to improve filling characteristics). Preheating should be carried out in ovens. Local heating with a gas torch is sometimes used, but this can introduce moisture from the combustion gases if moulds are not heated to a high enough temperature.

Refractory mould coats are often spray applied to the surfaces of the mould cavity. These minimise chances of metal reaction with the mould surface and for magnesium alloys, usually contain an inhibitor such as  $\text{KBF}_4$ .

As mentioned previously, moulds and cores can be made with sand mixtures without inhibitors, relying on the use of an inhibited mould coat to avoid reaction in the mould. In this instance, care is necessary in thicker sections where molten metal contact may be prolonged, causing “burn-out” of the inhibitor in the casting. Magnesium reaction with the uninhibited sand can then be exothermic and spectacular!

Finally, before casting, mould cavities are often flushed with an inhibiting gas to further minimise oxidation in the mould. This was often  $\text{SO}_2$ , but is now usually an inhibiting gas mixture such as  $\text{CO}_2 + 1\text{--}2\% \text{SF}_6$ .

Moulds should be flushed immediately before casting, long enough to ensure the cavity is filled with the inhibiting gas mixture.

6.1.1.5 Identification and Elimination of Defects

A range of defects can occur during the sand casting process. Types and origins may be summarised as listed in Table 6.6:

All these defects will affect the properties of the casting to a greater or lesser extent.

Typical defects are listed in Table 6.7, along with causes and corrective measures.

Table 6.6. Typical defects

Origin of defect	Type of defect
In the metal from the crucible	Oxide Segregated intermetallics
During pouring/mould filling	Oxide skins Segregated intermetallics Reacted sand inclusions
During solidification	Porosity Microshrinkage Eutectic segregation Hot tearing

**Table 6.7.** Typical defects – causes and prevention

Defect	Cause	Prevention
Gravity segregation (e.g. “pot bottoms”)	Poor melting practice Insufficient settling time Pouring contaminated metal from crucible bottom	Avoid excessive oxidation and disturbance of melt Allow adequate settling time Leave residue in crucible (10% minimum)
Oxide skins	Inadequate protection of pouring stream during casting Turbulent flow in mould	Ensure all pouring stream is protected Maintain even pouring into moulds Correct design of gating system Mould thoroughly preheated
Reacted sand inclusions	Moisture in mould Loose sand or inadequate binder level in mould. Insufficient inhibitor in mould	Increase binder and/or inhibitor levels
Shrinkage (e.g., in AZ type alloys)	Poor solidification pattern in mould Inadequate chilling	Improve chilling/mould design Optimise grain refinement of alloy
Microporosity (e.g., in Zr refined alloys)	Inadequate feeding during solidification	Optimise casting temperature Improve gating/feeding to eliminate “hot spots”
-	Inadequate grain refinement	Increase grain refinement
Hot tearing (healed or unhealed)	Stress in mould during solidification in “hot spot”	Modify gating to minimise “hot spots”

### 6.1.1.6 Sand Casting Techniques

**Conventional gravity casting** is still the most widely used method of sand casting magnesium alloys, particularly since relatively small numbers of castings are produced.

While perfectly adequate for many castings, this method does have a number of drawbacks.

Molten metal is poured directly from the crucible through air into a pouring bush and hence through a running and gating system into the cast shape (Fig. 6.5). The molten metal stream goes through several abrupt changes of direction, each of which can give rise to turbulence and possible formation of oxide inclusions or gas entrainment.

Furthermore, the rate at which the casting fills is a function of the height difference between the pouring bush and the metal level in the mould. Consequently, fill rate reduces towards the end of the cast. Where thin-sectioned castings are being poured, the reducing fill rate increases the difficulty of filling the thinner sections (Fig. 6.5). This increases the complexity of mould and running system design to ensure good quality metal is fed adequately to all parts of the casting.

**Counter gravity casting** overcomes most of these disadvantages. Metal is fed directly from the crucible into the base of the mould by applying either low pressure to the sealed crucible, or vacuum/reduced pressure to the mould.



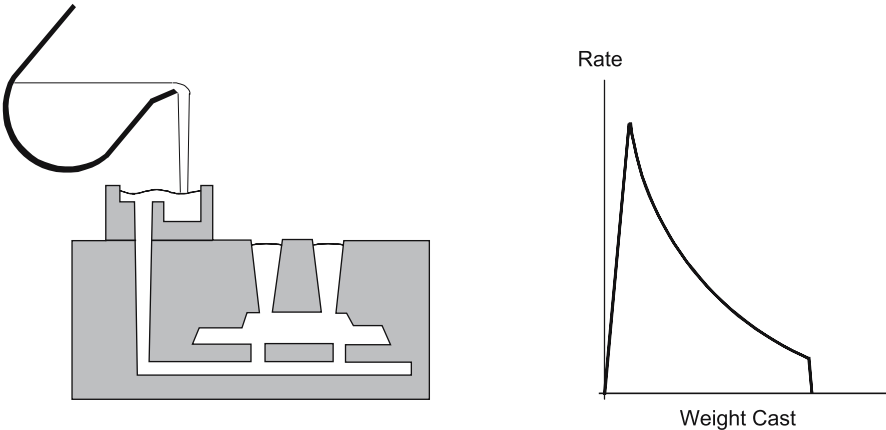


Fig. 6.5. Fill rate defined by mould geometry

The two main principles are illustrated diagrammatically in Figs. 6.6 and 6.7. The net result of both basic techniques is that a differential pressure is created between the surface of the metal in the crucible and that in the mould.

This forces metal from the crucible to the mould at a rate which can be varied at will by adjusting the differential pressure. The differential pressure and all other major parameters of the processes are amenable to measurement and computer control, so that once optimised casting parameters can be reproduced accurately from casting to casting.

The ability to feed metal directly into the bottom of the mould permits moulds, running and gating systems to be designed to minimise direction changes, reducing likelihood of turbulent flow. Maximum metal efficiency can also be achieved. Ideally, mould systems can be designed to allow directional solidification from the top of the mould to the bottom, where the hot metal is being fed in. This avoids the need for excessive risering and temperature inversion for effective solidification. Substantial reductions in casting ratios (casting: total poured weight) can be achieved for improved metal efficiency.

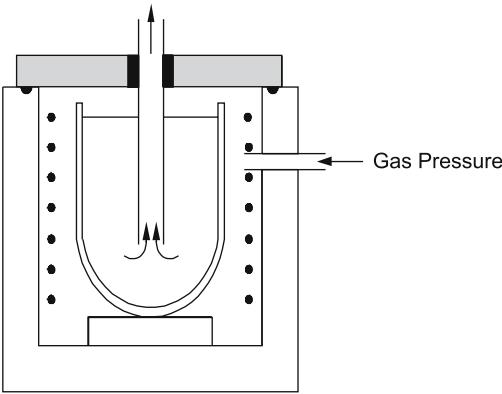


Fig. 6.6. Pressurised furnace

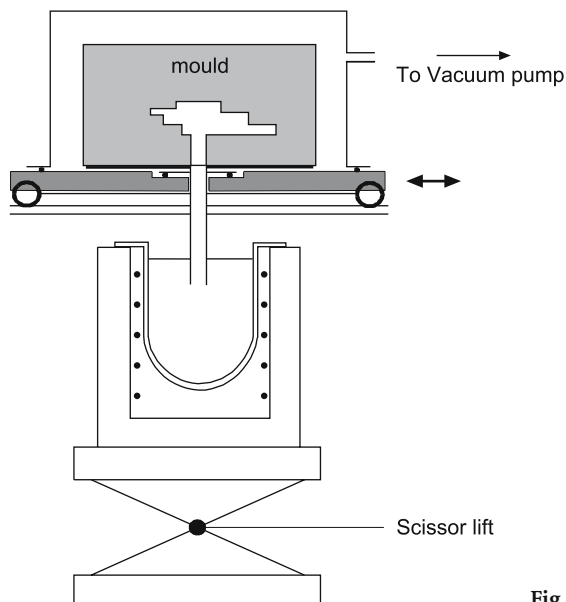


Fig. 6.7. Differential pressure casting

Figure 6.8 illustrates a casting made by the MEL DPSC system, in which total cast weight was reduced from 50 kg by conventional casting to 27 kg by DPSC as a result of inverting the casting and utilising directional solidification to eliminate most of the original gating and risering.

Sand casting systems utilising low pressure, vacuum and even combinations of the two have been developed and are now being increasingly used. Relative advantages and disadvantages of the various systems have been published [3, 4].

#### 6.1.1.7 Heat Treatment

Most magnesium alloy sand castings require some form of heat treatment before use. This may be to develop the required mechanical properties, achieve stress relief, or to “set” castings to specific dimensions.

Very few sand castings are used in the as-cast condition. Depending on the alloy, the following heat treatments may be applied:

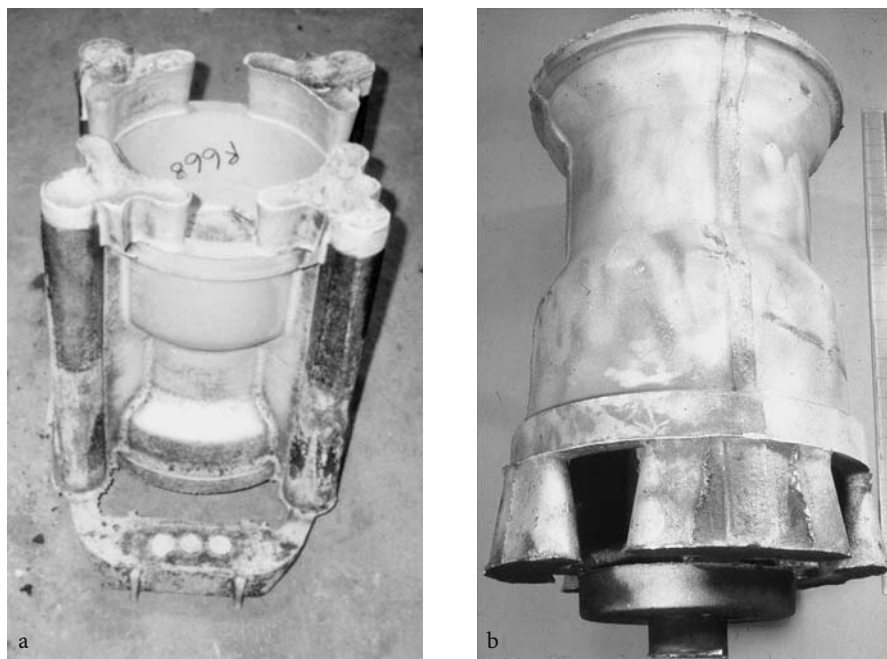
As-cast – solution treated – air cooled (T4)

As cast – precipitation treated – air cooled (T5)

As-cast – solution treated – air cooled or quenched – precipitation treated – air cooled (T6)

Full details of specific heat treatment parameters and resultant properties of the cast alloys are described elsewhere in this publication.

Stress relief is particularly relevant to sand castings. Most castings will contain some internal stresses due to differential cooling between different section thicknesses. Very little stress relief occurs in magnesium castings below 300°C. However, where permissible by other heat treatment parameters, stress relief for



**Fig. 6.8.** Improved casting efficiency by differential pressure casting; **a** Gravity sand cast, **b** differential pressure sand cast

around 2 hours at 330°C or above is effective. Where possible, this is incorporated in the full heat treatment schedule. Thus, for ZE41 (RZ5) – T5, a precipitation treatment of 2 hours at 330°C + 16 hours at 180°C is typically used. AZ91-T4/T6 would be solution treated to 410°C, then air-cooled. A problem arises for T6 heat-treated alloys, which require a rapid quench between solution treatment and precipitation treatment, since this can induce a higher level of internal stress than the original cast in stresses. Figure 6.9 illustrates the residual stress in WE43 cast rings with various quench treatments as indicated by the springback of cast cylindrical rings when cut. Fortunately, in WE43, the required mechanical properties can still be achieved by controlled air cooling, although this is not necessarily the case for some other alloys such as QE22 (MSR)-T6.

In all cases, it is customary for large and/or high precision casting to fix the castings on jigs prior to heat treatment and maintain the jigs in place throughout the heat treatment process. This helps to maintain dimensional accuracy and minimise distortion if internal stresses remain.

#### **6.1.1.8 Inspection of Castings**

Techniques used for magnesium sand castings are basically similar to those used for other metals. However, some specific issues related to magnesium alloys may be highlighted.

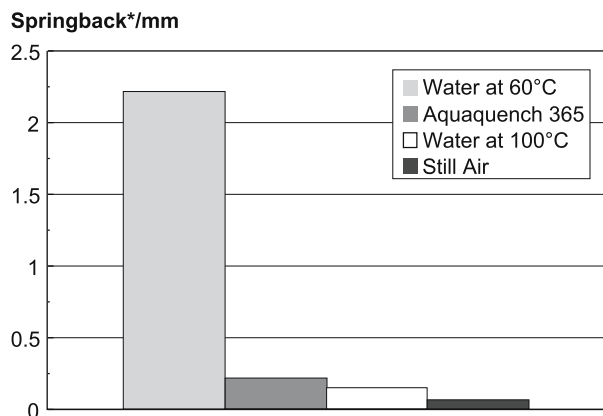


Fig. 6.9. Residual stress in WE43 cast rings after quenching

**Visual inspection** immediately after removing the casting from the mould will obviously identify major defects such as mis-runs and identify areas or defects, which may be recoverable by repair welding. It is customary to clean castings by blasting with an abrasive medium (e.g., iron or steel shot, alumina). Subsurface defects such as dross, blowholes, etc., may be revealed at this stage. It is important to note that use of practically any abrasive medium will impinge cathodic impurity contamination such as Fe, into the surface, which can have a very deleterious effect on corrosion resistance. For this reason, sensitive castings should be acid etched after blasting, sufficiently to remove any contaminated layers. This is normally carried out prior to any subsequent inspection.

**Dye penetrant crack detection** is commonly used for magnesium castings. A range of standard fluorescent dye penetrant and developer systems are available, which are applicable to magnesium alloys. These techniques will further reveal defects such as minute cracks, misruns, “cold shuts”, outcropping porosity or oxide defects.

For many commercial castings, this level of inspection is often adequate. For more critical castings, particularly for aerospace applications, **radiography** is required.

Radiographic density of magnesium is significantly less than that of say Al, so radiographic contrast for many defects or inclusions is enhanced, making this a very sensitive technique.

Sensitivity also varies from alloy to alloy depending on alloy content. In alloys containing Al, only gross oxide defects will be detected due to low contrast. However, for Mg-Zr alloys, even very fine oxide defects may be revealed due to the precipitation of very fine radiographically dense Zr rich particles on the oxide.

Specific radiographic techniques and parameters are usually developed on the basis of experience of individual alloys and castings. Graded radiographic standards have been developed for all typical defects in magnesium alloys by ASTM and are universally applied [5, 6]. Acceptable radiographic ratings will normally

be agreed for specific critical areas or general castings between the foundry and the casting user.

### 6.1.2 Die Casting

*Dieter Brungs, Andreas Mertz*

#### 6.1.2.1 Die Casting Process for Magnesium

High pressure die casting of magnesium is a proven manufacturing process by which products are being produced in volume, from tiny electronic parts to truck transmission cases. High pressure casting is a repetitive process where identical parts are cast at high production rates by injecting molten metal under pressure into a steel die. A die casting die or mould is a closed vessel into which molten metal is injected under high pressure and temperature, then rapidly cooled until the solidified part is sufficiently rigid to permit ejection from the mould. High-pressure die casting, has the unique ability to transform the injected molten magnesium into an accurately dimensioned and smoothly finished form in the shortest possible cycle time. With similarities to the plastic injection moulding process, die casting can make parts to the final shape, often with no additional machining or other operations required. Unlike plastics, however, magnesium die castings can generally be produced to tighter and dimensionally stable specifications.

A designer can plan for the execution of a product form as a net-shape die casting with far greater freedom and flexibility than with any other metal forming process. A die casting foundry is shown in Fig. 6.10.

Generally, two types of pressure die casting processes can be identified, the cold-chamber- and the hot-chamber process:

#### The Cold Chamber Die Casting Process (Fig. 6.11)

In this type of high pressure die casting machine (Fig. 6.12) the molten metal is transferred into the cold chamber cylinder through a port or pouring slot. A hydraulically operated plunger, advancing forward, seals the port forcing metal into the locked die at high pressures. Injection pressures range from 30 to over 100 MPa.

In the cold chamber machine, more molten metal is poured into the chamber than is needed to fill the die cavity. This helps sustain sufficient pressure to pack the cavity solidly with casting alloy. Excess metal is ejected along with the casting and is part of the complete shot.

A modified die casting process is the vacuum die casting process. In vacuum die casting the air in the die cavities is evacuated prior to the injection of the alloy. This process allows the part to “quick fill” by a combination of reduced back pressure and a high injection rate.

Using conventional pressure die casting dies, vacuum pressure of about 350 hPa in the cavity can be achieved. Additional internal die sealing leads to an actual vacuum in the cavity of less than 100 hPa.



Fig. 6.10. Die casting foundry

Vacuum die casting enables thin wall sections in large cavities, deep fins and narrow blind cavities to be filled without laps, swirls or holes.

Squeeze casting is a recently introduced high-pressure casting process which, through the use of very large gates and high hydraulic pressure, can cast liquid metal without turbulence or gas entrapment. The result is a heat-treatable component with thick walls and reduced porosity. Production costs will be higher than conventional high-pressure die casting, but squeeze-cast parts may replace permanent mould and iron castings in high strength applications.

The size of the required high pressure die casting machine is mainly determined by the projected area  $A_{\text{proj}}$  of the casting including runner, biscuit and gating system and the maximum pressure onto the melt  $p_{\text{sol}}$ . The necessary locking force  $F_{\text{lock}}$  can be calculated by Eqs. (6.3) and (6.4) (Fig. 6.13).

$$F_e = A_{\text{proj}} \cdot p_{\text{sol}} \quad (6.3)$$

$$F_{\text{lock}} = 1.1 \dots 1.25 \cdot F_e \quad (6.4)$$

Machine and process characteristics, typical for the cold-chamber die casting process for magnesium are shown in Table 6.8.

### The Hot Chamber Die Casting Process

In the hot chamber machine (Fig. 6.14), the injection mechanism is immersed in molten metal in a furnace attached to the machine. As the plunger is raised, a port opens allowing molten metal to fill the cylinder. As the plunger moves downward

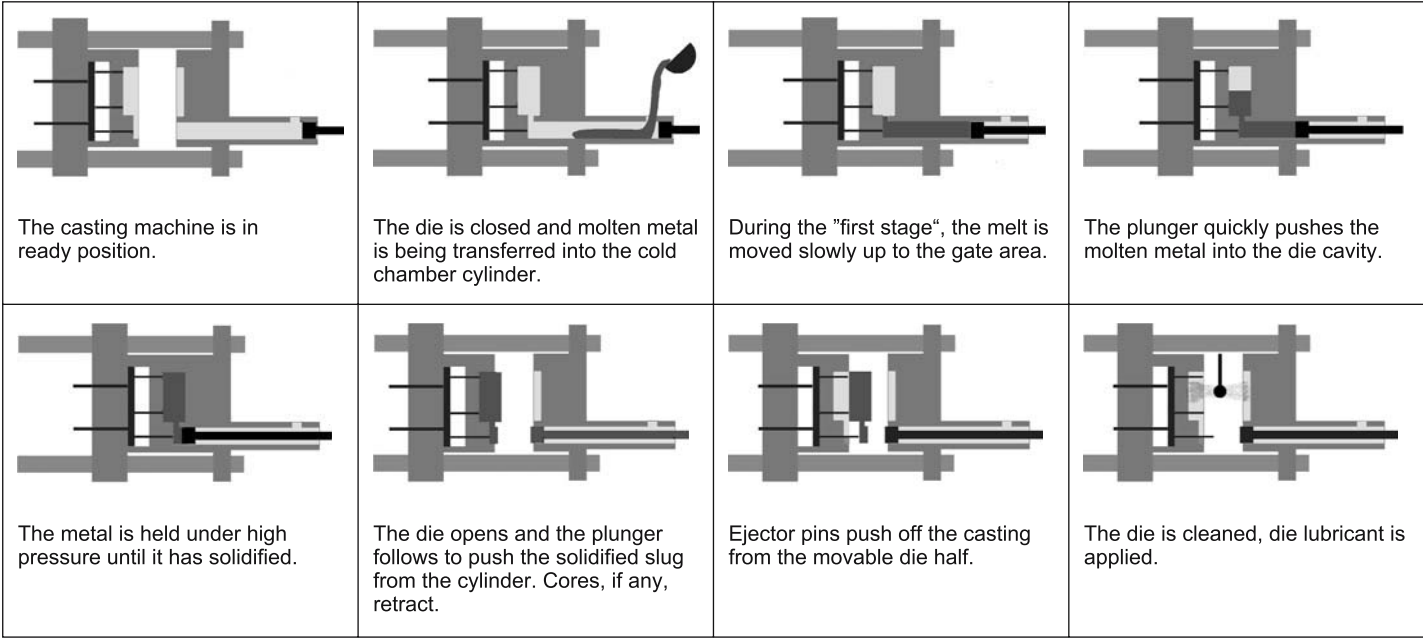


Fig.6.11. Cycle of the cold chamber die casting process

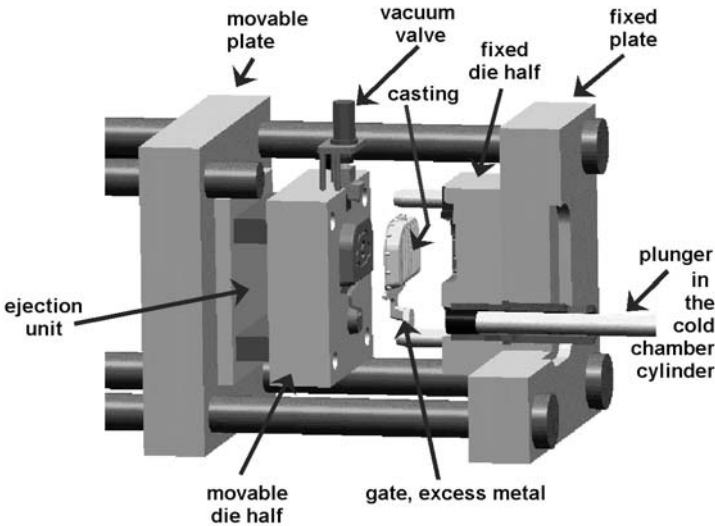


Fig. 6.12. Cold chamber high pressure die casting machine

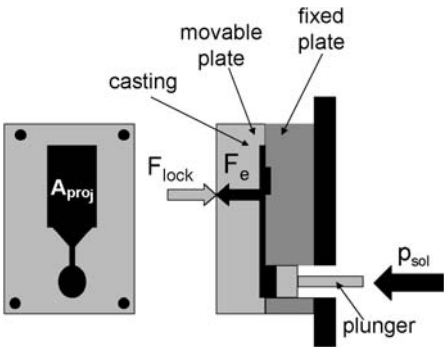


Fig. 6.13. Calculation of the necessary locking force of the pressure die casting machine

Table 6.8. Characteristics of the cold chamber die casting process

Holding furnace	Separated from pressure die casting machine
Locking force	1 MN–45 MN
Plate dimensions	max. 1750 · 1750 mm <sup>2</sup>
Projected area of the entire magnesium casting	max. 1.0 m <sup>2</sup>
Pressure during solidification	max. 120 MPa
Casting weight	50 g – 40 kg
Wall thickness	1.5 – 30 mm
Alloys	all Mg-alloys



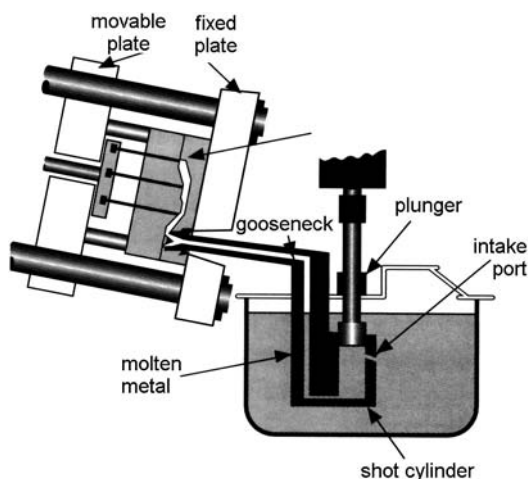


Fig. 6.14. Hot chamber die casting machine

sealing the port, it forces molten metal through the gooseneck and nozzle into the die. After the metal has solidified, the plunger is withdrawn, the die opens, and the resulting casting is ejected.

A typical cycle of the hot chamber process is shown in Fig. 6.15.

Hot chamber machines are rapid in operation. Cycle times vary from less than one second for small components weighing less than 10 g to 30 s for a casting of more than 1 kg. Dies are filled quickly (normally between 5 and 50 ms) and metal is injected at pressures from 15 to over 40 MPa. Nevertheless, modern technology permits fine control of these values, thus producing castings with fine detail, close tolerances and high strength.

Operation of a “hot chamber” machine is faster than a “cold chamber” machine because of lacking the dosing operation and the decreased solidification time of the runner system. Particularly, this is true for small die casting machines with locking force up to 5,000 kN. Cycle time varies with the maximum wall thickness of the casting. In contrast to the cold chamber process, the alloy range of hot chamber machines is limited to alloys with low melting temperatures. The most common alloy for the hot chamber process is the AZ91D. Cold chamber die casting machines have to be used for high melting point magnesium alloys because plunger and cylinder assemblies are less subject to attack since they are not submerged in molten metal.

Usually, pressure die casting machines are powered by hydraulic systems. However, especially for small hot-chamber die casting machines, electrically driven machines are available [7].

The casting industry generally has applied the word “miniature” to magnesium die castings that are produced at high volume and low cost using specialised hot chamber die casting machines (called 4-slide and 5-slide machines) that yield flash-free castings. They are cast with zero draft and to very close tolerances, and require no trimming. While very small die castings can be produced on larger, conventional die casting machines using multiple-cavity dies, 4- and 5-slide

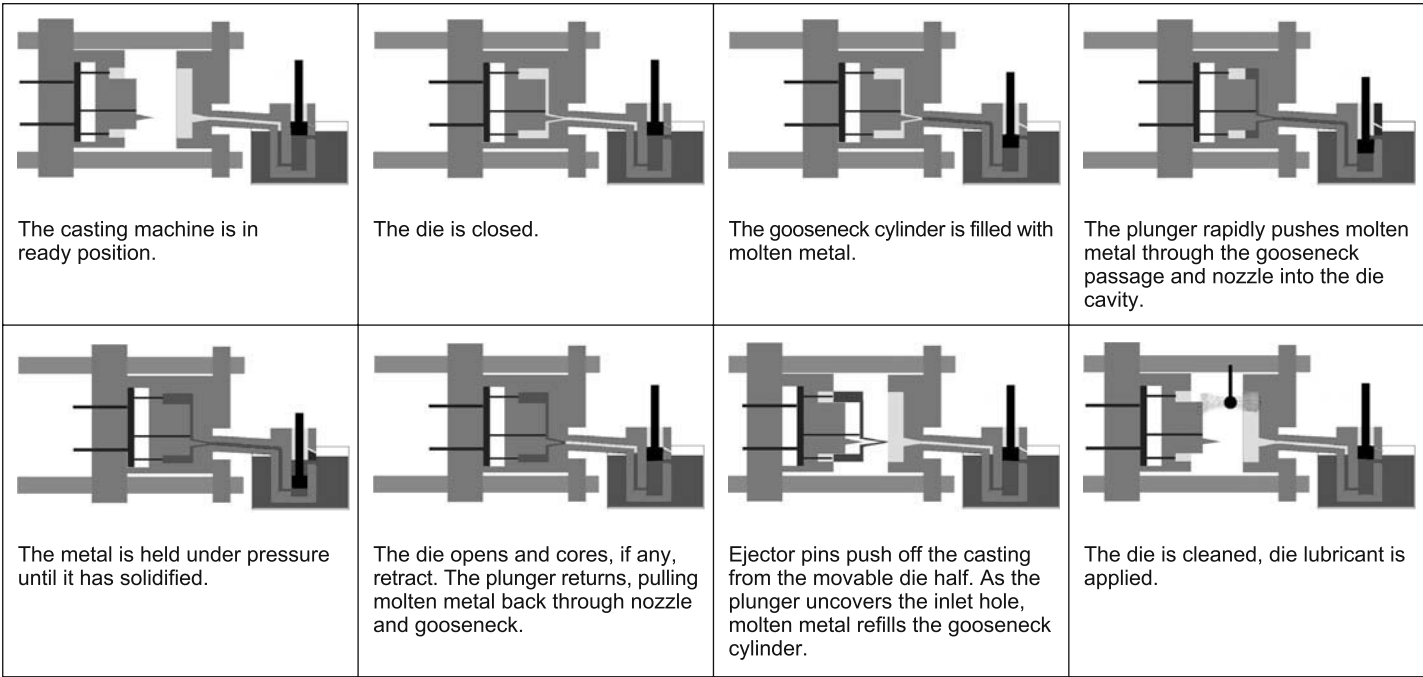


Fig. 6.15. Cycle of the hot chamber die casting process

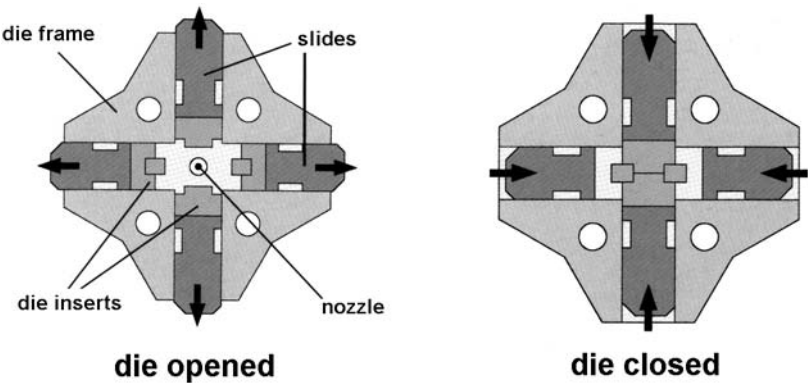


Fig. 6.16. The 4-slide process [8]

equipment may be the optimum method for casting flash-free, micro-miniature parts (Fig. 6.16).

Machine and process characteristics typical for the hot-chamber die casting process for magnesium are shown in Table 6.9.

Special Considerations for Magnesium Die Castings Compared with other Products/Processes

**Magnesium Sand Castings**

Compared with sand castings, die castings require little or no machining to meet specifications, can be made with thinner walls, can have all or nearly all holes cored to size, can be held within much closer dimensional limits, and are produced more rapidly in dies which can make many thousands of castings without replacement, rather than requiring new cores for each casting. Die castings have smoother surfaces and involve much less labour cost per casting. Sand castings, on the other hand, can be made from alloys not suitable for die casting which provide higher strength and wear resistance. Certain shapes not producible by die casting are available in sand castings. The maximum size can be greater, the tool cost is usually less and small quantities can be produced more economically.

**Table 6.9.** Characteristics of the hot chamber die casting process

Holding furnace	Integrated in pressure die casting machine, shot sleeve is submerged in liquid alloy
locking force	0.2 MN–8 MN
plate dimensions	max. 1400 × 1400 mm <sup>2</sup>
projected area	max. 0.4 m <sup>2</sup>
pressure during solidification	max. 25 MPa
casting weight	< 10 g–7 kg
wall thickness	0.8–10 mm
alloys	AZ91, AM50, AM60

The key to determining the lowest economic production quantity level for a conversion from sand casting to die casting, or from any other lower volume production process, depends largely on the configuration, size and complexity of the part. While the die casting process is most economic at higher volumes, die casting can achieve comparative savings at quantities at or below 2,000 pieces if extensive secondary machining or surface finishing can be eliminated.

### **Magnesium Permanent Mould Castings**

Compared with permanent mould castings, die castings can be made to closer dimensional limits and with thinner sections; holes can be cored. They are produced at higher rates with less manual labour; have smoother surfaces and usually cost less per casting. Permanent mould casting involves somewhat lower tooling costs and can be made with sand cores yielding shapes not available in die casting.

### **Magnesium Drawn Sheet Products**

Compared with stampings, one die casting can often replace several parts. Die castings frequently require fewer assembly operations, can be held within closer dimensional limits, can have almost any desired variation in section thickness, involve less waste in scrap; are producible in more complex shapes and can be made in shapes not producible in stamped forms. Stampings, on the other hand, have properties of wrought metals, can be made in alloys not suitable for die casting, are produced more rapidly in their simpler forms and may weigh less than die castings.

Stamping from sheet magnesium offers economy that is difficult to match when a component can be made from one relatively simple stamping. Magnesium stamping dies that perform a single operation are less costly than die casting dies. In contrary to stamping of aluminium or steel sheet, magnesium sheet and deep drawing tools have to be pre-heated. The relative costs for tooling and processing depend on the number and types of dies and presses needed. When a highly complex stamping or several stampings are required, die casting can be a cost-effective alternative. In the case of multiple stampings, costs of fixtures and welding adds to the costs of fabrication, can make die casting very competitive. Material costs for stamping may be substantially higher than indicated by published per kg costs due to high scrap rates. Stampings invariably consume more material than is contained in the end product, sometimes substantially more.

### **Aluminum-Die Casting**

It is true that the raw material cost of magnesium is higher than that of aluminium, however there are other factors that need to be considered when pricing a total program.

Magnesium die casts 25–50% faster than aluminium; decreased cycle time produces more parts per hour.

Magnesium's lack of affinity for tool steel allows the die-cast tools to last roughly two times longer than for aluminum. This greatly reduces the amount of money for replacement inserts and decreases piece price when amortised into the life of the program.

Magnesium is easily castable and able to hold tighter tolerances than aluminium. This may eliminate the need for additional machining steps. The fluidity of molten magnesium aids in the castability of complex and fine detailed components. The relatively low heat content results in reduced thermal distortion. This, coupled with its lower density, enable close tolerances to be held and allows designers to incorporate more features.

Magnesium’s superior machinability allows the use of high speeds and heavy feeds, which result in fewer machines, less capital investment, less floor space, and less labour overhead requirements than aluminum. Low cutting pressures, high thermal conductivity, and rapid heat dissipation provide four to five times greater tool life and less “downtime” than aluminum (Table 6.10).

Heat checking and washout of the cavity steel are two problems which have plagued die casters for years. It is not uncommon to see signs of washout and heat checking after as few as 10,000 shots on a die running aluminum. Once started, tool steel in the cavities slowly deteriorates leading to die or cavity replacement after 80,000–150,000 shots. Occasionally, this happens after even fewer shots.

Magnesium does not have the affinity for tool steel that aluminum has, so it will not attack the cavity steel like aluminum does. Die casters running magnesium report tool life four to five times greater than that normally experienced with aluminum. There are many magnesium production tools still in daily operation that have more than 500,000 shots on them. Many of these tools produce thin-wall castings that must have a high-quality surface appearance.

**Plastics Injection Mouldings**

Compared with plastic injection mouldings, magnesium die castings are stronger, stiffer, more stable dimensionally, more heat resistant, and are far superior to plastics on a properties/cost basis. They help prevent radio frequency and electromagnetic emissions. For chrome plating, magnesium die castings are much superior to plastic. Die castings have a high degree of permanence under load when compared to plastics, are completely resistant to ultra-violet rays, weathering, and stress-cracking in the presence of various reagents. Manufacturing cycles for producing die castings are much faster than for plastic injection mouldings.

Castings offer built-in shielding of electromagnetic interference (EMI) and radio frequency interference (RFI), which is often a difficult and costly secondary operation with plastic housings. However, plastics cost less on a unit volume basis. They have colour-inherent properties which tend to eliminate finishing, are temperature sensitive, and have a high degree of electrical resistance. While plastic mouldings offer integral colour properties, the die casting process may be se-

**Table 6.10.** Die cast tools for Magnesium vs. Aluminum

	Magnesium	Aluminum
Productivity [shots/h]	75–400	40–200
Average tool life [shots]	100,000–300,000	50,000–150,000

lected based on rigidity, impact strength, heat resistance, dimensional stability, and built-in EMI/RFI shielding characteristics.

### Design of Casting Die

#### **Fixed and Movable Die**

Die casting dies are made of tool steels in at least two sections called fixed die half and movable die half. The fixed die half is mounted on the side toward the molten metal injection system. The movable die half, to which the die casting adheres, and from which it is ejected when the die is opened, is mounted on the moveable platen of the machine.

The movable half usually contains the runners and gates which route molten metal to the cavity (or cavities) of the die. The movable half is also connected to an ejector box which houses the mechanism for ejecting the casting from the die. Ejection occurs when pins connected to the ejector plate move forward to force the casting from the cavity. This usually occurs as part of the opening stroke of the machine. Placement of ejector pins must be carefully arranged so that force on the casting during ejection will not cause deformation.

Location of the die casting parting line, affects part aesthetics, integrity, mechanical properties, dimensions and the simplicity with which the casting can be trimmed. For cosmetic surfaces, the small ridges of flash remaining where the two die halves join must be removed or the parting line relocated. An inappropriate parting line location can also result in more complicated and costly trimming operations.

Fixed and moveable cores are often used in dies. If fixed, the core axis must be parallel to the direction of die opening. If moveable, they are often attached to core slides. Should the side of a die casting design require a depression, the die can be made with one or more slides to obtain the desired result without affecting ejection of the casting from the die cavity.

#### **Die Materials, Coatings**

The parts of the die, which form the cavity are exposed to direct contact with the molten metal. Therefore, die inserts have to be made of steels that are resistant to thermal shock, e.g., X37CrMoV5 1.

After machining, die cavity parts are hardened and annealed to a hardness of about 46-48 HRC.

Components of the pressure die casting die, that are not directly in contact with the liquid alloy are usually made of medium carbon steel.

The lifetime of a magnesium die casting die is of the order of 100,000 to 300,000 shots, depending on casting geometry and surface requirements. That is about twice the lifetime of dies for aluminium die casting. Lifetime of areas of the die surface, that are exposed to wear by the high-speed melt flow, can be protected by special heat treatments or by applying thin hard PVD/CVD coatings.

#### **Gating System**

Position and shape of the gating system strongly influence the filling behaviour of the cavity. To obtain good surface and mechanical properties flow distance of the melt after the gate has to be kept reasonably short. Figure 6.17 shows an ex-

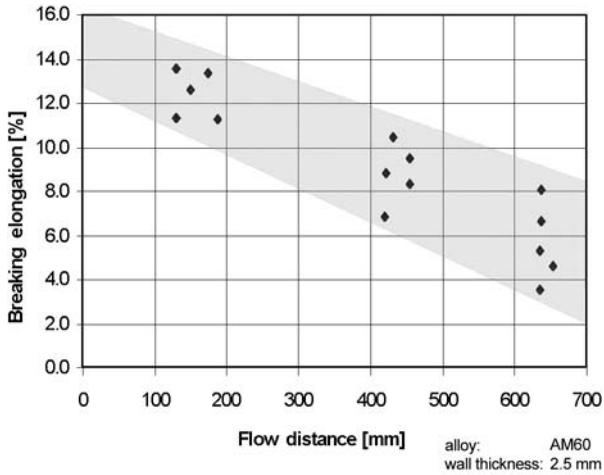


Fig. 6.17. Elongation to fracture with respect to the flow distance of the melt

ample for the dependence of the elongation to fracture from the flow distance in the cavity. An increased flow distance implies reduced elongation values together with increased. That means, especially when dealing with thin walled structural castings, the minimum recommended wall thickness (Fig. 6.18) should be observed.

When designing runner and gating system, different requirements have to be met. On the one hand, a proper feeding of the solidifying casting has to be assured. This leads to runner and gating systems, that usually have comparably big cross sectional areas, that solidify after the casting itself.

On the other hand, economical considerations lead to very thin runner and gating systems to allow easy removal of runner and gate and to minimize cycle material and cycle time. Depending on shape and quality requirements of the casting, an appropriate middle course has to be followed.

### Heating/Cooling

The die casting process is cyclic. For a reliable operation it is important, that the die reaches a virtually-static temperature distribution, which is repeated for each shot.

Compared with typical aluminum – silicon alloys, magnesium alloys have a low heat content. Though this fact may improve productivity by shortening the solidification time, on the other hand, low heat content of the melt usually leads to a much more sensitive heat balance of the die. The recommended cavity surface temperature, just before the shot, is of the order of 220–300°C. When producing thin walled castings, often heat dissipation by radiation, convection, conduction and vaporising release agent is more than the heat energy supplied by the liquid alloy. In this case, external heating of the die becomes most important.

External heating commonly is performed by oil based heating/cooling units. Cooling lines located in both die halves and are passed by a pre-heated or pre-

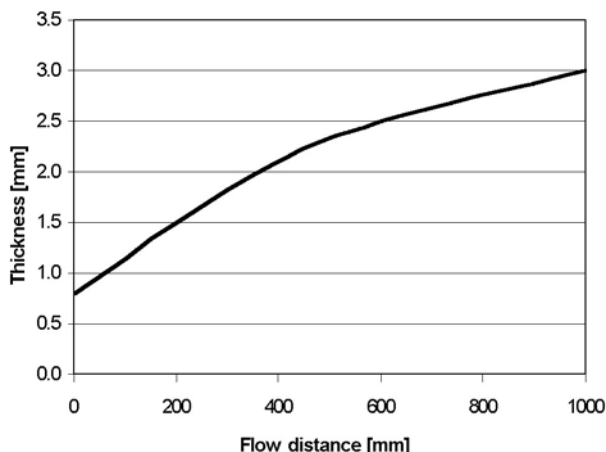


Fig. 6.18. Minimum recommended wall thickness for alloy AM50/60

cooled coolant. Such devices can be used for heating as well as cooling purposes. However, maximum coolant temperature is restricted to 240°C or in particular cases up to 300°C.

Alternatively electrically powered cartridges become more and more common, particularly in thin-walled magnesium die casting.

### Die Casting Techniques

#### **Melting/Metering**

In magnesium high pressure die casting, melting and holding are fluxless processes.

To avoid segregation in the melt, caused by temperature drops due to charging with magnesium pigs, usually melting and holding of the magnesium melt takes place in different furnaces or at least different chambers of a furnace. When transporting the melt from the melting into the holding furnace, air contact should be avoided.

Besides transferring molten metal by robots, closed holding/metering devices operated by gas pressure or metal pumps become more and more popular (Fig. 6.19). Another advanced concept for dosing magnesium alloy into the shot sleeve is the VACURAL-process (Fig. 6.20), where the melt is sucked into the shot sleeve by the vacuum applied to the cavity.

#### **Melt Protection**

If unprotected, magnesium melt exothermally reacts with the oxygen of the surrounding air. These reactions may become violent to uncontrollable. The eutectic phase  $Mg_{17}Al_{12}$  starts to oxidise at temperatures around 430°C. Thus, shielding of magnesium alloys containing aluminum may become necessary at temperatures above 400°C. Liquid magnesium alloys typical for the high pressure die casting process can be protected effectively by shielding gas mixtures listed in Table 6.11 [9].



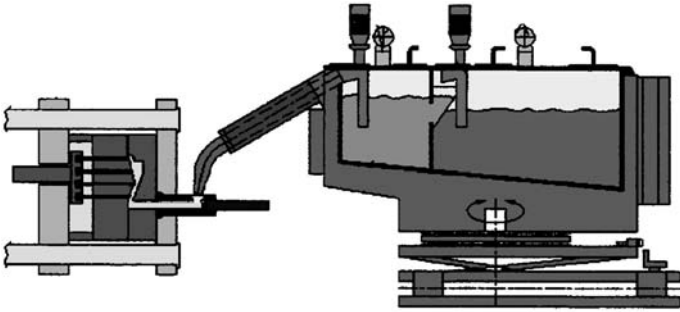


Fig. 6.19. Dosing furnace

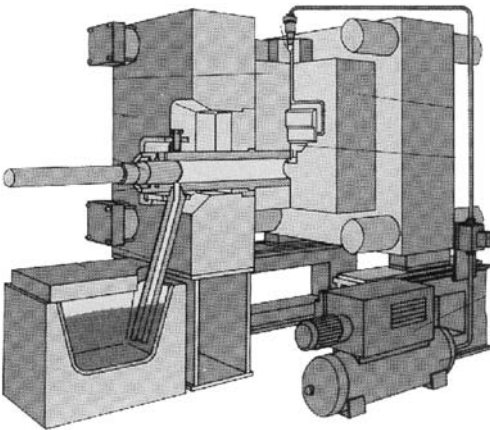


Fig. 6.20. VACURAL-process

Table 6.11. Shielding of magnesium melt

Melt temperature [°C]	Recommended shielding gas [vol%]	Working conditions		Melt protection
		Melt circulation	Salt impurities	
650–705	air + 0.04% SF <sub>6</sub>	no	no	excellent
650–705	air + 0.2% SF <sub>6</sub>	yes	no	excellent
650–705	75% air + 25% CO <sub>2</sub> + 0.2% SF <sub>6</sub>	yes	yes	excellent
705–760	50% air + 50% CO <sub>2</sub> + 0.3% SF <sub>6</sub>	yes	no	excellent

Alternatively,  $\text{SO}_2$ - $\text{CO}_2$ - $\text{N}_2$  mixtures may be used as shielding gas. In contrast to the sand casting process, in magnesium high pressure die casting, melt temperatures in the holding furnace can usually be kept below  $700^\circ\text{C}$ . At this temperatures level  $\text{SF}_6$  and  $\text{SO}_2$  additions may be replaced by environmentally friendly shielding gases like, e.g., Argon- $\text{CO}_2$ - $\text{N}_2$  mixtures with varying volume shares.

Furthermore, new alloys containing traces of beryllium, that are under development, can be handled without any protection atmosphere at all.

### **Casting Procedure**

The magnesium cold chamber high pressure die casting process is quite similar to that for aluminum alloys. To reduce heat loss, after dosing the melt into the shot sleeve, the slow plunger movement to transport the melt to the gate, is slightly accelerated, compared with aluminum die casting. During this stage of the process, the cavity may be evacuated to a remaining air pressure of 80–250 hPa. Particularly at the high melt velocities that are necessary for thin walled magnesium die castings, the flow resistance of the melt can be decreased significantly by removing the air from the cavity prior to the filling process. In this way, vacuum pressure die casting not only decreases the probability of air inclusions in the casting, but also expands the possible length/thickness ratio of the casting.

A key factor of the magnesium die casting process is the fill time of the cavity. Depending on wall thickness, alloy, flow distance and die temperature, typical fill times are of the order of 10–100 ms.

The in-gate velocity of the melt is about 30–50 m/s. For thin walled castings, in-gate velocity sometimes reaches 100 m/s. However, die wear increases significantly with metal velocity exceeding 70 m/s.

Especially for thin walled products, short fill time and high die temperatures usually improve strength and ductility of the casting (Figs. 6.21 and 6.22).

During the solidification process of the melt, a pressure between 40 and 100 MPa is applied onto the melt. This pressure allows the compression of possible gas inclusions and also supports the feeding process of the solidification shrinkage of the alloy. Particularly, when producing castings with wall thickness of more than 5 mm, usually, mechanical properties of the casting become better with increased solidification pressure.

To avoid sticking of the magnesium alloy to the die surface, die lubricants are applied. These lubricants usually are water-based and are used with dilution ratios of 1 : 10 to 1 : 100. Due to the comparably low heat content of magnesium alloys, usually there is no need to use the lubricant as cooling medium. Especially, when thin walled castings are produced, water based lubricants should be used very thriftily to avoid heat loss by vaporising water. New developments in lubricant application technology abandon water by depositing lubricant on the cavity surface as solid powder or by sublimating vapour.

#### **6.1.2.2 Design Guidelines for Magnesium Die Castings**

While product designers often call for an exact conversion of an existing non-die cast part to a die casting for reasons of package size and mating parts, dramatic

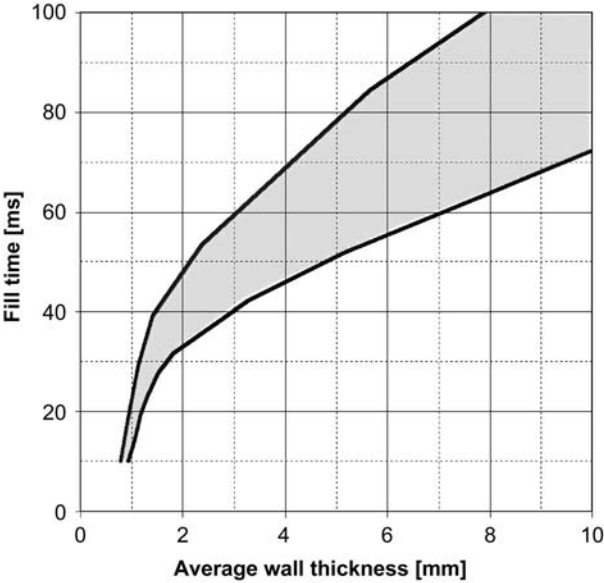


Fig. 6.21. Recommended fill time of the cavity

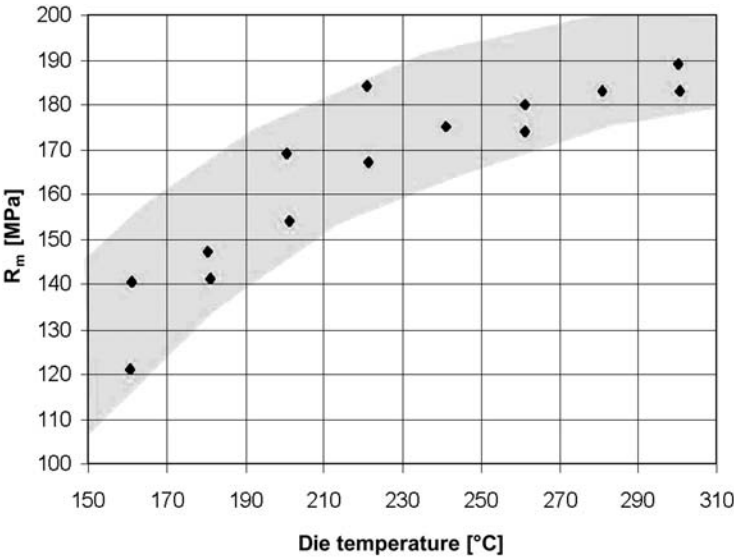


Fig. 6.22. Influence of die temperature to the ultimate tensile strength

savings can often be made if the part and its mating components are redesigned as one single die casting. Costly assembly and secondary operations can often be eliminated, with greater product integrity over assembled components.

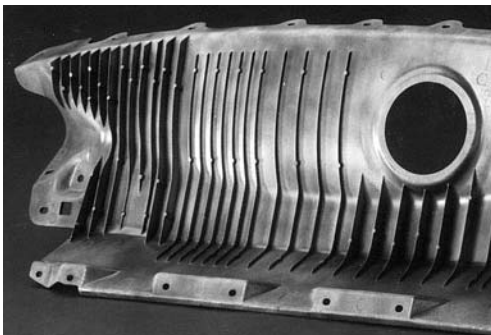
The part design itself must be configured so that die casting production will be capable of maintaining the proper metal flow to assure surface quality. The quality of the surface preparation of the die casting die will also be a key factor in the surface quality of the casting produced. Extra time and costs will be involved in the required die preparation, and the dies will require added surface maintenance during their expected life. The results are part surface finishes that cannot be duplicated by any other high-volume production process. Attention must also be given to the proper placement of the parting line, in-gates, overflow gates, and the ejector pins, so that the important cosmetic surfaces are not affected.

Following basic design guidelines should give a first help in designing magnesium cast structures [10]:

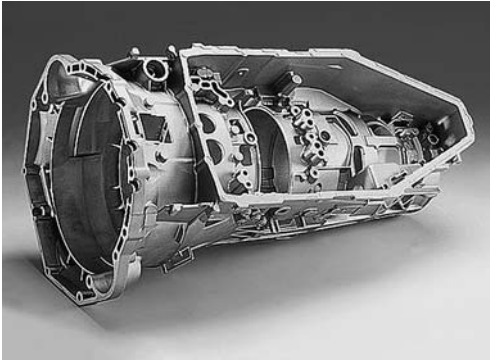
1. Specify thin sections which can easily be die cast and still provide adequate strength and stiffness. Use ribs wherever possible to attain maximum strength at minimum weight.

Typical wall thickness for a die cast design range from 1–5 mm, depending on alloy, part configuration, part size and application. In specific instances for smaller die castings, wall sections as thin as 0.50 mm can be cast (Fig. 6.23).

2. Keep sections as uniform as possible. Where sections must be varied, make transitions gradual to avoid stress concentration.
3. Keep shapes simple and avoid nonessential projections.
4. A slight crown is more desirable than a large flat surface, especially on plated or highly finished parts. Textures, from delicate stipples to deep grain patterns photoengraved into the die surface, can be cast into the surface of a part during die casting production, with no further texture treatment other than final painting, if required. In addition to providing a unique decorative surface, many of these textures enable parts to maintain their appearance during rough handling in use as well as providing a better grip for hand-held products. However, these advantages will entail added maintenance of the die surface at the end of the die's normal life, to reproduce the textured die surface.

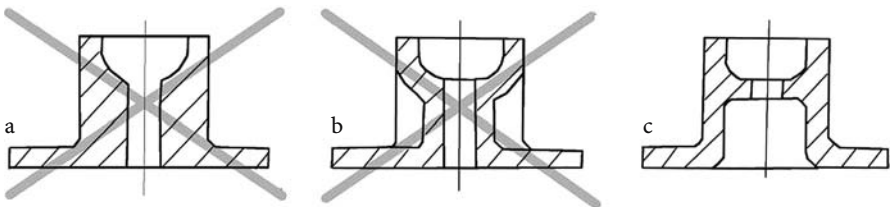


**Fig. 6.23.** Rib design of a structural casting (with kind permission of Honsel, Meschede)



**Fig. 6.24.** Transmission housing with cast bores (with kind permission of Honsel, Meschede)

5. Specify coring for holes or recesses where savings in metal and overall costs outweigh tooling costs (Fig. 6.24).
6. Design cores for easy withdrawal to avoid complicated die construction and operation. For lowest cost die cast production, undercuts should be avoided in a part design. To produce a die cast part with an undercut, as cast, requires the construction of special die members, such as retractable core slides. The increased tooling cost and increased cycle time would be offset by savings on secondary machining costs. Intricate features and the most complex shapes are common to die castings, with the basic limitation being that a part feature must not prevent removal of the casting when the die halves are parted. With the use of a variety of core slides, special features are cast in place, with the slides retracting to permit ejection. Such moving die parts may require the use of a larger machine and often rule out the use of a multiple-cavity die (Fig. 6.25).
7. Avoid small cores. Usually, cored hole diameter should be more than 2 mm. Small cores can be easily bent or broken necessitating frequent replacement. Drilling or piercing small holes in die castings is often cheaper than the cost of maintaining small cores.
8. Provide sufficient draft on side walls and cores to permit easy removal of the die casting from the die without distortion. Draft angles of more than two de-



**Fig. 6.25.** Avoiding heavy sections and retractable core slides. **a** Undesirable design because the heavy mass of metal. **b** Undesirable design because ejection is only possible with retractable core slides. **c** Ejection is possible without core slides, heavy sections are avoided

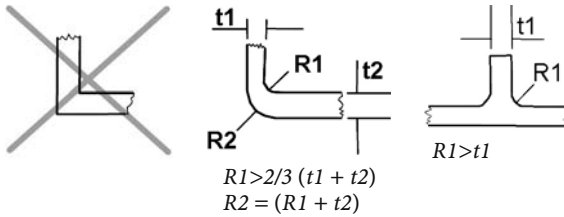


Fig. 6.26. Appropriate corner design

grees are generally recommended. In special cases draft angles can be reduced locally even to zero.

9. Provide fillets at all inside corners and if possible, avoid sharp outside corners. Radii should be generous, at least equal to the minimum wall thickness (Fig. 6.26).
10. Die casting design must provide for location of ejector pins. Ejector pins are used to push the casting out of the die after the casting has solidified. Each ejector pin will leave a slight impression on the cast surface. Take into consideration the effect of resultant ejector marks on appearance and function. The location of ejector pins is largely determined by the location and magnitude of metal shrinkage on die parts as metal cools in the die. To avoid fatigue cracking of the die steel, the minimum distance between the centre line of the ejector pin and the casting wall is 0.75 times the pin diameter (Fig. 6.27).
11. Cast-in inserts should be designed to be held firmly in place with proper anchorage provided to retain them in the die casting. Cast-in-place inserts used with magnesium die castings are commonly zinc coated, as well as some non-metals, are sometimes used. There are shape, galvanic and stress considerations to be addressed with the use of inserts.

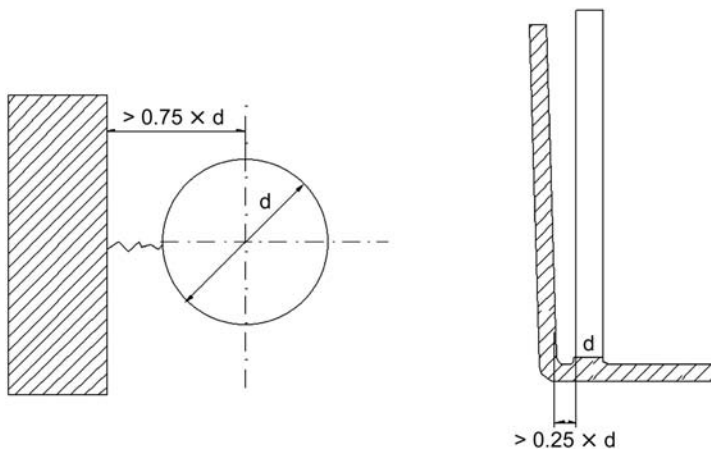


Fig. 6.27. Minimum distance between ejector pin and casting

12. Design parts to minimise flash removal costs.
13. Never specify dimensional tolerances closer than essential. This increases costs (see also Sect. 6.1.2.3).
14. Design die castings to minimise machining.
15. Where machining is specified, allow sufficient metal (nominal size + tolerance + 0.2 mm) for required cuts and consider the draft angles.

### 6.1.2.3 Properties of Magnesium Die Castings

Some typical advantages of magnesium die castings are:

- thin walls
- high dimensional accuracy
- design close to final shape
- long die life span and short casting cycles in production

Other qualities of magnesium die-cast materials are excellent machinability, good damping and good shielding characteristics. The high purity of magnesium die-casting alloys result in improved corrosion behaviour. The corrosion properties of the alloy AZ91D for example are comparable with those of the most common aluminium die-casting alloy AlSi8Cu3.

#### Alloy Characteristics and Typical Uses

##### **AZ91D**

##### **MgAl9Zn1**

The most widely used magnesium die-casting alloy with high strength properties for standard components in automotive and computer construction, household and sports equipment and many other applications. Excellent pouring characteristics with very good flow and die-filling abilities.

##### **AM60B**

##### **MgAl6Mn**

##### **AM50A**

##### **MgAl5Mn**

##### **AM20**

##### **MgAl2Mn**

Materials with enhanced elongation and energy absorption, high strength and good pouring qualities. Among the typical uses of the alloys AM60 and AM50 are large thin-walled automotive parts with higher elongation and deformation requirements. The lower aluminium content of AM20 compared with AM50 and AM60 results in increased elongation and impact strength with reduced yield and tensile strength as well as substantially reduced flow and die-filling abilities.

##### **AS21**

##### **MgAl2Si1**

##### **AS41B**

##### **MgAl4Si1**

Alloys with good creep properties up to 150°C. A reduced aluminum content in AS21 compared with AS41B results in increasing creep strength and higher elongation, but also in a decrease of tensile strength and castability.

##### **AE42**

##### **MgAl4RE2**

Alloy with good creep properties up to 150°C, similar to AS21 with the tendency to adhere to the die-casting tool and considerably higher metal cost.

### Mechanical Characteristics

Typical mechanical characteristics of die-casting alloys are listed in Table 6.12. The figures stated refer to room temperature. The average values for test bars (cast in a 400-ton cold-chamber machine with a 6-cavity die) are given in brackets [11].

The mechanical characteristics of a casting depend substantially on the manufacturing process, pouring and solidification conditions in the die, and the composition of the alloy.

A comparison between magnesium die-casting alloys and the most commonly used aluminum die casting alloys shows Fig. 6.28.

AZ91D shows a lower 0.2 limit in comparison to AlSi<sub>9</sub>Cu<sub>3</sub>, but an equally high tensile strength with similarly low elongation at rupture. The figures apply in the cast state.

As a non heat-treatable alloy in the as-cast state, AM60B has an elongation at rupture and an impact strength which are roughly equal to that of AlSi<sub>10</sub>Mg in the artificially aged state. The 0.2 yield and tensile strength are on the same level.

For applications in the automotive sector involving high demands on elongation at rupture, fracture toughness and energy absorption, magnesium alloys of the AM group are preferred. As the aluminum content decreases, the elongation at rupture increases while 0.2-limit and tensile-strength values decrease, in particular with reduced flow and die-filling abilities (Fig. 6.29).

The extent to which the high elongation values at reduced aluminum content can be utilised depends on dimensions and design of the casting, the gating system, the casting conditions and especially the die-filling time. The relation between the Al content of the alloy, its castability and the ductility achieved are shown in Fig. 6.30.

Best creep strength is achieved by the magnesium alloys AS21 and AE42, and to a lesser extent, the alloy AS41B. For applications requiring high creep strength,

**Table 6.12.** Mechanical properties of die cast components

Property	Unit	AZ91	AM60	AM50	AM20	AS41	AS21	AE42
Ultimate tensile strength	MPa	240 (250)	225 (240)	210 (230)	190 (210)	215 (240)	175 (220)	230 (230)
Tensile yield strength	MPa	160 (160)	130 (130)	1250 (125)	90 (90)	140 (140)	110 (120)	145 (145)
Compressive yield strength	MPa	160	130	125	90	140	110	145
Fracture elongation	%	3 (7)	8 (13)	10 (15)	12 (20)	6 (15)	9 (13)	10 (11)
Impact strength charpy un-notched test bars	J	6 (9)	17 (18)	18 (18)	18 (18)	4 (16)	5 (12)	5 (12)



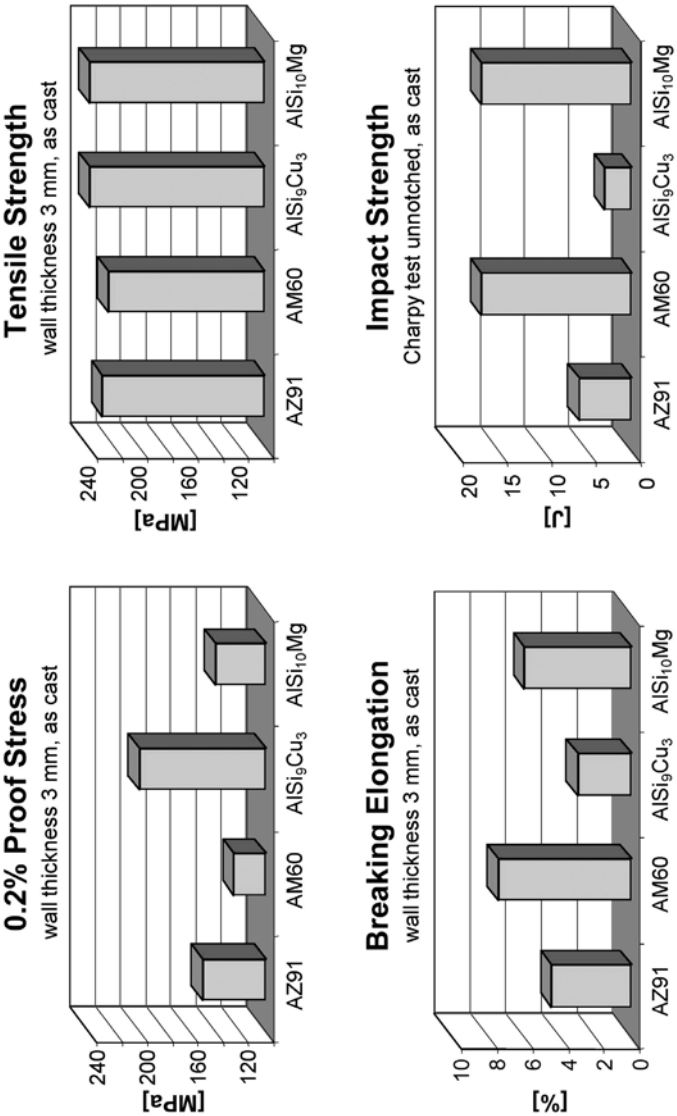


Fig. 6.28. Mechanical properties of common aluminum and magnesium die casting alloys [12]

the task of finding the optimum combination of alloy composition, castability and achievable creep strength is similar to that described above for applications with increased ductility requirements. Although AZ91D has a relatively low creep strength, die castings of AZ91 are used successfully in elevated-temperature automotive applications, e.g., for cylinder-head covers and in manual transmissions [13]. In view of the especially good castability of the alloy AZ91D, it is worth checking whether the demands made on the casting could also be met using AZ91D, before deciding in favour of other alloys with poorer castability (Fig. 6.31).

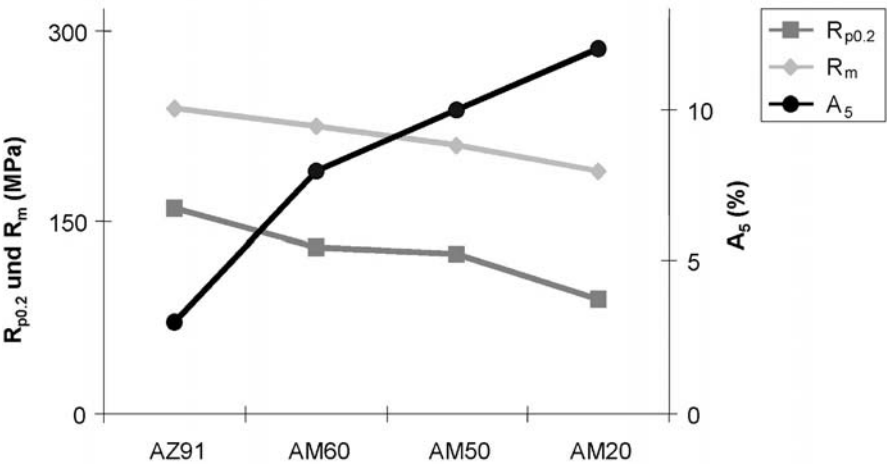


Fig. 6.29. Tensile properties of different Mg-alloys

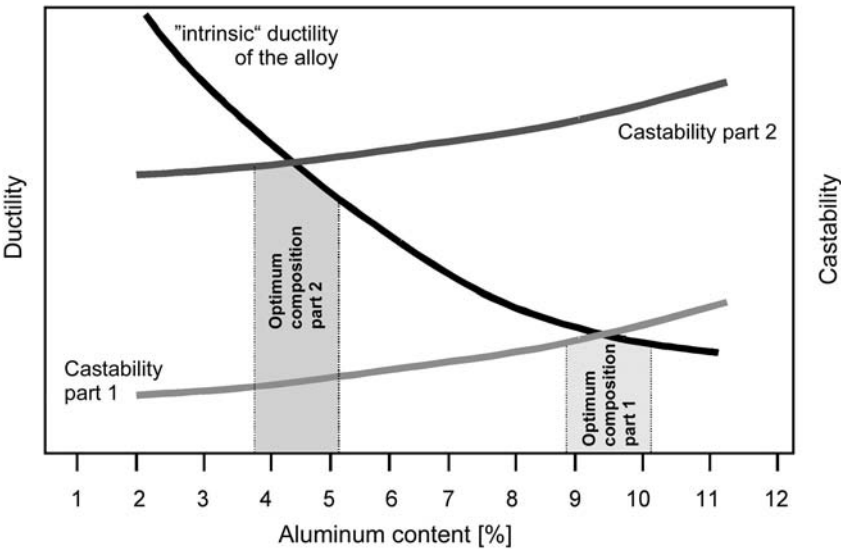


Fig. 6.30. Optimum alloy composition versus castability of the part

New economically priced alloys addressing better creep strength are under development and will be available for die casting soon.

**Dimensional Properties**

Die casting is a precision casting process. Casting tolerances not only depend on the accuracy of the die construction, but also on fluctuations of die temperature, ejection temperature and quenching rate of the casting. The tolerances that can

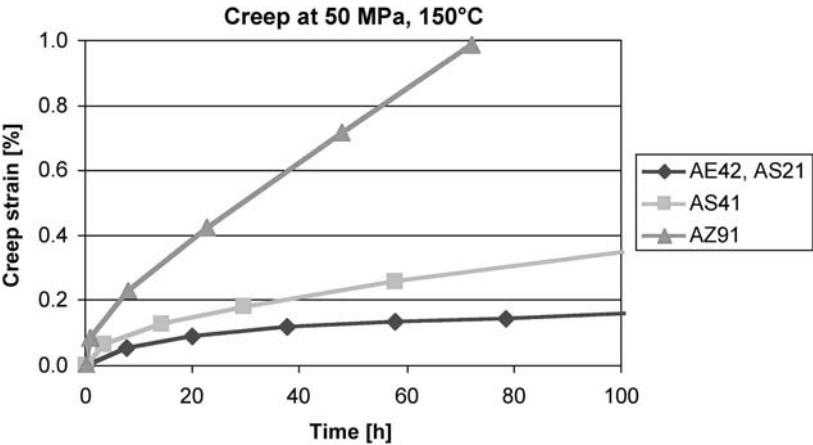


Fig. 6.31. Creep resistance of different die casting alloys

be specified on pressure die castings vary with the precise configuration of the part and whether a dimension is contained entirely in one half of the die, or falls across a parting line or is formed by a moving die component. Casting accuracy will also depend on the die casting machine being used and its control systems. Recommended tolerances for linear dimensions of magnesium pressure die castings between features formed in the same die part are plotted in Fig. 6.32.

Of course, smaller tolerances can be achieved by refinishing the die after casting and measuring first samples. Then, tolerances of e.g. less than  $\pm 0.014$  mm for a 3 mm nominal size or  $\pm 0.04$  mm for a 100 mm nominal size can be realized. When casting do not require additional machining, the draft angle of about  $0,5^\circ$  has to be considered [14]. Tolerances of dimensions, that fall across a part-

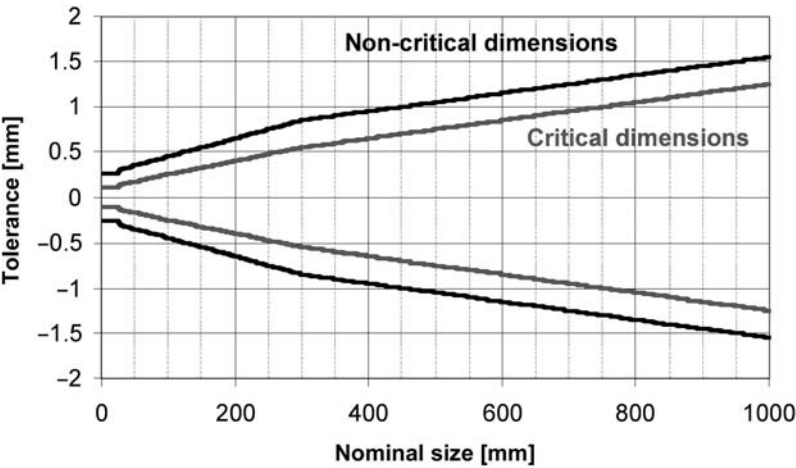


Fig. 6.32. Recommended tolerances for magnesium high pressure die casting [12]

ing line or are formed by moving die components, have to be increased by about 0.1 to 0.2 mm.

### **Surface Properties**

Magnesium die castings produced by the vacuum die casting process can be powder coated and wet painted without the characteristic surface disruption described as 'cissing'. These imperfections look like mini volcanic craters. They are caused by trapped gases and/or bound hydrogen that seep from pores within the casting and blow bubbles in the soft paint layer. In any case, the pre-treatment process has to be adapted to the applied release agent.

Particularly, when painting big sized structural castings sink marks, that usually are present on the opposite side of internal rib structures will lead to rejects. Even if not visible on the raw casting, also small sink marks with a depth of less than 0.01 mm become visible after the casting has been gloss painted. This effect can be avoided by using a textured coating or if gloss painting is necessary by interposing an additional grinding process. By lowering the ratio of rib thickness/wall thickness of the casting, the sink mark effect is less pronounced.

### **Soundness**

Vacuum-die casting, now being widely used in die casting plants, can greatly reduce gas entrapment in a casting and thus improve its integrity. Vacuum systems, however, should be considered an important supplement, but not as a substitute for an appropriate product, cavity, runner, gating and overflow design which addresses minimising the creation of porosity. Depending on the part configuration and porosity specifications, good part and die design can often provide all the casting integrity required for trouble-free machining without the use of vacuum. Where high structural integrity is required throughout the casting, high or ultra-high vacuum has to be used.

With special attention to controlling porosity in the design of the part, in die design, and in production processing, most die castings can be cast pressure tight, particularly if this requirement is not essential throughout the casting's entire cross section. The die caster should always be informed of pressure tightness requirements before any die design takes place. Where a part design with heavy sections, for example, will not allow modification and 100% pressure tightness is required, impregnation techniques may be a solution. Impregnation processing forces organic material into the surface pores of the casting, effectively sealing the parts.

#### **6.1.2.4 Environmental Impact**

The competitiveness of a product or its manufacturing process more and more depends on its environmental impact. Due to the good recyclability of magnesium alloys, yield of magnesium alloys put into the process is rather high. Scrap parts, biscuits and runners are easiest to recycle, because they are relatively clean and free from oxides. Other magnesium parts like machining chips, flash, sludge, ... contain higher quantities of oxides and require special precautions in recycling. Some die casters do an entirely own in-house-recycling. On the other hand specialized facilities are available to handle the more contaminated material.

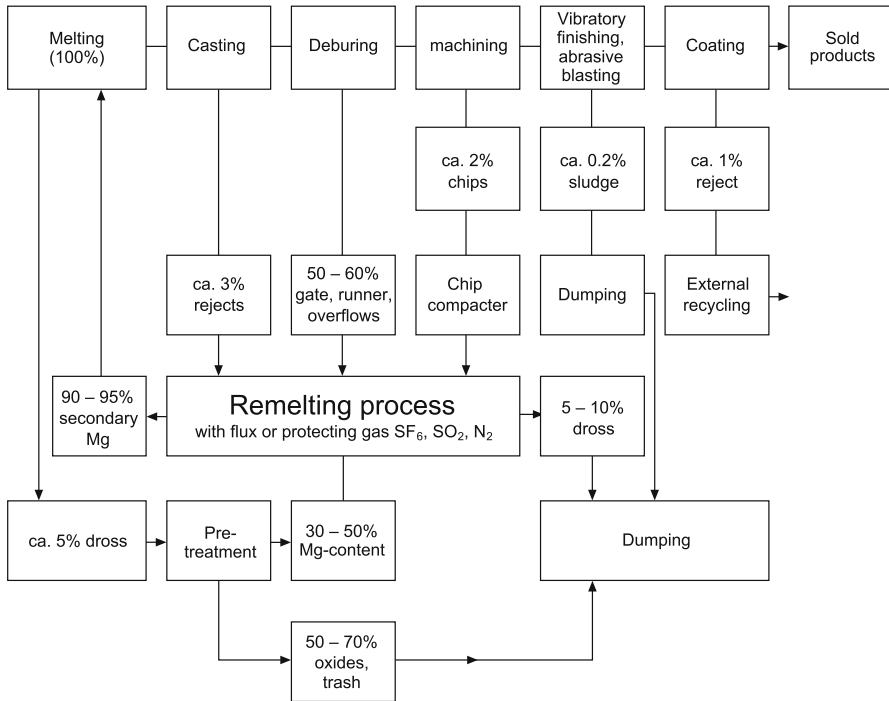


Fig. 6.33. Example of the material flow in a magnesium high pressure die casting foundry [18]

For 20 years, magnesium producers and casters have used the potent green house gas sulphur hexafluoride ( $\text{SF}_6$ ) to protect molten magnesium from burning in air. Very low volume of  $\text{SF}_6$  is needed for effective melt protection. However,  $\text{SF}_6$  has a global warming potential (GWP) of 24,000 times greater than that of carbon dioxide.  $\text{SO}_2$  can be used as an alternative to  $\text{SF}_6$ , whereas emissions of  $\text{SO}_2$  to the working atmosphere must also be controlled. Initiated by the 1997 “Kyoto Protocol for Climate Change”, a number of alternative shielding gases are under development and have already been tested successfully [15–17].

An example for a typical material flow in a magnesium die casting foundry is shown in Fig. 6.33.

### 6.1.3 Squeeze Casting, Thixocasting and Rheocasting

#### 6.1.3.1 Introduction

*Helmut Kaufmann, Simon Kleiner*

In this section three processes are introduced, that represent emerging technologies for the magnesium casting field, and are at present the subject of extensive research activities. Squeeze casting, thixocasting and rheocasting have

been studied in detail for aluminium alloys over the past 15 years and several products have been introduced into series production [18]. For Mg-alloys this R&D work is still quite young, but very promising.

The motivation for such development work is manifold: Manufacturing engineers are aiming for near-net-shape parts in order to reduce the high cost of machining. This is even more important in the field of magnesium alloys than in the field of aluminium alloys, because a safe and low-cost recycling concept for machining chips has yet to be developed.

Conventional high-pressure die-casting (HPDC) is the most frequently used and readily available casting technology for magnesium alloys and fulfils the aforementioned requirement widely, but HPDC has some inherent drawbacks. Generally, the die filling speed is very high and therefore, the flow very turbulent. In fact, it often sprays rather than flows, considering ingate velocities of 50 m/s and above. In conventional HPDC this results in castings with compressed gas inclusions, which cause porosity or blisters after heat treatment. Porosity and inclusions result in mechanical properties that are far below those acceptable for a given alloy. To improve this situation, vacuum assisted HPDC is under continuous development. The excellence of HPDC lies in the possibility to cast large-size castings with thin walls, but not necessarily in highly loaded parts.

Squeeze casting and the two semi-solid process routes, thixocasting and rheocasting, aim at low porosity levels, higher strength and higher elongation to fracture. It should become possible to cast new alloys other than the classical AZ91 or AM60 alloys. The castings should be heat treatable and weldable for high ductility in structural applications. Castings made with these processes should target forging quality at lower cost.

### 6.1.3.2 Squeeze Casting

The name “Squeeze Casting” is often used for rather different processes, and it is necessary to distinguish between “Direct Squeeze Casting” and “Indirect Squeeze Casting”. Direct squeeze casting has some equipment similarities with forging presses (Fig. 6.34). Liquid metal is poured into the lower die half before the upper die half moves downwards and closes the die. By doing so it forms the shape of the casting and applies pressure to the solidifying melt. This process has been frequently used for the production of MMCs with magnesium matrices [19] as well as the casting of monolithic magnesium parts [20].

A significant advantage of this process is the lack of any runner system, leading to high material yield and a cost benefit. But on the other hand, runners pro-

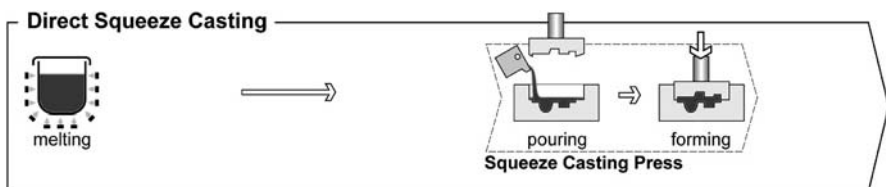


Fig. 6.34. Schematic diagram of the direct squeeze casting process

vide the foundrymen with the possibility to trap inclusions before entering into the die – which is especially crucial in semi-solid casting – while all impurities and inclusions of the melt are surely in the component in direct squeeze casting.

Since the solidification pressure is applied on the whole casting surface and feeding distances are short, castings made in direct squeeze casting are generally pore free. This process is mostly used for simple shapes without sliding cores, and a good method for infiltration of ceramic preforms.

Indirect squeeze casting machines are combinations of the low-pressure die-casting (LPDC) filling concept with HPDC shot units (see Fig. 6.35). The shot units are placed below the die and allow a vertical bottom-up die filling direction. This means that during filling the metal front velocity is perfectly controlled by the plunger speed of the shot unit. This filling speed has to be selected such that turbulent flow is avoided in order to produce castings without gas inclusions. Roughly speaking the ingate speed is about 1/100 of the speed applied in HPDC. This results from a generally lower plunger speed combined with larger ingate areas for better feeding of the casting during solidification.

This is possible also for magnesium alloys, because the considered castings differ in shape and wall thickness from classical HPDC parts. The wall thickness has to be thicker and the flow length shorter to permit this way of casting. Similar to direct squeeze casting, the indirect vertical squeeze casting process is well suited for the infiltration of preforms for MMC production [21].

The material yield is significantly lower than for direct squeeze casting and lies in the range of 50%. This requires a low cost separation process for castings and runners (the ingates are in most cases too thick for stamping) as well as a recycling process for this kind of class I scrap. Equipment for in-house recycling of Mg alloys as well as companies for external recycling are available today. For both types of squeeze casting processes it can be stated that the conventional metal supply unit can be used. There is no difference from HPDC.

Squeeze casting allows processing of alloys with a narrow solidification range, which are very difficult to cast by other casting processes. The low porosity level of squeeze castings is very beneficial for alloys that are amenable to age-hardening. No blistering occurs during heat treatment.

Figure 6.36 shows a typical microstructure of squeeze cast AZ91 with the brittle intermetallic  $\beta$ -Mg<sub>17</sub>Al<sub>12</sub> located in interdendritic areas. Grain size is quite large due to the slower cooling in thick-walled sections and only medium strength levels are therefore achieved in as-cast condition. Yield strength (YS) of about 120 MPa, ultimate tensile strength (UTS) of 190 MPa and an elongation of 4.5% are typical for AZ91 specimens machined from 15 mm thick castings. These

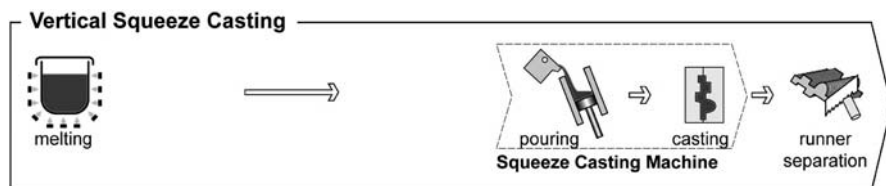


Fig. 6.35. Schematic diagram of the indirect vertical squeeze casting process



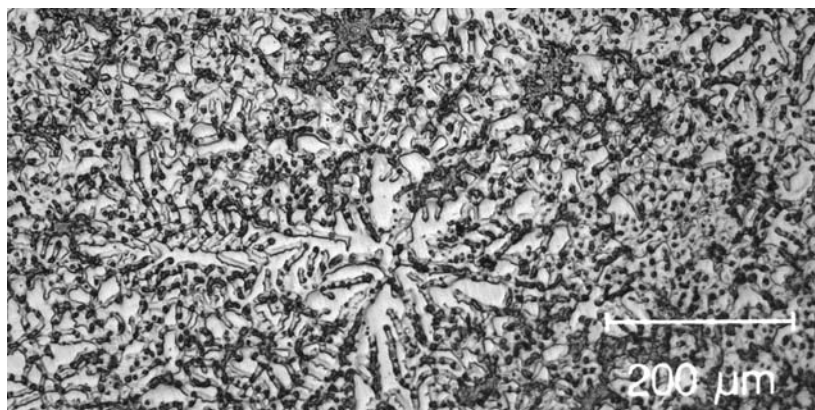


Fig. 6.36. Microstructure of squeeze cast AZ91

strength values are inferior to mechanical properties of thin-walled fine-grained high-pressure die-castings of the same alloy. The excellence of squeeze casting does not lie in especially high strength in as-cast condition but in the ability to cast thick-walled parts in various alloys with low porosity. Such parts are weldable and heat treatable and cannot be produced by means of HPDC.

### 6.1.3.3 Semi-Solid Casting

#### General considerations

The concept of semi-solid metal (SSM) processing started in the early 1970s with the discovery of the shear thinning and thixotropic behaviour of partially solidified alloys under stirring [22]. Two basic routes of SSM processing, termed “rheocasting” and “thixocasting”, were developed and their feasibility proved in industrial trials. The rheo-route involves the preparation of a SSM slurry from liquid alloys and transferring the prepared slurry directly to a die or mould for component shaping. The thixo-route is basically a two step process, involving the preparation of a feedstock material with thixotropic characteristics, reheating the solid feedstock material to semi-solid temperature and shaping the semi-solid slurry to components [23].

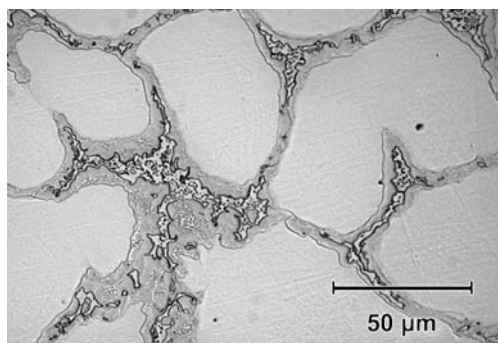
The most often stated advantages of SSM processing compared with conventional casting are the non-turbulent filling of the die, the reduced shrinkage porosity, the longer die life and the shorter cycle time. Semi-solid processed components are heat treatable, weldable and show superior mechanical properties. All these qualities were deduced from the properties of semi-solid slurries and most of them have been confirmed in practical experience for suitable aluminium alloys. In the past decade, SSM processing has experienced intensive research and development, predominantly on aluminum alloys, which has led to the series production of some semi-solid processed aluminum components. The situation for magnesium alloys, however, is somewhat different. Despite some 15 years of effort, SSM processing of magnesium has not made such remarkable progress. The



only semi-solid casting process that is in industrial use for magnesium alloys is thixomoulding [24]. This process is closely related to the well-known injection moulding of plastics and normally operates at very low solid fractions of 0–20%, i.e., thixomoulding is often not semi-solid casting but liquid casting with a non-superheated melt instead.

One reason for the different states of development of SSP for aluminum and magnesium may be the fundamental metallurgical differences of aluminum and magnesium casting alloys. While the usual Al-Si-Mg aluminum casting alloys are hypoeutectic alloys containing roughly 50% eutectic, the common Mg-Al and Mg-Al-Zn casting alloys solidify as single-phase alloys under equilibrium condition. Commercial casting processes involve cooling rates, which do not allow equilibrium solidification and it is for this reason that non-equilibrium eutectic is found in Mg-Al castings (Fig. 6.37). Semi-solid processing as well as the properties of the components are largely affected by the presence and morphology of eutectic phases.

Actual high-purity magnesium casting alloys contain 2–9 wt% aluminum, and these AZ- and AM-alloys have attracted most interest for SSM processing in the past. The binary phase diagram (Fig. 6.38) is the basis to estimate the suitability of different alloys for SSM processing. An adequate fraction of liquid is the prerequisite for successful SSM processing. It is generally accepted that a liquid fraction ( $f_L$ ) of 40–60% is suitable for semi-solid casting. Two very similar criteria for processability of an alloy in the semi-solid state have been established, namely the temperature range  $\Delta T^{40/60}$  corresponding to liquid fractions of 40–60% as a technical approach and the temperature sensitivity  $df_L/dT$  as a more scientific approach. Both of these criteria permit to estimate if it is technically possible to reach the desired fraction of liquid with sufficient accuracy and reproducibility. Figure 6.39 shows the temperature sensitivity of Mg-Al alloys at 50% liquid fraction in non-equilibrium condition. It becomes obvious that SSM processing becomes more difficult when the Al-content is lowered. The temperature sensitivity increases disproportionately to decreasing Al-content. In order to guarantee processability in the semi-solid state, a maximum value of  $\Delta f_L = 0.01 \cdot T \cdot df_L/dT < 0.06$  (at  $f_L = 0.4$ ) has been suggested [25]. According to this criterion, Mg-Al alloys containing less than 7% alu-



**Fig. 6.37.** Microstructure of SSM processed AZ91 showing non-equilibrium eutectic between primary  $\alpha$ -Mg particles

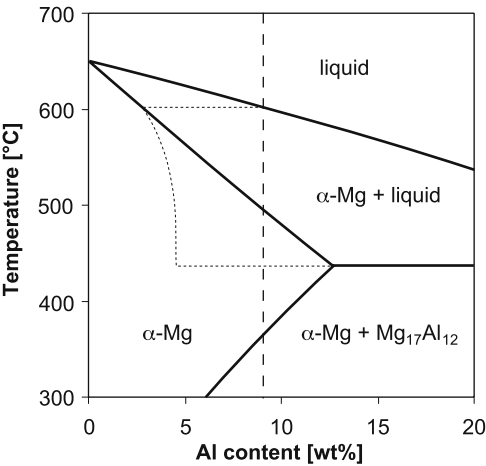


Fig. 6.38. Binary phase diagram Mg-Al, dashed line represents non-equilibrium solidification of Mg-9% Al alloy

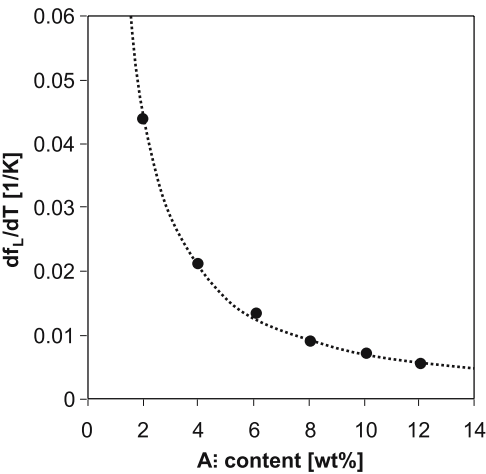


Fig. 6.39. Temperature sensitivity at  $f_L = 50\%$  for various Mg-Al alloys under non-equilibrium conditions

minum are not amenable to SSM processing, but in practical experience, AZ61 and AM50 have successfully been thixocast [24, 26, 27].

While high aluminium or zinc content is beneficial for processability, the ductility of the produced component is adversely affected by the presence of brittle intermetallic phases. The amount of non-equilibrium eutectic containing brittle  $\beta$ -Mg<sub>17</sub>Al<sub>12</sub> largely depends on the aluminium content of the alloy (Fig. 6.40). These opposite demands – processability vs. mechanical properties – are well known from magnesium die castings. The most commonly used die casting alloy AZ91 shows excellent casting behaviour but low ductility while the lower

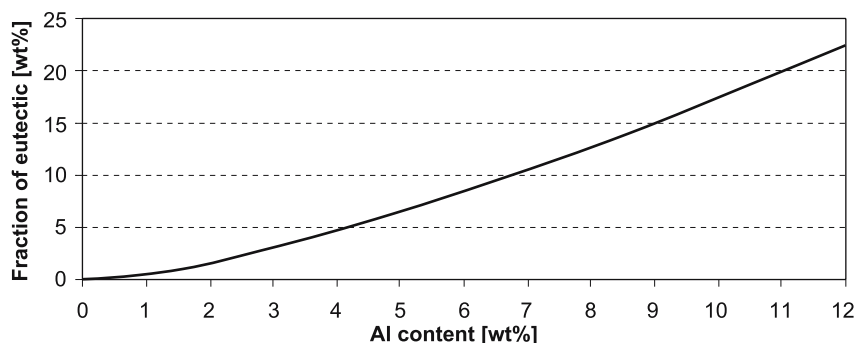


Fig. 6.40. Amount of non-equilibrium eutectic in Mg-Al alloys

alloyed AM50 or AM20 exhibit superior ductility but quite poor castability. This behaviour is even more pronounced in semi-solid casting.

Apart from an adequate volume fraction of solid, the morphology of the solid phase is a crucial factor in SSM processing. Grain size and sphericity or roundness of the solid particles are the most important parameters, and determine the quality of the SSM slurry. A maximum grain size of 150  $\mu\text{m}$  has been proposed for various aluminum and magnesium alloys [28]. Different expressions have been used in the literature to quantify roundness of particles [23] and an upper limit for the shape factor  $F^S = 2.0$  was introduced by Uggowitzer et al. [28].

Other microstructural aspects like distribution and agglomeration of particles also play an important role in SSM processing [23] but will not be dealt with in this article.

### Thixocasting

Thixocasting is the most widely known concept for semi-solid casting of metals, and for a limited number of alloys, the thixocasting process of aluminum is available in the market today.

Semi-solid casting requires a special type of material in terms of microstructure before casting. It was shown for many alloys that a globular primary phase, which is the solid portion of the slurry, is required for proper flow behaviour of the slurry [23]. Different production methods have been proposed to provide suitable feedstock material for thixocasting [29].

In classical thixocasting – which is today mostly used for Al alloys – this kind of globular microstructure is achieved by a magnetohydrodynamic (MHD) stirring operation during continuous casting of billets. To explain the observed fine particles and non-dendritic morphology under forced convection several mechanisms have been proposed including dendrite arm fragmentation, dendrite arm root remelting and growth controlled mechanisms [23]. Thixotropic aluminium alloy feedstock material produced by MHD stirring is commercially available.

No MHD stirred magnesium alloys have been produced so far but many alternative routes for precursor manufacturing of Mg have been developed. Direct chill casting with chemical grain refinement [30], pressure ingot die casting (PID)

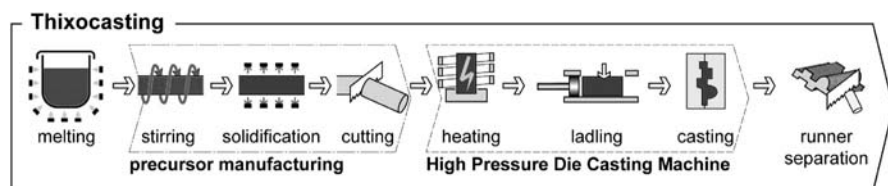


Fig. 6.41. Schematic diagram of the classical thixocasting process

[29], single slug production (SSP) and rapid slug cooling technology (RSCT) [26] are feedstock manufacturing processes, which are based on controlled cooling to avoid extensive dendrite formation while the SIMA (stress induced melt activation) [31, 32] and extrusion approach [33] take advantage of the recrystallisation phenomenon to transform the dendritic microstructure.

The precursor material is cut into slugs of appropriate length, reheated into the semi-solid region and cast to shape (Fig. 6.41). Inductive heating has been established as the preferred reheating method for semi-solid processing [34, 35]. The aim of the reheating process is to get a semi-solid slug with a defined amount of liquid phase and a homogeneous solid-liquid distribution all over the billets cross-section. This implies that a homogeneous temperature field in the billet at the end of the heating cycle has to be attained. A multiple-stage heating cycle with consecutive reduction of heating power is recommended to limit the temperature gradient between core and periphery to a few degrees Celsius. The use of a protective gas like SF<sub>6</sub> and/or a closed heating container is necessary to avoid severe oxidation of the semi-solid slug. Reheating is a very critical processing step in thixocasting as it largely affects the quality of the semi-solid slug. Several different methods have been developed in order to control the quality (softness, rheology, homogeneity) of the slug [36, 37] but manual cutting of the slug with a knife or blade is still the preferred method.

Casting machines used for thixocasting are normally conventional HPDC machines with stronger shot units, which are readily available in the market. The higher viscosity and the lower heat content of a semi-solid slurry compared to a superheated melt and the tendency to liquid-solid segregation cause difficulties in die filling, especially in geometrically complex parts. In order to avoid premature solidification during die filling, a sufficiently high filling speed and a high die temperature must be applied. A high die filling speed also reduces liquid-solid segregation [38]. Even under optimised conditions, it is not possible to cast such complex and thin-walled parts by thixocasting as can be done by HPDC, but thixocasting has its advantages when it comes to thick-walled parts where HPDC fails in terms of porosity. The increased viscosity of the slurry results in a closed metal front and less gas inclusions in the product. Thixocastings are therefore heat treatable and weldable. Since roughly 50% of the metal are already solid during casting, the amount of solidification shrinkage is reduced, which is beneficial especially for alloys that are critical for hot tearing. The lower temperature of the slurry increases the lifetime of the die and the solidification time can be reduced, especially in thicker wall castings. Whether all these possible advantages of semi-solid casting can finally be achieved depends strongly on the geometry of the part.

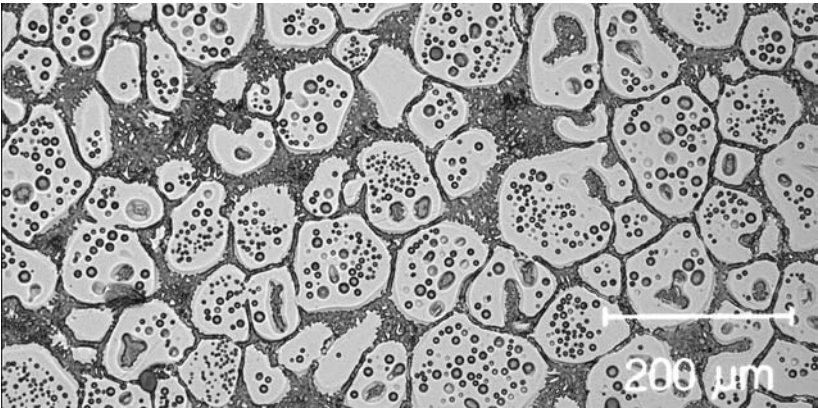


Fig. 6.42. Microstructure of thixocast AZ80

The recycling process of runners and scrap is quite costly in thixocasting because the foundry does not prepare the precursor in-house. Therefore, runners and scrap are either downgraded and used in HPDC or sent to an outside supplier of globular precursor for recycling as a thixocasting billet.

A typical microstructure of thixocast magnesium is shown in Fig. 6.42. Liquid inclusions in the globular  $\alpha$ -Mg particles are typical for a semi-solid slurry made from extruded feedstock material. Such entrapped liquid has been stated to be unfavourable [25] because it does not contribute to the ability of the material to flow. In practical experience, however, extruded feedstock material shows proper casting behaviour, which is attributed to good sphericity of solid phase particles in the slurry.

The brittle  $\beta$ - $\text{Mg}_{17}\text{Al}_{12}$  tends to form a continuous network in thixocast microstructure especially in higher alloyed AZ-alloys and ductility in as-cast condition is limited. Alloys with reduced aluminum content like AM50 and AZ61 show elongation values of up to 10% even in thick-walled sections but are more difficult to process in the semi-solid state. A solution heat treatment causes dissolution of  $\beta$ - $\text{Mg}_{17}\text{Al}_{12}$  and accounts for large improvements in elongation and fracture toughness. If we consider that the yield strength depends highly upon the grain size of Mg-alloys – the Hall-Petch coefficient of magnesium is four times larger than that of pure aluminum – it becomes obvious that thixocast parts featuring grain sizes of about 100  $\mu\text{m}$  show only a rather low yield strength. Typical values for thixocast AZ80 are presented in Table 6.13.

Table 6.13. Mechanical properties of thixocast AZ80

Alloy	Condition	YS [MPa]	UTS [MPa]	Elongation [%]
AZ80	As thixocast	105	185	3.5
	Solution treated	100	230	8.0

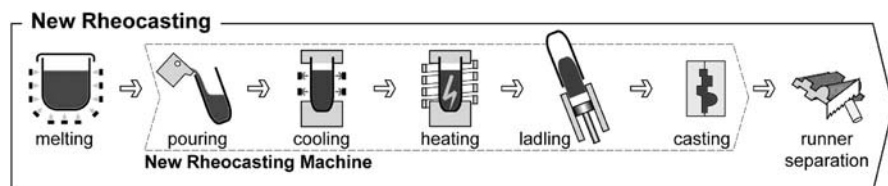


Fig. 6.43. Schematic diagram of the new rheocasting (NRC) process

### New rheocasting

New rheocasting (NRC) is a novel route for semi-solid casting, that is already in series production for aluminum alloys [39]. In this process the globular microstructure of the semi-solid slug is obtained by controlled solidification of regular light metal alloys (Fig. 6.43).

Since the process starts from conventional liquid alloys, the difficulties of metal supply and recycling can be avoided, while the benefits of semi-solid casting remain valid. A fully liquid melt is taken from the holding furnace and poured into specially designed steel cups, which are placed on a cooling carousel (slurry maker carousel) next to the NRC machine. By controlled cooling of the melt into the semi-solid region a globular microstructure is attained. In the final position of the carousel the temperature is equalized over the cross-section of the cup. The semi-solid slurry is then poured into the inclined sleeve of a squeeze casting machine, the sleeve docks to the die, and the slug is cast into shape. Final solidification occurs in the die at high pressure. After part extraction the runner system is cut off and returned to the melt shop of the foundry for in-house recycling. In the original development for aluminum the cooling station was added to a vertical squeeze casting cell. The on-going development work [40] for Mg-alloys follows this route as well. In the long run, the slurry making system can be added to both squeeze casting machines and conventional HPDC machines with stronger shot units.

The essential metallurgical feature of the process is the forced nucleation of  $\alpha$ -particles on the wall of the steel cup, which continue to grow in globular shape due to controlled cooling under conditions that avoid constitutional supercooling [41]. For the ladling of the cup the melt must not be superheated excessively, otherwise nuclei formation will not take place on the cup wall or nuclei already present in the cup will be destroyed again. From experimental observation 10–20°C superheat are recommendable. An ideal semi-solid slug with fine and spherical particles distributed uniformly in the liquid matrix can only be achieved with suitable alloys and proper process control. In NRC the semi-solid condition is controlled by temperature measurements with thermocouples directly in the melt and the resulting slug, respectively.

In order to perform the necessary control of the cooling profile and to provide thixotropic slugs for high production rates, NRC uses slurry maker systems with up to ten cooling stations on a carousel. Taking into account the lower heat content of Mg-alloys compared to Al-alloys, less cooling stations may be used.

The microstructure of new rheocast AZ91 (Fig. 6.44) has most features in common with a thixocast microstructure except for the fact, that no inclusions



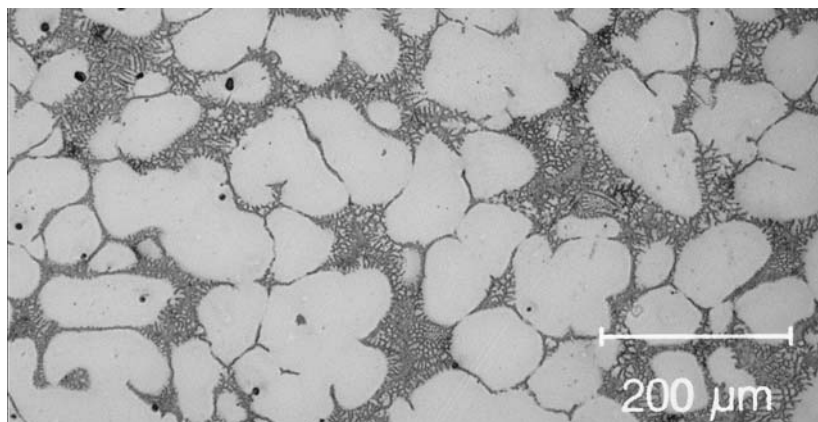


Fig. 6.44 Microstructure of new rheocast AZ91

Table 6.14. Mechanical properties of new rheocast AZ91

Alloy	Condition	YS [MPa]	UTS [MPa]	Elongation [%]
AZ91	As cast	115	180	3.4
	Solution treated	180	240	8.3

within the primary  $\alpha$ -Mg particles are observed. Grain size and distribution of  $\beta$ -Mg<sub>17</sub>Al<sub>12</sub> are similar to thixocastings and the comments made on ductility and strength of thixocast parts also apply to new rheocast components. Typical mechanical properties for new rheocast AZ91 are listed in Table 6.14. A solution heat treatment of 24 hours at 400°C is very beneficial for ultimate tensile strength and elongation but yield strength is slightly reduced.

Whereas thixocasting and new rheocasting do not differ much in mechanical properties, new rheocasting has noticeable economical advantages. For aluminum alloys it could be shown that NRC is approximately 20% lower in manufacturing cost, mainly due to the use of conventional alloys [42]. The possible use of recycling material for NRC in future may add a further benefit. For an overall energy consumption it could be shown that fully liquid squeeze casting requires about 2% less energy than NRC, but 95% less than classical thixocasting with slug stirring and inductive reheating. A detailed cost comparison is not possible at the moment for Mg-alloys due to the lack of commercially available feedstock material. Nevertheless, it can be stated that NRC is cheaper than any competing semi-solid process, because of no special alloy preparation before casting. Compared with thixomoulding, there will also be lower cost and energy consumption, because the machining of granules for thixomoulding adds about 25%, to the cost [43] and requires additional energy. At this point in time it is impossible, however, to name calculated or measured numbers of difference between these casting processes.

## 6.2 Forming

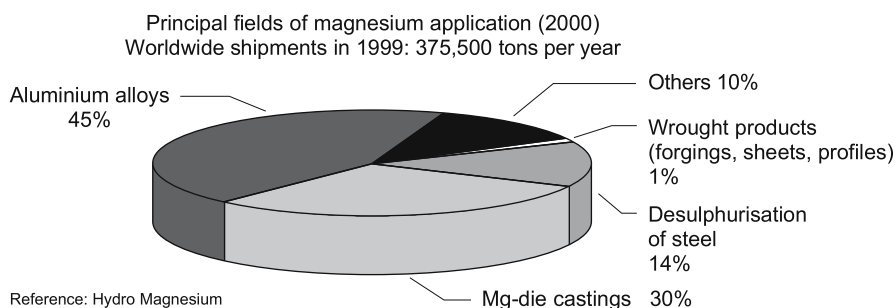
### 6.2.1 Rolling and Shut Forming

*Peter Juchmann*

#### 6.2.1.1 Situation and Potential of Magnesium Sheet

Arising from an increasing demand for lightweight construction, magnesium as the lightest structural metal enjoys renewed attention. The main driving force comes from the automobile industry. Future automobiles will have to fulfil growing customer requirements concerning mobility and individuality. Yet demand for improved power, comfort and safety standards partly contrast with a simultaneous need for environmental acceptance. Innovative car concepts, therefore, require new solutions to achieve optimised lightweight construction and functionality. Within a growing materials competition, the attraction of magnesium seems to increase continuously. One leading German automobile company is already talking about a new magnesium age in passenger cars [1, 2]. Magnesium die castings have already been established in a variety of series applications such as steering wheels, gearbox housings, seat frames and instrument panels [see Chap. 8].

In contrast to traditional materials like steel and aluminum, a very limited spectrum of wrought alloys and semifinished products exists today, especially for flat rolled material, necessary to open new fields of application with special ductility and surface requirements. In 1992, L. Barnes described the situation of magnesium wrought products, particularly of sheet and plate, as “the best kept secret in the non-ferrous industry” [3]. On the one hand, this niche position is due to the comparatively limited cold-workability of magnesium alloys; on the other hand, it mainly results from a more or less neglected alloy and product development in the last decades. All magnesium wrought products (forgings, extrusions and flat rolled products) represent less than 1% of the total annual magnesium use of roughly 400,000 t worldwide (Fig. 6.45). The market has decreased to 2.500 tons per year at the moment [4]. Today magnesium sheet, for example, is mainly used in the printing industry as photo-engraving plates.



**Fig. 6.45.** Use of magnesium in different areas [4]



Many examples from the past, however, illustrate the usability of magnesium sheet for complex structural applications in different fields of transportation e.g., cars, trucks, aeroplanes, satellites or missiles [5] (Fig. 6.46). As early as the late 30s of the last century, a small-series bus trailer completely constructed out of magnesium extrusions and sheet metal of MgMn-alloy was reported [6]. Car body applications show the outstanding forming and design potential of magnesium sheet. For example, the ultralight magnesium sheet metal construction of the early French sports car weighed only 64 kg. The materials' thickness varied between 1.3 and 2.0 mm and was shielded arc welded [7]. Mercedes also used body components for their competition racing cars of the 50s, which were planked on a steel tube chassis [8]. Furthermore, another premier application has been deep drawn Samsonite suitcase sides formed from 1.0 mm AZ31B sheet [3].

Today the technical property profile of magnesium wrought products still offers the best preconditions for complex ultralight components with high mechanical and surface requirements. Thus, this material group opens new application areas which can hardly be achieved by magnesium castings. The property profile of magnesium sheet is characterised by:

- large resources and universal recyclability,
- ultralight material (density below  $1.8 \text{ g/cm}^3$ ) and outstanding weight specific strength and stiffness properties: the resultant weight reduction capability for large thinwalled parts reaches up to 60% compared to steel and up to 25% compared to aluminum, and
- good damping capacity (depending on alloy) to absorb vibrations.

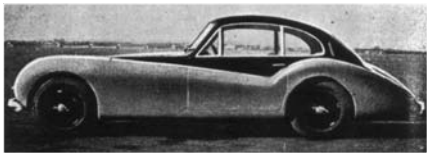
Compared to die castings, advantages mainly result from the homogeneous, fine crystalline and nearly fault free microstructure resulting from:

- balanced mechanical behaviour on a higher strength level,
- improved ductility and therefore better deformability and dynamic properties,
- uniform distribution of properties which simplifies an optimal part design and
- potential for large thinwalled parts including outer-skin quality.

The advantages compared to plastics are:

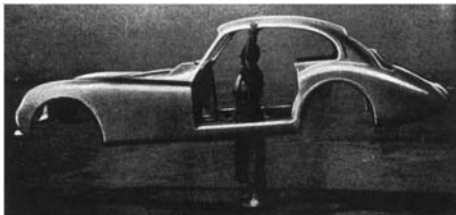
- higher thermal stability, smaller tolerances caused by lower thermal expansion,
- X-ray absorption capability (low neutron capture cross section) and
- shielding function against electromagnetic interference.

Focusing on automobile applications (Fig. 6.47), magnesium flat rolled products offer potential for nearly all car areas. Besides a significant reduction of weight and improved weight distribution in terms of a lighter front area, the lowering of the point of gravity and the reduction of unsprung masses should lead to better driving performance. Fields of application include the interior (e.g., bracket carrier, seat components); the body (large hang-on parts like doors, roof, bonnets, as well as body in white and front end parts); the drive system (cylinder head cover, oil pan), as well as the chassis (e.g., wheels).



**Series sports car Allard (1952)**

Car body out of Mg-sheet  
(thickness: 1.3 to 2.0 mm); Global weight (incl. doors and bonnet): 64 kg

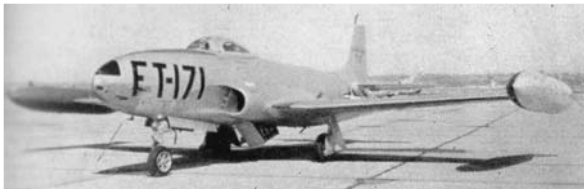


**Competition sports car Mercedes-Benz 300 LR Le Mans (1955)**

Car body components out of Mg-sheet metal, pressed at about 200°C and planked on a steel-tube chassis  
Reference: Daimler-Chrysler



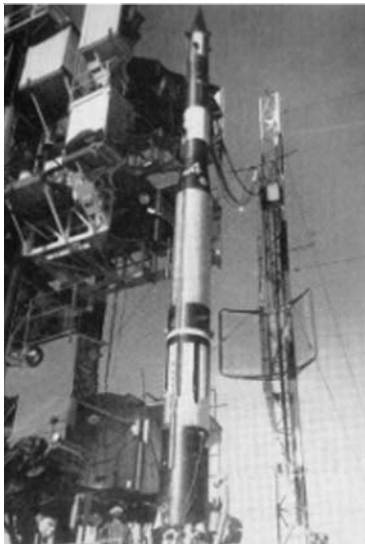
**Experimental all-magnesium aircraft with monocoque wing construction**



**Missile** containing about 18 kg Mg-sheet and 90 kg Mg-castings

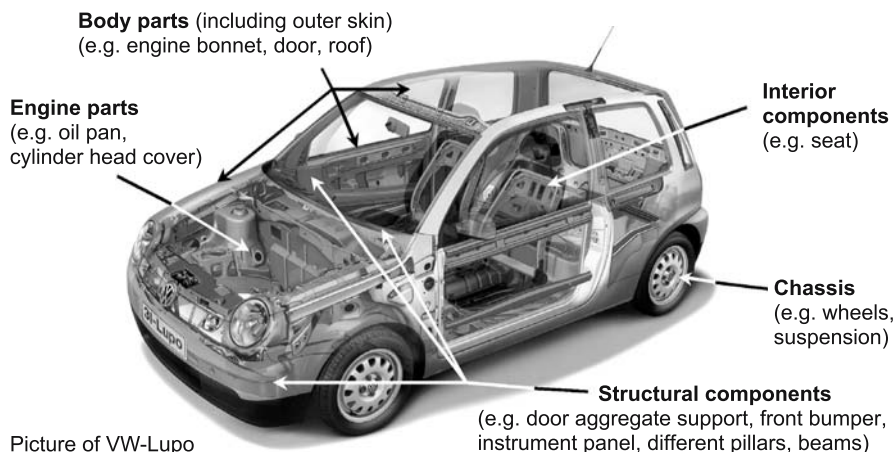


**Helicopter** skinned with Mg-sheet (about 113 kg)



**Vanguard satellite launching rocket**  
(using Mg for tail can, spacer section, 2nd stage skin and satellite skin)

**Fig. 6.46.** Structural applications of Mg-sheet for transportation [5–8]



**Fig. 6.47.** Perspectives of application of Mg-sheet for automotive lightweight construction

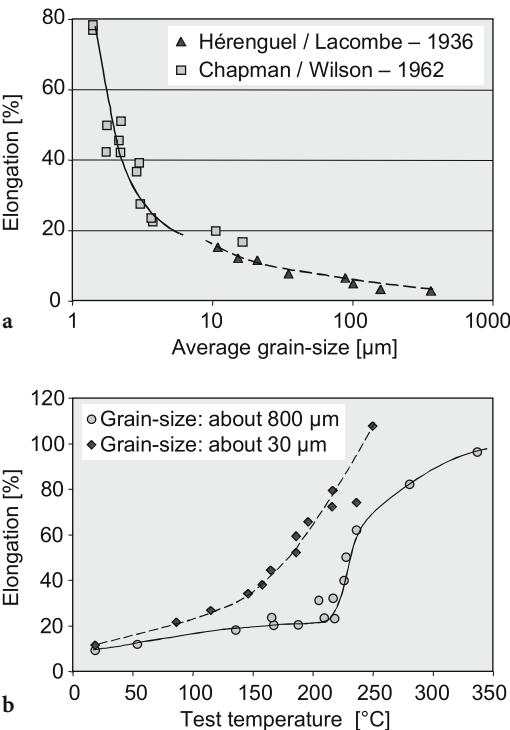
The breakthrough of magnesium wrought products in automotive use demands the availability of magnesium sheet, which can fulfil the high quality requirements and delivery performance for series applications. The main aim is to produce high purity wrought products with a corrosion resistance comparable to magnesium die castings. In this regard the ASTM-standard B90/B90M [9] at present used as a quality guide is not completely sufficient. Simultaneously missing material, production and experience in use have to be collected. Further alloy development can, for example, lead to an improved workability and deformation behaviour, as well as to higher thermal stability and corrosion resistance. At the moment, the wrought alloy AZ31 is used nearly exclusively. To a small extent further alloys like ZM21, AZ61 or M1 are employed for special applications. These materials are generally acceptable in terms of processing and performance, but leave space for a variety of significant improvements [10–15].

One additional key factor consists in the qualification of powerful process chains adapted to magnesium sheet including the raw material, the production and processing of semifinished products, the part design and fabrication and the recycling of production scrap and used parts. Therefore, during the last few years a variety of institutional and industrial R&D-activities have been started worldwide. At international conferences magnesium wrought products, meanwhile, play a nearly equivalent role with respect to die castings.

### 6.2.1.2 Forming of Magnesium and Magnesium Alloys

Based on the general deformation behaviour of magnesium alloys described in Chapter 3.2.1, the resultant consequences for the production, processes and use of magnesium wrought products shall be discussed briefly.

Due to their hexagonal lattice structure, magnesium alloys show a comparatively limited cold workability. Near room-temperature, plastic flow only occurs by basal slip. This anisotropic deformation behaviour of magnesium, which is



**Fig. 6.48.** a Grain-size dependency of ductility of pure magnesium [16, 17]; b Effects of grain-size and temperature on the formability of pure magnesium [5]

not effectively obstructed by the interaction of various slip systems, corresponds to a low basic strength. This behaviour causes critical stress concentrations at the grain boundaries. The results are strongly directional mechanical properties under tension and compression, as well as the danger of an early material failure.

The flow stress and ductility of magnesium depends significantly on grain-size [18]. In this context, early studies [16] pointed out a rapid increase of room temperature strength and ductility, which becomes obvious below an average grain diameter of 5  $\mu\text{m}$  (Fig. 6.48a). In general, the hall patch coefficient of magnesium is very high compared to aluminum.

The inhomogeneity of plastic deformation increases with coarser grains accompanied by a simultaneous promotion of twinning, because fewer grains are favourably oriented for sliding. Also, the intensity of twinning depends heavily on the orientation of the material's texture to the direction of external stresses. For magnesium sheet, twinning primarily occurs under tensile stresses vertically to the sheet plane and under compression at right angle to this direction [19].

Fundamentally, intensive twinning is connected with an early initiation of plastic flow and leads to reduced yield strength [20]. While they can improve the orientation of grains for subsequent slip, twin boundaries are impassable barriers

ers for dislocation movement. Such interactions cause local stress areas which may support the early development of microcracks.

Therefore, cold forming of magnesium has to be carefully performed. Resulting work hardening and unfavourable lattice defects can be eliminated or modified respectively by applying a controlled annealing. Above 200°C, however, the plasticity of magnesium wrought alloys increases dramatically due to the thermal activation of additional slip systems (Fig. 6.48b) [5, 6, 17, 19].

### **6.2.1.3 Magnesium Rolling**

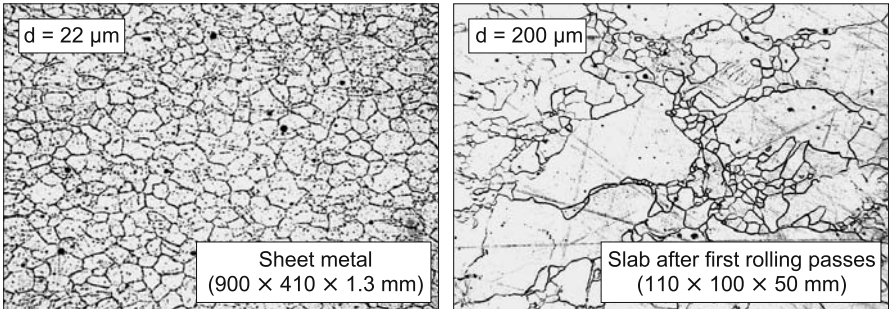
Hot rolling is usually carried out in the temperature range between 300°C and 480°C depending on the alloy and the pre-treatment of the feedstock material. Mg-Al-wrought alloys like AZ31 or AZ61 need, for example, an intensive homogenisation treatment of up to 24 h at 400°C to dissolve low melting intermetallic phases.

Initially the hot deformation process leads to an efficient break down of the comparatively coarse cast or solution treated structure (Fig. 6.49) into a fine-grained material, with a medium grain-size of 20 µm and below [14, 15, 21, 22]. A thickness reduction of 10–30% per pass can be realised without cracking, but the low volumetric heat content of magnesium combined with the comparatively limited process window of hot rolling normally requires several intermediate reheats. In some cases, lubricants like colloidal graphite, water based fluids or oils, as well as heated working rolls were used to reduce the number of rolling passes necessary [23]. Microstructural analyses [22] shows an inhomogeneous deformation structure, after a cumulative reduction of 50%, especially characterised by coarse shear bands and a completely recrystallised grain structure after finished hot rolling (reduction > 99.5%). Above a reduction of 90%, a pronounced basal texture was detected which remains nearly unaffected by further heat treatment. The grain orientation parallel to the sheet surface is tendentially less extensive transversally to the rolling direction and also attenuates towards the centre of the sheet.

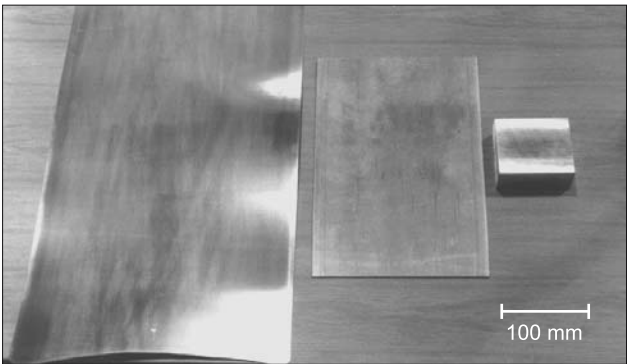
The finishing operations of magnesium sheet metal are normally carried out at lower temperatures to reach the maximum combination of mechanical properties, dimensional accuracy and surface quality. Cold rolling near room temperature is generally restricted to reduction values below 5%.

The mechanical properties of sheet metal are mainly determined by the final grain-size. Beneficial thermomechanical reactions can be activated by controlled interference of work hardening, recovery and recrystallisation effects, which are sensitive to alloy composition; process temperature; deformation parameters; reheating cycles; the final cooling to room temperature and an additional heat treatment.

An optimised thermomechanical treatment leads to finely recrystallised sheet metal (Fig. 6.49) [14, 15, 22]. Laboratory experiments have been verified in pre-industrial production trials. Salzgitter Magnesium-Technologie GmbH is able to produce large sheet metal plates in a quality acceptable for ongoing material tests and prototyping activities. A new industrial rolling mill adapted to the special requirements of magnesium flat rolled products has started operation.



Laboratory

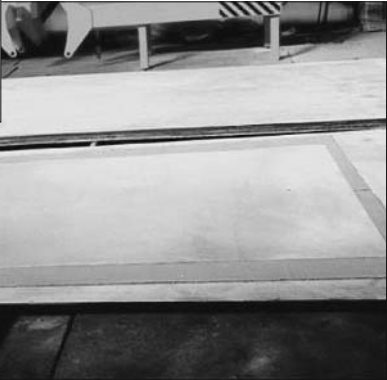


Pre-industrial trial

Raw material:  $\text{MgAl}_3\text{Zn}_1\text{wt\%slab}$  – 2100 × 1000 × 150 mm



Heavy plate  
8200 × 1030 × 39 mm



Sheet metal  
2850 × 1700 × 1.4 mm

Fig. 6.49. Rolling experiments and microstructure of Mg-sheet AZ31 [14, 15]



### 6.2.1.4 Magnesium Sheet

Magnesium flat rolled products are produced mainly according to the internationally accepted ASTM-standard B90/B90M [9]. During recent years, the list of standardised magnesium wrought alloys for sheet has been continuously reduced to AZ31 exclusively. Some other compositions with Li-, Th- or RE-content, for example, are no longer considered. This situation reflects the difficult niche position of magnesium sheet products.

AZ31 sheet material can be divided into two delivery qualities, “H24 – work hardened” and “O-annealed”. Table 6.15 gives an overview of the basic mechanical properties of magnesium sheet AZ31 in comparison to representative standard Al- and St-sheet products for automotive applications [9, 10, 15, 22, 24, 25, 26]. Table 6.16 contains the alloy composition and impurity levels of AZ31 (ASTM-B90). It becomes obvious that the wrought alloys need further improvements to be comparable to high purity die casting alloys e.g., AM50A [27]. This is necessary to reach an acceptable corrosion resistance.

The mechanical properties of commercial Mg-sheet metal AZ31 normally exceed the ASTM-limits significantly. They are competitive to conventional Al-sheet material used for car body applications (Fig. 6.50).

**Table 6.15.** Room temperature-mechanical properties of Mg-sheet AZ31

Properties	Symbol	Unit	AZ31 “O”	AZ31 “H24”	AZ31 exper- iment.	AZ31 com- mercial	AZ61 com- mercial	AlMg4.5 Mn0.4	DC04
Tensile strength	R <sub>m</sub>	MPa	221– 275	269– ...	230– 280	220– 290	290	279	306
Yield strength	R <sub>p 0,2</sub>	MPa	...	200– ...	130– 200	125– 220	190	146	160
Uniform elongation	A <sub>g</sub>	%	...	...	10–18	...	...	/	/
Elongation at rupture	A <sub>80</sub>	%	12	6–...	10–23	8–21	/	26	40
Anisotropy	r	–	/	/	1.2–2.0	/	2.0	0.74	1.68
Consolidation index	n	–	/	/	0.15– 0.20	/	0.20	0.32	0.25

**Table 6.16.** Composition of AZ31 compared to AM50 [9, 27]

Component	Al	Zn	Mn	Fe	Ni	Cu	Si	Ca	Others
AZ31B	2.5–3.5	0.6–1.4	0.20– 1.0	0.005 max	0.005 max	0.05 max	0.10 max	0.04 max	0.03 max
AM50A	4.4–5.4	0.22 max	0.26– 0.6	0.004 max	0.002 max	0.01 max	0.10 max	/	0.02 max

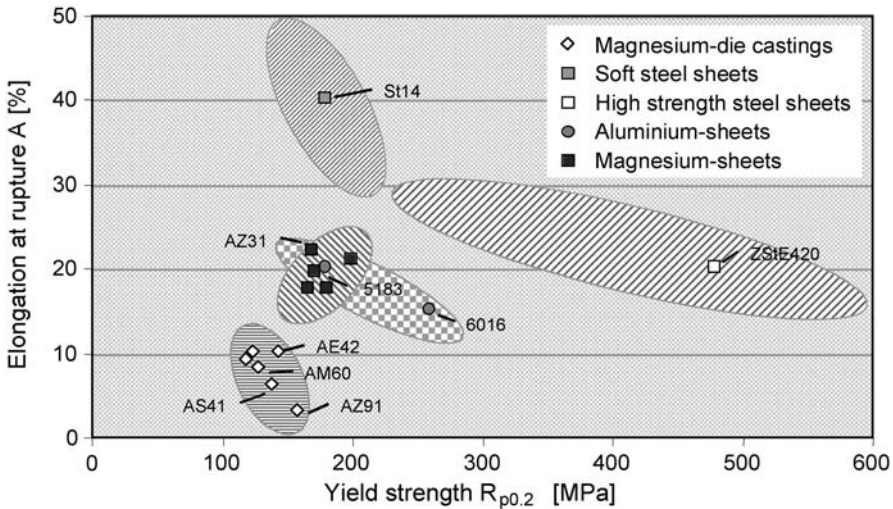


Fig. 6.50. Basic mechanical properties of different materials for car body construction [15]

Looking at tension tests of AZ31 sheet at room temperature, annealing, leads to a significant increase in uniform elongation and elongation to fracture, while a parallel decrease in strength can be observed. Independently of treatment, the properties are nearly equivalent in all directions of the sheet plane. Perpendicular to the rolling direction, slightly larger strength values are detected. Under compression, the yield strength is drastically reduced due to the early onset of twinning. N-values below 0.2 and r-levels up to 2 reveal a better deep-drawability than stretch forming potential of magnesium sheet.

For sheet metal forming of complex shapes, the material's behaviour at ambient temperatures is of special interest. While characterising the temperature-dependent properties up to 235°C, a continuous decrease in strength and of the r- and n-values down to the region of 1.0 and 0.1, respectively, has been measured [10]. Correspondingly, the elongation to fracture increases and reaches up to 50% for AZ31 and up to more than 80% for alternative alloys. The uniform elongation decreases, compared to room temperature, caused by a growing superposition of recovery reactions. The high deformability of the heated tensile specimen corresponds with an enlarged phase of continuous contraction before local necking takes place. The material predominantly flows out of the width [14, 15, 24].

The dynamic properties of magnesium sheet (cycle fatigue performance, crash) have also been analysed [28–30] more frequently. The results significantly depend on the material and surface condition, the surrounding atmosphere, as well as the mechanical test parameters. Generally, the load-dependent material reactions have to be further separated and understood. In this context, the data basis should be enlarged compared to competing materials and according to real application requirements. Nonetheless, the dynamic properties do not seem to be the limiting factor for using magnesium wrought alloys in less aggressive corrosion environments.



The surface quality of commercial and laboratory magnesium sheets has been analysed by [10, 14, 31] measuring roughness and peak numbers. The topography of the sheets sometimes changes significantly with the orientation to the rolling direction. For different sheet materials providing a clean and smooth surface,  $R_a$ -values between 0.3 and 1.0  $\mu\text{m}$  are measured. According to tests [31], the roughness is lower than for commercial steel sheet St14 and Al-sheet AlMg<sub>5</sub>Mn, but shows a slightly higher straggling of the data. Peak numbers  $P_{c0.5}$  of up to 120  $\text{cm}^{-1}$  underline the perspective of magnesium sheet for outer-skin applications. Improved rolling schedules, including a final skin pass rolling with specially textured rolls, may lead to further improvements of the overall surface quality.

### 6.2.1.5 Sheet Metal Forming

#### Flow behaviour

The deformation behaviour of magnesium sheet metal is basically characterised by flow curves documented in tension tests. Thereby, the flow stress  $k_f$  describes the external stress which is necessary for plastic flow under unidirectional load. The temperature dependent flow behaviour of 1.3 mm AZ31B (Fig. 6.51) shows an intensive cold work-hardening reaction. With growing temperature, flow stresses and consolidation exponents  $n$  decrease continuously, accompanied by a simultaneous increase of logarithmic deformability. At a typical hot forming temperature of Mg-sheet metal above 200°C, the flow curve becomes very flat, showing a large phase of decreasing flow stress (at  $\varphi > 0.2$ ) before local necking takes place. This curve characteristic represents a growing dominance of thermally activated recovery and recrystallisation effects. The formability of alloys with a higher Al-content (e.g., AZ61) is normally reduced, partially related to the growing presence of brittle intermetallic phases ( $\text{Mg}_{17}\text{Al}_{12}$ ). Different from room

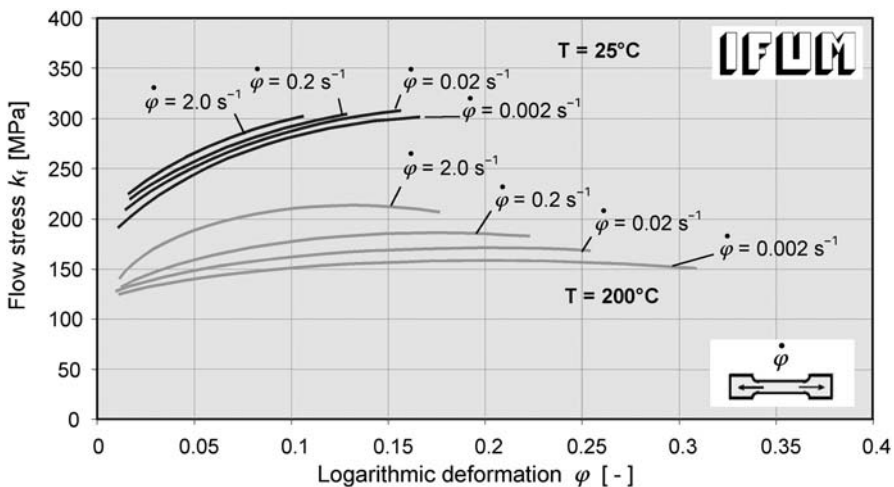


Fig. 6.51. Temperature and deformation rate dependent flow behaviour of AZ31 sheet metal [10]

temperature, the formability of magnesium sheet at elevated temperatures (200°C) is significantly influenced by the deformation rate. This behaviour is comparable to AlMg4.5Mn0.4-sheet and should be borne in mind when designing or adapting sheet forming operations [10, 25, 26].

### Drawing behaviour

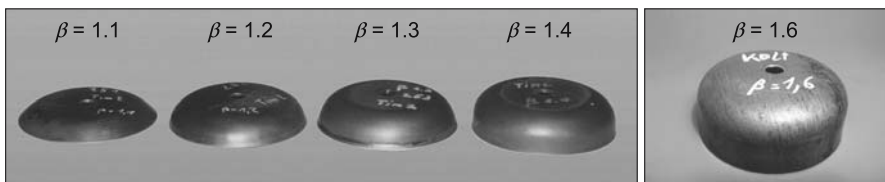
At present, much research work concentrates on the evaluation of the temperature-dependent deep drawing and stretch forming limits of magnesium sheet. The experiments were carried out using numerous different cylindrical, rectangular or ball shaped tool geometries. One main aspect is the analysis of tribological conditions e.g., the influence of lubricants, which is especially important at elevated process temperatures. As a general remark, the affinity between magnesium sheet and steel tool towards adhesion is much lower in comparison to aluminium.

### Cold forming

The transfer of the material properties under uniaxial loads to deep drawing, stretch forming or bending processes of multiaxial stresses is limited. This becomes obvious in the comparatively low cold formability of magnesium sheet. In Erichson's cupping tests AZ31 sheet reaches roughly 44% of the depth (maximum depth 4 mm, punch diameter 25.5 mm) measured for soft steel sheet St14 [32].

Deep drawing tests on annealed AZ31 sheet metal at room temperature, however, show acceptable results [32]. The cylindrical cups produced (Fig. 6.52) reach a limited deep drawing ratio  $\beta_0$  of 1.6 even at a high pressing velocity of 35 mm/s. The wall thickness increased continuously up to 18% from the bottom to the flange area of the cup. This behaviour is due to an overproportional tangential material flow caused by compression forces and correlates with comparatively high r-values above 2. The increase of hardness is moderate. An optimal punch and die design can significantly support the cold formability, and the flow behaviour can generally be improved by using increased tool radii. Special die profiles like a tractrix contour lead to significantly reduced deformation forces e.g., compared to circle geometry, and support a faultless pressing (Fig. 6.53). Figure 6.54 shows a pressing result using a tractrix contour which, by far, could not be reached with a circle die geometry.

Irrespective of the above a stepwise forming operation with intermediate annealings provides an effective opportunity for enlarging the cold drawing capabilities of flat rolled material.



**Fig. 6.52.** Cold deep drawing results: increasing drawing ratio until  $\beta = 1.6$  [31, 32]

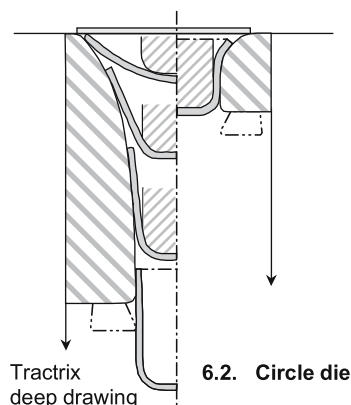


Fig. 6.53. Tractrix and conventional deep drawing processes (without blankholder) [31, 32]

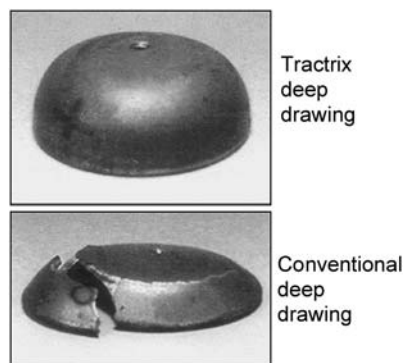


Fig. 6.54. Pressing results of different processes (parameters: room temperature, drawing ratio  $\beta = 1.5$ ) [31, 32]

For faultfree cold bending of AZ31 sheet metal a minimum bending radius of  $6t$  ( $t$  = sheet thickness) is recommended [13]. Therefore, sharp edge forming or lock-seaming operations are more or less excluded for magnesium sheet at room temperature. However, larger radii can be produced much more easily. Figure 6.55 shows a thinwalled tube of AZ31 sheet with a diameter of 60 mm and a length of 1500 mm. The geometry was cold formed in an industrial die forming process. The bending tolerances allow for a laser or electron beam welding of precision tubes such as those for hydroforming operations.

Compared to deep drawing stretch forming, which requires a material flow exclusively out of the sheet, thickness generally seems to be more critical. Nevertheless the room temperature ductility of AZ31 sheet metal seems to be sufficient to produce large thinwalled components of shallow design e.g., car body parts. Following Wagener and Lehnert [32], these prerequisites widely permit the use of established process routes and equipment of conventional sheet materials. A comparatively large springback of cold pressed magnesium parts can be ob-



Fig. 6.55. Thinwalled tube profil out of AZ31-sheet (thickness: 1.5 mm) (SZMT)

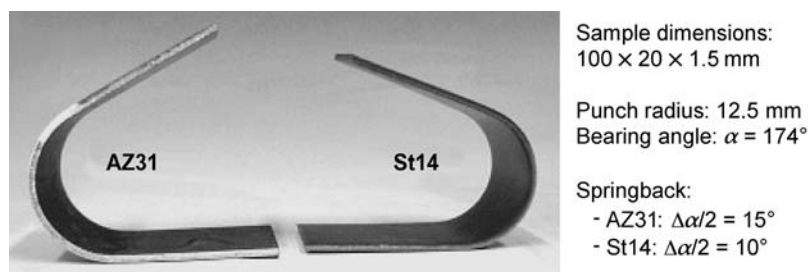


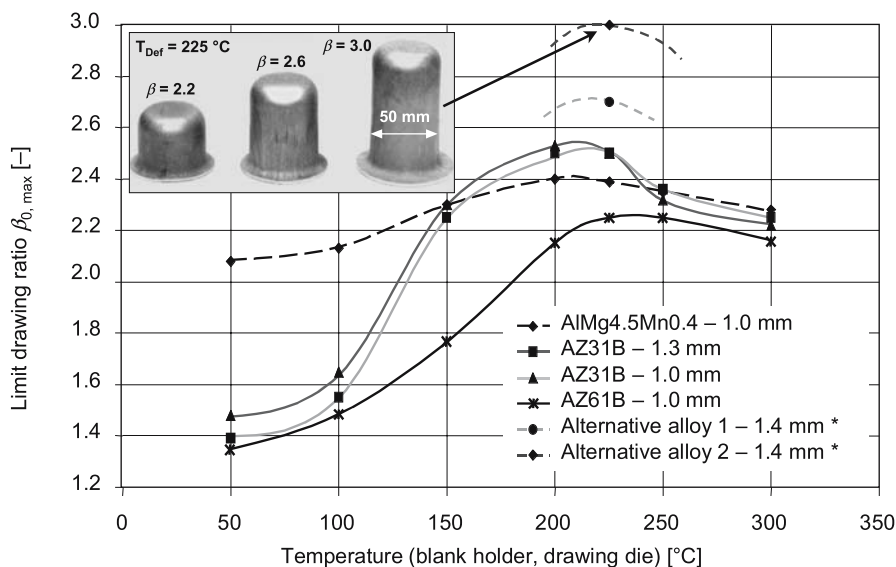
Fig. 6.56. Springback of magnesium sheet AZ31 [31, 32]

served due to the lower Young's modulus. In bending tests (Fig. 6.56), the spring-back angle measured for magnesium sheet is nearly doubled compared to steel sheet. Such effects have to be considered in tool design and can be additionally compensated by a final calibration step [31–33].

### Hot forming

On increasing the workpiece temperature, the sheet drawability increases significantly. Figure 6.57 shows representative results of single step cup drawing tests for various temperatures and alloys. The diameters of the cylindrical punches were 50 and 100 mm respectively [10, 14, 15, 34, 35]. The drawing equipment used in such operations is predominantly designed with a separately heatable punch, blankholder and die thereby offering the ability to adjust the temperature distribution in the blank before and during the forming process. Enlarged die and edge radii of up to 12 mm should be used to guarantee a successful forming operation.

In the region of 200°C, all magnesium alloy sheets show a jump-like increase in the limit deep drawing ratio, while the aluminum sheet AlMg4.5Mn0.4wt% shows a moderate increase in formability. The deep drawing ratio of the magnesium sheet AZ31 reaches a maximum level of 2.5, which was superior to the hot deformed aluminum reference material. On the one hand, new magnesium alloy alternatives offer the perspective of increasing the deformability up to  $\beta$ -values of 3.0. On the other hand, the process temperatures may be decreased down to the level of 150°C [10, 15, 34]. During the heated deep drawing operation, a slight thinning of the material is detected in the bottom radius. Turning to a rectangular part's geometry and higher press velocities, a reduced drawability has to be



**Drawing parameters:** punch diameter:  $d_0 = 100 \text{ mm}$  (\*50 mm) ; drawing rate:  $v_p = 5 \text{ mm} \cdot \text{s}^{-1}$

**References:** IFUM Hannover, Volkswagen AG, SZMT

**Fig. 6.57.** Deep drawing properties [10, 14, 15]

taken into account. Nevertheless, a box-like shape [10] reaches a limit drawing ratio of  $\beta_0 = 2.0$  using a velocity  $100 \text{ s}^{-1}$  at  $225^{\circ}\text{C}$ .

The data base for designing and simulation of forming processes (e.g., limit drawing curves) and part performance (e.g., material data under dynamic loads) has to be enlarged further. In this context, a powerful method to apply a temperature resistant surface grid to the magnesium sheet is of practical importance to carry out, for example, an automated laseroptical deformation analysis.

The excellent hot drawability of magnesium sheet offers the possibility to reduce forming and tool steps down to a single step press operation. In contact with steel tools magnesium sheet generally shows a favourable tribological behaviour which, among other things, is characterised by significantly lower adhesion effects when compared to aluminum. In the past, a variety of forming lubricants such as waxes, high-temperature oils, molybdenum disulphide or colloidal graphite, as well as different suspensions have been used with respect to the process temperature [10, 36]. Growing product requirements – especially surface quality and corrosion resistance – necessitate new lubricant solutions, which are thermally stable, health-protective and at the same time completely removable from the sheet surface. Alternatives may be friction-reducing and thermochemically stable tool coatings, which should permit a dry forming even of complex magnesium sheet parts.

In a variety of cases, therefore, the additional expenditure resulting from material heating, combined with a larger cycle time, may be overcompensated by lowering the overall tool costs.

Extensive stretch forming requires a more homogeneous heating of the sheet above 200°C. With increasing temperature, the bending properties of magnesium sheet metal are also improved. A hot bending operation of 90° using a bending radius of 2.5 may deliver acceptable results. However, a sharp edged lock-seaming operation as established for joining outer-skin car body components of steel and aluminium sheet does not seem to be the best solution for magnesium sheet. Alternative fastening concepts should be found, which are based on a more moderate sheet deformation.

### Process technology

A variety of principles are under evaluation to develop heated drawing processes and tooling systems adapted to the technological requirements of magnesium sheet.

At first, magnesium sheet can be hot worked by hammer forming quite successfully. The shaping may take place by a local gas-torch heating of the sheet and does not necessarily have to be supported by an additional heating of the tool bed. No difficulty has been found in meeting the standard tolerances of alternative materials. This method seems to be practicable for the very first prototyping of large thinwalled and complexly shaped demonstrators.

Press forming can be carried out by externally heating the sheet material e.g., using a resistance-heated furnace with active circulation to guarantee quick and homogeneous heating. For shallow shapes the drawing process then takes place in a cold tool. However, with growing complexity of the part, heated tooling systems are used. Resistance-, induction- and fluid-heating methods (e.g., oil circuit) are under evaluation. In most cases, the acting parts – punch, die and blankholder, if available, – are heated separately which offers the opportunity of a flexible and definite selection and control of the optimal temperature distribution. The sheet is heated up to the process temperature while being positioned in the nearly closed tool.

Deep drawing is predominantly carried out with a unheated cold or moderately heated punch. This leads to a favourable temperature distribution in the sheet, which allows for an intensive material flow in the heated flange. Simultaneously, the colder bottom and wall area ensure a stable transmission of the drawing forces without early material failure [5, 10, 37]. Hydraulic presses are preferred for forming magnesium sheet because of their moderate pressing velocity which can be controlled precisely. For the prototyping of magnesium sheet parts, conventional cast-iron or steel tools which have originally been constructed for processing steel or aluminum sheet are often used [38]. In some cases, the radii of the tool shape have to be modified. Droeder [39] reported about prototyping tools consisting of aluminium powder bonded with temperature-resistant epoxy casting resin, which should represent a cost- and time-saving alternative.

Further developments are focused on a segmented heating of blankholder and die according to local deformation requirements of the part. Investigations with a rectangular component geometry proved that a distinct extension of the forming limits is possible by increasing the flange-temperatures in the more severely formed corner areas and by reducing the temperatures in the straight sections

[10, 34]. As a basis for series operations, these measures generally increase the safety and reproducibility of the forming process leading to defined technological properties. In parallel, consequent heat isolation between the hot tool and press body should lead to an improved dimensional accuracy (close tolerances) of the pressed part.

As a future perspective, continuous coil-fed press operations are conceivable, with better materials' utilisation and productivity than the hot forming of single magnesium sheet. For retrofitting a conventional work station for magnesium, it was proposed to integrate only a stock preheater and a heated roll feed system [3].

Alternative techniques like superplastic forming [40] and hydroforming [41] with heated media are also discussed for magnesium sheet. They may have particular attraction for special products and small series applications. These processes seem to be able to further enlarge the design potential and surface quality of magnesium sheet parts. The superplastic forming of aluminium sheet outer-skin components has recently been established. Hot spinning operations should also be kept in mind with respect to rotationally symmetrical parts like car wheels [3].

#### **6.2.1.6 Prototyping and Application Perspectives**

Further prototyping examples (Fig. 6.58) show the perspectives of magnesium flat rolled products for a variety of different application areas.

Referring to the automotive sector, magnesium sheet offers new opportunities for ultralight constructions, primarily in the car body, but also in chassis, interior and motor components. The potential of magnesium sheet for dynamically loaded components was proved successfully.

Reports [25, 42] exemplarily describe the design, prototyping and testing of a front bumper system of a series vehicle. Magnesium bumper beams (Fig. 6.58a) were produced by Benteler Automotive in Paderborn, Germany, using a preheated AZ31 sheet metal blank and the cold tool of a series steel bumper. The hydraulic pressing needed no further modification of the process and was carried out without any lubricant. The mechanical properties of the thinwalled beam profile are nearly equivalent to the initial sheet quality. Tensile tests according to DIN EN 10002 lead to an ultimate tensile strength of  $R_m = 235$  MPa, a yield strength of  $R_{p0.2} = 140$  MPa, a uniform elongation of  $A_g = 16$  % and an elongation to a fracture of  $A_{80} = 20$ %. The magnesium bumper beam was joined to crash boxes out of stainless steel using a combination of riveting and adhesive bonding. First automobile standard crash tests reveal a good deformation characteristic of the magnesium beam without any cracks. The complete hybrid system showed a good impact strength and a satisfying energy absorption. A further optimised bumper system enables a weight reduction of about 2 kg compared to a similar construction of high strength steel sheet.

Furthermore, an instrument panel designed as a laser or electron beam-welded double shell or a thinwalled longitudinal seam profile represents another component belonging to the group of interior and non-visible parts with comparatively moderate corrosion resistance and surface quality requirements. In this respect Stoffig GmbH in Germany carried out various pilot production tri-



als using conventional press tools technology without blank holder. The modular die systems were heated by an oil radiator heating device. By means of complex shaped bracket elements (Fig. 6.58b), the reproducible fabrication in a series process could be demonstrated. Such parts may be used without any additional surface treatment and can lead to significant weight savings. According to these prototyping results, seat components may be another interesting area (Fig. 6.58c).

Pressing trials at Volkswagen also confirm the formability of large thinwalled car body components. The inner door panels of a passenger car (Golf 2) has been successfully formed at temperatures of roughly 220°C (Fig. 6.58d). The slightly modified series tool system was preheated using resistance mats. The large AZ31 single sheets (1700 × 1250 × 1.4 mm) required were produced by Salzgitter AG [14, 15]. Further developments are directed towards the hybrid engine bonnet of a 3L-Lupo [26] (Fig. 6.58e). The inner bonnet consists of Mg-sheet AZ31 with a thickness of 1.4 mm. Cutting and punching operations can be carried out cold with series equipment. The aluminium sheet outer skin (thickness 1.1 mm) of alloy AlMg0.4Si1.2 wt%) is joined using a combined lock-seaming and adhesive bonding process. Aluminium hinge and lock reinforcing sheets are fastened with Al-rivets. The weight reduction compared to a complete aluminum sheet construction amounts to nearly 1 kg. Sheet metal products of SZMT already perform successfully in Volkswagen's recently presented 1 L-car.

With respect to hybrid structures, a variety of mechanical joining techniques for integrating magnesium sheet are rapidly developing at the moment. Methods based on intensive material deformation like clinching or riveting generally require a sufficient local heating of the joining zone. This can be realized by heated tools, as well as external heating sources (e.g., laser beam). Fastening elements such as riveting or punching nuts are partly usable without heating [25, 43, 44].

Additional weight savings can be realised more efficiently by introducing magnesium sheet in outer-skin applications. In this regard, Opel AG, Germany presented the roof of its G90 demonstrator car in 1999, which was hand-formed at room temperature and adhesive-bonded to the body structure [45] (Fig. 6.58f). Recently, Salzgitter Automotive Engineering GmbH prototyped an ultralight front fender from 1.2 mm AZ31 sheet metal. This geometrically ambitious part could be hammer-formed successfully at temperatures of about 200°C (Fig. 6.58h). The magnesium sheet fender weighs less than 1 kg, whereas a conventional 0.75 mm steel part having comparable bending stiffness is more than 2.5 times heavier at 2.5 kg.

For prototype assembly or repair weldings, established processes like laser or shielded arc welding are qualified for magnesium sheet. Nearly faultless welding joints can be formed without porosity leading to very acceptable strength and ductility properties [46-48]. High quality filler wire of different wrought alloys is now available (Drahtwerke Elisenthal), which further enlarges the welding opportunities of magnesium sheet in terms of quality, flexibility and productivity (process automation). Alternative methods like non-vacuum electron beam or resistance welding have been evaluated less intensively.

Sandwich components can also lead to ultralight and extremely stiff structural material. Figure 6.58g shows the cold bended interior covering sheet for railway





**Fig. 6.58.** Further examples and perspectives of applications of Mg-sheet [15, 25, 42, 54–57].  
 a Prototype magnesium bumper beam (Benteler Automotive); b Bracket element (Stolfig);  
 c Seat component (IFUM); d Inner door panel (Volkswagen); e Hybrid Al/Mg engine bonnet  
 (Volkswagen); f Prototype car Opel G90 with Mg-sheet roof; g Sandwich component – Interior  
 covering panel (Rono Systemtechnik); h Prototype front fender (SZA); i Mg-tailored blank

vehicles, which consists of a polycarbonate honeycomb core structure conglomerated on both sides with a 1.0 mm magnesium sheet layer.

Further perspectives for magnesium sheet can be expected in the aircraft and aerospace industry. This also applies for the communication and electronic sector (e.g., housings for mobilephones or computers), where weight, mechanical stability, heat resistance, electromagnetic shielding, thermal conductivity and damping behaviour play a significant role. Additionally the large field of automation systems, aiming at a mass reduction of high precision and flexible handling facilities, as well as high speed production machines, seem to be of special attraction. Other fields are leisure, sports and medical technology, in addition to the classic areas of printing plates or batteries [3, 49].

The technical key factor for many potential series applications is an acceptable corrosion protection of the component. Treatment measures must be adapted to the different requirements of the part. Similarly, attention has to be paid to galvanic corrosion aspects depending on the assembly of hybrid structures.

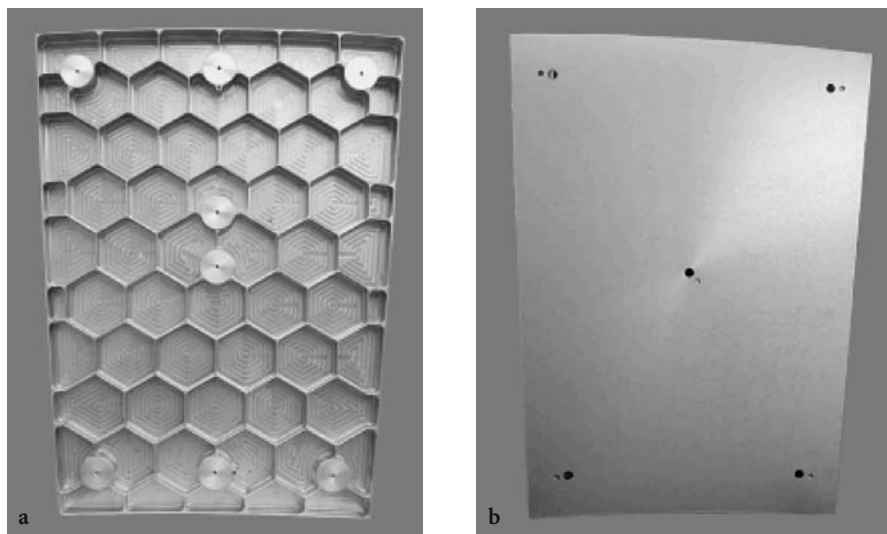
Currently, a surface treatment of magnesium sheet components should be applied to the pressed part. After cleaning, an etching process is normally carried out to remove the oxide skin developed during the rolling and sheet forming step. For further passivation, chromate free conversion treatments, as well as anodic oxidation methods are commercially available and environmentally acceptable [50–52]. They provide a powerful corrosion protection comparable to an ordinary chromatising (Chap. 7). The surface finish is done, if necessary, by a multi-layer organic coating. For hybrid structures the varying chemical behaviour of different materials have to be considered. For example, the Mg-sheet component of Al/Mg-engine bonnet (Fig. 6.58e) at first undergoes a separate dip- and powder-coating procedure. Afterwards, the joined hybrid part passes the conventional treatment for Al-sheet [53]. For future volume applications, surface treatment processes suitable for all construction metals will have to be developed.

Regarding the automotive sector, the corrosion treatments mentioned above should guarantee a satisfying protection of the interior or the non-visual area. In addition to that, further improvements have to be made for outer-skin applications being influenced by stoning and a more aggressive environment. The self-healing function of conversion coatings available seems to be mostly insufficient.

Especially in non-automotive applications Magnesium plate can also be used as a basis for structural parts. Figure 6.59 shows the ultralight prototype panel of a radiotelescope completely machined out of a single Mg-heavy plate of the alloy AZ31. Lightweight, stiffness and high geometric precision can be ideally combined. This component represent similar areas of application in aerospace, electric equipment and high performance machines.

#### **6.2.1.7 Concluding Remarks and Outlook**

In comparison to magnesium castings and other competing materials, magnesium sheet offers a variety of technical advantages. It has the potential to open new perspectives for ultralight constructions with high strength, ductility and surface requirements. The large resources and the high recycling potential predestines magnesium sheet as one of the future materials.



**Fig. 6.59.** Ultralight prototype magnesium telescope panel. Telescope component, machined out of a 50 mm-thick Mg-plate of AZ31; dimensions : 630 × 820 mm; **a** Panel rear side; ribbing structure designed by Böhm; **b** Panel front side; shape precision of the paraboloid < 10  $\mu\text{m}$  RMS (with kind permission of Böhm, Germany)

A remarkable amount of part developments and prototyping activities has already been started using magnesium sheet products delivered by Salzgitter Magnesium-Technologie GmbH [54, 55]. The hybrid engine bonnet, the front fender, as well as the crash-relevant parts previously mentioned impressively represent the design and application opportunities for the automotive sector.

Further improvements must be made in terms of sheet quality, material processing and treatment to use magnesium sheet components in series applications. Salzgitter Magnesium-Technologie GmbH has recently started an industrial production of tailor made and high quality Magnesium flat rolled products in Salzgitter, Germany. The company offers a complete technology and material partnership for product development and series applications [56]. Such strategic projects should help to overcome the niche position of Mg-wrought alloys.

At the moment, its comparatively high price limits a wider use of magnesium flat rolled products. This mainly results from the small scale and multi-step production processes rarely adapted to magnesium. Optimised process chains have to consider and fully utilise the material's working behaviour. They also need to include a powerful recycling loop to reuse significantly cheaper secondary alloys.

An economical use of magnesium sheet, competitive with aluminum, needs an intensive development of the market. For now an increased readiness of potential customers to test the material performance in niche products would be helpful. Increased demand will certainly be accompanied by the availability and acceptable delivery performance of high quality magnesium flat rolled products for series parts.

## Acknowledgements

Many thanks to my colleague Sébastien Wolff from Salzgitter Magnesium-Technologie GmbH for supporting the design of this chapter. The following companies and research institutes are also gratefully acknowledged for contributing new R&D results and photographs, as well as for giving further assistance:

- Salzgitter AG, Salzgitter, Germany
- Salzgitter Automotive Engineering GmbH (SZAE), Osnabrück, Germany
- Volkswagen AG, Wolfsburg, Germany
- DaimlerChrysler, Sindelfingen, Germany
- Institute for Metal Forming and Metal Forming Machine Tools (IFUM), University of Hanover, Germany
- Metal Forming Laboratory, University of Kassel, Germany
- Stolfing GmbH, Geisenfeld, Germany
- Adam Opel AG, Rüsselsheim, Germany
- Benteler Automobiltechnik GmbH & Co. KG, Paderborn, Germany
- Böhm Feinmechanik und Elektrotechnik GmbH, Seesen-Rhüden, Germany
- Rono Systemtechnik GmbH, Ilsenburg, Germany

### 6.2.2 Extrusion, Forging

*Bernard Closset*

#### 6.2.2.1 Production of Cast Stock

Pure magnesium (99.8%; 99.9%; 99.95%), with its hexagonal lattice ( $c/a = 1.624$ ) and atomic diameter (0.32 nm), is seldom used for structural applications. To obtain good mechanical properties for a wide range of applications it is necessary to add other elements to pure magnesium but still maintain a good castability. The alloying potential is influenced by the atomic sizes and the solid solubility of the added elements. In most cases, binary alloy phase diagrams exhibit in the magnesium – rich sections a eutectic transformation with few exceptions of elements such as, manganese and titanium, which show a peritectic reaction. Aluminum is the most widely used alloying element because of its favourable effect on castability. For example, the binary Mg-Al phase diagram, shown in Fig. 6.60, exhibits a maximum solid solubility of aluminum of 12.7% in magnesium at 437°C. For practical purposes, binary alloy systems are rarely employed to cast parts, billets and slabs. Today, the four most common wrought alloy systems used for industrial applications are:

- AZ series : Mg-Al-Zn
- ZK series : Mg-Zn-Zr
- AM series: Mg-Al-Mn
- RE series : Mg-Re-X

Table 6.17 summarises a few chemical compositions of the main wrought alloys currently in use.

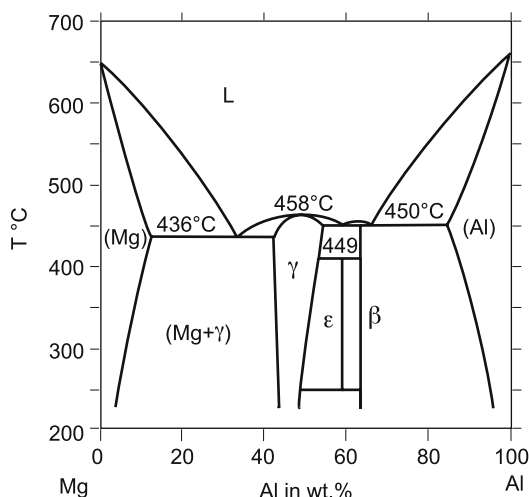


Fig. 6.60. Mg-Al phase diagram [57]

Table 6.17. Chemical composition of typical wrought magnesium alloys

Alloy	Al	Mn	Zn	Zr	RE	Fe	Other
M1	0.01	1.5–1.3	–	–	–	0.030	–
AZ21X	1.6–2.5	0.15	0.8–1.6	–	–	0.005	0.1–0.25 Ca
AZ31B	2.5–3.5	0.2–1.0	0.7–1.3	–	–	0.005	0.04 Ca
AZ61A	5.8–7.2	0.15–0.5	0.4–1.5	–	–	0.005	–
AZ80A	7.8 – 9.2	0.15–0.5	0.2–0.8	–	–	0.005	–
ZK40A	–	–	3.5–4.5	0.45	–	–	–
ZK60A	–	–	4.8–6.2	0.4	–	–	–

Notes: Fe: max.; Zr min.; Ca: max; Mn: max; Al: max.

The AZ series are at present of the highest commercial importance. The alloys are relatively inexpensive to produce due to the aluminum content and easy to fabricate. The presence of aluminium allows a significant solid solution strengthening. The alloys of the AZ series developed over a half a century ago have seen only some minor adjustments in the chemical composition. The importance to keep iron, copper and nickel levels well below 50 ppm is known to limit the corrosion of magnesium alloys. Lower impurity levels are usually obtained in magnesium produced by the thermal reduction process. In general, magnesium production by electrolysis has a tendency to contain higher iron levels. Therefore, a treatment based on the addition of manganese has been developed to iron. At an adequate manganese level and in a given temperature range, ternary aluminum – iron – manganese intermetallics are formed and precipitate out of the melt before the start of the casting step. For example, this explained the high manganese upper limit (1.0%) in the AZ31 B alloy. If the starting magnesium is very low in iron (<0.005%) then it is possible to produce

AZ31 alloys with a manganese level below 0.005%. Consequently the formation of manganese based compounds, most likely,  $Al_6Mn$ , is avoided resulting in higher ductility and better formability. Machining properties are also improved by extended tool life during cutting, milling and drilling operations.

The presence of zirconium in the ZK series, leads to a fine grain structure. As a result good formability is obtained making the ZK series well suitable for forging applications.

The fine grain structure is the main reason behind the excellent strength (including fatigue) but affects negatively the creep resistance. Stress corrosion cracking resistance in these alloys is moderate. The high zinc level reduces the weldability.

To overcome poor creep resistance of AZ and ZK alloys at elevated temperatures and the limited weldability, thorium and RE containing alloys are available or have been developed [58]. The elevated temperature properties of the extruded Mg-Y-RE-Zr alloys are significantly better when compared to the yield strength of an AZ80 alloy.

### **Melt preparation and Alloying**

Magnesium alloys are produced from liquid cell magnesium or by melting solid magnesium ingots in steel pots heated in oil, gas, electric or induction furnaces. Aluminum and zinc may be added by plunging a perforated cage in molten magnesium and kept in a temperature range of 700–750°C. A gentle stirring movement of the cage facilitates the alloying and minimises the possibility of segregation. Manganese is added generally in the form of a salt (manganese chloride). Metallic manganese or a manganese containing hardener is also a possible solution.

The addition of zirconium, rare earths, and thorium can be carried out at the smelter or at the foundry. Zirconium is added in the form of a hardener.

After alloying, the metal is kept still in a holding furnace to settle out impurities, particularly iron before ladelled or pumped into ingot moulds or single/multiple strands of a vertical direct chill caster.

During melting, alloying, refining and casting, the molten metal surface is protected by salt fluxes and/or a mixture of gases containing amongst others either  $SF_6$  or  $SO_2$ . Although  $SO_2$  is toxic at high concentrations and has a propensity to react with humidity, some smelters and foundries have been using this protective gas method successfully. The use of  $SF_6$  has grown gradually over the last few decades because of its non-toxicity and good molten magnesium surface protection capacity. Recently, at the Kyoto summit in 1997,  $SF_6$  was identified as having a high global warming potential (GWP). The European Union is planning to implement in the coming years legislation that will monitor and restrict the use of "F" gases such as HFCs, CFCs and  $SF_6$ . Research is being carried out to find a substitute for  $SF_6$  in the magnesium industry [59].

### **Metal Cleanliness**

Metal cleanliness has a strong influence on mechanical properties and corrosion resistance. The detrimental effects of heavy metals such as iron, copper and nickel on the corrosion resistance of magnesium castings alloys have been demonstrated [60]. In particular, iron should be kept below 0.002% to avoid an increase

in the corrosion rate and an excessive use of manganese additions to compensate for higher iron levels. Non-metallic inclusions decrease the metal fluidity [61]. This could result in poorer castability by changing the solidification parameters.

Porosity through macro and microshrinkage can occur. The most common non-metallic inclusion found in magnesium is magnesium oxide (MgO).

The introduction of ceramic filters between the launder and the casting table could greatly reduce the entrapment of oxides in ingots, billets and slabs. An apparatus measuring the size and distribution of inclusions online has been developed for magnesium [62]. It could provide magnesium producers and users with a good opportunity to control online liquid metal quality levels.

Hydrogen is soluble in pure magnesium and magnesium alloys [63]. At levels above the maximum solid solubility of hydrogen (29 ppm) in pure magnesium, it was found that large gas holes are formed. In AZ91, the maximum solid solubility of dissolved hydrogen was determined to be 24 ppm. Castings, made from metal containing more than 24 ppm of hydrogen, showed large gas holes. Below 24 ppm of hydrogen the casting microporosity was directly proportional to the dissolved hydrogen level. Degassing of non-zirconium containing melts is performed by adding compressed hexachlorethane tablets to the bottom of the melt. These tablets, through carbon inoculation, also provide a grain refining effect. In zirconium containing alloys both degassing and grain refining takes place with the addition of zirconium.

**Casting**

The vertical direct chill casting technique is the preferred method to produce wrought magnesium alloy billets and slabs. Casting in thick-walled iron or steel permanent moulds is a possible alternative to obtain billets and slabs. Horizontal direct chill casting could also be envisaged. Today only pure magnesium has been successfully cast using a Properzi-type technique. In the past, strip casting has also been envisaged. Currently, research is being conducted at a Canadian University on magnesium strip casting. Such a technique would be ideally suited to economically produce the pre-formed material for magnesium alloy sheet rolling. More recently, attempts have been made to develop a novel continuous casting process for magnesium [64]. This concept is characterised by the upward drawing direction of the billet. The main advantages are: easy molten metal dosage, little exposure of liquid metal to the atmosphere, excellent temperature control and safe casting.

Continuous casting of magnesium differs significantly when compared with the process used for more common metals such as steel, aluminum and copper. Besides the need to protect the liquid metal, thermophysical parameters, e.g., heat of fusion and thermal capacity differ significantly, as shown in Table 6.18.

**Table 6.18.** Comparison of specific heat of fusion and heat capacity

Metal	Mg	Al	Cu	Steel
Specific heat of fusion (KJ/dm <sup>3</sup> )	640	1074	1829	2143
Specific heat capacity at 530°C (KJ/dm <sup>3</sup> )	2.23	3.07	3.89	5.42



The thermophysical data of magnesium are very low over even when compared to aluminum. The mould design and the cooling system associated with the continuous casting equipment have to be engineered to take advantage of the relatively low-level of heat to be extracted during solidification.

Magnesium billets and slabs are best produced by the direct chill (DC) casting technology. The automated process has enabled the routine production of higher quality magnesium in large format shapes at attractive economical levels.

### **Billet Production**

The production of magnesium billets for extrusion is not yet as competitive as that for aluminium. Magnesium wrought products like those in aluminum have melting, alloying, and casting process stages as part of their production route. With the low heat capacity of magnesium, one would have assumed that the continuous casting rate should be at least as high as for aluminium or very significantly better. But in order to obtain competitive properties it is necessary to increase the alloy content of magnesium. As a result the tendency to hot shortness and the formation of cracks is increased.

Magnesium billets can be produced in a single or multistrand caster. For larger diameter billets, ranging from 500–600 mm the single or dual strand casting method is favoured. Slabs and T-bars up to 300 mm × 850 mm have been cast by the dual strand technique. For example, 55 tonnes of a 570 mm diameter ingot can be cast per day by using two strands [65]. Traditionally, magnesium billets of large diameter (500–550 mm) were produced with an open-top technique. As a result the cast speed was low and only 1000 kg of a 535 mm diameter ingot could be produced in an hour. By increasing the number of strands to 20 and reducing the ingot diameter to 180 mm the productivity could be tripled to reach 3,000 kg/h [66]. For a given billet diameter the casting speed is limited by the alloy composition and the metal temperature. Therefore, a higher number of strands, is one of the alternatives to increase productivity without causing casting defects such as centre cracks.

Hot-top processes can be adapted for the casting of magnesium extrusion billets. New mould technology and materials also have a positive effect on casting productivity and billet surface quality. The short mould design with graphite lining in an aluminium frame and a gas insulation cushion between the mould wall and the metal allow a narrow solidification zone. As a result a smooth casting surface is obtained with small defects such as cold shuts, dragmarks or segregation. Therefore, for the production of billets and slabs without surface scalping of approximately 10 mm from the ingot surface can be envisaged. Since the metal is protected from oxygen with inert gases during casting, the surface contamination is minimized. The presence of oxide particles is reduced to  $< 1$  count/cm<sup>2</sup> compared to a level as high as 100 counts/cm<sup>2</sup> for conventional gravity cast ingots.

During solidification pure magnesium undergoes a large volume contraction of the order of 4.5%. Therefore magnesium and magnesium alloys have a higher tendency to form shrinkage cavities. The direct chill casting technique through continuous feeding and controlled cooling of the mould during solidification avoids the formation of shrinkage porosity.



**Table 6.19.** Effect of grain refining on tensile properties [66]. Alloy: A31B

Extrusion speed	3.12 m/min		28 m/min	
	As cast billets	Grain refined billets	As-cast billets	Grain refined billets
Tensile strength (MPa)	255	260	245	255
Yield strength (MPa)	210	220	180	190

Generally, direct chill continuous cast billets are characterised by large columnar grains. An efficient grain refining method or product applied to AZ31 billets results in small equiaxial grains. Fine grains improve the extrudability of the billets. The extrusion pressure can be reduced and the extrusion speed increased by a small increment. Mechanical properties are only slightly increased (see Table 6.19).

Grain refining of billets increases the tensile and yield strength by 5%. An increase in the extrusion speed reduces the tensile strength slightly and the yield strength of the order of 10%.

### 6.2.2.2 Extrusion

#### Extrusion Methods

As with aluminum, magnesium billets are extruded into profiles of various shapes using all the different extrusion techniques: direct, lubricated and non-lubricated and indirect extrusion. Impact extrusion is mainly chosen for producing thin wall tubular forms with a length-diameter ratio between 5 and 1 and between 10 and 1.

The direct and indirect methods are the two preferred magnesium extrusion techniques. There are two possible routes to extrude magnesium billets:

- the pre-extrusion route, and
- the direct route

as illustrated in Fig. 6.61.

The pre-extrusion route is currently the favoured route to obtain extruded magnesium profiles. Large diameter billets, up to 550 mm or more, depending on the casting equipment and mould sizes, are DC cast in single or multi-strands. After cutting the DC cast product to an adequate length, the billets undergo a scalping operation, which consists of removing 5–10 mm from the rough as-cast surface. In order to obtain a homogenised structure, as-cast billets can be heated to a temperature in the 300–500°C range prior to this pre-extrusion phase.

Depending on the alloy composition and billet size, the pre-extrusion step is carried out at a relatively high extrusion speed in the 30–50 m/min range on a large capacity press (50,000 RN). The reduction in the cross-sectional area can vary from 5–1 to 10–1. The main objective of the pre-extrusion phase is to obtain fine and uniformly distributed grains. The grain size of the pre-extruded billets is mainly a factor of extrusion temperature and speed, and the deformation ra-

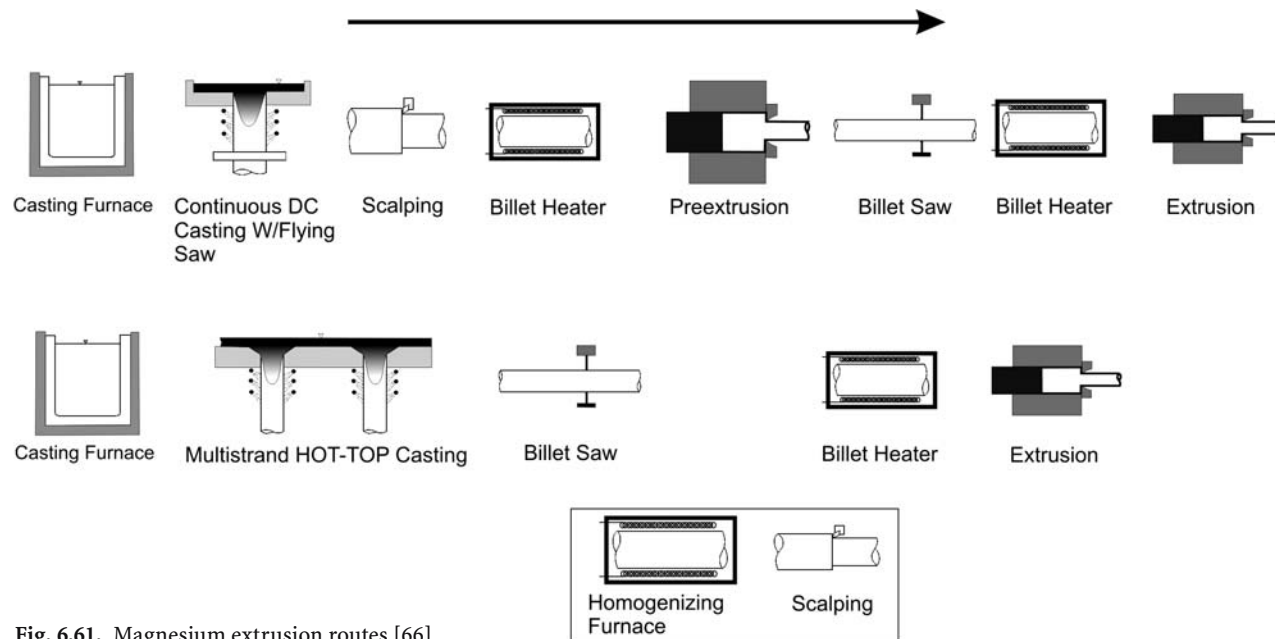


Fig. 6.61. Magnesium extrusion routes [66]

tio. Due to the presence of fine grains, the pre-extruded billets have an excellent extrudability.

Before the final extrusion step, the billets are cut to the desired length, which is a function of the final shape and then preheated to a temperature in the 300–450°C range. Direct extrusion of the final shapes is performed at speeds varying from 3–30 m/min. The AZ31 alloy is widely used for extrusion because it offers a good extrudability, which is synonymous with a high extrusion rate such as 20 m/min.

Other extrusion alloys such as AZ61A, AZ80A and ZK60A offer higher mechanical properties especially tensile strength but to the detriment of extrudability, which can be greatly reduced by a factor of 10. On the other hand, the extrusion economics can be substantially improved by constructing dies with multiple holes.

In a possible direct route the pre-extrusion step is eliminated. The good billet surface quality of multistrand hot-top casting and the smaller ingot diameters (150–200 mm) allow the elimination of the time consuming pre-extrusion phase. After cutting the billets to the required length it is recommended to homogenise the billets followed by a slight scalping if the maximum extrusion speed is sought. The billets are preheated in a 300–450°C temperature range prior to the extrusion.

In most instances the direct extrusion process is employed for magnesium alloys (Fig. 6.62). The container, dummy block and die are kept at the same temperature as the billet but 25–50°C below the extrusion temperature. Various plain and hollow shapes can be produced using the direct process. Tubes can be produced by extruding a hollow billet over a centred mandrel located inside the main ram.

Indirect extrusion is seldomly used for magnesium alloys. The die is pressed with a hollow ram towards the billet. The friction between the billet and the container is significantly reduced and less pressure is necessary. In this process the friction between the die and the container is avoided. As a result a higher deformation ratio is possible and more complicated shapes with thin walls can be obtained. Very often the indirect extrusion is used at the start of the direct extrusion process because the friction force is eliminated. The final extrusion phase is carried out by the direct method.

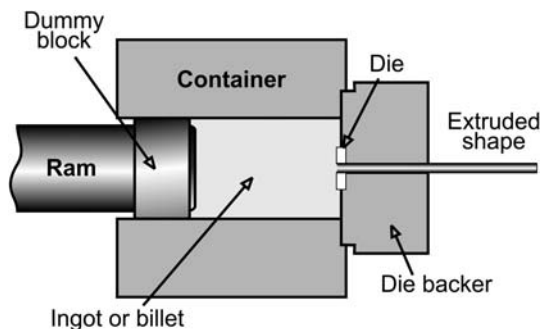


Fig. 6.62. Main components of the direct extrusion method [67]

Impact extrusion is limited to the production of tubular or other symmetric shapes. Magnesium alloy slugs or blanks are prepared by using pre-extruded bars and blanking sheets.

Dies, slugs and blanks are preheated to a minimum temperature of 175°C. Higher levels of deformation are achieved, such as length to diameter ratios between 10 and 1 and between 15 and 1.

Impact extrusion of magnesium alloys requires presses up to 900 kN capacity. Graphite coated slugs and dies are usually heated to the 175–370°C range, depending on the alloy composition and the operating rate could be as high as 100 extrusions/min. At increasing operating temperatures, the extrusion pressure is gradually reduced from 455 MPa at 230°C to 317 MPa at 400°C for an AZ31B alloy for a given reduction in area of 85%. A higher level of alloying elements increases the extrusion pressure. Impact extrusion can produce parts with a wall thickness as low as 0.5 mm and tolerances between 5 and 10%. Typical applications are cylindrical magnesium alloy AZ21 battery containers with a wall thickness of 1 mm, a height of 80 mm and an outside diameter of 20 mm.

### Extrudability

The extrudability of magnesium alloys can be measured by the extrusion speed. In general, magnesium alloys exhibit a lower extrusion speed than aluminum alloys and are carried out at a higher pressure level. Although higher extrusion speeds are sought for economical reasons there are limitations due to hot shortness tendencies and a reduction in mechanical properties. Indirect extrusion is a possible solution to achieve higher extrusion speeds but the mechanical properties could be negatively affected.

In evaluating extrudability not only extrusion speed has to be considered, but mechanical properties and surface quality of the shapes produced as well. In general the extrusion speed is limited by such parameters as:

- blistering
- hot shortness
- mechanical properties.

Blistering is directly related to the surface quality of the billets. The presence of surface oxidation and solidification segregation are the main causes for the formation of blisters during extrusion of profiles. By controlling the extrusion speed, and scalping and homogenising the billets before extrusion, blistering can be significantly reduced or even avoided. Various shapes can be produced from pre-extruded 180 mm billets with a cross-sectional area reduction ranging from 40–50% at an extrusion speed of 30 m/min without the formation of blisters. A good billet surface quality is a determining factor in achieving high extrusion speeds without blistering.

Hot shortness occurs when low melting phases in the billet are remelted during extrusion. Therefore, alloy composition, billet microstructure and extrusion temperature are the main parameters which influence hot shortness. Both billet homogenisation and a reduction in billet temperature have a beneficial effect on hot shortness and consequently allow a higher extrusion speed. Depending on

the extruded shape a billet temperature as low as 300°C is recommended for an AZ31B alloy.

An increase in extrusion speed from 3 m/min to 50 m/min results in a decrease of the yield strength of an AZ31 alloy extruded at 360°C into a 50 × 10 mm flat bar from 200 MPa to 180 MPa while the elongation is increased from 10 to 14% and the tensile strength at 250 MPa is maintained.

For the AZ type of alloys, the binary compound  $Mg_{17}Al_{12}$  forms as an incoherent precipitate. Its low melting point of 438°C causes hot shortness during extrusion. The presence of this compound in alloys containing high aluminum levels such as AZ61 and AZ80 is mainly responsible for the slow extrusion rates compared to AZ21 and AZ31 alloy. For greater formability at higher temperatures billet homogenisation is required especially for AZ61 and AZ80 alloys.

Generally, the higher alloy content reduces the process throughput of casting and forming equipment. The production rate of 200 mm diameter pre-extrusion billets is the highest for AZ21 alloy but is divided by 2 and 3 for respectively AZ61 and AZ80 and ZK60 alloys. The form factor must also be taken into account when extrudability of different alloys and shapes are compared. For a given shape the extrusion rate of an AZ61A pre-extruded billet can be 50 to 60% slower than for an AZ21 alloy.

### Extrusion – Shapes

Magnesium extrusions are available in several standard alloys and forms. For room temperature to moderately – elevated temperature applications, alloys from two alloy systems (Mg-Al-Zn and Mg-Zn-Zr) with a moderately low to high properties are selected. The extruded forms in which the main alloys may be obtained are given in Table 6.20.

Due to their poor weldability tubes and hollow shapes in AZ80A are not available. The extrusion forms and definitions are listed below:

Rod:	A round solid section with a diameter greater than 10 mm
Bar:	A symmetrical solid section which is square, rectangular, polygon with a distance between parallel faces greater than 10 mm
Tube:	A symmetrical hollow section which is square, rectangular, polygonal or elliptical with a uniform wall thickness. Tubes can be produced with and without seams

**Table 6.20.** Extruded magnesium alloys and forms

Extruded form	AZ21	AZ31B	AZ61A	AZ80A	ZK60A
Rod, bar, solid shapes	×	×	×	×	×
Structural shapes	–	×	×	×	×
Wire	–	×	×	–	–
Tube	×	×	×	–	×
Hollow & semi-hollow shapes	×	×	×	–	×

Solid shape:	Any extended solid shape with a non-symmetrical cross-section
Hollow shape:	An extruded shape section with a closed void. There are three classes of hollow shapes defined according to the size and the distribution of the void in a cross-section
Semi-hollow shape:	An extruded shape whose cross-section partially encloses a void
Form factor:	A calculated number that gives an indication of the expected difficulty to extrude a shape
Circumscribing circle:	The smallest diameter circle that will surround the extrusion or cross-section without touching the perimeter

Typical magnesium extruded forms are: rods, square, rectangular, hexagonal bars, equal and unequal angles, I-beams, H-beams, T-shapes, Z-shapes and channels. Section thickness and wall thickness are a function of shapes, cross-section sizes and alloy type. For rods, bars, solid, hollow, and semi-hollow shapes the minimum section thickness increases with the increase of the circumscribing circle diameter. For example, for a small circumscribing circle diameter (CCD) of 25 mm the minimum section thickness for AZ31A, AZ61A, AZ80A and ZK60A alloys extruded in the form semi-hollow shapes is 1 mm. For a higher CCD of the order of 190 mm the minimum section thickness is 2.8 mm for an AZ31B alloy and 3.2 mm for AZ61A, AZ80A and ZK60 alloys. Hollow shapes are more difficult to extrude than solid shape and semi-hollow shapes. For example, the minimum section thickness is 3.2 mm for hollow shapes with a 190 mm CDD extruded in an AZ31B alloy. The maximum wall thickness surrounding a void is of the order of 20 mm for hollow shapes and tubes extruded in AZ31B, AZ61A, ZK60A alloys. The minimum wall thickness for tubes increases with the outside diameter.

AZ21 and AZ31B alloys are extrudable with a smaller minimum wall thickness than the corresponding AZ61 and ZK60A alloys. AZ80A alloys are generally not extruded in the forms of hollow shapes and tubes. For an equivalent CDD, non-round tubes require a higher wall thickness than round tubes. The standard section thickness and wall thickness limits are a general indication of the extrudability of common magnesium alloys. Deviations from these limits are possible depending on the specific shape.

Magnesium extrusions can be produced with good dimensional tolerances. Cross-sectional and diameter tolerances of  $\pm 0.5\%$  to  $\pm 1.0\%$  are routinely achieved. Wall thickness tolerances of  $\pm 1\%$  can be achieved for a 130 mm diameter tube with a 15 mm wall thickness. Magnesium extrusion offers also good angularity, contour, flat surface, straightness twist and length tolerances. Surface roughness tolerances for magnesium bars, rods, shapes and tubes vary as a function of section thickness. A 0.1 mm depth of a defect is allowable for 10 mm section thickness.

### 6.2.2.3 Magnesium Extrusion Fundamentals

Extrusion of magnesium alloys is a typical case of hot-working practice where a heated billet is deformed into the required shape at a rate determined by the

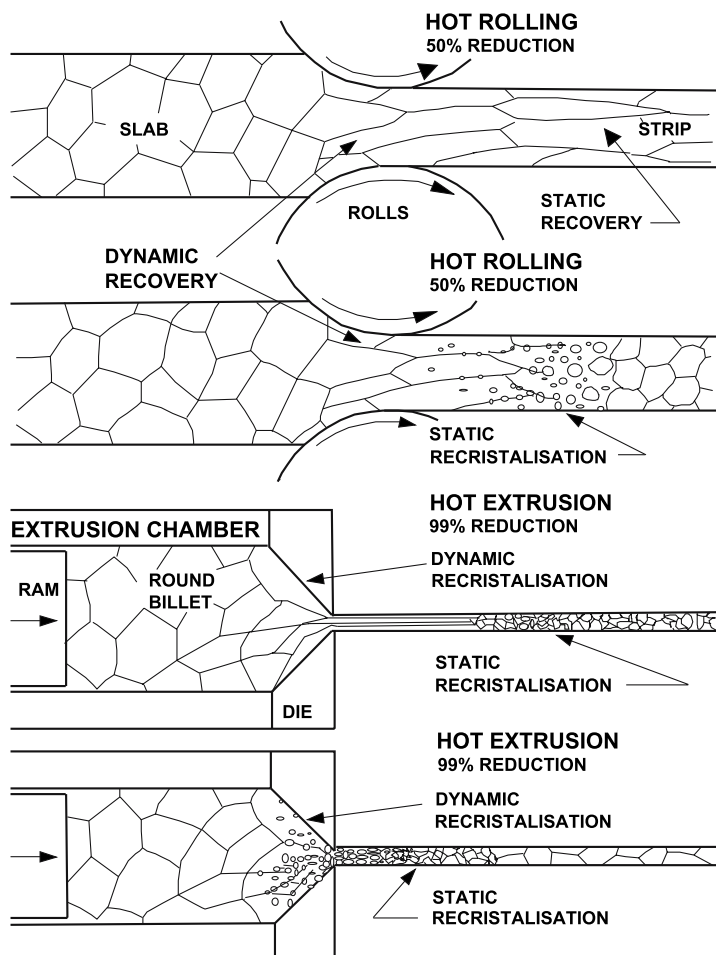


Fig. 6.63. Schematic representation of possible softening process during hot-working [68]

process equipment. The strain rate time profile is usually defined by the process. Hot-working operations such as extrusion are conducted in a high strain rate range of  $10^{-3}$  to  $10^3 \text{ sec}^{-1}$  and develop relatively high stresses. Under hot-working conditions all forms of softening processes occur; namely static recovery and recrystallisation, and dynamic recovery and recrystallisation. Some possible combinations of dynamic and static softening processes during hot working are shown in Fig. 6.63.

In magnesium the level of dynamic recovery is sufficiently low to allow dynamic recrystallisation above  $240^\circ\text{C}$ . Fine grains are formed at the initial grain boundaries. The product is strengthened due to the substructures from dynamic recrystallization or refined grains. Magnesium alloys such as AZ31B and ZK60A workharden in the  $180\text{--}240^\circ\text{C}$  range by deformation mechanisms induced by twinning [69]. At  $300^\circ\text{C}$ , the occurrence of dynamic recovery limits the work

hardening. Above 360°C dynamic recrystallisation is observed and ductility is significantly improved. The alloy ZK60A exhibits lower ductility than the alloy AZ31A but becomes stronger at 420°C.

At room temperature, deformation occurs mainly by slip on the basal planes in the close packed  $\langle 11\bar{2}0 \rangle$  directions and by twinning on the pyramidal  $\{10\bar{1}2\}$  planes. Above 250°C additional pyramidal  $\{10\bar{1}1\}$  slip planes are activated. As a result deformation is much easier and the importance of twinning is reduced. At relatively low temperatures, extrusion tends to occur on the basal planes and the  $\{10\bar{1}0\}$  directions approximately parallel to the extrusion direction.

The main hot working mechanisms for magnesium alloys are similar to other metals, but there are a few important differences. The initial deformation is characterised by a high degree of twinning and dynamic recovery. Gradually the occurrence of dynamic recovery increases and results in lower hardening and higher ductility. At 300°C and  $\dot{\epsilon} = 1.0 \text{ sec}^{-1}$  recrystallisation starts and gradually affects larger grains as the temperature increases and the strain rate declines. The ductility is improved due to the formation by dynamic recrystallization of new grains near the grain boundaries and twins intersections.

### Mechanical Properties

Magnesium alloys have a modulus of elasticity listed at 45 GPa. The modulus of rigidity (shear modulus) is 16.5 GPa. Poisson's ratio is 0.35. The modulus of elasticity is a useful parameter for comparing magnesium with other materials but is not a good value to use for the design of stressed parts. The exploitation of the specific properties resulting in a lower overall part weight is a key factor in the successful use of magnesium. Tensile properties give an initial indication on the strength of any material. Typical tensile properties at room temperature of selected magnesium alloys are given in Table 6.21 for common commercial extrusions.

The mechanical properties of non heat treated AZ types of alloys increase with the alloy content of elements constituting the alloys. The ratio of the yield strength in tension to the yield strength in compression for samples taken parallel to the extrusion direction varies from as low as 0.4 for an AZ31B alloys to 0.90 for an AZ80 alloy. The reverse is true for samples taken perpendicular to the direction of extrusion. Elongation decreases with the alloying content and heat treatment. The variation between yield and tensile strength becomes smaller with increasing alloy content. It means a greater work hardenability and more uniform properties. For ZK60A alloys the more uniform properties are most likely due to the finer grains.

For magnesium extrusions, there exists a great discrepancy between tensile samples taken from the direction parallel and perpendicular to the extrusion direction. Table 6.22 shows that the difference in tensile yield strength is particularly marked for non-heat treated AZ alloys. The tensile yield strength obtained from a direction perpendicular to the extrusion direction is 30–40% lower than the tensile yield measured in a direction parallel to the extrusion direction of AZ alloys.

For ZK alloy types this difference is of the order of 20%. It appears that both the heat treatment and the higher content of alloying elements have a beneficial



**Table 6.21.** Typical mechanical properties of magnesium extrusions [70].

Product	Alloy	Least dimension mm	Area [cm <sup>2</sup> ]	Tensile strength [MPa]	Tensile yield strength [MPa]	Elonga- tion [%]	Compres- sive yield strength [MPa]	Shear strength [MPa]	Bearing strength [MPa]	Bearing yield strength	Brindell hardness <sup>a</sup>
Bars, rods and shapes	AZ31B -F	Under 6.3		262	193	14	103	131	386	234	49
		6.3–38.1		262	200	15	97	131	386	228	
		38.1–63.5		262	193	14	97	131	386	228	
		63.5–127		262	193	15	97	131	386	228	
	AZ61A -F	Under 6.3		317	228	17		152	469	262	60
		63.3–63.5		310	228	16	131	152	469	276	
		63.5–127		310	214	15	145	152	469	290	
	AZ80A -F	Under 6.3		338	248	12		152	469	331	60
		6.3–38.1		338	248	11		152	469	331	60
		38.1–63.5		338	241	11		152	469	331	60
		63.5–127		331	248	9		152	469	331	60
	AZ80A -T5	Under 6.3		379	262	8	234	165	414	394	82
		6.3–38.1		379	276	7	241	165	414	400	82
		38.1–63.5		365	269	6	221	165	455	372	82
		63.5–127		345	262	6	214	165	469	469	82
	ZK60A -F	Under 12.9	Under 12.9	338	262	14	228	165	524	386	75
		12.9–19.3		338	255	14	193	165	524	345	75
		19.3–32.3		338	248	14	186	165	524	338	75
		32.3–259		331	255	9	159	165	517	303	75
	ZK60A -T5	Under 12.9		365	303	11	248	179	545	407	82
		12.9–19.3		359	296	12	214	179	538	365	82
		19.3–32.3		352	290	14	207	179	531	359	82

**Table 6.21** (continued)

Product	Alloy	Least dimension mm	Area [cm <sup>2</sup> ]	Tensile strength [MPa]	Tensile yield strength [MPa]	Elongation [%]	Compressive yield strength [MPa]	Shear strength [MPa]	Bearing strength [MPa]	Bearing yield strength	Brindell hardness <sup>a</sup>
Hollow and semi-hollow shapes	AZ31B	-F		248	165	16	83				46
	AZ61A	-F		283	165	14	110				50
	AZ60A	-F		317	234	12	172				75
	ZK60A	-T5		345	276	11	200				82
Tube			Wall thick- ness	OD, cm							
	AZ31B	-F	0.7–6.3 incl.	15.2 max	248	165	16	83			46
			6.3–18.9 incl.	38.7 max	248	165	12	83			
	AZ61A	-F	0.7–18.9 incl.	38.7 max	283	165	14	110			50
	ZK60A	-F	0.7–6.3 incl.	19.3 max	324	241	13	172			75
	ZK60A	-T5	0.7–6.3 incl.	19.3 max.	345	276	11	207			82
	ZK60A	-T5	2.4–48 incl.	19.3–54.8	338	269	12	179			

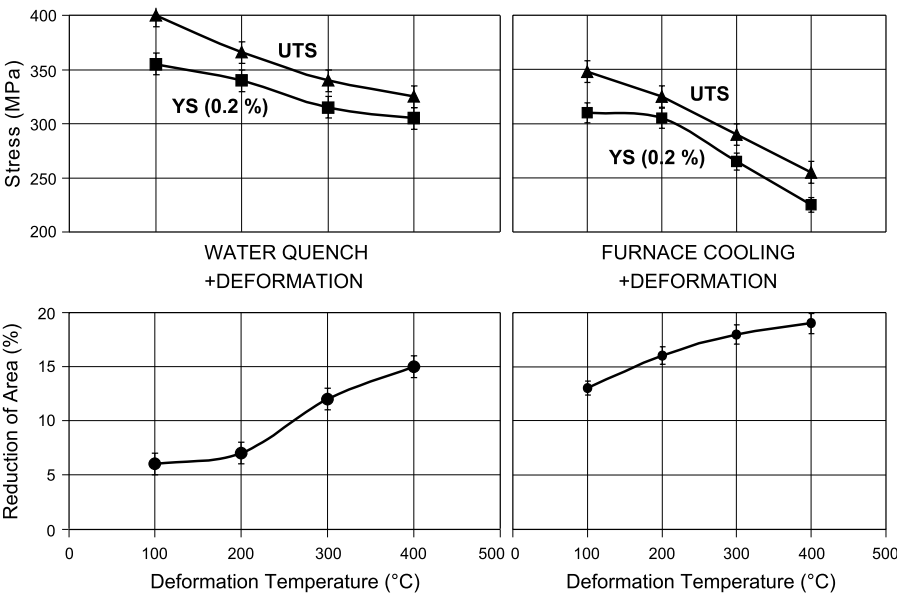
<sup>a</sup> 500 kg load; 10 mm ball.

**Table 6.22.** Tensile and compression strength of magnesium extrusions [71]

Alloy	Condi- tion	Tensile (↗)			Compression (↘) R <sub>p0.2</sub> (D) (MPa)	Tensile (↖)		
		R <sub>p0.2</sub> [MPa]	R <sub>m</sub> [MPa]	A <sub>5</sub> [%]		R <sub>p0.2</sub> [MPa]	R <sub>m</sub> [MPa]	A <sub>5</sub> [MPa]
AZ31	F	180	250	14	110	110	225	13
AZ61	F	220	300	12	130	137	294	12
AZ80	F	240	340	10	145	170	323	11
ZK30	T6	240	290	14	190	220	280	16
ZK60	T6	280	320	12	230	250	310	14
WE43	T6	170	260	12	165	165	250	14
WE54	T6	190	280	10	180	185	275	13

effect on the anisotropy induced by extrusion. It should be noted that the tensile yield strength in the perpendicular direction and the compression yield strength in the parallel direction are comparable. In addition, it seems that the newly developed WE43 and WE54 alloys do not suffer from anisotropic behaviour at room temperature. Elongation measured in both directions are relatively high and range from 10–16%.

Tensile strength and elongation can also be influenced by the billet deformation temperature. Extrusions of QE22 (Mg – 2.2 Mg – 2Nd – 0.5 Zr) show strengths that decrease with increasing billet temperature (Fig. 6.64). Furnace cooled billets exhibit greater ductility and lower tensile strength than solution



**Fig. 6.64.** Effect of deformation temperature and billet cooling on tensile strength and elongation [72]

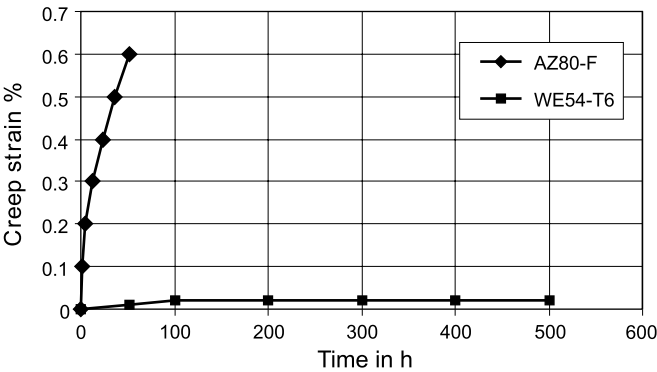


Fig. 6.65. Creep properties of WE54-T6 and AZ80A-F alloys [71]

treated billets. This is certainly due to the formation of coarse precipitates during slow cooling.

At elevated temperature (300°C) the presence of RE such as yttrium combined with a fine grained structure has a positive effect on tensile properties. The tensile and yield strength of a WE54-T6 alloy are stable at 275 and 200 MPa over a wide temperature range (25–250°C). For a AZ80-F alloy both the tensile and yield strength decrease linearly from respectively 350 to 100 MPa and 250 to 75 MPa.

The creep properties at elevated temperature (200°C) are better for a WE54 alloy compared to AZ80 alloy (Fig. 6.65). At subfreezing temperatures, the properties of extruded magnesium increase in tensile and yield strength, and in hardness with decreasing temperature [67].

The fracture toughness  $K_C$  of magnesium alloys is relatively low compared to aluminium and steel (Table 6.23). The AZ31B-F alloy offers relatively good fracture toughness. Other non heat treated alloys (AZ61A-F, AZ80A-F) exhibit a toughness significantly below the levels obtained for aluminum wrought alloys. In Table 6.24 some fracture toughness values of commonly used magnesium and aluminum wrought alloys are compared. The fracture toughness is significantly reduced for heat-treated magnesium alloys.

Table 6.23. Fracture toughness of various alloys [67]

Alloy	Mean Value, [ $J_C$ , J/mm <sup>2</sup> ]	Standard deviation, [ $J_C$ , J/mm <sup>2</sup> ]	Mean value, [ $K_C$ , MPa√m]	Standard deviation, [ $K_C$ , MPa√m]
6061-0	0.125	0.009	93.0	3.4
7075-0	0.075	0.008	71.7	3.5
AZ31B	0.052	0.003	48.4	1.4
1018	0.342	0.039	266.0	15.0
4130	0.218	0.021	212.0	10.0
HP-4-20	0.245	0.023	218.0	11.0

Compact-tension (CT specimens).

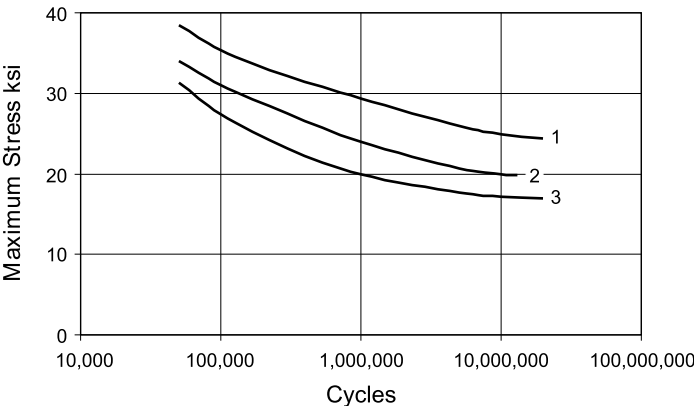
**Table 6.24.** Fracture toughness of common magnesium and aluminum alloys [71]

Alloy	Condition	Fracture toughness $K_{IC}$ [MPa m <sup>1/2</sup> ]	
		L-T	T-L
AZ 80	F	23	20
AZ 80	T 6	16	14
AZ 61	F	24	20
ZK 30	T 6	16	16
WE 54	T 6	16	17
AA6082	T 6	36	29
AA7075	T 6	29	24

For magnesium alloys the fatigue data are mostly represented by S-N curves. Strain – cycle ( $\epsilon$ -N) curves are also used to assess the fatigue strength of magnesium alloys. The best properties for magnesium are obtained for high cycles at low stress. Figure 6.66 represents typical mean fatigue curves in axial loading for several magnesium alloys. The S-N curves for magnesium exhibit a low slope, which tends to flatten with increasing life. Solid solution strengthening increases the fatigue life of magnesium alloys. Cold working and precipitation have little effect on the fatigue strength a higher cycles. The S-N curves should serve as a general guideline. The avoidance of stress raisers in a design and the surface smoothness are important considerations in fatigue properties.

The mechanical properties of as-extruded magnesium alloys vary with the form of the shape and the wall thickness. Table 6.25 summarizes the as-extruded tensile properties of samples cut parallel to the extrusion direction.

The AZ31B profile B exhibit a good elongation (11.2%) but relatively low tensile (232 MPa) and yield (131 MPa) strength. The higher alloy (AZ80A) shows a



**Fig. 6.66.** Axial load fatigue curves for magnesium alloys:

- 1. Forged or extruded AZ80A
- 2. Cast AZ91
- 3. Extruded AZ31B

**Table 6.25.** Tensile properties of As-extruded magnesium alloys

Shape	Profile	Alloy	UTS [MPa]	YS [MPa]	E [%]	Thickness [mm]
Semi-hollow	A	ZK60A	302	212	5.1	1.7
Channel	B	AZ31B	232	131	11.2	2.3
H beam	C	ZK60A	270	219	6.4	4.5
Hollow	D	ZK60A	288	238	6.5	2.1
Bar	E	AZ80A	294	207	11.4	1.3
Bar	E	AZ80A	319	248	9.5	2.5
Bar	E	ZK60A	284	230	9.9	1.3
Bar	E	ZK60A	326	262	9.0	2.5

good ductility (9.5% and 11.4%) in addition to a good tensile strength (207 and 248 MPa) and yield strength (294 and 319 MPa). The tensile properties of the ZK60A profiles reflect the influence of the shape and consequently of the extrusion conditions. Tensile strength, yield strength and elongation are not so much influenced by the wall thickness but by the shape. An increase in the wall thickness to 4.5 mm is very detrimental to tensile properties of profile C. The effect of the wall thickness on tensile properties is clearly seen by comparing the test results of profile E. The tensile strength and yield strength of both AZ80A and ZK60A alloys are significantly higher for the thicker wall (2.5 mm). For a thinner wall (1.3 mm) the ductility is markedly better. The tensile properties for both AZ80A and ZK60A alloys extruded into profile E differ mainly due to the yield strength which is higher for the zirconium containing alloy.

Material for superplastic deformation is produced via grain refinement by dynamic recrystallisation.

### Stretching

After extrusion, the profiles must be straightened in the extrusion direction to meet the straightness and twist tolerances given below.

- Bars, rods, shapes: Straightness tolerances:  $D = 4 \text{ mm} \times L$  or  $1 \text{ mm} \times L$
- Tubes: Straightness tolerances,  $D = 2 \text{ mm} \times L$  or  $1 \text{ mm} \times L$
- Bars, Shapes: twist tolerances:  $Y = 3^\circ$  or  $1.5^\circ$  or  $0.75^\circ \times L$   
But not respectively higher than  $7^\circ, 5^\circ, 3^\circ$

The stretching operation is carried out in the 200–300°C temperature range. Stretching is also possible at room temperature to improve the mechanical properties of the extrusions. Table 6.26 summarises the tensile properties of a ZK60A alloy treated for 24 hours at 360°C followed by furnace cooling and stretching corresponding to 0.5% elongation.

The application of a 0.5 % elongation prior to mechanical testing results in a significant improvement of the yield strength which is increased from 239 to 264 MPa. The elongation is only slightly improved from 14.5 to 16%.

**Table 6.26.** Effect of stretching on mechanical properties of ZK60A alloy

Alloy	Heat treatment cycle	UTS [MPa]	YS [MPa]	E [%]
ZK60A-T5	360°C/24 hours furnace cooled not stretched	294	239	14.5
ZK60A-T5	360°C/24 hours furnace cooled stretched	296	264	16.0
6066-T5	NA	291	253	9.8

### Heat Treatment

In AZ alloys containing more than 2% aluminum the  $\beta$ -phase  $\text{Mg}_{17}\text{Al}_{12}$  appears and forms at the grain boundaries. Annealing at 420°C causes some of the  $\beta$ -phase to redissolve resulting in a significant improvement of both tensile strength and elongation caused by solid solution strengthening. Ageing at 150–250°C improves further the tensile strength through the precipitation of the  $\beta$  phase in the matrix. Ageing of Mg-Zn alloys at 150°C results in coherent Mg  $\text{Zn}_2$  precipitates.

Precipitation mechanisms in Mg-RE alloys such as WE54 (Mg-5Y-2Nd-0.5 zr) and WE43 (Mg-4Y-2.5Nd-0.4 zr) are complex and not completely understood. Below 200°C fine  $\beta'$  plates are formed. At 250°C plates with the composition  $\text{Mg}_{12}\text{NdY}$  are precipitated.

AZ alloys containing a low amount of alloying elements are used in the as-extruded F state. AZ80A and ZK60A alloys are normally treated to T5 conditions. ZK60A and RE containing alloys can be fully heat treated by applying a T6 cycle. The effect of different T5 heat treatments on a ZK60A profile are shown in Table 6.27. At 150°C both tensile and yield strength are substantially increased to the detriment of elongation. At higher T5 treatment temperatures (200 and 400°C) ductility is restrained and improved but both tensile and yield strength are reduced. By optimising the heat treatment cycle the tensile and yield strength and elongation are further improved to reach levels that are now comparable to aluminum wrought alloys (Table 6.28). Samples from the same profile were T6 heat treated. Tensile and yield strength after a T6 treatment are now even higher than the data obtained after the T5 treatment (Table 6.29). But the elongation is

**Table 6.27.** Tensile properties extruded magnesium and aluminum profiles

Heat treatment		UTS [MPa]	YS [MPa]	E [%]
Alloy	Heat treatment cycle			
ZK60A-F	As-extruded	288	238	6.5
ZK60A-T5	150°C/24 hours air quenched	345	281	2.8
ZK60A-T5	200°C/16 hours furnace cooled	289	244	5.2
ZK60A-T5	400°C/8 hours furnace cooled	248	191	14.6
6066-T5	NA	291	253	11.2

**Table 6.28.** Effect of heat treatment on the tensile properties of ZK60A alloy

Alloy	Heat treatment cycle	UTS [MPa]	YS [MPa]	E [%]
ZK60A-T5	350°C/24 hours furnace cooled	295	247	14.4
ZK60A-T5	360°C/24 hours furnace cooled	294	258	13.8
ZK60A-T5	350°C/16 hours furnace cooled	300	248	14.0
ZK60A-T5	350°C/16 hours Air quenched	301	243	12.6
6066-T5	NA	291	253	9.8

**Table 6.29.** Mechanical properties of T6 heat treated ZK60A alloy

Cycle	Heat treatment schedule	UTS [MPa]	YS [MPa]	E [%]
1	450°C/3 hours; Air quenched; 135°C/48 hours	322	290	5.0
2	450°C/3 hours; Air quenched; 135°C/48 hours	324	297	5.0
3	475°C/3 hours; Air quenched; 150°C/36 hours	335	309	6.6
4	475°C/3 hours; Air quenched; 150°C/36 hours	331	305	7.6

significantly reduced from 14 to 7.6% (cycle #4). For a particular ZK60A alloy profile the heat treatment cycle can be tailored to the tensile properties required for specific applications.

The mechanical properties of WE54/43 extruded alloys when studied extensively [73]. An increase of the ageing temperature from 200 to 250°C decreases both the tensile and yield strength of the WE54 alloy (Table 6.30). Excellent tensile, strength and elongation are obtained after ageing at 200°C. An increase of the extrusion temperature from 400 to 450°C results in substantially lower tensile and yield strength. Alloy WE43 is less sensitive than alloy WE54 to an increase in the extrusion temperature.

Stress relief schedules of common welded magnesium extrusions are given in Table 6.31. Post-weld-stress-relief of AZ alloys is required to prevent possible

**Table 6.30.** Tensile properties of WE54/WE43 alloys [73]

Alloy	Ext [°C]	H.T.	Ext. RATIO	YS [MPa]	UTS [MPa]	El [%]
WE43	400		16:1	300	331	17.5
WE43	400	200°C/16 hr	16:1	325	342	12.2
WE54	425		16:1	274	319	18.9
WE54	425	200°C/16 hr	16:1	299	333	13.8
WE54	425	200°C/8 hr	22:1	247	299	21.3



**Table 6.31.** Stress relief treatments for some commercial magnesium alloys

Extrusions		
Alloy	Temp. [°C]	Time [min]
AZ31B-D	260	15
AZ61A-F	260	15
AZ80A-F	260	15
AZ80A-T5	200	60
ZK60A-F	260	15
ZK60A-T5	150	60

stress-corrosion. Post-heat treatment of ZK alloys is used mainly for straightening or stress-relief prior to machining.

#### 6.2.2.4 Alloy Developments

In order to improve primarily the mechanical properties of magnesium alloys research efforts have been directed towards the development of metal matrix composites (MMCs) and rapid solidification processes (RSP). Extrusion is a technique which would be well suited to form into useful shapes MMCs ingots and billets and rapid solidification products obtained after densification of powders.

Cast billets of magnesium composites containing 10 and 20% SiC particles were prepared by stirring into pure magnesium 40  $\mu\text{m}$  size SiC particles. After a two-hour homogenisation, the cast billets were extruded at a ratio of 13 : 1 [74]. The extrusions are free of SiC clusters. However, the presence of streaks of SiC was observed due to the orientation of the particles parallel to the extrusion direction. In general the SiC particles were well bonded to the matrix with the exception of when MgO was present at the interface.

Small billets of an AZ91 alloy reinforced with SiC whiskers were extruded at 360°C with a speed of 1.2  $\text{ms}^{-1}$  and an extrusion ratio of 12 [75]. Practically no porosity was observed in the extruded composites and the whiskers were randomly distributed. The elastic modulus of the extruded composites reaches 120 GPa for 30% volume fraction of SiC whiskers. The presence of a 20% volume fraction increases the tensile strength from 300 to 450 MPa. The tensile strength of the extruded composites decreases rapidly with the temperature and at 300°C only 50 MPa is achieved. At 300°C the elongation is close to 50% for a composite containing 13% SiC whiskers.

The rapid solidification process was utilized to produce WE54 alloy powders which were mechanically alloyed with either  $\text{Al}_2\text{O}_3$  or SiC particles [76]. After degassing at 400°C the mixtures were extruded at 380°C with an extrusion ratio of 30 to 1 to a 7 mm diameter. The tensile properties of the two mechanically alloyed materials were similar (Table 6.32). The yield strength is significantly higher than for conventionally extruded WE54 alloys and elongation is reduced from 22 to 8%.

A good improvement in higher temperature properties and creep behaviour is achieved by producing an extruded particulate ( $\text{Al}_2\text{O}_3$ ) reinforced ZC71 (Mg-

**Table 6.32.** Tensile properties of MA – WE – as extruded [76]

Alloy	Mechanical properties		
	0.2%PS [MPa]	UTS [MPa]	E [%]
WE54 + 3% Al <sub>2</sub> O <sub>3</sub>	318	321	7.5
WE54 + 3% SiC	321	331	8.0
WE54 (conventional)	271	314	22

6Zn-1.2Cu-0.7 Mn) material (77). A ZCM711 (Mg-7Zn-1Cu-1Mn) alloy was reinforced with 12%  $\beta$ -SiC particles with an average diameter of 10  $\mu$ m [78]. After extruding the DC cast billet most casting defects were eliminated and a better particle distribution observed. Vickers hardness measurements after an 8-hour solution treatment at 440°C followed by hot water (65°C) quenching and ageing at 200°C indicated that the DC cast ZMC711 + 12% SiC reached a peak hardness in a shorter time than that of the unreinforced matrix. The increase in modulus for the extruded ZMC711 + 12% SiC composite was 24%. Grain refinement of the ZMC711 + 12% SiC alloy occurs through the nucleation of grains on the SiC particles during dynamic recrystallisation. The grain size is reduced from 50 to 10  $\mu$ m after an 80% extrusion.

Different series of alloys based on the Mg-Li system were developed and studied [79].

After casting, the alloys were extruded between 75° and 300°C at an extrusion ratio of 3.7. For an Mg-3.75 Li alloy, the increase in the extrusion temperature from 75 to 300°C reduced both the tensile and yield strength while the elongation is maintained in the 13–16% range. By more than tripling the lithium level the hexagonal compact structure becomes body centre cubic. The tensile and yield strength of the Mg-12% Li alloy is much lower, of the order of 100 MPa. Elongation is now in the 30–35% range. The addition of Al and Si or RE (Ce) improves the tensile and yield strength and reduces the elongation of the Mg-5.3Li alloy. The alloy Mg-12.5Li extruded at 300°C exhibits an impact strength of 43 J/cm<sup>2</sup> compared to 7.7 J/cm<sup>2</sup> for pure magnesium.

Ternary Mg-Li-Al and Mg-Li-Si alloys were subjected to rapid solidification by a melt spinning technique [80]. After cold compacting, the microcrystalline ribbons were extruded at 250°C. The tensile strength and micro hardness of respectively Mg-Li-Al and Mg-Li-Si alloys are substantially higher when compared to the conventionally cast material.

The gas atomisation technique was chosen to produce powders of Mg-6Al, Mg-8Al-1 Si and Mg-6Al-1Si alloys [81]. The powders were cold compacted into 71 mm diameter billets and then hot extruded at various temperatures with a ram speed of 1.8 m/min and an extrusion ratio of 27:1. Mechanical properties of the as-extruded material measured at room temperature are shown in Table 6.33. The RS process improves the mechanical properties when these values are compared to similar commercial alloys. For the commercial alloy AZ61 the tensile and yield strength are respectively 310 and 230 MPa compared to 340 and 251 MPa for the RS Mg-6Al, extruded at 390°C. The elongation is similar. The response to ageing

**Table 6.33.** Mechanical properties of RS alloys

Alloys	Temp. of extrusion (°C)	0.2% Proof stress [MPa]		UTS [MPa]	Elongation [%]	K Short rod [MPa · m <sup>1/2</sup> ]
		Tensile	Compression			
Mg-7.9Al-0.76Si	300	270	266	366	12	7.1
Mg-7.9Al-0.76Si	400	291	275	405	19	–
Mg-5.7Al-0.70Si	270	283	290	354	12	9.5
Mg-5.7Al-0.70Si	285	281	295	352	9	8.3
Mg-5.7Al-0.70Si	300	291	295	354	12	9.6
Mg-5.7Al-0.70Si	350	285	284	358	12	11.5
Mg-6.3Al	270	242	226	301	10	9.0
Mg-6.3Al	300	238	226	311	10	9.0
Mg-6.3Al	390	251	230	340	14	12.0
Mg-6.3Al (aged)	390	251	231	341	13	9.4

of the Mg-Al alloys produced by RSP is small. After 8 h at 190°C there was no significant change in micro hardness and mechanical properties.

#### 6.2.2.5 Novel Extrusion Methods

##### Cold Extrusion

An AZ91 alloy was reinforced with a 15 volume % of C short fibres and extruded cold at 20°C [82]. The hardness is increased from 90.4 to 122.4 Hv. For comparison the hardness of an AZ91 alloy is 62 Hv before and 113.5 after extrusion. The tensile properties are also greatly improved. Tensile and yield strength of AZ91 are respectively 220 MPa and 160 MPa, compared to 280 MPa and 230 MPa for AZ91 + 15% C. Cold extrusion improves further the tensile properties of AZ91 + 15% C alloy by 15 to 20%.

##### Equal Channel Angular Extrusion

An AZ91 was used to obtain 40 mm diameter bars for normal extrusion at different temperatures and 20 mm diameter bars for equal channel angular extrusion (ECAE) at 85°C [83]. In Table 6.34 are summarised the grain size and the tensile properties of the extruded AZ91 alloy.

**Table 6.34.** The results of tensile tests at room temperature of the extruded AZ91 alloy

	Extrusion temperature (K)	0.2% Proof stress [MPa]	Tensile strength [MPa]	Elongation to failure [%]	Grain size [µm]
Extrusion	473	364	400	1.9	1.2
	523	278	302	1.4	2.1
	623	227	325	7.1	15.6
	723	158	274	11.0	59.1
ECAE	458	277	318	2.5	1.01

**Table 6.35.** Recommended minimum bend radii of magnesium alloys at room temperature [67]

Alloy and temper	Minimum bend radius (a) in terms of work piece thickness, t									
	At 20°C	At 100°C	At 150°C	At 200°C	At 230°C	At 260°C	At 290°C	At 315°C	At 370°C	At 425°C
Extruded flat strip 22.2 × 2.3 mm thick										
AZ31B-F	2.4						1.5			
AZ61A-F	1.9						1.0			
AZ80A-F	2.4						0.7			
AZ80A-T5	8.3				1.7					
ZK60A-F	12.0					2.0				
ZK60A-T5	12.0					6.6				

(a) Values based on bending a 152 mm wide specimen through 90° (99% success rate).

**Table 6.36.** Bending angles at room temperature of 20 mm diameter magnesium alloy extruded rods

Alloy	Bending Angle [°]	
	D = d	D = 5d
AZ31A	77°	180°
AZ61A	53°	180°
AZ80	30°	77°

Notes: D = Bending radius.  
d = Rod diameter.

**Table 6.37.** Stress relief treatments for the magnesium alloys most commonly cold formed

Alloy and temper	Temperature [°C]	Time at temperature [min]
Extruded flat strip		
AZ31B-F	260	15
AZ61A-F, AZ80A-F	260	15
AZ80A-T5	205	60

The grain size decreases substantially on lowering the extrusion temperature from 450 to 200°C. A small grain size of 1.2  $\mu\text{m}$  was obtained by the conventional extrusion process. By ECAE a slightly finer grain size of 1.0  $\mu\text{m}$  was attained. A 400 MPa tensile strength was measured for the AZ91 alloy extruded at 200°C. The flow stress of the AZ91 alloy processed by ECAE at 180°C was significantly lower than that of the AZ91 alloy extruded conventionally at 200°C.

### Hydrostatic Extrusion of Magnesium

As with conventional extrusion, hydrostatic extrusion uses a ram and a container. The main difference is that the ram is filled with a pressure medium [84]. Therefore the ram does not touch the container resulting in the absence of container friction. Tests were carried out with both ZM21 (Mg-2Zn-1Mn) and AZ61 alloys. Extruded ZM21 profiles were characterised by a smooth surface and the properties were comparable to those from standard profiles. The AZ61A alloy exhibited cracks due to hot shortness.

#### 6.2.2.6 Bending of Magnesium Extrusions

Bending is usually carried out around generous radii. Relatively minor deformation can be performed at room temperature. Bending is generally performed in the 160–290°C temperature range. For example, thin and flat profiles (suitcase profiles) are bent at 90° angles after the profiles, die and press have been heated to a temperature close to 200°C. The increased formability at elevated temperature is due to the hexagonal crystal structure of magnesium. When the metal

is heated, additional slip planes become available and plastic deformation is easier.

Table 6.35 gives the minimum radii for rapid bending in a press brake at room temperature. Also the radius decreases markedly as the angle becomes smaller than 90°. Table 6.36 provides the bending angles for 20-mm-diameter round-extruded magnesium alloy rods. The failure criteria is the formation of the first crack. Alloys containing higher alloying levels are more difficult to bend.

It is recommended to apply a stress relief treatment to cold formed AZ alloys to prevent stress corrosion (Table 6.37).

Bending stiffness for magnesium alloys is defined as

$$\sqrt[4]{E/\rho} \quad (6.5)$$

for solid beam and profiles. The specific stiffness of magnesium alloys is temperature dependant since the Young's modulus decreases with temperature.

## 6.3 Magnesium Matrix Composites

*Norbert Hort, Hajo Dieringa, Sanday T. Kumar, Karl Ulrich Kainer*

### 6.3.1 Introduction

Today, light metal automotive applications are the focus of interest due to the increasing cost of transportation. On one hand, the necessity of reducing environmental pollution by lowering fuel consumption and exhaust gases and on the other hand, protecting our natural resources has led to a renaissance in the use of magnesium and its alloys in automotive industries. At the same time, good casting properties as well as good recycling properties support this growing market for light metals. Most of the alloys used today have been known for a long time. Besides these alloys, there are new alloys and magnesium-based materials coming into service [1–7].

The advantage of using low-density common magnesium materials is often limited by unsatisfactory mechanical properties at elevated temperatures. To overcome this limitation, great efforts must be made to develop temperature resistant magnesium-based materials for use in power train applications. The preconditions for establishing magnesium materials in automotive engineering are creep resistance at temperatures > 130°C, low coefficient of thermal expansion (CTE) and a decreased rate of wear. Newly developed alloys serve these expectations partially. However, alloy development has reached its limit. Hence, magnesium matrix composites are expected to have a big potential to substitute the aforementioned alloys, e.g., aluminum alloys currently used in automotive applications. The magnesium matrix composites are able to extend the use of magnesium-based materials.

Metal matrix composite (MMC) consists of at least two phases. The phases can be totally different regarding their physical properties. One phase is normally the

metallic matrix and the second phase is the reinforcement. The minimum precondition for the combination of these different phases in order to manufacture a MMC is the chemical affinity that leads to the formation of reaction products at the interface. The loads and stresses are transferred through the interface between the two phases. The interface plays an important role for mechanical properties as well as for other properties required for different applications [8–17].

The given definition of MMC excludes materials that develop directional eutectic or even intermetallics during solidification. Even a high amount of precipitates or precipitation of intermetallic or ceramic character are not the phases in the sense of the definition of MMC.

Magnesium, or one of its alloys, is the phase in which reinforcements are incorporated. As reinforcements, a wide range of materials, mostly ceramics, such as carbides, borides or oxides can be used. Besides geometry, shape and volume fraction of the reinforcement, the interface, matrix composition and matrix properties are the most important parameters for developing MMCs.

The aim in developing MMCs is to reach an optimum of both mechanical and physical properties. For instance, the increase in strength at elevated temperatures as well as an increase in Youngs modulus and lowering of creep rate are expected by reinforcing magnesium alloys (Table 6.38). However, another goal of MMC development is the lowering of the coefficient of thermal expansion (CTE) compared to that of its matrix alloy. Generally speaking, MMC development is creating new materials in order to replace, for example, aluminum alloys, and is improving already existing parts by partial reinforcement or extending the field of application of magnesium based materials. The following list shows some properties that could be improved by the development of MMCs [9, 10, 16, 18, 19]:

- Youngs modulus
- Yield strength and tensile strength
- Strength at elevated temperature
- Thermal shock resistance
- Creep
- Fatigue resistance
- Damping capacity
- Wear resistance
- Coefficient of thermal expansion

**Table 6.38.** Properties of MMC with pure magnesium and RZ5-alloy as matrix in compression and tension [105]

Material	Youngs modulus [GPa]		0.1 yield strength [MPa]		Ultimate strength [MPa]		$d_U$ [%]	
	comp.	tens.	comp.	tens.	comp.	tens.	comp.	tens.
Mg	36	36	20	32	169	91	11.9	10
Mg-MMC	49	42	84	59	339	163	4.6	1
RZ5	46	47	69	54	320	176	18.4	8
RZ5-MMC	60	63	141	123	428	234	4.4	0.75

All these properties play an important role when a mechanical load is applied. But, there are more demands, for instance, in the electronic industries, that could be satisfied with composite materials. Applicability of MMCs has to be examined in every new case. That means that goals of development of MMCs are not only optimization of properties like Youngs modulus, creep resistance or thermal expansion but also criteria for choosing matrix and reinforcement. A closer look must also be given to the specific properties. It means that mechanical properties related to density, play an important role. Equation (6.6) shows this relation for the Youngs modulus. Table 6.39 and Figs. 6.67 and 6.68 show some examples of mechanical properties and their specific values.

$$E_{spez} = \frac{E}{\varrho \, g} \, [m]$$

(6.6)

Table 6.39. Specific properties of standard metals and alloys

Material	Density [g/cm³]	E-Modulus [GPa]	Rm [MPa]	Spec. E-Modulus [GPa/g¹ cm³]	Spec. strength [MPa/g¹ cm³]
Mg	1.7	45	100	25.9	57.5
AZ 91	1.8	45	230	24.9	127.1
QE 22	1.8	45	260	24.9	142.9
WE 43	1.8	44	250	24.0	135.9
Al	2.7	70	100	25.9	37.0
6061	2.7	70	115	25.9	42.6
2024	2.8	70	185	25.3	66.8
Fe	7.8	210	200	26.9	25.6
S235JR (St 37)	7.8	210	370	26.9	47.43
QStE 550 TM	7.8	210	600	26.9	76.9
35NiCrMoV 12 5	7.8	210	1780	26.9	228.2

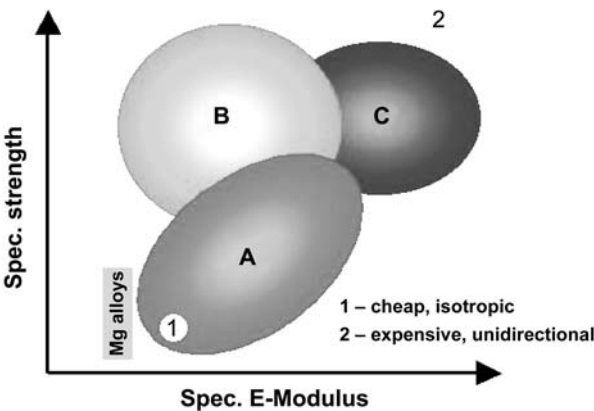
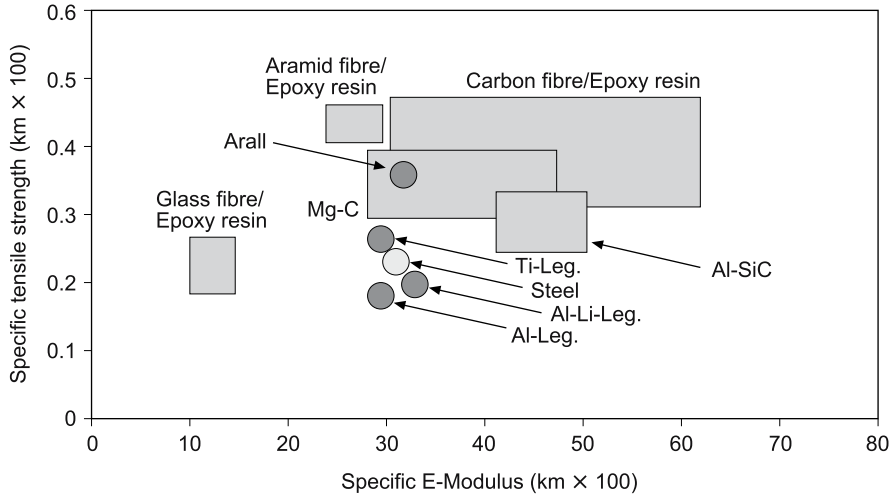


Fig. 6.67. Areas of specific strength and specific E-Modulus for Mg-MMC with different reinforcements. A Particle or whisker, B Monofilament fibres, C high modulus C-fibres





**Fig. 6.68.** Spec. strength and spec. E-Modulus of different quasiisotropic fibre reinforced composites and alloys

The different types of reinforcements have different influences on specific properties, such as, specific Youngs modulus or tensile strength. Figure 6.67 shows specific properties depending on type of reinforcement and also related to its cost. It is obvious that discontinuous reinforcement shows a lower effect of reinforcement but is cheap.

The rule of mixtures (ROM) is the first approximation to calculate mechanical properties of MMCs (6.7). Often yield strength is taken as matrix strength, because plastic deformation of matrix is equivalent to the plastic deformation of MMC. Equation (6.7) is strictly applicable only on unidirectional long fibres with perfect bonding and perfect distribution. By defining an effective length  $l_m$  calculated from the average fibre length and a factor of orientation  $C$ , this model can be applied to discontinuous unidirectional reinforcements as well. It is assumed that  $C = 1$  for unidirectional short fibres,  $C = 0.5$  for average fibre distribution and  $C = 0.375$  for planar isotropic fibre distribution [20–22].

In the case of discontinuous fibre-reinforcement three kinds of fibre lengths compared to their critical fibre length  $l_{crit}$ , have to be compared. The fibre length can be longer than, equal to or shorter than a critical fibre length (6.8–6.10).

$$\sigma_V = \sigma_V V_F + \sigma_M^* (1 - V_F) \quad (6.7)$$

$$1.) \ l_m > l_{crit} \quad \sigma_V = C V_F \sigma_F \frac{1 - d_F \sigma_F}{4 l_m \tau_{FM}} + (1 - V_F) \sigma_M^* \quad (6.8)$$

$$2.) \ l_m = l_{crit} \quad \sigma_V = C^* 0.5 V_F \sigma_F + (1 - V_F) \sigma_M^* \quad (6.9)$$

$$3.) \ l_m < l_{crit} \quad \sigma_V = C \sigma_M^* V_F \frac{l_m}{2 d_F} + (1 - V_F) \sigma_M^* \quad (6.10)$$

where

$\sigma_V$  – strength of MMC

$\sigma_F$  – strength of fibre

$V_F$  – fibre volume fraction

$\sigma_M^*$  – Yield strength of matrix

$\tau_{FM}$  – shear stress at interface fibre/matrix:  $\tau_{FM} \approx 0.5 \sigma_M^*$

$C$  – Factor of orientation

$d_F$  – fibre diameter

$l_m$  – average fibre length

$l_{crit}$  – critical fibre length

When  $l_m < l_{crit}$  the reinforcement cannot exercise their full strength. The optimum reinforcement properties as well as matrix properties can be reached by using a critical fibre length. This critical fibre length, which is derived from fibre strength is given as:

$$l_{crit} = d_F \frac{\sigma_F - \sigma_M^*}{\sigma_M^*} \quad (6.11)$$

There are other models available that describe the strength of MMCs, like inverse rule of mixture for laminate-structures (Reuss-model), Halpin-Tsai-model, shear-lag-model and Eshelby's model. The models for strength-calculation in MMCs are often based on unidirectional continuous fibres. Due to anisotropic mechanical properties of MMCs, those models are used only in a limited way [8–10, 15, 16, 19, 23–32].

### 6.3.2 Reinforcements

For magnesium MMCs, as well as for other MMCs, mainly ceramic materials or carbon fibres are used as reinforcement. The reinforced materials show a wide range of mechanical and physical properties. In addition to the type of reinforcement, the geometry and volume fraction of reinforcements are also responsible for properties of the MMCs. Therefore, the properties of MMCs can be tailored for a certain application. Recently, besides having only a particular type of reinforcement like fibre, whisker or particle, the combination of two or more types of reinforcements are also being used. They are called hybrid reinforcements and contain, e.g., fibres and particles. Given below is a list of classes of reinforcements used in combination with magnesium and its alloys.

- particles [10, 12, 15, 18, 19, 33–37, 106]
- short fibres [10, 15, 27, 38, 105]
- long fibres [10, 15, 27, 38]
- whiskers [10, 15, 38–41]
- hybrids (particle + short fibres/whisker) [42–45]

These different classes of reinforcements are shown schematically in Fig. 6.69. All the reinforcements above can be used for producing MMCs directly. But, very often they are used as so-called preforms. These preforms consist of either one type

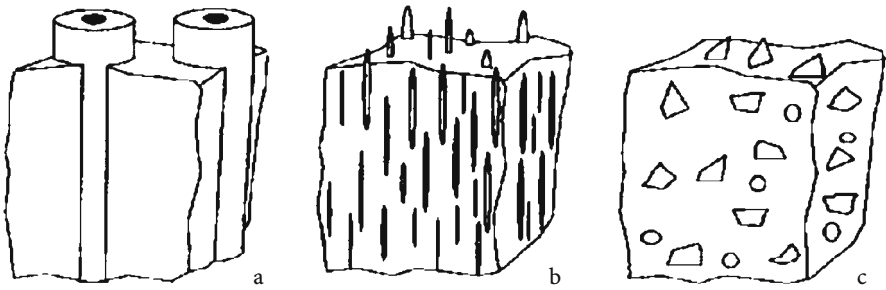


Fig. 6.69. Types of reinforcements for continuous and discontinuous reinforced materials. a Monofilament; b short fibres or whisker; c particles

of reinforcement or a combination of both as in the case of hybrid reinforcement. The preforms are very useful in the case of a partial reinforcement. A certain volume fraction of reinforcement is chosen to manufacture a preform and then a preform is introduced to a production process, which is mainly based on ingot metallurgy [46].

6.3.2.1 Particle-Reinforcement

The particles used as reinforcement in MMCs are mostly ceramics and have their origin in the grinding industry. Normally, oxides, borides, carbides or nitrides are used as particle reinforcements. The particles are classified on the basis of their geometry, size and size distribution [12, 35]. Table 6.40 shows some properties of commonly used particles. The chemical reaction between particles and matrix alloy has to be taken into consideration while choosing the particles for tailoring a MMC. The melt of magnesium alloy generally shows chemical reactivity to most other materials. As a result, the particles are often chemically attacked or even totally converted into a different phase. The particle reinforced MMCs always show isotropic behaviour due to the homogenous particle distribution. In the case of magnesium MMCs, the density also plays an important role, as they are often stirred into the melt. However, for a satisfactory distribution of reinforcement in the matrix, a short time of solidification and continuous stirring are necessary.

Table 6.40. Materials and properties of potential particle reinforcements (CTE – coefficient of thermal expansion) [12]

Partikel type	SiC	B <sub>4</sub> C	Al <sub>2</sub> O <sub>3</sub>	BN	AlN	TiB <sub>2</sub>
Crystal type	hex.	rhomb.	hex.	hex.	hex.	hex.
Shape	irregular	irregular	Platelet	Platelet	irregular	irregular
Density [g cm <sup>-3</sup> ]	3.21	2.5	3.9	2.25	3.26	4.51
CTE [10 <sup>-6</sup> K <sup>-1</sup> ]	4.7	5.0	3.6	0.8-7.5	5.5	4.6-6.4
Heat conductivity [W m <sup>-1</sup> K <sup>-1</sup> ]	40	29	25	25	10	27
E-Modulus [GPa]	480	450	410	90	350	370
Mohs hardness	9.7	9.5	9.0	1-2	7.0	9.5

### 6.3.2.2 Fibre-Reinforcement

In the case of fibre reinforcement, the distinction between short- and long-fibre-reinforcement must be made. Long-fibre-reinforcement is also called continuous reinforcement while whisker- and short-fibre-reinforcement, as well as particle reinforcement, are called discontinuous reinforcement. In the case of continuous reinforcement, distinction has to be made between mono- and multifilaments. The monofilaments have diameter in the range of 100–150  $\mu\text{m}$  and the multifilaments contain 500–1000 fibres in a strand with a fibre diameter of 6–20  $\mu\text{m}$ .

In the case of particle reinforcement, the particles are mostly introduced during the melt stirring process, whereas in the case of fibrous reinforcement, fibres are mainly used for manufacturing preforms by using powder metallurgy methods. These short-fibre- or whisker-reinforced MMCs have almost statistical or two dimensional statistical fibre distribution (planar isotropic). This planar isotropic fibre distribution is the result of preform manufacturing [46]. Hence, the mechanical properties are isotropic in the fibre plane but not in the direction perpendicular to the fibre plane.

The carbon fibres are often used as reinforcement for magnesium MMCs (Fig. 6.70) [44–53]. The poor wettability of carbon fibres by magnesium alloy is avoided by coating the fibres or using an infiltration technique with pressure or using alloying elements that react chemically with carbon [48, 52, 54–56]. Also, SiC- and  $\text{Al}_2\text{O}_3$ -fibres, as well as SiC whiskers, are in use for making Mg MMCs. There are a wide range of Youngs moduli and fibres strengths depending upon the fibre material and the manufacturing process. Table 6.42 shows some prop-

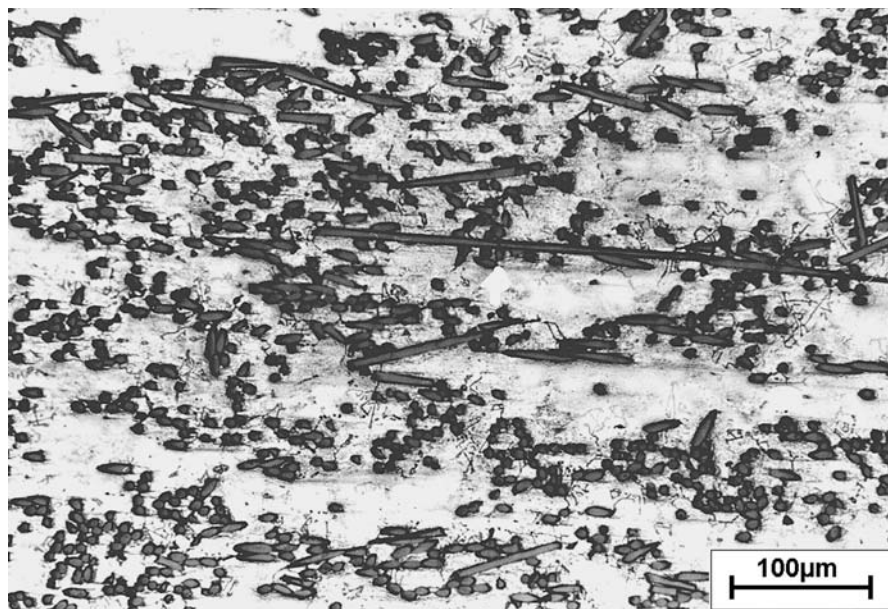


Fig. 6.70. C-fibre reinforced magnesium matrix composite (AS 41 + Sigrafil C) [51]

**Table 6.41.** Materials and properties for whisker and fibre reinforcements [12, 46]

	Diameter [μm]	Length [μm]	Density [g/cm <sup>3</sup> ]	E-Modulus [GPa]	Rm [GPa]	CTE [10 <sup>-6</sup> K <sup>-1</sup> ]
SiCw	0.5–1.7	10	3.2	400–500	1–5	5.1
Saffil (δ-Al <sub>2</sub> O <sub>3</sub> )	1–5	50–250	3.3	300	2	4.7
P 100 <sup>a</sup>	10	adjustable	2.1	720	2.2	k. A.
Sigrafil-C <sup>a</sup>	7		1.78	215–240	2.5	–0.3
Nicalon <sup>a</sup>	10–15		2.55	180–200	2.5–3.2	2.5
Nextel 610 <sup>a</sup>	10–12		3.9	373	2.9	7.9
Tyranno <sup>a</sup>	8.5		2.3	171	2.8	3.1
Altex <sup>a</sup>	10		3.3	210	1.8	k. A.
	<sup>a</sup> long fibres					

erties of common fibres. Furthermore, the type of preform fibres used influences strongly the properties of MMCs as in the case of fibre bundles or wovens [57].

Often the material used for short- and long fibres is the same. But the reinforcing effect is usually lowered by using short fibres as compared to long fibres. The advantages of using short fibres include cheaper production and more isotropic material properties. Usually, short fibres are produced by cutting and milling long fibres.

### 6.3.2.3 Whisker

The whiskers are fibre shaped single crystals with aspect ratios (length to diameter ratio) of about 10 or more while the diameter is in the range of 1 μm or less. The SiC-whiskers have been used due to their especially good wettability. In Europe, whiskers are no longer in use because of an increasing risk of cancer shown by clinical investigations. Table 6.41 shows some properties of usual fibres and whiskers.

### 6.3.2.4 Hybrids

The hybrid reinforcement, in general, is a mixture of particles and whiskers or short fibres. By using hybrids, it is possible to have material properties that could not have been obtained by using only one type of reinforcement [44, 45, 58].

In hybrids, the short fibres are used mainly as a framework containing the embedded particles. As compared to standard fibre preforms, the fibre volume fraction is low (in the range of 10 vol.-% or less). Moreover, with hybrid preforms, low volume fractions of particles can be realized that are lower than that of the particle preform actually used. Quite often, particles in hybrid reinforcement are chosen to react completely with the melt, in order to form precipitates having isotropic distribution that strengthen the MMC. This is called in situ reaction infiltration.

### 6.3.3 Manufacturing

For manufacturing of metal matrix composites, a number of processes have been introduced. Mostly, powder metallurgy (PM) and the processes based on ingot metallurgy (IM) are used. The use of mechanically based processes such as mechanical alloying is also possible but is seldom used. An increasing emphasis is currently being placed on the processes where one phase is changed to the reinforcement (in situ composites) during manufacturing itself.

#### 6.3.3.1 Ingot Metallurgy

Ingot metallurgy is presently widely used for producing Mg-MMCs and is more relevant than the powder metallurgy route. The processes available in ingot metallurgy are more effective, more acceptable in industry and much cheaper than those of PM-based MMCs. The processes mostly used are:

- compo casting or melt stirring [36, 72, 76–78]
- squeeze casting [50, 56, 80–83]
- gas pressure infiltration [50, 79, 80]

However, there are several other manufacturing processes known but irrelevant for industrial application [57].

#### Compo Casting, Melt Stirring

Both the names compo casting and melt stirring are commonly used for a process where the particle shaped reinforcement is directly incorporated into a light metal melt (Fig. 6.71). The reinforcement particles often tend to agglomerate when introduced in the melt but this can be overcome by using appropriate mixing parameters. During mixing of particles and melt, the absorption of gas has to be avoided that may lead to porosity in the final casting and also may lead to inhomogeneous distribution of the reinforcement in the melt matrix. Moreover, the combination of reinforcement particles and the matrix alloy must be chosen carefully because of the fact that in nearly in every case, a reaction will

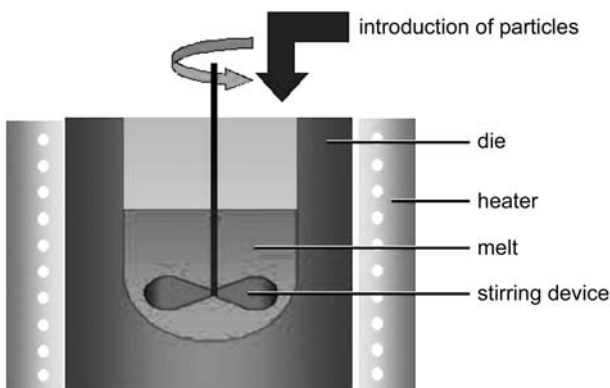


Fig. 6.71. Compo-casting

take place between the matrix, alloying elements and the reinforcement. In the worst case, this will lead to complete dissolution of the particles during melting, stirring and casting. The use of fibrous reinforcements is known to have some difficulties during stirring and subsequent processing steps. After stirring, the material can be cast directly to a near net shape or can be used as semifinished material for hot extrusion, forging, squeeze casting or thixoforming [36, 72, 76–78].

### Squeeze Casting

Squeeze casting is the most widely used process for manufacturing Mg-MMCs. In this process, after slow filling of the die, pressure is applied to infiltrate the preform. This allows the production of partially infiltrated materials. After infiltration, the MMC solidifies under pressure that leads to a fine microstructure and a fully dense material without gas entrapment. In squeeze casting, a distinction must be made between direct and indirect squeeze casting (Figs. 6.72 and 6.73). In direct squeeze casting, the pressure is directly applied to the melt. The ram is part of the die that leads to a simple machine setup. The disadvantage of direct squeeze casting is that the amount of melt has to be adjusted with the dimensions of the manufactured part, whereas, in indirect squeeze casting, a gate system is used that leads to easier filling of the die. Moreover, the oxides and other dross can be trapped in the gate system itself. An advantage of both methods is the slow filling speed in comparison to pressure die casting. This allows the use of preforms due to a non-turbulent flow of melt. It also avoids gas entrapment in the die and the infiltrated material. This leads to materials with a fine microstructure that are also suitable for heat treatment. Another advantage is the short time of manufacturing. It also permits the use of reinforcement materials which normally show higher reactivity with magnesium melts. Moreover, the infiltration by

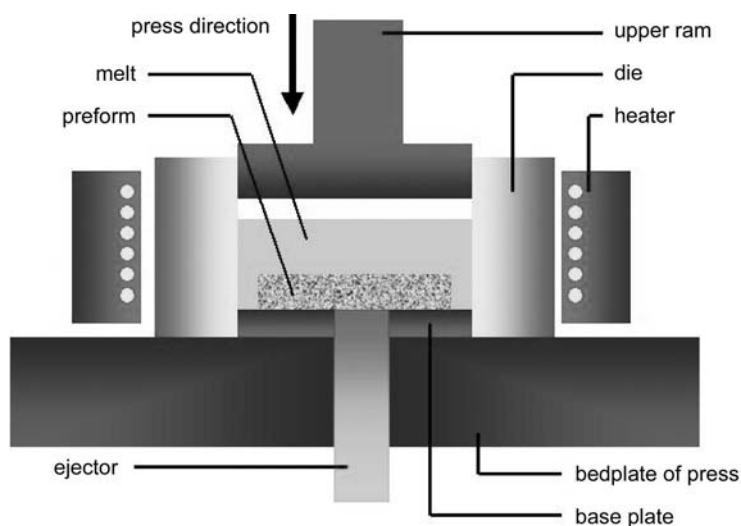


Fig. 6.72. Direct squeeze casting

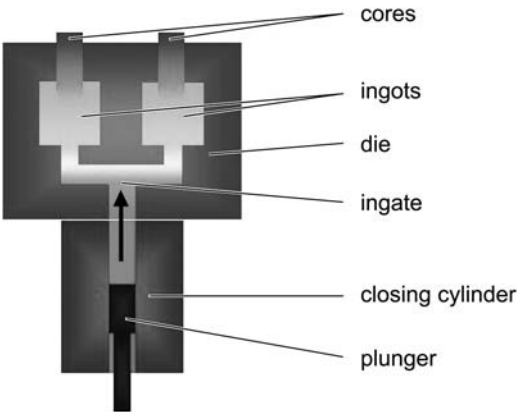


Fig. 6.73. Indirect squeeze casting

pressure also permits the use of non reactive reinforcements like carbon fibres with magnesium and magnesium alloys. By using squeeze casting as a manufacturing process, the production of partially reinforced components is also possible [50, 56, 80-83, 104, 107].

**Gas Pressure Infiltration**

Like the squeeze casting process, gas pressure infiltration also uses preforms for the manufacture of MMC (Fig. 6.74). This process also allows the production of partially reinforced material. Contrary to the squeeze casting process, the gas pressure infiltration process does not use the hydraulic press to infiltrate the preform with melt. In this process, the preheated preform is put into the melt then a pressure is applied by a gas on the melt surface. Due to the differential pressure, the preform is infiltrated. By comparing both processes, viz., squeeze casting and gas pressure infiltration, it has been found that the squeeze casting process has higher pressure with shorter infiltration time. The time for infiltration in gas pressure infiltration is approximately ten times longer than that for the squeeze casting process and thus, has a longer time for a reaction between the melt and

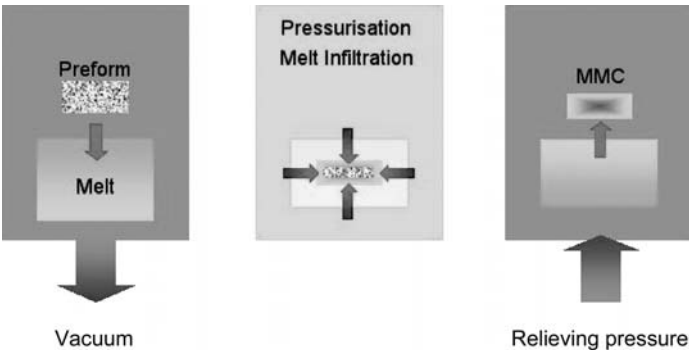


Fig. 6.74. Gas pressure infiltration



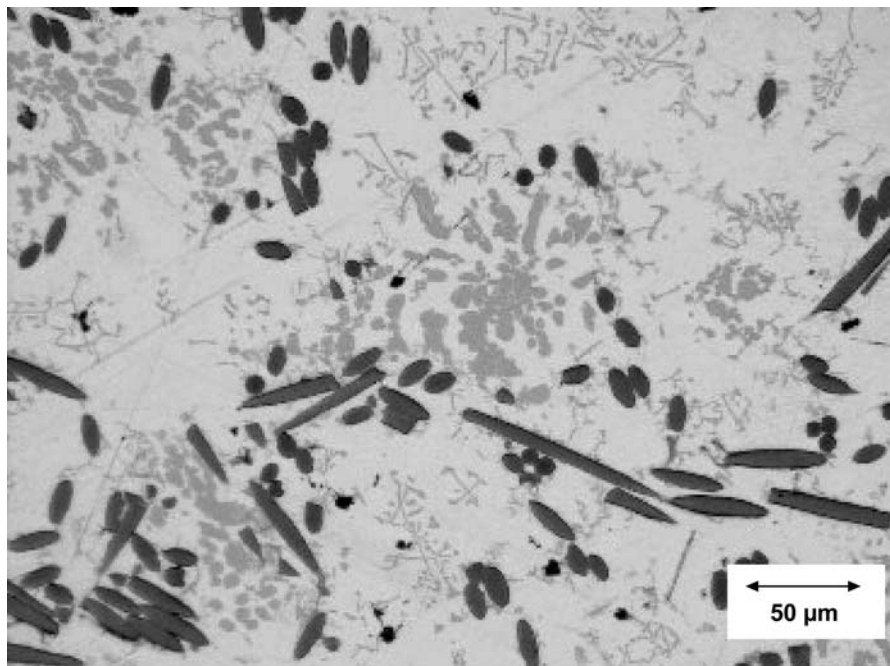
the reinforcement. For this reason, gas pressure infiltration is more suitable for manufacturing in situ Mg-MMCs [50, 79, 80].

### **In situ MMC**

Mostly, in situ MMCs do not fit into the definition of the MMCs given above. But, it is possible to start with a completely different material, in which the starting reinforcement may react completely with the matrix or alloying components. In the case of in situ MMCs, the original reinforcement will be completely dissolved into the melt and will form an entirely new phase, which is now being used for improving desired properties. In most of the cases, the reactive component is introduced as a particle via a hybrid preform. Figure 6.75 shows an example of in situ Mg-MMC based on AM50 alloy reinforced with carbon short fibres and silicon particles. The silicon particles react completely during infiltration to form  $\text{Mg}_2\text{Si}$  and this material contributes to the improvement of high temperature properties [44, 58].

#### **6.3.3.2 Powder Metallurgy**

The production of MMCs by blending the alloy powder with the reinforcement followed by consolidation and spray forming is also well known and often used, but is costly and time consuming. Both manufacturing processes fail to offer the possibilities given by standard ingot metallurgy. Moreover, it is impossible



**Fig. 6.75.** Light optical picture of a hybrid reinforced Mg-MMC (AM 50 RE 7C 4Si)

to manufacture continuous fibre reinforced MMCs without problems. Also, there are some limitations for producing short fibre reinforced composites. The processes used at present are:

- blending of alloy powders and reinforcement [19, 34, 35, 59–66]
- Spray forming [67–71]

Other production routes like mechanical alloying are known for producing PM based MMCs but are not suitable for Mg based MMCs. The reason behind this is the high reactivity of magnesium, mainly the formation of oxide layers on the surface of powder particles. This surface layer of magnesium oxide is a very effective diffusion barrier and prevents sintering. For this reason, any powder metallurgical production process based on magnesium powder is limited to processes that offer high shear forces to brake the surface layer. Processes like powder forging or hot extrusion can be used. Cold isostatic pressing (CIP), hot isostatic pressing (HIP), hot pressing or normal sintering are not suitable for the production of Mg-MMCs.

### Blending

Any blending process starts with a metal or alloy powder and a discontinuous reinforcement consisting of particles, whiskers or short fibres. For producing the metal powder, gas atomisation of the melt is normally used. The use of fibrous reinforcement is limited due to the fact that they will be broken during forging or hot extrusion and at the same time, an alignment of fibres occurs [41]. While using particles, it is necessary to choose an appropriate particle size distribution for both the matrix and reinforcement particles, otherwise, agglomeration of reinforcements on grain boundaries may occur (Fig. 6.76), followed by the failure of the MMC in service after consolidation [73–75]. After blending, the powder mixture has to be filled into cans and then gases have to be evacuated followed by a consolidation process such as hot extrusion or forging [62, 64]. Examples of Mg-MMCs produced by the PM route using SiC particles as reinforcement are given in Figs. 6.77 and 6.78.

### Sprayforming

The sprayforming (Fig. 6.79) process offers the possibility of manufacturing semifinished products. A standard gas atomizing apparatus is used for the pro-

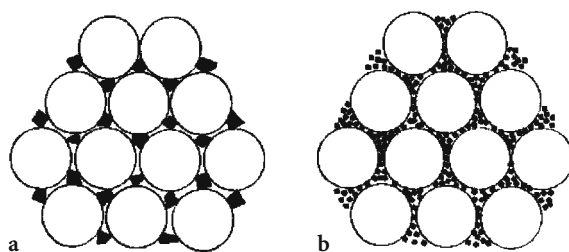


Fig. 6.76. Influence of particle size distribution on the distribution of reinforcements. **a** Homogeneous distribution (1:5), **b** formation of clusters (1:15)

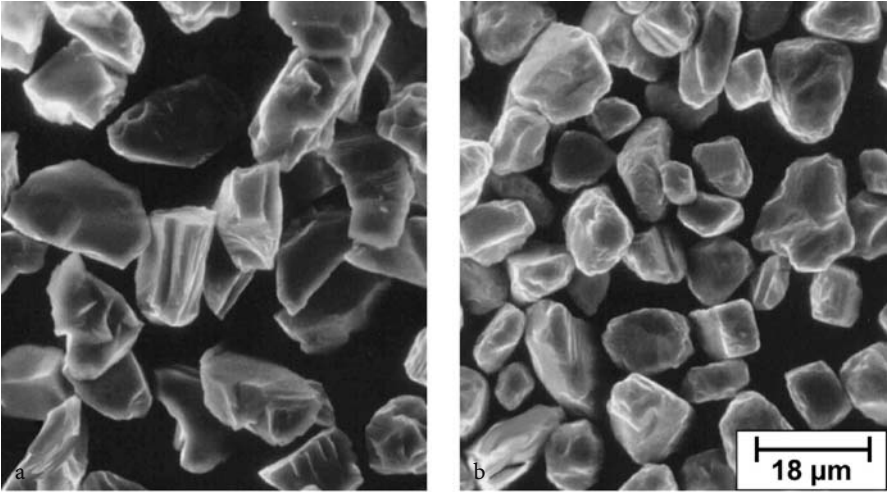


Fig. 6.77. Shape of SiC-particles, a blocky, b rounded [37]

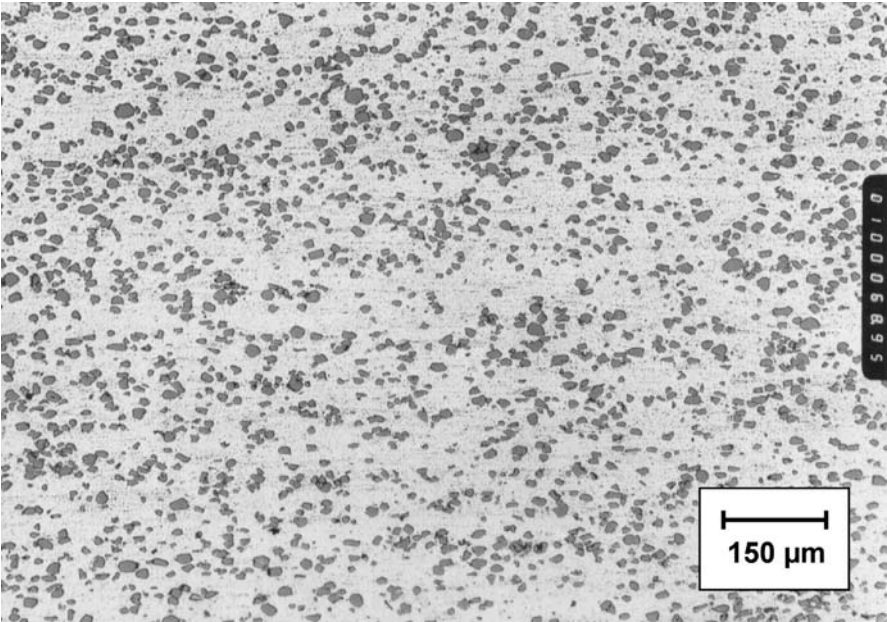


Fig. 6.78. QE22 15 Vol.% SiCp, powder metallurgically produced

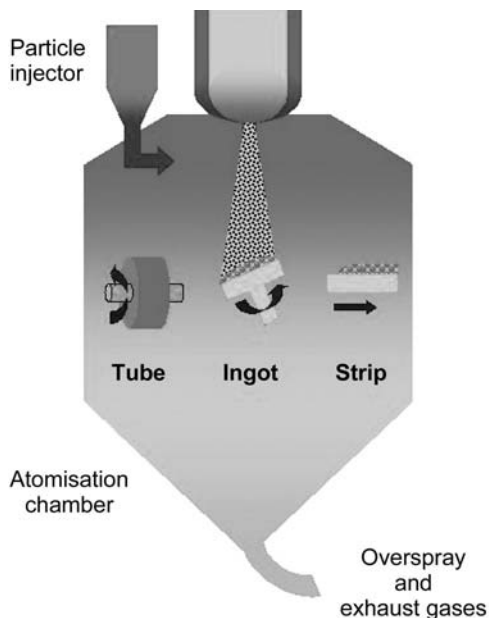


Fig. 6.79. Sprayforming

duction of alloy powder. A substrate is located directly beneath the atomisation unit, collecting solidified, partially solidified and still liquid melt particles. The substrate is moved in accordance with the production of the semifinished part that can be used afterwards for direct hot extrusion. The production of MMCs is also possible by co-spraying. Here the reinforcement is directly introduced into the melt stream and simultaneously deposited. By using this technique, several processing steps like blending, filling cans and evacuation can be avoided. Unfortunately, the production of spray formed MMCs is limited to particle reinforced materials [103].

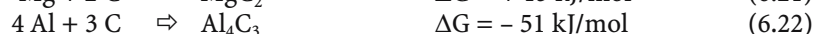
The MMCs manufactured by spray forming have a density of approximately 90–95 % of theoretical density. To reach the full density, a consolidation step is necessary. The consolidation can be performed by forging, hot extrusion or any other processing route. By adopting proper atomisation conditions, the oxide layers can be avoided. The other advantage of gas atomisation is the contribution to a homogeneous microstructure without segregation. This results in good mechanical properties of spray formed materials.

#### 6.3.4 Interfaces

The sharp region in which the reinforcement is in contact with the matrix is the interface between them. For MMCs, it is necessary to have some reaction between reinforcement and matrix to reach a certain bonding at the interface. This bonding at the interface transfers the forces from the matrix to the reinforcement. Two

major types of interaction occur at the interface between a liquid and a solid phase: (a) physical and (b) chemical. The physical interactions determine the wettability and the chemical interactions provide most of the bonding energy. An intimate contact between the reinforcement and the matrix needs to be established through satisfactory wetting of the reinforcement by the matrix to ensure adequate adhesion and the rate of chemical reaction at the interface should be very low and extensive interdiffusion between the component phases should be avoided so that the reinforcement will not be degraded. In the case of magnesium-based composites, the reactivity between the matrix and reinforcement limits the number of possible materials and suitable production processes. Mainly, the production process influences the amount of reaction products formed at the interface due to the time in which melt and reinforcement remain in contact. The composition of reinforcement is another influencing factor because of possible formation of brittle phases at the interface between matrix and reinforcement. In the case of the formation of a brittle phase at the interface, it can be assumed that the load during service will lead to an early breakdown of the MMC, far below the properties given by an unreinforced matrix [98, 99].

As mentioned above,  $\text{Al}_2\text{O}_3$ ,  $\text{SiC}$  as well as carbon fibres are the most commonly used reinforcements in Mg-MMCs. A reaction between Mg and carbon may occur, but normally the carbide that may form is unstable in solids. Only a proper process like squeeze casting, which applies high pressure, or the addition of suitable alloying elements is able to overcome this and helps to form an appropriate interface. In the case of  $\text{Al}_2\text{O}_3$  and  $\text{SiC}$ , certain reactions may occur that lead to the formation of stable interfaces [84, 85]:



Most of the above mentioned reactions are exothermic. They will occur in the melt as well as in the solidified material at elevated temperatures. Only the reaction between Mg and C are endothermic, but magnesium carbide is not stable in the solid. However, the reaction between Al and C is exothermic and forms a stable product in the solid. Due to the fact that nearly any reaction between magnesium and reinforcing components may occur, the time given for the reaction is one of the most important factors. Another very important factor is the temperature, which mainly influences the formation of reaction products by diffu-

sion. Being aware of the possible reactions, reaction enthalpies and time of formation of reaction products, makes it possible to find suitable Mg-MMCs in accordance to a particular manufacturing process.

6.3.5 Alloys and Composites

For the production of Mg-MMCs, nearly any alloying system can be used. Normally, however, the improvement in high temperature properties is one of the most important goals for the use of a reinforcement. Therefore, in most of the cases, alloys are used as a matrix that show good high temperature properties.

In Tables 6.42 and 6.43 are some examples of Mg-MMCs and their properties, comparing matrix and the reinforced composites. Besides, an improvement of tensile properties, wear behaviour or creep properties, the use of magnesium as a matrix alloy for producing MMCs exhibits other advantages. In comparison with aluminum alloys as a matrix material, using magnesium requires lower energy consumption for melting and casting. Moreover, there is usually no reaction between the dies (usually made out of steel), which means a longer life.

Mechanical properties of particle reinforced magnesium MMCs show a wide range depending upon the magnesium alloy used and the shape, volume fraction and type of particles. Youngs modulus, yield and tensile strength, as well as creep resistance, show increasing values by reinforcing magnesium alloys with particles. Four different mechanisms are thought to be responsible for increasing strength [108].

- Orowan mechanism: interdependence between particles and dislocations
- Strengthening by stabilising or reducing grain size.
- Increasing the amount of dislocation around the particles and the development of internal stress due to misfit during thermal expansion.
- Strengthening of matrix due to different strain properties of both matrix and particles.

Table 6.44 shows Youngs modulus and yield strength of some magnesium-based particle reinforced MMCs manufactured by powder metallurgy [109].

Table 6.42. Mechanical properties of a particle reinforced Mg-MMCs (ZC 63 + SiCp)

Temperature [°C]	E-Modulus [GPa]	Yield strength [MPa]	Tensile strength [MPa]	Elongation [%]
ZC 63				
RT	40	138	244	8.5
100	38	122	198	4.6
150	37	121	167	4.7
ZC 63 + 12% SiC				
RT	65	148	197	0.7
100	45	136	184	2.0
150	70	123	148	1.4

**Table 6.43.** Properties of different Mg-MMCs produced by ingot metallurgy [101, 102]

	cp Mg		AS41		AZ91		QE22	
	Matrix	MMC	Matrix	MMC	Matrix	MMC	Matrix	MMC
R <sub>p0.2</sub> [MPa] (RT)	70	220	151	225	160	230	180	250
R <sub>m</sub> [MPa] (RT)	80	240	185	270	220	280	250	300
A. [%] (RT)	5.0	2.2	2.2	4.3	4.8	1.8	4.5	1.6
E-Modul [GPa]	46	56	49.8	77.7	46	64	46	74
R <sub>m</sub> [MPa] (100°C)	65	240	175	250	200	270	240	285
R <sub>m</sub> [MPa] (200°C)	45	180	150	240	120	220	200	245
R <sub>m</sub> [MPa] (300°C)	30	120	70	145	60	130	125	180
HV 10 [kp/mm <sup>2</sup> ]	40	75	60	135	65	140	75	125
CTE [10 <sup>-6</sup> K <sup>-1</sup> ]	26.5	21.5	24.0	18.0	27.0	20.5	26.0	20.0

**Table 6.44.** Properties of particle reinforced Mg-MMCs [109]

Material	Youngs modulus [GPa]	Yield strength R <sub>p0.2</sub> [MPa]
AZ61A + 15vol% B <sub>4</sub> C	61	229
AZ61A + 20vol% B <sub>4</sub> C	64	254
AZ61A + 25vol% B <sub>4</sub> C	78	258
AZ90 + 25vol% B <sub>4</sub> C	91	460
ZK60A + 15vol% B <sub>4</sub> C	73	388
ZK60A + 20vol% B <sub>4</sub> C	78	393
ZK60A + 25vol% B <sub>4</sub> C	86	418
Mg + 10vol% B <sub>4</sub> C	57	260
Mg + 20vol% B <sub>4</sub> C	59	273
AZ31B + 20vol% SiC	102	466
Mg + 15vol% SiC (1μm)	62	422
Mg + 17vol% SiC (3μm)	68	409
Mg + 18vol% SiC (4μm)	69	382
Mg + 20vol% SiC (3μm)	72	386
Mg + 20vol% SiC (4μm)	70	368
ZK60A + 15vol% SiC	78	399
ZK60A + 20vol% SiC	84	428



The discontinuously reinforced MMCs show, in most of the cases, in contrast to particle reinforced MMCs, an anisotropic mechanical behaviour. This is due to the fact that a preform that is infiltrated by squeeze casting, for example, has a planar isotropic fiber distribution. The increase in strength, Youngs modulus and creep resistance is achieved in the direction parallel to the fibre plane but only a small increase or even decrease in strength is measured in a direction perpendicular to fibre plane. Due to the low number of fibres (maximum 25%), that is introduced by preform manufacturing process, the density hardly increases by using alumina or carbon fibres.

The strength of MMC at higher temperatures shows a significant improvement as compared to the matrix alloy. Table 6.45 shows some mechanical properties of monolithic and reinforced Mg-MMCs.

The unidirectional long fibre reinforced MMC shows its highest strength in the fibre direction and – corresponding to the rule of mixture – its lowest strength in the direction perpendicular to the fibre direction. Three categories of failure, depending upon the angle between fibre and applied stress, can arise [110]:

- Stress || fibre: failure will occur at critical stress of fibre
- Stress  $\perp$  fibre: failure will occur at critical transverse strength of the composite (i.e., interface, matrix or fibre)
- Off axis loads: failure mechanisms are influenced by a critical shear strength of the composite as well (i.e., interface, matrix)

Table 6.46 shows some longitudinal and transversal properties of continuous fibre reinforced magnesium matrix composites [110].

### 6.3.6 Machining and Recycling

In accordance with certain applications and a chosen production process, it is necessary to manufacture near net shape products. But, at the same time, it is initially possible to manufacture semifinished products that have to be shaped by an additional process like hot extrusion, hot pressing or thixoforming [86]. Due to the fact that the reinforcements used are normally hard materials, the tooling materials have to be chosen carefully to form the finished part. Any further tooling should be performed only with hard coated tools, diamond tools or by water jet cutting. The use of grinding may also lead to good results [87–89].

Recycling is also a field of investigation for Mg-MMCs. Unfortunately, the high reactivity of magnesium, and the reinforcement, limits the recyclability of

**Table 6.45.** Properties of fibre reinforced Mg-MMCs produced by squeeze casting

Material	$R_m$ [MPa]	$R_{p0.2}$ [MPa]	$A$ [%]	$E$ [GPa]	CTE [ $10^{-6} \text{ K}^{-1}$ ]
AZ91	180–220	120–150	2–8	44	27
AZ91 + 20% C-fibre	225–260	200–240	0.5	66	19–20
AZ91 + 20% Saffil	295	260	2	69	20.5
QE22	183	185	5.2	48	26
QE22 + 20% Saffil	230	270	1.2	70	20



**Table 6.46.** Properties of C-fibre reinforced Mg-MMCs produced by gas pressure infiltration [110]

Matrix	Vol%/Fibres	$E \parallel$ [MPa]	$R_m \parallel$ [MPa]	$R_m \perp$ [MPa]
AM60	65/M40B 6k 50B		1800	
AZ91	63/M40J	216	1340	51 shear
AZ91	63/T300J	155	520	
AZ91	65/M40B 6k 50B		1900	
AM20	63/M40J	196	1400/1050	45 shear
AM20	63/T300J	153	1250/840	68 shear
AM20	65/M40B 6k 50B		1600	
cp-Mg	63/M40J	203	1640	44 shear
cp-Mg	63/T300J	138	1300	36 shear
cp-Mg	65/M40B 6k 50B		1500	

Mg-MMCs. When the material needs to be remelted, damage to the reinforcement will definitely occur. A remelted material can be used again for casting, squeeze casting or other manufacturing processes, but the material will never reach the properties of the original composite. A second method of recycling would use only the matrix material again. Remelting is also necessary, but the reinforcements will be treated as dross and be removed from the process. After refining the melt, it can be used again for the production of magnesium-based materials [90–93, 101].

### 6.3.7 Corrosion

Mg-MMCs show nearly the same corrosion behaviour as standard magnesium alloys. Therefore, the same processes for corrosion prevention and protection can be used. Only in the case of carbon fibres, has more care has to be taken. Especially, in this case, the contact of the carbon reinforcement with the corrosive environment at the surface of the MMC has to be avoided. This can be done only by an appropriate surface protection or by using the C-Mg-MMC in an enclosed environment without any contact with the corrosive environment [90, 94–96].

### Conclusion

Magnesium matrix composites show a high potential for use in wear applications and also where high temperature properties are necessary. They are able to compete with aluminum and aluminum-based composites. The manufacturing processes used currently are capable of producing bigger series of Mg-MMCs with good process control. As compared to Al-based materials, Mg-MMCs exhibits lower properties but have advantages in energy consumption during manufacturing.

## 6.4 Joining

### 6.4.1 Motivation and Requirements

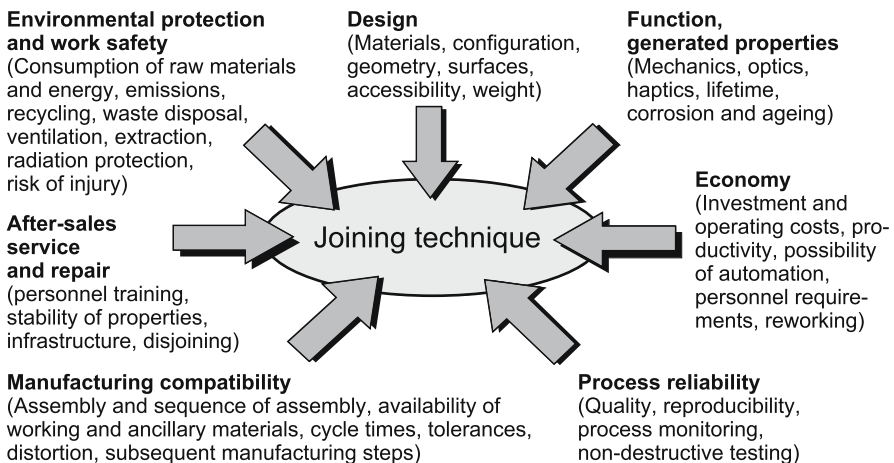
*Gerson Meschut*

In order to achieve further reductions in the weight of the body, efforts are being made in the field of car design to replace structural elements with magnesium components. The very good casting properties of magnesium mean that, in addition to the use of extrusion and sheet metal processes, die casting in particular is an especially important method of producing thin walled, highly integrated components. The integration of die cast components into a vehicle structure calls for joining techniques that offer the maximum use of the materials of the joined parts under operating loads. This chapter discusses the necessity of material-specific joining techniques for future magnesium body structures.

Integrating new materials into a vehicle structure calls for joining techniques which have a property profile better than or at least equal to that of established technologies. In addition to the material-specific boundary conditions, a joining process in car body construction must fulfil a large number of other requirements. Figure 6.80 shows the main criteria for selecting a joining process.

In addition to the selection criteria given in Fig. 6.80, a further decisive factor in the choice of a joining process for body manufacturing is the guarantee that the joints will maintain the required mechanical properties over the whole life-time of the vehicle. Figure 6.81 shows the significant stresses to which an automobile is exposed during operation.

With regard to the requirements to be met by a car body, the following mechanical properties are the most important:



**Fig. 6.80.** Selection criteria for a joining process in car body design

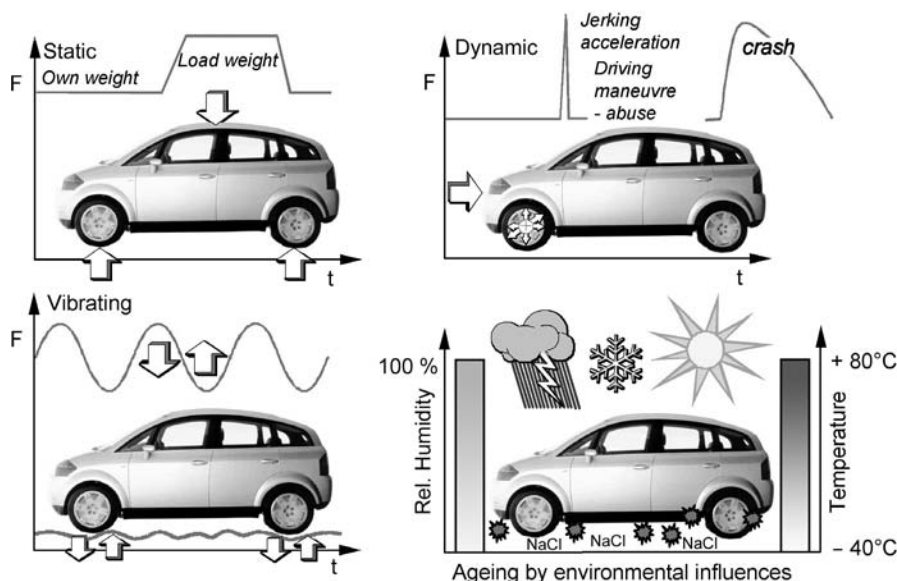


Fig. 6.81. Automobile operating stresses

- High stiffness to ensure functionality and driving comfort
- High fatigue strength in order to withstand safely dynamic stresses during operation of the vehicle
- High energy absorption in order to guarantee maximum passive occupant protection in the event of a crash

## 6.4.2 Joining Magnesium

Günter H. Deinzer

### Preface

Independent of the process applied to produce magnesium parts, there will always be a need to join magnesium to parts made of dissimilar materials. In this case the specific thermal, mechanical and chemical properties must be taken into account.

Nevertheless, a variety of industrial processes are available to join magnesium to similar or dissimilar materials. In what follows, the state of the art and the developments in this field of manufacturing will be discussed.

### Inserting Riv-studs and Riv-nuts

If magnesium die cast components are being used for structural parts like instrument panel carriers, numerous ambient parts have to be fixed to the central component. For such applications riv-nuts and riv-studs are inserted into both punched and machined holes (Fig. 6.82).

Riv-nut in high-pressure die cast structural component: misalignment due to incorrect positioning of the insertion tool

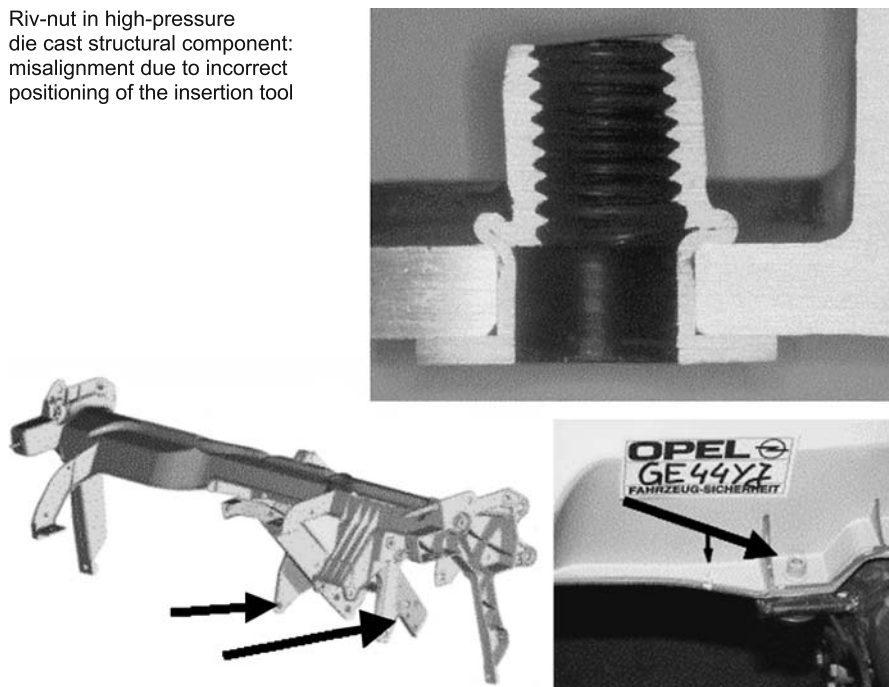


Fig. 6.82. Riv-studs on a magnesium instrument panel carrier

The inserts that are in use for aluminium applications also have to be adapted to magnesium with its poorer mechanical properties. It is very important to keep the tolerances tight and the edge shape of the punched hole rectangular in order to provide enough torque resistance. If this is not done, the studs or nuts will tend to fall loose and hinder the successful completion of the assembly process.

The inserts should be corrosion protected as required by the given environmental conditions. If applied to structural components in a dry climate, a standard zinc coating will meet all requirements as it is applied underneath the dashboard of conventional cars.

### Fastening

Joining magnesium components using fasteners is one of the most commonly used processes for this material. Two main aspects of this method must be analysed thoroughly in order to design to the requirements of the material [1, 2].

Galvanic corrosion must be avoided by coating the fasteners, preventing electrical between the two materials [3, 4].

Especially when using steel fasteners, the design must take into account the lower creep resistance of commonly used magnesium alloys as compared to aluminium or grey cast iron. Components like transmission cases, oil pans or engine blocks need to be designed accordingly to avoid relaxation, and thereby loosening, of the joint.

### Steel Fasteners

Steel fastener systems for magnesium components must provide a separation of the metallic surfaces of magnesium and steel bolts in the presence of electrolytes. This is not required in a dry atmosphere like the passenger compartment or underneath the cockpit of an automobile [5, 6].

Commercially available steel fastener systems are based mainly on the following concepts:

- Covering the bolt head and the surface under the head with Polyacrylnitril (nylon) layers
- Coating the bolts with chromate containing layers (e.g. Dacromet®)
- Coating the bolts with chromate free layers based on zinc flake pigments in an epoxy resin matrix (Deltatone®, Deltaseal®)

Additionally, the separation of the steel bolt and part can also be achieved by using a washer made of low-copper-content aluminium. It is recommend that the washer be fixed to the bolt in order to avoid both additional logistical work and failures caused by lost washers.

When steel fasteners are used for magnesium power train applications, the system will suffer from thermal cycling. Temperatures may range from ambient temperatures – which in severe cases might be  $-40^{\circ}\text{C}$  – to running temperatures of around  $+150^{\circ}\text{C}$ .

Due to the significantly lower thermal expansion coefficient of steel compared to magnesium, the surface pressure under the bolt heads will increase and exceed the maximum allowable surface pressure. Creep will occur and the bolts' preload will drop. This will result in leakage or in loosening of the joint [7].

To avoid this, bolts with an increased head diameter must be used in order to reduce the surface pressure under the head below the maximum tolerable value for the given magnesium alloy.

For the proper design of a fastener system, the minimum thread engagement  $m_{\text{eff,min}}$  needs to be applied. In case of overload, the bolts would be damaged and more easily removed than the threaded tap. Otherwise, time-consuming and costly reworking of the thread would be required [5].

For steel fasteners (grade 8.8), a minimum thread engagement  $m_{\text{eff,min}}$  of 2.5 times the diameter of the bolt is required. This may lead to design problems when there is insufficient space to meet this requirement.

To solve this problem, inserts to reinforce the thread area can be applied. Minimum thread engagement  $m_{\text{eff,min}}$  of 1.0 to 1.5 times the diameter of the bolt and more (Fig. 6.83) will then be sufficient. The use of push-in nuts is also acceptable.

With regard to design for recyclability, it should be mentioned that the use of steel fasteners always presents the possibility of dissolution of iron in the magnesium melt. This is detrimental to the corrosion resistance of the magnesium alloy produced by the addition of a secondary metal.

### Aluminium Fasteners

Promising new developments in the field show great potential for the use of aluminium fasteners in joining magnesium parts [1, 8 – 11]. The main advantages are:

- Avoidance of galvanic corrosion
- Reduction of preload of fasteners to avoid extensive plastification and long-term relaxation
- Avoidance of preload increase at elevated temperatures and thereby avoidance of loosening of joints through thermal cycling during use
- Reduction of minimum thread engagement  $m_{\text{effmin}}$
- Ease of recycling without polluting secondary molten magnesium with iron

**Length of Thread Engagement**

The length of the internal thread  $m_{\text{effmin}}$  required to meet the design parameters also depends on the ratio of the material strength between bolt and nut:

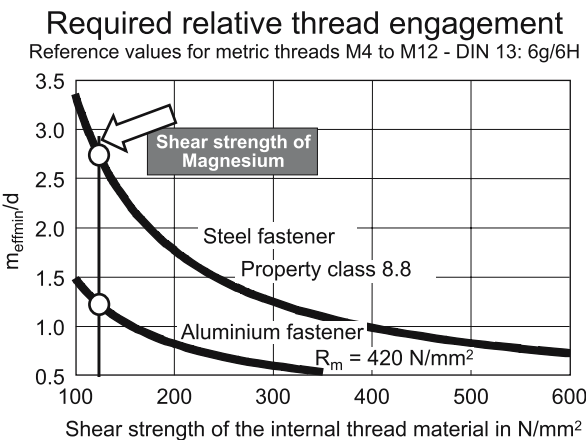
$$m_{\text{eff,min}} = \frac{R_{\text{mB}} \cdot A_{\text{s,nom}} \cdot P}{C1 \cdot C3 \cdot \tau_{\text{BM}} \cdot [P/2 + (d_{\text{min}} - D_{2\text{max}})\tan30] \pi \cdot d} + 0.8 P$$

where

- $R_{\text{mB}}$  = tensile strength of screw material
- $\tau_{\text{BM}}$  = shear strength of external thread
- $A_{\text{s,nom}}$  = thread nominal stress area
- $P$  = thread pitch
- $C1, C3$  = Alexander factors
- $d_{\text{min}}$  = screw thread major diameter, minimum
- $D_{2\text{max}}$  = internal thread pitch diameter, maximum

As a result, the required length of thread engagement will increase as the strength of the screw increases relative to the strength of the internal thread (Fig. 6.83).

For example, according to a well known design principle – in case of overloading a bolted joint, the fastener will fracture in its shank or in the free, stressed thread area – the threads of an 8.8-class screw used to join magnesium compo-



**Fig. 6.83.** Required relative thread engagement for aluminium and steel fasteners

nents made of a magnesium alloy with a shear strength of  $150 \text{ N/mm}^2$  should be engaged to a length of approximately  $2.3 d$  to prevent the internal thread from stripping immediately during the initial installation. Switching to an aluminium screw with a tensile strength of e.g.  $420 \text{ N/mm}^2$  would reduce the required length of thread engagement to a value of approximately  $1 \times d$ .

### Example M8

Screw made of steel, 8.8: Minimum length of thread engagement: 18.4 mm.

Screw made of aluminium: Minimum length of thread engagement: 8.0 mm.

When using an aluminium screw or a screw made of steel of a low strength rating, a shorter length of engagement may become feasible. This translates into lower manufacturing costs, lower costs for the fastener and, additionally, the possibility of thinner-walled bolting components.

### Surface Pressure

The permissible interface pressure for the particular clamped material should not be exceeded so as to avoid any excessive plastic deformation in the head contact area (bearing surface) of the screw, even when the bolted joints are in operation. As a rule, exceeding the interfacial pressure limit will result in a loss of the preload, jeopardising the operational reliability of the joint [2, 12].

In the event that a fastener of relatively high tensile strength is used to clamp components made of materials of a lower strength rating, special provisions should be made to comply with the requirements mentioned earlier. This may include the rather limited use of a fastener or the reduction of the surface pressure by enlarging the head-bearing diameter.

**Example:** Bolting of magnesium components, magnesium alloy tensile strength  $R_m = 240 \text{ N/mm}^2$ .

(a) Using a steel screw of property class 8.8:

- Normally, during installation it may not be possible to fully utilise a screw with a standard head, e.g. one per ISO 4014 (DIN 931). Whenever the strength of the screw is clearly greater than that of the clamped components and the head-bearing area is approximately equal to the thread stress area, only a limited utilisation of the fastener will be possible (utilisation factor  $v_s \ll v_p$ ; see Fig. 6.84). This also means that the above-mentioned design concept cannot be achieved and that there will always be the risk of premature damage to the bolted joint.
- However, if there is a bearing stress problem, the screw could be used if the compressive unit load were sufficiently reduced by enlargement of the head contact area. This may be accomplished by using washers or by configuring the screw head to provide a dimensionally adequate contact surface diameter.

where

$p$  = surface pressure

$A_s$  = nominal stress area of screw head

$A_p$  = head contact area

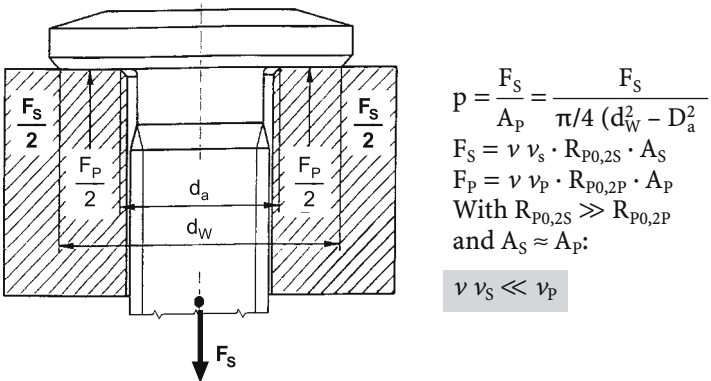


Fig. 6.84. Surface pressure under bolt head

b) Using an aluminium screw:

The use of screws made of a light metal, e.g. aluminium, is always beneficial when the components are also made of a light metal, e.g. magnesium alloys. The differences in the strength of both materials in this case are relatively small, which – with respect to the compressive load – makes any drastic enlargement of the head contact area unnecessary.

Most suppliers recommend a specific bolt geometry for fasteners being used for magnesium applications. For example, one supplier has conceptualised the geometry of the head contact area of screws made of aluminium having an external lobe hex for torque application (ASR) so that, even with a relatively low strength of the clamped components and a loss of strength due to the effects of temperature, plastic deformation of the clamped materials is largely prevented (Fig. 6.85).

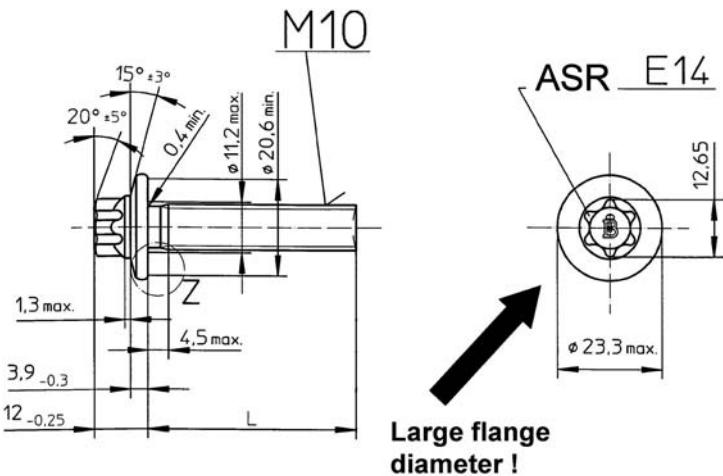


Fig. 6.85. Magnesium-specific bolt design



### Elastic Compliance

The elastic compliance  $\delta = l/(EA)$  of the screw and the clamped components has a major effect on the proportion of the operation force  $F_A$  to be transmitted by the screw. This force to be transmitted by the fastener, i.e. the added screw force  $F_{SA}$ , will decrease as the elastic compliance of the screw increases, that is the force ratio  $\Phi$  becomes smaller:  $\Phi = F_{SA}/F_A$ . The reduction of the force ratio is affected by three parameters: grip length  $l_K$ , Young's modulus for the material of the screw and the clamped components, and the screw diameter or the area of the clamped components.

Young's modulus values for light metals such as aluminium, titanium and magnesium rank considerably below those for steel.

In actual practice, to the threaded fastener engineer this means that, for the same operational force  $F_A$  and compared to a steel screw joint, the force ratio  $\Phi$ , and thus the added screw force  $F_{SA}$ , may be considerably reduced simply by using e.g. an aluminium alloy screw (Fig. 6.86).

### Stress/Strain Properties: Effects of Temperature

Environments with stable or unstable temperatures alike may cause a change in the installed preload due to the difference in thermal expansion factors. The change in Young's modulus for the screw and the clamped components due to exposure to temperatures may be disregarded; the preload change is the result of thermal expansion only [11, 12].

The following equation applies:

$$\Delta F_M = F_{MRT} - F_{MT} = (\alpha_s \Delta T_s - \alpha_p \Delta T_p) : (l/E_s A_s + l/E_p A_p),$$

where

$\Delta F_M$  = preload change

$F_{MRT}$  = preload at room temperature

$F_{MT}$  = preload at temperature T

$\alpha_s$  = thermal longitudinal expansion factor for screw material

$\alpha_p$  = thermal longitudinal expansion factor for the material of clamped components

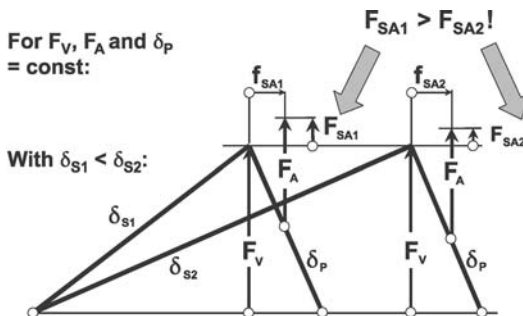


Fig. 6.86.

- $\Delta T_s$  = temperature change in screw
- $\Delta T_p$  = temperature change in clamped components
- $E_s$  = Young's modulus for screw material
- $E_p$  = Young's modulus for material of clamped parts
- $A_s$  = area of screw head
- $A_p$  = area of clamped components

When introducing the elastic compliance parameters  $\delta_s = l_s/(E_s A_s)$  and  $\delta_p = l_p/(E_p A_p)$  for uniform temperatures between the screw and the clamped components, and with  $l_s = l_p = l_K$  (grip length), this calculatory relationship is simplified and reads:

$$\Delta F_M = (\alpha_s - \alpha_p) l_K \Delta T : (\delta_s + \delta_p).$$

In particular, the use of steel screws for light metal joints may cause considerable preload changes due to critical differences in their thermal longitudinal expansion. For a temperature increase of 100°C, a bolted assembly involving magnesium components and a steel screw may sustain an increase in axial stress of up to approximately 150 N/mm².

Figure 6.87 also shows that the increase in axial stress due to an increase in temperature may be considerably reduced by reducing the differences in the thermal longitudinal expansion factors between the screw material and the material of the clamped parts.

Example: Bolting magnesium components with aluminium screws.

**Screws and Bolts Made of Aluminium Alloys – Test Results**

*Mechanical Properties at Room and Higher Temperatures*

Generally speaking, high mechanical strength and good corrosion characteristics in aluminium-type materials are mutually exclusive. An increase in strength during hardening is promoted by the alloy elements copper and zinc, which, on the other hand, have a detrimental effect on the corrosion properties. Especially in bolted joints for magnesium components, higher preload forces cannot generally be applied due to relatively low permissible compression loads.

$$\Delta F_V = \frac{(\alpha_p - \alpha_s) l_K \Delta T}{\delta_s + \delta_p}$$

Material of structural part Magnesium, $\alpha_p = 27$	$(\alpha_p - \alpha_s)$ $10^{-6}/K$		
		Screw-material:	
Titanium	ca. 27 – 8,6 = 18,4		
Steel	ca. 27 – 11 = 16		
Aluminium	ca. 27 – 23 = 4		

Fig. 6.87. Change of preload by thermal extension

The material strength of aluminium fasteners after exposure to higher temperatures (150°C) was barely lower, while screws made of e.g. 7075 (AlZn 5.5 Mg-Cu) showed a distinct drop. This characteristic is due to the relatively high thermal aging temperature for aluminium fasteners.

**Relaxation Properties**

The use of an aluminium screw has proved to be particularly beneficial in relaxation tests run with magnesium components. Thermal expansion of the aluminium screw is only slightly less than that of the clamped magnesium components.

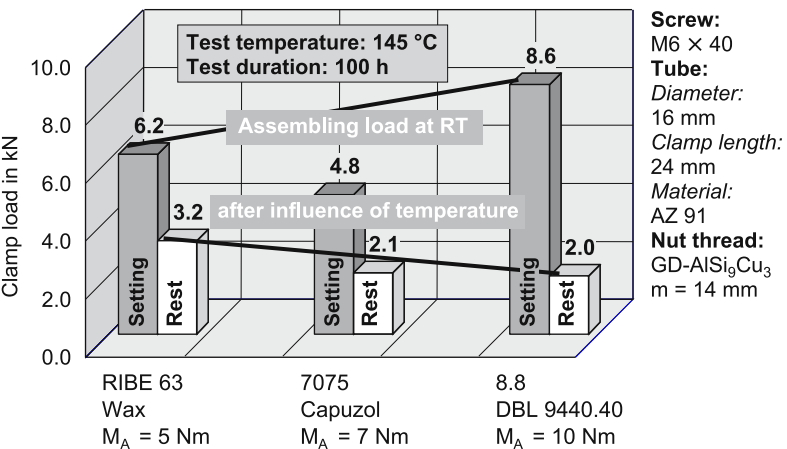
Therefore, the additional mechanical stress applied to the magnesium due to heat and, consequently, the creep process amount to less than it would have been with a steel screw. Tests have clearly shown that, despite an initially higher preload, after a longer exposure time at 145°C the preload level of a steel screw falls far below that of an aluminium screw. Preloads were always measured after the joint had cooled to room temperature (Fig. 6.88).

**Frictional Properties and Installation Behaviour**

Frictional conditions under the screw head and in the threads have a major effect on the amount and variance of the preload force generated, especially in torque controlled installations.

Experience also indicates that, in general, adverse frictional properties are to be expected whenever components of a similar material or finish are mated. As a rule, those conditions call for a custom lubricant. Also important is the behaviour of the lubricant during multiple installations.

Figures 6.89 and 6.90 show the frictional behaviour during installation. Frictional data for the threads and the screw head can be read directly from the graphs.



**Fig. 6.88.** Influence of fastener material on relaxation strength of bolted magnesium joints

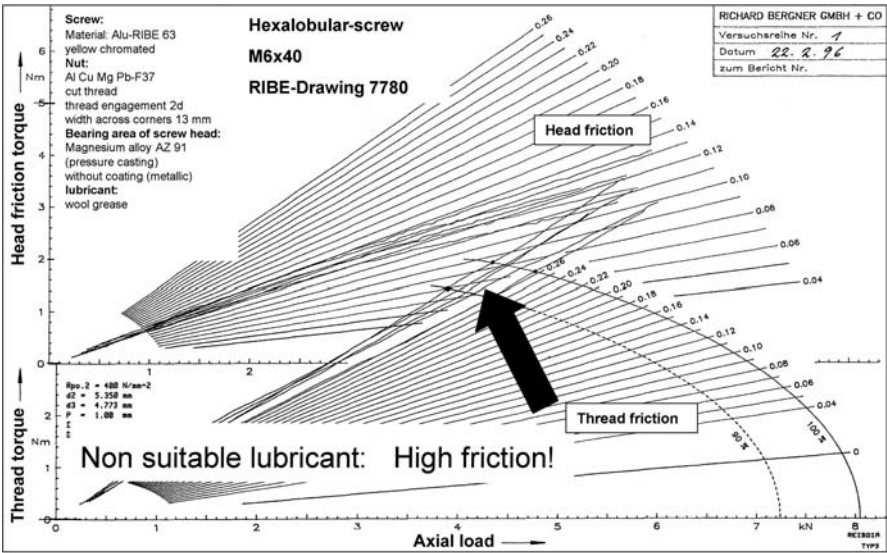


Fig. 6.89. Friction tests with M6 aluminium screws. Use of an unsuitable lubricant

The tests represented in Fig. 6.89 were run using a lubricant that in fact had tested well in other instances but was inadequate for the combination of an aluminium screw with an aluminium nut. The respective thread frictional readings were extremely high. Regarding friction, a product consisting of a mixture of synthetic waxes tested considerably better (Fig. 6.90).

In addition to certain design parameters (e.g. the grip of the bolted joint), the most important requirement for the use of torquing methods that exceed the yield point is sufficient ductility of the screw material. As our tests showed, aluminium screws made of aluminium alloy A 6013 may also be torqued using the yield point control or the angle control method.

The installation graph of Fig. 6.91 is an example of the characteristics of the preload force and the tightening torque versus the angle of rotation, up to screw fracture. In this case the uniform elongation, i.e. the plastic elongation of the threaded shaft up to the point where (at maximum preload) localised reduction in area occurs, was 0.9 mm. This is equivalent to an angle of rotation of 325°. This value shows that there is sufficient plastic strain capacity available for installations exceeding the yield point.

Fatigue Limits

Aluminium has a lower fatigue strength than steel. It is also known that anodising may have a detrimental effect on dynamic material behaviour. Figure 6.92 shows the results of alternating fatigue tests on M12 aluminium screws made of aluminium alloy A 6013. The fatigue limit was found to be only  $\sigma_A = \pm 20 \text{ N/mm}^2$ . The fatigue limit of an anodised screw at  $\sigma_A = \pm 10 \text{ N/mm}^2$  was only half as much as that of the non-anodised, bright screw (at room temperature). Basically, the



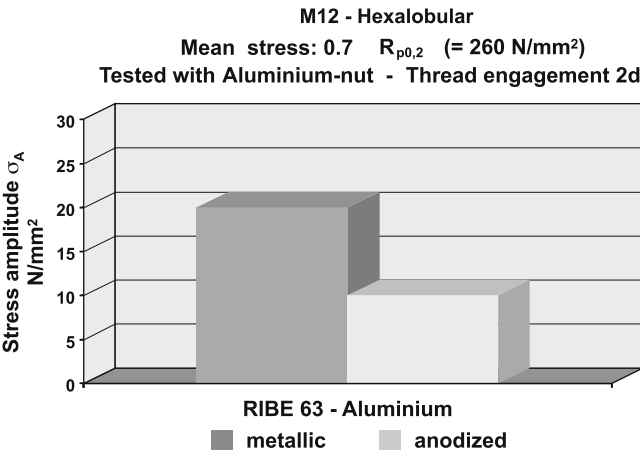


Fig.6.92. Fatigue of aluminium fasteners

**Corrosion Test Results**

Initially, corrosion tests were run according to DIN 50021 (salt spray test) using screws made of different aluminium alloys. The screws had one of the following finishes: (a) bright (heat-treated surface), (b) yellow chromated, or (c) anodised.

The best results were obtained from the material types 5056 and aluminium alloy A 6013, both having a yellow chromated finish. In comparison, anodic oxidation in general provided no substantial corrosion protection.

The favourable corrosion properties of 5065A are due to the very low content of its alloy elements copper and zinc. Starting at approximately 80°C, however, this type of material tends to develop stress corrosion. Therefore, it was not taken into consideration for screws joining magnesium components.

Additional tests were run to determine to what extent corrosion protection is diminished when the protective layer is damaged during installation – especially at the screw head. Yellow chromated ASRI screws were installed three times and then subjected to the spray test. Compared to 7075, aluminium alloy A 6013 showed clearly superior results.

Corrosion tests that are more closely adapted to actual in-service conditions are more informative than tests run according to DIN 50021. In this test, aluminium alloy A 6013 again proved to be superior to the 7075 and 7050 materials. Compared to anodising or oiling, yellow chromating provided the best corrosion protection.

**Joining by Casting Using Inserts**

Joining by casting is used in aluminium engine block manufacturing mainly for incasting of aluminium or grey cast iron liners. Recently, an aluminium–magnesium hybrid engine block for a six-cylinder engine was successfully introduced in high-volume production.

### Joining by Forming

In applications where fusion welding processes cannot be applied, joining by forming becomes an interesting alternative. This is the case when non-weldable or dissimilar materials have to be joined. Due to the absence of a liquid phase during the process, there is no threat of formation of brittle intermetallic phases.

Joining of precoated sheet metal has become more popular in the automotive industry. Additionally, there is a trend to join preassembled modules to the already trimmed body. Those applications require joining techniques with no or relatively low heat input. Furthermore, no dust, weld spatter or fumes may be generated as this would require an expensive cleaning operation. Joining by forming can be an alternative or a supplement to adhesive bonding.

Clinching, self-piercing riveting and friction stir welding have been investigated for joining magnesium sheets.

### Clinching

Clinching is a special application of joining material by local plastic deformation of parts by the use of mechanical forces. As the forming limits of magnesium at room temperature are comparatively low, the clinching operation should be performed at elevated temperature ( $< 260^{\circ}\text{C}$ ) of the joining material.

While this is easy under laboratory conditions, successful industrialisation of the process will require the development of machine tools capable of providing the right temperature conditions in an acceptably short time; it is believed that the use of a highly localised mechanism applied to the magnesium component only would make a cycle time of 5s achievable.

Figure 6.93 shows a schematic of a Mg/Al test joint and the cross section of a real joint highlighting the critical areas.

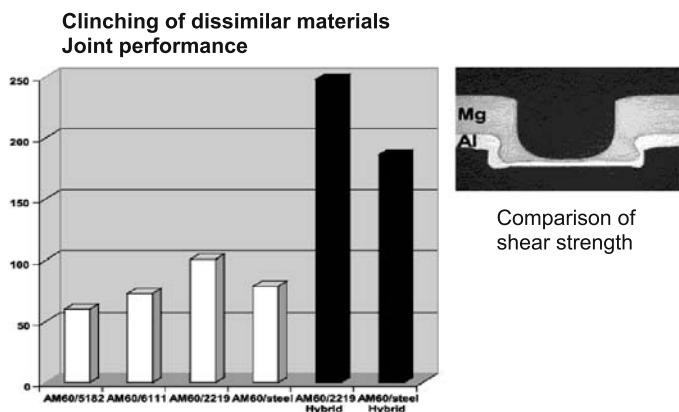


Fig. 6.93. Comparison of shear strength of clinched dissimilar materials

### Acknowledgement

The author wishes to thank Mr. Thomas Huehnert, Supervisor Fastening and Sealing at the International Technical Development Center of Adam Opel AG, Ruesselsheim and Dr. Wolfgang Thomala, Manager Research & Development, Richard Bergner Verbindungstechnik GmbH, Schwabach, Germany for their most valuable support.



### 6.4.3 Welding and Other Thermal Processes

*Günter H. Deinzer, Michael Rethmeier*

#### 6.4.3.1 Weldability of Magnesium Alloys

Welding of magnesium and its alloys has been known since 1924 and was described precisely between 1929 and 1931 [13]. The first results concerning welding of magnesium in Germany were published in 1938 and 1939 [14, 15]. Early results concerning short-circuiting-, impulse- and spray-arc-welding were presented between 1960 and 1970 mainly by L.F. Lockwood [16–20]. In the last years, great progress has been achieved, for the short-circuiting-arc, which is used for MIG-welding of thin sheet.

Magnesium puts high demands on the welding process because of its physical properties. Magnesium alloys show a relatively broad melting interval of about 420–620°C. In combination with low-melting eutectics one has to take a considerable risk of hot-cracking into account. In comparison with aluminum alloys, some important differences occur, so that it is not possible to transfer the knowledge of welding aluminum alloys directly to the welding of magnesium alloys: One needs only 60% of the energy to melt the same volume of magnesium compared to aluminum. The required energy for welding is reduced to 1/3 because of the lower heat conductivity. Furthermore, magnesium alloys have only half the vaporisation temperature, that is, about 1,100°C. The vaporisation pressure in the relevant temperature interval for welding is 3–4 powers of ten higher than that of aluminum. These properties lead to great problems concerning the heat input into the weld filler metal which can result in excessive spatter formation. As a consequence of the high thermal expansion coefficient which is more than twice that of mild steel and still 10% higher than that of aluminum alloys one has to consider high welding distortion and clamping forces.

The electrical conductivity is similar to mild steel and so the use of resistance welding for magnesium alloys is possible.

#### 6.4.3.2 TIG Welding

TIG welding of magnesium alloys can be compared with TIG welding of aluminum alloys. AC-welding is preferred because the oxide-layer on the base metal has to be destroyed without overheating the tungsten electrode. Removal of the oxide-layer immediately before the welding should be avoided because the oxide stabilises the welding-arc. With a variation of the helium ratio in the shielding gas, the penetration can be controlled. The main difference of TIG welding of aluminum alloys is the lower required energy input, as explained before. As a mainly manual process, TIG welding is considered to be the choice for welding prototype pieces.

#### 6.4.3.3 MIG Welding

The greatest difference between MIG welding of aluminum and magnesium alloys is seen in the heat input into the filler metal. With magnesium alloys the



possible temperature interval for heat input is very small (700–900°C). If the temperature of the filler metal exceeds ~900°C there is a great spatter loss (>50%). Therefore, one has to use a very low and exact heat input into the filler metal. The lowest heat input can be achieved with the short-circuiting-arc with very long periods between the single short-circuits. The result is voluminous drops at the tip of the filler metal with which a good weld-penetration can not be ensured.

For producing a better weld-penetration, impulse-arc-welding has to be used. But also with this technique it is impossible to increase the heat-input without getting much spatter-loss. If the energy is relatively low, it is impossible to warrant a secure drop detachment without a short-circuit. The spatter loss during some tenth of a second of the impulse-arc-welding-process (with short-circuits) is documented with the help of high-speed-photography. Metal loss due to spatter of about 50% appeared (see Fig. 6.94). If one tries to increase the energy to avoid short-circuits, the filler metal is heated above the vaporisation temperature. This leads to an irregular and disturbed drop detachment because of the vaporising filler metal which results again in great spatter-formation.

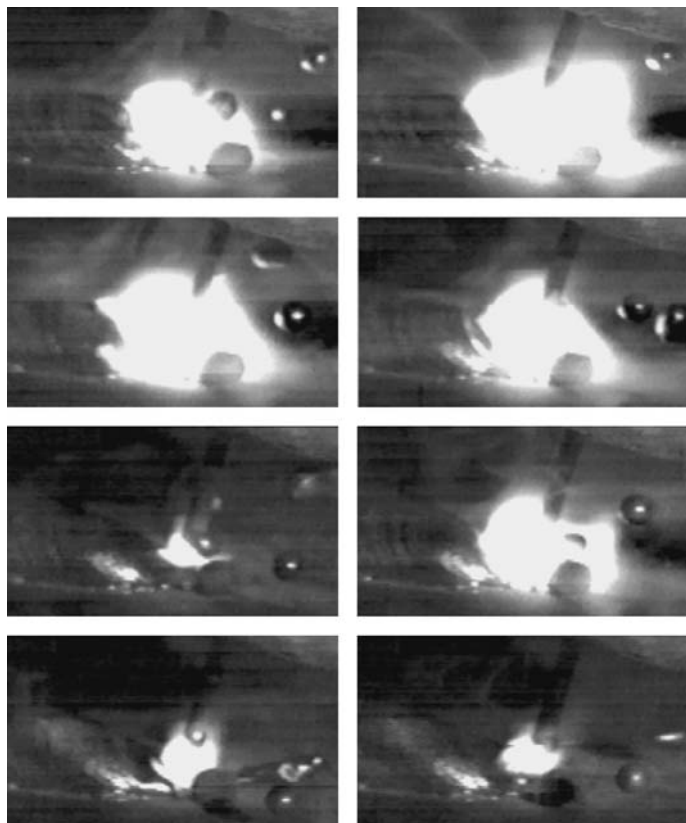


Fig. 6.94. Spatter-formation during MIG-impulse-welding



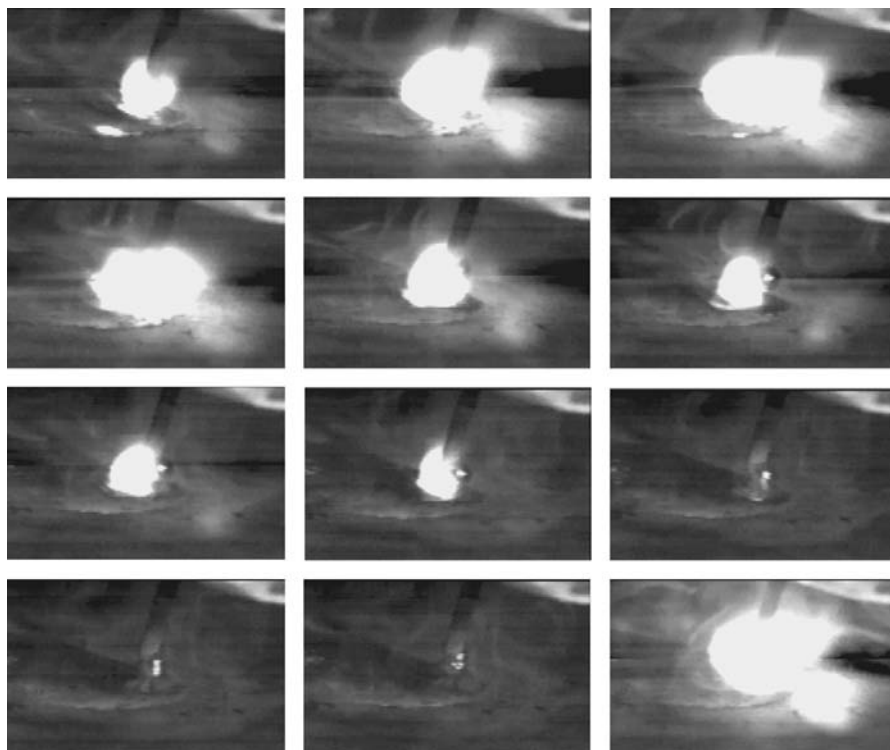


Fig. 6.96. Metal transfer during a triggered short-circuiting-arc

Furthermore, one has to consider a 10% higher thermal expansion coefficient compared to aluminum when taking into consideration the fixing of the work-pieces. This thermal expansion coefficient necessitates a very rigid clamping of the joining members to avoid any movement in the joining area.

**Metallographic investigations.** A typical microsection of base metal, heat affected zone and weld metal of MIG-welded AZ31 with AZ61 filler metal is shown in Fig. 6.98. The structural constituents are the same as those that can be found in the literature on this subject [21, 22].

A weld of AZ31 with overmatched filler wire AZ61 was analysed using polarised light, see Fig. 6.99. It is possible to show some differences between the base metal (top line) and the weld metal, with the heat affected zone (bottom line). In the base metal the grains are coarser than in the weld metal. The grain refinement in the weld metal is one result of the higher aluminum content of the filler metal. The other effect is the higher amount of the  $\beta$ -phase ( $\text{Mg}_{17}\text{Al}_{12}$ ) in the weld metal. It is obvious that this  $\beta$ -phase is arranged on the grain-boundaries. This has no negative influence on the mechanical behaviour of the joints.

Mappings taken with the electron-micro-probe-analyser (EMPA) show the distribution of alloying elements and can help to recognise any loss of them. In

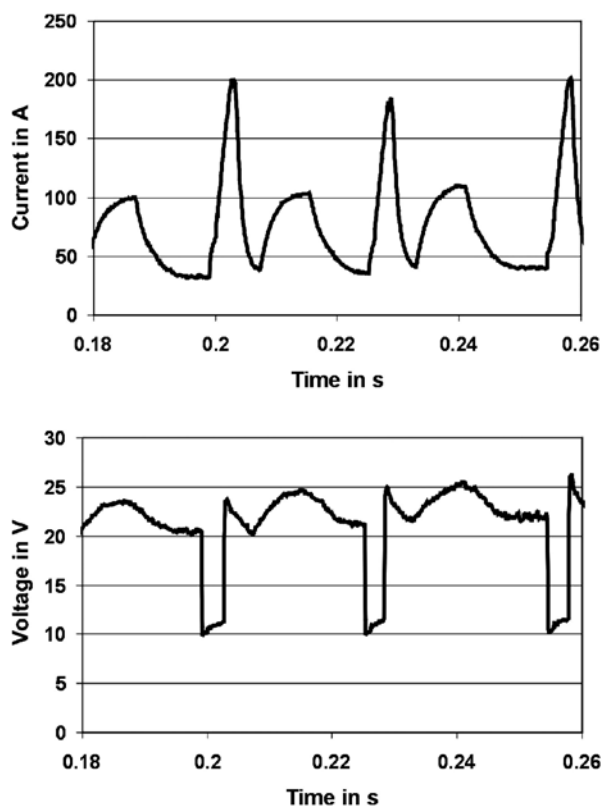
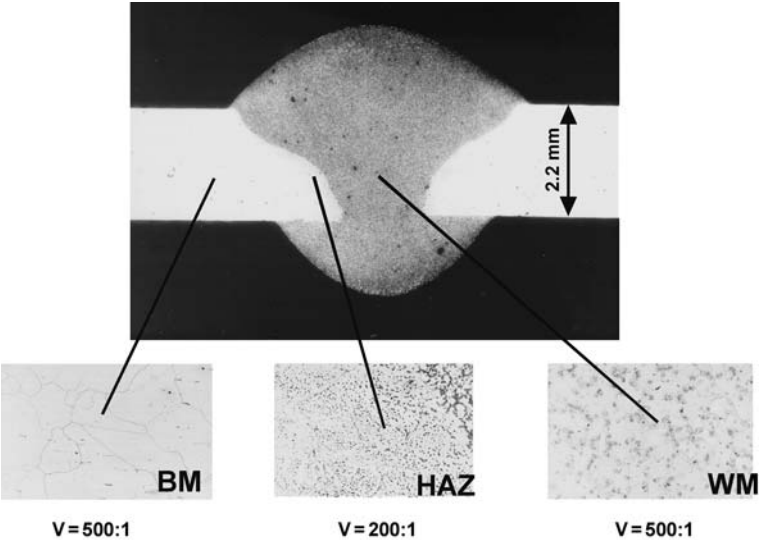


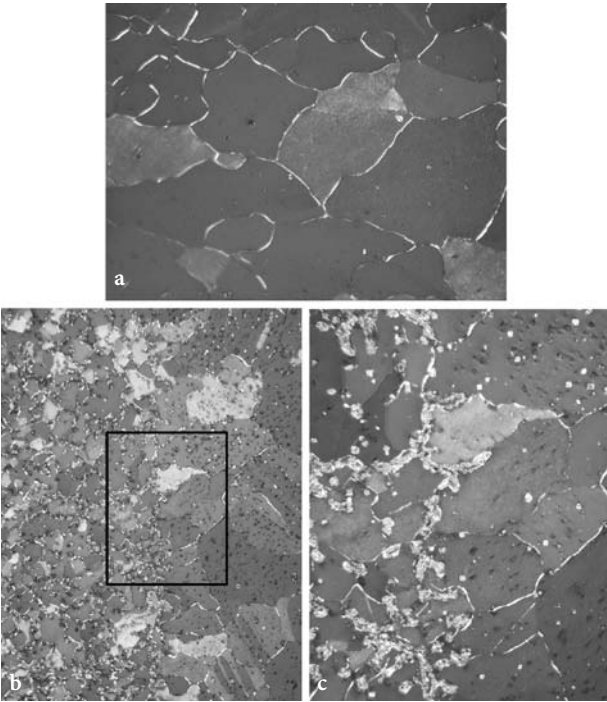
Fig. 6.97. Experimentally determined welding power source characteristic

the top line the magnesium (left) and aluminum (right) distribution is shown, whereas the base line displays the manganese (left) and zinc (right) content. Analyses of welded AZ31 extruded profiles with overmatched filler material (AZ61, Fig. 6.100) show a homogenous distribution of the elements. Differences occur only between filler and base metal. Loss of alloying elements during welding can thus be excluded. As to be expected, the element distribution in Fig. 6.100 shows a higher content of aluminum in the welding seam. Weld deposit dilution was determined to be 50% (see Fig. 6.100).

**Strength of MIG-welded joints.** Specimens welded at 1 m/min welding speed and a filler-metal feeding rate of 6.8 m/min were used for mechanical testing. The voltage reached 17.1 V and the short-circuit time was 15.9 ms. During the technological flexural test, bending angles up to 60° could be reached. Tensile tests of the butt welds – as welded and after removal of the weld reinforcement – revealed a strength from 80 to 100% of the base metal. Some typical results for AZ61 are shown in comparison with the specification of TIG-welded joints according to ASM in Fig. 6.101. One can see that it is possible to almost reach



**Fig. 6.98.** Microsections of base metal, heat affected zone, weld metal of MIG-welded AZ31 with AZ61 filler metal (magnification 200 and 500)



**Fig. 6.99.** Microsections using polarized light, **a** base metal, **b** weld metal, **c** magnified weld metal

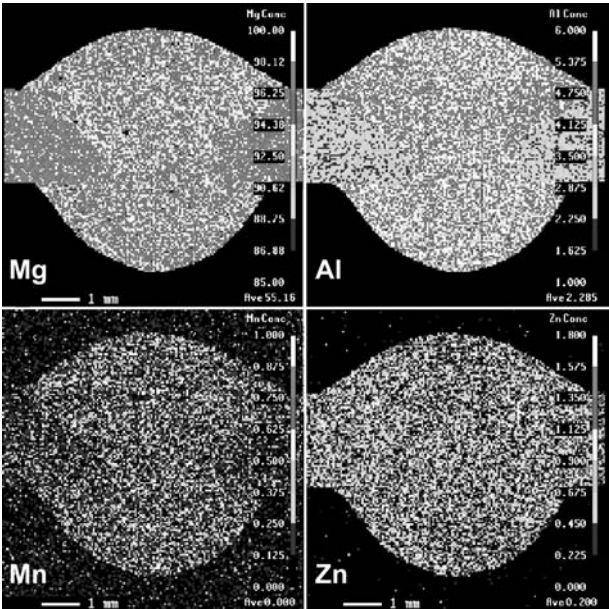


Fig. 6.100. Element distribution: AZ31 welded with overmatched filler wire AZ61

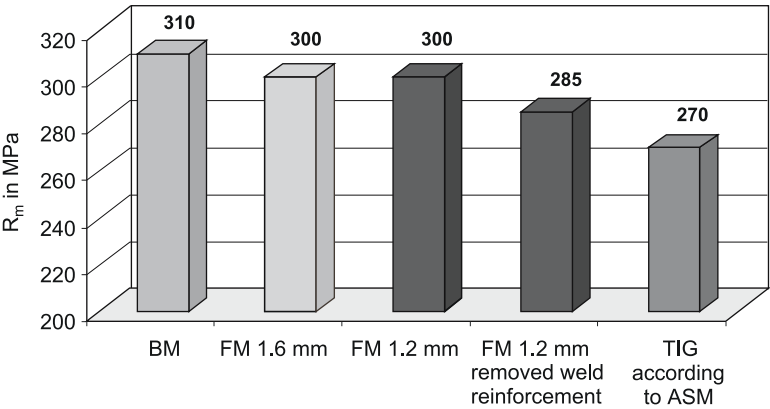


Fig. 6.101. Tensile tests of AZ61 (BM base metal, FM filler metal)

the strength of the base metal. In every case the specification of ASM is exceeded.

The fatigue behaviour under reversed plain bending without mean stress ( $R = -1$ ) is shown in Fig. 6.102. The results were analysed according to the statistical evaluation method arcus-sinus-squareroot-P. The fatigue strength of the as-welded joints reaches 50% of the strength of the base metal. If one is able to

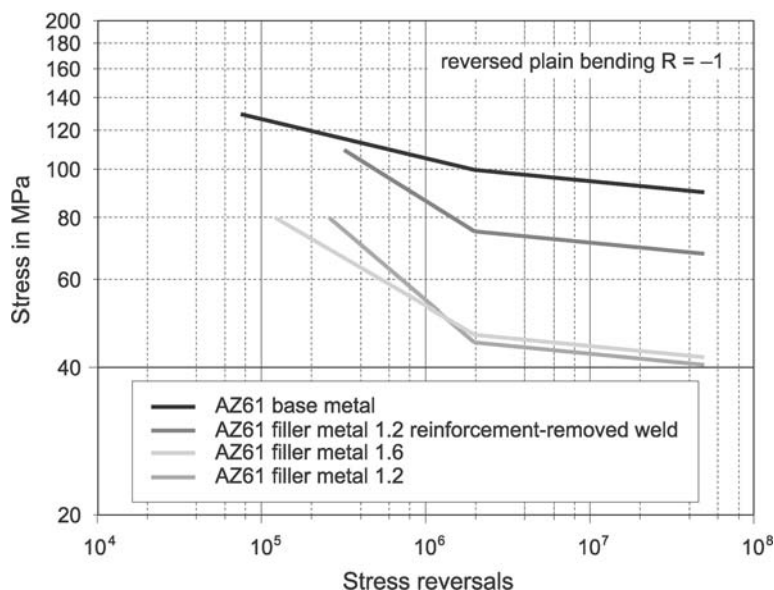


Fig. 6.102. S-N-curves of MIG-welded butt joints, AZ61, 2.5 mm thickness with matching filler wire, 50 % probability of failure

remove the reinforcement of the weld and therefore produce a macro notch free test specimen, the fatigue strength can reach 75% of the strength of the base metal.

#### 6.4.3.4 Laser-Beam Welding

Laser-beam welding of magnesium alloys offer the same potential advantages as it does with other metals: high speed, autogenous and neat, narrow welds. Because of the good coupling of the laser-beam and the low threshold energy density for initial coupling, magnesium alloys are particularly suited to laser-beam welding.

A microsection of a typical CO<sub>2</sub>-welded ZK60 of 5 mm thickness is displayed in Fig. 6.103. The laser power of 3 kW was used with a welding speed of 2 m/min. The view of the upper bead shows a high-qualitative weld seam without cracks.

In comparison to MIG-welding, laser-beam welding of magnesium alloys is uncomplicated. Difficulties occur mainly when a filler metal is used. Good welding results depend on the feeding of the filler metal. The coordination of laser beam, filler metal and base metal is therefore of crucial importance.

Laser beam welding is characterized by a very narrow interaction zone between beam and material surface and a high potential for automation and process control. Nd:YAG-solid state as well CO<sub>2</sub>-gas lasers are widely used for precision welding operations in industrial applications. Diode lasers are becoming more and more competitive while the mean output power is significantly increasing.



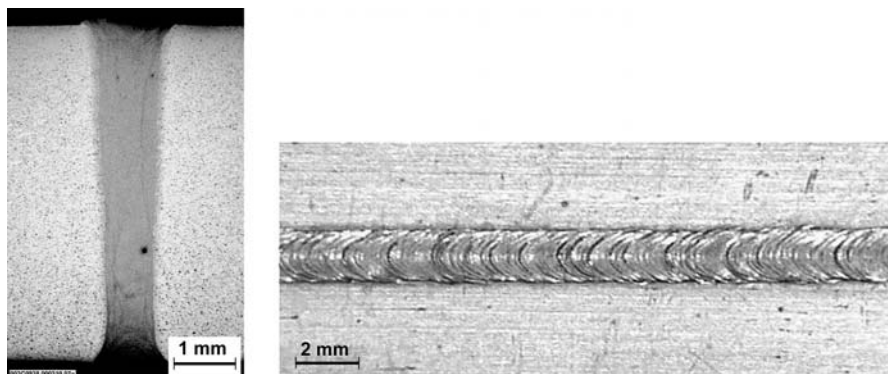


Fig. 6.103. Microsection and top view of laser welded ZK60

Nd:YAG lasers, with an output power in the range up to 4 kW, are operated in continuous wave or pulsed mode. The beam is transmitted from the source to the substrate through an optical fibre and a relatively small focusing head. Conventional multi-axis industrial robots are used to detect the relative motion of the laser beam and the substrate to be welded.

At present, CO<sub>2</sub> lasers, with an output power of up to 40 kW, are used in industrial applications mainly operating in the continuous wave mode. For most of the welding tasks an output power of 1 kW to 4 kW is sufficient. CO<sub>2</sub> laser beam guiding systems usually consist of a mirror system that is positioned by a gantry machine or a powerful industrial robot.

One characteristic of Nd:YAG or CO<sub>2</sub> laser welding is the formation of a laser induced plasma that increases the energy absorption on the material surface. It leads to a self-focusing of the incident laser beam and thereby generates a small but deep metal vapour pinhole. This results in a weld seam with a small width to depth ratio.

Diode laser welding is operated differently. Due to the high absorption of the laser wavelength, the head input, even without formation of a laser plasma, is high enough to melt a significant cross section of the bulk material (see Fig. 6.104).

Magnesium castings and wrought material can be successfully welded either with Nd:YAG, CO<sub>2</sub> or diode lasers. The main influences on the quality of the weld are given by the metallurgical consistency of the parts to be welded. Although the molten zone is relatively small for laser welding the level of porosity and inclusion still affect the results significantly.

The weld penetration and thereby the maximum weldable material thickness is mainly influenced by the line energy and thereby by the welding speed. A weld speed of 8 m/min at a beam power of 1.7 kW (cw) is achievable for 1.4 mm thick magnesium sheet without filler metal. Figure 6.105 shows a comparison of weld penetration as a function of welding speed for different materials. For magnesium, the figures at low welding speed are much higher than for steel or aluminum.

Investigations of the mechanical properties of welded joints show little decrease of strength figures. Yield strength and ultimate tensile strength can be



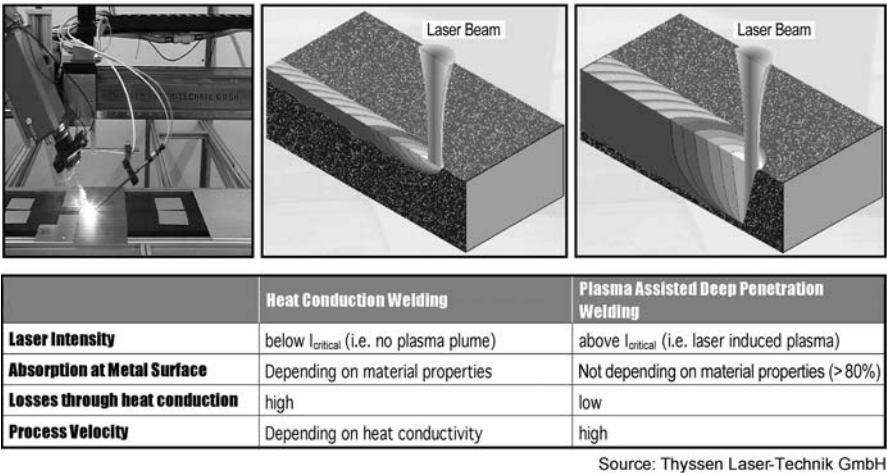


Fig. 6.104. Laser welding processes for joining magnesium sheet

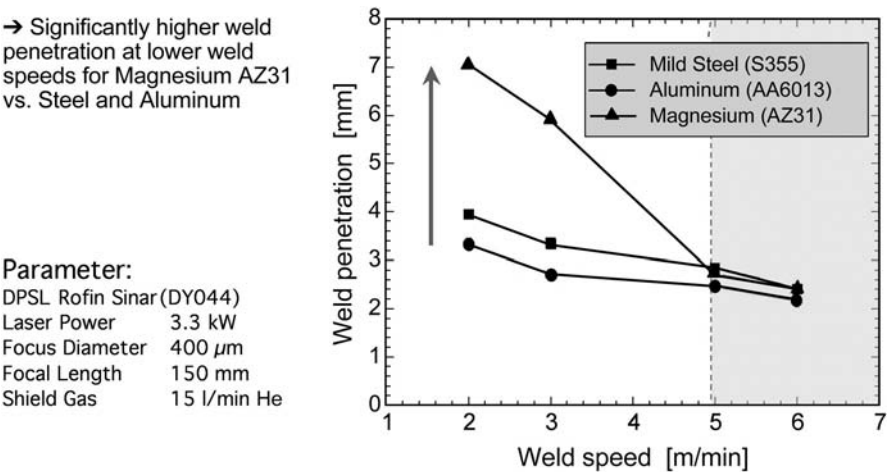


Fig. 6.105. Weldability of magnesium alloy vs. aluminum and steel

found in the range of 10% below the parent material in the case of butt welds. The use of filler metal improves the elongation to fracture figures significantly.

Investigations into the mechanical properties of laser welded sheet metals with a lap joint configuration show a decrease in sheer strength of 30–50%. In the latter case, this is due to the fact that the joint configuration of a single flange weld is very unfavourable to welding in general.

Modern light metal automotive body structures are designed as a framework of extrusions and castings. This requires welding techniques that are able to join parts manufactured using different process and different alloys. In laboratory

tests, AZ91 high pressure die cast parts and AZ31 extrusion have been successfully welded by laser beam welding using AZ61 filler metal. Welding of real body structures that require 3D operation is currently under investigation.

In the case of magnesium, heat conduction welding can also be applied. This process leads to improved weld seam quality, as there is much less turbulence in the molten material. No additional porosity through entrapped air is generated. Very homogeneous weld seams with no undercut or seam irregularities can be achieved at relatively high welding speeds.

#### 6.4.3.5 Electron-Beam Welding

Concerning the weldability of magnesium alloys, no crucial differences exist between laser and electron beam welding. Nevertheless electron beam welding is used to a limited extent, chiefly for repair, on commercial wrought and cast magnesium alloys. The main difficulties appear – in accordance with arc-welding – to be associated with the high vaporisation pressure of magnesium and zinc and also with their low melting point. It is usually impractical to electron-beam weld magnesium alloys that contain more than 1% zinc [23]. Circular oscillation of the beam or the use of a slightly defocused beam is helpful in obtaining sound welds [23].

#### 6.4.3.6 Friction Welding

Friction welding of magnesium alloys is possible, but has the known restrictions concerning the joint geometry of standard friction welding processes. An example of joining tubular shaped parts is shown in Fig. 6.109.

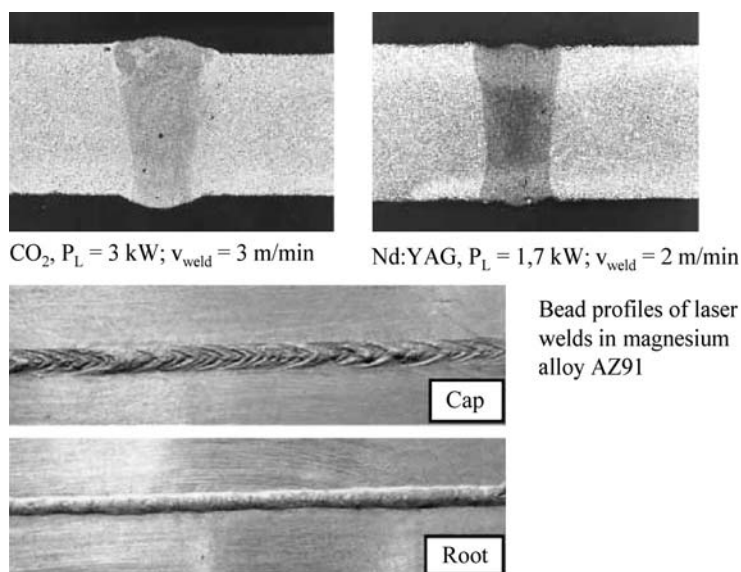


Fig. 6.106. Laser beam welding: cross section and bead profiles

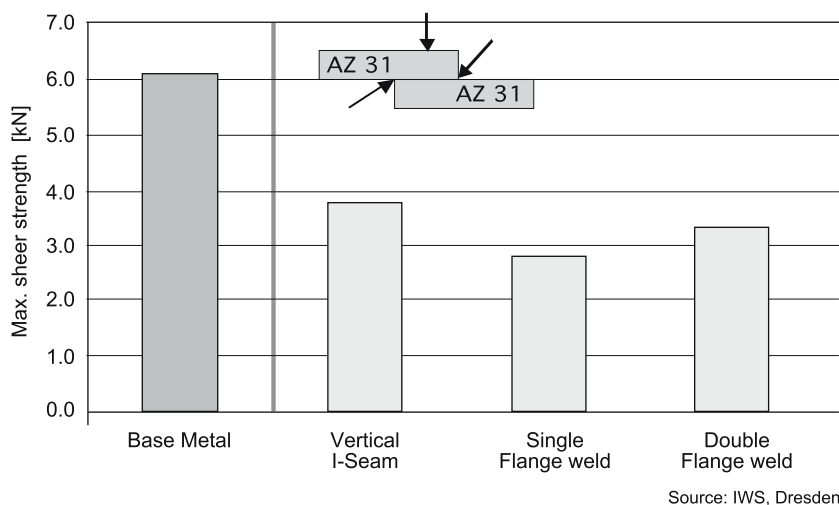
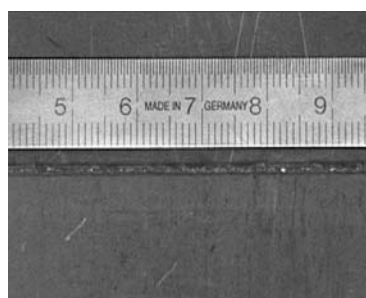
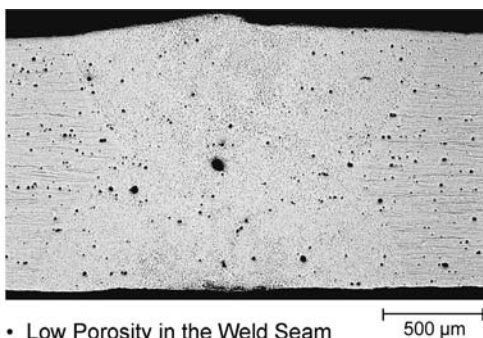


Fig. 6.107. Laser welding at the lap joint sheet metal alloy AZ31



- Material: AZ31
- Sheet Thickness:  $t_{1,2} = 1.4 \text{ mm}$
- Welding Speed.:  $7 \text{ m/min}$
- Type of Laser: Diode Laser



- Low Porosity in the Weld Seam
- No Cracks in the Weld Seam
- No Undercuts

Source: MgF Magnesium Flat Products GmbH/Thyssen Laser-Technik GmbH

Fig. 6.108. Heat conduction laser welding of magnesium sheet metal

An exception is the friction stir welding process (FSW). For FSW, in principle (see Fig. 6.110), the two pieces to be welded are brought into contact, placed on a backing plate and securely clamped. A specially designed cylindrical tool (see Fig. 6.111), consisting of a shoulder and a profiled pin is inserted into the joint. During welding, rotation of the shoulder (which is in intimate contact with the upper surfaces of the workpiece) and the pin produce frictional heat, bringing the material to the plastic state. As the tool translates along the joint line, plasticised material is stirred and forged behind the trailing face of the pin, where it con-

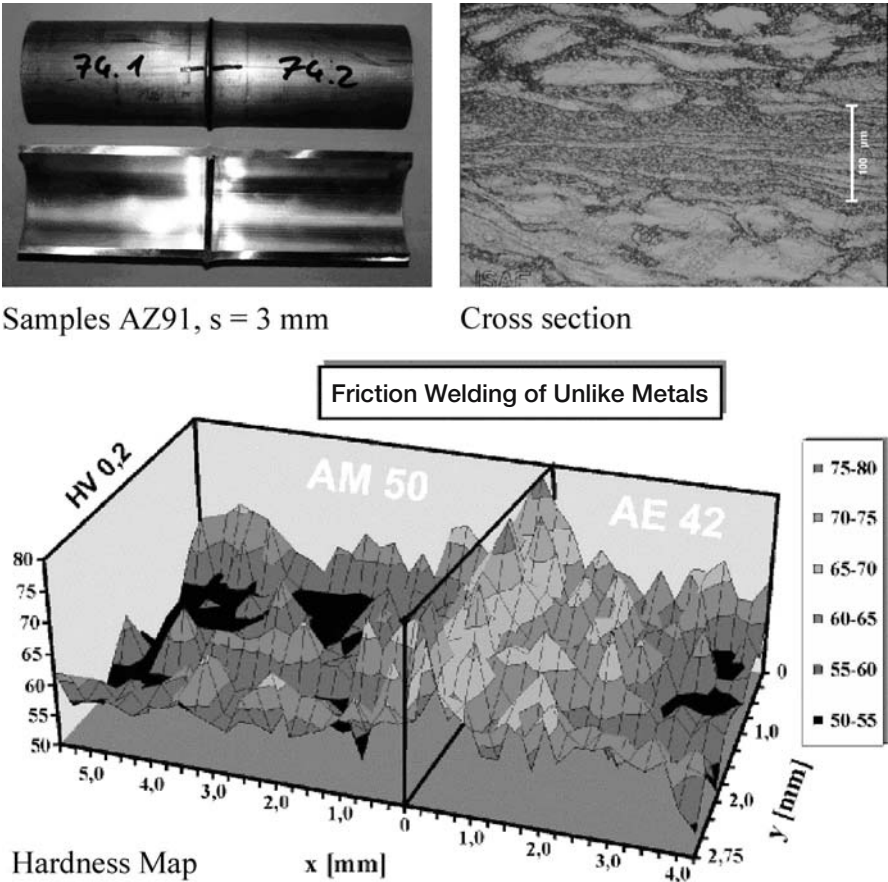


Fig. 6.109. Friction welding of forged magnesium tubes

solidates and cools down to form the solid state weld [24]. The tools are manufactured from a wear resistant material, which allows up to approximately 1000 m of welds in 5-mm-thick materials without changing the tool.

Friction stir welding is a patented joining process, which was invented at TWI in the 1990s. The welds are made below the melting point in the solid phase. The good mechanical properties, low distortion and residual stresses are attributed to the low heat input and the absence of melting [25]. Therefore it is a very suitable welding technique for magnesium alloys. Moreover, filler material is not required. A limitation of the process is that the best use is with long and straight welds. A typical weld seam and microsections are shown in Fig. 6.112.

The left picture in Fig. 6.112 shows the top of the weld seam with the typical hole at the end, where the tool leaves the plate. The three zones of FSW welding (nugget, thermo-mechanical-affected zone and heat-affected zone) are presented in the right picture with additional magnification, is indicated by the rectangle, in the middle picture.

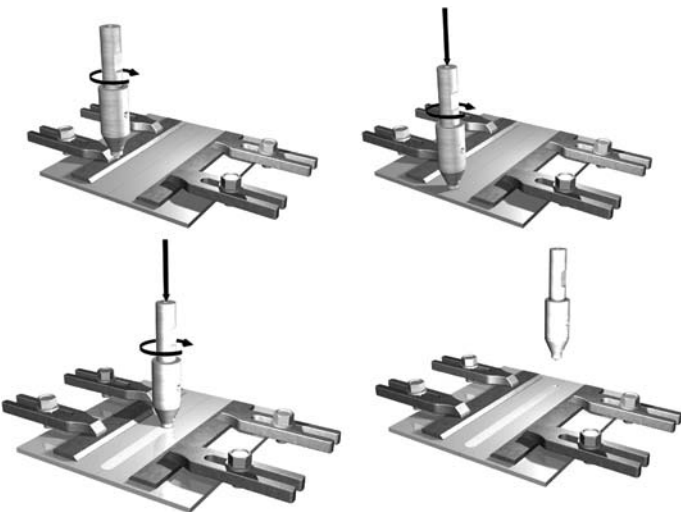


Fig. 6.110. Schematic FSW process [26]



Fig. 6.111. FSW-tool [26]

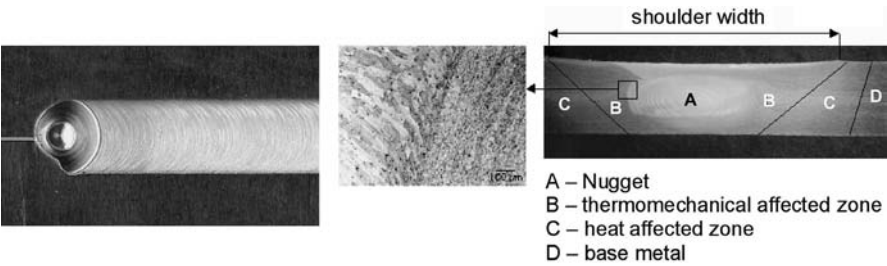


Fig. 6.112. Typical FSW weld seam (left) and microsection (middle and right) [26]

The effect of the welding speed on tensile properties of AZ91 and AM50 is shown in Figs. 6.113 and 6.114.

Possible joint configurations and the experimental set-up for Robotic FSW are displayed in Fig. 6.115.

Because of the high clamping forces, experiments with robotic friction stir welding are at a very early state of development. The welded geometries to date are still quite simple. FSW is also suitable for the joining of different materials in a multi-material design, for example, magnesium and aluminum alloys.

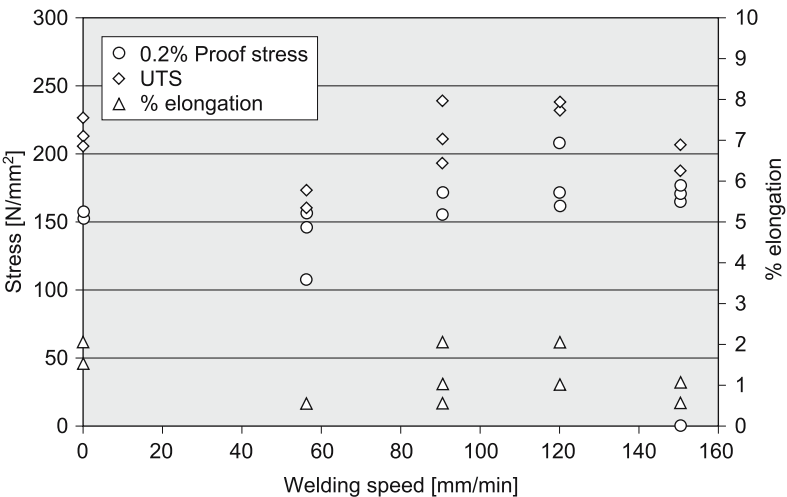


Fig. 6.113. Effect of friction stir welding speed on tensile properties magnesium alloy AZ91

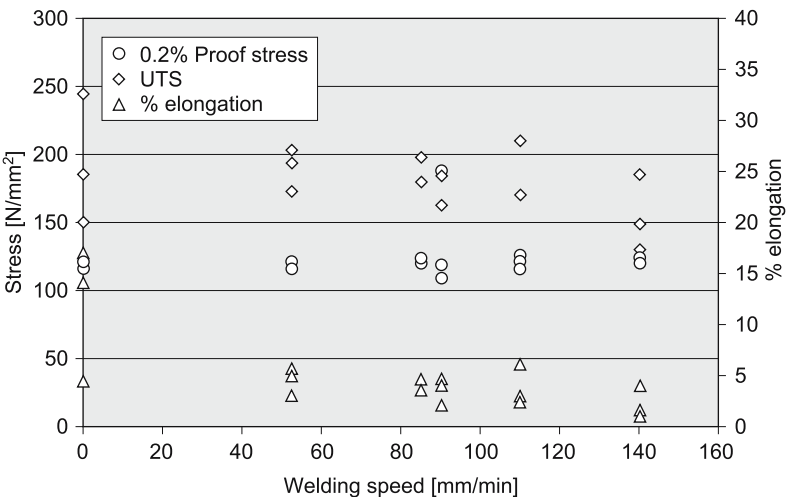


Fig. 6.114. Effect of friction stir welding speed on tensile properties magnesium alloy AM50

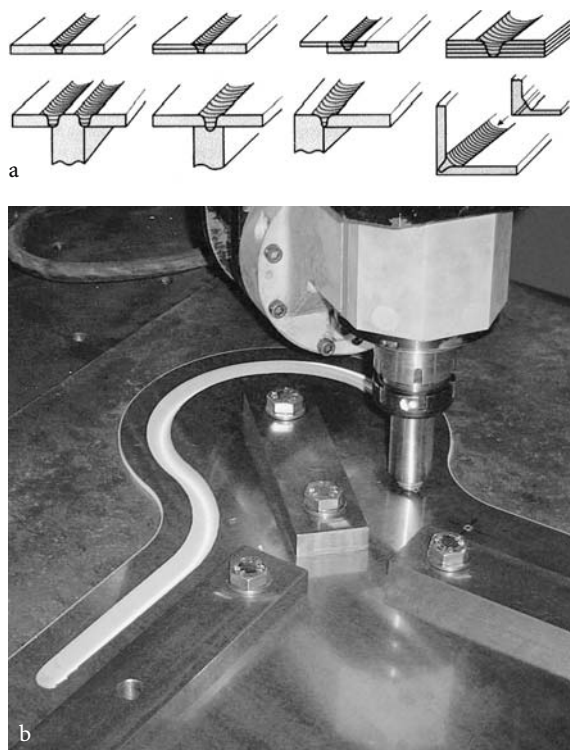


Fig. 6.115. Possible FSW joint configurations (a) experimental set-up for Robotic FSW (b) [26]

#### 6.4.3.7 Brazing and Soldering

Brazing and soldering processes are currently seldomly employed in the assembly of magnesium parts. They can be brazed by the furnace, torch and dip methods. The recommended method is dip brazing [22, 23].

Three filler metal alloys, with different ranges of melting and brazing temperatures, are used for brazing magnesium alloys: BMg-1 (for higher-melting alloys), AZ125A (for low-melting alloys) and GA432 (for very low-melting alloys such as ZK60A) [22, 23].

Prebrazing cleaning is important for successful brazing. All dirt, oil and grease must be removed by solvent degreasing. Surface films such as chromates or oxides must also be removed, either by mechanical or chemical cleaning. Alumina abrasive cloth or stainless steel wool can be used for mechanical cleaning [22, 23].

Joint clearance of 0.1 to 0.25 mm should be used to ensure good capillary flow of the molten filler metal throughout the joint [22, 23].

The high temperature at which brazing is carried out anneals the base-metal magnesium alloys used, which results in a reduction in their mechanical properties [22, 23].



No suitable flux is currently available to remove the oxide film on the surfaces to be soldered. Therefore, bare magnesium can be soldered only by using abrasion and ultrasonic methods to mechanically dislodge the film. Soldering should not be used to make joints in magnesium alloys that are subject to moderately high stress or will be exposed to corrosive salt environments [22, 23].

6.4.4 Adhesive Bonding

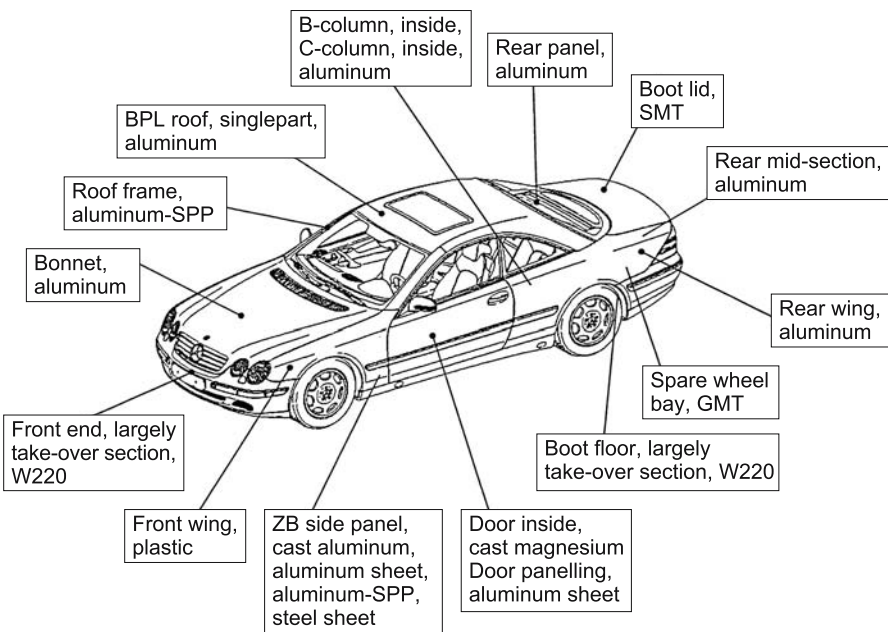
*Otto-Diedrich Hennemann*

6.4.4.1 Introduction

Lightweight construction is one of the major driving forces in the use of magnesium and magnesium alloys. This applies not only to applications in the automotive industry, in sensors or in domestic and industrial appliances, but also to applications that on first glance may seem unusual, e.g., piano frames [27].

In structures subjected to high mechanical stresses, use is primarily made of magnesium alloys, such as AM 50, AM 60, AZ 91, AZ31 and AZ 61, so it makes sense for adhesive bonding technology to concentrate on this group of materials [28, 29].

Lightweight construction can be achieved on one hand with components made completely from magnesium alloys, and on the other hand by consistent



**Fig. 6.116.** DaimlerChrysler, S-Class Coupé with adhesive bonded magnesium and aluminum composite inside door section



application of composite construction techniques, e.g., in the manufacture of car doors from AM 50 HP as shown in Fig. 6.116 [30].

The latest advances in thin-walled casting technology in the manufacture of geometrically complicated components [31] have paved the way for applications in lightweight construction. The use of composite construction techniques in lightweight construction, i.e., the combination of several lightweight materials, such as magnesium, aluminum and carbon-fibre-reinforced plastics (CFP), e.g., Tepex 201 [32], for the manufacture of high-strength components is not possible without the use of adhesive bonding technology. Particularly in the case of very lightweight and thin-walled structures, other assembly technologies, including welding, soldering and screwing [33] are unsuitable, or additional preparations are required (special weld seam preparation, specific welding conditions, additional corrosion protection in the case of screws primarily made of aluminum and chrome nickel alloys).

A further point to consider in the case of screwed connections is that the pre-tension forces fall off considerably at temperatures over 120°C, something that would not be acceptable with safety-relevant components. Due to its character as a lower temperature bonding process, adhesive bonding technology is therefore particularly suited to joining magnesium, because significant material changes (tempering effects) can be first observed at temperatures > 150°C.

Since other factors, in addition to lightweight construction, determine the use of magnesium alloys (favourable modulus of elasticity and  $R_{0.2}$  limit, high impact energy absorption capability [34]), adhesive joints must also meet these requirements. A particular adhesive bonding variant is the joining of magnesium alloys in combination with mechanical bonding processes, e.g., permeation bonding or punch riveting. These combinations are described as hybrid joining techniques [28, 32, 35]. They are arousing more and more interest as connection technologies, since little heat is required to create the connections, and they are high-strength, sound insulating, stable against corrosion, fluid-tight and capable of being dynamically stressed [28, 30]. Processes using plastic deformation are unsuitable for use with magnesium [36]. Aluminum punched rivets with an Al-mac-Zinc coating, by contrast, produce high-strength joints, even in damp room conditions. Maximum strength is obtained if the punched rivet is inserted after an application of adhesive and is followed by heat curing. As an alternative, cold-curing, gap-filling adhesives can be used, as the main load is borne by the punched rivets.

Rabbit adhesive bonding is an additional hybrid connection technology in composite construction. In this case, the fold is produced with a second component, capable of plastic deformation, and the joint is produced with a heat-curing epoxy resin. The combination of folding and adhesive bonding provides a good example of purpose-designed joints.

In order to be able to produce reliable adhesive joints between magnesium parts, it is essential to observe a few fundamental rules and underlying conditions, which apply generally to structural adhesive bonding. In addition, the experience gained, particularly in bonding aluminum, can be applied, because there are many comparable conditions that can be transposed to the adhesive bonding of magnesium [37].

The following factors determine the durability and reliability of adhesive bonded joints:

- Joint design (round joints, overlap, tapered overlap, size of the area to be bonded)
- Material combinations (other metals, ceramics, high-strength synthetics)
- Application of force (static, dynamic, in conjunction with media)
- Type of adhesive (cold or heat curing, reactive curing, non-reactive binding).
- Adhesive layer (thickness, modulus of elasticity, rigidity)
- Surface condition of the faces of the two elements being bonded (degree of contamination, roughness, surface energy, element composition, degree of oxidation, adhesion of oxide and conversion layers)
- Technological procedure of the production process (pre-treatment, application of adhesive, curing process in the case of reactive adhesive, vaporisation of solvent-based adhesives, cooling and solidification of hot-melt adhesives)
- Personnel qualification and skills in adhesive methods

The wide diversity of influences makes it clear that adhesive bonding of magnesium is a complex process, and that the reliability of these joints (as an expression of the survivability and long term durability) under specified loads requires a high degree of expertise in their design and implementation.

#### **6.4.4.2 Adhesives**

To facilitate classification, adhesives are divided into groups according to various criteria. There are (chemically) reactive and non-reactive adhesives. Bonding of non-reactive adhesives occurs as a result of the vaporisation of solvents or water, cooling of hot melt adhesives and heat-activated adhesive layers or as a result of adherent recipe constituents in pressure-sensitive masses.

Under comparable conditions, the adhesive strength of this group of adhesives is lower by a power of ten than the adhesive strength of reactive adhesives. For this reason, exclusive use is made of reactive adhesives for structural, high-strength adhesive bonds [28, 29]. It has been shown in recent years that viscoplastic adhesives are preferable to hard, brittle adhesives with a high modulus of elasticity [38], particularly for dynamic loads. In hybrid bonding technologies, however, pressure-sensitive masses, hot-melt adhesives or sealing adhesives can also be used, because the load-bearing capacity of these types of joints is primarily determined by the mechanical bonding technology.

A typical feature of reactive adhesives is that the transition from the original fluid condition (which frequently does not occur until they are heated) to the final solid condition is caused by chemical reactions – known as curing. The reactions are triggered by special hardeners or by various forms of energy. During the chemical reactions, the original materials change into polymer structures with thermoplastic, elastomer or durometer character. The reaction mechanisms produce various types of adhesive.

Two-component adhesives: these comprise a “resin” and a hardener, and cure at room temperature (cold-curing). The resin and hardener have to be mixed in a precisely specified stoichiometric ratio, whereby the curing reaction com-

mences immediately after mixing and cannot be halted. The most important adhesives for magnesium alloys are the two-component epoxy resins and two-component polyurethane. For sealing applications and in the cases of low adhesive strength requirements, two-component silicones are used, particularly since these adhesives ensure uniform adhesive strength up to around 150°C.

**One-component adhesives:** The hardener in this case is already contained in latent form in the resin. However, at room temperature, the hardeners are so inactive that no curing can take place. The curing reactions do not start to take effect until specific (limit) temperatures are reached, between approx. 100 and 220°C. There is a direct relationship between the minimum temperature that triggers the heat-curing of these adhesives and the modulus of elasticity or respective rigidity of the adhesive, which in turn helps determine the strength of the adhesive bonds, i.e., adhesives with very high curing temperatures frequently produce high-strength, but also rigid adhesive bonds. The most important heat-curing adhesives are made up of epoxy resins and polyurethanes.

**One-component, anaerobic-curing adhesives:** the original molecules are not capable of reaction unless there is no oxygen present, i.e., until anaerobic conditions prevail. This is the case where thin adhesive layers are present, e.g., in the case of form-fitting bonding parts or in the flanks of screws (screw locking). The reaction speed of anaerobic polymerisation is accelerated or delayed by metal ions, so that depending on the metal, very different levels of polymerisation and therefore strength values can be achieved with the same adhesive. Magnesium is one of the passive metals, so that this type of adhesive can be used only in conjunction with special activators.

**One-component, photo-curing adhesives:** the hardeners in the resins made from modified acrylates, polyurethanes and epoxy resins are reactive only under the effect of radiation with specific wavelengths. Depending on the individual type of hardener (also described as photo-initiators), the radiation wavelengths are between 200 and 400 nm. In practical terms, this radiation does not occur in closed rooms, so that the adhesive can be applied long before the hardening reaction. The photo-initiated curing is completed in a few seconds, and so these adhesives can be used in automated manufacturing processes.

However, for the process to work, radiation must actually reach the adhesive. This means that one of the elements being bonded must be permeable to the radiation (glass, transparent plastics).

**One-component, moisture-curing adhesives:** Due to their molecular structure, polyurethanes and silicones are capable of curing merely by the presence of moisture, i.e., the moisture is the “hardener.” The absorption of moisture and diffusion into the joint is a long process. Particularly in the case of thick joints or where gaps need to be sealed, complete curing takes several days.

Many epoxy and polyurethane-based adhesives contain fillers, such as aluminum powder and carbon black to increase their rigidity or flexibility. Due to the electric conductivity, these adhesive recipes carry the risk of corrosion of the magnesium. Additives (e.g., organic or inorganic phosphorous compounds, borates) in adhesives can also react with the magnesium, and these reactions can lead to significant losses of strength, particularly when subjected to climatic ageing. Irrespective of any additives, a factor that must always be taken into ac-

count is that magnesium adhesive bonds are susceptible to corrosion. In the case of ageing, the rupture frequently occurs at the oxide/metal boundary layer, so that the measured “shear strength” actually corresponds to the adhesion of this boundary layer. This corrosion effect can be reduced by special “protective measures,” including chromate pre-treatment, a suitable adhesive recipe and edge sealing of the adhesive.

In composite construction techniques, the adhesive selection is determined not just by the magnesium, but also by the other materials in the composite structure. This particularly applies to the pairing of magnesium and CFP.

#### **6.4.4.3 Pre-treatment**

Corresponding to manufacturing techniques, magnesium alloys have surfaces with low surface energies and uncontrolled chemical compositions that are very different from the bulk material. This also applies to the surface structures of die casting and extrusion alloys of a comparable composition. In particular, the atom percent of oxygen, magnesium and aluminum of die-cast and extruded profiles differs up to a thickness of around 0.3  $\mu\text{m}$ . Depending on their history, the oxide layers on the surface exhibit a greater or lesser degree of cracking, which can have a detrimental effect on the adhesion. It is therefore necessary to pre-treat the surfaces to ensure a uniform structure and atomic composition. In the case of magnesium alloys, dry blasting [29, 38], the standard process used with other metals, leads to explosive or combustible dusts, and therefore cannot be recommended. Brushing and grinding produces microcracks with negative effects on the dynamic loading capacity and the diffusion of humidity along the micro-furrows produced in the process. Treatment with water jets is also of little use, as the magnesium surfaces are very reactive, and layers would be produced in an uncontrollable process. For this reason, chemical pre-treatment (pickling), in which both corrosion protection layers and adhesion-enhancing layers are produced, is the most successful. Two variants are suited as methods of pre-treatment:

- Pre-cleaning with borate and phosphate-based alkaline “cleaners” (Ridoline 1561 or 1559 by Henkel)
- Pickling with highly concentrated sulphuric acid with special additives (De-oxidizer 395 H by Henkel).

Surface removal during pickling is around 4–10  $\mu\text{m}$ . In some cases, cleaning with the alkaline solutions is sufficient for adhesive bonding, removing/obviating the need for pickling.

In the following yellow chromating process [38], which is also described as passivation in industrial practice and provides a very good bonding base for adhesives, the pickled surfaces are treated with Alodine C 6100 from Henkel, Alotron 5 from BASF AG or using the NH 35 process from Hydro Magnesium Marketing. Frequently, chromating is sufficient on its own to create an adequate bonding base for high strength values [38]. Black chromating is less effective, producing lower adhesion of the passivation coating [38]. An intermediate organic coating with very good adhesion to magnesium can be one way of achieving high adhesive strength, if the adhesive in turn bonds well with the organic layer. The NH 35

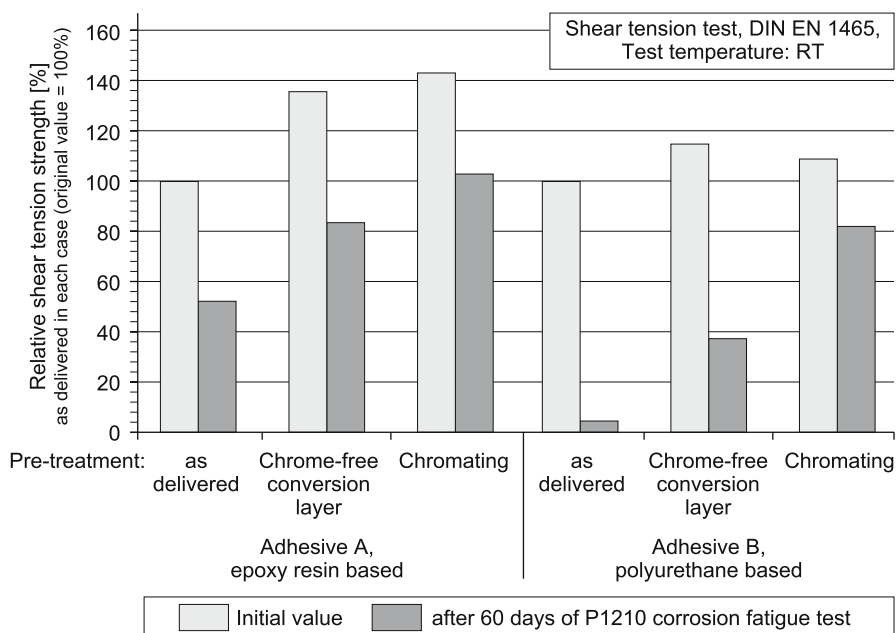
process uses a low chromate concentration, so that this process incurs lower costs for the disposal of the bath chemicals than other chromating processes.

In view of the  $\text{Cr}^{6+}$  problem (carcinogenic), use of this process is meaningful only if no other alternatives exist or in cases where maximum adhesive strength is required. Suitable products for the chrome-free treatment of the alloy AZ 91 HP are hexafluorozirconate solutions, such as NP-Bonder C 4740 from Chemetall, with which comparable pre-treatment effects can be achieved [32, 39]. An important criterion for adhesion is the micro-topography of the surface, with a roughness of about 5  $\mu\text{m}$  being particularly favourable.

At temperatures of 50 to 60°C, the pickling treatment times are around 2 minutes. Since chemicals are depleted during the pre treatment, the solutions must be continuously monitored and topped up as required. The solutions can be used in immersion or spray processes. The passivation processes require temperatures of 25 to 35°C and treatment times of 20 to 40 s.

In all processes using heavily caustic aqueous solutions (cleaning, pickling, passivation), rinsing processes are required; otherwise, even minimal traces of the salts used can significantly reduce the adhesive strength. In addition, it is essential to pay particular attention to health and safety regulations.

The pre-treatment does not just affect the adhesive strength, it also has a considerable influence on the stability of the adhesive bond subjected to alternating climatic stress (alternating climate test P 1210 from Volkswagen AG) as shown in Fig. 6.117.



**Fig. 6.117.** Relative adhesive strength of the magnesium alloy, AM50HP, with heat-curing epoxy and polyurethane adhesives (initial values and following a corrosion fatigue stress) based on [35]

Particularly in the case of the epoxy resins, pre-treatment increases the adhesive strength by around 40% in comparison with untreated specimens. In the case of polyurethanes, the increase in strength is only around 10%. The results of corrosion fatigue tests are a decisive factor in the evaluation of pre-treatment variants. Figure 6.117 underlines the particular effectiveness of passivation with chromate solutions for both types of adhesive.

The extreme loss of strength of polyurethane adhesives as a result of fatigue stress, indicates that the boundary layer is being undermined and that this undermining can partly be prevented by chromation. The chrome-free coatings are not as effective.

The wet-chemical heat treatment techniques described apply only to the treatment of magnesium. The following processes are suitable for aluminum – another lightweight construction material:

- To meet maximum requirements: chrome-sulphuric acid process with subsequent anodising,
- Plasma treatment
- Dry corundum blasting with subsequent Silicoater treatment
- For low-stress applications (e.g., no climatic stressing): jet treatment, grinding or brushing

Suitable treatments for CFP components are plasma treatment, blasting with fine-grain corundum in the bonding area, laser treatment or fluorination [32, 36].

Since wet chemical processes involve high costs in disposal of the bath solutions, “dry” pre-treatment processes are also used. Treatment with plasma at normal pressure is the most important alternative to wet-chemical treatment, in particular in combination with a chemical modification of the magnesium surface during plasma treatment. For this, suitable gas mixtures are introduced into the plasma. In order to ensure an increase in adhesion, the plasma treatment must lead to a micro-topographical and chemical change of the surface.

#### **6.4.4.4 Adhesive Bonding Technology**

When bonding magnesium, the adhesion process comprises several steps:

- Pre-treatment
- Application of the adhesive in the preliminary steps of measuring and mixing, and checking the adhesive application
- Precise bonding and, where necessary, positional correction
- Curing in a heating furnace (for heat-curing adhesives)

When using heat-curing adhesives with magnesium in composite components, account must be taken of the different expansion coefficients, particularly when used in combination with plastics. For example, the expansion coefficient of Al is  $24 \cdot 10^{-6}$  1/K, that of Mg is  $27 \cdot 10^{-6}$  1/K and that of adhesives 50 to  $70 \cdot 10^{-6}$  1/K. Tensions are generated during cooling which reduce the adhesive strength of rigid plastics [38]. Frequently, the spontaneous failure of adhesive bonds after several days or weeks is attributable to these cooling tensions. In alternating temperature tests (e.g., P-VW 1200), also, account has to be taken of

the different expansion coefficients, given that the ductility of the adhesive layers is significantly reduced at low temperatures.

#### 6.4.4.5 Strength and Testing

The best means of testing the strength of adhesive bonds is the shear tension test in accordance with DIN EN 1465. Typical values are shown in Table 6.47.

The values in Table 6.47 apply only to adhesive bonds under normal conditions. Under climatic ageing and following a salt spray test, total failure occasionally occurs [32]. Aluminum-adhesive bonds, by contrast, retain a residual strength under the same marginal conditions. This, therefore, once again underlines the fact that adhesive experience gained with aluminum cannot be transferred directly to the adhesive bonding of magnesium.

In evaluating the adhesives, reliance must not be placed solely on the absolute value of the combined tension and shear resistance, since in the case of climatic ageing, in addition to corrosion of the magnesium alloy at the boundary layer (adhesion), changes in the adhesive itself (cohesion) also lead to “strength losses.” In addition, during climatic ageing, the adhesion of the oxide to the metal is weakened, so that adhesive failure of the oxide on the metal can occur in shear tension tests. In contrast to this, if unsuitable adhesives are used, a typical adhesion break between the adhesive and the oxide occurs under normal conditions (23°C, 70 to 80% relative humidity).

With uniform specimen geometry, (so-called H-shear tension specimens from two U profiles), the hybrid bonding of blind rivets made of AZ91 and AZ61 alloys with heat-curing adhesives, produces the following tensile forces:

Adhesive bonding	118 kN
Blind rivet adhesion	114 kN
Welding	88 kN
Riveting	37 kN

Welding cannot be used for the material combination Mg/Al, therefore only adhesive bonding and blind riveting can be used. In view of the greater bonding surface, the separation forces involved in pure adhesive bonding are greater, allow-

**Table 6.47.** Combined tension and shear resistance of magnesium alloys AZ91, AZ31 and AM50HP

Bonding pairs	Adhesive	Shear strength MPa
AZ91/AZ91	EP resin, cold-curing	10.2
AZ91/PA 66	EP resin, cold-curing	5.3
AZ91/AZ91	Silicone, moisture-curing	2.2
AZ91/PA 66	Silicone, moisture-curing	2.1
AZ31/AZ31	EP, heat hardening at 180°C	16.0
AM50/AM50	EP, heat hardening at 180°C	19.8
AM50/AM50	PUR, heat hardening at 180°C	5.6
AM50/CFK	EP, heat hardening at 180°C	17.5
AM50/CFK	PUR, heat hardening at 180°C	5.3



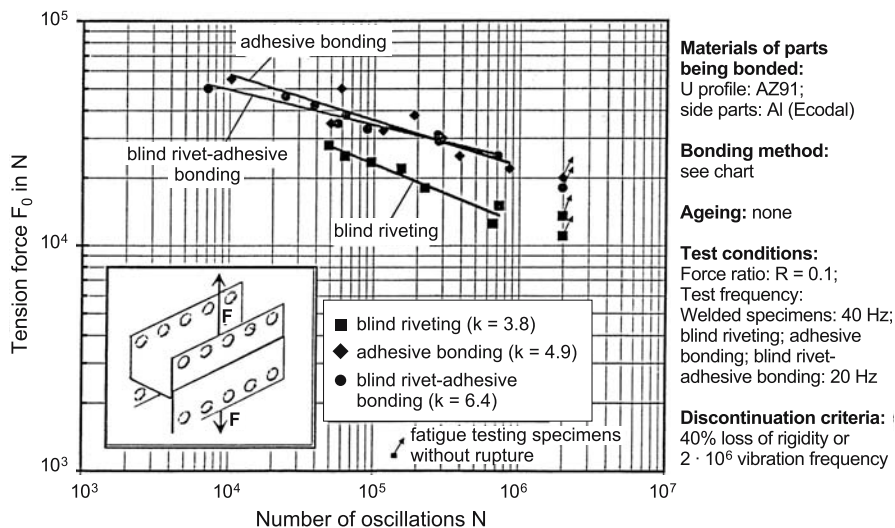


Fig. 6.118. Wöhler Stress-cycle diagrams of H-shear tension specimens of AZ91 and AlMg0.8Si0.9, test frequency 20 Hz, based on [28]

ing complete utilisation of the material properties. In addition to the absolute tensile forces, another key factor is that of the break patterns, since under vibration stresses, cracks radiate from blind rivets, which cannot be accepted. In addition, at the same frequency, higher over-forces are achieved with adhesive bonds than with pure blind rivet connections, as shown in Fig. 6.118.

Given the same specimen dimensions, the material combination AZ91/AZ61 allows larger over-forces for the blind rivet-adhesive bonds or higher vibration frequencies for the same over-forces.

#### 6.4.4.6 Development tendencies

Decisive advances in the application of adhesive bonding technology result from:

- A precise analysis of the adhesion processes in the zones near the boundary surfaces of the adhesive and magnesium
- The analysis of the dynamic molecular processes during the formation of the boundary layer and in medial and mechanical stresses to evaluate the long term behaviour
- The introduction of dry-chemical pre-treatment processes
- The application of calculation methods and simulation programs to predict stressing criteria and life expectancy
- The demonstration of the correlation of important microscopically acting material parameters and macroscopically measured variables, which are important for the adhesion and life

The simulation of microscopic adhesion phenomena is an important tool to be able to rapidly and reliably access the interaction of various factors. However,



the focus of development must not simply be on maximum adhesion of high-strength, structural adhesive bonds, but must also take into account a reliable life expectancy. In particular for the automotive industry, further development is necessary to determine crash behaviour and energy absorption, as these are important criteria in deciding on the application of adhesive bonding technology.

The development of adhesives has reached a high level, so that high-strength joints can be produced with the available epoxy resin and polyurethane-based adhesives. Using suitable additives, adhesives must be prepared that produce high adhesive strengths without any pre-treatment, and are specially adapted to adhesive bonding of magnesium. Reliable calculation methods represent an important pre-condition for the increase in acceptance among designers, since “safety factors” ranging from 2 to 10 in the consideration of various important variables in the calculation of adhesive bonded designs, are frequently a sure way of keeping designers from using of adhesive bonding technology.

#### **6.4.5 Mechanical and Hybrid Joining**

*Gerson Meschut*

##### **6.4.5.1 Clinching**

Single-stage, non-cutting clinching processes have gained acceptance in body building. A distinction is made between processes with a closed die and processes with a split die. In these standard clinching processes, the parts are joined by clinching in combination with hobbing and subsequent upsetting. The point at which the components are to be joined are first placed onto the die. The upper section of the clinching device, the punch, moves down onto the components. A force is exerted by the blank holder to secure and pre-tension the metal sheets between the blankholder and the die. The punch now presses the parts that are to be joined against the die. In clinching, locally limited joining areas are pushed against the adjacent parts. In this case, the initial sheet metal thickness of the joined parts is not changed significantly. The locally limited joining areas retain their connection with the original parts in full. In an uninterrupted joining process, the initial sheet metal thickness of the locally limited joining areas is reduced, and these are pressed into the die by hobbing and, in those processes involving a split die, subsequent upsetting. In combination with the punch, the blank-holder and the workpieces that are to be joined, the die specifies the form of joint which is to be generated. An adherent and positive joint is generated via extrusion. The return stroke occurs following a set maximum force (force-controlled) or pre-specified travel (travel-controlled). The joint once produced, does not require any subsequent treatment.

In the following, Fig. 6.119 shows the joining process schematically with a closed die, while Fig. 6.120 shows a split die.

According to the current state of the art, clinching at room temperature is not possible with the depicted standard joining systems. Due to its hexagonal lattice structure, magnesium has a severe tendency to crack at room temperature when

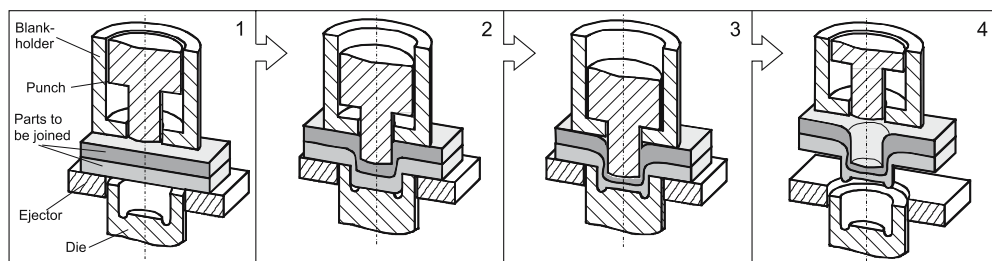


Fig. 6.119. Clinching procedure using a closing die [40]

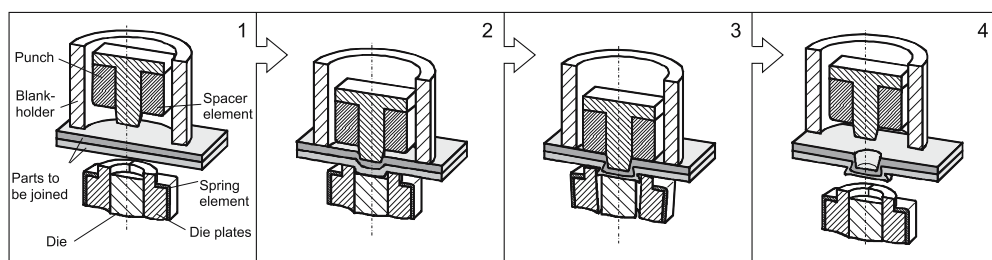


Fig. 6.120. Clinching procedure using a split die [40]

positioned on either the punch or the die side. When in its cold state, load-bearing joints cannot be produced to join magnesium.

One possibility of clinching both wrought magnesium alloys such as, AZ31 and AZ61, and cast magnesium alloys such as AM50 and AZ91 with standard systems is to heat both materials of the parts to be joined and the dies in order to avoid excessive thermal transition. Temperatures in excess of 300°C have proved highly suitable for achieving this.

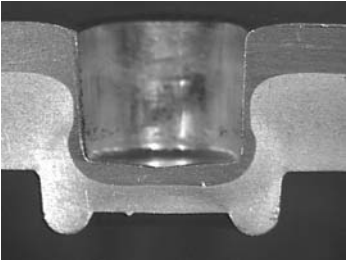
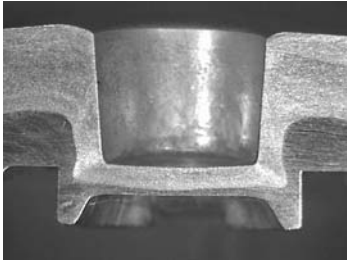
Table 6.48 shows the characteristics of clinched elements set at a joint part temperature of 300°C for AM50HP and AlMgSi0,7 sheet. A closed die was used if the magnesium was located on the die side, and a split die if the magnesium was located on the punch side. In each case, the force required to make the joint was 45 kN. No cracking was detected in the magnesium macroscopic section.

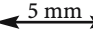
The load-bearing capacity of the joints when subjected to quasi-static shear stress is good. In particular, the AM50HP in AlMgSi0,7 joint transmitted a very high level of maximum force (3.9 kN) and high tensile energy absorption capacity (3 J), which is primarily attributable to the large neck thickness of the clinched element. The aluminum-magnesium joints failed in both joint directions as a result of a cracked neck.

#### Clinching using special clinching processes at room temperature

Clinching magnesium alloys with more ductile metals at room temperature can be carried out by employing special clinching processes which necessitate pre-

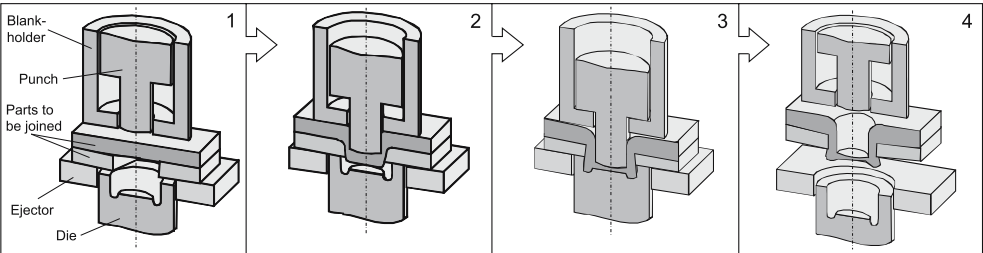
**Table 6.48.** Characteristic joining element characteristics of clinched connections manufactured at joining part temperatures of 300°C using a AlMgSi0,7 – AM50HP material combination [41]

AlMgSi0,7 in AM50HP Joined part temperature 300°C	AM50HP in AlMgSi0,7 Joined part temperature 300°C
	
Shear stress ( $F_{\max}$ ): 2 kN Tensile energy absorption (W): 2.4 J	Shear stress ( $F_{\max}$ ): 3.9 kN Tensile energy absorption (W): 3 J

Scale in all photographs: 

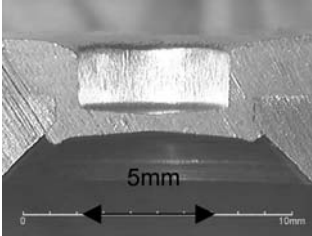
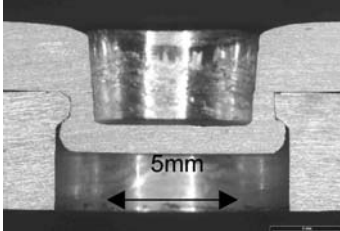
punching the die-side joined part. In these processes, the punch-side material is pressed in a single stage in the bore of the die-side material, and is anchored in a positive and adherent manner. This process is particularly suitable for joining material combinations, in which a material with a low forming capacity can be located in the die-side. Figure 6.121 shows such a setting process.

The geometrical design of the bore in the magnesium joined part varies from system supplier to system supplier. In the case of system A, the bore is designed cylindrically with a chamfer, in which the undercut has formed through the pressed aluminum material. In the case of system B, a stepped, cylindrical bore is also installed in the magnesium joined part, whereby only the bore step is chamfered. The specific bore geometries are designed in such a way as to minimise magnesium material stress as far as possible and therefore to combat crack formation. The process forces required to manufacture the joint are 35 to 40 kN. Table 6.49 shows the characteristic joining element characteristics of the processes using the AlMgSi0,7 – AM50HP material combination.



**Fig. 6.121.** Clinching procedure with pre-punched, die-side magnesium joined part [40]

**Table 6.49.** Characteristic joining element characteristics of the special clinching processes using the AlMgSi0,7 – AM50HP material combination [41]

System A	System B
AlMgSi0,7 in AM50HP	
	

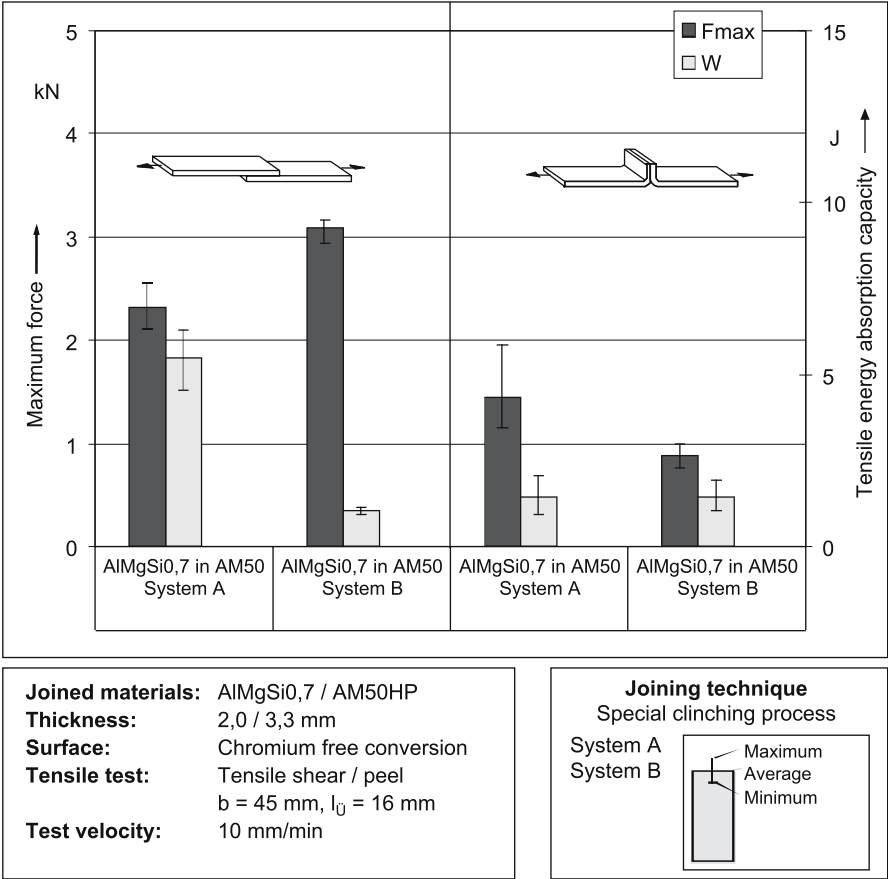
The maximum forces and tensile energy absorption that can be achieved by such joints under quasi-static shear and peeling stress are shown in Fig. 6.122. Under quasi-static shear stress, maximum forces in excess of 3 kN can be achieved at the joints in system B. The tensile energy absorption capacity of this joint lay at the low level of 1.05 J. In contrast, a high tensile energy absorption capacity of approx. 5.5 J was achieved at the A joint with a maximum force which was approximately 30% lower than that of the B joint. This is due to the fact that the neck area of the B element is relevant to failure under shear stress, whilst the A element fails due to the formation of slits in the magnesium located on the die-side. Under quasi-static peeling stress, the A joint is able to transmit a maximum force of 1.45 kN, approx. 40% higher than that of the B joint. This is primarily attributable to the more pronounced undercut in the A element, as both joints fail as a result of popping out.

In summary, it can be stated that, according to the current state-of-the-art, clinching magnesium materials using standard clinching processes only leads to crack-free joining elements and load-bearing joints at joined part temperatures in excess of 300°C. Intensive work is currently being carried out in various research projects to achieve process relevant processes for locally heating the joints in magnesium materials, e.g., by means of induction or resistance heating. Alternatively, however, special clinching processes are available. When the magnesium joint part is positioned on the die-side, this enables the production of highly stress-capable joints even at room temperature. Whilst the effort involved in heating can be omitted in this case, the increased effort involved in pre-punching the magnesium parts and precisely positioning the clinching dies on the pre-punched magnesium joined part must be taken into consideration.

6.4.5.2 Riveting

Self-piercing riveting

Self-piercing riveting processes are characterised by a high level of cost-effectiveness, process validity and universal applicability. Self-piercing riveting can be



**Fig. 6.122.** Maximum force and tensile energy absorption capacity of mixed joints joined using special clinching processes under quasi-static shear and peeling stress, AlMgSi<sub>0,7</sub> in AM50HP material combination [41]

used to join a multitude of different materials together, including those which are metallurgically incompatible. The general prerequisite for making use of this process is adequate ductility of the die-side material. Mettally, organically and inorganically coated materials may also be joined. The self-piercing riveting processes are sub-divided into two systems, self-piercing riveting using full rivets and self-piercing riveting using semi-tubular rivets.

**Self-piercing riveting using semi-tubular self-piercing rivets**

In the self-piercing riveting process using semi-tubular self-piercing rivets, a positive, adherent and impermeable joint, which does not necessitate any pre-punching operations on the joined parts, is achieved using a rotationally-symmetrical semi-tubular self-piercing rivet in a single-stage, low-noise and emission-free operation. As the self-piercing rivet and the die are largely responsible for the

formation of the joining element which is created as a result of their geometrical and material characteristics, the significant characteristics of the joint are dependent on suitable co-ordination of the joining dies and the auxiliary joined part with the overall thickness and material strengths of the joined parts.

In order to produce a joint using semi-tubular self-piercing rivets, the location of the joint is first positioned on the die. When the setting unit advances, the parts to be joined are secured by positioning the setting unit's blank-holder. The rivet is moved to the joining point. The semi-tubular self-piercing rivet then punches through the rivet punch-side material or materials and expands into the ductile die-side material via a die sink, whereby the rivet element is formed into a closed head via the formation of a collar. In this case, the form of the closed head is primarily determined by the die sink. The rivet shaft's expansion leads to the formation of an undercut in the die-side metal sheet, resulting in the creation of a positive joint in interaction with the undercut on the rivet head. Subsequent upsetting of the rivet generates an almost gap-free rivet shaft seat in the joined parts, thereby integrating the component of adherence into the joint. The material punched out of the joined part on the rivet punch-side, which is called the piece punched out, fills the hollow shaft of the rivet and is thereby irrevocably enclosed. After reaching the set maximum force in the case of a force-controlled joining process or pre-specified travel in the case of a travel-controlled joining process, the return stroke's made. The procedure involved in self-piercing riveting using semi-tubular self-piercing rivets is shown in Fig. 6.123.

Like clinching, self-piercing riveting using semi-tubular rivets with standard joining dies at room temperature leads to joints which are susceptible to cracking or which are incapable of bearing loads if the magnesium alloys are positioned on the die-side. If, however, a more ductile joined part material is positioned on the die-side, crack-free joints can be manufactured at room temperature if standard semi-tubular self-piercing riveting systems are used, Table 6.50.

As a result of material-specific optimisation of the die geometry, crack-free and load-bearing joints can be generated using commercially available semi-tubular self-piercing rivets if the thickness of the die-side joined part is sufficient. Table 6.51 shows the joint element characteristics for various die forms with otherwise constant joining parameters.

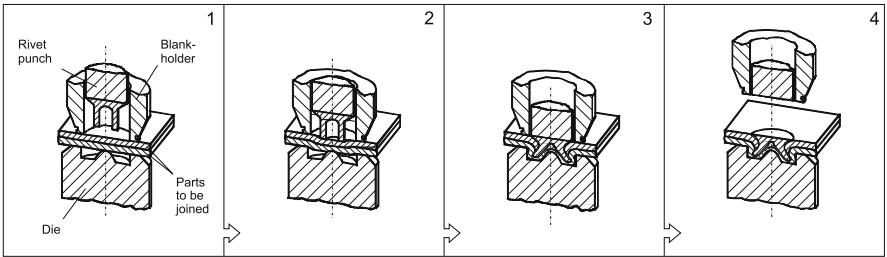
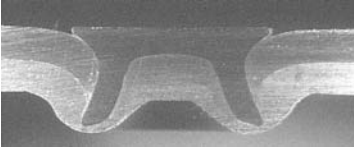
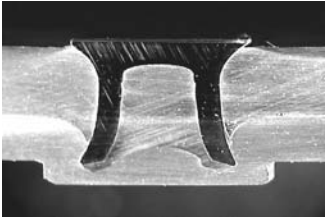
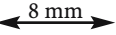
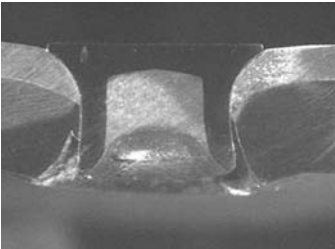

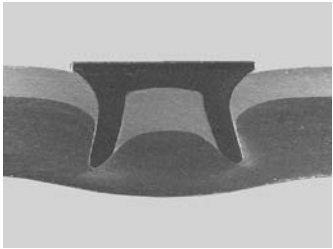
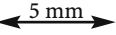


Fig. 6.123. Self-piercing riveting procedure using semi-tubular self-piercing rivets [40]

**Table 6.50.** Characteristic joining element characteristics of self-piercing riveting using semi-tubular rivets in magnesium-aluminum joints [41]

AZ31 in AlMg0,4Si1,2 Joined part temperature: RT	AM50HP in AlMgSi0,7 Joined part temperature: RT
	
Shear stress ( $F_{max}$ ): 2.94 kN Tensile energy absorption (W): 7.8 J	Shear stress ( $F_{max}$ ): 3.0 kN Tensile energy absorption (W): 6 J
Scale in all photographs: 	

**Table 6.51.** Characteristic joining element characteristics in the case of semi-tubular self-piercing riveting using the AlMg0,4Si1,2 in AM50HP material combination with different die sinks

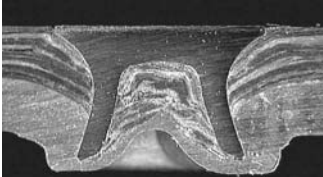

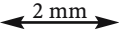
AlMg0,4Si1,2 in AM50HP (joined part temperature: RT)		
		
Punch die	Flat die	Spherical die
Scale in all photographs: 		

Whilst a punch die leads to break-out and a flat die to severe crack formation in the die-side joined part, crack-free and load-bearing joints can be manufactured with a spherical die, which considerably reduces the deformation of magnesium necessary to produce the joint. The joined parts do not have to be heated in order to produce a joint. The maximum joining force is 51 kN. A minimum overlap length of 20 mm is required to produce the joint as a result of the large die diameter. The joints transmit a maximum force in excess of 3.3 kN and achieve a tensile energy absorption capacity in excess of 18.2 J. The joints fail due to the aluminum material’s tearing out, starting from the head of the self-piercing rivet.

In the same manner as clinching materials which reveal improved forming capacity at higher temperatures, semi-tubular self-piercing riveting can also be



**Table 6.52.** Joining element characteristics of the semi-tubular self-piercing riveted joint manufactured with thermal support using the CRP in AZ31 material combination [41]

Micrograph	Closing head
	
Scale in all photographs: 	

used at elevated temperature. In this case, the joined parts are locally heated to approx. 300°C in the direct joining area using induction or resistance heating. In addition to magnesium mono-joints, mixed joints including carbon reinforced plastics can also be achieved (CRP), with the magnesium part positioned on the die-side. Table 6.52 shows the macroscopic section and the crack-free closing head of a CRP-AZ31 joint, which was self-piercing riveted using standard dies on a joined part at a temperature of approx. 300°C.

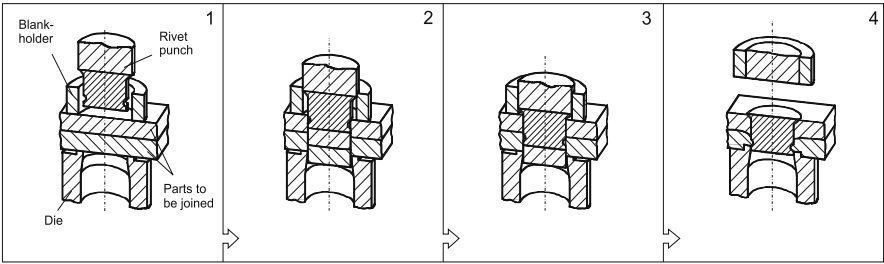
The load-bearing capacity of the joint was evaluated and found acceptable, particularly under shear stress. Despite the small self-piercing rivet diameter, maximum forces of over 1.5 kN and a tensile energy absorption capacity of approx. 2 J were achievable under shear stress. Only low characteristic load-bearing capacity values were achieved when the joint was subjected to peeling stress, as premature joint failure occurred due to popping out as a result of the low diameter of the self-piercing rivet head.

**Self-piercing riveting using full self-piercing rivets**

Self-piercing riveting using fully self-piercing rivets is a joining process with which sheet metal materials can be joined using an auxiliary joined part without pre-punching the joined parts. In this case, the self-piercing rivet cuts through all sheet metal layers and during the single-stage setting, the material of the lower sheet metal layer is pressed into the rotary groove in the rivet shaft. The formation of the full self-piercing rivet joint is determined by the geometry of the self-piercing rivet and the die and by the part material characteristics.

During self-piercing riveting using full self-piercing rivets, the self-piercing rivet is moved to the location of the joint using a setting die, and is vertically aligned with the parts joined and the die. The holding-down device serves a guiding and centering function. During the shearing process, the rivet acts as a single way cutting die. The sheet metal layers which are to be joined are punched through and the piece which is punched out is removed. The rotary elevation of the die presses the die-side material into the annular groove in the lower area of the rivet shaft. Due to the pronounced sheet metal undercut in the annular groove the joint so created is good; due to the pre-tension which results from the setting





**Fig. 6.124.** Procedure on self-piercing riveting using full self-piercing rivets [40]

process, it is adherent. Figure 6.124 shows characteristic phases of the setting process for a full self-piercing rivet.

As full self-piercing riveting makes fewer demands on the forming capacity of the joined parts, magnesium alloys can also be subjected to full self-piercing riveting under certain limiting conditions such as, adequate die-side joined part thickness, even at room temperature. Both crack free composite joints, Table 6.53, and magnesium mono-joints, Table 6.54, with good strength characteristics can be manufactured.

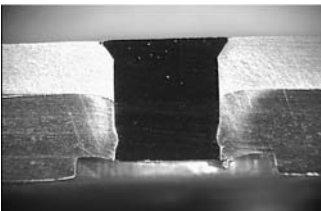
**Blind riveting**

Unilateral joining using rivet elements, so-called blind riveting, is a joining process which requires a pre-punching operation in both parts to be joined and which also enables the making of a joint if the joint location is only accessible from one side. The most important components of the blind rivet are the rivet punch and the rivet sleeve. The setting head, whose size and form may vary, is located on the processing side. Figure 6.125 shows the structure of conventional blind rivets.

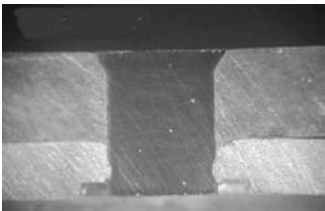
**Table 6.53.** Joining element characteristics on full self-piercing riveting in magnesium-aluminum-joints [41]

AlMgSi0,7 in AM50HP  
Joined part temperature: RT

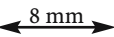
AM50HP in AlMgSi0,7  
Joined part temperature: RT



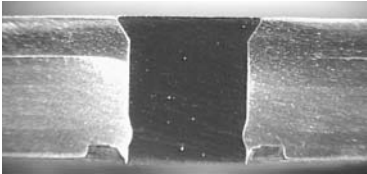
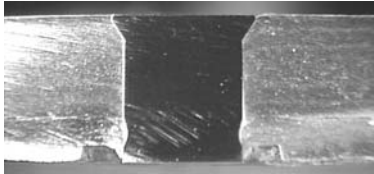
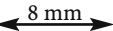
Shear stress ( $F_{max}$ ): 3 kN  
Tensile energy absorption (W): 6 J

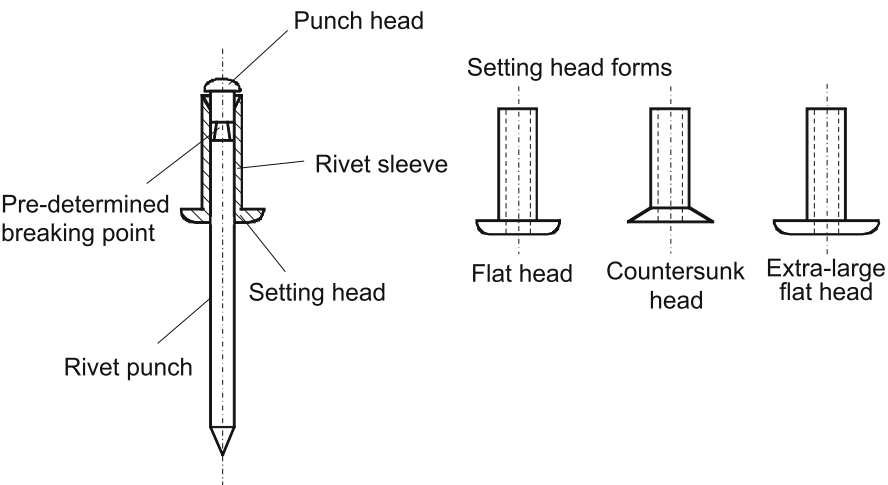


Shear stress ( $F_{max}$ ): 4.5 kN  
Tensile energy absorption (W): 12.5 J

Scale in all photographs:  8 mm

**Table 6.54.** Joining element characteristics on full self-piercing riveting in magnesium joints [41]

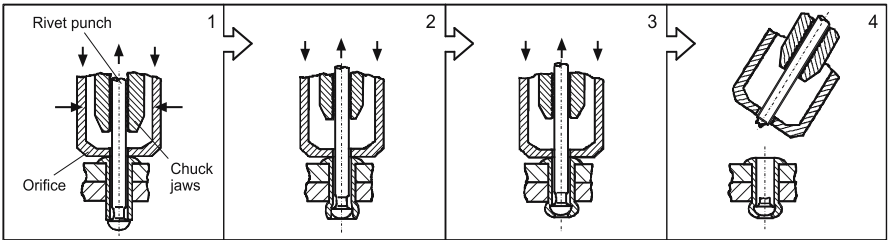
AZ31 in AM50HP Joined part temperature: RT	AM50HP in AZ31 Joined part temperature: RT
	
Shear stress ( $F_{\max}$ ): 2.3 kN Tensile energy absorption ( $W$ ): 4.4 J	Shear stress ( $F_{\max}$ ): 1.4 kN Tensile energy absorption ( $W$ ): 1.5 J
Scale in all photographs: 	



**Fig. 6.125.** Structure of conventional blind rivets [40]

When selecting blind rivet-material combinations, component requirements such as corrosion characteristics, temperature range and coefficients of thermal expansion must be taken into consideration in addition to the necessary strength. As the rivet punch’s tasks include plastically deforming the rivet sleeve, the demands made on the material to be used here are higher, in terms of strength, than those made on the rivet sleeve material.

With the exception of minor variations, all blind rivet processing is in principal the same. In the case of the standard blind rivet, the rivet punch serves to deform the rivet sleeve and to form the closing head. The blind rivet is inserted into the orifice by the rivet punch and into the bore hole by the rivet sleeve. On actuation of the device, the chuck jaws grip the rivet punch and pull it back. Due to

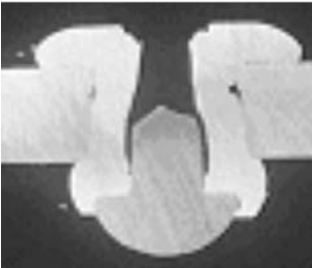
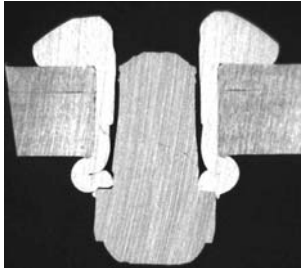
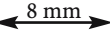


**Fig. 6.126.** Setting a blind rivet using a tension punch with a pre-determined braking point [40]

this pulling movement, the punch head begins to deform the rivet sleeve, simultaneously causing the workpieces which are to be joined to be pressed together. Inside the material bore, the rivet sleeve is pressed against the wall and, at the same time, is formed again on the opposite side radially to the closing head. The rivet punch breaks off at the pre-determined breaking point, whilst the remainder of the rivet punch is firmly encompassed by the rivet sleeve. The blind rivet joint has been manufactured and requires no subsequent treatment. Figure 6.126 shows schematically the setting process for a standard blind rivet.

In the case of a blind riveting system for magnesium alloys, the blind rivet sleeve, at the very least, should be manufactured from aluminum due to corrosion protection reasons. A steel punch usually leads to higher strengths in comparison with an aluminum punch. With regard to joining element formation, attention must be paid to complete hole filling, symmetrical closing head formation and gap-free seating. Table 6.55 shows the joining element characteristics on blind riveting the AZ31 in AM50HP material combination with different blind riveting systems.

**Table 6.55.** Joining element characteristics in blind riveting in magnesium joints [41]

AZ31 in AM50HP Joined part temperature: RT	
	
Shear stress ( $F_{\max}$ ): 2.8 kN Tensile energy absorption (W): 6.3 J	Shear stress ( $F_{\max}$ ): 1.5 kN Tensile energy absorption (W): 2 J
Scale in all photographs: 	

### 6.4.5.3 Direct Screwing (Self-piercing/-Tapping)

In order to reduce the weight of the body, consideration is being given to modern lightweight design concepts involving new materials. In this case, increasing importance is being attached to composite design, including that of space-frame structures and fibre reinforced plastics (FRP). Material and design friendly joining processes are a significant prerequisite for implementing these designs, Fig. 6.127. Hybrid space-frame structures, which may additionally be characterised by the use of flange-free profiles, pose a challenge to mechanical joining technology, particularly due to the unilateral accessibility of the joining points.

One solution to this technical joining task is blind riveting, which can be used to manufacture high-strength, insoluble joints even between different types of material. In addition to the actual joining process, however, this necessitates further operations such as punching the joined parts and aligning the components when inserting the blind rivet; these may lead to comparatively high joining system costs.

One alternative to the blind riveting technique is direct screwing; whilst this can be used in the event of unilateral joining point accessibility according to the state of the art, at least the setting side joined part has to be pre-punched. The further development depicted in the framework of this contribution enables the pre-punching operation to be dispensed with entirely, as a result of which the process costs can be significantly reduced, particularly in comparison with those of blind riveting. Direct screwing without pre-punching closes the gap between the mechanical joining process with an auxiliary joined part, without pre-punching and with unilateral accessibility, see Fig. 6.128.

A screw which has been specially developed for this joining process is equipped with a specially shaped tip with a conical transition to the subsequent threads, Figs. 6.129 and 6.130 shows the principle of the process in the total of six process steps. Four raised edges are distributed around the circumference of the tip; during the setting process in the joint, these generate the frictional heat nec-

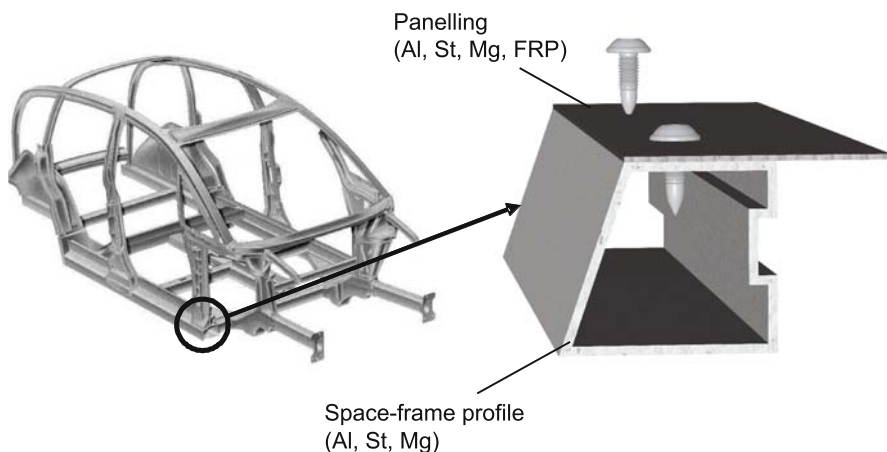


Fig. 6.127. Joining situation in space-frame panelling

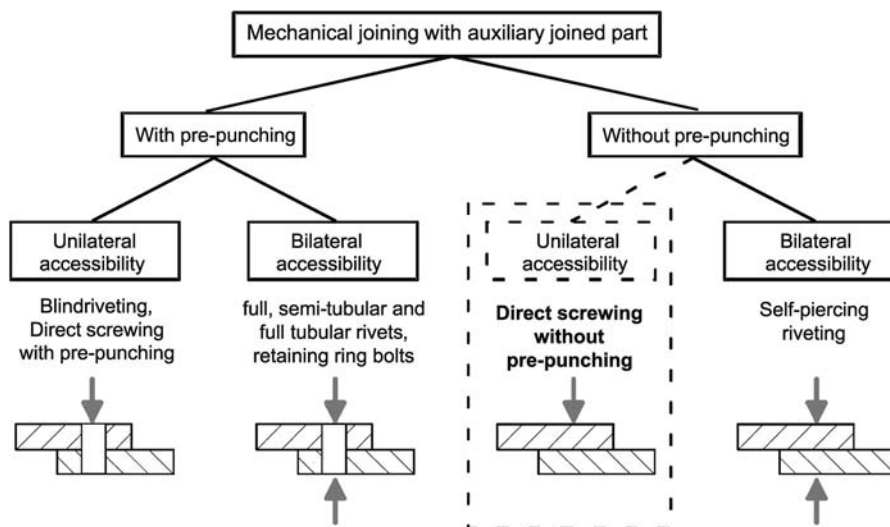


Fig. 6.128. Classification of pre-punching in the mechanical joining process system involving an auxiliary joined part

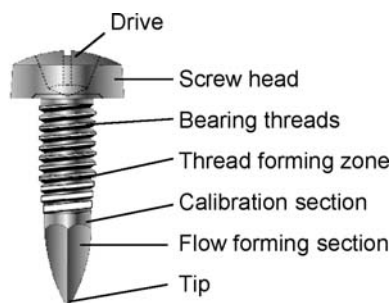


Fig. 6.129. Functional sections of a flow forming screw (source: EJOT)

essary to form the passage in combination with the moderate application of pressure and the required high spindle speed. The heated material flows axially around the shaped tip of the flow-hole forming screw, and a passage is formed with a constant rise in tapping moment. Depending on the material and the process parameters, the length of the passage which is formed is approximately three times the thickness of the joined part.

Non-cutting thread tapping follows on directly after the passage has been formed, see No. 4 in Fig. 6.129. In the final two stages of the screwing process, the screw is screwed through the tapped thread and is tightened with the selected tightening torque. When the joint zone cools, the passage shrinks and encloses the flow forming screw's threads without play. This additionally increases the screw's loosening torque and seals the joint. This screwed connection can be undone at any time and can be replaced by means of a metric screw [42, 43].

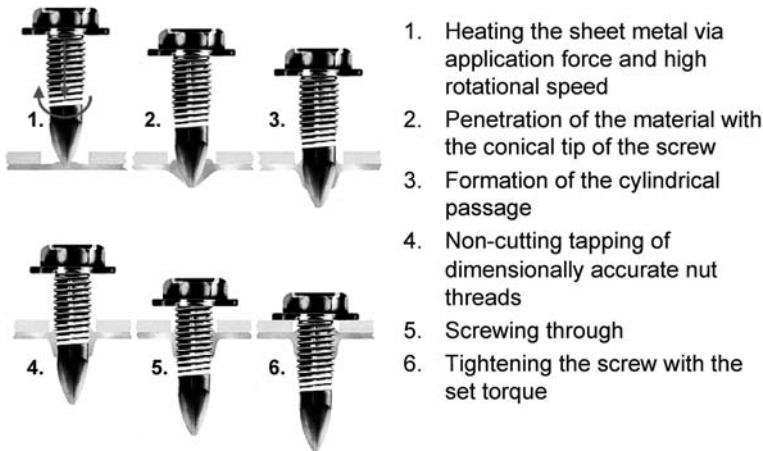


Fig. 6.130. Direct screwing process steps (source: EJOT)

A part of the joined part material – approximately  $1/3$  of the thickness of the joined part in the case of metallic materials – flows counter to the direction of screwing. The joined part located on the screw head-side is equipped with a passage in the case of direct screwing. This absorbs the increase, thereby enabling the creation of a gap-free joint. In addition to the effort involved in the pre-punching operation, it must also be guaranteed that the screw is positioned in the pre-punched hole, which must also be taken into consideration when planning systems for an automated series.

Direct screwing *without pre-punching* is a further development in which no preparatory process steps, such as pre-punching, are incurred. This enables the process costs and the time required to produce the joint to be reduced significantly. For the first time, direct screwing without pre-punching offers a joining technique with unilateral accessibility without pre-punching which also enables destruction-free separation. This is particularly advantageous in the event of repairs and on recycling.

In order to form the flow hole, high frictional heat is required during direct screwing. Depending on the type and thickness of the material, this is achieved by means of a high rotational speed in the range 1000 to 5000 rpm and an applied force of 0.3 to 1.5 kN. The process parameters of torque, travel and rotational speed during direct screwing without pre-punching are shown in Fig. 6.131 depending on the process time. In order to achieve an optimum joint, the process parameters must be adapted to the type of material and the thickness of the joined parts, which may result in several process steps. In comparison with the process sequence involved in direct screwing with pre-punching, the joined parts are heated via a higher screw application pressure and a high rotational speed (1) until plastification occurs (2), a passage through both layers of sheet metal is formed (3) and a thread is tapped in these passages without cutting (4). During thread tapping, the tapping moment increases to a peak value, declining again when the screw passes through. Once the technical forming process steps have

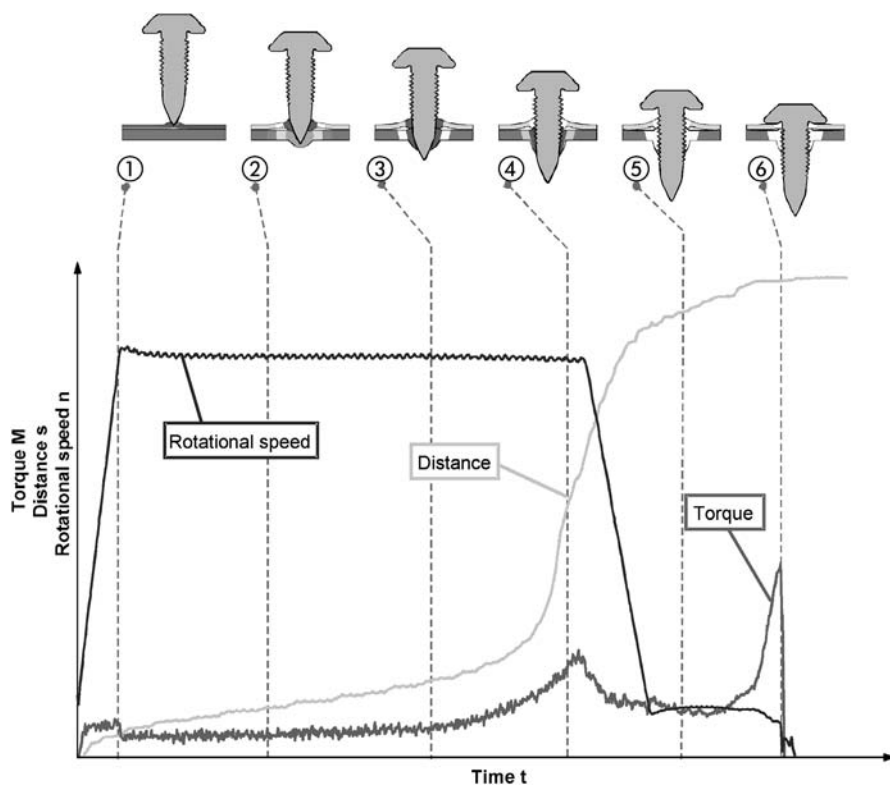


Fig. 6.131. Process sequence and parameters in direct screwing without pre-punching

been completed, the speed of the screwing device is reduced so that the thread is not damaged when the screw is screwed in and the selected tightening torque can be set with greater precision (5). As soon as the head of the screw comes to rest on the clamped part, the screwing torque increases to the intended tightening torque and the joining process is completed (6).

The entire joining process without pre-punching the joined part on the screw head-side takes slightly more time than screwing with pre-punching, as both joined parts have to be heated by means of the applied force and the screw speed, and the passage has to be formed through both parts to be joined. In Fig. 6.132, the characteristic process parameter curves of the variants with and without pre-punching are compared. The selected tightening torque must lie between the screwing-in torque  $M_s$  and overscrewing torque  $M_o$ , whereby the gap between these characteristic values should be as large as possible in order to guarantee the largest possible process window and a high degree of process validity. The screwing-in torques for direct screwing with and without pre-punching are approximately on a par. However, the overscrewing torque, in which the thread tapped in the joined parts is destroyed, is higher in the case of direct screwing without pre-punching, as the screw thread is engaged in both the joined parts on the side

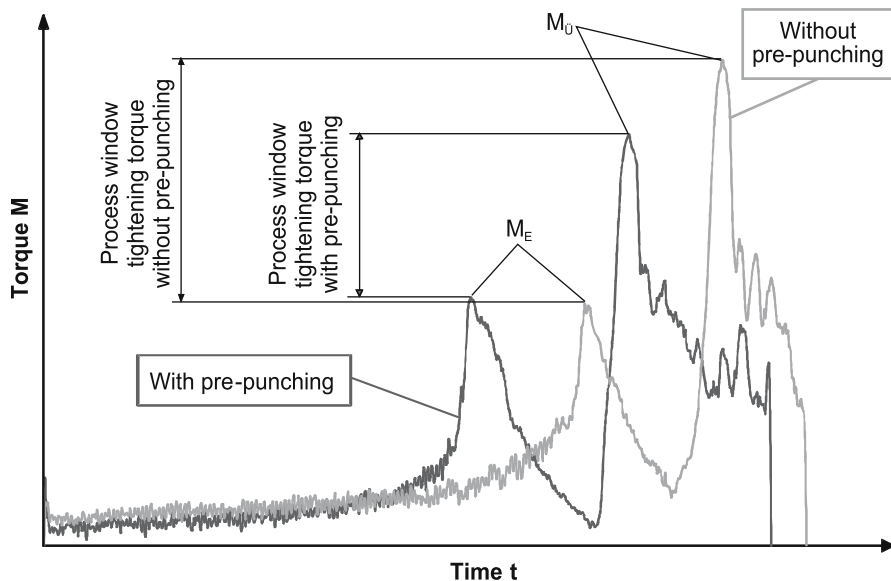


Fig. 6.132. Comparison of torque-time curves on direct screwing with and without pre-punching


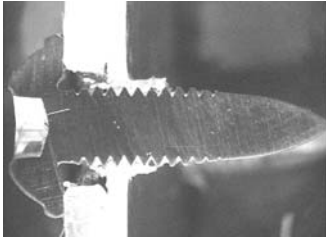
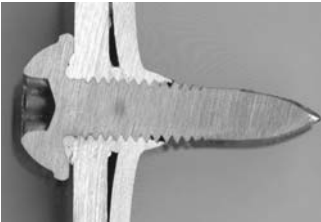
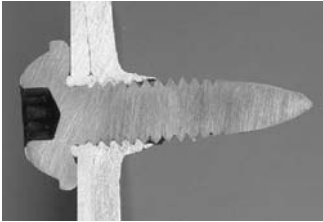
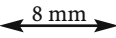
in which screwing-in occurs and the screw head-side. Although two nut threads are screwed using one screw in this case, a pre-tensioning force must be applied. As the process window for tightening the torque is larger in the case of direct screwing without pre-punching, this process variant offers greater process validity. In addition, higher tightening torques can be set for direct screwing without pre-punching; these also lead to higher release torques for the screwed connection without pre-punching.

Direct screwing is an ideal mechanical joining technique for magnesium materials, as a means of heating the joint location, which is advantageous in joining magnesium materials via technical forming, and is already part of the process and does not have to be additionally induced. Re-screwable magnesium joints with outstanding strength characteristics can therefore be manufactured. Table 6.56 shows the macroscopic sections of various directly-screwed magnesium joints.


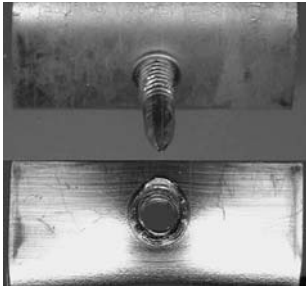
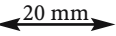
In the joints with pre-punching, Table 6.57 a and b, the play between the clamped part's bore wall and the screw shaft is clearly visible; the upper passage of the screwed-in part is integrated into this. However, if screwing is carried out without pre-punching, Table 6.57 c and d, the clamped part lies directly against the screw shaft and is reinforced by the displaced material, which increases the thickness of the sheet metal at the screw shaft. However, a gap is formed between the two layers of sheet metal, Table 6.57c, as the upper sheet material flows down between the two components and a lower percentage of the lower sheet flows upwards. This has a negative effect on the dimensional accuracy of the components, enabling the occurrence of gap corrosion and reducing the components' torsional rigidity. By specifically developing further the screwing process, however, the ma-



**Table 6.56.** Joining element characteristics of the direct screwing system using the AZ31 – AM50HP material combination [41]

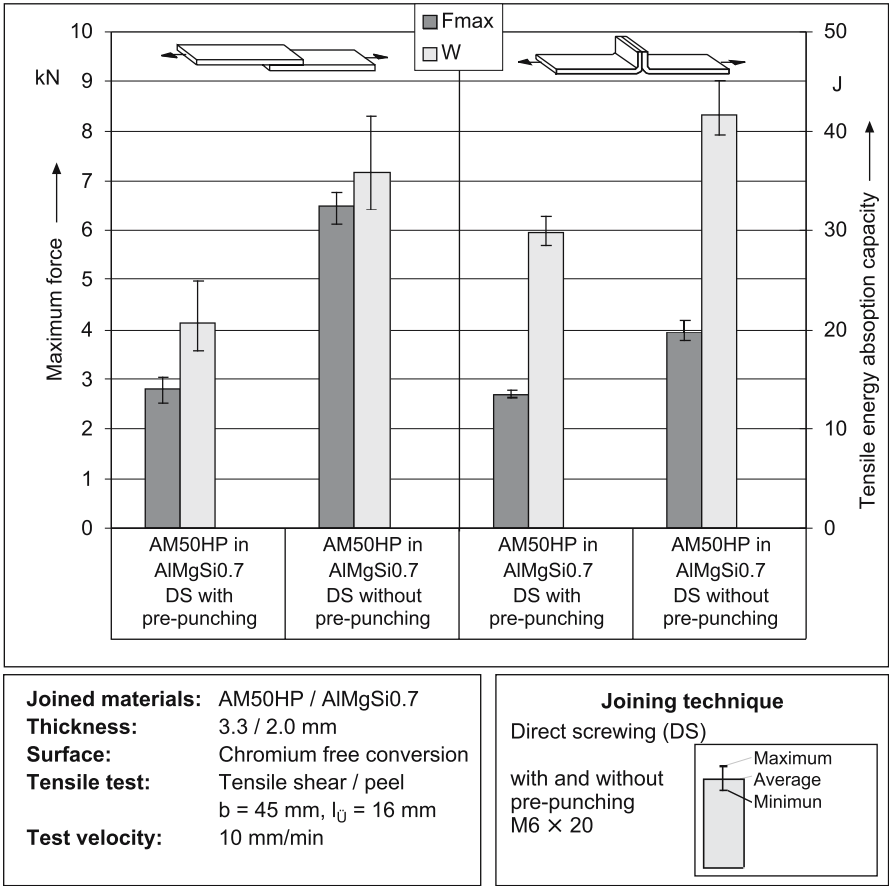
Direct screwing with pre-punching	
a) AZ31 in AM50HP	b) AM50HP in AZ31
	
Direct screwing without pre-punching	
c) AM50HP in AlMgSi0,7	d) AlMg0,4Si1,2 in AZ31
	
Scale in all photographs: 	

**Table 6.57.** Characteristic failure profiles of non-perforated joined parts in directly-screwed composite joints showing quasi-static shear and peeling stress; material combination AM50HP in AlMgSi0,7 [41]

Shear stress	Peeling stress
	
Scale in all photographs: 	

terial flow can be controlled in such a manner that a gap-free joint is created and the joined parts lie flush on one another, Table 6.57d.

In addition to simplifying the manufacturing process, direct screwing without pre-punching has the added advantage of better strength characteristics in comparison with joints with pre-punched setting-side joined parts. Figure 6.132 shows the maximum forces and tensile energy absorption capacity of punched and non-punched joined parts in directly-screwed composite joints under quasi-static shear and peeling stress for an AM50HP and AlMgSi0,7 material combination. Direct screwing without pre-punching enables the characteristic strength to be increased significantly by up to 130% both for shear stress and under peeling stress. Amongst other aspects, this is attributable to the increased percentage of positive engagement due to the larger hole surface in AM50HP positioned on the setting-side.



**Fig. 6.133.** Maximum forces and tensile energy absorption capacity of punched and non-punched joined parts in directly-screwed composite joints under quasi-static shear and peeling stress [41]

The aluminum material, which leads to the destruction of the joint as a result of slit formation under a shear stress and thread failure in the basic material under a peeling stress, is relevant to failure under both types of stress, Table 6.57.

The applied forces required in the case of direct screwing may cause undesirable deformation in low-rigidity joint zones. The part of the overall length of the screw which is used to form the flow hole and tap the thread projects relatively far out of the joint and is no longer required for the joint. As a result, the use of direct screwing is advantageous e.g., in the case of closed magnesium profiles which offer adequate rigidity and which are able to accommodate the projecting screw tips. Figure 6.134 shows a nodular joint in a magnesium space-frame (MSF) demonstrator floor, in which two extruded magnesium profiles are structurally joined together via a magnesium node by direct screwing and adhesive bonding.

#### 6.4.5.4 Folding

In sheet metal processing, folding refers to joining two bent, interlocking sheet metal edges which have been pressed together. A distinction is made between simple, double, horizontal and vertical flat and round folds. In the majority of cases, simple folds serve to join an optically effective visible surface to a supporting element. Double or multiple folds are used in vessels which are subject to high levels of mechanical stress [44].

In body building, folding is primarily used in the visible area to join the outer skin and the inner section in the case of attaching body parts such as, e.g., bonnets, boot lids and doors, but is also employed in roof cut-outs, window slots and wheel housings.

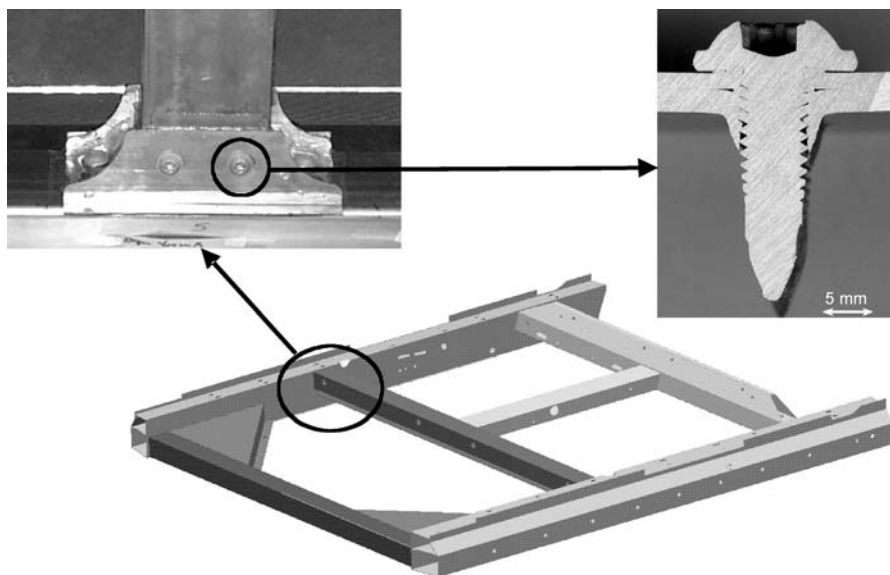


Fig. 6.134. Directly-screwed nodular joint in the magnesium space-frame (MSF)

Body parts are generally folded using dies integrated into body presses, whereby the flanges are bent by at least  $75^\circ$ , generally to  $90^\circ$ , from the plane of initial operation. In a second operation, they are then pre-folded by a further  $45^\circ$  to  $135^\circ$ , and are then fully-folded to  $180^\circ$  in a third operation. The pressure which is applied in this case must be selected so that the flange does not spring back and no pressure marks occur in the visible area of the outer skin. The high pre-deformation occurring in the folding area in a parts' drawing process impedes the folding of exterior panelling and internal reinforcements. In order to avoid coarse roughening and cracks, adherence to minimum bending radii is necessary depending on the deformation and work hardening behaviour of the outer material, which is to be folded and the degree of pre-deformation and the sheet metal thickness.

Hemming is especially cost-effective in body production, particularly for low to medium sheet magnesium component unit numbers, as it exhibits a high level of flexibility and enables multiple usage of the folding device. Figure 6.135 shows the principle of hemming together with the different process steps.

As in the majority of joining processes involving forming, the magnesium sheet has to be heated, especially when folding the flanges, which are generally pre-stretched in the component forming process. Both induction and hot air heating, which temporarily heat the component to approx.  $250^\circ\text{C}$ , may be used for this purpose. Using the example of a magnesium bonnet, Fig. 6.136 shows thermally-supported magnesium sheet hemming, in which crack-free folded and mechanically bonded joints are produced. Due to reasons of strength and corrosion protection, the gap has to be filled with an adhesive in this application. In order to avoid pre-coating during the thermally supported pre-folding steps adhesives must be used whose reaction kinetics have been adapted to the process.

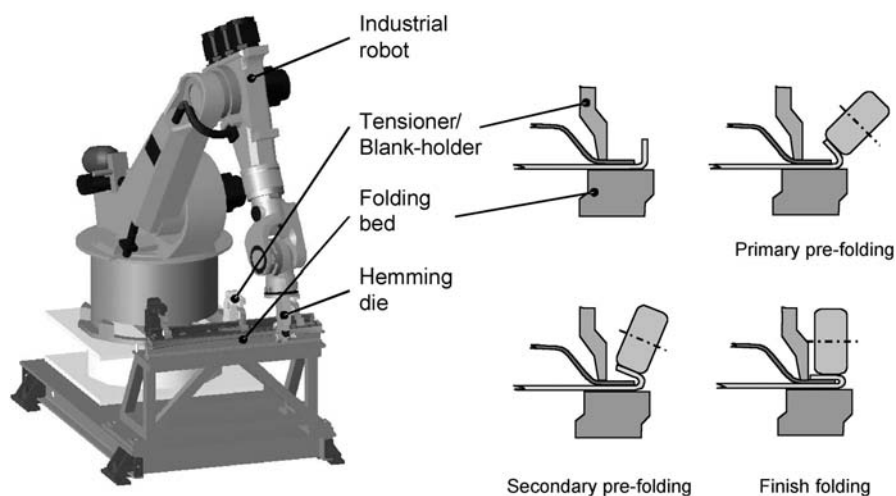


Fig. 6.135. Principle of hemming [45]

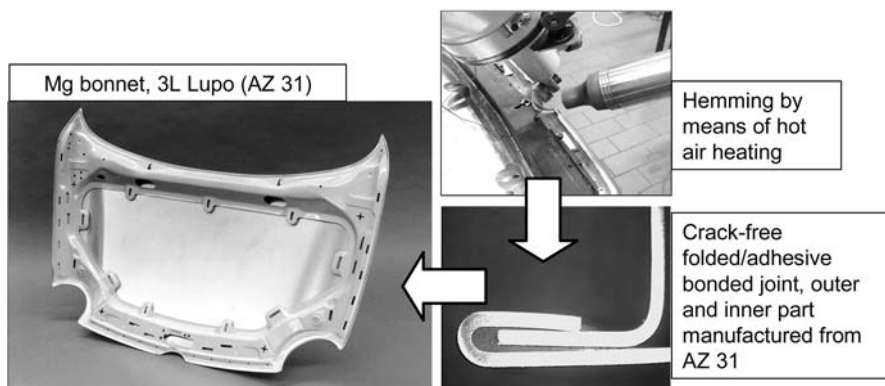


Fig. 6.136. Magnesium sheet hemming using the example of a magnesium demonstrator bonnet (3L Lupo)

#### 6.4.5.5 Hybrid Joining

Cold joining methods seem particularly suitable for integrating modern lightweight structural materials such as magnesium to steel and/or aluminum vehicle structures. Particularly for future vehicle structures with a multi-material design, the key technologies will be cold joining techniques of adhesive bonding and mechanical joining, since they generally allow different materials to be joined during the manufacturing process without subjecting them to temperature stresses.

The combination of adhesive bonding and mechanical joining results in the so-called *cold hybrid joining method*, which offers impressive synergy effects with regard to the manufacturing process and the property profile of the resultant joints, making innovative joining solutions for body design possible. This is primarily the result of the beneficial properties of adhesive bonding technology, which, apart from the possibility of joining dissimilar materials, also enables isolation of the joined parts and joint gap filling, thus avoiding both electrochemical and gap corrosion. Furthermore, since forces are transmitted over the whole surface of the joint, a quasi weight-neutral increase in structural strength is achieved, as well as maximum utilisation of the materials of the parts joined under both dynamic and impact loads. Secondly, the mechanical fastening processes involved in hybrid joining ensure that the parts joined are held in place until the adhesive has cured, as well as compensating for any losses in the properties of the bonded joint due to the ageing of the adhesive. The mechanical fastening processes used in car body construction include riveting, clinching and lock-seaming. Compared to adhesive bonding, these processes produce joints with point-centred force transmission or, in the case of lock-seaming, with linear force transmission. Although screwing has rarely been used until now as a joining method in body construction, it will become increasingly important in the future with the development of modern direct screwing techniques using self-piercing and self-tapping screws [43].

Based on the strength behaviour of magnesium joints which have been created using different methods, the performance of hybrid joining will be portrayed in the following under both rapid, quasi-static bending stress and dynamically-vibrating tensile/compression stress on joints which have not been aged. The samples which are to be used involve a cast node manufactured in AM50 and an AZ31 extruded profile with an octagonal cross-section manufactured using the following joining processes: MIG welding, blind riveting, adhesive bonding and a combination of blind riveting and adhesive bonding. An auxiliary wire is used in the welding process. This is AZ61 alloy with a diameter of 1.6 mm. The punch break blind rivet which is used has a nominal diameter of 6.5 mm and consists of an aluminum rivet sleeve and an aluminum rivet punch, in order to reduce the risk of corrosion in the location of the joint due to contact between the blind rivet and the parts joined. The adhesive which is used is a high-strength, single-component epoxy resin, which was hardened at a temperature of 170°C with a curing time of 30 min. For reference purposes, the joined parts were yellow-chromated for these tests, as Cr(VI)-free surface treatment processes are still being developed and tested at present.

Analysis of the force-deformation behaviour under quasi-static bending stress in Fig. 6.137 makes a greater distinction between the joining processes. For example, MIG welding reveals the highest strengths in the quasi-statically tested samples – over and above the strengths exhibited by elementary adhesive bonding or blind rivet adhesive bonding. Elementary blind riveting reveals by far the lowest strengths. The increase in sample stiffness due to additional adhesive bonding of the blind riveted/adhesive bonded joints in comparison with that of the joints manufactured via elementary blind riveting is also remarkable. The difference between adhesive bonded and hybrid joints can be attributed to the fact that, in the case of the profiled node joints which are created via elementary adhesive bonding, the cross-section of the joined parts is not weakened by the holes which are required in blind riveting and that the thickness of the adhesive layer is more even.

In the case of dynamically vibrating tensile/compression stress shown in Fig. 6.138, the joining process of adhesive bonding and blind rivet adhesive bonding offer advantages compared to MIG welding and show the highest vibration strengths. The blind riveting process is considerably easier to classify under dynamically-vibrating stress than under quasi-static stress, but fails to achieve the Wöhler curves attained by the MIG joints. Whilst the Wöhler curve slope is similar for all of the joining processes, there is considerable disparity between the levels. This mechanical behaviour is comparable to the results shown in chapter 6.4.4 on adhesive bonding.

The failure behaviour of the welded joints is characterised by break-away of the weld seam flank. Macroscopic sections clearly reveal that the cracks run in the transition from the weld seam to the base material. The cause of the cracks may be assumed to be geometrical notches and problems in the heat affected zone. The adhesive bonded and blind riveted/adhesive bonded joints fail in the node's transition from the drawn-in area to the rib-reinforced node shaft. Macroscopic sections clearly identify the even formation of the adhesive layer and therefore the function of the spacers.

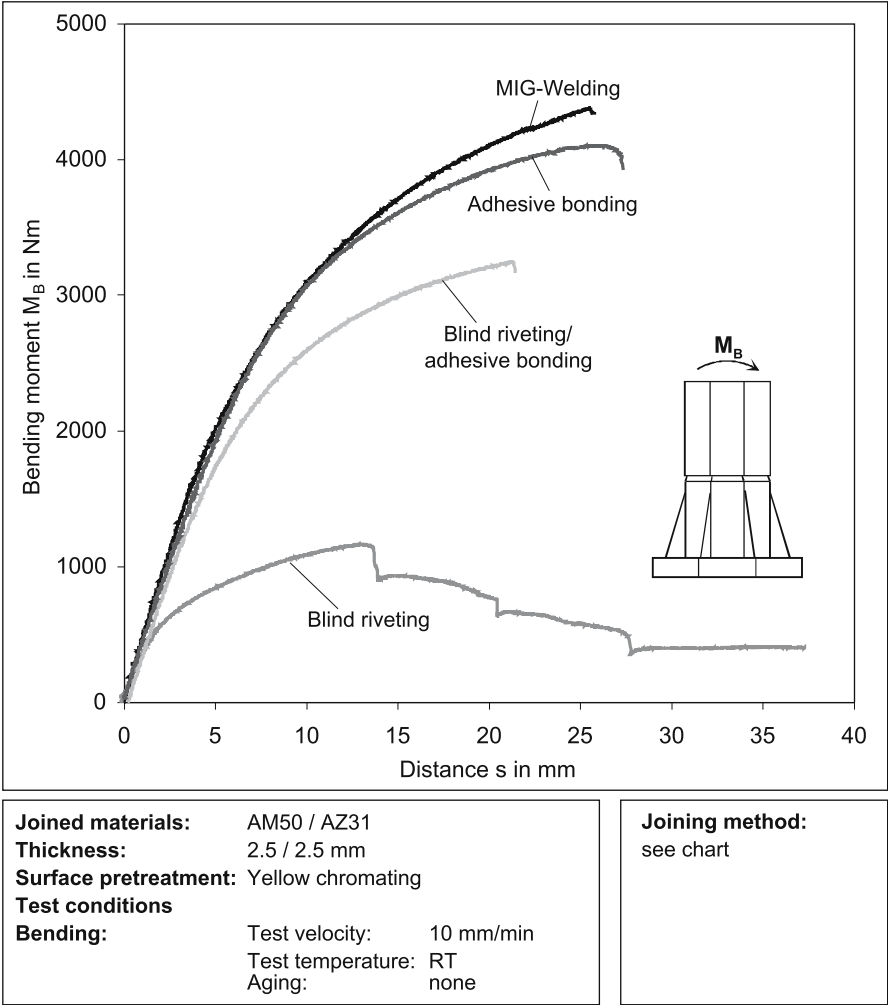


Fig. 6.137. Comparison of the force-deformation behaviour of profiled node joints manufactured using different joining processes to join AM50 and AZ31 magnesium alloys under quasi-static bending stress

6.4.5.6 Conclusion and OutView

The investigations presented here clearly demonstrate the efficiency of cold joining techniques with regard to the integration of modern lightweight materials for the implementation of future multi-material car body concepts. However, adhesive bonded joints in particular are subject to an occasional but considerable loss in properties during their lifetime due to ageing. These ageing processes are dependent not only on the mechanical stresses but also in particular on the thermal and media stresses as well as on the radiation stresses to which the joint is

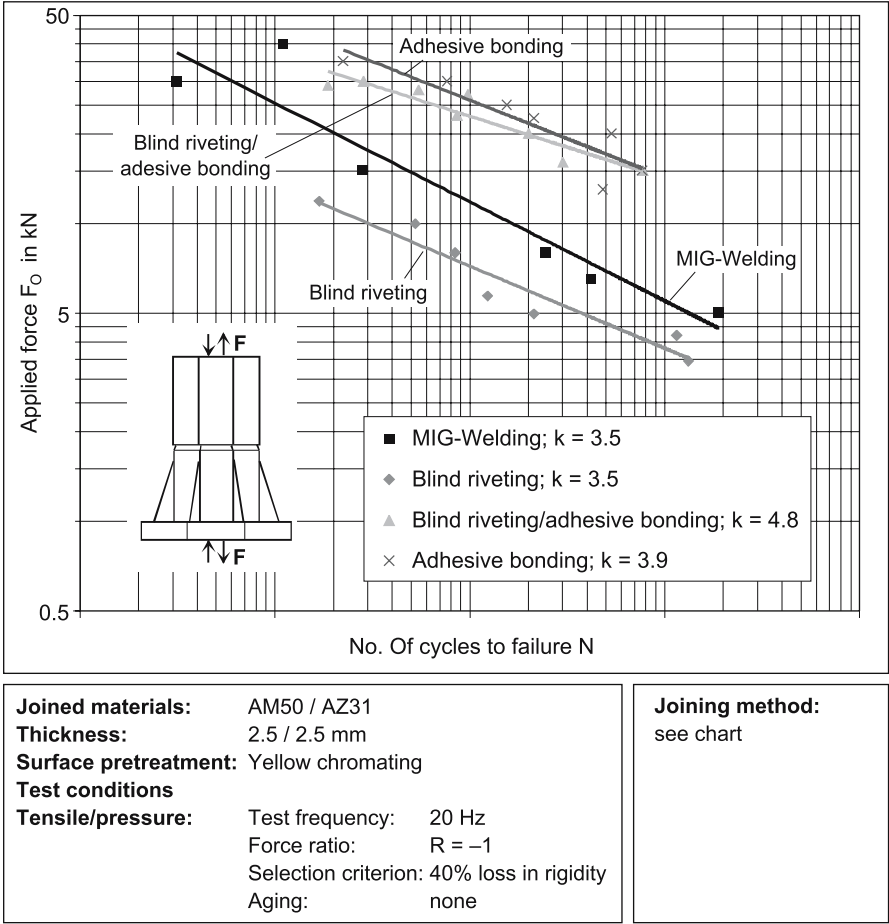


Fig. 6.138. Comparison of Wöhler curves for profiled node joints manufactured via different joining processes from AM50 and AZ31 magnesium alloys under tensile/compression stress

exposed. As a result, further studies regarding the ageing and corrosion behaviour of magnesium joints are being carried out. Furthermore, the aim is to determine the extent to which the – in some cases additive – use of adhesive bonding technology using crash-resistant structural adhesives is able to achieve a quasi-neutral increase in the ultimate strength of vehicle structures exposed to crash stresses, thus achieving an improvement in occupant protection.



## 6.5 Machining

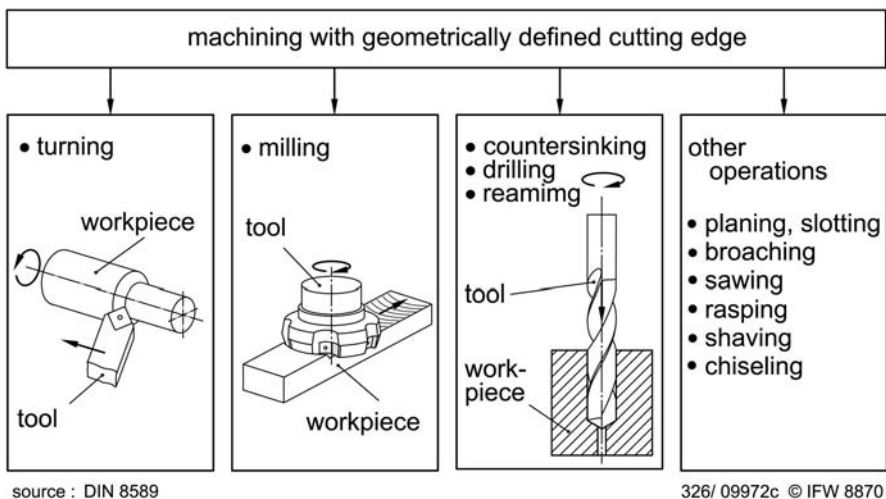
*Hans Kurt Tönshoff, Bernd Denkena, Jens Winkler, Christian Podolsky*

### 6.5.1 Machining

Manufacturing by material separation is known as machining. Material in the form of chips is mechanically separated from a raw workpiece, using one (turning), two (milling), or several (grinding) cutting edges of a tool. The number of cutting edges, the shape of the wedges, and their position to the workpiece are known and can be described in machining using geometrically determined cutting edges (Fig. 6.139). The following four criteria are relevant to the machining process:

- process forces
- tool wear
- workpiece topography
- shape of chips

In addition, environmental aspects must be taken into consideration. The process forces are important with regard to the design of machine drives and frame, the energy needed, the performance desired, the elastic deformation of the workpiece and tool, as well as the necessary fixing of the workpiece and tool. The efficiency of the process is determined mainly by the tool wear. The deviation of the workpiece topography from the desired shape indicates the workpiece quality. The shape of the chip is important for the tool design (flutes), the design of the working area of the machine, and for an undisturbed process [1].



**Fig. 6.139.** Manufacturing process: Machining with geometrically defined cutting edges (DIN 8589)

### 6.5.1.1 Machining of not Reinforced Magnesium Alloys

No reinforced magnesium alloys are considered to be easy to machine at low cutting speeds. The reasons are:

- low cutting forces
- As a consequence, low mechanical and thermal loads on the tool
- high achievable surface qualities
- short-breaking chips
- the possibility of dry processing [2, 3]

Dry processing, however, can result in adhesive effects (Fig. 6.140). Particularly at high cutting speeds, the formation of flank build-up on carbide tools can be observed. This results in higher process forces, a higher friction and an enhanced danger of chip inflammation. Furthermore, it leads to a reduced shape and dimension accuracy of the workpiece and a poorer surface quality [4–6].

In the following, results are presented on the machining of the magnesium wrought alloy AZ31 and the magnesium cast alloy AZ91. The cutting material or the coating of the cutting material has a significant influence on the formation of adhesive products machining. The influence of the cutting material and the coating of the tool when machining AZ91D can be seen in Fig. 6.141. The tools are applied along a tool travel of  $l_c = 750$  m at a cutting speed of  $v_c = 900$  m/min, a depth of cut of  $a_p = 1.5$  mm, and a feed rate of  $f = 0.4$  mm. At the tool flanks of uncoated and TiN coated carbides, flank build-up can be observed at the runout of the contact surfaces. When DP tools are used, adhesion between material and workpiece cannot be avoided in any case. It occurs at long turn travels of  $l_c > 750$  m, when the processed material and the cemented carbide substrate of the tool are in contact. This effect is not observed when using diamond coated

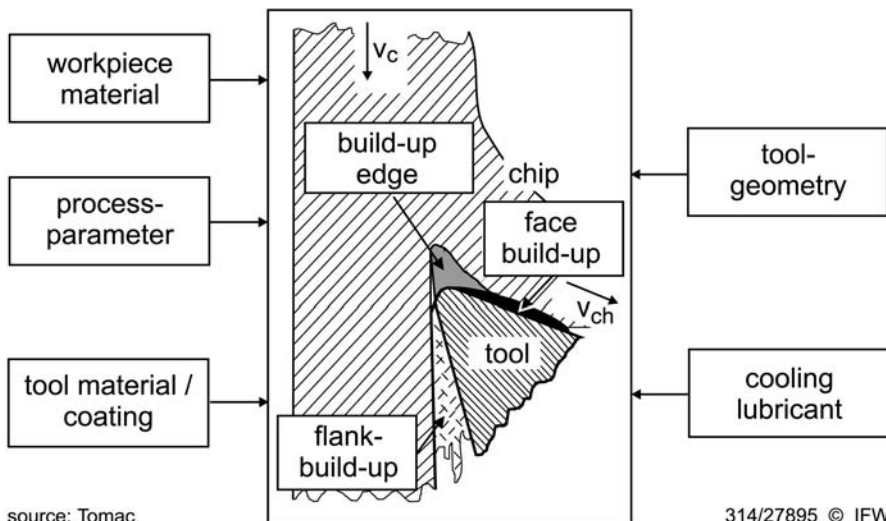


Fig. 6.140. Adhesive effects and reasons for their formation [7]

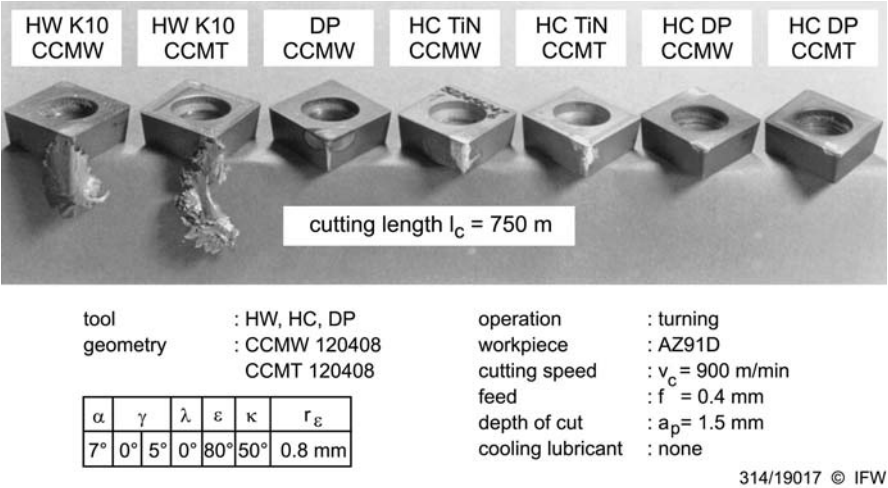


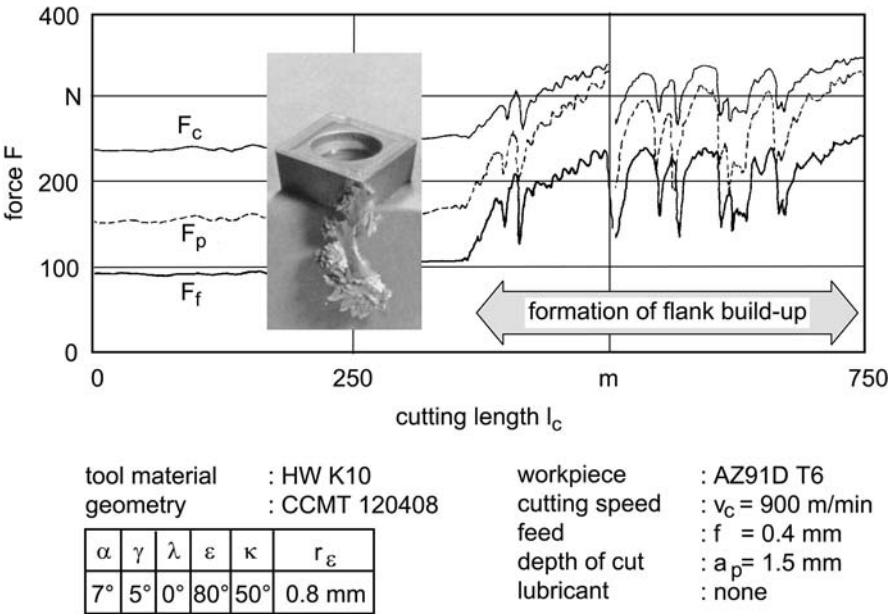
Fig. 6.141. Comparison between cutting materials with different geometries and coatings

tools. Their rakes and flanks are completely covered with diamond, so that flank build-up can be avoided reliably.

All tools investigated show material on their rakes after machining. As opposed to uncoated carbide and DP, coated tools show a significantly poorer surface quality on their rakes. The accumulation of material is due to mechanical clamping of material to roughness peaks. It cannot be observed, however, that flank build-up depends on the roughness and surface condition of the tools, so that mechanical adhesion as the sole cause can be ruled out.

Figure 6.142 illustrates the travel dependent process force components, which are cutting force  $F_c$ , feed force  $F_f$  and passive force  $F_p$ , on dry machining AZ91D (heat treatment T6) using uncoated cemented carbide in CCMT geometry. At a critical tool travel of  $l_{crit} \approx 350 \text{ m}$ , significant fluctuations in the forces can be observed, which result from flank build-up attaching to and detaching itself from the tool flanks. The peak forces of the cutting force  $F_c$  exceed the force level before flank build-up by approximately 45%.

Figure 6.143 illustrates the influence of the cutting speed  $v_c$  on the average values of cutting force  $F_c$ , passive force  $F_p$ , and average peak to valley height  $R_z$  of the workpiece surface, when machining AZ31B using carbide and DP tools. There is no influence of the tool material on the generated forces. Both cutting materials show no dependence of either the cutting force or the roughness on the cutting speed  $v_c$ . The passive forces decrease slightly on increasing the cutting speed. Using carbide tools, increasing adhesion between the processed material and the cutting material can be observed for a cutting speed of  $v_c = 300 \text{ m/min}$  at longer tool travels. This leads to material build-up on the rake-contact surface. Flank build-up forms at the rake behind the contact surface for a cutting speed of  $v_{crit} = 1800 \text{ m/min}$  and a tool travel of  $l_{crit} \approx 300 \text{ m}$ . Build up at the tool when machining AZ31B has no significant influence on the process forces, as opposed to flank build up at the tool when machining AZ91D. Adhe-



314/19001 © IFW 10203

Fig. 6.142. Flank build-up on uncoated cemented carbide after critical turn travel

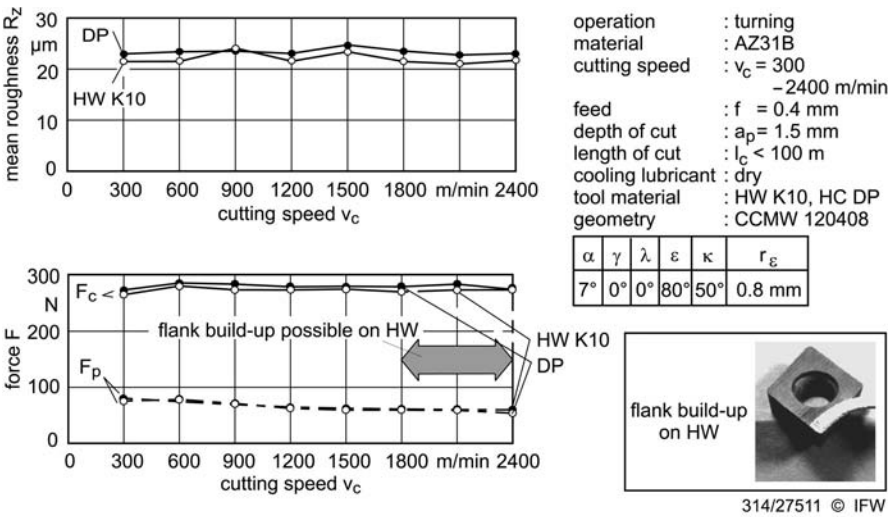


Fig. 6.143. Influence of the tool material on machining AZ31B at different cutting speeds

sion strength between flank build-up and cutting material is low compared with that of AZ91D.

Under identical cutting conditions, there is also no dependence of the cutting and passive force  $F_c$  and  $F_p$ , as well as of the average peak-to-valley height  $R_z$  on the cutting speed  $v_c$ , when machining AZ91D (Fig. 6.144). However, by using DP tools, the process forces can be reduced significantly, and the surface roughness of the machined surface can be improved slightly. The investigations show, especially on cemented carbide tools, adhesion between the processed material and the tool at all cutting speeds. At low cutting speeds, adhesion occurs in particular at the major flank. On increasing cutting speed, it extends to the minor flank and subsequently to the rake face at the major cutting edge. The critical cutting speed at which flank build-up occurs can be determined to be  $v_{crit} = 900$  m/min. For this cutting speed, a critical tool travel of  $l_{crit} \approx 350$  m was determined.

Apart from the lower process forces when machining AZ91D, resulting from the lower strength and ductility of the material, the dependence of the forces and roughnesses on the cutting speed  $v_c$  differs only slightly from the processing of AZ31B.

Metallographic investigation of the build-up at AZ31B and AZ91D shows significant plastic deformation (Fig. 6.145), opposed to the insignificant deformation in the subsurface layer of the workpiece. The build-up at AZ31B shows a partly recrystallized microstructure with a grain diameter of  $d = 5\text{ }\mu\text{m}$ , which is significantly smaller than that of the extruded matrix. The flank build-up of AZ91D, caused by successive material accumulation, is of a lamellar structure, in which the parent phases of the microstructure cannot be separated. Al-Mn-dispersions can be detected clearly in the form of point shaped inclusions.

In Fig. 6.146, chip roots of the two magnesium alloys are illustrated for  $v_c = 2100$  m/min. Chips form by shearing on machining AZ31B. The individual

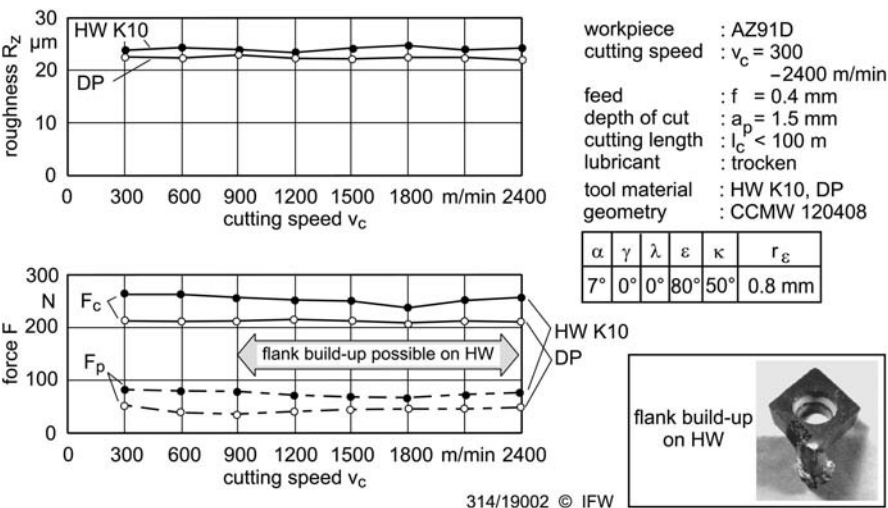


Fig. 6.144. Influence of the tool material when machining AZ91D at different cutting speeds

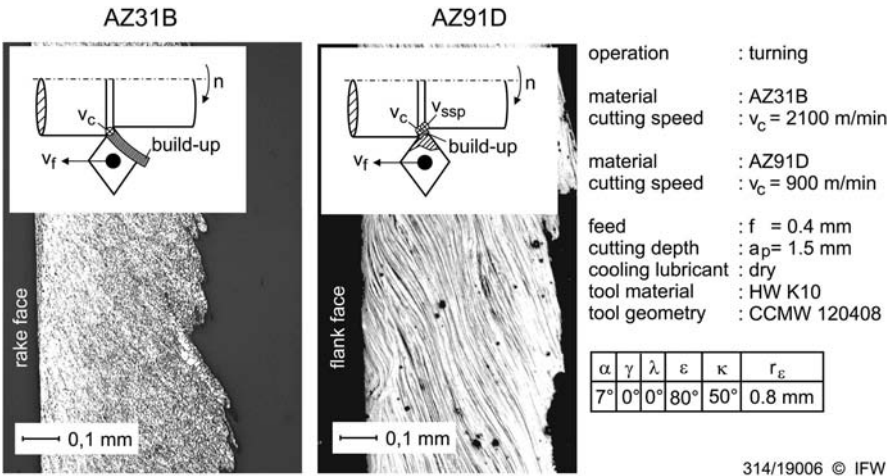


Fig. 6.145. Microstructure of flank build-up at AZ31 and AZ91

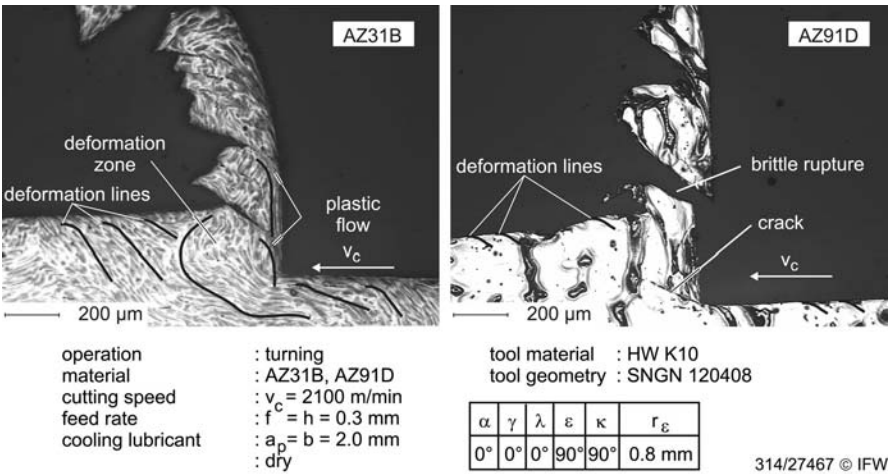


Fig. 6.146. Chip formation at AZ31 and AZ91

chip segments are held together by the highly plastically deformed material. Deformation lines in cutting direction can be identified in the material volume; the deformation zones can be seen clearly. Exceeding the yield stress  $k_f$  leads to plastic deformation of the workpiece surface at the contact surface.

Machining AZ91D at high cutting speeds results in the tearing of chips. A crack forms, which propagates along a shear plane and leads to brittle material separation. The chip surface has not yet been influenced by the chip formation. The low plastic deformability and the elastic yield of the base material (low elastic modulus) result in little plastic deformation of the subsurface layer.



Chip formation can be correlated with the ductile yield of magnesium alloys, depending on the content of aluminum. For extruded AZ31B, the ductile yield is  $A = 7\%$ , as opposed to  $A = 1\%$  for sand cast AZ91D. Reverse dependencies such as decreasing ductility due to high deformation speeds in the shear plane, and increasing ductility due to an increased material temperature, are not taken into account. Brittle separation of both materials show that the average thermal load in the shear plane is low. A temperature  $t > 120^\circ\text{C}$  would lead to a softening of the  $\gamma$ -phase and to sliding of the  $\delta$ -phase along the grain boundaries, particularly at AZ91D. This mechanism of plastic deformation, however, was not observed.

### Fire hazard

Most of the energy put into cutting processes is converted into heat. In the case of magnesium machining, this leads to a risk of fire due to chip ignition. Magnesium chips may ignite, if the temperature exceeds the inflammation temperature of  $t_F \approx 500^\circ\text{C}$ . Friction at the rake and flank can result in reaching the melting temperature at the bottom of the chip or the material surface of the alloys AZ31B and AZ91D. These melting temperatures exceed significantly the inflammation temperatures. Machining of AZ91D using carbide tools and high cutting speeds is particularly critical. The risk of chip heating is significant, due to:

- adhesion, increasing process forces when flank build-up occurs, and an increasing friction at the contact area of tool and workpiece
- short-breaking chips
- a low thermal conductivity of the cutting material ( $\lambda = 80 \text{ W/mK}$ )

The German government safety organisation published rules for safe machining and handling of magnesium [29, 30].

In the following, a chip temperature is calculated and a critical feed rate is determined under the condition, that the entire cutting power  $P_c$  put into the machining process is transformed into heat and carried off with the chips. This assumption is particularly valid at high cutting speeds [1]. Assuming that the cutting process is a stationary flow process in which the chip enters and exits the process as mass flow  $m$  at the cutting speed  $v_c$ , and its internal conditions change by taking up the entire process energy, the first main theorem of thermodynamics applies for the theoretical chip temperature:

$$t_{sp} = \frac{k_c}{c_p \cdot \varrho} + t_R \quad (6.28)$$

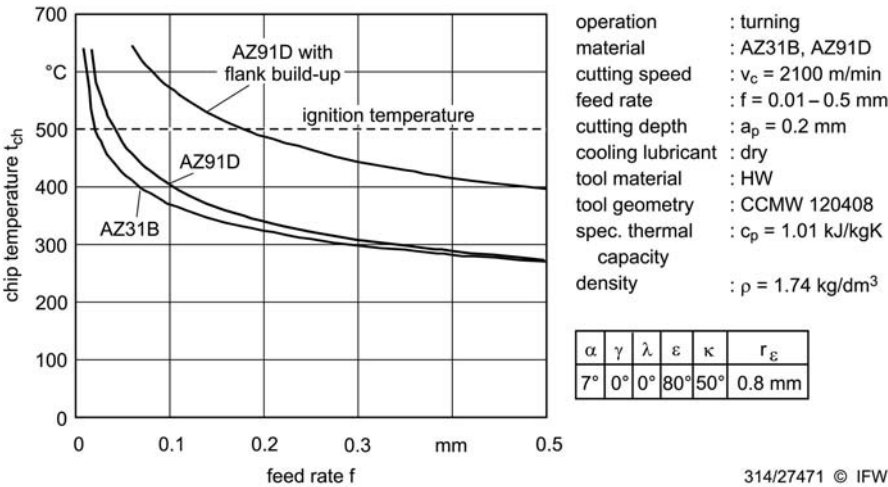
Or generally depending on the chip thickness  $h$ :

$$t_{sp} = \frac{k_{cb} \left( \frac{f \cdot \sin \kappa}{h_0} \right)}{c_p \varrho} + t_R \quad (6.29)$$

The specific cutting force  $k_{cb}$ , as well as the related rise values  $m_b$  (Table 6.58) are determined in experiments for the depths of cut used in preceding investigations.

**Table 6.58.** Specific cutting force depending on the depth of cut as basic value and related rise values ( $v_c = 2100$  m/min)

$a_p$	HW K10/AZ31B		HW K10/AZ91D	
	$k_{cb}$	$m_b$	$k_{cb}$	$m_b$
0.2 mm	359.6 MPa	0.21	344.9 MPa	0.26
1.5 mm	335.8 MPa	0.22	281.5 MPa	0.27



**Fig. 6.147.** Calculated chip temperatures  $a_p = 0.2$  mm

Depending on the feed rate, the chip temperature can be calculated for a constant depth of cut by using Equation 6.29. Taking into consideration that chipping only occurs at the cutting edge radius  $r_\varepsilon$  with a depth of cut  $a_p = 0,2$  mm and a cutting edge radius  $r_\varepsilon = 0.8$  mm, the effective setting angle is  $\kappa_{\text{eff}} \approx 31^\circ$ . Figure 6.147 and 6.148 show the theoretical chip temperatures  $t_{\text{sp}}$  versus the feed rate  $f$ . The chip temperatures rise progressively with a decreasing feed rate. The inflammation temperature  $t_i$  of the chips is exceeded when the critical feed rate  $f_{\text{krit}}$  is reached.

If flank build-up occurs when machining AZ91D, an increase in the cutting force by up to 45% must be expected (Fig. 6.142). An increase in the energy put into the process can lead to a significantly higher chip temperature during continuous cutting. Table 6.59 lists the calculated values of the critical feed rate  $f_{\text{krit}}$ .

If flank build-up does not occur, there is a risk of chip ignition as a result of the low critical feed rates  $f_{\text{krit}}$ , especially when the cutting edge enters and exits the material. AZ31B,  $f_{\text{krit}}$  is independent of the depth of cut  $a_p$ . On machining AZ91D, the critical feed rate increases with decreasing depth of cut.

If flank build-up leads to higher cutting power consumption, a significant increase in the critical feed rate can be observed. A risk of ignition already exists



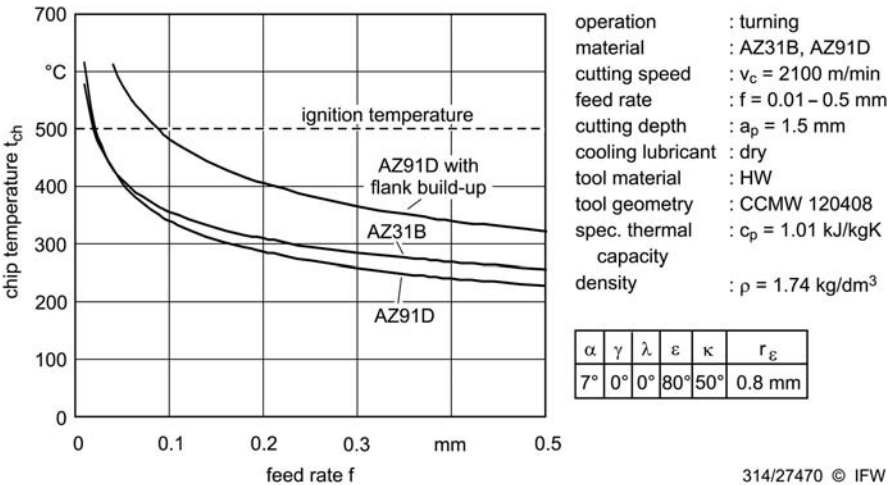


Table 6.59. Critical feed rates at given depths of cut ( $v_c = 2100$  m/min)

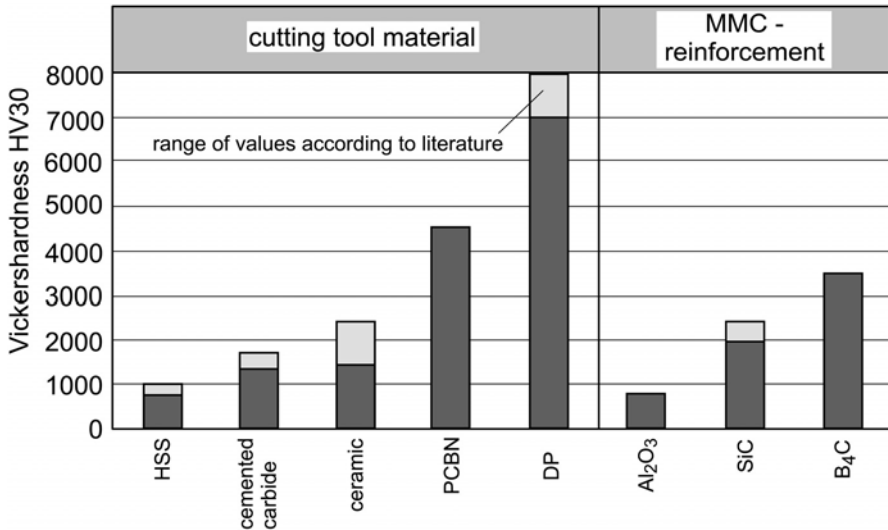
$a_p$	HW K10/AZ31B $f_{krit}$	HW K10/AZ91D $f_{krit}$ without/with flank build-up
0.2 mm	0.02 mm	0.04 mm/0.18 mm
1.5 mm	0.02 mm	0.02 mm/0.09 mm

at a feed rate of  $f = 0.2$  mm, particularly at a low depth of cut of  $a_p = 0.2$  mm. The risk of chip ignition can be reduced significantly when diamond cutting tools or coatings are used, since such as materials have a high thermal conductivity and can avoid flank build-up.

6.5.1.2 Machining of Reinforced Mg Alloys

In contrast to unreinforced light metals, there are completely different process requirements for machining of metal matrix composites, since the hardness of the reinforcement components usually exceed the hardness of the tool (Fig. 6.149). A strong abrasive tool wear can be observed [8–12]. According to Biermann, the fundamental wear mechanisms of carbide tools are surface disruption (micro-cracking), if the hardness of the tool is higher than that of the reinforcement component ( $\delta Al_2O_3$  short fibers), and microcutting, if the hardness of the tool is lower than that of the reinforcement components (SiC,  $B_4C$  particles). Using DP, self-grooving due to detached diamond grains of the tool is predominant [13].

The material used for the following investigations is ZC71 wrought alloy reinforced with 12 vol.% SiC particles. The average size of the SiC particles is 10  $\mu$ m, manufactured by Magnesium Electron Manchester, England.



after: Beitz, Küttner, Eastman, Lane, Tönshoff

314/22087c © IFW 10205

Fig. 6.149. Hardness of different tool materials and reinforcement components

The wear of coated carbides (HC TiN, HC DP) and DP versus tool travel  $l_c$  is illustrated in Fig. 6.150. TiN coated carbides fail immediately and are therefore not suited for processing of the material. Only a diamond coating results in a significantly higher tool life travel of  $l_c = 500$  m. The use of DP makes tool life travels of  $l_c > 13,000$  m possible.

Both TiN coated carbide and DP show pure abrasive wear. The continuous progress of wear of DP enables its safe use in the process. Although the cutting material contains 6% cobalt, the diamond coating shows a cohesive layer failure at the main cutting edge. The strong increase of the process force components  $F_c$ ,  $F_f$  and  $F_p$ , as well as the average peak-to-valley height  $R_z$  at the end of the tool life show, that the coating protects the substrate until the abrasive wear uncovers the substrate (Fig. 6.151). As a consequence, diamond coated tools can be used for the processing of particle reinforced magnesium materials until the protection of the coating ends. Diamond coatings can be generated up to a layer thickness of  $s = 20 \mu\text{m}$ . However, the coating time rises in proportion to the thickness of the coating, which also raises the costs.

### Drilling

SEM pictures in Fig. 6.152 show the wear of cemented carbide drills after machining fibre and particle reinforced magnesium alloys. Microcracking and fatigue are the main wear mechanisms when drilling  $\delta\text{-Al}_2\text{O}_3$  short fibre reinforced magnesium. Abraded parts of the substrate material cause tool wear when sliding over the rake and clearance face. A smooth topography of the worn surface is caused by small abraded carbide grains. Large cracks can also be observed.

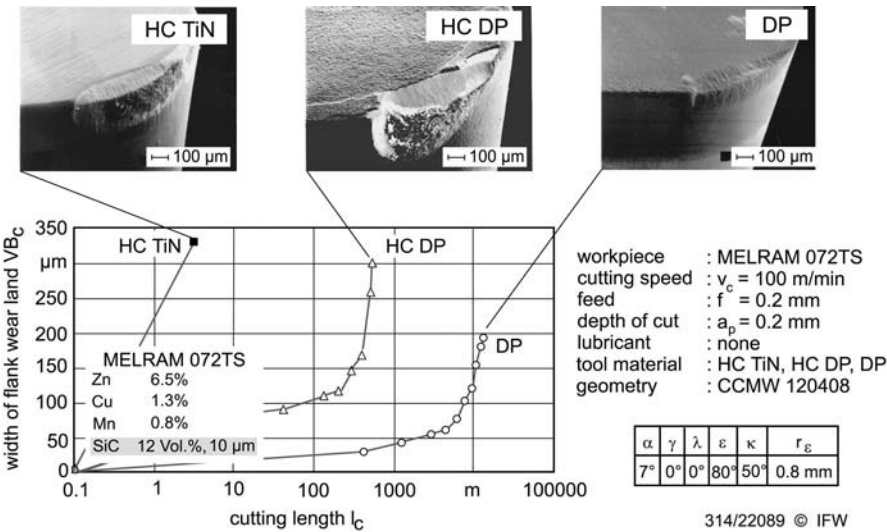


Fig. 6.150. Tool wear when machining magnesium MMC

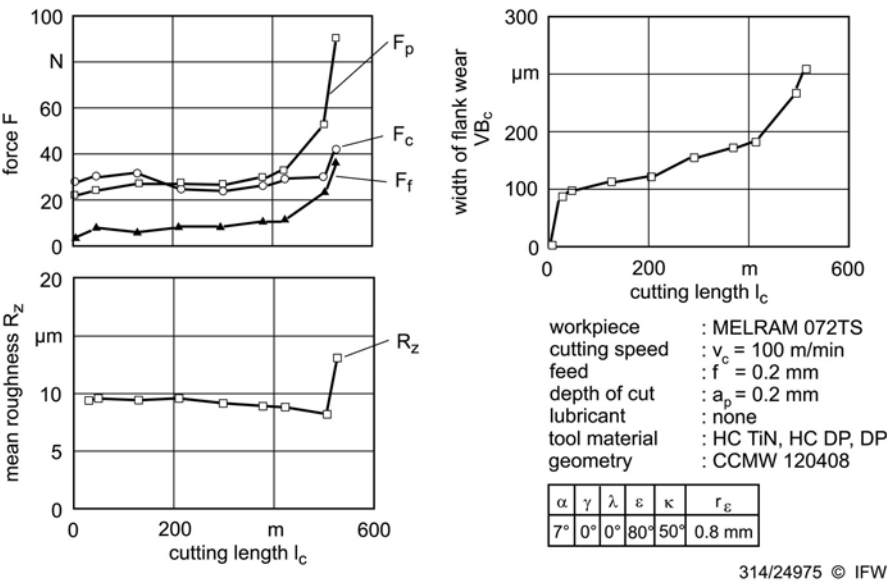


Fig. 6.151. Wear of diamond coated cemented carbide tools

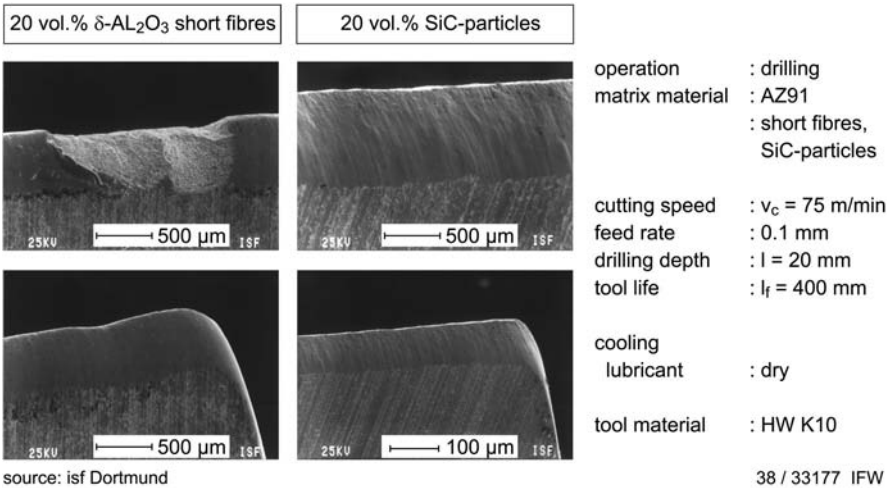


Fig. 6.152. Worn cutting edges after drilling MMC with  $\delta$ - $\text{Al}_2\text{O}_3$  short fibres and SiC particles after K. Weinert [14]

A different type of tool wear is found when drilling MMCs containing harder reinforcement components. The worn surface topography is characterised by grooves, which are oriented in the cutting direction. The high hardness of the SiC particles (2400 HV) exceeds the hardness of the cemented carbide grade and influences microcutting of the cutting edge. Extensive tool wear is the result. For these materials, DP tools or DP coated tools are needed.

Figure 6.153 shows the tool wear when drilling magnesium MMCs with different tools. Short  $\delta$ - $\text{Al}_2\text{O}_3$  fibres cause only a slight deterioration of the tool, depending on the hardness of the reinforcements. The uncoated cemented carbide drill shows the strongest wear. The results of the (Ti,Al)N coated drill are even better than those of the diamond coated drill. When drilling ZC63 + 12 vol.% SiC magnesium alloy, the wear of the uncoated and (Ti,Al)N coated drill is very high. Due to the high hardness of the SiC particles, the end of the tool life is reached quickly. The diamond coated drill shows good resistance against abrasive wear. No significant tool wear is observed after a drilling length of  $L_f = 400 \text{ mm}$ . Also for the machining of hybrid reinforcements, diamond coated tools are preferred.

6.5.1.3 Cooling Lubricants

The requirements on cooling lubricants can be divided into main and additional functions. Cooling, in order to remove heat from the tool, the workpiece and the machine, is one main function. Another main function is lubrication. The forces and energy needed for machining can be reduced and the surface quality can be improved by a decreased friction and adhesion tendency. The removal of chips and the protection of the workpiece surface are additional functions. Cooling lubricants also need to protect machine parts, be harmless to people, resistant to aging and biodegradable.

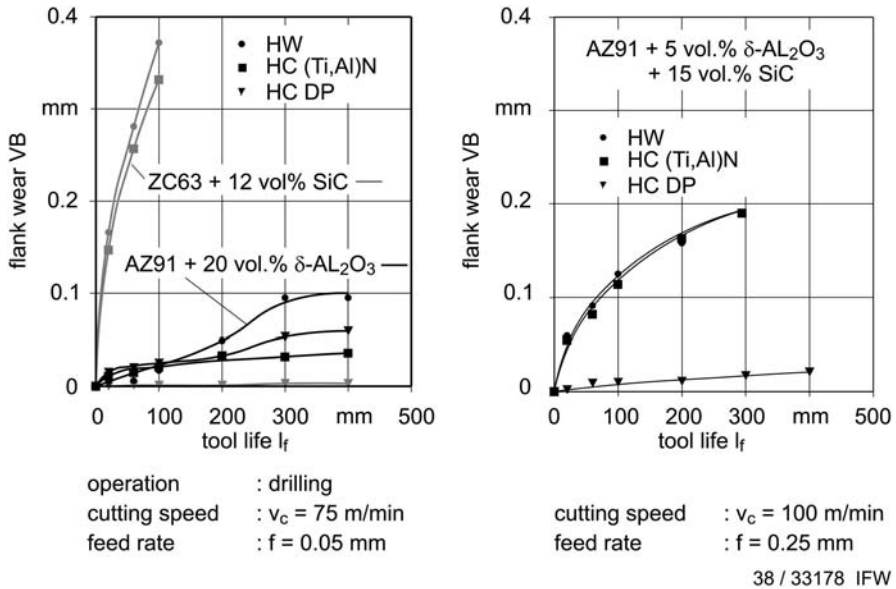


Fig. 6.153. Tool wear when drilling magnesium MMC after K. Weinert [14]

Media with cooling, lubricating or combined effects can be divided into

- one-phase media, such as gases and liquids and
- two-phase media, such as solid suspensions and liquid-gas mixtures.

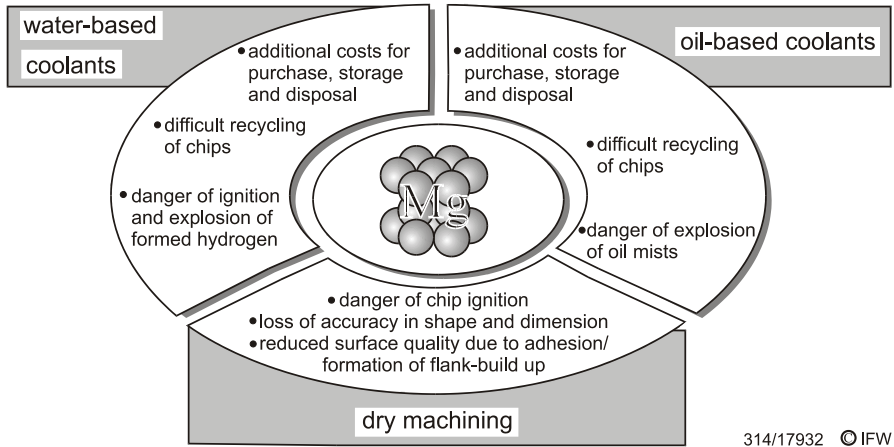
Liquid cooling lubricants are those mostly used in practice. They can be divided into water based cooling lubricants and those which are not water based.

Non water based cooling lubricants use basic mineral oils with or without additives. Cooling lubricants that are not water based are characterised by high lubrication and corrosion protection, but a low cooling capacity.

Water based cooling lubricants have better cooling properties due to their high heat capacity, thermal conductivity, and heat of evaporation. They are, however, susceptible to microorganisms, such as aerobic and anaerobic bacteria and fungi [1].

At present, cooling lubricants are generally used in series production of magnesium components. The risk of chip ignition in the working area of the machine tool exists during processing, when the ignition inflammation temperature of magnesium of  $t_F = 500^\circ\text{C}$  is exceeded. Particularly hazardous are chips of a small-volume, which form when pocket holes are drilled, radii are turned and during milling processes [4, 15, 16]. Another problem is the high thermal expansion of the material  $\alpha_{\text{Mg}} = 26 \cdot 10^{-6} \text{ 1/K}$  (Al:  $\alpha_{\text{Al}} = 24 \cdot 10^{-6} \text{ 1/K}$ , Ti:  $\alpha_{\text{Ti}} = 8.4 \cdot 10^{-6} \text{ 1/K}$ ). Thermal expansion, which results from heat conduction into the workpiece, can lead to loss of shape and dimensional accuracy, e.g., in drilled holes or on sealing surfaces. Therefore the use of cooling lubricants is often required [16–18].

Water-based cooling lubricants, however, bear the risk of hydrogen formation when reacting with magnesium. These reactions do not occur only within the working area of the machine, but also in the lubricant cooling cycle, chip con-



314/17932 © IFW

Fig. 6.154. Problems and hazards when machining magnesium

veyor, and chip storage [4, 16]. Hydrogen is inflammable in a concentration of at least 4 vol.% in the air. According to the observations of Tomac, Tønnessen and Rasch, the release of hydrogen decreases with an increasing concentration of free  $\text{OH}^-$  ions in the cooling lubricant. By law, water based cooling lubricants are limited to a pH value of  $\text{pH} = 9.5$  so that they are harmless to people [1]. A significant reduction in the release of hydrogen, however, can only be expected when a stable magnesium hydroxide cover forms at a pH value of  $\text{pH} = 10.4$ . Furthermore, water-based cooling lubricants may have a negative effect on the tool wear [7]. Magnesium hydroxide which deposits in the working area can lead to machine tool damage [4]. The use of cooling lubricants that are not water based can result in the formation of oil mists. Figure 6.154 summarises the problems when processing magnesium alloys wet or dry.

Cooling lubricants are always a strain on personnel and the environment. The risks are not only the basic oils and additives, but also bacteria, fungicides, reaction products and foreign substances. There is strain on the soil, water, and air caused by leakage loss in continuous chip removal, emissions, and wash water. In addition, costs for the investment, maintenance, and disposal of cooling lubricants must be evaluated economically. Therefore, dry processing is preferred, not only for ecological, but also economic reasons.

### 6.5.2 Burnishing

In many cases in technical practice, the surface and the subsurface layers of functional areas have to carry high loads [19]. A mechanical surface treatment changes the conditions of subsurface layers, e.g., hardness increase or decrease, as well as micro and macro residual stresses. In addition, the surface topography can be changed, depending on the process and process parameters. All effects can influence the behaviour of the components under dynamic load and change their fatigue strength [20, 21]. Compressive stress in the workpiece reduces the stress

intensity at cracks and hinders crack propagation [22, 23]. A direct overlapping of load and residual stress, however, is not valid since the material specific and strength dependent sensitivity to residual stress  $m$  must be taken into consideration [24, 25]. Due to  $m < 1$ , the effect of residual stresses in the workpiece surface is lower than of the load-stress amplitude  $\sigma_A$ . In the experiments, the influence of residual stresses can hardly be separated from other changes in the subsurface layer properties [26].

Particularly burnishing is used as mechanical surface treatment for rotationally symmetrical components. Rolling processes offer a higher penetration depth of the residual stresses and can improve surface quality, as opposed to shot peening, sandblasting or water jetting. Processing in one clamping of a small number of parameters is possible in almost all cutting machine tools [27]. Burnishing is a press polishing process to generate smooth and strengthened surfaces on metallic workpieces without cutting. Such surfaces have a high loadability, good running qualities, and an improved corrosion resistance [28]. Since this process does not involve removal of material, the influence on the dimensions is limited to levelling the roughness peaks, which were developed in the preceding machining process. Turned parts entail a change in diameter by the size of the peak-to-valley height  $R_z$ . The desired changes in the subsurface layer of the workpiece during burnishing are caused by local elastic-plastic deformation and possible changes in microstructure [19, 20].

### AZ31

Figure 6.155 illustrates the influence of the rolling force  $F_w$  on the average peak-to-valley height  $R_z$ , the integral surface hardness HV10, and the microhardness HV0,025 as a function of depth, on rolling AZ31B. The hardness of the workpiece after turning is 58 HV10. Burnishing leads to an increase in surface hardness. The increase is significant even when using a rolling force of only  $F_w = 0.5$  kN. Using a rolling force of 5 kN results in a maximum hardness of 90 HV10.

The microhardness shows a maximum hardness below the workpiece surface. The surface hardness is between 85 and 90 HV0,025. At increasing roll forces, the maximum hardness increases from 103 HV0,025 at a roll force of  $F_w = 0.5$  kN to 128 HV0,025 at a roll force of  $F_w = 5.0$  kN, and shifts slightly from the surface into the workpiece. The effective depth of rolling increases significantly with increasing roll force. Only at the maximum roll force of  $F_w = 5$  kN, can a higher hardness at a 2-mm distance from the workpiece surface than in the base material be detected.

After machining, the peak-to-valley height is  $R_z = 6.1$   $\mu\text{m}$ . All rolling forces show smoothing of the surface roughness. The smoothest surface roughness is generated at a roll force of  $F_w = 3$  kN. At this rolling force, the marks generated during machining are levelled, as can be seen in the SEM pictures in Fig. 6.156. At higher rolling forces, the surface gets rougher again, but damage by crack formation or pitting cannot be observed.

Figure 6.157 illustrates the influence of the rolling force on residual stress conditions in the subsurface layer of the workpiece. With an acceptable effort, values can be measured up to a distance of 1.5 mm from the surface by using X-ray diffractometry and chemical etching. The residual stresses can also be calculated at greater depths by means of FEM. With the exception of the immediate sub-



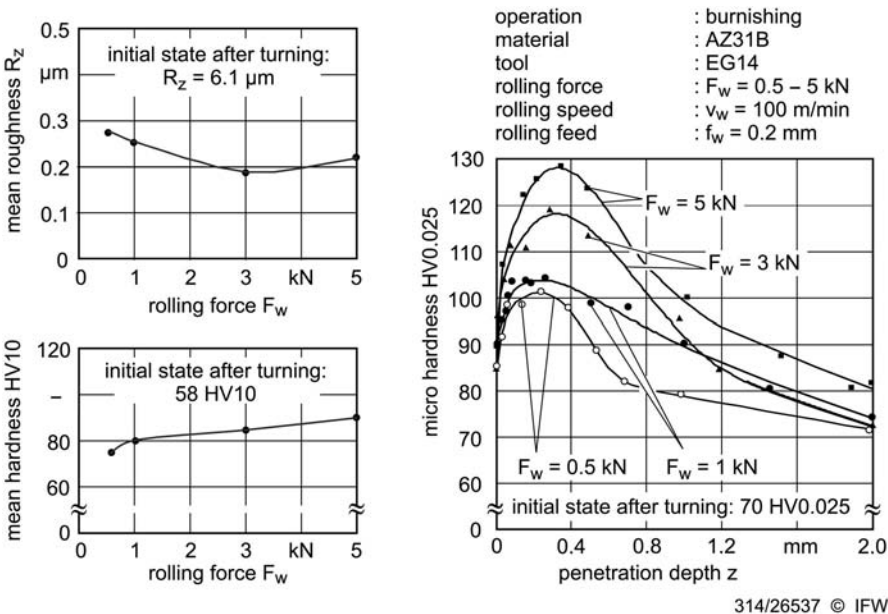


Fig. 6.155. Influence of the rolling force on the average peak-to-valley height and the hardness in the subsurface layer (AZ31)

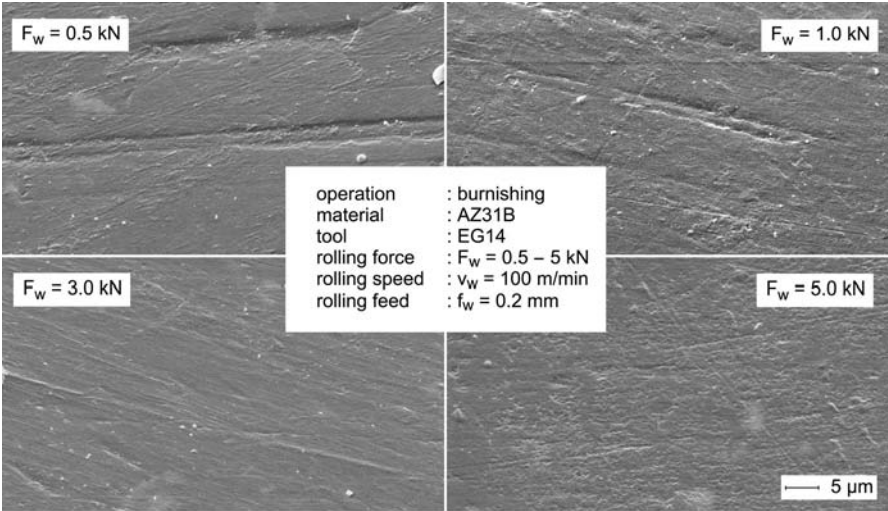


Fig. 6.156. Influence of the roll force on the surface (AZ31)



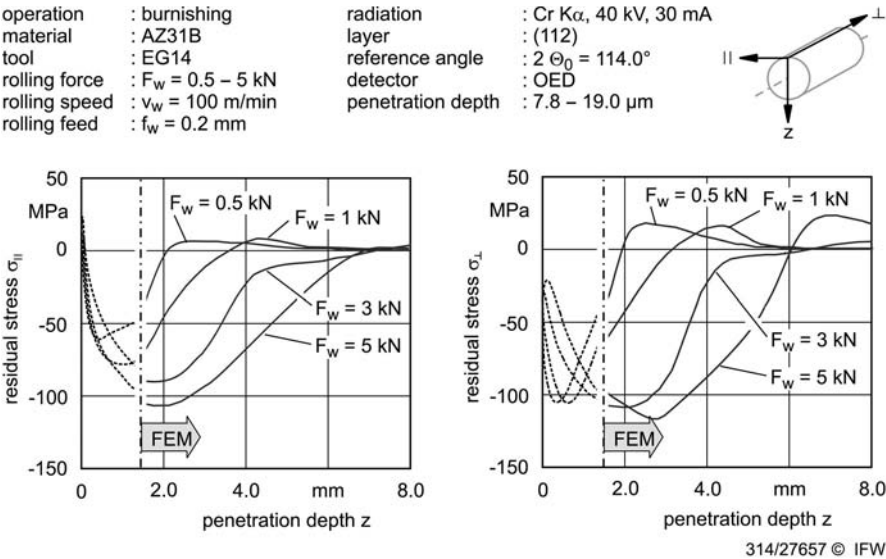


Fig. 6.157. Influence of the roll force on residual stress conditions in the subsurface layer

surface layer, the measured and calculated values correspond well, so that the measured values can be supplemented by calculated values over a surface distance of  $z \geq 1.5$  mm.

At an increasing distance from the surface, the residual compressive stress increases over the measurement range in the processing direction  $\sigma_{||}$ , without forming a distinct maximum. Higher rolling forces do not only lead to higher compressive stresses, but also to a higher effective depth in the  $z$  direction. The course of the residual stress in the axial direction  $\sigma_{\perp}$  shows low compressive stresses in the subsurface layer of the workpiece, which increase significantly with an increasing distance from the surface. The stress values  $\sigma_{\perp}$  are higher than those in the circumferential direction  $\sigma_{||}$ . On increasing the roll force, the stress maximum  $\sigma_{\perp, \max} \approx 105$  MPa shifts further into the workpiece, so that stresses near the surface can vary, depending on the roll force between  $\sigma_{\perp} = -20$  MPa ( $F_w = 5$  kN) and  $\sigma_{\perp} = -100$  MPa ( $F_w = 0.5$  kN).

AZ91

In Fig. 6.158, the influence of the roll force  $F_w$  is compared between AZ31B and AZ91D. Compared to AZ31B, the integral surface hardness of AZ91D is higher by approximately 20 HV10. On increasing the roll force, the integral hardness rises to 113 HV10 at  $F_w = 5$  kN.

To guarantee comparability, the microhardness is only determined in the  $\delta$ -phase of AZ91D. The  $\gamma$ -phase is the hardness carrier of AZ91, since the microhardness values in the  $\delta$ -phase are much lower compared to those of AZ31B. Using the highest rolling force  $F_w = 5$  kN enables a significant increase in the microhardness of AZ91D up to 110 HV0,025 to be made. Increasing rolling forces lead to a significant increase in the effective depth of rolling.

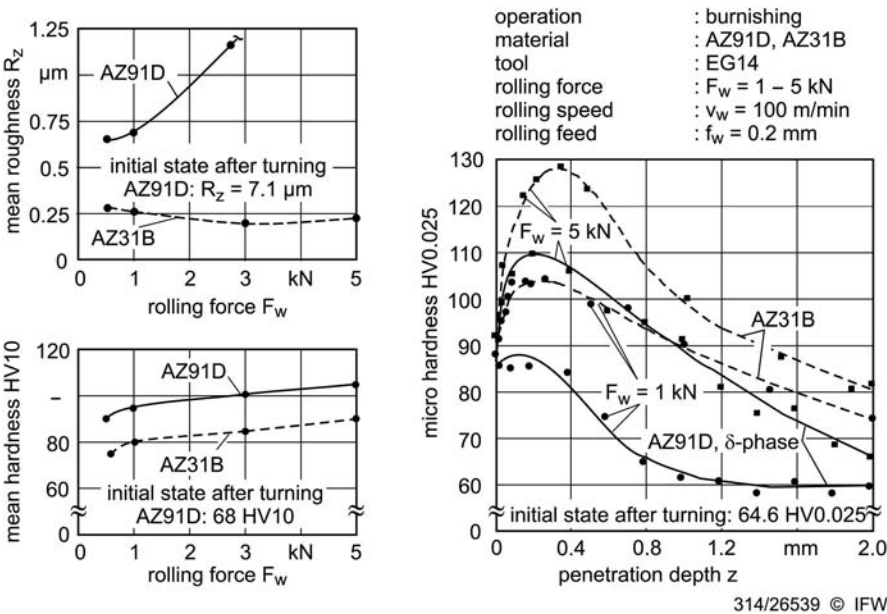


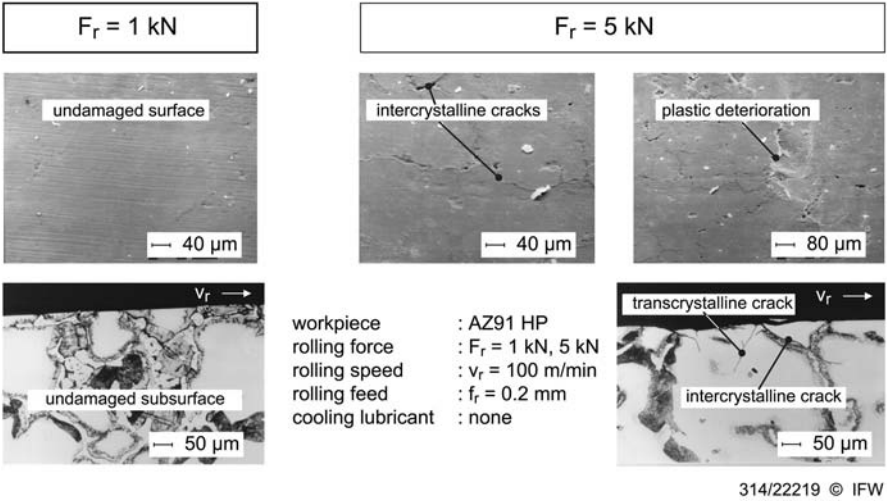
Fig. 6.158. Influence of the rolling force on the average peak-to-valley height and the hardness in the subsurface layer (AZ91D)

Compared to AZ31B, the deformability of AZ91D is much lower. Only at low rolling forces of  $F_w \leq 3 \text{ kN}$ , can the machined surface of AZ91D be improved significantly, as can be seen from the average peak-to-valley height values. In Fig. 6.159, SEM pictures and micrographs of the subsurface layers illustrate the influence of rolling forces. Pores near the surface are closed by low roll forces ( $F_w = 1 \text{ kN}$ ), and feed grooves are smoothed. By contrast, high roll forces ( $F_w = 5 \text{ kN}$ ) can result in damage of the workpiece surface and the subsurface layer by intercrystalline and transcrystalline cracking. In addition, too much load on the areas near the workpiece surface leads to pitting in the form of local plastic build-up. An influence of surface damage on the hardness values, however, cannot be observed.

Application behaviour

In order to examine the behaviour of rolled specimens rotary bend tests are carried out according to DIN 50113. The surface of the specimen is treated mechanically by means of a hydrostatic burnishing tool. A hydrostatically fixed ball is pressed against the workpiece at pressures up to  $p_w = 40 \text{ MPa}$ .

Figure 6.160 illustrates the results of the rotating bend tests for an AZ31B specimen. The number of stress cycles  $N$  until failure can be increased significantly by a burnishing treatment. The maximum average number of stress cycles  $N$  can be achieved by applying a high roll pressure of  $p_w = 10 \text{ MPa}$  at a low roll feed rate of  $f_w = 0.1 \text{ mm}$ . The scatter in the data increases, however, in contrast to the lower roll pressure of  $p_w = 4 \text{ MPa}$ . A doubling of the specimen lifetime with identical



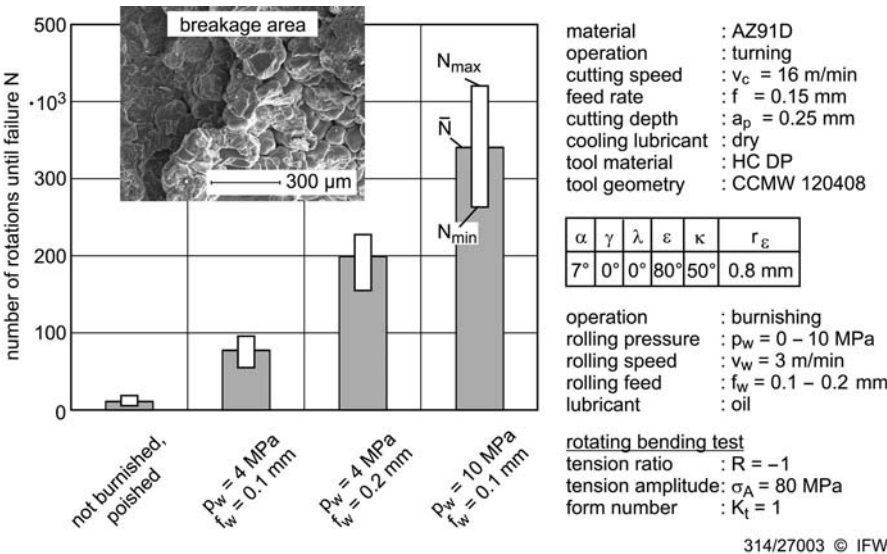


Fig. 6.161. Results of the rotating bending test at AZ91

lower (AZ31:  $\sigma_A = 155$  MPa), the specimen of the less strong AZ91D shows only a comparatively low average number of stress cycles until rupture  $\bar{N}$ .

Analogous to AZ31B, the average specimen lifetime can be improved and the scatter in the data is increased by raising the rolling pressure  $p_w$ . Damage of the surface in the form of crack formation and pitting of AZ91D already takes place at a rolling force which has no negative effect on AZ31B. In addition, the increase of stress cycles by means of an increased rolling feed rate at a rolling pressure of  $p_w = 4$  MPa indicates that the material is susceptible to fatigue as a result of the mechanical surface treatment. At fatigue rupture of AZ91D, crack propagation originates from micropores in the materials microstructure. Crack propagation takes place in an intercrystalline manner between the grains in the  $\delta$ -phase. A shift in the crack formation from the surface to inside the material, achieved by rolling, cannot be detected for AZ91D.

Corrosion investigations

Sulfuric acid or  $\text{CO}_2$  leads to sour media in contrast to synthetic sea water with a neutral pH value. This ensures that stable oxide and hydroxide layers form. The loss of material by corrosion can be determined reliably (Fig. 6.162). The pH value of a molar solution of 0.01 from the dissociation of sulfuric acid in water can be calculated and is  $\text{pH} = 1.9$ . A pH value of 5.3 is obtained for a solution of  $\text{CO}_2$  in water at a medium temperature of  $T = 20^\circ\text{C}$  in a state of equilibrium.

If there is no subsurface layer damage due to rolling, the corrosion behaviour of AZ91D is independent of the process in both acid media. Machined surfaces of AZ91D show a significantly better corrosion behaviour than those of AZ31B. In comparison, the corrosion behaviour of AZ31B is directly related to the pre-

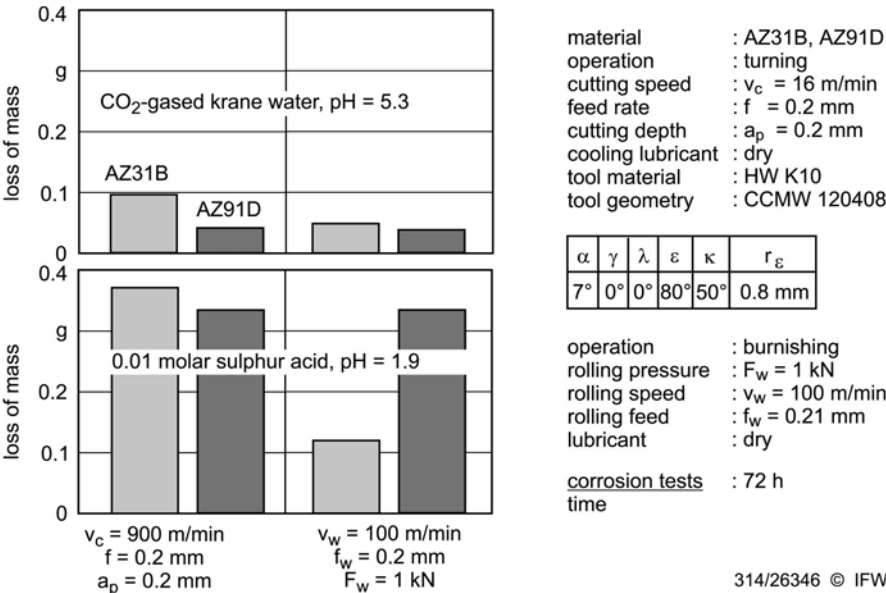


Fig. 6.162. Material loss of AZ31 and AZ91 in corrosive media

ceding treatment. Specimens which are simply machined show an increase in material consumption on increasing the cutting depth and feed rate in both media. The material loss can be reduced to 30% of the value of a simply machined specimen, by a burnishing process with a rolling force of  $F_w = 1$  kN. In 0.01 molar sulphuric acid, the material loss is less than 40% of the material loss of the untreated magnesium alloy AZ91D.

References to Chapter 6.1

1. Emley EF (1966) Principles of Magnesium Technology. Pergamon Press Ltd, Oxford, England, 1966.
2. Michels W (2002) "Magnesium Sand Casting-A Flexible Production Process for Complex Parts of High Volume" Proc. 10<sup>th</sup> Magnesium Automotive and End Users Seminar, Aalen Sept. 2002.
3. Hirose K et al. (1987) "Premium Quality Magnesium Alloy Castings by Low Pressure Pouring System" Proc. 44<sup>th</sup> Annual IMA World Magnesium Conference, Tokyo, Japan, May 1987.
4. King JF (1990) "The MEL Differential Pressure Sand Casting Process for Magnesium Alloys" Proc. 47<sup>th</sup> Annual World Magnesium Conference, Cannes, France, May 1990
5. ASTM (1964) ASTM-E155-64. Standard Radiographs for Inspection of Aluminium and Magnesium Castings. Series 2.
6. ASTM (1974) ASTM-E155-74. Standard Radiographs for Inspection of Aluminium and Magnesium Castings. Vol. 2. Magnesium Castings. Technology of Magnesium and Magnesium-Alloys
7. Beck, Frech GmbH (2000) Vorstellung einer elektrischen Warmkammer Druckgießmaschine, 8<sup>th</sup> Annual IMA Seminar on Magnesium in Automotive Applications, Aalen, Germany, 12–14 June
8. Dynacast (2001) Präzisionskleinteile aus Druckguss (Zn, Mg), technical information

9. Lockwood LF (1988) Recommended Practice for Melting High Purity Magnesium Alloys. IMA Technical Comitee Report
10. NADCA training papers (2000)
11. Hydro Magnesium, MAGNESIUM Die Casting technical information, 4.98
12. Mertz A, Brungs D, Honsel (1999) Opportunities to Combine Mg-Extrusions with Die Castings. IMA 1999 Annual World Magnesium Conference, Rome
13. Schumann F (2001) Volkswagen AG, Forschungsstrategien für ein zweites Magnesium-Zeitalter im Fahrzeugbau. Mat.-wiss. u. Werkstofftech. 32, 6–12
14. BMBF (1999) MADICA: Sichere Produktionsprozesse für die Magnesiumver- und -bearbeitung. Final Project Report, FH-Aalen
15. Cashion, Ricketts, Frost (2000) CAST Research Centre. The Protection of Molten Magnesium and ist Alloys during Die Casting 8th Annual IMA Seminar on Magnesium in Automotive Applications. Aalen, Germany, 12–14 June
16. Milbrath D, Owens M (2001) Performance Materials Division. New Flourochemical Cover Gases for Protection of Molten Magnesium. IMA Annual World Magnesium Conference, Brussels, May
17. King JF, MEL (2000) SF6 Replacement in Fluxless Melting. ELEKTRON GROUP MEETING 2000, 11–13th November, Sheraton – El Conquistador, Tucson, Arizona
18. Rhomberg A (2000) Stoffliches Recycling von Magnesiumbauteilen, Fortschritte mit Mg im Automobilbau. Praxis Forum, 2
18. Garat M, Maenner L, Sztur Ch (2000) State of the art of thixocasting. In: Chiarmetta GL, Rosso M (eds) Proc. 6th Int Conf on “Semisolid processing of alloys and composites”. Turin, Italy, Edimet, Brescia, pp 187–194
19. Kainer KU (1994) Herstellung und Eigenschaften von faserverstärkten Magnesiumverbundwerkstoffen. In: Kainer KU (ed) Metallische Verbundwerkstoffe. DGM-Verlag, Oberursel, pp 219–244
20. Chadwick GA, Yue TM (1989) Principles and applications of squeeze casting. Metals Mater 5: 6–12
21. Long S, Beffort O, Moret G, Thevoz P (2000) Processing of Al-based MMCs by indirect squeeze infiltration of ceramic performs on a shot control high pressure die casting machine. Aluminium 76 (1/2): 82–89
22. Fleming MC (2000) SSM: Some thoughts on past milestones and on the path ahead. In: Chiarmetta GL, Rosso M (eds) Proc. 6th Int Conf on “Semisolid processing of alloys and composites”. Turin, Italy, Edimet, Brescia, pp 11–14
23. Fan Z (2002) Semisolid metal processing. Int Mater Rev 47: 49–85
24. Walakus D, LeBeau S, Prewitt N, Decker R (2000) Thixomolding – technology, opportunities and practical uses. In: Chiarmetta GL, Rosso M (eds) Proc 6th Int Conf on “Semisolid processing of alloys and composites”. Turin, Italy, Edimet, Brescia, pp 109–114
25. Tzimas E, Zavaliangos A (1999) Materials selection for semisolid processing. Mater Manuf Process 14: 217–230
26. Fehlbier M, Aguilar J, Sahm PR (2001) Rapid-slug-cooling technology (RSCT): A new approach for the production of thixocasting prematerial billets. Int J Cast Metals Res 14: 71–78
27. Suk S, Collot J (2001) Study of mechanical properties of both magnesium alloys AZ91D and AM50A cast by thixomag process, Influence of microstructure. In: Light metal applications for the automotive industry: aluminium and magnesium. SAE, Warrendale, USA, pp 13–18
28. Uggowitzer PJ, Gullo G-C, Wahlen A (2000) Metallkundliche Aspekte bei der semisolid Formgebung von Leichtmetallen, In: Kaufmann H, Uggowitzer PJ (eds) Vom Werkstoff zum Bauteilsystem. Proc Ranshofener Leichtmetalltage 2000, LKR, Ranshofen, Austria, pp 95–107
29. Collot J, Scalo EL (1993) Survey of the technologies of preparation and shaping of semi-solid alloys. Application to magnesium alloy. In: Proc. Int. Conf Aluminium Alloys: New process technologies. Marina di Ravenna, Italy, pp 13–30
30. Gjestland H, Westengen H (1993) Method for production of thixotropic magnesium alloys. European Patent, Publication No. 0575796 A1



31. Kamado S, Kojima Y (1996) Semi-solid forming using strain-introduced Mg-Al based alloys. In: Proc 3rd Int Magnesium Conf, Manchester, UK, pp 123–136
32. Young KP, Kyonka CP, Courtois JA (1983) US Patent No. 4,415,374
33. Woodhouse GH (2000) Semi-solid metal forming process. US patent No. 6,079,477
34. Collot J (1997) Rheoformage et thixoformage des alliages de magnésium et d'aluminium: les avantages de l'induction, *Matériaux et Techniques*, No. 7–8: 13–18
35. Gräf T, Jürgens R, Gies J (2000) Controlled inductive heating for thixotropic materials into the semi-solid state. In: Chiarmetta GL, Rosso M (eds) Proc 6th Int Conf on "Semisolid processing of alloys and composites". Turin, Italy, Edimet, Brescia, pp 667–673
36. Young KP (1996) Recent advances in semi-solid metal cast aluminium and magnesium alloys. In: Kirkwood DH, Kapranos P (eds) Proc 4th Int Conf on "Semisolid processing of alloys and composites". Sheffield, UK, pp 229–233
37. Keist J, Apelian D (2000) Induction heating of SSM billets: Processing issues. In: Chiarmetta GL, Rosso M (eds) Proc 6th Int Conf on "Semisolid processing of alloys and composites". Turin, Italy, Edimet, Brescia, pp 203–208
38. Loue WR, Suery M, Querbes JL (1992) Microstructure and rheology of partially remelted AlSi-alloys. In: Brown SB, Flemings MC (eds) Proc 2nd Int Conf on "Semisolid processing of alloys and composites". Cambridge, Massachusetts, USA, TMS, pp 266–275
39. Kaufmann H, Limburg D, Uggowitzer PJ (2000) Das New Rheocasting – Konzept und aktuelle Bauteileigenschaften. *Gießerei-Praxis* 7: 300–304
40. Potzinger R, Fragner W, Kaufmann H, Uggowitzer PJ (2002) New Rheocasting von AZ71: Struktur und Eigenschaften. In: Kaufmann H, Wahlen A, Uggowitzer PJ (eds) Vom Werkstoff zum Bauteilsystem, Proc. Ranshofener Leichtmetalltage 2002, LKR, Ranshofen, Austria, pp 83–92
41. Kaufmann H, Uggowitzer PJ (2001) Fundamentals of the new rheocasting process for magnesium alloys. *Adv Eng Mater*: 963–967
42. Hall K, Kaufmann H, Mundl A (2000) Detailed processing and cost consideration for new rheocasting of light metal alloys. In: Chiarmetta GL, Rosso M (eds) Proc 6th Int Conf on "Semisolid processing of alloys and composites". Turin, Italy, Edimet, Brescia, pp 23–28
43. Hartmann D, Dworog A (2000) Magnesiumspritzgießen (Thixomolding). In: Krammer C (ed) *Magnesium-Taschenbuch*. Aluminium-Verlag, Duesseldorf, pp 534–544

## Additional References

- Siedersleben M, Honsel (1997) Vakuum-Druckguss von Magnesiumlegierungen für hochbelastete Bauteile. *Aluminium* Nr. 3
- Stummer F, Müller-Weingarten AG (1999) Innovationen in der Druckgießmaschinentechologie, *Gießerei-Erfahrungsaustausch*, June
- Mertz A, Weiß K, Vornhof R, Heller R, Honsel RWP, Recaro (1999) Near-Net-Shape Magnesium Structural Components for Automotive Applications EUROMAT, Munich
- Westengen H (2000) Magnesium, *Die Castings: From Ingots to Automotive Parts*, Light Metal Age, April
- ASM International (1988) *Metals Handbook*, 9th Edition, Vol 15, Casting
- VDG-Merkblatt S 700 (1994) Schmelzen und Schmelzebehandlung von Magnesiumlegierungen, Verein deutscher Gießereifachleute

## References to Chapter 6.2

1. Schumann S, Friedrich F (2001) Strategies to overcome technological barriers to increase the use of magnesium in cars, 58<sup>th</sup> Annual World Magnesium Conference. Int. Magnesium Association, May 20–22, Brussels, Belgium
2. Schumann S, Friedrich F (1998) The Use of Magnesium in Cars – Today and in Future, Proceedings of the Int. Conference on "Magnesium Alloys and Their Applications", Wolfsburg, Edited by Mordike BL, Kainer KU, MATINFO Werkstoffinformationsgesellschaft, pp 3–13

3. Barnes L (1992) Rolled Magnesium Products “What goes around, comes around”, 49. Annual World Conference. Int. Magnesium Association IMA, Chicago, May 12–15., Proceedings 29–43
4. Edgar RL (2000) Global Overview on Demand and Applications for Magnesium Alloys, Proceedings of the Int. Congress on “Magnesium Alloys and their applications”. München, Edited by Kainer KU, WILEY-VCH-Verlag GmbH, Weinheim, pp 3–8
5. Emley EF (1966) Principles of Magnesium Technology, Pergamon Press, 1. Edition
6. Beck A (1939) Magnesium und seine Legierungen, Springer-Verlag Berlin
7. NN (1952) Metal Industry, No. 21, Nov.
8. NN (2001) Company Information DaimlerChrysler
9. NN (2000) Annual Book of ASTM Standards, Section 2, Nonferrous Metal Products. Volume 02.02, Aluminium and Magnesium Alloys, pp 33–39
10. Dröder K (1999) Untersuchungen zum Umformen von Feinblechen aus Magnesium-Knetlegierungen. Dr.-Ing. Dissertation, Universität Hannover
11. Enß J, Evertz T, Reier T, Juchmann P, Schumann S, Sebastian W (2000) New Magnesium Rolled Products for Automobile Applications, Proceedings of the “Second Israeli International Conference on Magnesium Science & Technology”, Dead Sea, Israel, 22.–24.02., pp 19–26
12. Sebastian W, Dröder K., Schumann S (2001) Properties and Processing of Magnesium Wrought Products for Automotive Applications, in: see [4] pp 602–607
13. NN (2000) Magnesium-Taschenbuch, Edited by Aluminium-Zentrale Düsseldorf, 1. Edition
14. Enß J, Evertz T, Reier T, Juchmann P, Schumann S, Sebastian W (2001) Neue Magnesiumblechprodukte für den Automobilbau. Automobiltechnische Zeitschrift ATZ, Febr., pp 142–145
15. Enß J, Evertz T, Reier T, Juchmann P. Properties and Perspectives of Magnesium Rolled Products, in: see [4] pp 590–595
16. Chapman JA, Wilson DV (1962–1963) The room-temperature ductility of fine-grain magnesium, Journal of the Institute of Metals, Vol. 91, pp 39–40
17. Herenguel J, Lacombe P (1936) Métaux, Vol. 11, pp 185
18. Hehmann F (1996) WO-Patent, No. 9604409, Selected Processing for Non-Equilibrium Light Alloys and Products
19. Wilkinson RG, Fox FA. The hot working of magnesium and its alloys
20. Nobre JP, Noster U, Gibmeier J, Altenberger I, Kornmeier M, Dias A, Scholtes B (2000) Mechanical behaviour and residual stress in AZ31 Wrought Magnesium Alloy subjected to four point bending, in: see [4] pp 336–341
21. Chabbi L, Lehnert W, Kawalla R (2000) Hot and Cold Forming of Magnesium Alloys AZ31 and AZ61, in: see [4], pp 621–627
22. Hirsch J, Dumont C (1999) Fertigung und Gefüge von Magnesium AZ31-Blechen, Proceedings: Fortschritte mit Magnesium im Automobilbau, Bad Nauheim, pp 7–20
23. Roberts CS (1960) Magnesium and its alloys, Wiley-Verlag, pp 171–177
24. Juchmann P (2001) Einsatzpotenzial und Perspektiven von Magnesiumblechen im Karosseriebau, 8. Fachtagung des Internationalen Rohbau-Expertenkreises – “Prozeßkette Karosserie” Werkstoffe, Herstellung von Bauteilen und Oberflächenprozesse für den Karosseriebau, 5./6. April, Fellbach, Proceedings, pp 385–404
25. Juchmann P, Wolff S, Kordisch T, Rostek W, Härtel W, Lübbers R (2001) Mg-Blechhalbzeuge – Erweitertes Einsatzpotenzial für Magnesium im Automobilbau, 3<sup>rd</sup> Annual Expert and 1<sup>st</sup> European Automobile Conference “Progress with Magnesium in car body manufacturing”. 18./19. September, Bad Nauheim, Proceedings, pp 167–181
26. Dröder K, Sebastian W (2000) Einsatzpotential von Mg-Blech für Karosserieanwendungen, in: see [25] pp 147–161
27. Hillis JE, Mercer WE, Murray RW (1997) High purity die cast alloys – compositional requirements for quality performance. 5. Magnesiumguss Abnehmerseminar & Automotive Seminar, 8./9. October
28. Hilpert M (2001) Dauerschwingverhalten von Magnesiumlegierungen: Einfluss von mechanischen Oberflächenbehandlungen und Umgebungsmedien, VDI-Fortschrittberichte, Reihe 5, No. 627



29. Noster U, Scholtes B (2001) Schwingfestigkeit von AZ31 und AZ91 in Abhängigkeit der Einsatztemperatur, *Metall*, 55. Jahrgang, März, pp 112–116
30. Zenner H, Renner F (2001) Zyklisches Werkstoffverhalten von Magnesium-Druckguss- und Knetlegierungen. *Materialwissenschaft und Werkstofftechnik*, Vol. 32, No. 1, pp 68–75
31. Wagener H-W (2001) Private communication
32. Wagener H-W, Lehnert F (2000) Deep Drawing of Magnesium Sheet Metal at Room Temperature, in: see [4], pp 615–620
33. Wagener H-W, Hosse-Hartmann J (2001) Das Tiefziehen von Magnesiumblechen bei Raumtemperatur und mit partieller induktiver Erwärmung, EFB-Kolloquium “Prozeß-optimierung in der Blechverarbeitung”, 13./14. März
34. Doege E, Dröder K (1999) Sheet Metal Forming of Magnesium Wrought Alloys – Formability and Process Technology. *Proceedings of the Int. Conference “Sheet Metal”*, Erlangen-Nürnberg 27./28. September, pp 263–270
35. Dröder K, Janssen ST (1999) Forming of Magnesium Alloys – A Solution for Light Weight Construction, SAE-Paper 01-3172
36. NN (1950) Warmziehen von Leichtmetallblechen, *Mitteilungen der Forschungsgesellschaft Blechverarbeitung*, No. 27, (Aug.)
37. Kuretz E (1974) Die Anwendung von Wärme bei der Herstellung von Blechformteilen aus schwer umformbaren Werkstoffen. *Bänder Bleche Rohre*. Düsseldorf, Vol. 15, No. 5, 200–205
38. Wilkinson RG (1955–56) The hot forming of magnesium alloys, *Journal of the Institute of Metals*, Vol. 84, pp 217–228
39. Frank C, Dröder K (1999) Kunststoffwerkzeug für Prototypen aus Magnesiumfeinblech, Bänder – Bleche – Rohre, Mai, pp 28–30
40. Draugelates U, Schram A, Kedenburg CC. Superplasticity of Magnesium-based Alloys, in: see [4], pp 343–347
41. Hennige T (2000) Innovativer Leichtbau durch Innenhochdruckumformen, EUROFORUM-Fachkonferenz “Leichtbau – Werkstoffe und Fertigungstechnologien”, 06./07. Juni, Düsseldorf
42. Juchmann P, Wolff S, Kordisch T, Rostek W, Hartel W, Lubbers R (2001) Magnesium sheet for lightweight construction, *Materials Week*, Munich
43. Doege E, Dröder K, Elend L-E (2000) Tiefziehen und Clinchen von Magnesiumfeinblechen, *Praxis Forum-Tagung “Fortschritte mit Magnesium im Automobilbau”*, Bad Nauheim, pp 123–144
44. Ahlers-Hestermann G (2000) Fügen von Magnesium und Mischverbindungen mit Magnesium mittels Druckfügen. *Praxis Forum-Tagung „Fortschritte mit Magnesium im Automobilbau“*, Bad Nauheim, pp 148–170
45. Deinzer GH, Suess U (2001) Status and potential of magnesium rolled products, *Automotive Light Metals*, Vol. 1, No. 2, pp 34–38
46. Niemeyer M (1999) Strahl-Stoff-Wechselwirkung und resultierende Verbindungseigenschaften beim Laserstrahlschweißen von Magnesiumlegierungen, *Dissertation Universität Hannover*, Fortschrittberichte VDI, Reihe 5, No. 572
47. Haferkamp H, Codini P, Niemeyer M, Goede M, Schmid C (2000) Anwendungspotenzial des Laserstrahlschweißens für Magnesiumlegierungen, VDI-Seminar “Leichtbau mit metallischen Werkstoffen”, Bremen, 09.–10.05.
48. Rethmeier M, Wiesner S, Wohlfahrt H (2000) Influences on the Static and Dynamic Strength of MIG-welded Magnesium-Alloys, in: see [4], pp 200–204
50. Kurze P, Singe T, Diesing J (2000) Korrosionsschutz von Magnesium-Werkstoffen, *metallüberfläche*, Jahrg. 54, (Sept.), pp 22–24
51. NN. Diverse Produktprospekte der Firma AHC-Oberflächentechnik, Kerpen
52. Skar JI (2000) Corrosion Protection of Magnesium Alloys, *Schriftenreihe “Praxis-Forum, Fortschritte mit Magnesium im Automobilbau”*, Hrsg.: Ebert F, Woydt M, pp 53–68
53. Schreckenberger H, Lauden G (2000) Das Korrosionsschutzkonzept der Aluminium-Magnesium-Hybridheckklappe des VW-Lupo, *Praxis Forum-Tagung “Fortschritte mit Magnesium im Automobilbau”*, Bad Nauheim, pp 43–66

54. Juchmann P, Wolff S (2002) Magnesiumblech – neuer Ultraleichtbauwerkstoff für den Automobilbau, IIR-Fachkonferenz “Intelligenter Magnesium Einsatz im Automobil”, 15./16. April, Stuttgart
55. Juchmann P, Wolff S (2002) Magnesium sheet components for ultralight construction, 59<sup>th</sup> Annual World Magnesium Conference, International Magnesium Association. Montreal, Canada, May 19–21, Proceedings, pp 49–54
56. Juchmann P (2002) Magnesiumbleche. Entwicklungen bei der Salzgitter Magnesium-Technologie GmbH, Proceedings, 13. Expert conference/13. Fachtagung des Internationalen Rohbau-Expertenkreises – “Prozesskette Karosserie” Prozess und Fertigungsverfahren im Automobilleichtbau, 10.–12. Juli, Fellbach
57. Okamoto H (1998) I. Phase Equilibria. Vol. 19 (No. 6), p. 598
58. King JF, Thistlethwaite S (1992) New Corrosion Resistant Wrought Magnesium Alloys, DGM, “Magnesium Alloys and Their Applications”. Editor Mordike BL, Hehmann F, Garmisch-Partenkirchen, pp 327–334
59. Tranell G, Pettersen G, Aarstad K, Engh TA, Solheim I, Syversten M, Oye B (2001) A Systematic Approach for Identifying Replacements to SF<sub>6</sub>/CO<sub>2</sub> in the Magnesium Industry A IMA/SINTEF-NTNU Cooperative Project, IMA Proceedings, pp 69–73
60. Videm M, Skar JI, Bakke P (2000) Corrosion Properties of Die Cast AM Alloys, DGM, “Magnesium and Their Applications”. Editor Kainer KU, Munich, pp 432–438
61. Katsiv M, Lerer E, Zirkin D, Danguv M (1998) Fluidity as an Instrument for Indirect Evaluation of Primary and Recycled Magnesium Alloys Quality and Properties, MRI, “Magnesium 1997”. Editors Aghion E, Eliezer D, pp 100–107
62. Guthrie RIL, Isaac M, Li M, Byun JY (1998) An On-Line System for the Detection of Inclusions in Molten Magnesium Based on the Electric Sensing Zone Principle, MRI, “Magnesium 1997”. Editors Aghion E, Eliezer D, pp 81–87
63. Chearhouse JD, Mikucki BA (1994) The Origin of Microporosity in Magnesium Alloy AZ91, SAE, “Attributes of Magnesium for Automobile Design”. SP-1023, pp 53–63
64. Holzkamp U, Haferkamp H, Niemeyer M (2000) Magnesium Adapted Continuous Casting Technology, DGM, “Magnesium Alloys and Their Applications”. Editor Kainer KU, Munich, pp 564–570
65. Tripp T, Bassani R, Fox J (2000) Quality Review of Magnesium Corporation of America’s Direct Chill Cast Product, IMA Magnesium Conference Brussels, pp 45–48
66. Kittilsen B, Pinfold PMD (1992) Magnesium Extrusion – Recent Developments, DGM, “Magnesium Alloys and their Applications”. Editors Mordike BL, Hehmann F, Garmisch-Partenkirchen, pp 85–92
67. Handbook ASM (1999) Magnesium and Magnesium Alloys
68. Jonas JJ, McQueen HJ (1975) Recovery and Recrystallisation during High Temperature Deformation, CNRS, “Mise en forme des métaux et alliages”, Villars-sur-Ollon
69. Wemba AM, McQueen HJ, Herba E, Sauerborn M (1998) Hot Workability of Five Commercial Magnesium Alloys, DGM, “Magnesium Alloys and their Applications”. Editors Mordike BL, Kainer KU, Wolfsburg, pp 215–222
70. Brochure IMA. “Magnesium and Magnesium Alloys”
71. Becker J, Fischer G, Schemme K (1998) Light Weight Construction using Extruded and Forged Semi-Finished Products made of Magnesium Alloys, DGM, “Magnesium Alloys and their Applications”. Editors Mordike BL, Kainer KU, Wolfsburg, pp 15–28
72. McQueen HJ, Pekguleryuz M (1992) Hot Workability of Magnesium Alloys, DGM, “Magnesium Alloys and Their Applications”. Editors Mordike BL, Hehmann F, Garmisch-Partenkirchen, pp 101–108
73. King JF, Thistlethwaite S (1992) New Corrosion Resistant Wrought Magnesium Alloys, DGM, “Magnesium Alloys and Their Applications”. Editors Mordike BL, Hehmann F, Garmisch-Partenkirchen, pp 327–334
74. Wang RM, Song YG, You SY, Surappa MK (2000) Microstructure and Interface Structure of SiC – Reinforced Mg Metal – Matrix Composite, MRI, Magnesium 2000. Editors Aghion E, Eliezer D, pp 229–234

75. Kaneko J, Sagamata M, Kim JS, Kon M (2000) Fabrication and Properties of Cast and Extruded SiCu/AZ91 Composites, DGM, "Magnesium Alloys and Their Applications". Munich, pp 221–228
76. King JF, Hehmann F (1992) Mechanical Alloying for the Development of High-Temperature Mg-Alloys, DGM, "Magnesium Alloys and Their Applications". Garmisch-Partenkirchen, pp 309–316
77. Wilks TE, King JF (1992) The Development and Properties of Particular Reinforced Magnesium Alloys, DGM, Magnesium Alloys and Their Applications". Editors Mordike BL, Hehmann F, Garmisch-Partenkirchen, pp 431–437
78. Inem B, Pollard G (1992) Microstructure/Property Relationship in Cast and Extruded Magnesium Matrix Composites, DGM, "Magnesium Alloys and Their Applications", Editors Mordike BL, Hehmann F, Garmisch-Partenkirchen, pp 439–446
79. Haferkamp H, Bach F-W, Juchmann P (2000) New Magnesium Alloys of Higher Ductility, MRI, Magnesium 2000. Editors, Aghion E, Eliezer D, pp 173–180
80. Schemme K (1992) Rapid Solidification of Mg-Li-Y Alloys, Magnesium Alloys and Their Applications, DGM. Editors Mordike BL, Hehmann F. Garmisch-Partenkirchen, pp 519–525
81. Garboggini A, McShane HB (1992) Structural Magnesium – Aluminium Alloys Produced by Rapid Solidification, DGM. Magnesium Alloys and their Applications. Editors Mordike BL, Hehmann F, Garmisch-Partenkirchen, pp 503–510
82. Wagener K-W (1998) Cold Extrusion of Magnesium Alloys and MMCs, Magnesium Alloys and Their Applications, DGM. Editors Mordike BL, Kainer KU, Wolfsburg, pp 557–562
83. Mabuchi M et al. (2000) The Grain Size Dependence of Strength in the Extruded AZ91 Alloy. "Magnesium Alloys and Their Applications". DGM, Editor Kainer KU, Munich, pp 280–284
84. Savage K, King JF, Van Kooj A (2000) Hydrostatic Extrusion of Magnesium, Magnesium Alloys and Their Applications, DGM. Editor Kainer KU, Munich, pp 609–614

## References to Chapter 6.3

1. Beck A (1939) Magnesium und seine Legierungen. Julius Springer Verlag, Berlin
2. Roberts CS (1960) Magnesium and its Alloys. J. Wiley & Sons
3. Emley EF (1966) Principles of Magnesium Technology. Pergamon Press, Oxford
4. Neite G et al. (1996) Magnesium-based Alloys, in: Materials Science and Technology Vol. 8, Eds. Cahn RW, Haasen P, Kramer EJ, VCH Weinheim
5. Schumann S, Friedrich F (1998) In: Magnesium Alloys and their Applications. Eds.: Mordike BL, Kainer KU, Werkstoff-Informationsgesellschaft, Frankfurt, pp 3–13
6. Zeumer N (1998) In: Magnesium Alloys and their Applications, Eds.: Mordike BL, Kainer KU, Werkstoff-Informationsgesellschaft, Frankfurt, pp 125–132
7. Aluminium-Zentrale Düsseldorf (2000) Magnesium Taschenbuch. Aluminium Verlag,
8. Degischer HP et al. (2001) Composites: Part A 32, pp 111–1166, <http://mmc-assess.tuwien.ac.at>
9. Everett RK, Arsenault RJ (1991) Metal Matrix Composites: Mechanisms and Properties. Academic Press
10. Clyne TW, Withers PJ (1993) An Introduction to Metal Matrix Composites. Cambridge University Press
11. Bunk W, Schulte K (1988) Verbundwerkstoffe mit Metallmatrix. Mat.-wiss. u. Werkstofftech. 19, pp 391–401
12. Kainer KU (1994) Metallische Verbundwerkstoffe. Ed.: Kainer KU. DGM Informationsgesellschaft, Oberursel
13. Ziegler G (1995) Verbundwerkstoffe und Werkstoffverbunde. DGM Informationsgesellschaft, Oberursel
14. Schulte K, Kainer KU (1999) Verbundwerkstoffe und Werkstoffverbunde. DGM-Wiley VCH

15. Chawla KK (1993) *Composite Materials – Science and Processing*. Springer, Berlin 1987
16. Chawla KK (1993) In: *Materials Science and Technology*. Vol 13, Eds.: Cahn RW, Haasen P, Kramer EJ, VCH Weinheim
17. Ibe G (1994) In: Kainer KU, *Metallische Verbundwerkstoffe*, DGM Informationsgesellschaft, Oberursel, pp 3–42
18. Kainer KU (1992) VDI-Berichte 965.1, pp 159–169
19. Kainer KU et al. (1991) *Proc. Int. Conf. on Aerospace Materials*, MPR, pp 38.1–15
20. Kelly A, Davies GJ (1965) *Metallurgical Reviews*. Vol. 10, No. 37, pp 1–77
21. Kelly A (1973) *Strong Solids*. Oxford University Press, London
22. Friend CM (1987) *J Mater Sci* 22, pp 3005–3010
23. Taya M, Arsenault RJ (1987) *Scripta Met*, Vol. 21, pp 349–354
24. Mattei NJ, Mehrabi MM (1994) pp 261–272
25. Ashbee K (1993) *Fundamental principles of fiber reinforced composites*. 2<sup>nd</sup> Edition, Technomic Publishing, Lancaster, PA
26. Fan Z et al. (1992) *Mat Sci Tech* Vol 8, pp 922–929
27. Kelly A (1993) In: *Materials Science and Technology*. Vol. 13, Eds. Cahn RW, Haasen P, Kramer EJ, VCH Weinheim
28. Pedersen OB (1983) *Acta Metall.* 31, No. 11, pp 1795–1808
29. Halpin JC, Tsai SW (1967) *Air Force Materials Laboratory*, AFML-TR-67-423
30. Piggot MR (1980) *Load Bearing Fibre Composites*. Pergamon Press
31. Humphreys FJ (1988) *Proc. 9<sup>th</sup> Riso Int Symp on Materials Science*, p 51
32. Humphreys FJ et al. (1991) *Proc. 12<sup>th</sup> Riso Int Symp on Materials Science*, p 51
33. Kainer KU, Mordike BL (1990) *Metall.* Vol. 44, No. 5, pp 438–443
34. Schröder J et al. (1989) 3<sup>rd</sup> Int Conf on Composite Materials ECCM3, EACM, pp 221–226
35. Roos U et al. (1994) *Proc Powder Metallurgy World Congress PM94*, pp 2249–2252
36. Saravanan RA, Surappa MK (2000) *Materials Science and Engineering A276*, pp 108–116
37. Moll F (2000) *Dissertation TU Clausthal*
38. Parvizi-Majidi A (1993) In: *Materials Science and Technology*. Vol. 13, Eds.: Cahn RW, Haasen P, Kramer EJ (1993) VCH Weinheim
39. Zheng M et al. (2001) *Mat Lett* 47, pp 118–124
40. Wu K et al. (1996) *Scripta Materialia*. 35 (4), pp 529–534
41. Kaneko J et al. (2000) In Kainer KU: *Magnesium Alloys and their Applications*, Wiley-VCH, Weinheim, pp 221–228
42. Schröder J, Kainer KU (1991) *Mat Sci Eng A135*, pp 33–36
43. Kainer KU et al. (1999) In: *Verbundwerkstoffe und Werkstoffverbunde*. Eds.: Schulte K, Kainer KU, DGM. Wiley-VCH, Weinheim, pp 127–133
44. Kainer KU et al. (2000) In Kainer KU: *Magnesium Alloys and their Applications*, Wiley-VCH, Weinheim, pp 240–245
45. Gu M et al. (1999) *Mat Sci Eng A272*, pp 257–263
46. Hegeler H, Buschmann R (1994) In: Kainer KU, *Metallische Verbundwerkstoffe*. DGM Informationsgesellschaft, Oberursel, pp 101–116
47. Wurm D (1998) *Dissertation, Universität Erlangen*
48. Öttinger O (1996) *Dissertation, Universität Erlangen*
49. Kainer KU (1994) In: Kainer KU, *Metallische Verbundwerkstoffe*. DGM Informationsgesellschaft, Oberursel, pp 219–245
50. Degischer HP et al. (2000) In Kainer KU: *Magnesium Alloys and their Applications*, Wiley-VCH, Weinheim, pp 207–220
51. Sommer B (2000) *Dissertation, TU Clausthal*
52. Körner C (2000) *Advanced Engineering Materials*, 2, 6, pp 327–337
53. Degischer HP (1999) In: Schulte K, Kainer KU, *Verbundwerkstoffe und Werkstoffverbunde*, pp 525–530
54. Körner C et al. (2001) In: *Verbundwerkstoffe und Werkstoffverbunde*. Eds.: Wielage B, Leonhardt G, DGM, Wiley-VCH, Weinheim, pp 121–126
55. Than E et al (1994) In: Kainer KU, *Metallische Verbundwerkstoffe*. DGM Informationsgesellschaft, Oberursel, pp 65–100

56. Böhm E (1996) Dissertation, TU Clausthal
57. Schreiber K et al. (2001) In: Verbundwerkstoffe und Werkstoffverbunde. Eds.: Wielage B, Leonhardt G, DGM, Wiley-VCH, Weinheim, pp 127–133
58. Kainer KU et al. (1999) In: Schulte K, Kainer KU, Verbundwerkstoffe und Werkstoffverbunde, pp 201–206
59. Schröder J et al. (1991) Advances in Powder Metallurgy. Vol. 6, pp 281–292
60. Schröder J et al. (1990) Proc Int Conf on Powder Metallurgy, PM '90, pp 304–309
61. Kainer KU et al. (1991) Advances in Powder Metallurgy, Vol. 6, pp 293–305
62. Schröder J et al. (1992) In: Magnesium Alloys and their Applications. Eds. Mordike BL, Hehmann F (1992) DGM Informationsgesellschaft, Oberursel, 469–476
63. Schröder J et al. (1991) Proc. 2<sup>nd</sup> Europ. Conf. on Advanced Materials and Processes, pp 81–91
64. Schröder J, Kainer KU (1992) Proc. 5<sup>th</sup> Europ. Conf. on Composite Materials ECCM5, EACM, pp 665–670
65. Schröder J, Kainer KU (1990) Proc ASM Int Conf on Advanced Aluminium and Magnesium Alloys, pp 847–854
66. Mordike BL et al. (1990) Trans of PMAI, 17, pp 7–17
67. Ebert T et al. (1997) Powder Metall 40, p 126
68. Schröder J, Kainer KU (1993) In: Aldinger F, Materials by Powder Technology. DGM Informationsgesellschaft, p 739
69. Vervoort PJ, Duszczyc J (1993) Proc of the 2nd Int Conf on Spray Foming, Ed.: Wood JV. Woodhead Publishing Ltd. Cambridge, pp 409–425
70. Lavernia EJ, Grant NJ (1988) Mat Sci Eng 98, p 381
71. Srivatsan TS et al. (1995) Prog in Mat Sci 39, pp 317–409
72. Rohatgi P (1988) Modern Castings, pp 47–50
73. Nityanand N et al. (1986) Met Trans B, 17B, pp 247–257
74. Bytnar JH et al. (1995) Int. J Powd Met 31, 1, pp 37–49
75. Bhanu Prasad VV et al. (2000) Scripta Mater 43, pp 835–840
76. Asthana R (1997) Mat Synthesis and Processing, 5, pp 251–277
77. Laurent V et al. (1992) J Mat Sci, 27, pp 4447–4459
78. Luo A (1995) Met Mat Trans A, 26A, pp 2445–2455
79. Fritze C (1997) Dissertation TU Clausthal
80. Degischer HP (1994) In: Kainer KU, Metallische Verbundwerkstoffe, DGM Informationsgesellschaft, Oberursel, pp 139–168
81. Chadwick GA (1991) Mat. Sci Eng A135, pp 23–28
82. Hu H (1998) J Mat Sci 33, pp 1579–1589
83. Öttinger O, Singer RF (1993) Z Metallkd 84, pp 827–831
84. Kubaschewski O, Alcock CB (1979) Metallurgical Thermochemistry, Pergamon Press, Oxford, 5th edition
85. Barin I (1989) Thermochemical data of pure substances. VCH-Verlagsgesellschaft, Weinheim
86. Kainer KU, Tertel A (1991) Proc. 12<sup>th</sup> Riso Int Symp on Materials Science, pp 435–440
87. Biermann D, Meister D (1994) In: Kainer KU, Metallische Verbundwerkstoffe, DGM Informationsgesellschaft, Oberursel, pp 261–284
88. Weinert K et al. (2000) In Kainer KU: Magnesium Alloys and their Applications. Wiley-VCH, Weinheim, pp 412–417
89. Weinert K et al. (2000) In: Kainer KU, Magnesium – Eigenschaften, Anwendungen, Potenziale. Wiley-VCH, pp 137–160
90. Ditze A (2000) In: Kainer KU, Magnesium – Eigenschaften, Anwendungen, Potenziale. Wiley-VCH, pp 272–296
91. Kainer KU (1997) In: Leonhard G, Wielage B (1997) Recycling von Verbundwerkstoffen und Werkstoffverbunden. DGM Informationsgesellschaft, 39–44
92. Kiehn J et al. (1997) In: Leonhard G, Wielage B, Recycling von Verbundwerkstoffen und Werkstoffverbunden. DGM Informationsgesellschaft, pp 51–56
93. Kiehn J et al. (1997) In: Friedrich K, Verbundwerkstoffen und Werkstoffverbunde. DGM Informationsgesellschaft, pp 577–582

94. Kurze P (2000) In: Kainer KU, Magnesium – Eigenschaften, Anwendungen, Potenziale. Wiley-VCH, pp 236–243
95. Haferkamp H et al. (2000) In: Kainer KU, Magnesium – Eigenschaften, Anwendungen, Potenziale. Wiley-VCH, pp 244–259
96. Leyendecker F (2000) In: Kainer KU, Magnesium – Eigenschaften, Anwendungen. Potenziale, Wiley-VCH, pp 260–271
97. Kainer KU (1991) *Mat Sci Eng A135*, pp 243–246
98. Kainer KU (1990) In: *Haftung bei Verbundwerkstoffen und Werkstoffverbunden*. Eds.: Brockmann W. DGM Informationsgesellschaft Oberursel, pp 31–44
99. Mortensen A (1991) *Mat Sci Eng A135*, pp 1–11
100. Ünal A (1992) *Materials & Manufacturing Processes*, 7, 3, pp 441–461
101. Kainer KU (1992) In: Mordike BL, Hehmann F, *Proc Int Conf on Magnesium Alloys and their Applications*. DGM Informationsgesellschaft, pp 415–422
102. Kainer KU, Benzler T et al. (2000) In: Kainer KU, Magnesium – Eigenschaften, Anwendungen, Potenziale. Wiley-VCH, pp 59–75
103. Kainer KU, Moll F (1996) 29<sup>th</sup> int Symp on Automotive Techn and Automation. Florence, Italy
104. Sohn KE et al. (1998) *Met and Mat trans A*, 29A, pp 2543–2554
105. Towle DJ, Friend CM (1993) *Mat Sci Techn*, 9, pp 35–41
106. Wilks TE, King JF (1992) In: Mordike BL and Hehmann F. *Magnesium Alloys and their Applications*. pp 431–437
107. Kleine A, Duddek HJ (1992) In: Mordike BL and Hehmann F. *Magnesium Alloys and their Applications*. pp 447–454
108. Moll F, Kainer KU (2000) In: Kainer KU, Magnesium – Eigenschaften, Anwendungen, Potenziale. Wiley-VCH, pp 212–235
109. Mikucki BA (1990) *SAE Transactions* 90533, pp 597–605
110. Degischer HP et al. (1997) *Key Eng Mat* 127–131, pp 99–110

## References to Chapter 6.4

1. Thomala W (1999) Screws and bolts made of aluminum alloys. *ALUDetroit*
2. Westphal K (2002) Verschraubung von Magnesiumkomponenten. *Metalle Jg 56*
3. Senf J (2001) Untersuchung und Beschreibung von Magnesiumdruckgusslegierungen unter tribologischer, korrosiver und mechanisch-korrosiver Beanspruchung. Dissertation TU-Darmstadt, D17, Shaker, Herzogenrath, Germany
4. Schreckenberger H (2000) Korrosion und Korrosionsschutz von Magnesium-Werkstoffen für den Automobilbau – Problematik der Kontaktkorrosion. Dissertation TU – Darmstadt, D17, Shaker, Herzogenrath, Germany
5. Berger C, Arz U, Kaiser B, Landgrebe R (1986) Gebrauchseigenschaften von Schraubenverbindungen für Leichtmetalle. *DVM-Bericht 802*
6. Thomala W (1986) Notes on Guideline 2230, Sheet 1. Example: Bolted joints for passenger car connecting rods. *VDI-Z 128(12):128–143*
7. Friedrich C (2004) Designing fastening systems. In: Totten GE, Xie L, Funatani K (eds) *Modeling and simulation for material selection and mechanical design*. Dekker, New York. ISBN 0-8247-4746-1
8. Friedrich C (2004) Reliable light weight fastening of magnesium components in automotive applications. In: *SAE World Congress, Detroit, Paper No. 2004-01-0136*
9. Downs K (1996) Aluminum use in fastener manufacturing. *Fastener Technology International*, October 1996
10. ISO 8839: Mechanical properties of fasteners – bolts, screws, studs and nuts made of non-ferrous metals
11. Scheiding W (2001) Beitrag zur Ermittlung der Gebrauchseigenschaften von Schraubenverbindungen mit Magnesiumkomponenten. Dissertation TU-Darmstadt, D17, Shaker, Herzogenrath, Germany



12. Arz U (2003) Beitrag zur Ermittlung der Beanspruchbarkeit von Schrauben aus Aluminium-Legierungen. Dissertation TU-Darmstadt, D17, Shaker, Herzogenrath, Germany
13. West EG (1951) The welding of non-ferrous metals, London, Chapman and Hall
14. N.N. (1938) Werkstoff Magnesium, Berlin, VDI
15. Beck A (ed) (1939) Magnesium und seine Legierungen. Springer Verlag
16. Lockwood LF (1963) Welding Journal 42 (1963), p. 807
17. Koeplinger RD and Lockwood LF (1964) Welding Journal 43, p 195
18. Lockwood LF (1965) Welding Journal 44, p 213s
19. Lockwood LF (1967) Welding Journal 46, p 168s
20. Lockwood LF (1979) Welding Journal 49, p 464
21. Emley EF (1957) British Welding Journal, July, p 307
22. Avedesian MM (1999) Magnesium and Magnesium Alloys, ASM International, p 26
23. N.N. (1993) ASM Handbook Volume 06: Welding, Brazing, and Soldering, ASM International
24. Strombeck A v, dos Santos JF, Troster F, Laureano P and M. Kocak M (1999) In: Threadhill PL (ed.): First International Symposium on Friction Stir Welding
25. Kallee SW, Nicholas ED, Thomas WM (2002) In dos Santos JF, Strombeck A v and Schilling C (eds) Friction Stir Welding
26. N.N. (2003) Friction Stir Welding, GKSS Geesthacht
27. Klavierrahmen aus Magnesium (2000) VDI-Nachrichten, 15 Dezember
28. Bohling P et al. (2000) Eigenschaften von thermisch und wärmearm gefügten Al-/Mg-Verbindungen für den strukturellen Karosserieleichtbau. 7th Paderborn Symposium on Bonding Technology, Paderborn, Germany
29. Di Pardo, Micucci E (1998) Bonding of magnesium alloy and mechanical evacuation. EU-RAD '98, Garmisch
30. Jost R, Disse Th (2000) Kleben von Leichtbauwerkstoffen in Mischbauweise – Fügekonzept der Al-Mg-Tür des S-Klasse Coupe. 7th Paderborn Symposium on Bonding Technology, Paderborn, Germany
31. Immer mehr Konstrukteure lieben Leichtbau mit Magnesium. (2000) VDI-Nachrichten, 17 November
32. Kleben und mechanisches Fügen von Magnesium und CFK (1996) Investigation Report by Fraunhofer-Institut für Angewandte Materialforschung, Bremen
33. Scheiding W (2001) Magnesium verschrauben. Konstruktionspraxis 2, p 42
34. Schumann S, Friedrich F (1998) The Use of Magnesium in Cars – Today and in Future. DGM Event, Wolfsburg
35. Budde L, Widder Th, Bischoff J (1997) Wärmearmes Fügen von Magnesiumwerkstoffen im Fahrzeugbau. Adhäsion kleben&dichten 41, 10, pp 12–17
36. Kleben und Mechanisches Fügen von Magnesium und CFK (1996) Investigation Report by IFAM Bremen, Bremen
37. Habenicht G (1997) Kleben Grundlagen, Technologie, Anwendungen. Springer Berlin Heidelberg New York
38. Kötting G (2000) Oberflächenbehandlung und Korrosionsschutz für geklebte Magnesiumbauteile. 7th Paderborn Symposium on Bonding Technology, Paderborn, Germany
39. Chrome-free Pre-treatment of Magnesium Parts. Chemetall information sheets
40. Hahn O, Klemens U (1996) Fügen durch Umformen, Nieten und Durchsetzfügen – Innovative Verbindungsverfahren für die Praxis; Identifikation: Studiengesellschaft Stahlanwendung e.V. Documentation 707, 1st edition, Düsseldorf: Verlag und Vertriebsgesellschaft Stahlanwendung mbH, ISBN 3-930621-56-8
41. Hahn O. et al (2003) Concluding report on the BMBF project “Fügesystemoptimierung zur Herstellung von Mischbauweisen aus Kombinationen der Werkstoffe Stahl, Aluminium, Magnesium und Kunststoff”. Paderborn
42. Birkelbach R (1993) Neue Verbindungstechnik für Dünnbleche; VDI reports: Fügen im Vergleich. No 1072, p 1–16

43. Meschut G (2001) Hybridfügen – Grundlagen, Technologie, Anwendungen, DVM conference 2001 “Fügetechnik im Automobilbau”. DVM report 668, p 119–134, Berlin, ISSN 0946-5987
44. Radtke H (1989) Automatisieren des Falzens von Blechkonstruktionen; Bänder Bleche Rohre 10, p 24–30
45. Melcher A (2000) Rollfalzen – Flexibles Falzen mit Robotern; conference work on the event “Innovatives Fügen im Multi-Material-Design” on October 25th and 26th, Ulm, 12 pages, verlag moderne industrie

## References to Chapter 6.5

1. Tönshoff HK, Denkena B (2004) Spanen, Grundlagen, 2. erweiterte und neu bearbeitete Auflage, Springer
2. Hansen S, Rasch FO, Tomac N, Tønnessen K (1992) High Speed Machining of Mg-Castings, In: Mordike BL, Hehmann F (Hrsg.): Magnesium Alloys and their Applications. DGM Informationsgesellschaft Verlag, Oberursel, pp 61–68
3. Tokisue H, Kato K (1990) Turning Machinability of Magnesium Alloy Castings for High-Temperature Structures. Aluminium 5, pp 479–482
4. Spicer A, Kosi J, Billpus C, Pajek J (1991) Machining Magnesium with Water Base Coolants. SAE Technical Paper 910415
5. Tomac N, Tønnessen K (1991) Formation of Flank Build-up in Machining of Magnesium Alloys. Annals of the CIRP 40 1, pp 79–82
6. Tomac N, Tønnessen K, Rasch FO (1991) PCD Tools in Machining of Magnesium Alloys. European Machining 3, pp 12–16
7. Tomac N, Tønnessen K, Rasch FO (1994) The Specific Behaviour of Magnesium Alloys in Machining Processes. Eurometalworking, Udine
8. Chambers AR (1996) The Machinability of Light Alloy MMCs. Composites 2, pp 143–147
9. Lin JT, Bhattacharyya D, Lane C (1995) Machinability of Silicon Carbide Reinforced Aluminium Metal Matrix Composite. Wear 181–183, pp 883–888
10. Tönshoff HK, Winkler J (1997) The Influence of Tool Coatings in Machining of Magnesium. Surface Coating Technology 94–95, pp 610–616
11. Weinert K (1993) A Consideration of Tool Wear Mechanisms when Machining Metal Matrix Composites, Annals of the CIRP 42 1, pp 95–98
12. Weinert K, Biermann D, Buschka M, Liedschulte M (1999) Be- und Verarbeitungstechnologien für Verbundwerkstoffe – Optimierung der Schnittbedingungen, Poster zum Abschlußkolloquium des SFB 316 “Herstellung, Be- und Verarbeitung sowie Prüfung von metallischen und metall-keramischen Verbundwerkstoffen”. Dortmund
13. Biermann D (1996) Untersuchungen zum Drehen von Aluminiummatrix-Verbundwerkstoffen. Dr.-Ing. Diss., Dortmund
14. Weinert K, Lange M, Schroer M (2000) Spanende Bearbeitung von Magnesium und Magnesiumverbundwerkstoffen, in: Magnesium Taschenbuch. Aluminium Verlag, pp 577–599
15. Kurihara KT, Kato H, Tozawa T (1981) Cutting Temperature of Magnesium Alloys at Extremely High Cutting Speeds. Keikinzoku – Journal of Japan Institute of Light Metals 31, 4, pp 255–260
16. Tomac N, Tønnessen K, Rasch FO (1996) Safe Machining of Magnesium. AMST '96, Udine
17. Tønnessen K, Rasch FO, Tomac N (1992) Machining Magnesium Alloys with Use of Oil-Water Emulsions. Tribology 2000, Esslingen
18. Tönshoff HK, Friemuth T, Podolsky C, Winkler J, Haferkamp H, Niemeyer M, Kaese V, Janssen S (2001) Einfluss des Festwalzens auf die Oberflächen- und Randzoneigenschaften der Magnesiumlegierungen AZ31 und AZ91. Sonderband Magnesiumtechnologie in Materialwissenschaft und Werkstofftechnik
19. Scholtes B, Vöhringer O (1996) Grundlagen der mechanischen Oberflächenbehandlung, in: Broszeit E, Steindorf H (Hrsg.): Mechanische Oberflächenbehandlung. DGM Informationsgesellschaft Verlag, Oberursel, pp 3–20



20. Broszeit E, Adelman J (1996) Schwingfestigkeitssteigerung durch Festwalzen – Grundlagen und Anwendung, In: Broszeit E., Steindorf H (Hrsg) Mechanische Oberflächenbehandlung. DGM Informationsgesellschaft Verlag, Oberursel, pp 63–82
21. Scholtes B, Zinn W (1997) Mechanische Oberflächenbehandlung von Leichtbauwerkstoffen, in: Frieling E, Martin H, Tikal F: Neue Ansätze für innovative Produktionsprozesse. Kassel University Press, Kassel, pp 376–383
22. Kloos KH, Adelman J, Bieker G, Oppermann T (1988) Oberflächen- und Randschichteinflüsse auf die Schwingfestigkeitseigenschaften. VDI-Berichte 661, pp 215–245
23. Nüstedt H (1996) Beitrag zum Ermüdungsverhalten superleichter Magnesium-Lithium-Basislegierungen. Dr.-Ing. Diss., Hannover
24. Kroos F (1995) Randschichtverfestigung durch Hochdruckwasserstrahlen. Dr.-Ing. Diss., Hannover
25. Scholtes B (1990) Eigenspannungen in mechanisch randschichtverformten Werkstoffzuständen. DGM Informationsgesellschaft Verlag
26. Munz D, Schwalbe K, Caner P (1971) Dauerschwingverhalten metallischer Werkstoffe. Verlag Vieweg, Braunschweig
27. Ostertag A (1996) Dauerfestigkeit kostensparend steigern, DGM-Seminar “Mechanische Oberflächenbehandlung zur Verbesserung der Bauteilfestigkeit”. Braunschweig
28. Ecoroll AG (2002) Werkzeuge zum Glatt-, Festwalzen, Umformen, Anwendungsbeschreibung Nr. 5593, Celle
29. N. N. (1999) BGR 204, BG-Regeln “Umgang mit Magnesium”. Carl Heymanns, Köln
30. N. N. (1999) “Beschaffenheitsanforderungen für Maschinen und Einrichtungen zur Vermeidung von Brand- und Explosionsgefahren bei der Be- und Verarbeitung, beim Schmelzen und Gießen von Magnesium”, BG-Entwurf des Fachausschusses Eisen und Metall III, Carl Heymanns, Köln

---

# 7 Corrosion and Surface Protections

## 7.1 Surface Treatments and Protection

*Peter Kurze*

### 7.1.1 Introduction

Magnesium and its alloys are the lightest, but also the most basic, of light-alloy constructional materials. Table 7.1 lists the corresponding data in this respect.

The current challenge involves the increasing use of light alloys in high-technology sector constructional materials, with the aim of both reducing mass and of saving energy. Typical areas of application include vehicle construction, aeronautics and the space sector, along with the mechanical engineering and electrical industries.

The use of magnesium-based materials delivers, on one hand, the important advantages of reduced mass, while offering improved mechanical and physical properties. However, the characteristics of magnesium-based materials also make them highly susceptible to corrosion. Indeed, the existence of unfavourable ambient conditions (such as those caused by the spreading of salt on the roads during the cold months of the year), and the effect of airborne pollutants such as SO<sub>2</sub>, mean that the use of magnesium-based materials continues to be regarded with a great degree of scepticism. The problem here resides not only in the corrosion of the magnesium in a general sense, but also in the consequences of galvanic corrosion (also known as contact corrosion). Magnesium is normally used in so-

**Table 7.1.** Light alloys (symbol, crystalline structure, density, reaction and standard reduction potential)

Light alloy	Symbol crystalline structure	Density [g/cm <sup>2</sup> ]	Reaction	Standard reduction potential E° [V] taken from [1]
Magnesium	Mg (2)	1.7	$Mg^{2+} + 2 e \rightleftharpoons Mg$	-2.37
Beryllium	Be (2)	1.85	$Be^{2+} + 2 e \rightleftharpoons Be$	-1.85
Aluminium	Al (1)	2.7	$Al^{3+} + 3 e \rightleftharpoons Al$	-1.66
Titanium	Ti (2)	4.5	$Ti^{2+} + 2 e \rightleftharpoons Ti$	-1.63

(1) cubic, (2) hexagonal.

called “mixed-construction” applications. Differences in potential arise here due to the contact between noble components (e.g., steel) and the base-metal component provided by the magnesium-based material. The presence of the ambient conditions described above (saltwater, etc.) causes galvanic corrosion, which in turn leads to the magnesium base-metal acting as an anode and wearing away.

The following sections of this chapter show how the carefully targeted surface treatment of magnesium-based material can provide effective protection against corrosion.

### 7.1.2 Passivation Properties of Magnesium-Based Materials in Air

In moist air, magnesium-based materials naturally tend to form a thin ( $< 1 \mu\text{m}$ ) passivated surface-layer, which consists mainly of magnesium hydroxide  $\text{Mg}(\text{OH})_2$  and hydrated oxidic components of the alloying elements.

This behaviour is typical for all the light alloys listed in Table 7.1. Ono [2] displays – particularly in the case of magnesium and its alloys – a three-layer passivation structure, which is characterised by a hydrated inner layer closest to the magnesium metal, a thin and dense middle layer and a porous outer zone. The passivated layer also contains alloy components such as Al, Zn and rare earths (mostly in a hydrated state), which exercise a positive influence on the corrosion stability of the surface of magnesium. Pure magnesium counts as highly resistant in a normal atmosphere, if there are no defects in the passivated layer or impurities from noble elements (e.g., metals, graphite, etc.) that combine with electrolytes. In the case of magnesium, the pH-value of the passivated layer is increased by the presence of water (i.e., air humidity), which stabilises the passivated layer consisting of  $\text{Mg}(\text{OH})_2$ . Pourbaix [3] displays, by means of a redox potential pH-value diagram, the thermodynamic stability ranges of metallic magnesium and its compounds in an aqueous solution. The upshot is that  $\text{Mg}(\text{OH})_2$  does not become stable until the pH-value is greater than 8.5. This explains why magnesium, in contrast to aluminium-based materials, does not dissolve in alkaline media.

One result of the hexagonal lattice of magnesium (Table 7.1) is that there is geometric mismatching with the structure of the naturally formed passivated layer on the metal. There is then a high degree of compressive strain in the passivated layer, which leads to cracking. This allows corrosive substances to enter as far as the magnesium base-metal, thus resulting in corrosion. The passivated layer on the magnesium is not dense, even from a theoretical point of view, as the degree of coverage obtained from the quotient of the specific higher volume of the magnesium hydroxide and the metallic magnesium is less than 1. This quotient, which is referred to as the Pilling-Bedworth ratio, has a value of 0.81 for an existing passivated layer consisting mainly of  $\text{Mg}(\text{OH})_2$ . If a value of less than 1 is obtained for the degree of coverage corresponding to a natural oxidic passivated layer, this indicates that the underlying metal is not completely covered. It is important to understand at this juncture, that oxidic surface protection coatings applied to magnesium – the application and structure of which are described below – always require the use of an additional sealant. This supposes a difference with respect to aluminium, where the established Pilling-Bedworth ra-

tio is 1.38 and the surface of the metallic aluminium is thus fully-covered by its natural passivated layer. In the case of magnesium, the passivated layer – which is generally regarded as stable – is not resistant to aqueous electrolytes that contain ionogenic components such as  $\text{Cl}^-$ ,  $\text{SO}_3^{2-}$ ,  $\text{SO}_4^{2-}$ ,  $\text{NO}_3^-$ ,  $\text{PO}_4^{3-}$  or  $\text{CO}_3^{2-}$ , as it reacts with these ions. Magnesium salts are formed, which are water-soluble and thus dissolve the protective passivated layer.

$\text{F}^-$  ions provide an exception to this rule because they transform the oxidic passivated layer into  $\text{MgF}_2$ , which dissolves in water only with great difficulty. This explains why a relatively good level of protection can be achieved with electrolytes containing  $\text{F}^-$  ions. This natural passivated surface of the magnesium is resistant to many organic substances, such as hydrocarbons, common types of alcohol (*except* Methanol), aromatic compounds, ether and ester. Organic acids, however, *do* attack magnesium – as do glycerol and glycol. The corrosive action of these substances takes place mainly via the cracks and pores in the surface of the magnesium's passivated layer.

#### 7.1.2.1 Resistance of the Passivated Layer to Chemicals

An attempt is made, in Table 7.2, to provide a comparative evaluation of the resistance of magnesium (with its oxidic passivated layer) to a variety of different substances (taken partly from [4] and [5], and including my own additional research).

The composition shows that the natural passivated layer on magnesium cannot protect the metal in the long term.

### 7.1.3 Surface Treatment of Magnesium-Based Materials

Figure 7.1 summarises the main methods used for the surface treatment of magnesium-based materials.

The primary purpose of all the surface-treatment methods listed in Fig. 7.1 for use on magnesium-based materials is to provide corrosion prevention. Electroless electrochemical and normal electrochemical procedures are the methods most commonly used at the moment for the production of oxidic protective layers.

#### 7.1.3.1 Principles and Prerequisites for Optimum Surface Protection

In order to achieve the optimum surface protection for the magnesium-based material, the following principles, prerequisites and recommendations [6] should be observed:

- Magnesium, in comparison to other lightweight metals, is a highly sensitive material. Any error that occurs during processing or at the manufacturing or production stage will have a serious effect on the characteristics of the material – manifesting itself in particular is the highly increased sensitivity of the metal to corrosion. Not even the best of surface treatments can compensate for this type of imperfection.
- High-purity (HP) quality of the material  
Not even the best-available surface treatment will have an effect on magnesium-based material, if the metal is not of HP-grade quality. This is because

**Table 7.2.** Resistance of magnesium and its alloys to different substances

Substance group	Corrosive substance	Suitability
<b>Resistance to inorganic substances</b>		
Water	Water (water containing carbon dioxide, marsh or tap water)	–
	Seawater, salt spring water, at any temperature	–
	Distilled water, at temperatures of up to 100°C	+
Acids	Pure hydrofluoric acid, in any concentration	+
	All mineral acids, such as hydrochloric acid, sulphuric acid, sulphurous acid, nitric acid, phosphoric acid, siliceous hydrofluoric acid, boric acid in aqueous solution (applicable to all temperatures, concentrations and alloys), carbon dioxide (including gaseous type, insofar as there are traces of humidity)	–
Salts of halogen acids	Aqueous solutions of the salts of halogen acids (with the exception of fluorides), e.g., ammonium chloride, common salt, magnesium chloride, zinc chloride, barium chloride, potassium chloride, calcium chloride, nickel chloride, calcium hydrochloride, at any temperature, concentration and for all alloys	–
	Potassium fluoride, sodium fluoride, ammonium fluoride (applies to all alloys, with pure magnesium displaying the best properties)	–
Sulphur and sulphur-based compounds	Sulphur, in liquid or vapour form (applies to all alloys)	+
	Ammonium sulphide, carbon bisulphide (for all alloys)	+
	Aqueous solutions of sulphates (e.g., aluminium sulphate, aluminium potassium sulphate, iron sulphate, zinc sulphate, copper sulphate) in all concentrations for all alloys	–
Nitrogen-based compounds	Aqueous ammoniacal solutions (tested with concentrations of 5% and higher at room temperature)	+
	Ammonia-air mixture (applies to all alloys)	±
	Ammonium hydroxide, nitrous fumes, potassium nitrate and nitride	–
Miscellaneous compounds	Aqueous solutions of sodium hydroxide, potassium hydroxide (including high concentrations)	+
	Alkali silicate solutions (applies to alloys with respect to temporary effects only)	±
	Alkali chromate and alkali bichromate solutions (for all concentrations, temperatures and alloys)	+
	Quicklime, lime mixtures, concrete, mortar (applies only to pure magnesium and AM 50)	±
	Mercury at 20°C (assuming that no humidity is present)	±
	Mercury salts (for all temperatures, concentrations, alloys)	–

+ resistant, – not resistant, ± medium level of resistance.

**Table 7.2.** Resistance of magnesium and its alloys to different substances

Substance group	Corrosive substance	Suitability
<b>Resistance to organic media</b>		
Aliphatic compounds	Hydrocarbons such as methane, ethane, ethylene (dry), hexane, tar, benzene, petroleum, asphalt, lignite wax (for all alloys)	+
Halogen derivatives	Trichloroethylene, carbon tetrachloride, dichlorhydride, epichlorhydride	+
	Monochlormethane, monochlorethane as dry gas in aqueous and alcoholic solution	+
	Ethylene bromide	+
	Methylene chloride (alcohol/water-free)	+
Alcohols	Methanol	–
	Methanol as fuel additive (up to 10%)	+
	Ethanol (water-free)	+
	Methylated spirits	+
	Grain mash, wort	–
	Glycerol	–
	Radiator antifreeze	–
	Glycol and glycol-water mixtures	–
Ether	Ethyl ether, acetic ether	+
Aldehydes and ketones	Formaldehyde, acetaldehyde, trichloraldehyde	–
	Benzaldehyde	–
	Acetone	+
Acids	Formic acid, acetic acid, butyric acid, valerian acid, palmitic acid, oxalic acid, succinic acid, lactic acid, tartaric acid, citric acid, fruit juices, salicylic acid	–
Wax products	Acid-free wax products, beeswax	+
Fats and oils	Acid-free fats and oils	+
Nitrogen-based compounds	Urea in aqueous solution, cold	+
	Urea in aqueous solution, warm	–
Explosives-industry products	Nitroglycerine, trisinate, lead azide, (blasting oil), mercury fulminate (in general)	–
Carbo-hydrates	Acid-free sugar solutions, cellulose	+
Heterocyclic compounds	Gelatine, pyridine, if acid-free	+
Fuel products	Petroleum spirit	+
	Benzene	+
	Sodium benzoate (fuel additive)	+
Aromatic compounds	Crude tar and its fractions, benzene, toluol, xylol, phenol, cresol, tricresol, naphthalene, anthracene, lysol, creoline, salveol, tetraline	+
	Anthranilic acid, camphor, copal resins, natural rubber	+

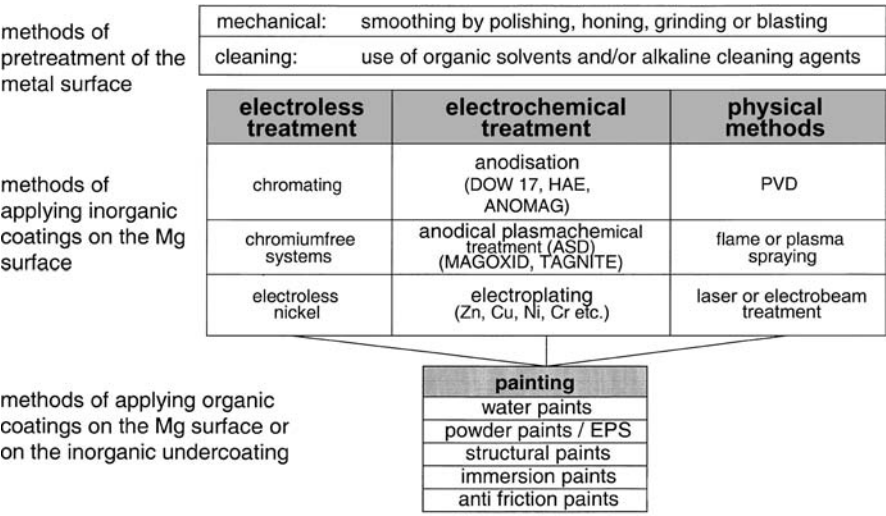


Fig. 7.1. Surface treatment of magnesium-based materials

impure magnesium-based materials suffer from build-ups containing galvanic elements such as heavy metals (Ni, Cu, Fe, etc.), which cause serious corrosion under the protective coating. The formation of hydrogen causes the coating to lift off, which in turn leads to gradual destruction of the metal beneath.

- Ratio of iron to manganese in the cast part  
When casting care should be taken to ensure that the molten metal from each batch is poured without interruption. Excessive idle time, in which the molten magnesium remains inside the smelting equipment, favours the separation of the elements that form the alloy. The result, in the case of AZ91 for example, is that the iron-content of the workpiece becomes excessive and the amount of manganese too low. Cast-magnesium parts of this type are then highly susceptible to corrosion.
- Incorporation of emulsifying salts into the cast part  
If emulsifying salts (i.e., substances containing  $\text{SO}_4^{2-}$  and  $\text{Cl}^-$ ) are inadvertently incorporated into the magnesium workpiece, the affected item will tend to corrode over time, thus causing irreparable damage to the workpiece. Not even surface treatment can prevent this occurring. Items so affected must be scrapped.
- The use of parting agents during casting  
Magnesium casting requires the use of specific parting agents, which must be compatible with the surface treatment subsequently applied. It may be necessary to carry out tests to determine the suitability of a given parting agent. Once the parting agent or its decomposition products (e.g., carbon) get deep inside the part of the magnesium part nearest the surface, they cannot be removed. This has negative consequences for the corrosion-resistance of the workpiece and is detrimental to the effectiveness of the protective coating.

- Function of the casting crust  
The casting crust is the most densely packed area of any casting or diecasting material, and its removal should be avoided wherever possible. Removal of the casting crust “activates” the metal and makes it more porous, thus allowing corrosive reactions to occur more quickly.
- Porosity of the magnesium-based material  
If the magnesium-based material is very porous, remains of electrolyte build up in these pores. The main effect of this is to release hydrogen, which leads in turn to the detachment of any protective coating applied.
- Particle-blasting of the magnesium surface  
Particle blasting does not cause compacting on magnesium surfaces. The blasting particles – e.g.,  $\text{Al}_2\text{O}_3$  (corundum) or glass – must however be chemically neutral. The use of impure particles (containing Fe, for example) has the effect of “doping” the magnesium surface with heavy metals. This results in galvanic corrosion beneath the applied surface-protection layer.
- Correct and wet-chemical processing  
Note that magnesium *only*, and no other light alloy (and, of course, no heavy metal), should be handled in the processing line (degreasing, pickling, rinsing, coating) used for the application of wet-chemical surface treatment of magnesium (see Fig. 7.1).  
If this condition is not observed, the “activated” magnesium surface will be contaminated. The consequence is that values such as those determined in corrosion tests (e.g., to ASTM-B117 standards) are widely distributed – thus resulting in confusing data with respect to the stability of the chemical baths used and the quality of the surface coating.

### 7.1.3.2 Preliminary Treatment

#### Physical preliminary treatment

The physical surface treatment of magnesium-based materials involves commonly-used methods such as grinding, abrasive-finishing, particle-blasting, polishing and brushing (Fig. 7.1). The method of physical treatment selected depends on the shape and surface quality of each component and also – of course – on the specified characteristics of the surface in its final state. Physical treatment should be carried out immediately before the surface treatment itself is applied. Note that it is often possible to eliminate the need for physical pre-treatment altogether if the part is shaped with great precision (e.g., by diecasting).

**IMPORTANT:** Note that special safety precautions apply to the physical pre-treatment of magnesium-based materials.

*Grinding.* Magnesium alloys are especially suitable for grinding. A basic distinction is made between wet- and dry-grinding. Speeds of between 900 and 1800 m/min are used when grinding magnesium on belts or discs. Grinding agents such as silicon carbide (carborundum) and aluminium oxide (corundum) with a coarseness of 60–400 mesh are recommended. Grinding produces ultra-fine particles of dust which, when mixed with air at certain ratios, can cause spontaneous explosive combustion. Grinding is precisely one process where there is a danger



of unexpected sparks occurring (e.g., due to accidental contact between the grinding disc and ferrous-metal components, the ricocheting against the grinding hood of fragments of disc, the tearing-off of paper linings, etc.). In order to eliminate the danger of ignition occurring, magnesium alloys are always wet-ground from the beginning, or the dust is removed by a suction device fitted just behind the grinding machine.

*Abrasive-finishing.* Abrasive-finishing can be used to remove burred edges from magnesium parts, and for final-machining of the surface. The reagents used must be neutral or alkaline.

DO NOT use acidic solutions, as this will result in the magnesium being etched during the abrasive finishing process.

*Particle-blasting.* The particle-blasting of magnesium surfaces can be carried out either “wet” or “dry”. As magnesium-based materials are relatively soft, the blasting pressure should be adjusted to ensure that the particles do not become embedded in the material being treated. Purified sand ( $\text{SiO}_2$ ), corundum ( $\text{Al}_2\text{O}_3$ ) and glass balls are all suitable for use as blasting particles. The blasting medium used must not be contaminated in any way (e.g., with ferrous metal). If iron-contaminated blasting particles *are* used to treat magnesium, its resistance to corrosion is drastically reduced and it is often then impossible to improve the surface of the magnesium (even with pickling). For this reason, the use of steel grit as a blasting medium should be avoided.

*Polishing.* Magnesium alloys are suitable for polishing. The process is normally carried out with the same equipment that is used for aluminium-based materials. The use of flexible cotton-covered discs (running at 1800–2500 m/min) is recommended.

*Brushing.* Brushing can be used to produce special decorative effects on the magnesium surface. It can also be used for removing impurities such as oxides or dirt. Brushes that have been contaminated or corroded by frequent use should not be used, for the reasons given above.

### **Chemical-based preliminary treatment**

This section covers the following procedures:

- Cleaning in organic solvents or emulsions
- Cleaning in alkaline baths
- Pickling in acid

*Cleaning in organic solvents or emulsions.* Organic solvents can be used to remove oil products, greases and wax-based substances from the magnesium surface. Established working procedures are to be strictly followed in all cases. Basic emulsions are preferred, in order to prevent erosion of the metal. The testing of the commonly-available emulsions used is recommended in order to determine their suitability for the pre-treatment of magnesium-based materials.

**Table 7.3.** Cleaning of the metal surface in alkaline baths

Composition of aqueous cleaning solution	50 g/l caustic soda (NaOH) 10 g/l sodium phosphate (Na <sub>3</sub> PO <sub>4</sub> ) 1 g/l surface-active agent
Parameters	Immersion: 5–20 min, T <sub>bath</sub> 80–95°C

*Cleaning in alkaline baths.* The resistance of magnesium alloys to high pH levels means that cleaning in alkaline solutions is the preferred method. Alkaline substances have a soap-like effect on any grease or oil products present on the surface of the metal. Aqueous tank solutions starting with a pH value of 11 are recommended (see examples listed in Table 7.3).

The cleaning of the magnesium surface using this alkaline-bath method can also be aided by electrolytic means, by treating the magnesium workpiece as a cathode ( $i = 1\text{--}4\text{ A/dm}^2$ ;  $U = 4\text{--}6\text{ V}$ ;  $t = 1\text{--}3\text{ min}$ ). The hydrogen produced at the cathode has the effect of removing impurities. The alkaline cleaning bath must only be used for magnesium-based materials. Care should be taken to ensure that only fresh chemical products are used and that no impurities – especially ions of heavy metals – are allowed to enter. Ions of this type tend to accumulate on the surface of the magnesium, leading to corrosion. Magnesium workpieces that have already been surface-treated (see Fig. 7.1) should not be de-greased in alkaline baths, as this will result in damage to the protective layer.

*Pickling in acid.* Pickling should be applied to magnesium-based materials only in limited circumstances, as it leads (with chromic or hydrofluoric acid excepted) to metal erosion. The associated decomposition of the casting crust and increase in the porosity of the pickled material do not improve the corrosion prevention properties of subsequent protective surface treatments. Pickling can also have a negative effect on the physical properties (strength, fatigue strength, etc.) of the magnesium alloy, as the various phases of the magnesium-based material dissolve in the pickling solution at different rates. The indentations that remain on the surface of the material tend to turn into cracks when the material is subjected to physical strain. Data relating to acid pickling baths have been taken from [7] and listed in Table 7.4.

**7.1.3.3 Conversion Coatings Provided by Electroless Electrochemical Surface Treatment**

After appropriate preliminary treatment, the magnesium parts being coated are brought into contact with the conversion electrolyte without the use of any external source of energy. Application can be by immersion, injection, spraying or brush, etc. The magnesium-based material reacts with the active components of the conversion electrolyte to form a conversion layer. This conversion layer is normally oxidic in nature. Layer thickness ranges from 1 to 5  $\mu\text{m}$ .

**Formation mechanism, structure and composition of the conversion coating**  
Referring to [2], it is clear that the formation mechanism of the conversion layer is an anodic reaction, and that the process is more complicated than it is gener-

**Table 7.4.** Acid pickling-bath treatments for magnesium alloys

Type	Application	Baths and conditions	Container material
Chromic acid <sup>a</sup>	Removal of oxide, products of corrosion, flux, old chromate deposits and anodic coatings Alloys: all	Chromium trioxide (CrO <sub>3</sub> ) 180 g/l, treatment duration 1–15 min, bath temperature 20–100°C Metal erosion: none	Stainless steel, aluminium 2 S, lead-lined steel
Hydrofluoric acid <sup>a</sup>	Activation prior to chemical surface treatment  Alloys: all	Hydrofluoric acid (70% HF) 160 ml/l, treatment duration 0.5–5 min, bath temperature 20–30°C Metal erosion: none	Lead-lined steel, natural or synthetic rubber, polyethylene
Acetic acid Sodium nitrate <sup>a</sup>	Removal of rolling scale Wrought alloys	Acetic acid (crystallisable) CH <sub>3</sub> COOH 200ml/l Sodium nitrate (NaNO <sub>3</sub> ) 50 g/l, bath temperature 20–30°C, treatment duration 3 min Metal erosion: 5–10 µm	Ceramic, glass, lead, rubber, polyethylene
Chromic acid nitrate <sup>a</sup>	Removal of rolling scale, oxides and burnt-on graphite lubricant Wrought alloys Cast alloys	Chromium trioxide (CrO <sub>3</sub> ) 180 g/l, sodium nitrate NaNO <sub>3</sub> 30 g/l, bath temperature 20–30°C, treatment duration 3 min Metal erosion: 5–10 µm	Stainless steel or steel container with lead or rubber lining PVC
Nitric or sulphuric acid <sup>a</sup>	Removal of impurities after sandblasting  Cast alloys	Nitric acid (65% HNO <sub>3</sub> ) 90 ml/l Sulphuric acid (98% H <sub>2</sub> SO <sub>4</sub> ) 20 ml/l, bath temperature 20–30°C, treatment time 10–15 s Metal erosion: 50 µm	Ceramic, glass, rubber, PVC

<sup>a</sup> Take care of waste water treatment!

ally described, or supposed to be. The development of the conversion layer begins, at the point of contact between the metal and the conversion electrolyte, with the formation of a hydrated oxidic film of  $\text{MgO}_x(\text{OH})_y$ . This film is then partially dissolved once more by the anodic action of the conversion electrolyte. Pores then form, which join together in the manner of cylindrical cell colonies. There then occurs an exchange of ions and charges via this barrier layer, which results in the formation of the conversion layer. Components of the conversion electrolyte, pre-treatment (e.g., activation) and the alloy are then incorporated into the oxidic matrix  $\text{MgO}_x(\text{OH})_y$ , thus producing a semi-crystalline protective layer. The conversion layer consists of a system of cylindrical cell colonies, with

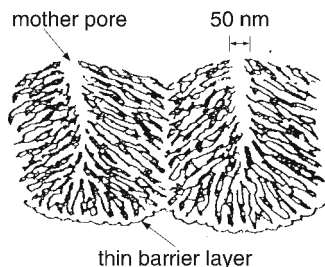


Fig. 7.2. Schematic illustration of cylindrical cell colonies in conversion layers produced with electroless methods

a pore diameter of around 5 nm, which radiate from a central pore (described in [2] as the “mother pore”) with an approximate diameter of 50 nm. Beneath this system of cylindrical cell-colonies, there is an ultra-fine barrier layer with an approximate thickness of 5nm.

Figure 7.2 provides the corresponding schematic illustration of the structure described above.

The use of XPS and Auger analysis reveals the presence in the conversion layer both of components of the conversion electrolyte and of reaction products that originate in the conversion electrolyte and magnesium alloy. These substances include, depending on the type of conversion electrolyte and magnesium alloy, such items as metallic oxides (e.g.,  $\text{Cr}_2\text{O}_3$ ,  $\text{MnO}_2$ ,  $\text{MgF}_2$ ,  $\text{NaMgF}_3$ ) – along with oxyhydroxide elements of the base-material (especially  $\text{MgO}_x(\text{OH})_y$  and  $\text{AlO}_x(\text{OH})_y$ ). Examination of the MIL 3171-standard conversion layer on AZ 91 has established that the conversion layer contains no zinc. If thoroughly rinsed chromated magnesium parts are placed in DI water, it is possible to detect the presence of significant components of the conversion electrolyte (e.g., Cr(VI)-ions), which originate in the cylindrical cell colonies described above. This Cr(VI)-content “trace” electrolyte is what causes the “self-healing” effect.

### Conversion coatings provided by chromating

(MIL-M-3171, types I and III; ASTM D 1732, CLASS I, type I and class I, type III)

See [8] for details of the methods commonly used for producing chromated layers on magnesium-based materials. Chromating constitutes one of the basic methods for the electroless application of surface coatings.

The magnesium is passivated by this process. The conversion layer formed by the chromate solution provides a primer base for organic finishes such as lacquer, paint or plastic-powder coatings. Note that chromate layers in themselves provide only temporary protection from corrosion. Tables 7.5 and 7.6 give a summary of the main processing parameters.

The colour of the conversion layers produced to standard MIL-M-3171 (types I and III) ranges from yellowish-brown to dark brown, depending on the type of magnesium alloy being treated. The non-homogeneity of magnesium diecasting often means that the coloration of the chromate film is somewhat irregular. This does not however have any effect on the corrosion-resistance of the chromate

**Table 7.5.** Processing parameters for chromating, MIL-M-3171 type I

Composition of electrolyte	180 g/l sodium dichromate $\text{Na}_2\text{Cr}_2\text{O}_7 \cdot 2 \text{H}_2\text{O}$ 190 ml/l nitric acid (65%) $\text{HNO}_3$
Parameters	Immersion and agitation of components for 30–120 sec., $T_{\text{EL}}$ 20–40°C IMPORTANT: Dimension adjustment-rate of 10–15 $\mu\text{m}/\text{min}$ Surface erosion
<b>Chromating procedure no. 2</b> (dichromate nitric acid/sulphuric acid)	
Composition of electrolyte:	140 g/l sodium dichromate $\text{Na}_2\text{Cr}_2\text{O}_7 \cdot 2\text{H}_2\text{O}$ 110 ml/l nitric acid (65%) $\text{HNO}_3$ 4 ml/l sulphuric acid (conc.) $\text{H}_2\text{SO}_4$
Parameters:	Immersion and agitation of parts for 10–30 s, $T_{\text{EL}}$ 20–40°C IMPORTANT: Dimension adjustment-rate (erosion) of 3–5 $\mu\text{m}$ Surface erosion

**Table 7.6.** Processing parameters for chromating, MIL-M-3171 type III

Activation	10% hydrofluoric acid $\text{H}_2\text{F}_2$ , immersion for 5 min, 20–30°C, RT
Composition of electrolyte	120–180 g/l sodium dichromate $\text{Na}_2\text{Cr}_2\text{O}_7 \cdot 2\text{H}_2\text{O}$ 2.5 g/l magnesium/calcium fluoride ( $\text{MgF}_2$ or $\text{CaF}_2$ ) pH value 4.1–5.5
Parameters	Immersion for 30 min. $T_{\text{E}}$ 100°C Parts do not undergo dimension adjustment

film. Excessive treatment times can make the chromate film powdery, which *does* have a negative effect on both corrosion protection and topcoat priming. One half to two-thirds of the chromate conversion layer is formed beneath the surface of the magnesium-based material, with the rest taking the form of a coating [9]. Note that chromate layers can only withstand temperatures of up to 200°C, and that they offer no protection against abrasive wear.

Corrosion protection conforming to ASTM-B117 or DIN 50021-SS should be regarded as slight. Chromate layers examined to these standards can withstand about 24 h of salt-mist testing. The chromate layer alone can only be regarded as a temporary corrosion-prevention measure. When this treatment is used in conjunction with organic coatings such as lacquer or paint however, there is an enormous increase in the amount of salt-mist testing that the workpiece can withstand (>1000 h). The chromate layer stops any increase in the pH value of the magnesium surface beneath the organic coating, thus preventing deterioration of the lacquer or paint. Within certain limits, it can also absorb and bind water – which is then diffused via the outer coating. It forms active chemical binding

**Table 7.7.** XPS quantitative analysis of a chromate conversion layer (MIL-3171, type III) on AZ91D

Element	at %	mole %
Mg	32	18
Na	0.42	1
Cr	25	3
Al	7.5	16
Fe	1.6	4
Mn	0.06	–
F	33	–
N	3.4	7
O	4.6	51
OH	15	–

points for the topcoat, thus improving the primer characteristics of the chromate layer. If there are any defects (cracking, scratches, etc.) in the chromate layer, what is generally described as the “self-healing” effect takes place beneath the outer coating. See [10] for a description of this phenomenon when applied to zinc (note that it has not yet been tested with magnesium). In the case of chromate layers on magnesium, soluble chrome (VI) compounds present in the layer are incorporated into the “defect”. The defective part is thus passivated once more. If a painted chromated magnesium surface is scratched (ASTM-B 117) and then subjected to salt-mist testing, slight infiltration of the outer coating is detected at the location of the scratch. Note that the following points must also be taken into account: When carrying out simple chromating, it should be observed that chrome (VI) ions are both toxic and – above all – carcinogenic. This evaluation is not generally accepted, however, with the point being argued all too often that the conversion layer contains no chrome (VI) whatsoever, or that the proportion that it does contain is insignificant. If there were no chrome (VI) ions in the cell colonies of the chromate layer, the “self-healing” process would not take place. See [2] for details of chromate layers produced to MIL 3171 type III standard. The analysis readings are listed in Table 7.7.

The chromate layer nevertheless contains 25 atom %  $\text{Cr}_2\text{O}_3$  with a proportion of Cr (VI) ions. Working on the basis of aqueous solutions with chromate and other substances, such as alum and manganates, a wide range of electroless surface-treatment procedures can be described (with special reference to [7] and [8]). However, none of these processes offers – in general – any improvement on the corrosion protection provided by surface treatments applied to MIL-M-3171 standards. This also applies to the phosphating and fluoridating of magnesium-based materials. It is therefore necessary to produce conversion layers on magnesium-based materials using equivalent chrome (VI)-free or even totally chrome-free procedures, with development proceeding as suggested in [11].

### Conversion coatings provided by chrome-free systems

The starting point for the use of Cr (VI) ions is provided by the elements that are listed nearest to chrome in the periodic table and which can thus – as “neigh-

**Table 7.8.** Processing parameters for phosphate-permanganate treatment as shown in [12]

Preliminary treatment	Acid-pickling 75% $\text{H}_3\text{PO}_4$ , 30 s, RT Neutralisation 10% NaOH, 30 s, RT
Composition of electrolyte	100 g/l ammonium dihydrogen phosphate $\text{NH}_4\text{H}_2\text{PO}_4$ 20 g/l potassium permanganate $\text{KMnO}_4$
Additive:	Phosphoric acid $\text{H}_3\text{PO}_4$ up to pH value of 3.5
Parameters:	Immersion 1–20 min, $T_{\text{EL}}$ 40°C, Dimensional erosion due to preliminary and main treatment

bouring elements” – be expected to display certain similar characteristics. The elements to which this applies in particular are Mn, V, Mo and W. They all form anions with a structure similar to that of chromate ions. They are, in part, very strong oxidants (e.g. permanganate) and can – like the element Cr – occur in numerous stages of oxidation. See [12] for a description of a phosphate-permanganate conversion coating for magnesium-based materials from Hydro Magnesium. Details of the production of this layer are listed in Table 7.8.

The conversion layer mainly consists of magnesium phosphate, but also contains oxidic components from the alloying elements (such as  $\text{Al}_2\text{O}_3$ ) and reduction products of the potassium permanganate (such as  $\text{MnO}_2$ ). The colour of the conversion layer, which depends on the treatment time of the magnesium alloy in the conversion solution, ranges from yellow to mid-brown – with a thickness of 4 to 6  $\mu\text{m}$ . See [12] for details of the positive evaluation of the corrosion-prevention properties, according to ASTM- B 117 standards, of the conversion layer with an acrylic finish applied. The main disadvantage of this process is that the acidic phosphate-permanganate solution decomposes at a high rate, thus limiting its use in industrial applications. The CHIBA Institute of Technology in Japan has published details [13] regarding the production of chemical conversion layers with the use of aqueous passivating electrolytes based on potassium permanganate, in combination with small quantities of acids ( $\text{HNO}_3$ ,  $\text{H}_2\text{SO}_4$ ,  $\text{H}_2\text{F}_2$ ). The treatment is carried out as listed in Table 7.9.

The conversion layer contains oxides of manganese, in various valency stages, and manganese oxide hydroxide. The components of the conversion layer that originate in the alloy itself are not indicated in [13].

The coloration of the conversion layers ranges, depending on the type of magnesium alloy involved, from yellow to brown. The corrosion protection offered by

**Table 7.9.** Processing parameters for potassium permanganate/acid treatment as shown in [13]

Preliminary treatment	De-grease in alkaline solution and activate in 46% $\text{H}_2\text{F}_2$
Composition of electrolyte	1–4 g/l potassium permanganate $\text{KMnO}_4$ 1–10 ml/l acid (e.g., $\text{HNO}_3$ , $\text{H}_2\text{SO}_4$ or $\text{H}_2\text{F}_2$ )
Parameters	Immersion for 5 min, $T_{\text{EL}}$ 40–80°C

passivated layers produced in this way is comparable to chromating that has been carried out to MIL-M-3171 standards. As with chromating, this conversion process must likewise be carried out at high temperatures (40–80°C). The main disadvantage when using this procedure is that the acidic potassium permanganate solution is not stable. It displays maximum oxidation performance with respect to its acidity, but the substance decomposes at a fast rate. Manganese dioxide quickly precipitates out, making the aqueous conversion electrolyte unsuitable for any further use. The result is a drastic reduction in the corrosion prevention performance of the conversion layer. Loose deposits, consisting mainly of manganese dioxide dust, also form on the surface of the conversion layer (although these can be wiped off). The conversion layers produced using the process described in [13] are not of consistent quality. See [6, 14, 15] for details of a conversion procedure for magnesium-based materials, supplied by German company AHC. The aqueous conversion electrolyte used in this procedure is potassium permanganate which – in combination with other substances – also contains at least one alkaline or ammonium salt of an anion from the group consisting of vanadate, molybdate and wolframate. This procedure, and the products manufactured using it, are protected by the registered trademark MAGPASS-COAT. The treatment is carried out as shown in Table 7.10.

While bearing in mind that the individual anions used in the MAGPASS-COAT process, in comparison to chromate ions, possess lower oxidation potential, it becomes clear that no synergic effect can be achieved without a combination of permanganate ions with the corresponding vanadate, molybdate and/or wolframate ions. This permits the formation of a corrosion preventing conversion layer on elements of the magnesium or its alloys and keeps the conversion electrolyte stable. This point is of special importance, as the aqueous conversion electrolyte containing potassium permanganate can only exercise this amount of influence on the electrolyte solution, with respect to oxidation, if the pH value drops and/or the temperature is increased (CHIBA). A possible explanation for this synergetic effect can be found in the formation of very strong heteropoly acids in the shape of their soluble ammonium or alkaline salts. A particular advantage of this procedure is the fact that the aqueous electrolyte remains stable even after an extended period, without the precipitation – in any considerable quantity – of the manganese dioxide that would render the aqueous electrolyte unsuitable for further use. Using the above procedure, it is therefore simple just to top up the chemical after it has been in use over a long period, without having to change the aque-

**Table 7.10.** Processing parameters for MAGPASS-COAT treatment [14]

Preliminary treatment	De-grease in alkaline solution, pickle in $\text{H}_3\text{PO}_4$ (75%), 30 s, RT; Neutralise with NaOH (10%), 30 s, RT
Composition of electrolyte	1–10 g/l potassium permanganate $\text{KMnO}_4$ , 1–10 g/l sodium or ammonium salts containing the anions vanadate, molybdate and wolframate, pH value 7.0–8.0
Parameters	Immersion for 2–10 min, $T_{\text{EL}}$ 20–30°C



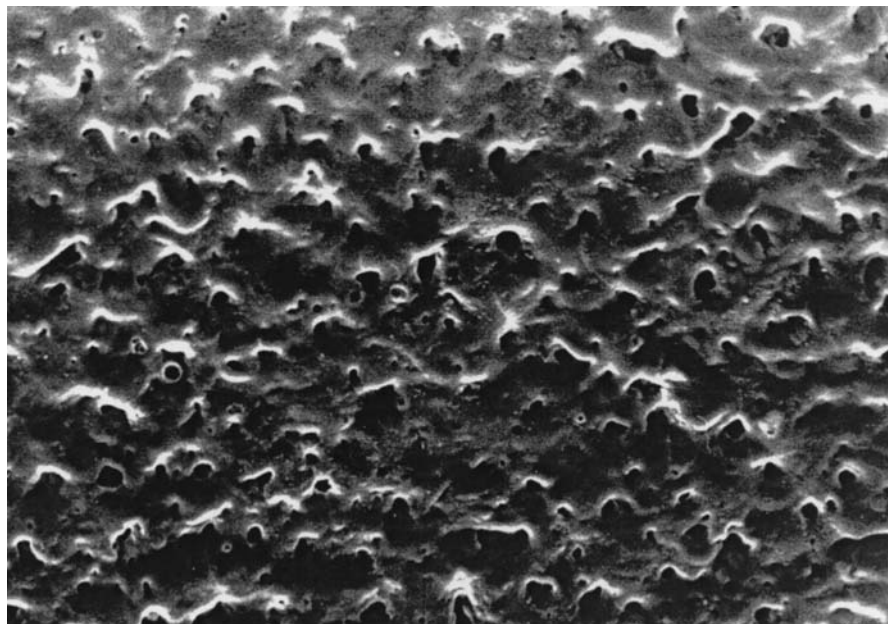


Fig. 7.3. REM-image of a MAGPASS-COAT layer applied to AZ91D

ous electrolyte itself. It is preferable to apply the coating within an aqueous electrolyte pH range of 7.0 to 8.0. The MAGPASS-COAT treatment can be applied to all common types of magnesium alloy. The colour of the conversion layer, depending on the magnesium-based material being treated, is golden-yellow to greyish-brown. The layer is approximately  $1\text{ }\mu\text{m}$  thick. The use of EDX and Auger analysis has determined that the conversion layer consists of  $\text{MgO}$ ,  $\text{Mn}_2\text{O}_3$ ,  $\text{MnO}_2$  and at least one oxide from the group of elements V, Mo and W. Figure 7.3 is a REM image of a MAGPASS-COAT layer applied to AZ91D.

There are – as in the case of the chromate layer applied to MIL-M-3171 standards – cracks in the surface, which are caused by the degree of coverage (Pilling-Bedworth ratio  $< 1$ ). As with all oxidic conversion layers applied to magnesium-based materials, the MAGPASS-COAT layer also requires additional sealing if it is to provide protection against corrosion. MAGPASS-COAT layers, again like their chromate counterparts, display outstanding “self-healing” properties, although – before being sealed – they have a low corrosion prevention rating in salt-mist testing carried out to DIN 50021-SS standards. Suitable sealants include wax products, lacquers and hydrosilicon combinations based on Sol-Gel solutions, which are made to react on the conversion layer. Sol-Gel solutions with titanium compounds, as used in [16] for the sealing of chromated zinc coatings on steel (and which are available under commercial names such as DELTACOLL 80), are also highly suitable for the sealing of MAGPASS-COAT finishes. The following section contains details of the corrosion prevention ratings (in hours) of chromate (MIL-M-3171) and MAGPASS-COAT finishes on AZ91D substrates.

**Table 7.11.** Comparison of the DIN 50021-SS-standard corrosion-protection ratings (in h) of chromating and MAGPASS-COAT on samples of AZ91D

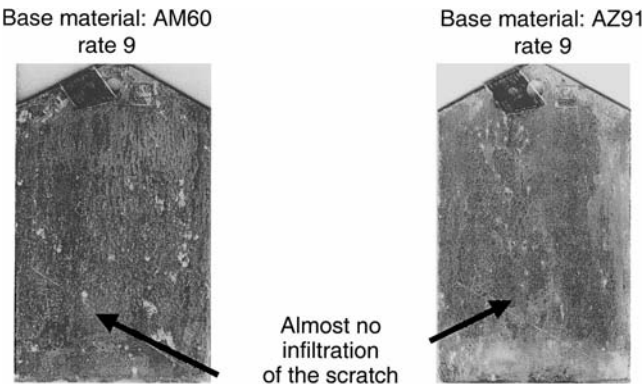
	Chromating according to MIL-M-3171 in [h]	MAGPASS-COAT in [h]
Electroless produced conversion layer without sealant	5–10	5–10
Electroless produced conversion layer + hydrosilicon combination DELTACOLL 80	412–495	451–608
Electroless produced conversion layer + epoxy polyester powder coating (Delta powder coating) 80 to 100 µm	505–603	528–607
Electroless produced conversion layer + hydrosilicon combination (DELTACOLL 80) + epoxy polyester powder coating (Delta powder coating) 80 to 100 µm	796–1038	818–1038

The lower value corresponds to the moment at which the first of three samples showed insufficient corrosion-protection properties. The larger value corresponds to the moment at which the last of the three samples displayed this insufficiency.

Table 7.11 contains comparative values obtained from standard DIN 50021-SS salt-mist testing.

The data in Table 7.11 show that very good corrosion protection performance can be obtained, relative to chromating, with MAGPASS-COAT. Figure 7.4 shows clearly how test GM 9540 P\* carried out on sealer-treated MAGPASS-COAT-finished magnesium plates made of AZ91HP and AM60HP (both materials supplied by Norsk-Hydro) reveals a high corrosion-prevention rating.

Figures 7.5 and 7.6 give a comparison, in terms of resistance to salt-mist spray testing to DIN 50021-SS standards, between chromate-content and chrome-free



**Fig. 7.4.** Test GM9540P (after 80 days) applied to MAGPASS-COAT treated with sealer (DELTACOLL 80)

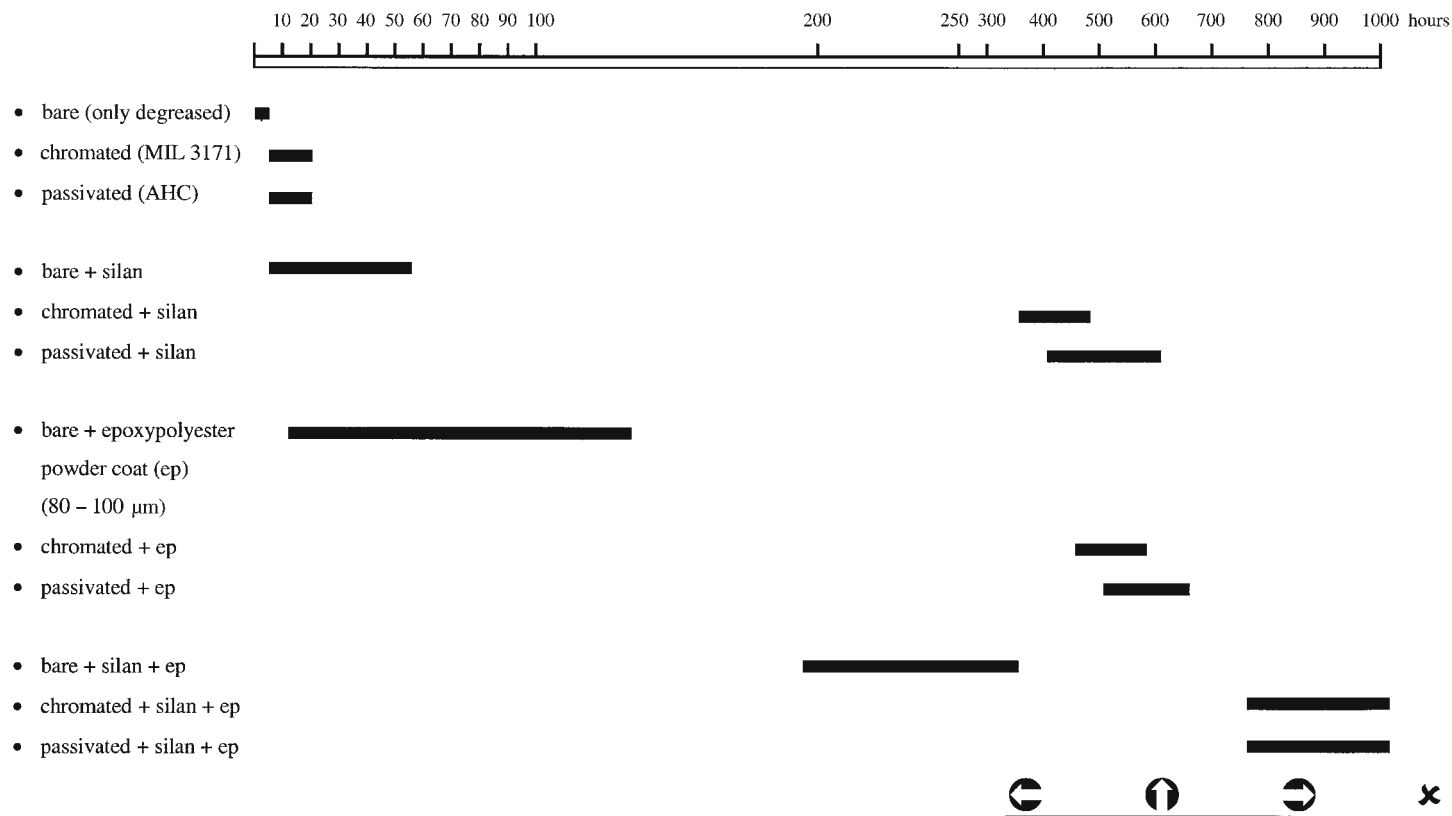


Fig. 7.5. Resistance to salt-mist testing (DIN 50021-SS) of chromate-content and chrome-free conversion layers on AZ91 HP

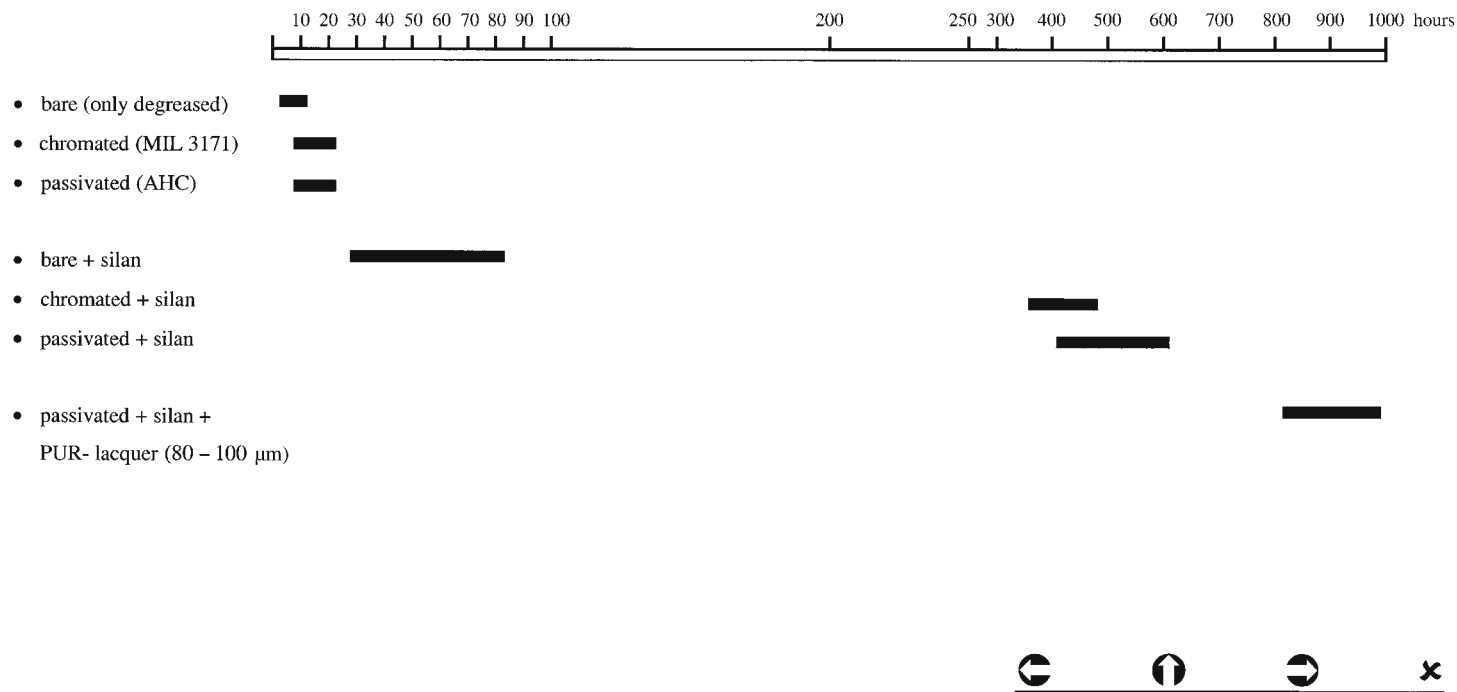


Fig. 7.6. Resistance to salt-mist testing (DIN 50021-SS) of chromate-content and chromate-free conversion layers on AM50

MAGPASS-COAT – conversion layers. The corrosion protection performance of both systems is roughly the same.

Pure phosphate or fluoride layers are also familiar types of conversion coatings for use on magnesium-based materials. Neither of these coating systems has a high corrosion prevention rating. Fluoride coatings should preferably be used for the pre-treatment of the magnesium surface. The surface is then “activated” by the formation, on the magnesium substrate, by a thin protective layer of  $\text{MgF}_2$ . Other familiar coatings are those based on zirconium fluoride. These are mainly designed for aluminium but can also be used on magnesium-based materials.

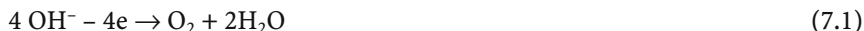
#### **7.1.3.4 Conversion Coatings Provided by Anodic Oxidation**

Given the excellent corrosion protection performance that the anodising of aluminium alloys provides, it is reasonable to suppose that magnesium alloys can be subjected to anodic oxidisation in the same way. It should however be made clear at this point that – for theoretical reasons – it is not possible to obtain the same level of protection as with aluminium-based materials, as the degree of coverage for  $\text{MgO}$  is 0.81 (i.e., the Pilling-Bedworth ratio is less than 1). For this reason, anodic oxide coatings applied to magnesium are porous and rough with a coarse surface structure. The nature of these characteristics is such that corrosive substances can infiltrate down to the base metal and cause its deterioration. The anodic finish, once applied, must therefore be sealed in order to make it corrosion-proof. A further property of magnesium oxide finishes is their relative lack of hardness in comparison to aluminium oxide, which negatively effects the wear resistance of anodic finishes applied to magnesium-based materials.

The conversion coatings provided by anodic oxidation involve costs which are almost twice as high as those for conversion coatings provided by electroless electrochemical surface treatment. This is due to the time-consuming handling, the consumption of electrical energy and a prolonged coating time.

#### **Formation mechanism, structure and composition of the conversion coatings**

The magnesium-based material that is being coated functions as an anode during the electrochemical process. The reactions, coarsely-defined, that take place in an aqueous electrolyte are as follows:



The result of this reaction is the formation of  $\text{MgO}$ . Note that alloying elements, such as Al, can also be oxidised. This produces double oxides such as spinel  $\text{MgAl}_2\text{O}_4$ . As with aluminium, the anodic layer that is formed from the metal adopts oxidic hexagonal cell structures. Each cell has a pore at its centre. The model originally published by Keller, Hunter and Robinson [17] (KHR model, Fig. 7.7) for anodic oxidation finishes on aluminium is also of relevance where the anodic coating of magnesium is concerned. The cell diameter of the porous section of the anodic layer on magnesium (anodised to DOW 17 standard) is 15 nm. This porous section of the anodic finish does not consist only of magnesium ox-

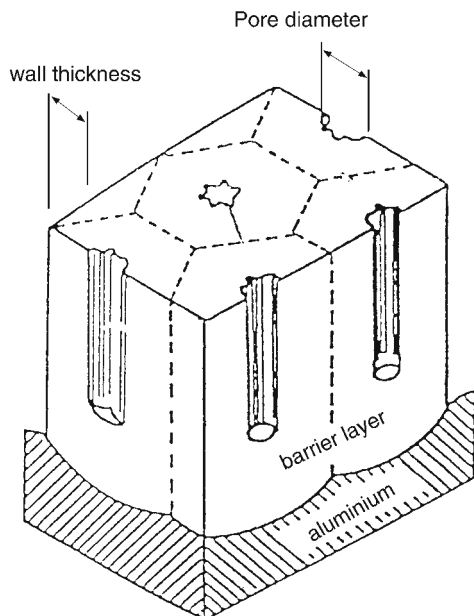


Fig. 7.7. KHR model [17]

ide – it also contains considerable quantities of the substances that go to make up the electrolyte.

The presence of a distinctive barrier layer beneath the porous anodic finish has already been mentioned in [18] and [19], and shown to exist in [2] by means of TEM tests on ultramicrotomy cross sections. The thickness of this barrier layer, in the case of magnesium, is approximately 10 nm. Its field strength has a high value of  $10^{10} \text{ Vm}^{-1}$ . It is made up of crystalline components such as  $\text{MgF}_2$ ,  $\text{NaMgF}_3$ , along with amorphous  $\text{MgO}$  and magnesium oxide hydroxide. The development of the anodic layer begins with the formation of a very thin film on the metal. This film consists of magnesium hydroxide and components of the electrolyte (e.g.,  $\text{MgF}_2$ ). The film is then partly dissolved by the action of the anodising electrolyte. A current flows from the external energy source (the anode) through these partly dissolved points and via the barrier layer. This current also transports ions belonging to the electrolyte. These ions crystallise out in the amorphous magnesium oxide hydroxide matrix. This process is kept active by the external energy source. The result is layers that are considerably thicker than conversion layers produced using electroless techniques. See [20] for a description of the function of the anions in the anodising electrolyte with respect to the formation and build-up of the anodic coating. It is generally established that the formation mechanism with respect to anodic layers on magnesium is, in detail, considerably more complicated than its aluminium equivalent.

### Anodic oxidation procedures and coating properties

There is a wealth of published source material related to anodic treatments. Indeed, details of a fluoride-based anodising treatment for magnesium were pub-

lished as early as the nineteen-twenties. See [21] for details of the “long-standing processes” used in the anodic oxidation of magnesium. More recent standard techniques are included in [22–24]. In [25], an attempt is made to give systematic details and an overview with respect to the development of the anodising of magnesium, with electrolytes organised into groups. The electrolytes employed are mainly aqueous solutions of ionogenic substances, used individually or in mixtures. Molten salt can also be used. Electrolyte components include chromic acid, hydrofluoric acid, phosphoric acid, boric acid and/or their corresponding salts. Anions such as manganates or permanganates, vanadates, wolframates, aluminates, silicates, carbonates and so on can also be added as electrolyte components. Normal practice also consists of adding a strong base-substance (KOH, NaOH,  $\text{NH}_3$ ) to the electrolyte, in order to make a large quantity of  $\text{OH}^-$  ions available for the anodic reaction. However, very few of the processes that have found practical application in the anodic surface-treatment of magnesium actually produce anodic conversion layers that guarantee a good level of protection against corrosion. The following section describes these processes and the protective layers they are designed to produce.

### *DOW 17 Treatment*

Specification: MIL-M-45202 A

This process, which was developed by the DOW CHEMICAL COMPANY [8], can be used on all types of magnesium alloy. Anodising takes place in an aqueous, acidic electrolyte consisting of a combination of phosphate, fluoride and chromate ions. Alternating current (AC) is used in preference to direct current (DC). Table 7.12 gives a summary of the processing parameters used in DOW 17 treatment.

Figure 7.8. shows a typical tension-time curve for the anodising of AZ 31 (note that a similar curve applies to other magnesium alloys) [8].

Treatments applied using the DOW 17 anodising process have a light- to dark green appearance and are thus described as “green type” finishes. Very thick coatings also have a somewhat mottled and coarse appearance. Thin coatings measure 2.5–7.5  $\mu\text{m}$ , while thick coatings measure 23–38  $\mu\text{m}$ . Sealed thick DOW 17 coatings display good resistance to corrosion. Thick DOW 17 coatings produced with DC energy are smoother than those using AC. About one half of the layer forms below the surface of the material, while the other 50% forms a coating above the original level of the metal.

**Table 7.12.** Processing parameters for DOW 17 [8]

Preliminary treatment	Alkaline
Electrolyte	240 g/l ammonium fluoride $\text{NH}_4\text{HF}_2$ 100 g/l sodium dichromate $\text{Na}_2\text{Cr}_2\text{O}_7 \cdot \text{H}_2\text{O}$ 90 ml/l phosphoric acid 85% $\text{H}_3\text{PO}_4$
Parameters for AC	$i = 0.5 - 5 \text{ A/dm}^2$ ; thin layer: $V_{\text{end}} 60-75 \text{ V}$ , 4–5 min; thick layer: $V_{\text{end}} 90-100 \text{ V}$ , 25 min $T_{\text{EL}} = 70-80^\circ\text{C}$
Sealing	Immersion in water glass (50 g/l), 95–100°C, 15 min

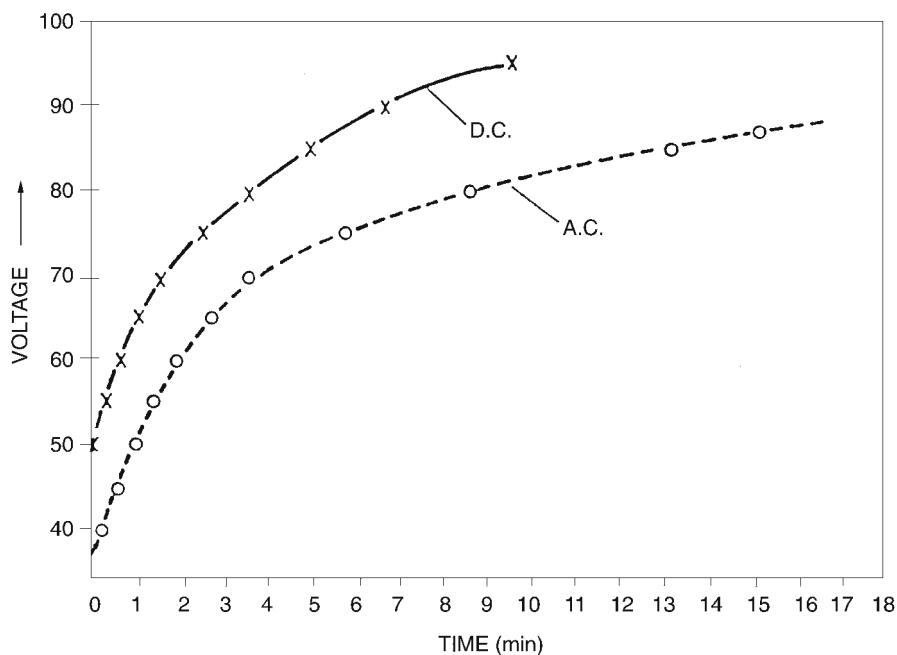


Fig. 7.8. A typical tension-time curve for the anodising of AZ31

### HAE Treatment

Specification: MIL-M-45202 A

This process, which is named after its inventor Harry A. Evangelides [26, 27], was first supplied by Pitman-Dunn Laboratories, Frankfort Arsenal, Phil. USA in 1951. HAE treatment can be used on all types of magnesium alloy. Anodising takes place in an aqueous, alkaline electrolyte consisting of a combination of hydroxide, aluminium oxide, phosphate, fluoride and manganate ions. Alternating current (AC) is used in preference to direct current (DC). Table 7.13 gives a summary of the processing parameters used in HAE treatment.

Treatments applied using the HAE anodising process have a matt light- to dark brown appearance and are thus described as “brown type” finishes. HAE coatings consist of spinels of the elements Mg, Al and Mn – i.e., of mixed oxides of bivalent and trivalent metallic ions – and contain a high proportion of  $\text{MgF}_2$ . Thin coatings are applied with a thickness of 5–10  $\mu\text{m}$  and thick coatings with a thickness of 25–80  $\mu\text{m}$ . Both thin and thick HAE coatings are porous (see also [9], p. 86 cross-sections and REM)). Sealed thick HAE coatings display better corrosion resistance than their DOW 17 equivalents. There is virtually no roughening of thin HAE coatings. Thick HAE coatings are very rough and relatively hard, but they are also very brittle. They have both corrosion prevention and abrasive wear protection functions. In [9, p. 89], it can be seen that HAE treatment, when compared to DOW 17 and chromate coatings, displays the best wear resistance in Taber abrasion tests. As the HAE layer is a strong electrical insulator, and is thus barely worn away by the electrolyte during the anodising process, this procedure



**Table 7.13.** Processing parameters for HAE [27]

Preliminary treatment	Alkaline
Electrolyte	35 g/l potassium fluoride KF 35 g/l sodium phosphate $\text{Na}_3\text{PO}_4 \cdot 12 \text{H}_2\text{O}$ 165 g/l potassium hydroxide KOH 35 g/l aluminium hydroxide $\text{Al}(\text{OH})_3$ (as a dry gel) 20 g/l potassium manganate $\text{K}_2\text{MnO}_4$
Parameters for AC	$i = 1.5\text{--}2.5 \text{ A/dm}^2$ ; thin layer: $V_{\text{end}} 65\text{--}70 \text{ V}$ , 7–10 min; thick layer: $V_{\text{end}} 80\text{--}90 \text{ V}$ , 60–90 min $T_{\text{EL}} = 27 + 5^\circ\text{C}$
Sealing (applies only to non-painted items)	Immersion (4 s–60 s) in solution of 20 g/l sodium dichromate $\text{Na}_2\text{Cr}_2\text{O}_7$ 100 g/l ammonium difluoride $\text{NH}_4\text{HF}_2$ , 20–30°C, parts are dried (without removing the sealing solution) and stored at 80°C for 7–15 h

permits the contoured coating of complicatedly shaped components. About one half of the HAE layer forms below the surface of the magnesium-based material, while the other 50% forms a coating above the original level of the metal. Thin HAE layers form an excellent primer coat for paint and lacquer finishes.

### ***ANOMAG Treatment***

The ANOMAG treatment was developed in New Zealand [28]. Publications [25], [29] and [30] contain little information on this technology. One point that is certain is that high voltages (of up to 500 V) are used [29]. These voltages must not be allowed to produce spark discharges onto the coating substrate. The electrolyte consists of ammonia with added phosphates. See [29, p. 299] for a schematic explanation (but without any details) of the ANOMAG treatment. The coating, which can be painted, is light grey in appearance and consists of magnesium oxides and magnesium phosphates. It builds up regularly at edges and can be applied in three coating classes [30]: 3–8  $\mu\text{m}$ , 10–15  $\mu\text{m}$  and 20–25  $\mu\text{m}$ .

As with all the electroless electrochemical and electrochemical surface treatments described above, its purpose is to act as a primer surface for lacquers and paints and to provide corrosion protection. The corrosion resistance of ANOMAG is shown below in terms of salt-spray testing to ASTM-B 117 standards on sample panels supplied by the company Norsk Hydro [29, p. 301].

AZ 91D	class 1 (3–8 $\mu\text{m}$ )	up to 150 h
	class 2 (10–15 $\mu\text{m}$ )	up to 400 h
	class 3 (20–25 $\mu\text{m}$ )	up to 1300 h
AZ 50	class 1 (3–8 $\mu\text{m}$ )	up to 300 h
	class 2 (10–15 $\mu\text{m}$ )	up to 446 h

In [29, p. 300] it is claimed that ANOMAG treatment seals and levels all irregularities in cast magnesium (such as cavities, cracks, etc.). One disadvantage that should be mentioned here is that ANOMAG treatment is carried out using sealed-off equipment and that  $\text{NH}_3$  must be removed from the exhaust gas and waste water produced.

### ***7.1.3.5 Conversion Coatings Provided by Anodic Plasma-Chemical Reaction in the Electrolyte***

This group of electrochemical coating techniques – which are variously described as anodic spark deposition (ASD), anodic spark discharge, microarc oxidation (MO), electrical breakdown and plasmachemical oxidation – were developed primarily for the surface treatment of aluminium. However, other light alloys can also be coated using these methods. The nevertheless revolutionary basic idea of this processing technology consists of combining anodic processes on valve-grade metals with plasma discharges in the electrolyte. This provides protective coatings of a crystalline ceramic nature, the thickness and hardness of which make them especially suitable for providing protection against both corrosion and wear. In comparison to other, more conventional, plasma processes (CVD, PVD) this anodic plasma-chemical oxidation process is easy to apply using normal electrochemical process plant techniques and without additional expense (e.g., for vacuum equipment). The important differences with respect to the classic anodic processes are that the achievable thickness of the oxide layer is increased (up to 150  $\mu\text{m}$ ), coating hardness is improved (up to 1500 HV 0.025 at 30–50  $\mu\text{m}$ ), along with wear resistance, and a good level of corrosion resistance can be guaranteed without any need for further treatment [25]. The surface treatment is carried out using relatively high voltages ( $> 100\text{ V}$ ) and with various types of power supply, such as DC, AC, three-phase current and pulsed current. The reaction mechanism in the case of the anodic plasma-chemical reaction allows edges, profiles sections and reliefs to be coated in a consistent manner.

Suitable electrolytes include aqueous solutions – preferably with the anions fluoride, phosphate, borate, silicate and aluminate – which work in the neutral-to-alkaline range [31–33]. Half of the protective layer that forms on the magnesium substrate is below the surface of the material, while the other 50% forms a coating above the original level of the metal. Apart from their excellent corrosion- and wear-prevention properties, coatings of this type also display a high amount of resistance to heat and radiation exposure. They are also good insulators of heat [thermal conduction approx.  $1\text{ W}/(\text{m}\cdot\text{K})$ ] and electricity (minimum of  $10\text{ V}/\mu\text{m}$  dielectric strength). In [34], it can be seen that the physical strength (yield stress, tensile strength, elongation to failure) of the magnesium-based material is not diminished by the use of a ceramic layer. A disadvantage that needs to be mentioned with respect to surface treatment using the anodic plasma-chemical reaction is the use of high voltages (requiring protection against accidental contact) and the dissipated energy that results from the exchange of energy within the electrolyte, which requires the corresponding cooling of the electrolyte.

#### **Formation mechanism, structure and composition of conversion coatings**

Günterschulze and Betz [35] are the first to publish investigation work dealing with anodic spark discharges in electrolytes on aluminium and tantalum. See [31–33] for details of basic work and monographs containing numerous references, which include descriptions of the formation mechanism and of how oxide ceramic layers build up on various metals, among them magnesium. Figure

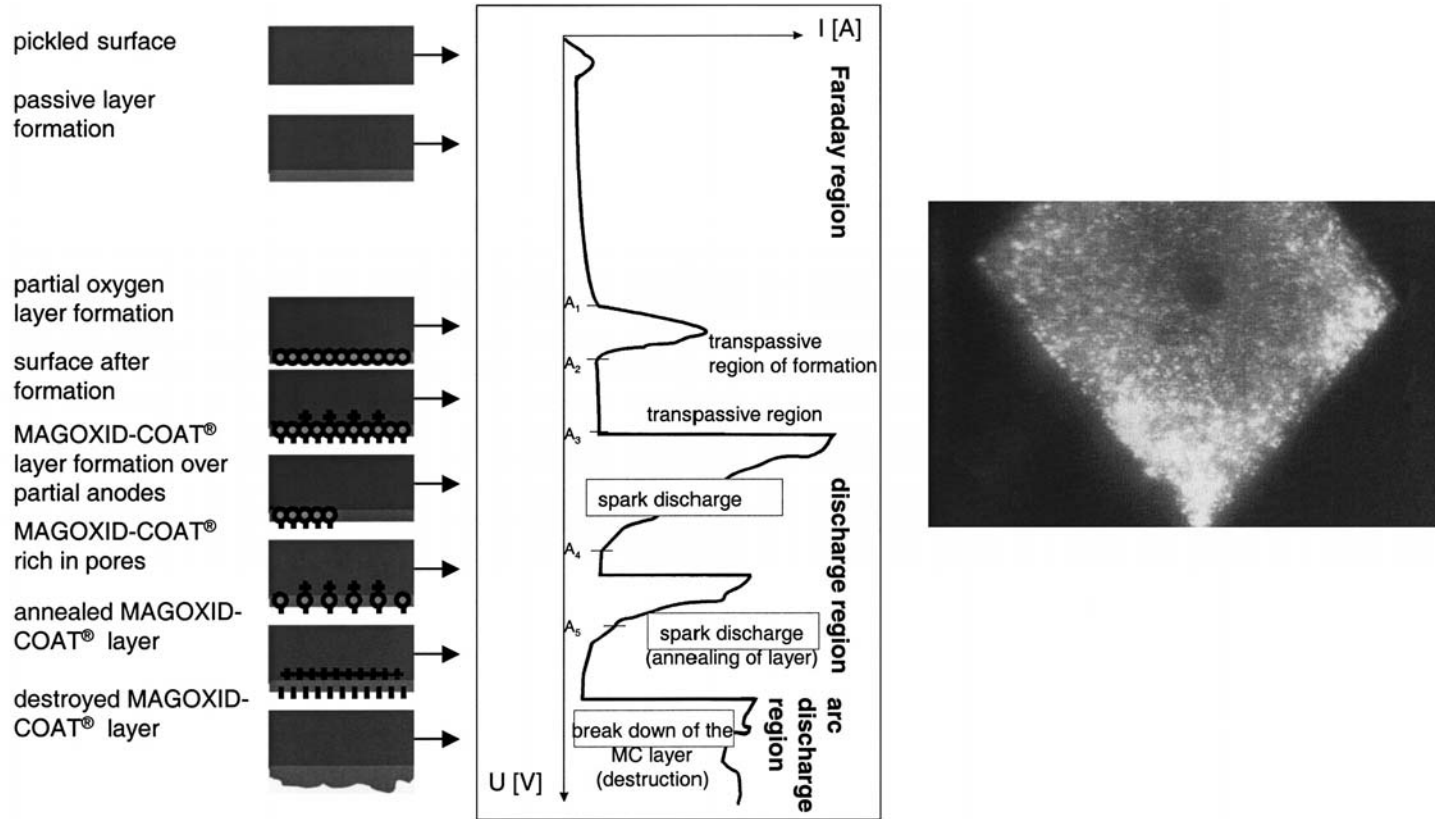


Fig. 7.9. Schematic current-voltage curve with respect to an anodic plasma-chemical reaction on magnesium-based materials

7.9 gives a schematic depiction of the reaction mechanism in the form of a current-voltage curve.

The schematic depiction in Fig. 7.9 shows three areas: the Faraday, spark-discharge and arcing ranges [33]. The voltage at the anode is slowly increased in the Faraday range.

Very little current actually flows. A very thin passivated layer (approx. 1  $\mu\text{m}$  thick) forms on the anode. A film of oxygen will now have stabilised on this passivated layer and charges will have formed. With voltages of  $> 100\text{ V}$ , there is a sudden increase in current and plasma discharges become visible as “sparks” (see Fig. 7.10 for details of spark discharge range).

This plasma discharge causes the partial destruction of the passivated layer formed within the Faraday range, and a charge exchange takes place at the metal/oxygen/electrolyte point of contact.

The amount of energy released by this process is so great that part of the magnesium on the surface melts and reacts immediately with the ionised oxygen. Crystalline oxides then form, and components of the electrolyte are incorporated into this hot zone and transformed. The plasma process continues until the entire magnesium surface has, point by point, become oxidised. As the plasma process ends, the current drops to around zero because the oxide layer has formed an electrically insulating surface on the anode. The spark discharge procedure can be forced several times by further increases in voltage.

However, if the voltage is too high, the discharge becomes stationary (arcing range), which destroys the layer that has formed. See [33] for details of the characteristics of impulse-type spark discharge:

Impulse rate	$10^5$ impulses/s
Impulse density	$10^4$ impulses/ $\text{cm}^2$
Impulse time	$2 \times 10^{-5}$ s
Estimated current density	$> 10^3$ A/ $\text{cm}^2$

Each discharge (impulse) has an approximate cathode spot diameter of 1  $\mu\text{m}$  on the magnesium surface, with a temperature of around 8000 K. In sum, the following can be said of the formation mechanism with respect to the anodic plasma-chemical reaction in the electrolyte: it is a gas-solid reaction, which takes place with partial discharges onto the magnesium surface, resulting in the formation of an oxide ceramic coating.

The oxide ceramic coatings produced by anodic plasma-chemical reaction consist of two sub-zones (Fig. 7.11): one on the barrier layer (with a low pore count) and another on top (with a high pore count). The layer with the low pore count prevents corrosion, while the section with the high pore count functions as a primer base for lacquers or paints, and as a reservoir for sealers or impregnation treatments (e.g., PTFE).

These oxide ceramic layers consist of partly crystalline  $\text{MgO}$ , spinels (e.g.,  $\text{MgAl}_2\text{O}_4$ ) and of components – such as  $\text{MgF}_2$  – that are derived from the electrolyte. The colour of these oxide ceramic layers ranges, depending on the type of alloy, from white to greyish-white. Black oxide ceramic coatings – and layers of other colours – can be produced in a single-stage process by the addition to the electrolyte of substance such as salts [36].

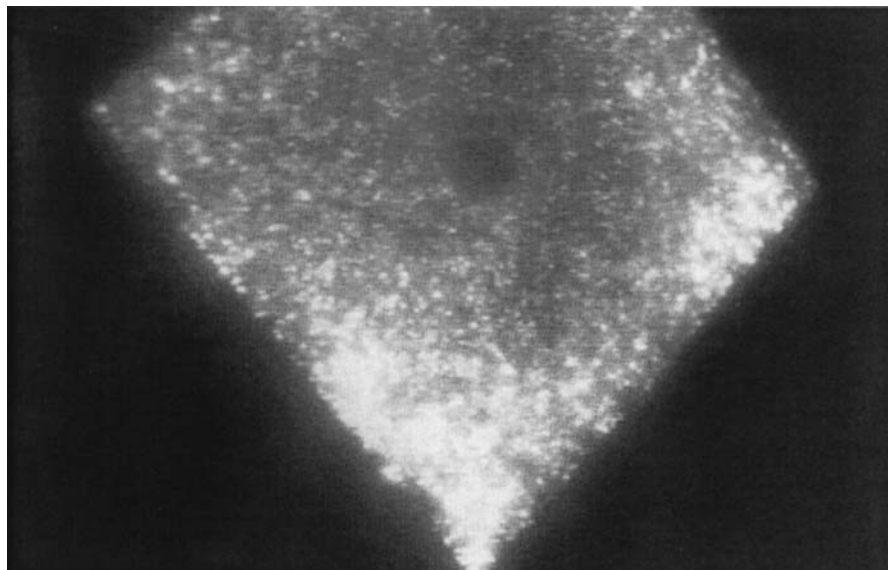


Fig. 7.10. Plasma discharges in the electrolyte on a magnesium surface

### **Anodic plasma-chemical reaction procedures and coating properties**

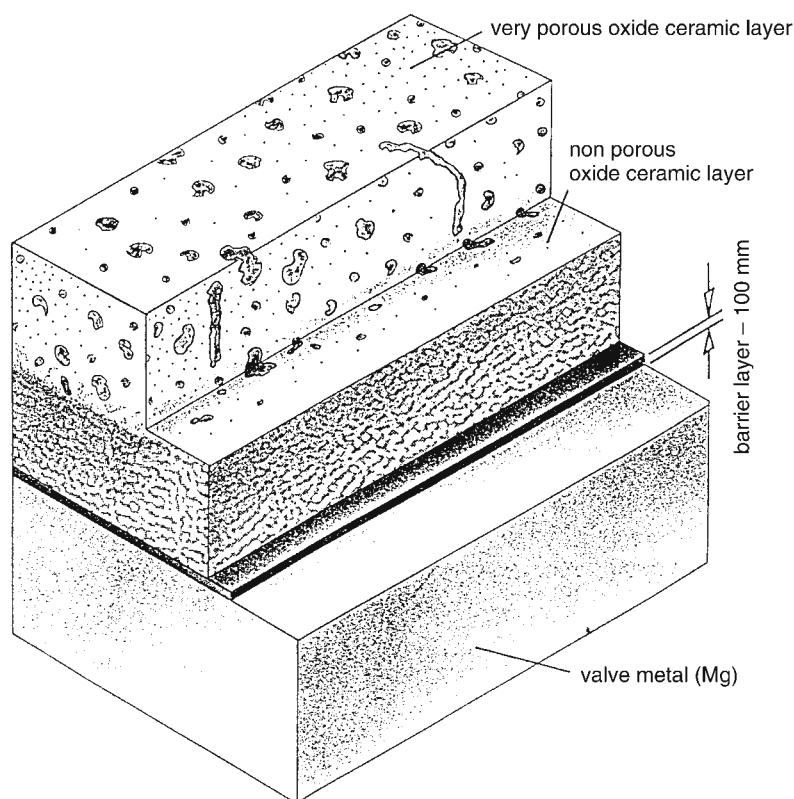
The following section describes the processes actually used in industry.

#### ***MAGOXID-COAT Treatment***

This process, which was developed by German company AHC [37], can be used on all types of magnesium alloy. This anodic plasma-chemical treatment is carried out in an aqueous, neutral electrolyte, which is a combination of mineral acids (fluoric, phosphoric and boric acid) and basic organic substances. The use of direct current (DC) is preferred. Table 7.14 gives a summary of the processing parameters used in MAGOXID-COAT treatment.

MAGOXID-COAT finishes have a white to greyish-white appearance. They are crystalline in structure and consist of spinels of the elements Mg, Al and Zn (i.e., they are built up of mixed oxides of bivalent and trivalent metallic ions, as revealed by X-ray diffraction). They also contain a high proportion of substances based on fluoride, phosphate and borate. If supplementary ions, such as vanadate or molybdate, are added to the conventional MAGOXID-COAT electrolyte, deep black fade-resistant spinels are formed which give the layer a smooth black appearance. See Fig. 7.12 for REM and micrograph images of a MAGOXID-COAT layer applied to AZ91 HP.

The REM image in Fig. 7.12a shows fused-together structures with pores. Figure 7.12b (fracture surface) appears as one-half dense layer relative to the magnesium substrate and one half pored layer. The micrograph images (Figs. 7.12c and 7.12d) show consistent layer-formation on surfaces and edges. Fine MAGOXID-COAT finishes produced to a thickness of approximately 5  $\mu\text{m}$  pro-



**Fig. 7.11.** Schematic depiction of the structure of an oxide ceramic coating applied to magnesium-based materials

**Table 7.14.** Processing parameters for MAGOXID-COAT [38]

Preliminary treatment	Alkaline
Activation	10% $\text{H}_2\text{F}_2$ , RT, 30–60 s
Electrolyte	30 g/l hydrofluoric acid ( $\text{H}_2\text{F}_2$ ) (40%)
	60 g/l phosphoric acid ( $\text{H}_3\text{PO}_4$ ) (85%)
	35 g/l boric acid ( $\text{H}_3\text{BO}_3$ )
	360 g/l hexamethylene-tetramine
Parameters	pH 7–7.2 (adjusted using ammonia)
	$i = 1\text{--}2 \text{ A/dm}^2$ , 400 V, $T_{\text{EL}}$ RT, coating formation rate
	$1.5 \mu\text{m/min}$ , thin coatings $5 \mu\text{m}$ , thick coatings $30 \mu\text{m}$
Sealing	1. Variant: Immersion in water glass (50 g/l)
	95–100°C, 15 min
	silicating out in $\text{CO}_2$
	2. Variant: Immersion in Sol-Gel solutions such as hydrosilicon combinations RT, dry at 80–100°C



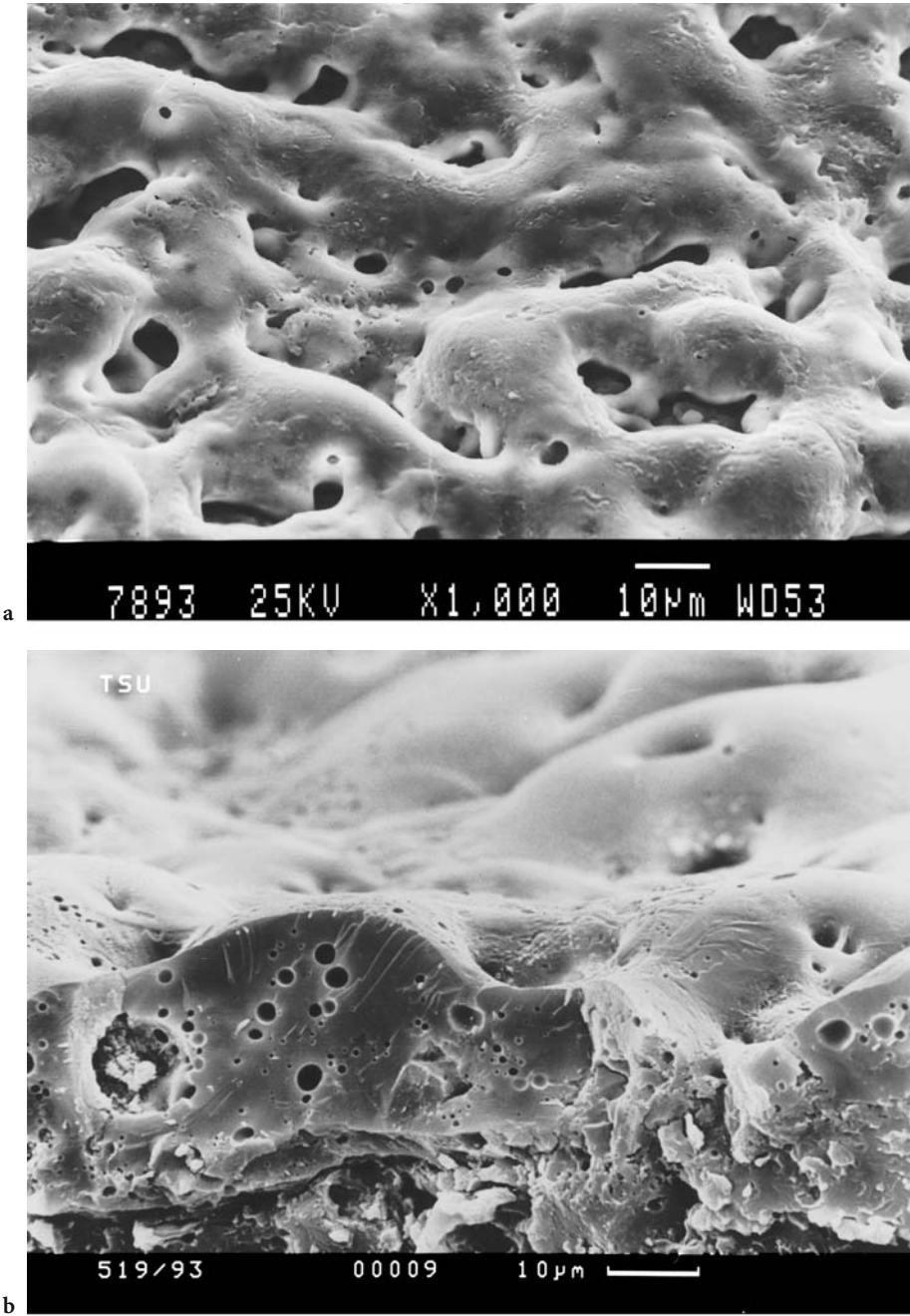
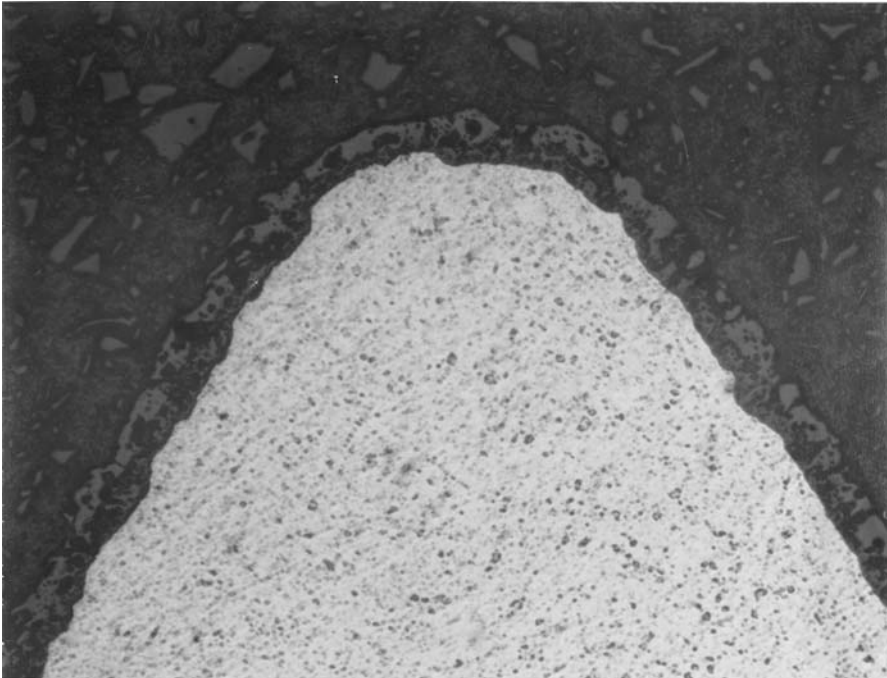
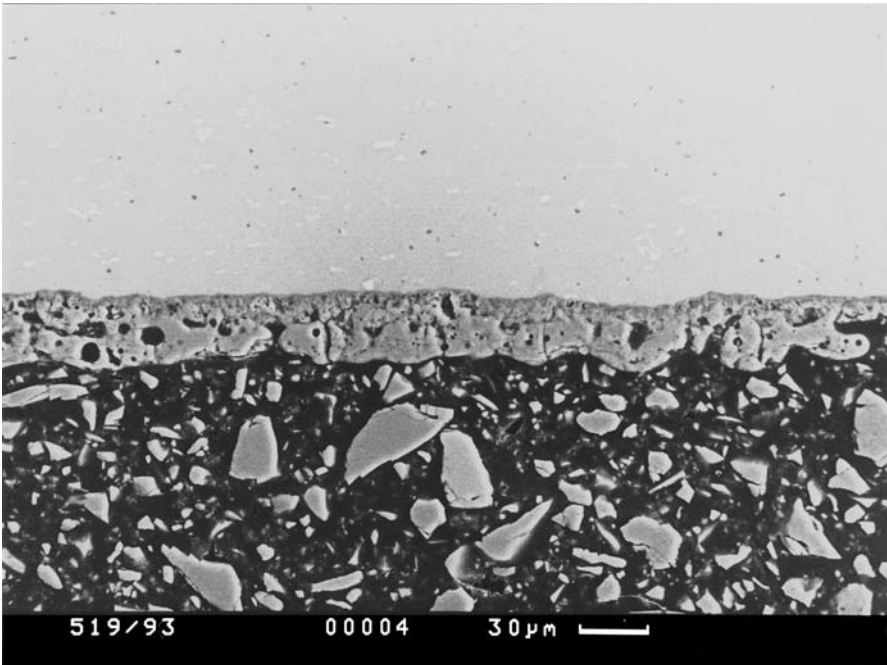


Fig. 7.12a–d. a REM image of a MAGOXID-COAT finish (1000 : 1). b REM image of a fracture surface of a MAGOXID-COAT finish



c



d

Fig. 7.12. c Metallographic cross-section on one edge (300 ×). d Metallographic cross-section on a flat surface (450 ×)



vide an excellent primer base for lacquers and paints. Thicker coatings (25–30  $\mu\text{m}$ ) provide outstanding protection against corrosion and very good friction-wear resistance. See Fig. 7.13 for details of the resistance to DIN 50021-SS-standard salt-spray testing of plain, sealed and painted MAGOXID-COAT finishes applied to AZ 91 HP.

It is apparent from the corrosion trial results shown in Fig. 7.13 that very high levels of resistance can be achieved with respect to salt-spray testing.

Figure 7.14 shows the GM9540P corrosion-test results (after 80 days) relating to a MAGOXID-COAT layer sealed with hydrosilicons. There is only slight infiltration at the site of the scratch.

The following section attempts to compare MAGOXID-COAT finishes with other anodic coating systems (DOW 17, HAE). Table 7.15 shows how HAE and MAGOXID-COAT finishes respond to salt-mist testing.

Electrochemical corrosion testing carried out to DIN 50918 standards (see Table 7.16) shows a clear difference, in terms of corrosion resistance, between MAGOXID-COAT and conventional anodic finishes (DOW 17, HAE). The time that elapses between arrival at maximum corrosion potential and 80% of the corrosion current of untreated magnesium samples provides a benchmark for gauging the corrosion resistance of coating systems. As shown in Table 7.16, MAGOXID-COAT requires the longest period and is thus – relative to the other coating systems – more resistant to corrosion.

Thick corrosion-protection coatings applied to magnesium-based materials do not just perform this function – they also help prevent wear caused by abra-

**Table 7.15.** Comparison of HAE and MAGOXID-COAT with respect to DIN 50021-SS-standard salt-mist test

System	Corrosion points/ $\text{dm}^2$ after 24 h	Corrosion points/ $\text{dm}^2$ after 100 h	Observations
HAE 25 $\mu\text{m}$	3	41	Medium-sized pores
HAE 40 $\mu\text{m}$	0	18	Small points
MAGOXID-COAT 25 $\mu\text{m}$	0	0	

**Table 7.16.** Electrochemical corrosion testing (to DIN 50918 standards) of DOW 17, HAE and MAGOXID-COAT finishes

Coating	Sealing <sup>a</sup>	Coating thickness [ $\mu\text{m}$ ]	Corrosion resistance [s]
None (material AZ91)	–	0	0
DOW 17	–	15	0
HAE	–	15	25
MAGOXID-COAT	–	15	100
DOW 17	+	15	820
HAE	+	15	520
MAGOXID-COAT	+	15	2200

<sup>a</sup> without sealing, + with sealing.

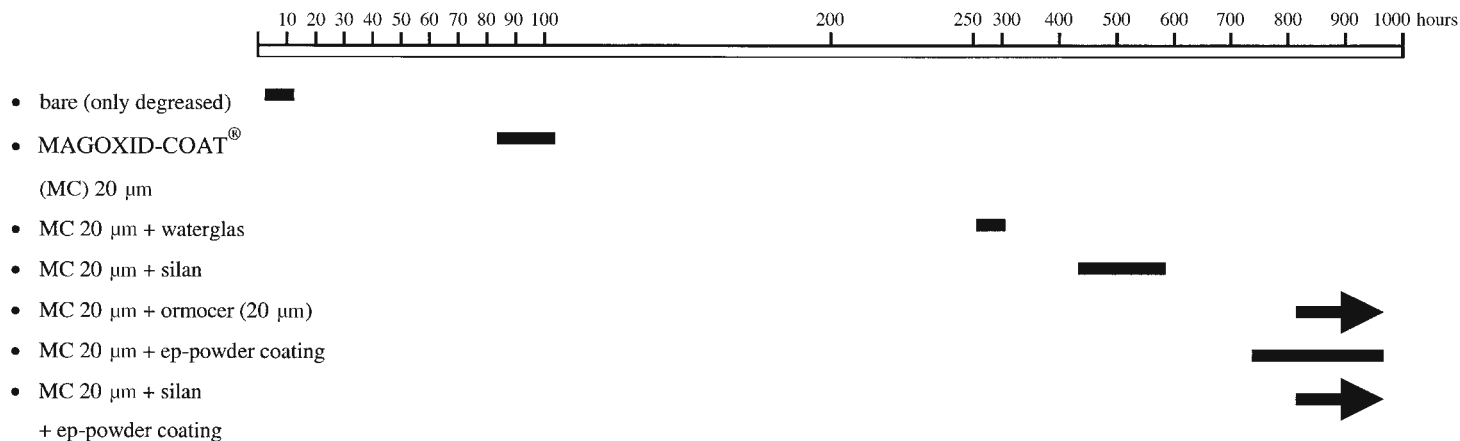


Fig. 7.13. Resistance to DIN 50021-SS-standard salt-spray testing of different surfaces treated with MAGOXID-COAT

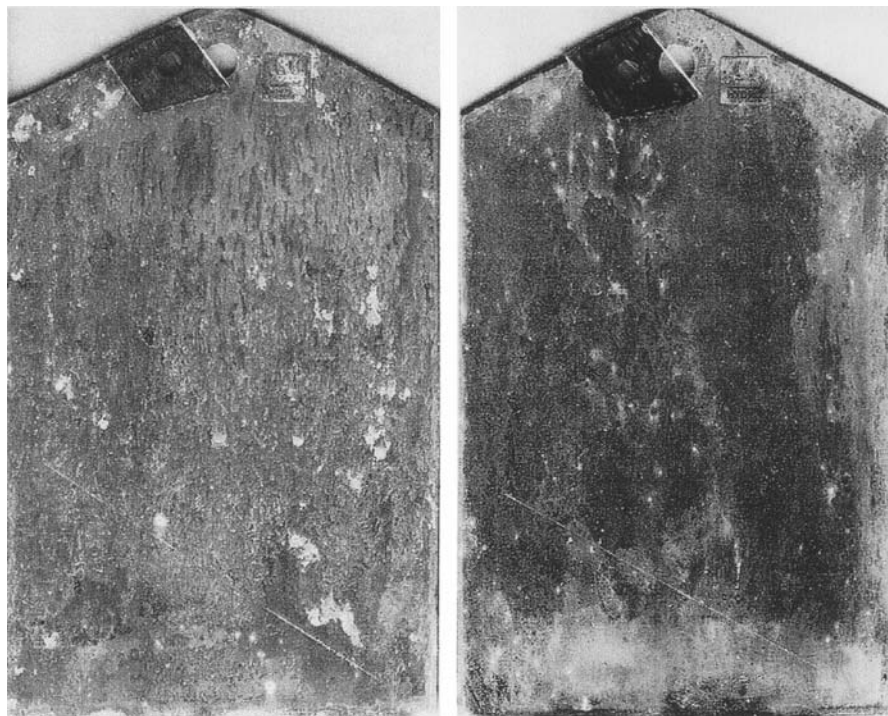
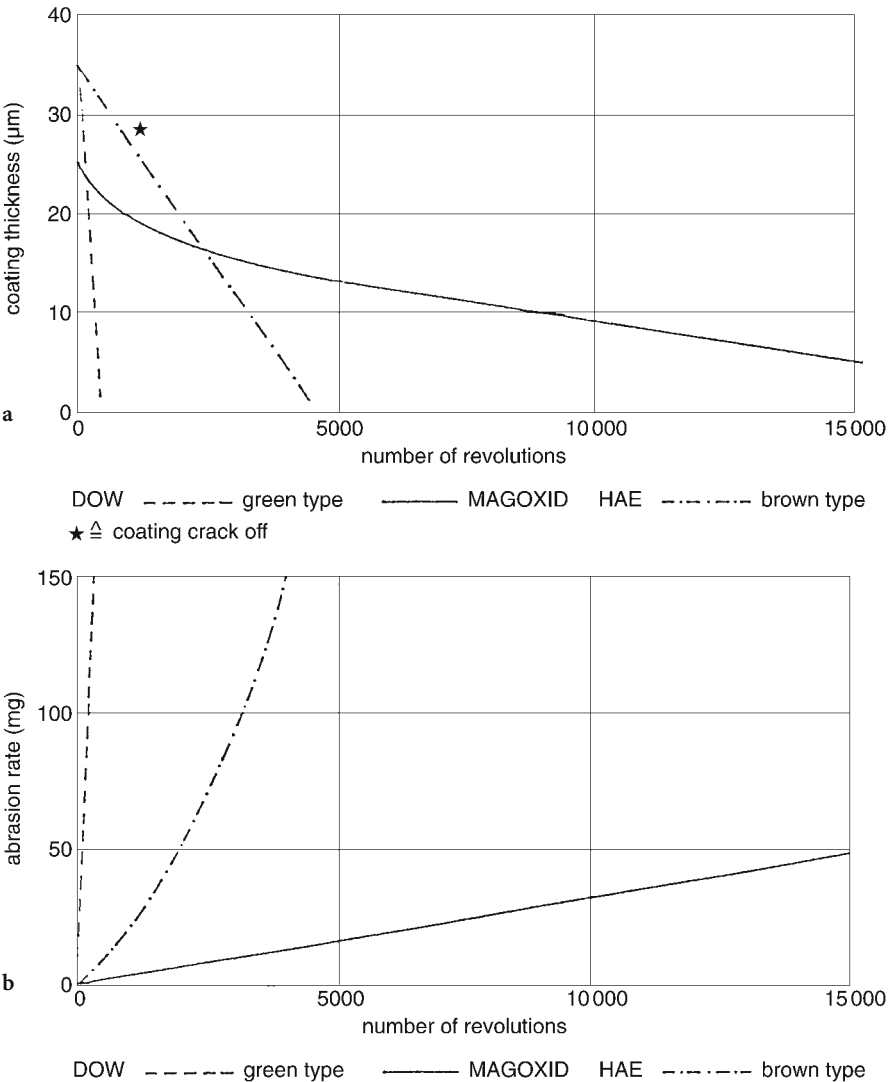


Fig. 7.14. Infiltration at site of scratch on MAGOXID-COAT

sion. The following section attempts to compare the coating systems DOW 17, HAE and MAGOXID-COAT in terms of their respective wear resistance properties. Existing Taber abrasion test results (test conditions: abrasive roller CS10, load 10 N, turning speed of 70 rpm) show that DOW 17 finishes suffer the greatest amount of abrasive wear. HAE coatings are worn right down to the base material after about 5,000 revolutions. MAGOXID-COAT finishes show the lowest amount of wear, with 5  $\mu\text{m}$  of coating still intact after 15,000 revolutions. See Fig. 7.15a for a summary of the test results. Figure 7.15b shows the mass loss rate for different types of coating, as revealed by Taber-abrasion testing. DOW 17 coatings display an abrasion loss of 150 mg after fewer than 1,000 revolutions while HAE systems suffer the same loss of mass after some 4,000 revolutions. MAGOXID-COAT loses just 50 mg to abrasion over 15,000 revolutions.

When the surface roughness of the various coating systems is compared (20  $\mu\text{m}$  coating thickness, initial roughness  $R_z$  of base material AZ 91HP = 2.25  $\mu\text{m}$ ), the MAGOXID-COAT finish emerges as the coating with the lowest surface roughness ( $R_z = 7.66 \mu\text{m}$ ) with respect to HAE (12.66  $\mu\text{m}$ ) and DOW 17 (18.26  $\mu\text{m}$ ). The following additional characteristics of MAGOXID-COAT finishes are also worth mentioning:

- High electrical insulating performance and dielectric strength (30 V/ $\mu\text{m}$ )
- Good thermal stability (up to 350°C)



**Fig. 7.15a, b.** a Coating-thickness loss for different types of finish in Taber-abrasion tests. b Mass-loss rates for different types of finish in Taber-abrasion tests

- The MAGOXID-COAT finish does not reduce the physical strength of the magnesium alloy (e.g., its fatigue strength). See [38–42] for comprehensive published MAGOXID-COAT material.

*TAGNITE Treatment*

This process, which was developed by US company Technology Applications Group [43], can be used on all types of magnesium alloy. It is a two-stage process, in which the first stage involves the electroless application – in a chemical bath

**Table 7.17.** Processing parameters for TAGNITE [43]

Preliminary treatment	Alkaline
Activation (stage one)	0.5–1.2 M $\text{NH}_4\text{F}$ , 70–80°C, 30–40 min
Electrolyte (stage two)	5–7 g/l potassium hydroxide KOH 15–20 g/l potassium silicate $\text{K}_2\text{SiO}_3$ 8–10 g/l potassium fluoride KF pH 12.5–13
Parameters	$i = 1\text{--}5 \text{ A/dm}^2$ , within 30 s increase voltage to 150 V → then continue to anodise at constant current of 3 A/dm <sup>2</sup> End-point voltage (depending on thickness) = 200–400 V $T_{\text{EL}} 10\text{--}20^\circ\text{C}$
Sealing	12% $\text{KH}_2\text{PO}_4$ , 5 min, 60°C

– of a fine conversion layer consisting of magnesium fluoride and/or magnesium ammonium oxofluoride. The second stage consists of an anodic plasma-chemical treatment carried out in an aqueous, strongly alkaline electrolyte, which is a combination of hydroxides, fluorides, fluosilicates and silicates. The use of pulsed direct current (DC) is preferred. Table 7.17 gives a summary of the processing parameters used in TAGNITE treatment.

TAGNITE finishes, which have a white to greyish-white appearance, consist of crystalline  $\text{MgO}$ ,  $\text{MgSiO}_3$  and  $\text{MgF}_2$ . They are produced in two coating classes: type I (5–10  $\mu\text{m}$ ) and type II (20–25  $\mu\text{m}$ ). The TAGNITE coating displays very good corrosion protection properties in salt-mist testing carried out to ASTM-B 117 standards (with a rating of 10 after 700 h) [43]. Referring to [44], it is also apparent that TAGNITE coatings deliver better corrosion- and abrasion-resistance performance – in terms of Taber abrasion testing – than HAE and DOW 17 finishes. The general conclusion to be drawn is that coating systems applied to magnesium-based materials with methods that involve anodic plasma-chemical reactions provide better protection against corrosion and wear than the familiar classic systems that rely on anodic oxidation.

### 7.1.3.6 Galvanic-deposit coatings

The large potential difference between magnesium and the metals used to treat its surface (Cu, Ni, Cr, Zn, Ag, Au, brass) makes the electrolytic precipitation of metallic coatings onto magnesium alloys a special case. Just the slightest imperfection in a metallic coating of this type can lead, in a damp atmosphere, to serious galvanic corrosion – which turns into widespread visible pitting of the underlying magnesium alloy as the metallic coating peels off.

This is why metallic coatings produced by galvanic precipitation should not be used to provide protection against corrosion. There is however a recent tendency to use galvanically deposited coatings in applications in the electronics industry, such as on the casings of laptop computers and mobile telephones. The basic steps involved in the galvanising of magnesium and its alloys are as follows:

1. Surface conditioning
2. Activating

3. Zinc immersion coating
4. Copper striking
5. Standard plating procedures

See [8] for details of formulae used in the galvanising of magnesium and its alloys and [45–47] for details of published research in the field.

Some very recent work refers to electroless precipitated nickel-phosphor coatings for magnesium. Referring to [48], it is apparent that – right after activation – (NB: see basic steps for galvanising) it is possible to precipitate nickel-phosphor coatings onto magnesium-based material. Sharma [49] has examined electroless nickel-phosphor coatings applied to magnesium, and gives data relating to applications and formulae. Depending on the type of application, it is also possible to incorporate particles of hard material (SiC, diamonds) or lubricant particles (PTFE) into the electroless precipitated nickel-phosphor coatings applied to magnesium (the former to provide wear resistance; the latter to reduce friction). Note that the conditions relating to galvanic corrosion with respect to pure metal coatings are likewise valid for electroless precipitated nickel-phosphor coatings applied to magnesium.

#### **7.1.3.7 Application of Coatings Using Physical Methods**

Attempts are currently being made to coat magnesium-based materials by means of physical methods (see Fig. 7.1). These techniques include PVD (Physical Vapour Deposition) and variations such as arc-PVD, plasma-oxidation and arc-PVD ion implantation. Additional alloyed boundary layers, such as the sub-surface implantation of aluminium into the magnesium by means of sputtering, are the object of current research. These boundary layers contain highly stable chemical compounds such as spinel  $\text{MgAl}_2\text{O}_4$ . However, the classical processes – as described in [50] – still serve the purpose of providing aluminium-based diffusion coatings for magnesium alloys with the use of heat treatment in powdered aluminium.

The coating of magnesium-based materials with physical methods is likewise an object of current research, although no actual applicable process is yet available for magnesium alloys.

#### **7.1.3.8 Organic Coating Systems**

Organic coating systems are applied to magnesium and its alloys in order to improve its resistance to corrosion and to enhance its appearance. Note however that this article cannot go into the regulations and standards to be observed in this respect. These matters should be discussed with the firm supplying the coating.

#### **General points**

As already described in Sect. 7.1.2, the thin “air oxide layer” does not cover the entire surface of the magnesium to which it is applied, it contains cracks and imperfections, is susceptible to the action of chemicals and therefore does not provide any long-term protection for the base material. Furthermore, this “air oxide

layer” has few anchoring points to provide a base for any subsequently applied finish, making it unsuitable as a primer coating. If any lacquer- or paint-based coating is in fact directly applied, it suffers from the same lack of long term stability. This is a result of the deterioration and loss of function caused by the strongly alkaline “air oxide layer” ( $\text{pH} > 12$ ). Depending on the application, magnesium should always be treated with conversion coatings (see Sects 7.1.3.3–7.1.3.5) that act as a primer base for further finishes. The conversion layer should be dried thoroughly, as humidity causes corrosion on magnesium, reduces the adhesion of the topcoat and causes bubbles to form while the piece is being fired. It is also important to note, where organic coating systems are concerned, that the methanol or short-warp organic acids contained in organic solvents can lead to serious corrosion of the magnesium-based material. Solvents of this type should therefore not be used.

### **Lacquer/paint-based coating systems**

Once the surface of the magnesium has been pre-treated with a conversion layer, it is suitable for the application of virtually any type of lacquer- or paint-based technique, such as wet-coating technology, electro-dip coating and powder coating. This involves the use of primer systems to improve the adhesion properties of the conversion layer and/or topcoat. The treatments used include such alkaline-resistant products such as acrylates, polyvinyl butyral, phenolic resins, polyurethane and epoxy resins. Personal safety considerations should be taken into account when handling the additives used for improving the corrosion-inhibiting performance of chromates, as these substances are carcinogenic and likely to cause mutations in living organisms.

Tried and tested topcoat systems include those based on alkyd resin, epoxy resin, polyester, acrylate and polyurethane. These all make the final coating harder after firing.

These coating systems possess a range of different properties: Acrylates display the greatest resistance to salts; vinyl-based compounds show a high level of thermal stability (up to  $150^{\circ}\text{C}$ ); alkyd resins are highly resistant to general ambient conditions and epoxy resins offer the best resistance to abrasion. Electro-dip coating is a good method of applying epoxy-based primer to the magnesium surface. This also provides for the consistent coating of objects with complicated shapes. The electro-dip coating technique is widely used in the automotive sector.

Powder coatings are applied to the pre-treated magnesium surface both by electrostatic and fluidised-bed coating. Neither technique involves the use of solvents, thus ensuring that there is no harm to the environment.

However, the particles used in the powder coating process (polyamides, epoxy resins, polyester) must be melted at very high temperatures, which can lead to “blistering” caused by gas escaping from the pores in the cast magnesium. This can be prevented by using cast magnesium with a low pore-count and by heating up the workpiece before it is powder-coated.

Sol-Gel processes [51] are also increasingly being used for the sealing of pre-treated magnesium surfaces.

## 7.2 Corrosion

*Jim Hillis*

### 7.2.1 Introduction

Magnesium alloys have had a poor reputation for corrosion resistance for many decades, particularly in salt-water environments. But the introduction of high purity alloys in the mid-1980s significantly altered the paradigm, providing one of several catalysts leading to growth in the automotive applications of high pressure die castings in the 1990s. The alloys with new limits on heavy metal contaminants provide salt-water corrosion performance that is consistent and competitive with common automotive aluminum die cast alloys. The performance of these alloys may be as much as 2–3 orders of magnitude better than their predecessors when tested in accelerated laboratory or road salt exposures.

The discussion that follows will summarize the requirements for achieving the optimum performance from magnesium alloys in corrosive environments. The factors involved are not unique to magnesium but may be more critical due to the metal's position in the electrochemical series. The factors include the alloy composition and contaminants, the fabricated form, microstructure, surface quality, and assembly practices. In salt-water exposures the assembly practice is important because galvanic attack on the magnesium component can be severe if the materials are not carefully chosen and the components are not designed to mitigate the severity of the corrosion experienced in aggressive environments.

### 7.2.2 Magnesium Protective Films

In general pure magnesium exhibits good resistance to corrosion at ambient temperatures. Electron diffraction studies of the film formed in humid air found that the film is amorphous with the oxidation rate reported to be less than  $0.01 \mu\text{m/y}$ . If the humidity level is sufficient to produce condensate on the surface of the sample, the amorphous film is found to contain at least some crystalline magnesium hydroxide (brucite). On immersion in deionized water, weight-loss studies indicate that a crystalline hydroxide film is formed, which is protective at room temperature. Aeration of the water during immersion was found to have no measurable effect on the composition of the film or the oxidation rate. If the temperature of the water was raised to near the boiling point, however, the protective capacity of the film was found to erode, particularly in the presence of contaminants in either the metal or the water [52, 53]. The chemical reactions then can be summarized as:



In extended atmospheric exposures of magnesium and magnesium alloys, the reaction of the magnesium hydroxide with acid gases (carbon dioxide and sulfur dioxide) was reported to play an important role in the stability and composition of the film. X-ray diffraction analysis of the oxidation products present on unal-



loyed magnesium revealed it consisted of a mixture of crystalline carbonates – hydromagnesite [ $\text{MgCO}_3 \cdot \text{Mg}(\text{OH})_2 \cdot 9\text{H}_2\text{O}$ ], nesquehonite [ $\text{MgCO}_3 \cdot 3\text{H}_2\text{O}$ ], and lansfordite [ $\text{MgCO}_3 \cdot 5\text{H}_2\text{O}$ ], while in an industrial atmosphere with high levels of  $\text{SO}_2$ , traces of  $\text{MgSO}_4 \cdot 6\text{H}_2\text{O}$  and  $\text{MgSO}_3 \cdot 6\text{H}_2\text{O}$  were detected in addition to the hydroxy-carbonate products for the unalloyed metal. It was suggested that  $\text{SO}_2$  exposures accelerate the corrosion of magnesium through the conversion of the protective hydroxide and carbonate compounds to the highly soluble sulfate and sulfite, which are then eroded. In the case of the common commercial aluminum alloy – AZ31 (magnesium, 3% aluminum, 1% zinc, 0.2% manganese) – analysis of the corrosion product by X-ray diffraction revealed only two crystalline phases – hydromagnesite and hydrotalcite [ $\text{Mg}_6\text{Al}_2(\text{OH})_{16}\text{CO}_3 \cdot 4\text{H}_2\text{O}$ ]. The hydrous character of the magnesium films formed in the natural environment means that these films absorb and release water as the moisture content of the atmosphere varies. This absorption/desorption process, in time, results in the disruption of the initially clear structure of the films turning them opaque or frosted in appearance similar to zinc films that are not stabilized by chemical treatments [52, 54]. Like zinc, magnesium alloys can be chemically treated to stabilize the surface film and retard the tarnishing process.

### 7.2.3 Metallurgical Factors in the Corrosion of Alloys

The metallurgical factors affecting the corrosion performance of a magnesium part are the alloy composition and microstructure. The alloy composition refers to both the intentional constituents and the common contaminants. The microstructural factors are the grain size and alloy temper, or heat treatment effects. While these factors are interdependent they will be discussed separately for convenience.

#### *Chemical Composition*

Figure 7.16 summarizes the effect of 14 elements on the salt-water corrosion performance of magnesium in binary compositions. Six of the elements included in the figure (aluminum, manganese, sodium, silicon, lead and tin) have no detrimental effect on the basic corrosion resistance of primary magnesium at levels up to 5% by weight [55]. In addition beryllium, cerium, praseodymium, thorium, yttrium and zirconium have been reported to have no detrimental effect on the salt-water corrosion performance of magnesium at levels exceeding their solid solubility or up to a maximum of 5% [52]. Four elements in Fig. 7.16 (calcium, cadmium, silver, and zinc) are shown to have mild to moderate accelerating effects on the corrosion rate, while four other elements (cobalt, copper, iron, and nickel) are shown to have extremely severe accelerating effects due to their low solid solubility and their ability to serve as active cathodic sites for the reduction of water at the sacrifice of elemental magnesium. Cobalt is not a common contaminant and cannot be readily introduced into magnesium melts; even through long immersion of high cobalt steels at elevated melt temperatures. In this writer's more than twenty-year experience dealing with magnesium corrosion and finishing issues, cobalt has never been encountered at detrimental levels in commercial alloys. The other three elements, however, are common cont-

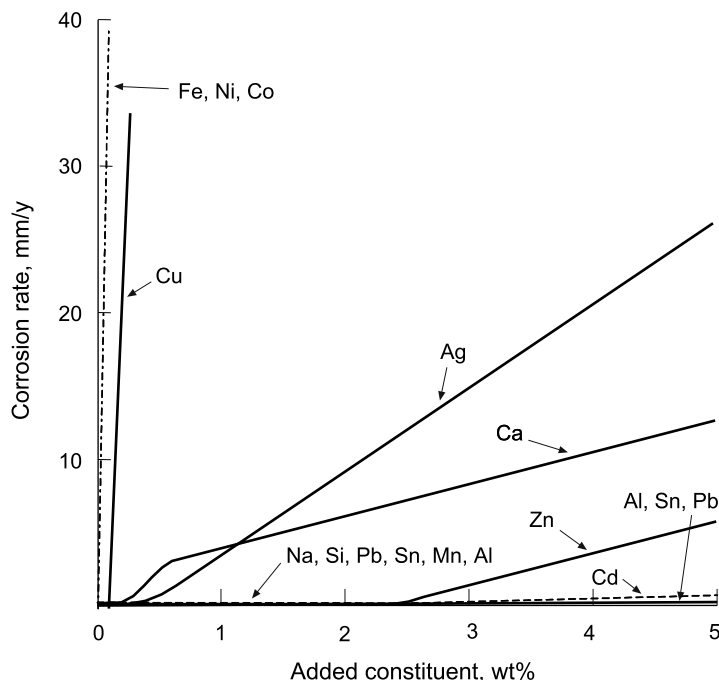


Fig. 7.16. Corrosion rates of binary alloys, by alternate immersion in 3% sodium chloride solution [55]

aminants, which can be easily introduced through normal alloy preparation and processing operations. In order to achieve good corrosion performance from a magnesium alloy it is apparent that the alloy composition should incorporate only compatible elements and that the common contaminants – iron, nickel, and copper – must be controlled to low levels.

Table 7.18 lists the common commercial alloys of magnesium plus three developmental alloys AE42, AJ52 and AX52 along with their nominal compositions. The alloys are described in accord with ASTM practice, as defined in standard B 275, and by European Alloy (EN-) designations, where assigned. The alloys can be divided into two separate families – those containing aluminum and those containing zirconium. These two elements play the critical role of nucleating the formation of magnesium grains during solidification of the alloys such that reasonably fine-grained structures are produced, imparting good mechanical properties, without a negative impact on the corrosion performance of the alloys. The aluminum content varies from 2–10 % depending on the product form and properties desired. In addition to improving the mechanical properties of the alloys aluminum is beneficial to the corrosion performance of the alloys through improved tolerance for the contaminants. The zirconium alloys consistently employ about 0.6% zirconium for the desired grain refining of the alloys. This content is near the solubility limit at normal processing temperatures in the foundry. In addition to improved mechanical properties the zirconium content is beneficial in

**Table 7.18.** Magnesium alloys and their nominal compositions

Alloy designation	Alloyed elements, nominal %										Product form <sup>c</sup>
	Al	Zn	Mn	Ag	Zr	Re <sup>b</sup>	Y	Sr	Ca	Si	
AE42X <sup>d</sup>	4		0.2	...	...	2	...				DC
AJ52X <sup>d</sup>	5	...	0.4	...	...	...	...	2			DC
AX52X <sup>d</sup>	5		0.4						2		DC
AM50A	5	...	0.4	...	...	...	...	...			DC
AM60A, B	6	...	0.2	...	...	...	...				DC
AS41A, B	4		0.4							1	DC
AS21X <sup>d</sup>	2		0.2							1	DC
AZ31B, C, D	3	1	0.2	...	...	...	...				W, A
AZ61A	6	1	0.2	...	...	...	...				W
AZ63A, B, C, D	6	3	0.2	...	...	...	...				C, A
AZ80A	8	0.5	0.2	...	...	...	...				C, W
AZ91B, C, D, E	9	1	0.2	...	...	...	...				DC, C
EZ33A	...	2.5	...	...	0.6	2.5	...				C
M1C			1								W, A
QE22A	...	...	...	2.5	0.6	2	...				C
ZE41A	...	4.5	...	...	0.6	1.5	...				C
ZE63A	...	5.5	...	...	0.6	2.5	...				C
ZK40A	...	4	...	...	0.6	...	...				C, W
ZK60A	...	6	...	...	0.6	...	...				C, W
WE43A, B	...	...	...	...	0.6	3	4				C
WE54A	...	...	...	...	0.6	4	5				C

<sup>a</sup> For complete details see ASTM-B 80, B 90, B 93, B 94, B 107, or B 843.

<sup>b</sup> Total rare earth content.

<sup>c</sup> DC – die cast, C – sand/permanent mold cast, W – wrought products, A – anodes for cathodic protection.

<sup>d</sup> A developmental alloy; see [11] (AE42), [57, 58] (AJ52), [59–61] (AX52X).

melting and processing the alloys by combining with any iron contamination that might be introduced and precipitating it in the pot prior to casting.

Aluminum Alloys

The poor reputation of magnesium alloys for salt-water corrosion resistance is in large part due to the lack of control of the common contaminants – iron, nickel and copper - as indicated in Fig. 7.16 and discussed above. Although the critical importance of these elements was known for more than 50 years, it was not until the mid-1980's that specific maximum limits for each of the contaminants was established in a commercial alloy [62–64]. Figure 7.17 illustrates the effect of increasing levels of each of the three contaminants individually on the ASTM B117 salt spray corrosion rate of high-pressure die cast AZ91 alloy. For comparison the range of salt spray corrosion rates obtained on 380 aluminum alloy parts and automotive cold rolled carbon steel is included in the composite plot. Figure 7.18 shows the visual contrasts in corrosion performance for high purity AZ91D versus AZ91B (~150 ppm each of iron and nickel contamination), cold rolled steel, and die cast 380 aluminum following a 240-hour exposure to ASTM B117 salt spray. As may be seen in the corrosion curves for each of the three contaminants, Fig. 7.17, there is a concentration below which the corrosion rate remains low and constant. This base corrosion rate in the laboratory salt spray test has been found to fall in the range of 0.1 to 0.2 mm/y (or, 0.05 to 0.1 mcd – mg/cm<sup>2</sup>/day), which is lower than the best samples of 380 aluminum die castings or cold rolled steel tested [63, 64]. By calculating the least squares intercept of the corrosion data above and below the area where the acceleration in corrosion begins the con-

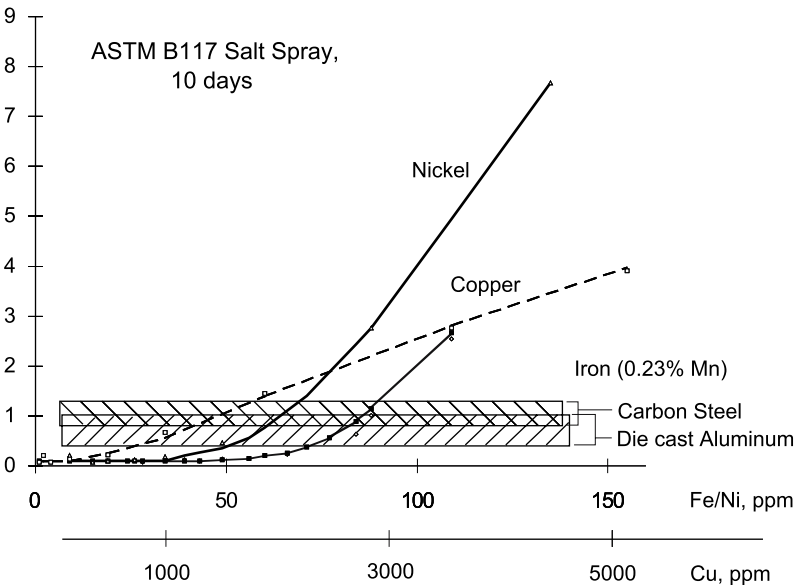
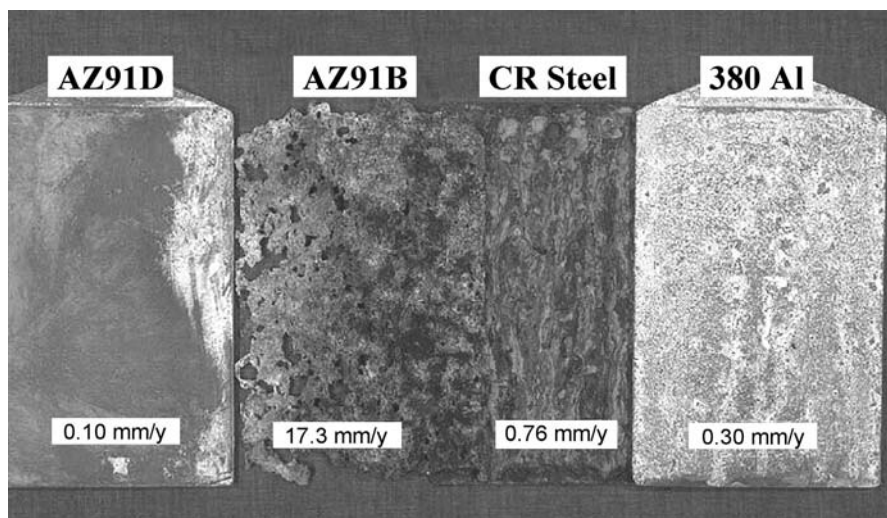


Fig. 7.17. Die cast AZ91 corrosion performance versus Internal contaminant content and versus cold rolled steel and 380 aluminum



**Fig. 7.18.** 240 hour ASTM B117 salt spray corrosion performance of AZ91D versus AZ91B, cold rolled steel and 380 aluminum alloy with measured corrosion rates except AZ91B, samples uncleaned

centration at which the break to higher corrosion rates occurs can be established for each of the contaminants. This has commonly been referred to as the contaminant tolerance limit. Table 7.19 summarizes the known contaminant tolerance limits established to-date for several commercial alloys and developmental alloy AE42 [56, 64–67]. While the specific contaminant tolerance limits have not been defined for the developmental alloys AJ52 and AX52, the corrosion performance at low contaminant levels has been demonstrated to be equivalent to the existing high purity alloys and the specific limits should be defined prior to commercialization alloys in order to assure consistent high purity performance [58, 59].

It should be noted in Table 7.19, that while the nickel and copper tolerance limits are given as absolute values in parts per million, the iron tolerance limit is given as a function of the manganese content – a specific content of 0.3%. This is because the tolerance for the iron contaminant is directly related to the manganese content of the cast alloy [64, 66]. The manganese addition to these alloys has long been known to control the soluble iron content in the alloy melts, but based on more recent data it has been clearly shown to not only affect the solubility of iron in the melt, but also the corrosion activity of the iron which remains dissolved in the melt and is cast to the mold in either high pressure die casting or low pressure sand or permanent mold casting. Thus the iron tolerance for the aluminum alloys is reported not as an absolute concentration but rather as an iron-to-manganese ratio. Table 7.19 includes this critical factor for each of the alloys listed.

Figures 7.19, 7.20 and 7.21 illustrate the impact of manganese on both the iron solubility and the corrosion activity of the residual content in high-pressure die cast AZ91 alloy [64, 66]. In Fig. 7.19 the variation in salt-water corrosion rates versus iron content is plotted for a series of castings produced from AZ91 alloy of

**Table 7.19.** Some aluminum-magnesium alloys nominal alloy element content and known contaminant tolerance limits

Alloy designation	Alloyed elements, nominal %							Contaminant tolerance, ppm				
	Al	Zn	Mn	RE <sup>b</sup>	Si	Sr	Ca	Fe (0.3 Mn)	Ni	Cu	Fe/Mn ratio	Product form <sup>c</sup>
AZ91D	9	1	0.2	...	...	...		96	50	400	0.032	DC
AZ91E-T6	9	1	0.2	...	...	...		138	20	400	0.046	SC
AM60A, B	6	...	0.2	...	...	...		63	30	100	0.021	DC
AM50A	5	...	0.4	...	...	...		48	30	100	0.016	DC
AS41B	4	...	0.4	...	1	...		30	40	200	0.010	DC
AE42X <sup>d</sup>	4	...	0.2	2	...	...		64	200	1000	0.02	DC
AJ52X <sup>d</sup>	5	...	0.4	...	...	2		under development			DC	
AX52X <sup>d</sup>	5	...	0.3	...	...	< 0.2	2				DC	
AZ31A	3	1	0.5	...	...	...		39	...	...	0.013	W
AZ61A	6	1	0.3	...	...	...		63	...	...	0.021	W

<sup>a</sup> For complete details see ASTM-B 80, B 93, B 94, or B 107.

<sup>b</sup> Total rare earth content.

<sup>c</sup> DC – die cast, SC – sand cast, W – wrought.

<sup>d</sup> A developmental alloy; see [56] (AE42), [57, 58] (AJ52), [59–61] (AX52X).

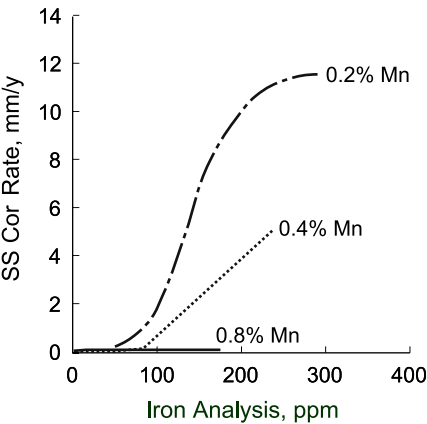


Fig. 7.19. Die cast AZ91 corrosion rates versus analyzed iron content at three levels of manganese content

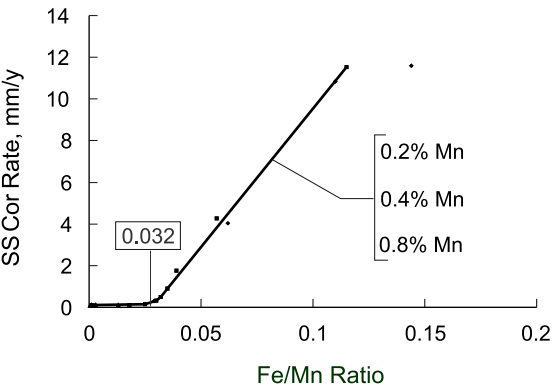
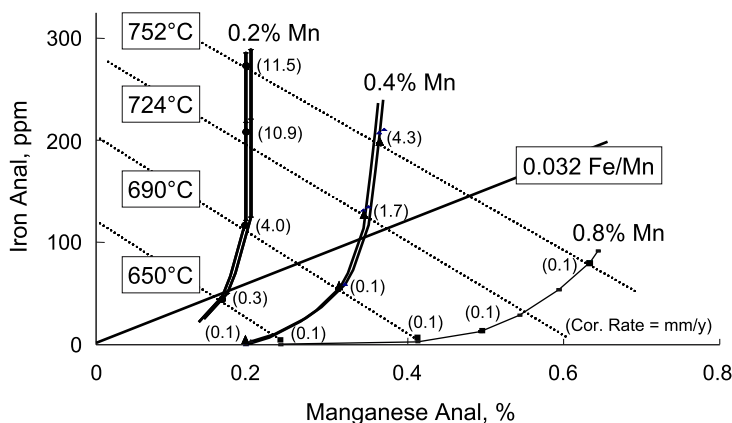


Fig. 7.20. Die cast AZ91 corrosion rates versus Fe to Mn ratio for alloy of three levels of manganese content

three differing levels of manganese content. Here the corrosion rates begin to accelerate at progressively lower iron contents as the manganese content drops in each series and the rate of rise for incremental increases in iron content is also greater for the lower levels of manganese content. In Fig. 7.20 the corrosion data for the same three series of castings is plotted not versus the iron content, but the iron-manganese ratio. This results in one corrosion response for all three alloys with the break to higher corrosion rates occurring at an iron-manganese ratio of 0.032 and with the same slope, or rate of rise in corrosion rates beyond the break for the differing manganese contents.

In Fig. 7.21 several trends are superimposed on the same plot of iron versus manganese content. The data summarized here is for the same three heats of AZ91 for which the corrosion performance of cast samples is summarized in Figs. 7.19 and 7.20. The vertical curves labeled – 0.2%, 0.4% and 0.8% manganese



**Fig. 7.21.** AZ91 iron and manganese mutual solubility and the critical iron-manganese ratio – derived from three alloy heats of differing nominal manganese content

– represent the trend in iron and manganese content as the melt was cooled from the manganese alloying temperature of  $\sim 750^{\circ}\text{C}$  to each of the successively lower melt temperatures indicated –  $724^{\circ}\text{C}$ ,  $690^{\circ}\text{C}$ , and  $650^{\circ}\text{C}$ . In each case the initial iron content of the Al-Zn-Mg melt analyzed  $\sim 390$  ppm prior to the manganese addition. The diagonal lines sloping downward, left to right, represent the mutual solubility limits for iron and manganese for each of the four temperatures indicated. The diagonal line sloping upward, left to right, is the iron-manganese tolerance limit ratio of 0.032. Examination of the plot reveals that indeed there is a linear decrease in iron solubility as the manganese content is increased at each of the four temperatures employed in the experiment. The data also reveals, that on cooling, the melt first loses iron and then iron and manganese simultaneously at the lower manganese contents. In all cases when the iron content drops below the critical ratio the loss of iron and manganese occurs simultaneously. The numbers noted adjacent to each data point along the curves represent the salt spray corrosion rate (mm/y) determined for die cast samples produced at that melt composition. From this data it is apparent that samples cast from the iron and manganese contents below the 0.032 ratio are all low corroding due to the separation of iron with manganese within the microstructure of the castings. The phase which precipitates is thought to be  $\text{Al}_5(\text{Mn-Fe})_2$ , based on x-ray diffraction analyses and chemical analysis of the intermetallic rich sludge found in the pot bottom. By inference it seems reasonable that the phase which precipitates free of manganese at compositions above the critical iron-manganese ratio is not iron but an iron-aluminum intermetallic,  $\text{Al}_5\text{Fe}_2$  or  $\text{Al}_3\text{Fe}$ , either of which would be active catalysts for the corrosion of the magnesium matrix and result in the elevated corrosion rates noted in Fig. 7.21.

The iron-manganese solubility and the iron-manganese tolerance were established for each of the alloys in Table 7.19 in the same manner outlined for AZ91 above [56, 64–67]. The interaction of the manganese, iron and aluminum content and the measured corrosion performance was much the same in each



case, with a consistent trend to lower iron-manganese ratios as the aluminum content of the alloys decline, with one exception – the AE42X alloy, where the tolerance limit for all three contaminants is 2–5 times higher than for AS41 alloy, apparently due to the rare earth constituent [56].

### *Zirconium Alloys*

The zirconium family of alloys should be capable of providing corrosion performance similar to that of the high purity aluminum alloys discussed above, however, many of these alloys contain zinc or silver at levels above that identified as moderately accelerating the corrosion of the magnesium matrix. While the corrosion resistance of these alloys should be anticipated to be worse than the high purity aluminum alloys, the performance is typically better than the aluminum alloys prior to the 1980s. The zirconium family of alloys is normally used in low-pressure sand cast or permanent mold cast applications. None of the alloys are commonly high-pressure die cast and they have not therefore participated in the recent growth of magnesium applications in the automotive industry.

The alloys based on yttrium and rare earths plus zirconium, WE54 and WE43, have been demonstrated to provide corrosion performance equivalent to the high purity aluminum alloys [68]. The recently introduced WE43B is an improved composition with tight limits on the common contaminants for improved salt-water corrosion resistance in sand or permanent mold cast applications. Due to the cost of the yttrium these alloys have been limited to premium aerospace applications or other weight critical applications, where good mechanical properties at elevated temperatures are required.

### *Wrought Alloys*

Based on the statistics from the International Magnesium Association for the year 2000, wrought magnesium alloys accounted for less than 1% of the total magnesium market and about 3% of all magnesium alloy shipments that year. Consequently, little data has been generated on these alloys in recent years. The aluminum alloys – AZ31, AZ80 and AZ61 – would appear to have the same potential for low corrosion rates as the die cast alloys, but to-date complete tolerance data for the alloys is not available, as indicated in Table 7.19. The published corrosion data available for the alloys, therefore, indicates that these alloys and the zinc-zirconium alloys- ZK60 and ZK40 – are generally comparable to the standard cast aluminum alloys of prior to the high purity development [52, 69].

### *Heat Treatment and Grain Size Effects*

In Table 7.19 it may be noted that low pressure cast alloy AZ91E is listed in the T6 condition (a “solution treated and aged” temper), and that the nickel tolerance limit is listed at less than half that of the die cast alloy, while the iron tolerance is about 50% greater. The variation in contaminant tolerance between the high-pressure die cast composition and the low pressure cast material is attributed to the slower solidification rates associated with the permanent mold cast samples used in generating the data (average grain size 70–150  $\mu\text{m}$ ) versus the high pressure die cast samples ( $<10 \mu\text{m}$ ). The behavior of the die cast material versus the

low pressure cast material has not been fully explained, but - in addition to the precipitation of active contaminants within the microstructure of the low pressure casting - it may involve simply the segregation of the contaminants between the magnesium phase and the aluminum rich grain boundary phase, which could activate the cathodic phase, leading to increased corrosion in salt water exposures. The variation in corrosion performance can be very pronounced for samples of identical composition. Low pressure cast AZ91 of low iron, nickel and copper content can yield "as-cast" (F temper) corrosion rates near 2 to 4 mm/y, where the same die cast composition would produce salt spray corrosion rates near the base rate of 0.1 mm/y. If the same "as-cast" material is either "solution treated and aged" (T6 temper) or simply "aged" (T5 temper) the corrosion rates will consistently be less than 0.2 mm/y, and often 0.1 mm/y, through standard ASTM salt spray (see Table 7.20) [64, 66].

Table 7.20 summarizes the behavior of several AZ91 melts cast at varying manganese and iron contents, with and without grain refining, and then salt spray corrosion tested in each of the common alloy tempers - F, T4, T6 and T5. The "unsanded" and "sanded samples" refer to the surface condition of the samples tested. The "Unsanded" - F temper results represent the salt spray corrosion rates determined for the "as cast" samples with the foundry finish unaltered. The other four columns of corrosion results represent the performance of castings that had been heavily sanded to remove all traces of the foundry finish and possible surface effects. Initially, disregarding the samples cast from melt 3a and 3b and looking only at the series of sanded samples - it is clearly evident that the F and T4 corrosion rates are significantly greater relative to the standard high purity die cast performance, with significant dependence on the grain refining process, or grain size, and with considerable variation associated with each result. In the T5 and T6 tempers, however, the variation is much reduced and the corrosion rates are consistently 0.2 mm/y or less, virtually the same as high pressure die cast material. Turning to corrosion data from melt 3, this represents the alloy composition and corrosion performance associated with the old sand cast alloy AZ91C, typically low in manganese and high in iron. Here the effect of temper and foundry finish is of no noticeable difference, due to the exceptionally high corrosion rates and the associated large scatter.

Figure 7.22 illustrates the contrast in salt spray corrosion performance associated with the high purity AZ91E versus the former standard AZ91C in the T6 temper. For the samples cast from high purity melts 1, 2, and 4, however the foundry finish ("F-unsanded") produced corrosion rates that were very high versus the sanded samples in the F temper. Examination of the surface by SEM/EDS revealed that the foundry finish was contaminated with steel particulate from the shot peening process used prior to the application of the chromate treatment. Although the samples had been acidized following the shot peening operation the acid bath had not been properly maintained and the acid content had declined, such that the treatment was insufficient to fully clean the surface prior to chromating [64]. Obviously, the use of high purity alloy in the casting of magnesium alloys is not sufficient to assure the corrosion performance of the finished components. The issues that can negate the use of high purity alloy in the production of magnesium parts whether produced as die castings, sand or permanent mold

**Table 7.20.** Sand cast corrosion results – AZ91 alloy

Melt	Grain size, $\mu$	Fe, ppm	Mn, %	Fe/Mn	Salt spray corrosion rates, mm/y				
					Unsanded		Sanded samples		
					F	F	T4	T6	T5
1a	146	20	0.23	0.008	$6.05 \pm 0.1$	$0.62 \pm 0.1$	$4.0 \pm 0.4$	$0.16 \pm 0.04$	$0.12 \pm 0.02$
1b	78	22	0.26	0.008	$8.3 \pm 0.6$	$2.26 \pm 0.10$	$1.8 \pm 0.4$	$0.12 \pm 0.04$	$0.12 \pm 0.04$
2a	135	23	0.37	0.006	$4.2 \pm 0.6$	$0.28 \pm 0.02$	$4.4 \pm 0.90$	$0.24 \pm 0.04$	...
2b	68	22	0.24	0.005	$8.8 \pm 1.2$	$2.0 \pm 0.2$	$1.3 \pm 0.4$	$0.18 \pm 0.04$	...
3a	187	161	0.18	0.87	$17 \pm 5$	$17 \pm 5$	$15 \pm 5$	$15 \pm 7$	...
3b	66	162	0.16	0.099	$25 \pm 2$	$17 \pm 1$	$15 \pm 5$	$16 \pm 10$	...
4a	160	12	0.33	0.004	$6.4 \pm 0.8$	$0.3 \pm 0.1$	$3.0 \pm 0.8$	$0.22 \pm 0.1$	$0.12 \pm 0.02$
4b	73	15	0.35	0.004	$7.0 \pm 0.2$	$0.4 \pm 0.2$	$0.8 \pm 0.2$	$0.10 \pm 0.08$	$0.10 \pm 0.02$

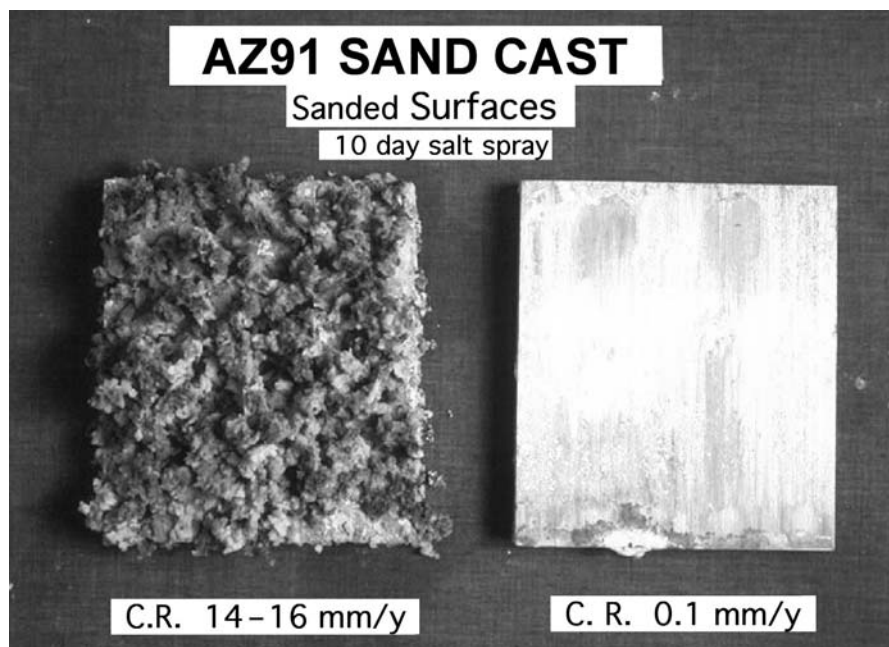


Fig. 7.22. Sand cast salt spray corrosion performance of AZ91 T6 alloy-typical AZ91C (left; Fe/Mn = 0.87) versus AZ91E (right; Fe/Mn = 0.004) performance clean sanded surfaces

castings, or fabricated from wrought products will be discussed later under “Common Causes of Corrosion Failures”.

#### 7.2.4 Stress Corrosion

Pure magnesium can be considered immune to stress-corrosion cracking (SCC) in both atmospheric and aqueous environments, with no reported failures occurring when loaded to its yield strength [53, 70, 71].

Aluminum containing alloys of magnesium are generally considered the most susceptible to SCC, with the tendency increasing with the aluminum content. Thus the alloys AZ61, AZ80, and AZ91 with 6, 8, and 9% aluminum, respectively, can show high susceptibility to SCC in laboratory and atmospheric exposures, while AZ31, a 3% aluminum alloy used in wrought product applications, is considered to show good resistance [70, 24, 72].

Magnesium-zinc alloys such as ZK60 and ZE41 that are alloyed with zirconium, or zirconium and rare earth elements are typically considered only mildly susceptible, while magnesium alloys, containing no aluminum or zinc, are the most SCC-resistant. Thus, M1 alloy, a 1% manganese alloy, like unalloyed magnesium itself, shows no evidence of SCC when placed under tensile stresses as high as its yield strength [53, 63].

In controlled laboratory exposures it has been shown that SCC occurs only when the relative humidity exceeds 85 to 98% with O<sub>2</sub> or CO<sub>2</sub> additions slightly

accelerating the rate [24, 73]. In atmospheric exposures rainfall, dew, and high humidity have been reported to accelerate SCC of magnesium alloys, with failures often occurring during the drying period following a rain [72, 74]. Yet, a comparison of identical materials in rural, industrial, and seacoast exposures produced nearly identical results, suggesting that SCC severity is not necessarily associated with the corrosivity of the environment [53, 75]. To-date, standard and preferred procedures for the evaluation of SCC in magnesium alloys have not been established.

In aqueous exposures, only strong alkalis, concentrated hydrofluoric acid, and chromic acid are considered not to induce SCC in magnesium alloys [53]. In other exposures from deionized water to a wide variety of aqueous salt solutions SCC failures have been observed in full, partial, or alternate immersion [76]. The most severe acceleration of failures has been found to occur with  $\text{NaCl} + \text{K}_2\text{CrO}_4$  solutions which have been used in many laboratory studies of magnesium SCC; however, the results have been found to correlate poorly with service experience [72, 75, 77].

Both transgranular and intergranular crack propagation have been reported for magnesium alloys, however, transgranular failures with significant secondary cracking, or branching, are the most common mode of failure. Of the many mechanisms proposed over the years, hydrogen embrittlement is best supported by experimental evidence such as: crack initiation and propagation are accompanied by hydrogen evolution; immersion in a cracking solution before the stress is applied produces a fracture similar to a SCC fracture; the effect of pre-immersion in a cracking solution is reversed by vacuum annealing or exposure to room temperature air; or testing in gaseous hydrogen results in the same crack characteristics produced in an aqueous solution test [78, 79].

As with other metals, the control of magnesium SCC failures has involved the control of the three factors required for SCC to occur: the long-term tensile stress above a critical level, on a susceptible alloy, in a SCC inducing environment. In practice this has been interpreted as designing to continuous loads of 30–50% of the yield stress and employing finishes which serve as effective corrosion barriers, combined with the selection of less susceptible alloys, where feasible. Design precautions should also include limiting the stresses in bolting and riveting components together, and the use of heat treatments to relieve the stresses induced by welding [76, 80].

### 7.2.5 Corrosion Fatigue

Magnesium alloys in die cast and wrought forms show fatigue properties, which are dependent on a number of factors similar to those for other materials – the mechanical process induced topography (or roughness), surface defects, residual compressive stresses, as well as the environmental exposure. In Fig. 7.23 the rotary fatigue performance of extruded AZ31 and high pressure die cast AZ91 samples, with various surface treatments are compared in air and a corrosive environment of 3.5% sodium chloride solution. The surface treatments include electro polished, shot peened and roller-burnished. The advantage of the compressive stresses induced by roller-burnishing is clear in both the air and corro-

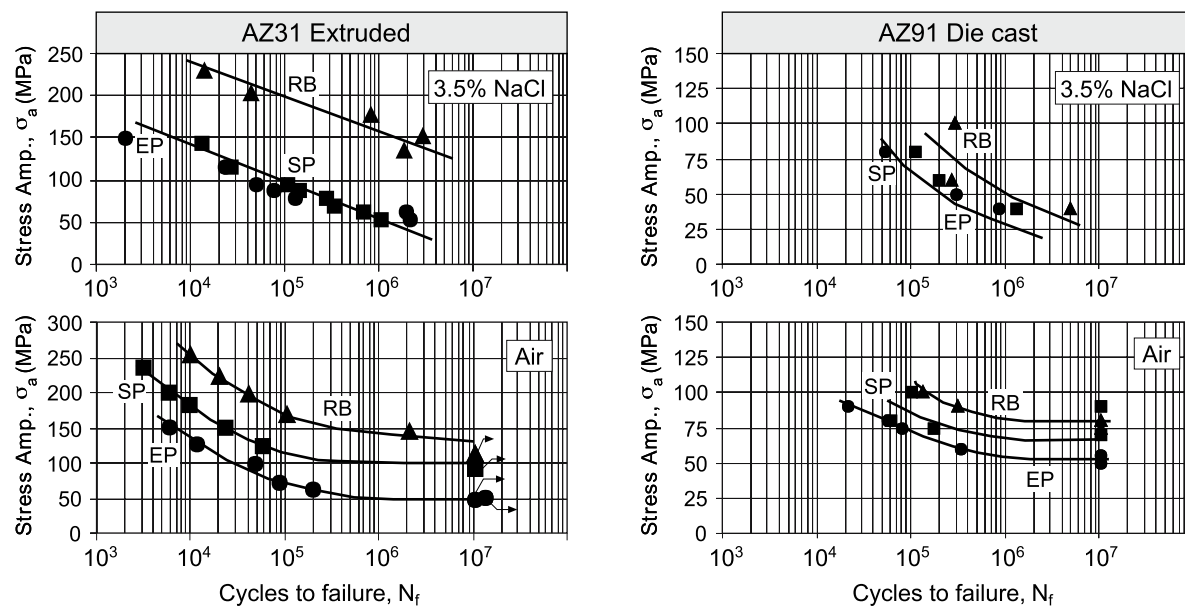


Fig. 7.23. S-N curves for extruded AZ31 and die cast AZ91 in NaCl and air: EP – electropolished; SP – shot peened; and RB – roller-burnished [81]

sive saltwater exposures, but in the case of the shot-peening, while the fatigue performance is improved when evaluated in dry air, in the corrosive salt-water environment the advantage of the compressive forces appears to be fully off-set by either the roughness of the surface [81], or perhaps the corrosion induced by embedded blast contaminants. In each case, however, the corrosive environment results in a significant reduction in the fatigue performance of similar samples. However, the effect on fatigue performance does not seem to correlate consistently with the severity of the environment in some cases as noted by Ferguson, Lui, Ross and MacCulloch [82]. For example, the bending fatigue limit for AM50 die cast samples tested in air and seawater was repeatedly found to be 105 MPa in both environments, but when tested in deionized water the endurance limit was reached at stress amplitudes as low as 70 MPa. Further evaluations of the environmental effects on magnesium fatigue will be required to resolve these seemingly anomalous results.

In earlier studies Loose [53] summarized data for AZ61A and AZ31A sheet subjected to plate bending at 1500 cycles per min in both a dry air exposure and in a 0.01% sodium chloride spray. At  $10^7$  cycles the observed fatigue strength was 103 MPa and 117 MPa (15 and 17 ksi), respectively, in air versus 34 MPa and 40 MPa (5.0 and 5.8 ksi), respectively, in the salt spray. In a summary by Bothwell [52] it was related that AZ31 subjected to an axial load cycled at  $10^5$  cycles per h in air and then subjected to increasing levels of humidity showed a slow decrease in the fatigue strength once the humidity exceeded 50%. At 93% relative humidity, the measured fatigue strength had declined to about 75% of that in dry air, or about 124 MPa (18 ksi), while in condensing humidity the strength was 89 MPa (13 ksi). Interestingly, in total immersion in deionized water, or deionized water saturated with magnesium hydroxide, the fatigue strength was reported to be 124 MPa (18 ksi). This improvement in the fatigue strength was suggested to be due to the reduced exposure to atmospheric carbon dioxide in the total immersion environment.

As with SCC the effects of the environment on corrosion fatigue have been found to be mitigated by painting the components with a suitable coating [52, 70, 82].

### 7.2.6 Common Causes of Corrosion Failure

The selection of a high purity alloy for the production of a magnesium component will not guarantee the finished part will not suffer from corrosion. Causes for corrosion failures with high purity magnesium alloys include contamination during melting and casting operations as well as surface contamination during secondary operations. Some of the more common causes are listed below.

#### 1) Internal Contamination Sources

- Iron Contamination (die, sand and permanent mold castings) – Iron contamination of high purity aluminum alloys is often a problem in start-up operations in the casting foundry. The use of new or freshly cleaned steel pots and transfer equipment lead to accelerated pick-up of iron by the magnesium melt. Under normal operating circumstances the manganese content of the alloy

will suppress the pick-up to levels within the alloy specification limits. However, in start-up operations problems are often encountered with the casting equipment, resulting in long delays, which can lead to excessive pick-up. In addition to the preceding factors the melt temperature is also a factor in the iron pick-up. The higher the temperatures employed the higher the rate of pick-up.

- Nickel Contamination (die, sand and permanent mold castings) – Nickel contamination of magnesium melts will occur where nickel bearing steels are immersed in the molten metal. While 400 series chrome steels and carbon steels can be used safely in magnesium melts, 300 series alloy steel containing nickel should be avoided. A few inches of a thermal well in a 300-series stainless steel immersed in a magnesium melt is sufficient to contaminate the melt with excessive nickel in a few short hours. Again, the rate is temperature dependent.
- Copper Contamination (die, sand and permanent mold castings) – The most common source of copper contamination in the foundry is aluminum alloys. It is not uncommon for an aluminum casting to find its way into the magnesium melt. Since aluminum alloys typically contain significant copper, the magnesium melt can easily exceed the specified limit. To minimize the potential for such problems, it is common for aluminum casting operations to be physically separated from magnesium operations. Where recycling operations are involved, it is also possible that parts with brass bushings may find a way into the recycle melt.
- Flux Contamination (Cast and Wrought alloys) – Until the early to mid 1970s magnesium alloys were commonly processed using molten salts for protection against excessive burning in the melting pot. Today fluorine compounds in blends with air or CO<sub>2</sub> are commonly used in die casting, permanent mold casting operations, but recycling and primary production of alloy ingot in many cases still employ magnesium salt fluxes in processing. Many sand casting operations also use salt fluxes in melting and refining operations. When used, the potential for flux-oxide contaminants occurs. Their presence in a casting, or wrought product, is typically noted by the formation of white corrosion products, which appear on bright machined surfaces after an overnight exposure to nothing more than atmospheric humidity. Humidity exposure of a fractured or machined surface is a common test for such inclusions [24].

## 2) Surface Contaminant Sources

- Blast residues (die castings and sand castings) – Parts are often blasted to improve the uniformity of appearance, smooth parting lines and “clean”, or brighten, the part surfaces. Regardless of whether the media used is steel shot, sand, ceramic grit, glass bead, plastic bead, aluminum wire, aluminum bead, or high purity aluminum oxide, the corrosion performance will be degraded to a degree. As noted in the earlier discussion on low-pressure sand castings, shot peening with steel media can have very detrimental effects on the surface quality of the sand casting. The other media here are listed in their approximate order of improving compatibility. Chopped aluminum wire and aluminum beads of 3, 5, or 6 thousand series alloy compositions can result in relatively modest effects as can high purity alumina. But, surface contamination of the media by the blast equipment can often be transferred to the magnesium eliminating the anticipated cleanliness and leading to disappointing cor-



rosion performance. A short acid etch of the blast treated parts, even steel shot peened parts, can restore the high purity performance [64, 68].

- Heat treating (low pressure castings) – Solution heat treatments used for the production of the T4 and T6 tempers is sometimes done under  $\text{CO}_2$  or  $\text{CO}_2 + \text{SF}_6/\text{SO}_2$  protective atmospheres. The high temperatures involved burn-in carbon contamination due to reactions with the  $\text{CO}_2$  content of the atmosphere. The result is a significantly elevated corrosion rate, although not as severe as that associated with blast residues. Mechanical or chemical cleaning can be used to reestablish the surface cleanliness and optimum corrosion resistance.
- Contaminants from the die surface (die castings) – The die cast corrosion performance of the “as cast” surface is often quite variable due to the history of the die and the die lube practice. Minimizing the die lubricant can produce part surfaces of good uniform appearance with few flow marks and little sticking tendency. However, test results, although of limited scope, suggest that the best-looking surfaces are sometimes higher corroding, apparently due to more iron pick-up from the die surface. Mechanical or chemical cleaning can be used to assure surface cleanliness and optimum corrosion resistance.
- Contaminants in the water used in dilution of the die lubricant (die castings)
  - tap water should not be used for dilution of lubricants without at least some controls on the water quality.
- In compatible lubes (die cast/wrought) – graphite-containing lubricants must be avoided.
- Surface Treatments (all metal forms) – Pre-paint chemical treatments should be carefully selected for compatibility with magnesium. Nickel or copper salts should be avoided but iron phosphates are compatible and effective non-chromate treatments for painting or adhesive bonding. Treatments of low acid content should only be used on well pre-cleaned surfaces. See the discussion below.
- Welds (low pressure cast/wrought products) – Weld materials should be carefully selected for purity consistent with the alloys involved, but the high temperatures involved have the potential for burning cathodic contaminants into the surface. New welding technologies and practices should be carefully evaluated, not only for the mechanical strength, but also for the impact they might have on the internal and surface quality of the affected area. Surface contaminants can be dealt with, but cathodic contamination within the weld metal could be a much more severe problem. In order to minimize the potential for SCC failures, all welds should be stress relieved.

### *Surface Cleaning*

The cleaning options available for dealing with the above sources of contamination are basically the same as those used with other metals, including – mechanical, solvent, alkaline, and acid treatments [30]. These are summarized in Table 7.21 with the method of application and common uses. Despite the potentially severe effects of shot blasting, it is often used on magnesium parts without consequence by using an acid pickle to remove the residual contamination from the part surfaces [64, 68]. A common, effective mechanical cleaning method for die cast parts is barrel, or vibratory bowl abrading using ceramic media and a

**Table 7.21.** Common cleaning processes for magnesium alloys

Type	Method	Use
Mechanical	Wire brushing; Sand, shot, grit, or wire blasting; Barrel or bowl abrading	Rapid removal of heavy layers of oxide, charred die lube, sand mold residues, and dirt. Also for smoothing surfaces of castings. (Should always be followed with an acid pickle for removal of residues)
Solvent	Dip or spray rinse, vapor degreasers, emulsion cleaners	Removal of excess oily matter following machining or prior to alkaline cleaning; touch cleaning prior to painting or adhesive bonding
Alkaline	Dip or spray soak, electrolytic immersion	Removes last traces of oils or waxes prior to application of chemical treatments for painting or adhesive bonding; removes old chemical treatments in many cases; effectively removes contaminants from cathodic areas of aluminum and zinc alloys
Acid pickle or etch	Dip or spray	Chemically mills imbedded contaminants from part surfaces; Conditions surface for selected chemical treatments

rinse solution. This method can be used without the problem of residual contamination when compatible media are used. It is often used in the lawn/garden and power hand tool applications as the only surface preparation prior to treating and painting. In the case of aluminum alloys of magnesium that have not been abrasively cleaned, it is important in chemically cleaning the part that both an alkaline and acid treatment are used in order to fully clean the part surface. Surfactants can be added to commercial phosphates to deal with small amounts of residual lubricants or machining oils on the part surface, but because there is often considerable surface segregation of the aluminum-phase they cannot serve as effective one-step cleaning and pre-paint treatments. This is due to the fact the aluminum phase, being cathodic to the magnesium surrounding it, is electrochemically protected from the etching action of the acid medium. Consequently the contaminants on the aluminum phase will remain and serve as catalysts for corrosion of the surrounding magnesium. Alkaline, high pH, cleaning with strong caustic solutions will etch the aluminum rich areas while passivating the surrounding magnesium and degreasing the entire surface. The acid treatment will then complete the cleaning process by etching the magnesium rich regions and providing a strong adherent film for painting or adhesive bonding.

Surface cleaning is a necessary first step in magnesium finishing and will be discussed in more detail in the following section on finishing.

## 7.2.7 Environmental Factors

### 7.2.7.1 Acidity/Alkalinity

The chemical resistance of magnesium and magnesium alloys is typically considered opposite to that of aluminum and its alloys. Magnesium resists attack by alkaline substances, but is attacked by acids, while aluminum is attacked by alkalis but has reasonable resistance to attack by mild acids. There are two notable exceptions to magnesium's lack of resistance to acids and these are chromic ( $\text{H}_2\text{CrO}_4$ ) and hydrofluoric (HF) acids. In both cases the resistance is the result of the formation of insoluble protective films. Consequently, both acids are employed in formulations for pretreatments for painting and surface anodize treatments [69]. While pure chromic acid has a very limited affinity for metallic magnesium, it will readily dissolve magnesium hydroxide corrosion products. Consequently, a boiling solution of 20% chromic acid is commonly used for the removal of magnesium corrosion products for refinishing parts as well as for establishing weight loss corrosion rates in the laboratory.

The strong alkalinity of the natural hydroxide film on magnesium means there is little tendency for the compound to give up a proton to strong alkalis; consequently, the film provides excellent protection even in strong hot alkali solutions that would readily attack aluminum or zinc alloys. Hot 10% caustic or caustic plus alkali metal phosphate solutions maintained at a pH of 11 to 13 or more are the preferred cleaning solutions for magnesium castings and extrusions [69]. The protective capacity of the magnesium hydroxide film at high pH apparently overwhelms the effects of impurities in both the metal and aqueous media. Loose [53] points out that the measured corrosion rate for magnesium in 4% NaCl is 0.15 to 0.30 mcd (0.30 to 0.60 mm/y) at 35°C, while in 48% caustic with the same 4% NaCl content the corrosion is only 0.01 to 0.02 mcd (0.02 to 0.04 mm/y). Magnesium's resistance to alkali attack combined with the metal's light weight has made it the preferred material for cement finishing tools for many years.

### 7.2.7.2 Specific Ions/Salts

Salt solutions vary in their corrosivity to magnesium. Alkali metal or alkaline-earth metal (chromates, fluorides, phosphates, silicates, vanadates, or nitrates) cause little or no corrosion. Chromates, fluorides, phosphates, and silicates in particular are frequently used in the chemical treatment and anodizes for magnesium surfaces due to their ability to form somewhat protective films [69, 73, 83–86]. Alkali or alkaline-earth metal (chlorides, bromides, iodides, and sulfates) will normally accelerate the corrosion of magnesium in aqueous solutions. Ammonium salts usually show greater activity than the alkali metal salts, apparently due to the acidity of these salts. Practically all heavy metal salts are likely to cause corrosion, since magnesium will normally displace heavy metals from solution due to its high chemical activity. Such displaced metals may tend to plate on the magnesium surface and provide cathodic sites for galvanic corrosion [53, 69]. There is at least one notable exception to this anticipated activity of heavy metal salts and that is iron phosphate solutions. Iron phosphates react to form surfaces

suitable for paint application. Even parts treated at elevated temperatures or baked at high temperatures (300 to 400°F) show no evidence of active heavy metal deposits even on high purity alloys [73, 83]. This is consistent, however, with the ability of phosphate systems to sequester or strongly complex metal ions at moderate to high pHs.

#### **7.2.7.3 Elevated Temperature**

Magnesium's corrosion performance in pure water is strongly dependent on temperature. In distilled water the corrosion rate of AZ61 alloy is reported to increase from less than 25  $\mu\text{m/y}$  to 500  $\mu\text{m/y}$  at the boiling point. This is typical of the commercial magnesium-aluminum and magnesium-aluminum-zinc alloys and these are reported to be among the best alloys for their resistance to aqueous corrosion environments [52, 53, 69]. Pure magnesium in distilled water is reported to corrode at 16 mm/y at the boiling point. Fluoride ion has been reported to be an effective inhibitor for the corrosion of magnesium in water, while sodium carbonate, sodium silicate, and sodium phosphate are not. Thus, A3A alloy (magnesium-3% aluminum-0.2% manganese) when boiled for 31 days in a 0.025 N  $\text{NH}_4\text{F}$  solution showed no discernible attack while the corrosion rate in pure distilled water was reported to be 1.0 mm/y [52].

Magnesium corrosion resistance is typically considered to be good in dry air to about 400°C and to about 350°C in moist air. Magnesium with small alloy additions of zirconium or beryllium has been used in gas-cooled nuclear reactors in England and France, where operating temperatures exceed 350°C. These alloys are reported to have adequate corrosion resistance in wet  $\text{CO}_2$  and wet air at temperatures to 500°C [24, 52].

#### **7.2.7.4 Organic Compounds**

Organic compounds, with a few exceptions, have little effect on magnesium and its alloys. Reference [70] contains a large summary of specific organic and inorganic substances with their compatibility with magnesium appropriately noted. Magnesium is usable in contact with aromatic and aliphatic hydrocarbons, ketones, esters, ethers, glycols, phenols, amines, aldehydes, oils, and higher alcohols. Ethanol causes slight attack, but anhydrous methanol causes severe attack unless significant water content is introduced. Gasoline-methanol fuel blends in which the water content equals or exceeds about 0.25% of the methanol content were found not to attack magnesium [87]. At room temperature ethylene glycol solutions produce negligible corrosion of magnesium alone or in galvanic couple with steel. At elevated temperatures such as 115°C (240°F), however, the rate rises and unless an effective inhibitor level is maintained significant corrosion will develop.

Most dry chlorinated hydrocarbons cause little attack on magnesium up to their boiling points. Chlorinated solvents have been used for years to degrease magnesium components without incident. (Parts that have been so cleaned, however, should be thoroughly baked to ensure that entrapped solvent is driven off, since it may cause degradation of subsequently applied coatings.) In the presence

of water, particularly at high temperatures, chlorinated hydrocarbons may hydrolyze to form hydrochloric acid, causing corrosive attack of the magnesium [52, 69].

Magnesium forms a highly stable fluoride film and consequently has good resistance to hot fluorine gas, HF solutions, and fluorinated hydrocarbons, such as refrigerants. Fluorocarbons and hydrofluorocarbons have recently been found to not only be non-corrosive at room and elevated temperatures, but very effective oxidation inhibitors at a few tenths percent in air over magnesium melts at temperatures up to 700°C [52, 69, 88, 89].

In acidic foodstuffs, such as fruit juices and carbonated beverages, attack of magnesium is slow but measurable. Milk causes attack, particularly when souring. Continuous poultices of wet organic matter have also been noted to cause corrosive attack, as has continuous contact of wet wood products. In both cases the presence of organic acids produced by the decay process has been assumed to be the cause of the attack [69].

### 7.2.8 Galvanic Corrosion/Selection of Fasteners

A discussion of magnesium corrosion issues is not complete without a discussion of the galvanic corrosion issue. Figure 7.24 summarizes the basic requirements for active galvanic corrosion – there are just four. There must be an anode (1; the magnesium) in direct electrical contact (2) with a cathode (3; the dissimilar metal) and the interface between the anode and cathode must be bridged by an electrolyte such as salt water [4].

If any one of these elements is missing the galvanic circle will not be complete and galvanic corrosion will not occur. Therefore direct couples to magnesium alloys in dry environments free of electrolytes will produce no galvanic attack. Likewise if the magnesium and the cathodic material are not in direct electrical contact there will again be no attack [69, 90].

In the electrochemical series of elements magnesium is near the top of the list as indicated in Table 7.22, which lists some common structural metals. Due to this active position in the series, magnesium alloys will serve as the sacrificial anode

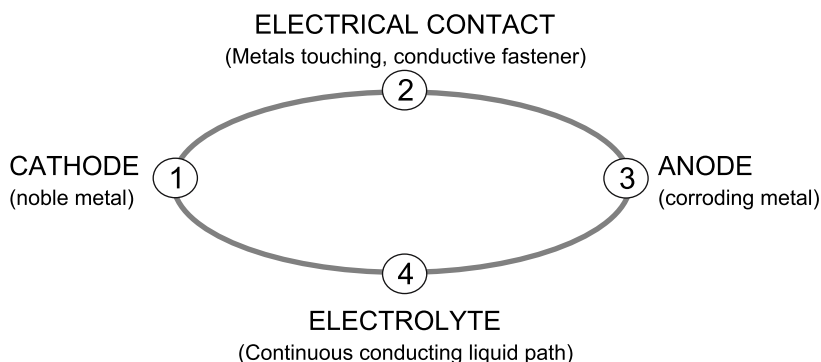



Fig. 7.24. The galvanic corrosion circle – the requirements for galvanic corrosion

**Table 7.22.** Electrochemical series of selected elements

Element	Potential, volts	Relative activity
Lithium	-3.04	
<b>Magnesium</b>	<b>-2.38</b>	
Aluminum	-1.66	
Manganese	-1.03	
Zinc	-0.76	
Iron	-0.44	
Cadmium	-0.42	
Nickel	-0.23	
Tin	-0.14	
Hydrogen	-0.0	
Copper	0.34	
Silver	0.80	
Gold	1.42	
		inert

in almost every couple with other metals and suffer significant galvanic attack unless care is taken in designing the components and in the selection of the dissimilar metals. Controlling galvanic corrosion is basically an exercise in Ohm's law, which allows few options in limiting the galvanic corrosion current as illustrated in the equation below.

$$I(\text{cor}) = [E_{\text{p-c}} - E_{\text{p-Mg}}] / [R_e + R_m] \quad (7.5)$$

Where  $I(\text{cor})$  is the galvanic corrosion current,  $E_{\text{p-c}}$  and  $E_{\text{p-Mg}}$  are the polarized chemical potentials for the cathode material and the magnesium, respectively, in the corrosion environment and where  $R_e$  and  $R_m$  are the circuit resistance –  $R_e$ , being the electrolyte resistance and  $R_m$ , being the resistance in the metal-metal contact between the anode and cathode [90].

The chemical reactions driving the corrosion process at the anode and cathode are



Looking at Eq. (7.5), the options are just two basic choices – minimize the difference in chemical potentials between the magnesium and the cathodic material or – maximize the circuit resistance. Looking first at minimizing the potential differences, it is fortunate that the critical chemical potentials are not the standard potentials, but rather the polarized potentials. While magnesium alloys show little or no tendency to polarize anodically, a number of metals do show significant cathodic polarization in couple with magnesium in salt water environments – for example aluminum alloys such as 5056, 6061, 5052 and 6063. When coupled to magnesium these alloys serve as poor cathodes for the reduction of water and the potentials become more negative, approaching a value near that of magnesium, resulting in very little corrosion. These aluminum alloys are low in copper and iron content, which would serve to catalyze the water reduction if present in significant levels. When the aluminum alloys are 2- or 7-thousand series

alloys or 380 alloy, where the copper content is 2–4%, the polarization does not occur effectively and significant galvanic attack will occur on magnesium coupled with these alloys. In addition to aluminum tin, cadmium, and zinc also polarize and show good compatibility. These metals are commonly used coatings on steel fasteners to minimize the galvanic attack that would occur on magnesium if the steel faster was used in an uncoated state. The order of compatibility is as listed and they are typically applied as electroplates, although they have also been applied mechanically and by ion vapor deposition as well. Critical to the performance of these coatings is the absence of cathodic contaminants. Thus electroplated zinc is of greater compatibility than a dip zinc coating, which is often contaminated with significant levels of iron from successive exposure to steel at the high, melt temperature. Fused zinc coatings have also been tested but found very poor for the control of galvanic attack on magnesium, apparently due to the contamination of the zinc by an active cathodic phase (possibly iron or carbon from the fused organic binder, employed in the process). Ion vapor deposited aluminum on steel fasteners would seem a good method for adding aluminum of high purity to the fastener surface, but again the compatibility was found to be very poor on testing, possibly due to the high energy involved with the process and the back diffusion of iron into the aluminum coating.

The ion vapor deposited aluminum and the fused zinc coating are part of a summary chart of the relative activities of variously coated steel fasteners shown in Fig. 7.25 [90, 91]. The relative activities were determined by exposing magnesium AZ91D test panels with 3 to 5 identical bolts to 7 days of ASTM B117 salt

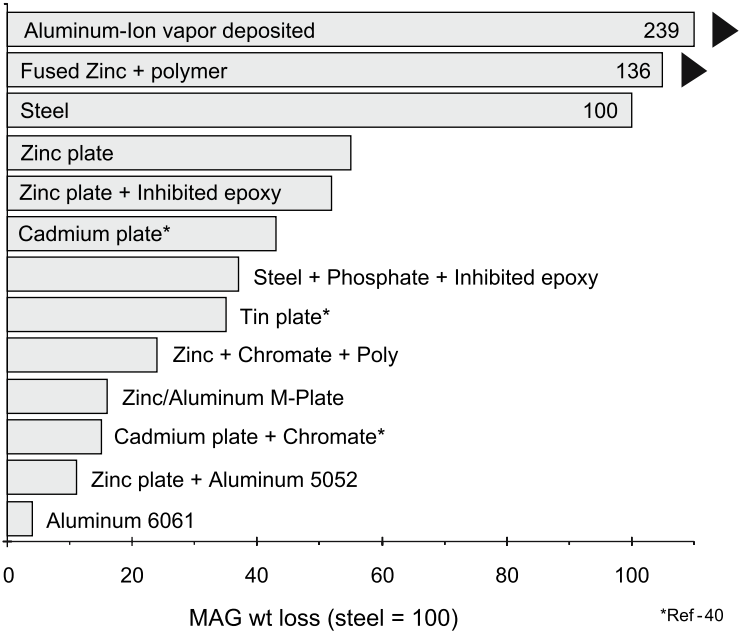


Fig. 7.25. Galvanic activity of variously coated steel fastener coupled to AZ91D alloys in ASTM B117 Salt Spray

spray. Then removing the bolts cleaning and determining the magnesium metal loss due to the corrosive attack. The weight loss associated with uncoated steel fasteners was used to normalize the results to bare steel at 100. As can be quickly seen the fused zinc and vapor deposited aluminum are 36% and 139% more aggressive to the magnesium than were the bare steel fasteners. The use of a zinc electro plate reduced the attack to about 55% while a proprietary coating of electrolytic zinc, a chromate dip treatment and a silicate sealer reduced the weight loss measured to just 22% of the steel. A 6061 bolt that gave a corrosion weight loss of <5% of that of the steel fasteners, produced the least attack.

Returning to Eq. (7.5) the other alternative to minimizing the potential difference in the equation for control of the galvanic current involved maximizing the resistance in the galvanic circuit. The options here again are relatively few [90].

- Electrically isolate the magnesium or cathodic material – this serves to break the corrosion circle or in this model it raises the anode-cathode contact resistance to infinity.
- Paint the cathodic material – painting the cathodic material with an alkali and water resistant coating will prevent the formation of the electrolyte bridge to the active cathodic surface thus raising the effective electrolyte resistance to a level near infinity.
- Design to prevent electrolyte pooling – by eliminating pooling the electrolyte resistance is raised due to the lower conductivity of a thin film and the thin film will dry quickly limiting the time of activity.
- Seal fraying surfaces – this is typically listed since electrolyte that infiltrates a crevice between the dissimilar materials would have a very short path and consequently low resistance, however unsealed surfaces in automotive applications do not show evidence of galvanic attack. This may be due to the fact that at the typical clamping loads water cannot infiltrate, or alternately, the captive volume of electrolyte would rapidly rise in pH to the passive region for magnesium alloys, which is 10.5, or above.

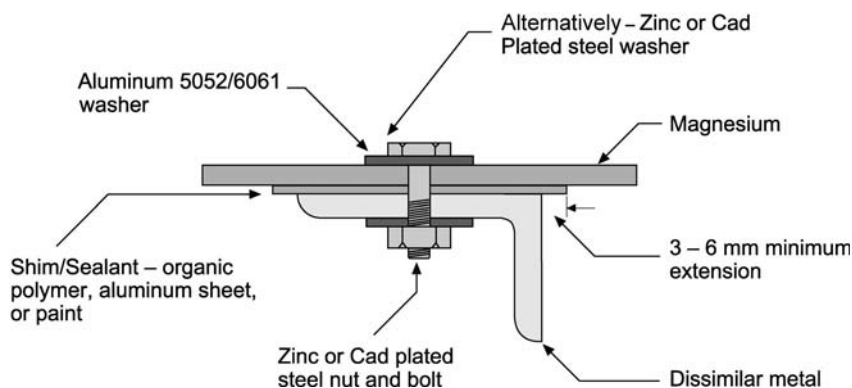


Fig. 7.26. A bolted magnesium assembly using good assembly practices for the control of galvanic corrosion



- Use compatible shims or washers – shims may be either conductive or non-conductive materials that serve to extend the electrolyte path at the interface between the dissimilar metals. In automobiles this is most commonly one of the compatible aluminum alloys mentioned above. Because the potentials involved are less than one volt the effective range of the galvanic current through typical saltwater electrolytes is typically less than 3/16ths inch. Therefore a shim or washer, which has a combined thickness plus extension of 1/8th to 3/16th inch, will significantly limit the galvanic current if not eliminate it. Figure 7.26 illustrates the use of shims and washers in a simple bolted assembly of magnesium plate to a dissimilar metal angle shape.

Controlling galvanic corrosion is one of the continuing challenges associated with the use of magnesium alloys in automotive road salt exposures. Although current practice has provided satisfactory performance, low cost alternatives with improved performance continue to be an opportunity for further development initiatives in both North America and Europe.

## References to Chapter 7.1

1. Weast RC (1986–1987) CRC Handbook of Chemistry and Physics, 67th Edition, CRC Press, Inc., Boca Raton, Florida
2. Ono S (1998) Metallurgical Science and Technology, Vol. 16, Nos. 1–2, Nov. Surface phenomena and protective film growth on magnesium and magnesium alloys, pp. 91–104
3. Pourbaix M (1974) Atlas of Electrochemical Equilibria in Aqueous Solutions, Second English Edition, National Association of Corrosion Engineers, Houston
4. Schichtel G (1954) Magnesium-Taschenbuch, VEB Verlag Technik, Berlin
5. Beck A (1939) Magnesium und seine Legierungen, Springer-Verlag, Berlin
6. Kurze P (1999) Korrosionsschutz durch neue chromfreie Passivierung von Magnesiumwerkstoffen, 7. Magnesium Automotive Seminar der Europäischen Forschungsgemeinschaft Magnesiumguss e.V., Tagungsband, Aalen, 29./30.09.1999
7. Norsk Hydro, Datenblatt Oberflächenbehandlung
8. DOW MAGNESIUM (1990) Operations in Magnesium Finishing, The Dow Chemical Company
9. Simon H and Thoma G (1985) Angewandte Oberflächentechnik für metallische Werkstoffe, Carl Hanser Verlag, München-Wien
10. Blumenthal G et al. (1999) Chromatierungen auf Zinkschichten, Metalloberfläche 53 (10), pp. 10–17
11. Jimenez A and Schmidt HA (1999) Chrom(VI)-freie Nachbehandlungsverfahren, Metalloberfläche 53 (9), pp. 46–49
12. Hawk D and Albright DL (1995) Metal Finishing 10, pp. 34–38
13. Takaya M (1996) The Formation Manganese-Type Chemical Conversion Coating for Magnesium Alloys, Tagungsband Interfinish 96. World Congress 10.–12. September, pp. 425–441
14. DE 19913242
15. Kurze P, Singe T and Diesing J (2000) Korrosionsschutz von Magnesiumwerkstoffen, Metalloberfläche 54 (9), pp. 22–24
16. DE 4138218
17. Keller F, Hunter MS and Robinson DL (1953) J. Electrochem. Soc. 100, pp. 411
18. Bradford PM et al. (1976) Corros. Sci. 16, pp. 747
19. Gulbrandsen E, TaAo J and Olsen A (1993) Corros. Sci. 34, pp. 1423
20. DE 3715663

21. Gmelin (1952) Handbuch der anorganischen Chemie, Syst. Nr. 27 Magnesium, Teil 1, Verlag Chemie GmbH, Weinheim, 8. Auflage, pp. 760–818
22. Dettner, Elze (1969) Handbuch der Galvanotechnik, Band III, Carl Hanser Verlag, pp. 179–190
23. Metals Handbook (1982) 9. Edition, Vol. 5, ASM, Ohio, pp. 628–649
24. Emeley EF (1966) Principles of Magnesium Technology, Pergamon Press, Oxford, London, Edinburgh, N.Y., Paris, Frankfurt, pp. 670–735
25. Rauscher G (2000) Jahrbuch Oberflächentechnik 2000, Die Entwicklung der Anodisation von Magnesium, Band 56, Giesel Verlag GmbH, Isernhagen/Germany, pp. 185–210
26. Evangelides HA (1958) Magnesium and Protective Coatings for Magnesium, Plating 45 (5), pp. 493–498
27. US 2, 723, 952
28. WO 96/28591 WO 98/42892
29. Magnesium Taschenbuch (2000) Herausgeber Aluminium-Zentrale Düsseldorf, Aluminium Verlag, Düsseldorf, 1. Auflage
30. Magnesium – Anwendungen, Potenziale, Eigenschaften (2000) Herausgeber Kainer KU, WILEY-VCH Verlag GmbH, Weinheim, Germany
31. Nikolaev AV, Markov GA and Pishchevitskii BI (1977) A new phenomenon in electrolysis, Izv. SO AN SSSR, Ser. Khim Nauk, 5 (12), pp. 32–33
32. Wirtz GP and Brown SD (1991) Ceramic Coatings by anodic spark deposition, Materials & Manufacturing Processes 6 (1), pp. 87–115
33. Kurze P (1990) Anodische Oxidation unter Funkenentladungen auf Metalloberflächen in wäßrigen Elektrolyten-Grundlagen und Anwendungen, Dechema-Monographien Band 121, VCH-Verlagsgesellschaft, pp. 167–181
34. Mobley C, Brevick J, Murray M and Rodrigo D (2000) The Effect of Coatings on Selected Mechanical Properties of Magnesium Alloy Die Castings, Die Casting Engineer Juli/Aug., pp. 36–39
35. Günterschulze A and Betz H (1934) Z. Physik (78), pp. 196–210 (1932) Z. Physik (91), pp. 70–96
36. Kurze P, Krysmann W, Schreckenbach J, Schwarz T and Rabending K (1987) Cryst. Res. Technol. 22 (1), S. 53–58
37. EP 0333048
38. Olbertz B and Haug AT (1989) Metalloberfläche 43 (4), S. 174–178
39. Kurze P (1992) Electrochemicals Coatings of Magnesium Alloys, DGM-Jahrestagung Garmisch-Partenkirchen, April, pp. 127–132
40. Kurze P (1994) Magnesium elektrochemisch beschichten, Metalloberfläche 48(2), pp. 104–105
41. Kurze P and Banerjee D (1996) Eine neue anodische Beschichtung zur Verbesserung der Korrosions- und Verschleißbeständigkeit von Magnesiumwerkstoffen, Gießerei – Praxis (11/12), pp. 211–217
42. Kurze P (1998) Herstellung keramischer Schichten auf Leichtmetallen mittels plasma-chemischer Verfahren in Elektrolyten, Mat.-wiss. u. Werkstofftech. 29, pp. 85–89
43. US 5, 470, 664
44. Zozulin AJ and Bartak DE (1994) Anodized Coatings for Magnesium Alloys, Metal Finishing 3, pp. 39–44
45. Rogers R and Boyd ML (1948) Galvanische Metallüberzüge auf Magnesiumlegierungen, Sheet Metal Ind. 25, pp. 959–962
46. De Long HK (1948) Elektroplattieren von Magnesium, Materials and Methods 27, pp. 63–65
47. Thews ER (1953) Englische Verfahren zur Elektroplattierung von Magnesium und seinen Legierungen, Metalloberfläche 5, pp. 110–111
48. Holländer A (1995) Chemische Vernickelung von Magnesium, Metalloberfläche 49 (4), pp. 265–267
49. Sharma AK et al. (1998) Electroless Nickel Plating on Magnesium Alloy, Metal Finishing 3, pp. 10–18
50. Shigematsu I et al. (2000) Surface Treatment of AZ 91D Magnesium Alloy by Aluminium Diffusion Coating, Journal of Materials Science 19 (6), pp. 473–475
51. Klein LC (1988) Sol-Gel-Technology for Thin Films, Fibers, Preforms, Electronics, and Specialty Shapes, Noyes Publications, Park Ridge, New Jersey, USA

## References to Chapter 7.2

52. Bothwell MR (1967) Magnesium Corrosion, in *The Corrosion of Light Metals*, Godard H, Jepson WB, Bothwell MR, Kane LR, Editors, Wiley J and Sons, Inc., New York, pp. 259–311
53. Loose WS (1948) *The Corrosion Handbook*, Uhlig HH, Edt., Wiley J and Sons, New York, pp. 218–252
54. Bengough GD and Whitby L (1933) *Trans. Inst. Chem. Eng.*, Vol. 11, pp. 176–189
55. Hanawalt JD, Nelson CE and Peloubet JA (1942) Corrosion Studies of Magnesium and Its Alloys, *Transactions AIME*, Vol. 147, pp. 273–299
56. Mercer WE and Hillis JE (1992) The Critical Contaminant Limits and Salt Water Corrosion Performance of Magnesium AE42 Alloy, Paper 920073, Society of Automotive Engineers, Detroit, MI
57. Pekguleryuz M and Baril E (2001) Development of Creep Resistant Mg-Al-Sr Alloys, *Magnesium Technology 2001*, (Hryn JN, ed.), The Minerals, Metals and Materials Society, Warrendale, PA, pp. 119–125
58. Labelle P, Pekguleryuz M, Argo D, Dierks M, Sparks T and Waltematte T (2001) Heat Resistant Magnesium Alloys for Power-Train Applications, *Light Metal Applications for the Automotive Industry – Aluminum and Magnesium*, Paper 2001-01-0424, Society of Automotive Engineers, Detroit, pp. 47–54
59. Luo AA and Powell BR (2001) Tensile and Compressive Creep of Magnesium-Aluminum-Calcium Based Alloys, *Magnesium Technology 2001*, (Hryn JN, ed.), The Minerals, Metals and Materials Society, Warrendale, PA, pp. 137–144
60. Powell BR, Luo AA, Rezhets V, Bommarito JJ and Tiwari BL (2001) Development of Creep-Resistant Magnesium Alloys for Powertrain Applications; Part 1 of 2, *Light Metal Applications for the Automotive Industry – Aluminum and Magnesium*, Paper 2001-01-0424, Society of Automotive Engineers, Detroit, pp. 29–36
61. Luo AA, Balogh MP and Powell BR (2001) Tensile Creep and Microstructure of Magnesium-Aluminum-Calcium Based Alloys for Powertrain Applications – Part 2 of 2, *Light Metal Applications for the Automotive Industry – Aluminum and Magnesium*, Paper 2001-01-0424, Society of Automotive Engineers, Detroit, pp. 37–45
62. Aune TK (1983) Minimizing Base Metal Corrosion on Magnesium Products. The Effect of Elemental Distribution (Structure) on Corrosion Behavior, *Proceedings of the International Magnesium Association*, Toronto
63. Hillis JE (1983) The Effects of heavy Metal Contamination on Magnesium Corrosion Performance, Paper 830523, Society of Automotive Engineers, Detroit, MI
64. Reichel KN, Clark KJ and Hillis JE (1985) Controlling the Salt Water Corrosion Performance of Magnesium AZ91 Alloy, Paper 850417, Society of Automotive Engineers, Detroit, MI
65. Hillis JE and Reichel RN (1986) High Purity Magnesium AM60 Alloy: The Critical Contaminant Limits and the Salt Water Corrosion Performance, Paper 860288, Society of Automotive Engineers, Detroit, MI
66. Hillis JE, Murray RW and Mercer II WE (1998) Compositional Requirements for Quality Performance with High Purity Magnesium Alloys, *Proceedings of the International Magnesium Association*, San Diego, pp. 74–81
67. Shook SO and Hillis JE (1989) Composition and Performance of an Improved Magnesium AS41 Alloy, Paper 890205, Society of Automotive Engineers, Detroit, MI
68. Clark KJ (1986) AZ91E Magnesium Sand Casting Alloy, *The Standard for Excellent Corrosion Performance*, *Proceedings of the International Magnesium Association*, Los Angeles
69. Hawke DL, Hillis JE, Pekguleryuz M and Nakatsugawa I (1999) Corrosion Behavior, in *Magnesium and Magnesium Alloys*, (Avedesian A and Baker H, Editors), ASM International, Materials Park, OH, pp. 194–210
70. *Stress Corrosion Cracking* (1999) in *Magnesium and Magnesium Alloys*, (Avedesian A and Baker H, Editors), ASM International, Materials Park, OH, pp. 211–215
71. Beck A (1940) *The Technology of Magnesium Alloys*, 2nd ed., F. A. Hughes and Co. Ltd., London, pp. 294–297

72. Logan HL and Helsing H (1950) Stress Corrosion of Wrought Magnesium Base Alloys, *Journal of Research of the National Bureau of Standards*, Vol. 44, pp. 233–243
73. Murray RW and Hillis JE (1990) Magnesium Finishing: Chemical Treatment and Coating Practices, Paper 900791, Society of Automotive Engineers, Detroit, MI
74. Pelensky MA and Gallaccio A (1967) Stress Corrosion of Magnesium Alloys – Environmental Factors, in *Stress Corrosion Testing*, ASTM STP 425, American Society for Testing and Materials, Philadelphia, pp. 107–115
75. Loose WS and Barbian HA (1945) Stress-Corrosion Testing of Magnesium Alloys, in *Symposium on Stress Corrosion Cracking of Metals*, American Society for Testing and Materials, Philadelphia, pp. 273–292
76. Miller WK (1992) Stress Corrosion Cracking of Magnesium Alloys, in *Stress-Corrosion Cracking: Material Performance and Evaluation*, ASM International, Metals Park, OH, pp. 251–263
77. Sager GF, Brown RH and Mears RB (1945) Tests for Determining Susceptibility to Stress-Corrosion Cracking, in *Symposium on Stress-Corrosion Cracking of Metals*, American Society for Testing and Materials, Philadelphia, pp. 15–36
78. Liu HW (1970) Stress-Corrosion Cracking and the Interaction Between Crack-Tip Stress Field and Solute Atoms, *Transaction of the ASME, Journal of Basic Engineering*, Vol. 92, pp. 633–638
79. Ebtehaj K, Hardie D and Parkins RN (1988) The Influence of Chloride-Chromate Solution Composition on the Stress-Corrosion Cracking of Mg-Al Alloy, *Corrosion Science*, Vol. 9, pp. 849–851
80. Ogarevic VV and Stephens RI (1990) Fatigue of Magnesium Alloys, *Annual Review of Materials Science*, Vol. 20, pp. 141–177
81. Wendt J, Hilpert M, Kiese J and Wagner L (2001) Surface and Environmental Effects on the Fatigue Behavior of Wrought and Cast Magnesium Alloys, *Magnesium Technology 2001* (J. Hryn, editor), TMS, New Orleans, LA, February, pp. 281–285
82. Ferguson WG, Liu W, Ross P and MacCulloch J (2001) Corrosion Fatigue of High Pressure Die Cast Magnesium Alloys, *Magnesium Technology 2001* (J. Hryn, editor), TMS, New Orleans, LA, February, pp. 269–274
83. Hillis JE and Murray RW (1987) Finishing Alternatives for High Purity Magnesium Alloys, Paper G-T87-, Society of Die Casting Engineers 14th International Congress and Exposition, Toronto
84. Bartak DE, Schleisman TD and Woolsey ER (1991) Electrodeposition and Characteristics of a Silicon-Oxide Coating for Magnesium Alloys, *Proceedings of the International Magnesium Association*, Quebec City, pp. 55–60
85. Skar JI and Albright D (2000) Phosphate-Permanganate: A Chrome Free Alternative for Magnesium Pretreatment, *Magnesium Alloys and Their Applications*, Wiley VCH, Weinheim, Germany, pp. 469–474
86. *Cleaning and Finishing* (1999) in *Magnesium and Magnesium Alloys*, (Avedesian A and Baker H, Editors), ASM International, Materials Park, OH, pp. 138–162
87. Hawke DL (1986) Compatibility of Magnesium Alloys with Methanol Fuels, Paper 86025, Society of Automotive Engineers, Detroit, MI
88. Milbrath DS and Owens JG (2001) New Fluorochemical Cover Gases for Protection of Molten Magnesium, Presentation at the Annual World Magnesium Conference, International Magnesium Association, Brussels, May
89. Tranell G, Pettersen G, Aarstadt K, Engh T, Solheim I, Syvertsen M and Oye B (2001) A Systematic Approach for Identifying Replacements to  $\text{SF}_6/\text{SO}_2$  in the Magnesium Industry – An IMA / SINTEF-NTU Cooperative Project, *Proceedings of the International Magnesium Association*, Brussels, pp. 69–73
90. Hawke DL, Hillis JE and Unsworth W (1988) Preventive Practice for Controlling the Galvanic Corrosion of Magnesium Alloys, *International Magnesium Association*, McLean, VA
91. Hawke DL (1987) Galvanic Corrosion of Magnesium, Paper G-T87-004, Society of Die Casting Engineers 14th International Die Casting Congress and Exposition, Toronto

# 8 Engineering Requirements, Strategies and Examples

## 8.1 Automotive Applications in Europe

Sönke Schumann, Horst Friedrich

### 8.1.1 Introduction

Successful vehicle concepts were well accepted by customers primarily due to a combination of low fuel consumption and a very good performance.

The successful attempts by the car industry to reduce fuel consumption have been already documented in the past. Figure 8.1 shows the reduction in fleet consumption. Here the progress for the respective model of the next generation is shown as an example for some vehicles. The 3L Lupo also meets the Euro IV standards in terms of exhaust emissions. In this context, the voluntary commit-

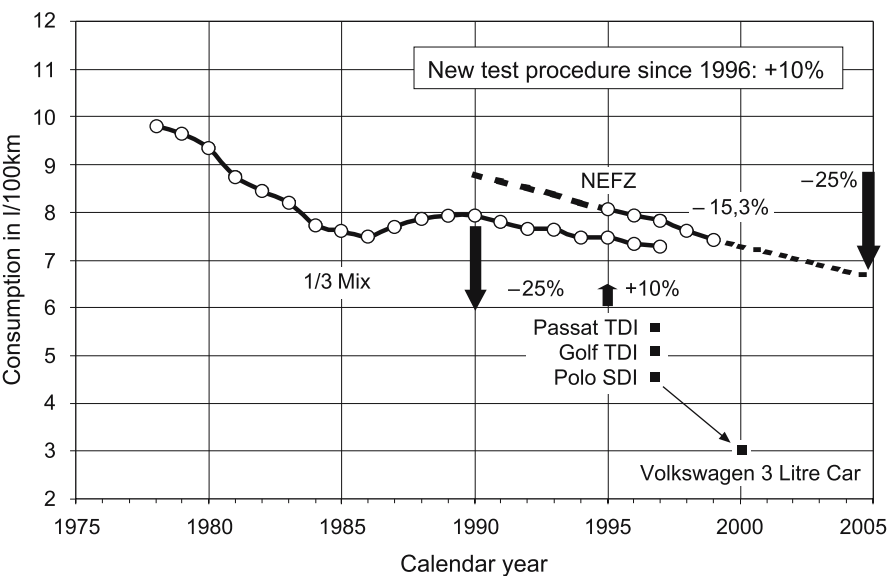


Fig. 8.1. Reduction in fuel consumption in Germany (voluntary commitment by the german car industry) [1]

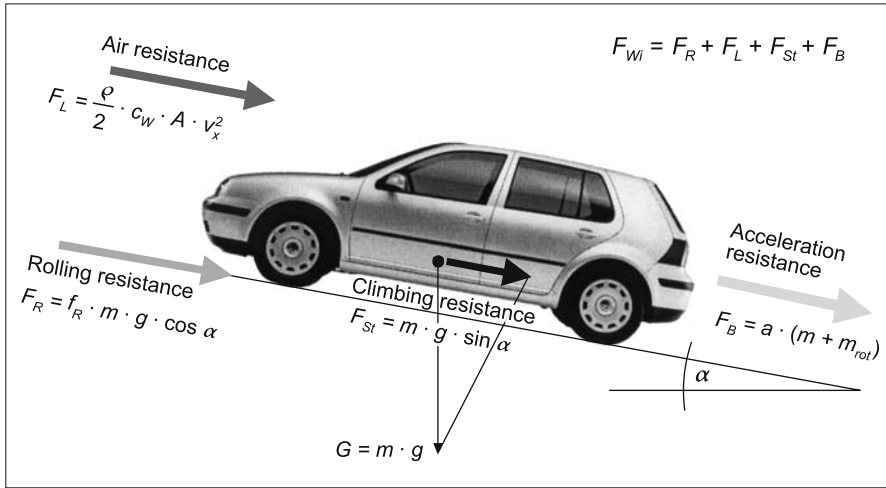


Fig. 8.2. Driving resistances

ment by the German car industry to reduce fuel consumption by 2005 by 25% compared to the levels in 1990 should be noted.

At the beginning of the 1990s, protecting the atmosphere and reduction of CO<sub>2</sub> traffic emissions grew in importance in the social discussion. The international commitment by the car industry ("ACEA agreement") set the trend to reduce CO<sub>2</sub> emissions by 2008 by 25% compared to that in 1990. The above-mentioned reduction in fuel consumption for motor vehicles therefore had a significant influence on CO<sub>2</sub> emissions [2].

Society and the market have achieved a remarkable position in the product development process of material technologies and constructions (lightweight construction) in order to fulfil the desires for frugal vehicles.

The influence of consumption-determining parameters has an influence on the driving resistance equation [3]. Based on this, the total driving resistance  $F_W$  is sub-divided as follows (compare Fig. 8.2):

Air resistance	$F_L = \frac{\rho \cdot A \cdot c_w \cdot v^2}{2}$
Rolling resistance	$F_R = m \cdot g \cdot f_R \cdot \cos \alpha$
Acceleration resistance	$F_B = a(m + m_{rot})$
Climbing resistance	$F_{St} = m \cdot g \cdot \sin \alpha$

Note that three of the four terms in  $F_W = F_L + F_R + F_B + F_{St}$  are determined by mass. This causes the motivation towards a reduction in mass by means of lightweight construction, particularly since the necessary engine performance  $P$  is a result of the sum of the driving resistance's  $F_W$ , multiplied by the driving speed  $v$ . Here the total resistance  $\eta$  of the drive train is taken into consideration:

Engine performance  $P = \frac{F_W \cdot v}{\eta}$

The fuel consumption  $B$  over a determined distance is also linked to the specific fuel consumption  $b_e$  of the engine and the previously mentioned formule in terms of the relation:

$$B = \frac{\int b_e \cdot \frac{1}{\eta} [m(f_R \cdot g \cdot \cos\alpha + a + g \cdot \sin\alpha) + m_{\text{rot}} \cdot a + \frac{\rho}{2} c_W \cdot A \cdot v^2] \cdot v \cdot dt}{\int v \cdot dt}$$

This includes the following:

Vehicle mass	$m$	[kg]
Air resistance	$c_W$	[-]
Rotating mass	$m_{\text{rot}}$	[kg]
driving speed	$v$	[m/s]
Vehicle acceleration	$a$	[m/s <sup>2</sup> ]
Gravity	$g$	[m/s <sup>2</sup> ]
Rolling resistance	$f_R$	[-]
Air density	$\rho$	[kg/m <sup>3</sup> ]
Cross-sectional area of vehicle	$A$	[m <sup>2</sup> ]
Gradient	$\alpha$	[°]
Degree of transmission efficiency from drive train	$\eta$	[-]
Specific fuel consumption	$b_e$	[g/kWh]
Fuel consumption	$B$	[g/m]

If one compares the effects of vehicle weight ( $m$ ), aerodynamics ( $c_W \cdot A$ ) and rolling resistance ( $f_R \cdot m \cdot g$ ) to the NEFZ consumption (New European Driving Cycle), the determining influence of the vehicle weight becomes apparent. Thus a reduction in vehicle mass by 10% leads to approximately 5% reduction in fuel consumption (Fig. 8.3). The same reduction in fuel consumption, as a result of a reduction in rolling resistance or improvement in aerodynamics, would have required disproportionately greater modifications (which are not technically perceivable for series production vehicles). This comparison applies to similar driving behaviour with the prerequisite of adapted gearbox/engine layouts.

Equally valid is that apart from improvements in the drive train, the decisive role in reduction of fuel consumption, is dependent on lightweight construction.

The fuel consumption target of 3 l/100 km (MVEG driving cycle) in a series produced vehicle was first achieved in a VW Lupo [5]. In addition to an efficient drive train, a reduction in weight of approx. 100 kg, compared to a conventional Lupo, played a primary role in reducing fuel consumption (Fig. 8.4). Among a wide range of lightweight construction measures, there are also applications in Mg alloys, e.g. for the steering wheel frame or the tailgate.

Magnesium alloys, with their low density of approx. 1.8 g/cm<sup>3</sup>, are considered seriously contenders for lightweight vehicle manufacture.



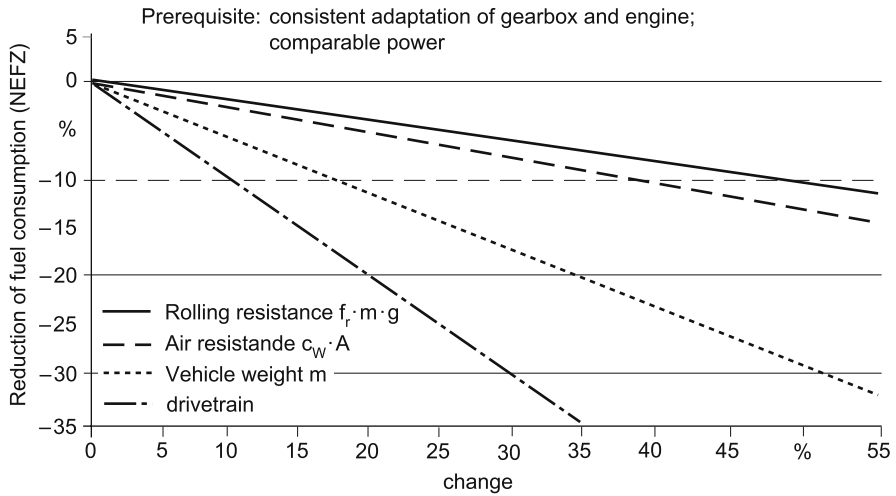


Fig. 8.3. Effect of important parameters in consumption [4, 5]

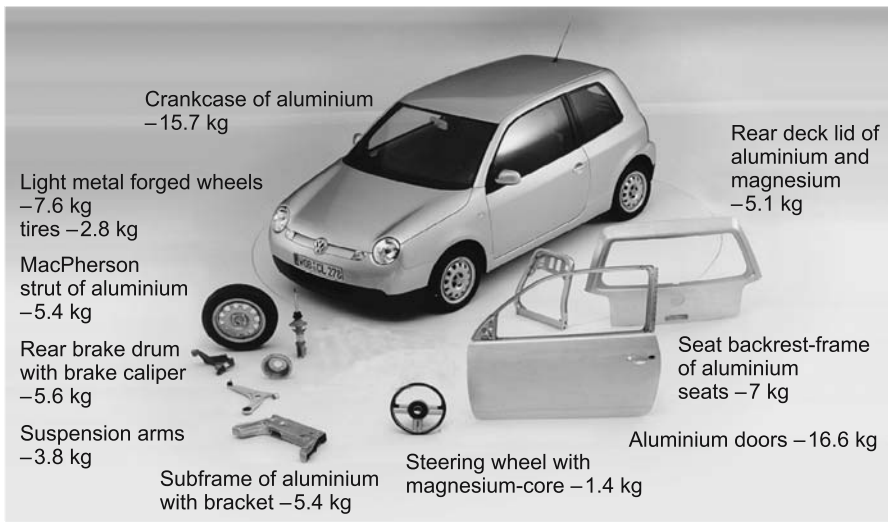


Fig. 8.4. Lightweight construction measures 3L Lupo

However, when determining the method of construction, all physical characteristics of a magnesium alloy for the relevant component in a mg-compatible design must be considered. This is as equally important as adequate manufacturing processes, e.g. high pressure die casting, vacuum die casting or forging/reshaping technology to achieve optimal material/component properties.



Some good examples for this type of integral optimisation of

- method of construction (design)
- material (properties)
- processes

are gearbox housings, die cast in the alloy AZ 91 (see Fig. 8.5). Here the low elastic modulus is compensated (integrated approach) by a reduction in the wall thickness and strengthening of the complex cast component by greater use of ribbing (compared with aluminum alloys). The good casting properties of alloy AZ 91 enables thinner walls and ribs to be possible.

A total weight of 12.7 kg has been achieved with three individual components of the B80 gearbox housing, the same gearbox used in a manual version in the VW Passat and AUDI A6 [7, 8]. This is a reduction of 25%, compared to an existential lightweight aluminium design. Due to the design/construction and manufacturing procedure, a reduction in weight virtually corresponding to the difference in density of aluminum to magnesium alloys was possible.

### 8.1.2 Potential Use of Magnesium in Vehicles

The use of magnesium for a certain component is determined essentially by the requirement profile. Priority is given to the influences on and loads in operation, for example, and the resulting requirements for rigidity, and strength deriving from it as well as the influences of temperature and media. In addition there is a whole series of primary or associated requirements to which priority is assigned such as safety, comfort, weight, cost efficiency, manufacturability and environmental safety (Fig. 8.6).

The essential demands on potential magnesium components affect four vehicle modules: drive train, interior, body and chassis (Fig. 8.7). This modular break-

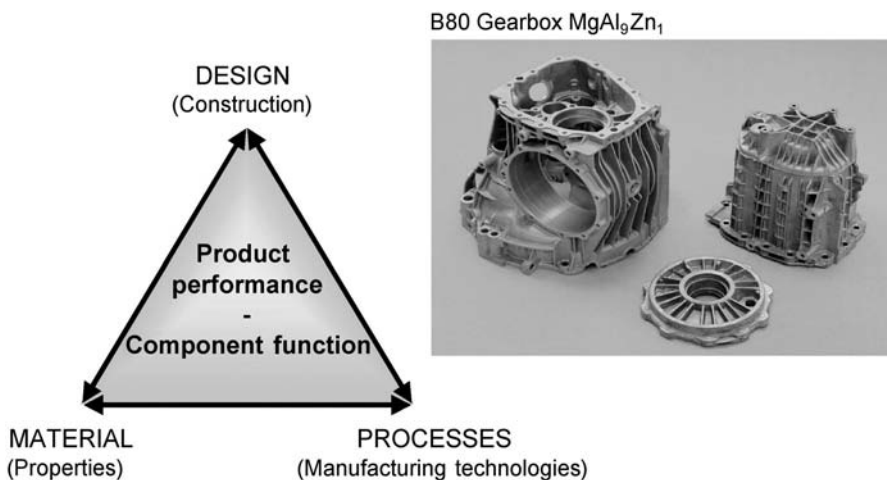


Fig. 8.5. Integrated approach, example B80 gearbox housing

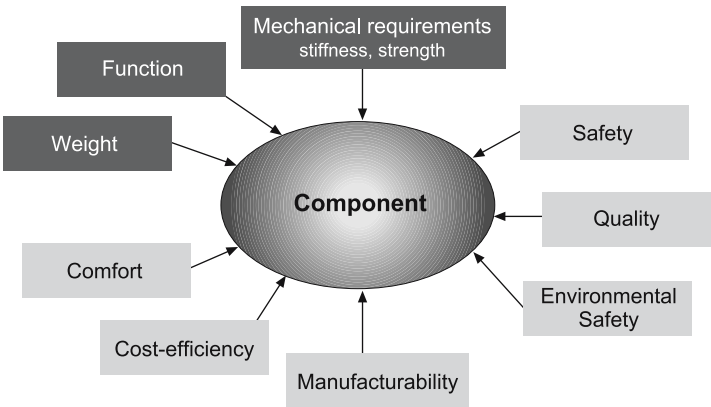


Fig. 8.6. Profile of component demands

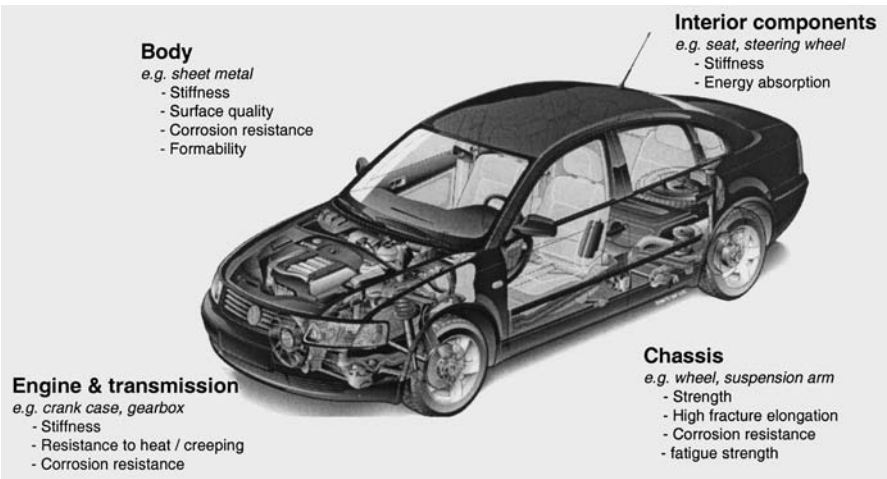


Fig. 8.7. Essential demands on potential magnesium components in the vehicle

down of vehicle components should also continue to serve as a basis for further explanation of the use of magnesium in the vehicle.

The use of magnesium in vehicles today and in the future depends thus on numerous technical and economical factors, and in particular the lost.

How might the use of magnesium in vehicles develop, what prerequisites are necessary, and what R&D efforts are required? These questions will be addressed as follows based on component and project examples and will be answered by a Mg strategy.

The starting point is an analysis in which, for the four vehicle modules, magnesium components are listed which have already been implemented or which are possible in the future, differentiated according to their probability (Table 8.1).

**Table 8.1.** Implemented and potential uses of magnesium in vehicles

Components	Implemented in various VW-/Audi cars	Possible short-term < 5 years [kg]	Possible mid-term > 5 years [kg]	Possible long-term > 10 years [kg]
<b>Drive train</b>				
Gearbox housing manual/automatic	×	×		
Intake manifold	×			
Cylinder head cover	×			
Mountings, supports		×		
Oil sump, oil pump housing		×		
Crankcase			×	
SUM	18	6–11	14–20	
<b>Interior components</b>				
Steering wheel core	×			
Pedal cluster mounting	×			
Steering wheel components	×			
Seat components, rear seat		×		
Other components	×	×	×	
SUM	4	8–12	2–4	
<b>Body</b>				
Tailgate/boot lid	×			
Door inner part 2 (4)		×		
Instrument panel/cross car beam		×		
Mg-sheet applications (interior/exterior)			×	×
Mg-extrusion applications			×	×
SUM	3,4	20–34	8–12	15–20
<b>Chassis</b>				
Engine cradle/Sub-frame			×	
Wheels (5)				×
Suspension arms (front, rear)				×
SUM	0	0	4–6	30–34
Total sum	25	34–57	28–42	45–54
Cumulative total		→ 59–82	→ 87–124	→ 132–178

Magnesium components have already been installed in various vehicles of the Volkswagen Group. The components add up to approx. 25 kg. The main focus of current magnesium applications is in the drive train and in the interior. In a short term (< 5 years); these applications will be further developed and even doubling the present amount is feasible. The currently developed Mg alloys with extended application potential (creep strength) will support this. A first step in the use of magnesium applications in body construction is also feasible. Here the technical prerequisite is, as in other applications, alloy development with the aim of achieving ductility, simpler manufacturing and high processing qualities.

The magnesium components already in use (which are described in the following chapters), together with those that are capable of introduction in the short

term suggest that a total weight of between 60 and 80 kg of magnesium in a vehicle is entirely realistic. In these cases, it is not so much the technical but rather the economic aspects that are the limiting factors. In order to be able to bring about the predicted medium-term use of magnesium, R&D work into creep-resistant alloys and forging alloys must continue in greater depth. The considerable jump to a figure of 90–120 kg and above can only become reality by a rigorous process of bringing together the entire chain of production from semi-finished product manufacture (e.g. alloys, sheets, extrusions) to finished component in an overall R&D strategy. This means that the end user – in this case the vehicle manufacturer – will have to co-operate closely with the semi-finished product manufacturer/developer.

Magnesium manufacturers will co-operate worldwide, if need be, to make use of quantitative and logistical effects and thus to organise the cost/price structure. One can assume that the price for magnesium metal will come closer to that of aluminum in the long-term.

### **8.1.3 Automotive Applications – Examples**

#### **8.1.3.1 Drive train Applications**

The essential components in the drive train are the engine with attachments (e.g. intake manifold), ancillaries (alternator, starter motor, etc.), the gearbox/clutch and the drive shafts for transmitting power. The high operating temperatures in the drive train is one particular demand, specifically for magnesium applications. As an example for the use of magnesium in the drive train, applications in the gearbox, intake manifold and cylinder head covers are shown in addition to possible magnesium applications in the engine.

#### ***The Gearbox Housing***

There was a renaissance of magnesium at VW/Audi with the B80 gearbox housing in AZ91 in 1996 (Fig. 8.8). In the years that followed, several gearbox housings for longitudinal and transverse installation in vehicles were produced in magnesium. The strong motivation for this was a weight reduction of approx. 20–25% compared to similar aluminium housings.

The VL300 was the first CVT gearbox (continuous velocity transmission) with a magnesium housing (Fig. 8.9) installed in a series production vehicle (MD = 310 Nm). The saving in weight compared to an already lightweight aluminium version was approx. 8 kg.

**The basics of gearbox design:** Direct substitution of aluminium by magnesium (e.g. by using the same cast form), there would, theoretically, be a reduction in housing weight of 34% relative to the difference in density. However, a greater use of ribbing (advantageous also for acoustics) and an increase in the wall thickness must be made to compensate for the loss in stiffness, since the elastic modulus is decreased in the same properties as the density and also only the slightest deformation is tolerated for gearboxes. Due to the very good castability of the

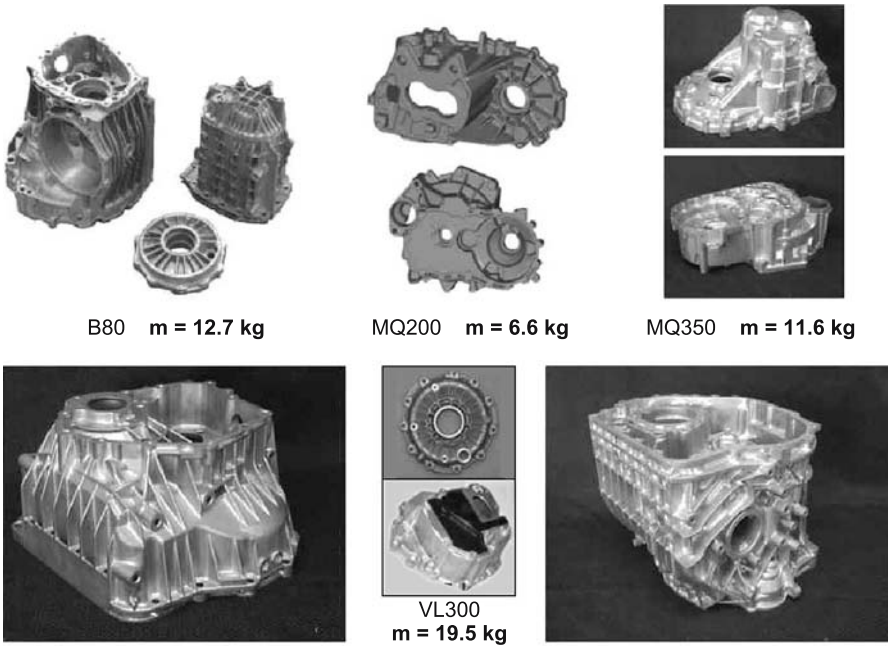


Fig. 8.8. Magnesium gearbox housing (VW, Audi) [7]

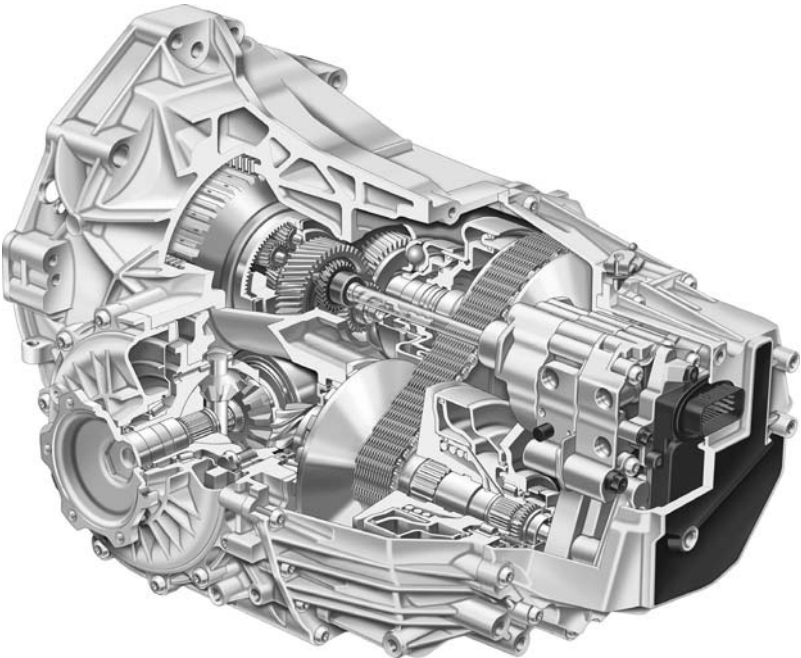
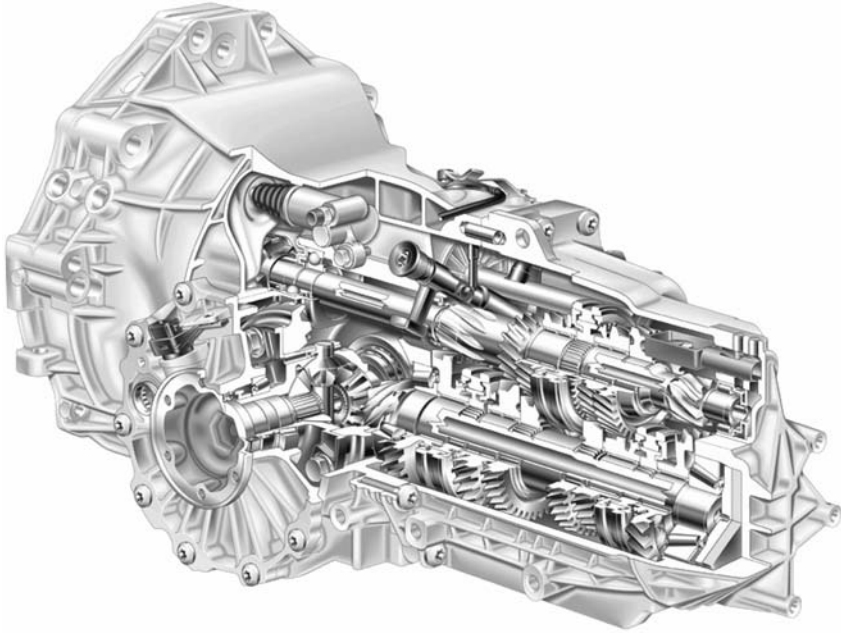


Fig. 8.9. VL300 CVT gearbox (Audi) [9]



**Fig. 8.10.** B80 gearbox for longitudinal installation; Transmission of engine torque up to 280 Nm (VW/Audi) [10]

alloy, less stressed areas, mainly housing walls can be constructed with thinner walls.

This results in a final weight reduction of 4.5 kg for the gearbox housing B80 (equating to 26%) (Fig. 8.10).

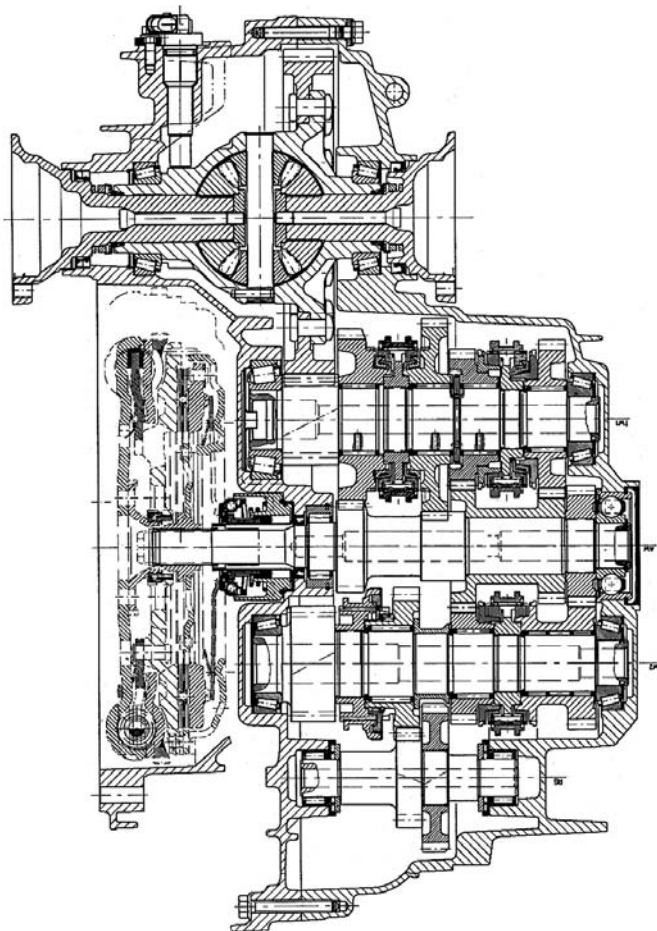
**Alloy selection:** The permanent operating temperatures of today's manual gearboxes are between 90 and 110°C, depending on the type of gearbox. The peak temperature can reach 140°C. Due to the set demands the decision was made to select the AZ91-HP alloy for the B80. The alternative AS21-HP was not selected despite better creep results. The lower-yield strength, the unfavourable corrosion behaviour and castability were the decisive factors. The higher tendency to creep and contact corrosion and the lower heat resistance of the AZ91-HP compared to the AlSi9Cu3 were addressed constructively. The high purity alloy AZ91-HP enables, however the use of housings without chromating and wax coating.

**Stress from tooth gearing and bearing forces** [10]. The wall thickness of the housing is determined by the strength required, permitted deformation, castability of the alloy used and acoustic requirements. FEM calculations were used to determine the reinforcement and wall thickness of the gearbox such that the calculated frequency of the engine and gearbox settles above that of the engine operating speed. A noticeable stress occurs only in the bearing areas.



**Demands on bearings.** The differences in thermal expansion of a steel bearing ring and magnesium housing makes pressing in of the shaft bearing outer ring necessary. Without adequate press fitting, the bearings outer rings would work into the magnesium seat too quickly under load. The press fit in magnesium must be increased compared to an aluminium housing so that the forced fit effect only starts to break down at gearbox temperatures above 90°C (equating to oil temperatures of about 105°C). Housing hubs, especially with bearings under high radial loads, should be designed with 30% thicker walls.

The main shaft is affected by stress under normal operating conditions. If the bearings work into the metal, clearance or imbalance could lead to noisy operation and bearing damage. To compensate, an axial clearance of the input shaft angular contact ball bearings can be replaced by e.g. a ball bearing/needle-bearing set-up. See cross section of MQ 350 gearbox (Fig. 8.11).



**Fig. 8.11.** Cross section of MQ350 gearbox (VW), bearing set up and bolt connection

**Demands on bolt connections.** The tightening torque of bolted assemblies in magnesium housings can relax because under a load and increased temperature time dependent plastic deformation (creep) can occur. Experience has shown, however, that this different behaviour does not lead to complete loosening of the bolts or to leaks. The following measures are recommended to avoid the tendency towards creep deformation:

- Select bolts with threads up to head or bolts with a shaft diameter relative to the mean diameter
- The head seating area should be increased by 20% for magnesium housings
- Increase of minimum screw-in depth by 2.5 times nominal thread diameter
- Allowance of more Mg volume at the flange surface. This would decrease the stress and reduce the tendency to creep
- Preference of highly durable aluminium bolts rather than steel bolts, since the lower thermal coefficient of expansion of aluminium results in reduced stress

**Corrosion protection measures.** An almost better optical result can be seen after salt spraying and endurance tests on Z91-HP housings without chromate treatment and wax coating compared to housings from the standard  $\text{AlSi}_3\text{Cu}_3$  alloy. In contrast to the alloy AZ81 previously used, the low Fe, Ni and Cu values in the AZ91-HP alloy have an advantageous effect.

High purity Mg alloys (HP quality) are obligatory.

In terms of contact corrosion, measures have to be taken, such as:

- Bore holes for the bolt threads and dowel sleeves
- Steel bolts acid dip galvanised and chromate treated; galvanic separation of Al,
- Mg alloy
- Aluminium washers hard coated (e.g.  $\text{AlMgSi}_1\text{-F31}$ ); polyamide coated heads (expensive)
- External drive bolts with collars to avoid surface damage or internal hexagon screw
- Contact aluminium parts should only contain max. 1% Cu (Al alloy  $\text{AlSi}_{12}$  (Cu) would be suitable) or a coating
- Aluminium bolts

**Forecast: Mg for drive train applications.** The limited heat and creep resistance of AZ91 compared to the commonly used aluminium pressure cast alloys, have reduced or restricted the use of magnesium in drive train components up to now, that is, they make constructional solutions necessary and this at the expense of the weight reduction potential.

If one considers higher gearbox performances and the use of crankcase alloys, at temperatures beyond 130°C at given stress loads solutions should be found. This was one reason, amongst others, for worldwide scattering of Mg manufacturer development programmes (e.g. NORSK HYDRO, NORANDA, and DSM). Volkswagen has initiated a research project with the aim of developing a cost effective, heat and creep resistant Mg high pressure diecasting alloy and is work-



ing via the Magnesium Research Institute (MRI) in Beer Sheva with international partners on alloy and process development [11].

The alloy should have the following property profile compared to conventional alloys:

- Room temperature properties at least as good as AZ91
- Heat resistance above 120°C better than AZ91
- Minimal creep rate better than AE42
- Castability similar to AZ91
- Corrosion resistance similar to AZ91
- Costs similar to AZ91

The information was based on an alloy matrix of approx. 40 alloys (based on the alloy system Mg Al (Zn) in addition to various elements such as Ca, Mn, Si), which appear to be promising from a metallurgical and processing point of view. The target-orientated optimisation of materials becomes particularly apparent in terms of the creep behaviour. The new alloys show a secondary creep rate with a load of 85 MPa at 135°C (this load collective was selected exemplary for the loads that occur during gearbox operation), which is up to one power of ten less than the corresponding values for the conventional alloys AZ91 and AE42 (see Fig. 8.12) [11].

Additional tests also show a balanced property profile for the projected area of application. As the characteristics of test rods cannot be applied directly to real components in terms of their casting properties and e.g. hot cracking tendency, their potential for substitution of aluminium alloys by magnesium alloys currently in use was examined during the manufacture of series production parts

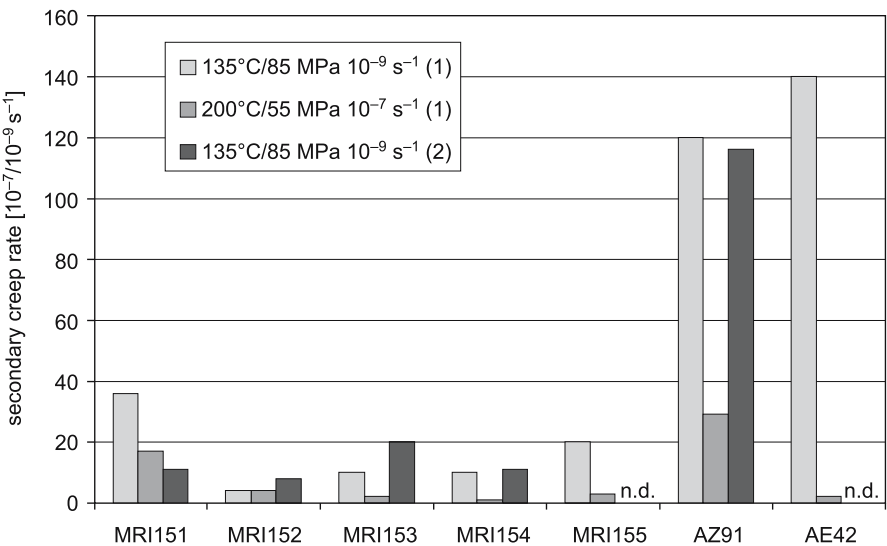
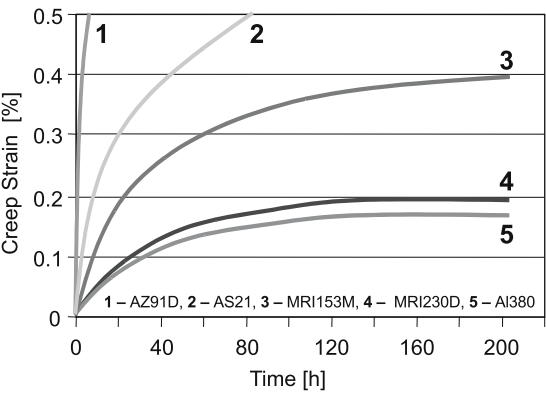


Fig. 8.12. Secondary creep rates of the alloys MRI151–155 with different load spectra, compared with AZ91 and AE42 [11]. (1) tensile (2) compression



**Fig. 8.13.** Creep curves of MRI/DSM - Mg-alloy (140°C/70 MPa) in comparison with different alloys

**Table 8.2.** Properties of new Mg-alloys, compared with standard alloys

Property	MRI 153M	MRI 230D	AZ91	AE42	AS21
Tensile Yield Strength [MPa]					
20°C	170	180	160	135	125
150°C	135	150	105	100	87
Tensile Strength 20°C [MPa]	250	235	260	240	230
Elongation to fracture (%)	6	5	6	12	16
Impact strength [J]	8	6	8	12	14
Fatigue strength [MPa] <sup>a</sup>	120	110	100	90	90
Corrosion rate [mg/cm <sup>2</sup> per day] <sup>b</sup>	0.09	0.10	0.11	0.12	0.34

<sup>a</sup> Rotation bending tests 10<sup>8</sup> load cycles; R = -1.

<sup>b</sup> 200 h salt spray test (ASTM B-117).

and component tests. After these tests some further alloy modifications were made and as a result two very attractive alloys came out, MRI153M for the temperature application range up to 150°C and MRI230D for temperatures up to 200°C (see Table 8.2 and Figs 8.13 and 8.14 [12]). These alloys are capable of use in high-performance gearboxes and crankcases and their ancillaries, and match the reference properties of Al.

**Lightweight construction in drive train: example – intake manifold [13]**

Intake units have the task of supplying the engine with air for combustion. Often several components are integrated into the intake manifold e.g. exhaust gas re-circulation valve or switch elements to vary the intake path. For manifolds with exhaust gas re-circulation temperatures up to 130°C are possible. Due to the fact that sulphuric acid in a very low concentration can arise, a specific corrosion load has to be considered. The lightweight construction of intake units can be

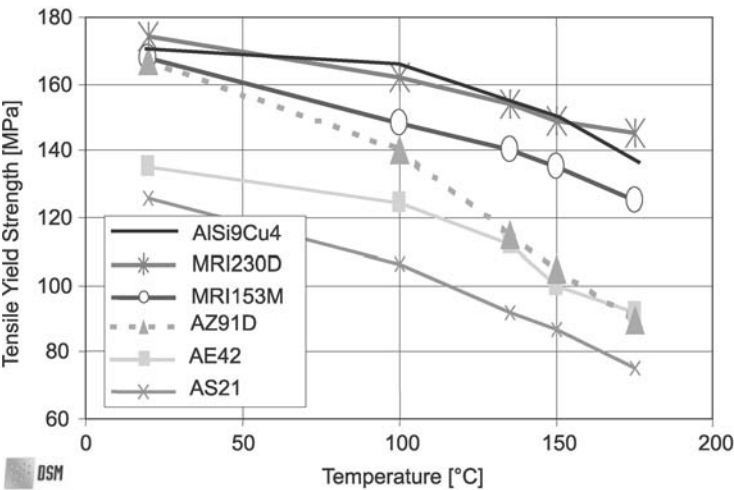


Fig. 8.14. Tensile yield strength for different alloys

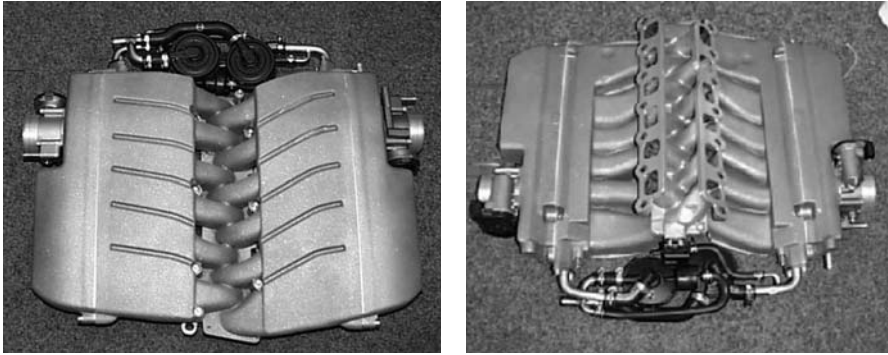
achieved with the aim of weight and cost reduction through good design in terms of effective material usage and component integration. Weight and cost reduction can be achieved by the following measures:

- Low density material (Mg, plastic)
- Low wall thickness
- Avoidance of material accumulation
- Integration of parts and components

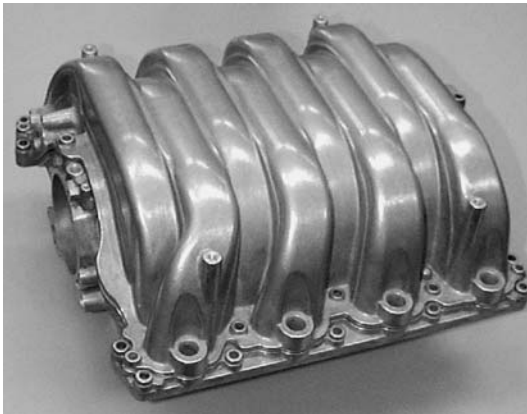
A standard cost-effective way of manufacturing today is by sand casting or permanent mould casting of aluminium with the disadvantages of heavy weight (wall thickness > 3.5 mm), rough surface and more machining. The high-pressure diecasting process offers advantages because of possibly lower wall thickness and smoother surfaces (low flow resistance, see Fig. 8.15). The shell concept can be used to balance limited die design possibilities for diecasting in contrast to sand casting (see Figs. 8.16, 8.17: four-shell construction).

The demands on intake manifolds, in terms of strength and stiffness, require a wall thickness in large areas of approx. 1 mm for aluminium, approx. 1.5 mm for Mg, and approx. 2.0 mm for plastic (PA 6) due to stiffness. The wall thickness of intake manifolds varies greatly due to the manufacturing process and material (compare Table 8.3), and attains a minimum of > 1.5 mm with magnesium die casting.

By using the manufacturing process dependent weight advantage of Mg compared to Al and plastic and whilst considering the design in terms of effective material usage e.g. reinforcement by use of ribbing, a weight reduction of approx. 25–30% can be achieved for a Mg intake manifold compared to Al. The acoustic properties of an intake manifold are determined, among other things, by the material's stiffness and its damping properties. Magnesium has other advantages as well.



**Fig. 8.15.** Left: 12 cyl. intake manifold 8.43 kg (Audi) AZ91; Right: Lower view of intake manifold



**Fig. 8.16.** Intake manifold; total weight 5,490 g (AZ91)/Audi V8

Material accumulation on intake manifolds can be found anywhere where an interface is necessary. These are areas where shells are assembled and components attached or the manifold itself is bolted to the engine. Particularly at bolted joints, Mg and Al have an advantage over plastic. Due to the low heat resistance, plastic flanges have to be made approx. twice as thick and inserts or sleeves are necessary. Further differences in terms of joining techniques/thread types can be seen in Table 8.3.

Contact corrosion is usually considered necessary with the use of coated steel bolts or aluminium bolts.

**Forecast.** Due to the high temperatures coming from exhaust gas re-circulation, hybrid intake units are only partly necessary, that means in the higher loaded, lower part aluminium can be used and in the upper part magnesium. Using heat and creep resistant die cast alloys (see Fig. 8.14), magnesium could be used fully in these cases.

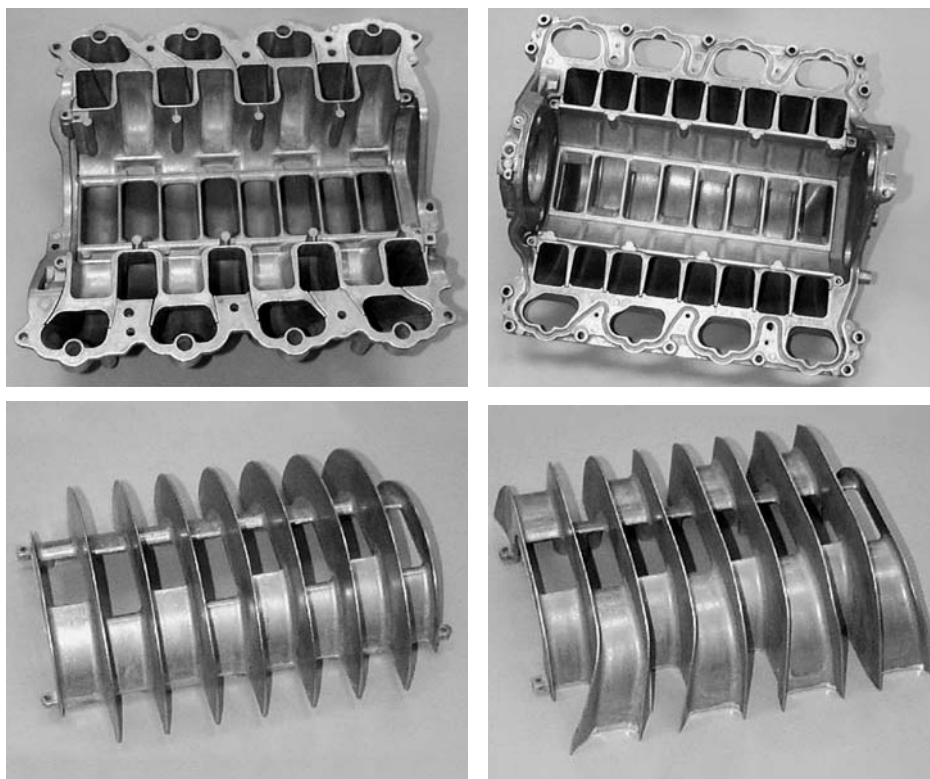


Fig. 8.17. Intake manifold parts

The most favourable weight advantage can be achieved currently by means of Mg die casting. By good design in terms of effective pressure casting with minimised use of materials and exploitation of manufacturing technology advantages (up to double die life compared to Al; 15–20% faster cycle times; better tolerance values), the costs per part can equate approximately to that of an aluminium pressure cast intake manifold. The advantage of integration is not only the lightweight construction, but also a considerable saving in costs and improvement in reliability due to fewer parts and avoidance of interfaces.

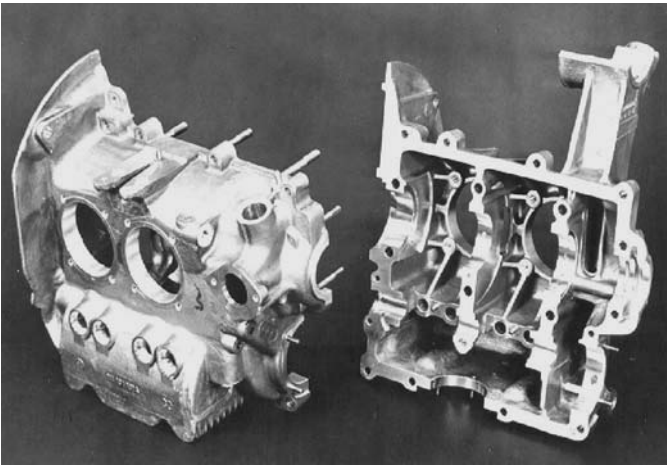
### ***Crankcase and cylinder head cover***

**Crankcase.** The load on the rear of the VW Beetle, developed in the 1930s, was an essential reason to produce the crankcase out of magnesium (Fig. 8.18). Today there is an urge, especially on front-wheel drive vehicles, to save weight at the front axle. Thus the drive train, in particular, with engine and gearbox is an obvious choice.

The achievable saving in weight of approx. 20–25 % compared to aluminium would mean an absolute maximum of 4–10 kg, depending on the type of engine. The particularly high material demands on Mg (temperature/stress of e.g.

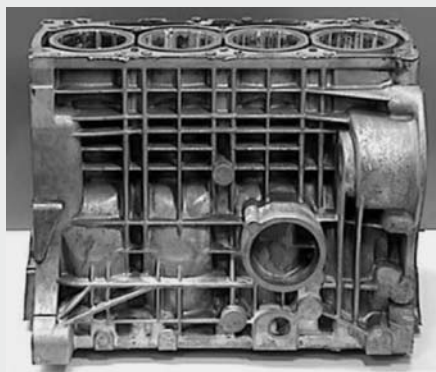
**Table 8.3.** Various manufacturing procedures and materials for Intake manifolds [13]

Process, material feature	Permanent mould cast, sand cast	Shell die-casting aluminium	Shell die-casting magnesium	Shell injection mould PA 6.6 GF30	Melt core, built core PA 6.6 GF30
Material density [kg/dm <sup>3</sup> ]	2.7	2.7	1.8	1.4	1.4
Required wall thickness[mm]	> 3	> 1.8	> 1.5	> 2.5	> 3
Flange width for connection of shells [mm]	–	approx. 5	approx. 5	approx. 10	–
Type of connection between shells;	–	Bolting, welding, bonding M4 1.5 × d = 6 mm	Bolting, welding, bonding M4 1.5 × d = 6 mm	Vibration-, hot wire-fusing –	–
Flange thickness to engine[mm]	> 10	> 10	> 12	> 20	> 20
Type of connection to attachments	Cuttetd or self forming thread	Cuttetd or self forming thread	Cuttetd or self forming thread	Threaded insert or sleeves	Threaded insert or sleeves
Intake manifold weight [%]	> 200	100	60	85	100



**Fig. 8.18.** Beetle-engine; alloy: AS41 (1973 changed to AS21), weight: 9.7 kg, boxer engine, air-cooled

- **Mg-alloys:** - AZ91  
- AE42  
- MRI153
- **High pressure diecasting**
- **Weight Mg-crankcase:**  
approx. 10.6 kg
- **Weight reduction in comparison  
to Al-crankcase:** approx. 4.4 kg



**Fig. 8.19.** Mg-crankcase prototype

150–200°C/50–100 MPa) will need to be satisfied by an even better heat and creep resistant alloy. A further essential pre-requisite is a special coolant for water-cooled Mg crankcases.

A Mg crankcase produced by high-pressure die casting is feasible if it is constructed efficiently in terms of the magnesium properties. This applies also to the bolted area, but in particular to the crankshaft bearings and the webbed area between the cylinders in the vicinity of the cylinder head gasket. From a technical standpoint as far as casting is concerned, a compact crankcase can be more easily cast than a gearbox housing with long flow channels and thinner walls. The relevant development work was done (Fig. 8.19).

Another example is shown in Fig. 8.20, the design principle of the Mg-Hybrid cylinder block from Audi [14]. The alloys AZ91/MRI153M /230D were used to build prototypes.

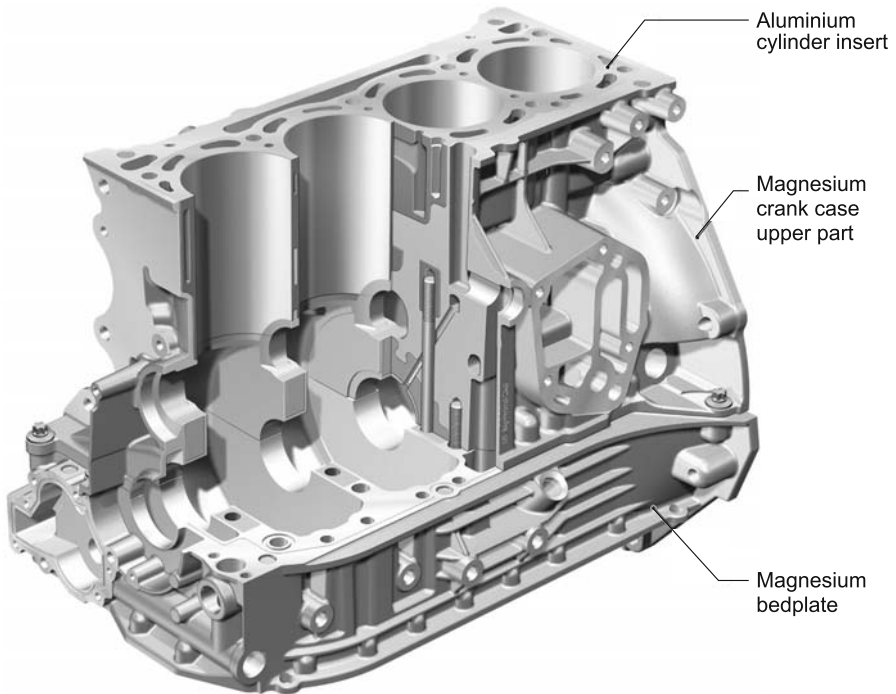
The distinguishing feature of the mg-hybrid cylinder block is the use of aluminium in severely loaded regions to solve localised materials engineering problems. The engine block has a modular structure with a compact, multi-functional cylinder insert in aluminium, which is cast-in during the diecasting process. Due to the stringent requirements of the acoustic properties of the power unit, a very stiff crankcase bedplate, also made of magnesium, is fitted to the Mg-Hybrid motor.

On the other hand, the use of Mg in sport and racing engines manufactured by sand casting has already attained traditional status. Special alloys such as WE 43/54, QE22, ZE41, EQ21 (see Fig. 8.21) are common. There are now cost-effective alternatives for premium car engine applications available (MRI201S/ 202S/203S) [12].

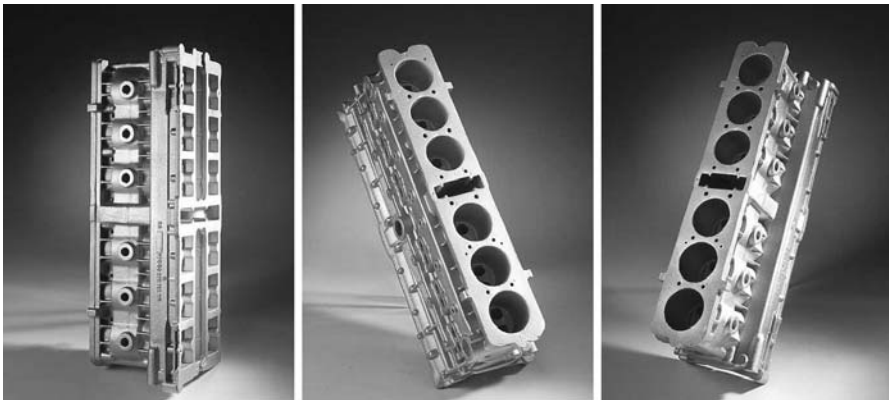
### Cylinder head covers

Cylinder head covers produced by die-casting AZ91 can be found in a number of vehicles. Competitive materials are aluminium and plastics. Cylinder head covers are installed both painted and unpainted depending on the manufacturer. The Fig. 8.22 show two examples.





**Fig. 8.20.** Sectioned view of the Audi Hybrid-Mg-cylinder block



**Fig. 8.21.** Mercedes M291 prototype sports engine-crankcase and cylinder block (12 cylinder Boxer engine; Alloy EQ21/RZ5) [15]



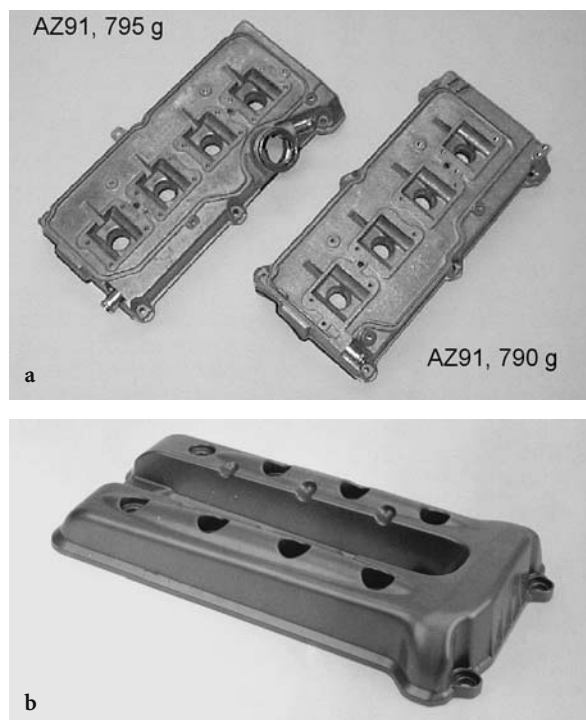


Fig. 8.22. a Cylinder head cover (Audi V8/AZ91); b BMW (AZ91/929 g)

### 8.1.3.2 Interior Applications

For interior applications in the vehicle, magnesium is in particular competition with the lightweight materials aluminium and plastic. The demands on the components here are extremely varied. The highest demands must be fulfilled for safety-related components such as steering wheel and seats in terms of strength and energy absorption and relatively low demands for various trim and small parts. The common requirements for all are low corrosion and a moderate load capacity temperatures at up to approx. 80°C. The component demand profile is thus extremely varied compared to the drive train profile, and the use of other Mg alloys is also possible. With the right design, magnesium is much superior to the plastics normally used in respect to the property profile. This is the reason why today most of the component applications can be found in the interior for many vehicle manufacturers. Often, magnesium solutions are also the most attractive choice in terms of costs. The alloy AM50/60 is used in many cases with elongation to fracture values of approx. 8–10%.

#### **Steering Column System; Steering Wheel**

The steering column must be balanced with the whole retaining system and vehicle structure. The resistance to imbalance from the wheels is an important com-

fort factor of the steering wheel. The steering column should be very rigid and also have little mass so that the natural frequency of the steering column/steering wheel composition is displaced to higher frequencies. A reduction in weight in the steering column system has the effect of improving the dynamic vibration response caused by wheel imbalance and bumps in the road.

The demands of load on a steering wheel in terms of operational and functional loads are:

- transfer of steering force i.e. steering wheel must be strong enough in shape under static load;
- static stress on torsion and bending (special test called coat-test)
- endurance strength under dynamic load
- at dynamic loads, e.g. crash and airbag operation, a defined deformation of the steering wheel is required, i.e. energy should be absorbed and the steering wheel should not break below a defined force level.

As an alternative lightweight construction to the composite design of sheet steel, Al and Mg die casting steering wheel cores prevail. The following demands must be fulfilled:

- elongation to fracture of at least 10–12%
- similar strength to  $\text{AlMg}_2\text{Mn}$ ,  $R_m$  approx. 180–230 MPa;  $R_{p0.2} = 90\text{--}120$  MPa
- good castability; high impact resistance

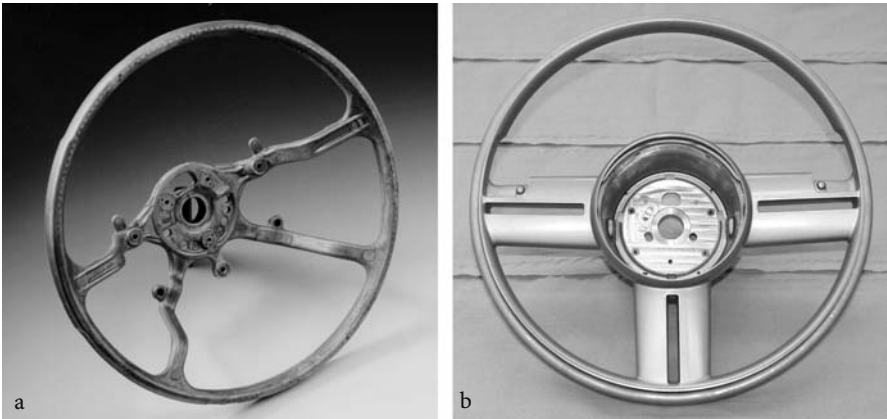
Alloy AM 50 shows the best-balanced property profile in contrast to AM20 and AM60 for demands on the steering wheel. The increased notch sensitivity compared to the  $\text{AlMg}_2\text{Mn}$  alloy must be taken into account constructively. Mg steering wheel skeleton frames can be manufactured at low cost by the cold chamber, pressure casting method with two cavities in one mould. Some proven advantages over Al steering wheel cores:

- approx. 20% weight saving (Fig. 8.23, Table 8.4)
- similar to equal manufacturing costs; among other things by a gain in productivity compared to Al steering wheels of approx. 30–40%, as mould filling is more efficient, mould life and casting frequency higher
- increase in natural frequency (70–90 Hz against 65–82 Hz for Al)

When designing the die casting mould, particular care should be taken in the mould temperature control (use of various cooling circuits) and in the use of a large flat ingate system to reduce the mould filling time. Generally, when designing the component, larger radii and stronger reinforcement should be implemented compared to aluminium, and larger cross sections and a wall thickness of approx. 4–6 mm are necessary.

The Mg steering wheel core as a deforming safety-related component is an example of the potential of magnesium to replace even aluminium. The prerequisites for this are a magnesium-compatible design and a reliable production process with high die cast quality.

Other magnesium components used frequently in the steering column/steering wheel composition are e.g. a steering column console (Fig. 8.24) and the steering lock (Fig. 8.25; previously frequently a Zn die cast part).



**Fig. 8.23.** a VW Golf steering wheel core AM50/515 g; b VW 3L Lupo steering wheel core (AM50)

**Table 8.4.** Comparison of different skeleton frame concepts (TRW) [16]

	Weight [%]	Part costs [%]	Advantage	Disadvantage
Present solution steel skeleton	100	100	easy to develop variation in inertia moment proven solution	high inertia moment
Present solution assembled aluminium skeleton	70	125	low weight variation in inertia moment	high costs
Full diecasting aluminium skeleton	70	80	low weight low inertia moment low costs easy to recycle	high investment high delvelopment costs
Full diecasting magnesium skeleton	50	78	low weight low inertia moment easy to recycle	high investment high development costs
Steel skeleton pressed	60	75	low weight low costs easy to recycle	high investment high inertia moment not yet tried out
Full plastic skeleton	60 expected	95 expected	low inertia moment vibration damping	high investment high development costs not yet tried out

**Seat Applications**

Seats must withstand high dynamic loads in case of a crash. The demands in terms of energy absorption have prevented greater use of Mg seats up until now (in addition to reasons of cost). An example of a mixed construction is the Alfa Romeo seat (Fig. 8.26). The elongation necessary in case of an accident is



Fig. 8.24. Audi A6 steering column consoles AZ91/920 g



Fig. 8.25. VW steering lock AZ91/295 g

achieved via the steel recliner. The relatively low weight reduction of 22% compared to steel clearly shows the high demands.

The DaimlerCrysler integral seat system (500 SEL Roadster) used the particular advantages of Mg die casting in terms of integration possibilities (see integrated belt retainer Fig. 8.27) and manufacturing advantages such as minimal achievable tolerances and the smaller draught angles [17] possible compared to Al permanent mould casting. The seat frame consists of five-Mg die cast parts. Due to the high strength requirements the backrest supporting structure and the seat frame (4 parts) are made in AM50. The backrest shell is made in AM20 (1.5 kg) (Fig. 8.28).

Especially in the MPV vehicle concepts (multi-purpose vehicle), the variability of the interior by means of repositioning the seat layout is an essential aspect. Lightweight Mg seats will play an important role in this in the future.

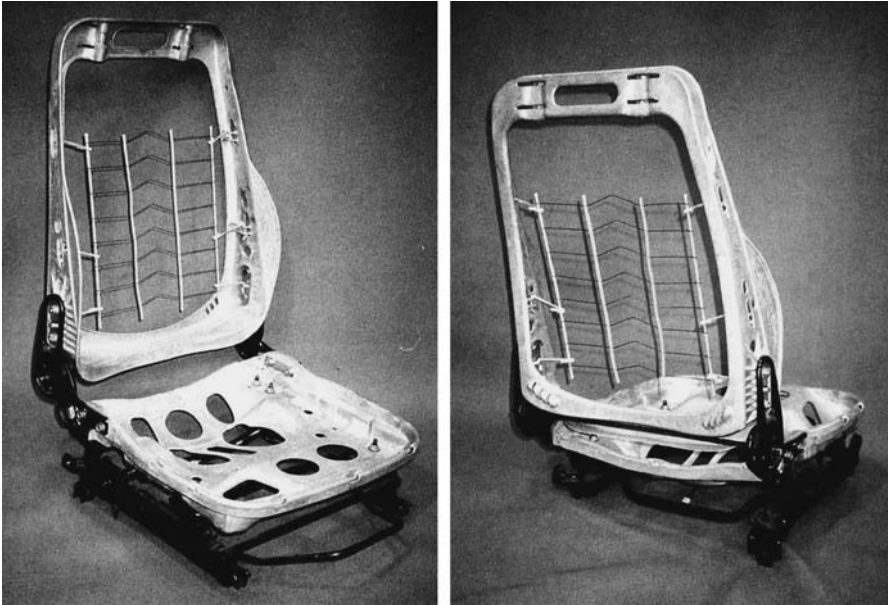


Fig. 8.26. Alfa Romeo seat

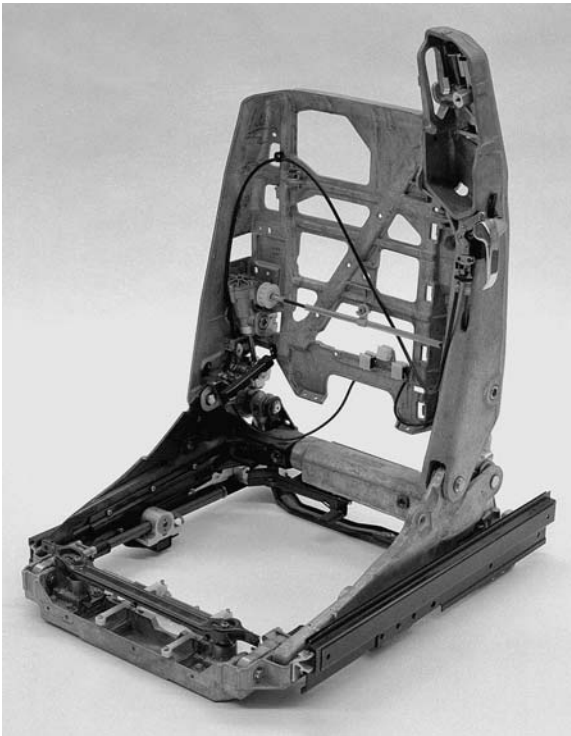


Fig. 8.27. DC integral seat [17]

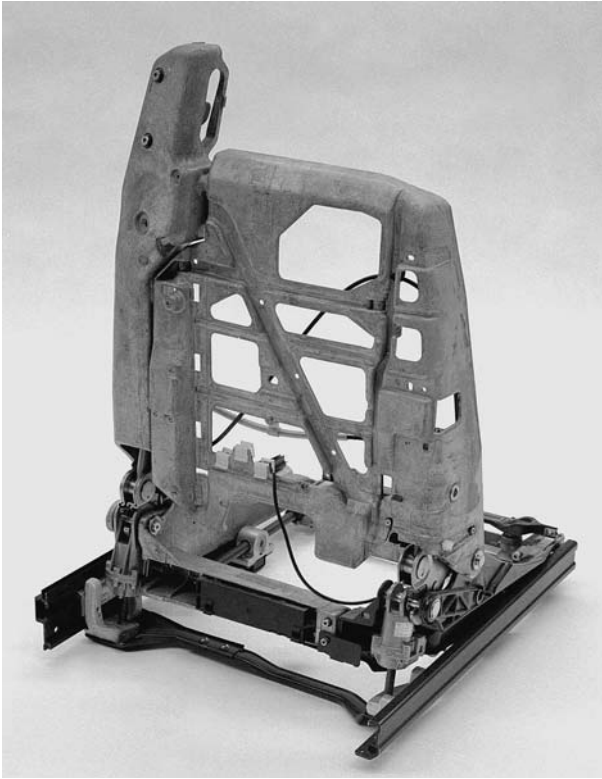


Fig. 8.28. Backrest shell AM20/backrest supporting structure AM50

### ***Other Interior Parts***

The frame of the navigation system is taken here as an example (Fig. 8.29). The weight of the additional parts which need to be mounted, created a problem in terms of stiffness for a plastic design due to the load. A solution was found in a thin-walled integral Mg die cast part.

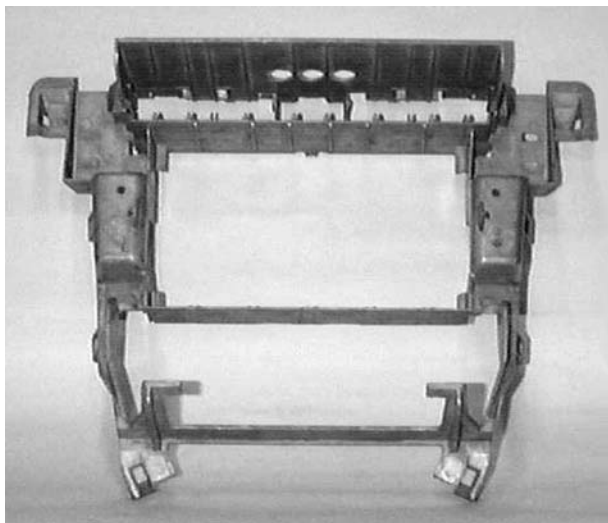
Good surface quality with stiffness requirements are further reasons for the use of magnesium such as for the radio trim shown in Fig. 8.30 or the dash board panel trim (Fig. 8.31).

The housing for mounting the selector (gear) lever is another example (Fig. 8.32), which is manufactured as a thin-walled die cast part to replace a steel/aluminium component. The possibility of casting thin walls up to 1 mm with an advantage in stiffness and weight over the standard solution speaks for magnesium.

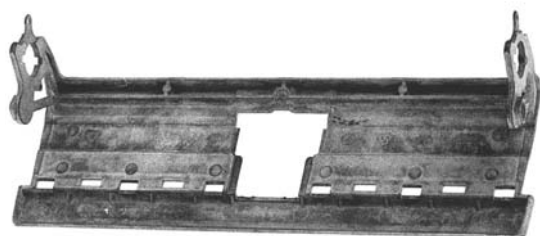
Further component examples in the interior are: rear-view mirror frame; handbrake lever with cover (Fig. 8.33) and the airbag housing (Fig. 8.34).

A general increase in applications requires a reduction in cost by means of optimising the processes e.g. by using magnesium casting and processing advantages and also by applying lightweight construction know-how.

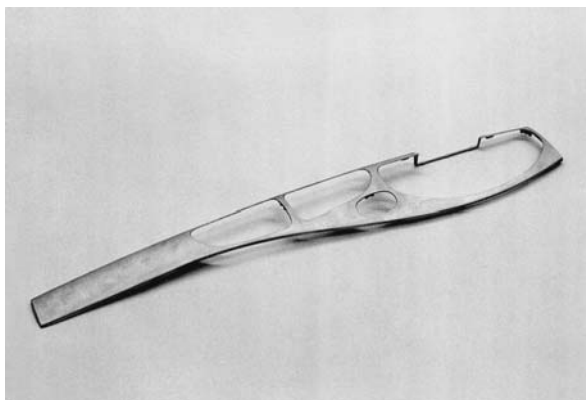




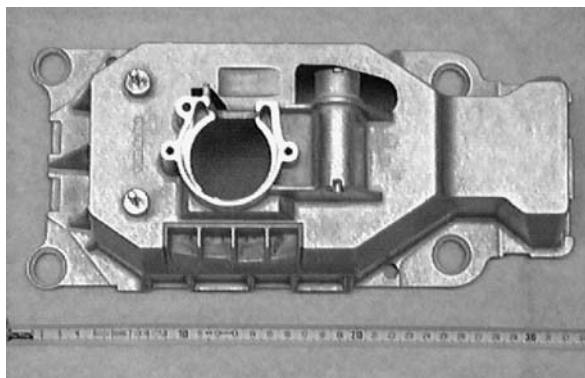
**Fig. 8.29.** Frame, console NAV (Audi) AZ91/435 g



**Fig. 8.30.** Radio trim: AZ91/74 g



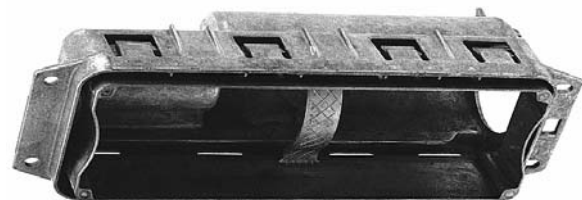
**Fig. 8.31.** Instrument panel trim Jaguar/AZ91



**Fig. 8.32.** Unitary switching VW (housing of selector lever)



**Fig. 8.33.** Handbrake lever with cover/920 g (Porsche)



**Fig. 8.34.** Airbag housing



### 8.1.3.3 *Body*

The body in white of today's series production vehicles is manufactured mainly as a body structure from sheet steel in sheet panel (monocoque) design. The Audi A8 and A2 were the first series production of vehicles to be built with a space frame (ASF) completely from aluminium. The ASF concept is a frame structure consisting of extrusions, cast nodes and sheet panels in which every surface part is integrated to provide the necessary structural support. The use of high performance fibre reinforced plastics (FRP) for passenger compartments in conjunction with e.g. an aluminium frame structure is reserved at the moment mostly for sports vehicles. In the future a mixed construction for bodies in terms of material usage and design concept will become more evident. For this, magnesium can also be used via Mg sheet, Mg extrusions and Mg die-cast components in the structure and as attachments to the basic body.

#### **Cast components**

The integration of individual parts, complex, thin-walled components such as door and tailgate/boot lid inner parts should be looked at as a challenge, in terms of whether manufacturing is possible. With such applications the emphasis is on the integration of parts in addition to weight reduction as these parts generally replace Aluminium – or steel sheet designs. Hang-on applications offer the means of using magnesium without changing the whole vehicle concept. For this, the demands in terms of energy absorption, surface quality and costs must be met.

#### **Tailgate/boot lid, die cast inner part**

For the tailgate of the VW 3L Lupo (Fig. 8.35), the following variations were compared within the framework of a concept evaluation process: aluminium (outer/inner), synthetic material (outer/inner), plastic outer/magnesium inner and aluminium outer/magnesium inner. An Aluminium sheet panel inner part would be problematic in terms of shaping (therefore two panel parts would be necessary). An aluminium die cast inner part would have thicker walls than a part from magnesium cast due to reasons of castability but not of strength. The weight advantage compared to a steel component would be lost with for aluminium die cast part. The additional integration of six steel sheet parts in Mg die cast version, e.g. hinge reinforcements, which are essential for weight reduction, makes the Mg cast version most advantageous. The following component solution was finally selected at the beginning of the series production of the VW 3L Lupo:

- integral Mg die cast inner part, Al outer panel and Al lock reinforcement

Figure 8.36 shows the load application situation, which is used for tailgate design in terms of rigidity, torsion, buckling and load of gas struts. The mountings, the applied forces and the test parameters can be seen. The selected variation shows the best values in terms of weight and torsion.

The aims of the development were as follows: high level of integration, weight minimisation and satisfaction of requirements with regard to features such as

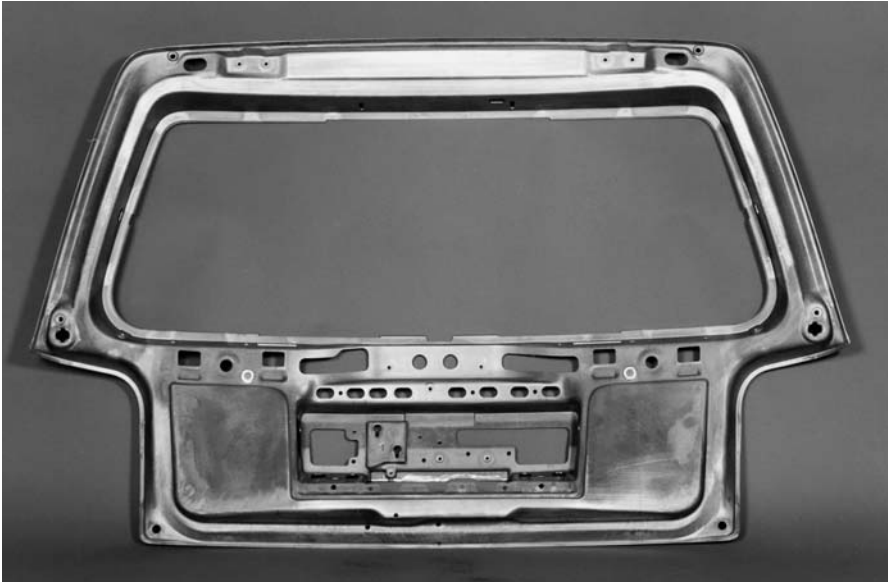


Fig. 8.35. Mg tailgate inner part VW 3L Lupo

stiffness, crash safety and surface quality. A direct weight comparison for the Lupo tailgate reveals the following figures: steel (10.5 kg); aluminium (8.5 kg); magnesium-aluminium tailgate 3L Lupo (5.4 kg).

#### Types of joining:

The Al outer panel is flanged onto the Mg inner part, and for reasons of strength and insulation, also both parts are bonded along the flange using an epoxy resin adhesive. Threaded inserts made out of high strength aluminium are pressed into the Mg die cast part for the necessary threaded joints of assembly parts such as hinges or wiper motor mountings.

#### Corrosion/surface technology:

A die cast component has been used in a visible area for the first time with the tailgate. This required great effort from the cast component manufacturer and painter. Here the aim for cost reduction would be via casting optimisation and suitable coating systems to allow Mg die cast components to be installed also in the area of view with class-A-demands without additional work. Contact corrosion on aluminium and steel parts is prevented by coating the magnesium inner part, by insulating the individual parts to each other and by surface coating fastening elements and partly by using insulation foils between surface contact points.

#### Casting technology/manufacture:

To improve the surface quality, all non-visible and non-functional surfaces are textured to prevent heat cracks which are caused during the cooling process. The casting process was previously supported by a vacuum.

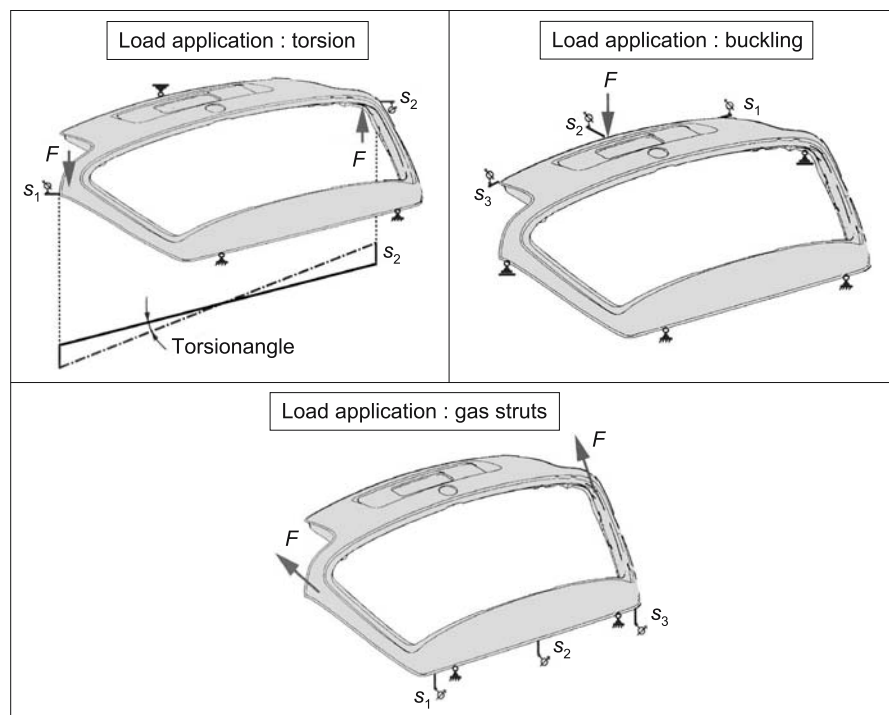


Fig. 8.36. Standard load applications of tailgate

### Door die cast inner part

As an example of a Mg application with hang-on parts, the research demonstrator, a door of the VW-car called Polo, was chosen (Fig. 8.37). The achievable degree of integration and the saving in weight, the joining technology, the castability, the achievable mechanical properties and the crash behaviour were to be examined.

#### Component description/construction notes:

A vehicle door must fulfil various requirement in the case of an accident. The specified response is defined for front and side tests. Static and dynamic load situations were the basis for the layout/construction (Fig. 8.38). The FEM calculations resulted in a necessary wall thickness of between 2 and 4 mm.

The Mg/Al door described is a hybrid door consisting of a Mg inner part, an Al outer panel and an inner window slot reinforcement and side impact bar made from Aluminium extrusions. The Al outer panel was integrated as part of the supporting structure for the whole door. To join the inner door to the outer skin, flanging and bonding were selected as the joining technique. The side impact beams were riveted and bonded for the prototype as well (Door dimensions:  $1.35 \times 1.15 \times 0.2$  m). The Mg die cast part integrates 7 parts, which were produced in the reference door out of steel sheets. The following savings in weight could be achieved (Table 8.5).



Fig. 8.37. Mg door inner part (prototype) AM60

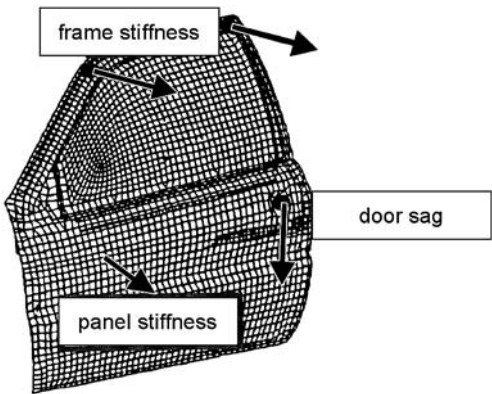


Fig. 8.38. Demands on doors

Table 8.5. Weight distribution of steel and Mg/Al-door

Door inner part	Steel – reference (comparable to Mg)	12.5 kg
	Mg – die cast part	6.4 kg
Remaining assembly	Steel – reference	10.5 kg
	aluminium	5.0 kg
Whole door body in white	Steel – reference	23.0 kg
	Mg/Al door	11.4 kg

**Component manufacture/casting:**

The Mg inner part was manufactured using the Mg alloy AM60 in a cold chamber pressure casting machine with vacuum support (closing force 47 MN). The gate system lines the breast area of the window (Figs. 8.39 and 8.40). The first attempts at casting resulted in several modifications, such as cast belts, reinforcements etc. in order to reach an adequate casting quality for the whole component. Typical achievable strength and elongation to fracture figures are given in Table 8.6. Here the cill area had to be optimised. The dimensional accuracy of the assembly was satisfactory.

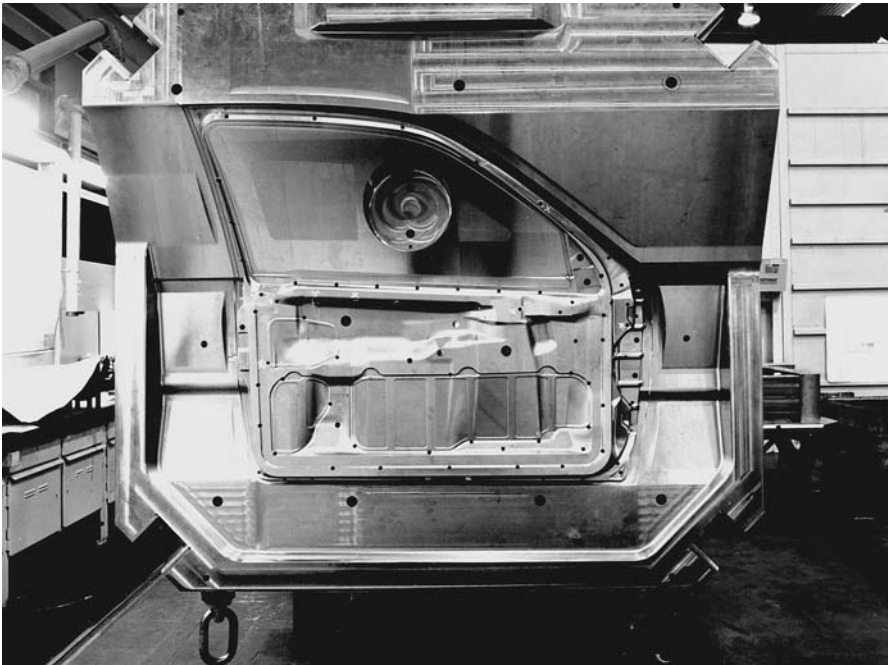


Fig. 8.39. Pressure cast mould (movable side)

Table 8.6. Elongation to fracture of die cast inner part; Yield strength measured: 120–135 Mpa

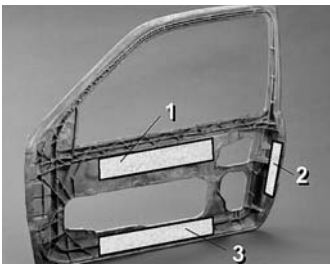
	Door area	No. 1	No. 2	No. 3	No. 4
	Window slot area (1)	10.3	11.8	10.1	8.3
	Lock area (2)	4.0	8.2	6.4	4.5
	Cill area (3)	3.6	7.1	4.9	2.8
	Elongation to fracture figures A 5 [%]				



Fig. 8.40. Pressure cast mould (fixed side)

### Test results:

The Mg door was tested with Al window slot reinforcement, side impact protection, and lock, hinge and window i.e. as full door assembly. The static tests to evaluate the door characteristics such as door sag, panel- and frame stiffness were successful. The elastic and plastic deformation results were below that required based on the steel door used as a reference. Furthermore, quasi static longitudinal and side compression tests were carried out that could be used as a good comparison basis to estimate the dynamic crash response (see Figs. 8.41–8.44).

Figure 8.42 shows the results of the quasi-static longitudinal compression test in which a ram applies a quasi-static force to the B pillar in a forward direction (Fig. 8.41). When comparing the different response to that of a steel door, it is clear that the door offers a higher stiffness and has a slightly higher energy absorption capacity up to the relevant ram travel of approx. 60 mm.

Several crash results are described as an example of the energy absorption of die cast components. These results were achieved with the Mg/Al door mentioned. Quasi-static compression tests and dynamic tests (side crash, frontal crash) served also as verification for crash simulation calculations with Pam-Crash.

### Side crash:

Although unsatisfactory elongation to fracture figures were achieved in the cill area of the Mg-die-cast part, the door assembly attained a pass in the crash test

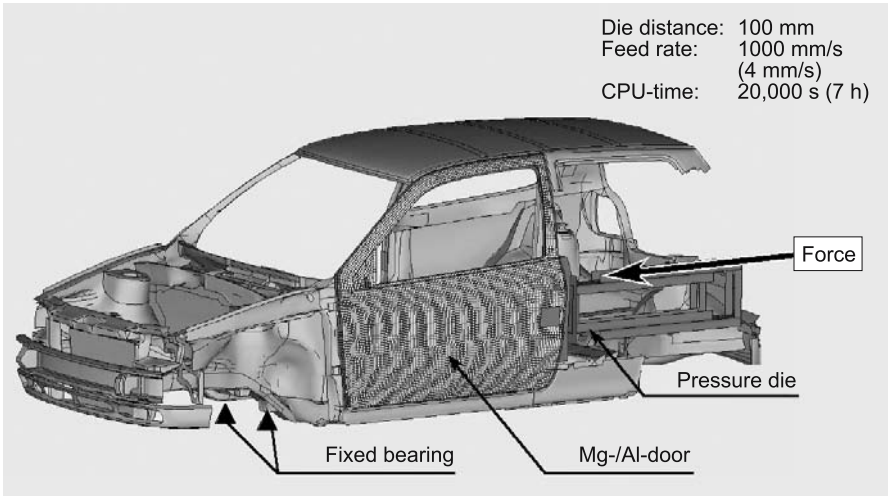


Fig. 8.41. Longitudinal compression test (principle)

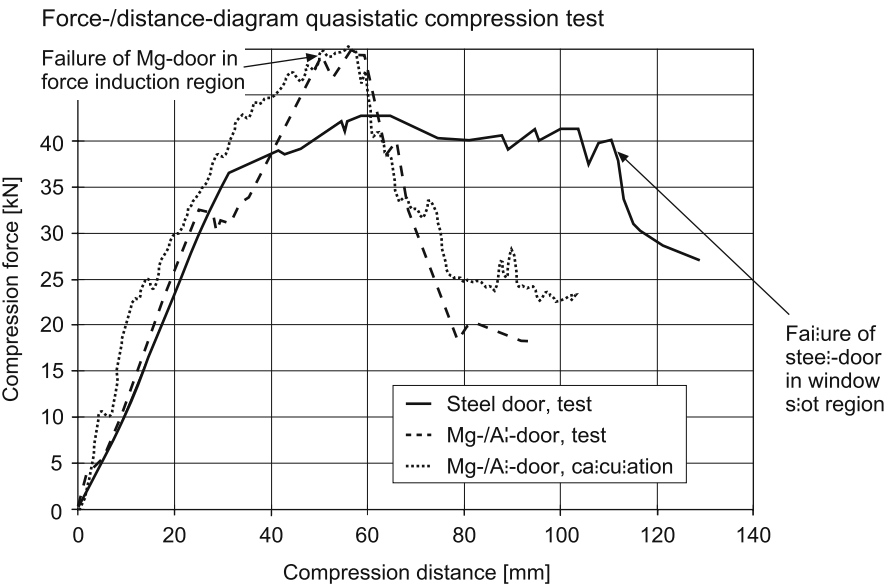


Fig. 8.42. Longitudinal compression test result

(Fig. 8.45). There were no signs of the Mg/Al door being pushed over onto the cill and it had a more homogeneous deformation than the steel door. The doors remained closed during the crash and the dummy results were also satisfactory (Test conditions: stationary car; speed: 27 mph; rectangular direction of impact; deformable mobile barrier).



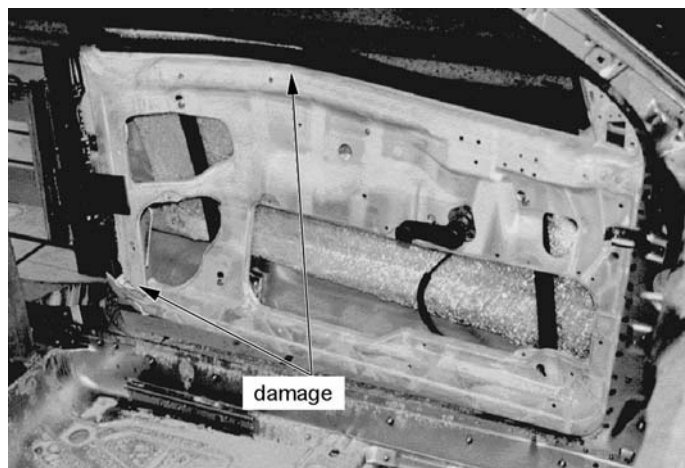


Fig. 8.43. Longitudinal compression test

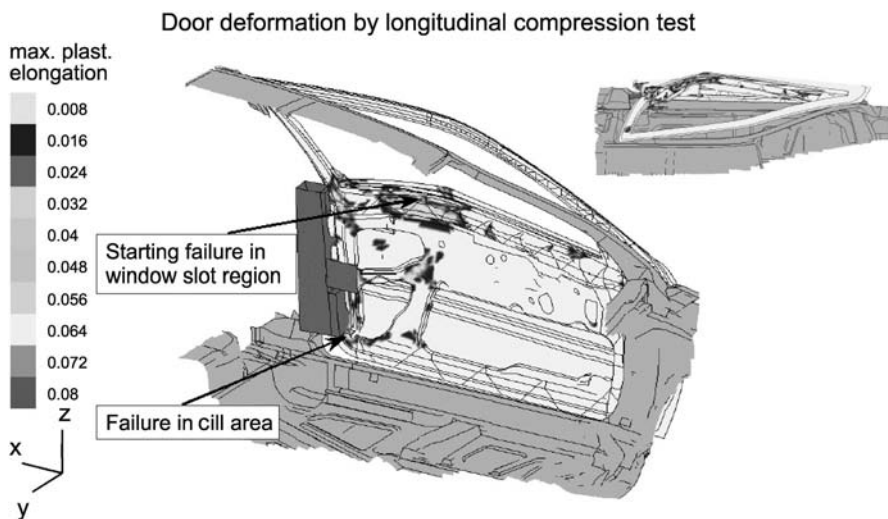


Fig. 8.44. Mg door inner part; longitudinal compression test

#### Frontal crash:

The collision speed on the AMS frontal crash was 30 mph. The stiff barrier offset was 50% of the vehicle width. The doors were easy to open after the crash, the Mg/Al-door was neither broken nor buckled and the crash-test dummy results were satisfactory (Fig. 8.46).

The decision to go to series production depends on many factors. The vehicle and door concept is important; a frameless door, i.e. without an upper doorframe, would mean fewer problems in terms of casting. A Mg door inner part would





Fig. 8.45. Mg door – side crash

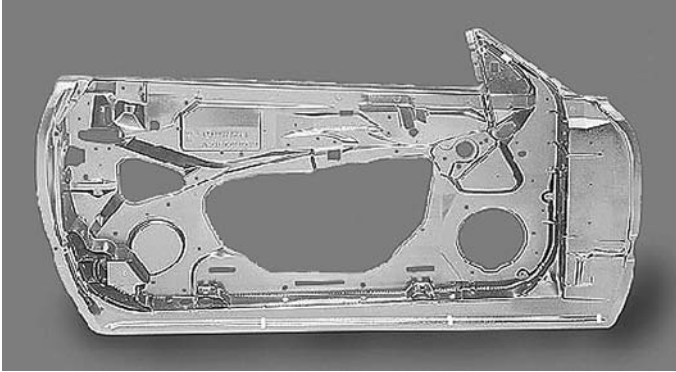


Fig. 8.46. Offset Front crash

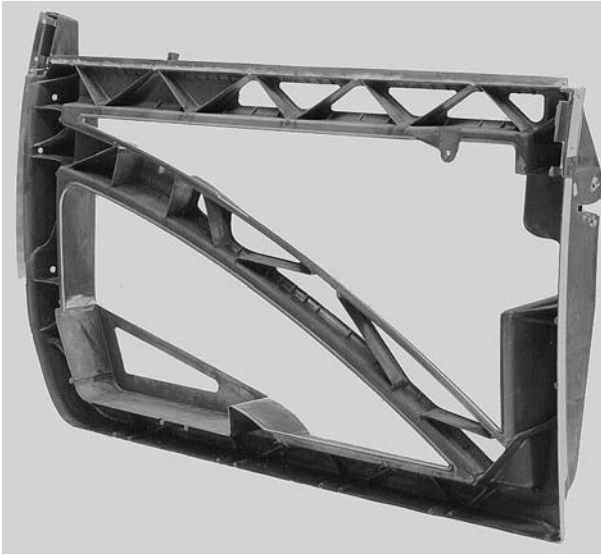
only make sense in conjunction with Mg, Al or plastic planking. This currently limits use to upper class and niche vehicles. DaimlerCrysler made the decision for the CL 500 to install a Mg inner door without an upper frame (Fig. 8.47). The inner part consists of a Mg die-cast part (AM50) and is reinforced partly with Al extrusion profiles and Al panels (outer skin AC120). The powder coated inner part is flanged using a 1K – epoxy resin adhesive [18]. A different Mg-door concept is shown in Fig. 8.48.

### **Structural parts**

An A-pillar made of AM50 was installed as a highly loaded structural part for a VW research vehicle. The component (Fig. 8.49) weighs 4.7 kg and connects the front end and the cill.



**Fig. 8.47.** Die cast inner door without window frame (Daimler/Chrysler-SL) AM50 4.5 kg; 1,450 × 800 × 150 mm; powder-painted, casting surface covered



**Fig. 8.48.** Door inner part; concept car CC1 (VW) AM50/4.3 kg

The tank cover in the Mercedes SLK (Fig. 8.50) can be seen as a genuine basic structural component. It serves as a partition between the luggage compartment and rear seat bench to reinforce the body. A welded steel panel construction and a welded aluminium construction were evaluated with a die cast magnesium part as an alternative. In addition to the weight advantage of the magnesium solution in AM60 (3.2 kg compared to 7–8 kg), there were further advantages with regard to the dimensional stability, less processing and lower package space requirements as well as the fact that coating is no longer required (dimensions 1.28 × 0.45 m; wall thickness approx. 2 mm) [19].



Fig. 8.49. A-pillar of concept car CC1 (VW) AM60/4.7 kg

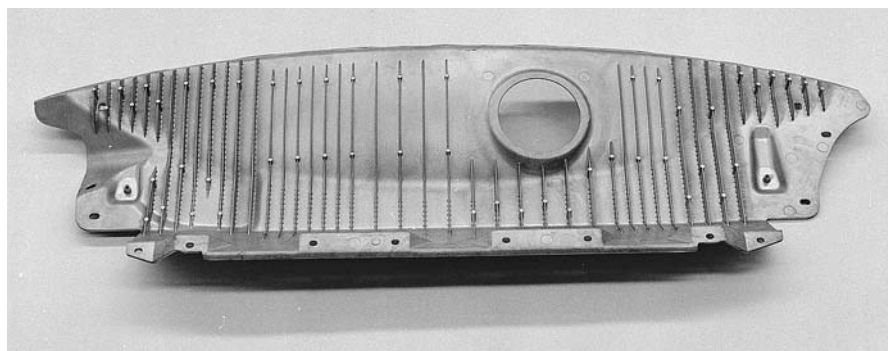


Fig. 8.50. Tank cover (DaimlerChrysler SLK) [19] AM60/3.2 kg

The cross car beam in the Fiat Marea is a structural component that joins the A pillars and replaces an existing steel panel construction consisting of 24 panel parts (Fig. 8.51). With a wall thickness of 2.5 to 1.8 mm, a weight reduction of 41% can be achieved (3.4 kg compared to 6.1 kg). The component manufactured in AM60B by vacuum pressure casting shows, in addition to weight reduction, advantages concerning part integration, reduced knocking and squeaking noises and coating is not required.

The largest weight and cost saving potential can be achieved by consistent use of the possibility to integrate a large cast part that can replace up to 30 or more

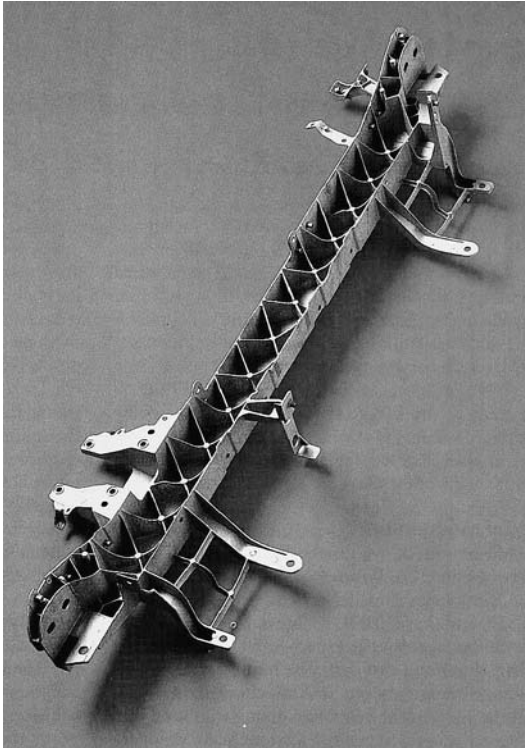


Fig. 8.51. Cross car beam (Fiat-Marea)

individual parts (Norsk Hydro [20]) and offers the means of mounting airbags, air conditioning systems, steering column connections, pedal clusters, etc. and joining the A-pillar structurally. Examples of this strategy are the instrument panel structure of the Fiat-Stilo (Fig. 8.52) and the BMW Mini (Fig. 8.53).

As in the US market more vehicles in Europe have now also been equipped with a magnesium instrument panel structure or a Mg-crosscar beam (Figs. 8.54 and 8.55) because the following further benefits can be achieved:

- Reduction of part numbers results in fewer interfaces and better tolerances
- Improvement of body stiffness and crash behaviour
- Increased vertical steering column frequency
- Weight reduction of 40% in comparison with steel
- Cost advantages are possible

Due to their design these types of integral components have many interfaces with other components and vehicle modules. This is why a design-freeze in the vehicle development phase is not possible until very late on. The time consuming production of such a complex die casting tool and the optimisation in terms of casting and also component tests stand in the way of this. If, in addition, a platform concept is pursued during vehicle development, a heavily integrated, instrument



Fig. 8.52. Dash board panel carrier (Fiat-Stilo)

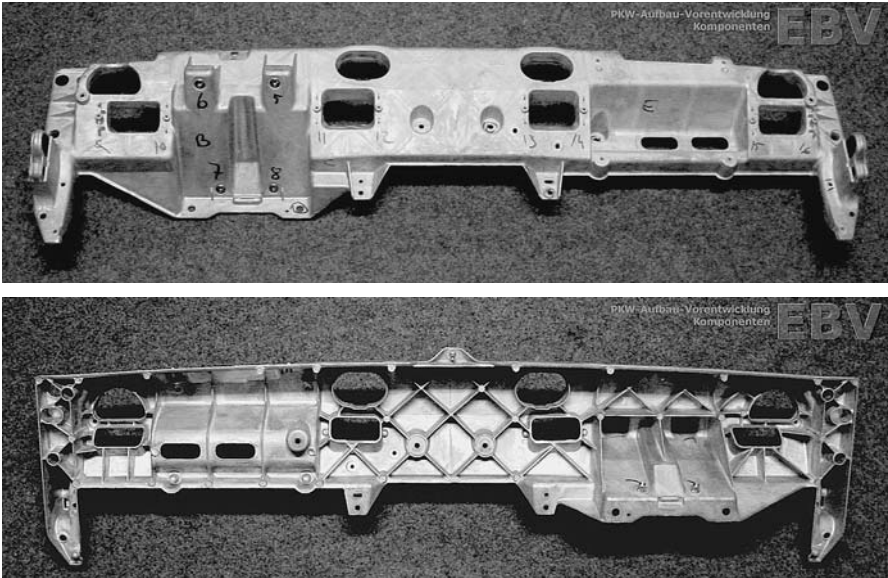
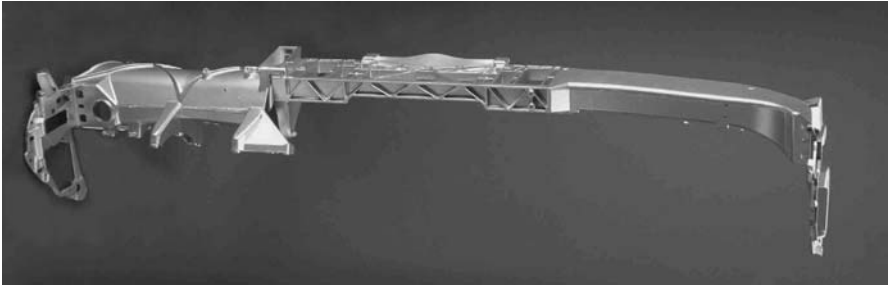
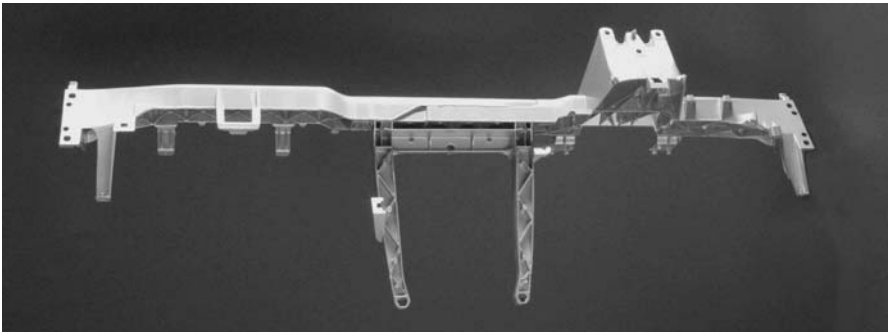


Fig. 8.53. Dash board panel carrier (BMW-Mini)





**Fig. 8.54.** Crosscar beam Audi-D3 (driver side: Aluminium; co-driver side Mg:2 kg)



**Fig. 8.55.** DC-E-class (4,26 kg) three parts

panel, carrier concept will be hardly flexible enough. The reduction of development and testing time is therefore a very important aspect in increasing these Mg applications. The main prerequisites of a standard application of the instrument panel include the use of casting and crash simulation tools (validation is necessary), early design freeze and the use of prototyping tools to obtain parts with near-series characteristics at a very early stage. In addition, parts must be approved by means of integral test procedures such as drop tower tests; test specimen results are not relevant for such complex parts. An alloy with improved castability and high elongation to fracture would greatly assist these applications.

Nowadays, the number of niche cars, cross over vehicles, MPVs and sports/fun cars with low or medium unit numbers is increasing very rapidly. Cost advantages arise with regard to die costs in comparison with the cost of several sheet steel dies.

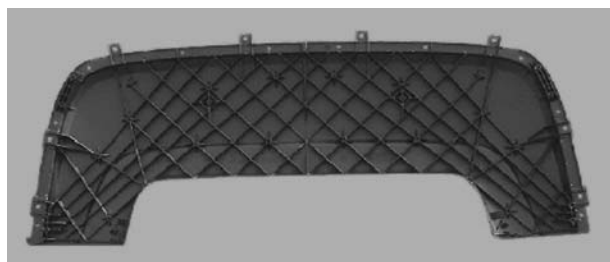
Examples for sport car applications (roof cover, top covers) are shown in Figs. 8.56–8.59.

### ***Mg Panel Components***

The full potential of magnesium for lightweight construction is realised above all when sheet metal components with a large surface area and thin walls, which are



**Fig. 8.56.** Roof cover (Porsche Boxter)



**Fig. 8.57.** Top cover BMW; AM50; 4.5 kg; 1,500×800×300 mm; powder painted, cast surface covered by imitation leather

subject primarily to bending stresses and thus need to satisfy requirements for flexural/buckling stiffness, i.e. the outer panels of body components (doors, boot, bonnet). In such cases, weight savings of around 50% compared with steel and 20% compared with aluminium can be achieved depending on stress profiles relevant to practical applications (Fig. 8.60).

Due to the only recently occurring demand for Mg sheets, the availability of sheet dimensions relevant to the car industry and also expectations of quality in regard to surface quality (peak number, medium roughness) and corrosion at

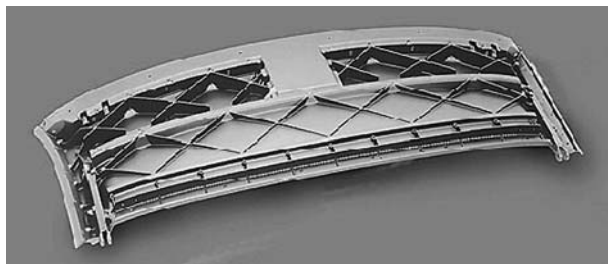


Fig. 8.58. Part of the top system of Porsche 911 (AM50; 2.8 kg;  $400 \times 800 \times 140$  mm)

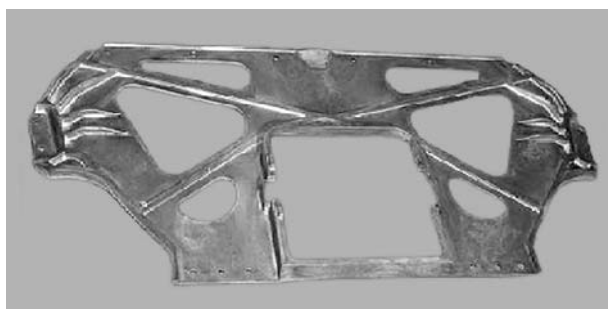


Fig. 8.59. Rear panel; DC AM50; 2.4 kg  $1,250 \times 500 \times 70$  mm without coating

competitive prices are still very limited. The mechanical properties of commercially available Mg sheets are in the range of Al panels and Mg sheets can typically be found in vehicles, such as AC120. As to the layout of the component, the lower elastic modulus must of course be considered. Due to the hexagonal lattice structure, the forming properties of magnesium sheets at room temperature are limited. Basic investigations into hot forming, however, reveal that at  $225^{\circ}\text{C}$  an AZ31 sheet has similar deep-drawing capabilities to steel-and-aluminium sheets at room temperature. The recommended temperature range for deep drawing operations is between  $200^{\circ}\text{C}$  and  $250^{\circ}\text{C}$  and for stretch drawing above  $250^{\circ}\text{C}$ . To produce components, heated deep drawing tools are a necessary prerequisite.

Customary Mg sheets are not capable at present of meeting the corrosion resistance and surface finish requirements placed on vehicle-body outer skin components. For that reason, current research activities are concentrating primarily on the design and testing of sheet metal components for the vehicle interior. In the medium term, production and corrosion resistance strategies for exterior applications need to be developed.

Mg panels were used mainly for military purposes in the 1940s to 1970s, for building aircraft, for space travel but also for vehicle prototypes. Currently there are only a few applications in highly priced cars. In preparation, prototypes are still being built.



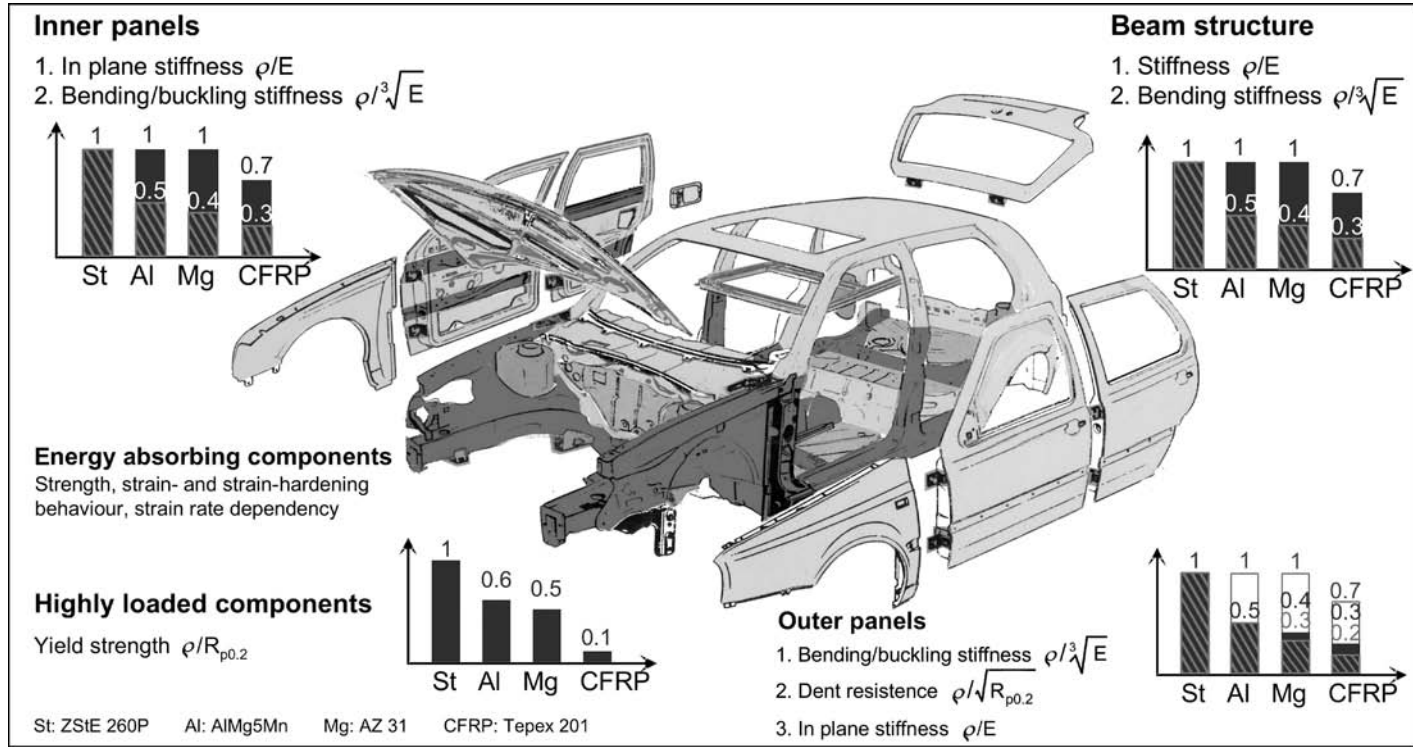


Fig. 8.60. Lightweight construction potential of different materials; criteria for load oriented material selection

For example, the inner part of the VW 3L Lupo bonnet (currently in Al for series production) was manufactured from Mg sheets using a heated tool (Fig. 8.61) and joined by means of flanging and bonding with the Al outer panel (Fig. 8.62). Reinforcement parts such as hinge and lock reinforcements were joined with punch rivets (Fig. 8.63). The mechanical behaviour of the hybrid boot was evaluated similarly by determining the rigidity under various loads in comparison to Al and steel bonnets. The simpler outer part of the bonnet as far as deep drawing is concerned require the highest standards in sheet panel quality (Fig. 8.64). The flanging technique for joining the Mg inner and outer panels is carried out

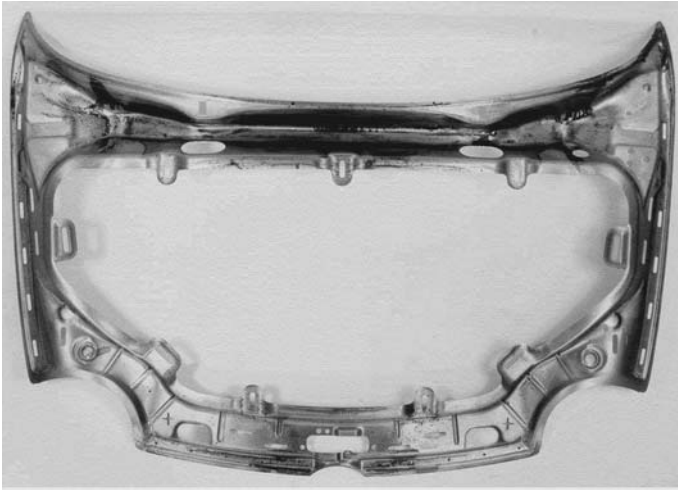
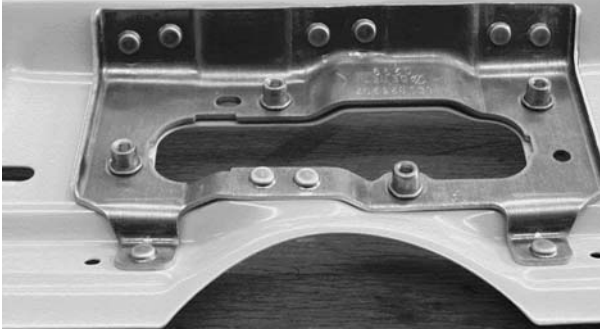


Fig. 8.61. Bonnet inner part (mg sheet) (VW – 3L-Lupo)



Fig. 8.62. Bonnet assembly

Schloßverstärkung gefügt mit RIBE ALUFORM RIFIT 5,3 x 5,5 - Ansicht: Matrizen-seite erste

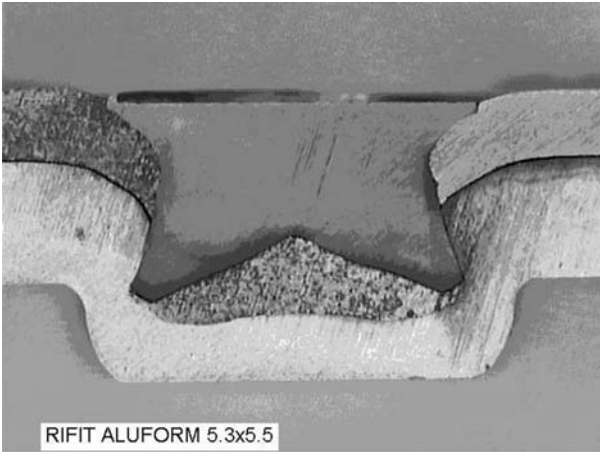


a

Scharnierverstärkung gefügt mit RIBE ALUFORM RIFIT 5,3 x 5,5 - Ansicht: Matrizen-seite



b



c

**Fig. 8.63.** a Punch rivets, lock reinforcement; b Punch rivets, hinge reinforcement; c Punch rivet with Al rivet

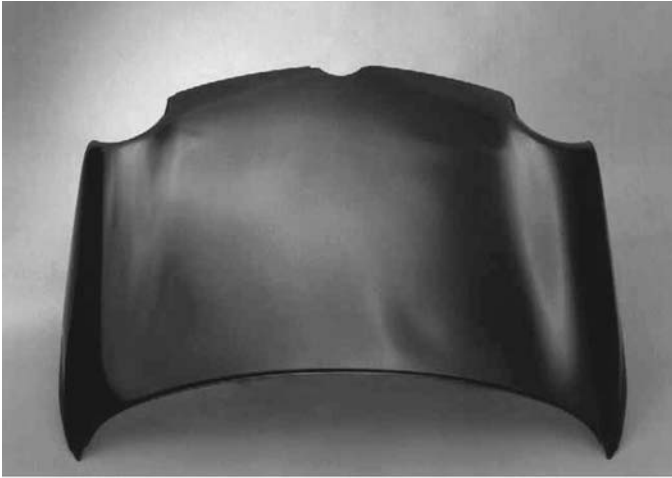


Fig. 8.64. Mg door inner part

using the application of heat. Weight saving in the Mg-bonnet (inner and outer part) will be about 50% compared to the steel-bonnet and about 15–20% compared to the Al-bonnet (respectively 1–1.3 kg). The offset-crash behaviour of the Mg bonnet was very similar to that of an Al bonnet (see Fig. 8.65); no tearing open. Although Mg has a hexagonal lattice, component behaviour is quite good. Several companies are striving to produce sheets of an adequate quality, which meet the corrosion resistance and surface finish requirements for the outer vehicle body outer skin, using Mg-oriented processes [21].

Further examples for prototype applications can be seen in Fig. 8.66/67. The Mg panel roof of the Opel G90 concept car (Fig. 8.66) also shows a potential ap-



Fig. 8.65. Mg bonnet after offset crash, ODB-64 km/h (VW-31 – Lupo)



**Fig. 8.66.** a Concept car with Mg panel roof (Opel G90); b Mg panel roof

plication. Another part involving high expectations in terms of forming is the door assembly carrier (Fig. 8.67), which is installed in the vehicle door. The demonstrator has a weight of just 0,8 kg (reduction compared to steel: 48%). The future success of Mg sheet applications depends on a competitive price and quality. We are still a long way away from this situation (Mg-sheet price today is about



Fig. 8.67. Door – assembly carrier (research demonstrator VW-Golf)

four to five times that of the Al sheet price). Formability and corrosion protection methods are technical aspects and will be dealt with in the short to medium term.

### ***Mg Extrusion Applications***

The use of Mg-extrusions in motor-vehicle production is dependent primarily on the stresses to which the particular component is subjected. Appropriate mass-requirement characteristics as a criteria for the choice of material based on suitability for loading requirements are known for essential single-axis stresses. A comparison of those mass-requirement characteristics shows that in comparison with steel and aluminium, magnesium offers the potential for reducing component mass particularly with regards to requirements of strength (tensile and bending stress). For stiffness requirements, weight advantage is only achievable with regards to bending stress [22]. In the particular case of tubular magnesium extrusions, weight advantages are obtainable particularly where the manufacturing technology allows very thin walls to be produced and the component cross section can be correspondingly enlarged.

Taking those parameters into account, areas of application such as window frames, and seat and supporting structures are suitable. The substantial advantage of magnesium extrusions consists in better mechanical properties in comparison to cast components. Thus extrusions of the alloy AZ31 achieves elongation to fracture of up to 15%. Under dynamic axial stress, the energy absorption capabilities are lower than aluminium due to the hexagonal lattice (Fig. 8.68). With dynamic transverse and diagonal loading, the difference is much less marked. Figure 8.69 shows deformation tests that simulate a pillar impact. Newly developed Mg wrought alloys reveal the potential for improved energy absorption capabilities. Thus the folding characteristics of Mg alloys with modified lattice structures was found to be similar to comparable steel and aluminium extrusions with ultimately higher specific energy absorption figures [22] (Fig. 8.68).



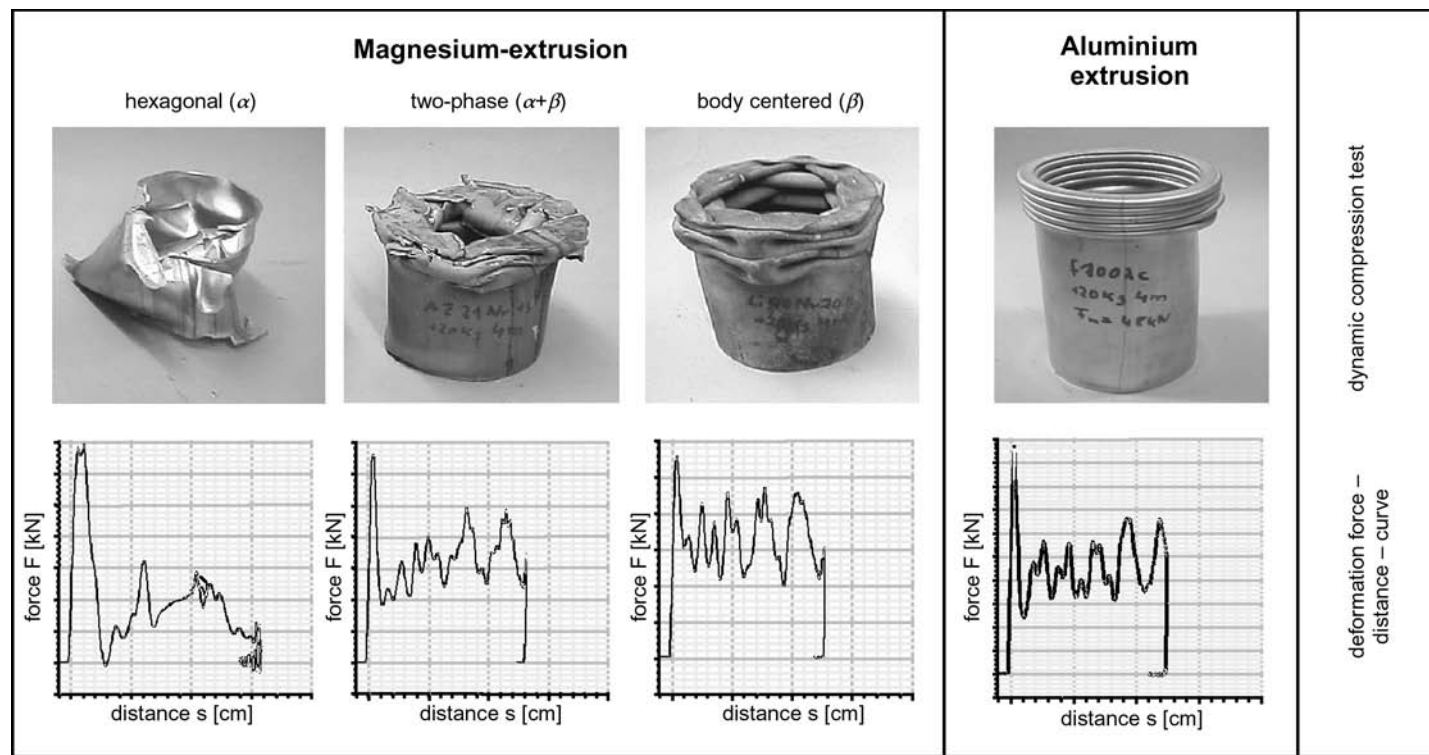


Fig. 8.68. Dynamic axial pressure test

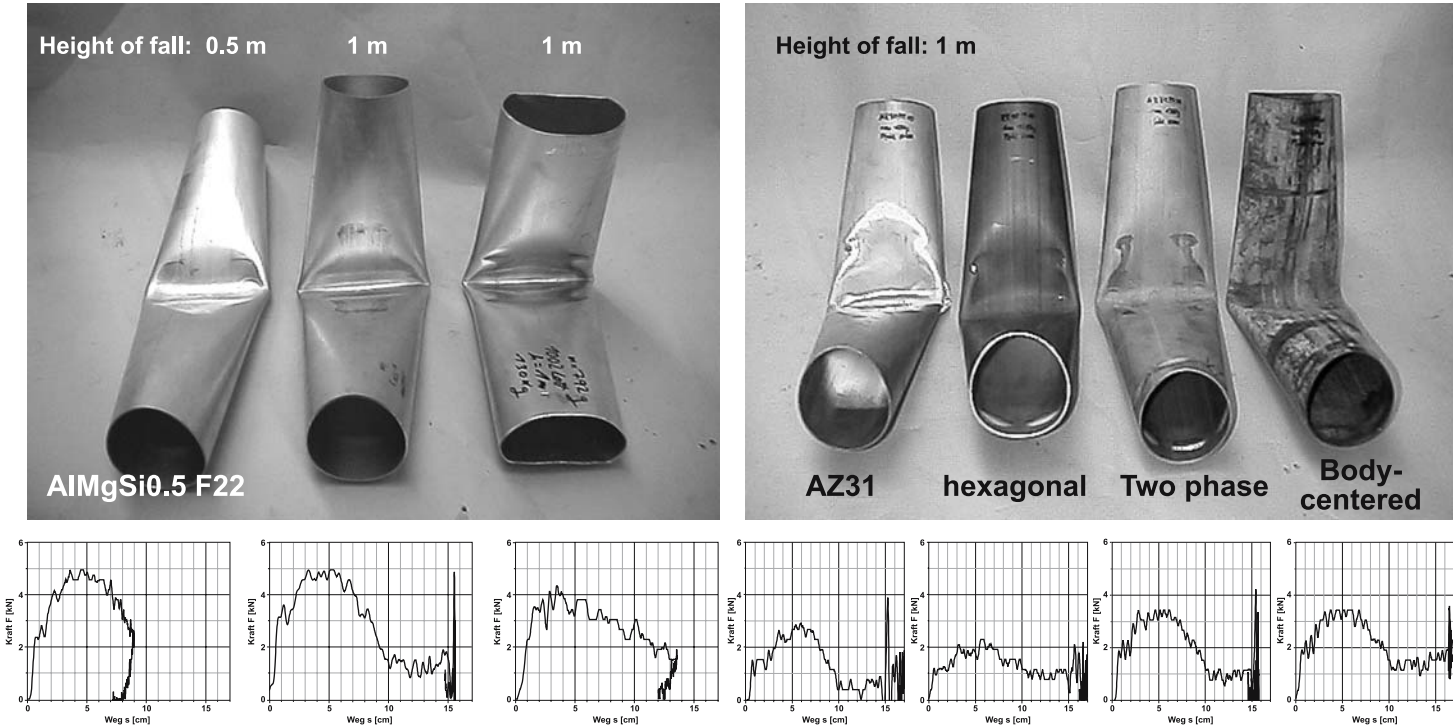


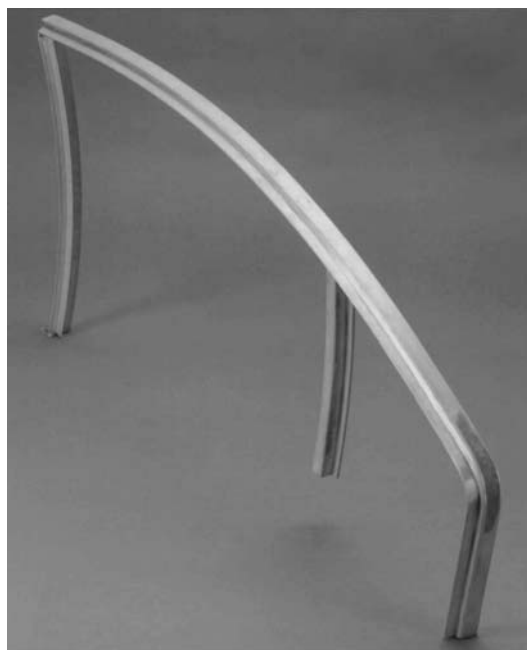
Fig. 8.69. Pillar collision tests



This is achieved with the addition of the lightest metallic element Lithium ( $0.534 \text{ g/cm}^3$ ), which leads to a two-phase or cubic-body centred grid structure. Thus at the same time a reduction in density from just  $1.6\text{--}1.4 \text{ g/cm}^3$  can be achieved.

To exploit the Mg lightweight construction potential in the body, it would be technically logical to pursue the use of Mg extrusions in a spaceframe structure, the use of Mg sheets for the bottom (bearing shear and bending loads) and for the outer skin. The joining technique is now available [23]. Three-dimensional bent extrusions can be manufactured by stretch bending at room temperature similar to Al extrusions (Fig. 8.70). Figure 8.71 shows a spaceframe demonstrator made using Mg extrusions (cross-section up to 150 mm diameter see Fig. 8.72). The welding process was carried out automatically with MIG welding equipment and modified arc, and manually with WIG-AC.

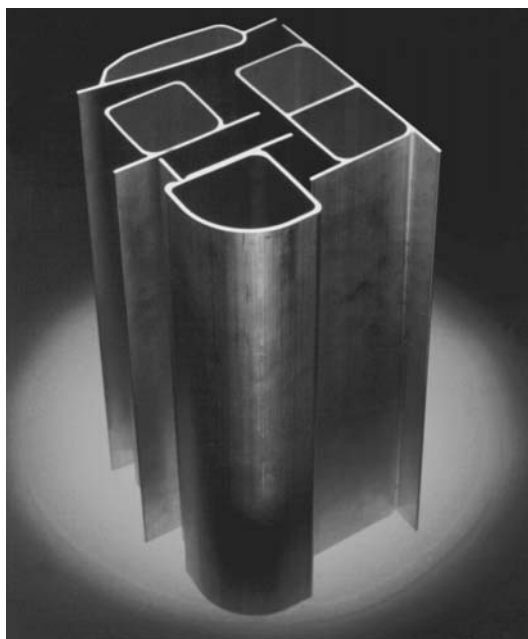
The research demonstrator (Fig. 8.73), the Volkswagen 1-LITRE CAR (1-litre fuel consumption per 100 km), makes extensive use of the mg-spaceframe design [24] (Fig. 8.74). In this case a combination was chosen of a Mg-spaceframe and an outer skin of carbon fibre composite material. With a weight of some 76 kg for the bodywork including the frame (without closures), this version was 13 kg lighter than a combination of an Al-spaceframe with a carbon fibre outer skin. Figure 8.74 shows the multi-material design with about 36 kg of magnesium, thin wall Mg-casting nodes (see also Fig. 8.75), Mg-extrusions and Mg-sheets.



**Fig. 8.70.** Mg extrusions window frame (VW – Research demonstrator)



**Fig. 8.71.** Mg-spaceframe (research demonstrator – VW)



**Fig. 8.72.** Different profile cross sections



**Fig. 8.73.** Volkswagen 1-LITRE CAR [24]. Key-figures: Vehicle weight: 290 kg; top speed: 120 km/h; engine: 1-cyl. Diesel with unit injection (output: 6.3 kW); consumption: 0.99 litres/100 km

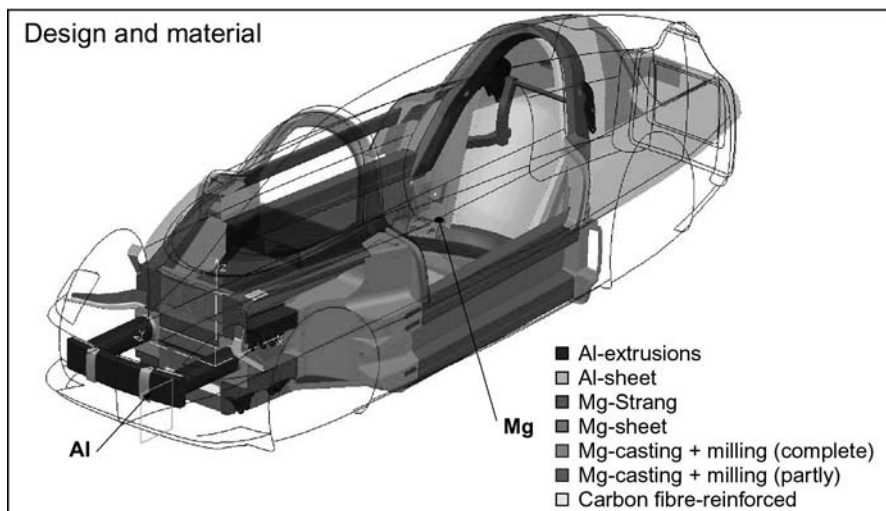


Fig. 8.74. Mg-Spaceframe of Volkswagen 1-LITRE CAR

#### 8.1.3.4 Chassis

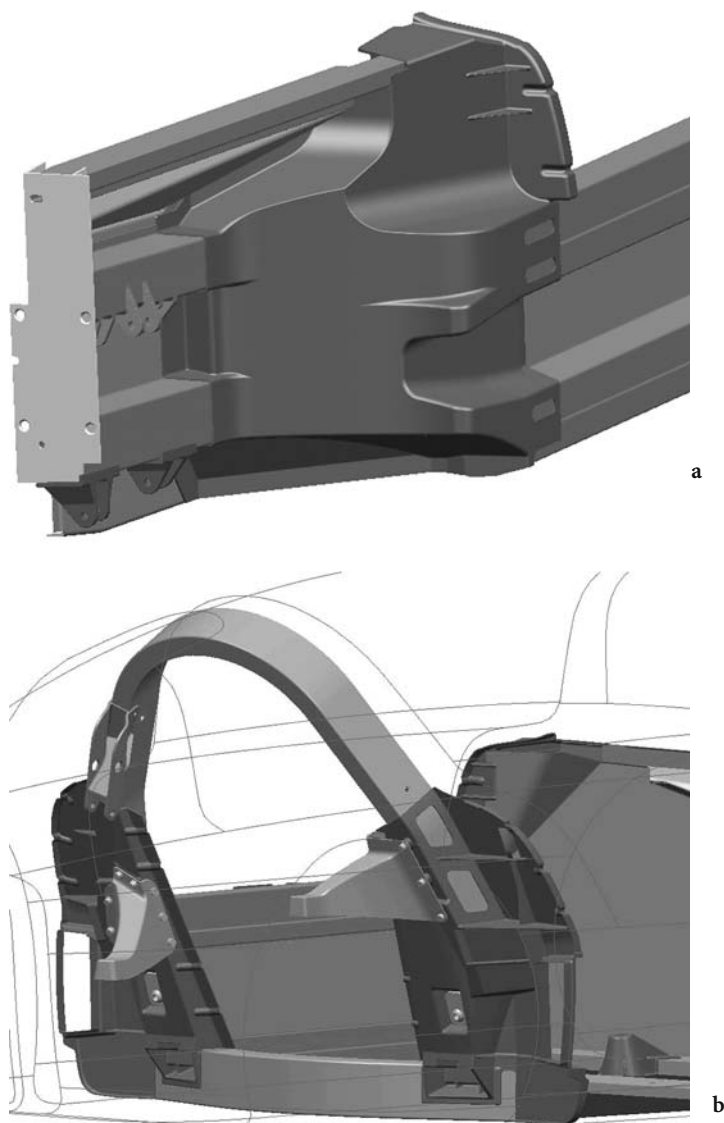
Due to the high safety requirements for chassis components, the use of Mg is a major challenge in this case. At the same time, exploitation of the lightweight design potential of components also means borderline design, i.e. maximum achievable tensile stresses are calculated in the FEM design, and the prerequisite for the component is therefore the achievement of optimum material characteristics and mechanical values (minimum porosity, inclusions) during manufacturing. This borderline design therefore also inevitably necessitates considerable additional effort during component testing. Wheels and suspension arms will be discussed as an example of this module.

#### Wheel

As the historical outline of the use of Mg shows, applications in chassis existed in the 1930s and subsequently from the 1950s to the 1970s.

As the wheel is an unsprung mass, lightweight design enables a very valuable improvement in vehicle handling in this case. The use of Mg wheels in racing is therefore traditional (e.g. touring car championships, Indy car, and Formula 1). Lightweight design takes priority in this case but dynamic strength and corrosion requirements are by no means comparable to the requirements of on-road vehicles.

Since the 1960s, Mg prototype wheels, and also wheels approved for on-road use in niche vehicles, have continuously been designed and manufactured via sand casting, permanent mould casting or die casting (Fig. 8.76). For example, Porsche series-diecast AM60 wheel for the 914/6 model taken from 1970. The  $5.5 \text{ J} \times 15$



**Fig. 8.75.** a A-pillar (weight: 3 kg/AM50); b B-pillar (weight: 1.8 kg/AM50)

wheel weighed 4.4 kg and was therefore 19% lighter than a forged Al wheel at the time. In approx. 1983, Porsche developed a  $7J \times 15$  AZ91HP Mg wheel via low-pressure permanent mould casting (5.9 kg) for the 944 model (Fig. 8.77). The comparable  $AlSi_{12}Mg$  wheel (permanent mould) weighed 22% more [24].

In addition to certain design conditions, such as wheel load, wheel offset, etc. and design requirements; the following material characteristics must especially be taken into consideration with the development of Mg wheels:



Fig. 8.76. Corvette-wheel (9.5×18"; AZ91; 8.6 kg)



Fig. 8.77. Porsche-wheel

- Fatigue resistance under corrosion
- strength
- corrosion behaviour (contact corrosion)
- creep behaviour (bolt seating)

Wheels are components, which are subjected to high levels of dynamic stress. During their service life (the current basis is approx. 300,000 km, this results in stress cycle numbers of  $N = 2 \cdot 10^8$ ). They have to withstand high levels of operational stress, but also considerable peak loads due to impacts or stress due to misuse. In the laboratory, such peak loads are simulated via:

- rim flange striking test: simulates driving against the edge of a kerb
- impact test with tyres: accident-like impact against the edge of a kerb

On the one hand, numerous tests are carried out in the laboratory with the levels of stress which occur during operation (e.g. ZWARP – dual-axis wheel test rig) in order to verify the service life, and on the other hand test drives are carried out to validate the results achieved in the laboratory.

The rotational bending fatigue test, in particular, is important for verifying the necessary dynamic strength of the wheel disk, because this is primarily subjected to rotational bending with superimposed spoke torsion. The test simulates stress on the wheel during cornering.

This stress scenario is also used as the design scenario in the FEM calculations, in order to determine the stress, which occurs in the wheel design from the wheel load and transverse force. The equivalent calculated stress (von Mises stress) is compared with the permissible stress (generally determined from test rod fatigue strength under reversed bending stress tests  $R = -1$ ). This generally leads to design modifications on the basis of iterative optimisation with repeated FEM calculation. The permissible reference stress depends on the:

- alloy, casting procedure, influence of corrosion, number of cycles, type of load

#### **Casting technique/manufacturing procedures (Fig. 8.78/Table 8.7):**

In addition to the costs, the manufacturing procedures which are used, also influence:

**Table 8.7.** Characteristic material values of Mg and Al alloys for wheels

Alloy	Manufacturing procedure	$R_{p0.2}$ [Mpa]	$R_m$ [Mpa]	A5 [%]	Fatigue Strength [Mpa]
AlSi <sub>7</sub> Mg (T6)	Perm. mold	200	300	5–9	8–115
AlMgSi <sub>1</sub> (T6)	Forging	250	300	10	150 <sup>a</sup>
ZK60 (T6)	Forging	150–240	280–300	7–14	120–140 <sup>a</sup>
AZ80 (T4)	Forging	210	300–320	9–11	120–145 <sup>a</sup>
AZ91 (T4)	Perm. mold	75–120	155–230	3–7	80 <sup>a</sup>

<sup>a</sup>  $N = 5 \cdot 10^7$  rotating bending (test rods from wheels).

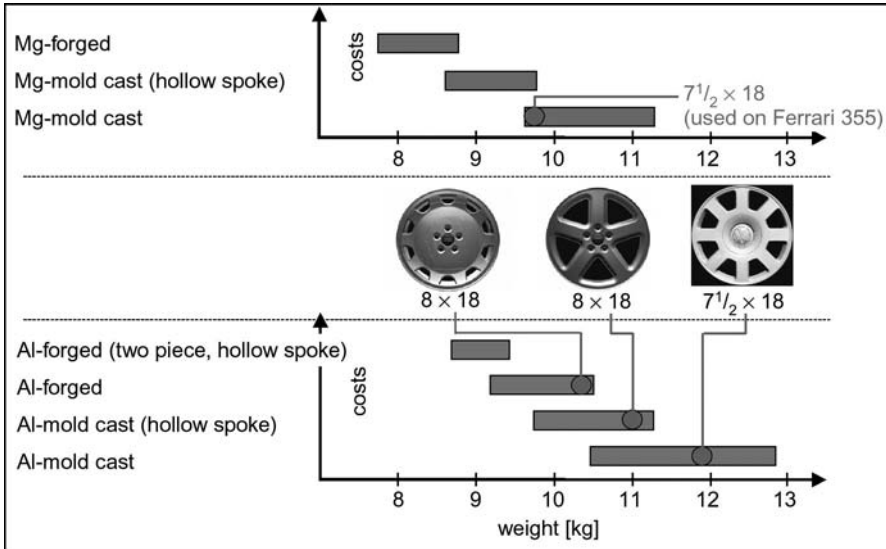


Fig. 8.78. Mg/Al wheel weight comparison by using different design and manufacturing procedures (18''-wheels)

- corrosion behaviour (sand casting is unfavourable)
- dynamic strength (die casting is unfavourable, due to increased porosity and defects)
- achievable strengths (thermal treatment possible in case of permanent mould casting)
- forging (is advantageous, due to the presence of small grain sizes, and a considerable reduction in porosity and defects)

Contact corrosion at the threaded wheel connections and the contact surface at the brake disk must be combated with special design measures. The use of Al disks, Al calottes, coated steel bolts or Al/titanium bolts are recommended. The contact surface at the brake disk may, e.g. be insulated with an intermediate plastic ring or a suitable intermediate Al alloy (AlMgSiF31) disk is used (Fig. 8.79).

The special requirements caused by stone impact or kerb damage in the coating structure must be taken into account. An example of a coating structure: vibratory grinding, chromating or chromate-free pre-treatment, CDP, powdered primer, base coat, clear coat.

### **Suspension arms/subframe**

Due to the requirements placed on them, suspension arms must reveal ductile component behaviour and high strength. In the event of component overload, considerable deformation is intended to occur prior to the final failure (breaking strain >6–8%).

Chassis components such as the wheels and suspension arms are subject to maximum requirements with regards to component quality (casting quality and



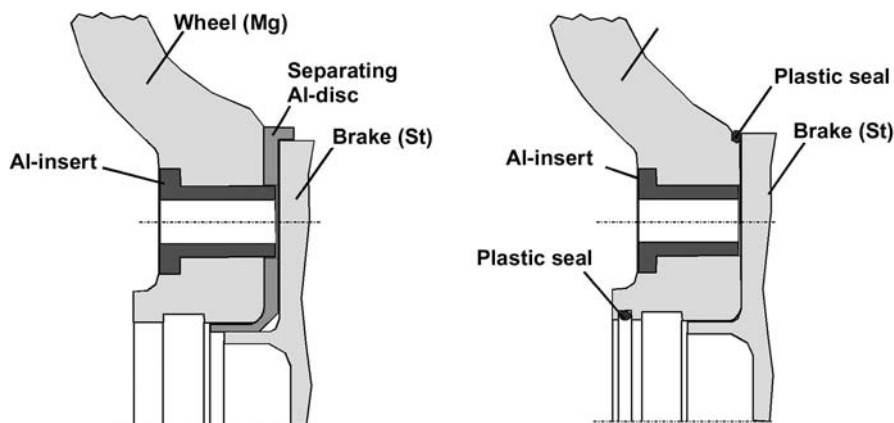


Fig. 8.79. Measures against contact corrosion

mechanical material properties). These results cannot be achieved via standard alloys and processes such as sand casting or die casting. In particular, the topic of dynamic strength for fatigue loading subject to corrosion still necessitates considerable R&D work. Up to now, neither squeeze casting nor tests involving the thixocasting procedure have revealed any improvements regarding durability in comparison with optimised die casting. These are reasons for regarding the use of Mg as a rather a long-term venture. However, improved component quality due to adapted and new procedures such as e.g. rheo casting, optimised wrought alloys and the production of components via forging reveal a potential for application.

#### 8.1.4 Life Cycle Assessment

Nowadays, in addition to the optimisation of product and system characteristics with the minimisation of manufacturing and operating costs, the focal point of interest as an important criterion of technical developments is the improvement of environmental compatibility.

In order to achieve this, the analysis and optimisation of the entire product life cycle is necessary. Effects on the environment must be minimised via the efficient use of non-renewable resources and low pollutant emissions. This affects the entire product cycle, from material extraction and product manufacturing to product utilisation and recycling for the next cycle or environmentally safe disposal. As a result of the interaction between the individual phases of the overall cycle, this involves an optimisation task, which may also necessitate compromises in individual phases to the benefit of the overall balance.

With the generation of an ecological audit, all material and energy flows that affect the environment must basically be taken into consideration, weighed against one another, weighted and finally evaluated. The models available for this purpose (life cycle assessment tool) are extremely complex and time-consuming.

Individual emissions of CO<sub>2</sub>, nitrogen oxides and other gases are examined, and the effects of these – i.e. on the greenhouse effect – are comprised to form effect audits. Experience has shown that the energy audit can be used effectively to support the optimisation strategy to reduce the strain placed on finite resources and to reduce undesired emissions and the effects of these, because pollutant emissions and the consumption of resources can be reduced to a common denominator in the energy audit.

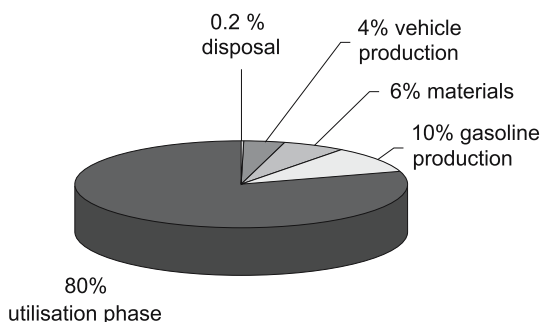
#### 8.1.4.1 Life Cycle Inventory of Vehicles

In the automotive industry, concentration has therefore been targeted towards the energy audit, which influences significantly the ecological audit [26]. As the CO<sub>2</sub> audit is also causally linked to the energy audit and this makes the greatest contribution towards the green-house effect in comparison with all other emission sources, the latter is a very suitable instrument for evaluating different materials in combination with specific components or modules and is also suitable for evaluating entire vehicle concepts as a whole.

The ecological benefit of recycling also becomes clear in the audits. Wherever material recycling succeeds, it is also generally ecologically advantageous. Wherever it fails, attempts must at least be made to utilise the energy content in the case of organic substances. Also regarded as a very efficient ecological procedure in this case is so-called metallurgical recycling in the reduction zone of the blast or cupola furnace. Figure 8.80 shows the result of a study regarding the overall energy audit of a Golf [27].

The main result of this audit is that the utilisation phase involves significant energy consumption. Some 10% of the total energy is required to manufacture the vehicle, a further 10% to provide the gasoline. The remaining 80% is concealed in the calorific value of the gasoline, which is combusted over the 150,000 km covered. The recognition of how little energy is required to manufacture the vehicle, and the fact that the percentage of energy required to acquire the materials is higher than that required to produce the vehicle, is new [27].

Due to the dominance of vehicle operation in the overall audit – approx. 80% of energy requirements are determined by fuel requirements – the acceptance of



**Fig. 8.80.** Breakdown of the primary energy consumption of a Golf (545 GJ = 150 MWh) mileage 150,000 km in 10 years; consumption 8.1 l/100 km [27]

higher expenditure during the phases of recycling, and material, component or vehicle manufacture, may be entirely ecologically advantageous if the strain on the environment were reduced during vehicle operation – e.g. via lightweight design methods.

These facts can be seen, e.g. in the case of vehicles which make extensive use of aluminium or low consumption vehicles such as the 3-litre Lupo (Fig. 8.81) or the 1-LITRE CAR by VW.

Comparison of the audit results achieved by the Golf A3 and the 3-litre Lupo reveals significant differences since, on the one hand, two functionally different vehicles are compared, and due to the fact that these vehicles are separated by several years of development (Fig. 8.82). The VW 3-litre Lupo shows what is now technically feasible for series production with regards to low fuel consumption in this vehicle class, whilst the Golf is a typical mass-produced vehicle. Primary energy consumption is halved, whereby the reduction of fuel consumption makes the most significant contribution. The absolute amount of effort involved in the production of the 3-litre Lupo is comparable to that of the Golf, resulting in a changed breakdown between production and utilisation (see Fig. 8.81).

The primary energy consumption required for producing a few selected materials (standardised for the weight of 1 kg) is mentioned merely as an example in Fig. 8.83. In order to properly audit a vehicle, primary energy consumption has

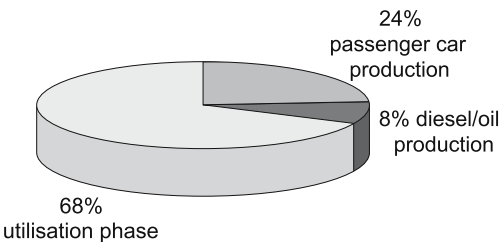


Fig. 8.81. Breakdown of the primary energy consumption of a VW 3-litre Lupo (256 GJ = 71 MWh) mileage 150,000 km in 10 years; consumption 3.0 l/100 km [29]

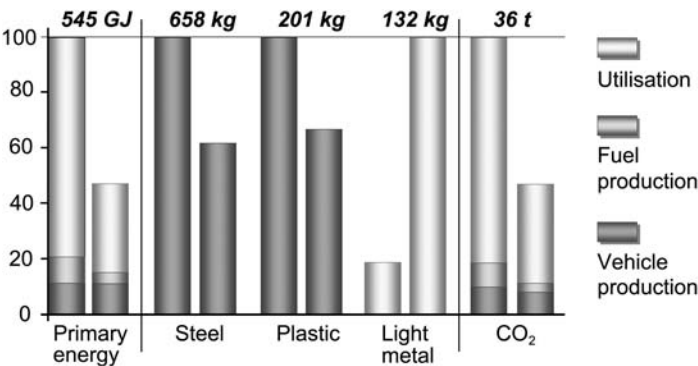


Fig. 8.82. Comparison of the breakdown of primary energies (left column: Golf [29], right: 3-litre Lupo)

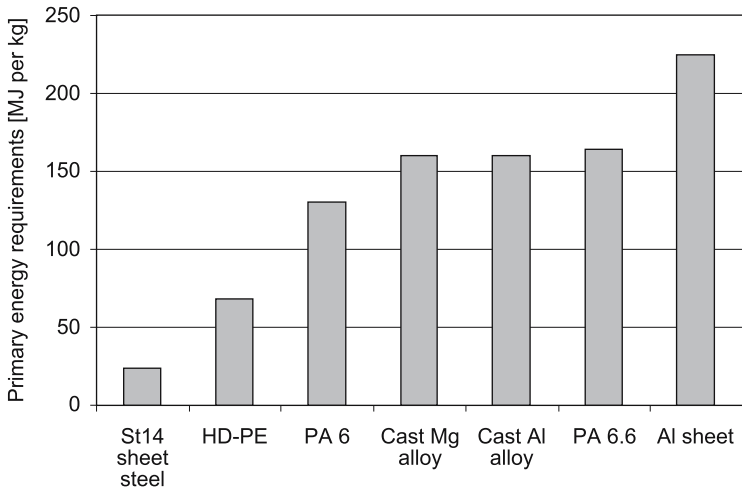


Fig. 8.83. Primary energy requirements for construction materials [27]

to be determined according to the vehicle's material composition. Extensive databases are available for this purpose.

#### Reduction of fuel consumption:

The characteristic figures specified in the literature, describing the influence of a reduction in weight of fuel consumption (fuel reduction coefficients) differ according to the boundary condition/vehicle and the driving cycle, which is used as the basis. Relatively low fuel reduction coefficients (0.1–0.36 l/100 km) are revealed for a weight reduction of e.g. 100 kg both in tests [28] and simulation calculations [26]. If, however, the drive train is adapted to the same performance with integration of the engine, values of between 0.3–0.5 l/(100 km · 100 kg), depending on the vehicle, are realistic, e.g. in the NEDC cycle [29, 31] (NEDC = New European Driving Cycle). This value may also be higher depending on the driving style.

If the weight of a vehicle is reduced due to the lightweight material design, e.g. in the body-in-white, additional weight savings may be achieved whilst retaining performance. Measures such as engine and gearbox adaptations, smaller brakes, chassis adaptations, etc. must be mentioned at this point (displacement of the operating point; re-dimensioning of components). These so-called secondary lightweight design effects act additionally to reduce consumption as a result of weight savings, but also as a result of consumption-reducing measures on the part of the drive train. As the above mentioned secondary effects and measures only become possible in cases in which weight savings of 100–200 kg are achieved, which is only generally possible in the case of lightweight vehicle design such as e.g. in Audi's A8 and A2 vehicles with the Aluminium Space Frame, secondary lightweight design effects are evaluated in very different manners. On examination of component comparisons in a standard vehicle, the secondary effects can hardly be emphasised if they are merely integrated into a lightweight design concept such as that mentioned above.

8.1.4.2 Life Cycle Inventory of Magnesium

Life cycle inventory results for magnesium production account for energy consumption, the use of raw materials extracted from the earth, emissions to air and water, and solid waste. The primary results, which were dedicated by Norsk Hydro for Porsgrunn, are listed in Table 8.8. The die casting process was also analysed in [30]. A simplified model for energy use and emission shows that the environmental strain resulting from die casting and re-melting is low in comparison with the production of primary metal.

The energy consumption for re-melting is only a small percent of what is otherwise required. Similarly, energy consumption in die casting is less than 5% of what is required for the production of primary metal. However, the consumption of SF6 is of concern both during the die casting process and during the casting of defined recycled alloy ingot products. The environmental “hot spot” highlights a focal point for the attention of industry. Of course, the LCI study results are dependent on the specific production site, and the resources and processes that are used [30].

The primary energy required to produce Mg lies between 150 and 190 MJ/kg depending on the production location and the mix of energy which is used. According to [32], recycling requirements amount to approx. 5% of the energy required to produce new material. These requirements refer to material qualities which are suitable for internal recycling (e.g. scrap type 1A), and increase for other qualities of scrap.

In addition to the environmental evaluation of vehicle concepts, individual vehicle components must also be evaluated.

Example: Mg/Al door:

The Mg/Al door was audited with the Gabi software [32].

Figure 8.84 shows the weight breakdown of both variants. The energy difference and its results for the production and utilisation phase in comparison with

Table 8.8. Life cycle inventory results for Mg production [30]

	Pure Mg	Mg Alloy AZ91	Mg Alloy AM60
Total energy consumption (MJ/kg metal)	144	151	149
Global warming effect incl. SF <sub>6</sub> (kg CO <sub>2</sub> equivalents/kg metal)	19	19	19
Global warming effects excl. SF <sub>6</sub> (kg CO <sub>2</sub> equivalents/kg metal)	6	6.5	6.5
Acidification (kg/kg metal)	0.02	0.025	0.02
Winter smog (kg/kg metal)	0.015	0.017	0.016
Solid waste (kg/kg metal)	0.5	0.5	0.5
Dioxins to air (µg/kg metal)	0.24	0.21	0.21
CHC to air (mg/kg metal)	13.7	12.4	12.4

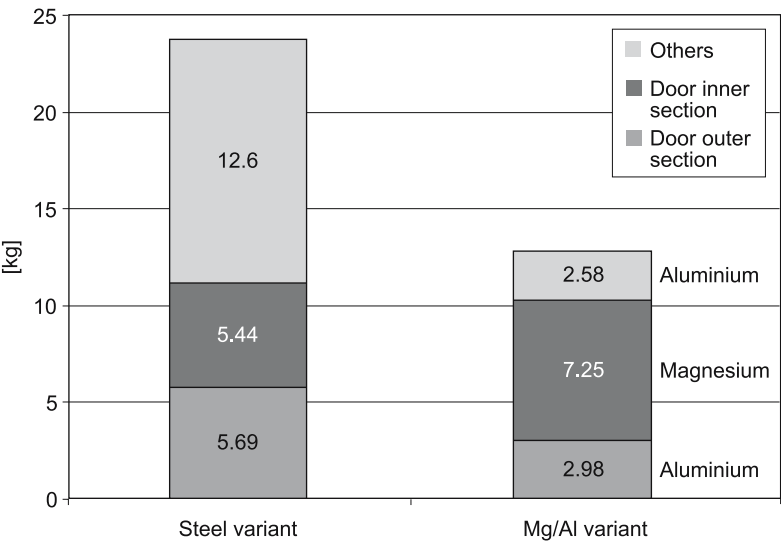


Fig. 8.84. Weight comparison of door variants; steel and magnesium/aluminium [32]

the steel reference door, is shown in Fig. 8.85. The energy requirements, which are approximately 620 MJ higher in production, and are more than compensated during the utilisation phase due to fuel savings, leading to the possibility of energetic amortisation at approx. 47,000 km.

The following recycling scenario was assumed in this case: Due to the high material content, a 100% rate of metal return into the Mg/Al cycle is assumed, which saves the corresponding volume of primary Mg/Al (thereby saving the high primary metal energy requirements). The considerably lower energetic requirements for secondary Mg/Al thereby come into play.

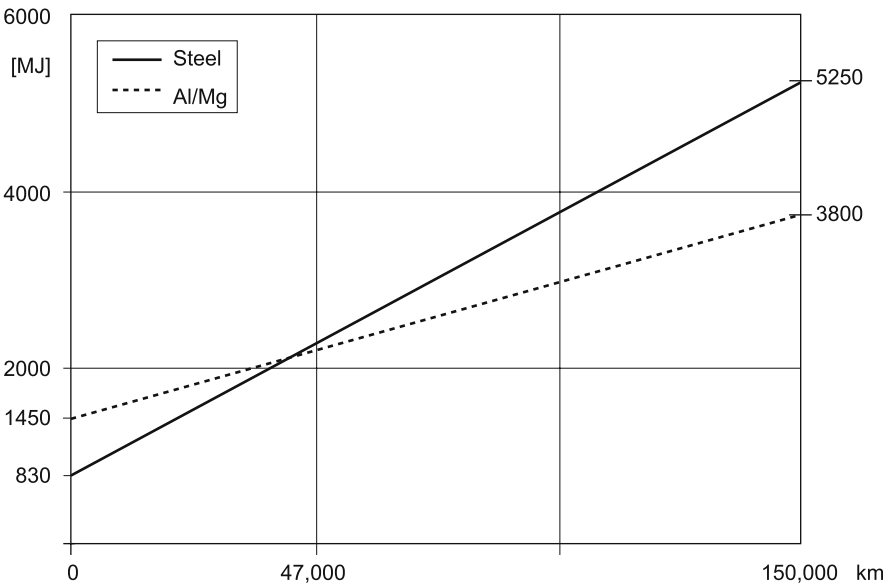
Following the disassembly of the vehicle, the Mg content is used as a secondary material for cast Mg alloys or as an alloying element for Al-alloys. As e.g. the cast alloys are generated from primary Mg if there is a deficit of available secondary scrap, the equivalent volume of primary Mg is saved due to recycling.

**Example: Transmission housing**

The B80 transmission housing, with a weight reduction of 4.5 kg, was selected as an example of the energetic evaluation of the substitution of an Al component by a Mg component. Figure 8.86 shows the primary energy difference for the production and utilisation phase in comparison to the aluminium housing.

From the very beginning, the Mg transmission housing offers advantages due to its lower weight, as it requires less production energy than the Al housing. This applies if both housings are produced from either primary or secondary material.

If a 0.4 l/(100 km · 100 kg) reduction in fuel consumption is taken as the basis in the case of a weight saving of 4.5 kg and mileage of 150,000 km, this leads to a saving of 25–30 l per vehicle. This does not appear to be a great deal in ref-



**Fig. 8.85.** Primary energy requirements for the production and utilisation phase of two body-in-white door variants (steel; Mg/Al) (second life cycle: secondary material usage) basis: VW Polo: 6.63 l/100 km; approach: 4.5% reduction in fuel consumption with 10% weight reduction

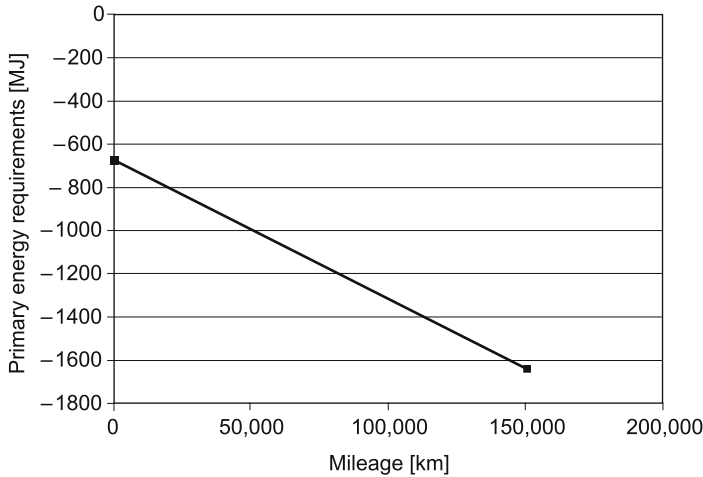
erence to one individual vehicle, but when regarded as a whole, taking an overall volume of e.g. 1.5 million vehicles into consideration, it results in fuel savings of up to 45,000 m<sup>3</sup> and a reduction of approximately 110,000 t in carbon dioxide emissions.

The results of several studies, including [30, 33], show that energetic advantages are revealed on analysis of the entire life cycle of Mg components in comparison with Al or steel components, especially if re-melted material is used.

Although the CO<sub>2</sub> audit is linked directly to the energy audit, evaluation is, in the final analysis, dependent upon SF6 consumption (1 kg SF6 corresponds to the global warming potential (GWP) of 23,900 kg CO<sub>2</sub> +/-35% [34]). Only the substitution of SF6, especially for the ingot production, will lead to greenhouse gas audit advantages in comparison with Al components.

**8.1.5 Strategy and Outlook**

Lightweight construction using magnesium is in competition with lightweight construction using aluminium, plastics and steel. The aim is, wherever it makes technical sense and is economically possible, to establish magnesium in series production vehicles also a large scale. Naturally, for the introduction of new technologies, series production vehicles on a smaller scale and niche vehicles will be selected (Fig. 8.87).



**Fig. 8.86.** Cumulative energy difference between a vehicle with an Mg and Al transmission housing

The midterm prognosticated increase in the use of Mg and the considerably large jump from 90–120 kg (through body applications among other things) and beyond (see Sect. 8.1.2), can only become reality if the entire production chain, starting from half-finished products (castings, sheets, extrusions) to component processing, is addressed consistently in an all-encompassing R&D strategy and if the vehicle manufacturer or supplier co-operates with the manufacturer of the half-finished product at the outset. Since the entire Mg industry cannot be compared to the structure of the aluminium industry (R&D capacity and number of companies), co-operative work should be concentrated on building up the engineering database also on an international basis (R&D).

Only by integral consideration of construction (design), material (properties) and process (production) can lightweight construction with Mg be achieved at competitive prices. For this integrated approach we still see deficits but at the same time the key to an increased use of Mg in vehicles [35].

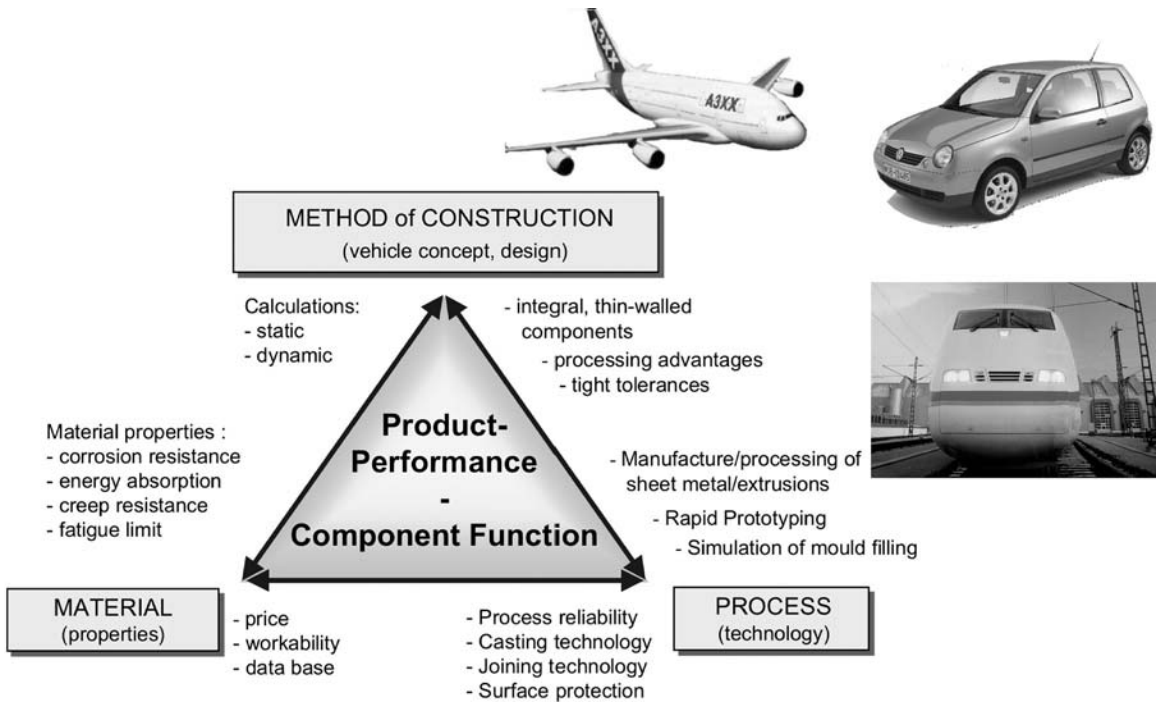
The prerequisites for this type of development even at midterm high Mg prices are:

- greater use of in-house recycling (cost reduction)
- Secondary material circuit
- Adaptation of existing casting and forming techniques and development of new ones
- Development of new Mg alloys with improved property profile
- magnesium-compatible design (integrated approach)
- incorporation in a multi-material design concept
- Expansion of the knowledge base (database)

The strategy regarding the use of Mg in vehicles to achieve a “second Mg age” is based on the applications for cast components; here further development of Mg



Fig. 8.87. Integrated approach



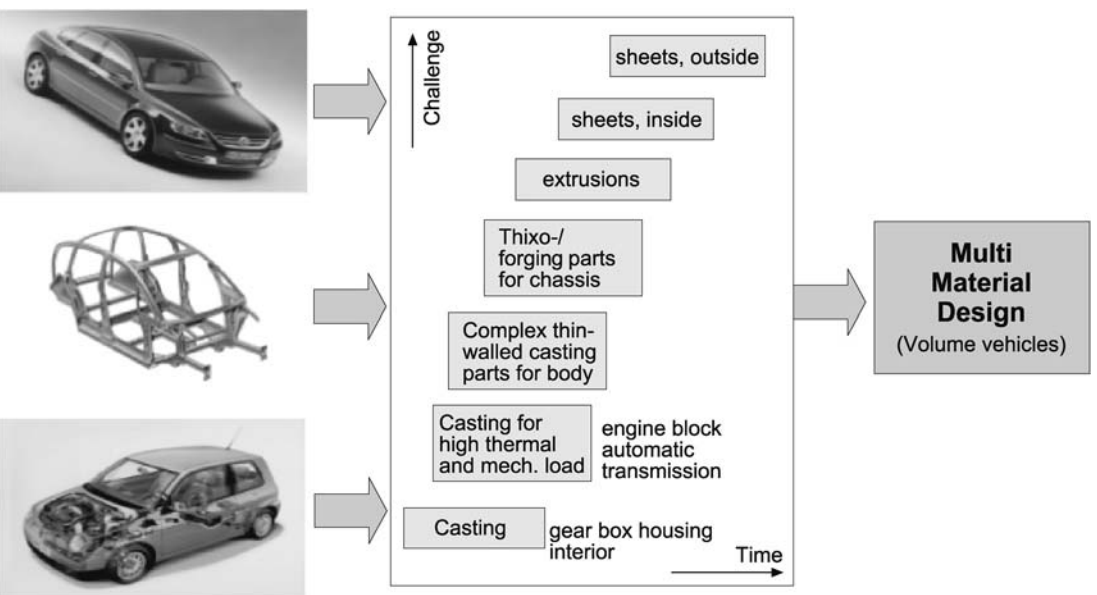


Fig. 8.88. Strategy for magnesium applications in vehicles

properties (e.g. improved creep resistance) will be helpful. Mg components in body, sheet and extrusion applications will follow in niche and premium vehicles supported by new Mg alloys with improved ductility and energy absorption (Fig. 8.88).

In this way the increased use of magnesium in volume models can be prepared and implemented within the framework of multi-material design. Further prerequisites for this are innovative manufacturing and processing techniques, recycling and secondary market strategies and, in particular, cost effectiveness from using the advantages of world-wide logistical organisations in the entire production chain.

## **8.2 Automotive Applications in North America**

*Gerald Cole*

### **8.2.1 Transportation Industry**

#### **8.2.1.1 Introduction and Background**

Magnesium use in North America (NA) has a particularly exciting history. During the past decade the automotive industry has taken a great liking to its properties for vehicle lightweighting. Unlike Germany, which essentially invented magnesium, and developed many uses for it, there was only a minor interest in magnesium prior to the late 1980s. The Society of Automotive Engineers (SAE) in the United States has been the major outlet for technology associated with transportation. The first mention of magnesium is in a 1931 [36] paper by John Gann of Dow Chemical. Dow dominated the NA magnesium scene for over 80 years, first through its production at Midland Michigan, mining natural brines, and then at its Freeport Texas plant where it produced magnesium from sea water. Dow's impact on the NA use of magnesium cannot be overstated both through its marketing efforts to "sell" magnesium, as well as through its significant R&D activities. (Dow Chemical ceased production of magnesium in 1998.) Gann's data showed that pure magnesium ingot production in NA grew from 45 m in 1916 to 418 mt in 1929 (other data has shown that alloy production was 25 m in that year). Most of the applications were from the aircraft industry, where extreme lightness coupled with strength and toughness were important; all the examples were from the German and Italian aircraft industry. They included crankcases, housings, covers, fuel tanks, ribs, struts, sheet covering, furniture and trimmings. Gann also discussed the limited automotive applications of the time. Again the examples were from Germany. An interesting application was bus wheels, where magnesium saved 237 kg over steel wheels, which weighed 363 kg. This unsprung weight reduction allowed greater acceleration, improved braking, better road clinging, less shimmying, less pounding against the springs, and improved (> 60%) tire life.

In 1938, Harvey [37] indicated that alloy magnesium production had grown to 360 m by 1936 (from 25 mt in 1928). He indicated that 70% of the metal produced went into aircraft use: engines (crankcases, blowers, housings-accessory/oil pump/starter, oil sumps, manifolds, gear cases, supercharger), cockpit fittings, pedals, air scoops, control boxes, levers, door hinges, landing gear apparatus, pulleys, etc.), landing and tail wheels from 18–160 cm diameter. Uses outside the aircraft industry were associated with applications where reducing weight was important. These included portable parts for pneumatics and grinding/drilling tools, machine frames for bread slicing, book binding, printing machinery, motion picture equipment and sound boxes, foundry (flasks, patterns, match plates, core boxes), machining (jigs and fixtures), and automotive parts for trucks and buses.

After World War II, aircraft applications began to dry up, based on the problems with corrosion and the significant efforts by the aluminum industry to address issues of manufacturability.

The first SME paper on vehicle applications was presented in 1946 [38], and discussed rolling using formed magnesium sheet to reduce the weight of body panels. In fact Dow had produced a small fleet of trucks using magnesium panels to demonstrate the feasibility of this technology and to show the weight reduction advantage versus aluminum. The next paper to appear, three years later, continued with a forming theme, this time extrusion technology associated with a new alloy developed by Dow [39]. The first casting application in the SAE appeared in 1952 [40], with a presentation of a magnesium alloy truck wheel. The paper described how, after a considerable redesign of the current steel wheel, and with 40,000 km of lab testing, a truck wheel and hub were feasible and gave a 45% mass savings.

During the next 30 years, there was the odd paper (one in each of 1966, 1971, 1974 and 1977). This indicated the lack of magnesium interest in the North American market. There were no vehicles as exciting as the 1946 VW Beetle, which used 19 kg of magnesium components (all in powertrain). Interest in magnesium waned in Europe after the demise of the Beetle in the mid 1970s while continuing at the slow pace in NA during the next few years.

### **8.2.1.2 Magnesium in the 1970s**

By 1980, the North American automotive industry was consuming around 3,000 mt of cast magnesium products, or about 0.25 kg per vehicle. These were described in a 1977 paper by Erickson [41] who detailed transportation applications in the first really serious automotive paper presented at SAE. Powertrain components included fan spacer, fuel pump air body, transmission stator blade, and limited use of clutch housings. There were also several chassis and body parts described (glove compartment door, turn signal housing, heater blower fans, grills and bezels and steering column shroud-bracket and clamp).

### **8.2.1.3 Magnesium in the 1980s**

Interest in magnesium technology accelerated in the 1980s, particularly due to the worldwide petroleum shortage and the resulting demand for fuel efficient,

and therefore lighter weight vehicles. This interest was mirrored in the presentations at SAE congresses. In 1980 there were four papers; again in 1983 there were another four presentations; in 1985 and 1986 there were six each, in 1987 there were three, in 1988 there were 7, and in 1989 an additional 4 giving a total of 34 papers in this decade, or twice the output from the previous 50 years. By 1985, the North American auto industry was consuming 5,500 mt of magnesium or approximately 0.5 kg per average vehicle [42]. Typical applications included the brake and clutch pedal support and bracket introduced by Ford Motor Company in 1982 in its Bronco and Ranger trucks, and the steering column lock housing introduced about the same time. Small parts included mirror trim covers and ashtray doors. At the same time Ford introduced the first low volume powertrain part, a bell housing for a manual transmission on the small Ranger truck.

#### **8.2.1.4 Magnesium in the 1990s**

It was in the 1990s that interest in magnesium mushroomed. At the beginning of the 1990s the North American automotive fleet (at least that proportion produced by the Big Three, GM, Ford and Chrysler) used ~11,000 m of castings (or 1.2 kg per vehicle). By the turn of the millennium the volume had grown to between 40 and 48,000 m (or ~3.5 kg per vehicle). There are no exact numbers since all magnesium producers, recyclers, die casters, Tier One suppliers and OEMs keep their production and metal purchase information closely held. NA was significantly ahead of Europe in all automotive magnesium applications, which were at ~0.5 kg/vehicle.

The list of parts currently (2001–2002) used in North American vehicles is shown in Table 8.9. The Figs. 8.89–8.103 show photos of the various major families of components listed in this table (steering wheels and related parts such as steering lock housing and shafts, transfer cases, instrument panels and brake/clutch pedals). The tabulated components are listed by system: chassis, interior, exterior and powertrain; the number of applications (car lines or nameplates) for each component is also shown. The list does not show the future programs under development, since that is proprietary to each company. But there is a page of photos that show where the interest is highest: body parts (cast lift gates and door inners), powertrain (oil pan, bed plate), and chassis (wheels). GM had cast magnesium wheels as an option on its Corvette sports car for 2 years; but they were removed this year (in place of forged aluminum).

The casting volume produced for each of the big three is quite different. At the beginning of the 1990s Ford with Ford at 7,500 m cast parts, used twice the amount of magnesium castings as GM, which purchased 3,500 m, and eight times the 900 m purchased by DaimlerChrysler. By the end of the decade GM's use of magnesium had increased beyond Ford's to 28,000 m (or 3.8 kg per vehicle). Ford used 16,000 or 2.7 kg/v and DCX used 9,000 (or 2.3 kg/v). The total NA consumption is around 53,000 m. These figures belie the fact that the distribution of magnesium components is not uniform across the NA fleet. The majority of the NA magnesium use is with trucks, for example, GMs full size pickup trucks contain 12 kg. Very little is used in cars, for example, small 'C' class cars (such as the Ford Focus) contain ~1 kg.

**Table 8.9.** Details of current (2001–2002) North American magnesium components used in vehicles

System	Component	OEM	Name plates
Interior	Chaptainchair seat base	DCX	1
	Bench seat riser	GM	1
	Console bracket	Ford	1
	IP cross car beam	DCX	1
		GM	4
		Ford	2
	Reinforcement	DCX	2
	Console support bracket	Ford	2
	Brace	Ford	1
	Support beam	GM	5
	Support bracket assembly	GM	2
	ABS housing passenger side	GM	1
	Steering wheel armature	DCX	8
		Ford	13
		GM	11
		Toyota	3
	Steering column bracket	DCX	4
		GM	7
	Hub	DCX	3
	Jacket assembly	DCX	1
	Lower bearing housing	DCX	2
	Shell housing fixed	DCX	3
	Shell housing tilted	DCX	3
	Tilt head	DCX	3
	Upper mounting bracket	DCX	2
	Lock housing	DCX	1
		Ford	3
	Housing	GM	3
	Actuator housing	Ford	6
		GM	3
	Lower bearing retainer	Ford	2
	Retainer	Ford	Multi
	Glove box door	GM	Multi
	Radio housing	Ford	Multi
Exterior	Sunroof cover/cap assembly	Ford	2
		GM	2
	Outside mirror armature	GM	1
Electrical	Amplifier housing	Ford	Multi
Powertrain	Alternator/A-C bracket	DCX	3
	Alternator bracket	DCX	1
	Alternator/idler bracket	DCX	1
	Misc engine bracket	DCX	1
	Valve cover	DCX	4
		Ford	Multi
		GM	1
	Cam cover	Ford	Multi
		GM	1
		Dihatsu	1
		Toyota	1

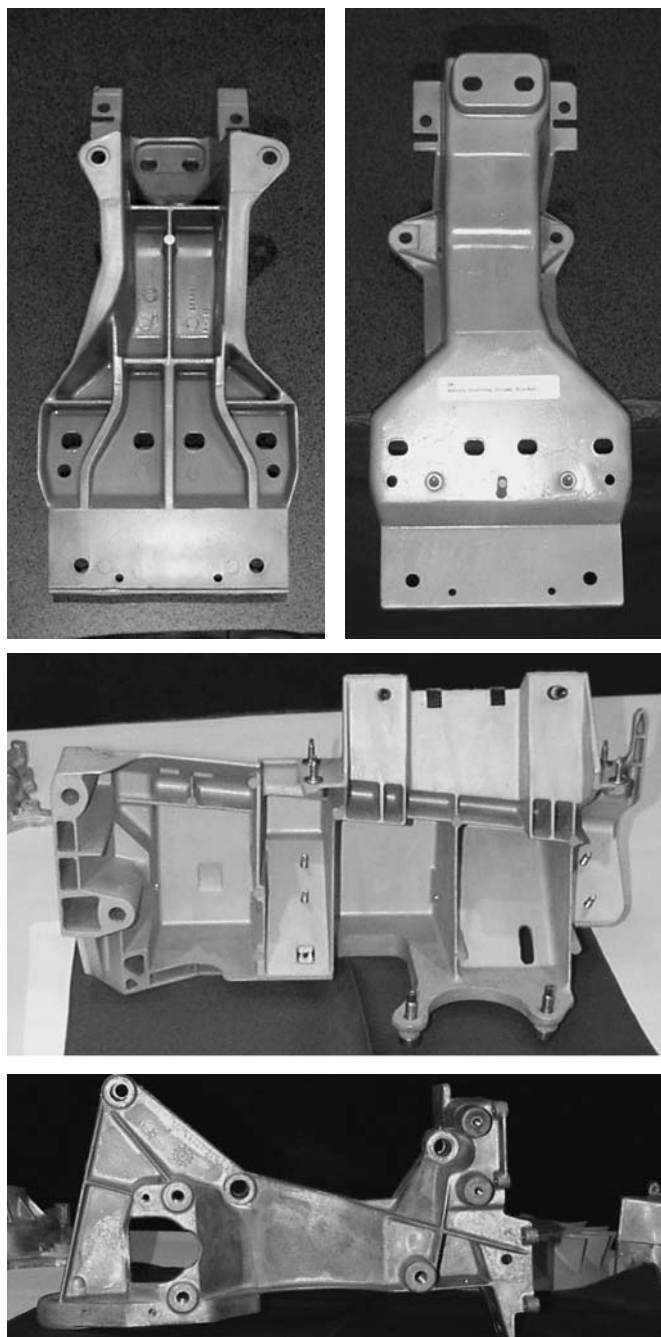
**Table 8.9** (continued)

System	Component	OEM	Name plates
Chassis	EGR valve plate	GM	Multi
	Oil filter adapter	GM	Multi
	Transmission stator	GM	Multi
	Clutch housing and piston	GM	Multi
	Transfer case (Frt/Rt)	GM	4
		Ford	2
	Intake manifold	GM	1
	ABS brake bracket	DCX	1
	ABS mounting bracket	GM	1
	Pass air bag housing	DCX	1
	Brake bracket assembly	DCX	1
	Brake/clutch pedal bracket	Ford	2
	Clutch pedal assembly	GM	4
	Clutch pedal bracket	GM	1
	Brake pedal bracket	GM	2
Total 2000–2002 volumes		GM	28,000 m
		Ford	16,000 m
		DCX	9,000 m

In 2000, there were 60 different parts used in NA vehicles (see Table 8.9). GM used the most with some full sized vans, such as the Savana and Express having up to 26 kg, and the minivans Safari and Astro having up to 16.7 kg of magnesium parts. Ford uses less magnesium in total; the largest application, is in its Ford explorer which has about 16 kg and the F-150 truck some 14 kg. DCX is further back in the pack with its minivan having 5.8 kg. In the car arena, the Buick Park Avenue has the most magnesium in NA at 9 kg, compared the VW Passat and Audi at 13.6–14.5 kg.

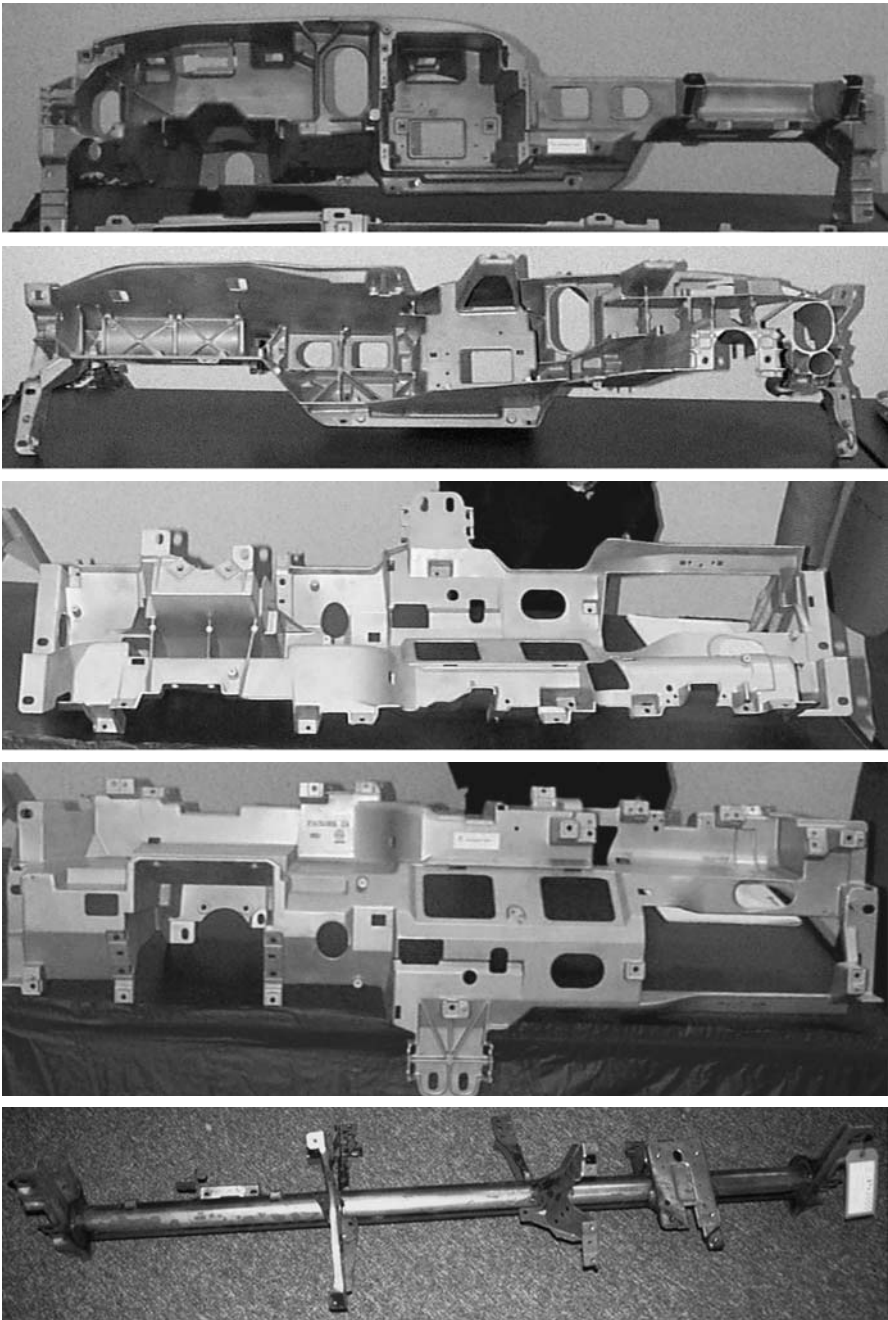
### 8.2.1.5 Magnesium in NA vs Europe

The reasons for the significant difference in magnesium usage are based on the economic climate and infrastructure of the North American automotive industry and on politics. In North American over 50% of vehicles sold are pick-up trucks, Sports Utility Vehicles (SUVs) and mini-vans. These are the vehicles where the auto manufacturers make their highest profits. These are therefore the vehicles where the auto industry can afford to pay the extra cost for the more expensive lightweight components that can improve driveability and fuel efficiency. There is not very much profit on the smaller vehicles produced in North America, in fact the smaller more fuel efficient vehicles are sold so that the industry can meet its Corporate Average Fuel Economy (CAFE) requirements for cars of 27.5 mpg (8.6 l/100 km). This allows the industry to sell the large more profitable cars that have poorer fuel consumption. There is more cost competitiveness among materials and component options for the smaller vehicles, and magnesium has been too expensive for the mass-reductions that are achieved.



**Fig. 8.89.** Steering column bracket, inner and outer, showing structure required for rigidity. The shape and dimension are controlled by the crash loads and the IP design architecture

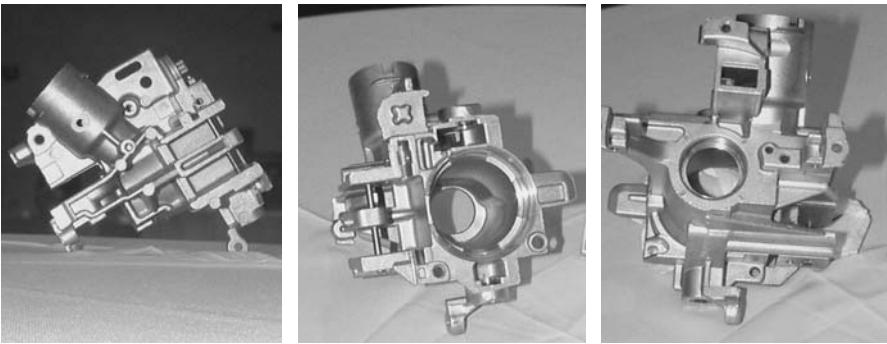




**Fig. 8.90.** Instrument Panel architecture. Lowest section show conventional steel with weldments. Next lower 2 sections show inside and outside views, in car position of an angular IP. Upper 2 sections show a more rounded structure. Both designs are to provide crashworthy crush and prevent steering column rotation. (Meridian products limited)

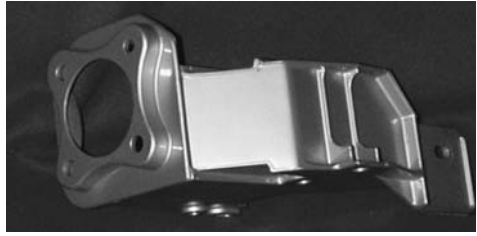
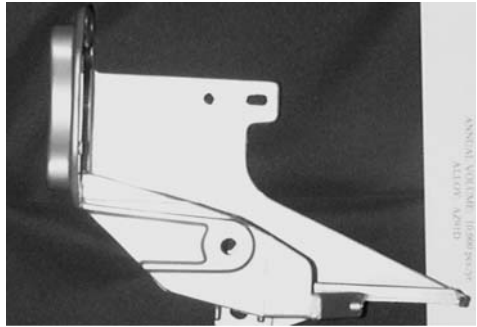
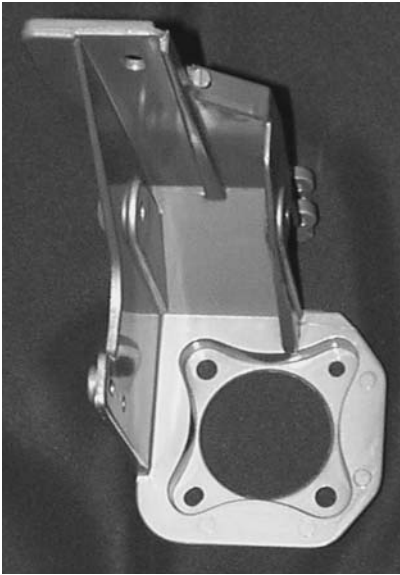


Steering Column and Steering Column Actuator Assembly (Intermet)

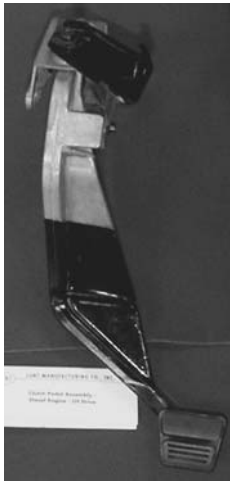


Steering Column Keylock Cylinder (Intermet)

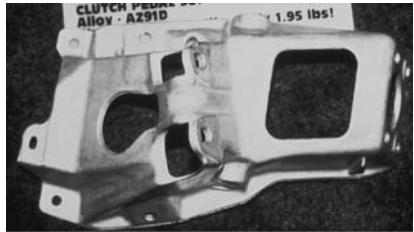
**Fig. 8.91.** Steering column elements, including cylinder lock housing. Note rib details to obtain stiffening



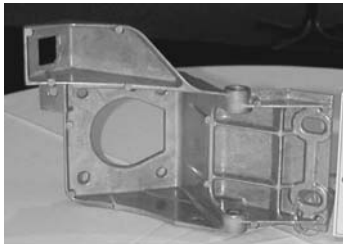
Brake Pedal Bracket (Magnesium Aluminium Corporation)



Clutch Pedal Assembly



Explorer Clutch Pedal Support Bracket



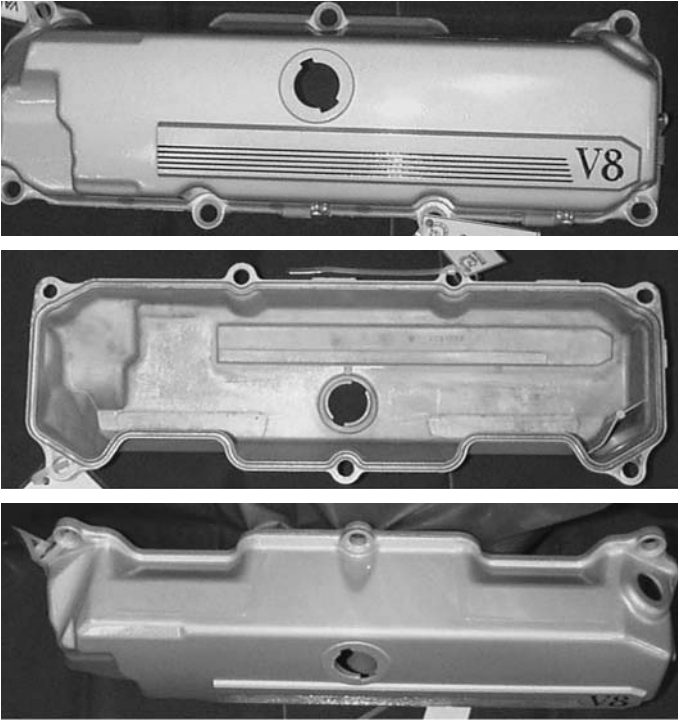
Brake & Clutch Pedal Support Bracket



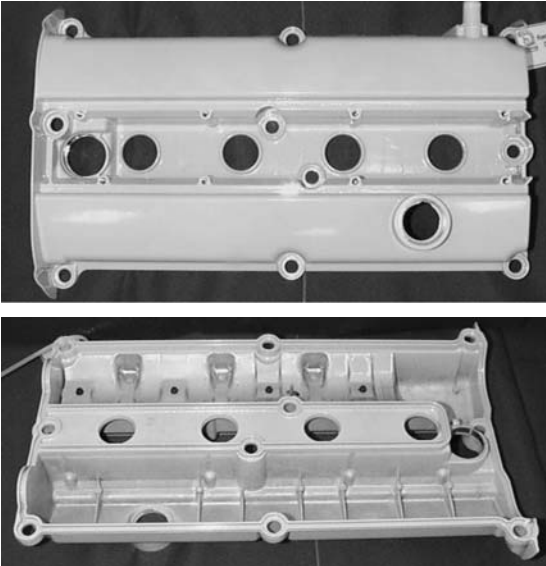
Brake End Clutch Bracket



**Fig. 8.92.** Various shaped clutch and brake pedal support brackets. Note details of ribbing and surface edges/ledges to provide stiffness

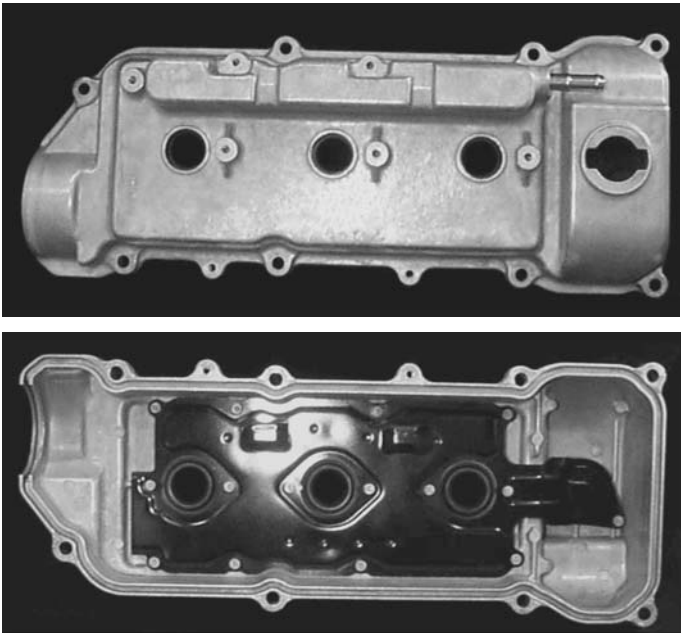


Calve Cover, Spartan Light Metal Products

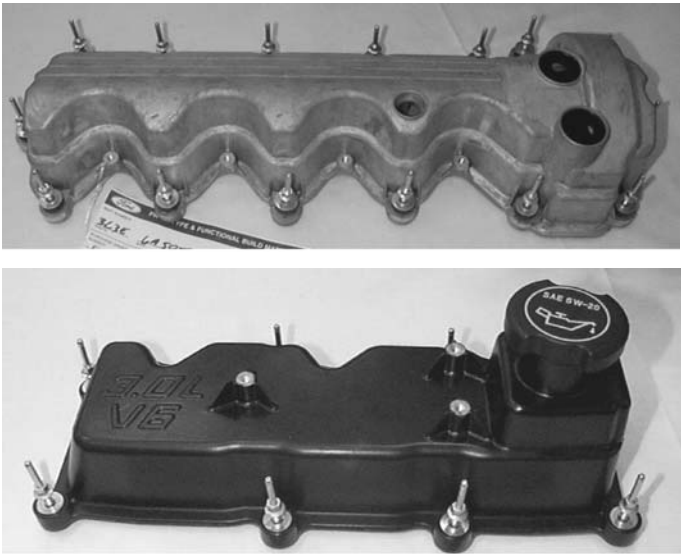


Cam Cover,  
Spartan Light Metal Products

**Fig. 8.93.** Valve and cam covers or sealers. Note details of ribbing to provide stiffening. The spacing between the fasteners is critical to ensure no leakage

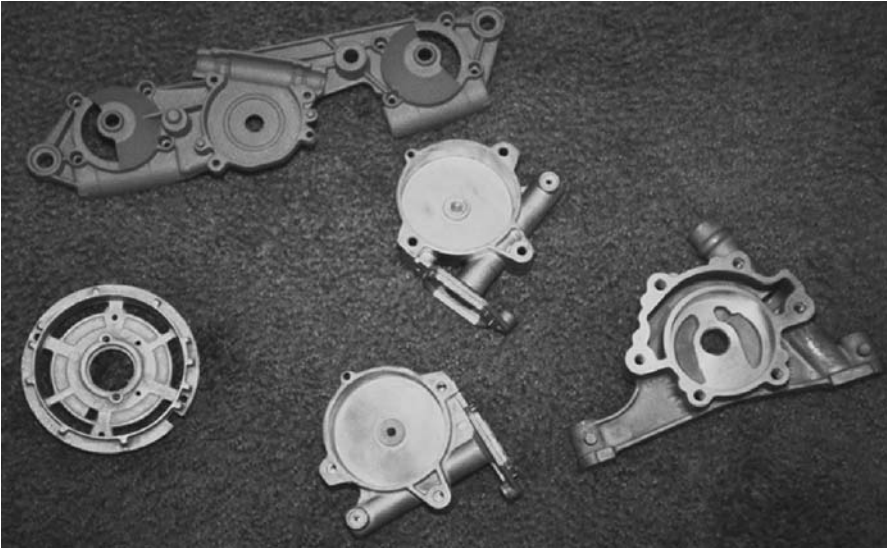


Cam Cover. Left top view, right inner view with assembly of splash shield



Various Shaped Valve Covers with fasteners in place ready for assembly  
Fig. 8.93 (continued)

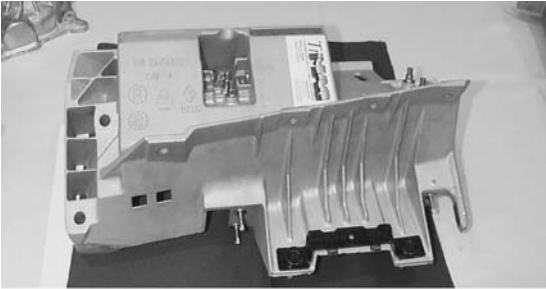




Various Small Motor Housings in Magnesium

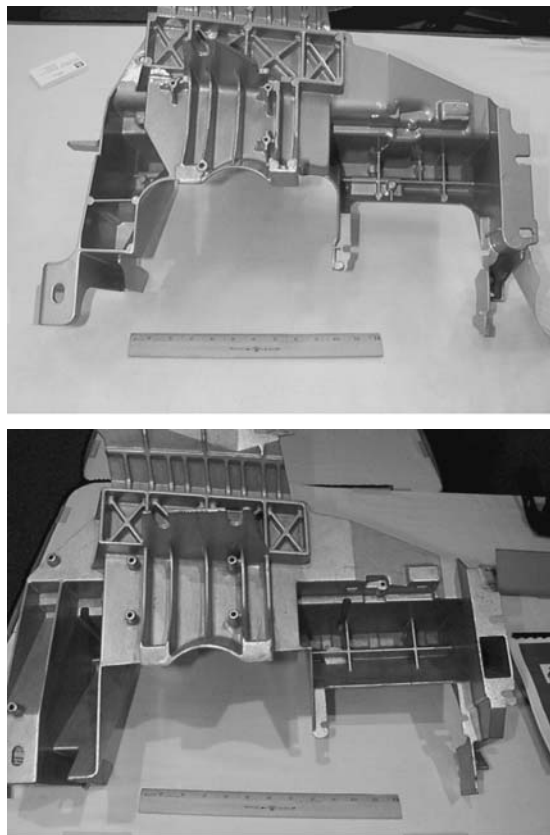


Instrument Panel Bracket  
Assembly  
(Meridian Products Limited)



Instrument Panel Bracket  
Assembly  
(Trimag)

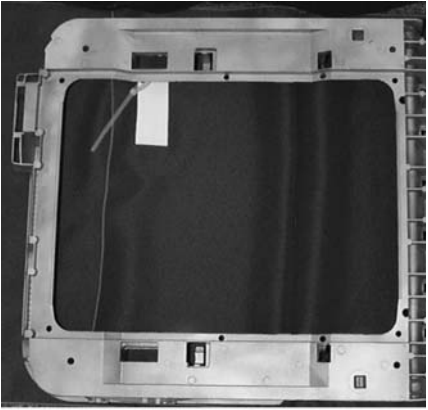
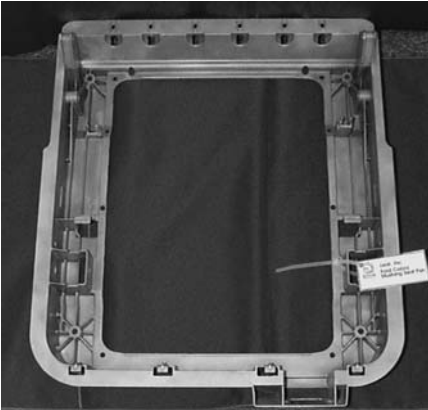
**Fig. 8.94.** Mixture of interior magnesium components associated with instrument panel and motor drives



One-half Instrument Panel, for GM Vehicles (Intermet). Each half is joined by an adhesive bonding technique.

**Fig. 8.94** (continued)

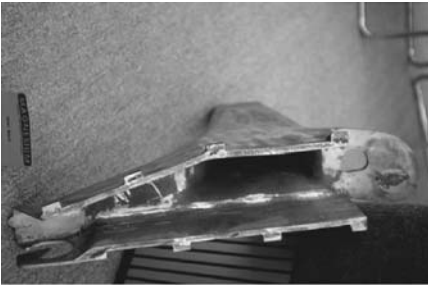
While fuel efficiency in North America is considered when buying a vehicle, it has not been a major issue with consumers. Only the U.S. government has taken an active role in fuel efficiency, for cars as noted above as well as for trucks (minivans, sports utility vehicles-SUVs, and small pick-ups... which comprise more than 50% of the North American market) setting a truck CAFÉ of 20.7 mpg (11.5 l/100 km). There are two reasons for this lack of interest. First, the price of gasoline is low (~\$0.25–0.30/l) based on low taxes by the federal and state governments, which can not increase them because that would be politically unacceptable. Second, while there is a societal demand for clean air in North America, it is not as strong as in Europe, where there are political “green” parties focused on emissions control and other environmental issues. The direct correlation between fuel efficiency, emissions and light weight is well-marketed by the European auto industry. In North America, lightweight vehicles are considered unsafe in comparison to the larger, heavier behemoths currently on the road.



Seat Base Architecture, for Ford

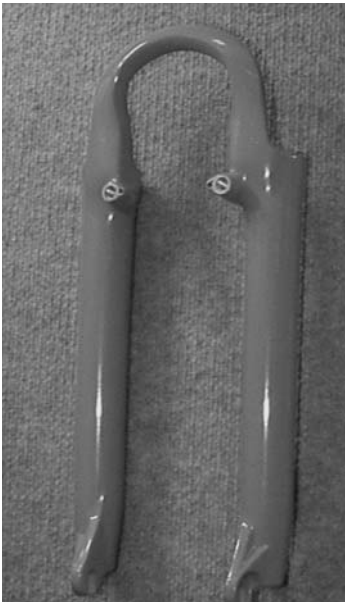


Seat Stanchios for Ford Windstar. Note ribbing details to increase stiffness. Product converted back to steel to reduce cost



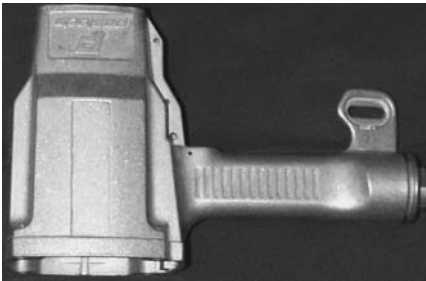
**Fig. 8.95.** Interior (seat) and seat stanchion architecture. None of the casting shown here survived more than three years in production because of cost





Camcorder Frame

Bicycle



Hand Held Tool  
(Thompson Casting Company)

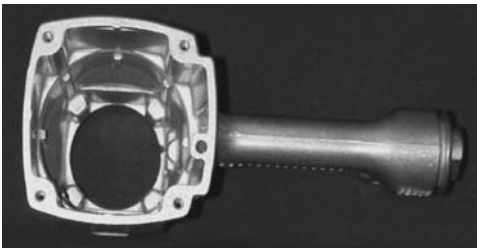


Fig. 8.96. Various non-automotive applications of magnesium

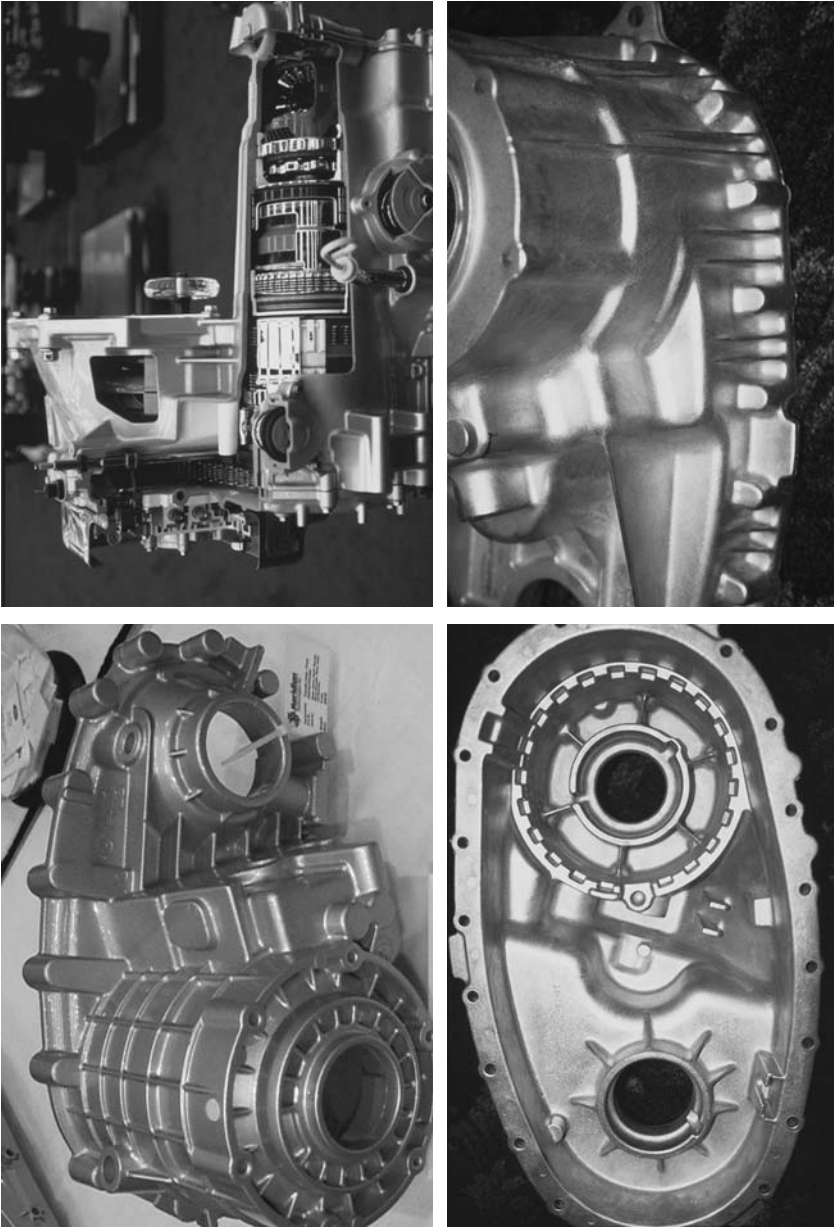
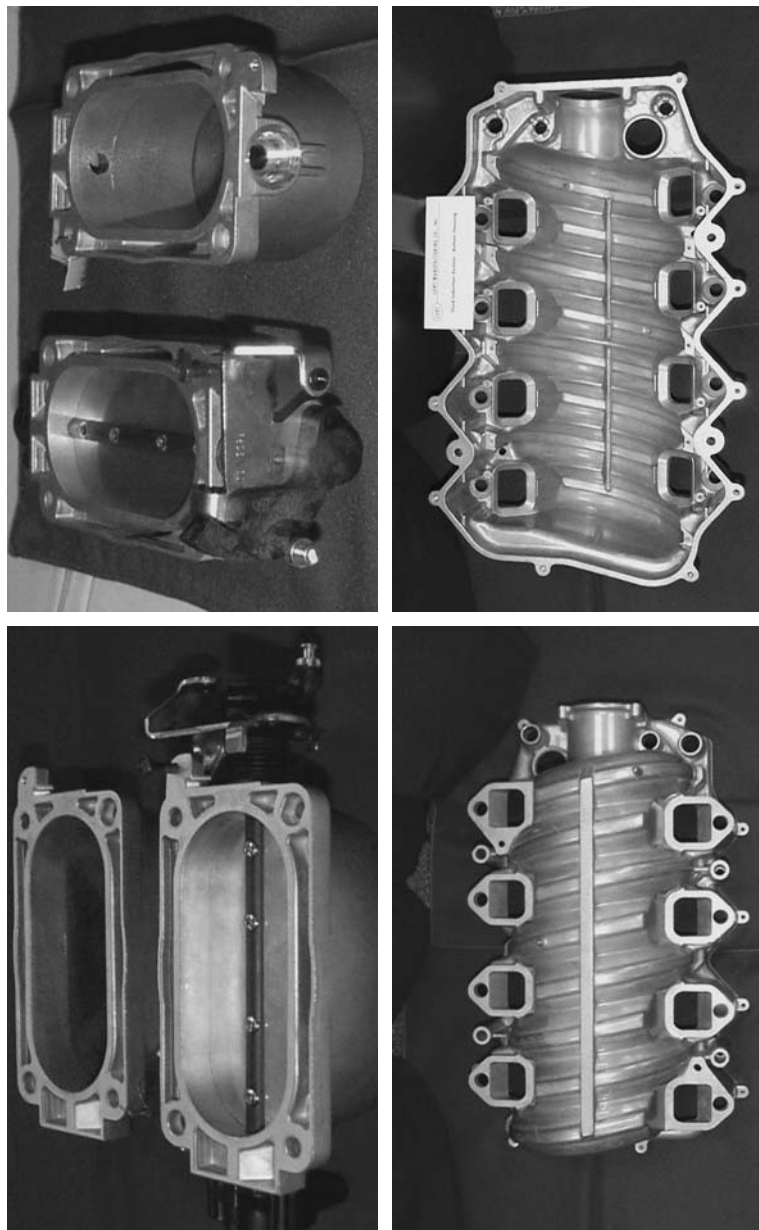
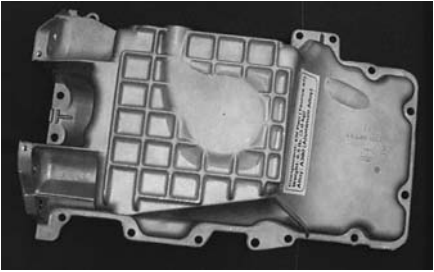
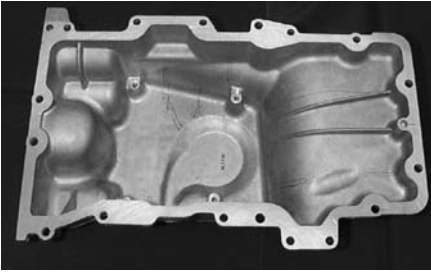


Fig. 8.97. Various powertrain applications for magnesium

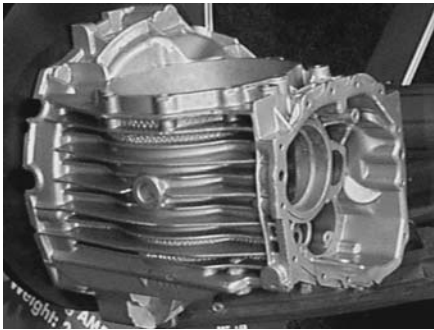




Potential Application for an Oil Pan in Magnesium



Magnesium Bed Plate Concept for an Magnesium Engine



Magnesium Transmission, currently in an Audi Vehicle

**Fig. 8.98.** New applications of magnesium technology in powertrain. In a North American truck application the concern is the high temperature ( $\sim 180^{\circ}\text{C}$ ) and high compressive creep loads that are experienced. Current alloys are insufficient, but there are new materials on the horizon that are being tested in Europe and in North American, that may not be cost prohibitive

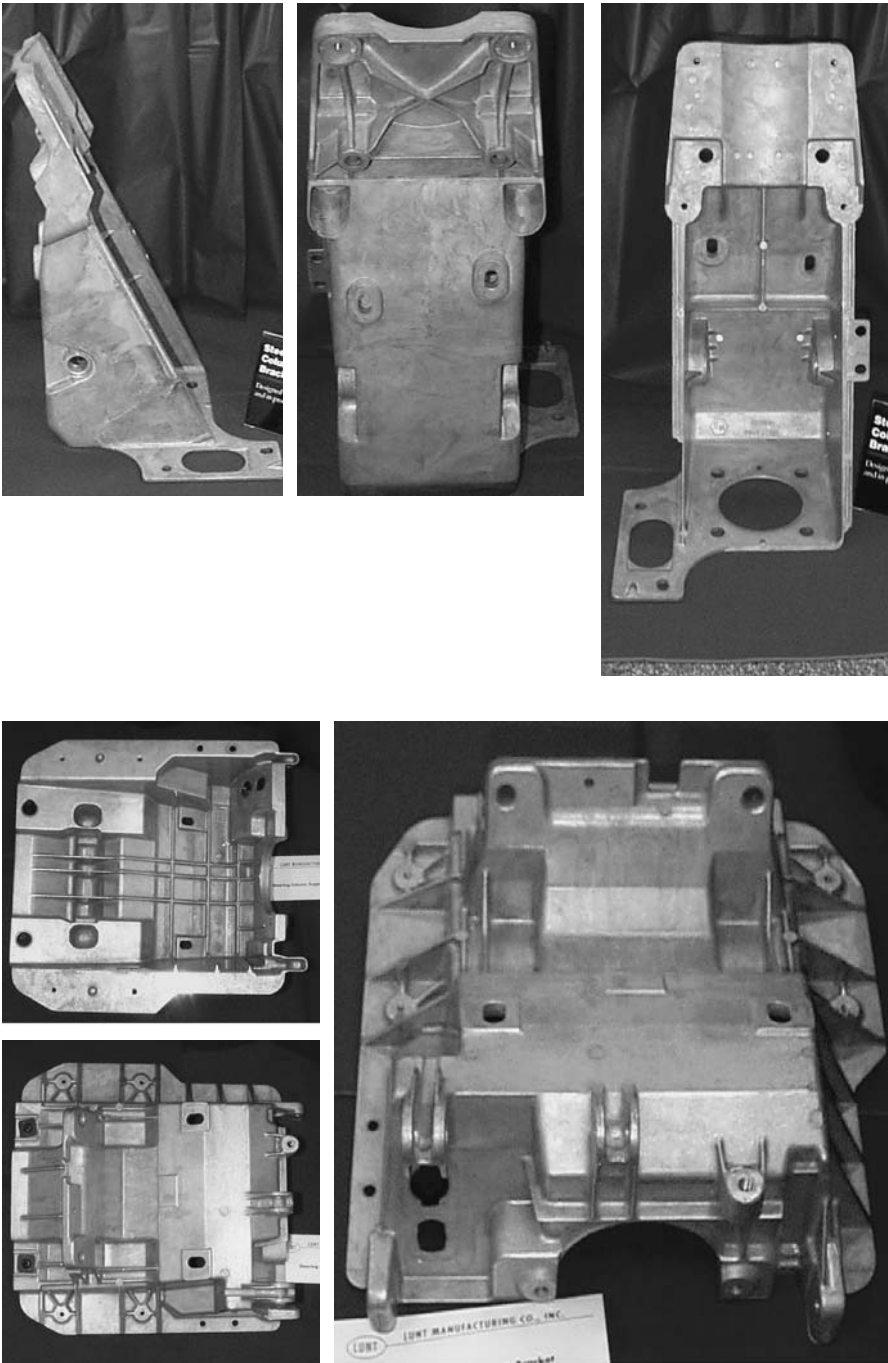
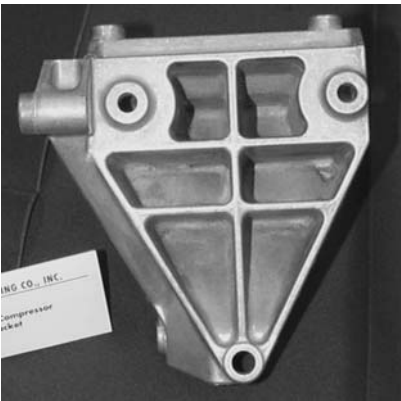
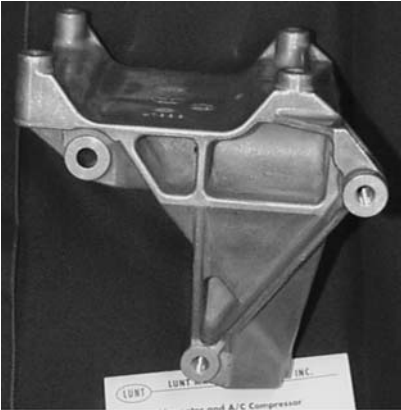


Fig. 8.99. Different steering column support brackets. Lower lunt engineering, upper harvard industries





Alternator and Air Conditioner Compressor Mounting Bracket (Lunt Engineering)



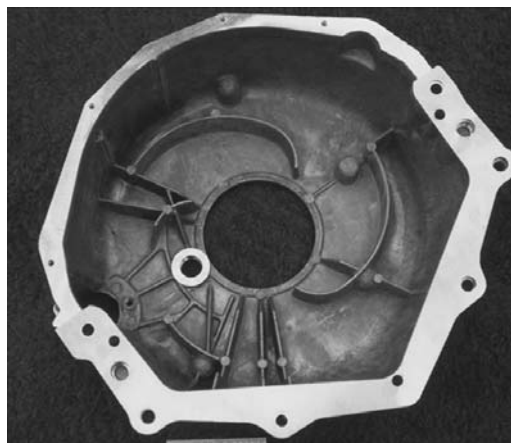
Various Engine Accessory Mounting Brackets (Lunt Engineering)



**Fig. 8.100.** Various powertrain applications, mounting brackets and transmission



Torque Converter Stator (Lunt Engineering)



Transmission Bell Housing For  
1980's Ranger Truck (Meridian  
Products Limited)

Fig. 8.100 (continued)

#### 8.2.1.6 Engineering Magnesium Applications

The growth in magnesium applications has been mirrored in SAE publications. Whereas in the 1980s there were 34 presentations, in the 1990s there were 112.

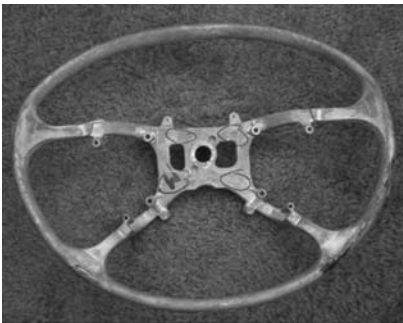
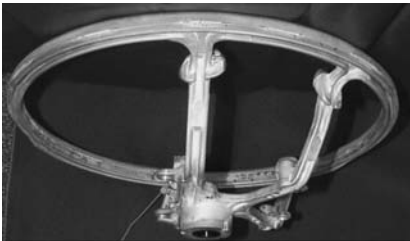
The details of the engineering criteria that govern conversions from steel, aluminum or plastics, are often described in the SAE literature and the interested reader can obtain these from the SAE website: [www.SAE.org](http://www.SAE.org).

The key issues for North American engineering is to be able to fully explain the magnesium replacement so that the part is as light as possible (to reduce cost and to improve the cost/weight ratio). This requires a full dynamic model of the machine tool (HPDC machine functions) the tool design (parting lines, gate/runner and overflow conditions), the filling and solidification, the optimal component shape required to fulfill the vehicle functions (casting thickness and position in the tool), the dynamic and static loads on the part (critically loaded location/position in the die), and issues of fastening loads. In turn this requires



**Fig. 8.101.** Various magnesium body applications lower. Door inner modules and assembled door closures upper. Lift gate example of VWs lupu

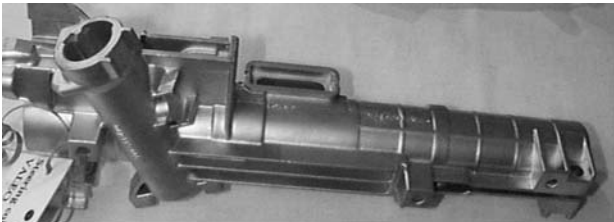




Steering Wheel Armature After Deformation in a Crash Simulation. The AM50 alloy passed the test by not fracturing

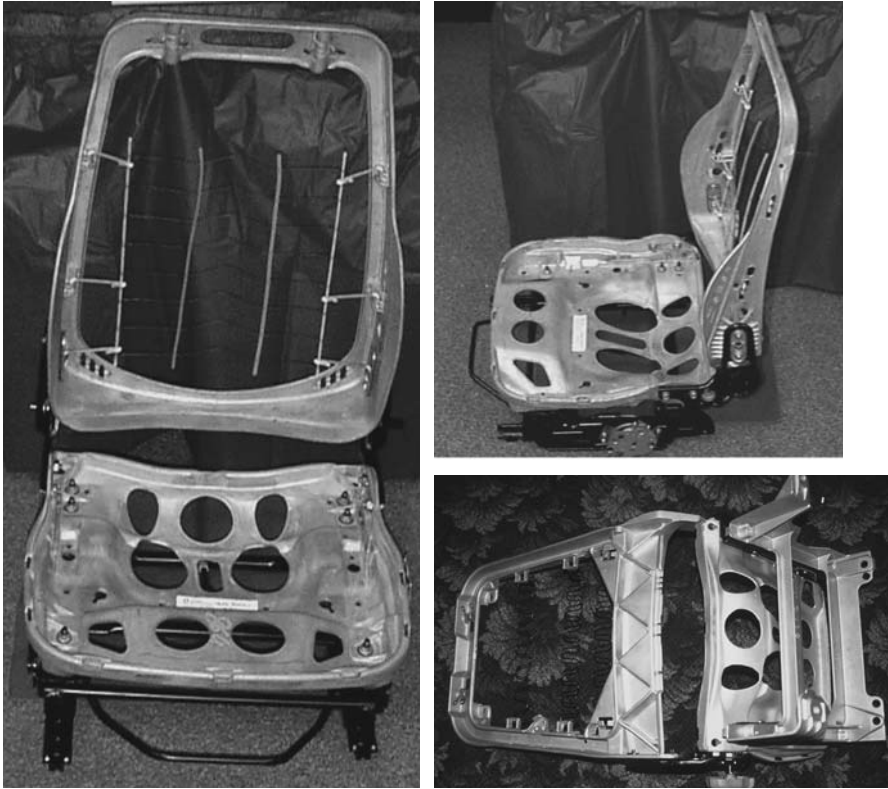


Steering Wheel Armature (Gibbs DC). The bottom 2 views show the upside and underside (lowest view)



Steering Column (Valeo)

Fig. 8.102. Steering applications for magnesium



Magnesium Seat Demonstrators for Lear Corporation, Cast by Meridian Products Limited Italy



Lower Control Arm R&D Demonstrator for Ford (Gibbs DC)

**Fig. 8.103.** Various automotive applications of potentially new components in chassis and interior. There are limited us of seats in two GM trucks; the GM corvette used to offer magnesium wheels as a very expensive option

a complete database of actual material properties from similarly shaped/produced castings, not necessarily as produced, but after exposure and possible damage by the environment during 200 km of vehicle operation.

Because these answers are not immediately available for the critical components, the rate of magnesium introduction will continually be hampered. As long as North American engineers live and work in a risk-averse society, there will always be a conservative view to product and materials changes, especially with a metal that is still not as well understood compared to aluminum and plastics. The amount of aluminum on a typical North America vehicle is over 120 kg; the amount of magnesium is 3.5 kg. This has taken the efforts of a significant amount of R&D in the past at the laboratories of Alcoa, Alusuisse, Alcan, Pechiney, Reynolds, Kaiser, and many others. The polymer proportion on a vehicle is about equal that of aluminum. The polymer industry is petrochemical derived, so it certainly has the resources to support the engineering and commercial issues that affect material substitution. The magnesium industry does not currently have the depth and financial resources to support a large-scale introduction of magnesium components.

But the need for weight reduction will grow in North American as the need for emissions reduction and fuel efficiency grow, both from social concerns as well as from the North American political requirements for oil independence. Magnesium has a potentially great future in North American.

## **8.2.2 Non-Automotive Uses for Magnesium**

### **8.2.2.1 Electronics/Communication**

Lightweighting and downsizing are challenges for mobile electronic/communications equipment. First, for the same fuel and energy savings during shipping, whether land-based or aerospace-based. Second, light and small laptop computers, cameras, cell phones and hand-held devices are desirable for many other reasons: human ergonomics (low mass/thinner walls, down to 0.4 mm), EMI/EMF shielding (both from inside and outside fields), vibration and noise reduction, thermal management to reduce internal heat loads on electronic components, rigidity and impact resistance, low inertia for moving components such as actuator arms, and metallic look and feel compared to polymers. Electronic/communication systems that currently use magnesium are laptop computers, cellular phones, digital cameras, digital projectors, TVs, hand-held devices and electronic enclosures.

### **8.2.2.2 Hand Tools**

To reduce fatigue and increase safety for workers, the hand tool industry has incorporated many lightweight parts into their assembled devices. Examples are chain saws, drills, handsaws, impact nailers and garden tools.

### **8.2.2.3 Sports Equipment**

This field is characterized by high interest in new materials for speed and performance. Net shape lightweight parts are now used in bicycles (Hayes), fishing reels (Shimano), archery bows, and snow boards (K2).

### **8.2.2.4 Aerospace**

This industry has been wary of lightweight cast alloys because of concerns with porosity and corrosion. Yet savings by lightweighting could be as high as US \$300 per pound of weight saved for commercial aircraft or US \$30,000 for spacecraft. A power boost of 30% can be gained by a mass reduction of 40%. Thus the incentives are high to upgrade structure/processing/properties.

## **8.2.3 Magnesium Manufacturing in North America**

More than 90% of all magnesium components are pressure die cast, since this is the lowest cost manner to produce magnesium components; only a small number of applications are sand or permanent mold castings. The two common pressure die cast processes are hot chamber, for smaller castings weighing ~3 kg and cold chamber, for larger pieces. The North American Die Casting Association (NADCA) is the main repository of North America's die casting knowledge and runs an annual conference (and biannual exposition) where issues of die casting technology including magnesium metallurgy (as well as other metals) are discussed in detail. The interested reader can contact NADCA [43] to obtain copies of their publications and annual transactions, which contain considerable information on the technology of magnesium. The International Magnesium Association (IMA) also provides a forum for exchange of magnesium manufacturing, trade and technical information; their address is listed in reference [44]. Magnesium die casting technology is discussed elsewhere in this volume. There are no particular differences between Europe and North America except that the world's largest magnesium die caster, Meridian Products Limited (a Canadian company), and Meridian Products America (in Michigan USA) is in North America. Since North America uses twice the amount of magnesium as Europe, this is understandable, and it has led to a magnesium infrastructure that is North American in overtone.

The mechanical properties of cast metals and alloys are strongly influenced by a variety of casting defects and artifacts, all of which reduce strength and ductility. These include entrapped gas porosity, shrinkage porosity, oxide, flux, and dross inclusions and planar defects such as cold shuts and folded oxidized surfaces. Die castings are especially prone to high levels of porosity due to high velocity turbulence of molten metal entering the die and oxide and flux inclusions resulting from melting and liquid metal transfer systems. Elimination of defects and reductions of porosity will lead to improvements in the quality and performance of metal castings. Cast metals structure, including the size, distribution, and location of precipitates, the size and morphology of crystalline phases, the amount and location of porosity and the final grain size of the material have a direct impact on the resulting properties.

### **8.2.3.1 Semi-Solid Metal Casting (SSM)**

One of the earliest reports of casting benefits was associated with casting mushy melts in the UK. In this procedure, molten alloys were stirred as they were cooled into a slushy stage and then cast into molds; reductions in porosity and improvements in strength were observed. The benefits of semi-solid processing of cast metals has been the subject of considerable research dating back to the early work performed at the Massachusetts Institute of Technology (MIT) in the 1960s. During this time, foundry studies led by the students of Professor Merton Flemings developed the Rheocasting process. This was the first well-known semi-solid metal casting process. A molten metal bath was stirred while it was cooled into the semi-solid state; at the appropriate mushy level (i.e. at the appropriate proportion of solid and liquid), the metal could be successfully pressure die cast. The MIT research capitalized on the discovery that the solid dendritic phase has its morphology altered into small (100–200  $\mu\text{m}$ ) almost spherical elements as a result of stirring through the solid-liquid boundary (rather than stringer-like interconnected solid dendrite threads). At greater than 50% solid, the resultant material displays thixotropic behavior, i.e., it can support itself (as a solid) in an unloaded condition, but flows like a liquid when it is stressed.

SSM has several potential advantages over traditional pressure die casting. In contrast to pressure die casting where the metal enters the die as turbulent streams of atomized sprays, semi-solid/thixotropic metal can fill the mold in an essentially planar non-turbulent flow manner, but only when the fraction solid is high enough (>25%). High volume fraction semi-solid parts can theoretically be produced with lower porosity than can pressure die castings.

There is currently a considerable amount of R&D effort toward developing “mush-on-demand” (or semi-solid metal produced directly during cooling, bypassing an initial freezing and then remelting process). These techniques can mimic the Rheocasting approach. Or, as in the case of Ube, use controlled cooling into the liquid solid region (followed by a short burst of induction to remove all temperature gradients) of the liquid magnesium alloy contained inside a small cup, the size of the required charge. For thinner parts, low solid fractions (near 0.01) are required, because of filling and rapid solidification difficulties. For thicker cross-sections, higher solid fractions in the thixotropic region are allowable.

The mechanical behavior of SSM-processed parts exhibit improvements over die cast counterparts, principally due to a reduction in porosity (sometimes up to 50%) and other casting defects. The reduction in porosity and absence of continuous porosity leads directly to improvements in both ductility and tensile properties.

### **8.2.3.2 Thixomolding (TXM)**

TXM was introduced in 1990, based on fundamental work by Dow engineers searching for a way to produce magnesium components in a similar manner to making injected molded polymers. The end result of over 10 years intensive R&D has achieved a robust process that has produced a typical TXM machine that is shown schematically in Figure 8.104. It is similar to a plastic injection molding machine. Mg alloy



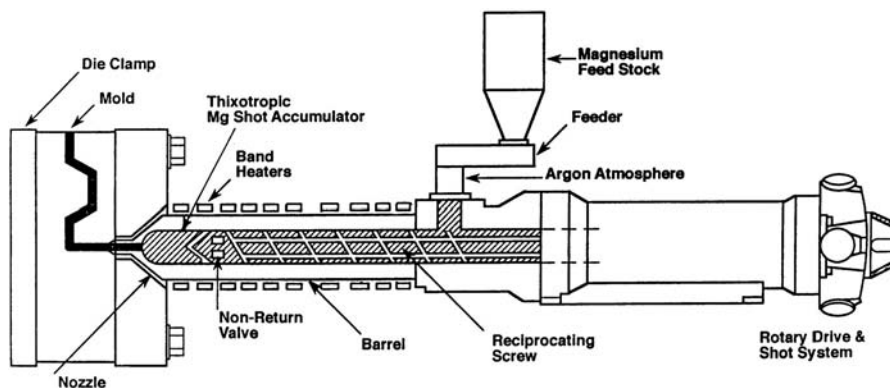


Fig. 8.104. Schematic of Thixomolding machine

feedstock (in the form of metal granules at room temperature) is introduced into a heated barrel and screw of a modified injection molding machine. In plastic injection molding the temperature of the material is raised to a plastic state under high shear rate mixing. With TXM, external heating is required as shown in the figure. The semi-solid slurry, consisting of nearly spherical solid particles suspended in a liquid matrix is propelled through a non-return valve into an accumulation zone, which is sealed off from air at the nozzle by a frozen plug. After a sufficient volume of slurry has been collected to fill the die (about 15–30 seconds), the screw is driven linearly at high velocity to inject the slurry into the heated mold. The clamping forces compare to hot chamber units and are in the range from 75 to 1,600 tonnes.

In HPDC, a protective gas of  $\text{SF}_6$  or  $\text{SO}_2$  is required to protect the molten magnesium surface from burning. During TXM processing, pellets of the desired alloy composition are fed under an argon atmosphere; in addition all melting and molding takes place in this same protective in Ar atmosphere.

The TXM process permits the production of parts over a wide range of solid fractions, nominally on the order of 0.05–0.60. This is a unique advantage over SSM methods that use semi-solid billets (processes which stir the melt during freezing into a solid billet, which is then reheated back up into the semi-solid region). These are restricted to solid fractions greater than 0.60. In addition, there is a possibility to recycle TXM produced scrap without secondary refining operations, since the alloy has low oxide content by virtue of it having been melted under an argon cover gas.

The tensile mechanical properties for TXM-produced AZ91D, AM60, and AM50 components meet or exceed ASTXM die casting specifications, for 0.3 or lower solid fraction; at higher solid fractions, heat treating is required to achieve maximum strength levels. In addition, steady state creep rates in both AZ91D and AS41 are reportedly improved compared to counterpart die cast structures. The improvement, which is enhanced with increasing solid fraction, is attributed to the duplex microstructure consisting of the primary  $\alpha$  phase distributed uniformly in a divorced eutectic continuous matrix of  $\text{Mg}_{17}\text{Al}_{12} + \alpha\text{Mg}$ .

Thin wall hot chamber die casting, SSM forming and TXM offer similar opportunities to expand the industrial application of magnesium. In a recent review

of magnesium applications in Japan [48], out of 192 different thin wall applications, half were TXM and half were HPDC. Because of its unique marketing approach TXM has been at the cutting edge of applying thin wall magnesium castings in commercial components that historically, have been produced from polymers and polymer composites. The following information was provided by Thixomat [49], and is reproduced here, since it succinctly describes how and where magnesium components can supplant current polymer parts.

### **8.2.3.3 Magnesium Can Replace Polymers**

Thin wall magnesium is replacing plastics in many applications, due to its favorable physical and mechanical properties. Density is only 50% higher than for plastics (unique for a low cost metal), EMF/EMI shielding is enhanced, parts have greater stiffness (flexural modulus of 45 vs 2.2–6.7 GPa) and greater tensile strength (223 vs 35–104 MPa), sections can be thinner (0.35 mm vs 1 mm), draft angles can be lower (0–1.5 vs 2–3 degrees), and dimensional tolerance is more precise ( $\pm 0.001$  vs  $\pm 0.002$  mm/mm). And, of course, and most important, magnesium is almost 100% recyclable.

### **8.2.3.4 Magnesium Can be Fabricated into Macro-composites of Plastics and Metals**

Magnesium has its shortcomings in corrosion, joining, touch and feel, and color. Net shape assemblies can be produced with plastic overlays and internals that ameliorate the shortcomings of magnesium, while retaining the virtues of plastics. Engineered plastics can serve to “join” magnesium components, rather than welding. Likewise, plastic portions of the composite can serve as the fastening interface with other metals to evade magnesium’s usual galvanic corrosion problems. Plastic coatings can provide decorative color and touch and corrosion protection. Both hot chamber die castings as well SSM parts and TXM require special tolerances to ensure that the plastic can be overlayed onto a magnesium armature to produce successful composite components. This requires innovative designers who can select the polymer compositions with appropriate modulus of elasticity, strength and adhesion to compliment magnesium’s properties.

### **8.2.3.5 Alloys Designed Especially for SSM and TXM**

- Commercial production to date by TXM has used standard magnesium alloys; AZ91D, AM60 and AM50. Although the properties are excellent, it has become evident that the process offers new opportunities to develop new alloys specifically designed to improve on process/alloy/composition/microstructure/properties and process. The phase separation inherent in semi-solid processing produces dual-phase microstructures. To improve mechanical properties, the second (solid) phase can be optimized in both volume % and composition by controlling the barrel temperature. Molding fluidity is enhanced when the action of the screw both spherodizes and reduces the amount of solid phase, and when high shear (injection) rates are employed.

- Mold design to control solidification rates can also control grain size and eutectic spacing. Many semi-solid castings have low porosity. Unlike conventional HPDCs, they can often be T6 heat treated to modify microstructure without blistering.
- Some of the newer magnesium alloy compositions (such the new Ca containing alloys) can only be die cast using specialized HPDC processing. However, they can often be easily semi-solid molded. ZAC alloys with 0.6 Ca have exhibited moldability comparable to AM50 and superior creep resistance with 33% solid phase [46].
- Metal matrix composites (MMCs) can be more easily produced in TXM using the screw action to suspend particulates uniformly in Mg; this has already been demonstrated with  $\text{Al}_2\text{O}_3$  and SiC reinforcements.
- As a final note, it is possible to conceive “just-in-time” alloy manufacturing, wherein tailored compositions can be ordered up and blended much like colored paints are at a hardware store.

#### **8.2.3.6 Redesigning Parts and Assemblies**

Both hot chamber die casting and TXM have the ability to make a range of thicknesses from 0.9 to 25 mm (TXM has reported castings as thin as 0.35 mm). Both processes hold very tight dimensions, and can produce zero draft holes. This offers the part designer opportunities to simplify parts and assemblies and allow multiple parts to be combined in one, so that machining can be eliminated. One hand-held tool user has moved nine parts from die casting into TXM at a considerable cost saving.

#### **8.2.3.7 Thermal Management and Improvement of TXM**

One of the most interesting recent TXM developments has been in thermal management of the injected slurry as it progresses from the barrel nozzle to the extremities of the part in the mold, using hot runner technology borrowed from plastic-injection molding. Previously this had not been feasible in metal casting. But heating and maintaining the slurry all the way to the gate can eliminate the sprue and runner. Using multiple pin gates, flow distances can be shortened and shot yields raised from 50 to 90%. At the same time, parts can be moved to smaller machines using multi-part dies. All these improvements in processing significantly reduces costs by over 40%.

Another new development has been in the barrel heating area. Previously, electric resistance heaters have been used to heat up the barrel, container and the metal, causing a multitude of materials' problems (excessive wear on the barrel and auger, and short life-time of heaters). A new approach, using inductive heating has just been developed which could change the manufacturing and cost paradigm of the TXM process. Machine maintenance, downtime and therefore component costs should be able to be reduced significantly. Now, even with the higher base machine cost and license fees, TXM could be cheaper than HPDC.

The commercial progress of TXM has been considerable, especially over the past three years as measured by the growth of machines. In 1996 there were only





Fig. 8.105. Auto seat back (560 × 460 mm)

20 machines installed. But in 1999 there were 145, in 2000 there were 188, and by the end of 2001 more than 225 were expected to be operating around the world to 45 licensees. Initially it is more expensive to purchase a TXM machine and its license than an equivalent hot chamber die casting machine; for this reason almost no existing die casters have purchased them. However, there are many companies who do not wish to be involved in a foundry process situation. TXM appeals to those companies who are uncomfortable with the dirtier, noisier environment of a conventional die casting foundry.

In North American, where there are a large number of die casting installations, there are few TXM machines. However, it is in Asia, where there are fewer die casters, that most of the installed capacity is found. The initial impetus was in electronics/communication applications. Mini-notebook computers led the field, with cellular telephones now following closely. Other components include mini-notebook PCs, digital VCRs, minidisks, digital cameras, cellular telephones, TV cameras, TV consoles, digital projectors, control panels, and copiers. There are now activities beginning in hand-held tools, fishing reels, fans, and bicycle parts.

Current activities are also expanding into automotive applications as represented by an auto seat from a 850-ton machine (see Fig. 8.105) and a quiet exhaust fan that replaced an Al assembly (see Fig. 8.106).

#### 8.2.3.8 Summary

Semi-solid molding and especially the Thixomolding process are in their commercial and technological infancy. As the technology evolves, with more robust machines, better heating and less wear on auger and barrel, there should be more impact in industries where cost, productivity and reliability are important, such as the automotive industry. This uniquely North America development will then



Fig. 8.106. Copier exhaust fan. (202 × 45 mm and 260 × 99 mm)

be able to play an increasingly valuable role in growing magnesium component applications throughout industry.

#### **8.2.4 Magnesium R&D in North America**

The magnesium industry is dynamic, and changing continuously with new applications, new problems, and often new solutions. Unlike in Europe, and unlike the other materials aluminum and plastics, there are no organizations and institutions in North America solely devoted to solving issues that effect function and that can add to the value of magnesium alloys. There is one major activity that is noteworthy in sponsoring R&D in North America and that is the United States Council of Automotive Research (USCAR). The results of USCAR efforts will be long-lasting in promoting new magnesium developments in North America. A short summary will be presented here to describe to organizations activities to those readers of this volume who may not be aware of them.

##### **8.2.4.1 USCAR Programs**

###### **(a) Structural castings**

In 1994, the Department of Energy (DOE) and USCAR together created the Partnership for a Next Generation of Vehicles (PNGV) with the goal of developing a “Supercar” which could attain 80 mpg. It was quickly recognized that weight reduction would be a necessary enabler for this aggressive increase in fuel efficiency from the current 27.5 mpg (8.6 l/100 km) and a new partnership was created, the Automotive Materials Partnership (USAMP) to manage this aspect of

the Supercar program. In 1995, under the USAMP umbrella, a 5-year cast light metals project was initiated whose goal was to eliminate 50% of the weight of structural/chassis components, primarily by utilizing aluminum castings. Only a small amount of investigatory R&D was performed on magnesium components. By 1999, there was a growing concern that aluminum technology had matured, but magnesium still had "a long way to go" before it could play an important role in vehicle weight reduction. In order to promote a more aggressive stance with magnesium, a new Cast Structural Magnesium program was initiated in early 2000 to focus on resolving critical issues that limit the application of magnesium castings in automotive components.

There are two major issues with magnesium R&D: (1) There are no major R&D/technical institutions fostering the necessary infrastructure to support automotive magnesium applications, unlike aluminum, plastics and steel. (2) The North American automotive producers do not manufacture any of the cast magnesium components used in its vehicles; they only assemble them. Castings and sub-assemblies are produced by a relatively small industry base, that is not sufficient in size to conduct the R&D necessary for large-scale magnesium component development. Consequently, if the auto industry wishes to take advantage of magnesium's potential weight-reduction opportunities, it will have to nurture it itself. The project combines efforts of the Big 3 (Ford, GM and DCX), the DOE, three DOE National Laboratories, North America technical societies (in casting and materials), and approximately 35 North America corporations involved in manufacturing castings, testing, casting equipment and software simulation. Canada is an important partner in this program, and the Canadian Light Metal research Institute, CLIMRI (in Ottawa) is devoting significant resources toward magnesium technology; its efforts are directed mainly to galvanic and atmospheric corrosion R&D.

The activities of the 5-year, US \$5 million Cast Structural Magnesium project center on developing the science and technology necessary to overcome technical and manufacturing issues that limit the light weighting application of cast magnesium automotive components. To widen the application of ductile castings the scientific understanding of magnesium alloys must be improved. Comprehensive design guidelines, improved casting processes and gate/runner designs, improved component corrosion resistance, failure (fail-safe) mode analysis and improved joining technologies are required to produce low cost, high integrity, ductile (as-cast) structural magnesium castings that have significantly reduced porosity over current high pressure turbulent die casting processes. In addition, the program will investigate galvanic (bi-metallic) and atmospheric corrosion behavior of common alloys, especially as related to fastening magnesium components to aluminum, cast irons and steels. The goal is to develop suitable low cost corrosion-protection systems to ensure durability of chassis components against stones, fatigue and corrosion.

Cast magnesium microstructure will be linked to fracture, and monotonic/cyclic mechanical properties. Math-based models will be developed that simulate key cast microstructural features using boundary conditions of mold temperature, metal temperature, mold fill, solidification and possibly the influence of heat treatment. These will be used to simulate corrosion and stress corrosion behav-

ior of the component. Radioscopic inspection standards and quality indicators for thin wall magnesium castings will be integrated with process sensor development to improve casting processing and with quantitative x-ray or other non-destructive evaluation (NDE) methods to analyze casting discontinuities.

Current North America cast magnesium applications include components that generally are considered non-cyclic load situations in friendly (i.e. non-corrosive) environments. But aggressive weight saving applications will require high strength, ductile castings in body and chassis areas of the vehicle, which require the ability to function in cyclic loading and harsh corrosive environments. To demonstrate the relevance of the R&D, an aggressive application was selected, front and rear cradles, which are currently fabricated from aluminum and steel. Such components offer all of the difficult manufacturing issues including casting processing (HPDC, SSM, low pressure, squeeze) and joining, along with harsh service environment challenges, such as corrosion, fatigue, and stress relaxation associated with fasteners. A prototype cradle will be produced during the program that meets automotive durability, strength, crashworthiness and NVH requirements, and at an affordable cost target. The project's findings and simulation models will be applicable to other components in chassis (control arms, steering knuckles, road wheels), body (door and lift gate inner, A/B pillars), and interior (front cross-car beams and seats).

### **(b) Powertrain applications**

In early 2000, it was recognized that if the North American auto industry was going to be able to incrementally add significant amounts of lightweighting, it would have to be in the vehicle powertrain (engine and transmission). New high temperature ( $T > 150^{\circ}\text{C}$ ) magnesium alloys for powertrain application were beginning to be discussed in the literature, based on calcium and rare earth additions to conventional AZ and AM alloys. The new magnesium companies, Noranda, Dead Sea Magnesium (DSM) and the Australian Magnesium Corporation (AMC), and the older companies, Avisma/Solikamsk (Russia), Norsk Magnesium and Magnesium Electron (MEL), had recently patented interesting and potentially valuable alloys. As well, R&D investigators within the automotive industry at GM, Toyota, Honda, Nissan and Mitsubishi were working on new alloys that had considerable possibility for utilization in powertrain applications. A new Cast Powertrain Magnesium project was formulated and commenced work in early 2001. Like the Cast Structural Magnesium project, there was an identifiable product at the end of the project, and that was the design, casting, manufacturing and verification of the functionality of magnesium in an engine block and other high temperature components associated with a block.

There are considerable problems using magnesium alloys for a high temperature block application in comparison with current aluminum engines. They include tensile strength, fatigue strength and stiffness (as a function of operating temperatures, pressures and loads), creep (stress relaxation at bolts), heat transfer (thermal conductivity), thermal expansion (at bores and bearings), corrosion (from coolant, environment and bimetallic/galvanic joining), leak resistance, and bore liner materials and design. In addition, issues of manufacturability (casting in sand and/or permanent molds), machinability, component assembly and alloy

recyclability will affect engine functionality and the cost effectiveness of using magnesium alloys in these severe applications.

It is expected that these problems will be solved during the next few years, and that the newer class of creep resistant, corrosion resistant magnesium alloys will find a growing use in high temperature applications, especially engine blocks, front covers, oil pans, bed plates and automatic transmission cases.

8.3 Magnesium Aerospace

*Francis H. Froes, Dan Eliezer, Eli Aghion*

8.3.1 Background

The use of a structural material is dictated by a number of factors including mechanical and physical properties and cost (which relates in part to availability). The latter factor plays a major role in use levels (Fig. 8.107), and in the industries in which they are used i.e. (Fig. 8.108 and Table 8.10).

Magnesium is the lightest of all commonly used metals and is thus very attractive for transportation applications Figs. 8.109 and 8.110 [50–63]. It also has other desirable features including reasonable ductility, better damping characteristics than aluminum and excellent castability. Magnesium can be joined by

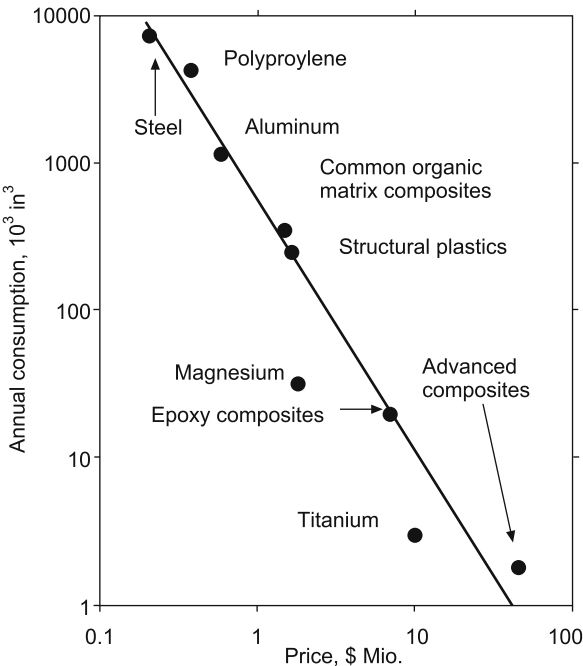
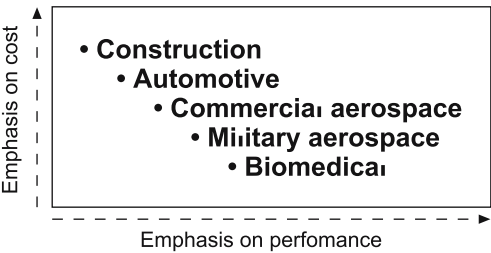


Fig. 8.107. Influence of price on amount of material consumed

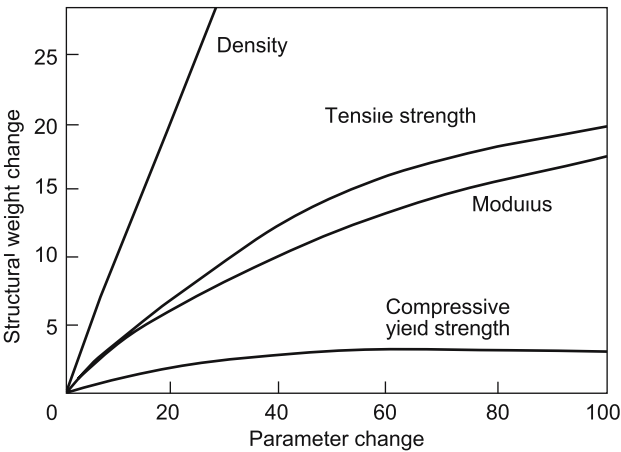


**Fig. 8.108.** Relative importance of cost and performance in material user industries

**Table 8.10.** Value of a pound in weight saved in various industrial segments

Aerospace segment	Value of a pound in weight saved (US \$)
Commercial/transport	300
Fighter	3,000
Space	30,000
Automobile <sup>a</sup>	3

<sup>a</sup> For comparison purposes, although, in reality this number is probably more like US \$1.50 per pound.



**Fig. 8.109.** Effect of mechanical property improvement on aircraft structural weight (Courtesy Lockheed Corp.)

riveting or any commonly used welding methods. Magnesium can be machined faster and has the best strength-to-density ratio of any of the commonly used structural metals. All of these characteristics make magnesium attractive to the aerospace industry. However, magnesium exhibits a number of negative features including inferior strength/ductility, fracture toughness, fatigue and creep compared to aluminum and a generally less than desirable corrosion behavior and

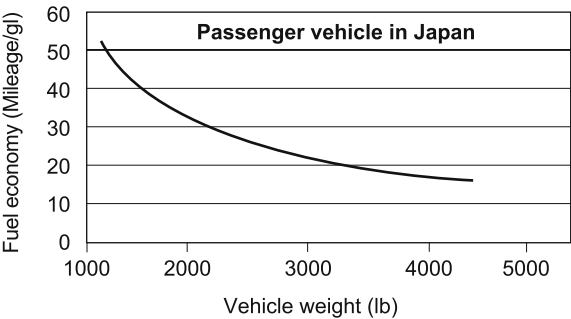


Fig. 8.110. Effect of weight reduction on automobile fuel consumption

Table 8.11. Comparison of Light Metals

Feature	Aluminum	Titanium	Magnesium
Price	+	–	0/–
Mech. Properties	+	++	–/0
Corrosion Behavior	+	++	–/0
Processability	0	–	+
Fabricability	+	–	–
Knowledge Base	++	+	–

+ Positive; –Negative; 0 Neutral.  
Processability: cast products.  
Fabricability: cast-and-wrought mill products.

Table 8.12. Metal shipments (metric tons) \*1997 estimates

Metal	Estimate × 10 <sup>3</sup>
Titanium	50
Magnesium	320
Aluminum	25,000
Steel	700,000

\* World Totals × 10<sup>3</sup>, Courtesy B. Clow, IMA.

galvanic corrosion resistance, which has been described as “awful.” Magnesium also suffers from the perception that it readily burns – a legacy from a demonstration by a high school science teacher.

There is also a limited supply base, a lack of fundamental knowledge on the behavior of magnesium alloys, and a cost which is about twice that of aluminum. A comparison of magnesium with the two other widely used light metals, aluminum and titanium, is given in Table 8.11, and use levels in Table 8.12.

There are an increasing number of processing and synthesis techniques available, all competing with the baseline ingot metallurgy (I/M) approach, Table 8.13,

**Table 8.13.** Comparison of the characteristics of a number of advanced processing/synthesis techniques

Process	Characteristics						
	Cost				Commercial viability		
	Mechanical properties	Starting material	Finished product	Capital	Lot size	Compatibility with existing infrastructure	Range of product forms
I/M (base-line)	M	L-M	L-M	L*	H	H	H
RSP (RS, MA, VAPOR, etc.	H	H	H	M	L	L	M
Net shape P/M (Press & Sinter BE)	L	L-M	L	L	L-M	M	L
Semi-solid processing	L-M	M	L-M	M	M	L	L
Casting	L	L	L	L	M-H	H	L
Spray forming	M-H	M	L-M	M	M	M	M

Key: H = high; M = medium; L = low.

\* Existing infrastructure, depreciated.

IM = ingot metallurgy; RSP = rapid solidification processing; RS = rapid solidification; MA = mechanical alloying; BE = blended elemental.

Vapor = Vapor deposition; P/M = powder metallurgy.



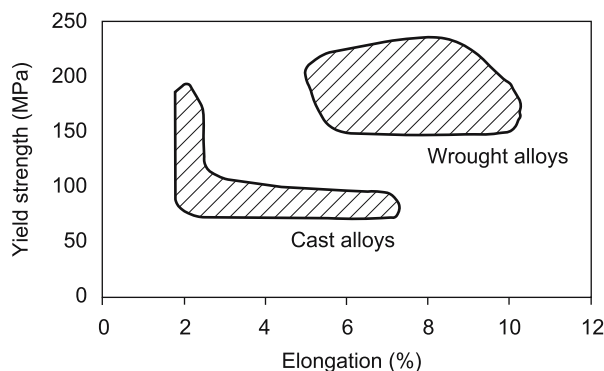


Fig. 8.111. Comparison of strength-ductility (specification minimum)

although in the case of magnesium, castings are the baseline. However, I/M mechanical properties are better than those of casting (Fig. 8.111), and in the case of very demanding aerospace applications, wrought magnesium components account for a larger percentage of use than terrestrial applications [63].

Magnesium metal for structural applications are processed into castings (die, sand, permanent mold, and investment), extrusions, forgings, and flat-rolled products. Castings far exceed cast and wrought products, and die castings account for 70% of the castings shipped; demand for automobile parts produced by this technique (about 85% of the total die castings) is projected to reach more than 100,000 tonnes per year worldwide early in the third millennium. Magnesium's use in a variety of applications will expand as knowledge of the interactions between forming processes, components design, component function/properties, and cost increases. However, this knowledge is less comprehensive than desirable, particularly for newer alloys.

Because of increasing pressures to improve automobile gas mileage in most parts of the world, in combination with the required property combinations of the automobile industry, use of magnesium in cars and light trucks is increasing significantly [50, 52–54]. Use of magnesium in the aerospace industry is more difficult and challenging [45] because of the much more stringent requirements. The purpose of Sect. 8.3 is to review the past use of magnesium in aerospace, to determine the present use, and to comment on how use can be increased.

### 8.3.2 Past Aerospace Use

Magnesium has seen quite extensive use in conventional aircraft and helicopter engines and in airframes. However, in recent years these levels have dropped dramatically because of real and perceived corrosion problems and the resultant construction mandates against using magnesium. However, even into the 1980s, a number of US government reports were quite positive on aerospace use of magnesium [64–70]. This also extended to reports on how “non-equilibrium” techniques such as rapid solidification could greatly alleviate the corrosion problem with extended solubility levels leading to a more protective oxide surface [69].

The Italian company, Isotta Fraschini, made the first serious efforts to incorporate magnesium into aircraft in 1926, when they started producing magnesium parts in Milan by casting and forging [63].

Wrought magnesium was used in aircraft fuel tanks and later propellers. Starting in 1930 and continuing to 1932 and 1934, special light planes participated in a flight around Europe. In 1930, 25 of 31 engines used magnesium crankcases and 28 had magnesium fuel tanks. Later flights saw most aircraft equipped with magnesium propellers. The Italian Breda engines used many magnesium parts. The "Round-Europe" aircraft had a maximum allowed empty weight of 400 kilograms [63].

In 1931, the first transatlantic formation flight led by Italo Balbo flew from Orbetello, Italy to Rio de Janeiro. Isotta Fraschini engines on these planes used many magnesium parts including housings, propeller shafts, oil sumps, distributors, oil tanks, carburetor housings, etc. [63].

In 1934, the Italian pilot Donati flew to a world record altitude of 14,335 m (47,000 ft) in a Caproni 113, which had magnesium gas and oil tanks and used magnesium in its body surfaces. The French pilot, Raymond Delmotte established a land speed record of 502.5 km/h (310 mph) in a Caudron 460, which had magnesium engine cases, body surfaces, fuel tanks, seats, fittings, wheels, oil pump, carburetor and several other parts [63].

The British de Havilland Comet which flew to Australia in 1934 in 71 hours contained more magnesium than any other British aircraft. The crankcases and other parts of its twin Gypsy VI engines and the under carriage, wheels, instrument panel, control lever, seats, wheel fairings, nose piece, front and rear engine cowlings and wing fairings were also fabricated from magnesium [71].

Jean Piccard and his wife made an ascent at Dearborn, Michigan in 1934 using a balloon carrying an eight foot in diameter spherical magnesium gondola. They reached an altitude of 17,550 m (57,564 ft.). In 1935, another balloon ascent by Stevens and Anderson, using a similar large magnesium gondola, reached an altitude of 22,066 m (72,376 ft). The gondolas were fabricated from a heavy flat magnesium plate, cut in an "orange peel" configuration and heated and welded into a sphere [72].

In 1929, a single engine training plane was built in which magnesium was used for all sheet, extrusion, and tubing material. In particular, the wing beams and wing ribs, the fuselage, including the sheet cowlings, the rudders and controls were made of magnesium [73].

Many magnesium parts were designed and used in aircraft production with initial use civilian aircraft. Many of the original civilian aircraft, particularly the Focke Wulf Condor 200, became vital parts of the military air service. The Condor used magnesium sheet for the engine cowlings, lower covering of fuselage and wings, the transitional fairings between the wing and tail unit, as well as the fuel tanks and several other fairings with parts being partly riveted and partly welded. The original civilian passenger plane model used seats made from welded Elektron (magnesium) tubes. The total weight of magnesium alloys used in the Condor was 650 kg (1,430 lbs) of which over 500 kg (1,100 lbs) were magnesium sheet. This was primarily AM503 alloy that was considered to be the most weldable of all light metal alloys [74].

The prewar Arado 196, a seaplane made to be launched from battleships, was called an “all magnesium” aircraft. It was also used in reconnaissance duty from shore-based airfields. The Messerschmitt 109 used forged Elektron AZ855 engine bearers (mounting brackets) and several other Messerschmitt liquid cooled engines used this type of mounting bracket. The magnesium forging concept was used in several other engine mounts, including the Focke Wulf 190, which had a BMW 801D radial engine. The 801D engine also used 20 kg (44 lb) of magnesium forgings. Both Messerschmitt and Focke Wulf used magnesium sheet in their airframe construction [63].

Heinkel used 80–100 kg (176–220 lb) of magnesium in the airframe of the HE-111. The HE-177, 4 engine bomber used 400–500 kg (880–1100 lb) in the airframe in the form of castings, forgings and sheet. Junkers was the largest user of magnesium in Germany for aircraft. The JU88A-4 (exclusive of engines) had over 350 kg (770 lb) of magnesium parts, of which 96 kg (211 lbs) were forgings. The company made extensive use of magnesium sheet and forgings. Prof. Hertel, Junkers design chief, was responsible for the adoption of the forged magnesium engine bearers (widely used in German Aircraft) and advocated the use of magnesium to the exclusion of aluminum in all forgings for aircraft except those subjected to elevated temperatures, such as pistons. The forging of these parts and of magnesium propeller blades was originally done on a 7,000-ton press and in 1938, more presses were added, including a 15,000-ton press [74].

The Northrup XP-79B Flying Ram, was a rocket engined flying wing interceptor, with a heavy magnesium sheet usage. The magnesium wings had special  $\frac{1}{4}$ -inch, case-hardened, steel-leading edges. It was designed to fly into enemy bomber formations and slice off wings or tails and survive, but it never went into production [75].

At the peak of magnesium production for World War II, thousands of tons of magnesium sheet were produced each month and fabricated into aircraft parts.

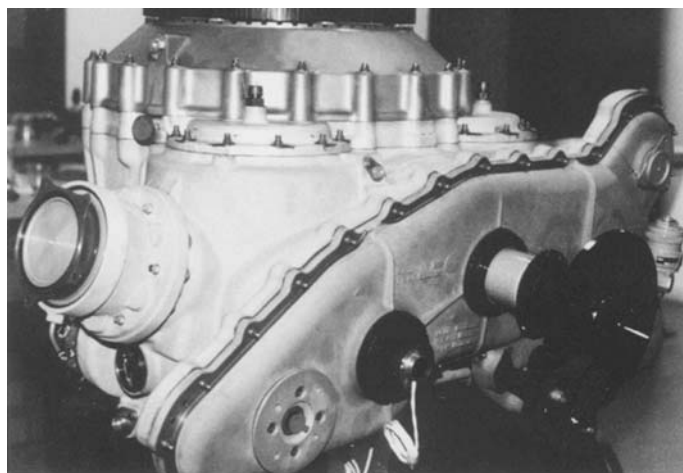


Fig. 8.112. An example of a magnesium helicopter transmission system

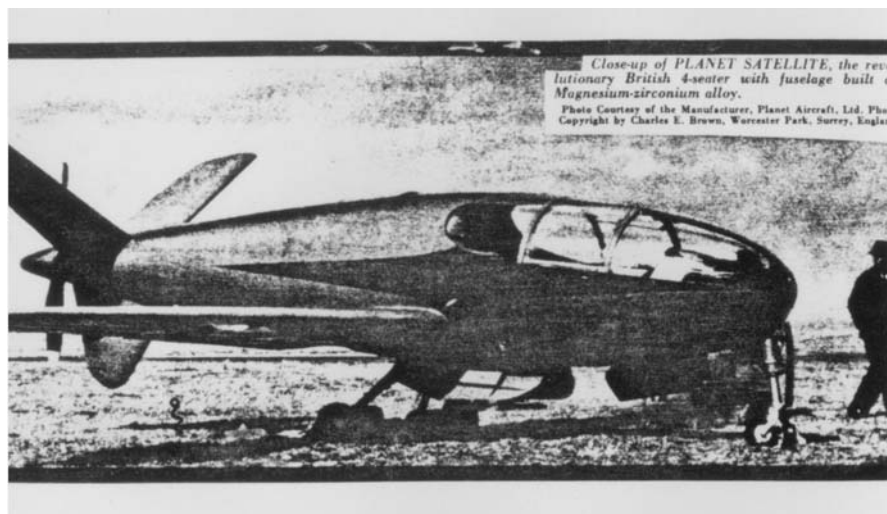


Fig. 8.113. Planet Satellite, British 4-seater with a Mg-Zr fuselage

Several aircraft were made of all magnesium extrusions, sheet and castings. These included the German Arado 196 and the US XP56 and F-80. Many other aircraft used large quantities of rolled magnesium [63].

Magnesium is the material of choice from a component weight/cost point-of-view in many helicopter transmission systems (Fig. 8.112), leading to a generic power increase in the rotor system [76]. Aluminum would increase weight, adversely affecting payload, while titanium is expensive. A series of corrosion-protection coatings must be applied.

Past use of alloy magnesium in aerospace applications included Mg-Zr alloy use in the fuselage of the British 4-seater planet satellite (Fig. 8.113), the Talon supersonic jet trainer, which had 11% (644 lbs) of the airframe fabricated from magnesium (Fig. 8.114) (360 lbs of sheet, 280 lbs of castings and minor amounts of extrusions, bar and tubing), and the B-52, which utilized 3600 lbs of magnesium (Fig. 8.115) (199 extrusions, 19 forgings, 542 sand castings and 380 lbs of sheet). Specific components included gearbox (8 kg) and cover (5 kg) castings for the Rolls-Royce/Turbomeca Adour Engine (Fig. 8.116), the power plant for the Jaguar, magnesium doors for the B-47 (Fig. 8.117), drop corrugation and nose skins (Fig. 8.118) and tail cones (Fig. 8.119). Another interesting, potential application of magnesium was as the material of construction in the platform of aerial delivery systems (Fig. 8.120).

Design of the B-36 bomber, “the Magnesium Wonder of the World,” was started prior to the end of World War II and development continued with the development of the largest bomber ever built; 385 aircraft were constructed. The gross weight of the production model was 162,727 kg (358,000 lbs). It was the largest single user of magnesium sheet, with 50% of the external skin using over 4,000 kg (9,000 lbs). The model of the B-36 built utilized 5,555 kg (12,200 lbs) of sheet, 700 kg (1,500 lbs) of forgings, and 300 kg (660 lbs) of castings [77]. The B-36 was



**Talon, supersonic jet trainer, has 644 lbs. of magnesium (11% of airframe weight). There is 361.25 lbs. of sheet; 276.52 lbs. castings; 2.47 lbs. extrusions; 2.44 lbs. bar; 1.42 lbs. tube.**

**Fig. 8.114.** The T-38 Talon, 11% magnesium airframe

unique in that 25% of the exterior surface of the plane was covered with a magnesium skin which had its stiffeners attached with metal adhesive. In a wing trailing edge section, magnesium replaced an aluminum design that fatigue-cracked due to vibrations from the six pusher engines [77].

After the B-36 came the B-47 jet bomber which had a total of 5,500 kg (12,000 lbs) of magnesium sheet, extrusions and castings. Magnesium was extensively used as a skin material on wing and tail leading edges, jet engine pods, and cowlings, gun enclosures and for miscellaneous doors. The tail cone of the B-47 was fabricated primarily of magnesium with some aluminum. In the B-52, 1600 kg (3,600 lbs) of magnesium was used with 636 kg (1,400 lbs) of sheet. The KC-135 jet tanker had 818 kg (1,800 lbs) total with 590 kg (1,300 lbs) of sheet [63].

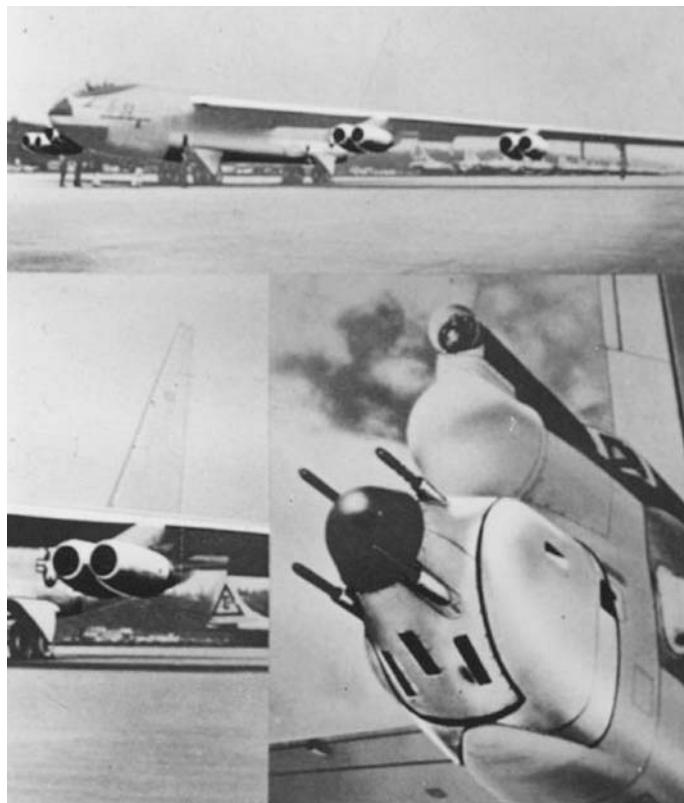


Fig. 8.115. The B-52, 3600 lbs of magnesium

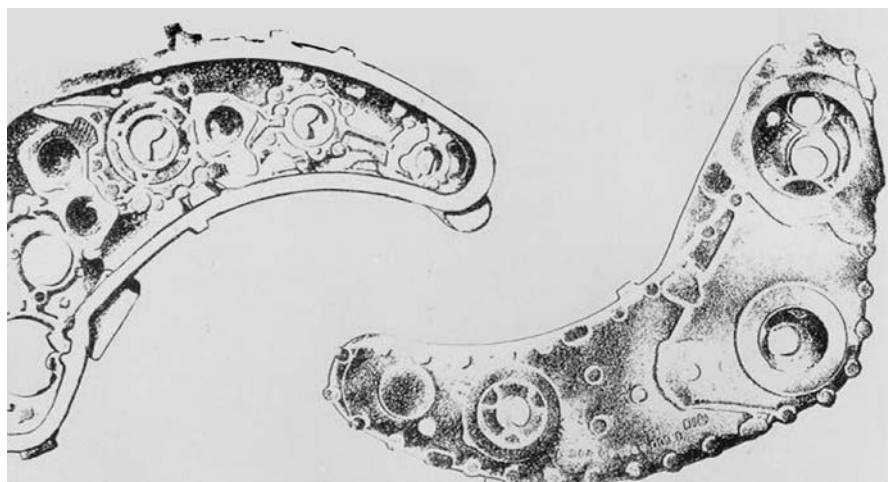


Fig. 8.116. Brequet/BAC Jaguar gearbox and cover made from magnesium



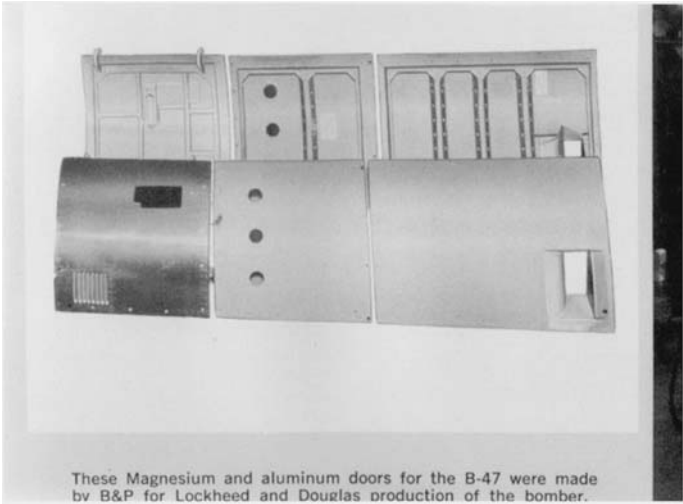


Fig. 8.117. Magnesium and aluminum doors for the B-47

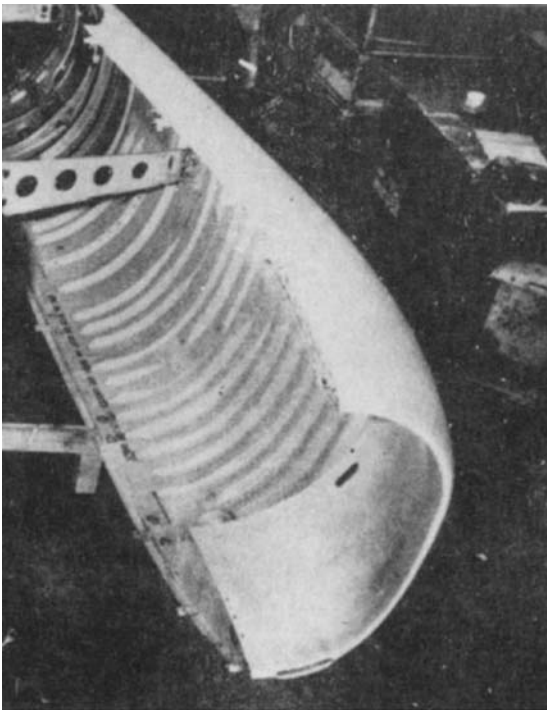
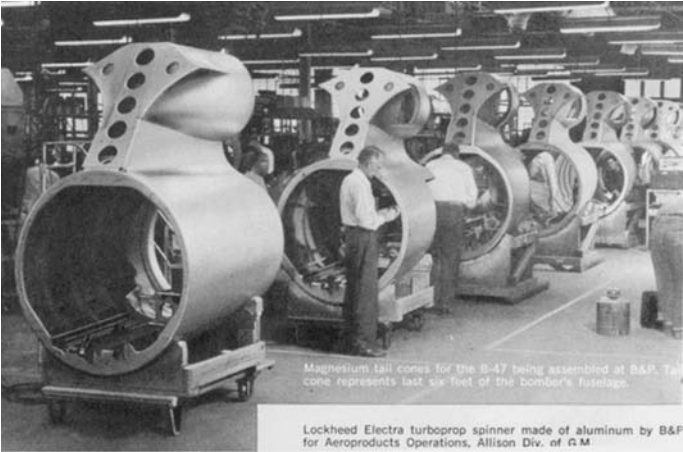
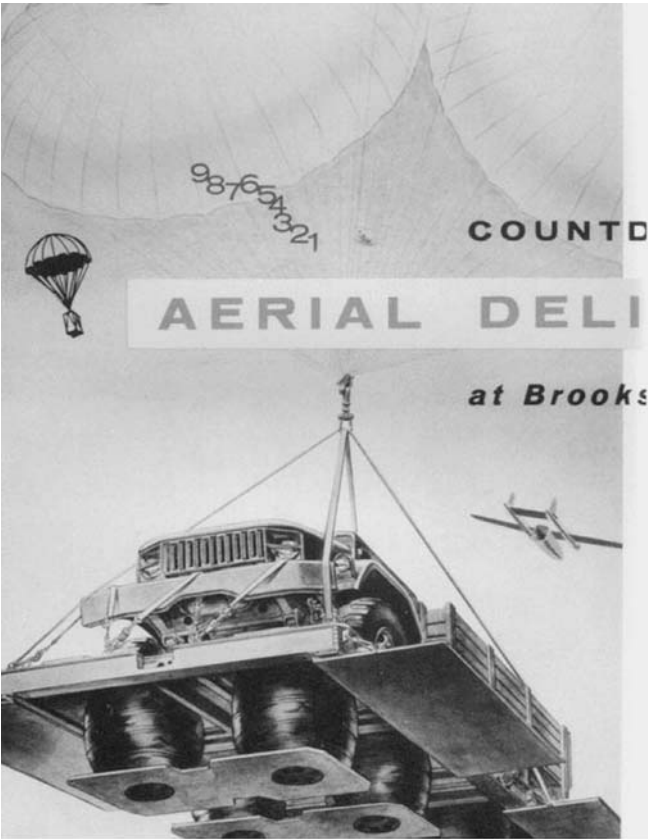


Fig. 8.118. Annealed magnesium drop hammer formed corrugation and nose skin



**Fig. 8.119.** Magnesium tail cones for the B-17, representing the last six feet of the bombers fuselage



**Fig. 8.120.** Magnesium platform body for an aerial magnesium delivery system



Extruded magnesium floor beams were first used in the C-47 cargo planes. Later they were installed in C-54s (DC-7). The Douglas C-124 Globemaster used magnesium for the main floor beams and also for the fold up second deck for troop transfer. The C-133 Cargomaster used ZK60B extrusions in the cargo deck and ramp, however, there were problems with these floors due to galvanic and other corrosion problems [78].

An entire F-80 "Shooting Star" jet fighter was made from magnesium and flown in 1955. The thick skin magnesium design that was successful on the monocoque wing design was applied to the fuselage, empennage, ailerons, flaps and other structural components by East Coast Aeronautics, Inc.

Beech Aircraft changed to magnesium control surfaces on the Bonanza in 1947. Using magnesium reduced the number of parts by 337, weight by 3 kg (6 lbs), man-hours by 10 per aircraft and production tools required by 57.

The Agena, Titan and Atlas long-range intercontinental ballistic missiles used large quantities of magnesium sheet. The thorium based alloy, HM21 and HK31 sheet was used for the magnesium skins of the vehicles. Much of the radar control equipment, antennas, electronic cabinets, plotting boards, etc., were made from magnesium sheet [63].

The former Soviet Union [79] has been producing and using magnesium for many years. There are no details on the rolling or extrusion of magnesium, however, stampings from magnesium alloys were used in the Vostok, Soyuz, Mars, Venus and Lunokhods space vehicles. It has also been reported that KUMZ was the leading producer of magnesium alloys and products in the former USSR. The Stupino plant produced large aviation panels from MA14 alloy by stamping. KUMZ developed complex ribbed stamping of rocket wings from alloy MA2. BKMPO has used the VILS (All Russian Institute for Light Alloys, Moscow, Russia) process to produce thin sheet manufactures and extruded articles from alloys based on the Mg-Y system (alloys VMD-10 and VMD-10-1).

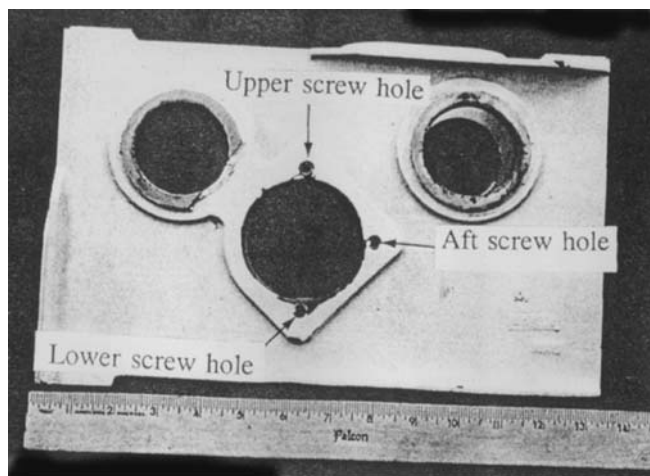


Fig. 8.121. Magnesium door handle box with cracks at screw holes

VILS have developed and introduced two lightweight alloys based on the Mg-Li system into commercial production. Alloy MA21 has a density of 1.69 g/cm<sup>3</sup> and the alloy M18 has a density of 1.48 g/cm<sup>3</sup>. These alloys have been used to reduce the weight of on-board devices in the space industry.

However, in-service problems have soured continued use [Ontko N, 1999; Hyatt M, 1999; Turzil J, 1999; Linc and McGuire, 1999; all private communications], and has led to the present negative attitude towards magnesium use in aerospace. One example is door handle box, where cracks were detected at screw holes in the magnesium structure (Fig. 8.121 and 8.122). This was attributed to stress corrosion cracking (Fig. 8.123).

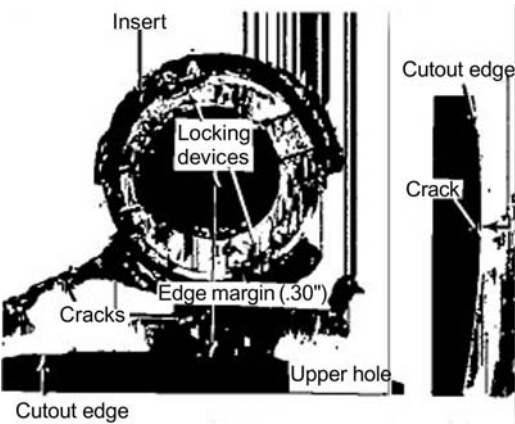


Fig. 8.122. As Fig. 8.121, showing crack locations

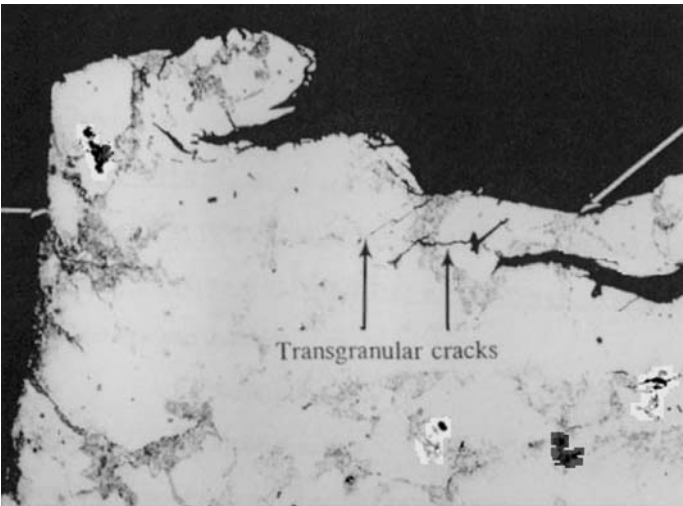


Fig. 8.123. Metallographic cross-section of screw holes shown in Figs. 8.121 and 8.122, indicating stress corrosion cracking

As noted above designers have also made extensive use of magnesium alloys in missiles [63]. The use of magnesium in missiles and space applications has been widespread because of magnesium's strength and rigidity at minimum weight coupled with ease of fabrication. However, it possesses other desirable characteristics, such as the ability to withstand temperature extremes, proximity of some components to liquefied fuels, exposure to ozone and free radicals in the upper atmosphere, and bombardment by short-wave electromagnetic radiation, high-energy particles and small meteorites. An example of missile use includes the Falcon GAR-1, an air-to-air missile, which was virtually a 90% magnesium structure. The body was made of 0.040-in AZ31B-H24 sheet which was rolled, longitudinally welded, and then stretch formed to size. ZK60A-T5 magnesium tubing is also used in the body. The four stabilizer frames were AZ91B die-castings and the rudders ZK60A-T5 forgings.

### 8.3.3 Barriers to Magnesium Use in Aerospace

Magnesium is potentially a very valuable metal for use in aerospace applications because of its low density (Fig. 8.109). However, use has dramatically declined. It is, therefore, very important to determine why magnesium use has decreased, broadly define what needs to be done to lead to increased aerospace use of magnesium both in the commercial and military segments of aerospace, and suggest how that increased use can be achieved.

In an attempt to answer the questions posed above, detailed discussions were held with aerospace system producers and users, for example: the US Armed Forces (AF, Army and Navy), NASA, airframe fabricators such as Boeing, Lockheed-Martin, engine manufacturers including Pratt and Whitney, GE and manufacturers of interior components (all the way from cockpit parts to seat frames and storage devices) [80, and Dimbrek GG, 1999; Ontko N and Thompson S, 1999; Dimbrek GG, 2000; Ontko N, 2001; all private communications]. Most contacts were in the USA, but discussions were also held with aerospace personnel in Europe and the former Soviet Union. The study encompassed a determination of the status of the use in aerospace applications, defining why magnesium use is low, learning the barriers which must be overcome to increase magnesium use in aerospace, and making recommendations on what needs to be done to increase use of magnesium in aerospace systems. This included both a study of the performance of magnesium parts (were there any real or perceived problems, or was use considered to be satisfactory?) and a determination of whether magnesium was a serious candidate either as original equipment or as a replacement for other materials in existing systems (e.g., for weight savings). The results of the study are summarized in this paper, and of more importance the hurdles which must be overcome to increase magnesium use in aerospace. Recommendations are also made on what various potential users will require in terms of databases and specification (e.g., MIL handbook 5 type data). The "emotional" factor is also addressed regarding the current strong negative feeling towards magnesium residing in most segments of the aerospace community.

Magnesium is currently used in aerospace systems but at low levels [60, 76]. Clearly, the low density of magnesium is its major asset, inferior corrosion be-

havior, particularly galvanic corrosion, the major deficiency (followed by a fear of fires and inferior mechanical properties compared to aluminum). Boeing uses magnesium in a number of their commercial aircraft (small wing components, parts of the doors, etc., on B707, B727, B737 and B747) and military planes (the B29 canopy nose being an obvious example). In fact, one Boeing source noted “[that] magnesium was used ‘everywhere’ on World War II systems.” Helicopter gearbox use is a clear example of an application where (with suitable protection systems, e.g., Rockhard, Tagnite, etc.) magnesium works beautifully. Space is another area of magnesium use (no corrosion problem) with magnesium metal matrix composites (MMC) seeing quite widespread use. However, overall there has been a significant decrease in use of magnesium mainly because both commercial airlines and the military insist on improved maintainability and longer life-time.

The use of magnesium in the interior of commercial airplanes was also addressed [Hyatt M, 1999; Turzil J, 1999; both private communications]. Here again there is a strong negative attitude. Quite surprisingly the use of magnesium is permitted in the cockpit (joy-sticks for example), but not in the passenger cabin (fear of fires). The greatly increased fear of hijacking since “11 September 2001” will clearly show designers much more reluctant to use materials that may burn (or are perceived to burn) such as magnesium.

So magnesium use, except for a few isolated examples, is rare in the aerospace industry, with the reason being partly technical (corrosion behavior being the major concern) and to a great extent emotional (“my science teacher in high school showed me how magnesium burns”).

Space offers a virtually corrosion-free environment where weight saving is critical (Table 8.10). So that for space applications when weight can be saved it will be saved by use of monolithic magnesium or magnesium MMCs. However, whenever we can get real world application experience it helps other potential applications, so space can help possible commercial/military use.

Increased commercial use is an uphill battle with the “maintainability” issue being of paramount importance. Boeing personnel, for example, are uneasy that “they may be missing something” with magnesium but they are negative on having to have elaborate protection systems – “these can be accidentally damaged leading to catastrophic corrosion problems.” However, protection systems are used in certain situations at Boeing, for example, the new C17 composite tail has aluminum ribs in “contact” with the polymeric composite skin.

One Boeing engineer noted that a number of the Allied-Signal rapidly solidified rare-earth containing alloys performed very well in laboratory corrosion tests where they were as good as some Al alloys (admittedly not the best). However, these magnesium alloys looked “very ugly” after ten years exposure on Whidbey Island in the Puget Sound area (a sea-coast environment). Probably the best approach in the commercial arena is to work for replacement parts (i.e. substitute magnesium or aluminum with a weight savings). The probable scenario is that the airlines would make the recommendation asking for a “part specific” approval (which could be overridden) by Boeing. Flying applications, building up confidence would gradually lead to further magnesium use and eventually original equipment manufacturer (OEM) use. Good experience outside the USA also

helps use in the USA (see below). Within the USA, the Federal Aviation Authority (FAA) has broad authority for safety concerns.

Military use is also an uphill battle. For example, at the USAF Materials Directorate, Systems Support Division (SSD) at Wright-Patterson Air Force Base (AFB) in Dayton, Ohio there is a legacy that “magnesium corrodes, and it always will.”

There is a chance to increase magnesium use in aerospace applications working with the AF Systems Support and System Program Office (SPO) personnel. But the system is rigid. For an OEM to recommend a certain material for use generally the material must be in MIL-Handbook 5 (the US-generated “bible” used throughout the world that contains statistically valid data generally from 10 heats for materials used in military systems). The OEMs define their materials of choice, but they must be approved by the SPO often with advice from the SSD people. Part by part material use can be approved without a MIL-Handbook-5 entry but it’s again an uphill battle. Also, part replacement is another (and probably easier) route, which can be pursued at Logistic command centers. A number of discussions have been conducted with Hill AFB personnel and the trend has been in the “wrong” direction – replacement of magnesium components with Al 2014 in particular.

For increased US military use, a knowledge of how MIL-Handbook-5 works is mandatory. Assuming we have statistically valid mechanical property data from the required 10 heats, the designer must first confirm that the desired alloy temper has adequate corrosion resistance. So for the voluminous aluminum section of MIL-Handbook-5 the initial page is a summary of acceptable (“can use”) and non-acceptance (“propose at your peril”) alloys/temperatures. Assuming acceptance from the corrosion perspective the designer then proceeds into the guts of the mechanical properties, and assuming SPO concurrence the material alloy/temper is proposed as bill-of-materials and goes into “dem-val” (a demonstration and validation version of the airplane), onto the prototypes, and assuming successful competition with competing designs (e.g., on the F22, Boeing versus Lockheed-Martin) to the production version. However, for magnesium there is a major problem: there is no initial corrosion page. There is also a scarcity of statistically valid mechanical property data. So the task here is to work with SSD and their contractor Battelle Columbus to compile the corrosion page (probably with appropriate caveats regarding protection systems). This is not a trivial task and requires a dedicated commitment.

AF Systems Support personnel mentioned that part by part exceptions are possible, but a really strong justification is necessary. For example, a significant weight reduction in a critical location of the airplane relative to the center of gravity. However, at least a statistically developed data base is needed (three heats, versus 10 heats for MIL-Handbook-5), and use in a foreign country (European generally) helps significantly. Use in a foreign country could be OEM or as a replacement. However, it is unlikely that, for example, replacement of an aluminum part by a magnesium part would occur.

Typically, an organization such as OGMA (Aeronautical Industry of Portugal) are only allowed to make changes to OEM components that “do not affect form, function and fitting (so-called first level concessions),” which translates to

changes such as small modifications to heat-treatment procedures (Portugal has systems such as the Lockheed-Martin F-16 Falcon, Lockheed-Martin C-130/L-100, Allison T-56 series, and Pratt and Whitney Canada PT-6A series). The ability to make more significant changes does reside in countries with more sophisticated indigenous aerospace industries such as the UK, France, Germany, and perhaps Israel.

The situation in the Former Soviet Union [79] (FSU) appears to be very similar to that in the West. Magnesium alloys have been employed in airplanes of the Antonov family from the very first AN-2 plane designed in 1947. Magnesium alloys were used mainly in the flight-control systems of planes in the form of castings of the ML-5 alloy (Mg-Al-Mn system). Use of magnesium alloys has included production of parts such as rocking-bars, brackets, shells, steering wheels and control columns. Since 1965, the ML-5 alloy has been used instead of the earlier ML-5PCh alloy (improved purity), with a decreased iron, silicon, and nickel content that allowed improved corrosion resistance. Since 1960, the formable BM65-1 alloy (MA-14) has been used in airplanes for production of small die forgings. Magnesium alloys are employed predominantly because of their low density. However, low corrosion resistance (in general, and galvanic), environmental danger and relatively high price have restricted wide-spread use in the aerospace industry. The high-strength ML-8 alloy (Mg-Zn-Zr system) of the ZK61 type has been evaluated and exhibited good strength characteristics, but due to technological difficulties it has not been used in full-scale production. Application of magnesium in Antonov systems will only be increased with a reduction in cost, coming from simplified component production methods, and a significantly more reliable corrosion protection methodology.

## Conclusion

The task of getting increased magnesium use in aerospace is not impossible. New alloys (including cast and wrought alloys) with better mechanical properties would be attractive, but are probably not mandatory at this point; reliable and “maintainable” protection systems are of paramount importance along with a “corrosion” page in MIL-Handbook 5. There must also be a solid commitment to achievement of these latter two goals by the magnesium producers working closely with the users.

## 8.4 Consumer Applications of Magnesium

*Steve Erickson*

The attributes of magnesium alloys along with their ability to be fabricated by forging, extrusion, rolling, gravity casting, pressure casting, and semi-solid forming processes, have resulted in a wide variety of consumer applications. It is typ-



ically the low density of magnesium that leads to its initial consideration as a material of construction in consumer applications. Its final selection as the material of choice most always comes from a combination of multiple values derived from the mechanical and physical properties of its alloys and the capabilities of the fabrication process. When evaluating the economics of using different materials for an application, it is important to consider not only the price relationship between the materials, but also the cost of conversion and other inherent values that are specific to the application. The excellent growth rate of the magnesium alloy market during the last part of the 20th century – when this raw material was often at a cost disadvantage – is testament to the value that magnesium can offer.

Most of the fabrication processes for magnesium are represented in the manufacture of consumer applications, although high-pressure die-casting (HPDC) constitutes the majority. The attributes of HPDC, together with the many benefits of magnesium alloys, create an environment where magnesium is highly competitive with other materials including steel, aluminum, and zinc.

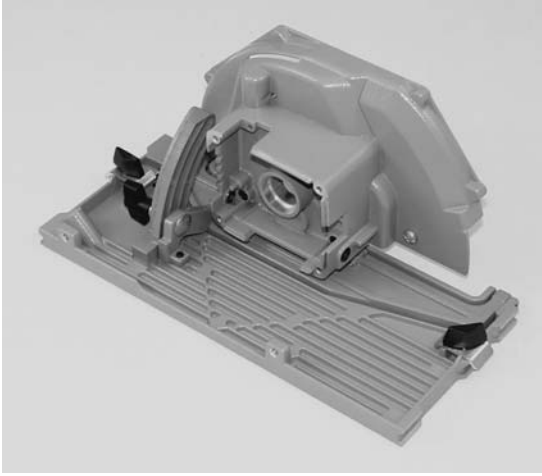
To illustrate the broad utility of magnesium alloys and their wide range of applications in the commercial field, everyday examples are presented, grouped according to the general industry in which they are used.

#### **8.4.1 Logistics**

The logistics and material transport industry effectively uses ramps, handcarts, and appliance trolleys that are fabricated from magnesium alloys. Magnesium castings, sheet, plate, and extrusions are extensively used in this type of equipment. A good example is a delivery truck loading ramp that uses die-cast magnesium grid sections to form the support surface. Magnesium die castings are also used as the nosepiece for some utility/luggage handcarts. Fabrication of the wrought forms of magnesium used for logistics equipment is normally accomplished by mechanical fasteners or welding techniques. The processes are similar to those used for aluminum fabrication. Weight reduction is the chief advantage in using magnesium for material handling products, which is extremely important for equipment that must be moved by workers or, when transported, becomes a part of the payload.

#### **8.4.2 Power Hand Tools**

Power hand tools vastly improve worker efficiency, but the mechanization, which allows this improvement, adds undesirable mass to the equipment. The weight advantage that magnesium offers has resulted in an excellent market in the power hand tool industry. The ability to form thin-walled, complex die castings and moldings from magnesium alloys is an excellent match for the needs of this industry. Here, designs require lightweight housings for intricate mechanisms and are often uniquely shaped to meet the ergonomic requirements of workers. The ability to apply protective and decorative finishes to magnesium is an important characteristic, and allows manufacturers to offer products with a surface that has an attractive appearance with the durability to maintain that appearance under harsh service conditions.



**Fig. 8.124.** Die-cast magnesium base and blade guard for a circular power saw (photo courtesy of Stihl)

Magnesium die castings, as illustrated in Fig. 8.124, are used for the housings and blade guards on circular and reciprocating saws. Hand drills make use of magnesium die casting for housings and gear mounting plates where their dimensional accuracy adds considerable value beyond weight savings. Pneumatic nail guns (Fig. 8.125) are critical to the productivity of carpenters. Magnesium is used extensively for their housings, cylinders, and nail guides to reduce weight and worker fatigue. Since the early days of their development, chainsaws have made use of magnesium die castings for their housings (Fig. 8.126). The low density of magnesium alloys and their ability to absorb vibration, because of the material's excellent damping capacity, are key elements in the success of this important forestry tool.



**Fig. 8.125.** Pneumatic nail gun with die-cast magnesium housing and cylinder (photo courtesy Lunt Manufacturing)





Fig. 8.126. Die-cast magnesium chain saw housing (photo courtesy of Stihl)

#### 8.4.3 Lawn and Garden Equipment

Lawn and garden is another environment where equipment portability and mobility is an important attribute. Here, as in the power tool industry, the low density of magnesium and its ability to be die-cast into complex, near-net-shape parts have been a major advantage in a variety of tools. Die-cast magnesium decks for power lawn mowers offer a lightweight solution to other material options with additional benefits of impact resistance, noise and vibration reduction. Trimming is a tedious job that is made easier by the application of lightweight magnesium die castings in the engine and gear housings (Fig. 8.127) of these hand-held machines. Handles for hand shears are a natural product for magnesium die-casting, which benefit from the low density, the ability to form complex shapes, and the finishing characteristics of magnesium alloys.

#### 8.4.4 Concrete Handling Tools and Equipment

Magnesium's excellent resistance to high alkalinity makes it a preferred construction material for concrete tools and equipment. Much of this work is done

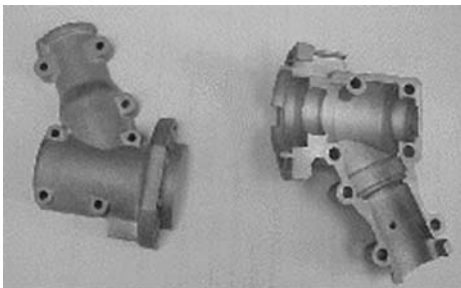


Fig. 8.127. Die-cast magnesium gear case for a string trimmer (photo courtesy of Mag-tec Casting)

with hand tools, where the low density of magnesium is invaluable. Examples of this application, most of which are manufactured from extrusions, include trowels, screeds, floats, and float handles. When working with concrete or other building materials it is important to keep things straight, flat, and true. Magnesium extrusions and castings are used here as frames for levels that are usually found in the manufacturer's premium product line. All levels benefit from magnesium's low density, rigidity, and dimensional stability. Especially in concrete finishing, the ability of a magnesium level to resist alkalinity is an important attribute.

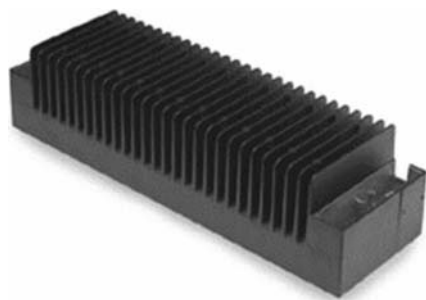
#### 8.4.5 Computers and Computer Hardware

The ability to cast and mold magnesium alloys into strong, intricate, lightweight housings has resulted in an excellent market within the computer industry. Housings for laptop computers, such as the one shown in Fig. 8.128, and other portable data collecting and transferring equipment, exemplify the benefits that magnesium die castings and semi-solid moldings offer in this sector. The high-pressure die-casting and Thixomolding processes are used to manufacture complex, thin-walled housings, which rival the intricacy of structures that can be produced in plastics. Magnesium alloys offer substantial improvement in durability, heat transfer, and RFI and EMI shielding without adding to the weight of this equipment. Within the housings of computers, magnesium alloys are used in the form of die castings, moldings, and extrusions, for both heat sinks and hard drive reader arms. Hard drive reader arms benefit from the ability to form magnesium alloys into intricate shapes as well as from the low density of the material which allows rapid movement of reader heads over the surface of data storage disks. Heat sink applications, such as the one in Fig. 8.129, take advantage of the excellent heat transfer and dissipation properties of magnesium alloys.

Digital image projection equipment is a growing application for magnesium castings and moldings. This equipment has displaced the slide projector as the preferred method for presenting images. Magnesium alloy die castings and Thixomoldings are widely used in this equipment for housings because of their



Fig. 8.128. Die-cast magnesium laptop computer case (photo courtesy of Stihl)



**Fig. 8.129.** Die-cast magnesium heat sink for an electronics application (photo courtesy Lunt Manufacturing)

low density, their resistance to the high temperatures generated by this equipment, and the ability to form intricate shapes for satisfying functional and design requirements.

#### **8.4.6 Electronic Equipment**

Personal, portable electronic equipment requires components that are stylish, rugged, and lightweight. Magnesium die castings and Thixomoldings meet these requirements while providing the added benefit of electronic shielding where needed. Housings for cellular phones and portable music playback systems are excellent examples that take advantage of the ability to cast or mold intricate, thin-walled parts that are as light as their plastic counterparts but vastly superior in strength and rigidity. Audio speakers for high performance systems and for automotive applications have benefited from the low density and excellent damping capacity of die-cast magnesium alloy frames, such as the ones shown in Fig. 8.130.

The television and video industry is using magnesium for housings that vary in size from compact digital video cameras to mid-size cabinets for receiver-monitors. The selection of magnesium over plastic for TVs is encouraged in some countries by regulations that require television housings to be recycled at the end of their useful life.

#### **8.4.7 Optical Equipment**

Magnesium die castings and semi-solid moldings are used in a variety of optical products. Cameras for both film and digital image capturing require intricate, durable, and attractive housings for these systems. Magnesium Thixomoldings® are used for the cases of several popular digital cameras. Magnesium Thixomolding has also been chosen to produce the eyewear frames shown in Fig. 8.131. The process enables molding of a highly sculpted form while magnesium alloy AM60B provides a strong, light, and flexible structure, which can be bent for adjustment and is resistant to breakage from handling. Binoculars are another optical product that benefits from the attributes of magnesium alloy die castings



**Fig. 8.130.** Audio speaker frames die-cast from magnesium alloy (photo courtesy of Laukutter GmbH)



**Fig. 8.131.** Eyewear with Thixomolded magnesium alloy frame (photo courtesy of Oakley, Inc.)

and semisolid moldings. Magnesium alloy field glasses are optically stable and easy to carry to spectator and field activities. Rifle scopes are another optical product that benefit from a magnesium alloy body, contributing to optical stability and reduces weight.

#### **8.4.8 Sports Equipment**

Equipment for sporting and recreational endeavors is a market that finds many interesting applications for magnesium alloys in both the cast and wrought forms. The excellent strength to weight ratio of magnesium structures and the ability to form intricate, highly decorated shapes is a combination which allows designers the ability to meet the high expectations of enthusiasts and fulfill their competitive desire to have the latest technical innovation in equipment. One example is a weight saving cooking stove for backpacking, with a die-cast magnesium alloy support stand. Handles for archery bows are a common application for magnesium die castings.



Fig. 8.132. Bicycle with magnesium frame (photo courtesy of Merida Industry, Ltd.)



Fig. 8.133. Bicycle frame fabricated from tubular magnesium extrusions (photo courtesy of Merida Industry, Ltd.)

For sports that translate muscle power into motion, the strength, rigidity, and low-density of magnesium die castings and moldings allow for the creation of equipment that maximizes efficiency and control. Top of the line bicycles such as the one pictured in Fig. 8.132 are fabricated from specially designed extruded magnesium tubes. The structure allows for a frame (Fig. 8.133) that is strong and stiff while keeping the weight to a minimum. The excellent damping capacity of magnesium alloys helps to absorb shock and vibration, reducing rider fatigue. Other bicycle components available that make use of magnesium alloys are shock absorbers, yokes, and brake mechanisms. The chassis for several inline skates is produced by the die-casting process, and the base plate for a popular snowboard binding is produced by the Thixomolding process. Magnesium castings and extrusions are occasionally used in golf clubs, tennis rackets, baseball bats, and other sports products that tend to change on a seasonal basis to attract customers to the newest, latest innovations in materials and design.

#### 8.4.9 Galvanic Applications

Although today's high purity magnesium alloys are known for their excellent corrosion resistance, they also have a high electro-chemical potential compared to

many other metals. This property can be used to advantage in certain environments to establish a controlled galvanic reaction where the magnesium alloy can serve as an anode, facilitating the cathodic protection of a more noble metal structure, or to accomplish a mechanical action, initiated by the alloy's dissolution in the reaction. Extruded magnesium anodes are used in water heaters to galvanically protect the steel tank from corrosion in the likely event of the failure of the tank's protective coating. Special magnesium alloys are used in galvanic timed-release devices, which are designed to dissolve in a controlled electrochemical reaction and facilitate the timed release of a fishing trap buoy or the opening of a fishing trap escape door, as required by the laws of some countries. Batteries are another product group that make use of magnesium's high electrochemical potential, where magnesium serves as the anode in a variety of high performance power sources.

#### 8.4.10 Miscellaneous Consumer Applications

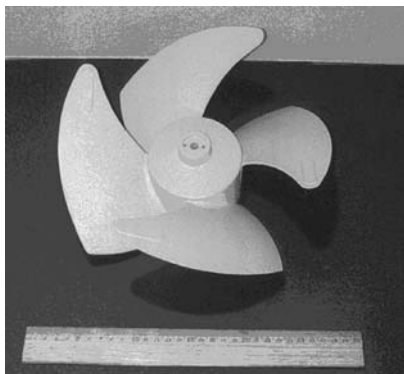
There are numerous other consumer products that take advantage of the utility and versatility of this metal. Wheels for both power and manual wheelchairs (Fig. 8.134), furniture structures, lighting fixtures (Fig. 8.135), cooling fans (Fig. 8.136), and luggage frames are a few examples of the growing and ever-changing list of magnesium applications.



Fig. 8.134. Die-cast split wheel for motorized wheel chair (photo courtesy of Lunt Manufacturing)



Fig. 8.135. Lighting fixture components die-cast in magnesium alloy (photo courtesy of Laukouter GmbH)



**Fig. 8.136.** Thixomolded magnesium alloy cooling fan (photo courtesy of Thixomat)

## References to Chapter 8.1

1. Friedrich H, Gänssicke T: Strategies and Trends in Lightweight Construction-Design and Material in Competition. VDI-Bericht 1653: Vehicle concepts for the 2nd Century of Automotive Technology
2. Friedrich H (2001) IIR-Werkstoffkongress, Stuttgart
3. Braess H-H, Seiffert U (Hrsg) (2000) Handbuch Kraftfahrzeugtechnik. Vieweg-Verlag, Braunschweig/Wiesbaden
4. Gebhard P, Wilk T, Kroll S (2000) Gesamtfahrzeugparameter und die Auswirkungen auf Fahrleistungen und Verbrauch. AUDI A2 Sonderausgabe von ATZ u MTZ, Vieweg Verlag, Braunschweig/Wiesbaden
5. Engelhart D, Mödl C (1999) Die Entwicklung des AUDI A2, ein neues Konzept in der Kompaktklasse. VDI-Berichte 1505, Düsseldorf
6. Dick M (1999) Die 3 ltr.-Lupo-Technologien für den minimalen Verbrauch. VDI-Berichte 1505, Düsseldorf
7. Friedrich H, Schumann S (2000) The second age of Magnesium, 2nd International Israeli Magnesium Conference, Sdom
8. Schumann S, Friedrich H (2003) The Route From The Potential of Magnesium to Increased Applications in Cars. 60th Annual World Magnesium Conference, May 11–12, Stuttgart, Germany
9. Nowatschin K et al. (2000) Multitronic- das neue Automatikgetriebe von Audi. ATZ Automobiltechnische Zeitschrift 102 Teil 1: Heft 7/8, pp 548–553; Teil 2: Heft 9, pp 746–752
10. Barnreiter K, Eichberg O (1997) Leichtbaumaßnahmen am manuellen Schaltgetriebe Audi B80. ATZ/MTZ Sonderausgabe März, pp 74–82
11. Von Buch F, Schumann S, Friedrich H et al. (2002) New die-casting alloy MRI153 for power-train applications. Magnesium Technology, (Warrendale, TMS 2002, pp 61–68)
12. Aghion E, Bronfin B, Eliezer D, Schumann S et al. (2003) The Art of Developing New Magnesium Alloys for High Temperature Applications. Magnesium Alloys 2003, Proceedings of the Second Osaka International Conference on Platform Science and Technology, OSAKA January 26–30
13. Sanders M, Kühnel H-U (1996) Leichtbau von Ansauganlagen durch werkstoffgerechte Auslegung und Integration von Komponenten. S. 104–115, Leichtbau im Antriebsstrang, Hrsg. Oetting, H.; expert Verlag
14. Böhme J, Doerr J et al. (2004) Audi Hybrid Magnesium Technology – A New Approach to the Lightweight Engine Block. 61st Annual World Magnesium Conference, May 9–12, New Orleans

15. Abthoff J, Gelsow W, Lang J (1996) Magnesium Alloys and Their Application as Housing Material for Sports Prototype- and Passenger Cars; Proceedings of the Third International Magnesium Conference 10–12 April. Manchester, UK
16. TRW-Mitteilung
17. Hector B, Heiß W (1989) Integralsitz mit Magnesiumrahmen. Ingenieur Werkstoffe VDI Heft 5–6 pp 62–66
18. Jost R, Disse T (2000) Kleben von Leichtbauwerkstoffen in Mischbauweise – Fügekonzept der Al-Mg-Tür des S-Klasse Coupe. 7. Paderborner Symposium Fügetechnik, 12–13. Oktober
19. Siedersleben M (2000) Vakuum-Druckguss von Magnesiumlegierungen für hochbelastete Bauteile. pp 48–58; in Kainer KU: Magnesium – Eigenschaften, Anwendungen, Potenziale; Wiley-VCH-Verlag
20. Magers M (1998) Magnesium – a good choice for weight reduction and other benefits in instrument panel substrates; presented at the 31st ISATA Symposium June 1998, Düsseldorf, Germany
21. Moll F, Mekkaoui M, Schumann S et al. (2003) Application of Mg sheets in car body structures. 6th International Conference Magnesium Alloys and Their Applications, Sept. 2003, Wolfsburg, Germany, pp 936–942
22. Sebastian W, Dröder K, Schumann S (2000) Properties and Processing of Magnesium Wrought Products for Automotive Applications. pp 602–608. Proceedings of “Magnesium Alloys and their Applications” Munich 26.–27.9.
23. Kaese V, Greve L, Jüttner S, Goede M, Schumann S et al. (2003) Approaches to Use Magnesium as Structural Material in Car Body. 6th International Conference Magnesium Alloys and Their Applications, Sept. 2003 Wolfsburg, Germany, pp 949–954
24. Volkswagen AG, press information (2002) The 1-LITRE-CAR 16.04.
25. Schnell R, Hönes R, Käumle F (1990) Erfahrungen mit Magnesium-Rädern in Sport- und Serienautos. Tagungsband DVM
26. Schäper S, Leitermann W (1996) “Energie-, Emissions- und Wirkbilanzen von PKW in aluminiumintensiver und in konventioneller Bauweise” in “Ganzheitliche Betrachtungen im Automobilbau”. VDI Report No. 1307, p 223
27. Schweimer GW, Schuckert M (1996) “Sachbilanz eines Golf” in “Ganzheitliche Betrachtungen im Automobilbau” VDI Report No. 1307, p 235
28. Untersuchung des Zusammenhangs zwischen Pkw-Gewicht und Kraftstoffverbrauch – Messungen an 11 Fahrzeugen auf dem dynamischen Rollenprüfstand – Institut für Kraftfahrwesen. ika Report 6746, Jan. 1998
29. Schweimer GW (1999) Sachbilanz des 3 Liter Lupo in Technologien um das 3-Liter-Auto. Braunschweig, 16–18.11.99; VDI Report No. 1505
30. Albright D L, Haagensen J O (1997) Life Cycle Inventory of Magnesium; IMA Annual World Conference, June, Toronto, Canada
31. Eberle R (1999) Die ökologischen und ökonomischen Grenzen des Leichtbaus. VDI Report 1505, Braunschweig
32. Universal auditing of CFRP and magnesium components using the example of door systems (Internal VW Report, 1997)
33. Deinzer G, Kiefer B, Haagensen JÖ, Wetengen H (1998) Life Cycle Inventory of Magnesium-Comparison of steel and mg in a car cross beam; in Conference Magnesium Alloys and their applications; April, Wolfsburg, Germany; p 119
34. Houghten JT et al. (2001) IPCC – Report, Cambridge University Press
35. Schumann S (2004) Future Use of Magnesium in Cars – Potential and Prerequisite. 12<sup>th</sup> Magnesium Automotive and End User Seminar, Aalen, Germany, September 13–14



## References to Chapter 8.2

36. Gann J (1931) "Magnesium-Industry's Lightest Structural Metal", Society of Automotive Engineers Transactions, paper # 310044, SAE Journal p. 620
37. Harvey WG (1938) "Manufacture, Characteristics and Use of Magnesium Castings", SAE Transactions, paper # 380123, SAE Journal p. 43
38. Dunn JH (1946) "Aluminum and Magnesium in Highway Transportation Bodies" SAE Transactions #460042
39. Schuette EH ZK60-An Improved Magnesium Extrusion Alloy-History, Characteristics, Service Experience and Future Prospects", SAE Transactions #490016, SAE Journal
40. Polzin MH (1952) "A Researchers Casebook on Magnesium Truck Wheels", SAE Transactions #520056
41. Erickson SC (1977) "Magnesium: A Proven Material for Light Weight Automotive Die Castings", SAE Transactions, #770323
42. Cole GS, Finstad RA and Grebetz JC (1995) "Magnesium in the Automotive Industry", Proceedings International Magnesium Association
43. North American Die Casting Association, Rosemont, IL 60018, USA. Website: [www.nadca.org](http://www.nadca.org)
44. International Magnesium Association, McLean, VA 22101, USA. Website: [www.intlmag.org](http://www.intlmag.org)
45. LeBeau S and Decker R (1998) Proc. 5th Int. Conf. Semi-Solid Processing of Alloys and Composites, Colorado School of Mines, p. 387–395
46. Carnahan R, Decker R, Nyberg E, Jones R and PiTXMan S (2000) Magnesium Technology 2000, TXMS, p. 403–409
47. Carnahan R, Kilbert R and Pasternak L (1994) 51st World Magnesium Conference, IMA
48. Ito T, Sato M and Kojima Y (2000) "Today's Magnesium Technologies and Applications in Japan", Transactions IMA, p. 33
49. Decker R, private communication

## References to Chapter 8.3

50. Froes FH (August 1997) Light Metal Age, p. 46
51. Aghion E, Bronfin B and Schwartz I (1996) Magnesium Applications in the Aerospace Industry
52. Eliezer D, Aghion E and Froes FH (1998) Dead Sea Magnesium Conference
53. Eliezer D, Aghion E and Froes FH (Dec. 1998) Advanced Performance Materials, vol. 5, No.3, p. 201
54. Froes FH, Eliezer D and Aghion E (Sept. 1998), JOM, Vol. 50, No. 9, p. 30
55. Froes FH (October 1997) Light Metal Age p. 18
56. Froes FH (February 1998) Light Metal Age p. 54
57. Gerald Cole, Magnesium Applications in Ford's PNGV Mondeo, p. 24
58. Proceedings of the Int. Magnesium Conf. (1995) (McLean, VA:DMA)
59. Proceedings of the Int. Magnesium Conf. (1995) (McLean, VA:DMA)
60. Proceedings of the Int. Magnesium Conf. (1998) (McLean, VA:DMA)
61. Magnesium Alloys and their Applications, ed. Mordike BL and Kainer KU, German: Werkstoff-Informationsgesellschaft
62. Polmear IJ (1994) Materials Science and Technology, 10, p. 1
63. Robert E (2000) (Bob) Brown, Magnesium Wrought and Fabricated Products Yesterday, Today and Tomorrow, Magnesium Technology 2002, Ed. Kaplan H, TMS, Warrendale, Pa, to be published in the Proceedings
64. Anon (1948) Design in Logic - The Planet Satellite Flight, July 15, p. 8
65. Tooley DA (1951) B-36 Service Experience with Magnesium, Proc. Seventh Annual Meeting of the Magnesium Association, p. 101
66. Dale H. (1952) Black, Magnesium in Military Aircraft, Ibid, p. 201
67. Kenneth King (1954) Magnesium Floors in Convair Aircraft, Ibid, p. 500B
68. Thos. T (1954) Tobin, Ibid, p. 500A

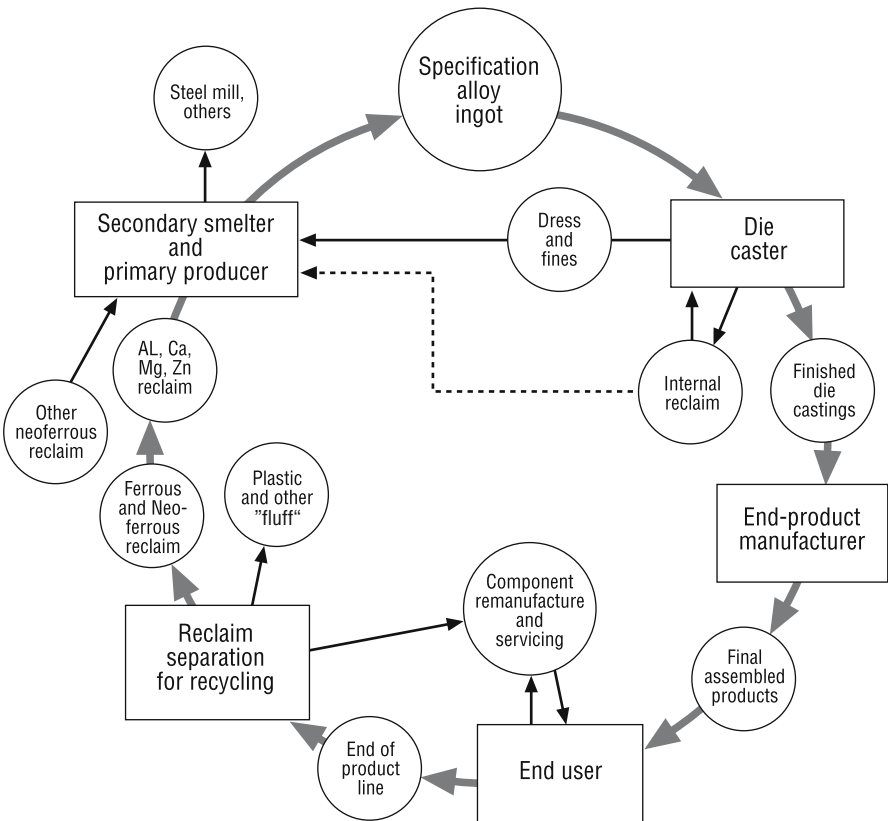
69. Bomberger HB (1986) The Potential for Magnesium Alloy Development using Rapid Solidification", AFWAL-TR-86-4114, Dayton, OH
70. Isserow S and Busk RS (1987) Workshop on Viability of Magnesium in Military Hardware, Ramada Inn, U.S. Army Laboratory Command, Boston, MA, Dec.
71. (1959) This is Magnesium, Magnesium Industry Council, London, Winter
72. Brown R (1995) Magnesium in Automotive and Aerospace, Design with Aluminum and Magnesium for the Automotive Industry, Society of Manufacturing Engineers, Dearborn, Michigan
73. Altwicker H (1939) Use of Magnesium Alloys in the European Automotive Industry, SAE Journal, Vol 45, No. 3, September
74. McConica III TH (1945) The German Magnesium Industry, unpublished report, August
75. Mizrahi J (1998) The Cutting Edge, Airpower, Vol. 28, No. 4, July
76. Leontis TE (1959) Magnesium in Missiles and Aircraft, Metallurgical Laboratory, Dow Metal Products Co., Div. Dow Chemical Co., Midland, Mich.
77. Tooley DA (1951) Magnesium in the B-36 Bomber, Proceedings of Magnesium Association, 7th Annual Meeting
78. Comstock H (1961) Magnesium and Magnesium Compounds, US Bur of Mines, Washington, DC, IC 8201, p. 20
79. (1999) Light Metals in the CIS, Roskill Information Services, ISBN 086214 832-4
80. (1997) MIL-HDBK-5CD-ROM, May 31, Systems Support Division, Materials Directorate, WPAFB, Dayton, OH

# 9 Recycling

*Håkon Westengen*

## 9.1 Introduction

Environmentally sound and cost effective use of magnesium alloys in automotive applications assumes efficient closed loop recycling of die casting returns and post-consumer scrap. Closed loop recycling (Fig. 9.1), is defined as recycling die casting returns and post-consumer scrap back to the quality needed to cast the same part, as produced originally [1–3].



**Fig. 9.1.** The die casting recycling circle. From North American Die Casting Association [3]

The success of closed loop recycling is important for the magnesium industry because unlike aluminium, there is no other major market or source for returns/scrap outside the die casting community. This forces recycling processes to be capable of regaining the original chemical composition and cleanliness of the magnesium alloys. It is also the objective of the industry to minimise life cycle costs, energy consumption and CO<sub>2</sub> emissions of magnesium products. It is also important for the industry to improve continuously the recycling friendliness of magnesium, both through developing recycling friendly alloy specifications, and through more efficient technologies for recycling die caster returns and post-consumer scrap [2].

Based on life cycle assessments, estimating the total energy consumption for producing a “typical” magnesium application, the importance of closed loop recycling of both die caster returns and post-consumer scrap can be visualised. The CO<sub>2</sub> emissions will in general follow the trend of the energy consumption [1]. The energy requirement for melting and recycling magnesium is only about 5% of the energy to produce the same quantity of primary material. As an example, parts produced from a mixture of primary and recycled alloys, assuming closed loop recycling of all die caster returns, represent only 50–70% energy consumption compared to parts produced from primary magnesium only, assuming a die casting yield of 50%. Parts produced from a mixture of primary, recycled die caster returns and post-consumer scrap, assuming that 50% of the net metal is produced from post-consumer scrap, represent only 30–40% energy consumption compared to parts produced from primary metal only.

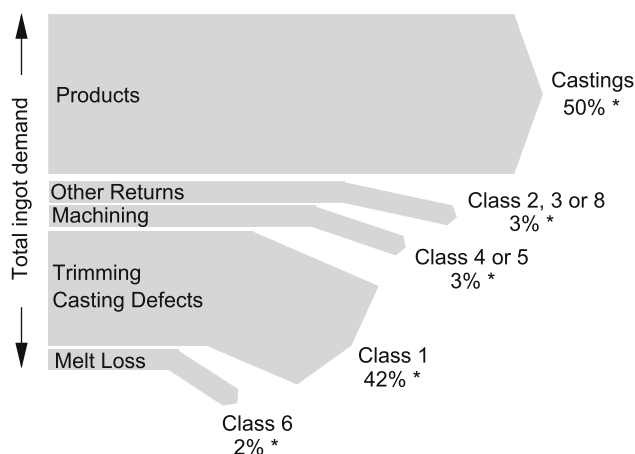
The growth in magnesium alloy consumption is driven by an increasing demand for automotive applications [4]. The automotive industry accounts for 90% of the casting demand. While this consumption generates considerable amounts of process scrap today, in the long run it will give significant amounts of post-consumer magnesium scrap as well. The need for recycling will more or less follow the same trend, illustrating the need for recycling capacity either by the die casters themselves, by primary producers, or by independent recyclers [5].

## 9.2 Classification System

In typical magnesium die-casting operations, only around 50% of the purchased ingot appears as finished castings [6], the remainder is scrap. This is illustrated in Fig. 9.2.

There are various classification systems for magnesium scrap. A generic classification system for typical recyclable material was derived by Hydro Magnesium [7, 8] and another fairly similar system by Magnesium Elektron [9, 10]. A third system was developed by Dow [11], while other variants have also been suggested [12]. The classification system applied by Hydro Magnesium divides the scrap into the following classes:

1. Sorted clean returns
2. Sorted clean returns with inserts
3. Sorted oily/painted returns
4. Sorted dry chips



\* Typical numbers in % of ingot demand

Fig. 9.2. Typical fractions of the various classes relative to ingot demand

5. Sorted oily/wet chips
6. Dross – salt-free
7. Sludge – with salt
8. Mixed and off-grade returns

Clean and sorted scrap generated at die-casting plants, i.e., runners, biscuits, trimmings and rejected cast parts are referred to as class 1 scrap. As seen from Fig. 9.2, most of the scrap produced by die-casters will normally belong to class 1. Class 2 scrap comprises clean scrap with inserts. The three first classes require no special precautions on packaging and shipping, except that the material should be kept away from moisture. The classes 4 and onwards need special attention as the material is subjected to certain transport regulations (ARD/RID). Classes 4 and 5 (chips, dry and oily/wet) should be packed in ventilated steel drums and classified according to paragraph 4.1 item 13 c) bearing UN no. 1869. Classes 6 (dross) and 7 (sludge) are classified in accordance with paragraph 4.3 item no. 20 b) with UN no. 2813. In addition, class 6 is classified as dangerous goods and should be treated in accordance with IMDG regulations. Regardless of classes, all material should meet the specifications of ASTM alloy series, AZ, AM, AS and AE. Other material, or material segregated otherwise belongs to class 8.

In principle, the classification system covers internal scrap at the primary alloy producer, process scrap from e.g., die casters and post-consumer scrap. However, as post-consumer scrap, e.g., End of Life Vehicle (ELV) scrap, is typically insufficiently sorted, this will belong to class 8.

### 9.2.1 Process Overview

Regardless of class, except for ELV scrap, recycling of magnesium will follow a general route. This is illustrated in Fig. 9.3.

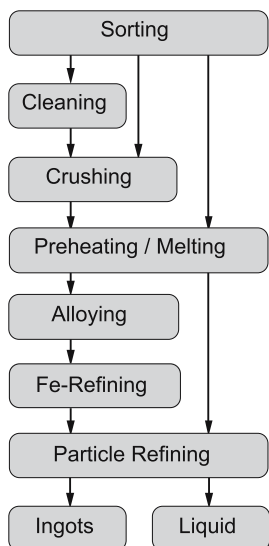


Fig. 9.3. General process steps for magnesium alloy recycling

The key issues in the process route described in Fig. 9.3 start with sorting by alloys and classification, which is a prerequisite. If necessary, cleaning can be undertaken. In order to increase melting rates (exposing larger surfaces for increased heat transfer) crushing of large sized scrap may be considered. Thorough preheating is generally a prerequisite as moisture represents a safety hazard. Exceptions may be certain processes for melting with salt where considerable amounts of surface water may be tolerated. Melting will either take place with flux or under a cover gas. Most of the inclusions are separated from the metal during or immediately after melting, generating dross and/or sludge. Iron-refining is performed by adding Mn (e.g., as salt or AlMn hardener) at a temperature higher than the casting temperature. Additional inclusion removal can be done by:

- Addition of a refining flux and agitation followed by settling,
- Settling in multi-chamber furnaces,
- Gas purging for floatation of inclusions towards the surface or compacting of dross,
- Filtration,
- Combinations of the above.

Each item will be discussed in greater detail later in this text. Recycling of magnesium from ELV scrap will also be mentioned.

### 9.2.2 Class 1

Two principally different methods for treatment of scrap may be utilized [11]:

1. Flux-based metal protection and refining, and

2. Protective gas ( $\text{SO}_2/\text{SF}_6$ ) for melt protection and settling, possibly assisted by argon-gas purging or filtration for removal (flux-free refining).

Flux-based protection and refining has been most widely used, and is probably still the most important in terms of tonnage. However, as in-house recycling, that is recycling of class 1 returns inside the die casting shop, is developed further [13–17], flux-free solutions are continuously attracting more interest.

### 9.2.2.1 Flux-based Systems

The traditional method for flux refining (Fig. 9.4), which is also used in the industry today, is to melt scrap and flux batchwise and stir in additional flux and alloying elements if necessary [5, 18]. Then, after allowing some time for separation and refining by settling (killing), the metal is transferred into a second furnace from where the metal is cast, either batchwise or continuously. In the second furnace (holding/casting furnace), additional separation of salt and metal takes place, and only small amounts of salt are used. The use of two furnaces increases the capacity, improves the temperature control, and has the potential to improve the quality of the metal. However, single furnace systems are also used. Metal is transferred and cast either by tilting and pouring of the crucible or by pumps/siphons. Normally, the furnaces are either induction heated or gas fired. Between each batch, bottom sludge consisting of salt, oxides and metal droplets is removed by grabbing. The sludge typically belongs to class 7. Starting with an empty furnace, the scrap charged melts from below. Thus, the scrap higher up in the furnace is preheated by the hot liquid metal gradually building up from the bottom. Normally no auxiliary preheating is necessary.

The crucibles can be made of mild steel, but due to creep problems it is more common to use stainless steels with an inner cladding of mild steel. Nickel containing stainless steel directly in contact with molten magnesium should be avoided due to dissolution of nickel into the metal. Crucible-free furnaces with a magnesium resistant refractory may also be used.

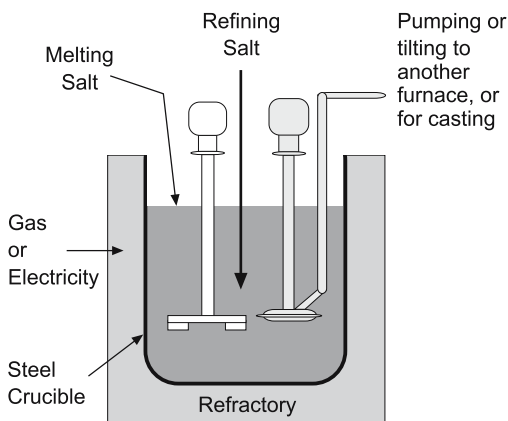


Fig. 9.4. Traditional batchwise recycling by use of salt

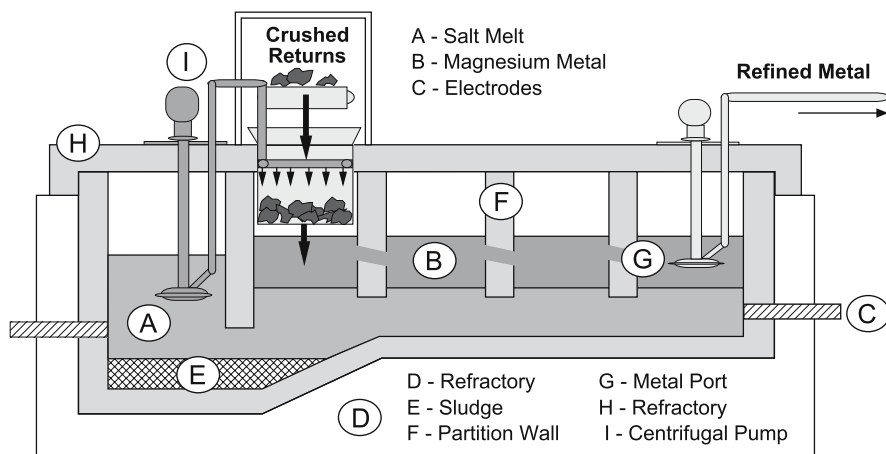


Fig. 9.5. Multi-chamber, AC-heated recycling furnace with salt

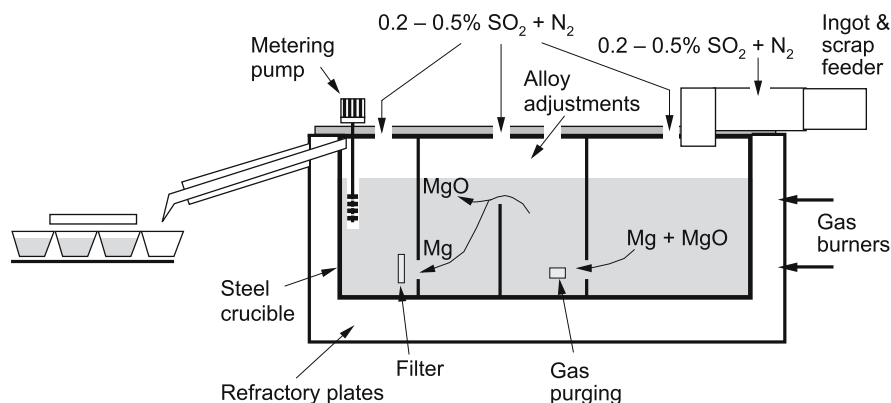
Hydro Magnesium has a system for continuous melting under flux (Fig. 9.5). Metal is melted in one end of a large multi-chamber furnace and pumped out or cast from the far end of the same furnace [19]. The salt is heated by AC electrodes in chamber one, and continuously pumped over a stream of scrap metal being fed into the melting basket. The excess heat content of salt heats up and melts the scrap, which falls into chamber two together with the salt.

Here, the salt and metal separates, and the metal is further refined through the remaining chambers of the furnace. It is not necessary to preheat the metal, as evaporating moisture is effectively vented through sprinkling salt during the melting process. The oxides present on the surface are removed by the salt and are carried down to the molten salt phase, thereby separating from the metal. Manganese salts can be used for alloy adjustments, if necessary. Molten salts with a composition of 40–60% calcium chloride and 3–7% calcium fluoride are preferred. In addition, the salt melt may contain sodium chloride and magnesium chloride, but a considerable amount of calcium chloride can be used. This method also gives protection against oxidation.

#### 9.2.2.2 In-house Recycling

Although in-house recycling of clean scrap like biscuits, runners and internal rejects, has been practiced for years at some die casters [10], systematic use is new, and little work has been published. However, in-house recycling systems are usually based on salt-free solutions. As an example, the companies Rauch and Schmitz & Apelt have developed a multi-chamber flux-free furnace for recycling class 1 returns (Fig. 9.6). Preheated scrap is fed into one end, and the metal is refined through the three-chamber furnace-equipped with baffles [20]. Metal is cast into ingots from the downstream end of the furnace. Molten metal refining includes inert gas purging and filtration.





**Fig. 9.6.** Example of a salt-free, multi-chamber magnesium recycling furnace (redrawn from [21])

For the past 30 years SF<sub>6</sub> and dry air sometimes mixed with CO<sub>2</sub> has been used as cover gases in the magnesium industry. Due to the global warming SF<sub>6</sub> is now being replaced by SO<sub>2</sub>. Dry air is still considered as a prerequisite component in the SO<sub>2</sub> based cover gas, as moisture leads to the formation of sulphuric acid [22]. In the Rauch system, a mixture of SO<sub>2</sub> and N<sub>2</sub> is added for melt protection. The humidity content of air leaking in and providing the necessary oxygen is thus not controlled due to the humidity.

A continuous flux-free process for recycling of class 1 process scrap based on a two-furnace system has recently been described [13, 23]. The company Rauch in Austria has recently put up a pilot plant for continuous flux-free in-house recycling based on a two-furnace system with electrically heated transfer pipes [24].

### 9.2.2.3 In-cell Recycling

In-cell recycling is defined as systems where class 1 returns, biscuits, runners and gating systems are charged directly back to the die casting furnace.

Some years ago, before the term in-cell recycling was introduced, Øymo et al. described fluxless remelting of magnesium die-casting scrap in a two-furnace system [17]. In this method, preheated primary magnesium ingots and scrap were melted in a 100 kW resistance-heated furnace with a steel crucible containing about 500 kg of metal. From the melting furnace, metal flows through a siphon tube into a casting furnace (Fig. 9.7). From the casting furnace, the metal was metered intermittently through a siphon tube into a large ingot mould simulating the die-casting process. Melt surfaces were protected with a mixture of 20% CO<sub>2</sub>, 0.2% SF<sub>6</sub>, and dry air. At a metal flow rate of 4 kg/min giving a metal residence time in the two furnaces of nearly two hours, an average yield of approximately 93% was attained independent of scrap content fraction.

For in-cell recycling a two-furnace system is considered superior to a traditional one-furnace system because it offers additional space for dross and sludge

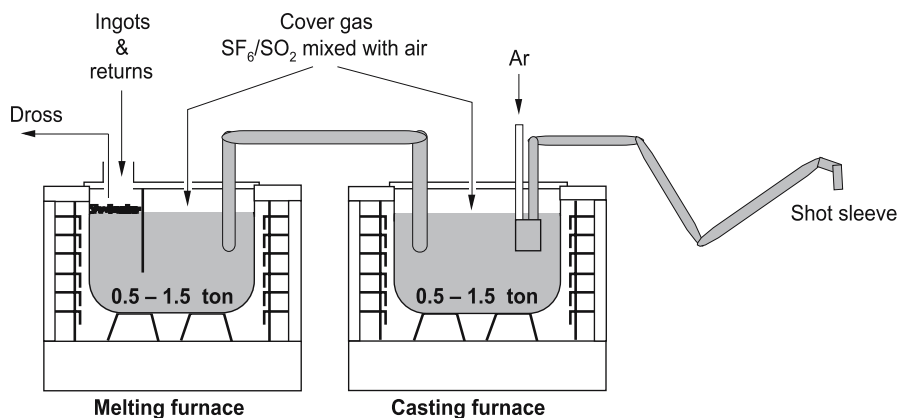


Fig. 9.7. Example of an in-cell recycling system based on a two-furnace system

accumulation and removal. Furthermore, it provides more evenly distributed residence time, which improves particle refining due to settling. Also, the two-furnace system offers superior temperature control upon casting, as temperature gradients generated during melting of ingots and scrap in the melting furnace are smoothed out in the casting furnace [25].

Although leading die-casters work on various solutions for in-cell recycling, very little has been published. It is expected that there may be logistic problems related to the return of runner systems, biscuits, etc., back into the furnace. Partly due to escape of cover gases during the more frequent charging, and partly due to the scrap being introduced to the melt, an increased frequency for dross and sludge removal may be unavoidable. This may increase production costs as well as melt losses. It may also have a negative impact on the HES performance.

### 9.2.3 Class 2

For class 2, basically the same methods as for class 1 may be used. If the insert materials do not dissolve excessively in molten magnesium, as is the case for steel, class 2 does not present any problem as the inserts in principle may be removed from the metal or salt. However, brass and bronze inserts may lead to Cu and other heavy metal contamination, and this material cannot be recycled back to high purity alloys. It may find its use as raw materials for anodes, for desulphurisation of steel melts, or as alloying elements in the (secondary) aluminium industry.

### 9.2.4 Class 3

In the case of flux-free melting, it is important that the paint/oil be burned off in advance, before the parts are immersed in molten metal. This is because the paints/oil may lead to evolution of toxic gases, and contamination of the metal in terms of unwanted dissolved elements and inclusions. When melting under

flux, one may expect the salt to absorb most of the remaining contaminants on the scrap surfaces.

Regardless of where the paint/oil is burned off, it is extremely important to treat the emitted gases at high temperatures (afterburning) to avoid emission of toxic compounds like dioxines, toxic furans and PCBs, which may form at intermediate temperatures when organic compounds decompose in the presence of chlorine. In order to fully decompose any chlorinated substances the temperature in the combustion chamber should exceed 1100°C [26]. Afterburning of furnace gases is standard technology in the aluminium recycling industry [27]. Depending on the energy content of the gases, additional energy may be introduced to reach the desired temperatures.

#### 9.2.5 Class 4

Dry chips (class 4) present limited problems, particularly when remelting with salt. Due to the large surfaces, high melting rates may be achieved. However, the large surfaces may cause additional salt to be used to avoid excessive oxidation during the melting, and to absorb the oxides from the same surfaces. Class 4 material can be remelted and refined back into high purity alloys, but with a considerably lower recovery compared to, for instance, class 1.

The large surfaces present great problems when melting without salt; it is difficult to get sufficient protection by the cover gas to completely avoid burning.

Leaving the principle of closed loop recycling, desulphurisation in the steel industry may be an outlet for chips.

#### 9.2.6 Class 5

Most of the chips arising from the production process today is contaminated with either oil or oil/water emulsions. It is technically feasible to recover the metal from wet/oily chips (class 5), but at present the costs may be higher than the actual value of the metal. As liquids represent a considerable volume of the class 5 material, large efforts must be in the cleaning step; that is, removing the main fraction of the liquids before melting can be undertaken. Even with long draining times it is not possible to reduce the oil content below 10% [5].

A special hydraulic press was developed by the company Rauch in which the chips are compacted and heated, causing the main fractions of the liquid to be squeezed out [40]. The remaining product is a rod consisting of compacted chips, which is considerably easier to handle during melting. The high forces involved in the press causes considerable development of heat, with fumes and smoke as a result. Liquid still present in the compacted material presents a problem, as the fumes tend to burn during the remelting of the compacted material. There are also more simple systems available for briquetting the oily chips, capable of reducing the overall oil content to < 5% [28].

Alternatively, mineral oil lubricants covering the chips can be removed by aqueous alkaline degreasing solution followed by a washing/centrifuging/drying system [10]. However, with this type of treatment, aqueous emulsion lubricants used for high-speed machining are more difficult to remove. Treatment in su-

percritical CO<sub>2</sub> might also provide a solution for cleaning wet chips as well as other metals in waste streams [29, 30].

Saxena [31] describes a process where the oily chips are heated to 200–400°C in a rotating furnace (higher temperatures may cause ignition of the chips). The oil evaporates and is conducted out of the furnace and coalesced. A US patent [32] reports a process where wet/oily chips are entrained in a gas and introduced to a cyclone separator. The walls of the cyclone are heated to temperatures causing vaporisation of the liquids. Gases/vapour may, in principle, be condensed and recovered.

Recently a vacuum distillation process has been adapted to magnesium chips [33]. A Pidgeon type furnace [18] is used. Pure Mg crowns with only Zn as a likely contaminant, crystallise in the cold end. The other elements remain in the residue. In order not to contaminate the system, it is recommended to remove most of the oil or other surface contaminants before charging the scrap to the reactor. A similar process [34] uses an installation that aids the production of magnesium by electrothermal reduction of magnesite or dolomite, for instance, the Magnetherm type of reactor [18]. The waste (any class) is introduced into an alternating current electric furnace in the presence of a flux having a density higher than Mg. The temperature is raised to 900–1100°C by the Joule effect at a pressure < 0.1 torr. Magnesium is recovered with, if appropriate, the elements which are more volatile than magnesium, in the form of vapour, which is condensed, while the less volatile elements are recovered in the form of a molten residual alloy at the bottom of the furnace.

With respect to the formation of dioxines or other chlorinated hydrocarbons, the same precautions as for class 3 apply.

### 9.2.7 Class 6

Surface dross from die caster operations may contain 70–90% metal; the remainder is oxides. Die caster sludge contains intermetallic particles, as well as oxides [1, 12]. As die caster sludge is salt-free, this also belongs to class 6. In order to maintain a reasonable quality of the die caster dross, the dross can be put into small steel vessels during skimming. As soon as the vessel is full, a cold and thick-walled steel cover is placed on top of the dross, not the vessel, preventing air from coming into contact with the dross and causing the surface to solidify quickly. This increases the metal content and the value of the dross [5].

The metal fraction in die caster dross can be recovered to high purity alloys by melting and refining with salt [12]. This can be done in systems as indicated in Fig. 9.3, or in rotary furnaces. The clue is to use sufficient amounts of salt and mix salt and metal very well in order to absorb all oxides to the salt phase. As the magnesium containing material to be melted may contain 10–100 times more oxides than class 1 scrap, it is quite obvious that a considerable amount of salt is needed.

It is notoriously difficult to recover dross by salt-free processes. Dross may be considered as a by-product from salt-free processes, and further stratification of dross may not occur by separation due to gravity, unless, possibly, if assisted by gas purging. The latter is discussed later in this text.

### 9.2.8 Class 7

The significant inhomogeneity of the phases and the wide size range of the metallic particles complicate processing of class 7 [35]. The material usually consists of a mixture of salt, oxides and alloy particles in the size range from  $< 100 \mu\text{m}$  to 10 cm. The alloy globules often contain a lot of intermetallic particles. Due to the precipitation processes in the preparation of high purity alloys mentioned elsewhere in this text, intermetallic particles collect at the metal side of the metal-salt interface. The wetting properties are such that the intermetallic particles preferentially stay inside the metal phase. When the density locally exceeds some critical level, a metal drop with intermetallic particles inside detaches, and sinks towards the sludge. Due to the wetting properties in the system, the oxides preferentially stay in the salt phase rather than with the metal, hence in the bottom sludge in a metal-salt system considerable amounts of oxides accumulate. It is reported from Solikamsk [35] that the metal content in sludge is in the range 18–50%, while oxide contents range from 12 to 25%. At Norsk Hydro, metal contents in the range 0–30% are more typical.

Sludge can be melted batchwise with additional salt, fairly similarly to traditional flux-based processing of classes 2–7 [36, 37]. After additions of  $\text{CaF}_2$  (a so-called thickening agent; the mechanisms are discussed later) the melt is stirred and metal globules coalesce. The metal is then decanted [36]. The  $\text{CaF}_2$  addition, stirring and decanting can be repeated to improve the recovery of metal. During melting of sludge cakes, one should always be aware of liberation of moisture, which has been picked up by the highly hygroscopic salt during storage.

Metal can be recovered dry by crushing and sieving the solidified sludge cake. Salts can also be removed by dissolving in water, but this also causes some loss of magnesium due to formation of  $\text{Mg}(\text{OH})_2$  and evolution of hydrogen gas. These processes increase the metal fraction in the product and it becomes more uniform. The metal globules may thus become attractive material for desulphurization of steels without remelting, casting and grinding. Due to the altered chemistry of the Mg globules, sometimes with exceptionally high contents of e.g., Mn, Ni and Cu, it is very difficult to make high purity alloys from the metal fraction in the sludge only. However, if the Ni content is low the metal may still be useful for applications not requiring high purity alloys like for instance sacrificial anodes. The metal may also be applicable for alloying purposes in the aluminium industry.

Sludge being melted and diluted by additional salt can be subjected to dispersion into granules by means of a centrifugal system and solidified whereafter the mixture undergoes mechanical treatment for separating off the salts and oxides [38]. The remaining metallic fraction (60–80% metal) can be used for desulphurization purposes.

A German patent [39] suggests a process where alkali salts, magnesium metal and magnesium oxides are converted into chlorides by reaction of the sludge with dilute hydrochloric acid. Other metallic elements (including Al) are separated as hydroxides.

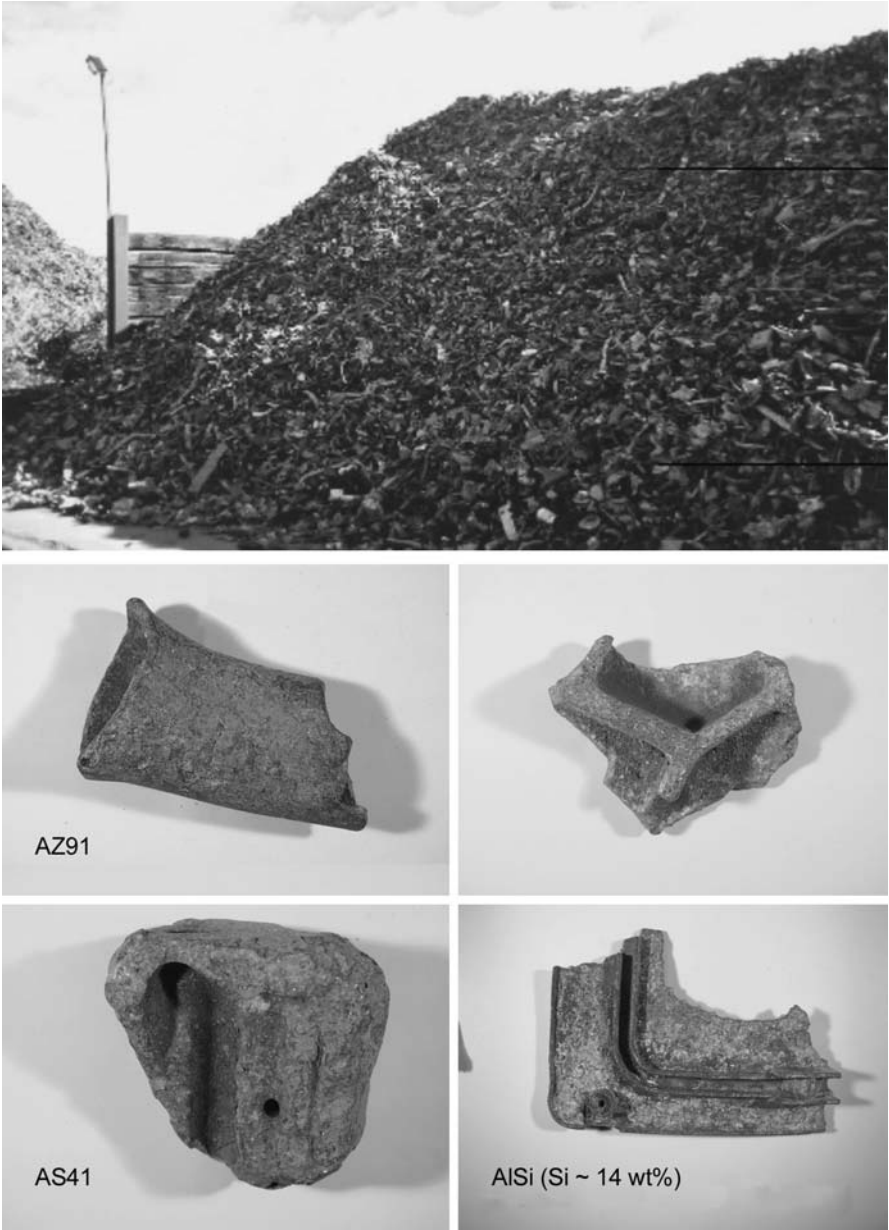


Fig. 9.8. Examples of ELV scrap

### 9.2.9 Class 8

Most of the aluminium and magnesium alloys from automobiles being scrapped today end up as shredded material sorted for heavy metals and plastics/fluff. Very often, magnesium and aluminium are not sorted. The magnesium fraction, normally constituting only a very small percentage, either burns off as the aluminium is remelted, or is removed in subsequent refining steps, for instance, by injection of a chlorine containing gas (demagging). Nevertheless, various methods are being used to separate the magnesium fraction from aluminium, including manual sorting, by means of laser or X-ray fluorescence analysis, or floatation in a liquid media having a density higher than magnesium but lower than aluminium [27]. Today, when a magnesium fraction is prepared on an industrial scale, all the common magnesium alloys are mixed. Examples are shown in Fig. 9.8. In addition, aluminium casting alloys are unavoidably present, giving very high Al content and contamination with Si if the magnesium alloy fraction is melted. As a result, ELV shredded scrap at present belongs to class 8. However, due to new directives on recycling of cars in the EU stating that any vehicle approved before 1 January, 2005 should meet a reuse/recovery target of 95% by weight, and a recycling target of 85%, it is obvious that ELVs will become increasingly important as a metal source. As a result, efficient methods to distinguish the various alloys need to be developed. For instance, systems based on electrical conductivity measurements may be useful for distinguishing magnesium alloys with varying aluminium content [40].

When cars on the roads today are to be scrapped, it is not likely that dismantling will be widely used, except for parts having value on the second-hand market or for reuse in new models. Dismantling for subsequent remelting of metals like Al and Mg is presently considered to be too costly, unless the parts are easily accessible. Cars not yet produced may be designed for increased use of dismantling.

## 9.3 Recycling Using Flux

Flux technology was developed in Germany in the 1920s [41]. Fluxes used for protection only should melt at a low temperature so that they cover the metal during melting. Near-eutectic compositions in the system  $\text{CaCl}_2\text{-NaCl-KCl-MgCl}_2$  are effective [18]. Refining fluxes should, in addition to this, contain thickening or inspissating agents such as fluorides or oxides. This improves separation of metal and flux, i.e., when pouring, causing less salt inclusions in the metal.

### 9.3.1 Principles

When magnesium alloy scrap covered with an oxide layer is in contact with molten salt, the wetting properties of the system promotes the oxides being transferred to the salt phase, leaving the molten metal parts free to coalesce.

When refining with flux, the principle is to use sufficient flux to absorb all the oxides present in the molten metal. As mentioned earlier, the salt must be inti-



mately mixed with the metal to achieve a large contact area so that virtually all metal gets in contact with the salt. Afterwards, the salt, to which the main fraction of oxides is transferred, and metal phase are allowed to separate.

The magnesium oxide films covering the magnesium alloy scrap parts constitute a barrier to coalescence. In aluminum-salt systems, fluoride ions facilitate removal (stripping) of the oxides from the surfaces of the metal drops [42, 43]. Such removal of oxides from the droplets must take place before coalescence of metal droplets can occur. The oxide stripping is not a thermodynamically spontaneous process and the reasons for it happening are not completely understood. Interfacial tension gradients, electrochemical dissolution (crevice corrosion) and modification of oxide surfaces have been suggested [43]. When the oxides are removed, it can be shown that coalescence of metal droplets is thermodynamically spontaneous [42].

The observations of Emley [18] agree with this. Emley explains that two factors are important in coalescence of finely divided metal thinly dispersed in a salt. Firstly, the salt must strip the oxide films from the droplets, and secondly, sufficient amounts of fluorides must be present in the salt to set up a contact angle between the salt and the droplet. The latter means that the salt tends to withdraw from the surfaces of metal leaving the metal drops free to coalesce. Salts consisting of alkaline chlorides are ineffective, and  $\text{MgCl}_2$  (or  $\text{CaCl}_2$ ) must be present. As the content of  $\text{MgCl}_2$  increases, so does the metal recovery up to a certain concentration [44]. Beyond this concentration, further increase in  $\text{MgCl}_2$  leads to lower recoveries. It is found in aluminum that as the concentration of  $\text{MgCl}_2$  increases in the  $\text{MgCl}_2$ -KCl system the ability for aluminum droplets to coalesce decreases [45]. According to Emley [18], there is a threshold concentration of  $\text{CaF}_2$  in the salt that must be reached before coalescence occurs. This content depends on the alloy content of the dispersed metal and also varies with the  $\text{MgCl}_2$  content in the salt melt. As the concentration of fluoride additives increased in both NaCl-KCl and  $\text{MgCl}_2$ -KCl salt systems, coalescence of aluminum drops also improves [45].

The temperature during refining is also important. Waltrip [11] suggests that temperatures  $< 700^\circ\text{C}$  results in entraining flux and other impurities in the metal, and too high temperatures may cause excessive oxidation and reduced crucible life. The melt is refined by using 2–3% flux, and stirred for 15 minutes so that melt and flux mix intimately. For heavily contaminated scrap, more salt may be necessary to get satisfactory refining and avoid “dry” sludge. Dry sludge means that the salt contains so much oxide that it affects the viscosity of the sludge and thereby its ability to separate from the metal.

The droplets being formed when the scrap parts melt have a maximum critical size [46], which is smaller than the size of ingots and the largest scrap parts, but larger than, for instance, flash and chips. When the large parts melt, fresh surfaces are formed that do not restrict heat transfer to the drops, and the drops can coalesce readily with the molten Mg and thereby dissolve. If the parts to be melted are *smaller* than the critical size, no fresh surface will be formed, and alloy droplets will be enveloped in their original oxide skin. Therefore, when melting small parts a salt composition facilitating oxide stripping is a prerequisite. The smaller the parts to be melted, the more important the salt composition.



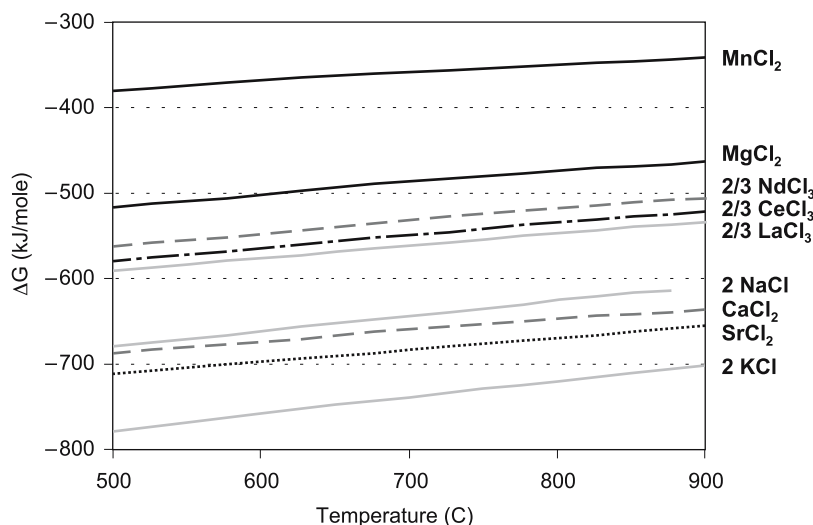


Fig. 9.9.  $\Delta G^\circ$  for some chlorides. Based on thermodynamic data from Kubaschewski and Alcock, 1979 (from [47, 48])

The density of the salt is also important in separating salt from metal, and to maintain a certain density difference between the alloy and salt phase.  $\text{CaCl}_2$  alone can be used to increase the density of salt.  $\text{BaCl}_2$  is considerably heavier and was widely used in the past [18, 37], but due to its toxicity it is no longer accepted.  $\text{SrCl}_2$  may also be an alternative.

### 9.3.1.1 Thermodynamic Restrictions

It must be noted that not all alloys are suitable for flux refining. If any of the alloy elements form chlorides that are more stable than  $\text{MgCl}_2$ , these will react with the molten salt and eventually be removed from the alloy. Figure 9.9 shows Gibbs free energy of formation for some chlorides. It is seen that magnesium alloys with Ca and Sr cannot be flux-refined without losing Ca and Sr to the salt ( $\text{CaCl}_2$  and  $\text{SrCl}_2$  are more stable than  $\text{MgCl}_2$ ). Likewise, a magnesium-chloride-containing salt will also affect alloys containing rare earth elements (Cl, La, Nd and Pr). However, kinetic factors may, in practice, limit the loss of these elements. The most common alloying elements: Al, Zn, and Mn will not be affected. In fact,  $\text{MnCl}_2$  is often used as a source for manganese, as it reacts and dissolves forming  $\text{MgCl}_2$ .

Scrap containing elements such as heavy rare earths, scandium and lithium may be treated by special salt compositions and special processes [49].

## 9.4 Fluxless Refining

Recycling of magnesium employing salt fluxes has the potential to improve the recovery. But the disadvantages with the salt flux are that it is corrosive for the

surrounding equipment and environment (HCl fumes), and it combines with impurities in the molten metal and/or with moisture in the atmosphere to form a sludge in the lower section of the crucible [5]. It also creates the possibility of having salt inclusions in the cast product. In addition, as mentioned earlier, chlorides may combine with organic residuals coming with the scrap, forming highly toxic compounds, creating the need for comprehensive emitted gas treatment systems.

### 9.4.1 Principles

Flux-free refining includes all refining processes where salt is not used. Settling/floatation and filtration are among these. It has been claimed that gas purging of magnesium alloys removes “a lot of” inclusions [9, 14, 16, 50]. However, quantitative results are to a great extent missing. Although the systems are different, a reduction by roughly a factor of two is reported in aluminum [51]. This indicates that gas purging may be an additional method, not the only refining method.

Fluxless refining requires the use of a protective gas atmosphere, based on  $\text{SF}_6$  or  $\text{SO}_2$ . Particles (inclusions) are to be removed from the bulk melt and transferred either to the melt surface, settle to the bottom, or stick to the walls. The purified metal may then be transferred from the bulk melt through a hole into a holding container, removed through a siphon tube or poured gently. Stirring must be limited since otherwise the inclusions will be re-entrained into the bulk melt. This usually means that the only mechanism for removal is gravity. Since magnesium is a light metal, one might expect that the heavier inclusions would settle to the bottom. However, most particles float up [52]. The explanation is probably that they are covered with a gas layer, thus lowering the mean density. Such gas layers have been detected for  $\text{Al}_2\text{O}_3$  in aluminium [53]. Perhaps water vapor and dissolved hydrogen play a role in creating the gas layers. The fact that there is a gas layer shows that the particles prefer gas to the magnesium melt, the particles are “wetted” by gas. This fact indicates that particles may be floated up by gas purging. Essentially, only inert gas can be employed since the presence of reactive gases such as chlorine or fluorine-containing gases would produce salts. When gas is purged through a melt, the impurities come into contact with the bubbles by various effects such as inertia, interception, gravitation, and diffusion. If the impurities are wetted by the bubbles but not by the melt, there is a high probability that the impurities remain trapped at the bubble-melt interface and are carried up to the dross or top-slag layer [47, 48].

It is important for a number of reasons that the purge gas is fed in as small bubbles [54]: (1) The melt/surface contact area is inversely proportional to the bubble size. (2) Small bubbles rise slowly up through the melt. (3) The contact area is proportional to the residence time of the bubbles. Finally, (4) small bubbles will only to a limited extent disturb and break up the protective layer of magnesium oxide on the bath surface. It is important that the bubbles are dispersed evenly over the cross-section of the melt. Small bubbles may be formed employing rotors, perforated tubes or porous plugs [54].

Taking gas cost, metal loss due to oxidation of continuously forming surfaces and evaporation of Mg to bubbles to form MgO dust and increased need for cover

gas, gas purging of Mg alloys has its obvious drawbacks. In salt-metal systems, however, gas introduced into the underlying salt phase [5] may be used effectively to distribute salt into the metal phase as a salt layer still surrounding the bubbles even when the bubbles are in the metal phase. This may have a refining effect, probably not due to the gas itself, but rather due to the salt being effectively distributed in the metal. In salt-metal systems, one may consider employing inert gases and reactive gases like nitrogen.

### 9.4.2 Systems Involving Filters

Reding [55] presents a method for melting magnesium without requiring a salt-flux cover on the magnesium surface. The method describes the refining of magnesium containing solid contaminant particles. Magnesium is melted in a container. The molten magnesium flows through a hole into a holding container. It is claimed that the solid particles are retained within the melting container. Purified molten magnesium is removed from the holding container. Melting is carried out using a protective gas cover. As pointed out earlier, oxide films and other contaminants usually rise to the surface of the melting container. They are excluded from the holding container by a position wall. The magnesium melt is removed from the holding container by a pump. It is claimed that the metal can be used for producing commercial castings without further refining.

Petrovich and Waltrip [16] discuss a process that utilizes the protective-atmosphere of air,  $\text{CO}_2$ , and 0.3–0.5%  $\text{SF}_6$  that incorporates a filtering system, which is said to give effective reduction of non-metallic inclusions (see Fig. 9.10). Utilizing a pump equipped with a suitable suction filter, molten metal is transferred into ingot moulds, to a transfer pot, a holding pot, or die-cast shot sleeve.

A flux-free process incorporating inert-gas purging and filtering techniques to remove non-metallic inclusions from molten magnesium scrap is described by Housh and Petrovich [50]. The process is claimed to have several advantages over

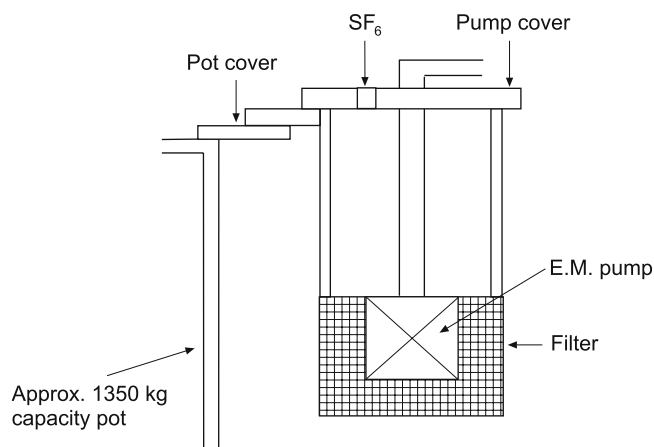


Fig. 9.10. A section of pump and suction-filter assembly [16]

a flux-refining system, including the removal of dissolved gases, decreased melt losses, and the elimination of chlorides. However, as will be discussed later, a significant effect of inert gas purging on the removal of hydrogen cannot be expected [56, 57].

A common feature of all the filter types described above is that the inclusions must be captured in front of the filter (cake filtration) rather than inside the filter (depth filtration). If these filters prove to be effective, the operating time (lifetime) necessarily must be short [54]. On the contrary, if the filters last for a long time without being blocked, it is rather unlikely that the filters are very effective.

## 9.5 Contamination Control

Generally, impurities in metals can be classified into five main groups [54]:

- I Volatile elements
- II Reactive elements
- III Non-reactive elements
- IV Reactive inclusions
- V Non-reactive inclusions

Impurity elements are defined as elements present in solution in the molten alloy that have deleterious effects on the metal properties [54]. These may either be volatile, or reactive and non-reactive (groups I, II or III). Hydrogen is an example of a volatile element. In molten magnesium, calcium and strontium are examples of reactive elements as these react with  $\text{MgCl}_2$ , while nickel is an example of a non-reactive element. Reactive or unstable inclusions (group IV) hardly exist in magnesium.

The most important non-reactive inclusions (group V) in magnesium and magnesium based alloys are [58]:

- Oxides, appearing as lumps, films and apparently loosely connected agglomerates or clusters
- Intermetallic particles
- Chlorides

Oxide films and clusters are expected to be reaction products from the melt surface, entrapped in the melt due to turbulence during processing; examples may be stirring, pumping, charging and ladling. Ingots and scrap are covered with a layer of oxide. The thickness of the oxide layer may depend on alloy composition, cooling and storing conditions. Upon charging and remelting, these oxide films may be introduced. Oxide films and oxide clusters have large surface/volume ratios and are thus not readily removed by settling. Magnesium nitrides,  $\text{Mg}_3\text{N}_2$ , may appear together with oxide clusters [59, 60]. However, thermodynamic calculations indicate that magnesium nitride will not form unless the partial pressure of oxygen becomes extremely low. The double oxide  $\text{MgO} \cdot \text{Al}_2\text{O}_3$  (spinel) is the most stable oxide in magnesium alloyed with aluminum. Nitrides, carbides, sulphates, sulphides and fluorides are rarely observed [61].

Intermetallic particles are usually a result of the iron removal process. Due to the relatively high density of the intermetallic particles ( $4\text{--}7\text{ g/cm}^3$ ) the main fraction of intermetallic particles formed during the iron precipitation process is removed before ingot casting. However, the solubility of iron and manganese decrease with decreasing temperature [62–64]. Decreasing temperatures thus facilitate formation and growth of intermetallic particles. As a result, temperature fluctuations in in-house as well as in die casting furnaces may lead to the formation of intermetallic particles, accompanied by decreased manganese content and increased iron content. Good temperature control in the furnaces is, therefore, mandatory in order to avoid iron pick-up and excessive formation of intermetallic particles. Intermetallic particles in pure magnesium as well as in magnesium base alloys are usually smaller than  $15\text{ }\mu\text{m}$ .

Due to the small relative difference in density the smallest salt particles are difficult to remove by settling. Fortunately, the wetting properties of most molten salts appearing in molten magnesium – magnesium oxide – salt system result in adhesion of salts to oxides and agglomeration of salt inclusions, resulting in increased size and thereby improved settling properties [18].

### 9.5.1 Additional Sources of Trace Elements and Inclusions During Recycling

Recycling introduces additional sources for contamination of all groups of impurities. Process scrap returned from the die casting machines may have surfaces 10–100 times larger than the surfaces of the ingots, and this represents a considerable source for inclusions.

Associated with the die casting process (classes 1 and 2) are die lubricants, usually water based, containing various organic components including petroleum oils, waxes (vegetable, mineral or synthetic) and bactericides. Silicones are normally also included in the recipes [65]. It is reported that a higher silicon level is a fingerprint of recycled class 1 metal [66]. The presence of hydrocarbons indicates that even when melting class 1 (and 2) scrap with salt, precautions to avoid formation of chlorinated hydrocarbons (i.e., dioxines) should be taken.

Magnesium alloy components may be coated with either organic or inorganic coatings for corrosion protection. Remelting of coated metal may thus introduce unwanted elements into the magnesium. Most inorganic pigments used in standard powder coatings do not introduce harmful elements in recycled magnesium. However, some colour pigments can cause concern when re-melting coated magnesium [67]. A survey of pigments is given in Table 9.1.

If the effect of colour pigments on recycling of magnesium is overlooked, a selection of coatings can cause trouble for the magnesium recycling industry in a long perspective. As will be discussed later, phosphorus may be an unwanted impurity element in magnesium. A source for phosphorus is phosphate conversion coatings. Although phosphate treatments have shown very good performance as a basis for subsequent coatings, they may be less attractive from a recycling point of view. As far as we know today, processes based on complex fluoro-compounds do not contain elements that cause problems for recycling of magnesium and are therefore preferred over phosphate treatments [67].

**Table 9.1.** Colour pigments that can give unwanted elements when remelting coated magnesium [67]

Colour	Pigment	Harmful elements
Blue	Cu-phthalocyanin	Cu
	Spinel ( $\text{CoAl}_2\text{O}_4$ , $\text{Co}(\text{Al,Cr})_2\text{O}_4$ )	Co
Green	Cu-phthalocyanin	Cu
	Spinel ( $\text{Co,Ni,Zn}_2(\text{Ti,Al})\text{O}_4$ )	Co, Ni
Yellow	Nickel titanium yellow ( $\text{Ti,Ni,Sb})\text{O}_2$ )	Ni
Red	Iron oxide ( $\text{Fe}_2\text{O}_3$ )	Fe
Black	Iron oxide ( $\text{Fe}_3\text{O}_4$ )	Fe

Thin-walled components for the electronic industry may be coated with an electroless nickel coating (typically 10  $\mu\text{m}$ ) possibly contributing to as much as 1 wt% of the component. For some applications, magnesium components may be electrolytically coated with zinc, copper, nickel and chromium [68].

### 9.5.2 Effects and Removal of Some Trace Elements

In this sub-section some common impurity elements and their negative effects on magnesium properties will be discussed. The elements discussed include nickel, iron, copper, cobalt and hydrogen.

#### 9.5.2.1 Nickel

Nickel is almost two orders of magnitude worse than copper in promoting corrosion of both die-cast and permanent mould-cast AZ91 [69] and AZ81 [70]. At 650°C liquid magnesium dissolves approximately 32 wt% nickel [71], so the solubility presents no restrictions for contamination. Alloying elements such as aluminum reduce the solubility of nickel considerably due to the formation of the AlNi phase [48]. For instance the solubility of nickel reduces to 0.15% at 650°C with addition of only 3% aluminum. If manganese is also added, the solubility of nickel decreases even further [72].

An American patent [73] describes a process for reducing the nickel content from about 2% to about 0.2% in pure magnesium by the use of zirconium, and further down to 0.001% by adding zirconium and aluminum. The mechanism is probably that the precipitating AlZr phase dissolves some Ni. Removal of Ni by Zr is also mentioned by Emley [18]. One should note that when adding Zr to an Al containing Mg melt, Zr and Al precipitate; there is no mutual solubility of these elements [18]. It is reported [74] that addition of excess Mn (as Al-75%Mn master alloy) at 720°C reduces the Ni content of a AZ91 melt made of scrap painted with a Ni-containing coating to 5 ppm. Baseline experiments with the same alloy material, but without addition of Mn, gave 0.0064 and 0.008% Ni.

Although it is documented that some nickel may precipitate alongside iron in the various Al-Mn-Fe phases, no industrial process is known for removal of

nickel from commercial molten magnesium-base alloys except by dilution with “nickel-free” material and possibly vacuum distillation.

### 9.5.2.2 Iron

The solubility of iron in pure magnesium is 0.018 wt% at 650°C increasing to approx. 0.04 wt% at 750°C [69]. A content of 200–400 ppm Fe is thus characteristic for commercial pure Mg. The principles for removing iron by means of manganese and aluminum, thereby getting a considerably more corrosion resistant alloy, was discovered more than 70 years ago [75, 76]. However, the industrial importance of this was not recognized until the 1980s. The metallurgical principles for removal of iron by addition of manganese are extensively discussed, and the mutual liquid solubilities of iron and manganese in various alloys have been investigated by Holta et al. [62].

Other ways reported to remove iron include the addition of boron [77] beryllium (AlBe master alloy or  $\text{BeCl}_2$ ) [78], zirconium (as flux containing  $\text{ZrCl}_4$ ) [79] or titanium (as flux containing  $\text{TiCl}_4$ ) [80].

### 9.5.2.3 Copper

As with Ni the solubility of Cu in molten magnesium presents no restrictions to contamination. At 650°C the solubility is about 70 wt% in the two-component system [71]. Copper has an adverse effect on the corrosion on AZ and AM alloys but is considerably less harmful than nickel and iron [69, 70]. The sand-casting alloy ZC63 contains 3 wt% Cu in addition to 5 wt% Zn and 0.5 wt% Mn [81], but the corrosion properties are reported to be acceptable. Most of the copper is incorporated in the eutectic  $\text{Mg}(\text{Zn,Cu})_2$  phase [82], which appears to be rather harmless. On introducing aluminum, the copper-containing phase is different and the Mg-Al-Zn-Cu alloy is heavily attacked by corrosion [83].

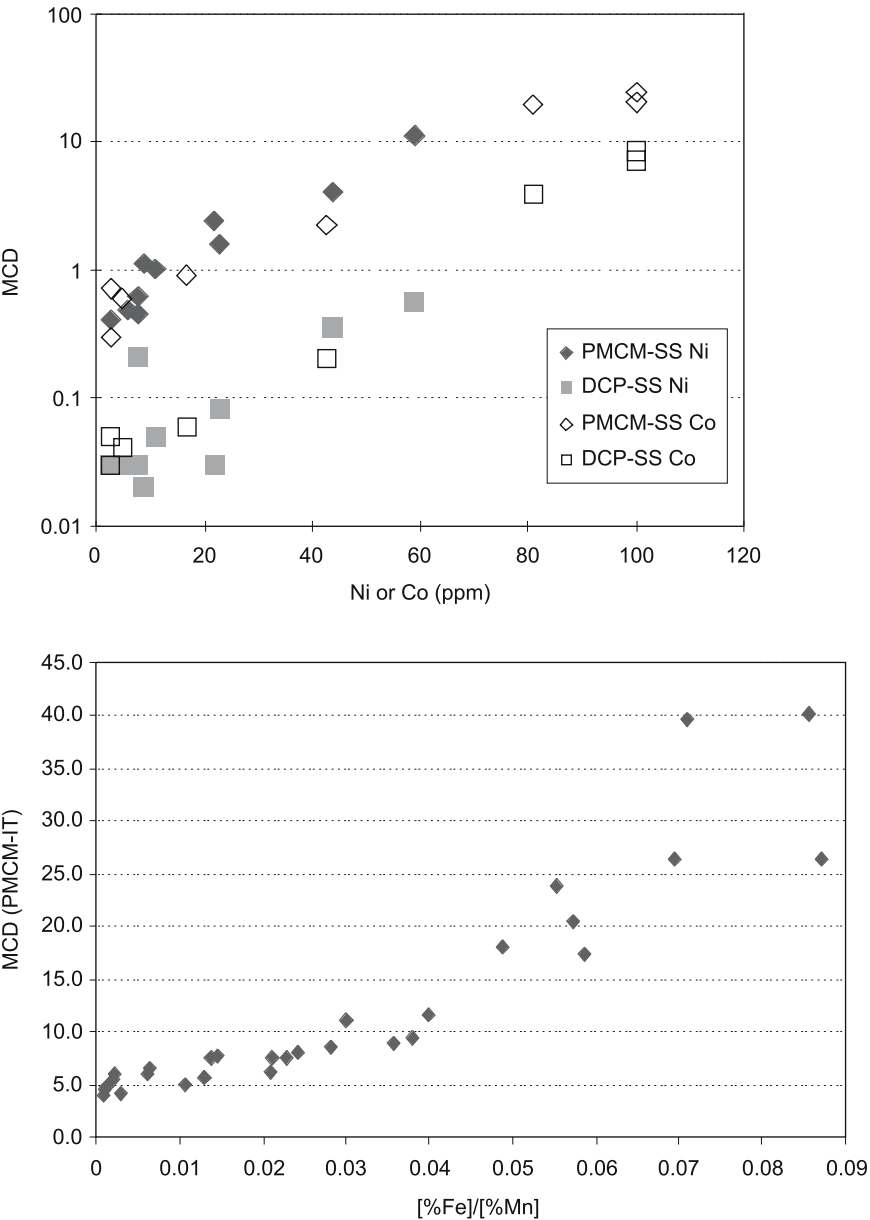
Although some copper may precipitate along with iron in the various Al-Mn-Fe phases, there is no known process for removal of copper from magnesium alloys except for dilution and vacuum distillation.

### 9.5.2.4 Cobalt

The elements Fe, Ni and Cu are quite common in materials that may be considered for use with magnesium. Although cobalt is present in some steel qualities, the main problem with cobalt may be its presence in some pigments that are used on magnesium-alloy parts, resulting in contamination during recycling.

Although Hanawalt et al. [84] demonstrated very early that cobalt is as harmful as nickel, very little attention has been given to cobalt and no standards are specified for it. Recent results showed the same effect of nickel and cobalt on AZ91 [69]. Like copper and nickel, cobalt cannot be removed from a molten Mg alloy except by dilution or vacuum distillation.

In Fig. 9.11 the influence of Fe, Ni and Co on the corrosion properties of AZ91 is illustrated [62, 68]. It can be seen that increasing Ni from 10 to 20 ppm results in five to ten times higher MCD values. At for instance 0.2% Mn, increasing Fe



**Fig. 9.11.** The influence of Ni, Co (left) and Fe on the corrosion properties of AZ91. Notice that the tests are different, so the MCD values cannot be directly compared. However, the effect of increasing contents of Ni, Co and Fe is clear



from 40 to 80 ppm ( $[\%Fe]/[\%Mn]$  ratio from 0.02 to 0.04) results in an increase of MCD values by less than a factor of two. This demonstrates that in AZ91 Ni and Co are the most important elements with respect to corrosion, and that iron is of secondary importance.

### 9.5.2.5 Hydrogen

Hydrogen present in magnesium is partly due to the pick-up of hydrogen from moisture in air and in flue gas from gas or oil burners [57].  $MgCl_2$ , as well as other salt components, are strongly hygroscopic and easily pick up water. Dissolved  $MgOHCl$  is reduced at the cathode during electrolysis, resulting in the evolution of hydrogen. Moisture and  $Mg(OH)_2$  from the surface of scrap, is probably an equally important source. When hydrogen from  $H_2O$  enters the metal, oxidation takes place, leading to metal losses and possibly contamination of the melt.

Magnesium has a much higher solubility for hydrogen than aluminum. While gas purging, as mentioned earlier, may reduce hydrogen in molten Al or Al-Mg alloys fairly easily, this is not the case in molten Mg due to unfavorable thermodynamics [56, 57]. Due to the high vapour pressure of Mg, it is hardly an alternative to remove hydrogen by means of vacuum extraction. However, hydrogen in magnesium die cast parts is not normally considered a problem as possible hydrogen porosity adds to the porosity usually present anyway. For gravity cast alloys, hydrogen may be important. Molten magnesium saturated with hydrogen rejects only 32% during solidification as compared to aluminum, which rejects 95% [57].

### 9.5.2.6 Other Elements

**Phosphorus.** Emley et al. [85] found that 0.09% P can be introduced into pure Mg held in graphite crucibles. If iron crucibles are used, a P content up to 0.4% can be achieved. It thus seems that Fe increases the solubility of P, possibly indicating that Fe and P may form compounds that remain suspended in the melt. Emley et al. [85] also reported that P disturbs the precipitation of Fe with Mn in A8 alloy resulting in incomplete iron removal. Findings by Fenn [86] and Fenn and Turner [87] at the same time supported Emley's results. In recent work [88] it was found that the presence of P (0.03%) in AM60 increases the level of iron and thereby aggravates the corrosion properties. It is reported [85] that phosphorus can be removed to < 20 ppm by adding zirconium alone or a zirconium aluminium master alloy. However, as mentioned elsewhere, precipitation with Zr is not applicable to Mg-Al alloys.

**Beryllium.** Beryllium is normally added to magnesium alloys (typically 5–15 ppm) to reduce the oxidation of the molten alloy [89]. The restricted solubility of Be in Mg alloys prevents larger concentrations. Recently Be has also entered the ASTM standards. The beryllium is gradually “lost” during processing, and a melt consisting of remelted die cast parts may contain < 5 ppm. This means that when recycling Mg alloys, either in-house or externally, the lost Be may have to be replaced. AlBe master alloys are normally used for this purpose. Due to the fact

that Be is classified as a carcinogen and finely-dispersed Be (or Be-containing) dust may lead to serious diseases, there are certain statutory regulations to follow and precautions to be taken with respect to handling this material. Ichikawa and Saito [90] investigated the concentration gradient of Be from the surface and inwards and found that when the Mg alloy is exposed to oxygen containing gases, Be segregates towards the surface. As mentioned earlier, Holdeman [78] added Be for removal of iron. At the temperatures of molten magnesium the vapour pressure of Be is insignificant. All this strongly indicates that the Be lost during processing accumulates in dross and sludge. Recent results confirm this as 0.007 and 0.037% Be is found in oxide/salt fractions from dross and sludge processing, respectively [12].

**Silicon.** Although silicon is added to some Mg alloys for improving the creep properties, it is considered to be an impurity in most other alloys at excess concentrations ( $> 0.1\%$ ) may lead to reduced ductility. According to Emley [18], silicon can be removed by adding zirconium or cobalt (as chloride). For reasons described earlier, it is unlikely that these principles can be utilised in practical recycling of commercial Mg alloys.

### 9.5.3 Effects of Inclusions

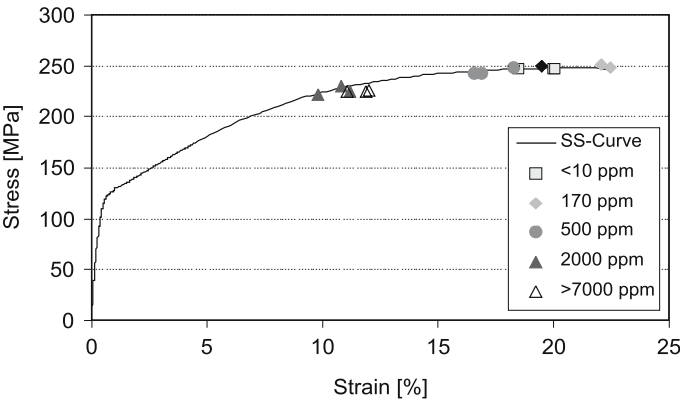
The impact of oxide inclusions on the mechanical properties of die-cast products is extremely difficult to quantify. The reason is that the oxides are not the only defect, they can be added to other casting defects such as porosity, cold shuts and hot tears [91, 92]. Recent findings (Fig. 9.11), indicate that depending on the presence of casting defects, deterioration typically starts at 500 ppm oxide content. In high quality castings this is in contrast to earlier findings indicating 2000 ppm as a critical content [93, 94].

From Fig. 9.12 it can be seen that the best values in each series constitutes three regimes with respect to elongation to fracture: (1) the clean metal ( $< 10$  ppm) and 170 ppm oxides, (2) 2000 and  $> 7000$  ppm, and (3) 500 ppm oxides in between.

Another aspect is the indirect influence of inclusions on mechanical properties. Inclusions (particles and films) have a significant influence on fluidity in die casting. Inclusions can then directly indicate cold shuts or other surface defects in the castings. Inclusions can also nucleate tears either in the semi-solid material or later in the completely solidified metal [91, 92]. There are also reasons to expect the larger inclusions to be more harmful than the small ones. Therefore, representing inclusions by their content (one figure only) is an oversimplification. Rather, inclusions should be represented by their number and size distribution.

### 9.5.4 Measurements of Inclusions

Metal cleanliness is a key feature in magnesium recycling, and the availability of methods for measurements of inclusions are important for assuring the quality of the recycled material. Two independent papers [58, 95] review the history of metal cleanliness assessment within the Mg industry up to 1997. A summary is



**Fig. 9.12.** Impact of inclusions on mechanical properties. The symbols represent the three best values of elongation at fracture in each casting series [92]

**Table 9.2.** Methods for metal cleanliness assessment used or considered for use in the magnesium industry [61]

Method	Equip- ment	Response time	Information	Detection limits	Sample size	Cost
HMIAM	OM/OM- IAS/SEM- EDS	Hrs/Days	Qualitative, Total content each type, NSD each type	1–2 µm/ ~ 4 ppm <sup>a</sup>	0.4–1.9 kg	Low/ Mod. <sup>b</sup>
DOW- method	Brighti- meter	seconds/ minutes	Total particle contents	0.2 %	Fractures	Low
Electrical resistivity		Min./Hrs	Total non-cond. particles	0.1%	1–10 g	Low
LECO		Min./Hrs	Total oxide	0.1–1 ppm	~ 1 g	High
GD-MS/ AES	Min./Hrs	Min./Hrs	Total oxide	0.1–1 ppm	~ 1 g	High
LiMCA	On-line		NSD, Total non- cond. particles	10–20 µm		High <sup>d</sup>

OM = Optical Microscopy, SEM = Scanning Electron Microscopy, EDS = Energy Dispersive Spectro-scopy, IAS = Image Analysis Systems, GD = Glow Discharge, MS = Mass Spectroscopy, AES = Atomic Emission Spectroscopy, NSD = Number Size Distributions.

<sup>a</sup> Detection limit 4 ppm refers to the Intersecting Lines Method. Lower detection limits can be achieved by other quantitative methods.

<sup>b</sup> Costs depend on which type of information wanted. Strictly, SEM-EDS is required for qualitative assessment. However, with some training, only an OM is needed to assess total contents of oxide particles, films, intermetallic particles and salts. NSD's requires an OM with IAS.

<sup>c</sup> Estimates.

<sup>d</sup> These technologies are not yet available for Mg.

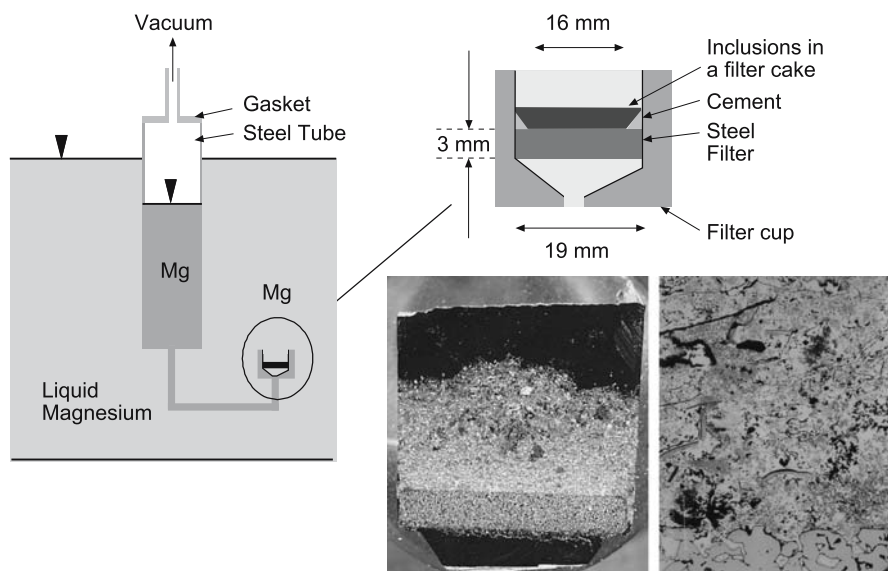


Fig. 9.13. Hydro magnesium inclusion assessment method

given in Table 9.2. Since then, there have been some efforts to establish methods giving rapid feedback to the user. The major developments since 1996/97 are briefly summarised.

In the Hydro Magnesium Inclusion Assessment Method (HMIAM) (Fig. 9.13), liquid metal is sucked through the sintered stainless steel filter into a canister holding up to 1.9 kg of magnesium [56, 60]. When the sampler is cold, the filter cup is cut off from the sampler and sectioned parallel to the flow direction. After metallographic preparation, inclusions on the filter are measured by means of optical microscopy, image analysis (optional) and SEM-EDS (optional). It is also possible to correlate filter cake thickness to inclusion content, thereby obtaining an estimate of the metal cleanliness fairly quickly [23]. The major advantage of Norsk Hydro's Inclusion Assessment Method is that sampling is performed directly in the melt, thus ladling or remelting steps are completely eliminated. Inclusions possibly generated during such operations are thus non-existent. HMIAM needs dedicated and skilled personnel to assure a high level of quality control throughout preparation of sampler, sampling, metallographic preparation and quantitative analyses. Unavoidably, the costs associated with inclusion assessment may be considered as high. Also, because a lot of work is involved, the time needed for analysing a sample may be extensive.

In North America there has been a big effort to measure oxides in ingot samples by fast neutron activation analysis (FNAA) [96]. Although there is only one institute (in Texas) that has developed analysis skills, this method has become an important tool for ingot evaluation. Others have focused on measuring oxides on arbitrary surfaces of ingots [97]. While evaluation of ingots might be a tool (although expensive) for ranking, e.g., in-house recycled metal during process

development and optimisation, it must be underlined that evaluation of ingots is not a good measure for metal cleanliness in die casting shops and die cast parts [91, 92]. Electrical resistivity as a tool for detecting oxide inclusions in Mg alloys is excluded [40]. As mentioned earlier, this is due to the electrical resistivity being extremely sensitive to the Al content.

The LECO method may be applicable for detecting oxides in solid magnesium samples [98]. The principle is that in presence of carbon and high temperatures (up to 2,300°C) magnesium oxide will be reduced to Mg and CO. The amount of CO developed can be quantified and related to the original MgO content. A recent paper from China [99] describes a technique based upon filtering the molten magnesium through two steel tubes, one with filter, and one without. The times needed for the melt to pass through the tubes are used to assess the cleanliness of the molten metal. This approach may be interesting, but probably more experience is needed to fully evaluate its usefulness.

The LiMCA instrument offering on-line measurements of non-conducting particles has been adapted to magnesium [100]. The problems related to ceramic probes have been overcome by using a concept of a concentric steel tube probe which is electrically insulating. The cost for this instrument probably makes it unattractive for magnesium die casters. Instruments such as Prefil and Qualiflash [101, 102] used in the aluminium industry can be adapted to magnesium, but the cost of the instruments as well as the adaptation costs probably prevent these instruments from widespread use in the magnesium industry.

Work has also been undertaken at SINTEF, Norway, aiming to develop an ultrasound based instrument for cleanliness monitoring in molten aluminium. The experimental results support the feasibility of using ultrasound to measure oxide content in molten Mg. However, considerable development is needed to establish an ultrasound based instrument for routine measurements in Mg alloys, for instance, in connection to in-house or in-cell recycling.

## 9.6 Concluding Remarks

Recycling of magnesium has until now mainly been associated with remelting of process scrap, consisting of clean returns from die casting operation and primary production. Traditionally, recycling by melting with flux has been used, but over the last decade, flux-free solutions have emerged, partly linked to in-house recycling in die casting shops. While the industry today effectively recycles the clean process scrap (class 1) in closed loop, the challenge in the short term is to close the loop for the lower grade scrap such as dross and chips. As magnesium alloys today have mainly automotive applications, in a market which is growing, the challenge in the longer term is to provide solutions for effective use of magnesium scrap from used cars.

## References

1. Albright DA, Haagenen JO (1997) Life cycle inventory of magnesium. 54<sup>th</sup> IMA Conference, June
2. Aune TK, Bakke P, Westengen H, Møllerud T, Albright DA (1997) Potential for improving the recycling friendliness of high purity magnesium die casting alloys. NADCA 97, Minneapolis, Minnesota, Nov. NADCA, Rosemont, Illinois, USA
3. NADCA (nn) NADCA Product Specification Standards for Die Castings, Die Casting Development Council, La Grange Illinois, USA
4. Edgar RL (2000) Global overview on demand and applications for magnesium alloys. In Kainer KU (ed) *Magnesium Alloys and their Applications*. Wiley VCH Verlag GmbH, Weinheim, Germany, pp. 3–8
5. Franke G (2000) Industrial recycling of magnesium alloys. *Automotive Light Metals* 1 (2), pp. 48–54
6. Edgar RL (1999) Magnesium supply and demand 1998. 56<sup>th</sup> IMA Conference, Rome Italy, pp. 1–6
7. Brassard C, Riopelle L (1997) Recycling of magnesium scrap a necessity. In Huglen R (ed) *Light Metals 1997*. TMS-AIME, Warrendale, PA, USA, pp. 1111–1114
8. Møllerud T, Andersen PK, Strømhaug SI, Lie O (1994) Hydro Magnesium opens a new plant for recycling of magnesium in Porsgrunn, Norway. 1st Intl. Conference on Recycling, Amsterdam, The Netherlands, October. ASM International
9. King JF, Thistlethwaite S (1994) Magnesium recycling for the European die casting industry. EFM-Aalen Magnesium Abnehmerseminar, Sept. 15–16, Aalen Germany
10. King JF, Hopkins A, Thistlethwaite S (1996) Recycling of by-products from magnesium die casting. In Lorimer GW (ed) *Proceedings of the 3rd Intl. Magnesium Conference*. Inst. of Materials, London, pp. 51–61
11. Waltrip JS (1990) Magnesium scrap and residual magnesium: Trash or treasure. SAE Technical Paper, 900789. SAE International, Warrendale, PA, USA
12. Ditzel A, Scharf C (2000) Utilization of Residues from Fluxless remelting of Compact Magnesium Scrap. In Kainer KU (ed) *Magnesium Alloys and their Applications*. Wiley VCH Verlag GmbH, Weinheim, Germany, pp. 753–760
13. Berkemortel R, Wang GG, Bakke P (2000) Fluxless in-house recycling of high purity magnesium die cast alloys at Meridian operations. 57<sup>th</sup> IMA Conference, Vancouver BC, Canada, May, pp. 22–27
14. Jacques RP, DasGupta R, Haerle AG (1997) Evaluation of recycled AZ91D magnesium alloy for steering column components. SAE technical paper 970332. SAE International, Warrendale, PA, USA
15. Leynedecker T, Rauch M (1998) Economical process for the in-house remelting in Magnesium die casting shops. In Mordike BL, Kainer KU (eds) *Magnesium Alloys and their Applications*. Werkstoff-Informationsgesellschaft mbh, Frankfurt, Germany, pp. 703–707
16. Petrovich VW, Waltrip JS (1989) Flux-free refining of magnesium die cast scrap. In Campbell PG (ed) *Light Metals 1989*. TMS-AIME, Warrendale PA, USA, pp. 749–755
17. Øymo D, Holta O, Hustoft OM, Henriksson J (1992) Magnesium recycling in the die casting shop. Proc. of the 1992 conf. on the recycling of metals, Düsseldorf/Neuss, Germany, May, ASM International, pp. 143–150
18. Emley EF (1966) *Principles of magnesium technology*, 1st ed. Pergamon Press, Oxford, UK
19. Wallevik O, Rønhaug JB (1991) Method and apparatus for remelting and refining of magnesium and magnesium alloys. US Patent 5,167,700, Oct. 21
20. Schroder D, Rauch E (1994) *Magnesiumschmelzöfen und Verfahren zum Schmelzen von Magnesium*. German Patent DE 44 39 214 A1, Nov. 3
21. Schmitz & Apelt (2000) Fluxless Recycling in Continuous Operation. Schmitz & Apelt LOI marketing material, Wuppertal, Germany
22. Schubert W, Gjestland H (2000) Use of SO<sub>2</sub> as protection gas in magnesium die casting. In Kainer KU (ed) *Magnesium Alloys and their Applications*. Wiley VCH Verlag GmbH, Weinheim, Germany, pp. 761–766

23. Berkmortel R, Wang GG, Bakke P (2001) Continuous fluxless recycling of high purity magnesium die cast alloys, Paper to be published at CIM, Ottawa, Ontario, Canada, August
24. Galowsky U, Kuhlein M (2001) A new conti-process for the fluxless recycling of high purity magnesium. In Hryn JN (ed) *Magnesium Technology 2001*. TMS-AIME, Warrendale PA, USA, pp. 49–54
25. Holta O, Hustoft OM, Strømhaug SI, Albright DL (1993) Two furnace melting system for magnesium, NADCA 93, Cleveland Ohio, USA, October. NADCA, Rosemont, Illinois, USA, pp. 49–53
26. Dioxines and PCBs (1999): Environmental and health effects. Final study. Scientific and Technological Options Assessment (Ref: EP/IV/STOA/99/ENVI/02. European Parliament, Directorate General for Research, The STOA Programme
27. Krone K (2000) Aluminium-recycling. Vereiniger Deutsche Schmelzhütten e.v. Dusseldorf, Germany
28. RUF (2000) From waste materials to raw materials. RUF GmbH & Co marketing material, Zaisertshofen, Germany
29. Beckman A, Russel AJ (1997) Extraction of metals in carbon dioxide and chelating agents therefor. US Patent 5,641,887, June 24
30. Kwang YH, Lin Y, Wai CM, Smart NG (1998) Fluid extraction using carbon dioxide and organophosphorus chelating agents. US Patent 5,840,193, Nov. 25
31. Saxena SK (1994) Method for treatment of oil contaminated filings of magnesium and magnesium alloys. US Patent, 5,338,335, Aug. 16
32. Areaux LD, Dudley RH (1998) Method and apparatus for cleaning and drying metal chips. US Patent 4,721,457, Jan. 26
33. Zhu T, Li N, Mei X, Yu A, Shang S (2001) Innovative vacuum distillation for magnesium recycling. In Hryn JN (ed) *Magnesium Technology 2001*. TMS-AIME, Warrendale PA, USA, pp. 55–60
34. Faure P (1994) Process for the recovery of magnesium from magnesium alloys waste. US Patent 5,476,529, Nov. 24
35. Kulinskii A, Zuev NM (1995) Processing of foundry wastes from magnesium production Russian Journal of non-ferrous metal 36 (4), 28–34
36. Foerster GS (2000) Recovery of metal from sludge and dross. Foundry management technology, Sept. p. 70
37. Gribov VI, Belkin NA, Shaibakov TI, Belkin MI (1988) Material balance for the processing of magnesium scrap and waste in a liquid salt bath. *Tsvetnye Metally: The Soviet Journal of non-ferrous metals*, pp. 63–65
38. Barannik IA, Devyatkin VN (1992) Magnesium alloys usage in the USSR. Secondary metal processing, In Mordike BL, Hehmann F (eds) *Magnesium Alloys and their applications* DGM Informationsgesellschaft, Oberursel, Germany, pp. 43–49
39. Rohman M, Scherzberg H (1995) Verfahren zur Aufarbeitung von aus der Magnesiumherstellung anfallenden Schlacken oder Kratzen. European Patent EP 0 693 563 B1, July 15
40. Fuerst CD, Dasch CJ (2000) Conductivity measurements on ingots of magnesium die-casting alloys. In Kaplan HI, Hryn JN, Clow B (eds) *Magnesium Technology 2000*. TMS-AIME, Warrendale PA, USA, pp. 107–111
41. Beck A (1940) *The Technology of Magnesium and its Alloys* (English Translation from German), Hughes FA & Co. Ltd, London, UK
42. Ho FK, Sahai Y (1990) Interfacial phenomena in molten aluminium and salt systems. In van Linden JHL, Stewart D, Sahai Y, (eds) 2nd Intl. Symp. – *Recycling of Metals and Engineered Materials*. TMS-AIME, Warrendale PA, USA, pp. 85–103
43. Ye J, Sahai Y (1996) Interfacial behaviour and coalescence of aluminium drops in molten salts. *Materials Trans, JIM*, 37 (2), 175–180
44. Komura A, Imanga H, Watanabe N (1973) Dispersion of Mg in the electrolysis of  $MgCl_2$ -KCl melts. *Denki Kagaku* 41 (4), 281–286
45. Friesen KJ, Utigard TA, Dupuis C, Martin JP (1997) Coalescence behaviour of aluminium droplets under a molten salt flux cover. In Huglen R (ed) *Light Metals 1997*. TMS-AIME, Warrendale PA, USA, 857–864



46. Clift R, Grace JR, Weber ME (1978) Bubbles, drops and particles. Academic Press, New York, USA
47. Tathgar HS, Bakke P, Engh TA (2000) Impurities in magnesium and magnesium based alloys and their removal. In Kainer KU (ed) *Magnesium Alloys and their Applications*. Wiley VCH Verlag GmbH, Weinheim, Germany, pp. 767–780
48. Tathgar HS, Bakke P, Øvrelid E, Fenstad J, Frisvold F, Engh TA (2000) Solubility of nickel in molten magnesium-aluminium alloys above 650°C. In Kaplan HI, Hryn JN, Clow B (eds) *Magnesium Technology 2000*. TMS-AIME, Warrendale PA, USA, pp. 181–189
49. Ditzel A, Schwerdtfeger K (1998) Concepts for recycling of new alloys. In Mordike BL, Kainer KU (eds) *Magnesium Alloys and their Applications*. Werkstoff-Informationsgesellschaft mbh, Frankfurt, Germany, pp. 709–714
50. Housh SE, Petrovich V (1992) Magnesium refining: A fluxless alternative. SAE Technical Paper, 920071, SAE International, Warrendale, PA, USA
51. Frisvold F, Bakke P, Øvrelid E, Hald NE, Engh TA (1996) Hydrogen and inclusion content in recycled aluminium at Holmestrand Rolling Mill. In Hale W (ed) *Light Metals 1997*. TMS-AIME, Warrendale PA, USA, 1011–1016
52. Hillis JE, Mercer II WE (2000) Separation of non-metallic contaminants in fluxless melting and refining of magnesium alloys. SAE Technical Paper 2000-01-1125. SAE International, Warrendale, PA, USA
53. Haugland E (1988) Removal of inclusions by gas purging. Dr. Ing. Thesis, Department of Metallurgy NTNU, Trondheim, Norway
54. Engh TA (1992) *Principles of Metal Refining*. Oxford University Press, Oxford, UK
55. Reding JN (1976) Apparatus and method for refining magnesium. US Patent 1,424,543
56. Bakke P (1992) Measurement and removal of inclusions and hydrogen. Dr. Ing. Thesis, Department of Metallurgy NTH, Trondheim, Norway
57. Øvrelid E (1997) Hydrogen in magnesium and magnesium alloys. Dr. Ing. Thesis, Institute of Metallurgy NTNU, Trondheim, Norway
58. Bakke P, Karlsen DO (1997) Inclusion assessment in magnesium and magnesium base alloys. SAE Technical Paper 970330. SAE International, Warrendale, PA, USA
59. Simensen CJ, Oberländer B (1980) A survey of inclusions in magnesium. *Z. Praktische Metallographie* 17 (3), 125–136
60. Øymo D, Karlsen DO, Pinfold PMD, Møllerud T, Lie O (1994) Particle removal in pure magnesium. In Mannweiler U (ed) *Light Metals 1994*, TMS-AIME, Warrendale, PA, USA, pp. 1017–1024
61. Bakke P, Laurin JA, Provost A, Karlsen DO (1997) Consistency of inclusions in pure magnesium. In Huglen R (ed) *Light Metals 1997*. TMS-AIME Warrendale, PA, USA, pp. 1019–1026
62. Holta O, Westengen H, Røen J (1996) High purity magnesium die casting alloys. Impact of metallurgical principles on industrial practice. In Lorimer GW (ed) *Proceedings of the 3rd Intl. Magnesium Conference*. Inst. of Materials, London, UK, pp. 75–88
63. Simensen CJ, Oberländer BC, Svalestuen J, Thorvaldsen A, (1988) The phase diagram for Magnesium – Aluminium – Manganese above 650°C. *Z. Metallkunde* 79 (11), 696–699
64. Thorvaldsen A, Aliravci CA (1992) Solubility of manganese in liquid Mg-Al alloys. *Adv. prod. and fabr. of light metals and metal matrix composites*, Edmonton, Alberta, Canada, Aug. 23–27, pp. 277–288
65. Kruszynski EA (1993) Die lubricants: Questions and answers. *Die Casting Engineer*, 37 (1), 16–18
66. Pinfold PMD, Øymo D (1993) An evaluation of refined recycled AZ91D alloy. SAE Technical Paper, 930420. SAE International, Warrendale, PA, USA
67. Skar JJ, Willekens J (2001) Perspective in Magnesium Applications. *Leichtmetall-Anwendungen. Neue Entwicklung in der Oberflächentechnik. Berichtsband – Nr 46, der Tagung am 13. und 14 März 2001, Münster*. Deutsche Forschungsgesellschaft für Oberflächentechnik e.V.
68. Olsen A (1992) Korrosionseigenschaften von neuen Magnesiumlegierungen. *Metall* 46 (6), 570



69. Bakke P, Sannes S, Albright DL (1999) Effects of Ni, Cu, Si and Co on the corrosion properties of permanent mould cast medallions and die cast plates of magnesium alloy AZ91. SAE Technical Paper 1999-01-0926. SAE International, Warrendale, PA, USA
70. Höllrigl-Rosta F, Just E, Köhler J, Melzer HJ (1980) Magnesium in Volkswagen. 37th IMA Conference, pp. 38–45
71. Nayeab-Hashemi AA, Clark JB (1988) Phase diagrams of binary magnesium alloys, ASM Intl., Metals Park, Ohio, USA
72. Tathgar HS (2001) Solubility of Nickel in Mg-Al, Mg-Al-Fe, and Mg-Al-Mn systems. Dr.-Ing. Thesis, Institute of Metallurgy NTNU, Trondheim, Norway
73. Foerster GS (1975) Removal of nickel from molten magnesium metal. US Patent 3,869,281, March 4
74. Inoue M, Iwai M, Kamado S, Kojima Y, Itoh T, Sugama M (1998) A new recycling process for thin walled AZ91D magnesium alloy die castings with paint finishing. In Mordike BL, Kainer KU (eds) Magnesium Alloys and their Applications. Werkstoff-Informationsgesellschaft mbh, Frankfurt, Germany, pp. 697–702
75. Bakken HE (1926) Magnesium – aluminium ally. US Patent 1,584,688
76. Beck A, Schmidt W (1929) Verfahren zur Entfernung von suspendierten Teilchen von Eisen und ähnlichen fein verteilte Verureinungen von nicht salzartigem Charakter aus Magnesium und hochprozentigen Magnesiumlegierungen. German Patent No. 604,580
77. Hillis JE, Green WG (1988) Method for removing iron contamination from magnesium. US Patent 4,773,930
78. Holdeman GE (1941) Removing iron from magnesium alloys. US patent 2,304,093. Dec. 16
79. Fox FA, Bushrod CJ (1944) Improvements in or relating to the production of magnesium base alloys. British patent 591,225, Aug. 8
80. Emley EF, Fox FA (1945) Improvements in or relating to the treatment of magnesium and magnesium base alloys. British patent 594,152, March 22
81. Unsworth W, King JF (1986) Recent casting alloy development. Proc. Intl. Conf. on Magnesium Technology, London. The Institute of Metals, London UK, pp. 25–29
82. Polmear IJ (1994) Magnesium alloys and applications. Materials Science and Technology 10, 1–15
83. Hillis JE (1983) The effect of heavy metal contamination on magnesium corrosion performance. SAE Technical Paper, 830523. SAE International, Warrendale, PA, USA
84. Hanawalt JD, Nelson CE, Peloubet JA (1942) Corrosion studies of magnesium and its alloys. Trans AIME 147, 273–299
85. Emley EF, Jessup AC, Higgins WF (1951–52) The effect of phosphorus on the corrosion-resistance of magnesium and some of its alloys. J. Inst. Met. 80, pp. 23–32
86. Fenn RW (1951) Effect of minor impurities on the corrosion rate of pure Mg. Prepared discussion for Gordon Research Conference, May 23
87. Fenn RW, Turner AM (1951) The preparation of high purity magnesium and the effect of minor constituents on its corrosion characteristics Fall Scientific Meeting, Midland, USA
88. Skar JI, Bakke P (2001) Effect of phosphorus on the corrosion properties of magnesium alloy AM60, To be published
89. Spiegelberg W, Ali S, Dunstone S (1992) The effects of beryllium additions on magnesium and magnesium containing alloys. In Mordike BL, Hehmann F (eds) Magnesium Alloys and their applications DGM Informationsgesellschaft, Oberursel, Germany, pp. 259–266
90. Ichikawa R, Saito R (1965) The distribution of beryllium in solid magnesium alloys containing beryllium at high temperatures. Trans. JIM, 6: 78–82
91. Bakke P, Fuerst CD, Westengen H (2000) Solidification induced inhomogeneties in magnesium-aluminium alloy AZ91 ingots. In Kaplan HI, Hryn JN, Clow B (eds) Magnesium Technology 2000. TMS-AIME, Warrendale, PA, USA, pp. 201–210
92. Bakke P, Pettersen K, Guldborg S, Sannes S (2000) The impact of metal cleanliness on mechanical properties of die cast magnesium alloy AM50. In Kainer KU (ed) Magnesium Alloys and their Applications. Wiley, Weinheim, pp. 739–745

93. Haerle AG, Mikucki BA, Mercer II WE (1996) A new technique for quantifying non-metallic inclusion content in magnesium. *Light Metal Age* (Aug.), pp. 22–29
94. Haerle AG, Murray RW, Mercer II WE, Mikucki BA, Miller MH (1997) The effect of non-metallic inclusions on the properties of die cast magnesium. SAE Technical Paper 970331, SAE International, Warrendale, PA, USA
95. Hu H, Luo A (1996) Inclusions in molten magnesium and potential assessment techniques. *Journal of Metals* 48 (10), 47–51
96. Fuerst CD, James WD (1998) Fast Neutron Activation analysis of oxide inclusions in magnesium alloy ingots. 15th Intl. Conf. on the Applications of Accelerators in Research and Industry, Denton, TX, USA, Nov.
97. Tartaglia JM, Grebetz JC (2000) Observations of intermetallic particle and inclusion distributions in magnesium alloys. In Kaplan HI, Hryn JN, Clow B (eds) *Magnesium Technology 2000*. TMS-AIME, Warrendale PA, USA, pp. 111–121
98. Aina L, Stella G, Conti M, Mattiel M (1999) The determination of oxides in magnesium based alloy AM60. *Metallurgical Science and Technology* 17 (2): 48–49
99. Fang Y, Shixian S (2001) A new self-gravitation filtering technique for rapid assessing cleanliness of magnesium alloy melt. In Hryn JN (ed) *Magnesium Technology 2001*. TMS-AIME, Warrendale PA, USA, pp. 67–74
100. Carozza C, Lenard P, Sankaranarayanan R, Guthrie RIL (1997) On the development of a LiMCA probe for liquid magnesium. *Light Metals 1997 Metaux Legers, CIM, Sudbury, Ontario, Aug.*
101. Enright PG, Hughes R (1996) A shop floor technique for quantitative measurement of molten metal cleanliness of aluminium alloys, *Foundryman*, (Nov.), pp. 390–395
102. Roberge JL, Richard M (1997) QUALIFLASH – An instrument for instantaneous evaluation of inclusion quantity in liquid aluminium alloys. BOMEM marketing material, Quebec, Canada

---

## Subject Index

### A

- Acid pickling 439
- Adhesive bonds 365
  - –, joints, durability/reliability 367
  - –, strength 372
  - –, structural, high-strength 367
- Adhesives, heat-curing 371
  - , one-component 368
  - , polyurethane-based 368
  - , reactive/non-reactive 367
  - , two-component 367
- AE 42 252
- Aerospace industry 604, 607
- Afterburning 641
- Ag 81
- Ageing 372, 397
- Agena, intercontinental ballistic missile 615
- Agglomerates 650
- Agitation 636
- Ailerons 615
- Air 639–655, 659
- Air Force, U.S. 617
- Al (aluminum) 80, 262, 645–655, 659
- AlBe 653, 655
- Al-Mn 636
- Al-Mn alloy, liquid 117
- Al-Mn-Fe 652
- Al<sub>2</sub>O<sub>3</sub> 648
- Al-5% Be master alloy 120
- Alabama Metallurgical Corp. 15
- Alais, Froges et Camerque 2
- Alcoa 14, 16
- Alkaline earth elements, Ca 122
- Allison T-56 series 620
- Alloy development 96
- Alloy M18 616
- Alloy MA21 616
- Alloy systems 298, 511
- Alloy systems, compatible 132
- Alloying 109
- Alloying elements 63, 149
- Alloying principles 146
- Alloys 510
  - , BM65-1 620
  - , characteristics 252
  - , diecasting 166
  - , –, Zr free 93
  - , high purity 164, 643
  - , highly creep resistant 97ff
  - , Mg-Al 225
  - , Mg high-performance 87
  - , preparation 146
  - , rare-earth containing, rapidly solidified 618
  - , sand casting 198
  - , super light-weight 86
  - , wrought alloys 289
  - , zirconium 128
- Aluminium 80, 262, 645–655, 659
  - , adding 115
- Aluminium alloys 343
- Aluminium Company of Canada (Alcan) 13
- Aluminium fasteners 338
- Aluminium und Magnesiumfabrik Hemelingen 3
- Aluminium-die casting 241
- Aluminothermic processes 56
- AM20 252
- AM503 alloy 608
- AM50A/AM60B 252
- Amati 6
- AMC process 50
- American Magnesium Corporation (AMC) 8, 16
- AN-2 plane 620
- Anderson, balloon ascent (1935) 608
- Anodes 640
- Anodic oxidation procedures 451
- Anodic plasma-chemical reaction procedures/coating properties 458
- Anodic spark deposition/discharge (ASD) 455

- Anodising 371  
 ANOIMAG treatment 454  
 Antennas 615  
 Antonov, airplanes 620  
 Application automotive 499, 506  
   – –, body 527  
   – –, chassis 554  
   – –, crankcase 515  
   – –, crash 532  
   – –, cross car beam 537  
   – –, cylinder head covers 517  
   – –, door 527  
   – –, instrument panel 538  
   – –, interior 519  
   – –, lightweight construction 512  
   – –, Mg extrusion 548  
   – –, Mg sheets 541  
   – –, panels 541  
   – –, potential use 503  
   – –, seat 521  
   – –, spaceframe 551  
   – –, steering column system 519  
   – –, steering wheel 519  
   – –, structural parts 535  
   – –, tailgate 527  
   – –, wheel 554  
 Arado 196 609, 610  
 Army, U.S. 617  
 AS21 252  
 AS41B 252  
 Asbestos fibers 32  
 Atlas, intercontinental ballistic missile 615  
 Automobile 269, 287  
 Automobile gas mileage 607  
 Automobile parts 252, 607  
 Avisma 8  
 AZ series 290  
 AZ31B-H24 617  
 AZ61A/AZ80A 296  
 AZ91B 617  
 AZ91D 252  
**B**  
 B29 618  
 B36 bomber 610  
 B47 610  
 B707 618  
 B727 618  
 B737 618  
 B747 618  
 Backer, Christian 8  
 BaCl<sub>2</sub> 135, 647  
 Ball, Major C.J.P. 5  
 Bar 298, 610  
 Barriers 617  
 Basic principles 219  
 Bauxite 52  
 Be 119, 653, 655, 656  
 BeCl<sub>2</sub> 653  
 Bedworth factor 111  
 Beech Aircraft 615  
 Bending 280, 314  
 Bending tests 415  
 Berezniki titanium/magnesium 18  
 Beryllium 119, 653, 655, 656  
   – –, diseases 121  
 Billets and slabs 292, 293  
 Bill-of-materials 619  
 Bischofite 31  
 Biscuits 635, 638–640  
 Bitterfeld 3  
 BKMP0 615  
 Black, Joseph 1  
 Blasting, abrasive medium 233  
 Blistering 297  
 BM65-1 alloy 620  
 BMW 801D radial engine 609  
 Body surfaces 608  
 Boeing 618, 619  
 Bolt connections 510  
 Bolzano process 56  
 Bonanza 615  
 Bonnet 544  
 Boron 653  
 Brackets 620  
 Brasmag 18  
 Brass 640  
 Breakdown temperatures 221  
 British de Havilland Comet 608  
 Broken Hill Proprietary Company (BHP) 2  
 Bronze 640  
 Brushing 369, 438  
 Bubble size 648  
 Bubbling nitrogen 125  
 Build-up 399, 402  
 Bunsen, Robert Wilhelm 1  
 Burnishing 412  
 Burns 605, 618  
**C**  
 C-124 Globemaster 615  
 C-133 Cargomaster 615  
 C-17 618  
 C-47 615  
 C-54 (DC-7) 615  
 Ca 80, 122, 123, 647, 650  
 CaCl<sub>2</sub> 646, 647  
 CaCl<sub>2</sub>-NaCl-KCl-MgCl<sub>2</sub> 645  
 CaF<sub>2</sub> 643  
 Cake filtration 650

- Calcium 122, 123, 647, 650  
Calcium chloride 638  
Calcium fluoride 638  
Calder Hall, nuclear power 63  
Caproni 113 608  
Car body 284  
– components 285  
Car mould, cast iron chill 136  
Carbides 650  
Carbon reinforced plastics 381  
Carbothermic process 57  
Carburettor 608  
– housings 608  
Castability 154, 603  
Caster, single/multistrand 293  
Casting 607–610, 620  
–, chill, vertical direct 292  
–, counter-gravity 229  
–, parting agents 436  
–, semi-solid 261, 595  
–, structural 600  
Casting alloys 145  
Casting crust, function 437  
Casting defects 656  
Casting furnace 637  
Casting procedure 247  
Casting returns 633  
Caudron 460 608  
Cavity surface temperature 244  
Cell colonies, cylindrical 441  
Cell recycling 659  
Ceramic fibre sleeves 226  
Cerium 122  
Charging 640, 642, 650  
Chemically bonded systems 220  
Chemische Fabrik Griesheim Elektron 3  
Chill casting, vertical direct 292  
Chills 226  
Chips 641, 642, 646  
–, ignition 410  
–, roots 402  
–, sorted, dry 634  
–, –, oily/wet 635  
–, wet/oily 641  
Chlorides 643–650  
Chlorinated hydrocarbons 642, 651  
Chlorine 641, 647, 648  
Chrome-sulphuric acid process 371  
Chromite sands 221  
Chromium 652  
Circumscribing circle 299  
Class 1 635–642, 651  
– scrap 635  
Class 2 635, 637, 651  
Class 3 640, 642  
Class 4 635, 641  
Class 5 635, 641  
Class 6 635, 642  
Class 7 637, 643  
– sludge 635  
Class 8 635, 645  
Classification systems 634–636  
Clean returns, sorted 634  
Cleaning 287, 641  
–, alkaline baths 439  
–, organic solvents/emulsions 438  
Cleanliness 634  
Clinching 285, 348, 374  
–, room temperature 375  
Clusters 650  
Co (Cobalt) 652–655  
CO 659  
CO<sub>2</sub> 560, 565, 634, 639, 649  
– /SF<sub>6</sub> 137  
–, supercritical 641  
CO<sub>2</sub> laser 357  
Coalescence 642–646  
Coating systems, lacquer/paint-based 468  
– –, organic 467  
Coatings 399, 651, 652  
–, application, physical methods 467  
Cobalt 652–655  
Cockpit 618  
–, parts 617  
Cold chamber die casting process 234  
Cold forming 279  
Cold isostatic pressing (CIP) 327  
Cold rolling 274  
Cold shuts 656  
Columns, controls 620  
Compo casting, melt stirring 323  
Composites, extruded 310  
–, magnesium matrix 315  
Compression properties 182  
Consistency 112  
Consumer applications 620  
Consumer magnesium scrap 634  
Contact angle 646  
Contact area 648  
Contact corrosion 431, 508  
Contamination 640, 645, 650, 651, 655  
Controls 608  
Conversion coatings 439  
– –, anodic oxidation 450  
– –, anodic plasma-chemical reaction, electrolyte 455  
– –, chromating 441  
– –, chrome-free systems 443  
– –, formation 439, 455  
Conversion layers, color 441

- Conversion treatments 287
- Cooling lubricants 409
- Cooling rate 164
- Copper 82, 640, 643, 652, 653
- Cornallite 31
- Corrosion 334, 366, 397, 431, 607, 652–655
  - , contact 431, 508
- Corrosion behavior 604, 617, 618
- Corrosion problems, galvanic 615
- Corrosion protection 287, 510
  - –, coatings 610
  - –, methodology 620
- Corrosion resistance 619, 620
- Counter-gravity casting 229
- Cover 610
- Cover gases 636, 639, 641, 648
- Cowling 611
- Crankcases 608
- Crash 532, 534
- Creep, secondary 511
- Creep behavior 310, 604
- Creep properties 190, 305
- Creep resistance 121, 510
- Cross-sectional area reduction 297
- Crucibles 637, 639, 646, 648, 655
- Crushing 636, 643
- Cu 82, 640, 643, 652, 653
- Current density, estimated 457
- Current-voltage curve 457
- Cutting speed 400
- Cycle times 238
- D**
- Damping behaviour 287
- Damping capacity 68, 159
- Damping characteristics 603
- Davy, Sir Humphrey 1
- Dead Sea –, Ltd. 18
- Deep drawing 279, 283
  - – ratio 279, 281
- Deformation 272, 281
  - behaviour 74
- Degree of coverage 432
- Delivery systems, aerial 610
- Delmotte, R. 608
- Dem-val, airplanes 619
- Demagging 645
- Density 65, 157
  - , low 620
  - , radiographic 233
- Density fluxes, higher 135
- Depth filtration 650
- Design guidelines 247
- Design of casting die 243
- Desulfurisation 640–643
- Deville and Caron 2
- Die 607
  - , closed 374
  - , slugs and blanks 297
- Die caster returns 634
- Die casting 25, 234, 617
- Die casting alloys (Zr free) 93
- Die casting process 234, 245
  - – –, hot chamber 235
- Die forgings 620
- Die half, fixed/movable 243
- Die lubricants 247
- Die materials, coatings 243
- Diffusion 65
- Dimensional properties 255
- Diode laser 357
- Dioxins 641, 642, 651
- Dip brazing 364
- Direct route 294
- Direct screwing 385
- Dislocation strengthening 76
- Dismantling 645
- Dissolution 123
- Distributors 608
- Dolomite 31
- Dominion Magnesium 13, 15
- Donati, pilot (1934) 608
- Doors 529, 610
  - , parts 618
- Dow, Herbert H. 8
- Dow Chemicals 8, 12–16, 569, 634
- Dow process 46
- Downsprues 223
- Drawing 279, 283
- Drawn sheet products 241
- Drop corrugation 610
- Dross 636, 639–642, 648
  - , salt-free 635
- Dry air 639
- Dry blasting 369
- Dry chips 641
- DSM and Russian process 44
- Ductility 273, 603
- Dye penetrant crack detection 233
- Dynamic properties 277
- Dynamic recovery 300
- E**
- East Coast Aeronautics, Inc. 615
- Edges, leading 611
- Ejector pins 243
- Elastic moduli 68
- Electrical breakdown 455
- Electrical resistivity 157
- Electrochemical methods 33

- Electrodes, mono-polar/multi-polar 40  
Electrolytic manganese 116  
Electromagnetic interference (EMI) 242  
Electromagnetic shielding 287  
Electron states 64  
Electron-beam welding 359  
Electronic cabinets 615  
Electronic equipment 625  
Elektron (magnesium) tubes, welded 608  
Elektron Metall Bad Cannstatt 3, 4  
Elements, dissolved 640  
–, incompatible 131  
–, non-reactive 650  
–, reactive 650  
–, trace 651, 652  
–, volatile 650  
Elongation 304  
Elongation to fracture 277  
ELVs 635, 636, 645  
Empennage 615  
End of Life Vehicle (ELV) 635  
Energy consumption 560, 563, 634  
Engine, 801D 609  
–, radial, BMW 801D 609  
Engine bearers 609  
Engine cases 608  
Engine cowlings 608  
Engine pods 611  
Environmental impact 257  
Epoxy 368  
Eshelby's model 319  
Etching 287  
Extrudability 297  
Extrusion 289, 294, 301, 569, 607–611, 615  
–, methods 294  
–, pre-extrusion 294  
–, shapes 298  
–, speed 297, 298
- F  
F.A. Hughes & Co. Ltd. 5  
F-22 619  
F-80 610  
Fabrication, ease 617  
Failure 333, 415  
Falcon GAR-1 617  
Faraday, Michael 1  
Fast neutron activation analysis 658  
Fasteners, steel 338  
Fatigue 306, 604  
Fatigue properties 184  
Fatigue strength 355  
Fe 82, 653, 655  
– /Mn ratio 116  
Fe pick-up 120  
Federal Aviation Authority (FAA) 619  
Feeding 244  
Feeding distances 225  
Fibre distribution 318  
Fibre length 318  
Fibre reinforced plastics 385  
Fibre reinforcement 321  
Fill time 247  
Films 650  
Filters 223, 650, 658, 659  
Filtration 636–638, 648, 659  
Fine-grained structure 129  
Finishing, abrasive 438  
Fires 618  
First level concessions 619  
Fittings 608  
Flaps 615  
Flash 646  
Flat-rolled products 607  
Flight-control systems 620  
Floatation 636, 645, 648  
Floor beams 615  
Fluidity 225, 656  
Fluorides 645, 646, 650  
Fluorine 648  
Fluorocarbons 115  
Flux 636–642, 645, 646  
–, BaCl<sub>2</sub> containing 135  
–, Mg-Zr alloys 135  
–, refining 645  
Flux free melting practice 138  
Flux inclusions 111  
Flux melting 109, 125  
Flux refining 637, 647  
Flux-free melting 640  
Flux-free refining 637, 648  
Fluxless melting 113  
Fluxless refining 647  
FNAA 658  
Focke Wulf 190 609  
Focke Wulf Condor 200 608  
Folding 392  
Forged Elektron AZ 855 engine bearers 609  
Forgings 289, 607–610  
Form factor 299  
Formability 278, 279  
Fracture toughness 305, 604  
France 620  
Freeport, Texas 9  
Friction stir welding 360  
Fuel, liquefied 617  
Fuel consumption 499, 501  
Fuel tanks 608  
Furakawa Magnesium Company 17

- Furans 641  
 Furnace 640  
 –, multi-chamber 638  
 Furniture 628  
 Fuselage 608, 615  
 –, lower covering 608  
 Fushan Aluminum 19
- G**
- Galvanic applications 627  
 Galvanic corrosion 431, 617  
 – – resistance 605  
 Galvanic-deposit coatings 466  
 Galvanisation, magnesium 466  
 Garden equipment 623  
 Gas cover 649  
 Gas mileage, automobile 607  
 Gas pressure infiltration 325  
 Gas purging 636–638, 642, 648, 649, 655  
 Gating systems 243, 639  
 GE 617  
 Gearbox 506, 509, 610  
 Germany, aerospace 620  
 Global warming potential 113, 565  
 Graetzel process 3  
 Grain refinement 136  
 – –, direct assessment 138  
 – –, mechanism 128  
 – –, strengthening 78  
 Grain refining 128, 151, 294  
 Grain size, direct estimation 134  
 – –, estimation 136  
 Grains, columnar 294  
 –, fine hexagonal 129  
 Gravity casting, conventional 229  
 Green sand mixes 220  
 Greenhouse effect 560  
 Grinding 369, 437  
 Gun enclosures 611  
 Günterschulze and Betz 455  
 Gypsy VI engines 608
- H**
- HAE treatment 453  
 Halpin-Tsai-model 319  
 Hand tools 621, 624  
 Hansgirk, F.J. 2  
 Hardening, solid solution 76  
 Hardness properties 188  
 Hardware 624  
 HE-111 609  
 HE-177 609  
 Heat affected zone 352  
 Heat checking 242  
 Heat resistance 287  
 Heat treatment 231, 308  
 Heating /cooling 244  
 –, external 244  
 Heavy metals 640, 645  
 Heavy rare earths 647  
 Helicopter gearbox 618  
 Helicopter transmission systems 610  
 Hemming 393  
 HES 640  
 High ductility 164  
 High purity alloys 164, 643  
 High-energy particles 617  
 Higher systems (ternary/quaternary) 90, 91, 92  
 HK31 615  
 HM21 615  
 HMIAM 658  
 Hollow shape 299  
 Hot chamber die casting process 235  
 Hot-cracking 349  
 Hot forming 281  
 Hot isostatic pressing 327  
 Hot pressing 327  
 Hot rolling 274  
 Hot shortness 297  
 Hot tears 656  
 Hot-top processes 293  
 Hot-working practice 299  
 Housings 608, 621, 624  
 Hybrid joining techniques 366, 394  
 Hybrid reinforcement 322, 319  
 Hybrid structures 285  
 Hydro magnesium inclusion assessment method (HMIAM) 658  
 Hydro magnesium process 47, 634, 638  
 Hydrocarbons 651  
 Hydroforming 284  
 Hydrogen 410, 643, 648–654  
 Hydroxides 643  
 Hygroscopicity 113
- I**
- IG Farben 2, 3, 13  
 Image analysis 658  
 Impact extrusion 297  
 Impact properties 186  
 Impulse-arc-welding 350  
 Impulse density/time/rate 457  
 Impulse-type spark discharge 457  
 Impurities 648, 651  
 Impurity elements 650  
 Inclusion content 658  
 Inclusions 636, 640, 648, 651, 656, 658  
 –, non-metallic 649  
 –, non-reactive 650



–, reactive 650  
Indirect extrusion 294, 296  
Inert gases 648, 649  
Inert-gas purging 649, 650  
In-gate velocity 247  
Ingot metallurgy 323, 605  
Ingots 650, 658, 659  
–, pre-alloyed 139  
Inhibiting gas 228  
Inhibition 221  
Insert materials 640  
Inspissated flux 110  
Instrument panel 608  
Intake manifold 512  
Interface 329  
Interior components 617  
Intermetallic particles 642, 643, 650, 651  
Investment 607  
Iron 651–656  
– /manganese, cast part 436  
Iron refining 636  
Iron removal 651  
Isotta Fraschini 608  
Israel, aerospace 620  
Italian Breda 608  
Italo Balbo 608

## J

Jaguar 610  
Joining 285, 528  
–, mechanical and hybrid 374  
Joy-sticks 618  
JSC Avisma 18  
JSC Oriana 19  
JSC UKTMK 19  
JU88A-4 609  
Junkers 609

## K

Killing (settling) 637  
Kulush magnesium plant 19  
KUMZ 615

## L

La (lanthanum) 122, 647  
Laser 645  
Laser-beam welding 356  
Lattice parameters 64  
Lever, control 608  
Li (lithium) 80, 124, 647  
LiCl–LiF 124  
Life cycle assessment 559, 634  
Life cycle inventory 560, 563  
Lifetime, MMC 618

Lightweight construction 269, 365, 500, 501, 540, 551, 565  
Lightweight design effects, secondary 562  
Lightweight materials 366  
LiMCA 659  
Lithium 80, 124, 647  
Lockheed-Martin 617, 619  
– – C-130/L-100 620  
– – F-16 Falcon 620  
Locking force  $F_{\text{lock}}$  235  
Logistic command centers 619  
Long-fibre-reinforcement 321  
Lubricants 641, 651  
Lumps, oxides 650  
Lunokhods, space vehicle 615

## M

M8 340  
M18 616  
MA2 615  
MA21 616  
Machinability 242  
Machines, 4-slide/5-slide 238  
Machining 333, 398  
Magcan 34  
MagCorp process (US Mag) 47  
Magnesite 31  
Magnesium 80, 269, 315  
–, creep resistant 510  
–, galvanisation 466  
–, hexagonal-grid structure 432  
–, impurities 82  
–, increased use in aerospace systems 617  
–, joining 336  
–, MMCs 618  
–, permanent mould castings 241  
–, properties 63  
–, pure 146  
–, uses 63  
–, wrought 608  
Magnesium adhesive bonds, corrosion 369  
Magnesium alloys 80  
– –, casing characteristics 225  
– – systems, commercial 93ff  
Magnesium-based material, porosity 437  
Magnesium chloride 638  
Magnesium corrosion 619  
Magnesium Elektron (MEL) 6, 12, 634  
Magnesium flat rolled products 270, 276  
Magnesium gondola, spherical 608  
Magnesium hydroxide 432  
Magnesium matrix composites 315  
Magnesium Metal Co. 6  
Magnesium nitrides 650  
Magnesium oxide 648

- Magnesium plate 608  
 Magnesium rolling 274  
 Magnesium sand castings 240  
 Magnesium sheet 269, 272, 276  
 Magnesium skin, aircraft 611  
 Magnesium strip casting 292  
 Magnesium surface, particle-blasting 437  
 Magnesium wrought products 269  
 Magnetherm process 53, 642  
 Magnohrom 18  
 Magnolia process 49  
 MAGOXID-COAT treatment 458  
 MAGPASS-COAT 445  
 Maintainability 618  
 Manganese 81, 116, 636, 638, 643, 647, 651–655  
 Manufacturing, North America 594  
 Mars, space vehicle 615  
 Mathey, J. 5  
 Matrix composition/properties 316  
 Mechanical properties 160, 335, 618–620  
 MEL DPSC system 231  
 Melt losses 640  
 Melt protection 245  
 Melting 245, 636, 642, 643  
 –, flux-free 113, 138  
 Melting furnace 639, 640  
 Melting interval 349  
 Melting procedure 136  
 Messerschmitt 109 609  
 Metal, molten, reactivity 150  
 Metal cleanliness 291, 656, 659  
 – – assessment 656  
 Metal matrix composites (MMC) 310, 315, 618  
 Metal spinning 25  
 Metallic hardeners 133  
 Metallostatic pressure 220  
 Meteorites 617  
 Mg (magnesium) 80, 269, 315  
 Mg alloys, classification 82  
 Mg phase diagrams 84  
 Mg-Ag 88  
 –, alloys 96  
 Mg-Ag-Re-Zr 133  
 Mg-Al 84  
 –, alloys 225  
 –, material combination 372  
 Mg-Al-Zn 298  
 Mg-Zn-Zr 298  
 MgBe<sub>13</sub> 119  
 MgCl<sub>2</sub> 646, 647, 654  
 MgCl<sub>2</sub>/KCl 646  
 Mg-Li 86, 87  
 Mg-Mn 85  
 Mg<sub>3</sub>N<sub>2</sub> 650  
 Mg-Nd 87  
 MgO 659  
 MgO-Al<sub>2</sub>O<sub>3</sub> 650  
 Mg(OH)<sub>2</sub> 643, 654  
 Mg-RE-Zn-Zr alloys 94  
 Mg-Sc 89  
 Mg-Th-Zr 133  
 Mg-Y 88  
 –, alloys 96  
 Mg-Y-RE-Zr 133  
 –, alloys 141  
 Mg-Zn 84  
 Mg-Zn-RE-Zr 133  
 Mg-Zn-Zr 94, 133  
 Mg-Zr 89, 610  
 –, alloys 225  
 –, –, flux 135  
 Microarc oxidation (MO) 455  
 Microporosity 225  
 Microscopy, optical 658  
 Microstructures 167, 266  
 Midland 8  
 MIG welding 349, 395  
 MIL-Handbook 5 617, 619, 620  
 Minhe Magnesium 19  
 Mischmetal 121  
 Missiles 617  
 ML-5 alloy 620  
 ML-5PCh alloy 620  
 ML-8 alloy 620  
 MMC 310, 315, 618  
 –, in situ 326  
 Mn 81, 116, 636, 638, 643, 647, 651–655  
 MnCl<sub>2</sub> 116, 647  
 Modulus of elasticity 301  
 Moisture 226, 638, 639, 643  
 Molten metal, transferring 245  
 Monofilaments 321  
 Mould, moisture 226  
 –, permanent 607  
 Mould coats, refractory 228  
 Mould design 223  
 MPLC 14  
 Multifilaments 321  
 Murex process 2–6  
  
 N  
 N<sub>2</sub> 639, 649  
 NaCl-KCl 646  
 Nanjing Hwahong Magnesium Industry Corporation 20  
 Nanjing Ube Magnesium Company 17  
 NASA 617  
 National Lead 17

- Navy, U.S. 617  
Nazionale Cogne S.A. 6  
Nd 140, 647  
Nd:YAG laser 357  
Ni (nickel) 82, 637, 643, 650–655  
Nitrides 650  
Nitrogen 639, 649  
Non-automotive uses 593  
Non-equilibrium techniques 607  
Noranda 13, 14  
Nordisk Lettmetall 7  
Norsk Hydro 7, 14, 16, 643  
Northrup XP-79B Flying Ram 609  
Nose piece 608  
Nose skins 610  
Nucleation 129  
Number size distribution 656
- O**  
Off-gas 641, 648  
OGMA (Aeronautical Industry of Portugal) 619  
Oil pump 608  
Oil sumps 608  
Oil tanks 608  
Oily chips 641, 642  
Optical equipment 625  
Orowan 331  
Osaka Titanium 13  
Österreichisch-Amerikanische Magnesit AG 2  
Outer-skin applications 287  
Oxidation 646  
–, plasmachemical 455  
Oxide ceramic layers 457  
Oxide clusters 650  
Oxide films 646, 649, 650  
Oxide inclusions 656  
Oxide layers 369  
Oxide stripping 646  
Oxides 637–646, 650, 651, 656, 659  
Ozone, exposure 617
- P**  
P (phosphorus) 651, 655  
Painting 257  
Panel 544  
Particle-blasting 438  
Particle reinforcement 320  
Parting agents, casting 436  
Parting line 243  
Passenger cabin 618  
Passivated layer, chemicals resistance 433  
Passivation 287, 432  
PCBs 641  
Pechiney 2, 7  
Peritectic reaction 128  
Peritectic temperature 129  
Permanent mould 607  
– –, sand/investment casting alloys 94, 95  
Phosphorus 651, 655  
pH-value diagram 432  
Physical properties 192, 603  
Piccard, Jean 608  
Pidgeon, Lloyd M. 8, 13  
Pidgeon process 8, 13, 53  
Pigments 651, 653  
Pilling factor 111  
Pilling-Bedworth ratio 432  
Pistor, G. 3  
Planet satellite 610  
Plasma treatment 371  
Plastics /fluff 645  
Plastics injection mouldings 242  
Plotting boards 615  
Plugs, porous 648  
Polishing 438  
Polymers vs. magnesium 597  
Polyurethane-based adhesives 368  
Porosity 257, 656  
Porsche 4  
Post-consumer scrap 633–635  
Pourbaix 432  
Pouring bushes 223  
Pouring streams 223  
Powder forging 327  
Powder metallurgy 326  
Powertrain applications 602  
Pr 647  
Pratt & Whitney 617, 620  
Pre-alloyed ingot 139  
Precipitation 643  
Precipitation strengthening 77  
Pre-extrusion route 294  
Prefil 659  
Preheating 636, 637  
Preliminary treatment, chemical-based 438  
Pressing, hot isostatic 327  
Pressure tightness 257  
Pretreatment, chemical 369  
Primary energy 563  
– – consumption 561  
Process force 400  
Process scrap 634, 635, 651  
Processing, correct/wet-chemical 437  
Propeller blades/shafts 608, 609  
Propellers 608  
Protection systems 618  
– –, maintainable 620

- Protection systems  
– –, Rockhard/Tagnite 618  
Protective gas ( $\text{SO}_2/\text{SF}_6$ ) 637  
Protective oxide surface 607  
Prototyping 284  
Puddling 134–136  
Purging 648  
Purity, high 433  
Purity control 150  
Push-pull torch 351
- Q**  
Qualiflash 659
- R**  
Radar control equipment 615  
Radenthein process 6  
Radio frequency interference (RFI) 242  
Radioactivity issues 133  
Radiographic standards/density 233  
Radiography 233  
Rakowics, P. 3  
Rapid solidification processes (RSP) 310, 607  
Rare earths 81, 121, 140  
– –, alloys, rapidly solidified 618  
– –, Gd, Dy, Er, Tb 141  
– –, Nd-rich 140  
Ravelli 7  
Reactivity 124  
Rear engine cowlings 608  
Recovery 115, 641, 643–647  
Recovery rates 124  
Recrystallisation 274, 300  
– –, dynamic 301  
Recycling 257, 333, 633  
– –, closed loop 633, 634, 641  
– –, in-cell 639, 640  
– –, in-house 637–639  
Recycling friendliness 634  
Refining 109, 636, 638–645  
– –, fluxless 647  
Refining fluxes 645  
Reinforcements 316, 319  
Remelting 645  
Replacement parts 618  
Residence time 639, 648  
Residual stress 412  
Residue 642  
Returns, clean, sorted 634  
– –, mixed and off-grade 635  
– –, sorted oily/painted 634  
Rheocasting 267, 595  
Ribbed stamping 615  
Rigidity 617  
Riken Metal Manufacturing Co. 1  
Riser design 226  
Riveting 285, 377, 604, 608  
– –, blind 382  
– –, self-piercing 377  
Rivets, full self-piercing 381  
– –, semi-tubular self-piercing 378  
Riv-nuts 336, 337  
Riv-studs 336, 337  
Rocking-bars 620  
Rods, extrusion 298  
Roll force 412  
Rolling 269  
Rolls-Royce/Turbomeca Adour Engine 610  
Rotary furnaces 642  
Rotors 648  
Roughness 400  
Rudders 608  
– –, ZK60A-T5 forgings 617  
Rule of mixture 318  
Runners 635, 638, 639
- S**  
Safety 619  
Salt 637–648, 651  
– –, emulsifying 436  
Salt fluxes 647  
Salt-free 638, 642  
Salt inclusions 645, 648  
Salt phase 649  
Samsonite luggage 23  
Sand 607  
Sand casting 219, 610  
Sand systems 220  
Scalping 293  
Scandium 647  
Scrap 636–646, 650, 654  
– –, internal 635  
– –, post-consumer 633–635  
– –, process 634, 635, 651  
– –, shredded 645  
Screwing without pre-punching 387  
Sealing adhesives 367  
Seat frames 617  
Seats 608  
Seawater 32  
Second deck 615  
Selection criteria 335  
Self-healing 441, 446  
SEM-EDS 658  
Semifinished products 272  
Semi-hollow shape 299  
Semi-solid casting 261, 595  
Sensitive material 433  
Sensitivity 121, 233

- Serpentine 32  
Settling 636–640, 648–651  
SF<sub>6</sub> 113, 137, 639, 649  
Shearing chips 402  
Sheet 269, 569, 608–611, 615  
Sheet cowlings 608  
Sheet metal 278  
Sheet rolling 292  
Shells 620  
Shenyang Al & Mg Engineering and Research Institute 19  
Shielding 245  
Shooting Star (F-80) 615  
Short-circuiting-arc processes 351  
Short-fibre-reinforcement 321  
Short-wave electromagnetic radiation 617  
Shredded material 645  
Shrinkage porosity 293  
Shut forming 269  
Si 81, 115, 121, 645, 651, 656  
Sieve gradings 221  
Silicon 81, 115, 121, 645, 651, 656  
Silicones 651  
Silicothermic processes 52  
Silver, age hardening response 81  
SIMS 120  
Sintering 327  
Siphon tube 639  
Slabs 293  
Sludge 637–646  
–, salt 635  
SO<sub>2</sub> 113, 639  
Società Magnesio e Leghe di Magnesio 6  
Société d'Electro-Chimie & Aciéries Electrique 2  
Société Général du Magnesium 2  
Sodium 125  
Sodium chloride 638  
Sol-gel processes 468  
Solid shape 299  
Solidification 155  
Solidification pressure 247  
Solikamsk 8, 18  
Solubility 120  
–, extended levels 607  
Sorting 636, 645  
Soundness 257  
Southern Magnesium and Chemicals 19  
Soviet Union (former) 615–620  
Soyuz, space vehicle 615  
Space, corrosion-free 618  
Sparging 115  
Spinels 457, 650  
Split die 374  
Sports equipment 626  
Sprayforming 327  
Springback 281  
Squeeze casting 235, 259, 324  
– –, thixocasting/rheocasting 258  
Sr 122, 123, 647, 650  
SrCl<sub>2</sub> 647  
Stainless steel 126  
Stampings 615  
–, ribbed 615  
Standard Magnesium Corporation 16  
Static recovery 300  
Steel, deoxidation 63  
Steering wheels 620  
Stevens, balloon ascent (1935) 608  
Stirring 648  
Storage devices 617  
Strain rate 300  
– – sensitivity 172  
Strength/ductility 604, 617  
Strength-to-density ratio 604  
Strengthening mechanisms 75  
Stress, internal 231  
–, residual 412  
Stress corrosion cracking 616  
Stress relief 231, 309  
Stretch forming 280, 283  
Stretching 307  
Stripping 646  
Strontium 122, 123, 647, 650  
Structural applications 270  
Structural material 603  
Stupino plant 615  
Sulphates 650  
Sulphides 650  
Sumitomo Sittix 13  
Superplastic forming 284  
Surface pretreatment 369  
Surface properties 257  
Surface protections 431  
Surface quality 278, 282  
Surface tension 120  
Surface treatment 411, 431  
– –, magnesium-based materials 433  
Surface-layer, passivated 432  
Systems Support Division (SDD) 619
- T  
T-bars 293  
Tagnite treatment 465  
Tail cones 610  
Talon, supersonic jet trainer 610  
Tamil Nadu Magnesium 19  
Tanks, gas and oil 608  
Tantalum 126  
Tearing chips 403

- Temperature bonding process, lower 366  
 Temperature control 637, 640, 651  
 Temperature extremes 617  
 Tensile properties 172  
 Terrestrial applications 607  
 Thermal conductivity 66, 67, 105, 106, 157, 287  
 Thermal expansion 65  
   – coefficient 316, 349, 352  
 Thermal parameters 64  
 Thermal reduction methods 52  
 Thermodynamic properties 65  
 Thermomechanical treatment 274  
 Thin sheet 615  
 Thin-walled structures 366  
 Thixocast 266  
 Thixocasting 264  
 Thixomolding 595  
 Thorium, creep resistance 81  
 Thread engagement, length 339  
 Three-layer-passivation structure 432  
 $\text{TiCl}_4$  653  
 TIG welding 349  
 Timminco 8, 15  
 Titan, intercontinental ballistic missile 615  
 Titanium 653  
 Titanium Metals Corporation of America 15  
 Tolerances 256  
 Tool travel 400  
 Tooling systems 283  
 Torsion properties 190  
 Toxicity 120  
 Trace elements 651, 652  
 Transitional fairings 608  
 Transport industry 621  
 Transportation applications 603  
 Trimmings 635  
 Tubing 298, 610, 617  
 Twinning 273, 301  
 Two-furnace system 639, 640  
 Typical defects 228
- U**
- UK, aerospace 620  
 Ultralight constructions 284  
 Ultrasound 659  
 US Armed Forces 617  
 US XP56 610  
 USAF Materials Directorate 619  
 Use levels 603
- V**
- Vacuum die casting process 234  
 Vacuum distillation 642, 653  
 Vacuum extraction 655  
 Vacuum ladle 42  
 Venus, space vehicle 615  
 VILS (All Russian Institute for Light Alloys/Moscow) 615  
 Viscosity 125, 646  
 Visual inspection 233  
 VMD-10 615  
 Volkswagen 20  
 Vostok, space vehicle 615
- W**
- Wall thickness 299  
 Washout, cavity 242  
 Water vapour 648  
 Weight reduction 508  
 Weld filler metal 349  
 Welding 349  
   –, laser-beam 356  
   –, methods 604  
   –, TIG 349  
 Weld-penetration 350  
 Wetting properties 643, 645, 651  
 Wheel fairings 608  
 Wheels 608  
 Whisker 322  
 Whitney Canada PT-6A series 620  
 Wing beams 608  
 Wing components 618  
 Wing fairings 608  
 Wing ribs 608  
 Wing trailing edge section 611  
 Wings 608, 609, 611  
 Wintershall 5  
 Wrought alloys 289  
 Wrought magnesium 608
- X**
- X-ray fluorescence analysis 645
- Y**
- Youngs modulus 316  
 Yt 81
- Z**
- Zaporoshe 8  
 Zaporozhyre Titanium and Magnesium Works 19  
 Zinc 81, 642, 647, 652–655  
 Zircon 221  
 Zirconium 81, 133, 652–655  
 Zirconium grain refining, fluxed/flux-free melts 135, 137  
 Zirconium hydride 131  
 Zirmax 133, 134

- ZK series 291
- ZK60A 296
- ZK60A-T5 617
- ZK60B 615
- Zn (zinc) 81, 642, 647, 652–655
- Zr (zirconium) 81, 133, 652–655
  - , “active” form 133
  - , inhibiting element 131
  - , maximum solubility 131
  - , reservoir 134
  - , soluble/insoluble 138
- Zr alloys, Mg-RE-Zn 94
- Zr-containing alloys 132
- Zr-containing salt mixtures 133
- Zr grain refinement 133
- Zr halides, direct reduction 133
- Zr residue 134
- Zr-rich coring 129, 130
- Zr-rich insoluble particles 135
- Zr-rich layer 134
- ZrCl<sub>4</sub> 653